

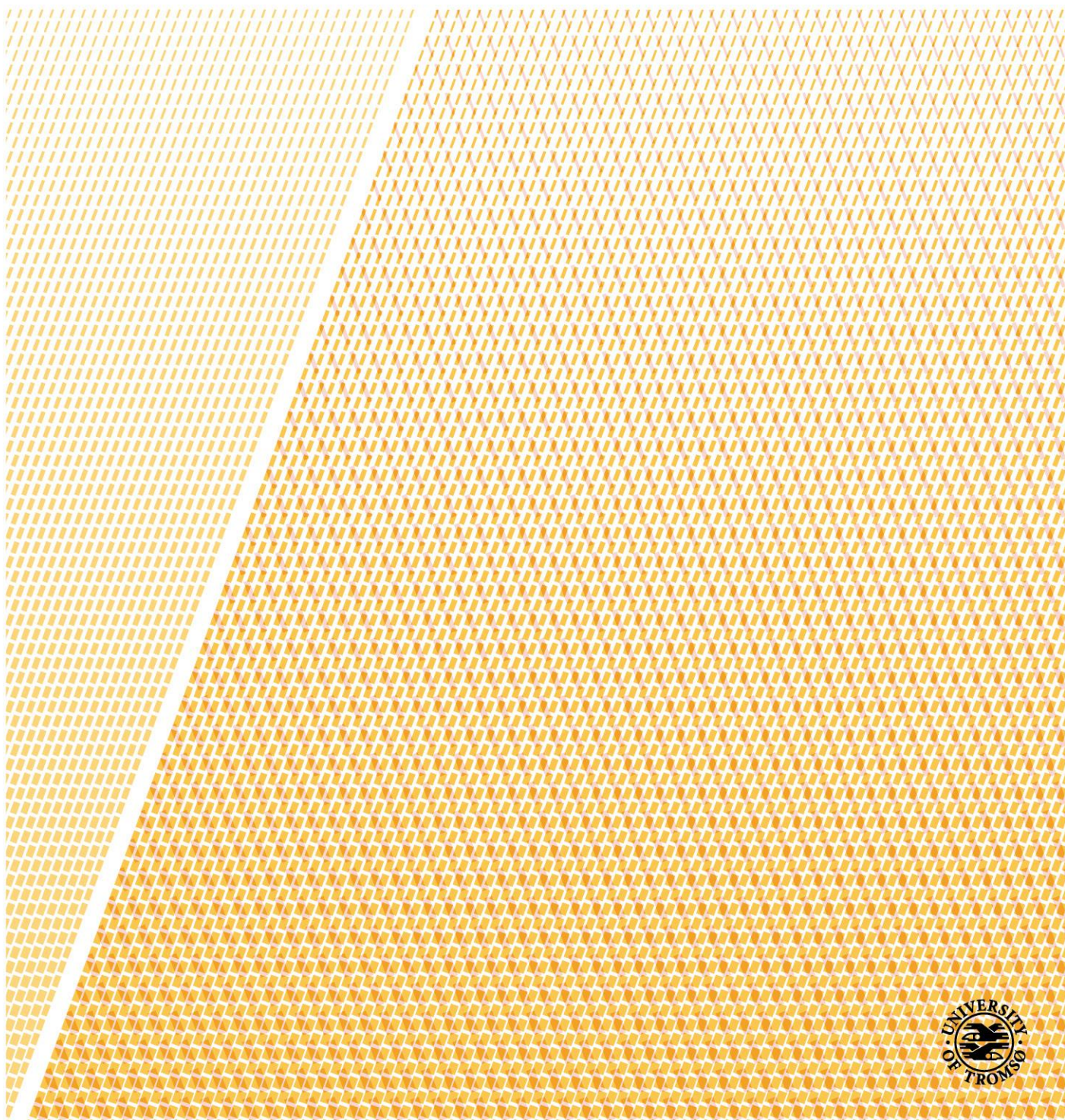
Two approaches to novel anticancer agents

Small-molecule library synthesis and evaluation

—

Marc Boomgaren

A dissertation for the degree of Philosophiae Doctor – December 2019



Acknowledgment

Doing a PhD is a journey with a known beginning and an approximately predictable end. In between, a lot of different experiences can be gained. Along my PhD journey, I had the pleasure to meet many new friends and the possibility to benefit from the knowledge and help of colleagues and my supervisors.

First of all, I want to thank my supervisor Associate Professor Jørn Hansen for the opportunity to do my PhD in his group. Jørn, I appreciated your help and the freedom you gave me to make own decisions and to find my way. Thank you so much to you and Stephanie for believing in me and supporting me.

I am grateful to my cosupervisor Professor Richard Engh for his help and the chance to start my career in Tromsø. The internship with you and Jørn was the start of a big adventure.

A thank you goes to Johan Isaksson for bringing me in contact with the dUTPase topic and for the NMR-support.

Without engineers, no research: a big thank you goes to Arnfinn Kvarsnes, Jostein Johansen, Truls Ingebrigtsen and Frederick Leeson for keeping the institute running. Arnfnn, I really learned a lot from you.

I am grateful to Marte Albrigtsen and Kirsti Helland for their work with the cell assays and Professor Jeanette Hammer Andersen for the support with the data analysis.

The contact to Professor Ole Morten Seternes and Henrike Bruckmüller changed a lot in my PhD-journey. I am thankful for every help and discussion I had with you.

Bjarte Aarmo Lund, Zuzana Kutová and Marcin Pierechod were fighting with the biochemical assays. I am grateful that you accepted this challenge and brought the project forward.

I am deeply grateful to Associate Professor Annette Bayer for her support. It would have been impossible to get this thesis finished without your help. It is really a pleasure to work for you and to have you as a friend.

Over all, I want to thank my colleagues, especially my lab and office fellows for all the support and good moments.

An extra big thank you goes to the members of my thesis correction and torture team: Hanna Bähr, Manuel Langer, Philip Rainsford, Tone Kristoffersen, and Yngve Guttormsen. I am

sure you really enjoyed torturing me with comments in the writing process. But yes, it would have been impossible to finish this journey without you. Be sure, I will do the same for you. Hanna and Manuel, you both brought me back on track in the right moment. I will not forget this.

The last lines are for my family at home. Lena, you know that I count you as a family member. Thank you so much for your friendship and help. It was so great that you came up to Tromsø for a few months. Without the support of my parents and grandparents, I would have never come so far in my life. The support was infinite and I returned it by moving to another planet. Sorry for that. I know this was not easy for you. You helped me to live my dream. I am endlessly grateful for that and I hope I will now find more opportunities to visit you at home.

Tromsø, December 2019

Marc Boomgaren

Abstract

The work presented in this dissertation combines two fully independent approaches to achieve compound libraries for anticancer drug research.

Project 1: Development of compounds inhibiting human dUTPase as an amplifier of a thymidylate synthase inhibitor based cancer therapy

The human dUTPase has received increased attention as a drug target in the recent years. Its inhibition can increase the efficacy of thymidylate synthase inhibitors in anticancer therapy. TAS-114 is the first human dUTPase inhibitor in clinical trials (phase 2). Based on the structure of TAS-114 and similar experimental dUTPase inhibitors, new dUTPase inhibitors were designed. Complex structure elements of the existing inhibitors were reduced to a simplified structure to form a new template. Literature described dUTPase inhibitors feature pyrrolidine, sulfonamide and triazole structures; these were replaced by imidazole as a core element in the newly designed compounds. The imidazole had further function in this simplified structure as the diversity platform for attempts to generate five different inhibitor scaffolds.

One scaffold included a N,O-acetal structure element, connecting uracil with the imidazole scaffold. The thesis describes the attempts to synthesize the N,O-acetal by use of protected N¹-chloromethyl uracil building blocks as alkylation agents. The synthesis of the four other scaffolds start from 2-imidazolecarboxaldehyde and ethyl imidazole-2-carboxylate as diversity platforms. The Mitsunubo reaction revealed a high potential for the connection of the imidazole building blocks with uracil and allowed short synthesis routes for new dUTPase targeting compounds. The synthesis routes were designed in a way that various scaffold types can be obtained from the intermediates. Overall, nearly 50 inhibitors were synthesized. The compounds were tested in different biochemical assays for their affinity to human dUTPase. ITC-measurements delivered thermodynamic data for the tested compounds and exhibited low micromolar target affinities. Further, initial cell assay screenings are described.

Project 2: Synthesis of dasatinib analogs enabled to form covalent connections with tyrosine kinases

Covalent binding tyrosine kinase inhibitors have been the subject of increasing interest in the last decade and there are now several FDA-approved inhibitors. These inhibitors form a covalent bond with cysteine containing kinases, increasing their affinity and selectivity for a specific target.

In project 2, the synthesis of potentially covalent binding dasatinib analogs is described. The bioactive core of dasatinib was modified for covalent binding. Diamine linkers of different

lengths and rigidity were attached to the bioactive core and connected to Michael acceptor groups, forming acrylic acid amides. To evaluate covalent binding effects, corresponding compounds with no Michael acceptor were synthesized. The compounds were tested for their affinity to different cysteine containing kinases. Covalent binding was not confirmed for the kinase BTK and KIT. Cell assays with different cancer cell lines expressing the kinases FLT3, BTK, and ITK, showed that three compounds significantly decreased cell viability relative to their reference compounds and dasatinib. These results indicate that covalent binding effects for some inhibitors may be present.

Abbreviations

ABL	Abelson-Kinase
addt	Additive
ATP	Adenosine triphosphate
BER	Base excision repair-Pathway
Boc	tert-Butyloxycarbonyl
BOM	Benzyloxymethyl-
BTK	Bruton-Tyrosinkinase
conc.	Concentrated
DCM	Dichloromethane
dCTP	Deoxycytidine triphosphate
DFT	Density functional theory
DHFR	Dihydrofolate reductase
DIAD	Diisopropyl azodicarboxylate
DIBAL-H	Diisobutylaluminum hydride
DIPEA	N,N-Diisopropylethylamine
DMAP	4-Dimethylaminopyridine
DMF	Dimethylformamide
DMSO	Dimethyl sulfoxide
DNA	Deoxyribonucleic acid
dTMP	Deoxythymidine monophosphate
DTT	Dithiothreitol
dTTP	Deoxythymidine triphosphate
dUMP	2'-Deoxyuridine, 5'-monophosphate
dUTP	2'-Deoxyuridine, 5'-monophosphate
e.g.	for example
EGFR	Epidermal growth factor receptor
eq	Equivalent
EtOAc	Ethyl acetate
EtOH	Ethanol
FdUMP	2'-Deoxy-5-fluorouridine 5'-monophosphate

FdUrd	5-Fluoro-2'-deoxyuridine
FdUTP	5-Fluorodeoxyuridine triphosphate
FLT3	Fms like tyrosine kinase 3
FTIR	Fourier-transform infrared spectroscopy
GSH	Glutathione
HMDS	Hexamethyldisilazane
HRMS	High Resolution Mass Spectrometry
ITC	Isothermal Titration Calorimetry
ITK	Interleukin-2-inducible T-cell kinase
MeCN	acetonitrile
MeOH	Methanol
MOM	Methoxymethyl
MTM	Methylthiomethyl
NBS	N-Bromosuccinimide
n.d	Not determined
NRTK	Non-receptor tyrosine kinase
O/N	overnight
POM	Pivaloyloxymethyl-
rt	Room temperature
RTK	Receptor tyrosine kinase
SAR	Structure activity relationship
SEM	2-(Trimethylsilyl)ethoxymethyl
solv	Solvent
TBAF	Tetrabutylammonium fluoride
TBAI	Tetrabutylammonium iodide
temp	Temperature
TFA	Trifluoroacetic acid
THF	Tetrahydrofuran
TKI	Tyrosine kinase inhibitor
TLC	Thin-layer chromatography
TMS	Trimethylsilane
TS	Thymidylate synthase
UDG	Uracil-DNA glycosylase

Table of Contents

1.	INTRODUCTION TO CANCER	1
1.1	General facts.....	1
1.2	Risks factors and processes leading to cancer	1
1.3	Chemotherapy	3
1.4	Resistances and negative side effects	3
2.	PROJECT 1: INTRODUCTION.....	7
2.1	Preventing uracil incorporation: The influence of uracil and thymine on DNA integrity.....	7
2.2	The thymidylate synthase: <i>De novo</i> synthesis to access the nucleobase thymine for DNA-synthesis	10
2.3	TS: the target for anticancer treatment.....	11
2.4	The deoxyuridine triphosphatase: A pyrophosphatase with uracil-gatekeeper function.....	13
2.5	The human dUTPase counteracts TS-cytotoxicity in cancer treatment	15
2.6	Examples of known dUTPase inhibitors	16
3.	PROJECT 1: AIM OF THE PROJECT	25
4.	PROJECT 1: DISCUSSION AND RESULTS	27
4.1	Design of human dUTPase inhibitors.....	27
4.2	Synthesis of N,O- acetal linked dUTPase compounds	30
4.3	N ¹ -chloromethyl uracils as electrophiles for N,O-acetal formation in type A and type B compounds.....	37
4.4	Synthesis of: alternative linkages replacing the N,O-acetal	54
4.5	Synthesis of: amide linked dUTPase compounds (Type H).....	56
4.6	Synthesis of: ether linked dUTPase compounds (type E).....	60
4.7	Synthesis of: plain hydrocarbon linked dUTPase compounds (type C/D).....	69
4.8	Biological activity evaluation of the compounds	74
5.	PROJECT 1: CONCLUSION	83

6.	PROJECT 1: FUTURE PERSPECTIVES	85
6.1	Options for scaffold optimization.....	85
6.2	Screening for carbonyloxymethyl-groups as protecting groups and prodrugs	87
7.	PROJECT 2: INTRODUCTION.....	93
7.1	Protein kinases as “on-off switches” in cell processes.....	93
7.2	Malfunction of tyrosine kinases	96
7.3	Tyrosine kinase inhibitors (TKIs) and resistance	97
7.4	Covalent binding in kinase inhibitors: Revival of an emitted interaction.....	100
8.	PROJECT 2: AIM OF THE PROJECT	107
9.	PROJECT 2: RESULTS AND DISCUSSION	109
9.1	Inhibitor design and strategy	109
9.2	Synthesis.....	111
9.3	Biological evaluation of the inhibitors.....	120
10.	PROJECT 2: CONCLUSION	135
11.	EXPERIMENTAL SECTION	137
11.1	General	137
11.2	Supporting information project 1.....	138
11.3	Supporting information project 2.....	210
12.	REFERENCES.....	224
13.	APPENDIX	235

1. Introduction to cancer

1.1 General facts

Cancer describes a group of over 100 different diseases that are characterized by uncontrolled cell- growth, division, and survival, with potentially life-threatening consequences for the host.^{1,2} The World Health Organization (WHO) estimates that approximately 9.6 million people died of cancer in 2018 world wide – equivalent to one in six reported deaths.² The risk of cancer under the age of 75 in Norway is 30% for women and 36 % for men.³ The Norwegian cancer statistic registry (Krefregisteret) registered 34 190 new cases in Norway in 2018, and 11016 deaths in 2017.³

1.2 Risks factors and processes leading to cancer

Cell growth, cell division, and apoptosis are well controlled in healthy cells, keeping the tissue homeostasis and blood formation in check.^{1,4-6} Risk factors can affect these controlled processes and can lead to a transformation of normal cells to cancer cells.^{7,8}

Potential risk factors for cancer are numerous and often not fully understood. Known risk factors are inherited defects and an unhealthy lifestyle e.g. consumption of alcohol and smoking.^{1,2,8,9} Further sources are radiation, a broad range of chemicals, infections e.g. human papillomavirus (HPV) or Helicobacter pylori, and hormones.^{2,9} These risk factors can induce mutations and alter gene transcription (epigenetic modification) of proto-oncogenes and tumor suppressor genes (Figure 1). Proto-oncogenes express proteins that are related to cell growth and cell division. The induced changes in the cell can lead to their transformation to oncogenes.^{1,6,10,11} These can have higher genetic activity, expressing more proteins or more active proteins. In order to keep these processes in check, and to prevent rampant cell growth and division, tumor suppressor genes express proteins, which mediate DNA-repair and apoptosis.^{5,11,12} Prolonged exposure to risk factors can result in the tumor suppressor genes being damaged or deactivated.^{4,8,13} This can result in uncontrolled cell growth, as well as decreased DNA-repair and apoptosis in affected cells (Figure 1).^{1,4,8,10,12}

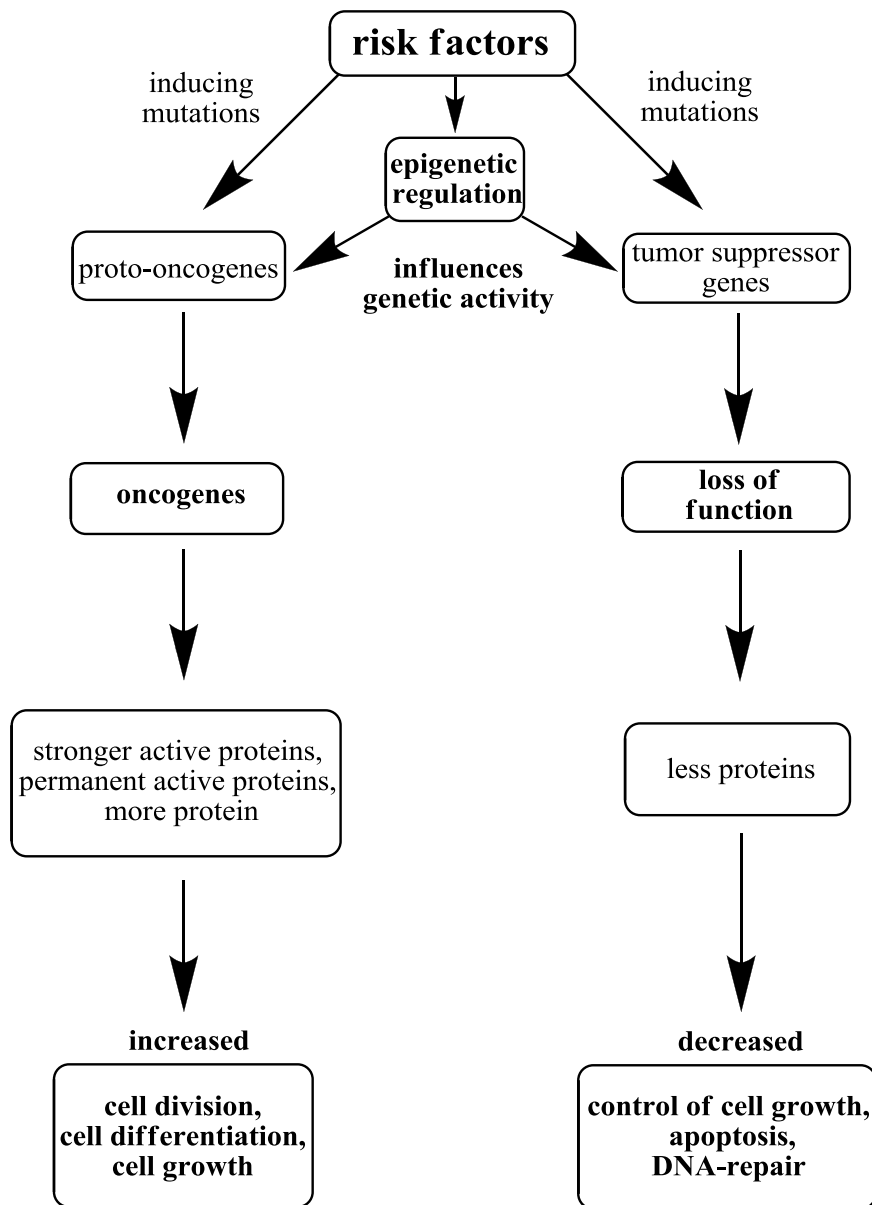


Figure 1: Risk factors can induce mutations and modification of proto-oncogenes or tumor suppressor genes. Oncogenes can express more, or due to modification, stronger active proteins involved in cell growth and related processes. Tumor suppressor genes can lose their function and express less proteins involved in cell growth control mechanism, apoptosis and DNA-repair.

Complex control systems prevent single mutations and/or epigenetic modifications from having serious consequences for the affected cells.^{14,15} If the control system fails however, an accumulation of synergistic mutations facilitate permanent changes and lead to malignant cells and cancer.^{7,14,15} With the exception of blood cancers (e.g. leukemia), most malign cells build solid tumors, damaging surrounding tissues and forming new tumors through cancer cell migration.⁷ Faster growing and less specialized tumor cells lead to a loss of function of the affected tissue.¹ This process is called metastasis and one of the main reasons for the high mortality rate of cancer patients.^{7,8}

1.3 Chemotherapy

Cancer can be treated by radiation, biologicals, and chemotherapy or by the removal of the tumor with surgery.¹⁶⁻¹⁸ Often, combinations of different methods are used. Despite the access to a multitude of strategies, the full remission is heavily dependent on the kind of cancer and for example the age of the patient.^{2,3} Chemotherapy is used to destroy cancer cells in a number of ways. “Traditional” chemotherapy focuses on turning the cancer’s biggest strength, rapid cell division, into its weakness.¹⁹ The rapid cancer cell division implies a high replication rate of DNA. To impede these processes, cytotoxicity is achieved through the cross-linking of DNA strands irreversibly, interruption of DNA-building block synthesis, and disturbance of the DNA replication process.^{13,19} Other drugs hinder the ability of the replicated DNA to migrate into newly formed cells.¹³ Newer anticancer strategies target proteins that are involved in growth and apoptosis signaling pathways. Targets are receptors and signal transducers that recover control over cell activity. Especially protein kinases as cell signal relays are the subjects of interest, and part of intensive research for new drugs.^{13,20}

1.4 Resistances and negative side effects

Often chemotherapy has to overcome selectivity problems and efficiency changes. Cytotoxic agents have an increased effect on rapidly dividing cancer cells, but also target quickly dividing healthy cells like hair follicles cells or the bone marrow, responsible for the proliferation of blood cells.^{13,18,21} These side effects make chemotherapy a huge physical stress for the entire body.

Drug resistance is another prominent problem in anticancer therapy. The high rate of DNA replication in cancer cells can result in increased mutations due to reduction of the DNA control mechanisms.^{8,22} These mutations can change the structure and function of expressed proteins, lowering the drug affinity of chemotherapeutic agents. Further reasons for reduced drug efficiency are:^{4,13,22}

- Drug efflux of the cell
- Reduced drug uptake
- Partial or full inactivation of the drug
- Higher activity of DNA-repair and DNA gatekeeper enzymes
- Higher expression of the target protein

The loss of drug efficiency and negative side effects are the driving forces for the development of new anticancer therapies.

Project 1:

**Development of compounds inhibiting human
dUTPase as an amplifier of a thymidylate synthase
inhibitor based cancer therapy**

2. Project 1: Introduction

2.1 Preventing uracil incorporation: The influence of uracil and thymine on DNA integrity

DNA is the genetic memory and operating manual for living cells, and is therefore of high value.²³ Especially, the complexity of the cell division process opens the DNA up to damages and replication failures from internal and external sources.^{24,25} The consequence of any error might be permanent mutations, reduced cell division or apoptosis. Therefore, the integrity of the genetic information needs to be ensured, and this is done through several proofreading-, repair- and supporting enzyme systems.

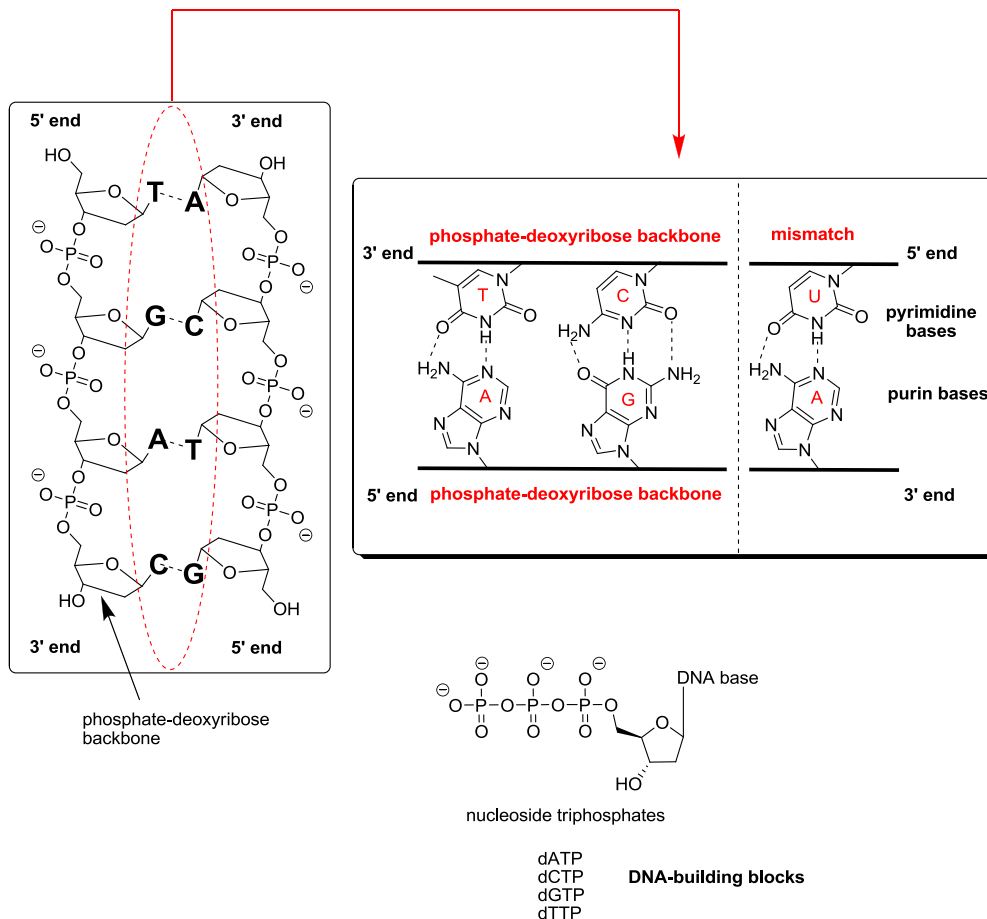


Figure 2: The DNA double helix is formed by two single strands. The phosphate-deoxyribose backbone carries the DNA nucleobases.^{23,26} The strands are connected by hydrogen bonding between a pyrimidine DNA base (T = thymine or C = cytosine) and a purine DNA base (A = adenine or G = guanine) resulting in the pairing AT and GC. The pyrimidine DNA base uracil (U) differs from thymine by a methyl group and pairs with adenine.²⁷ In most organisms, uracil is not part of the DNA. DNA is synthesized from nucleoside triphosphates (dATP, dCTP, dGTP and dTTP), consisting of the specific DNA nucleobase, a deoxyribose, and a triphosphate group.²³

DNA has a double helix structure formed by two antiparallel polynucleotide strands connected by hydrogen bonds. The backbone of both strands is made up by a phosphate-deoxyribose chain (Figure 2).^{23,26} Every deoxyribose contains a pyrimidine or purine nucleobase. The pyrimidine nucleobases cytosine (C) and thymine (T) form pairs with the purine nucleobases guanine (G) and adenine (A) on the opposite strand *via* hydrogen bonding.²³ The order and combination of pairs along the DNA strand codes the genetic information.²³ DNA replication and DNA repair requires that the nucleotides are in the form of their respective DNA building blocks: the nucleoside triphosphates dATP, dCTP, dGTP and dTTP.

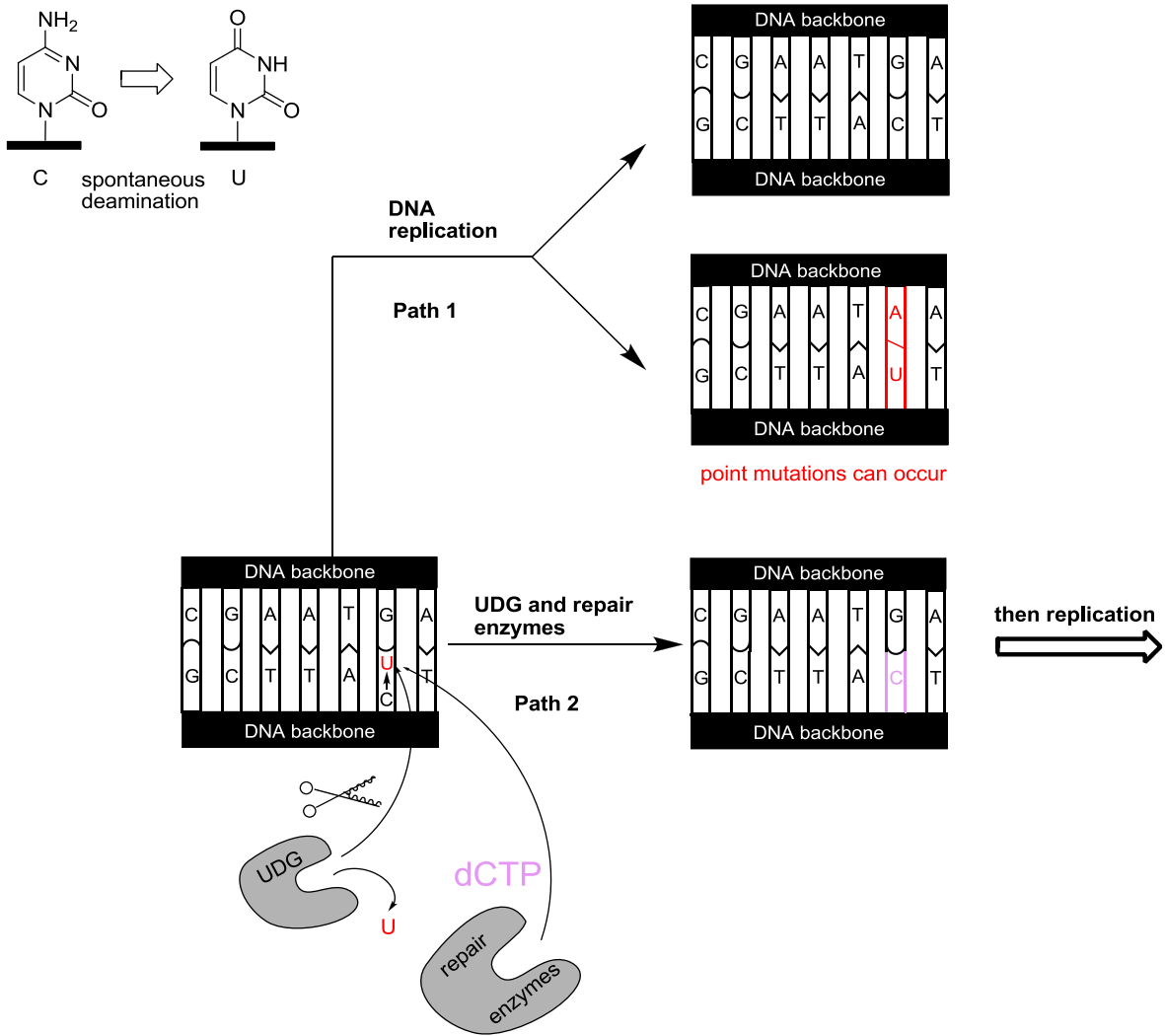


Figure 3: The pyrimidine base cytosine undergoes spontaneous deamination resulting in uracil (C → U). During DNA replication, the double stranded helix is separated, and both strands serve as template for new strands (path 1). One single-strand forms the correct GC pair, whereas in the other strand, uracil hybridizes with adenine (AU, in red) resulting in a change of the genetic information (point mutation). Enzymes of the BER system can detect uracil and exchange it for cytosine before replication (violet) (path 2).

The sensitivity of DNA nucleobases towards hydrolysis, methylations, and oxidations is one reason for the need of DNA replication systems.²⁴ The instability of the pyrimidine nucleobase cytosine plays a primary role; it is well established that cytosine undergoes spontaneous deamination to the pyrimidine nucleobase uracil (Figure 3).^{24,25,28} Uracil does not affect the stability of the double helix, but it affects DNA replication. The DNA single strands serve as templates for the incorporation of the correct nucleoside triphosphates during the synthesis of the new strand (Figure 3).²⁷ Spontaneous deamination of cytosine leads to a change in one of the single strands - that single strand contains uracil instead of cytosine, while the other single strand still contains guanine. During the replication process, the guanine-containing strand forms the correct GC-pair while the uracil-containing strand pairs with adenine (Figure 3, path 1).²⁷ The result is a point mutation (GC to AU), and a change of the genetic information.²⁷ The mutagenic impact of uracil explains its exclusion as DNA nucleobase in most organisms and the preference of thymine, which differs by a methyl from uracil, over uracil as hybridizing partner for adenine (Figure 2).^{27,29}

To avoid a mutagenic effect by uracil, enzymes like Uracil-DNA glycosylases (UDG) and deoxyuridine triphosphatase (dUTPase) are specialized in minimizing uracil levels in DNA.^{27,30} UDGs remove uracil from DNA (Figure 3, path 2) whereas dUTPase prevents deoxyuridine incorporation into DNA using its nucleoside, deoxyuridine triphosphate (dUTP) (1) (Figure 4).^{27,30,31} As such, the methyl group of thymine works as a selectivity marker for UDGs.²⁷ It allows UDGs to detect uracil in DNA as errors, and to excise them while AT-pairs remain unaffected.^{31,32} UDGs are part of the Base Excision Repair System (BER). Other enzymes of the BER system open the DNA-strand after uracil excision and insert a new deoxycytidine (Figure 3, path 2) in the form of its nucleoside triphosphate dCTP to recover DNA integrity.^{27,31}

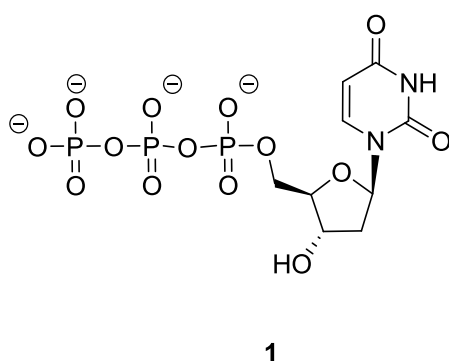


Figure 4: Structure of deoxyuridine triphosphate (dUTP) (1).

2.2 The thymidylate synthase: *De novo* synthesis to access the nucleobase thymine for DNA-synthesis

To get thymine as a nucleobase a more complex synthesis is required. Thymine is synthesized as a substituent of deoxythymidine monophosphate (dTMP) (**3**); the uracil group of deoxyuridine monophosphate (dUMP) (**2**) is methylated to a thymine group.^{33,34} The resulting dTMP (**3**) is further phosphorylated to deoxythymidine triphosphate (dTTP) (**4**) and used in DNA synthesis (Figure 5).³³ In this cascade of transformations, the rate-determining step is the methylation of uracil by the enzyme thymidylate-synthase (TS).³⁴ The cofactor and methyl group donor is 5,10-methylenetetrahydrofolate (5,10-CH₂-THF) which is an intermediate of the folate cycle. The enzyme dihydrofolate reductase (DHFR) is involved in the cofactor production.³⁴ The flawless function of the thymidylate synthase is crucial to obtain sufficient amounts of dTTP (**4**) for DNA synthesis and DNA-repair. Therefore, TS is seen as one of the “bottlenecks” in DNA synthesis.^{33,34} Disturbances of the TS-complex can have severe effects on DNA integrity.

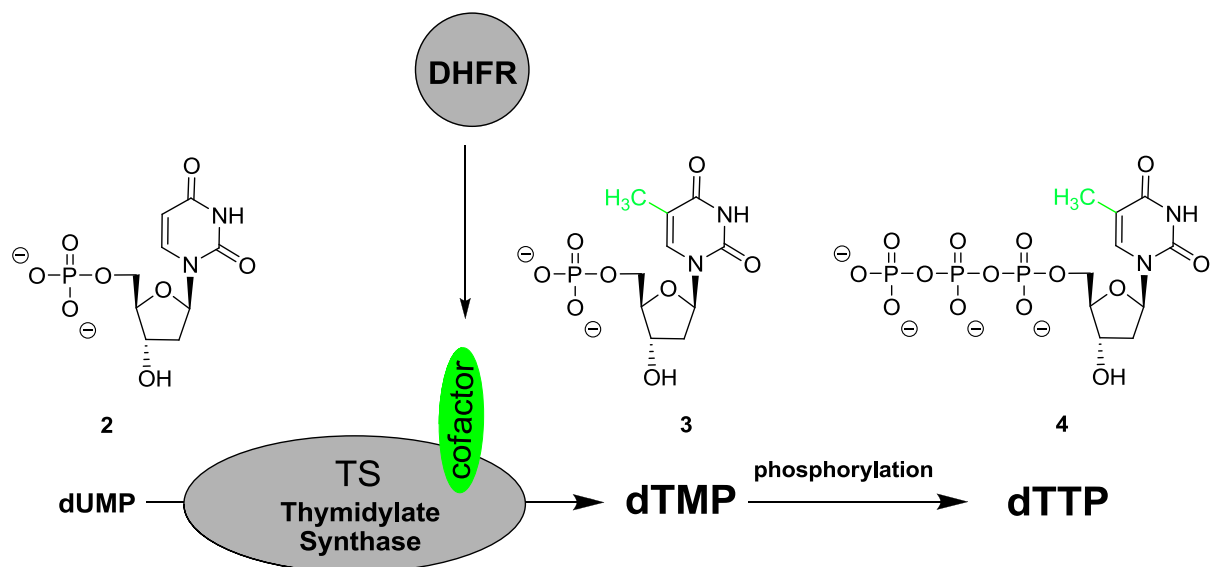


Figure 5: The nucleotide dTTP (**4**) is used as a building block for the incorporation of deoxythymidine in DNA. TS catalyses the methylation of uracil to thymine with the help of the cofactor 5,10-CH₂-THF (green). The dihydrofolate reductase (DHFR) is involved in cofactor production. dTMP (**3**) is further converted to dTTP (**4**).

2.3 TS: the target for anticancer treatment

For many centuries the thymidylate-synthase has played an important role in cancer treatment.³⁴ TS-inhibitors are used against a wide range of cancer types including colon-, breast- and lung cancers.³⁴ The administered compounds are divided into fluoropyrimidines and antifolates (Figure 6).³⁴ Fluoropyrimidines are mainly represented by 5-fluorouracil (5-FU) (**5**) and prodrugs like tegafur (**6**) or capecitabine (**7**) (Figure 6).³⁴ Free 5-FU (**5**) is metabolized to 5-fluorodeoxyuridine monophosphate (FdUMP), forming a stable ternary complex with the cofactor and TS through covalent binding.^{35,36} Thus, the natural substrate dUMP cannot enter the nucleotide binding site of the enzyme, and is therefore not converted to dTMP (**3**). Antifolates like Raltitrexed (**8**) and Pemetrexed (**9**) inhibit the TS cofactor binding site and the DHFR, thus suppressing the cofactor production (Figure 5 and Figure 6).^{34,37,38}

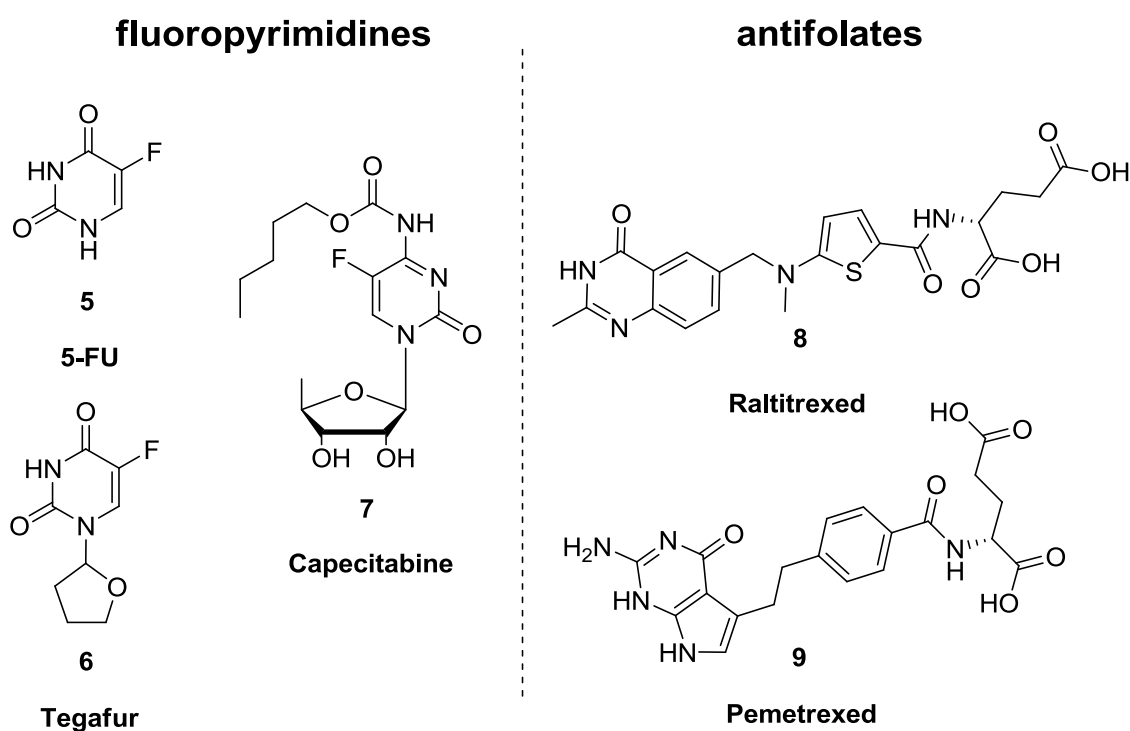


Figure 6: Structures of selected commercially available drugs used in anticancer therapy.

The inhibition of TS results in depletion of dTMP (**3**) and dTTP (**4**) and leads to an imbalance of the entire nucleoside pool (dATP, dCTP and dGTP) by a feedback systems (Figure 7, I).^{39,40} Normally, the DNA replication is restricted under these conditions (Figure 7, II).^{35,40} The concentration of dUMP (**2**) increases, and leads to increased formation of dUTP (**1**) by phosphorylation (Figure 7, III). If the ratio dUTP/dTTP is high, more dUTP (**1**) is used as a

substrate for DNA replication. UDGs remove the incorporated uracils leading to depyrimidated gaps in the DNA double helix (Figure 7, IV).^{28,30,41} Insufficient amounts of dTTP (4) (Figure 7, V) do not allow for efficient DNA-repair, and leads to double strand breakage and cell death; this process is often referred to as “thymidine-less death”.^{30,35} These mechanisms are the main reason for the cytotoxicity of TS inhibitors and their efficiency in anticancer treatment.^{35,42} Further cytotoxic effects are a result of fluoropyrimidine metabolites like 5-fluorodeoxyuridine triphosphate (FdUTP).³⁵ FdUTP can be incorporated into DNA just like dUTP (1), thereby damaging the DNA and impairing the RNA integrity. Due to these different modes of actions, fluoropyrimidine drugs are highly valuable.³⁵

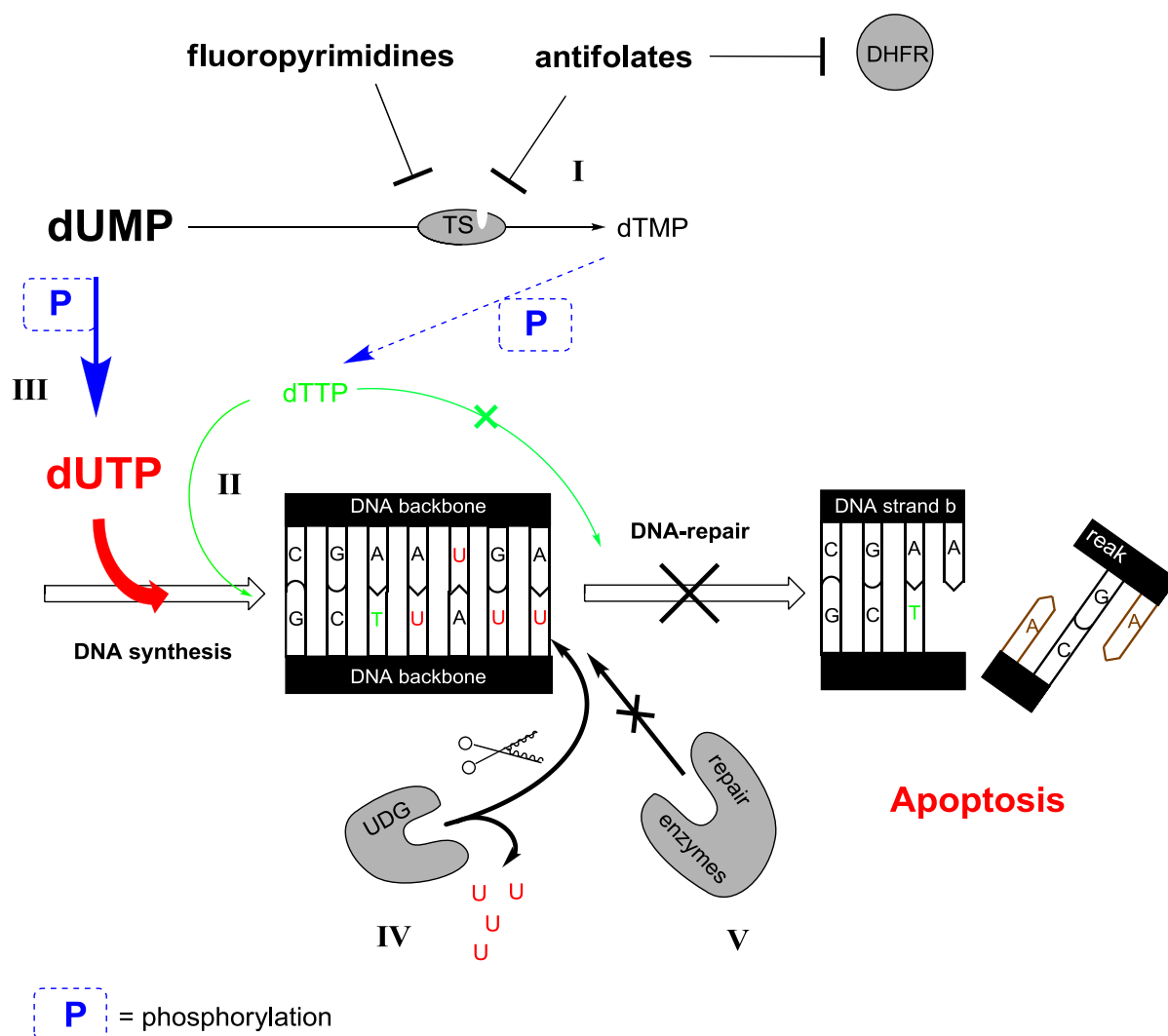


Figure 7: The inhibition of TS results in increased dUMP (2) and dUTP (1) concentrations. Statistically more dUTP (1) than dTTP (4) is available for DNA synthesis, and more uracil is incorporated. The excision of uracil by UDG results in depyrimidated gaps. Low amounts of dTTP (4) do not allow an efficient DNA repair and lead to apoptosis of the cell.

2.4 The deoxyuridine triphosphatase: A pyrophosphatase with uracil-gatekeeper function

The attempt to keep intracellular dUTP (**1**) levels low and dTTP (**4**) levels high is integral for DNA protection mechanisms against mutagenic effects caused by uracil.^{27,30,43} The enzyme deoxyuridine triphosphatase (dUTPase) hydrolyses dUTP (**1**) to dUMP (**2**) and pyrophosphate (PPi) (**10**) to avoid deoxyuridine in DNA (Figure 8).²⁷ Therefore, dUTPases are significant for DNA integrity and cell viability and are expressed in the majority of organisms.⁴⁴⁻⁴⁷

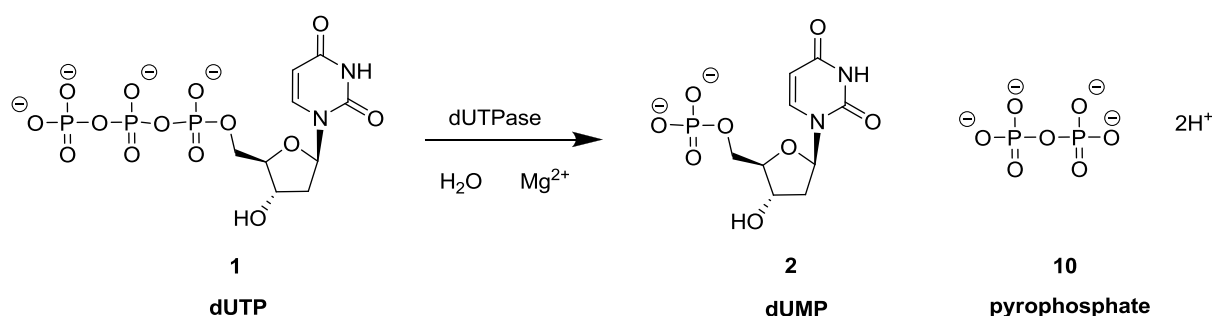


Figure 8: The dUTPase hydrolyses dUTP (**1**) to dUMP (**2**) using water and a stabilizing magnesium ion. dUMP (**2**) is used to build new dTTP (**4**) for DNA replication and to lower the chance of deoxyuridine incorporation into DNA.

dUTPases are mainly homotrimers constituted by monomers with jelly roll beta barrels folding and comprise three active sites (Figure 9).^{27,48} The monomers can be subdivided into five conserved structural motifs 1-5.⁴⁸ Every subunit (here: A, B, C) has a flexible C-terminal arm covering one active site between the surface of the two other subunits.^{27,49,50} A beta-hairpin motif is responsible for the high dUTP (**1**) selectivity.⁴⁸ The main concept is to bind uracil in a narrow pocket to discriminate other nucleobases by steric hindrance. This selection process avoids the destruction of the other nucleoside triphosphates by hydrolysis.^{27,48}

Magnesium ions play an important role in the catalytic process. They coordinate the triphosphate moiety of dUTP (**1**) in a gauge conformation for the attack of catalytically active water molecules. Thereby, the triphosphate chain and the magnesium ions are stabilized by motif 1, 2 and 4, as part of two monomers.^{27,48} A flexible C-terminal arm (motif 5) is involved in the catalytic process. It is assumed that the C-terminal arm becomes conformationally constrained due to substrate binding, closes the active site, removes bulk solvent, and initializes the catalytic process.^{48,50} Stacked conformations between phenylalanine of the C-terminal arm, with the uracil of dUTP inhibitors, are interpreted as indication for this function. Figure 9 shows the interactions of the C-terminal arm with the non-hydrolysable dUTP analog α,β -imino dUTP (**11**) in the active site of human dUTPase.⁵⁰

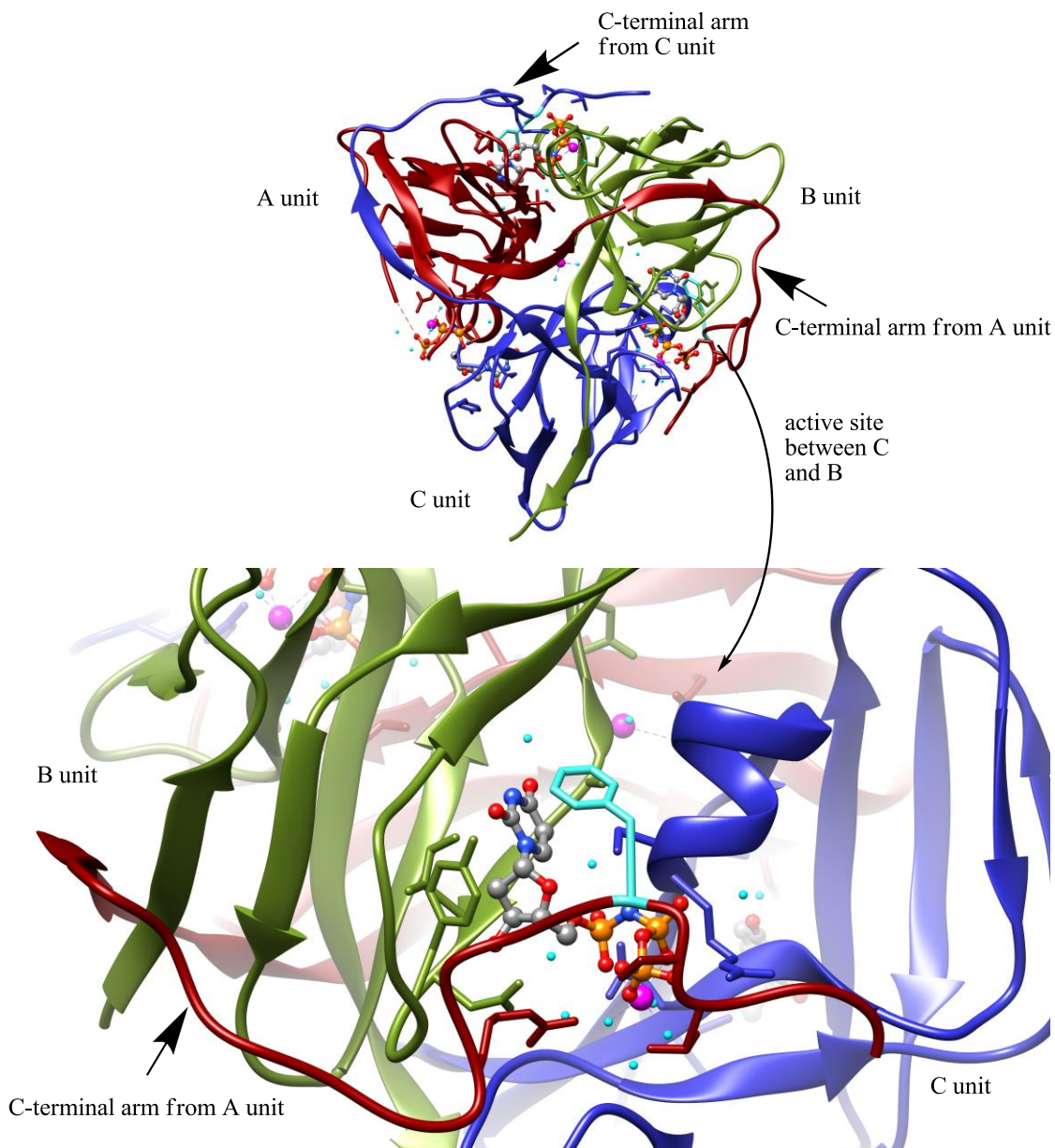


Figure 9: Most dUTPases are homotrimers (units A, B, C). The active site is on the surface between two subunits. The C-terminal arm from the third subunit becomes ordered when the substrate is bound to the active site (here α,β -imino dUTP (**11**)). The lower picture shows the dUTP analog α,β -imino-dUTP (**11**) (in element-specific colors, stick-ball model) in the active site formed by the B unit (green) and C unit (blue). The C-terminal arm of the A unit (red) is close to the active site. A phenylalanine of the C-terminal arm (highlighted in cyan, Phe 158) stacks over the uracil. (magnesium ions in magenta, water molecules are spheres in cyan). (PDB code: 2HQU).⁵⁰ Figure made with Chimera.

2.5 The human dUTPase counteracts TS-cytotoxicity in cancer treatment

The human dUTPase prevents deoxyuridine incorporation into DNA through the hydrolysis of intracellular dUTP (1) (Figure 10, A).^{27,30} Upon depletion of dUTP (1) the dUMP (2) concentration is elevated and induces a higher production of dTTP (4) by TS.^{27,30} This, in combination with the DNA-repair system, leads to subcritical amounts of deoxyuridine in DNA.^{27,30} TS-inhibitors (Figure 10, B) reduce the dTMP/dTTP production and lead to higher dUTP (1) concentrations and in case of fluoropyrimidines to the production of FdUTP.³⁵

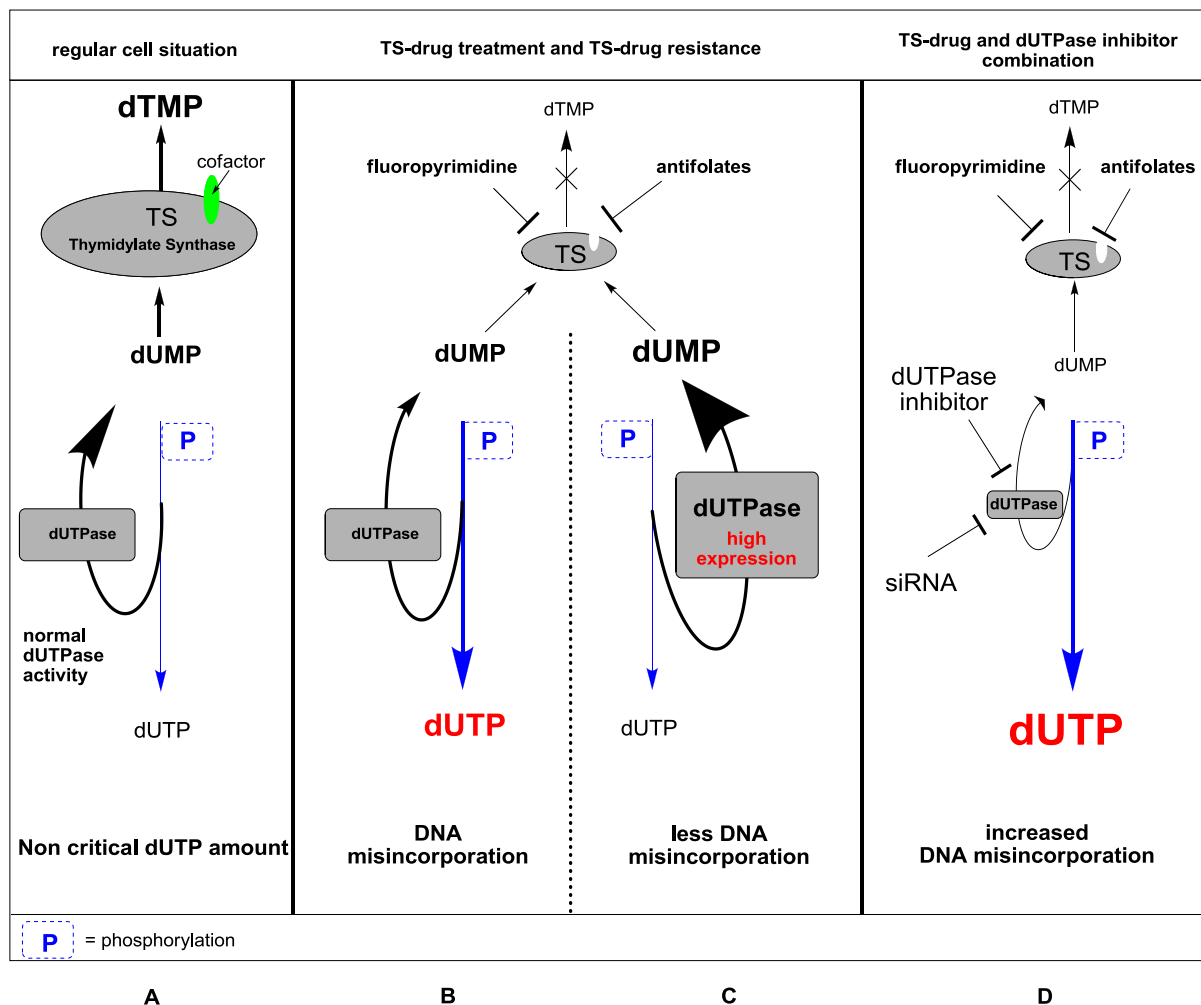


Figure 10: (A) Untreated cell; dUMP (2) is mainly converted to dTMP (3) by TS. Smaller amounts of dUMP (2) are phosphorylated to dUTP (1). A normally functioning dUTPase is able to convert dUTP (1) back to dUMP (2). Cytotoxic levels of dUTP (1) are not reached. (B) Treatment with drugs reduces TS activity. dUMP (2) can not be converted to dTMP (3) efficiently. Increased dUMP (2) levels result in higher dUTP (1) production which cannot be lowered by dUTPase. Cytotoxic levels of dUTP (1), as well as FdUTP, are reached. (C) An increased expression of dUTPase (resistant cells) in combination with TS inhibition results in an insufficiently cytotoxic effect of dUTP (1) and FdUTP. (D) Silencing of the dUTPase expression by siRNA or dUTPase inhibitors has the potential to increase the cytotoxic effects of dUTP (1).

A normal functioning human dUTPase hydrolyses parts of the produced dUTP (**1**) and FdUTP but still allows sufficient cytotoxic effects during anticancer therapy.⁴¹ However, a high dUTPase expression (Figure 10, C) can counteract TS-inhibitor effects and lower the drug activity significantly or lead to resistances.^{41,51-54}

The correlation between human dUTPase expression and lower TS-inhibitor efficiency was proven by using small interfering RNA (siRNA) for silencing dUTPase activity in cells (different lung-, breast- and colorectal cancer cell lines).^{47,51} Cells treated with a combination of siRNA and TS-inhibitors showed significantly higher sensitivity to drug treatment than to TS-inhibitor treatment alone. These correlations were proven by small molecule inhibitors like TAS-114 (**23**) (Figure 10, D; Figure 13).^{47,55}

2.6 Examples of known dUTPase inhibitors

The fact that human dUTPase reduces the efficiency of TS-inhibitors and siRNA silencing recovers cytotoxicity underlines the human dUTPase as a possible anticancer drug target.^{47,51} Therefore, the research towards the development of human dUTPase inhibitors has increased in recent years. However, research into human dUTPase inhibitors is still in an early stage in comparison to other anticancer drug research. Some important developments are described below.

2.6.1 Example: Structure analogs of the natural substrate

The high substrate selectivity of dUTPases for dUTP (**1**) offered a good starting points in the early development of dUTPase inhibitors.^{56,57} The design of these inhibitors was based on structural similarities to the natural substrate. Small structural changes are enough to convert the natural substrate into an inhibitor. One of the first structures that were developed are methylene-dUTP (M-dUTP) (**12**) and BM-dUTP (**13**).⁵⁶ The dUTPase hydrolyses dUTP between the α,β -oxygen bridge of the triphosphate. The exchange of the hydrolysis sensitive oxygen against a methylene group resulted in the slow, or non-hydrolysable structure analogues **12** and **13** (Figure 11, in red labeled). The benzyl group in **13** was introduced for lipophilicity to enhance membrane permeability (Figure 11, in red labeled).⁵⁶ Tests with E.coli dUTPase exhibited moderate K_i values of 3.5 μM for **12** and 0.3 μM for **13**. Assays with human cancer cell lines exhibited significant cytostatic and cytotoxic effects.⁵⁶ Besides the good affinities and cell assay results, no further drug development steps for compounds **12** and **13** are reported.

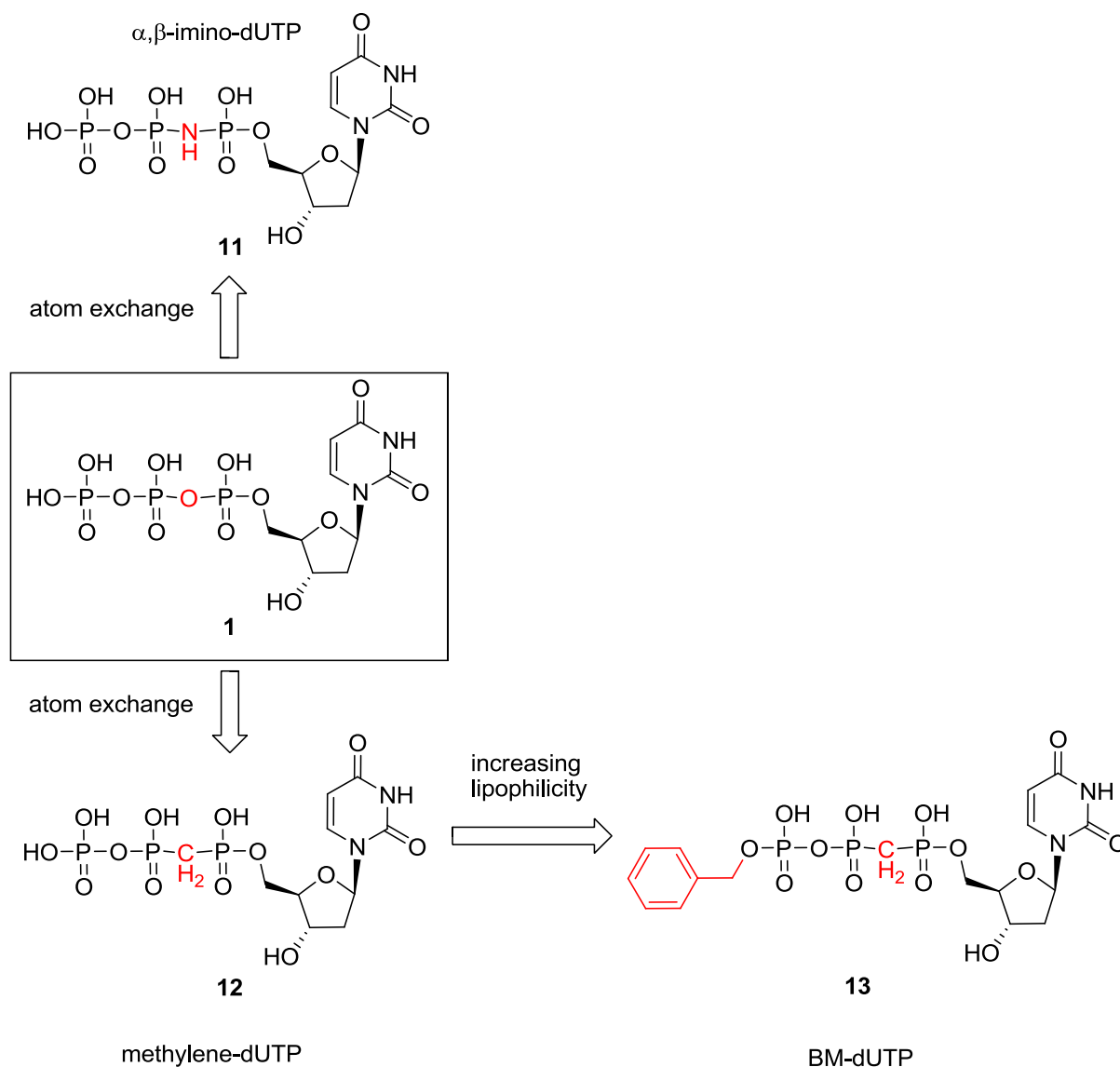


Figure 11: First attempts for designing dUTPase inhibitors based on the natural substrate dUTP. The exchange of the α,β -oxygen bridge of the triphosphate by a methylene or amino group delivered non-hydrolysable inhibitors. The benzyl group of BM-dUTP increases the membrane permeability (molecule changes in red).^{56,57}

The nitrogen analog α,β -imino-dUTP (dUpNpp) (**11**) is used frequently. **11** has K_i values of 5 μM against E.coli dUTPase and an IC_{50} value of 15 μM for human dUTPase.^{57,58} α,β -imino-dUTP (**11**) is used as a ligand in protein structure determination, as a reference compound in enzyme assays, and to study kinetics of dUTPases.^{50,57-60} The high similarity of the inhibitors with the natural substrate does however pose some problems. dUTP analogs are seen as being unsuitable drug candidates because of their poor physico-chemical properties leading to low bioavailability.^{59,61} However, dUTP analogs gave a deeper insight into the function of dUTPases and thereby contributed to the design of other inhibitors.

2.6.2 Example: Malaria dUTPase inhibitors

High target selectivity for a specific dUTPase is of importance when human dUTPase is not the subject of interest. This applies in particular to dUTPases relevant in diseases like malaria and tuberculosis.^{27,62,63} Treatment with unselective inhibitors can also affect the human dUTPase leading to negative consequences for the patient. In the case of malaria, several successful attempts for specific dUTPase inhibitors are described in literature.^{61,64-66} Trimeric dUTPases are structurally quite conserved, although the sequence homology between dUTPases can be small. Yet, these small differences at the active site are the key for selectivity.⁶²

The dUTPase of malaria caused by the parasite *Plasmodium falciparum* (*PfdUTPase*) was subject of intensive research for selective dUTPase inhibitor designs.^{61,62,66} The binding site of *PfdUTPase* is slightly more lipophilic than the human dUTPase due to an insertion of over 20 amino acids.⁶² Several libraries of inhibitors exploiting these differences have been synthesized, reaching 1000 fold higher selectivity factors towards *PfdUTPase* over human dUTPase.^{61,62,64,66} Many of the potent *PfdUTPase* inhibitors are also low micromolar human dUTPase inhibitors thus having low selectivity factors (Figure 12).^{61,64}

A few examples of *PfdUTPase* inhibitors with effect on human dUTPase are shown in Figure 12. The design contrasts the design of dUTP analogs like **11-13**. The first *PfdUTPase* inhibitors were based on deoxyribose-uracil structures (Figure 12). In these compounds, bulky trityl or diphenyl groups replaced the triphosphate chain to address the more lipophilic active site of *PfdUTPase*.^{61,66} Compound **14** (example 1) reached a K_i value of 1.8 μM for *PfdUTPase* but also showed a moderate binding affinity for the human dUTPase ($K_i = 18 \text{ M}$). Some other libraries replaced the sugar moiety with acyclic structures without losing affinity (**15**, example 2) to the human dUTPase.^{61,64} Even structures with low structural similarity (example 3-5) reached moderate to good affinities for the human dUTPase.

Introduction of heteroatoms (**16**), different bulky substituents (**17**), branched structures (**19**) (example 3-5), and rotational restriction through double bonds (**21-22**, example 5) were tolerated by both enzymes.^{61,64} Other examples also show how affinity can drop as a result of minor changes in the scaffold (example 4 and 5). Introduction of a methylene group into the linker of compound **18** lowered the affinity from 1.4 μM to over 1000 μM for human dUTPase (**20**). An insertion of an extra OH-group, however, restored affinity (**19**). The same effects were observed for the rigid structures **21** and **22** (example 5); while the *Z*-isomer **21** had a K_i value of 5.2 μM , the *E*-isomer **22** exhibited a K_i -value of over 1000 μM for human dUTPase (Figure 12).⁶¹ None of these described inhibitors have reached clinical trials as anticancer drugs. However, similar structures were starting points for human dUTPase inhibitors developed by Taiho Pharmaceuticals.⁵⁸

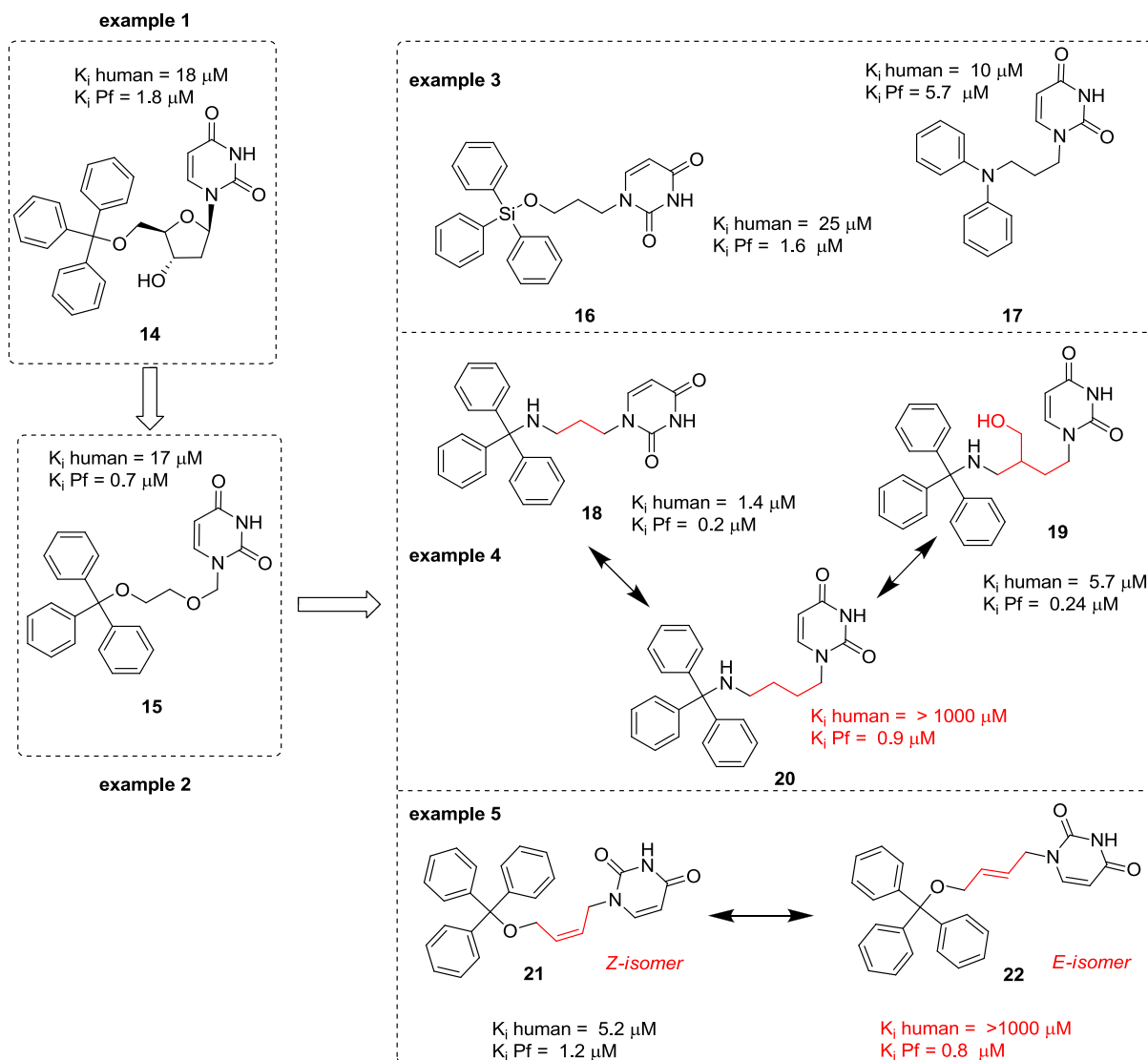


Figure 12: Examples of unselective *Pfd*UTPase inhibitors with affinity to the human dUTPase and *Pfd*UTPase.^{61,64-66}

2.6.3 Breakthrough: The way to human dUTPase inhibitor TAS-114

TAS-114 (**23**) is the first oral drug in clinical trials targeting human dUTPase and DPD (dihydropyrimidine dehydrogenase) (Figure 13).⁶⁷ This compound can be considered as a breakthrough in the development of human dUTPase inhibitors. Studies with different cancer cell lines proved the concept of amplified TS-inhibitor efficiency if used together with TAS-114. The dUTPase inhibitor alone showed only weak cytotoxicity.^{55,67}

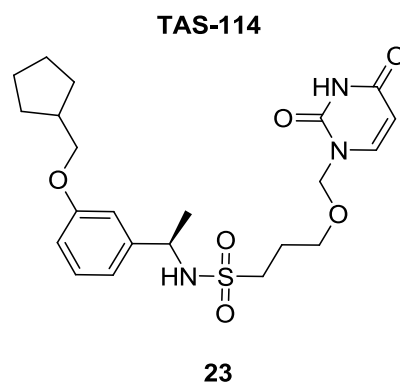


Figure 13: TAS-114 is the first human dUTPase inhibitor in clinical trials.^{55,67}

TAS-114 (**23**) was developed by Taiho Pharmaceuticals. Four papers based on patents were published (Miyakoshi and Miyahara et al.) between 2011-2012.^{58,59,68,69} They describe the synthesis, the rational design based on crystal structures, and the biological activity of numerous scaffolds similar to TAS-114 (**23**). Further patents followed.

Several reported compounds reached IC_{50} values lower than 50 nM making them the strongest human dUTPase inhibitors known so far (examples in Figure 14).⁵⁹ *In vivo* studies of these compounds showed synergistic effects when co-administrated with TS-inhibitors against HeLa S3 cells and in MX-1 xenograft models.⁵⁹ These findings confirmed the high potential of dUTPase inhibitors for anticancer drug therapies. Evaluations of protein-inhibitor complexes in crystal structures gave information about the binding mode in the active site and allowed for the proposal of a mechanism for target inhibition.^{58,59}

Uracil containing libraries were the starting point for these new classes of human dUTPase inhibitors. Hit-prescreenings were based on biological activity (enzyme assays and cell assays) and Lipinski rules.⁵⁹ The initial hits **24** and **29** had IC_{50} values of 97 μ M and 100 μ M, respectively (Figure 14).^{58,59} The structures were developed further in different compound libraries.

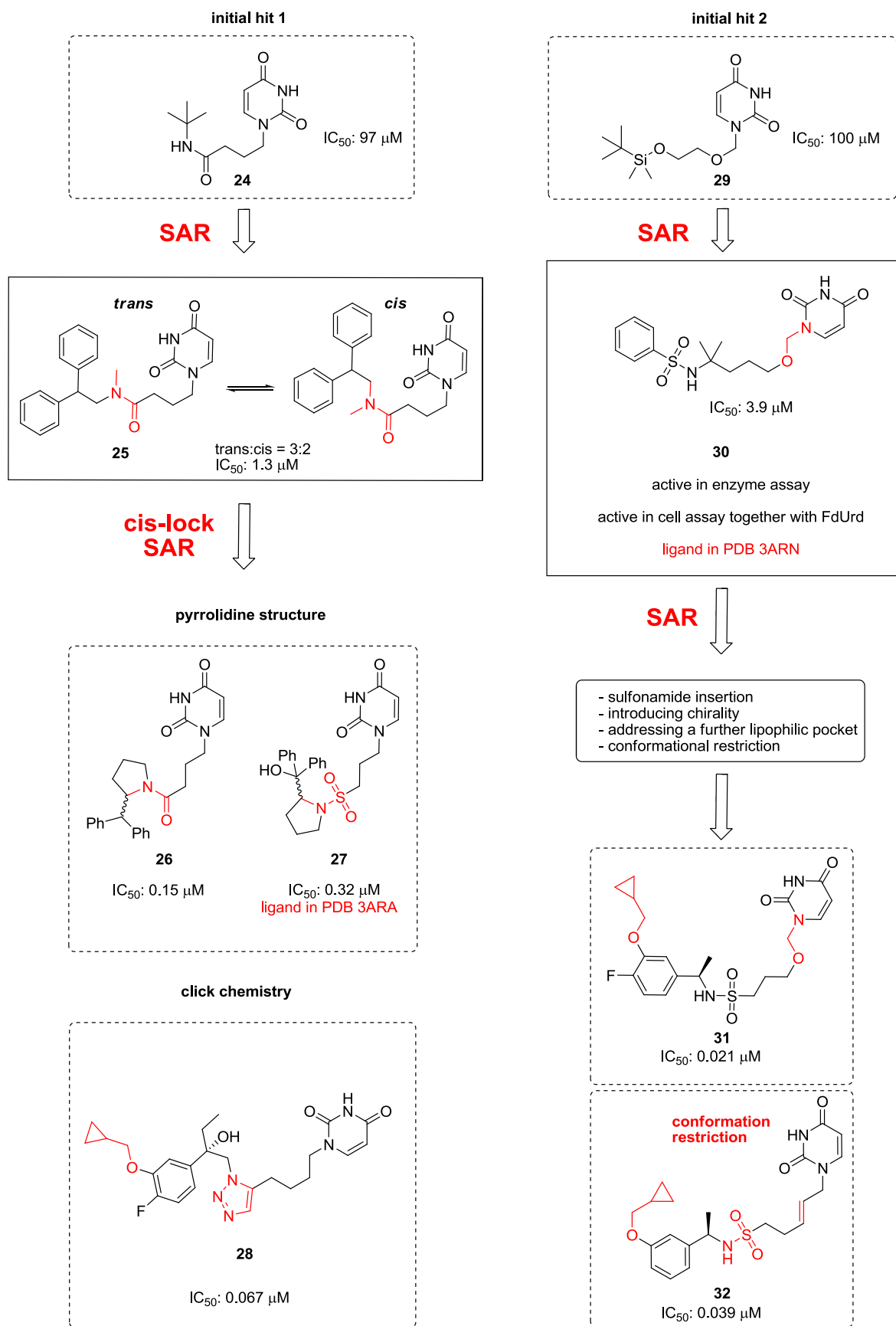


Figure 14: Summary of the main strategies for the development of dUTPase inhibitors by Taiho Pharmaceuticals.^{58,59,68,69}

2.6.4 SAR-studies at Taiho Pharmaceuticals

Using **24** as a starting point, amides containing uracil compounds were synthesized. Diphenyl-, phenyl- or *tert*-butyl groups were directly attached to the amide nitrogen or linked by small acyclic or cyclic hydrocarbon chains (Figure 14).⁵⁸ Compound similarities to *Pfd*UTPase inhibitors with trityl- and diphenyl-groups and acyclic structures (section 2.6.2) are recognizable (Figure 12).^{61,64} A comparison of *cis* and *trans* connected amides revealed that the *cis*-conformation of **25** has a higher target affinity. Thus more compounds were synthesized with locked *cis*-conformation (*cis*-lock) such as pyrrolidine amides, and pyrrolidine sulfonamides. The inhibitors **26** and **27** reached IC_{50} values lower than 320 nM (Figure 14).⁵⁸ The concept of *cis*-lock was further exploited by a “click chemistry” approach resulting in triazole based compounds like **28**. The triazole element imitates the *cis*-lock of amide moiety of pyrrolidine. These compounds showed good affinities and good pharmacokinetics (Figure 14).⁶⁹

Compounds like TAS-114 (**23**) are based on structure optimization of the N,O-acetal containing uracil derivative **29** (Figure 14).⁵⁹ SAR studies led to the development of the sulfonamide containing structure **30**. This structure was active in enzyme assays as well as in cell assays in combination with the experimental TS-inhibitor FdUrd. Further SAR studies revealed positive effects of the sulfonamide structure for physicochemical properties. The introduction of chirality, the restriction of linker flexibility, and the addition of lipophilic cycloalkyl methoxy groups led to increased inhibitor affinities represented by compound **31** and **32**. Especially chirality and cycloalkyl ethers as structural elements enhanced the inhibitor affinities and therefore, a typical feature of many inhibitors.^{59,68,69}

2.6.5 Proposed mechanism of dUTPase inhibitor activity

Taiho Pharmaceuticals conducted X-ray crystallography for SAR studies and proposed a general mechanism for their inhibitors. Therefore, inhibitors were cocrystallized with human dUTPase.⁵⁸ Superimposition of the inhibitor **27** (ligand PDB 3ARA, blue) and α,β -imino-dUTP (red) (in PDB: 2HQU) shows a fixed position of uracil in the active site (Figure 15, A). The diphenyl group of the sulfonamide compound points through the cis-lock into a hydrophobic pocket formed by the amino acids alanine (Ala 90, Ala 98) and valine (Val 65, Val 112) (Figure 15, B). The bulky group blocks space that is normally occupied by phenylalanine 158 (green, Figure 15, A) as part of the flexible C-terminal arm of dUTPase.^{58,59} It is proposed that this occupation disturbs the ordering of the entire C-terminal arm (Figure 16). This ordering process seems to be essential to conduct the catalytic hydrolysis of dUTP (**1**).^{48,50,58,59} Additionally, the scaffold of the inhibitor excludes dUTP (**1**) from the active site and inhibits the dUTP (**1**) hydrolysis. Similar observations were made for different inhibitor scaffolds of Taiho Pharmaceuticals.^{58,59}

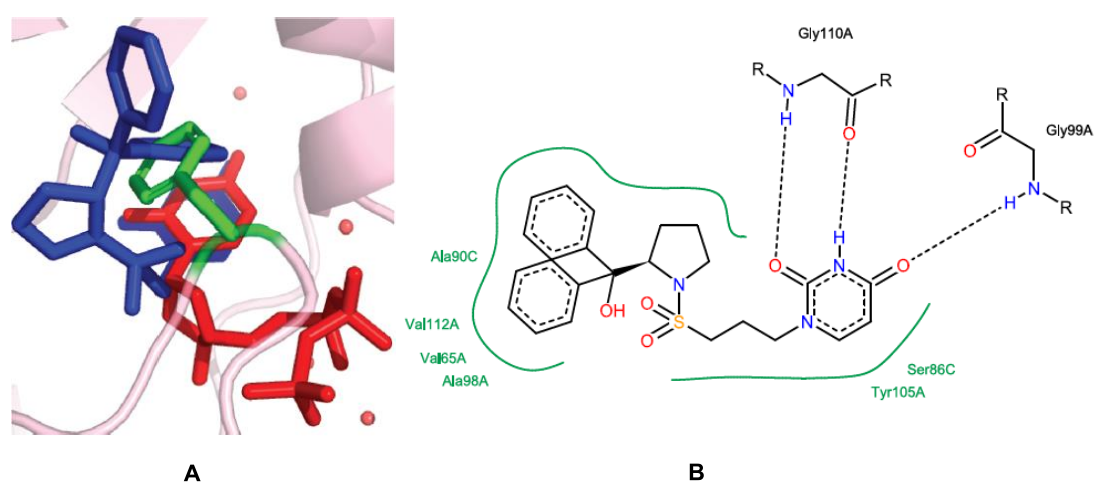


Figure 15: (A) **27** (blue, PDB 3ARA) superimposed with α,β -imino-dUTP (**11**) (red) in the active site of human dUTPase (PDB-code 2HQU). (B) Interactions of compound **27** with the active site. Many dUTPase inhibitors interact with a lipophilic pocket formed by alanines and valines (A used with permission, B was created with PoseView based on PDB file 3ARA)⁵⁸

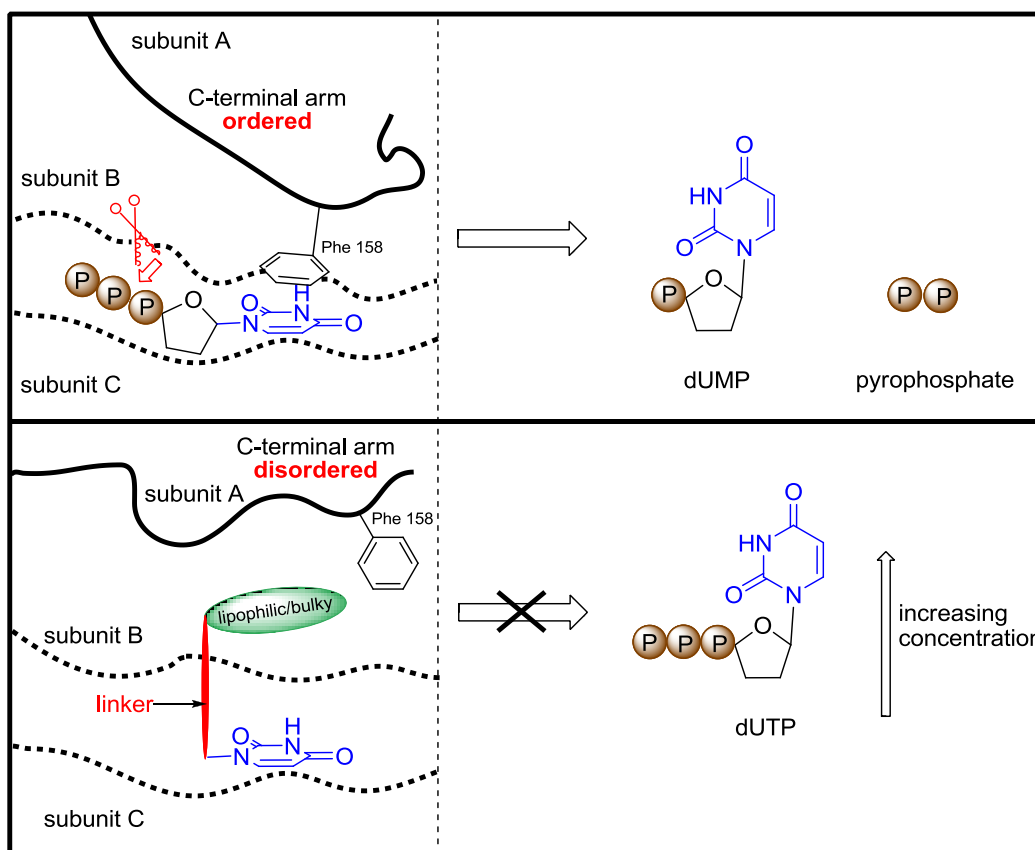


Figure 16: Proposed mechanism for dUTPase inhibitors. Schematic view of the active site formed between the subunits B and C. Upper representation: The C-terminal arm of subunit A becomes ordered when dUTP (1) or dUTP analogs bind. Phe 158 stacks with the uracil of the substrate and is thereby closing the active site. This closure initiates the catalytic process leading to substrate cleavage and dUMP (2) and pyrophosphate formation. Lower representation: The bulky lipophilic group of the dUTPase inhibitors prevents Phe 158 from stacking with uracil and closing the active site. The dUTPase loses its activity and the cellular dUTP (1) concentration increases to cytotoxic levels. Figure adapted and modified from Miyahara et al. based on their findings.⁵⁹

2.6.6 TAS-114 as a template for more dUTPase inhibitor development in the future

Based on these successful scaffolds, more patents have been published in the recent years containing similar structures.⁷⁰⁻⁷² In most cases, only slight changes to the original scaffolds were made. Modification attempts to exchange the uracil against hydantoin or uracil analogs can be considered as the most noticeable differences.⁷⁰ Robert Ladner (CEO of CV6) and coworkers conducted a lot of this research. Robert Ladner and coworkers presented a novel dUTPase inhibitor (CV6-168) at the 30th EORTC-NCU-AACR Symposium in Dublin in November 2018.⁷³ CV6-168 is to enter clinical trials, and is described as a selective inhibitor with activity against 21 of 22 tested cancer cell lines. The K_i value was measured to be 251 nM. This development can be seen as the starting point for the race for new dUTPase inhibitors.

3. Project 1: Aim of the project

The aforementioned importance and potential of dUTPase inhibitors in a combinatorial therapy with TS-inhibitors was the driving force for the development of new compounds in this project. The research interest of the scientific community increased with the publications of Taiho Pharmaceuticals and will most likely further increase through the development of TAS-114. However, in comparison to other anticancer research fields, the potential for discovery of novel inhibitor scaffolds is vast.

It was therefore of interest to synthesize novel compounds to investigate new scaffolds as lead structures and to gain a better understanding of the target enzyme human dUTPase.

The main objectives for the PhD-project were:

- To find new structural scaffolds while retaining activity against human dUTPase.
- To conduct chemical synthesis of compound libraries for SAR-studies to achieve higher affinity and improve inhibition properties relative to known compounds.
- To develop new compounds with affinities in a low micromolar to low nanomolar range towards human dUTPase.

4. Project 1: Discussion and Results

4.1 Design of human dUTPase inhibitors

A general structure of dUTPase inhibitors was deduced from the analysis of known inhibitors. The compounds from Taiho Pharmaceuticals and *Pfd*dUTPase inhibitors were used as templates and their structural analysis revealed four main units (Figure 17):^{58,59,61,68,69}

- **Uracil:** Works as an anchor to target the dUTPase active site.
- **Linker:** Connects uracil with the aromatic substituent/diversity platform. Must allow for the correct folding in the active site, and requires regulation in length and flexibility.
- **Bulky/lipophilic substituents:** Interacts with side pockets around the active site and improves affinity and selectivity. This moiety promotes its activity *via* hydrophobic interactions.
- **Diversity platform:** Connecting the linker and the aromatic substituent. It can have multiple functions such as:
 - Building block connection obtained by alkylation, acylations and sulphonamide formation or click chemistry.
 - Controlling conformational restriction (pyrrolidine cis-lock, triazole cis-lock).
 - Fine-tuning of solubility and other physicochemical properties like solubility or appearance (sulphonamide insertion, triazole structure; oil or solid).

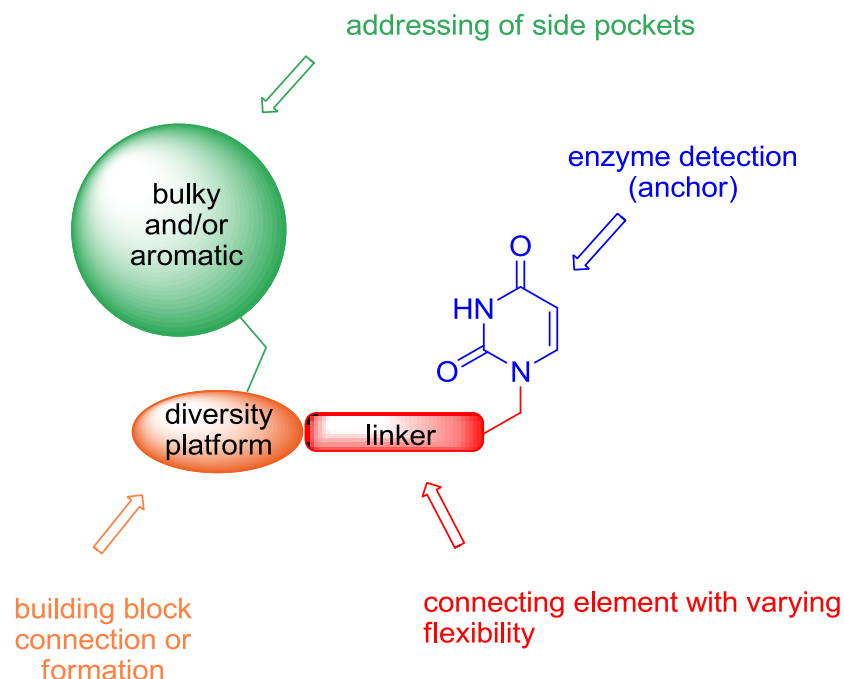


Figure 17: General structural elements and functions of dUTPase inhibitors. Most dUTPase inhibitors can be divided in four units. The uracil moiety serves as an anchor and is connected to the diversity platform by a linker with varying flexibility. The diversity platform enables chemical connection of building blocks, controls conformational restriction and physico-chemical properties. Mainly aromatic moieties are connected to the diversity platform to address the lipophilic side pockets around the active site of dUTPase.

As all of these units have a crucial function for the activity of the inhibitors the general units and their connection were kept unaltered. To simplify the reported structures no chiral centers were implemented. (Figure 18). The structures for the four units in the new template are the following (Figure 18):

Uracil: This structural element stayed untouched to address the active site.

Linker: The linker consists of an unsaturated hydrocarbon chain combined with an N,O-acetal and combines linker elements of previously reported inhibitors.^{59,68}

Bulky/lipophilic substituents: The aromatic substituent was simplified to a benzyl group as a starting point. Most substituents in dUTPase inhibitor libraries have benzyl groups as partial structure elements (diphenyl, trityl and phenethyl group). Substituent exchange with other commercially available substituted benzyl groups should enable fast compound library building. Based on biological test results the bulkiness and lipophilicity can be adjusted.

Diversity platform: Following the cis-lock strategy, previously achieved by pyrrolidines and triazols (Figure 18), an imidazole moiety was chosen.^{58,69} Besides the aforementioned function possess imidazoles more positive properties:

- Broad range of interactions to surrounding molecular structures including H-bonding, π -stacking as well as ionic and van der Waals forces.⁷⁴
- Isostere of other five-membered heterocycles including triazoles.^{74,75}
- Even better H-bond acceptor than triazoles and pyrrolidines—a feature that can modify binding.
- Can change physicochemical properties leading to better solubility and pharmacokinetics.⁷⁴
- Potential for further chemical modifications at the NH-functionality to create compound diversity.

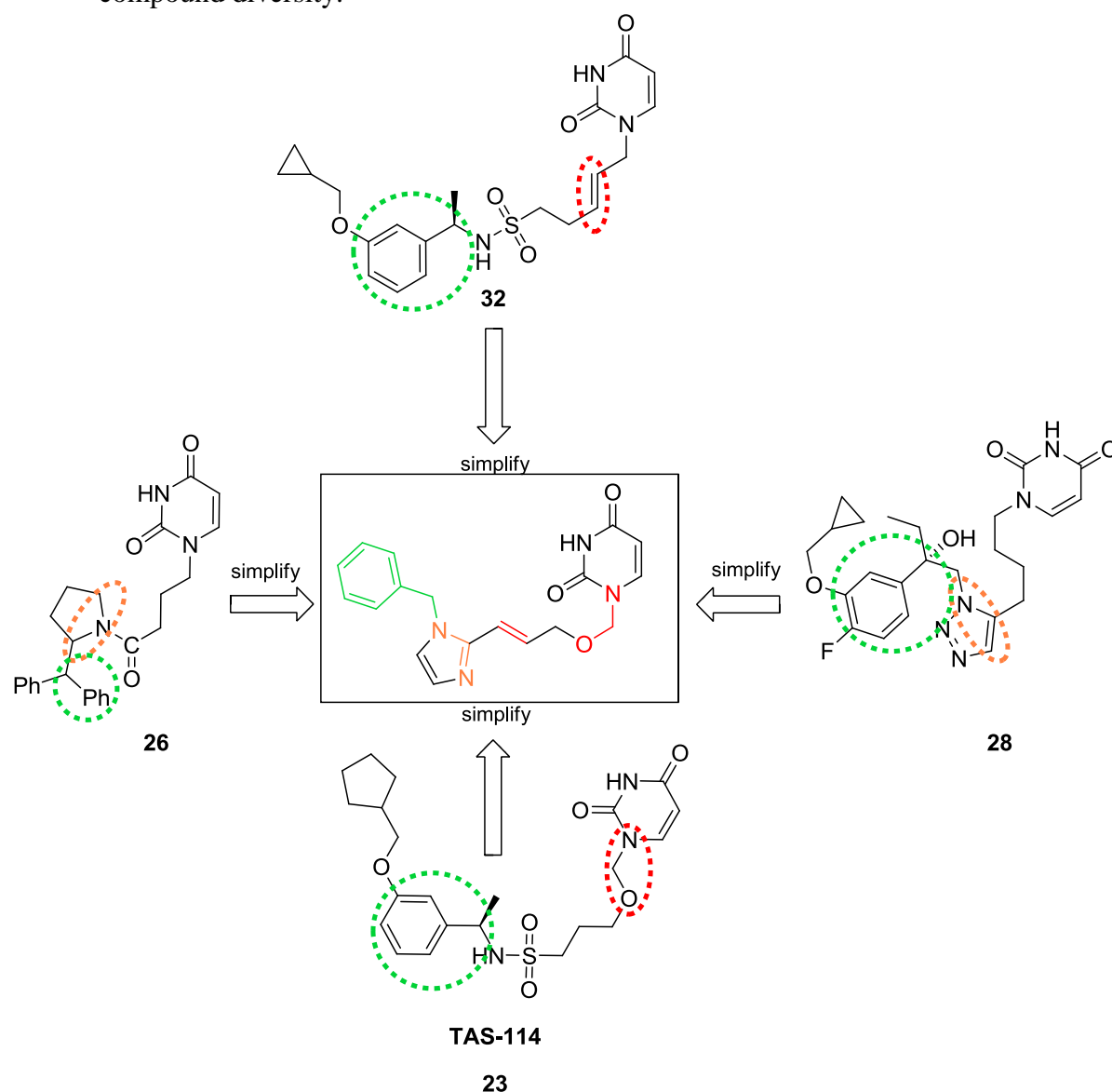


Figure 18: The structural elements of different dUTPase inhibitors were combined and simplified to form a template for the development of new inhibitors. Red: linker elements, orange: conformational restriction by imidazole following cis-lock strategy, green: benzyl group as partial element of most known dUTPase inhibitors.

4.2 Synthesis of N,O- acetal linked dUTPase compounds

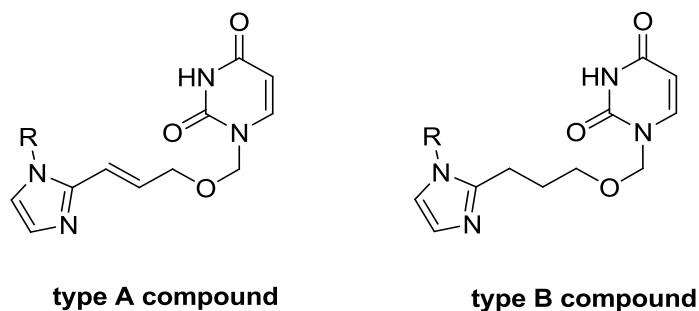
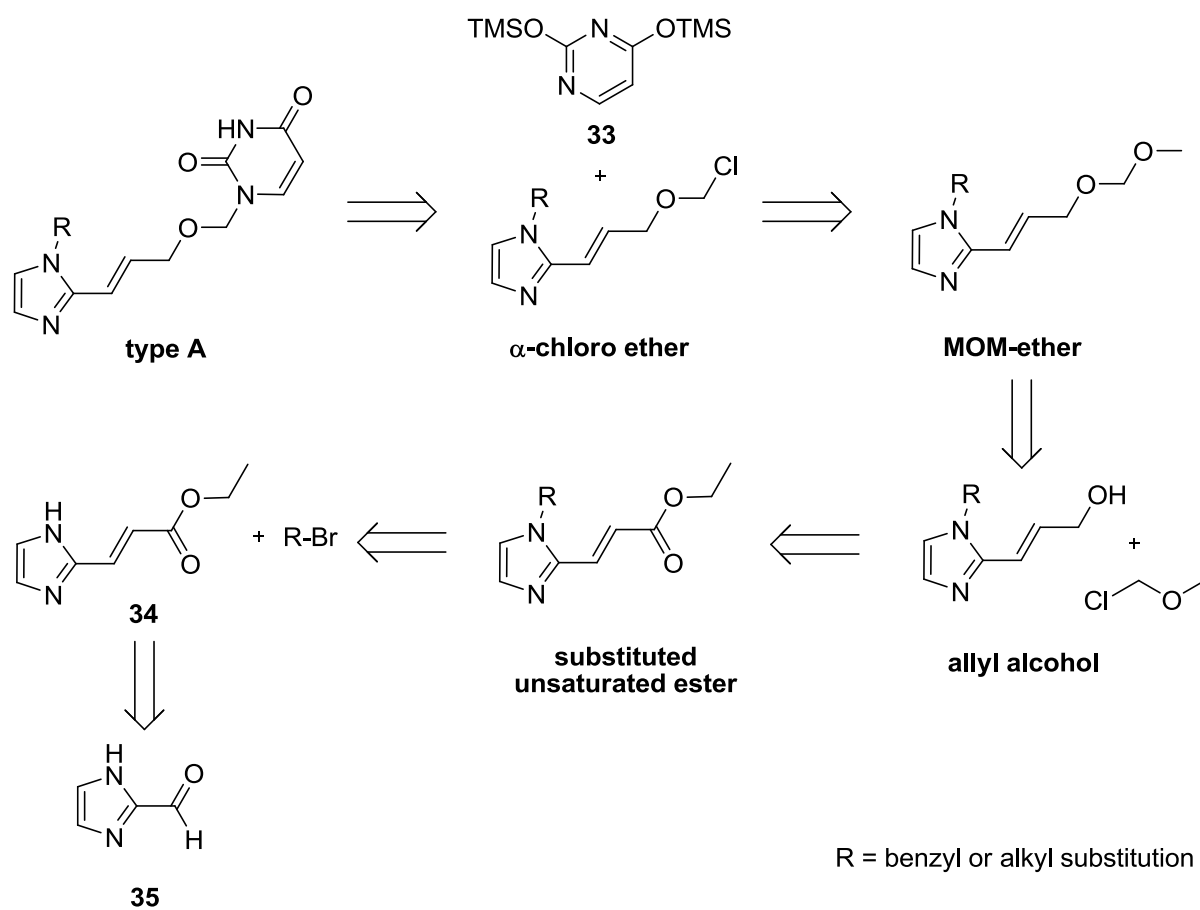


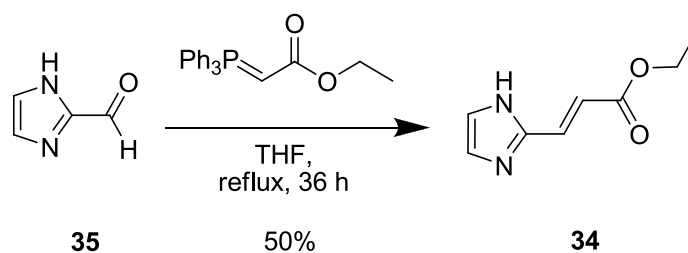
Figure 19: General structures of N,O-acetal linked compounds. R = benzyl or alkyl substitution.



Scheme 1: Retrosynthetic approach of type A compounds.

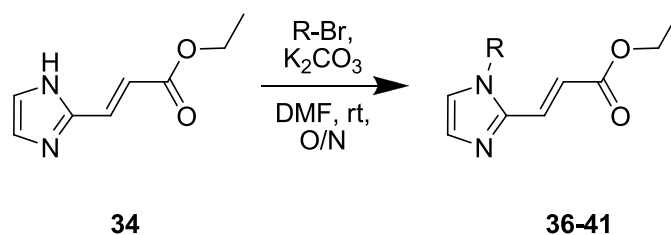
Based on the described design concept for inhibitors two alternative compound scaffolds are proposed: N,O-acetal containing structures named type A compounds (Figure 19); Along with structures with a saturated hydrocarbon linkage (type B) to compare in biological testing. Type B compounds were considered later in the synthesis process. The first retrosynthetic approach for type A compounds is shown in (Scheme 1). The N,O-acetal linkage was planned as a reaction between α -chloro ethers with trimethylsilyl-protected uracil (**33**), and was based on a procedure by Miyahara et al. for their N,O-acetal dUTPase inhibitors.⁵⁹ α -chloro ethers can be formed *in situ* through the activation of MOM-ether derivatives with boron trichloride (BCl₃). The MOM ethers were obtained by reduction of unsaturated esters and subsequent protection with chloromethyl methyl ether (MOMCl) while the allyl alcohols are obtained through reduction of unsaturated ester derivatives. (*E*)-ethyl 3-(1*H*-imidazol-2-yl)acrylate (**34**) was employed as the starting material for the synthesis of the unsaturated ester derivatives, generated by a Wittig reaction from aldehyde **35**.

(*E*)-ethyl 3-(1*H*-imidazol-2-yl)acrylate (**34**) was prepared according to the procedure of Leclaire et al. (Scheme 2).⁷⁶ The reaction of 2-imidazolecarboxaldehyde (**35**) with (Carbethoxymethylene)triphenylphosphorane in THF at reflux afforded the *E*-isomer in 50% yield.⁷⁶



Scheme 2: Synthesis of (*E*)-ethyl 3-(1*H*-imidazol-2-yl)acrylate (**34**) by the Wittig reaction.

Compound **34** had a central role for further synthesis steps and was synthesized in multi-gram scale. (*E*)-ethyl 3-(1*H*-imidazol-2-yl)acrylate (**34**) was the platform for *N*-alkylation and was the decisive step for diversification for further compound types. It was alkylated in the 2-position with different benzyl bromides at room temperature using potassium carbonate as base and DMF as solvent (Scheme 3). Products **36-41** were obtained in moderate to good yield after extraction and purification by column chromatography (Table 1).

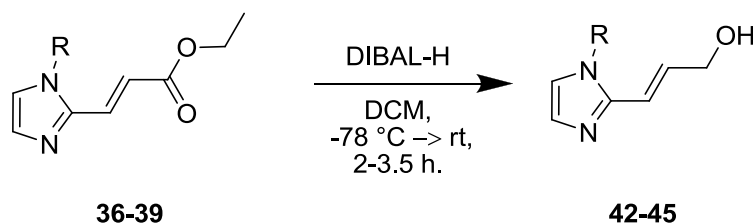


Scheme 3: Decisive step for diversification of type A compounds.

Table 1: Structures and yields of the substituted (*E*)-ethyl 3-(1*H*-imidazol-2-yl)acrylates **36-41**.

Substituent R			
yield	36, 81%	37, 75%	38, 70%
Substituent R			
yield	39, 74%	40, 65%	41, 69%

The reductions to the corresponding allyl alcohols were carried out with diisobutylaluminum hydride (DIBAL-H) to ensure the integrity of the double bond in the products. The applied procedure was a modified version of previously reported procedure by Leclaire et al.⁷⁶ Reactions were initialized by the addition of DIBAL-H (1M in DCM) to solutions of the starting materials **36-39** in DCM at -78 °C. Compounds **42-45** were afforded in moderate yields (Table 2).



Scheme 4: Reduction of the substituted (*E*)-ethyl 3-(1*H*-imidazol-2-yl)acrylates **36-39** with DIBAL-H.

Table 2: Isolated yields of the substituted (*E*)-3-(1*H*-imidazol-2-yl)prop-2-en-1-ols **42-45**.

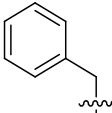
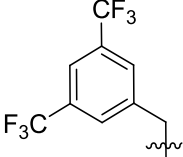
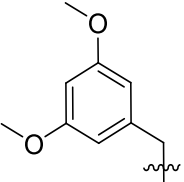
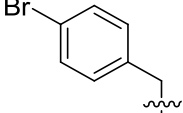
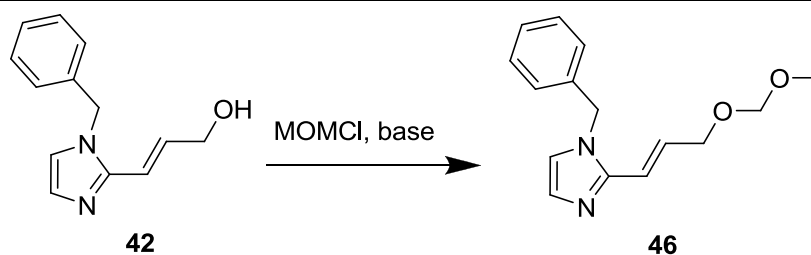
Substituent R				
yield	42 , 65%	43 , 66%	44 , 75%	45 , 73%

Table 3: Reaction conditions for MOM protection of the allyl alcohol **42**.

entry	MOMCl [eq]	base	[eq]	solvent	temp	time	remarks
1	1.0	DIPEA	1.1	DCM	0 °C to rt	O/N	byproduct
2	1.1	DIPEA	1.1	DCM	-10 °C to rt	6 h	byproduct
3	1.2	DIPEA	1.2	DCM	0 °C to rt	O/N	byproduct
4	1.4	DIPEA	1.3	DCM	-5 °C	40 min	byproduct
5	1.0	NaH	1.0	THF	rt	1 h	byproduct and 42
6	1.05	NaH	1.1	THF	-10 °C to rt	O/N	46 , poor conv.
7	1.3	NaH	1.1	THF	0 °C to rt	2 h	46 , poor conv., byproduct
8	1.4	NaH	2.0	THF	0 °C to rt	2 h	46 , poor conv., byproduct
9	1.4	NaHMDS	1.2	DMF	-50 °C to r.t	1 h	46 , 84% yield

Further synthesis route exploration was performed with allyl alcohol **42**. The synthesis of the MOM-ether derivative **46** proved to be challenging (Table 3). For the first test reactions different equivalents of MOMCl and *N,N*-diisopropylethylamine (DIPEA) in DCM at different temperatures were utilised (entry 1-4), similar to conditions used by Miyahara et al. for their *N,O*-acetal inhibitors.⁵⁹ Nonetheless, the variation of equivalents, temperatures, and reaction time resulted only in traces of the product and a highly polar byproduct. Having the target mass and high water solubility suggested *N*-alkylation, forming a quaternary ammonium compound. The use of sodium hydride (entry 5-8) increased the product formation and suppressed strong byproduct formation.⁷⁷ The reaction did not achieve

completion even though the yields increased. Further addition of MOMCl along with additional base resulted in low conversion and led again to more byproduct formation (entry 7-8). Product **46** could finally be obtained by using NaHMDS and DMF as solvent in combination with low temperature. The starting material was consumed completely and no relevant byproduct formation was observed (Table 3, entry 9). Product **46** was isolated in 84% yield and was used without further purification.

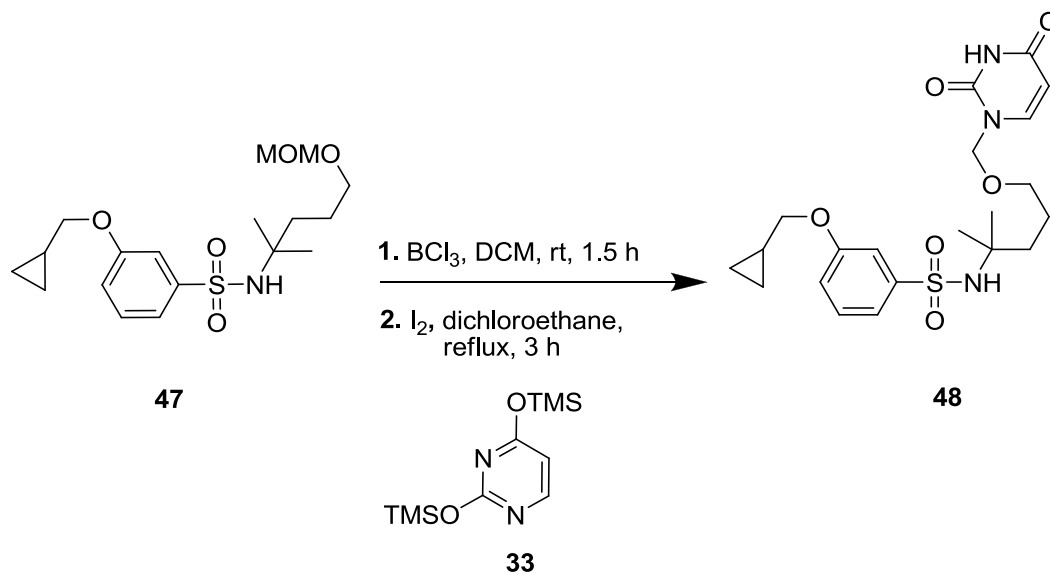
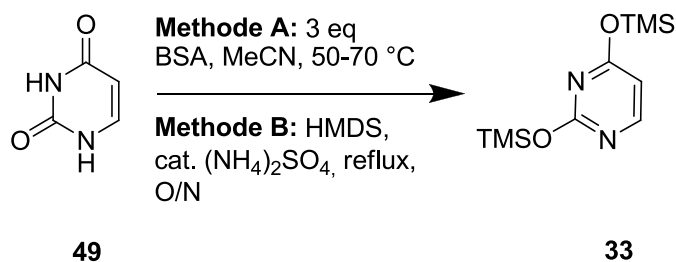


Figure 20: Reaction conditions used for the synthesis of N,O-acetal inhibitors by Miyahara and coworkers.⁵⁹

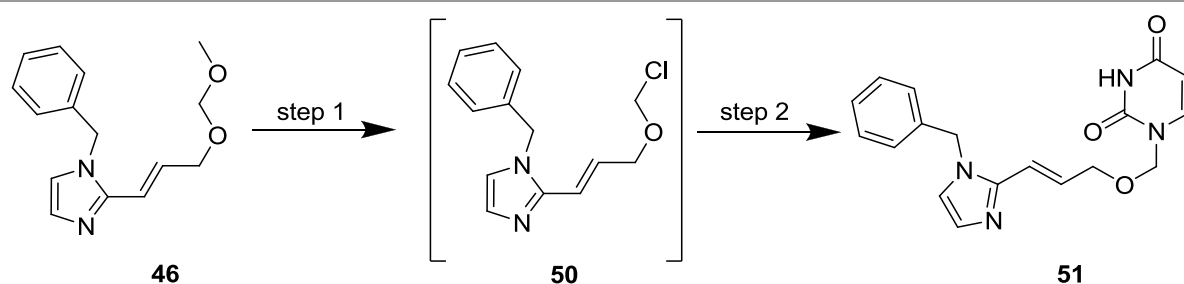
The coupling procedure of the imidazole scaffold with the essential uracil moiety was initially based on reaction conditions described by Miyahara et al. for the synthesis of their dUTPase inhibitors.⁵⁹ They conducted the N,O-acetal formation step by treating MOM-ether derivatives like **47** with boron trichloride (BCl_3) yielding the corresponding α -halo ethers (Figure 20, step 1). The active intermediates reacted directly with TMS-protected uracil and iodine in dichloroethane under reflux (step 2, Figure 20). The TMS groups of **33** increase the selectivity for N^1 -alkylation and is therefore often used in pyrimidine nucleobase synthesis.⁷⁸⁻⁸²

The synthesis of **33** was carried out according to two different silylation methods described in literature (Scheme 5). In the procedure of Kita et al. N,O-bis(trimethylsilyl)acetamide (BSA) was used as silylation agent (procedure A).⁸³ Uracil (**49**) was heated together with excess of BSA in MeCN at 50-70 °C until the solution cleared up. After solvent evaporation the crude was used directly in the coupling reaction (Table 4, step 2). As an alternative procedure, uracil (**49**) was refluxed in hexamethyldisilazane (HMDS) with a catalytic amount of ammonium sulfate until the solution cleared up (procedure B).



Scheme 5: *In situ* TMS protection methods for uracil **33**.

The excess of HMDS was removed under reduced pressure and the crude was used directly for the next step (based on procedures of Li et al. and Khare et al).^{82,84} **33** is highly unstable making reaction control difficult.⁸³ The protection of uracil must therefore be carried out directly prior to the coupling reaction. Table 4 shows the reaction conditions used for the activation of the MOM-alcohol derivative, **46**, (conditions 1), and for the reaction with the uracil moiety **33** (conditions 2). At the beginning similar reaction condition were used as described by Miyahara et al. (entry 1).⁵⁹ **46** was treated with 0.33 equivalents of BCl_3 in the temperature range of 0 °C and room temperature (step 1). The volatiles were removed and the crude was dissolved in dichloroethane and **33** and iodine were added (step 2). No product formation could be detected after heating to reflux for several hours, and remaining starting material **46** indicated insufficient α -chloro ether activation (Table 4, entry 1). It was observed that the use of more than 0.33 equivalents BCl_3 yielded the distinct conversion of the starting material (entry 2-3). The use of 1.0-1.33 equivalents BCl_3 resulted in full conversion of **46** (3-10), but led also to the formation of byproducts like allyl alcohol **42** and dimers of allyl alcohol **42** (acetal). Temperature and reaction times seemed to have a minor effect on the activation. The crude activated material was used after reagent removal under reduced pressure in reaction step 2. The reactions between crude activated material and **33**, were performed in MeCN or DMF. Product formation could be detected by MS and TLC for both solvents and both uracil silylation methods, regardless of the use tetrabutylammonium iodide (TBAI) (entry 4, 6, 8-10). Unfortunately, the product isolation was not successful, and the overall product conversion was not satisfying. Reactions with a modified MOM-ether activation protocol and original coupling conditions were not carried, but the general approach was changed.

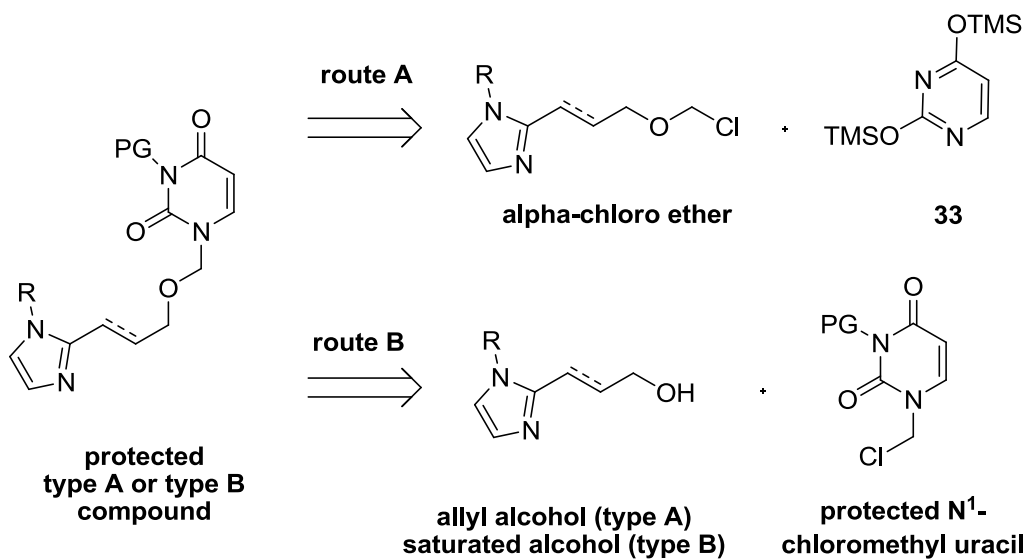
Table 4: Attempts towards the formation of the α -halo ether **50** and coupling with protected uracil **33**.

step 1				step 2					
entry	BCl_3 [eq]	temp	time	SP	solv	temp	time	addt	remarks
1	0.33	0 °C to rt	2 h	B	DCE	reflux	4 h	I_2	no 51 detected
2	0.5	-10 °C	1 h	A	MeCN	rt	O/N	-	no full conversion to 50
3	0.5	-78 °C to rt	40 min	A	MeCN	rt	O/N	-	no activation until 1.3 eq BCl_3
4	1.0	-78 °C to rt	1.5 h	A	DMF	70 °C	n.d	TBAI	50 detected
5	1.3	-78 °C to 0 °C	1.5 h	A	MeCN	50 °C	3 h	-	51 detected
6	1.3	-78 °C to rt	2 h	A	MeCN	rt	O/N	TBAI	51 detected
7	1.3	-78 °C to -40 °C	2 h	A	MeCN	rt	O/N	-	51 detected
8	1.33	-78 °C to rt	2.5 h	A	DMF	80 °C	O/N	TBAI	51 detected
9	1.33	-78 °C to rt	3 h	A	DMF	80 °C	3 h	TBAI	51 detected
10	1.33	-78 °C to rt	1 h	B	MeCN	-60 °C to rt	n.d	TBAI	51 detected

SP = silylation procedure

4.3 N¹-chloromethyl uracils as electrophiles for N,O-acetal formation in type A and type B compounds

The *in situ* activation of MOM-alcohols and the *in situ* protection of **33** was an inconvenient methods to afford compound libraries. Reasons were the limited reaction control possibilities and repeating activations steps for every test reaction to optimize conditions (Scheme 6, route A).



Scheme 6: Synthesis route A is a linear synthesis with strong focus on the α -halo ether formation. Route B is a convergent synthesis giving the uracil moiety a more important role. PG = protecting group, R = benzyl or alkyl.

Therefore, it was of great interest to change the strategy for the N,O-acetal synthesis. At least one building block should be possible to produce in bulk and the N,O-acetal formation should be easier to monitor. A way to realize this concept was identified by switching the role of nucleophile and electrophile in the N,O-acetal formation. Allyl alcohol derivatives or saturated alcohol derivatives and protected N¹-chloromethyl uracil were the intended new building blocks. The essential uracil moiety got, as a result, a higher importance through bearing of the leaving group. This changed the overall strategy from a linear synthesis to a convergent synthesis (route B, scheme 6). Expected benefits of the convergent synthesis pathway (route B) were:

- A possibility to design a standardized procedure for the formation of the electrophile.
- Fewer synthetic steps to form the different imidazole building blocks.
- BCl₃ sensitive functional groups can be used on the imidazole scaffold.
- Possibility to use the chloromethyl uracil derivative for other scaffolds.

4.3.1 Synthesis attempt for N,O-acetal formation with N³-benzoyl-protected N¹-chloromethyl uracil

Building block **52** was chosen as a surrogate for concept studies to form N,O-acetals (Figure 21). The chloride-leaving group was thought to enable the alkylation of alcohols and the benzoyl group prevents side reaction at the N³-position. The benzoyl protecting group can be removed under basic conditions after successful activation and N,O-acetal formation.

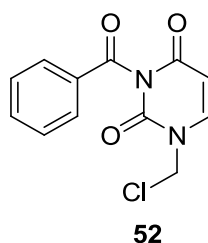
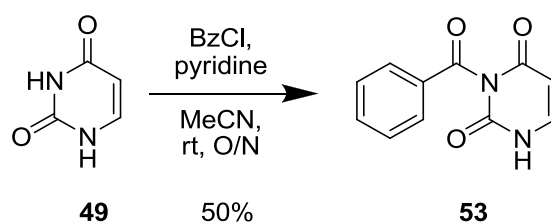
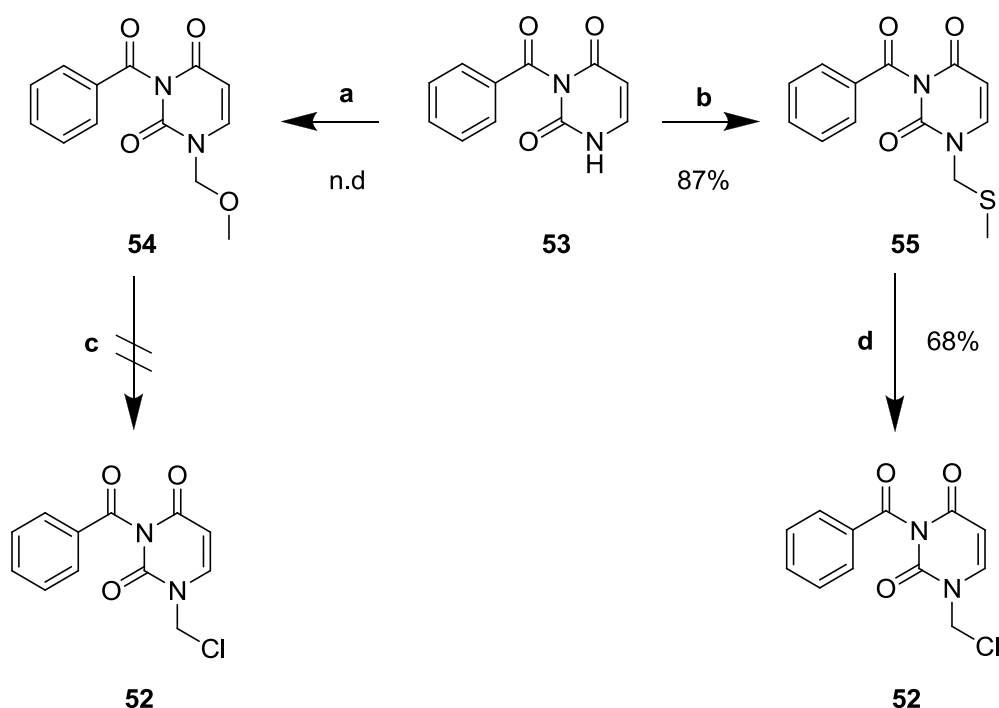


Figure 21: **52** represents the first activated uracil building block for synthetic Route B.

The starting point for the synthesis of **52** was the synthesis of N³-benzoyl uracil **53** (Scheme 7). The benzoyl protected uracil derivative **53** allows, similar to TMS-Uracil **33**, for selective alkylation at the N¹-position of uracil but has the advantage that it is more stable towards moisture and can be deprotected controllably.⁸⁵ Unsurprisingly, some dUTPase inhibitors of Miyakosi et al. and Miyahara et al. were also synthesized *via* intermediate **53**.^{58,68,69} The synthesis of **53** was realized by combining different published methods.⁸⁶⁻⁸⁹ **52** was obtained in 50% yield by treating uracil with 2.4 equivalents of benzoyl chloride and pyridine and hydrolyses of the N¹-benzoyl group as part of the work up. (Scheme 7).



Scheme 7: Synthesis of N³-benzoyl uracil **53**.



Scheme 8: (a) MOMCl, K₂CO₃, DMF, rt, O/N; (b) MTMCl, K₂CO₃, DMF, rt, O/N; (c) BCl₃, DCM, -78 °C or 0 °C → rt; (d) SO₂Cl₂, DCM, -78 °C → rt, 2h. .n.d = yield were not determined.

Starting from **53** two approaches were tested to achieve the N¹-chloromethyl uracil derivative **52**. The first approach was to synthesize the chlorinated material by introduction of a MOM group at the N¹-position of uracil, and to use BCl₃ as an activator. The other attempt was based on the introduction of a methylthiomethyl group (MTM) followed by chlorination using sulfuryl chloride (SO₂Cl₂). This system was inspired by the work of Edstrom et al., who used the MTM-group on pyrrolo[2,3-d]pyrimidin-2,4-dione to form a N-chloromethyl intermediate.⁹⁰

The precursors **54** and **55** were synthesized in small scale using MOMCl or MTMCl with potassium carbonate in dry DMF with good conversion (Scheme 8). The MOM-derivative **54** was dissolved in DCM and treated with 0.33 eq BCl₃ at 0 °C and -78 °C resulting in immediate precipitation of a solid. No chlorinated product **52** could be detected *via* HRMS after stirring 1-2 hours at room temperature. (Scheme 8). Analogously, the MTM-derivative **55** was dissolved in DCM and treated with 2.0 equivalents of sulfuryl chloride at -78 °C. The expected chlorinated product was detected by MS. Therefore, it was continued with **55** for further explorations. A synthesis repetition for **55** delivered the product in 87% yield after work up and purification (Scheme 8).

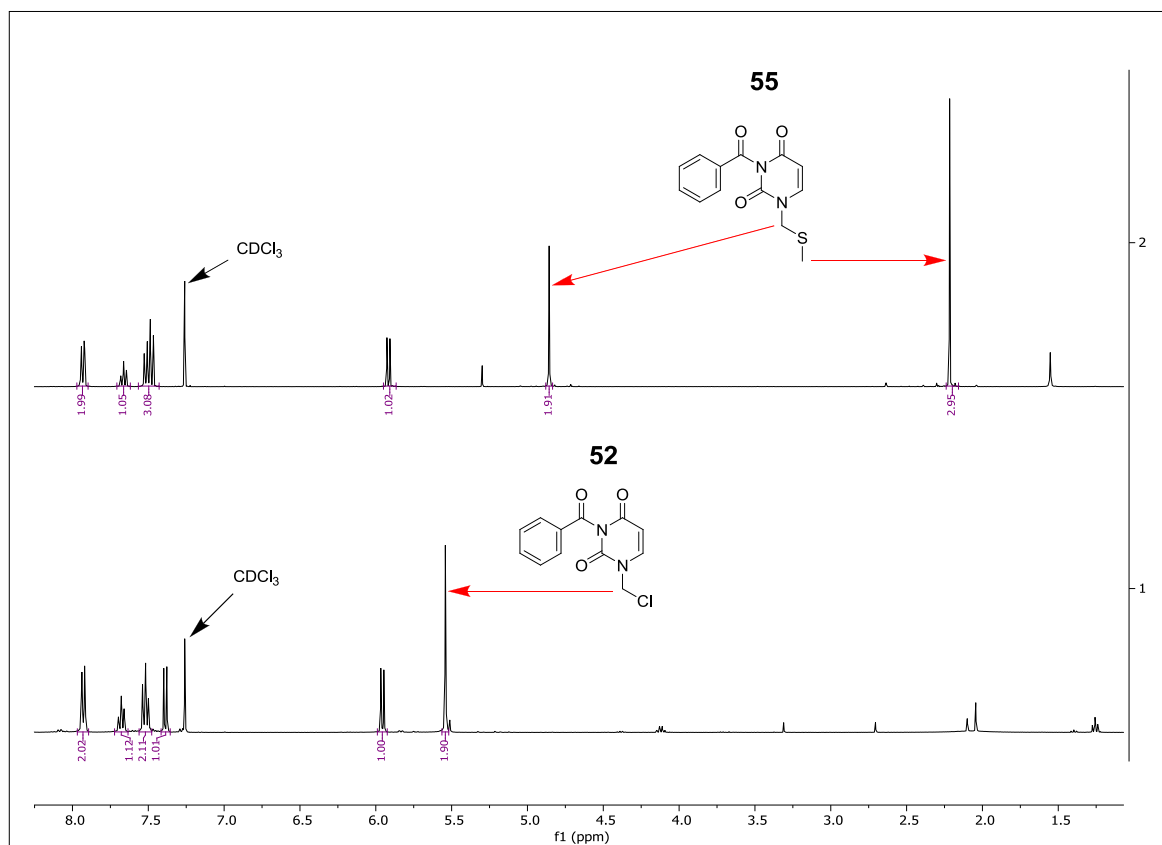


Figure 22: The figure shows the NMRs of compound **52** and **55** in comparison. The MTM group of **19** shows a signal for the CH₃-group at ~2.25 ppm and for the CH₂-group at ~4.9 ppm. The transformation of **55** to compound **52** led to the signal disappearance for the CH₃-group and to a deshielded CH₂-group.

The reaction repetition for **52**, with 2.0 equivalents SO₂Cl₂, showed full conversion of **55** after one hour (Scheme 8). The chlorinated compounds exhibited high stability and allowed reaction control by NMR, as well as isolation of the activated intermediate. The NMR confirmed the absence of the methyl signal of the MTM group and the formation of a deshielded methylene group (Figure 22). Compound **52** was used as crude material in the following reactions after removal of the volatiles. The purification by silica column chromatography removed small byproduct traces but lowered the yield to 68% due to strong surface absorption of the wax-like compound.

Compound **52** was reacted with the allyl alcohol **42** to obtain compound **56** (Table 5). The reaction was carried out at room temperature as well as at elevated temperature, but resulted only in product traces (entry 1-2), not converted start material as the bulk (entry 2) and byproducts (entry 1). The reactivity of the chlorinated compound and/or the nucleophilicity of the allyl alcohol **42** were too low. The use of the stronger base NaHMDS to increase nucleophilicity led to quick removal of the benzoyl protecting group; this was rather expected as this protecting group can be removed by alkoxides, hydroxyl ions, and nucleophilic amines.⁸⁵

Table 5: Reaction of the activated uracil **52** with allyl alcohol **42** under mild basic conditions.

42 **52** **56**

entry	solvent	42 [eq]	52 [eq]	DIPEA [eq]	temp	time	addt	remarks
1	DCM	1.0	1.2	1.0	rt	10 d	cat. TBAI	traces of 56
2	DMF	1.0	1.0	1.1	rt; then 50 °C	O/N; then 2 h	-	traces of 56

4.3.2 Search for alternative uracil protecting groups

The instability of the N³-benzoyl group of uracil led to the investigation of other imide protection groups that could withstand the harsher reaction conditions that are needed for the N,O-acetal formation. Hereby, several possible problems must be considered (Scheme 24):

- Adequate base stability is needed to reduce cleavage in the N,O-acetal formation.
- Acidic deprotection conditions can destroy the N,O-acetal.
- Hydrogenolysis sensitive protecting groups can cause a reduction of the uracil double bond and the alkene.
- The protecting group should be not sensitive to SO₂Cl₂.

Hydrogenolysis sensitive protecting groups, like the benzyloxymethyl protecting group (BOM), are used to protect pyrimidine nitrogen with differing levels of success.⁹¹ Typical deprotection methods for the BOM-group are palladium on carbon or similar palladium catalysts in the presence of hydrogen gas. The expected reduction of the uracil double bond (C5-C6) has been previously described in literature (Figure 23, A).

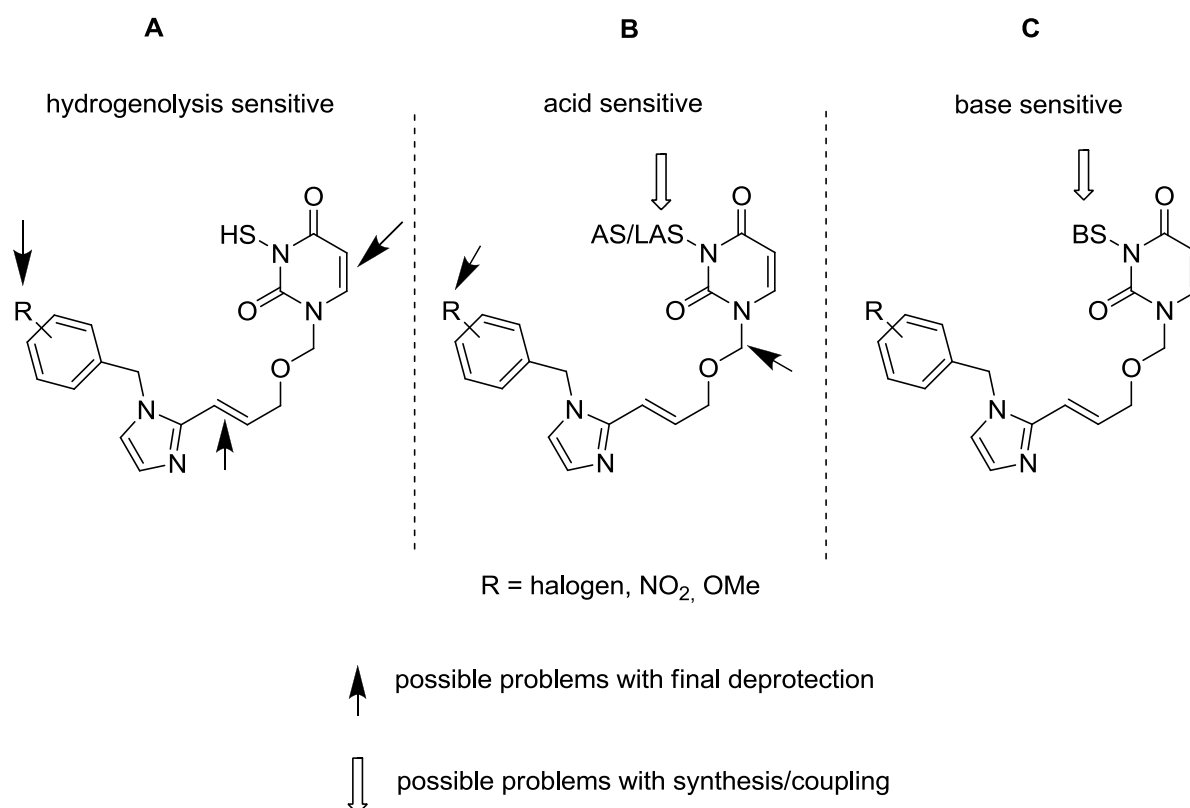


Figure 23: Possible problems for the use of different uracil protecting groups. The protecting group can be effected through either the chlorination reaction or the coupling conditions in the N,O-acetal formation. The removal of the protecting group can also affect the structural elements of the final compounds. (A) Hydrogenolysis, e.g of the BOM protecting group can lead to partial reduction of the uracil double bond. The alkene linker structure and substituents like NO₂ are most likely not stable under this conditions (B) Acid sensitive groups like MOM can form N,O-acetals. The deprotection with lewis acids could interfere with the N,O-acetal of the linker with uracil. The stability of the protecting groups against SO₂Cl₂ must also be considered. (C) Base sensitive acyl protecting groups are in most cases not very stable under strong basic conditions afforded for the N,O-acetal formation. Abbreviations of the protecting groups: HS = hydrogenolysis sensitive, AS = acid sensitive, LAS = lewis acid sensitive, BS = base sensitive.

The reaction resulted in inseparable mixtures when no acidic additives were used in the hydrogenation process.⁹¹ Other authors stated low byproduct formation, under neutral conditions, in limited reaction condition margins using Pd black in methanol and short reaction times.⁹² Overall, the BOM-group was not considered as an option due to the incompatibility with the alkene structure in type A compounds, or with substituents like halogens or nitro groups (Figure 23, A).

Acid/Lewis acid sensitive N,O-acetal based protecting groups (for example MOM, BOM, SEM, and others) were seen as problematic due to the fact that the compounds also contain an N,O-acetal structure in the N¹-position (Figure 23, B). It could not be ruled out that deprotection agents like BCl₃, BBr₃ or TFA would also cleave the desired junction. However, the SEM-protecting group additionally offers the possibility for cleavage with fluoride ions.

93-95

The imido nitrogen at the N³-position of uracil forms rather instable benzoyl amides making them sensitive to alkaline cleavage (Figure 23, C).⁸⁵ Bulky and electron rich benzoyl protecting groups are described in literature for uracil. They show increased stability towards different basic deprotection conditions compared to a normal benzoyl group. Overall, they are not stable for long periods of time under strongly basic reaction conditions and were not seen as a viable choice for the N,O-acetal synthesis.⁸⁵

Based on the analysis of different types of protecting groups, it was decided to continue with the 2-(trimethylsilyl)ethoxymethyl protecting group (SEM). The deprotection with fluoride ions was seen as possibility to reduce the interference with other structure elements in the molecules.

4.3.3 Synthesis attempt for N,O-acetal formation with N³-SEM -protected N¹-chloromethyl uracil

The SEM group is known for its stability towards a broad range of reaction conditions.^{94,95} It is used mainly for the protection of hydroxyl groups and nitrogen-containing heterocycles.^{93,94} Deprotection is typically done with hydrochloric acid as well as with TFA, SnCl₄ or BF₃·Et₂O or MgBr₂.^{93,94,96-98} The SEM protecting group, as previously noted, can be further cleaved by fluoride ion sources such as TBAF or CsF.⁹³⁻⁹⁵

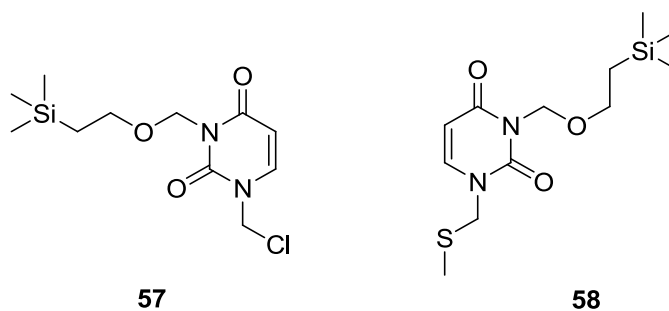
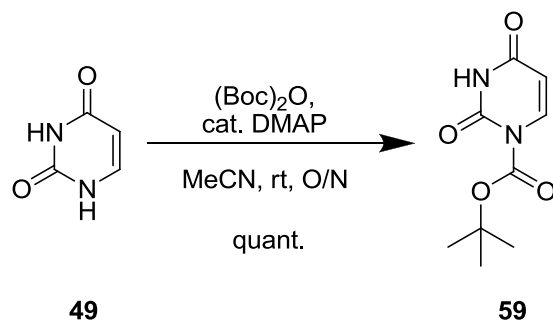


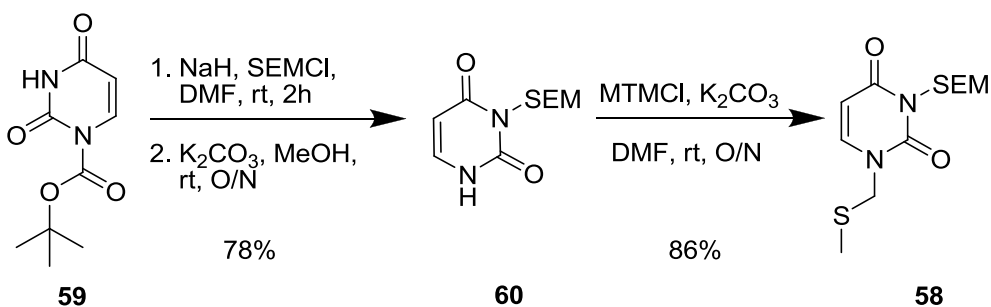
Figure 24: SEM-protected chloromethyl uracil **57** and MTM-uracil precursor **58**.

The SEM-protected chloromethyl uracil derivative **57** was synthesized from the MTM-precursor **58**. Compound **58** was generated in a four step synthesis starting from uracil **49** (Scheme 9). One equivalent di-*tert*-butyl dicarbonate and a catalytic amount of 4-(dimethylamino)pyridine (DMAP) converted uracil to N¹-Boc uracil (**59**) in an overnight reaction.⁹⁹ The crude product **59** was used without purification after removal of the solvent. The Boc-protecting group in the N¹-position exhibited low stability against moisture and long storage time.



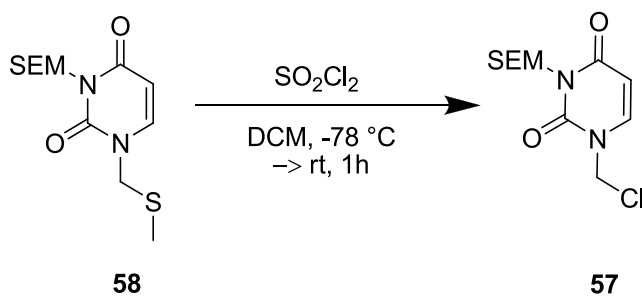
Scheme 9: Synthesis of N¹-Boc uracil **59**.

The synthesis pathway from **59** to **60** was based on a procedure of Jaime-Figueroa et al. for the general N³-alkylation of uracils (Scheme 10).⁹⁹ The SEM-protecting group was introduced by using 2-(trimethylsilyl)ethoxymethyl chloride (SEMCl) and sodium hydride (60% in mineral oil) in dry DMF. The alkylated Boc-protected intermediate was not isolated as per the original procedures of Jaime-Figueroa et al. and directly deprotonated with K₂CO₃ in MeOH overnight.⁹⁹ The product **60** was obtained in good yield (78%) (Scheme 10).



Scheme 10: Synthesis of the N³-SEM protected MTM uracil building block **58**.

Compound **58** was obtained in an overnight reaction from **60** with MTMCl, and K₂CO₃ in DMF. **58** was isolated in 86% yield after work up (Scheme 10). Activation reactions of **58** to generate **57** were performed with SO₂Cl₂ in DCM (Scheme 11). The reactions were monitored by TLC and NMR (Figure 25) for completion (1 hour). The crude was used directly in following reactions after solvent removal. Figure 25 shows a comparison of the crude **57** with the starting material **58**. The methyl signal of the MTM-group disappeared and the CH₂-group of **57** is deshielded.



Scheme 11: Chlorination of the SEM-protected uracil building block **58**.

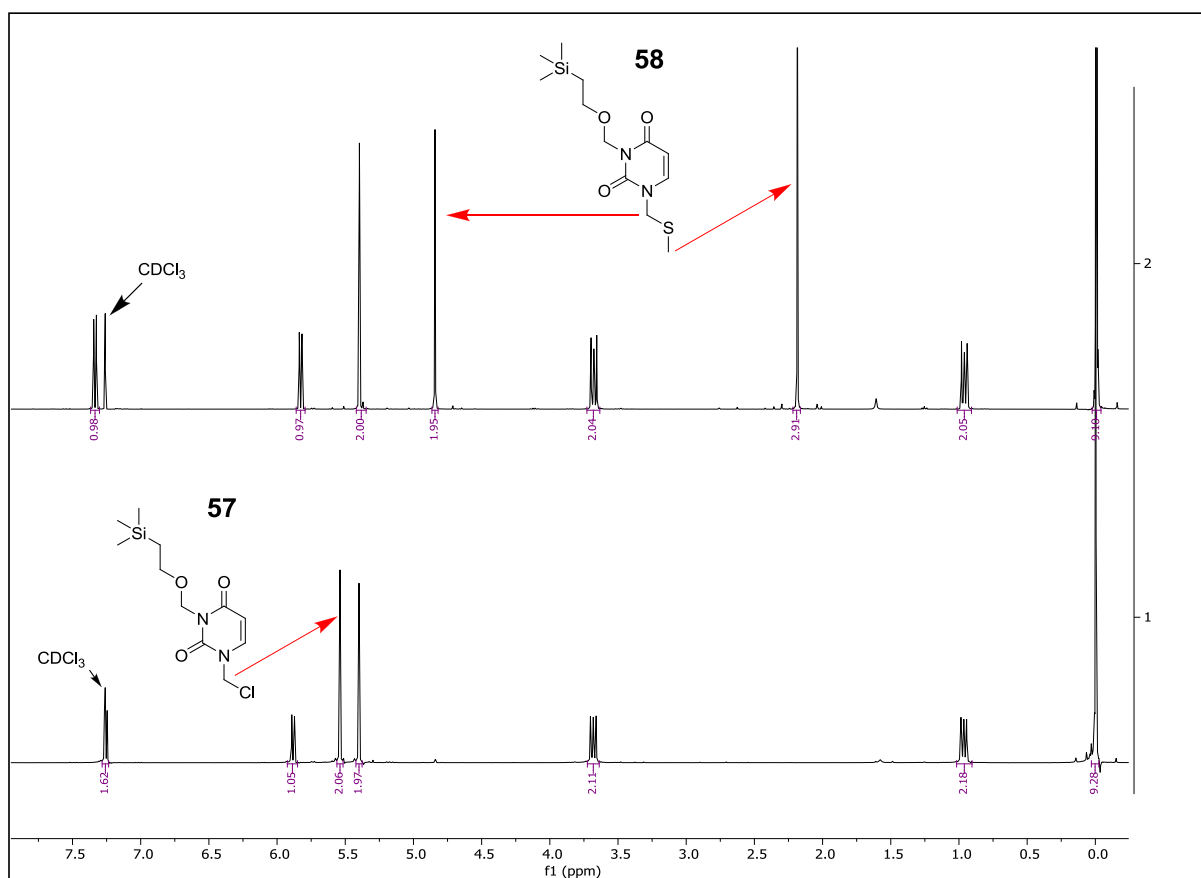


Figure 25: The figure shows the NMR spectra of compound **57** and **58** in comparison. (A) The MTM-group of **58** has its signals at 2.2 ppm (CH_3) and 4.9 ppm (CH_2) in the NMR. (B) *In situ* activation of **58** by sulfuryl chloride led to compound **57**. The CH_3 -group signal disappeared and the CH_2 -group is deshielded. The NMR of **57** was conducted with material from the reaction mixture after reagent removal under reduced pressure.

Attempts were made to convert chloromethyl derivative **57** with the allyl alcohol **42** under strong basic conditions to increase the nucleophilicity of **42** (Table 7). Compound **42** was treated with NaH in dry DMF at 0°C for 30 to 60 min before **57** (dissolved in DMF) was slowly added. The mixtures were stirred at room temperature overnight. Table 6 shows the different ratios of **42**, **59** and NaH used. A 1:1 ratio of allyl alcohol **42** and uracil **57** with a

slight excess of base resulted in product formation, but also left some starting material unreacted, along with the formation of some side products (Table 6, entry 1). Only small product amounts could be isolated. Unconsumed allyl alcohol **42** was the main obstacle for product separation

Table 6: Reaction conditions for the N,O-acetale formation with uracil building block **57**.

entry	42 [eq]	57 [eq]	NaH [eq]	solvent	temp	time	remarks
1	1.0	1.0	1.1	DMF	rt	O/N	61 , byproducts and starting material present
2	1.0	1.0	1.2	DMF	rt	O/N	61 , byproducts and starting material present
3	1.0	1.3	1.3	DMF	rt	O/N	61 (26% yield), byproduct formed

The equivalents of NaH (entry 2) were hereupon increased to ensure full allyl alcohol deprotonation. Clear product formation could be observed after several hours but **42** was still present and byproducts were formed. Therefore, the amount of **57** was increased to enable full allyl alcohol consumption and eliminate the purification problem (entry 3). Unfortunately, **61** could only be isolated with a yield of 26%. The main byproduct was identified to be the SEM-protected uracil dimer **62** (Figure 26).

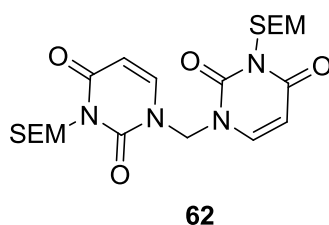


Figure 26: **62** was the main byproduct of the N,O-acetal formation.

Compound **61** was used to find suitable conditions for the deprotection of the SEM-group to obtain the final compound **51**. Therefore, **61** was treated with an excess of tetrabutylammonium fluoride (TBAF) and heated for the time indicated (Table 7). Using this method, only trace amount of product, together with starting material and byproducts, could be detected (entry 1-3). The outcome is correlating with experimental results described in literature. The high stability of the SEM protecting group, when incorporated into pyrimidines, was also observed by Phadtare et al. and by Chandra et al.^{96,100}

Table 7: Experimental conditions for SEM-deprotection of **61**.

entry	reagent	reagent [eq]	solvent	temp	time	remarks
1	1M TBAF (THF)	13	THF	reflux	1.5 d	decomposed
2	1M TBAF (THF)	3.8	THF	reflux/50 °C	O/N	51 traces, starting material decomposed material detected
3	1M TBAF (THF)	4.0	THF	50 °C	O/N	51 traces, starting material, decomposed material detected
4	SnCl ₄	1.2	DCM	0 °C	1 h	decomposed

Based on the procedure of Chandra et al. attempts were made to deprotect **61** with SnCl₄ (entry 4) at 0 °C leading to full decomposition of **61**. On one hand, the high stability of the SEM-protecting group was promising for further optimization of N,O-acetal formation reactions. On the other hand this high stability reveals problems to obtain the final product without using harsh conditions. These results led to no further optimisation of the N,O-acetal production with SEM-protecting groups and resulted in a new search for alternatives.

4.3.4 Attempts toward N,O-acetal formation with N³-carbonyloxymethyl-protected N¹-chloromethyl uracil

The previous analysis of different protecting groups in section 4.3.2 revealed that deprotection conditions for base sensitive protecting groups at uracil are most likely tolerated by other structural elements of the compounds. Unfortunately, the stability of acyl protecting groups is reduced when directly attached to the imido-nitrogen.⁸⁵ A possibility to increase the stability is by the introduction of a spacer between the carbonyl group and the imido nitrogen.

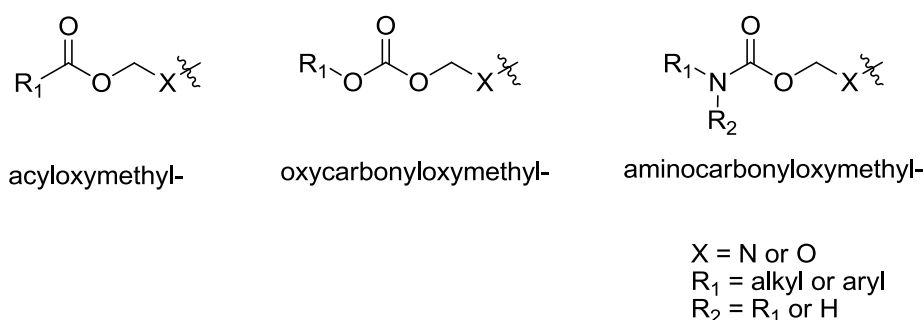
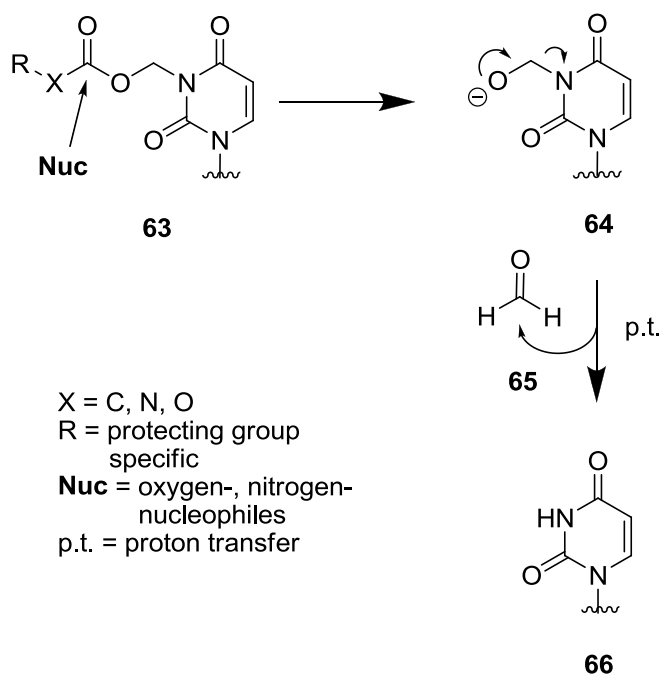


Figure 27: Overview of three different carbonyloxymethyl-protecting groups types used in synthetic and prodrug chemistry.

This strategy is represented by carbonyloxymethyl-protecting groups (Figure 27).¹⁰¹ These groups are mainly used as prodrug structures (for example Pivampicillin, 1-ACOM-5-FU) but can also be utilized as protecting groups in synthetic chemistry.¹⁰²⁻¹⁰⁴ The overall stability of carbonyloxymethyl-protecting groups is dependent on their stability towards nucleophilic attack at the carbonyl group. Therefore, the stability is tunable by varying the neighboring atoms and functional group resulting in acyl-, carbonate- or carbamate structures (Figure 27).¹⁰⁴ An attack at the carbonyl group results in the formation of a deprotonated hemiacetal/hemi-N,O-acetal **64** which further decomposes under liberation of formaldehyde (**65**) to the deprotected compound **66** (Scheme 12).^{101,105}



Scheme 12: Proposed mechanism for deprotection of carbonyloxymethyl-protecting groups at uracil. The stability of carbonyloxymethyl-protecting groups depends on the electronic and steric parameters of the substituents R (alkyl/aryl) and on X giving acyl groups, carbonates or carbamates. Nucleophiles as part of enzymes or as part of synthetic chemistry (OH^- , NH_3 and others) can attack at the carbonyl group of **63** and cleave the connection to the related (N,O)-acetal function. The formed (N,O)-hemiacetal is instable and releases formaldehyde (**65**). The unprotected structure **66** is obtained.

Two different classes of carbonyloxymethyl protecting groups for the N,O-acetal synthesis were investigated. The commercially available pivaloyloxymethyl group (POM-group) **67** is widely used as a prodrug structure for phosphates and pyrimidine derivatives, as well as a temporary protecting group for pyrimidines and triazoles in synthesis (Figure 28).^{104,105} Typical deprotection procedures involve nucleophilic bases like ammonium hydroxide or sodium hydroxide.^{104,106} In case of triazoles, the POM protecting group (**67**) is cleaved with sodium hydroxide for 10 minutes at room temperature.¹⁰⁴

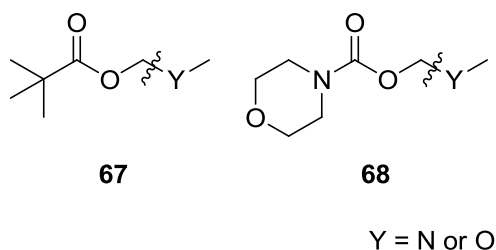
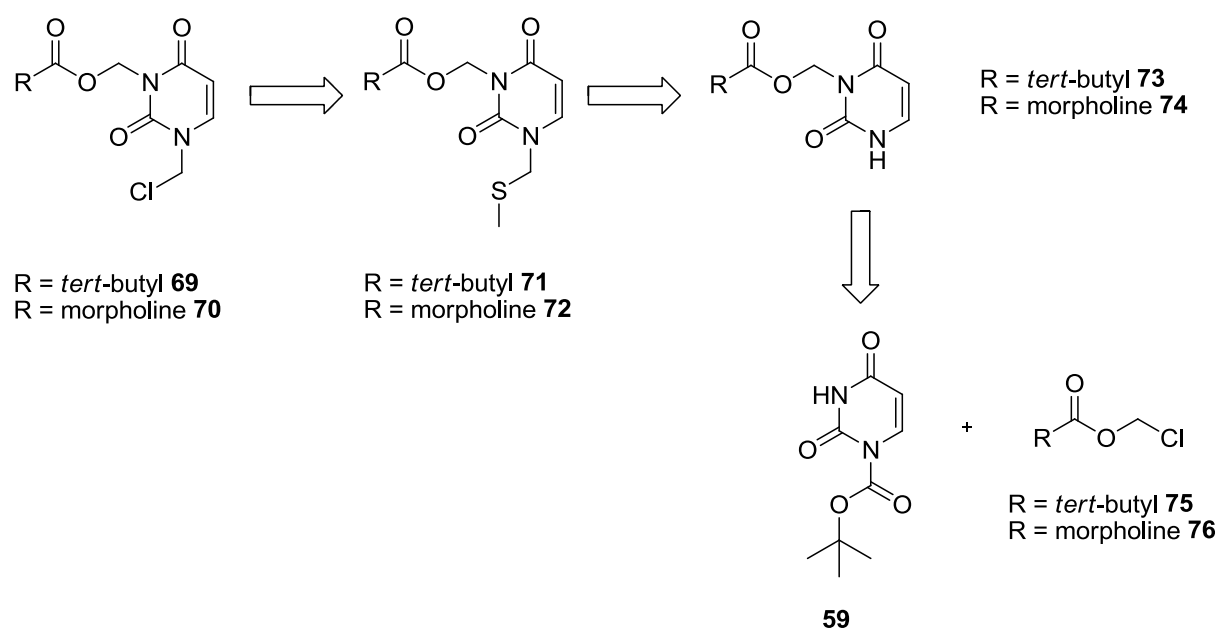


Figure 28: Carbonyloxymethyl-protecting groups used for uracil protection.

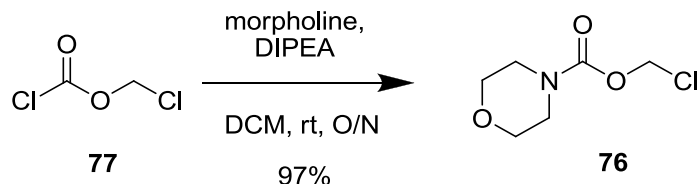
This protecting group was figured as potentially too instable for the N,O-acetal formation step, but attempts were made regardless. The aminocarbonyloxymethyl protecting group **68** was likewise described by Loren et al. for the protection of triazoles. The use of **68** increased the deprotection time to 24 h at room temperature and was therefore of interest to test for the protection of uracil (Figure 28).¹⁰⁴

The carbonyloxymethyl protected chloromethyl uracil analogs **69** and **70** required the synthesis of their respective MTM-precursors **71** and **72** (Scheme 13). The MTM derivatives **71** and **72** were planned as reaction of the N³-protected derivatives **73** and **74** with MTMCl. Compounds **73** and **74** were planned as products of the reaction between N¹-Boc uracil (**59**) with **75** and **76** as reactants (Scheme 13).



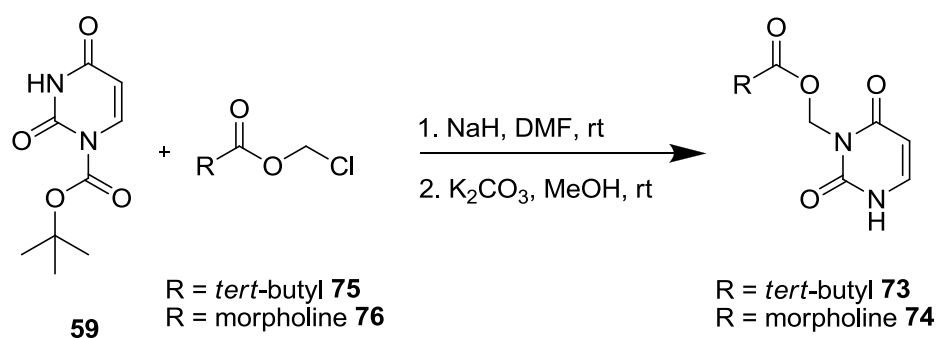
Scheme 13: Retrosynthesis for the carbonyloxymethyl protected chloromethyl uracil analogs **69** and **70** starting from N¹-Boc uracil (**59**).

Pivaloyloxymethyl chloride (POMCl) **75** is commercially available while **76** must be synthesized. Chloromethyl morpholine-4-carboxylate (**77**) was obtained in a reaction of chloromethyl chloroformate with morpholine and DIPEA that was based on a literature procedure (Scheme 14).^{104,107}



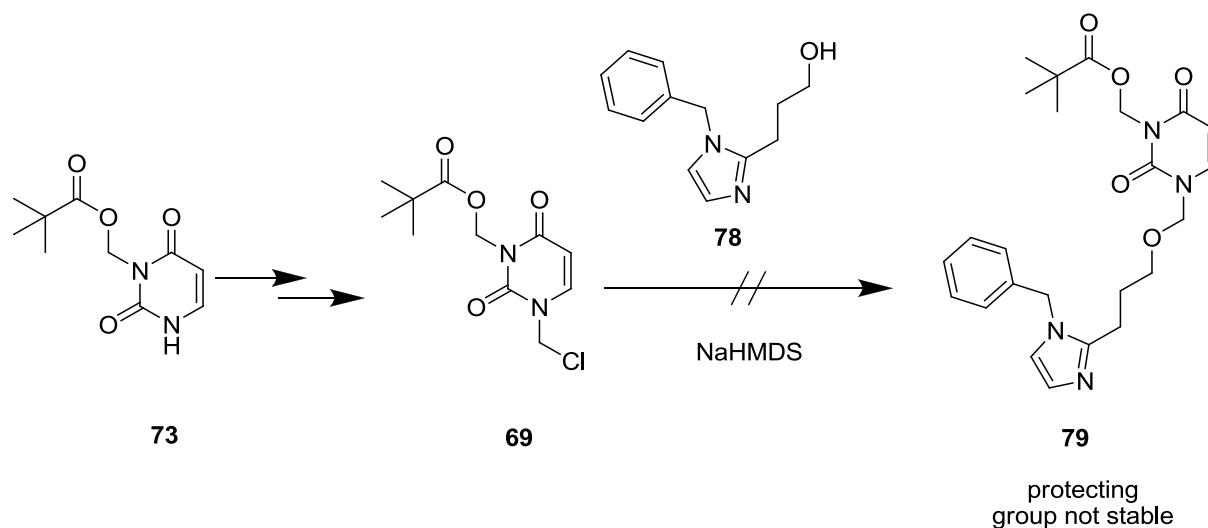
Scheme 14: Synthesis of chloromethyl morpholine-4-carboxylate (**76**).

To find suitable conditions towards N³-protected uracil derivatives **73** and **74** with the N¹-Boc uracil (**59**) and **75** or **76** were conducted (Scheme 15). The conversion was slow and by-products were formed in the reaction with sodium hydride yielding in small amounts of impure product in the cases of **74** (Scheme 15). For **73**, a sufficient amounts of product was afforded to test the next reaction steps.

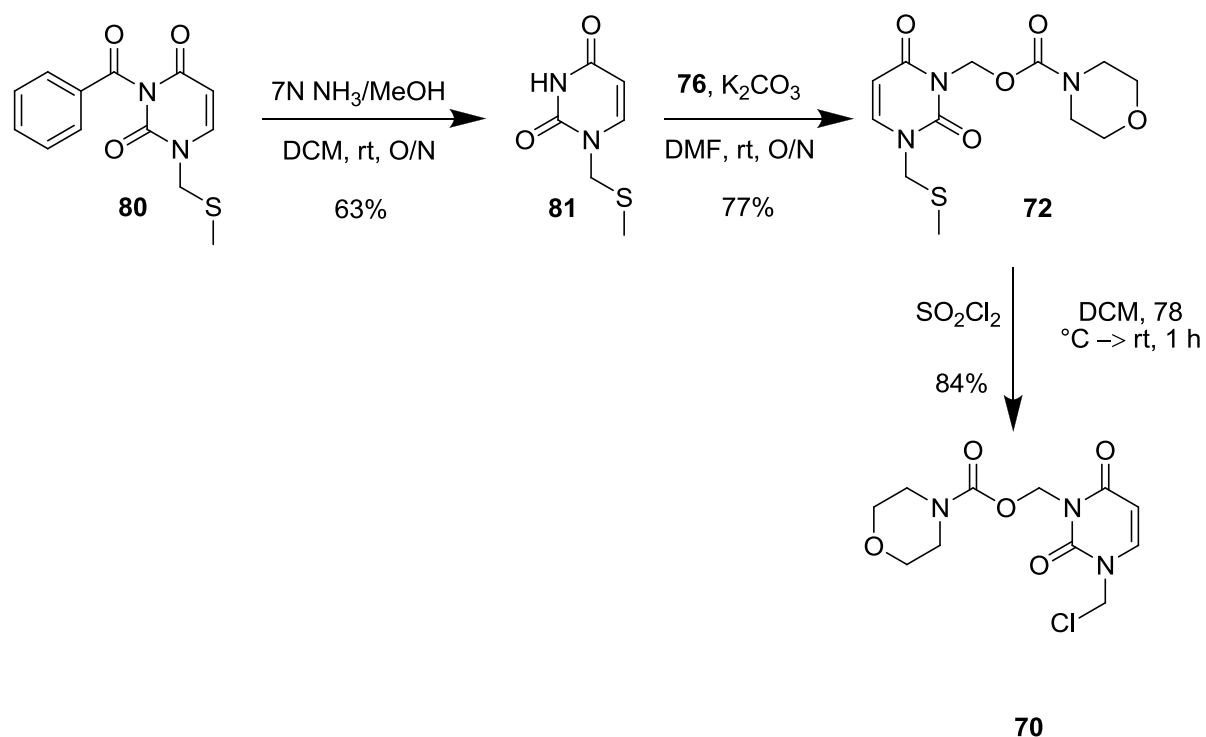


Scheme 15: Test reactions to afford the protected uracil building blocks **73** and **74**.

With **73**, the MTM-derivative **71** was formed in a test reaction and further activated with SO₂Cl₂ to the chloromethyl derivative **69** (Scheme 16). A reaction of **69** with **78** (type B approach, synthesis of **78** described in section 4.7) with NaHMDS as base failed. Unfortunately, the protecting group of **69** showed insufficient stability under strongly basic conditions and the type B compound **79** could be not generated using this approach.



Scheme 16: **73** was converted to **69**. The protecting group showed insufficient stability under strong basic conditions in a reaction with **78** to obtain the type B compound **79**.



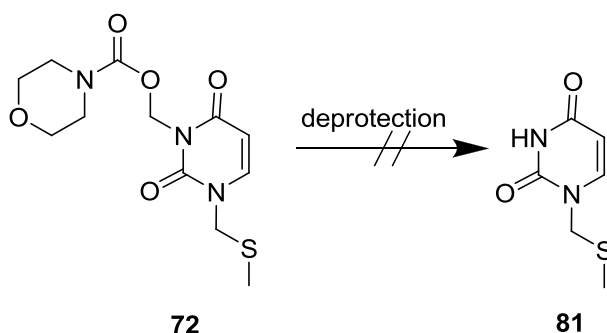
Scheme 17: Synthesis pathway for the synthesis of the chlorinated building block **70**.

Therefore, it was continued with the MTM-building block **72** to generate the chloromethyl uracil derivative **70**. The synthesis route for **72** was changed and the N¹-MTM uracil **81** was used as new starting material (Scheme 17). **81** was synthesized from **80** by debenzoylation with 7 N ammonia in methanol in 63% yield. **81** was treated with **76** and K₂CO₃ in DMF at room temperature overnight. **72** was isolated in 77% yield (Scheme 17). **72** was successfully transformed with SO₂Cl₂ into the corresponding chloromethyl uracil derivative **70** in up to 84% yield (Scheme 17). **70** was used in test reactions with the imidazole scaffolds **82** and **83** (synthesis described in section 4.7) to afford type B compounds. The use of NaOtBu or NaHMDS together with **70** resulted in 40-50% conversion to **84** and **85** respectively (Table 8, entry 1-2). The protecting group showed high stability under these reaction conditions. Reaction controls could be conducted by reverse-phase liquid chromatography only due to the high polarity of the products. Further optimization reactions were not carried out due to time constraints.

Table 8: Reactions conditions for N,O- acetal formation of **84** and **85**.

entry	R	70 [eq]	base	base [eq]	solvent	temp	time	remarks
1	82 , OMe	1.2	NaOtBu	3.0	THF	rt	O/N	40-50% conversion, starting material left
2	83 , CF ₃	1.2	NaHMDS	2.0	THF	rt	O/N	40-50% conversion, starting material left

Instead, two attempts with remaining starting material **72** and primary amines were conducted to find deprotection systems for the carbonyloxymethyl protecting group (Scheme 18). Primary amines should cleave the protecting group and trap released formaldehyde. **72** was treated with 7N ammonia in methanol for three days at room temperature. Only product traces of **81** could be detected by TLC. The protecting group stayed mainly intact. Therefore, **72** was stirred in 1,2-diaminoethane at 50 °C overnight leading to undefined compounds. Just as for the coupling reaction no further systematic testing could be conducted due to time constraints. It might be possible that this protecting group is too stable towards basic deprotection and that the morpholine moiety has to be replaced.



Scheme 18: The deprotection of the aminocarbonyloxymethyl protecting group of **72** failed.

4.4 Synthesis of: alternative linkages replacing the N,O-acetal

The difficulty in producing compounds with N,O-acetal structure (type A/B) led to a wider interpretation of what structural elements were required and necessary for dUTPase inhibitors. The N,O-acetal structure element is not an essential element for good inhibition and has been replaced in several similarly potent inhibitors.^{58,68,69} Using this knowledge, compounds without an N,O-acetal functional group were synthesized in parallel to the attempts to obtain N,O-acetal containing compounds.

Two points were thereby put forward to find new and alternative scaffolds:

- Find alternative linkages between the imidazole and the essential uracil based on the structure of known inhibitors.
- Reuse intermediates from the N,O-acetal synthesis approaches.

Structural elements of known inhibitors were compared with the intermediates afforded from the N,O-acetal syntheses to design new compound scaffolds.^{58,68,69} Structural elements of interest were alkyl/alkenyl chains that could be directly connected with the uracil. Amide structures, as well as ethers or amines as part of the linker were also considered. The structures were based on the three main starting materials shown in Figure 29. The unsaturated ester **34** was used for the synthesis attempts of type A and B compounds. The developed synthesis pathways were implemented in the synthesis of new type C and D compounds, which are characterized by a plain hydrocarbon linkage. Starting material **35** was used for the synthesis of the unsaturated ester **34** but due the carbonyl group, **35** was also of interest for the synthesis of ether linkages (type E).

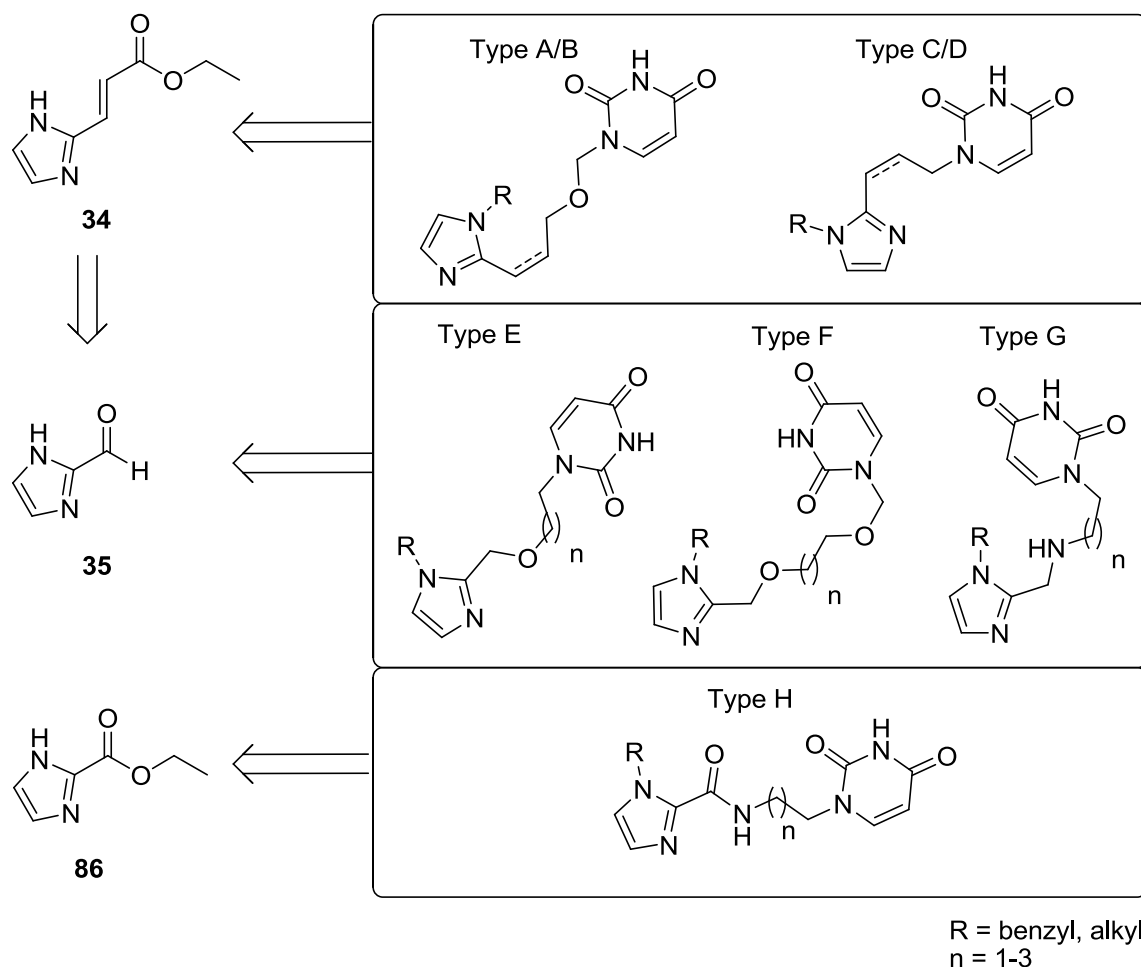
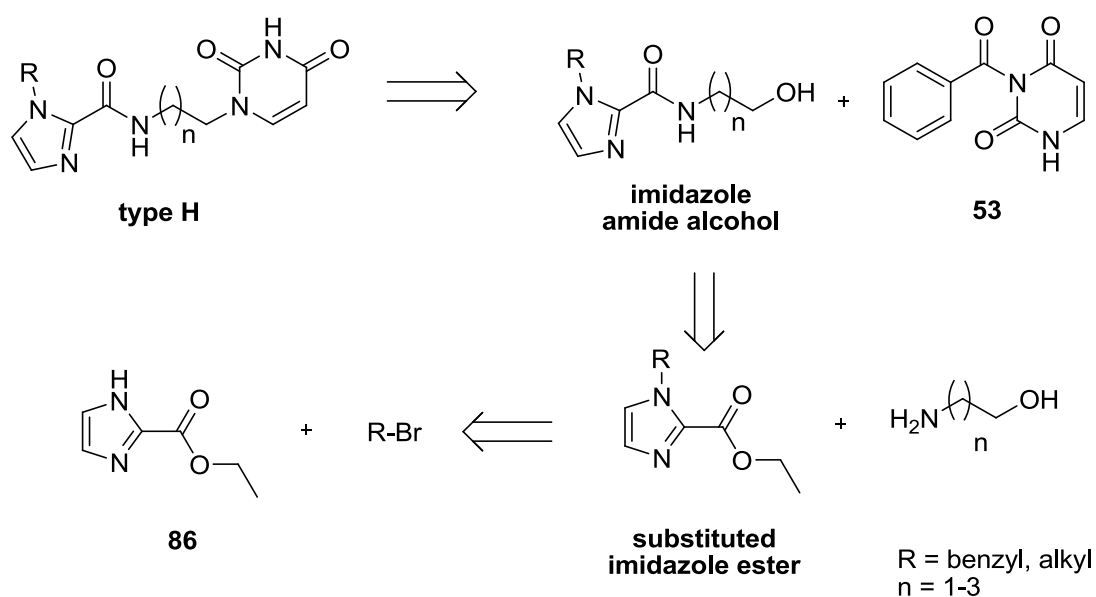


Figure 29: Possibilities to redesign the compounds. Shown are the three main starting materials for the synthesis of new compound scaffolds. Intermediate **34** was the precursor for type A/B compounds and was used to build plain-hydrocarbon compounds (type C/D). The aldehyde **35** was used for ether-linked type E compounds and could be used for ether/N,O-acetal linked type F compounds or amine linked type G compounds. Starting material **86** was new implemented to obtain type H compounds.

Further possibilities were identified in an extended structure with N,O-acetal (type F) once the attempts of the type A/B-compound syntheses were successful. The aldehyde group of **35** offered a possible route to amine linked compounds (type G) by reductive amination. Amide-linked compounds (type H) were seen moreover as interesting as active dUTPase compounds containing an amide group have previously been described in literature. Therefore, starting material **86** was additionally considered as a suitable starting material. Synthesis attempts for Type F and type G compounds were considered but postponed in favour of the other compound scaffolds. The use of protecting groups for late stage diversification was considered. Through the re-use of intermediates for different compound scaffolds and the in parts short synthesis routes, the use of protecting groups was not prioritized.

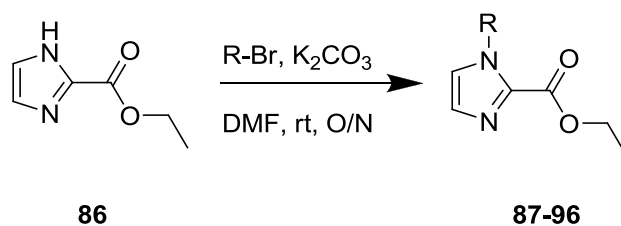
4.5 Synthesis of: amide linked dUTPase compounds (Type H)

Amide linked dUTPase inhibitors are described in the paper of Miyakoshi et al.⁵⁸ They played a central role in the first library screening to find lead structures for optimization and in the development of the cis-lock strategy.⁵⁸ The scaffold formation *via* an amidation reaction was seen as a possibility to quickly build a compound library for biological testing. The retrosynthetic analysis of type H compounds is shown in Scheme 19.



Scheme 19: Retrosynthetic analysis of type H compounds.

The connection of imidazole amide-alcohol intermediates with N³-benzoyl uracil (**53**) was planned as the key step of the synthesis. Mitsunobu-reactions should allow the direct coupling without a further activation step.¹⁰⁸ Subsequent deprotection under basic conditions leads the products. The amide-alcohol derivatives were planned to be obtained by the direct reaction of substituted imidazole ester derivatives with the corresponding amino alcohols; this is done to avoid ester hydrolysis and acid activation steps. The linker length should therefore be analogous with the linker length described for literature dUTPase inhibitors. The ester derivatives are generated by the alkylation of imidazole-2-carboxylic acid ethyl ester (**86**) with benzyl/alkyl bromides. The *N*-substituted imidazole-2-carboxylic acid ethyl esters **87-96** were synthesized under mild conditions (Scheme 20). Imidazole-2-carboxylic acid ethyl ester **86** was reacted with alkyl/benzyl bromides and potassium carbonate in dry DMF. The reaction conditions are similar to those described in literature by Jeannot et al. using acetonitrile instead of DMF, and Sindac et al. using sodium carbonate as the base.^{109,110} The products were afforded in good yields and purity with the exception of **92** (Table 9).

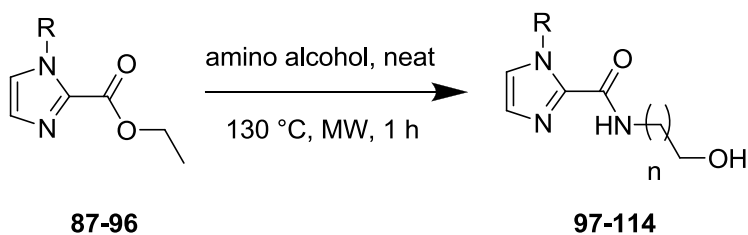


Scheme 20: Synthesis of *N*-substituted imidazole-2-carboxylic acid ethyl esters.

Table 9: Structures and yields of the *N*-substituted imidazole-2-carboxylic acid ethyl esters **87-96**.

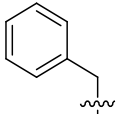
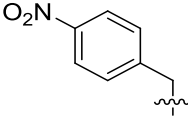
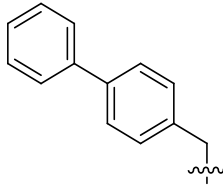
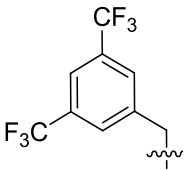
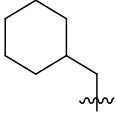
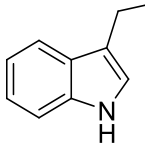
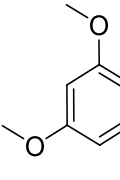
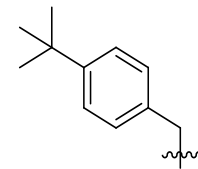
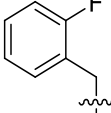
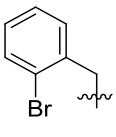
Substituent R					
yield	87 , 89%	88 , quant.	89 , 85%	90 , 99%	91 , 91%
Substituent R					
yield	92 , 18%	93 , 94%	94 , 92%	95 , 93%	96 , 93%

The corresponding imidazole amide-alcohol derivatives **97-114** were directly obtained from the ester intermediates **87-96** by reactions with amino alcohols (Scheme 21, Table 10). The length of the linker was chosen to be two or three carbons, corresponding to the known dUTPase inhibitors.⁵⁸ Full conversion was obtained by microwave irradiation at 130 °C and a reaction time of one hour (Scheme 21). It is reasonable to assume that most reactions proceeded faster, but the high conversion after one hour allowed for easier product isolation without the need of reaction monitoring. Using 4-amino-1-butanol and **96** led to **112** in 96% yield thus showing that also longer chains can be incorporated (Table 10). The intermediates **97-114** were afforded in high yield and purity (Table 10).



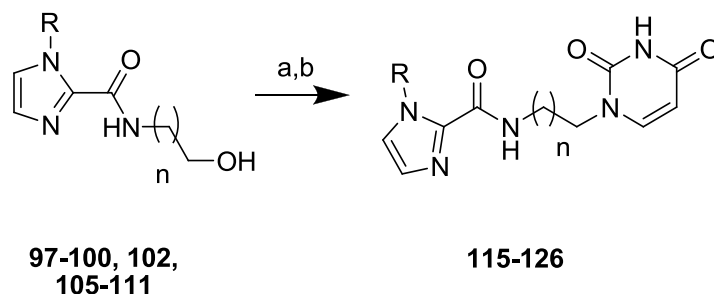
Scheme 21: Synthesis of imidazole amide alcohols

Table 10: Structures and yields of the imidazole-amide alcohols **97-114**.

Substituent R						
yield	n = 1	97 , 94%	-	-	101 , 91%	103 , 96%
	n = 2	98 , 95%	99 , 98%	100 , 93%	102 , 95%	104 , 95%
Substituent R						
-yield	n = 1	-	106 , 89%	108 , 98%	110 , 93%	113 , 86%
	n = 2	105 , quant.	107 , 89%	109 , 93%	111 , 93%	114 , 96%
	n = 3	-	-	-	112 , 96%	-

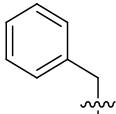
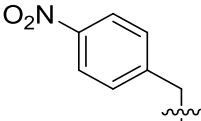
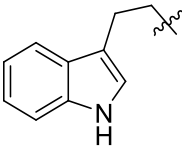
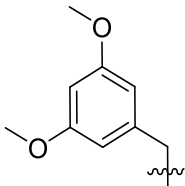
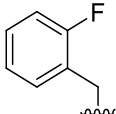
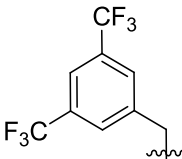
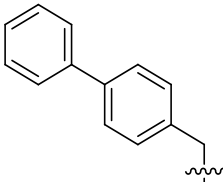
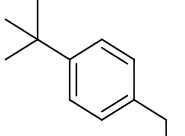
- = not conducted or not isolated.

The key step for the type H compound synthesis was a Mitsunobu reaction, *vide supra*.¹⁰⁸ This reaction allowed *in situ* coupling reactions of the imidazole amide-alcohol derivatives with N³-benzoyl uracil (**53**) and rendered additional activation steps. The Mitsunobu reactions were based on the procedure of Miyakoshi et al. using two equivalents diisopropyl azodicarboxylate (DIAD) and two equivalents triphenylphosphine (PPh₃).⁵⁸ The reactions for the target structures **97-100**, **102**, **105-111** were performed in a similar manner in overnight reactions (Scheme 22).



Scheme 22: Conditions: (a) N³-benzoyl uracil (**53**), PPh₃, DIAD, THF, rt, overnight; (b) 7 N NH₃/MeOH, rt, 3-4 h.

Table 11: Structures and yields of the type H compounds **115-126**.

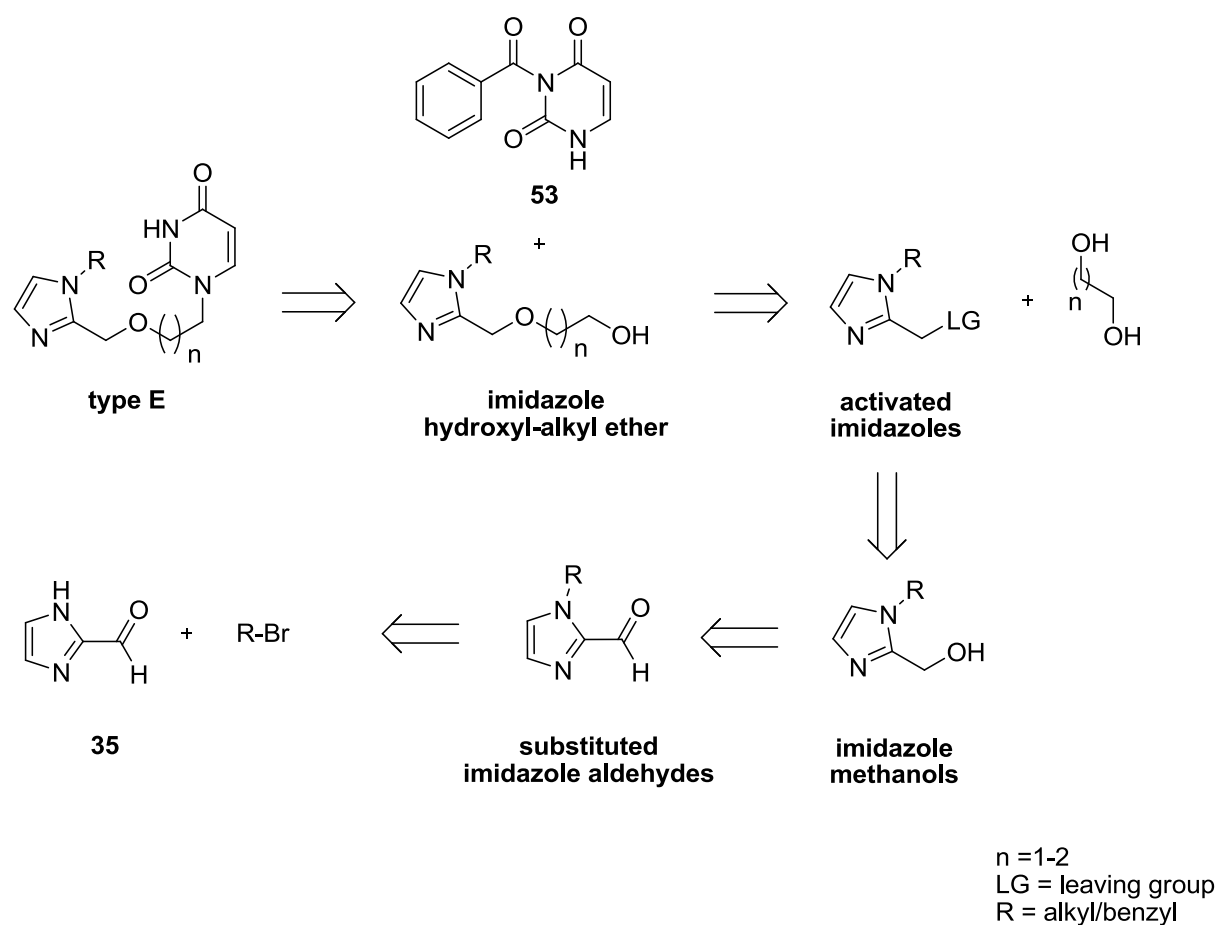
Substituent R				
	yield	n = 1 115 , 34%	-	-
	n = 2 116 , 31%	117 , 25%	118 , 41%	120 , 40%
Substituent R				
	yield	n = 1 121 , 41%	-	-
	n = 2 122 , 50%	123 , 33%	124 , 44%	126 , 48%

- = not conducted or not isolated.

With the high excess of DIAD and PPh_3 , no major side reaction with the less acidic amide was observed. The reaction mixtures were purified by silica column chromatography to afford the N^3 -benzoyl protected products which were directly deprotected with 7 N ammonia in methanol (7 N NH_3/MeOH) (Scheme 22). Some products precipitated directly from the reaction mixture. However, the product isolation was generally by filtration with DCM or EtOAc due to the low solubility of the products in most organic solvents. The first attempts to purify the products by silica column chromatography or recrystallization resulted only in low to moderate yields (compounds **115-126**) (Table 11). Many type H compounds showed low solubility in organic solvents as well as in water and had weak compound affinities in the first dUTPase enzyme assay (see section 4.8). Since there were alternative scaffolds at hand, the type H compounds were not investigated further. As a result not all intermediates were converted to final compounds.

4.6 Synthesis of: ether linked dUTPase compounds (type E)

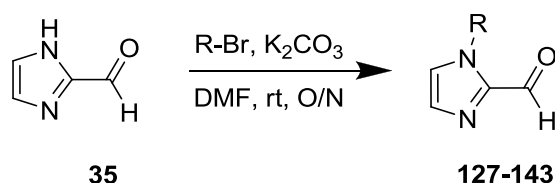
The ether linked compounds can not be deduced directly from inhibitors of Taiho pharmaceuticals, but they share this structure element with some malaria dUTPase inhibitors.⁶¹ The retrosynthetic analysis for type E is shown in Scheme 23. Since the introduction of the uracil moiety *via* the Mitsunobu reaction worked very well this strategy was also applied in this approach; therefore, the synthesis of imidazole hydroxyl-alkyl ethers was necessary. The imidazole hydroxyl-alkyl ethers were planned as a reaction between imidazoles, as alkylation agents (activated imidazoles), and diols.



Scheme 23: Retrosynthesis for ether-linked compounds (type E).

These activated imidazoles are afforded by the transformation of the hydroxyl group of imidazole methanols into better leaving groups. The imidazole methanols are obtained from the corresponding substituted imidazole aldehydes by reduction. The starting material for the substitution reaction was, as previously suggested, 2-imidazolecarboxaldehyde (**35**).

N-substituted imidazoles were synthesized by the alkylation of 2-imidazolecarboxaldehydes (**35**) with alkyl/benzyl bromides and potassium carbonate in DMF (Scheme 24). Similar conditions are described in literature for selected compounds.¹¹¹⁻¹¹³ Attempts to conduct the reactions in acetonitrile resulted in reaction conditions that were not superior to the mild conditions of DMF and room temperature. Most products were isolated in moderate to good yield (Table 12). **139** was isolated in 35% yield as a result of insufficient conversion. **143** could not be obtained in satisfying yield under varying reaction conditions.

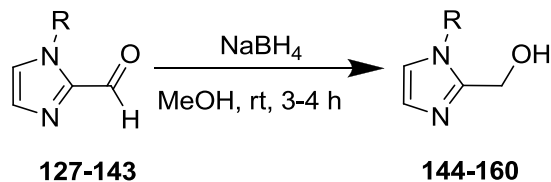


Scheme 24: Synthesis of *N*-substituted imidazole aldehydes **127-143**.

Table 12: Structures and yields of the *N*-substituted imidazole aldehydes **127-143**.

Substituent R					
yield	127 , 78%	128 , 63%	129 , 61%	130 , 74%	131 , 77%
Substituent R					
yield	132 , 67%	133 , 72%	134 , 72%	135 , 72%	136 , 77%
Substituent R					
yield	137 , 76%	138 , 68%	139 , 35%	140 , 61%	141 , 61%
Substituent R					
yield	142 , 59%	143 , 28%			

The aldehyde groups of **127-143** were reduced with sodium borohydride in methanol to the corresponding alcohol derivatives as described in literature for *N*-substituted imidazole-2-methanols (Scheme 25).¹¹⁴ Compounds **144-160** were obtained in high yields and purity (Table 13).

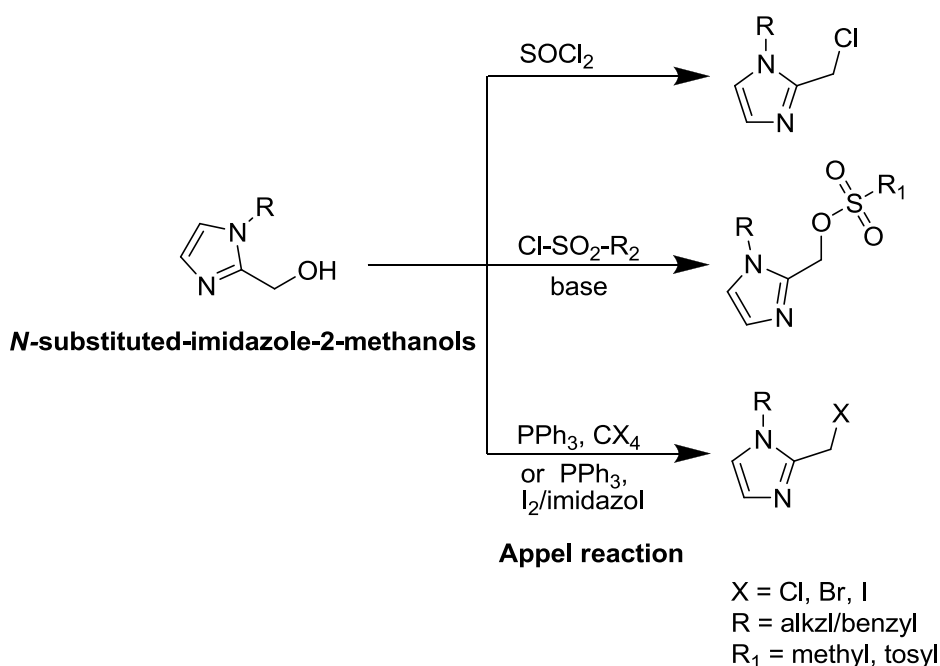


Scheme 25: Reduction of the *N*-substituted imidazole aldehydes **127-143**.

Table 13: Structures and yields of the *N*-substituted imidazole-2-methanols **144-160**.

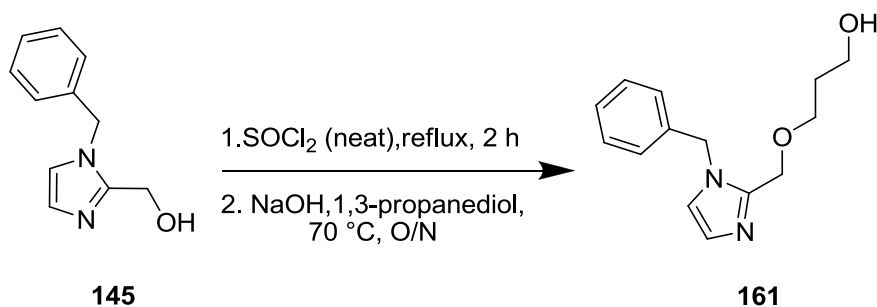
Substituent R					
yield	144, 93%	145, 95%	146, 85%	147, 97%	148, 86%
Substituent R					
yield	149, 95%	150, 95%	151, 94%	152, 93%	153, 91%
Substituent R					
yield	154, 95%	155, 94%	156, 94%	157, 99%	158, 98%
Substituent R					
yield	159, 90%	160, 98%			

For the transformation of the hydroxyl-group into a good leaving group, there are a number of options. Typical reactions are the formation of sulfonic esters by sulfonyl chlorides (tosyl or mesyl chloride), the use of the Appel reaction, or the halogenation by thionyl chloride (Scheme 26). The activation of the hydroxyl-group as sulfonate ester requires a workup to remove reagent excess and additives like base or must be conducted in equimolar amounts of reagents to avoid side reactions in the next reaction. The Appel reaction offers mild conditions but has the drawback of using triphenylphosphine.^{115,116} Removing the latter as well as any byproducts requires more intensive workup, which made this approach unfavorable. Thionyl chloride-based reactions often require no further additives and have simple workups. The byproducts are gaseous and excess thionyl chloride can be removed under reduced pressure leading to pure products. These conditions made thionyl chloride favorable over the other possibilities.



Scheme 26: Examples for the activation of the hydroxy-group to form a good leaving group.

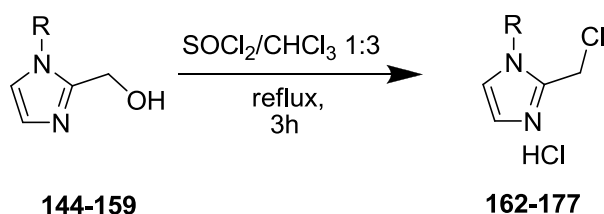
Chlorination reaction conditions with thionyl chloride for some imidazole methanols are described in the literature. Many procedures use the reagent neat under reflux, or in combination with solvents like chloroform.^{117,118} The workups are typically based on the removal of the reagent and solvent, and the direct use of the crude in following reactions. The first attempt to activate **145** with SOCl_2 was connected with the following reaction step to afford **161**. **145** was treated with thionyl chloride (neat) under reflux. The excess of SOCl_2 was removed by evaporation and the crude was used directly in the reaction with 1,3-propanediol and NaOH in an overnight reaction at 70 °C to generate **161** (Scheme 27).



Scheme 27: First attempt to form imidazole hydroxy-alkyl ether.

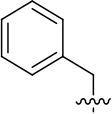
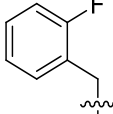
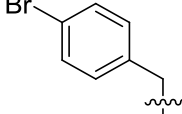
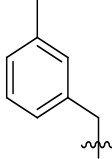
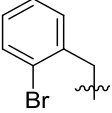
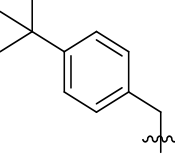
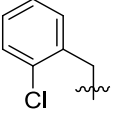
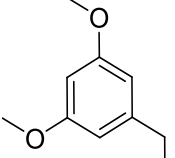
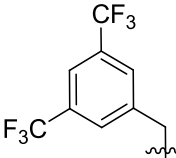
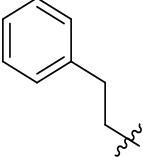
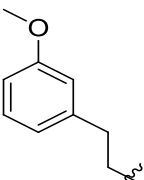
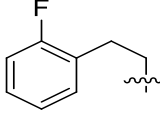
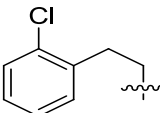
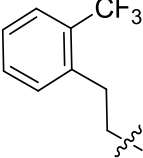
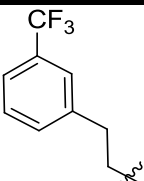
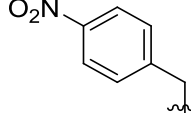
The use of the diol in excess should suppress the formation of dimers; a similar synthesis for chlorinated imidazoles is described by Zimmerman et al. using sodium hydride with ethanediol as solvent.¹¹⁹ **161** was isolated in 48% yield. The moderate isolated yield, and purity of this two step reaction and the limited possibility for diversification led to the decision to perform the synthesis of imidazole hydroxy-alkyl ethers in two distinct reactions. The purified chlorinated imidazoles should act as platform for different alkylation reactions.

The chlorinated products were finally obtained by treating the alcohol derivatives **144-159** with a mixture of 3:1 CHCl₃/SOCl₂ under reflux conditions (Scheme 28). The solvent and reagent excess were evaporated and the crude solids were washed with diethyl ether to obtain **162-177** as HCl salts in high yields and purity (Table 14).¹¹⁸ The 3,5-dimethoxy derivative **169** was not stable under these reaction conditions and could not be isolated as pure compound. An optimization for this intermediate was not of interest at this point. Milder reaction conditions, such as the use of SOCl₂ at room temperature or other activation agents could be potential alternatives to achieve this intermediate in higher purity. Compound **160** yielded no product for undetermined reasons.

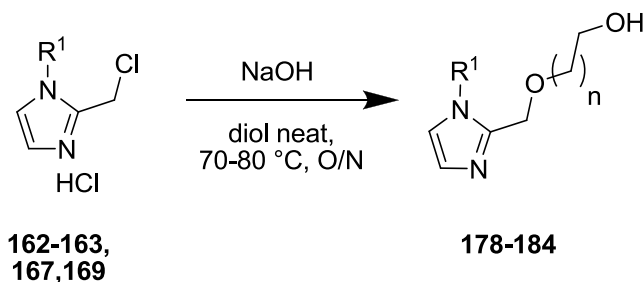


Scheme 28: Formation of the chloromethyl imidazole HCl salts **162-177**.

Table 14: Structures and yields of chloromethyl imidazole salts **162-177**.

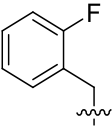
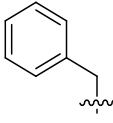
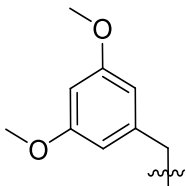
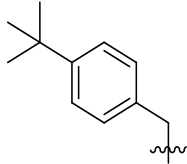
Substituent R				
yield	162 , 96%	163 , 93%	164 , 93%	165 , 93%
Substituent R				
yield	166 , 87%	167 , 84%	168 , 91%	169 , 92%
Substituent R				
yield	170 , 89%	171 , 95%	172 , 84%	173 , 97%
Substituent R				
yield	174 , 91%	175 , 82%	176 , 93%	177 , 80%

The imidazole hydroxy-alkyl ethers **178-184** were synthesized using NaOH and 1,2-ethanediol or 1,3-propanediol as solvents. The reaction were conducted at 70-80 °C overnight (Scheme 29). The yields of **178-184** are shown in Table 15. The purity and products yields were not satisfying due to byproducts formation.



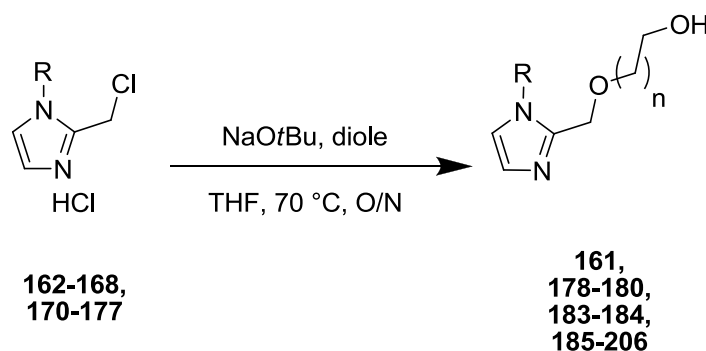
Scheme 29: Imidazole hydroxy-alkyl ether formation of diols with NaOH as base.

Table 15: Structures and yields of the hydroxy-alkyl ethers **178-184** obtained with NaOH as base.

Substituent R					
yield	n = 1	178 , 40%	180 , 42%	181 , 31%	183 , 21%
	n = 2	179 , 64%	-	182 , 43%	184 , 71%

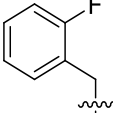
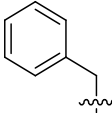
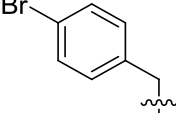
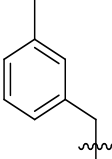
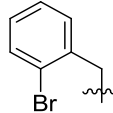
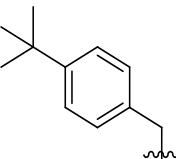
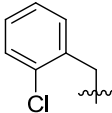
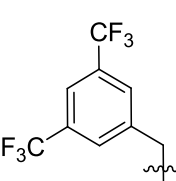
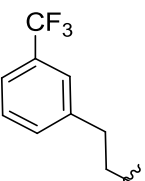
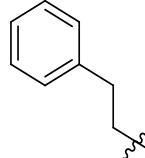
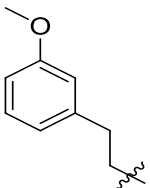
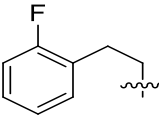
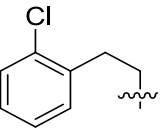
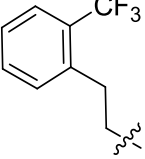
(-) = not conducted.

For that reason, water was excluded to prevent potential side reactions and to allow for the use of stronger bases. The diols were predried over anhydrous Na₂SO₄ for several days. Dry THF replaced the diols as solvent, and NaOH was exchanged for NaOtBu. The higher basicity when compared with NaOH or primary-alkoxides (for example the deprotonated starting material) should help to increase the nucleophilicity of the diols, and give cleaner reactions.

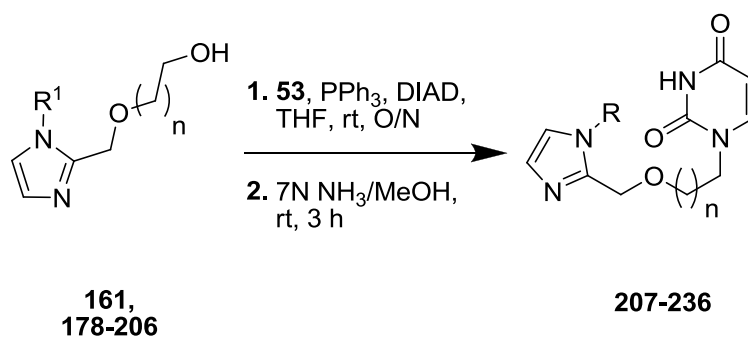


Scheme 30: Imidazole hydroxyl-alkyl ether formation with NaOtBu .

Table 16: Structures and yields of the imidazole hydroxy-alkyl ether **161**, **178-206** using sodium *tert*-butoxide.

Substituent R						
yield	n = 1	178 , 82%	180 , 74%	185 , 65%	187 , 80%	189 , 84%
	n = 2	179 , 84%	161 , 76%	186 , 81%	188 , 79%	190 , 83%
Substituent R						
yield	n = 1	183 , 80%	191 , 82%	193 , 91%	195 , 84%	197 , 71%
	n = 2	184 , 98%	192 , 84%	194 , 87%	196 , 90%	198 , 81%
Substituent R						
yield	n = 1	199 , 67%	201 , 78%	203 , 75%	205 , 80%	
	n = 2	200 , 62%	202 , 68%	204 , 87%	206 , 87%	

The imidazole hydroxyl-alkyl ethers were obtained by using sodium *tert*-butoxide and the corresponding diols. Compounds **161**, **178-180**, **183-184** and **185-206** were mainly obtained in good yields (Scheme 30, Table 16). It appeared that this condition was superior to reaction conditions with NaOH (Scheme 29 and Table 15). Because of missing starting materials **181** and **182**, these were not resynthesized under optimized conditions. The reaction of **177** failed for unknown reasons. In the final step N^3 -benzoyl uracil (**53**) was introduced *via* a Mitsunobu reaction, followed by deprotection with 7 N ammonia in methanol (Scheme 31). **207-236** were obtained in moderate to good yields over two reaction steps (Table 17).



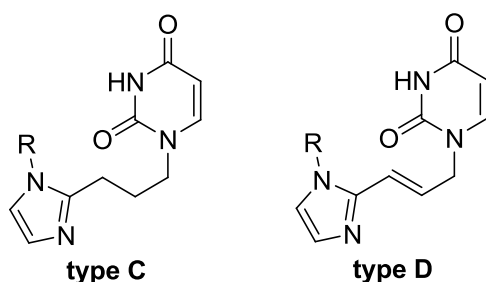
Scheme 31: Synthesis of the final compounds (type E).

Table 17: Structures and yields of the type E compounds **207-236**.

Substituent R						
yield	n = 1	207 , 46%	209 , 47%	211 , 63%	213 , 74%	215 , 60%
	n = 2	208 , 53%	210 , 68%	212 , 69%	214 , 71%	216 , 87%
Substituent R						
yield	n = 1	217 , 66%	219 , 59%	221 , 66%	223 , 76%	225 , 73%
	n = 2	218 , 71%	220 , 60%	222 , 67%	224 , 67%	226 , 83%
Substituent R						
yield	n = 1	227 , 61%	229 , 68%	231 , 61%	233 , 50%	235 , 50%
	n = 2	228 , 60%	230 , 64%	232 , 68%	234 , 64%	236 , 59%

4.7 Synthesis of: plain hydrocarbon linked dUTPase compounds (type C/D)

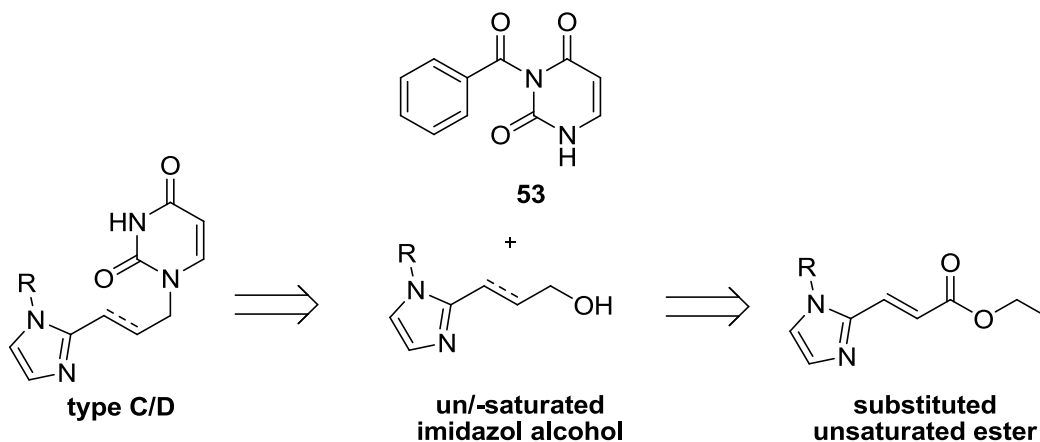
The attempts to synthesize type A compounds led to a synthetic route for the production of unsaturated imidazole esters. These derivatives gave the option for the synthesis of two plain hydrocarbon linked compounds types (type C and D, Figure 30) with a relative short linkage similar to some triazole containing dUTPase inhibitors described by Miyakoshi et al.⁶⁹



R = alkyl, benzyl

Figure 30: Structures of type **C** and type **D** compounds.

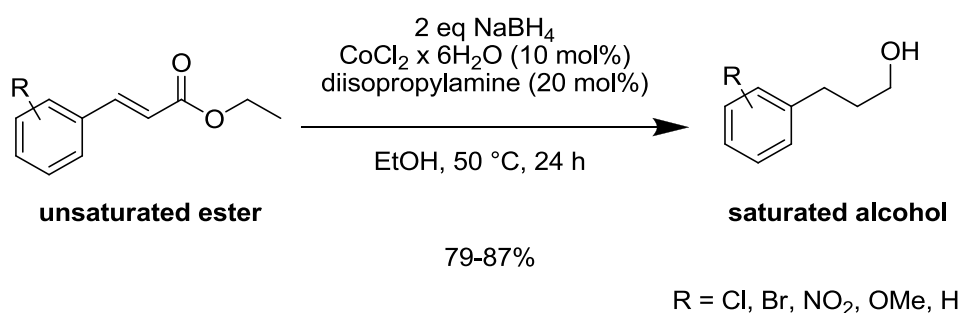
The retrosynthetic approach is shown in Scheme 32. A Mitsunobu reaction of saturated and unsaturated imidazole alcohol derivatives with N^3 -benzoyl uracil (**53**) is the key step following the established concept described for the other linkages. The imidazole alcohol derivatives are synthesized by reduction of the corresponding substituted unsaturated esters (Figure 30, Scheme 32).



Scheme 32: Retrosynthesis of type C/D compounds.

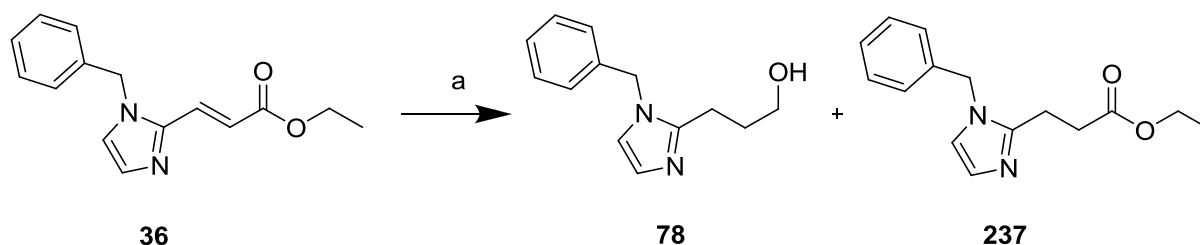
4.7.1 Synthesis approaches for type C compounds

It was of interest to access saturated linkers directly from the unsaturated esters derivatives to shorten the synthesis. The synthesis of saturated imidazole alcohols was based on sodium borohydride systems. NaBH₄ is an effective reducing agent for aldehydes, ketones, acid chlorides and imines, but it is not typically used for ester reduction and alkene reduction.^{120,121} These can be made accessible by adjusting the solvent properties and through additives such as copper-, nickel- or cobalt salts.¹²⁰ The *in situ* produced copper-, nickel- or cobalt-borohydrides are known as strong reduction agents which are also able to reduce esters, nitriles and nitro groups.¹²⁰ Jagdale and co-workers describe the combined reduction of unsaturated esters to the corresponding saturated alcohols.¹²¹

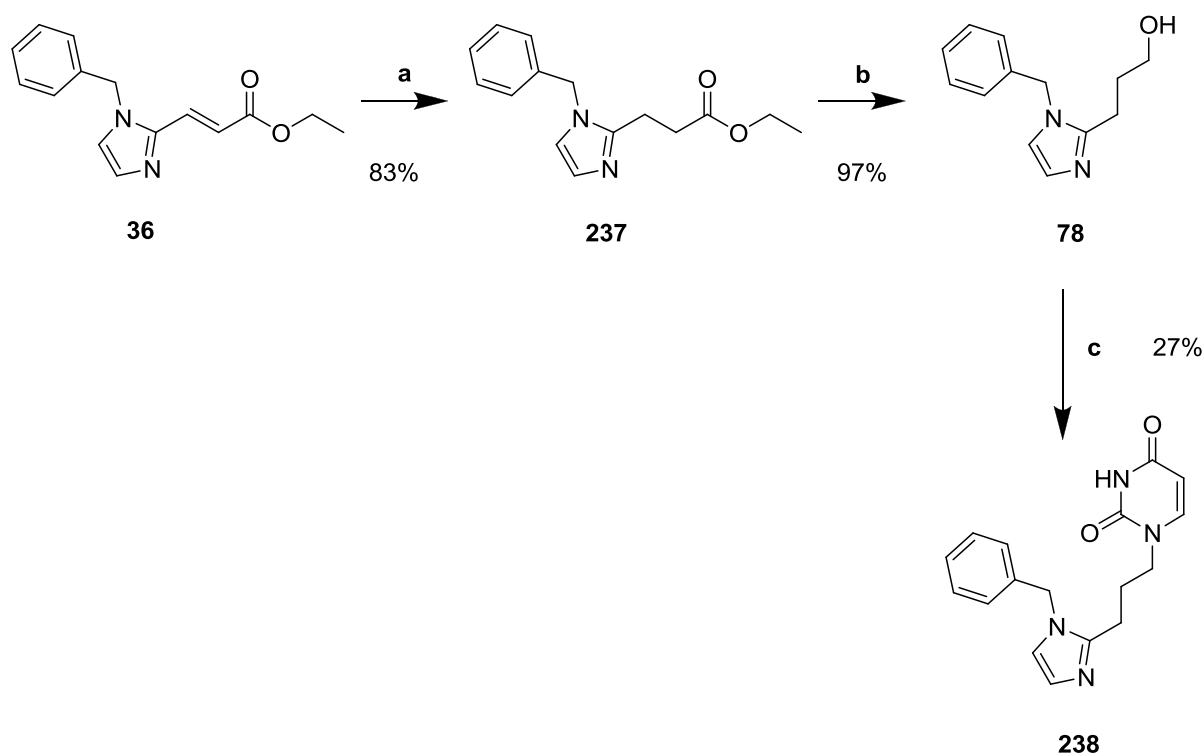


Scheme 33: Literature conditions to afford saturated alcohols from the unsaturated ester.¹²¹

The use of sodium borohydride together with 10 mol% cobalt(II)chloride hexahydrate and 20 mol% diisopropylamine was able to reduce different unsaturated aromatic ester derivatives in high yields (79-87%) (Scheme 33). These conditions are mild and do not affect halogens and nitro groups. Jagdale and co-workers showed that the absence of the cobalt catalyst leads only to 5% yield of the saturated alcohol.¹²¹ The use of cobalt catalyst without diisopropylamine leads to 95% yield of the saturated ester. Replicating the conditions of Jagdale and co-workers with **36** resulted in no sufficient amounts of saturated alcohol **78**, but instead led to the saturated ester **237** (Scheme 34, Scheme 35).

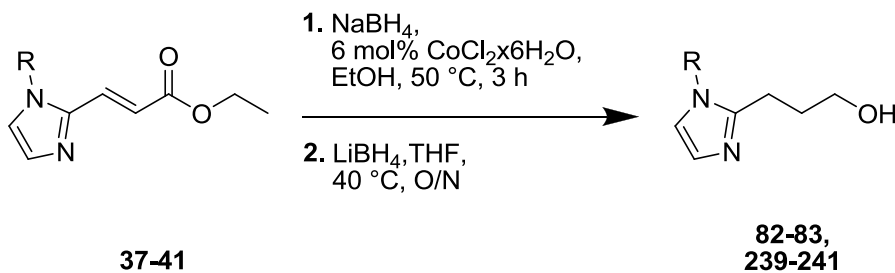


Scheme 34: (a) NaBH₄, CoCl₂ x 6H₂O (10 mol%), diisopropylamine (20 mol%), EtOH, 50 °C, 16 h.



Scheme 35: (a) 3 eq NaBH₄, 3 mol% CoCl₂ x 6H₂O, EtOH, rt, O/N; (b) DIBAL-H, DCM, -78 °C → rt, 2.5 h; (c) i. N³-Bz uracil (**53**), PPh₃, DIAD, THF, rt, O/N, ii. 7 N NH₃/MeOH, rt, 3 h.

Increasing amount of NaBH₄ did little to change the situation. Therefore, no further attempts to optimize the reaction conditions were conducted. Instead, the saturated ester derivative **237** was isolated in 83% yield as test material for further reaction steps. The reduction of the saturated ester **237** was conducted with DIBAL-H (Scheme 35). The product **78** was isolated in 97% yield. Compound **78** was used in a Mitsunobu reaction with N³-benzoyl uracil (**53**). The deprotected compound **238** was obtained as white solid (27% yield) (Scheme 35). Next, a one-pot reaction for the synthesis of the saturated linkers was tested (Scheme 36).



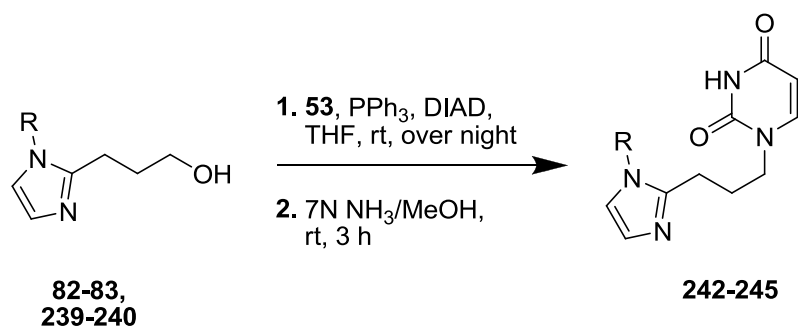
Scheme 36: Double reduction system to afford saturated alcohols.

Table 18: Structures and yields of the saturated alcohols.

Substituent R					
Yield	82 , 54%	83 , 49%	239 , 36%	240 , 50%	241 , n.d

n.d = not determined

The starting materials **37-41** (Table 1, section 4.2) were treated with cobalt(II)chloride hexahydrate and NaBH₄ to reach the saturated ester derivatives and directly converted to the reduced alcohol derivatives using lithium borohydride (LiBH₄). The saturated alcohols **82-83** and **239-240** were obtained in 36-54% yield (over two steps) (Table 18). For compound **241**, no product signal was detected in MS, and therefore no isolation conducted. The yields and overall reaction times were not optimized. Optimization was not done due to time constraints. The intermediates **82-83** and **239-240** were converted to the final compounds using the established Mitsunobu reaction/ 7 N NH₃/MeOH deprotection system. Compounds **242-245** were obtained in 50-62% yield (over two steps) (Table 19, Scheme 37).

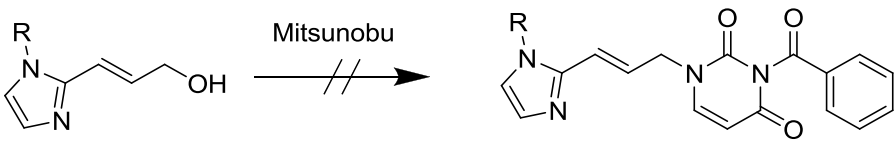
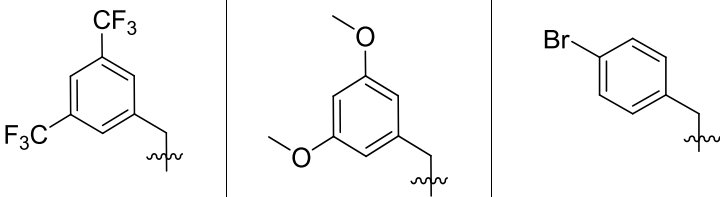
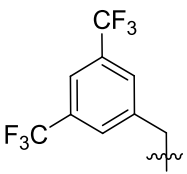
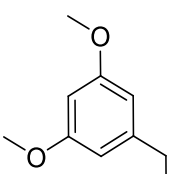
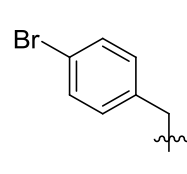
**Scheme 37:** Synthesis of final compounds of type C compounds.**Table 19:** Structures and yields of the type C compounds.

Substituent R				
yield	242 , 55%	243 , 52%	244 , 50%	245 , 62%

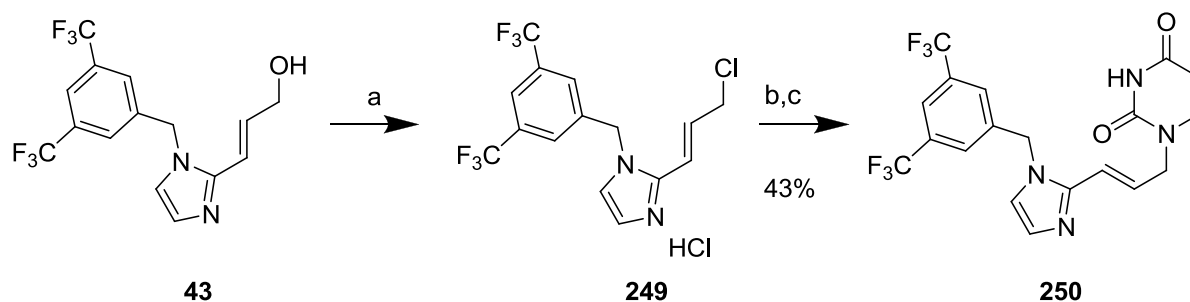
4.7.2 Synthetic approaches for type D compounds

For the synthesis of the unsaturated final compounds (type D) allyl alcohols were reacted under the previously used Mitsunobu conditions (Table 2, Scheme 4, 4.2). Surprisingly, there was very low conversion to the benzoyl protected products **203-205** (Table 20). A repetition to obtain **203** with prolonged reaction time resulted in poor conversion and gave insufficient amounts of product. Therefore, **43** was used to investigate an alternative reaction pathway.

Table 20: Results of the Mitsunobu reaction with allyl alcohols.

	
	
43-45	246-248
substituent R	<div style="display: flex; justify-content: space-around;"> <div style="text-align: center;">  203 </div> <div style="text-align: center;">  204 </div> <div style="text-align: center;">  205 </div> </div>
remarks	<div style="display: flex; justify-content: space-around;"> <div style="text-align: center;">no conversion (TLC)</div> <div style="text-align: center;">no conversion (TLC)</div> <div style="text-align: center;">traces of product (TLC)</div> </div>

Similar to the synthesis of chloromethyl imidazole HCl salts (Scheme 28), the hydroxy group of **43** was converted with thionyl chloride into a chlorine leaving group. The intermediate **206** was converted with N³-benzoyl uracil (**53**) and K₂CO₃ to the benzoyl protected product. (Scheme 38). The crude benzoyl protected product was isolated and deprotected with 7 N NH₃ in methanol. The product **207** was obtained in 43% yield (over two steps). Due to time reasons no further reactions were conducted.



Scheme 38: (a) SOCl₂, CHCl₃, reflux, 3 h; (b) N³-benzoyl uracil (**53**), K₂CO₃, DMF, rt, O/N; (c) 7 N NH₃/ MeOH, rt, 3h.

4.8 Biological activity evaluation of the compounds

4.8.1 SPR screening for compound affinities

The first evaluation for biological activity was executed with surface plasmon resonance (SPR), conducted at NorStrukt/UiT Tromsø by Marcin Pierechod to determine compound-target affinities. The first set of compounds consisted of eight type H and one type C and type E compound. Their obtained K_d values are listed in Table 28 (appendix) and visualized in Figure 31 with the approximate contribution of the compounds and scaffolds. Most type H compounds exhibited limited solubility in DMSO/water, and showed overall similar or weaker target affinities than the type C compound **238**, and the type E compound **210** (Figure 31).

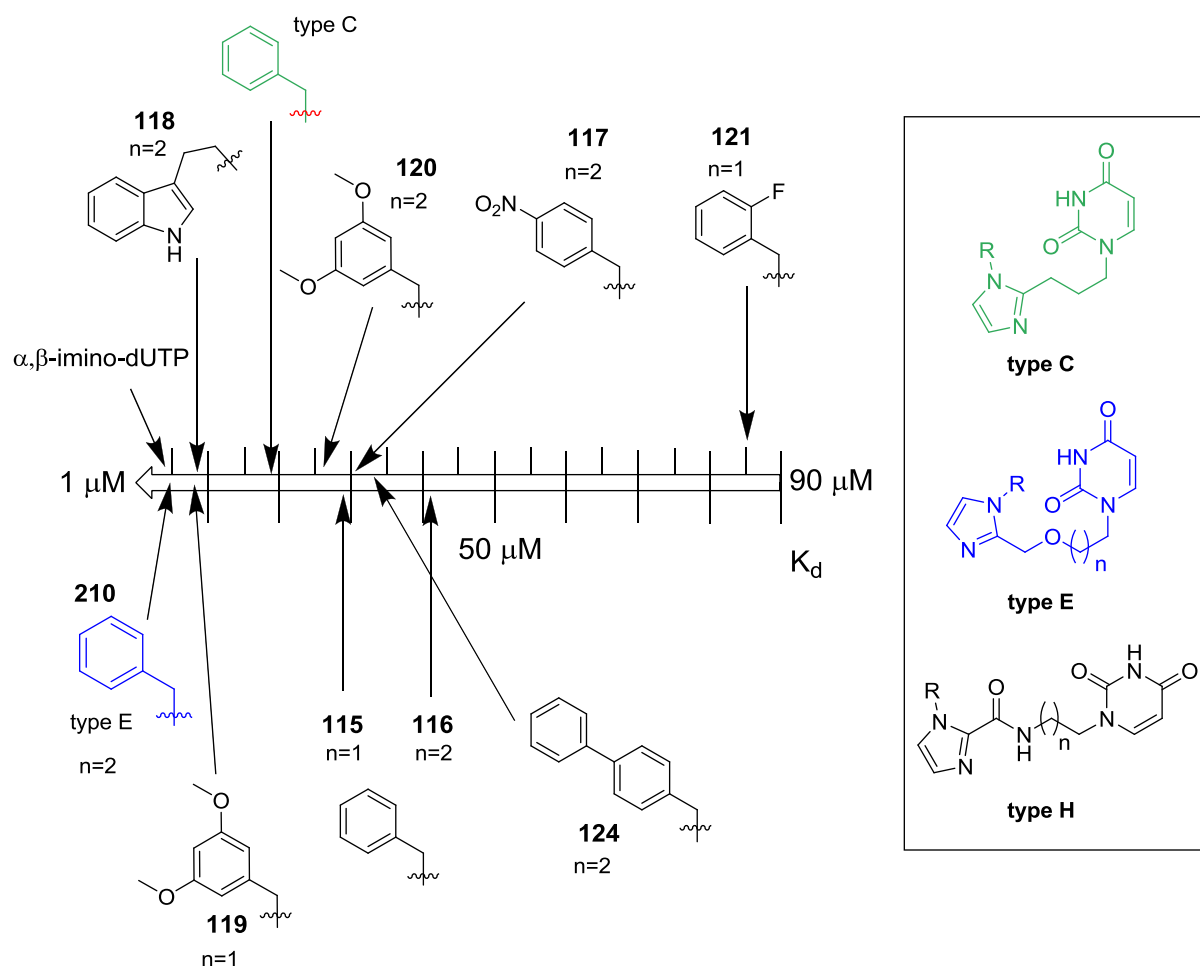


Figure 31: Overview of the approximately compound contribution in the first SPR screening. From all compounds tested compound **210** (scaffold type E) revealed the highest affinity to human dUTPase. K_d values are presented in μM . The linker length (CH_2 groups) of type E and type H compounds is represented with n .

Partially precipitation in the assay medium lowered the overall informative value for the K_d values of type H compounds. Therefore, the synthesis of type H compounds was not continued and compounds with similar or even higher lipophilicity not tested. The type C and type E compounds showed better solubility and, especially in case of **210**, interesting activity in comparison to other compounds. **210** showed also reasonable activity in independently conducted tests with good line fitting for K_d -value analysis (Figure 32). Compound **210**, and even **238** with their benzyl group substitution, exhibited a distinct affinity difference compared to the type H compounds **115** and **116** with benzyl groups. In combination with the better solubility, the type C and type E scaffold were found to be the better scaffolds for further investigations in combination with other substituents.

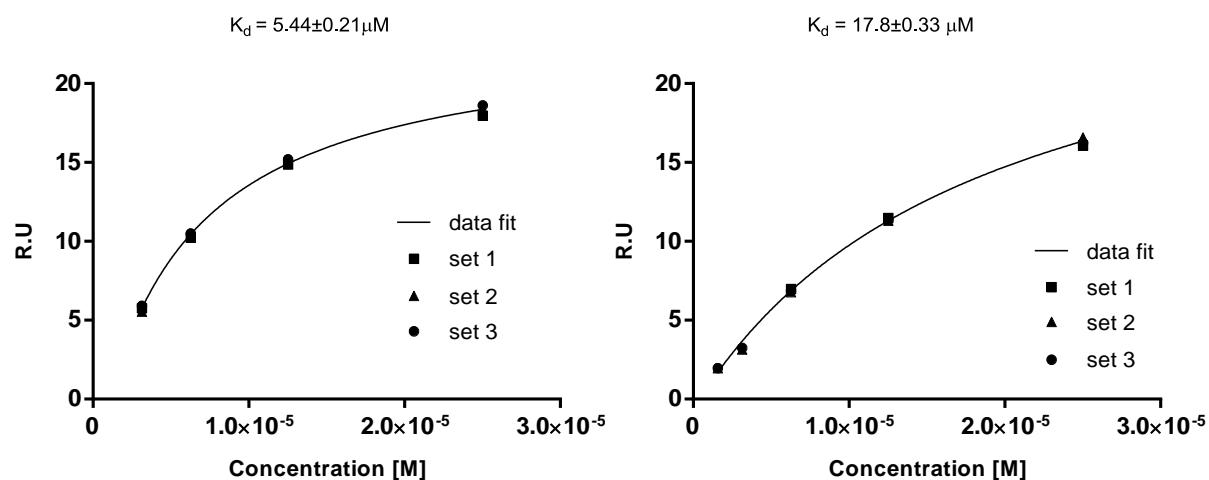


Figure 32: Line fitting curves for the ligands **168** (left) and **198** (right) in SPR experiments with immobilized dUTPase.

A screening with new synthesized type E and C compounds revealed rather low to moderate micromolar bindings of type E and type C compounds (full overview in the appendix Table 28). However, no values could be obtained for several compounds. The affinity of three compounds stood out in the screened library. Compounds **216**, **223** and **225** reached K_d values of 50 nM to 322 nM, but the numbers have very high standard deviation. The value of **216** was repeated twice with approximately 50 nM but it had a standard deviation of 40 nM (Figure 33). Data for the similar compounds **215**, **224** and **226** (different linker lengths) could not be obtained at this time. Time limitations and practical reasons made it necessary to continue with compound synthesis based on these screening results without further proof of activity.

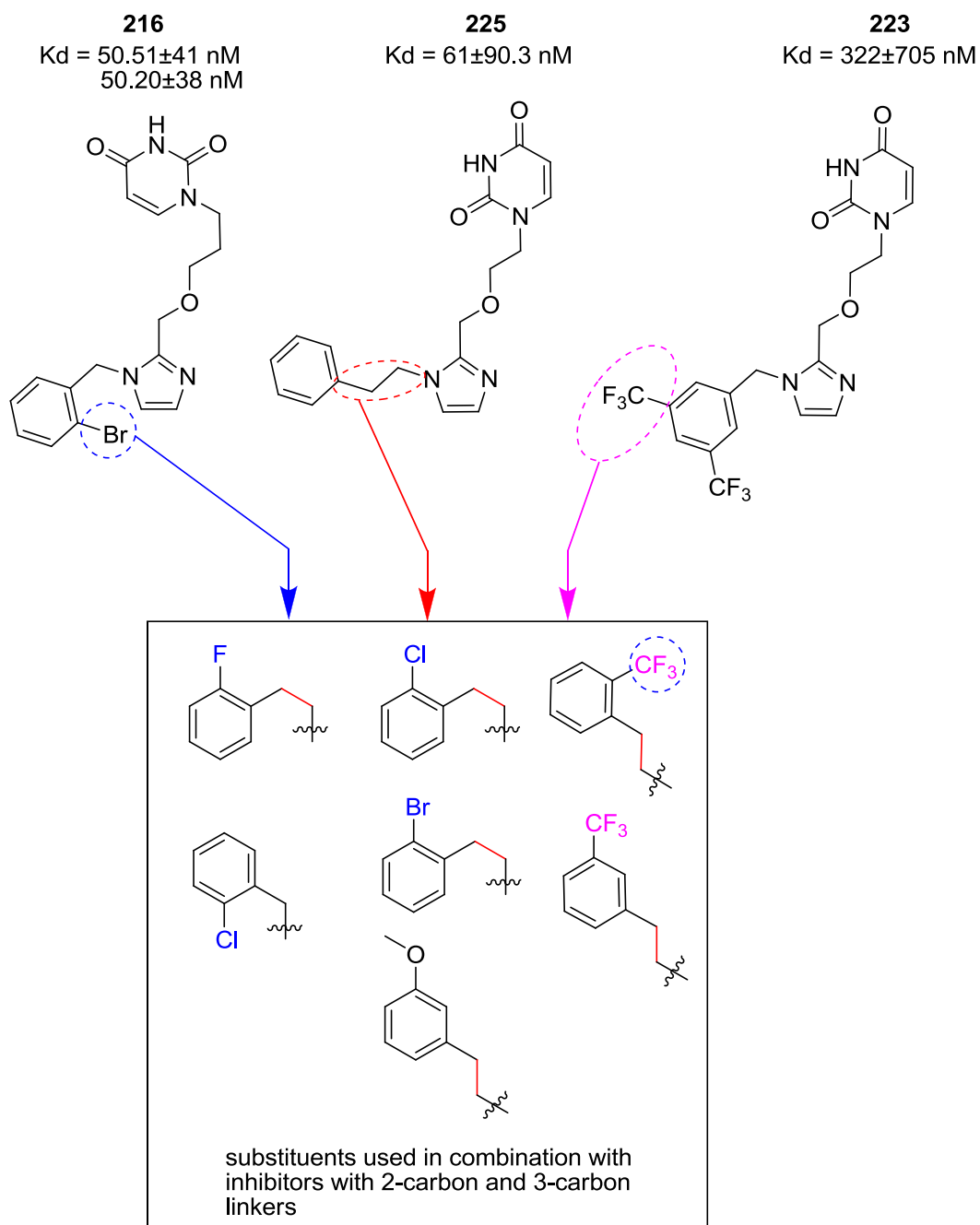


Figure 33: The activities of **216**, **223** and **225** in comparison to other tested type C and E compounds were distinctly higher, but the values had very high standard deviations. Combining these structure elements with new substituents, new compound structures were designed.

The selection of substituents was inspired by the analysis of the structure elements of the compounds **216**, **223** and **225** and is presented in Figure 33.

Of particular interest for the selection of new substituents was:

- Investigation of the role of halogens in the ortho-position of the benzyl group by substitution with chlorine or a CF₃-group (fluorine was previously tested).
- The effect of the extension from a benzyl group to a phenethyl group
- Investigation if halogens in ortho position shows additive effects when combined with phenylethyl groups.
- Determination if compound activity increases when substitution in the meta-position is combined with a phenethyl group.

The new compounds showed no increased compound affinities against human dUTPase, but several compounds with low μM values were found. An overview of the SPR measurements is shown in the appendix (Table 28). Unfortunately, problems with determining K_d -values for different compounds continued leading to bad line fitting curves in for K_d -value determination. Indications pointed to unspecific binding effects, and decreasing protein batch quality as two possible reasons. These problems meant that this screening method had limitations and was not suitable to obtain a full overview of compound activities. It was not possible to conduct further SAR-studies at this time. Later, other test methods (*vide infra*) could not confirm the obtained K_d values for several compounds, including the result of the most promising compounds **216**, **223**, and **225**. This led to the decision to state all obtained SPR K_d -values as questionable.

4.8.2 Pyrophosphate assay as pretest for ITC

A new approach for biological testing was based on the measurement of pyrophosphate (PPi) liberation as result of dUTP cleavage by human dUTPase. The experiments were conducted by Bjarte Aarmo Lund (NorStruct/ UiT Tromsø). The inhibition of the human dUTPase was determined by comparison of pyrophosphate release in presence and absence of the test compound. The pyrophosphate concentration was measured with a fluorescence assay and was conducted as single concentration tests (100 μ M compound concentration) in duplicate. The screening was used as a pretest to set up a compound affinity ranking for subsequent ITC measurements. Human dUTPase was freshly expressed for these experiments, and all relevant compounds from the previous SPR tests and untested compounds were included in the screening. An overview of the obtained inhibition values (in percent) compared to the uninhibited control reaction are shown in the appendix (Table 28).

4.8.3 ITC-measurements

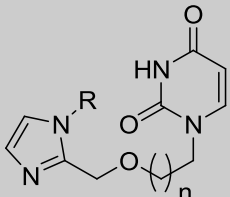
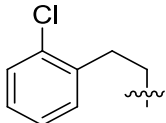
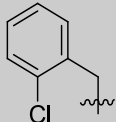
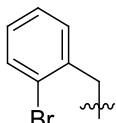
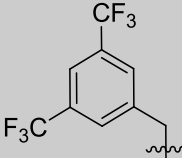
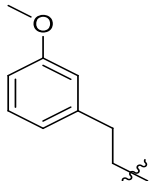
Based on the pyrophosphate pretests, compounds were ranked for more detailed ITC measurements to determine K_d values and thermodynamical insights of the binding events. The ITC measurements were conducted by Bjarte Aarmo Lund and Zuzana Kutová ((NorStruct/ UiT Tromsø). Compound binding energies can give information about the effects responsible for compound-target affinities and help to optimize lead structures for selectivity and affinity.^{122,123} Enthalpic binders rely more on polar interactions like hydrogen bonding, while entropic effects are more correlated to lipophilic interactions and the space filling of protein pockets.

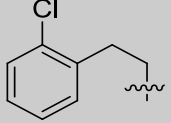
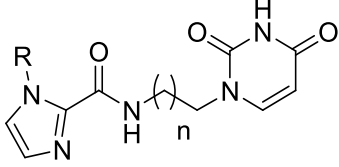
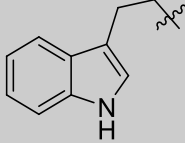
The compounds **216** and **223**, with strong but questionable K_d values, were tested together with compounds identified as even stronger by the pyrophosphate pretests. Unfortunately, the ITC measurements revealed that the pyrophosphate assay is not reliable as a single concentration assay. Stronger binders in the ITC-testing got distinctly weaker values in the pretest and vice versa (for example **220** and **231**). Repeated measurements of the pyrophosphate assay for a few selected compounds underlined this finding. Table 21 shows the ITC results together with the related data of the pyrophosphate assay and the SPR screening. No measured affinities were able to support the findings of the SPR screenings, for example **216** shows $K_d:10.57\pm0.03 \mu$ M vs 50 ± 41 nM.

Of particular interest are the binding energies of the tested compounds. For compound **223** and **216** similar K_d values were measured, but the binding energies differ significantly ($-8.92 \pm 0,01$ kcal/mol to $-14.81 \pm 0,01$ kcal/mol). The same tendency was observed for the compounds with higher and lower K_d values than the one of **223**. The substituent of **223** has the most bulky and lipophilic structure tested with ITC so far. The reference inhibitor α,β -

imino-dUTP (dUpNHpp) (**11**) in comparison was found to be a more enthalpic binder. Due to its conformity to dUTP, **11** is relying on highly specific polar interactions to the dUTPase. The ITC methods produced reproducible data and will be further used for the determination of all compounds, independent of the pyrophosphate screening. However, only seven out of approximately 40 relevant compounds could be tested due to time constraints. More data is necessary to interpret the structure-affinity relationships to get an overview of how to continue, and of how to optimize the compounds.

Table 21: ITC test results of seven compounds. The data is presented together with the corresponding pyrophosphate and SPR data (not confirmed) compound concentration. ITC values were measured in triplicate with exception of **220**, **231** and **232** which were measured in duplicate.

substituent	n	cpd	ITC K_d (μM)	ITC ΔH (kcal/mol)	PPI single concentration assay (100 μM)	SPR data (K_d) (not confirmed)
 type E						
	1	231	8.65±0.03	-15.67±0,01	49%	1.23 μM
	2	220	10.48±0.03	-15.16±0,01	71%	n.d
	2	216	10.57±0.03	-14.81±0,01	52%	50.51±41 nM 50.20±38 nM
	1	223	10,65±0.05	-8.92 ±0,01	58%	322±705 nM
	1	227	12.88±0.04	-16.65±0,01	61%	n.d

	2	232	13.08±0.06	-13.25±0,01	71%	n.d
 <p>type H</p>						
	2	118	18.57±0.06	-16.34±0,01	59%	8.6±0.13 μM
α,β-imino- dUTP	-	11	14.87±0.03	-22.58±0,01	45%	3.05±0.36 μM

n.d = not determined

4.8.4 Cell based assay attempt

The uncertainties with the enzyme based assays led to attempts to conduct cell based assays (conducted by Marte Albrigtsen/Kirsti Helland, Marbio/ UiT Tromsø) before pyrophosphate and ITC screening. The idea was to investigate possible synergistic effects of a fluoropyrimidine TS-inhibitor with the dUTPase compounds on cell viability of cancer cell lines. α,β -imino-dUTP (**11**) was used as control compound. HT-29 (colorectal adenocarcinoma) and MCF-7 (human breast adenocarcinoma) cancer cell lines were used for these experiments.^{124,125} Both cell lines are described in literature with respect to the influence of dUTPase expression for TS-inhibitor resistances.

The experiments were segmented into three parts to measure synergistic effect in cancer cells similar described in literature:⁵⁹

1. Determination of effects on cell viability of a TS-inhibitor alone (fixed concentration) against the cancer cell lines. The concentration was to be adjusted to get approximately 75-85 % cell survival.
2. Determination of the cell viability of the tested dUTPase compounds against the cell cancer lines.
3. Determination of cell viability of dUTPase compounds (changing concentrations) with the TS-inhibitor (fixed concentration).

The fixed TS-inhibitor concentration was adjusted to a concentration such that approximately 75-85% cancer cells were unaffected and survived. This allows for the observation of the remaining vital cells for assay evaluation in the case of strong synergistic effects with dUTPase compounds. Strong synergistic effects are known for TAS-114 in combination with the TS-inhibitor FdUrd (10 μ M) in different cell lines such as HeLa cells (increase of cytotoxicity by a factor of 339) and HT-29 cells (factor of 30.1).⁶⁷ FdUrd (5-fluoro-2'-deoxyuridine) was also used to test some of the synthesized compounds. The concentration to reach approximately 75-85% cell survival was determined as 10 nM for HT-29 and 500 nM for MCF-7 (Table 22 example for HT-29). The reference compound α,β -imino-dUTP (**11**) and a selection of synthesized dUTPase compounds were measured together with FdUrd at different concentrations (Table 22, extraction of the overview table Table 33 in the appendix) in a range of 20 μ M to 100 nM. The compounds showed no effects on cell viability at 10 μ M (Table 32 and Table 34 in the appendix).

Table 22: Effects on cell viability of 10 nM FdUrd on HT29 cells and effects of FdUrd (10 nM) with dUTPase compounds (extraction of the overview Table 33 in the appendix).

compound	assay name	survival (in %)	concentration	unit
10 nM FdUrd influence on HT-29 cells				
FdUrd	HT29_MTT	81.5 ± 1.05	10	nM
10 nM FdUrd in combination with different concentrations of dUTPase compounds				
α,β-imino-dUTP (11)	HT29_MTT	90	20	μM
α,β-imino-dUTP (11)	HT29_MTT	83	2.5	μM
α,β-imino-dUTP (11)	HT29_MTT	83	100	nM
231	HT29_MTT	87	20	μM
231	HT29_MTT	80	2.5	μM
231	HT29_MTT	80	100	nM
118	HT29_MTT	87	20	μM
118	HT29_MTT	82	2.5	μM
118	HT29_MTT	80	100	nM

Unfortunately, no concentration dependency on cell viability could be observed for all tested compounds in both cell lines compared to the effect of FdUrd alone (Table 22, Table 31 and Table 33 in appendix). The lack of effect for the known dUTPase compound **11** led to a questioning of the right experiment settings to achieve valid results.

It is possible that the compounds are not active enough, or their cell uptake or stability are too low under the tested conditions. **11** is highly polar due to the phosphate groups. This likely reduces the cell permeability, making this compound the wrong choice as a reference compound and is consistent with the finding described in section 2.6.1. It cannot be ruled out that the high polarity is also responsible for the negative results of the tested compounds. More tests are necessary to find the cause of the missing activity in the assays. Prodrug structures could be an option for compounds with established activity to adjust cell permeability in the future.

5. Project 1: Conclusion

In total, 48 compounds, of four different types, and approximately 130 other derivatives were synthesized for this project. The synthesis of the originally planned compound type A could not be finished in time. Several attempts for the N,O-acetal formation and cleavage of the protecting groups failed but led to interesting intermediates such as the N¹-chloromethyl uracil derivatives **52**, **57** and **70**. However, the possibility to form N,O-acetals with N¹-chloromethyl uracils could be verified. It requires optimization and the search for better protecting group or deprotection conditions. The bottle neck for the systematic synthesis and optimization was the lack of biological activity data to conduct better SAR-based approaches. The synthesis based on SPR data led to a very narrow and probably erroneous substituent and linker selection to combine the best properties of previously tested compounds. ITC measurements displayed the most reproducible results and gave further insights into the thermodynamic properties of seven compounds. The ITC determinations revealed better K_d values of six compounds in comparison to the reference compound α,β -imino-dUTP (**11**). The goal to obtain sub-micromolar compounds was not possible to fulfill. So far, none of the compounds showed activity in cell assays including the reference compound α,β -imino-dUTP (**11**). Therefore, it is required that the cell assay conditions must be optimized or that all compounds, including the reference compound, were not able to penetrate the cell membrane. Overall, further project activities are dependent on more ITC-measurements.

6. Project 1: Future perspectives

6.1 Options for scaffold optimization

The compound synthesis, and especially the testing for biological activity, were more challenging than anticipated at the beginning of the project. Therefore, and based on interim test results, the compound scaffolds were only substituted with commercially available benzyl bromides, phenylethyl bromides, and other related alkyl bromides. That should avoid further undirected synthesis steps as long as no comprehensive compound activity overview existed. Although not complete, the current test results indicate a limited prospect for sub-micromolar K_d values with the remaining untested compounds. Further optimisations are needed in order to obtain better compounds. Possible suggestions for improvement can be found in the analysis of Taiho Pharmaceuticals inhibitors in section 2.6.4-4.1. Significantly higher inhibitor affinities were obtained through the introduction of chirality or/and further substitution of the aromatic moieties with additional lipophilic residues like cycloalkanes.^{59,69} While the introduction of chirality can result in a more complex precursor synthesis, modifications of the aromatic moieties are theoretically possible with existing intermediates. Several final compounds and intermediates exhibit a halogen substitution pattern, and are possible to use for modification by palladium cross coupling reactions. The Suzuki coupling in particular, using aryl halides and boronic acid derivatives, opens up the possibility for late stage diversification of intermediates or even final compounds. As a result, known synthetic routes can be further, and more diversely, used for a structurally diverse compound library.¹²⁶

The introduction of cycloalkanes or aromatic moieties at the stage of the hydroxyl group containing intermediates can lead to modified building blocks, that can be used for different linkages with uracil (N,O-acetal, plain carbon linker). Additionally, established methods like the Mitsunobu reaction can be further exploited for the synthesis of the final compounds. (Figure 34 A). Substitution at the level of the final compound requires less intermediates to obtain different final compounds and is normally preferred. In this case, the synthesis at the stage of final compounds (protected/unprotected) could cause purification problems due to the questionable stability of the benzoyl-protecting group under Suzuki conditions or the high polarity of the unprotected compounds (Figure 34, B). The separation possibilities using normal phase chromatography is already limited. Reverse phase chromatography could be an option to overcome this hurdle.

For the synthesis of eligible intermediates, containing the combination of a free hydroxy group, an imidazole and benzyl ring no literature procedure could be found. However, synthetic approaches can be based on procedures for example for reactions of brominated benzyl alcohols or bromobenzyl imidazoles with cycloalkane- or aromatic boronic acids.¹²⁷⁻¹²⁹

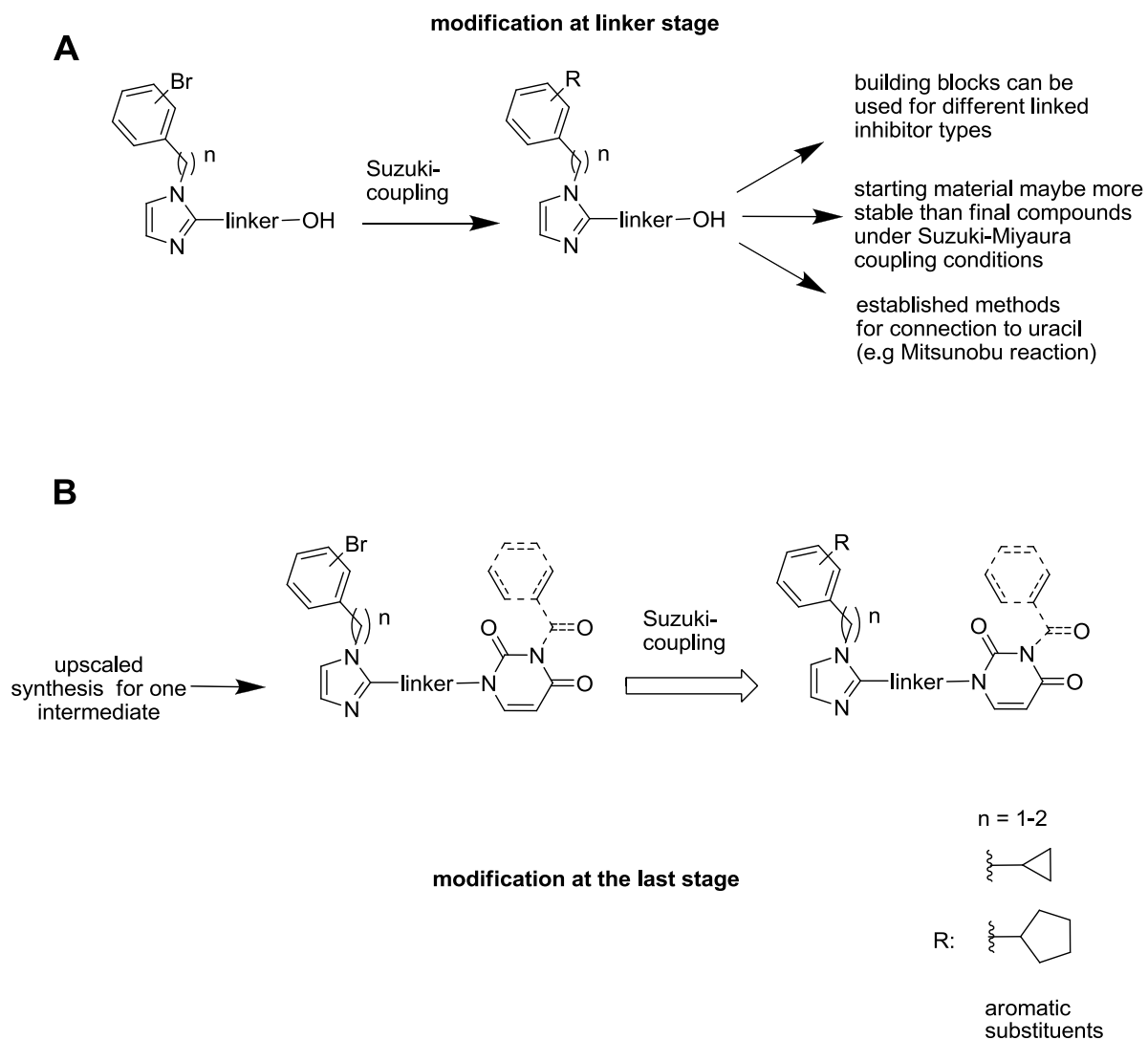


Figure 34: The Suzuki-Miyaura coupling reaction might allow for modification of the compounds to reach better affinities to human dUTPase. Introduction of e.g cycloalkanes at the aromatic moiety is possible at different stages in the synthesis process. A: The Suzuki-Miyaura coupling at the linker intermediate stage allow the use of the modified building blocks for different connections with uracil (e.g. N,O-acetal, plain hydrocarbon linkage). B: The Suzuki coupling as final stage modification (unprotected/N³-Bz protected) in the synthetic route allows for the use of fewer intermediates to produce different final compounds.

6.2 Screening for carbonyloxymethyl-groups as protecting groups and prodrugs

The synthesis of N,O-acetal containing compounds caused problems due to the lack of suitable protecting groups for the N³-position of uracil. While some protecting groups were too unstable in strongly basic media other protecting groups were too stable in the following cleavage processes. Carbonyloxymethyl-derivatives showed a promising potential for controllable stability. Unfortunately, the stability of the carbonyloxymethyl group **68** (section 4.3.4) was too high in the final deprotection. A systematic search for alternative carbonyloxymethyl protecting groups or improved deprotecting conditions is therefore of interest. Promising carbonyloxymethyl protecting groups can also be tested as prodrug groups to increase the cell's drug uptake of different compound types.

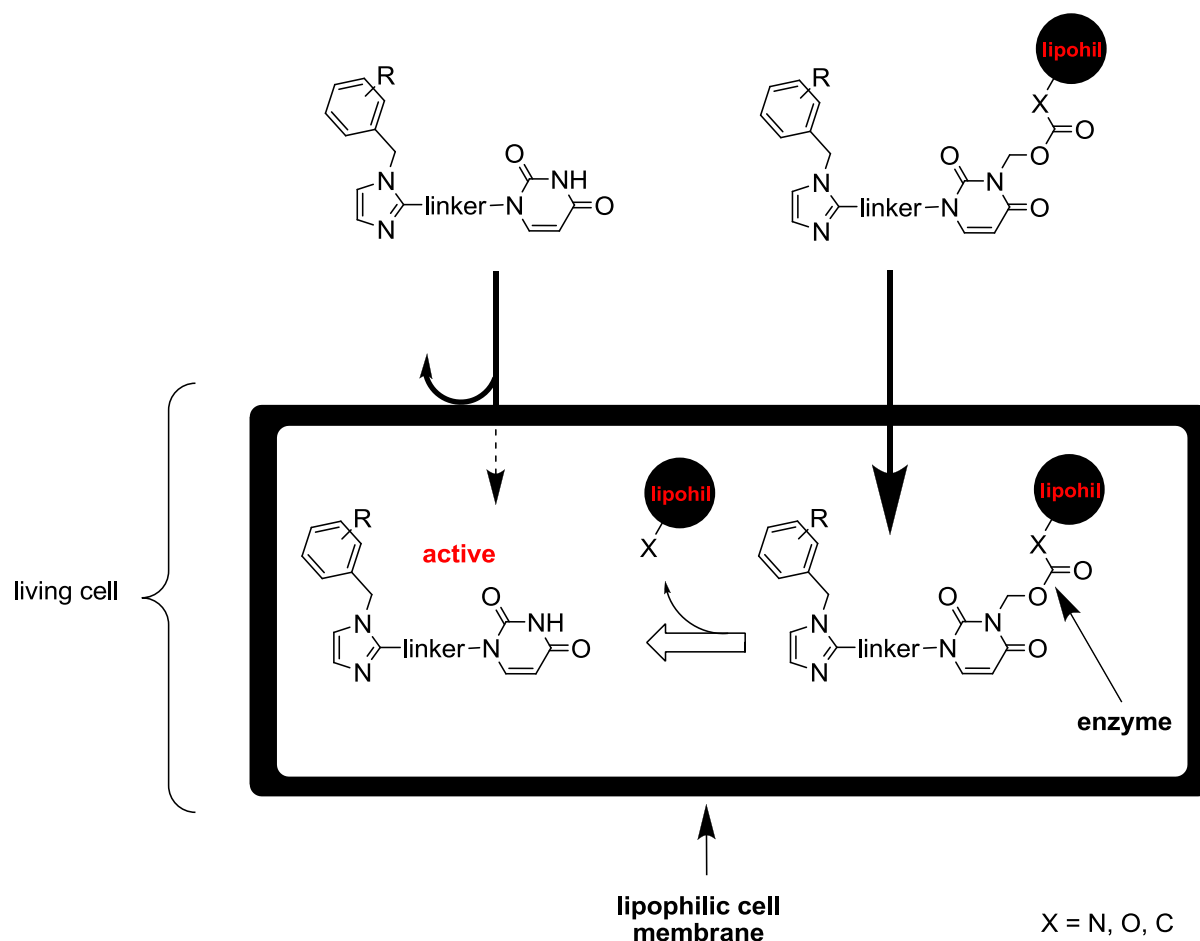
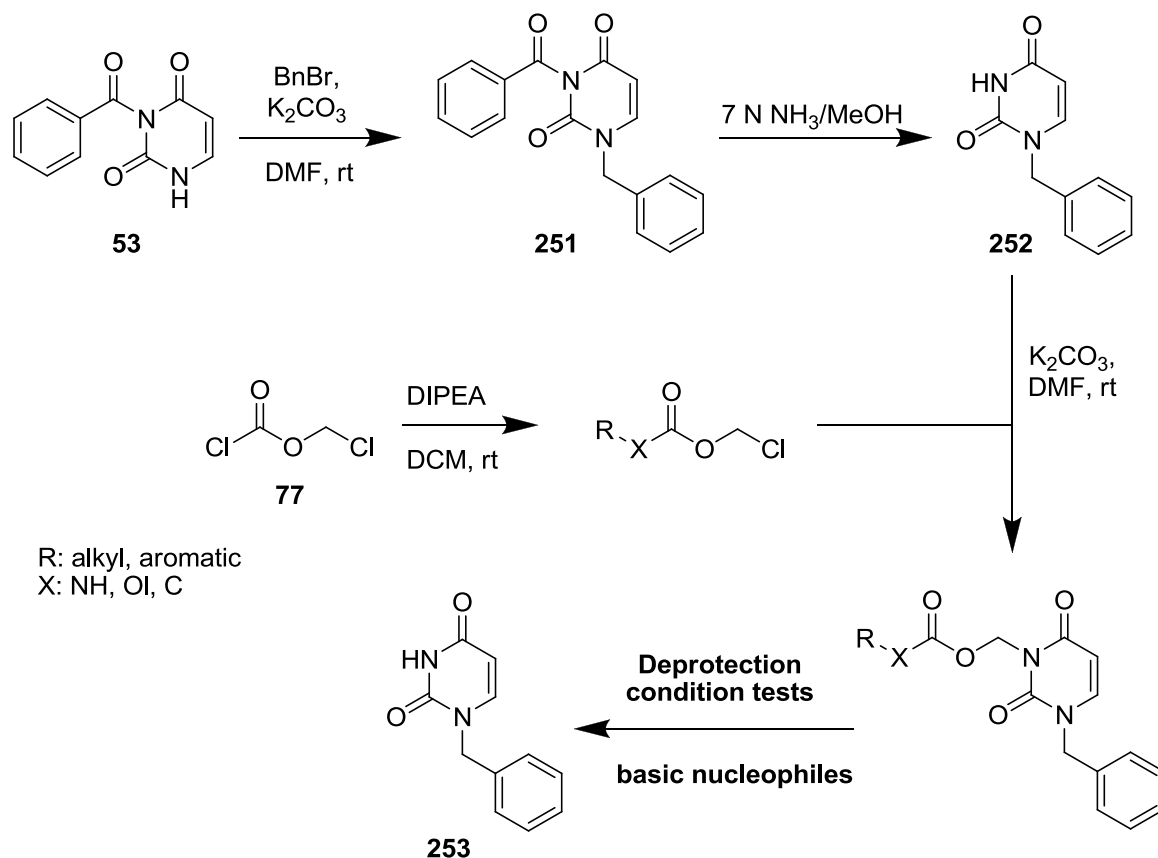


Figure 35: Carbonyloxymethyl-protecting groups for N,O-acetal formation reactions can also be of interest as prodrugs. Compounds with exhibited activity in cell assays can be compared with their unprotected precursors to evaluate increased compound cell uptake.

Many successful attempts to adjust lipophilicity and related cell permeability are described in the literature (see also section 4.3.4).^{102,103,105} The deprotection is mainly dependent on the cleavage by the cell's internal carboxylesterases (Figure 35).¹³⁰ Screening of protecting groups for the synthesis of different protected uracil derivatives is necessary (Scheme 39). The focus on protecting group stability enable the use of any stable N¹-substituted uracil derivative as testing platform.



Scheme 39: Compound **252** could work as testing platform to find carbonyloxymethyl protecting groups suitable for N,O-acetal synthesis or for prodrug structures in different compound scaffolds.

Compound **252** could be a good testing platform because it can be synthesized from existing starting materials. The benzylation at the N¹- position of uracil should increase the lipophilicity of the uracil derivatives for better reaction control by TLC and exclude side reaction at the N¹-position (Scheme 39). **252** could be synthesized from N³-benzoyl uracil (**53**) by benzylation to yield **251** following deprotection with ammonia in methanol. The carbonyloxymethyl protecting groups could be synthesized from chloromethyl chloroformate (**77**) with different amine and alcohols, and further reacted with **252** (Scheme 39).

The intermediates could be screened for stability against alkoxides, hydroxides, amines and other nucleophiles. Good candidates should withstand nucleophilic alkoxides for at least

12-18 h when used in a 1:1 ratio (ratio: imidazole building block alkoxide to protecting group in N,O-acetal formations). This should simulate the conditions as in a N,O-acetal synthesis. On the other side, the protecting group must be cleavable to **253** when the nucleophile is used in strong excess, or in combination with increased temperature (Scheme 39). However, further synthesis attempts are dependent on new ITC-results.

Project 2

**Synthesis of dasatinib analogs enabled to form
covalent connections with tyrosine kinases**

7. Project 2: Introduction

7.1 Protein kinases as “on-off switches” in cell processes

The regulation of protein activity, signal transduction, and gene transcription plays a crucial role in balanced cell proliferation and apoptosis processes. Many of these operations are controlled by protein kinases.¹³¹⁻¹³³ Imbalances of these processes, due to regulation failures, can lead to cancer development. Protein kinases transfer phosphate groups from ATP to hydroxy groups in proteins. Temporary conformational modifications can lead to activity changes or initialize further signal transduction cascades.¹³⁴ Therefore, the reversible addition of phosphate groups can be considered as one of the most important post-translational modifications of proteins.^{132,134} Protein phosphatases counteract these modifications by hydrolysis of the attached phosphates and recover the basal activity.¹³⁴ The combination of both processes acts as an “on-off switch” for cell signaling (Figure 36) and is a central element of regulation.¹³⁴

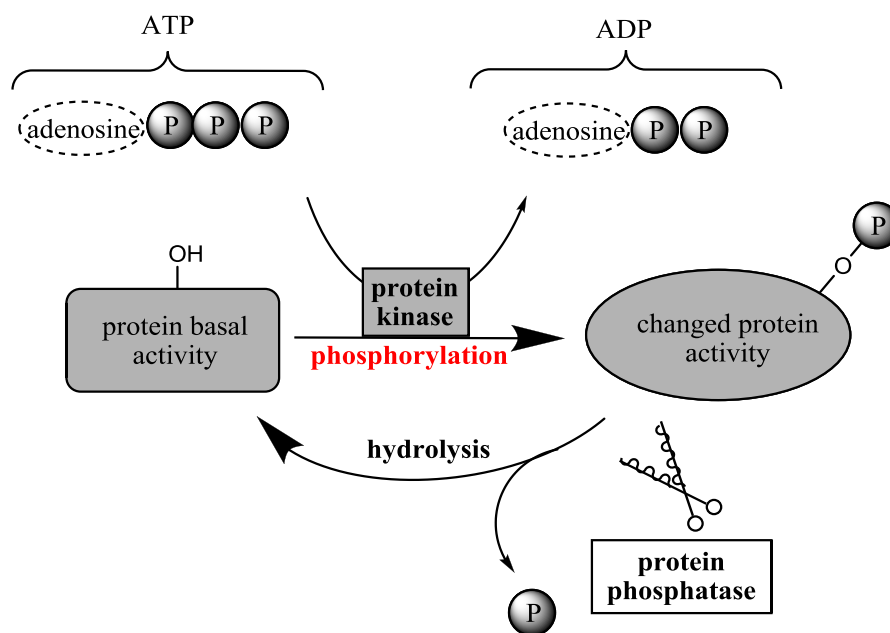


Figure 36: Protein kinases transfer phosphate groups from ATP to a functional group of a substrate protein or to themselves (autophosphorylation). Thereby they change the activity of the acceptor protein. To obtain a tightly controlled system, protein phosphatases hydrolyse the phosphorylated residues and recover the basal activity of the substrate. The figure is based on a literature graphics.¹³⁵

More than 500 human protein kinases are currently known.^{134,136} Many kinases are grouped into serine/threonine and tyrosine kinases, depending on which type of amino acid side chain becomes phosphorylated.¹³⁷ Furthermore, kinases can be classified as non-receptor kinases or receptor kinases. Receptor kinases have an extracellular receptor and an intracellular catalytic site connected by a transmembrane domain.^{138,139} They transduce extracellular signals, from

growth factors for example, into intracellular signal cascades.¹³⁸ Non-receptor kinases lack an extracellular receptor domain and are positioned in the cytoplasm. However, non-receptor kinases can interact with other proteins, lipids and DNA by specialised protein domains and relay downstream extracellular and intracellular cell signals by phosphorylation.¹³³ Both subclasses are present in tyrosine kinases (TK). They conduct a broad range of processes like cell growth, cell differentiation, apoptosis and immune system control among others.¹³³ Out of 90 tyrosine kinases, 58 are receptor tyrosine kinases (RTK) and 32 are non-receptor tyrosine kinases (NRTK).^{133,140}

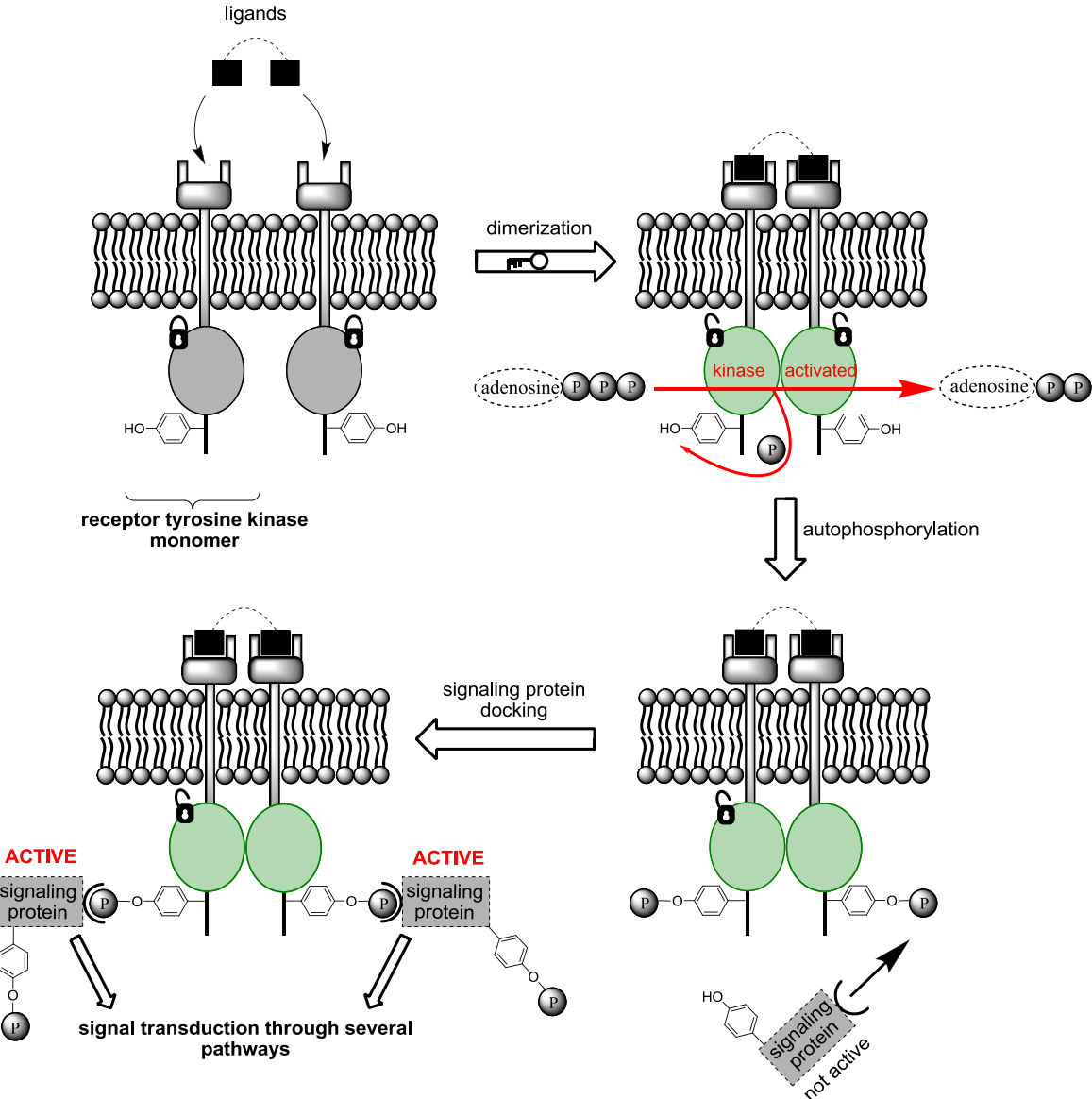


Figure 37: Simplified scheme of receptor tyrosine kinases with focus on the tyrosine receptor domain. Ligand binding leads to a dimerization of to RTK monomers. This process unlocks the autoinhibition of the kinase domains and results in phosphorylation of the tyrosine residues of the dimer. This activated RTK can bind inactivated signaling proteins and phosphorylate their tyrosine residues. The activated signaling proteins conduct further signal transduction. Figure based on literature graphics.^{138,141,142}

Most RTKs share similar structural elements, and have a similar method of activation and signal transduction.¹³⁸ RTKs are autoinhibited monomers, activated by ligand binding at the extracellular receptor domains. (Figure 37). Two monomers dimerize and unlock the autoinhibition by conformational changes leading to autophosphorylation of the RTK tyrosine residues. Inactivated signaling proteins can bind to these modified tyrosines and become activated by phosphorylation. The modified proteins can induce further signal transduction via different pathways.¹³⁸

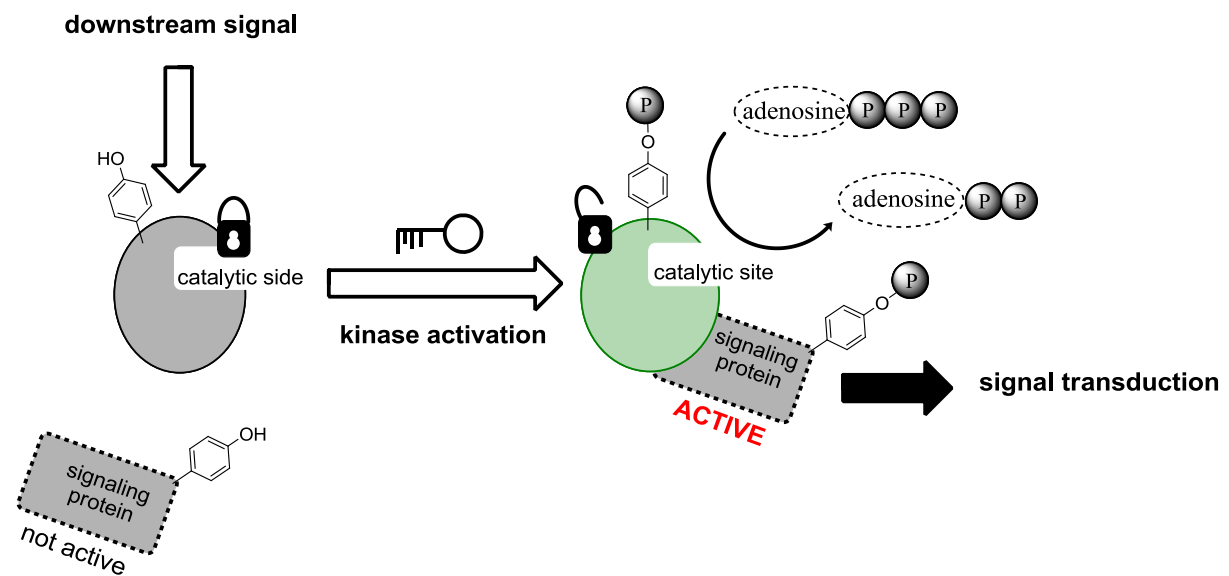


Figure 38: Simplified scheme of a non-receptor tyrosine kinase. NRTKs differ more in their domains and activation processes. Some kinase families undergo complex structural rearrangement for their activation. Incoming signals lead to unlocking of the autoinhibition and to autophosphorylation of the kinase. Signaling proteins can bind at different protein-protein interaction points like phosphorylated tyrosines at the kinase and be activated by phosphorylation. The activated signaling proteins can fulfill further signal transduction. Figure based on literature graphics.¹⁴³

Non-receptor tyrosine kinases (NRTK) display more structural variability in their protein domains than RTKs, and are categorized according to sequence similarity.¹³³ Many NRTKs are bound to membranes or are closely located to the nucleus where they work as signal relays. NRTK activations are more complex and vary between the kinases. Kinase activation is normally initialized by ligand binding at domains e.g. for protein-protein interactions (Figure 38).¹³³ Conformational changes unlock the autoinhibition and lead to kinase domain activation by autophosphorylation.^{144,145} Bound signaling proteins become phosphorylated and initiate further signal transduction (Figure 38).¹⁴⁴

7.2 Malfunction of tyrosine kinases

Disturbance in the vital role of TKs in cell growth and apoptosis processes results in dire consequences when their ability to perform is disturbed. The malfunction of tyrosine kinases can disable regulation mechanisms, leading to uncontrolled signal transduction and potential cancer development. These processes are a result of modified kinases with ligand independent activation, stronger kinases, or increased expression of the kinases.^{138,146} Trigger for changes are mutations or epigenetic modifications transforming proto-oncogenes to oncogenes.

The protein BCR-ABL is an important example of a malfunctioning kinase, and is related to chronic myelogenous leukemia (CML).¹⁴⁷ BCR-ABL is a fusion protein expressed from the BCR-ABL gene - a hybridization product resulting from a chromosome translocation.¹⁴⁷ The Abelson Kinase (ABL) is usually an autoinhibited non-receptor tyrosine kinase with the ability to travel between the cell nucleus and cytoplasm, transducing growth factor signals.^{144,147,148} The Breakpoint Cluster Region protein (BCR) is usually a signaling protein.¹⁴⁷ It has many structure elements to interact with other molecules/proteins.¹⁴⁷ In BCR-ABL, the BCR protein structure permanently interrupts the autoinhibition of the ABL kinase domain leading to constantly kinase activity and autophosphorylation.¹⁴⁸ Numerous protein-protein interactions possibilities and phosphorylated tyrosines of BCR-ABL enable more contact with signaling proteins and their activation.¹⁴⁸ The consequence is a stronger downstream signal transduction of growth factor signals (Figure 39).¹⁴⁹

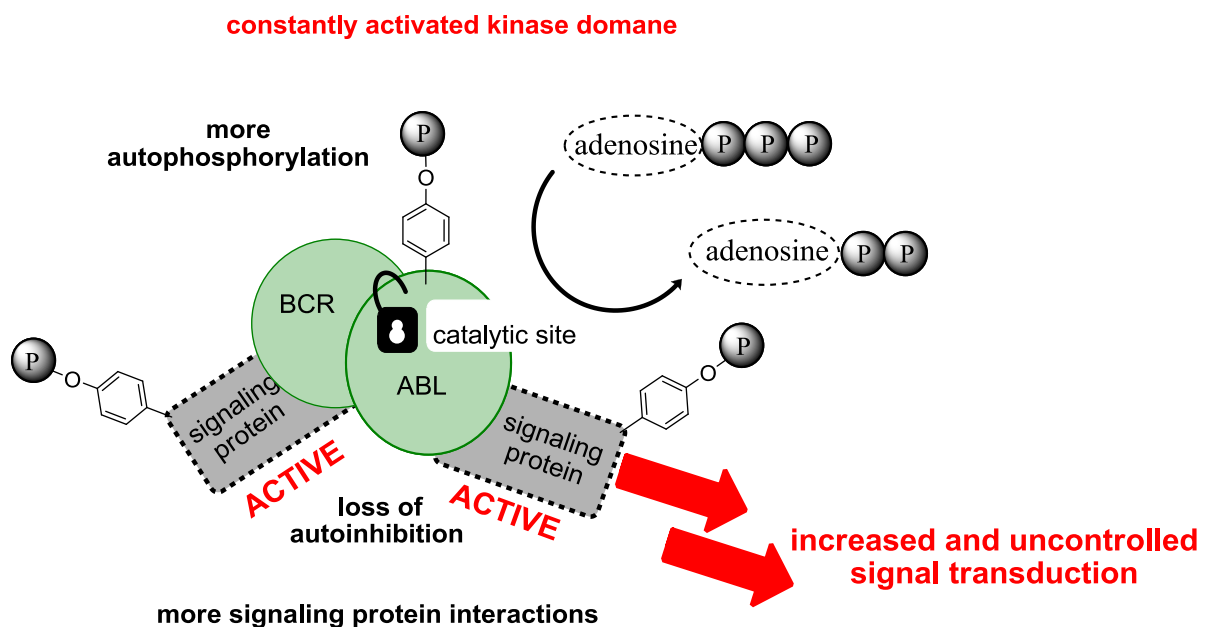


Figure 39: Simplified scheme of the malfunction of the tyrosine kinase BCR-ABL. BCR-ABL is a fusion protein. ABL is normally an autoinhibited kinase. The BCR protein part of the fusion protein interrupts permanently the autoinhibition and stimulate stronger autophosphorylation. The result is more signaling protein activation and more signal transduction. The figure is based on a literature graphic.¹⁴³

7.3 Tyrosine kinase inhibitors (TKIs) and resistance

Tyrosine kinase inhibitors (TKI) can limit the consequences of BCR-ABL and other malfunctioning tyrosine kinases. TKIs downregulate kinase activity and rebalance signal transduction of subordinated cell proliferation and apoptosis processes.^{143,150} Imatinib (**254**) was the first FDA approved TKI that targeted BCR-ABL, and is the first line drug for CML treatment (Figure 40).^{151,152} The use of imatinib (**254**) improved the life quality and life expectation of CML patients significantly.^{153,154}

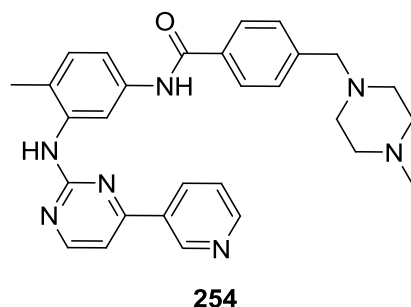


Figure 40: TKI inhibitor imatinib.

After the approval of imatinib (**254**) in 2001, more TKIs have entered the market. Currently, the FDA has approved more than 35 TKIs against a broad range of cancer types.¹⁵² Many of these compounds are multi-target kinase inhibitors targeting several kinases with different affinity. But the amount of therapeutic relevant targeted kinase is low in comparison to the total amount of existing tyrosine kinases.¹⁵² Many of the approved inhibitors focus on the Epidermal Growth Factor Receptor (EGFR), Vascular Endothelial Growth Factor Receptor (VEGFR) and BCR-ABL.¹⁵²

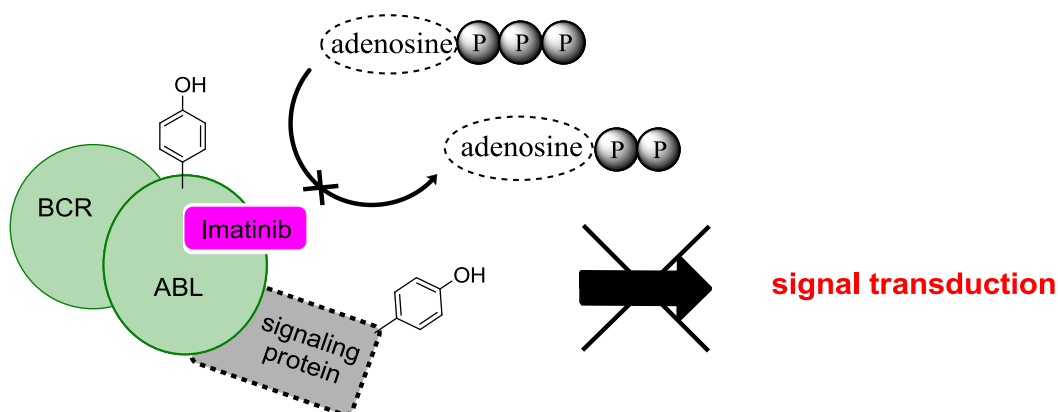


Figure 41: The fusions protein BCR-ABL is inhibited by TKIs like imatinib (**254**). Binding in the catalytic site of the tyrosine kinase disturbs the binding of ATP for the phosphorylation of the substrate protein. The figure is based on a literature graphic.¹⁴³

The majority of TKIs, like imatinib (**254**), competitively inhibit the ATP binding site of kinases and interrupt the phosphorylation of signaling proteins (Figure 41).¹³⁴ The ATP binding site of most protein kinases have similar structural features to conduct the catalytic process.¹³⁴ This situation is a challenge for the development of TKIs: Affinity and selectivity for specific tyrosine kinases, while normal functioning kinases remain undisrupted is difficult to achieve. A closer look at the ATP binding site shows structural elements essential for the binding of ATP, but also possibilities for inhibitor targeting (Figure 42). For the transfer of phosphate groups to the substrate protein, ATP has to bind in a favorable position. Therefore, the ribose and the triphosphate group of ATP is placed in a ribose and phosphate binding pocket. The triphosphate is further stabilized by essential magnesium ions. The purine base, adenine, of ATP interacts via hydrogen bonding with amino acids in the hinge region - the recognition motif for adenine.^{134,155}

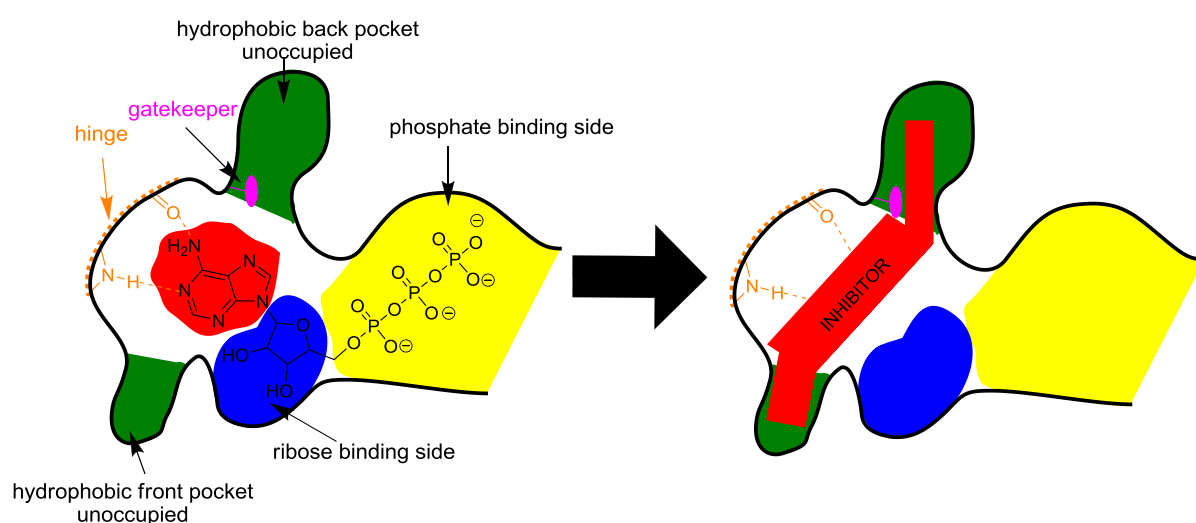


Figure 42: Simplified scheme of the ATP-binding site in kinases. The triphosphate group and the ribose are fixed in pockets. The adenosine is recognized by the hinge region via hydrogen bonding. Inhibitors are normally binding to the hinge-region. Around the active site, inhibitors can address e.g. two unoccupied hydrophobic pockets to form further interactions. A gatekeeper residue, which is a challenge in drug development, limits the entrance to the back pocket. The figure design based on literature graphics .^{134,156,157}

To compete with the high amount of ATP molecules and to get selective inhibition, inhibitors require stronger interactions with the active site than ATP does.¹⁵⁸ Besides the ATP binding site, two unoccupied hydrophobic pockets are also present. These pockets vary between kinases and are not required for ATP interactions; they are open space for more specific interactions.¹³⁴ The access to the back pocket is limited by the steric hindrance from a “gatekeeper” - an amino acid side chain pointing into the opening of the pocket.¹³⁴ TKIs interact mainly with the hinge region and address among others these unoccupied side pockets.¹⁵⁹ The affinity and selectivity of inhibitors is further influenced by the conformation of the kinase. A so-called “DFG-motif” is involved in the catalytic process and stabilizes the essential magnesium ions in the catalytic process.^{134,159} When ATP is present, the DFG-motif

interacts with the magnesium ions and is in close proximity to the triphosphate chain of ATP (active form of the kinase, DFG-in). In the inactive form of the kinase, the DFG-motif turns out from its position (DFG-out) and disrupts the coordination of the magnesium ions.¹³⁴ These conformational changes affect the electronic and steric parameters around the active site and result in different binding environments for inhibitors between active and inactive kinase.¹⁵⁹ The structural homology of kinases is higher in their active conformation; therefore, inhibitor selectivity increases if the inactive form is targeted and stabilized.¹³⁴

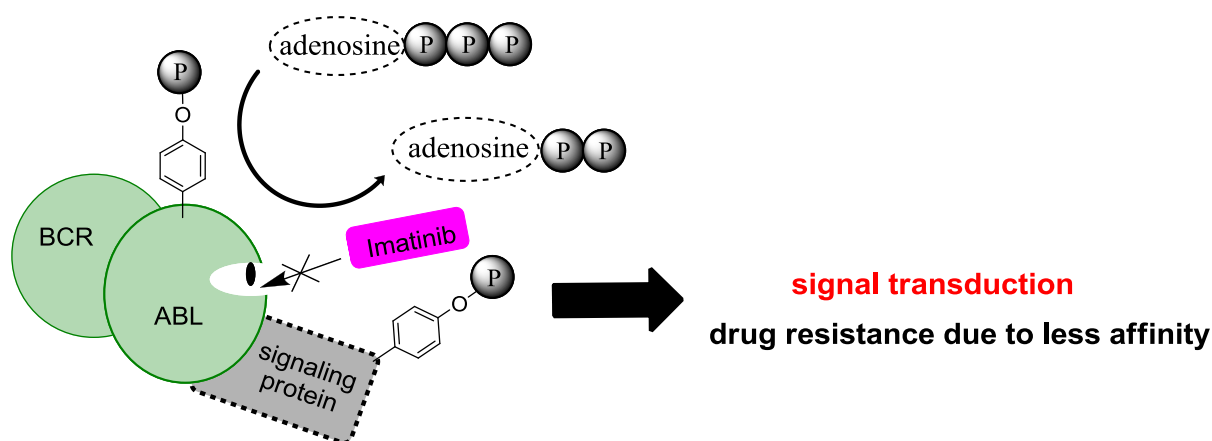
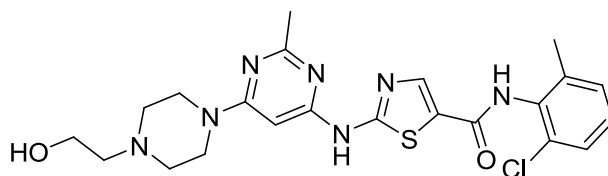


Figure 43: Mutations can lead to changes in the ATP binding pocket (e.g increased steric hinderance or loss of main interaction like H-bonding) preventing the binding of imatinib or other TKI inhibitors in the ATP binding site leading to drug resistance. The figure is based on a literature graphic.¹⁴³

TKIs have often to fight with upcoming resistance in therapy resulting in loss of effectivity. This is one of the reason for the development of many different TKIs against a small amount of kinase targets like EGFR and BCR-ABL.^{160,161} In the case of BCR-ABL and imatinib (254), numerous mutations are known that influence imatinib's (254) inhibitory abilities. The exchange of amino acids can interrupt essential H-bonding interaction with imatinib or lead to steric hinderance lowering imatinib's affinity and decreased drug response in therapy (Figure 41).^{162,163}



255

Figure 44: TKI inhibitor dasatinib.

The second generation BCR-ABL inhibitor dasatinib (**255**) was the answer to overcome most resistance problems in order to continue the anticancer therapy in case of imatinib resistances (Figure 44).¹⁶⁴ Dasatinib (**255**) is a multitarget kinase inhibitor with high affinity against BCR-ABL and other kinases such as c-KIT, BTK, as well as Src-kinase members.¹⁶⁵ It binds in the active kinase conformation of BCR-ABL, and is approximately 325 fold stronger.¹⁶⁶ Additionally, dasatinib exhibits a higher interaction flexibility to the active site of BCR-ABL than Imatinib (**254**), making it less sensitive towards imatinib specific mutations.¹⁶⁴ The development of different inhibitor generations is also observed for EGFR. A gatekeeper mutation from threonine (T) to methionine (M) (T970M-mutation) leads to 1000 fold loss of affinity towards noncovalent TKIs, leading to the development of covalent binding inhibitor generations.¹⁶⁰

7.4 Covalent binding in kinase inhibitors: Revival of an emitted interaction

Many tyrosine kinase inhibitors exhibit very strong interactions with their kinases. Low nanomolar or even picomolar affinities are not uncommon.¹⁶⁷ Most inhibitors get their binding strength through numerous interactions with the protein. Thereby, hydrogen bonding, ionic-, π -stacking- and hydrophobic interaction play an role.

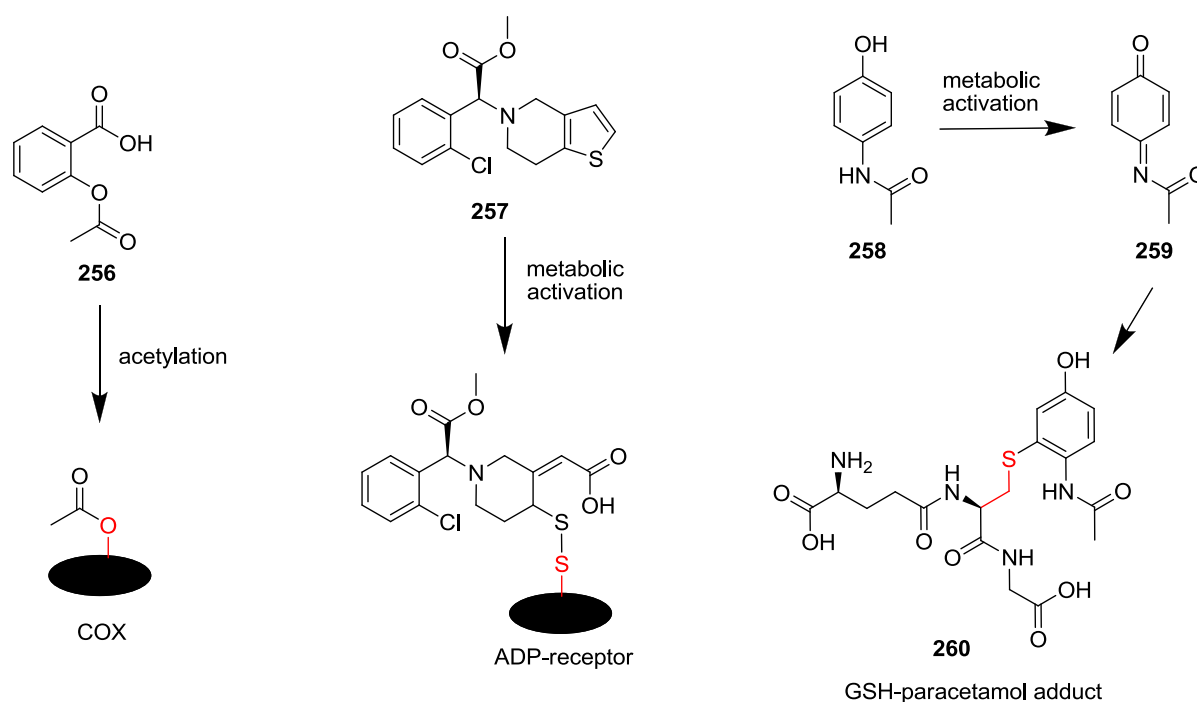


Figure 45: Examples for covalent binding in approved drugs.

Covalent interactions are another way to gain binding strength, but are much rarer in approved inhibitors, the main exceptions being antibiotics and anticancer drugs.^{168,169} The great benefit of covalent binding is the prolonged interaction and the concentration independent effects with the target.¹⁶⁸⁻¹⁷⁰ Especially in a situation with a high concentration of competing substrates e.g. ATP and kinases or unreliable noncovalent interactions due to mutation related affinity loss, the use of covalent binding can lead to better inhibitors.^{160,168} Despite these advantages, covalent binding inhibitors were for a long time the exception; they were often limited to drugs based on natural sources like β -lactam antibiotics, or they were part of unintended developments like acetylsalicylic acid (**256**).¹⁶⁸ In both cases, serine hydroxyl groups are acylated. The mechanism of action is the blockade of the D,D-transpeptidases, which are responsible for bacteria cell wall formation, and the inhibition of the cyclooxygenase (COX), which is involved in inflammation processes and platelet aggregation (Figure 45).^{168,171} Further prominent covalent binding drugs are omeprazole, which acts against reflux esophagitis, and clopidogrel (**257**), a platelet aggregation inhibitor effective against heart attacks and strokes (Figure 45).^{168,171} Both rely on disulfide formation between the drug and a cysteine in the target protein. The needed thiol group become available after the metabolic activation of the drugs.

Reasons for a reduced use of covalent binding inhibitors are mainly explained by expected side effects. While disulfide groups are cleaved by metabolism induced redox reactions and ester are cleaved by esterases, other covalent connections can be more problematic. The critical view on covalent binding inhibitors is to some extent related to observed negative immun response due to β -lactam antibiotics and hepatotoxic effects of paracetamol (**258**), used as an analgesic drug (Figure 45).^{169,171} Metabolic processes can transform paracetamol (**258**) into the intermediate **259**. **259** is a Michael acceptor that can react with thiol groups of the glutathione system (GSH) and form the adduct **260**. In high doses, **259** can lead to serious toxic effects.¹⁷² In recent years, the view on covalent binding inhibitors is slowly changing, and the number of applications for approval of new covalently binding drugs is increasing. This affects in particular protein kinase inhibitors. In the period of 2010-2013, more than 60 covalent binding kinase inhibitors were enclosed in patents.¹⁷³ The risk of negative side effects is still recognized, but set in context with possible benefits like high target selectivity afforded by the combination of strong noncovalent target affinities, and covalent binding as an additional feature.¹⁶⁸ Further, the chance of prolonged drug resident times in the active site can lead to reduced drug doses and can lower side effects.¹⁶⁹ The amino acid cysteine is the preferred target for covalent binding in protein kinases. The thiol group has a pronounced nucleophilicity that can be addressed by electrophiles. Liu et al. summarized tested electrophiles also known as thiol traps/warheads that are used in experimental, and approved inhibitors.¹⁷⁴

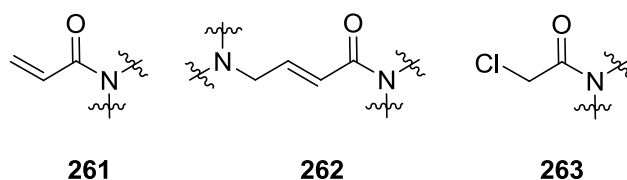
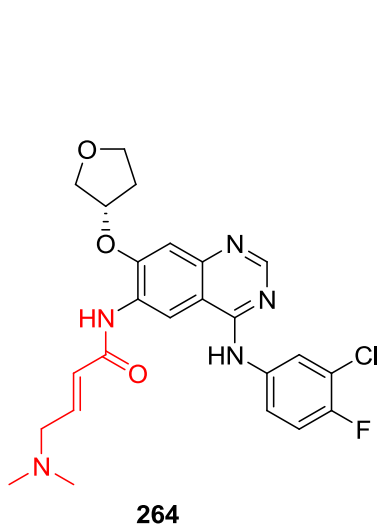


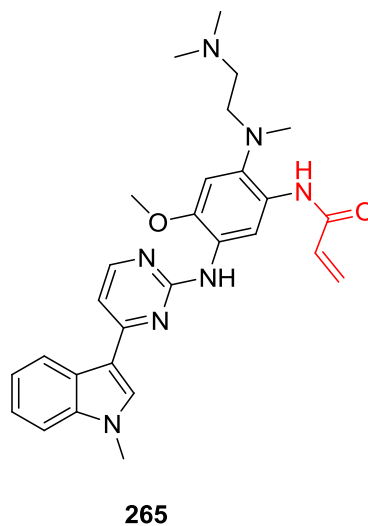
Figure 46: Typical structural elements found in covalent binding TKIs.

Commonly used electrophiles are Michael acceptors like **261** and **262** and α -halo carbonyl groups like **263** (Figure 46), forming thioethers with the target protein.¹⁷⁴ Cysteines are present in many protein kinases, but in unequal amounts and with varying degrees of accessibility. In recent years, several publications focused on the analysis of the cysteine contribution in the human kinome and their drugability.¹⁷⁴⁻¹⁷⁸ Liu et al. identified 18 spatial cysteine positions by sequence alignment studies of 442 protein kinases. The analysis revealed 196 protein kinases with accessible cysteines. 27 of these kinases were tyrosine kinases.¹⁷⁴ Leproult et al. showed that the accessibility of cysteines is higher in the active kinase conformation than in the inactive conformation even though the inactive conformation exhibited additional approachable cysteines.¹⁷⁶ Zhao et al. conducted DFT calculation on 2774 human kinases-ligand complexes.¹⁷⁵ 1599 complexes, belonging to 169 kinases showed one or more cysteines located along the active site of the protein kinases. An analysis of 124 covalent binding kinase inhibitors with connections to 44 kinases of different kinases classes revealed information about the location of the targeted cysteines residues. 119 inhibitors bound to cysteines close to the ATP binding site. 74 of the 119 inhibitors had a preference for the front pocket followed by the phosphate binding loop with 31 inhibitors.¹⁷⁵ Further, nine, previously untargeted kinases were recently tested with a covalent binding inhibitor.¹⁷⁷ This raises the number of successful targeted protein kinases to approximately 50, including the tyrosine kinases BMX, BTK, EGFR, EpHB3, FGFR1-4, FLT3, Her2, Her4, ITK, JAK3, KDR, KIT, PDGFR α , SRC, YES1.¹⁷⁷⁻¹⁷⁹ The number of potentially approachable cysteines exhibits the gap between theoretical knowledge and practical application strategies to target these presumeable accessible cysteines. This result is reflected in the amount of inhibitors on the market: Only six covalent binding kinase inhibitors are FDA approved. All of these are TKIs, and are directed against three kinases: EGFR, BTK, and Her2.¹⁵² The six FDA approvals between 2013 and 2018, in comparison to none between 2001 and 2013, illustrates the increased interest in covalent TKIs in recent years¹⁵². The focus on covalent EGFR inhibitors exhibits the potential of covalent binding for this kinase. Inhibitors like Osimertinib (**265**) have drug affinity against the highly important EGFR gatekeeper mutants like T970M, where other noncovalent EGFR-inhibitors like gefitinib (**270**) (Figure 48), and even afatinib (**264**) are not successful.¹⁶⁰



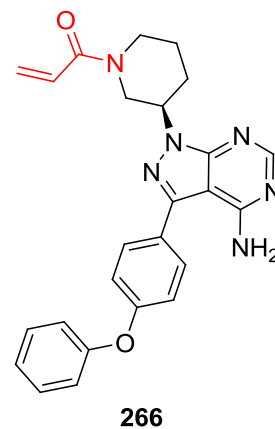
Afatinib

covalent EGFR inhibitor
(approval 2013)



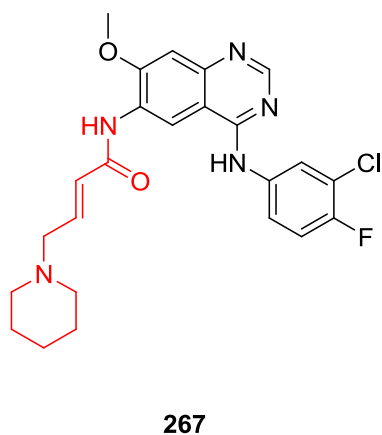
Osimertinib

covalent EGFR T970M inhibitor
(approval 2015)



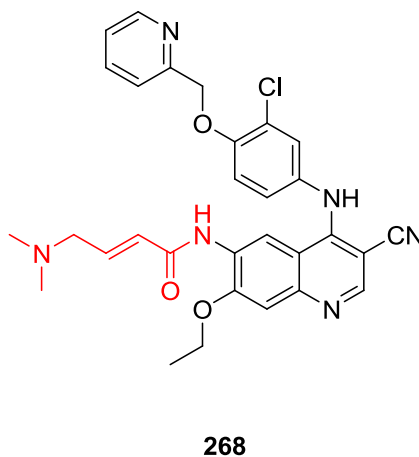
Ibrutinib

covalent BTK inhibitor
(approval 2013)



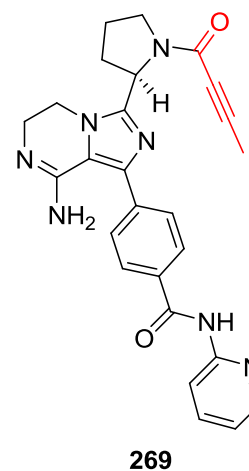
Dacomitinib

covalent EGFR inhibitor
(approval 2018)



Neratinib

covalent Her2 inhibitor
(approval 2017)



Acalabrutinib

covalent BTK inhibitor
(approval 2017)

Figure 47: Six covalent binding TKIs are FDA approved. Especially for EGFR, covalent binding TKIs can help against mutation induced loss of activity of other TKIs.

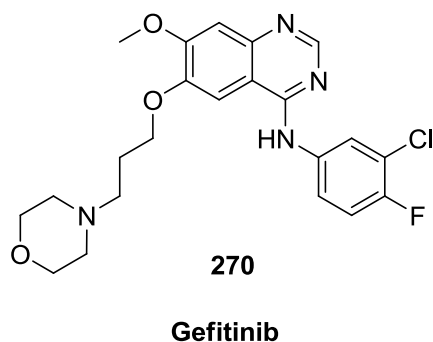


Figure 48: The noncovalent EGFR-inhibitor Gefitinib was the template for covalent EGFR-inhibitors.

The development of covalent binding inhibitors are often based on known noncovalent inhibitors. The noncovalent interactions define the binding position in the targeted kinase and enable sufficient selectivity. With modification on the bioactive scaffold it is tried to access nearby cysteines to form a covalent bond. Examples for this strategy can be found within the EGFR inhibitors **264**, **267** and **268**, which exhibit structural conformity with the reversible inhibitor gefitinib (**270**) (Figure 47, Figure 48).¹⁷⁸ Not surprisingly, approaches for covalent binding inhibitors based on imatinib (**254**) and dasatinib (**255**) are also described in literature (Figure 49). Leproult et al. synthesized covalent inhibitors based on imatinib (**254**).¹⁷⁶ The piperazine group was exchanged against different thiol traps and tested against 20 kinases. The inhibitor **271** formed covalent connections with cysteines close to the binding position of imatinib (**254**) in KIT and PDGFR α , shifting the spectrum of targeted kinases. Kwarcinski et al. made a similar approach with dasatinib (**255**).¹⁸⁰ Dasatinib (**255**) exhibits with an IC₅₀ of 14300 nM a very weak affinity to the T338M mutation of the kinase c-Src. The inhibitor **272** overcame the resistance by covalently binding lowering the IC₅₀ to 5.5 nM.¹⁸⁰ The possibility to change selectivity patterns towards kinases and to compensate loss of affinity due to mutations, reveals the potential of covalent binding and the advantage of screening known TKIs for their potential as platform for new covalent binding inhibitors.

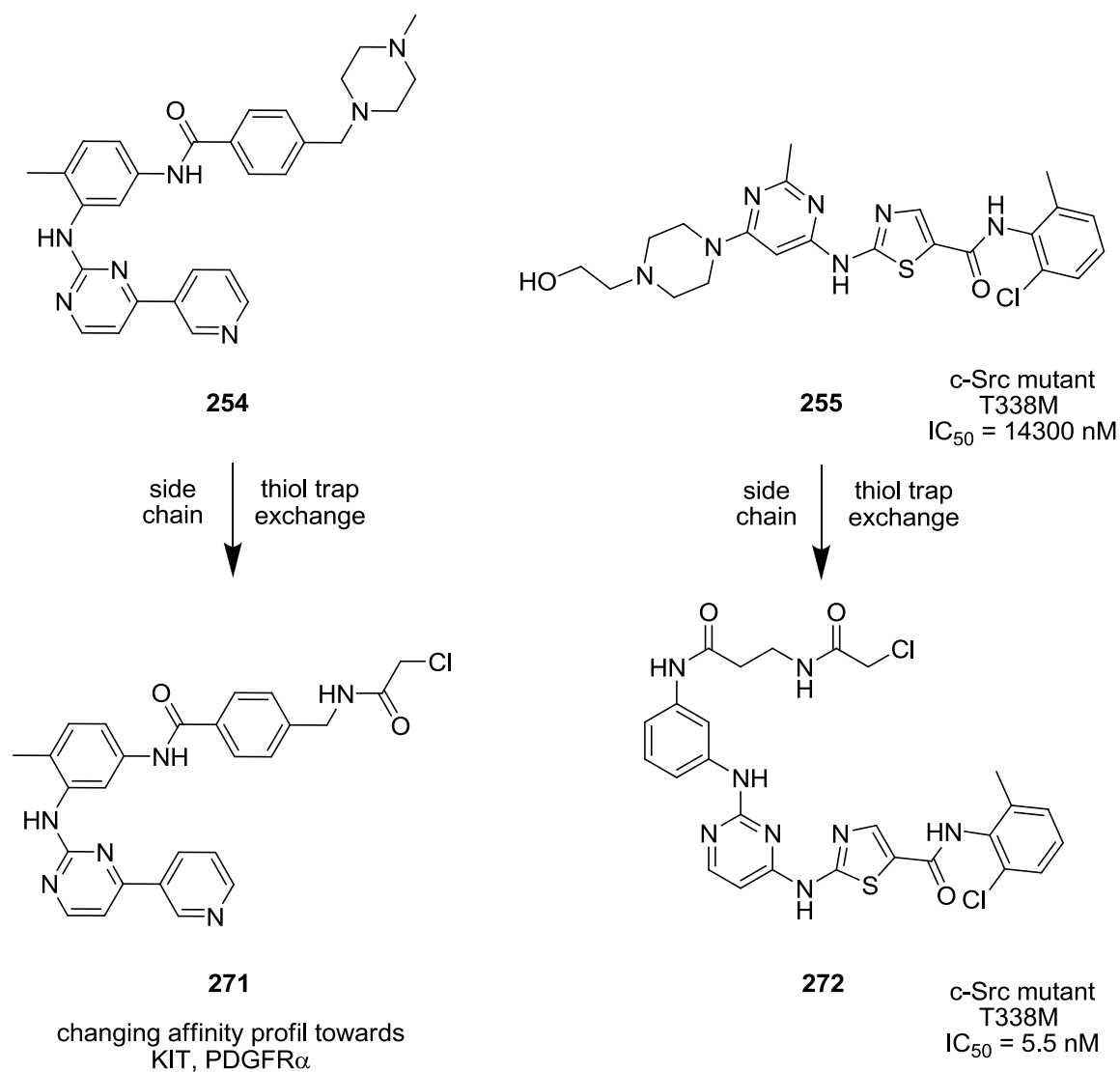


Figure 49: Examples of applied covalent binding on known noncovalent TKIs. The changes led to new affinity profile in case of **254** with compound **271** and increased affinity to a mutated kinase in case of **255** with the new compound **272**.

8. Project 2: Aim of the project

The multitarget kinase inhibitor dasatinib reveals the potential to act as a platform for new inhibitor libraries. Many major kinase targets of dasatinib exhibit accessible cysteine residues in the active site and open the opportunity for covalent connections with inhibitors. The idea, to turn the noncovalent inhibitor dasatinib into new covalent binding inhibitors followed the strategies presented in the introduction for EGFR inhibitors and modified imatinib compounds.

The aims of the project were;

- the development of a focused chemical library incorporating covalent binding moieties.
- design and test synthesis routes for the modification of dasatinib towards covalent binding inhibitors, while keeping dasatinib`s basic interactions to different kinases intact.
- test novel dasatinib analogs in kinase binding assays and in cancer cell lines.
- to improve selectivity and affinity profiles compared to dasatinib and potentially generate enhanced anticancer agents.

9. Project 2: Results and discussion

9.1 Inhibitor design and strategy

It was of interest to design and synthesize covalent binding inhibitors that maintain a high degree of structural similarity with dasatinib. This was done to conserve the main interactions with different kinases, and to gain new interactions through covalent bonds. Therefore, the required molecular changes must be made at positions with the least impact on the general sides of interaction of dasatinib.

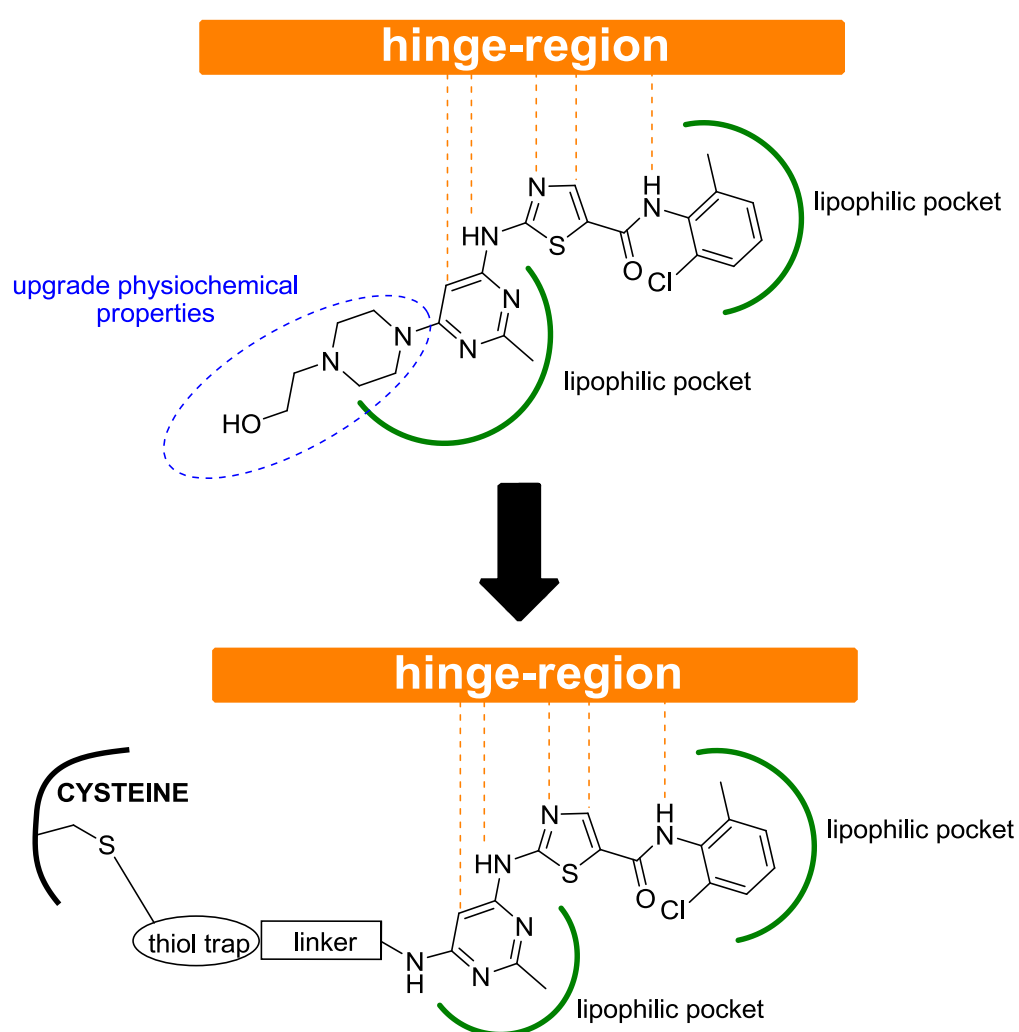


Figure 50: Upper part: Dasatinib has numerous interactions with the hinge region and with the lipophilic pockets around the ATP binding site. The 1-(2-hydroxyethyl)piperazine moiety also interacts with the active site, but is not integral to the binding. Lower part: The design for the intended covalent binding inhibitors is based on an exchange of this structure element with linker structures that contain electrophilic substituents. These thiol traps can form covalent bonds with nearby cysteine.

The essential interactions of dasatinib are hydrogen bonding of the amide NH, the thiazol nitrogen, and the NH linking the thiazol and pyrimidine moiety with the hinge region (Figure 50).¹⁸¹ In the case of the kinase ABL, further interaction between the CH group of the pyrimidine ring and thiazol heterocycle are described in literature.^{152,164} Hydrophobic interactions contribute also to dasatinib's affinity, in addition to hydrogen bonding. The aniline moiety, the pyrimidine ring and parts of the piperazine structure point into the lipophilic pockets around the ATP binding pocket. Different interactions of the 1-(2-hydroxyethyl)piperazine moiety are described in literature, but have less impact on the overall binding affinity of dasatinib.^{164,181} Replacement of this moiety during the development process of dasatinib exhibited only minor affinity changes in enzyme tests.¹⁸¹ However, the 1-(2-hydroxyethyl)piperazine structure element improved physiochemical properties such as water solubility and drug uptake, making dasatinib superior to similar compounds.¹⁸¹

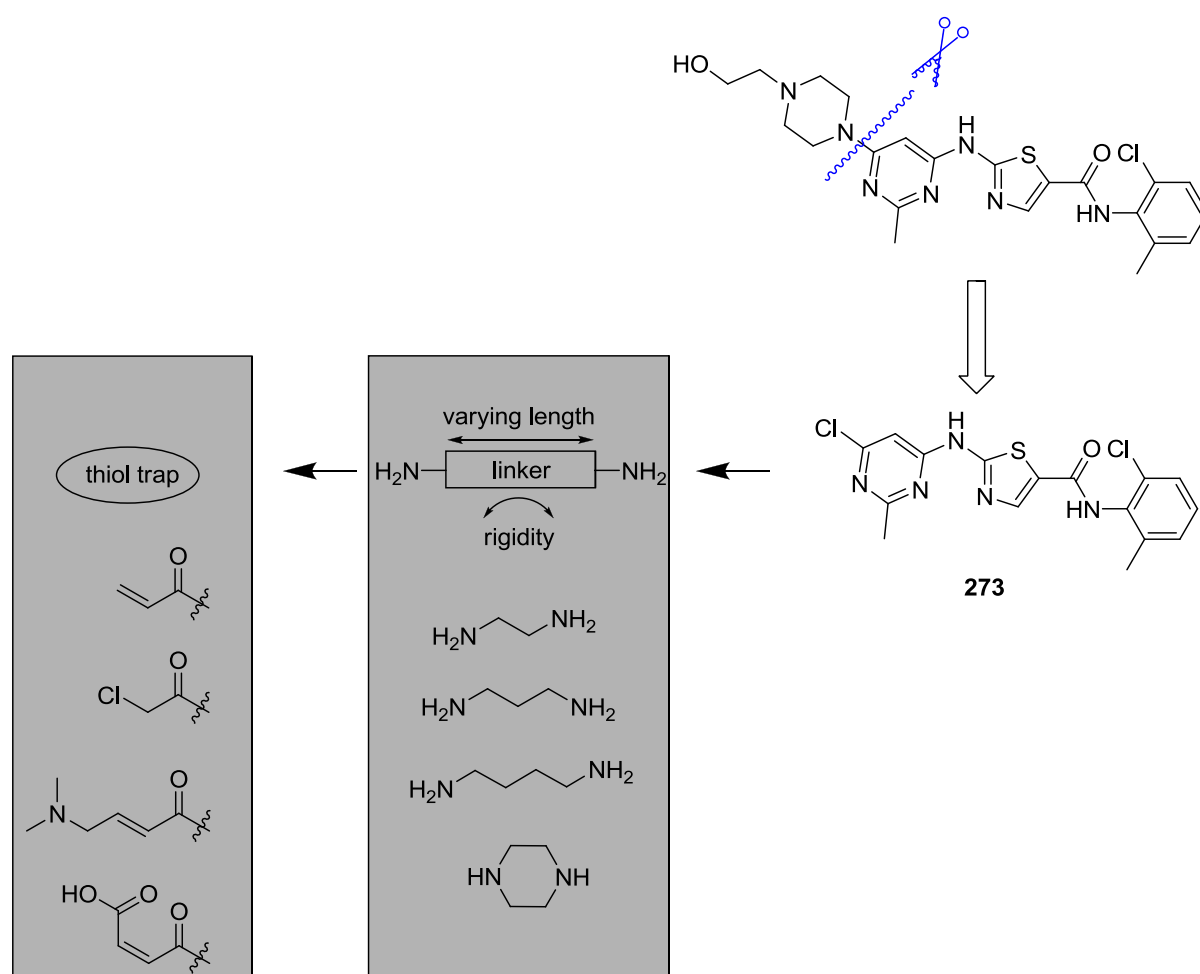


Figure 51: Strategy for the transformation of dasatinib in potential covalent inhibitors. Diamine structures of different lengths can act as linkers between the dasatinib scaffold and the thiol traps. The starting point of the synthesis of the new library is the dasatinib intermediate **273**.

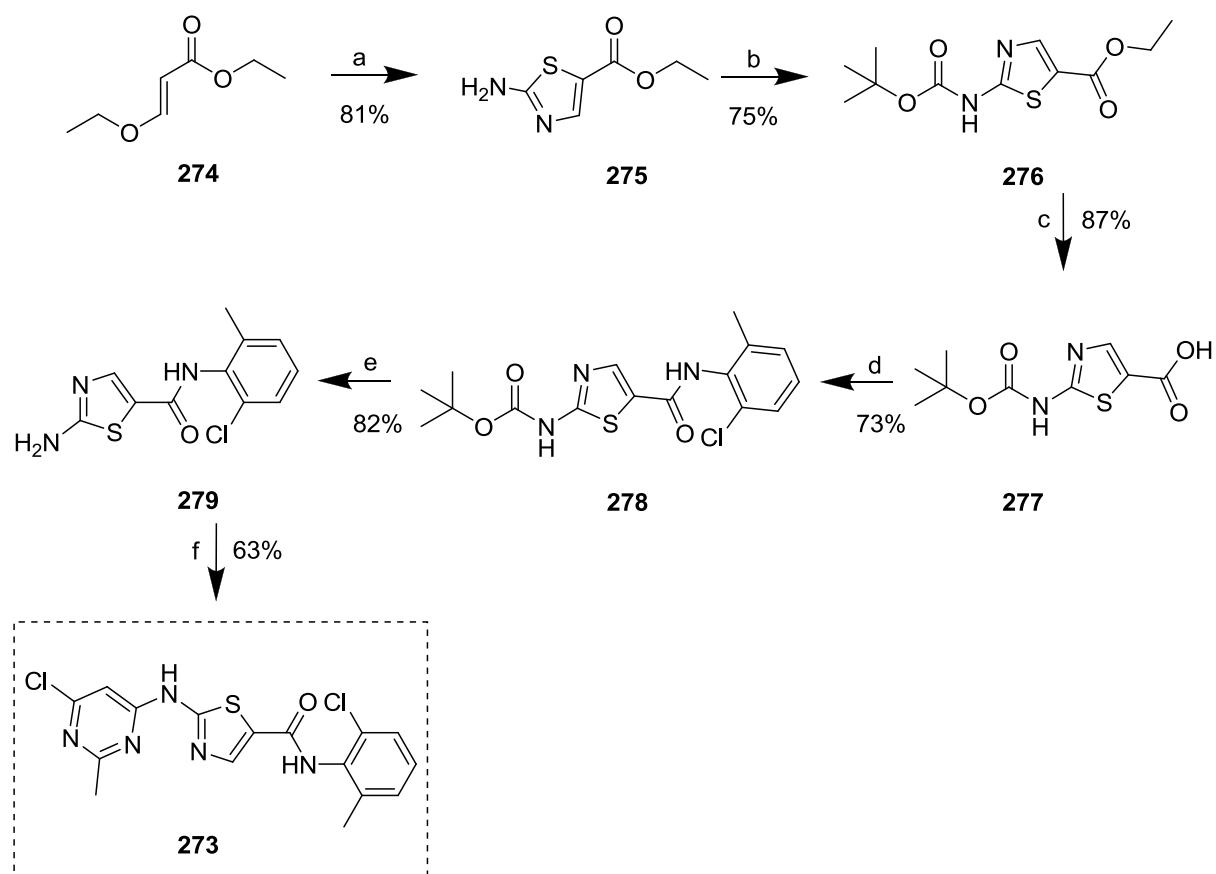
Modifications for covalent inhibitors were planned to be realized by the exchange of this 1-(2-hydroxyethyl)piperazine sidechain with linkers of different length and rigidity. Each of the linkers should bear a “thiol trap” that enables the “fishing” of accessible cysteines in proximity of the active sites in different kinases (Figure 50, Figure 51).

The dasatinib precursor **273** was chosen as the starting point for these modifications. This intermediate is used for the introduction of the 1-(2-hydroxyethyl)piperazine moiety into the dasatinib scaffold by nucleophilic aromatic substitution (S_NAr). Diamines of different lengths and rigidity (1-4 carbons) can act as linkers to the pyrimidine ring in the same manner. The other end of the diamine should be connected the thiol trap *via* an amide bond. For the thiol traps, “classical” Michael acceptors were prioritized. Namely acrylic acid, 4-dimethylamino crotonic acid, and chloroacetic acid (Figure 51). Maleic acid was also investigated as a potential active thiol trap.

9.2 Synthesis

9.2.1 Scaffold synthesis

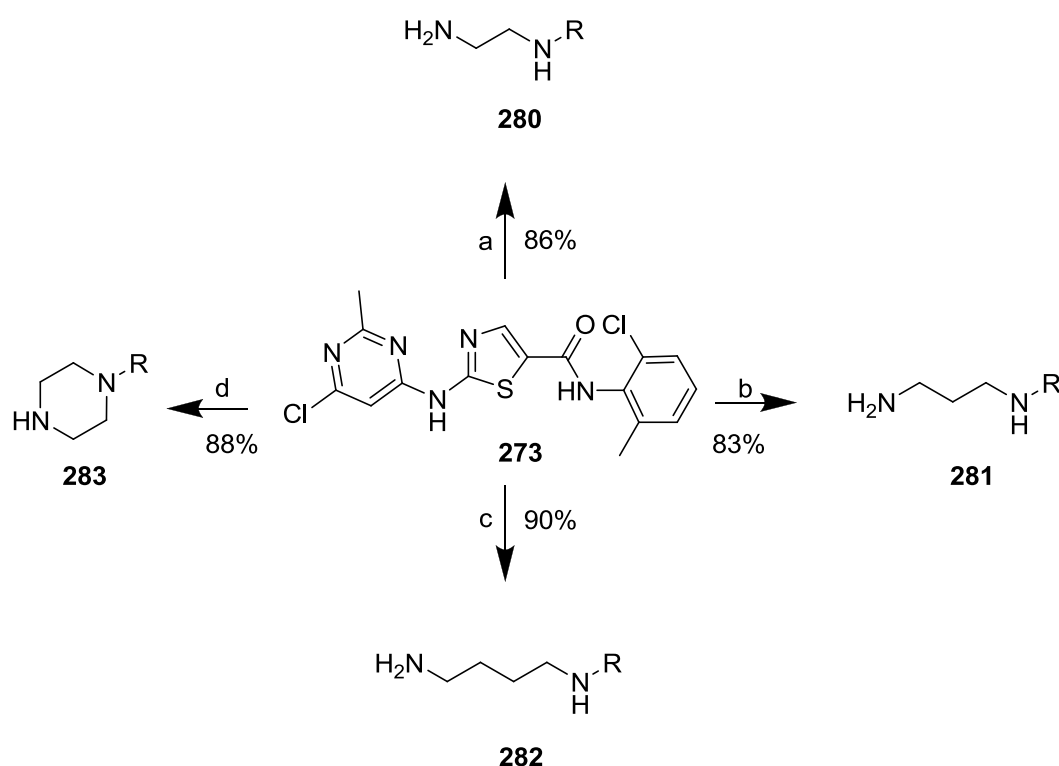
The synthesis of the dasatinib precursor **273** was carried out according to a synthesis route of Bristol-Myers Squibb (Scheme 40), and published procedures for single reaction steps.^{181,182} Intermediate **275** was obtained in a two step process from ethyl 3-ethoxy-2-propenoate **274** following a procedure from Zhao et al.¹⁸³ The reaction of **274** with NBS in a water/dioxane mixture formed an α -formyl- α -bromoacetate hemiacetal, which was further converted with thiourea under heating (Scheme 40). The following three reaction steps were conducted based on procedures of Das et al.¹⁸¹ To avoid side reactions in reaction step d, the amino group of **275** must be protected. Therefore, compound **275** was stirred together with di-*tert*-butyl carbonate and DMAP in an overnight reaction.¹⁸¹ In the next step, the ester of **276** (Scheme 40) was saponificated with 6N NaOH to yield the free acid for an ensuing carboxylic acid activation.¹⁸¹ The addition of concentrated HCl and pH-adjustment to pH 1 resulted in product precipitation with only minimal deprotection of the Boc-protecting group. For the amidation reaction, the carboxylic acid **277** was converted with oxalyl chloride into the corresponding acid chloride and stirred with 2-chloro-6-methylaniline and DIPEA overnight to obtain **278**.¹⁸¹ The introduction of the pyrimidine moiety in **279** required the removal of the Boc group from **278**. The treatment of **278** with neat TFA resulted in **279**.¹⁸¹ The key intermediate **273** was afforded by the reaction of **279** with 4,6-dichloro-2-methylpyrimidine and NaOtBu in THF in 63% yield. The synthesis was based on the literature procedures of Chen et al. and Allentoff et al.^{184,185}



Scheme 40: Conditions: (a) i. NBS, 1,4-dioxane/H₂O, -9 °C → r.t., 1.5 h; ii. thiourea, 80 °C, 1.5 h; (b) (Boc)₂O, DMAP, THF, rt, O/N; (c) aq. 6N KOH, THF/EtOH, 55 °C, O/N; (d) i. oxalyl chloride, cat. DMF, DCM, rt, 2 h; ii. 2-chloro-6-methylaniline, DIPEA, DCM, rt, O/N; (e) TFA neat, 0-5 °C, 3.5 h; (f) 4,6-dichloro-2-methylpyrimidine, NaOtBu, THF, 2-3 h, rt.

9.2.2 Linker intermediate synthesis

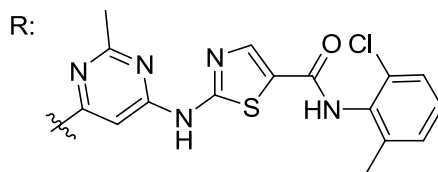
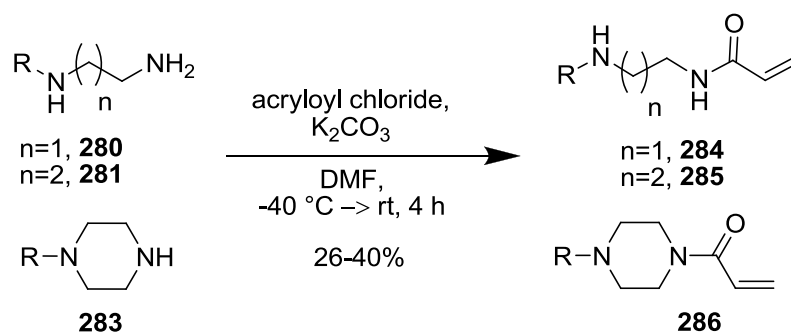
The linker compounds **280-283** were synthesized from **273** in an S_NAr reaction with diamines at 70 °C overnight.¹⁸² **280** and **281** were converted using 1,2-ethanediamine and 1,3-propanediamine as the solvents respectively. **282** and **283** required DMSO as solvent to dissolve the solid 1,4-butanediamine and piperazine. All diamines were used in excess (at least 10 eq.) to avoid dimerisation byproducts. The compounds **280-283** were isolated by filtration in 83-90% yields and used without further purification for the preparation of final compounds. Similar reaction conditions for **280** are described in literature.¹⁸⁶



Scheme 41: Conditions: (a) 1,2-ethanediamine neat, 70 °C, O/N; (b) 1,3-propanediamine neat, 70 °C, O/N; 1,4-butanediamine, DMSO, 70 °C, O/N; (d) piperazine, DMSO, 70 °C, O/N.

9.2.3 Synthesis of acrylic acid amide derivatives

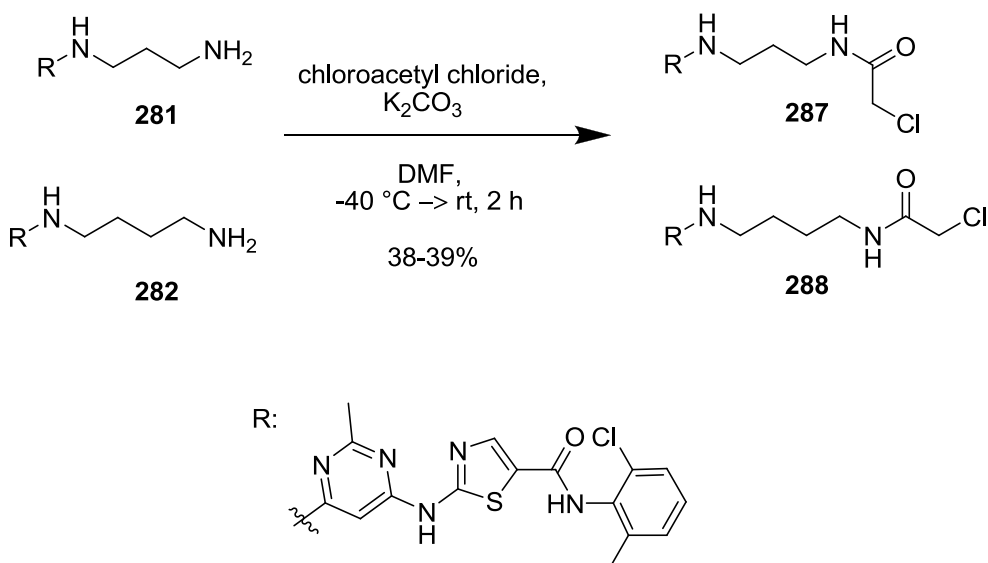
The synthesis of acrylic acid amide inhibitors was conducted with acryloyl chloride and potassium carbonate in DMF. Due to its high reactivity, acryloyl chloride was diluted with DMF and added dropwise to the reaction mixture at $-40\text{ }^{\circ}\text{C}$. The crude products were precipitated by the addition of 0.1 M acetic acid to the reaction mixture. Purification by flash reversed-phase chromatography afforded **284-286** in 26-40% yield. Compound **286** was described later in a patent from another group after this synthesis was already carried out.^{187,188}



Scheme 42: Synthesis of the acrylic acid amide derivatives **284-286**.

9.2.4 Synthesis of α -chloroacetic acid amide derivatives

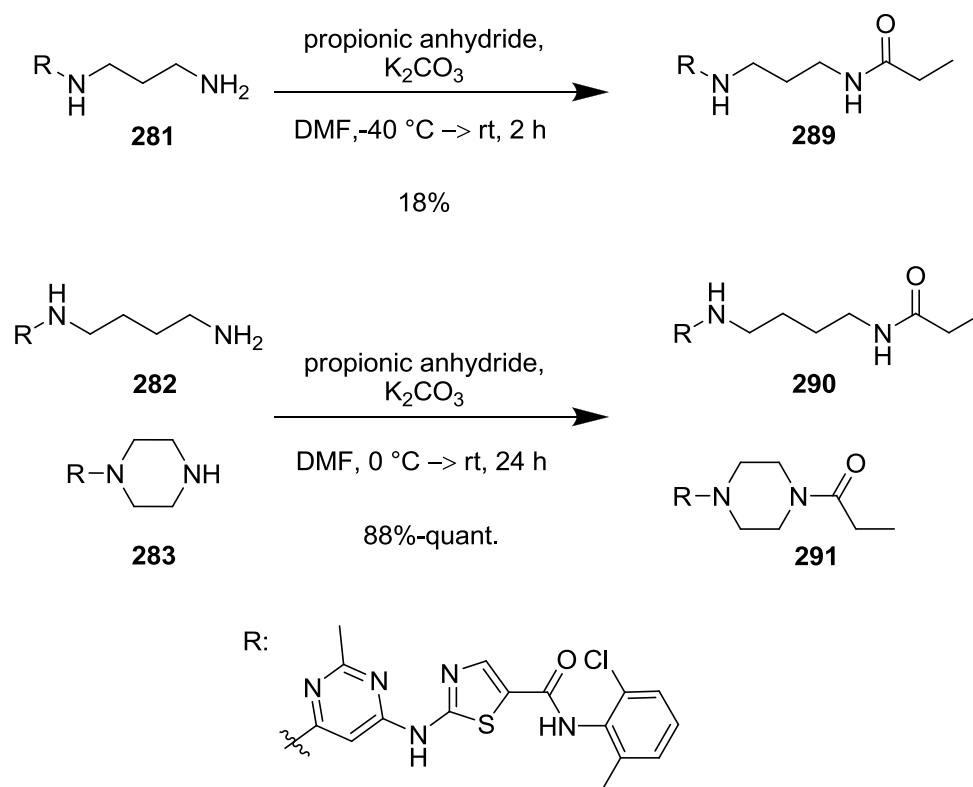
The syntheses of α -chloroacetic acid amides were conducted with chloroacetyl chloride and K_2CO_3 in dry DMF. To avoid side reactions, **281-282** and chloroacetyl chloride were used in equimolar amounts. The acid chloride was added dropwise as a solution in DMF at $-40\text{ }^\circ\text{C}$. As for the acrylic acid amides **284-286**, the crude products were obtained by addition of 0.1 M acetic acid and further purified by flash reverse-phase chromatography. **287** and **288** were afforded in 38-39% yields. Solubility problems also lowered yields in the final purification as with the acrylic acid amide derivatives.



Scheme 43: Synthesis of the α -chloroacetic acid amide derivatives **287** and **288**.

9.2.5 Synthesis of propionic acid amides for activity comparison

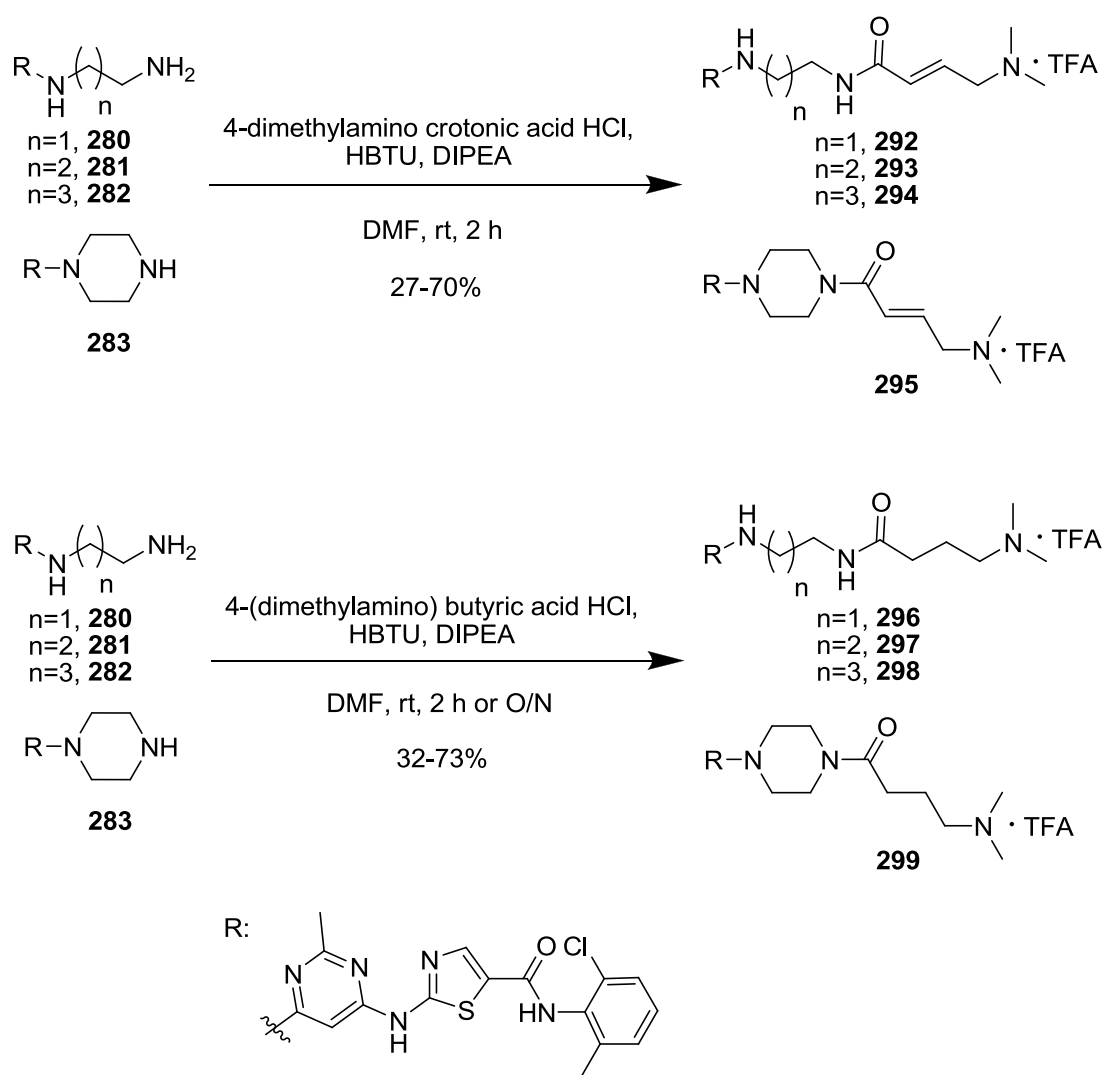
Propionic acid amides were synthesized as reference compounds without an acceptor group. They were used to evaluate the activity and mode of interactions of the acrylic acid amides and α -chloroacetic acid amides. The ethyl group has similar steric demand as the Michael acceptor and the chlorine leaving group and can help to distinguish between noncovalent and covalent binding interactions. A similar strategy was used by Kwarcinski et al. and Rao et al. to reference the activity for their covalent inhibitors.^{177,180} The reactions for **289-291** were carried out with propionic anhydride and potassium carbonate in DMF. In the first attempt towards **289** it was cooled to $-40\text{ }^{\circ}\text{C}$ because of the expected high reactivity of the reagent, but this proved to be unnecessary. Therefore, the reactions for **290** and **291** were started at $0\text{ }^{\circ}\text{C}$ and the reaction mixtures stirred at room temperature for 24 hours. The crude products precipitated after addition of 0.1 M acetic acid to the reaction mixture. **289** was afforded in 18% yield after flash reverse phase chromatography, **290** and **291** were filtrated and washed with water. The products **290** and **291** were obtained in 88% to quantitative yield.



Scheme 44: Synthesis of propionic acid amides **289-291**.

9.2.6 Synthesis of 4-dimethylamino crotonic acid amides and their deactivated analogs

The low water solubility of the final compounds **284-291** was a consequence of the removal of the *N*-(2-hydroxyethyl)piperazine moiety of dasatinib. Therefore, 4-dimethylamino crotonic acid amides were synthesized to enable “thiol trapping” while keeping the good physicochemical properties. 4-dimethylamino crotonic acid and derivatives combine the features of acrylic acid derivatives and allow salt formation through the nearby dimethylamino group.



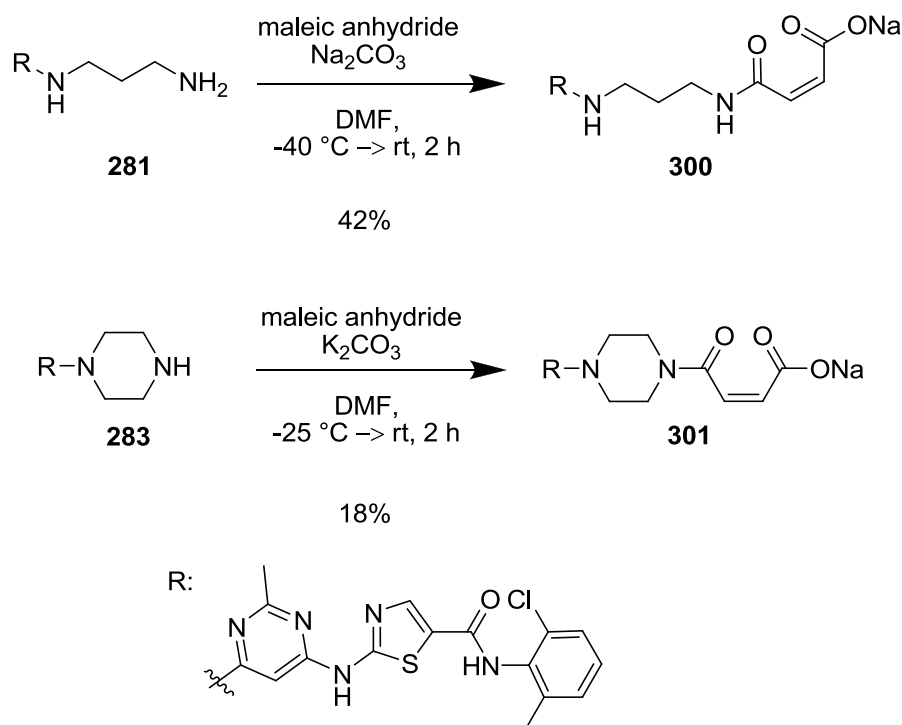
Scheme 45: Synthesis of 4-dimethylamino crotonic acid amides **292-295** and their saturated analogs **296-299**.

The final compounds **292-295** were afforded from the linker intermediates **280-283**. The amide bond was formed under peptide coupling conditions with HBTU, DIPEA and 4-dimethylamino crotonic acid HCl. The crude products **292-295** precipitated upon water addition and were purified by flash reverse phase chromatography. The products **292-295** were obtained as TFA salts in 27-70% yields.

The saturated compounds **296-299** were synthesized to compare the influence of covalent binding on the overall compound affinity, equal to the propionic acid amides **289-291**. The synthesis was conducted in the same way as for the inhibitors **292-295**, but with 4-(dimethylamino)butyric acid HCl as the starting material. The compounds **296-299** were obtained as TFA salts after purification in 32-73% yields. Compound **295** was later described in a patent from another group after the synthesis was already carried out.^{187,188}

9.2.7 Synthesis of maleic acid amides

The maleic acid amides **300** and **301** were synthesized to afford derivatives with Michael acceptors and better overall physicochemical properties due to a free acid structure in the thiol trap. **300** and **301** were synthesized from **281** and **283** by using maleic anhydride as an acylation agent and potassium carbonate or sodium carbonate as base in DMF. The reactions were started at low initial temperatures (-25 to -40 °C) and were further stirred at room temperature.



Scheme 46: Synthesis of maleic acid amides **300** and **301**.

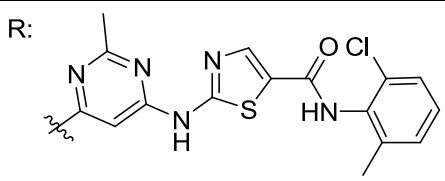
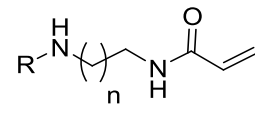
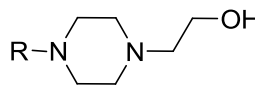
The use of sodium carbonate for compound **300** helped to obtain the sodium salt of the inhibitor directly from the reaction mixture. The crude product was precipitated by the addition of DCM and diethylether to the reaction mixture. The obtained solid was further purified with flash reverse phase chromatography and led to a 42% yield. For **301**, potassium carbonate was used as base and the free acid was precipitated from the reaction mixture by the addition of 1 M HCl solution. The filtrated crude product was treated with sodium carbonate solution and purified by flash reverse phase chromatography. **301** was generated in 18% yield.

9.3 Biological evaluation of the inhibitors

9.3.1 Kinase screening and first affinity evaluation

Kinase affinity screenings were purchased from DiscoverX using the KINOMEscan™ platform. An initial screening included the first synthesized compounds **284** and **285** and 8 different kinases. With the exception of ABL1, all kinases contained potentially accessible cysteines. The kinases ABL-1, BLK, TXK, BTK and KIT are known targets of dasatinib (**255**). The result of the screening is presented in Table 23. The test revealed an overall higher affinity of all kinases towards **285** over **284**. Of most interest were the outcome for the kinases BTK and KIT. BTK plays an important role in B-cell development, while KIT is related to gastrointestinal stromal tumors (GIST).^{189,190}

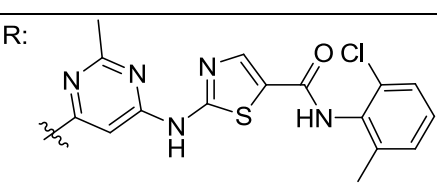
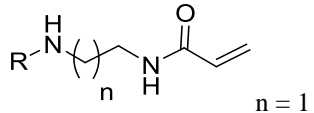
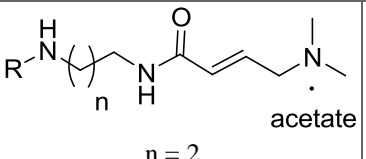
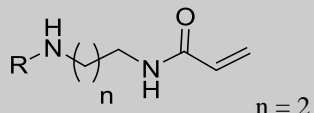
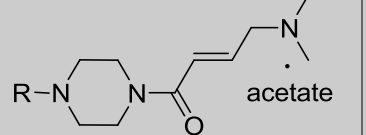
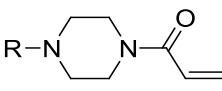
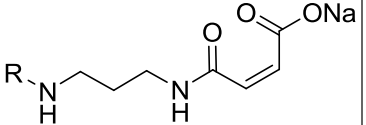
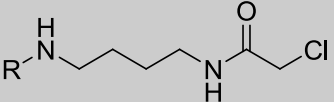
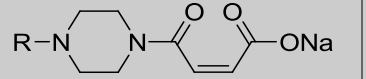
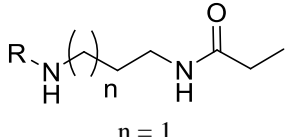
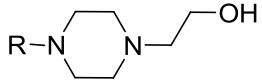
Table 23: Results of the initial DiscoverX screening.

R:			
			
			
compound	284 , n = 1	285 , n = 2	dasatinib (255)
target	K_d (nM)	K_d (nM)	K_d (nM) ¹⁶⁷
ABL-1 phosphorylated	0.12	0.03	0.046
BLK	0.64	0.16	0.21
BTK	7.6	0.91	1.4
EGFR (L858R)	1300	610	120
EGFR (L858R, T790M)	>30000	>30000	2300
JAK3 (JH1 domain-catalytic)	3300	860	640
KIT	0.73	0.1	0.81
TXK	18	3.9	2.1

Compound **285** exhibited a 1.5 fold higher affinity to BTK compared to literature values of dasatinib (**255**), but **284** was noticeably weaker.¹⁶⁷ **285** and **284** differ only by one CH₂-group in the linker length. For KIT, the difference of **285** to dasatinib (**255**) was 8 fold. The acrylamides **284** and **285** showed significantly lower affinity to the EGFR mutants and JAK3 compared to dasatinib (**255**).¹⁶⁷ The affinity to TXK and BLK was lower or similar to dasatinib (**255**).

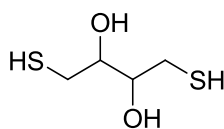
For KIT and BTK, kinetic studies with **284** and **285** were conducted by DiscoverX. They revealed characteristic association/disassociation rates for noncovalent binding. A second affinity screening for KIT with **285**, **284** and other inhibitors could not replicate the significant higher affinity for **285** obtained from the previous testing (Table 24).

Table 24: Results of the kinetic studies (K_d determination) for different inhibitors against KIT.

					
cpd	structure	K _d (nM)	cpd	structure	K _d (nM)
284		0.6	293		0.43
285		0.41	295		0.25
286		0.34	300		1.1
288		0.26	301		0.29
289		0.28	dasatinib (255)		0.81

The saturated reference compound **289** showed similar or better affinities than the Michael acceptor compounds and the chloroacetic acid amide **288** (Table 24). This indicates that there is no kinase specific covalent binding for the tested library with KIT. The inhibitory effects of compounds **286** and **295** towards KIT and BTK, as well as other kinases like DDR1, DDR2, ABL and SRC, was later described in literature.^{187,188} **286** and **295** were part of a dasatinib based compound library, conducted by Liu et al, including different Michael acceptor compounds and similar noncovalent compounds. Compounds with Michael acceptors, including **286** and **295**, were in many cases weaker than similar noncovalent binding inhibitors in their studies. This indicates limited success in obtaining superior interactions by covalent bonds for the library of Liu et al. and supports the findings for the compounds for KIT.^{187,188}

Another screening of the produced inhibitors with a different set of kinases was not conducted. A deeper analysis of the assay parameters of DiscoverX raised the question about the reliability of the assay method to investigate covalent binding inhibitors. Problems were seen in the limited possibility to optimize assay parameters in “real time”, such as the incubation time of the compounds with the target kinase. A sufficiently long incubation of the test compounds and the kinase is required to form the covalent bond. The incubation time can influence the extent of covalent bond formation. Of even bigger concern was the use of antioxidants in the buffer solution. Cysteine containing proteins in particular, can be sensitive to oxidation reactions such as disulfide formation leading to impaired, or loss of, function.



302

Figure 52: DTT (**302**) is an antioxidant often used in biochemical assays.

For that reason, thiol containing molecules like mercaptoethanol or 1,4-dithiothreitol (DTT) **302** (Figure 52) are used as antioxidants in high concentrations in biochemical assays. Analysis of the test results and conditions used by DiscoverX revealed the use of DTT (**302**) in mM concentration.

factor 10000-60000

e.g 0.1 μ M

e.g 1-6 mM

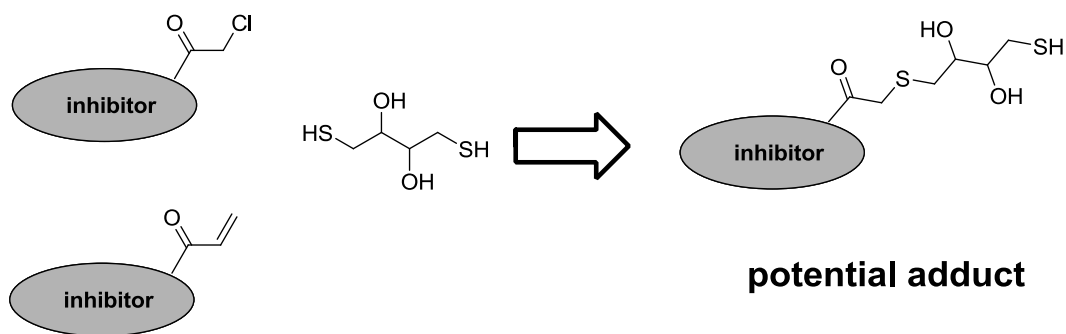


Figure 53: The assay conditions used by DiscoverX involved high inhibitor-antioxidant ratios. It was expected that the inhibitors could react with the antioxidant influencing assay results.

Table 25: Dragovich et al. tested covalently binding inhibitors for the influence of DTT.¹⁹¹

 HRV-3CP			 HRV-3CP		
compound	R	DTT deactivation	compound	R	DTT deactivation
303		no	306		yes
304		no	307		yes
305		no	308		yes

Kinase assays with e.g. 0.1 μM inhibitor and 1-6 mM DTT (**302**) in the buffer leads to concentration ratios of 1 to 10000-60000. The main concern for the interpretation of the assay results was the formation of inhibitor-DTT adducts preventing the formation of inhibitor-kinase adducts. The result can be seemingly weaker binding affinities due to loss of the potential covalent binding to the kinase. Further, basic noncovalent interactions of the scaffold with the kinase can be weakened by the DTT adduct. Dahlin et al. stated to be aware of the influence of DTT (**302**) in high throughput assays due to its reactivity with electrophiles leading to the wrong interpretation of test results.¹⁹² They suggest that comparison experiments with and without DTT (**302**) in the biochemical assays are utilized. Dragovich et al. developed Human Rhinovirus 3C protease inhibitors and tested also the effect of DTT (**302**).¹⁹¹ They preincubated their inhibitors with 5 mM DTT (**302**) for 2-3 minutes at 23 °C. Some of the compounds formed their respective DTT adduct partially or even fully (Table 26- extraction of a bigger table). Esters and electron rich amide derivatives (e.g. **303-305**) were not converted, but unsaturated ketones (e.g. **306, 307**) and compounds like **308** showed reactivity towards DTT (**302**). Overall, these thiol traps are sterically more hindered than terminal unsaturated systems. Therefore, the reaction of less hindered thiol traps with DTT (**302**) can be not excluded.

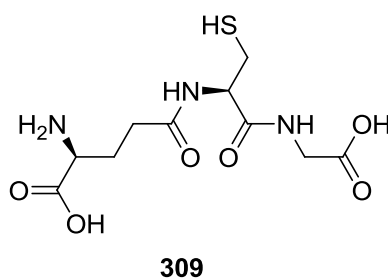


Figure 54: GSH (**309**) is present in the liver redox system and is used for the measurement of the intrinsic activity of covalent binding inhibitors.

The influence of steric effects was investigated for reactions with GSH (**309**) in literature. GSH (**309**) is part of the liver redox system and can bind drug molecules covalently (paracetamol, section 7.4). GSH (**309**) is also used to test the intrinsic reactivity of covalent binding inhibitors towards nucleophiles. Flanagan et al. made extensive tests of different thiol traps with GSH (**309**) and measured the half-life of the conversion to the thiol trap-GSH adducts.¹⁹³ Table 26 shows an excerpt of the test results they have obtained. The acrylic acid amide **311** shows adduct formation with GSH in less than one hour.

Table 26: Reactions of GSH (10 mM) with different thiol traps (1 mM). The intrinsic activity of the compounds was measured as time of the half conversion ($t_{1/2}$) to the GSH adduct. Extracted data from Flanagan et al.¹⁹³

<div style="text-align: center;"> </div>					
compound	structure	$t_{1/2}$ (h)	compound	structure	$t_{1/2}$ (h)
310		0.53	314		33
311		0.88	315		>60
312		3.2	316		>60
313		17	317		>60

By either increasing the steric demand of groups close to the nitrogen, or by increasing the double bond substitution, the half-life increased from 0.88 hours (fragment **311**) to greater than 60 hours (fragment **316**). Of relevance for the inhibitors produced in section 9.2 are fragments **312-315**: fragment **312** reveals a short half-life for chloroacetic acid amides like the TKI inhibitors **287** and **288** in contact with exogenous thiols. No relevant effect of deactivation could be observed for the fragment **315**, represented in the TKI compounds **292-295**. Therefore, a different influences of exogenous thiols for the TKI library can not be excluded.

Experiments to explore the covalent binding TKIs with exogenous thiol sources like DTT (**302**) and GSH (**309**) show different results regarding their influence on the cell assays. Kwarcinski et al. tested their inhibitor **318** (Figure 55) for the kinase c-Src in presence of 1 mM GSH (**309**) and DTT (**302**). The incubation time was 120 minutes.¹⁸⁰ They found no relevant differences between the obtained IC_{50} values between no DTT (93 ± 20 nM) and with DTT (95 ± 15 nM) present. The use of GSH increased significantly the efficiency of inhibitor **318** (Figure 55) from an IC_{50} value of 93 ± 20 nM to less than 30 nM.

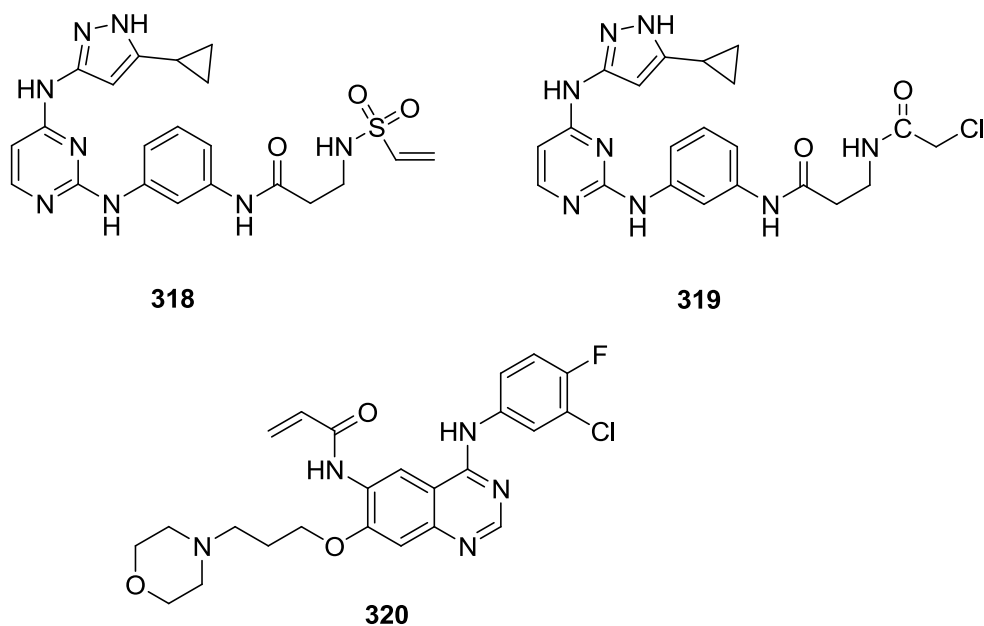


Figure 55: Compound **318** was tested as part of an IC_{50} determination for the influence of 1mM GSH (**309**) or DTT (**302**) in presence of the target kinase c-Src (120 min incubation time). No adduct formation could be detected. **320** was tested with GSH (**309**) without the presence of a kinase. After 10 minutes, half the amount of **320** was converted to the GSH adduct.

Even if not directly comparable, these results are interesting because of the otherwise high reactivity of non-sterically hindered vinyl sulfonamides like **310** (Table 26). This indicates the low influence of exogenous thiols and an even faster reaction of Michael acceptors with cysteines in the active site. Unfortunately, Kwarcinski et al. have tested only one inhibitor and did not show data for the chloroacetic acid amide **319** (Figure 55).^{180,193}

Schwartz et al. used GSH (**309**) to evaluate the intrinsic activity of their covalently binding EGFR-inhibitors.¹⁹⁴ They incubated compound **320** (Figure 55) at a concentration of 0.1 μ M with 5 mM GSH at 37 °C at pH 7.4 (no kinase present). Compound **320** showed a half-life of 10 minutes. These differences in the results between Kwarcinski et al. and Schwartz point out how assay conditions can influence the results.^{180,194} On the one hand, the presence of antioxidants with the test compound alone might lead to deactivation, especially if strong thiol traps are used. On the other hand, the presence of antioxidant and protein together with the test compound, can have fewer consequences or ensure even better affinities.

9.3.2 Summary and interpretation of the kinase screening

The results for the compound library shown in Table 24 indicated no covalent binding for the kinase KIT. This is in agreement with IC₅₀ determination of Liu et al. for **286** and **295** and other similar compounds for different kinases (KIT, BTK, DDR1, DDR2, ABL, and SRC).^{187,188} Noncovalent inhibitors were superior to potentially covalent inhibitors with similar structure.

Further investigations were stopped because of the unknown influence of antioxidants like DTT for the assay results. The presented literature examples showed inconclusive results regarding DTT and GSH in assays, and were mainly dependent on if the target kinase and the antioxidant are present at the same time, or if the compound is incubated only with the antioxidant. Considering the numerous known covalent inhibitors, and there existing only a few reports about the influence of DTT (**302**), it is reasonable to assume that in most cases DTT (**302**) does not lead to any relevant negative effects.

Therefore, the kinase assays for the TKI library were likely stopped unnecessarily and can be continued. Commercially available assay kits can help to conduct in-house testing to maintain sufficient control over the assay conditions. However, the tested compounds presented in Table 24 showed no indication of covalent binding. Therefore, a broader kinase screening would be necessary to find new target kinases.

9.3.3 Cell assay based approaches

Cell assays were performed in addition to the kinase assays. The aim was to detect reduced cell viability in different cancer cell lines due to compound treatment. The general effect on normal/healthy cells was also documented. This data should help to give an impression about the suitability of the compounds for further kinase and cell assays. To evaluate possible covalent binding effects in the cell lines, more noncovalent reference compounds (thiol trap inactivated/saturated compounds) with similar sterics were synthesized. Notable differences in the cell viability between the thiol trap containing compounds and the corresponding inactivated reference compounds were interpreted as possible signs of covalent binding effects. The experiments were conducted at Marbio/UiT in Tromsø by Marte Albrigtsen. The cell lines Ramos, MV4-11, MOLM-13, and MRC-5 were tested for their sensitivity against the TKI library shown in Table 27. Dasatinib (**255**) was used as a reference and DMSO and sodium trifluoroacetate (NaTFA) as controls. The cells were incubated for 48 h with eight different concentrations (0.1 μM-20 μM) of inhibitor and the cell viability was measured by an MTS-assay. The cell viability was compared to untreated cells. The tests were run at least in triplicate. Only the best inhibitors were further tested in MOLT-4 cells as an additional control.

The cell lines and their expressed kinases:

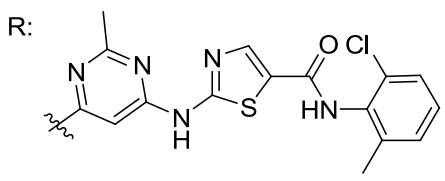
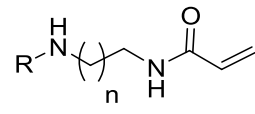
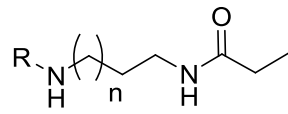
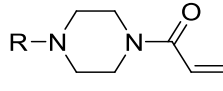
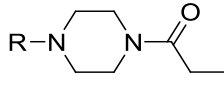
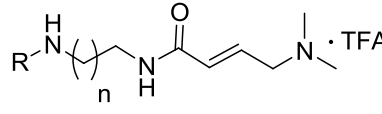
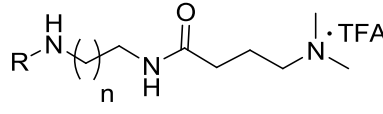
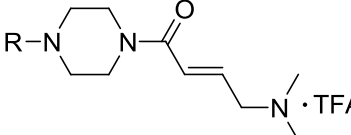
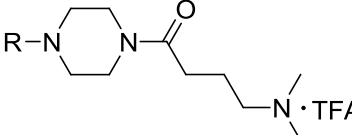
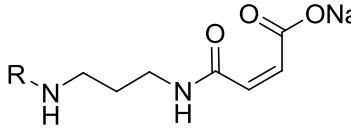
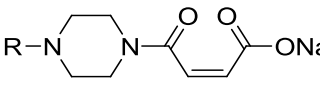
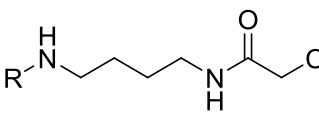
Ramos cells are related to Burkitt's lymphoma and are described as cell lines for the test of covalent BTK-inhibitors in literature.¹⁹⁵ Mv4-11 and MOLM-13 are related to acute myeloid leukemia (AML) and MOLT-4 to acute lymphoblastic leukemia (ALL). The cell growth of MV4-11 is driven by an activated FLT-3 kinase (FLT-3 ITD positive, *internal tandem duplication*) which leads to a continuous growth stimulus and high dependency on an uninhibited FLT3 kinase.¹⁹⁶ MOLM-13 cells carry the FLT-3 ITD mutant but also the wild type allele, which does not necessarily lead to a continuous growth stimulus.¹⁹⁶ Both cell lines are described in context with covalent binding FLT-3 inhibitors in literature.¹⁷⁹ MOLT-4 expresses a lower concentration of FLT-3 than MV-4-11 and was therefore used to assess the results for MOLM-13 and MV4-11 in the context of FLT-3 inhibition.¹⁹⁷ MRC-5 cells (fetal, normal lung fibroblast cells) with no oncogenic expression of specific kinases were used as the cytotoxicity control.

General observations for the references and the compound library:

The full overview of all assay results can be found in the appendix (Figure 59-Figure 64, primary sorted as thiol trap active/inactive pairs). DMSO revealed no relevant influence on the assay results. NaTFA was used to analyse the effect of the counter-ion as some inhibitors were obtained as TFA salts. No relevant effects were detected. The cell lines exhibit different sensitivity for dasatinib (**255**) as a reference compound. A cell viability of 50% or lower was reached with ~5 μM dasatinib for MV-4-11, with ~10 μM for MOLM-13, with >10 μM for MRC-5 and Ramos and ~15 μM for MOLT-4. Only the three compounds **286**, **288** and **295** showed significantly stronger effects on cell viabilities than dasatinib (**255**) in all cell lines (all graphs in the appendix, Figure 59-Figure 64). These compounds will be described and discussed in more detail. The effects on cell viability of all compounds compared to dasatinib (**255**) are summarized in Table 27.

Compounds **19** and **61** at high inhibitor concentrations of 15 and 20 μM possess no relevant activity and were notable weaker in all cell lines in comparison to dasatinib. Weak effects were detected for the dimethylamino crotonic acid amides **292-294**, as well as for the saturated analogs 4-(dimethylamino)butyric acid amides **296-298**, in all cell lines (graphs in the appendix, Figure 59-Figure 64). In most cases, the unsaturated derivatives were stronger than the deactivated analogs. The acrylic acid amides **284** and **285** showed similar or weaker effects. Only in MOLM-13 cells, did **285** show a better effect than dasatinib at high concentrations. The saturated reference compound **289** showed similar or lower efficiencies than dasatinib (**255**) with the exception of in the MRC-5 cell line. Surprisingly, **289** revealed in this cell line a greater effect than dasatinib. An explanation for this can not be given with the conducted analysis (graphs in the appendix, Figure 59-Figure 64).

Table 27: Summary of the finding in the cell based assays. More details in the text and in the appendix (Figure 59-Figure 64).

R: 				
n		effect compared to dasatinib		effect compared to dasatinib
				
1	284	similar or weaker	289	inconclusive
2	285	inconclusive	290	inconclusive
		stronger		similar or weaker
				
1	292	similar or weaker	296	weaker
2	293	weaker	297	weaker
3	294	similar or weaker	298	weaker
		stronger		inconclusive
		weaker		weaker
		stronger		

Observations in the MV4-11 and MOLM-13 cell line:

Compound **295** was the only dimethylamino crotonic acid amide with significantly increased effects in all cell lines in comparison to dasatinib (including MOLT-4). The cell viability curves of **295** have a similar shape for MV4-11 and MOLM-13 cells with slightly lower cell survival rates in MV4-11. The same situation applies to the inactivated derivative **299**. The cell viability values of **295**, **299** and dasatinib (**255**) are shown in Figure 56 (A, B). Cell viability differences of approximately 50% (measured for 2 μ M in MV4-11) between **295** and **299** were reached in these assays.

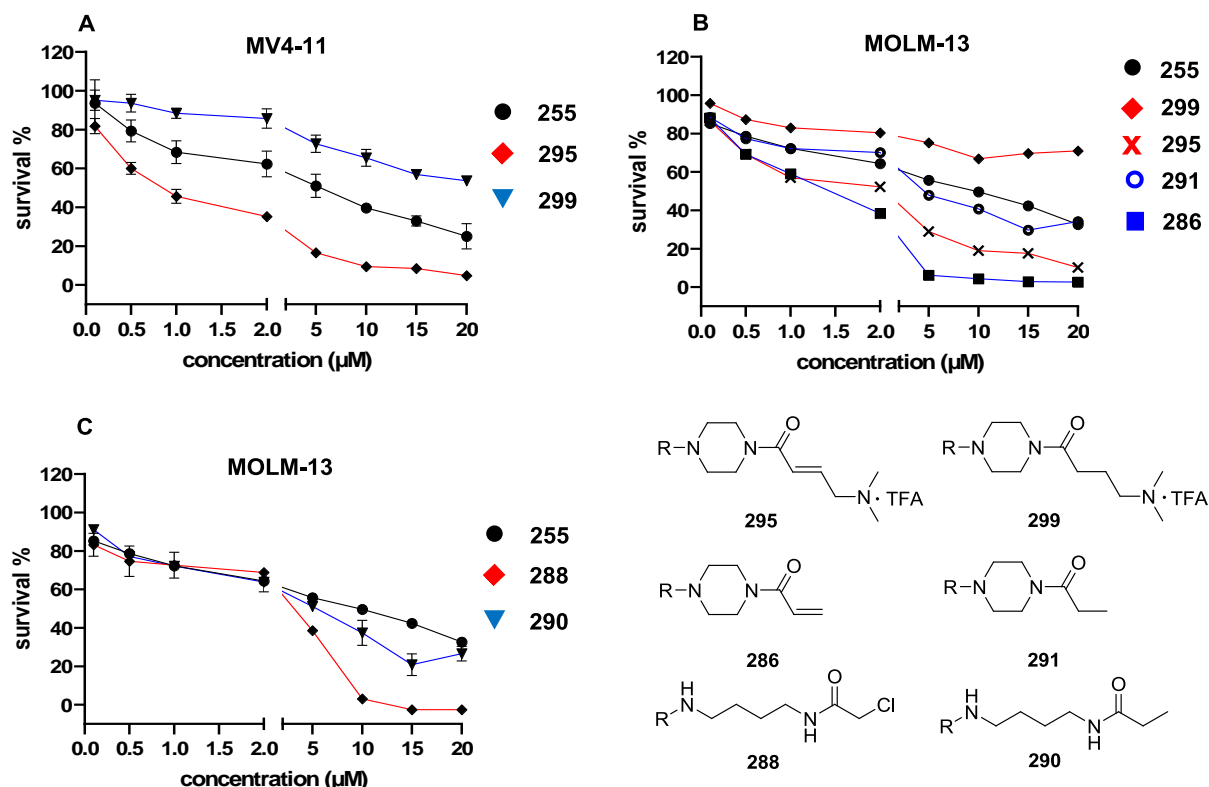


Figure 56: Representative findings of the cell viability assay for the most active compounds **286**, **288**, **295** and their corresponding inactivated analogs **290**, **291**, **299** in MV-4 and MOLM-13. The compounds were measured in triplicate. The reference compound dasatinib (**255**) was measured 3 times in triplicate. More details can be found in the appendix (Figure 59-Figure 64). The figures were made with GraphPad Prism 8.

Compound **286** has the highest structural conformity with dasatinib (**255**). It had markedly lower cell viabilities in MV4-11 and MOLM-13 than dasatinib (**255**) over a broad concentration range (Figure 56 B). The effects were stronger than for **295** and led to full loss of cell survival. The saturated reference compound **291** showed similar effects on cell viability in MOLM-13 and MV4-11 in comparison to dasatinib (**255**). **288** showed a strong effect at high concentrations for both cell lines (Figure 56 C). In comparison to **286** and **295**, the effect is concentration dependent and drops faster, while the two other inhibitors remain superior to dasatinib (**255**). The reference compound **064** showed at higher concentrations a

slightly better effect when compared on the cell viability when compared to dasatinib; in MOLM-13 (Figure 56 C) and in MV4-11 it has almost the same effect as dasatinib (**255**).

Interpretation: A significant cell viability difference between the potential covalent binders **286**, **288**, and **295** and their inactivated analogs as well as to dasatinib (**255**) could be identified. Covalent binding is most likely present. Kinase specific effects for **295** and **286** cannot be excluded, but unspecific covalent binding must be considered in all cases.

Observations in the Ramos cell line:

The noticeable effects on cell viability of compounds **286**, **288** and **295** were not as pronounced in Ramos cells. **295** showed a strong effect on cell viability at high concentrations. Only **288** led to the full loss of viability at high concentrations. Even at 5 μM , **288** had a significantly stronger effect on cell viability than dasatinib (**255**). Compound **286** showed at 6 μM the same efficiency as dasatinib (**255**). The inactivated reference compounds **290**, **291** and **299** showed lower or similar effects to dasatinib (**255**).

Interpretation: The comparison of **286** and **288** with their inactive reference compounds **291** and **299** make covalent binding effects plausible.

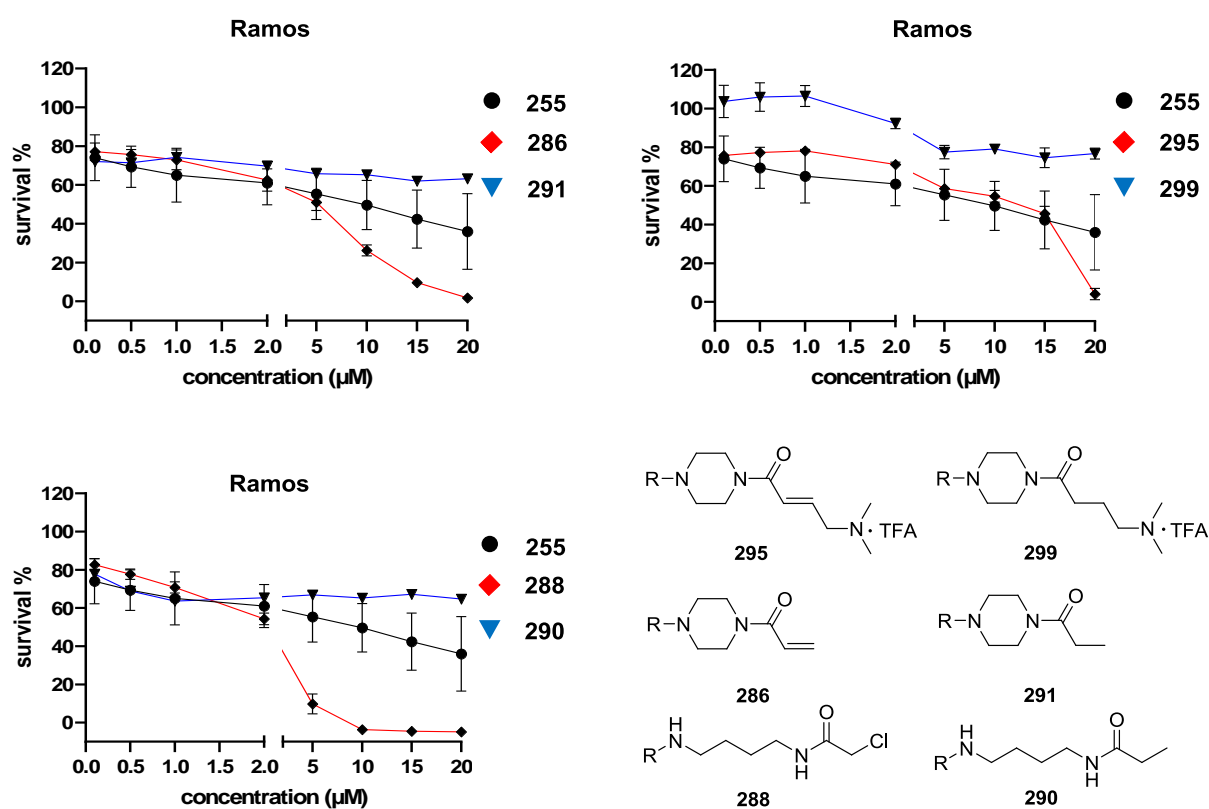


Figure 57: Representative findings of the cell viability assay for the most active compounds **286**, **288**, **295** and their corresponding inactivated analogs **290**, **291**, **299** in Ramos cells. The compounds and dasatinib (**255**) were measured in triplicate. More details can be found in the appendix (Figure 59-Figure 64). The figures were made with GraphPad Prism 8.

Observations in the MRC-5 cell line:

MRC-5 cells were used to determine unspecific effects on cell viability due to the TKI library. With the exception of **289** and **285**, and the three more active compounds **286**, **288** and **295**, no other compound showed any relevant decrease in cell viability when compared to dasatinib (**255**). Compound **288** led to full loss of cell viability in the MRC-5 cell line at high doses. In addition, compound **286** showed decreased cell survival. The effects of **295** were clearly weaker. The negative influence of the compounds **286**, **288** and **295**, when compared to dasatinib, is persistent down to $\sim 1 \mu\text{M}$.

Interpretation: At least compound **288** shows clear cell viability reducing effects, most likely due to unspecific covalent binding because MRC-5 expresses no oncogenic cysteine containing kinase.

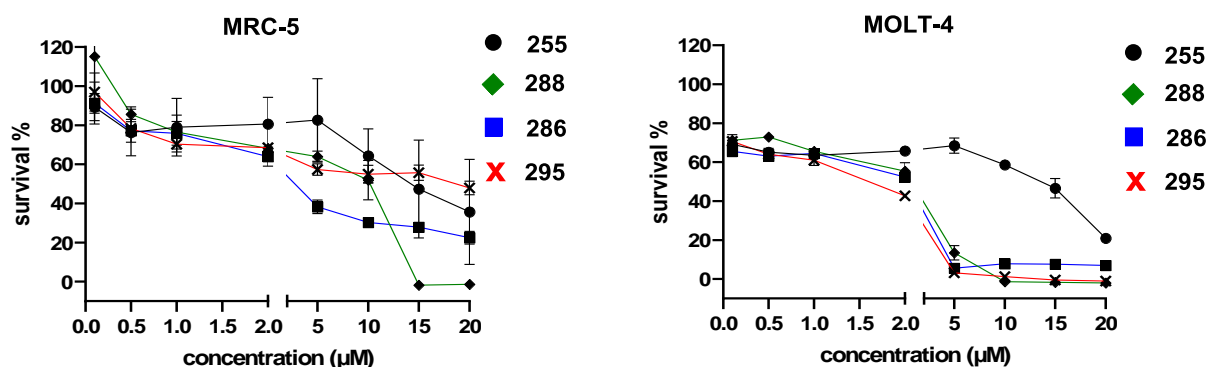


Figure 58: Representative findings of the cell viability assay for the most active compounds **286**, **288**, **295** in MRC-5 and MOLT-4. The compounds and dasatinib (**255**) were measured in triplicate. More details in the appendix (Figure 59-Figure 64). The figures were made with GraphPad Prism 8.

Observations in the MOLT-4 cell line:

The inhibitors **286**, **288** and **295** revealed strongly decreased cell viabilities in MV4-11 and MOLM-13 cells. These compounds were therefore also measured in MOLT-4 cells to evaluate the influence on the FLT-3 kinase. MV4-11 expresses higher amounts of FLT-3, and the cell growth/survival is dependent on FLT-3.¹⁹⁷ MOLT-4 cells express a lower amount of FLT-3 and as a result, are less dependent on this kinase.¹⁹⁷ Surprisingly, the compounds **286**, **288** and **295** exhibited strong influences on the cell viability. Even at 5 μM , cell survival was less than 10%.

286 reached similar values in MOLT-4 compared to those in MOLM-13 and MV4-11. At approximately 1 μM , the activity was comparable with dasatinib (**255**). Compound **299**, an inactivated compound, was measured in MOLT-4 cells (appendix, Figure 59-Figure 64). Even **299** at high doses was slightly more active than dasatinib, but otherwise comparable with dasatinib (**255**). The overall cell viability at the inhibitor concentration of 0.1 μM was lower in this cell line in comparison to other cell lines. Through the limited amount of tests, other reasons for the greatly decreased cell viability in MOLT-4 cannot be excluded.

Interpretation: Strong inhibition over a broad concentration range in comparison to dasatinib (**255**) and to the inactivated compound **299** make covalent binding effects plausible. Possible inhibition of other kinases like the in MOLT-4 cells expressed kinase ITK (interleukin-2-inducible T-cell kinase) must be considered.

9.3.4 Summary and interpretation of the cell assays

The big activity differences between **286**, **288**, and **295** and their inactivated counterparts **291**, **290** and **299**, suggest in parts Michael acceptor or chlorine leaving group related alkylation effects in the cell lines. These effects are most likely not related to specific kinases because decreased cell viability can be observed for different cell lines and different expressed kinases. **288** in particular exhibits a strong cell viability decreasing effect on the control cell line MRC-5. This cell line expresses no oncogenic activated kinases. The reason for reduction of cell viability by **286** and **295** (down to 50%) in MV4-11 and MOLM-13, with approximately 0.5-1.0 μM must be further investigated. **295** showed weaker effects on the Ramos and MRC-5 cell line than **286** and **295** and was more specific for MV4-11 and MOLM-13.

Presuming the effects of **286**, **288**, and **295** would be driven by inhibition of specific kinases in the cell lines; the therapeutic range would be small. Many significant effects were observed at the same concentration range were also strong and unwanted effects on the control cell line MRC-5 were observed. In contrast to known covalent inhibitors for BTK and FLT3, the values are high. The covalent FLT3 inhibitor FF-10101 reaches 50% growth inhibitions (GI_{50}) at 1.1 nM for MOLM-13 and 0.83 nM for MV4-11 after 48 h.¹⁷⁹ Also, the non-covalent inhibitor Quizartinib reaches GI_{50} values of 1.6 nM and 0.95 nM in the cell lines. The covalent BTK inhibitor QL47 reaches GI_{50} of 370 nM in Ramos cells.¹⁹⁵

Not fully understood are the results for MOLT-4. This cell line was planned to be used as control for the MV4-11 and MOLM-13 cell line. Due to lower growth dependency on FLT3, less loss of cell viability in comparison to MV4-11 and MOLM-13 was expected, but **286**, **288** and **295** showed unexpectedly strong effects on cell viability. These results could be related to unspecific covalent binding and possible cytotoxic effects. On the other side, MOLT-4 cells express the BTK related kinase ITK.¹⁹⁸ While BTK is a typical dasatinib

target, ITK is not.¹⁹⁹ ITK is involved in T-cell development and has an accessible cysteine residue and was covalently targeted before.²⁰⁰ Therefore, effects against this target cannot be negated and could be interesting to investigate deeper, for example in a new kinase screening.

10. Project 2: Conclusion

Kinase inhibitor research is still an expanding field and covalent inhibitors are becoming more relevant, especially in cases where there is resistance against approved inhibitors. The use of dasatinib as a template for covalent inhibitors should increase the chance to afford irreversible binding with dasatinib relevant kinases. The first aim of the project was to synthesize the bioactive core of dasatinib as a platform for new potentially covalently binding inhibitors. Based on that, new inhibitors with different linker lengths and rigidity as well as different classes of thiol traps were synthesized. The first two synthesized inhibitors were the acrylamide derivatives **284** and **285**. Affinity studies with different cysteine containing kinases, like KIT and BTK, were concluded with no covalent binding taking place for the both compounds. Another affinity screening, including **284**, **285** and new synthesized compounds for KIT showed even better affinities for a noncovalent inhibitor and were interpreted as most likely no covalent binding for the tested TKI library. The results were in agreement with literature results for the compounds **286** and **295**, when against different kinases including KIT and BTK. Unfortunately, the dependence on external screening platforms, and raised concerns about the right testing conditions, led to problems on how to continue with the project. Possible negative effects of the antioxidants DTT (**302**) on the test results due to possible adduct formation could not be excluded. Literature references draw differing conclusions as to the influence of DTT (**302**) and GSH (**309**) on covalently binding inhibitors/thiol traps. Most likely is that these effects are strongly dependent on the assay conditions and as such, require more control experiments.

The inhibitor library was screened for their influence on the cell viability of a range of different cancer cell lines. To evaluate covalent binding effects in general, more noncovalent binding inhibitors were synthesized to compare with the corresponding potentially covalent binders: this also allowed for the possibility of hits against unexpected kinases. From 17 tested compounds, only three showed stronger effects in reducing the cell viability than dasatinib. The concentrations to reach a 50% reduction of cell viability were generally high, and in many cases an effect only manifested at higher concentrations. Unspecific cytotoxic effects could not be excluded. Potentially interesting effects were seen for **295** and **286** in the MOLM-13 and MV4-11 cells, with noticeably stronger effects at lower concentrations. The results for the MOLT-4 cells were surprising and need further investigation; A kinases specific effect is a possibility that should be explored. Many further possible modifications of dasatinib for new inhibitors are already covered by other research groups. Therefore, it is required to find new relevant kinase targets or to change the project strategy in the future.

11. Experimental section

11.1 General

General:

Solvents and reagents were mainly acquired from the commercial suppliers Merck, AK Scientific, VWR and Combi Blocks and were used without further purification. Dry solvents were bought (DMF) or prepared by drying over molecular sieve. Air and moisture sensitive reactions were performed by using dry solvents in combination with inert gas (nitrogen gas, Schlenk-line). The reactions were conducted under inert atmosphere if not differently stated.

Compound analysis:

Reaction controls were realized by TLC using Silica 60 F254 precoated aluminum sheets from Merck. UV light or stain solutions were used for visualization. Instruments for compound characterization: High resolution mass spectrometry (HRMS-ESI) was conducted by an LTQ Orbitrap XL spectrometer with electrospray ion source ION-MAX (Thermo Scientific, Bremen, Germany). NMR spectra were recorded on a 400 MHz Bruker Avance III HD equipped with a 5mm SmartProbe. The signals shifts were reported in ppm relative to the residual NMR solvent peak. In brackets is shown the multiplicity description (abbreviation, s = singlet, br = broad singlet, d = duplet, dd = doublet of doublets, dt = doublet of triplets, td = triplet of doublets, t = triplet, q = quartet, p = pentet, m = multiplet), the coupling constancies *J* in Hz and the amount of protons. IR-spectra were reported on an Agilent Cary 630 FTIR spectrometer. Compound purity controls were conducted with an Acquity UPLC H class from Waters with BEH C18 1,7µm. 2,1x50nm column and PDA detector at 50 °C column temperature.

Purification:

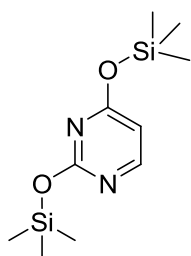
Normal phase flash column purification was conducted with silica (40-63 micrometer) from VWR. Reverse phase purifications were conducted on a Biotage SP1 system ® with a 12 g C18 RP column using 10-100% acetonitril in water gradients with a flow rate of 15 mL/min. The compounds were detected at 254 nm. Samplet ® precolumns were used for sample loading and water-acetonitrile gradients as mobile phase.

Purity: Compounds for biological testing had a purity between 94-100% if not differently stated.

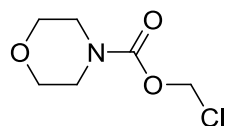
11.2 Supporting information project 1

11.2.1 Uracil building block synthesis

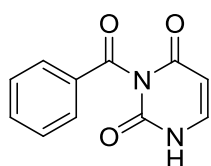
2,4-Bis(trimethylsilyloxy)pyrimidine (33). **33** was synthesized based on literature procedures.⁸¹⁻⁸³ The Product is highly unstable. **Method A:** Uracil (0.043 g, 0.38 mmol) was dissolved in dry MeCN (0.5 mL). BSA (0.24 mL, 1.68 mmol) was added and the mixture was heated to 70 °C until the uracil went into solution. The solvent and the reagent were removed under vacuum and the crude product was used directly. **Method B:** Uracil (0.280 g, 2.50 mmol) and a catalytic amount ammonium sulfate (7 mg) were dissolved in HMDS (6 mL) under inert gas and heated to reflux overnight. The volatiles were removed under reduced pressure and the crude product was used without further purification.



Chloromethyl morpholine-4-carboxylate (76). **76** was synthesized based on a literature procedure.¹⁰⁷ A stirred mixture of morpholine (0.98 mL, 11.23 mmol) and DIPEA (1.96 mL, 11.23 mmol) in DCM (5 mL) was cooled to 0 °C. Chloromethyl chloroformate (**77**) (1.00 mL, 11.23 mmol) was added dropwise. The reaction mixture was allowed to warm to room temperature and stirred overnight. Water was added to the solution and the mixture extracted with DCM (3x). The combined organic layers were washed with water (1x) and brine (1x) and further dried over Na₂SO₄. The solvent was removed under reduced pressure affording **76** (1.96 g, 10.91 mmol, 97%) as colorless liquid. ¹H NMR (400 MHz, CDCl₃) δ 5.79 (s, 2H), 3.73 – 3.62 (m, 4H), 3.56 – 3.47 (m, 4H). ¹³C NMR (101 MHz, CDCl₃) δ 152.8, 71.0, 66.6, 66.5, 44.6, 44.3.

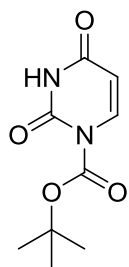


3-Benzoylpyrimidine-2,4(1H,3H)-dione (N³-benzoyl-uracil) (53). The compound **53** was synthesized based on published procedures.⁸⁶⁻⁸⁹ Benzoyl bromide (12.5 mL, 107.7 mmol) was added to a stirred suspension of uracil (5.0 g, 44.6 mmol) in dry acetonitrile (15 mL) and dry pyridine (9 mL) at 0 °C. The yellow suspension was allowed to warm to room temperature and stirred for 22 h. The reaction mixture was concentrated and afterwards mixed with water (100 mL) and DCM (20 mL). The aqueous layer was neutralized with saturated Na₂CO₃ solution and the resulting white suspension was stirred for 1h. The solid was filtered off and washed with water. The crude product was recrystallized from 96% ethanol. **53** (4.81 g, 22.2 mmol, 50%) was obtained as white solid. **R_f**: 0.31 (EtOAc): ¹H NMR (400 MHz, DMSO-*d*₆) δ 11.60 (s, 1H), 7.95 (d, *J* = 7.2 Hz, 2H), 7.78 (t, *J* = 7.4 Hz, 1H), 7.66 (d, *J* = 7.7 Hz, 1H), 7.60 (t, *J* = 7.7 Hz, 2H), 5.74 (d, *J* = 7.7 Hz, 1H). ¹³C NMR (101 MHz, DMSO-*d*₆) δ 170.0, 162.9, 150.1, 143.3, 135.4, 131.3, 130.2, 129.5, 100.1. **FTIR** (neat): 3324, 3219, 3182, 3085,

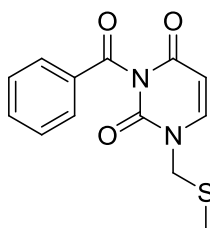


2970, 2888, 1707, 1652, 1629, 1599, 1417, 1231, 1212, 1182, 937, 788, 765, 680 cm^{-1} .
HRMS (ESI): calculated for $\text{C}_{11}\text{H}_8\text{N}_2\text{O}_3\text{Na}$ $[\text{M}+\text{Na}]^+$ 239.0427; found: 239.0428.

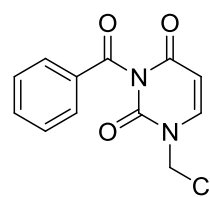
tert-Butyl 2,4-dioxo-3,4-dihydropyrimidine-1(2H)-carboxylate (59). **59** was synthesized based on literature procedures.^{99,201} Di-*tert*-butyl dicarbonate (6.55g, 30.0 mmol) and 4-dimethylaminopyridine (0.30 mmol) were added to a suspension of uracil (**49**) (3.36g, 30.0 mmol) in dry acetonitrile (200 mL) at room temperature. The resulting suspension was stirred overnight. The solution was concentrated *in vacuo* to afford **59** (quantitative) as white solid. **59** was used without further purification. **R_f**: 0.51 (EtOAc). **¹H NMR** (400 MHz, $\text{DMSO-}d_6$) δ 11.43 (bs, 1H), 7.89 (d, $J = 8.3$ Hz, 1H), 5.70 (d, $J = 8.3$ Hz, 1H), 1.52 (s, 9H). **¹³C NMR** (101 MHz, $\text{DMSO-}d_6$) δ 162.8, 148.0, 147.4, 140.3, 103.1, 85.6, 39.5, 27.3. **HRMS** (ESI): calculated for $\text{C}_9\text{H}_{12}\text{N}_2\text{O}_4\text{Na}$ $[\text{M}+\text{Na}]^+$ 235.0689; found: 235.0688.



3-Benzoyl-1-(methylthiomethyl)pyrimidine-2,4(1H,3H)-dione (55). Chloromethyl methyl sulfide (0.80 mL, 9.6 mmol) was added to a suspension of *N*³-benzoyl uracil (**53**) (1,730 g, 8.0 mmol) and K_2CO_3 (1.327 g, 9.6 mmol) in dry DMF (8 mL) at 0 °C. The reaction mixture was allowed to warm to room temperature and was stirred overnight. The suspension was concentrated and the resulting residue was mixed with water and EtOAc. The water layer was extracted with EtOAc (3x) and the combined organic layers washed with water (2x) and brine (1x). The solvent was removed under reduced pressure after predrying over Na_2SO_4 . The crude product was purified by silica column chromatography (pure DCM). The product **55** (1.930 g, 6.98 mmol, 87%) was obtained as colorless wax. **R_f**: 0.57 (EtOAc). **¹H NMR** (400 MHz, CDCl_3) δ 7.97 – 7.90 (m, 2H), 7.71 – 7.62 (m, 1H), 7.57 – 7.43 (m, 3H), 5.92 (d, $J = 8.1$ Hz, 1H), 4.86 (s, 2H), 2.22 (s, 3H). **¹³C NMR** (101 MHz, CDCl_3) δ 168.6, 162.1, 150.2, 142.6, 135.3, 131.5, 130.6, 129.4, 103.5, 51.2, 15.0. **HRMS** (ESI): calculated for $\text{C}_{13}\text{H}_{12}\text{N}_2\text{O}_3\text{SNa}$ $[\text{M}+\text{Na}]^+$ 299.0461; found: 299.0465.

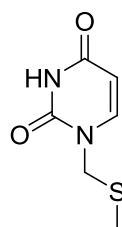


3-Benzoyl-1-(chloromethyl)pyrimidine-2,4(1H,3H)-dione (52). **52** (0.276 g, 1.00 mmol) was dissolved in dry DCM (2 mL) and cooled to -78 °C. Sulfuryl chloride solution (2.0 mL, 2.00 mL, 1M solution in DCM) was added dropwise and the reaction mixture was allowed to warm to room temperature. The reaction was stirred for 1 h and then concentrated under reduced pressure. The crude was further purified by a silica filter column with EtOAc. **52** (0.180 g, 0.68 mmol, 68%) was obtained as a colorless gum. **¹H NMR** (400 MHz, CDCl_3) δ 7.97 – 7.89 (m, 2H), 7.72 – 7.63 (m, 1H), 7.56 – 7.48 (m, 2H), 7.39 (d, $J = 8.1$ Hz, 1H), 5.96

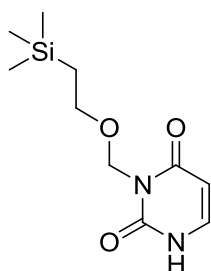


(d, $J = 8.1$ Hz, 1H), 5.54 (s, 2H). ^{13}C NMR (101 MHz, CDCl_3) δ 167.9, 161.7, 148.7, 142.2, 135.5, 131.2, 130.7, 129.4, 104.8, 55.2.

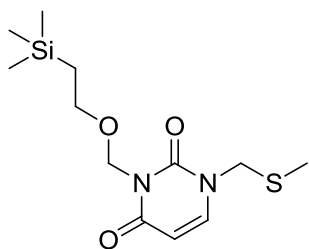
1-(Methylthiomethyl)pyrimidine-2,4(1H,3H)-dione (81). **80** (1.271 g, 4.60 mmol) was dissolved in dry DCM (10 mL). 7 N NH_3/MeOH (1 mL) was added at 0 °C. The solution was allowed to warm to room temperature and was stirred overnight. The reaction mixture was concentrated and the crude solid product washed with chloroform. The obtained filtrate was concentrated again and the solid washed with MeOH. The solids were combined and dried. The product **81** (0.497 g, 2.89 mmol, 63%) was obtained as a white solid. R_f : 0.31 (EtOAc). ^1H NMR (400 MHz, $\text{DMSO}-d_6$) δ 11.35 (bs, 1H), 7.71 (d, $J = 7.9$ Hz, 1H), 5.63 (d, $J = 7.8$ Hz, 1H), 4.83 (s, 2H), 2.14 (s, 3H). ^{13}C NMR (101 MHz, $\text{DMSO}-d_6$) δ 163.5, 150.7, 144.6, 101.6, 50.2, 14.1. FTIR (neat): 3149, 3093, 3022, 2869, 2821, 1670, 1633, 1424, 1383, 832, 762 cm^{-1} . HRMS (ESI): calculated $\text{C}_6\text{H}_9\text{N}_2\text{O}_2\text{S}$ for $[\text{M}+\text{H}]^+$ 173.0379; found: 173.0379.



3-((2-(Trimethylsilyl)ethoxy)methyl)pyrimidine-2,4(1H,3H)-dione (60). **60** was synthesized based on a literature procedure.⁹⁹ Sodium hydride (60% dispersion in mineral oil, 0.396 g, 9.90 mmol) was added in portions to a stirred solution of N^1 -Boc-uracil (**59**) (2.00 g, 9.40 mmol) in dry DMF (15 mL at 0 °C. The suspension was stirred for 30 minutes at 0 °C. 2-(Trimethylsilyl)ethoxymethyl chloride (2.0 mL, 11.3 mmol) was added slowly. The reaction mixture was stirred for 2 h at room temperature. The reaction was quenched with MeOH and the solvents were removed under reduced pressure. K_2CO_3 (1.30 g, 9.40 mmol) and MeOH (50 mL) were added to the residue and the mixture was stirred overnight at room temperature. The solvent was removed under reduced pressure. Water was added to the residue and the aqueous layer extracted with EtOAc (3x). The combined organic layers were washed with brine (1x) and were further dried over Na_2SO_4 . The solvent was removed under reduced pressure. The obtained solid was washed with pentane to afford **60** (1.777 g, 7.33 mmol, 78%) as white solid. R_f : 0.37 (EtOAc). ^1H NMR (400 MHz, $\text{DMSO}-d_6$) δ 11.13 (bs, 1H), 7.45 (d, $J = 7.5$ Hz, 1H), 5.59 (d, $J = 7.6$ Hz, 1H), 5.16 (s, 2H), 3.61 – 3.52 (m, 2H), 0.88 – 0.78 (m, 2H), -0.04 (s, 9H). ^{13}C NMR (101 MHz, $\text{DMSO}-d_6$) δ 163.1, 151.5, 141.5, 99.8, 68.6, 66.2, 17.5, -1.3. FTIR (neat): 3238, 3178, 3111, 2955, 2899, 1711, 1655, 1428, 1216, 1074, 866, 832, 773 cm^{-1} . HRMS (ESI): calculated for $\text{C}_{10}\text{H}_{18}\text{N}_2\text{O}_3\text{SiNa}$ $[\text{M}+\text{Na}]^+$ 265.0979; found: 265.0981.



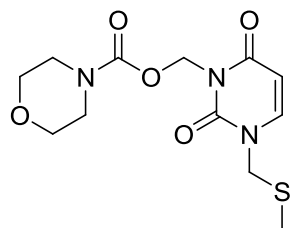
1-(Methylthiomethyl)-3-((2-(trimethylsilyl)ethoxy)methyl)pyrimidine-2,4(1H,3H)-dione



(58). Chloromethyl methyl sulfide (0.6 mL, 6.90 mmol) was added to a stirred suspension of **60** (1.400 g, 5.75 mmol) and K_2CO_3 (0.875 g, 6.33 mmol) in dry DMF (8 mL) at 0°C. The reaction mixture was allowed to warm to room temperature and was stirred overnight. The suspension was concentrated under reduced pressure and the residue was purified by a silica column chromatography.

The product **58** (1.500 g, 4.96 mmol, 86%) was obtained as a colorless gum. R_f : 0.69 (EtOAc). 1H NMR (400 MHz, $CDCl_3$) δ 7.33 (d, J = 8.0 Hz, 1H), 5.83 (d, J = 8.0 Hz, 1H), 5.40 (s, 2H), 4.84 (s, 2H), 3.73 – 3.64 (m, 2H), 2.19 (s, 3H), 1.02 – 0.91 (m, 2H), -0.01 (s, 9H). ^{13}C NMR (101 MHz, $CDCl_3$) δ 162.7, 152.0, 141.5, 103.1, 70.4, 67.8, 51.7, 18.3, 14.9, -1.3. HRMS (ESI): calculated for $C_{12}H_{22}N_2O_3SSiNa$ $[M+Na]^+$ 325.1013; found: 325.1019.

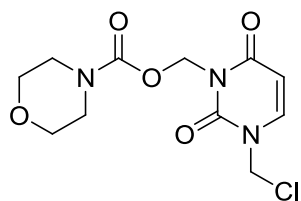
(3-(Methylthiomethyl)-2,6-dioxo-2,3-dihydropyrimidin-1(6H)-yl)methyl morpholine-4-carboxylate (72)



76 (0.332 g, 2.40 mmol) was added to a suspension of **81** (0.344 g, 2.00 mmol) and K_2CO_3 (0.395 g, 2.20 mmol) in dry DMF (4 mL) at 0 °C. The mixture was allowed to warm to room temperature and was stirred overnight. EtOAc and water were added and the aqueous layer extracted (3x). The combined organic layers were washed with water (1x) and brine (1x)

and were dried over Na_2SO_4 . The solvent was removed under reduced pressure. **72** (0.485 g, 1.54 mmol, 77%) was obtained as a colorless gum which solidified to a white solid after a while. R_f : 0.23 (EtOAc). 1H NMR (400 MHz, $CDCl_3$) δ 7.36 (d, J = 8.1 Hz, 1H), 6.00 (s, 2H), 5.84 (d, J = 8.0 Hz, 1H), 4.84 (s, 2H), 3.74 – 3.53 (m, 4H), 3.54 – 3.33 (m, 4H), 2.19 (s, 3H). ^{13}C NMR (101 MHz, $CDCl_3$) δ 161.8, 153.9, 151.3, 141.9, 102.9, 66.6, 65.6, 51.9, 44.0, 15.0. FTIR (neat): 3089, 2970, 2921, 2862, 1693, 1663, 1436, 1354, 1238, 1220, 1115, 1074, 966, 769 cm^{-1} . HRMS (ESI): calculated for $C_{12}H_{17}N_3O_5SNa$ $[M+Na]^+$ 338.0781; found: 338.0784.

(3-(Chloromethyl)-2,6-dioxo-2,3-dihydropyrimidin-1(6H)-yl)methyl morpholine-4-carboxylate (70)



Sulfuryl chloride (1M in DCM, 4 mL, 4 mmol) was added dropwise to a solution of **72** (0.640 g, 2.00 mmol) in dry DCM (4 mL) at -78 °C. The solution was allowed to warm to room temperature. The solvent was removed after 1 h. The crude product was purified by silica column chromatography (EtOAc). The

product **70** (0.510 g, 1.68 mmol, 84%) was obtained as white solid. 1H NMR (400 MHz, $CDCl_3$) δ 7.29 (d, J = 8.1 Hz, 1H), 6.01 (s, 2H), 5.91 (d, J = 8.0 Hz, 1H), 5.54 (s, 2H), 3.74 – 3.54 (m, 4H), 3.54 – 3.30 (m, 4H). ^{13}C NMR (101 MHz, $CDCl_3$) δ 161.2, 153.7, 149.8, 141.2, 104.3, 66.5, 65.4, 55.9, 44.0. FTIR (neat): 3089, 2966, 2925, 2866, 1711, 1678, 1439, 1235,

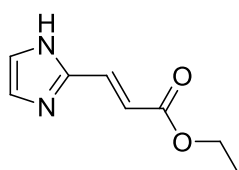
1119, 1082, 773 cm^{-1} . **HRMS** (ESI): calculated for $\text{C}_{11}\text{H}_{14}\text{ClN}_3\text{O}_5\text{Na}$ $[\text{M}+\text{Na}]^+$ 326.0514; found: 326.0516.

11.2.2 Synthesis discussed in section 4.2

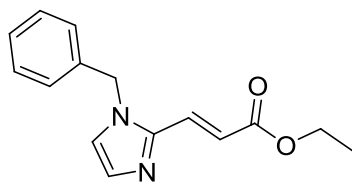
General procedure A: Alkylation of (*E*)-ethyl 3-(1*H*-imidazol-2-yl)acrylate

A stirred suspension of (*E*)-ethyl 3-(1*H*-imidazol-2-yl)acrylate (**34**) (1.0 eq.) and K_2CO_3 (1.2 eq.) in dry DMF (0.8 mL per mmol) was cooled to 0 °C. The alkyl halide (1.05 eq.) was added dropwise or in portions over 2 minutes. After completion, the reaction mixture was allowed to warm to room temperature and was stirred overnight. The suspension was concentrated under reduced pressure and the residue was diluted with water and extracted with DCM (3x). The combined organic layers were washed with water and brine and dried over Na_2SO_4 . The solvent was removed under reduced pressure. The crude product was purified by silica column chromatography (EtOAc).

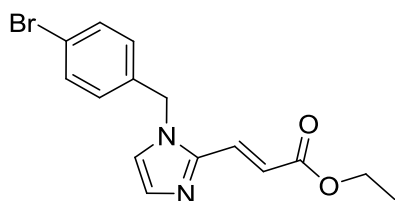
(*E*)-Ethyl 3-(1*H*-imidazol-2-yl)acrylate (34**).** **34** was synthesized according to a literature procedure of Leclaire et al.⁷⁶ 1*H*-imidazole-2-carbaldehyde (8.65 g, 90.0 mmol) was suspended in dry THF (50 mL). A suspension of (Carbomethoxymethylene)triphenylphosphorane (34.47 g, 98.9 mmol) in dry THF (250 mL) was added at room temperature over 5 minutes. The mixture was refluxed for 36 h and the solvent was removed under reduced pressure. The solid residue was washed with cold DCM to obtain **34** (7.52 g, 45.3 mmol, 50 %) as grey-white solid. **R_f**: 0.29 (EtOAc). **¹H NMR** (400 MHz, CD_3OD) δ 7.49 (d, $J = 16.0$ Hz, 1H), 7.21 (s, 2H), 6.59 (d, $J = 16.0$ Hz, 1H), 4.26 (q, $J = 7.1$ Hz, 2H), 1.33 (t, $J = 7.1$ Hz, 3H). **¹³C NMR** (101 MHz, CD_3OD) δ 168.1, 144.4, 132.6, 120.4, 61.9, 14.6. (imidazole CH carbons not visible). **FTIR** (neat): 3115, 2981, 2880, 2750, 2698, 2609, 1711, 1648, 1194, 1119, 970, 750 cm^{-1} . **HRMS** (ESI): calculated for $\text{C}_8\text{H}_{11}\text{N}_2\text{O}_2$ $[\text{M}+\text{H}]^+$ 167.0815; found: 167.0815.



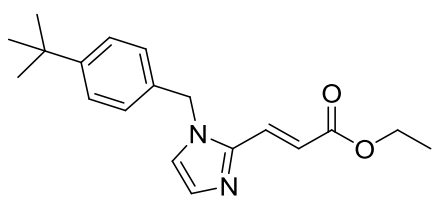
(E)-Ethyl 3-(1-(benzyl-1*H*-imidazol-2-yl)acrylate (36). The synthesis of **36** was conducted according to general procedure A with **34** (2.310 g, 13.90 mmol) and benzyl bromide (1.74 mL, 14.60 mmol). The product **36** (2.900 g, 11.30 mmol, 81%) was obtained as an orange oil. **R_f**: 0.44 (EtOAc). **¹H NMR** (400 MHz, CD₃OD) δ 7.58 (d, *J* = 15.6 Hz, 1H), 7.41 – 7.26 (m, 4H), 7.21 – 7.13 (m, 3H), 6.67 (d, *J* = 15.6 Hz, 1H), 5.40 (s, 2H), 4.22 (q, *J* = 7.1 Hz, 2H), 1.29 (t, *J* = 7.1 Hz, 3H). **¹³C NMR** (101 MHz, CD₃OD) δ 168.0, 144.0, 137.9, 130.6, 130.1, 129.7, 129.2, 127.9, 125.1, 121.8, 61.9, 50.7, 14.5. **HRMS** (ESI): calculated for C₁₅H₁₆N₂O₂Na [M+Na]⁺ 279.1104; found: 279.1104.



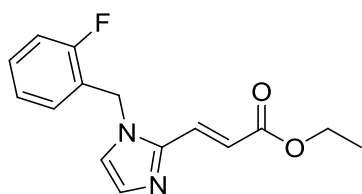
(E)-Ethyl 3-(1-(4-bromobenzyl)-1*H*-imidazol-2-yl)acrylate (39). The synthesis of **39** was conducted according to general procedure A with **34** (0.997 g, 6.00 mmol) and 4-bromobenzyl bromide (1.575 g, 6.30 mmol). The product **39** (1.491 g, 4.45 mmol, 74%) was obtained as a yellow solid. **R_f**: 0.43 (EtOAc). **¹H NMR** (400 MHz, CD₃OD) δ 7.60 – 7.49 (m, 3H), 7.36 (s, 1H), 7.18 (s, 1H), 7.13 – 7.06 (m, 2H), 6.69 (d, *J* = 14.7 Hz, 1H), 5.39 (s, 2H), 4.23 (q, *J* = 7.1 Hz, 2H), 1.30 (t, *J* = 6.7 Hz, 3H). **¹³C NMR** (101 MHz, CD₃OD) δ 167.9, 144.0, 137.3, 133.2, 130.7, 129.9, 129.5, 125.0, 123.0, 122.1, 61.9, 50.0, 14.5. **FTIR** (neat): 3108, 2981, 2940, 1704, 1640, 1305, 1264, 1164, 1015, 970, 739 cm⁻¹. **HRMS** (ESI): calculated for C₁₅H₁₆BrN₂O₂ [M+H]⁺ 335.0390; found: 335.0393.



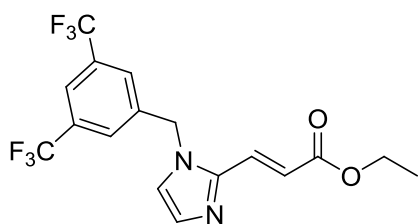
(E)-Ethyl 3-(1-(4-*tert*-butylbenzyl)-1*H*-imidazol-2-yl)acrylate (41). The synthesis of **41** was conducted according to general procedure A with **34** (0.997 g, 6.00 mmol) and 4-*tert*-butylbenzyl bromide (1.16 mL, 6.3 mmol). The product **41** (1.292 g, 4.13 mmol, 69%) was obtained as a white solid. **R_f**: 0.47 (EtOAc). **¹H NMR** (400 MHz, CDCl₃) δ 7.53 (d, *J* = 15.4 Hz, 1H), 7.40 – 7.32 (m, 2H), 7.19 (d, *J* = 1.1 Hz, 1H), 7.07 – 6.96 (m, 3H), 6.85 (d, *J* = 15.4 Hz, 1H), 5.20 (s, 2H), 4.24 (q, *J* = 7.1 Hz, 2H), 1.35 – 1.26 (m, 12H). **¹³C NMR** (101 MHz, CDCl₃) δ 167.0, 151.6, 143.2, 132.8, 130.7, 128.4, 126.7, 126.2, 122.8, 121.3, 60.8, 49.6, 34.7, 31.4, 14.4. **FTIR** (neat): 2970, 2907, 2873, 1696, 1633, 1264, 1171, 1112, 978, 866, 747 cm⁻¹. **HRMS** (ESI): calculated for C₁₉H₂₅N₂O₂ [M+H]⁺ 313.1911; found: 313.1916.



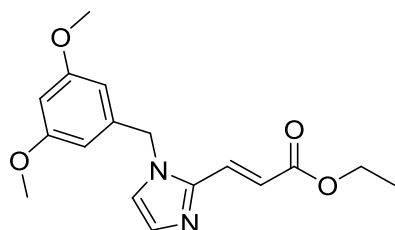
(E)-Ethyl 3-(1-(2-fluorobenzyl)-1H-imidazol-2-yl)acrylate (40). The synthesis of **40** was conducted according to general procedure A with **Z** (0.997 g, 6.00 mmol) and 2-fluorobenzyl bromide (0.76 mL, 6.30 mmol). The product **40** (1.068 g, 3.89 mmol, 65%) was obtained as a white solid. R_f : 0.49 (EtOAc). $^1\text{H NMR}$ (400 MHz, CDCl_3) δ 7.55 (d, $J = 15.4$ Hz, 1H), 7.36 – 7.28 (m, 1H), 7.22 – 7.18 (m, 1H), 7.15 – 7.06 (m, 2H), 7.05 – 7.00 (m, 1H), 6.94 (td, $J = 7.5, 1.8$ Hz, 1H), 6.87 (d, $J = 15.4$ Hz, 1H), 5.27 (s, 2H), 4.24 (q, $J = 7.1$ Hz, 2H), 1.31 (t, $J = 7.1$ Hz, 3H). $^{13}\text{C NMR}$ (101 MHz, CDCl_3) δ 166.9, 160.3 (d, 247 Hz), 143.1, 130.7, 130.6 (d, 8 Hz), 129.0 (d, 4 Hz), 127.9, 125.0 (d, 4Hz), 123.1 (d, 15 Hz), 122.7, 121.8, 116.0 (d, 21 Hz), 60.8, 43.8 (d, 4 Hz), 14.4. **FTIR** (neat): 3104, 3000, 2951, 2903, 1700, 1648, 1477, 1305, 1216, 1175, 1119, 1037, 966, 765, 747 cm^{-1} . **HRMS** (ESI): calculated for $\text{C}_{15}\text{H}_{16}\text{FN}_2\text{O}_2$ $[\text{M}+\text{H}]^+$ 275.1190; found: 275.1194.



(E)-Ethyl 3-(1-(3,5-bis(trifluoromethyl)benzyl)-1H-imidazol-2-yl)acrylate (37). The synthesis of **37** was conducted according to general procedure A with **34** (0.997 g, 6.00 mmol) and 3,5-bis(trifluoromethyl)benzyl bromide (1.32 mL, 6.30 mmol). The product **37** (1.770 g, 4.51 mmol, 75%) was obtained as pale yellow solid. R_f : 0.54 (EtOAc). $^1\text{H NMR}$ (400 MHz, CDCl_3) δ 7.85 (s, 1H), 7.49 (bs, 2H), 7.41 (d, $J = 15.4$ Hz, 1H), 7.29 (d, $J = 1.2$ Hz, 1H), 7.02 (d, $J = 1.2$ Hz, 1H), 6.89 (d, $J = 15.4$ Hz, 1H), 5.38 (s, 2H), 4.24 (q, $J = 7.1$ Hz, 2H), 1.30 (t, $J = 7.1$ Hz, 3H). $^{13}\text{C NMR}$ (101 MHz, CDCl_3) δ 166.7, 143.2, 138.6, 132.9 (q, 34 Hz), 131.7, 127.2, 126.8 (m), 123.0 (q, 273 Hz), 122.8 (m), 122.7 (m), 122.4, 61.0, 48.8, 14.3. **FTIR** (neat): 3137, 3111, 1991, 1907, 1693, 1279, 1264, 1175, 1130, 1048, 989, 750, 687 cm^{-1} . **HRMS** (ESI): calculated for $\text{C}_{17}\text{H}_{15}\text{F}_6\text{N}_2\text{O}_2$ $[\text{M}+\text{H}]^+$ 393.1032; found: 393.1032.



(E)-Ethyl 3-(1-(3,5-dimethoxybenzyl)-1H-imidazol-2-yl)acrylate (38). The synthesis of **38** was conducted according to general procedure A with **34** (0.997 g, 6.00 mmol) and 3,5-dimethoxybenzyl bromide (1.456 g, 6.30 mmol). The product **38** (1.330 g, 4.20 mmol, 70%) was obtained as a white solid. R_f : 0.37 (EtOAc). $^1\text{H NMR}$ (400 MHz, CDCl_3) δ 7.47 (d, $J = 15.4$ Hz, 1H), 7.19 – 7.16 (m, 1H), 7.00 – 6.98 (m, 1H), 6.82 (d, $J = 15.4$ Hz, 1H), 6.36 (t, $J = 2.2$ Hz, 1H), 6.19 (d, $J = 2.3$ Hz, 2H), 5.13 (s, 2H), 4.21 (q, $J = 7.1$ Hz, 2H), 3.72 (s, 6H), 1.28 (t, $J = 7.2$ Hz, 3H). $^{13}\text{C NMR}$ (101 MHz, CDCl_3) δ 166.9, 161.5, 143.1, 138.1, 130.6, 128.3, 122.9, 121.3, 104.9, 99.9, 60.7, 55.4, 49.8, 14.3. **FTIR** (neat): 3134, 3115, 3033,

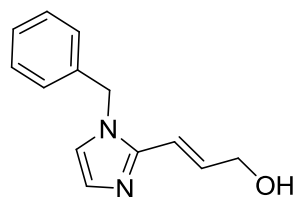


3007, 2977, 2948, 2843, 1693, 1596, 1264, 1208, 1149, 1048, 992, 832, 788, 747 cm^{-1} .
HRMS (ESI): calculated for $\text{C}_{17}\text{H}_{21}\text{N}_2\text{O}_4$ $[\text{M}+\text{H}]^+$ 317.1496; found: 317.1503.

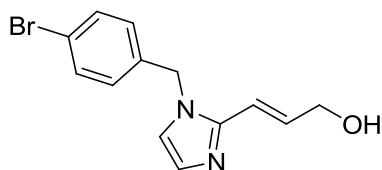
General procedure B: DIBAL-H reduction of alkylated (*E*)-ethyl 3-(1*H*-imidazol-2-yl)acrylates

Substituted (*E*)-ethyl 3-(1*H*-imidazol-2-yl)acrylate was dissolved in dry DCM and was cooled to -78°C . 1M DIBAL-H in DCM (2.2 eq.) was added dropwise (5 minutes) to the solution. The reaction mixture was allowed to warm to room temperature and was stirred for 2 h. The DIBAL-H excess was quenched with a small amount of MeOH (1-2ml). Saturated Rochelle-salt solution was added and the mixture was stirred overnight. The aqueous layer was extracted with DCM (3x). The combined organic layers were washed with brine (1x) and dried over Na_2SO_4 . The solvent was removed under reduced pressure. The residue was purified by silica column chromatography (DCM:MeOH).

(*E*)-3-(1-(benzyl-1*H*-imidazol-2-yl)prop-2-en-1-ol (42). **36** (1.985 g, 7.74 mmol) was dissolved in dry DCM (50 mL) and was cooled to -78°C . 1M DIBAL-H in DCM (17 mL, 17.00 mmol) was added dropwise (5 minutes) to the solution. The reaction mixture was allowed to warm to room temperature after 20 minutes and was stirred for 3.5 h. The DIBAL-H excess was quenched with MeOH and saturated Rochelle-salt solution (40 mL) was added. The mixture was stirred overnight and the aqueous layer was extracted with DCM (3x). The organic layers were washed with brine (1x) and dried over Na_2SO_4 . The solvent was removed under reduced pressure. The residue was purified by column chromatography (DCM:MeOH 9:1). The product **42** (1.070 g, 4.99 mmol, 65%) was obtained as a yellow oil. **R_f**: 0.43 (DCM:MeOH 9:1). **¹H NMR** (400 MHz, CD_3OD) δ 7.39 – 7.25 (m, 3H), 7.17 – 7.10 (m, 3H), 7.00 (s, 1H), 6.75 – 6.56 (m, 2H), 5.28 (s, 2H), 4.23 (d, $J = 4.4$ Hz, 2H). **¹³C NMR** (101 MHz, CD_3OD) δ 146.5, 138.4, 136.2, 129.9, 128.9, 128.6, 127.9, 122.3, 115.9, 62.8, 50.3. **HRMS** (ESI): calculated for $\text{C}_{13}\text{H}_{15}\text{N}_2\text{O}$ $[\text{M}+\text{H}]^+$ 215.1179; found: 215.1182.

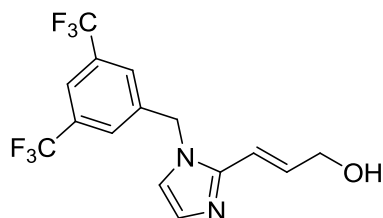


(*E*)-3-(1-(4-Bromobenzyl)-1*H*-imidazol-2-yl)prop-2-en-1-ol (45) The synthesis of **45** was conducted according to general procedure B with **39** (0.335 g, 1.00 mmol). The product **45** (0.214 g, 0.73 mmol, 73%) was obtained as a yellow solid. **R_f**: 0.17 (EtOAc:MeOH 9:1). **¹H NMR** (400 MHz, CDCl_3) δ 7.49 – 7.40 (m, 2H), 7.05 (d, $J = 1.3$ Hz, 1H), 6.96 – 6.89 (m, 2H), 6.87 – 6.77 (m, 2H), 6.47 (dt, $J = 15.5, 2.0$ Hz, 1H), 5.08 (s, 2H), 4.30 (dd, $J = 4.7, 2.0$ Hz, 2H), 3.17 (bs, 1H). **¹³C NMR** (101 MHz, CDCl_3) δ 145.3,



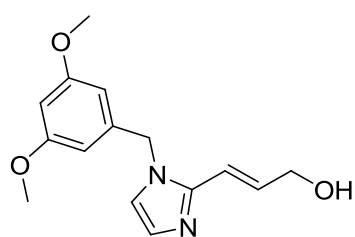
136.1, 135.4, 132.3, 128.7, 128.4, 122.2, 120.5, 114.5, 62.5, 49.0. **FTIR** (neat): 3115, 3175, 3137, 2840, 1436, 1287, 1078, 1015, 996, 799, 743, 691 cm^{-1} . **HRMS** (ESI): calculated for $\text{C}_{13}\text{H}_{14}\text{BrN}_2\text{O}$ $[\text{M}+\text{H}]^+$ 293.0284; found: 293.0290.

(E)-3-(1-(3,5-Bis(trifluoromethyl)benzyl)-1H-imidazol-2-yl)prop-2-en-1-ol (43). The



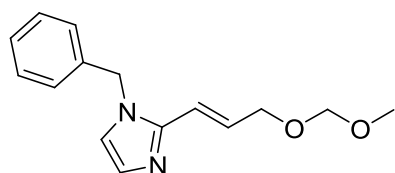
synthesis of **43** was conducted according to general procedure B with **37** (0.392g, 1.00 mmol). The product **43** (0.230 g, 0.66 mmol, 66%) was obtained as a yellow solid. **R_f**: 0.26 (EtOAc:MeOH 9:1). **¹H NMR** (400 MHz, CD_3OD) δ 7.92 (s, 1H), 7.67 (s, 2H), 7.23 (d, $J = 1.4$ Hz, 1H), 7.08 (d, $J = 1.3$ Hz, 1H), 6.74 (dt, $J = 15.6, 4.6$ Hz, 1H), 6.58 (dt, $J = 15.6, 1.9$ Hz, 1H), 5.51 (s, 2H), 4.23 (dd, $J = 4.6, 1.9$ Hz, 2H). **¹³C NMR** (101 MHz, CD_3OD) δ 146.7, 142.1, 137.3, 133.3 (q, 33 Hz), 129.3, 128.2 (m), 124.6 (q, 272 Hz), 122.7 (m), 122.3, 121.6, 115.2, 62.7. **FTIR** (neat): 3156, 3067, 2873, 2840, 1283, 1167, 1127, 1093, 736, 687 cm^{-1} . **HRMS** (ESI): calculated for $\text{C}_{15}\text{H}_{13}\text{F}_6\text{N}_2\text{O}$ $[\text{M}+\text{H}]^+$ 351.0927; found: 351.0932.

(E)-3-(1-(3,5-Dimethoxybenzyl)-1H-imidazol-2-yl)prop-2-en-1-ol (44). The synthesis of **44**



was conducted according to general procedure B with **38** (0.316g, 1.00 mmol). The product **44** (0.205 g, 0.75 mmol, 75%) was obtained as a pale green solid. **R_f**: 0.19 (EtOAc:MeOH 9:1). **¹H NMR** (400 MHz, CDCl_3) δ 7.08 (d, $J = 1.3$ Hz, 1H), 6.93 – 6.83 (m, 2H), 6.51 (dt, $J = 15.6, 2.0$ Hz, 1H), 6.37 (t, $J = 2.3$ Hz, 1H), 6.20 (d, $J = 2.2$ Hz, 2H), 5.07 (s, 2H), 4.32 (dd, $J = 4.7, 1.9$ Hz, 2H), 3.74 (s, 7H), 2.68 (bs, 1H). **¹³C NMR** (101 MHz, CDCl_3) δ 161.5, 145.2, 138.5, 135.7, 128.3, 120.7, 114.8, 104.9, 99.8, 62.8, 55.5, 49.6. **FTIR** (neat): 3141, 3007, 2936, 2840, 1599, 1458, 1432, 1208, 1156, 1097, 1060, 963, 832, 739, 887 cm^{-1} . **HRMS** (ESI): calculated for $\text{C}_{15}\text{H}_{19}\text{N}_2\text{O}_3$ $[\text{M}+\text{H}]^+$ 275.1390; found: 275.1394.

(E)-1-Benzyl-2-(3-(methoxymethoxy)prop-1-enyl)-1H-imidazole (46). **42** (0.471 g, 2.20



mmol) was dissolved in dry DMF (10 mL) and cooled to -50 $^{\circ}\text{C}$. NaHMDS-solution (2.64 mL, 2.64 mmol, 1 M in THF) was added and the reaction mixture was stirred for 30 minutes. MOMCl (0.23 mL, 3.08 mmol) was added and the reaction mixture was allowed to warm to room temperature. The reaction was stirred for 1 hour and then quenched by the addition of a small amount of MeOH and water. The reaction mixture was further diluted with water and the aqueous layer was extracted with DCM (3x). The combined organic layers were washed with water (1x) and brine (1x) and dried over Na_2SO_4 . The solvent was removed under reduced pressure. **46**

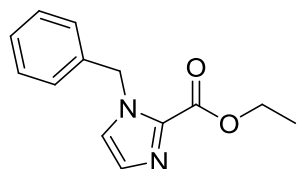
(0.478 g, 1.85 mmol, 84%) was obtained as a pale orange oil and was used without further purification. $^1\text{H NMR}$ (400 MHz, CDCl_3) δ 7.38 – 7.26 (m, 4H), 7.11 – 7.04 (m, 3H), 6.86 (d, $J = 1.3$ Hz, 1H), 6.76 (dt, $J = 15.6, 5.2$ Hz, 1H), 6.49 (dt, $J = 15.5, 1.8$ Hz, 1H), 5.15 (s, 2H), 4.63 (s, 2H), 4.21 (dd, $J = 5.2, 1.8$ Hz, 2H), 3.33 (s, 3H). $^{13}\text{C NMR}$ (101 MHz, CDCl_3) δ 145.0, 136.4, 131.2, 129.1, 129.0, 128.2, 126.8, 120.7, 116.7, 95.8, 67.0, 55.4, 49.5. **HRMS** (ESI): calculated for $\text{C}_{15}\text{H}_{19}\text{N}_2\text{O}_2$ $[\text{M}+\text{H}]^+$ 259.1441; found: 259.1444.

11.2.3 Synthesis discussed in section 4.5

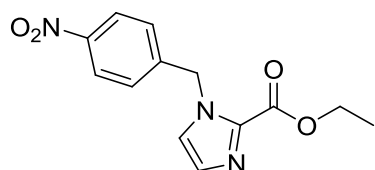
General procedure C: Alkylation of ethyl 1*H*-imidazole-2-carboxylate

A stirred suspension of ethyl 1*H*-imidazole-2-carboxylate (1.0 eq.) and K_2CO_3 (1.2 eq.) in dry DMF (1 mL per mmol) was cooled to 0°C . The alkyl halide (1.05 eq.) was added dropwise or in portions over 2 minutes. The reaction mixture was allowed to warm to room temperature and stirred overnight. EtOAc and water were added and the aqueous layer was extracted (3x). The combined organic layers were washed with water (2x), brine (1x) and then dried over Na_2SO_4 . The solvent was removed under reduced pressure. The intermediate was used without further purification unless described otherwise.

Ethyl 1-benzyl-1*H*-imidazole-2-carboxylate (87). The synthesis of **87** was conducted according to general procedure C with ethyl 1*H*-imidazole-2-carboxylate (0.981 g, 7.00 mmol) and benzyl bromide (0.87 mL, 7.35 mmol). The product **87** (1.430 g, 6.21 mmol, 89%) was obtained as a pale yellow oil. **R_f**: 0.34 (EtOAc). $^1\text{H NMR}$ (400 MHz, CDCl_3) δ 7.37 – 7.27 (m, 3H), 7.20 – 7.14 (m, 3H), 7.06 (d, $J = 1.1$ Hz, 1H), 5.63 (s, 2H), 4.39 (q, $J = 7.1$ Hz, 2H), 1.40 (t, $J = 7.1$ Hz, 3H). $^{13}\text{C NMR}$ (101 MHz, CDCl_3) δ 159.2, 136.4, 136.4, 129.8, 129.0, 128.3, 127.5, 125.4, 61.7, 51.8, 14.4. **FTIR** (neat): 3108, 3067, 2985, 2940, 1707, 1421, 1257, 1112, 713, 672 cm^{-1} . **HRMS** (ESI): calculated for $\text{C}_{13}\text{H}_{15}\text{N}_2\text{O}_2$ $[\text{M}+\text{H}]^+$ 231.1128; found: 231.1131.

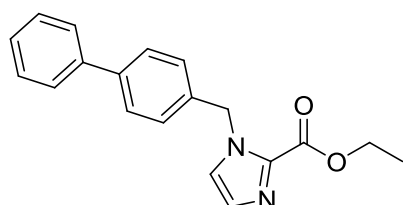


Ethyl 1-(4-nitrobenzyl)-1*H*-imidazole-2-carboxylate (88). The synthesis of **88** was conducted according to general procedure C with ethyl 1*H*-imidazole-2-carboxylate (0.561 g, 4.00 mmol) and 4-nitrobenzyl bromide (0.907 g, 4.20 mmol). The product **88** (1.110 g, quant.) was obtained as a pale red solid. **R_f**: 0.31 (EtOAc). $^1\text{H NMR}$ (400 MHz, CDCl_3) δ 8.22 – 8.14 (m, 2H), 7.32 – 7.24 (m, 3H), 7.15 (d, $J = 1.1$ Hz, 1H), 5.74 (s, 2H), 4.36 (q, $J = 7.1$ Hz, 2H), 1.38 (t, J



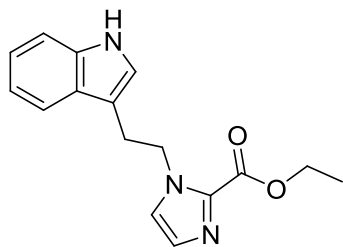
= 7.1 Hz, 3H). ^{13}C NMR (101 MHz, CDCl_3) δ 159.1, 147.8, 143.7, 136.4, 130.3, 127.8, 125.6, 124.3, 62.0, 51.1, 14.3. FTIR (neat): 3141, 3119, 2985, 2940, 1719, 1518, 1428, 1350, 1272, 1201, 1112, 1074, 784, 736, 665 cm^{-1} . HRMS (ESI): calculated for $\text{C}_{13}\text{H}_{14}\text{N}_3\text{O}_4$ $[\text{M}+\text{H}]^+$ 276.0979; found: 276.0978.

Ethyl 1-(biphenyl-4-ylmethyl)-1H-imidazole-2-carboxylate (89). The synthesis of **89** was



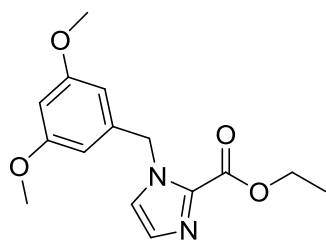
conducted according to general procedure C with ethyl 1H-imidazole-2-carboxylate (0.280 g, 2.00 mmol) and 4-phenylbenzyl bromide (0.519 g, 2.10 mmol). The crude product was purified by silica column chromatography (EtOAc). The product **89** (0.540 g, 1.70 mmol, 85%) was obtained as a colorless oil. R_f : 0.34 (EtOAc). ^1H NMR (400 MHz, $\text{DMSO}-d_6$) δ 7.69 – 7.60 (m, 5H), 7.49 – 7.41 (m, 2H), 7.39 – 7.31 (m, 1H), 7.29 – 7.22 (m, 2H), 7.16 (s, 1H), 5.66 (s, 2H), 4.26 (q, J = 7.1 Hz, 2H), 1.26 (t, J = 7.1 Hz, 3H). ^{13}C NMR (101 MHz, $\text{DMSO}-d_6$) δ 158.7, 139.6, 139.5, 136.7, 135.5, 129.2, 128.9, 127.6, 127.5, 126.9, 126.7, 126.6, 60.7, 50.3, 14.0. FTIR (neat): 3137, 3111, 3033, 2988, 2944, 2910, 1693, 1421, 1383, 1305, 1268, 1201, 1112, 1078, 791, 754, 702, 672 cm^{-1} . HRMS (ESI): calculated for $\text{C}_{19}\text{H}_{19}\text{N}_2\text{O}_2$ $[\text{M}+\text{H}]^+$ 307.1441; found: 307.1438.

Ethyl 1-(2-(1H-indol-3-yl)ethyl)-1H-imidazole-2-carboxylate (92). The synthesis of **92** was

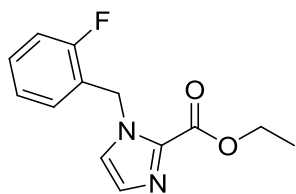


conducted according to general procedure C with ethyl 1H-imidazole-2-carboxylate (0.561 g, 4.00 mmol) and 3-(2-Bromoethyl)indole (0.941 g, 4.20 mmol). The reaction mixture was stirred for 3 days. The crude product was purified with silica column chromatography (EtOAc:MeOH 9:1). The product **92** (0.201 g, 0.71 mmol, 18%) was obtained as a yellow oil. R_f : 0.49 (EtOAc:MeOH 9:1). ^1H NMR (400 MHz, CDCl_3) δ 8.09 (s, 1H), 7.62 (d, J = 7.8 Hz, 1H), 7.37 (d, J = 8.1 Hz, 1H), 7.26 – 7.19 (m, 1H), 7.19 – 7.13 (m, 1H), 7.09 – 7.04 (m, 1H), 6.87 – 6.75 (m, 2H), 4.70 (t, J = 7.1 Hz, 2H), 4.38 (q, J = 7.1 Hz, 2H), 3.25 (t, J = 7.1 Hz, 2H), 1.42 (t, J = 7.1 Hz, 3H). ^{13}C NMR (101 MHz, CDCl_3) δ 158.9, 136.4, 135.9, 128.7, 127.1, 125.7, 122.7, 122.4, 119.9, 118.6, 111.6, 111.4, 61.8, 49.3, 27.6, 14.4. FTIR (neat): 3152, 3059, 2985, 2925, 1715, 1424, 1257, 1112, 1071, 732, 665 cm^{-1} . HRMS (ESI): calculated for $\text{C}_{16}\text{H}_{18}\text{N}_3\text{O}_2$ $[\text{M}+\text{H}]^+$ 284.1394; found: 284.1393.

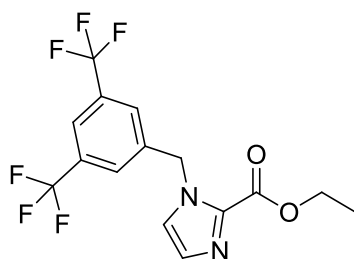
Ethyl 1-(3,5-dimethoxybenzyl)-1*H*-imidazole-2-carboxylate (93). The synthesis of **93** was conducted according to general procedure C with ethyl 1*H*-imidazole-2-carboxylate (0.561 g, 4.00 mmol) and 3,5-dimethoxybenzyl bromide (0.971 g, 4.20 mmol). The product **93** (1.097 g, 3.78 mmol, 94%) was obtained as an orange oil. **R_f**: 0.51 (EtOAc:MeOH 9:1). **¹H NMR** (400 MHz, CDCl₃) δ 7.18 (s, 1H), 7.06 (s, 1H), 6.37 (t, *J* = 2.3 Hz, 1H), 6.30 (d, *J* = 2.2 Hz, 2H), 5.56 (s, 2H), 4.39 (q, *J* = 7.1 Hz, 2H), 3.74 (s, 6H), 1.41 (t, *J* = 7.1 Hz, 3H). **¹³C NMR** (101 MHz, CDCl₃) δ 161.3, 159.1, 138.5, 136.3, 129.6, 125.4, 105.6, 99.9, 61.8, 55.5, 51.8, 14.4. **FTIR** (neat): 3108, 2940, 2843, 1707, 1599, 1465, 1421, 1303, 1253, 1208, 1153, 1112, 1067, 788, 754, 672 cm⁻¹. **HRMS** (ESI): calculated for C₁₅H₁₉N₂O₄ [M+H]⁺ 291.1339; found: 291.1337.



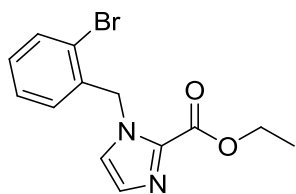
Ethyl 1-(2-fluorobenzyl)-1*H*-imidazole-2-carboxylate (96). The synthesis of **96** was conducted according to general procedure C with ethyl 1*H*-imidazole-2-carboxylate (0.561 g, 4.00 mmol) and 2-fluorobenzyl bromide (0.51 mL, 4.20 mmol). The product **96** (0.928 g, 3.74 mmol, 93%) was obtained as a white solid. **R_f**: 0.37 (EtOAc). **¹H NMR** (400 MHz, CDCl₃) δ 7.34 – 7.25 (m, 1H), 7.19 – 7.03 (m, 5H), 5.70 (s, 2H), 4.39 (q, *J* = 7.2 Hz, 2H), 1.40 (t, *J* = 7.1 Hz, 3H). **¹³C NMR** (101 MHz, CDCl₃) δ 160.7 (d, 247 Hz), 159.4, 136.5, 130.3 (d, 8 Hz), 129.9, 129.9 (d, 4 Hz), 125.6 (d, 2 Hz), 124.7 (d, 4 Hz), 123.8 (d, 14 Hz), 115.7 (d, 21 Hz), 61.7, 45.5 (d, 4 Hz), 14.4. **FTIR** (neat): 3115, 2988, 1711, 1424, 1272, 1231, 1201, 1127, 1112, 795, 762, 668 cm⁻¹. **HRMS** (ESI): calculated for C₁₃H₁₄O₂N₂F [M+H]⁺ 249.1034; found: 249.1037.



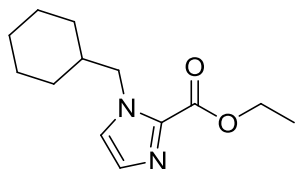
Ethyl 1-(3,5-bis(trifluoromethyl)benzyl)-1*H*-imidazole-2-carboxylate (90). The synthesis of **90** was conducted according to general procedure C with ethyl 1*H*-imidazole-2-carboxylate (0.561 g, 4.00 mmol), and 3,5-bis(trifluoromethyl)benzyl bromide (0.77 mL, 4.20 mmol). The product **90** (1.446 g, 3.95 mmol, 99 %) was obtained as a white solid. **R_f**: 0.40 (EtOAc). **¹H NMR** (400 MHz, CDCl₃) δ 7.82 (s, 1H), 7.62 (s, 2H), 7.27 (s, 1H), 7.15 (s, 1H), 5.76 (s, 2H), 4.39 (q, *J* = 7.1 Hz, 2H), 1.40 (t, *J* = 7.1 Hz, 3H). **¹³C NMR** (101 MHz, CDCl₃) δ 159.2, 139.1, 136.5, 132.5 (q, 34 Hz), 130.7, 127.5 (m), 125.3, 123.1 (q, 273 Hz), 122.3 (m), 62.0, 50.8, 14.3. **FTIR** (neat): 3108, 3007, 2974, 1715, 1283, 1261, 1186, 1167, 1119, 1078, 806, 687, 668 cm⁻¹. **HRMS** (ESI): calculated for C₁₅H₁₃O₂N₂F₆ [M+H]⁺ 367.0876; found: 367.0880.



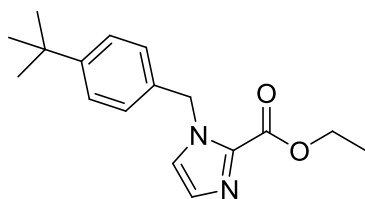
Ethyl 1-(2-bromobenzyl)-1*H*-imidazole-2-carboxylate (95). The synthesis of **95** was conducted according to general procedure C with ethyl 1*H*-imidazole-2-carboxylate (0.561 g, 4.00 mmol) and 2-bromobenzyl bromide (1.05 g, 4.20 mmol). The product **95** (1.155 g, 3.74 mmol, 93%) was obtained as a white solid. **R_f**: 0.39 (EtOAc). **¹H NMR** (400 MHz, CDCl₃) δ 7.59 (dd, *J* = 7.9, 1.4 Hz, 1H), 7.31 – 7.13 (m, 3H), 7.05 (s, 1H), 6.81 – 6.71 (m, 1H), 5.72 (s, 2H), 4.37 (q, *J* = 7.1 Hz, 2H), 1.38 (t, *J* = 7.1 Hz, 3H). **¹³C NMR** (101 MHz, CDCl₃) δ 159.1, 136.8, 136.0, 133.1, 130.1, 129.7, 128.5, 128.1, 125.4, 122.9, 61.7, 51.9, 14.3. FTIR (neat): 3130, 3108, 2981, 1704, 1417, 1268, 1108, 806, 750, 668 cm⁻¹. **HRMS** (ESI): calculated for C₁₃H₁₄O₂N₂Br [M+H]⁺ 309.0233; found: 309.0237.



Ethyl 1-(cyclohexylmethyl)-1*H*-imidazole-2-carboxylate (91). The synthesis of **91** was conducted according to general procedure C with ethyl 1*H*-imidazole-2-carboxylate (0.561 g, 4.00 mmol) and (bromomethyl)cyclohexane (0.59 mL, 4.20 mmol). The product **91** (0.856 g, 3.62 mmol, 91%) was obtained as a white solid. **R_f**: 0.35 (EtOAc). **¹H NMR** (400 MHz, CDCl₃) δ 7.14 (s, 1H), 7.03 – 6.99 (m, 1H), 4.39 (q, *J* = 7.1 Hz, 2H), 4.23 (d, *J* = 7.3 Hz, 2H), 1.85 – 1.55 (m, 6H), 1.42 (t, *J* = 7.1 Hz, 3H), 1.27 – 1.09 (m, 3H), 1.03 – 0.89 (m, 2H). **¹³C NMR** (101 MHz, CDCl₃) δ 159.3, 136.4, 129.2, 126.1, 61.5, 54.7, 39.3, 30.6, 26.3, 25.7, 14.4. **FTIR** (neat): 3104, 2985, 2925, 2858, 1704, 1413, 1249, 1112, 810, 672 cm⁻¹. **HRMS** (ESI): calculated for C₁₃H₂₀N₂O₂Na [M+Na]⁺ 259.1417; found: 259.1418.



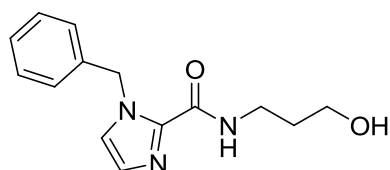
Ethyl 1-(4-*tert*-butylbenzyl)-1*H*-imidazole-2-carboxylate (94). The synthesis of **94** was conducted according to general procedure C with ethyl 1*H*-imidazole-2-carboxylate (0.561 g, 4.00 mmol) and 4-*tert*-butylbenzyl bromide (0.77 mL, 4.80 mmol). The product **94** (1.055 g, 3.68 mmol, 92%) was obtained as pale yellow oil. **R_f**: 0.37 (EtOAc). **¹H NMR** (400 MHz, CDCl₃) δ 7.38 – 7.32 (m, 2H), 7.16 (s, 1H), 7.15 – 7.09 (m, 2H), 7.05 (s, 1H), 5.60 (s, 2H), 4.39 (q, *J* = 7.1 Hz, 2H), 1.41 (t, *J* = 7.1 Hz, 3H), 1.29 (s, 9H). **¹³C NMR** (101 MHz, CDCl₃) δ 159.3, 151.3, 136.5, 133.4, 129.8, 127.4, 125.9, 125.4, 61.6, 51.4, 34.7, 31.4, 14.4. **FTIR** (neat): 3104, 2962, 2907, 2873, 1707, 1421, 1257, 1108, 788 cm⁻¹. **HRMS** (ESI): calculated for C₁₇H₂₃O₂N₂ [M+H]⁺ 287.1754; found: 287.1758.



General procedure D: Aminolysis of alkylated ethyl 1*H*-imidazole-2-carboxylates

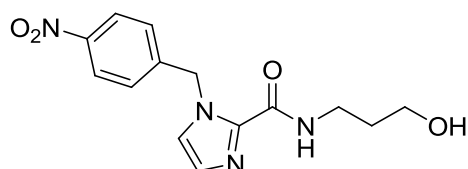
The alkylated ethyl 1*H*-imidazole-2-carboxylate was mixed with amino alcohol (2-3mL) in a microwave tube and heated to 130 °C in a microwave reactor. The temperature was held at 130 °C for 1 h. The obtained solution was diluted with EtOAc and water. The aqueous layer was extracted (3x). The combined organic layers were washed with water (3x) and brine (1x). The solution was dried over Na₂SO₄ and the solvent removed under reduced pressure to afford the product. The product was used without further purification in the next reaction step.

1-Benzyl-*N*-(3-hydroxypropyl)-1*H*-imidazole-2-carboxamide (**98**). The synthesis of **98**



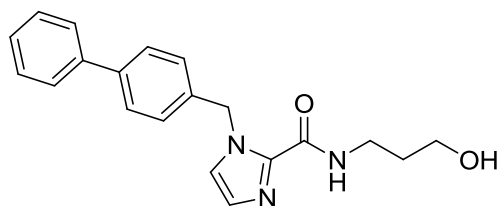
was conducted according to general procedure D with **87** (0.115 g, 0.50 mmol) in 3-amino-1-propanol (3 mL). The product **98** (0.123 g, 0.47 mmol, 95%) was obtained as a colorless oil. **R_f**: 0.43 (EtOAc:MeOH 9:1). **¹H NMR** (400 MHz, DMSO-*d*₆) δ 8.47 (t, *J* = 5.9 Hz, 1H), 7.45 (d, *J* = 1.1 Hz, 1H), 7.36 – 7.19 (m, 5H), 7.01 (d, *J* = 1.1 Hz, 1H), 5.68 (s, 2H), 4.50 (t, *J* = 5.2 Hz, 1H), 3.48 – 3.39 (m, 2H), 3.26 (q, *J* = 6.7 Hz, 2H), 1.63 (p, *J* = 6.6 Hz, 2H). **¹³C NMR** (101 MHz, DMSO-*d*₆) δ 158.8, 138.4, 138.1, 128.5, 127.5, 127.5, 127.3, 125.0, 58.8, 50.0, 36.0, 32.2. **FTIR** (neat): 3320, 2948, 2877, 1655, 1544, 1499, 1465, 1261, 762, 713, 661 cm⁻¹. **HRMS** (ESI): calculated for C₁₄H₁₇N₃O₂Na [M+Na]⁺ 282.1213; found: 282.1218.

N-(3-hydroxypropyl)-1-(4-nitrobenzyl)-1*H*-imidazole-2-carboxamide (**99**). The synthesis



of **99** was conducted according to general procedure D with **88** (0.413 g, 1.50 mmol) in 3-amino-1-propanol (4 mL). The product **99** (0.445 g, 1.46 mmol, 97%) was obtained as an orange oil. **R_f**: 0.37 (EtOAc:MeOH 9:1). **¹H NMR** (400 MHz, DMSO-*d*₆) δ 8.52 (t, *J* = 5.9 Hz, 1H), 8.25 – 8.17 (m, 2H), 7.54 (d, *J* = 1.1 Hz, 1H), 7.45 – 7.37 (m, 2H), 7.09 (d, *J* = 1.1 Hz, 1H), 5.82 (s, 2H), 4.50 (t, *J* = 5.2 Hz, 1H), 3.43 (q, *J* = 5.9 Hz, 2H), 3.25 (q, *J* = 6.6 Hz, 2H), 1.62 (p, *J* = 6.6 Hz, 2H). **¹³C NMR** (101 MHz, DMSO-*d*₆) δ 158.6, 146.8, 145.8, 138.4, 128.1, 127.8, 125.3, 123.7, 58.8, 49.7, 36.1, 32.1. **FTIR** (neat): 3335, 3111, 2940, 2877, 2659, 1547, 1521, 1465, 1346, 1268, 765, 724 cm⁻¹. **HRMS** (ESI): calculated for C₁₅H₁₆N₄O₄ [M+H]⁺ 305.1244; found: 305.1246.

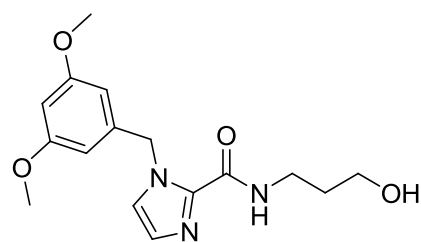
1-(Biphenyl-4-ylmethyl)-N-(3-hydroxypropyl)-1H-imidazole-2-carboxamide (100). The



synthesis of **100** was conducted according to general procedure D with **89** (0.306 g, 1.00 mmol) in 3-amino-1-propanol (3 mL). The product **100** (0.313 g, 0.93 mmol, 93%) was obtained as a white solid. R_f : 0.43 (EtOAc:MeOH 9:1). $^1\text{H NMR}$ (400 MHz, DMSO- d_6) δ 8.50 (t, J = 6.0 Hz, 1H), 7.67 – 7.58 (m,

4H), 7.55 – 7.39 (m, 3H), 7.39 – 7.29 (m, 3H), 7.03 (s, 1H), 5.73 (s, 2H), 4.51 (t, J = 5.2 Hz, 1H), 3.45 (q, J = 5.9 Hz, 2H), 3.28 (q, J = 6.6 Hz, 2H), 1.65 (p, J = 6.6 Hz, 2H). $^{13}\text{C NMR}$ (101 MHz, DMSO- d_6) δ 158.8, 139.7, 139.4, 138.4, 137.3, 128.9, 127.9, 127.5, 127.5, 126.9, 126.6, 125.0, 58.8, 49.7, 36.1, 32.2. **FTIR** (neat): 3316, 3108, 3033, 2936, 2873, 1655, 1547, 1465, 1261, 1063, 922, 747, 724, 698 cm^{-1} . **HRMS** (ESI): calculated for $\text{C}_{20}\text{H}_{22}\text{N}_3\text{O}_2$ $[\text{M}+\text{H}]^+$ 336.1707; found: 336.1711.

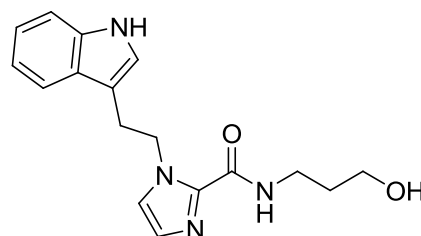
1-(3,5-dimethoxybenzyl)-N-(3-hydroxypropyl)-1H-imidazole-2-carboxamide (107). The



synthesis of **107** was conducted according to general procedure D with **93** (0.435 g, 1.50 mmol) in 3-amino-1-propanol (4 mL). The product **107** (0.425 g, 1.33 mmol, 89%) was obtained as a pale beige solid. R_f : 0.41 (EtOAc:MeOH 9:1). $^1\text{H NMR}$ (400 MHz, DMSO- d_6) δ 8.48 (t, J = 6.0 Hz, 1H), 7.44 (s, 1H), 7.00 (s, 1H), 6.46 –

6.33 (m, 3H), 5.60 (s, 2H), 4.50 (t, J = 5.2 Hz, 1H), 3.44 (q, J = 5.9 Hz, 2H), 3.27 (q, J = 6.6 Hz, 2H), 1.63 (p, J = 6.5 Hz, 2H). $^{13}\text{C NMR}$ (101 MHz, DMSO- d_6) δ 160.6, 158.9, 140.3, 138.4, 127.4, 125.0, 105.4, 98.9, 58.8, 55.1, 49.9, 36.0, 32.2. **FTIR** (neat): 3201, 2940, 2843, 1659, 1603, 1559, 1465, 1428, 1294, 1208, 1160, 1060, 825, 762 cm^{-1} . **HRMS** (ESI): calculated for $\text{C}_{16}\text{H}_{22}\text{N}_3\text{O}_4$ $[\text{M}+\text{H}]^+$ 320.1605; found: 320.1606.

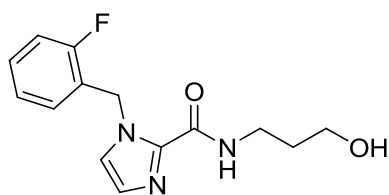
1-(2-(1H-indol-3-yl)ethyl)-N-(3-hydroxypropyl)-1H-imidazole-2-carboxamide (105). The



synthesis of **105** was conducted according to general procedure D with **92** (0.142 g, 0.50 mmol) in 3-amino-1-propanol (3.0 mL). The product **105** (0.158 g, 0.51 mmol, quantitative) was obtained as a white solid. $^1\text{H NMR}$ (400 MHz, DMSO- d_6) δ 10.84 (s, 1H), 8.42 (t, J = 6.0 Hz, 1H), 7.65 (d, J = 7.8 Hz, 1H), 7.37 – 7.28 (m, 2H), 7.12 – 7.02

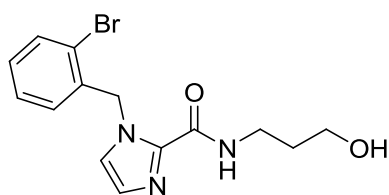
(m, 2H), 7.03 – 6.94 (m, 1H), 6.93 (s, 1H), 4.71 – 4.61 (m, 2H), 4.52 (t, J = 5.2 Hz, 1H), 3.47 (q, J = 5.9 Hz, 2H), 3.36 – 3.26 (m, 2H), 3.17 – 3.09 (m, 2H), 1.66 (p, J = 6.5 Hz, 2H). $^{13}\text{C NMR}$ (101 MHz, DMSO- d_6) δ 158.9, 138.3, 136.2, 127.1, 126.9, 124.9, 123.0, 121.0, 118.4, 118.3, 111.3, 110.5, 58.8, 47.9, 36.0, 32.2, 27.4. **HRMS** (ESI): calculated for $\text{C}_{17}\text{H}_{20}\text{O}_2\text{N}_4\text{Na}$ $[\text{M}+\text{Na}]^+$ 335.1478; found: 335.1461.

1-(2-Fluorobenzyl)-*N*-(3-hydroxypropyl)-1*H*-imidazole-2-carboxamide (111). The



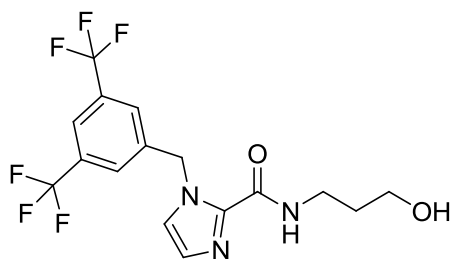
synthesis of **111** was conducted according to general procedure D with **96** (0.273 g, 1.10 mmol) in 3-amino-1-propanol (2.5 mL). The product **111** (0.283 g, 1.02 mmol, 93%) was obtained as a colorless gum. **R_f**: 0.17 (EtOAc). **¹H NMR** (400 MHz, CDCl₃) δ 8.49 (t, *J* = 6.0 Hz, 1H), 7.39 – 7.29 (m, 2H), 7.26 – 7.17 (m, 1H), 7.17 – 7.10 (m, 1H), 7.08 – 7.02 (m, 1H), 7.00 – 6.91 (m, 1H), 5.76 (s, 2H), 4.49 (t, *J* = 5.2 Hz, 1H), 3.43 (q, *J* = 5.9 Hz, 2H), 3.25 (q, *J* = 6.6 Hz, 2H), 1.62 (p, *J* = 6.6 Hz, 2H). **¹³C NMR** (101 MHz, CDCl₃) δ 159.7 (d, 246 Hz), 158.4, 138.6, 129.7 (d, 8 Hz), 128.8 (d, 4 Hz), 127.6, 125.2, 125.0 (d, 14 Hz), 124.7 (d, 3Hz), 115.3 (d, 21 Hz), 58.8, 44.3 (d, 4 Hz), 36.0, 32.1. **FTIR** (neat): 3335, 2940, 2877, 1659, 1544, 1495, 1462, 1235, 754, 695, 661 cm⁻¹. **HRMS** (ESI): calculated for C₁₄H₁₇FN₃O₂ [M+H]⁺ 278.1299; found: 278.1303.

1-(2-Bromobenzyl)-*N*-(3-hydroxypropyl)-1*H*-imidazole-2-carboxamide (114). The



synthesis of **114** was conducted according to general procedure D with **95** (0.340 g, 1.10 mmol) in 3-amino-1-propanol (2.5 mL). Product **114** (0.357 g, 1.06 mmol, 96%) was obtained as a colorless gum. **R_f**: 0.17 (EtOAc). **¹H NMR** (400 MHz, DMSO-*d*₆) δ 8.51 (t, *J* = 6.0 Hz, 1H), 7.66 (d, *J* = 7.8 Hz, 1H), 7.37 (s, 1H), 7.36 – 7.28 (m, 1H), 7.28 – 7.19 (m, 1H), 7.09 (s, 1H), 6.51 (d, *J* = 7.6 Hz, 1H), 5.74 (s, 2H), 4.48 (t, *J* = 5.2 Hz, 1H), 3.42 (q, *J* = 5.9 Hz, 2H), 3.22 (q, *J* = 6.6 Hz, 2H), 1.60 (p, *J* = 6.6 Hz, 2H). **¹³C NMR** (101 MHz, DMSO-*d*₆) δ 158.6, 138.8, 137.3, 132.5, 129.3, 128.2, 127.7, 127.3, 125.2, 121.5, 58.8, 50.7, 36.0, 32.1. **FTIR** (neat): 3316, 2936, 2877, 1659, 1544, 1503, 1465, 1443, 1030, 747, 661 cm⁻¹. **HRMS** (ESI): calculated for C₁₃H₁₂O₄N₃Br [M+H]⁺ 338.0499; found: 338.0506.

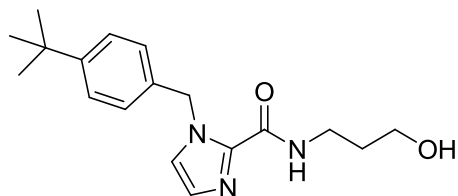
1-(3,5-Bis(trifluoromethyl)benzyl)-*N*-(3-hydroxypropyl)-1*H*-imidazole-2-carboxamide



(102). The synthesis of **102** was conducted according to general procedure D with **90** (0.403 g, 1.10 mmol) in 3-amino-1-propanol (2.5 mL). The product **102** (0.414 g, 1.05 mmol, 95%) was obtained as a pale yellow oil. **R_f**: 0.22 (EtOAc). **¹H NMR** (400 MHz, DMSO-*d*₆) δ 8.56 (t, *J* = 6.0 Hz, 1H), 8.05 (s, 1H), 7.93 (s, 2H), 7.62 (s, 1H), 7.07 (s, 1H), 5.83 (s, 2H), 4.48 (t, *J* = 5.2 Hz, 1H), 3.41 (q, *J* = 5.9 Hz, 2H), 3.25 (q, *J* = 6.6 Hz, 2H), 1.61 (p, *J* = 6.6 Hz, 2H). **¹³C NMR** (101 MHz, DMSO-*d*₆) δ 158.7, 141.5, 138.4, 130.4 (d, 33 Hz), 128.2 (m), 128.0, 125.1, 123.2 (q, 273 Hz), 121.5 (m), 58.7, 49.2, 36.1, 32.1. **FTIR** (neat): 3346, 2951, 2884, 1659, 1547, 1469,

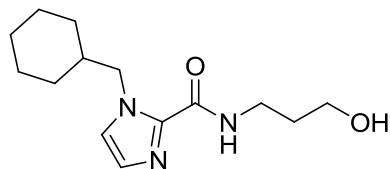
1383, 1357, 1279, 1171, 847, 758, 709, 687 cm^{-1} . **HRMS** (ESI): calculated for $\text{C}_{16}\text{H}_{16}\text{F}_6\text{N}_3\text{O}_2$ $[\text{M}+\text{H}]^+$ 396.1141 ; found: 396.1144.

1-(4-*tert*-Butylbenzyl)-*N*-(3-hydroxypropyl)-1*H*-imidazole-2-carboxamide (109). The



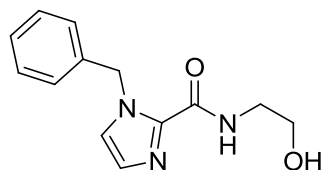
synthesis of **109** was conducted according to general procedure D with **94** (0.315 g, 1.10 mmol) in 3-amino-1-propanol (2.5 mL). The product **109** (0.324 g, 1.03 mmol, 93%) was obtained as a white solid. **R_f**: 0.18 (EtOAc). **¹H NMR** (400 MHz, $\text{DMSO-}d_6$) δ 8.47 (t, J = 6.0 Hz, 1H), 7.44 (s, 1H), 7.37 – 7.30 (m, 2H), 7.20 – 7.13 (m, 2H), 7.00 (s, 1H), 5.64 (s, 2H), 4.50 (t, J = 5.2 Hz, 1H), 3.44 (q, J = 5.9 Hz, 2H), 3.27 (q, J = 6.6 Hz, 2H), 1.64 (p, J = 6.6 Hz, 2H), 1.24 (s, 9H). **¹³C NMR** (101 MHz, $\text{DMSO-}d_6$) δ 158.9, 149.9, 138.3, 135.1, 127.4, 127.1, 125.3, 124.9, 58.8, 49.6, 36.0, 34.2, 32.2, 31.1. **FTIR** (neat): 3387, 3149, 2962, 2936, 2869, 1655, 1555, 1514, 1462, 1428, 1268, 1071, 925, 769, 709 cm^{-1} . **HRMS** (ESI): calculated for $\text{C}_{18}\text{H}_{25}\text{N}_3\text{O}_2\text{Na}$ $[\text{M}+\text{H}]^+$ 338.1839; found: 338.1843.

1-(Cyclohexylmethyl)-*N*-(3-hydroxypropyl)-1*H*-imidazole-2-carboxamide (104). The



synthesis of **104** was conducted according to general procedure D with **91** (0.260 g, 1.10 mmol) in 3-amino-1-propanol (2.5 mL). The product **104** (0.276 g, 1.04 mmol, 95%) was obtained as a colorless oil. **R_f**: 0.41 (EtOAc:MeOH 9:1). **¹H NMR** (400 MHz, $\text{DMSO-}d_6$) δ 8.39 (t, J = 6.0 Hz, 1H), 7.32 (s, 1H), 6.95 (s, 1H), 4.50 (t, J = 5.2 Hz, 1H), 4.26 (d, J = 7.3 Hz, 2H), 3.44 (q, J = 5.9 Hz, 2H), 3.26 (q, J = 6.6 Hz, 2H), 1.78 – 1.55 (m, 6H), 1.49 – 1.41 (m, 2H), 1.20 – 1.06 (m, 3H), 1.00 – 0.85 (m, 2H). **¹³C NMR** (101 MHz, $\text{DMSO-}d_6$) δ 158.9, 138.6, 126.8, 125.4, 58.8, 52.7, 38.7, 36.0, 32.2, 29.7, 25.9, 25.1. **FTIR** (neat): 3335, 3111, 1915, 2854, 1659, 1544, 1503, 1469, 1451, 1264, 1078, 758, 665 cm^{-1} . **HRMS** (ESI): calculated for $\text{C}_{14}\text{H}_{24}\text{N}_3\text{O}_2$ $[\text{M}+\text{H}]^+$ 266.1863; found: 266.1865.

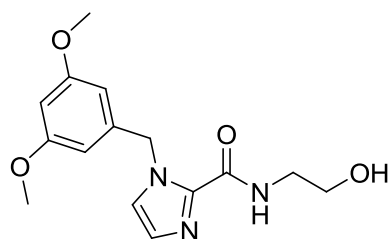
1-Benzyl-*N*-(2-hydroxyethyl)-1*H*-imidazole-2-carboxamide (97). The synthesis of **97** was



conducted according to general procedure D with **87** (0.460 g, 2.00 mmol) in 2-aminoethanol (3 mL). The product **97** (0.460 g, 1.88 mmol, 94%) was obtained as a colorless oil. **R_f**: 0.20 (EtOAc). **¹H NMR** (400 MHz, $\text{DMSO-}d_6$) δ 8.30 (t, J = 5.9 Hz, 1H), 7.46 (d, J = 1.1 Hz, 1H), 7.38 – 7.19 (m, 5H), 7.02 (d, J = 1.1 Hz, 1H), 5.69 (s, 2H), 4.75 (t, J = 5.5 Hz, 1H), 3.47 (q, J = 6.0 Hz, 2H), 3.28 (q, J = 6.1 Hz, 2H). **¹³C NMR** (101 MHz, $\text{DMSO-}d_6$) δ 158.9, 138.2, 138.0, 128.5, 127.6, 127.5, 127.3, 125.1, 59.6, 50.0,

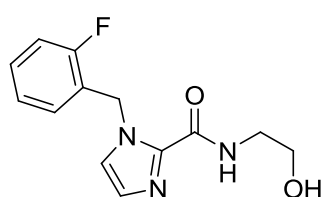
41.1. **FTIR** (neat): 3320, 3033, 2933, 2877, 1655, 1544, 1499, 1458, 1060, 713 cm^{-1} . **HRMS** (ESI): calculated for $\text{C}_{13}\text{H}_{16}\text{N}_3\text{O}_2$ $[\text{M}+\text{H}]^+$ 246.1237; found: 246.1239.

1-(3,5-Dimethoxybenzyl)-*N*-(2-hydroxyethyl)-1*H*-imidazole-2-carboxamide (101). The



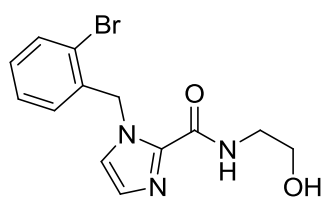
synthesis of **101** was conducted according to general procedure D with **93** (0.435 g, 1.50 mmol) in 2-aminoethanol (4 mL). The product **101** (0.406 g, 1.33 mmol, 89%) was obtained as pale beige solid. **R_f**: 0.40 (EtOAc:MeOH 9:1). **¹H NMR** (400 MHz, DMSO-*d*₆) δ 8.32 (t, *J* = 5.9 Hz, 1H), 7.46 (d, *J* = 1.0 Hz, 1H), 7.02 (d, *J* = 1.0 Hz, 1H), 6.43 – 6.34 (m, 3H), 5.60 (s, 2H), 4.75 (t, *J* = 5.5 Hz, 1H), 3.69 (s, 6H), 3.48 (q, *J* = 6.0 Hz, 2H), 3.29 (q, *J* = 6.1 Hz, 2H). **¹³C NMR** (101 MHz, DMSO-*d*₆) δ 160.6, 158.9, 140.3, 138.2, 127.5, 125.2, 105.5, 98.9, 59.6, 55.1, 49.9, 41.1. **FTIR** (neat): 3383, 3193, 3015, 2933, 2869, 2847, 1663, 1599, 1547, 1465, 1421, 1205, 1149, 1164, 1071, 758 cm^{-1} . **HRMS** (ESI): calculated for $\text{C}_{15}\text{H}_{19}\text{N}_3\text{O}_4$ $[\text{M}+\text{H}]^+$ 306.1448; found: 306.1450.

1-(2-Fluorobenzyl)-*N*-(2-hydroxyethyl)-1*H*-imidazole-2-carboxamide (110). The synthesis



of **110** was conducted according to general procedure D with **96** (0.273 g, 1.10 mmol) in 2-aminoethanol (2.5 mL). The product **110** (0.270 g, 1.03 mmol, 93%) was obtained as a colorless gum. **R_f**: 0.17 (EtOAc). **¹H NMR** (400 MHz, DMSO-*d*₆) δ 8.49 (t, *J* = 6.0 Hz, 1H), 7.39 – 7.29 (m, 2H), 7.26 – 7.11 (m, 2H), 7.04 (d, *J* = 1.1 Hz, 1H), 7.00 – 6.91 (m, 1H), 5.76 (s, 2H), 4.49 (t, *J* = 5.2 Hz, 1H), 3.43 (q, *J* = 6.0 Hz, 2H), 3.25 (q, *J* = 6.6 Hz, 2H), 1.62 (p, *J* = 6.6 Hz, 2H). **¹³C NMR** (101 MHz, DMSO-*d*₆) δ 159.7 (d, 245 Hz), 158.7, 138.5, 129.7 (d, 8 Hz), 128.8 (d, 4 Hz), 127.6, 125.3, 125.0 (d, 15 Hz), 124.7 (d, 4 Hz), 115.3 (d, 21 Hz), 59.6, 44.3 (d, 5 Hz), 41.1. **FTIR** (neat): 3394, 2936, 2880, 1659, 1544, 1495, 1462, 1235, 1063, 754 cm^{-1} . **HRMS** (ESI): calculated for $\text{C}_{13}\text{H}_{15}\text{FN}_3\text{O}_2$ $[\text{M}+\text{H}]^+$ 264.1143; found: 264.1146.

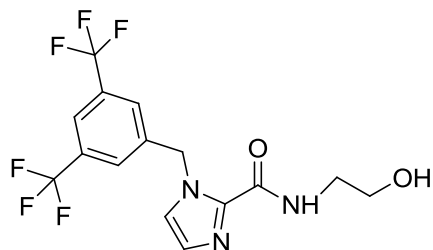
1-(2-Bromobenzyl)-*N*-(2-hydroxyethyl)-1*H*-imidazole-2-carboxamide (113). The



synthesis of **113** was conducted according to general procedure D with **95** (0.340 g, 1.10 mmol) in 2-aminoethanol (2.5 mL). The product **113** (0.306 g, 0.94 mmol, 86%) was obtained as a white solid. **R_f**: 0.17 (EtOAc). **¹H NMR** (400 MHz, DMSO-*d*₆) δ 8.34 (t, *J* = 5.9 Hz, 1H), 7.70 – 7.63 (m, 1H), 7.39 (s, 1H), 7.35 – 7.27 (m, 1H), 7.27 – 7.19 (m, 1H), 7.10 (s, 1H), 6.55 – 6.48 (m, 1H), 5.74 (s, 2H), 4.74 (t, *J* = 5.5 Hz, 1H), 3.45 (q, *J* = 6.0 Hz, 2H), 3.24 (q, *J* = 6.1 Hz, 2H). **¹³C NMR** (101 MHz, DMSO-*d*₆) δ 158.6, 138.6, 137.2, 132.5, 129.3, 128.2, 127.8, 127.3, 125.3, 121.5, 59.6, 50.7, 41.1. **FTIR**

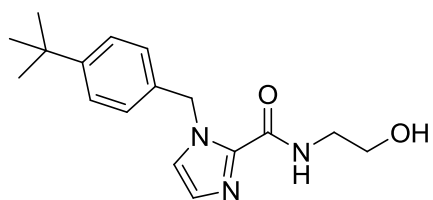
(neat): 3346, 3197, 3130, 3111, 2929, 2880, 1648, 1573, 1469, 1432, 1078, 1026, 747, 665 cm^{-1} . **HRMS** (ESI): calculated for $\text{C}_{13}\text{H}_{15}\text{O}_2\text{N}_3\text{Br}$ $[\text{M}+\text{H}]^+$ 324.0342; found: 324.0341.

1-(3,5-Bis(trifluoromethyl)benzyl)-*N*-(2-hydroxyethyl)-1*H*-imidazole-2-carboxamide (101).



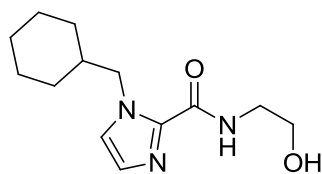
The synthesis of **101** was conducted according to general procedure D with **90** (0.403 g, 1.10 mmol) in 2-aminoethanol (2.5 mL). The product **101** (0.380 g, 1.00 mmol, 91%) was obtained as a pale yellow oil. **R_f**: 0.22 (EtOAc). **¹H NMR** (400 MHz, DMSO-*d*₆) δ 8.39 (t, *J* = 6.0 Hz, 1H), 8.05 (s, 1H), 7.94 (s, 2H), 7.64 (s, 1H), 7.11 – 7.06 (m, 1H), 5.82 (s, 2H), 4.74 (t, *J* = 5.5 Hz, 1H), 3.45 (q, *J* = 6.0 Hz, 2H), 3.27 (q, *J* = 6.1 Hz, 2H). **¹³C NMR** (101 MHz, DMSO-*d*₆) δ 158.7, 141.4, 138.3, 130.4 (q, 33.0 Hz), 128.3 (m), 128.0, 125.2, 123.2 (q, 273 Hz), 121.5 (m), 59.5, 49.2, 41.2. **FTIR** (neat): 3346, 2951, 2884, 1659, 1547, 1469, 1383, 1357, 1279, 1127, 1063, 907, 758, 709, 687 cm^{-1} . **HRMS** (ESI): calculated for $\text{C}_{15}\text{H}_{14}\text{F}_6\text{N}_3\text{O}_2$ $[\text{M}+\text{H}]^+$ 382.0985; found: 382.0988.

1-(4-*tert*-Butylbenzyl)-*N*-(2-hydroxyethyl)-1*H*-imidazole-2-carboxamide (108).



The synthesis of **108** was conducted according to general procedure D with **94** (0.315 g, 1.10 mmol) in 2-aminoethanol (2.5 mL). The product **108** (0.324 g, 1.08 mmol, 98%) was obtained as a white solid. **R_f**: 0.18 (EtOAc). **¹H NMR** (400 MHz, DMSO-*d*₆) δ 8.31 (t, *J* = 5.9 Hz, 1H), 7.46 (s, 1H), 7.38 – 7.31 (m, 2H), 7.21 – 7.14 (m, 2H), 7.02 (s, 1H), 5.65 (s, 2H), 4.77 (t, *J* = 5.5 Hz, 1H), 3.49 (q, *J* = 6.0 Hz, 2H), 3.30 (q, *J* = 6.1 Hz, 2H), 1.25 (s, 9H). **¹³C NMR** (101 MHz, DMSO-*d*₆) δ 158.9, 149.9, 138.2, 135.1, 127.5, 127.1, 125.3, 125.1, 59.6, 49.6, 41.1, 34.2, 31.1. **FTIR** (neat): 3432, 3316, 3115, 2962, 2866, 1655, 1551, 1469, 1052, 773, 721 cm^{-1} . **HRMS** (ESI): calculated for $\text{C}_{17}\text{H}_{24}\text{N}_3\text{O}_2$ $[\text{M}+\text{H}]^+$ 302.1863; found: 302.1867.

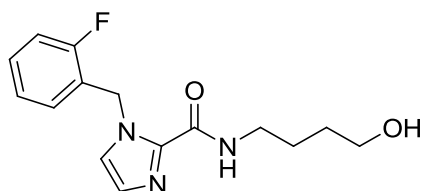
1-(Cyclohexylmethyl)-*N*-(2-hydroxyethyl)-1*H*-imidazole-2-carboxamide (103).



The synthesis of **103** was conducted according to general procedure D with **91** (0.260 g, 1.10 mmol) in 2-aminoethanol (2.5 mL). The product **103** (0.266 g, 1.06 mmol, 96%) was obtained as a colorless oil. **R_f**: 0.41 (EtOAc:MeOH 9:1). **¹H NMR** (400 MHz, DMSO-*d*₆) δ 8.23 (t, *J* = 6.0 Hz, 1H), 7.33 (s, 1H), 6.96 (s, 1H), 4.75 (t, *J* = 5.5 Hz, 1H), 4.27 (d, *J* = 7.3 Hz, 2H), 3.48 (q, *J* = 5.9 Hz, 2H), 3.28 (q, *J* = 6.0 Hz, 2H), 1.80 – 0.84 (m, 11H). **¹³C NMR** (101 MHz, DMSO-*d*₆) δ 158.9, 138.5, 126.8, 125.6, 59.7, 52.8, 41.1, 38.7, 29.7, 25.9, 25.1. **FTIR** (neat): 3398, 2925, 2854, 1659, 1540, 1503,

1469, 1451, 1268, 1063, 762, 739, 713 cm^{-1} . **HRMS** (ESI): calculated for $\text{C}_{13}\text{H}_{22}\text{N}_3\text{O}_2$ $[\text{M}+\text{H}]^+$ 252.1707; found: 252.1709.

1-(2-Fluorobenzyl)-N-(4-hydroxybutyl)-1H-imidazole-2-carboxamide (112). The

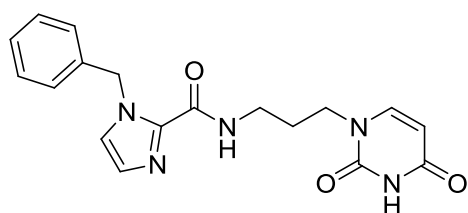


synthesis of **112** was conducted according to general procedure D with **96** (0.273 g, 1.10 mmol) in 4-amino-1-butanol (2.5 mL). The product **112** (0.308 g, 1.06 mmol, 96%) was obtained as a white solid. **R_f**: 0.14 (EtOAc). **¹H NMR** (400 MHz, $\text{DMSO}-d_6$) δ 8.47 (t, $J = 6.2$ Hz, 1H), 7.39 – 7.29 (m, 2H), 7.26 – 7.18 (m, 1H), 7.18 – 7.10 (m, 1H), 7.06 – 7.02 (m, 1H), 6.99 – 6.91 (m, 1H), 5.76 (s, 2H), 4.37 (t, $J = 5.2$ Hz, 1H), 3.38 (d, $J = 5.8$ Hz, 2H), 3.18 (q, $J = 6.7$ Hz, 2H), 1.55 – 1.44 (m, 2H), 1.44 – 1.33 (m, 2H). **¹³C NMR** (101 MHz, CDCl_3) δ 159.7 (d, 246 Hz), 158.4, 138.6, 129.7 (d, 8 Hz), 128.8 (d, 4 Hz), 127.6, 125.2, 125.0 (d, 14 Hz), 124.7 (d, 3Hz), 115.3 (d, 21 Hz), 60.4, 44.3 (d, 4 Hz), 38.3, 29.9, 25.8. **FTIR** (neat): 3435, 3331, 3175, 3041, 2940, 2869, 1633, 1559, 1491, 1462, 1428, 1231, 758, 665 cm^{-1} . **HRMS** (ESI): calculated for $\text{C}_{15}\text{H}_{19}\text{O}_2\text{N}_3\text{F}$ $[\text{M}+\text{H}]^+$ 292.1456; found: 292.1460.

General procedure E: Synthesis of amide-type final compounds (type H)

The imidazole amide alcohol (1.0 eq), N^3 -benzoyl uracil (**53**) (1.1 eq) and PPh_3 (2.0 eq) were suspended in dry THF. DIAD (2.0 eq) was added dropwise at 0 °C. The mixture was allowed to warm to room temperature and was stirred overnight. The solvent was removed under reduced pressure. and the residue was purified by silica column chromatography (EtOAc \rightarrow EtOAc:MeOH 9:1) to afford the benzoyl-protected product. The N^3 -benzoyl protected product was dissolved in cold 7 N NH_3/MeOH . The resulting solution was allowed to warm to room temperature and was stirred for 2-3 h. The formed suspension was concentrated with a stream of nitrogen gas. The crude product was purified by filtration, recrystallization or silica column chromatography.

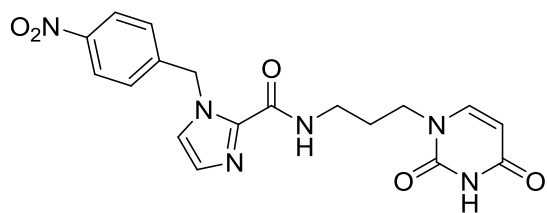
1-Benzyl-N-(3-(2,4-dioxo-3,4-dihydropyrimidin-1(2H)-yl)propyl)-1H-imidazole-2-



carboxamide (116). The synthesis of **116** was conducted according to general procedure E with **98** (0.259 g, 1.00 mmol) in dry THF (3 mL). The benzoyl protected product was treated with 7 N NH_3/MeOH (5 mL) for 2 h. The crude product was purified by silica column chromatography (EtOAc \rightarrow EtOAc:MeOH 9:1). The product **116** (0.111 g, 0.31 mmol, 31%) was obtained as a white solid. **R_f**: 0.29 (EtOAc:MeOH 9:1). **¹H NMR** (400 MHz, $\text{DMSO}-d_6$) δ 11.23 (s, 1H), 8.60 (t, $J = 6.1$ Hz,

1H), 7.66 (d, $J = 7.9$ Hz, 1H), 7.46 (d, $J = 1.1$ Hz, 1H), 7.37 – 7.18 (m, 5H), 7.03 (d, $J = 1.0$ Hz, 1H), 5.68 (s, 2H), 5.53 (d, $J = 7.8$ Hz, 1H), 3.66 (t, $J = 6.9$ Hz, 2H), 3.22 (q, $J = 6.6$ Hz, 2H), 1.79 (p, $J = 6.9$ Hz, 2H). ^{13}C NMR (101 MHz, DMSO- d_6) δ 163.7, 159.0, 151.0, 145.7, 138.3, 138.1, 128.5, 127.5, 127.5, 127.3, 125.1, 100.8, 50.0, 45.5, 35.6, 28.7. FTIR (neat): 3305, 3037, 2948, 2813, 1711, 1681, 1659, 1436, 765, 728 cm^{-1} . HRMS (ESI): calculated for 354.1561 [M+H] $^+$ 354.1561; found: 354.1568.

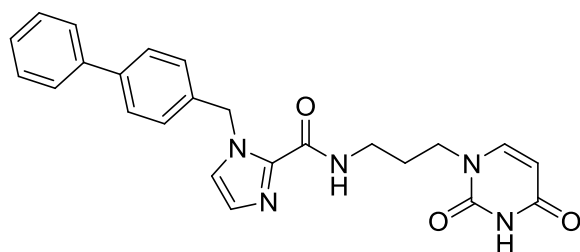
***N*-(3-(2,4-dioxo-3,4-dihydropyrimidin-1(2*H*)-yl)propyl)-1-(4-nitrobenzyl)-1*H*-imidazole-2-carboxamide (117).**



The synthesis of **117** was conducted according to general procedure E with **99** (0.304 g, 1.00 mmol) in dry THF (6 mL). The benzoyl protected product was treated with 7 N NH_3/MeOH (3 mL) for 2 h. The crude product was purified by recrystallization from

chloroform. The product **117** (0.100 g, 0.25 mmol, 25%) was obtained as a solid. R_f : 0.23 (EtOAc:MeOH 9:1). ^1H NMR (400 MHz, DMSO- d_6) δ 11.22 (s, 1H), 8.63 (t, $J = 6.1$ Hz, 1H), 8.24 – 8.15 (m, 2H), 7.64 (d, $J = 7.9$ Hz, 1H), 7.54 (d, $J = 1.1$ Hz, 1H), 7.44 – 7.37 (m, 2H), 7.09 (d, $J = 1.1$ Hz, 1H), 5.80 (s, 2H), 5.51 (d, $J = 7.8$ Hz, 1H), 3.63 (t, $J = 6.9$ Hz, 2H), 3.19 (q, $J = 6.6$ Hz, 2H), 1.77 (p, $J = 6.8$ Hz, 2H). ^{13}C NMR (101 MHz, DMSO- d_6) δ 163.7, 158.7, 151.0, 146.8, 145.7, 145.7, 138.3, 128.1, 127.8, 125.4, 123.7, 100.8, 49.7, 45.4, 35.6, 28.6. FTIR (neat): 3331, 3115, 3007, 2799, 1693, 1659, 1514, 1346, 799, 728 cm^{-1} . HRMS (ESI): calculated for $\text{C}_{18}\text{H}_{19}\text{N}_6\text{O}_5$ [M+H] $^+$ 399.1411; found: 399.1407.

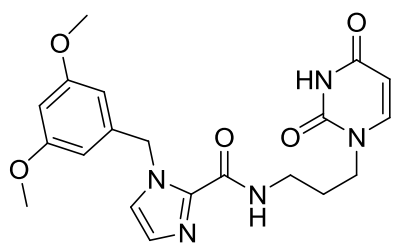
1-(Biphenyl-4-ylmethyl)-*N*-(3-(2,4-dioxo-3,4-dihydropyrimidin-1(2*H*)-yl)propyl)-1*H*-imidazole-2-carboxamide (124).



The synthesis of **124** was conducted according to general procedure E with **100** (0.268 g, 0.80 mmol) in dry THF (5 mL). The benzoyl protected product was treated with 7 N NH_3/MeOH (3 mL) for 2 h. The crude product was purified by recrystallization from

chloroform. The product **124** (0.150 g, 0.35 mmol, 44%) was obtained as white solid. R_f : 0.26 (EtOAc:MeOH 9:1). ^1H NMR (400 MHz, DMSO- d_6) δ 11.24 (s, 1H), 8.62 (t, $J = 6.1$ Hz, 1H), 7.68 – 7.58 (m, 5H), 7.54 – 7.49 (m, 1H), 7.48 – 7.40 (m, 2H), 7.39 – 7.28 (m, 3H), 7.07 – 7.02 (m, 1H), 5.72 (s, 2H), 5.51 (d, $J = 7.8$ Hz, 1H), 3.66 (t, $J = 6.9$ Hz, 2H), 3.23 (q, $J = 6.6$ Hz, 2H), 1.80 (p, $J = 6.9$ Hz, 2H). ^{13}C NMR (101 MHz, DMSO- d_6) δ 163.7, 159.0, 151.0, 145.7, 139.7, 139.4, 138.3, 137.3, 128.9, 127.9, 127.6, 127.5, 126.9, 126.6, 125.2, 100.8, 49.7, 45.5, 35.6, 28.7. FTIR (neat): 3331, 3029, 2802, 2685, 16555, 1436, 750, 6698 cm^{-1} . HRMS (ESI): calculated for $\text{C}_{24}\text{H}_{24}\text{N}_5\text{O}_3$ [M+H] $^+$ 430.1874; found: 430.1874.

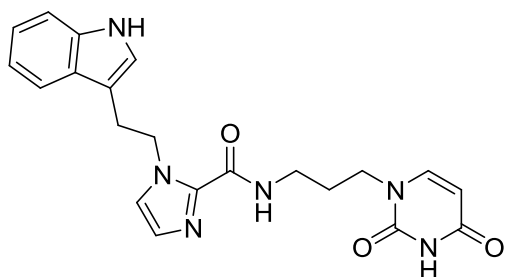
1-(3,5-Dimethoxybenzyl)-N-(3-(2,4-dioxo-3,4-dihydropyrimidin-1(2H)-yl)propyl)-1H-



imidazole-2-carboxamide (119). *dutpase164* The synthesis of **119** was conducted according to general procedure E with **107** (0.319 g, 1.00 mmol) in dry THF (6 mL). The benzoyl protected product was treated with 7 N NH₃/MeOH (5 mL) for 3 h. The crude product was purified by washing with EtOAc. The product **119** (0.166 g, 0.40 mmol, 40%) was

obtained as a white solid. **R_f**: 0.29 (EtOAc:MeOH 9:1). **¹H NMR** (400 MHz, DMSO-*d*₆) δ 11.23 (s, 1H), 8.61 (t, *J* = 6.1 Hz, 1H), 7.65 (d, *J* = 7.8 Hz, 1H), 7.46 (s, 1H), 7.02 (s, 1H), 6.41 – 6.36 (m, 3H), 5.64 – 5.49 (m, 3H), 3.75 – 3.61 (m, 8H), 3.22 (q, *J* = 6.6 Hz, 2H), 1.79 (p, *J* = 6.8 Hz, 2H). **¹³C NMR** (101 MHz, DMSO-*d*₆) δ 163.7, 160.6, 159.0, 151.0, 145.7, 140.3, 138.3, 127.5, 125.1, 105.5, 100.8, 98.9, 55.1, 50.0, 45.5, 35.6, 28.7. **FTIR** (neat): 3331, 3007, 2951, 2840, 1689, 1663, 1462, 1432, 1208, 1164, 1149, 829, 762 cm⁻¹. **HRMS** (ESI): calculated for C₂₀H₂₃N₅O₅Na [M+Na]⁺ 436.1591; found: 436.1595.

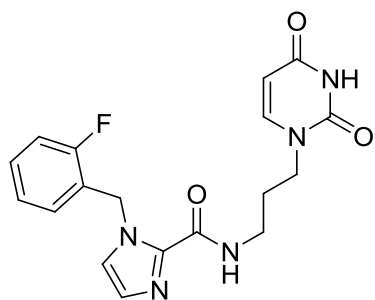
1-(2-(1H-indol-3-yl)ethyl)-N-(3-(2,4-dioxo-3,4-dihydropyrimidin-1(2H)-yl)propyl)-1H-



imidazole-2-carboxamide (118). *dutpase168* The synthesis of **118** was conducted according to general procedure E with **105** (0.150 g, 0.48 mmol) in dry THF (3 mL). The benzoyl protected product was treated with 7 N NH₃/MeOH (3 mL) for 3 h. The crude product was purified by washing with EtOAc. The product **118** (0.080 g, 0.20 mmol, 41%) was

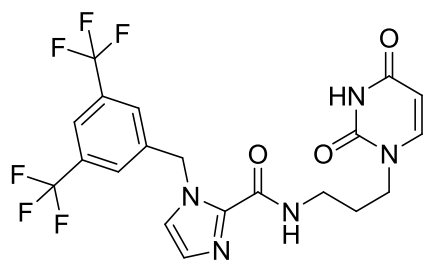
obtained as a white solid. **R_f**: 0.21 (EtOAc:MeOH 9:1). **¹H NMR** (400 MHz, DMSO-*d*₆) δ 11.25 (s, 1H), 10.83 (s, 1H), 8.55 (t, *J* = 6.1 Hz, 1H), 7.71 (d, *J* = 7.8 Hz, 1H), 7.65 (d, *J* = 7.8 Hz, 1H), 7.36 – 7.30 (m, 2H), 7.11 – 7.02 (m, 2H), 7.02 – 6.93 (m, 2H), 5.54 (d, *J* = 7.8 Hz, 1H), 4.67 (t, *J* = 7.7 Hz, 2H), 3.69 (t, *J* = 6.9 Hz, 2H), 3.26 (q, *J* = 6.6 Hz, 2H), 3.18 – 3.09 (m, 2H), 1.82 (p, *J* = 6.9 Hz, 2H). **¹³C NMR** (101 MHz, DMSO-*d*₆) δ 163.8, 159.0, 151.0, 145.8, 138.2, 136.2, 127.1, 126.9, 125.0, 123.0, 121.0, 118.4, 118.4, 111.3, 110.5, 100.8, 47.9, 45.5, 35.6, 28.8, 27.4. **FTIR** (neat): 3264, 3003, 2966, 2921, 2880, 2802, 1685, 1637, 1547, 1465, 1428, 1398, 1242, 743, 706 cm⁻¹. **HRMS** (ESI): calculated for C₂₁H₂₃N₆O₃ [M+H]⁺ 407.1826; found: 407.1827.

***N*-(3-(2,4-dioxo-3,4-dihydropyrimidin-1(2*H*)-yl)propyl)-1-(2-fluorobenzyl)-1*H*-**



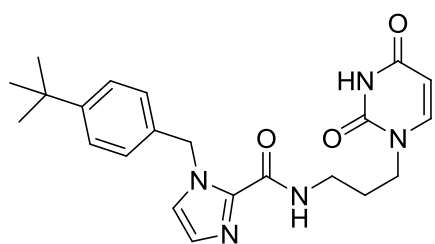
imidazole-2-carboxamide (122). The synthesis of **122** was conducted according to general procedure E with **111** (0.222 g, 0.80 mmol), in dry THF (5 mL). The benzoyl protected product was treated with 7 N NH₃/MeOH (4 mL) for 2 h. The crude product was purified by washing with DCM. The product **122** (0.148 g, 0.40 mmol, 50%) was obtained as a white solid. **R_f**: 0.29 (EtOAc:MeOH 9:1) **¹H NMR** (400 MHz, DMSO-*d*₆) δ 10.36 (s, 1H), 8.63 (t, *J* = 6.1 Hz, 1H), 7.66 (d, *J* = 7.8 Hz, 1H), 7.41 – 7.29 (m, 2H), 7.27 – 7.18 (m, 1H), 7.15 (t, *J* = 7.5 Hz, 1H), 7.09 – 7.04 (m, 1H), 6.96 (t, *J* = 7.4 Hz, 1H), 5.76 (s, 2H), 5.53 (d, *J* = 7.8 Hz, 1H), 3.66 (t, *J* = 6.9 Hz, 2H), 3.26 – 3.15 (m, 2H), 1.79 (p, *J* = 6.9 Hz, 2H). **¹³C NMR** (101 MHz, DMSO-*d*₆) δ 163.7, 159.7 (d, 245 Hz), 158.8, 151.0, 145.7, 138.5, 129.6 (d, 8 Hz), 128.8 (d, 4 Hz), 127.6, 125.2, 125.0 (d, 15 Hz), 124.7 (d, 4 Hz), 115.4 (d, 21 Hz), 100.8, 45.5, 44.3 (d, 5 Hz), 35.6, 28.6. **FTIR** (neat): 3290, 3123, 3037, 2981, 2802, 1704, 1678, 1655, 1439, 810, 762, 721 cm⁻¹. **HRMS** (ESI): calculated for C₁₈H₁₉FN₅O₃ [M+H]⁺ 372.1466; found: 372.1470.

1-(3,5-Bis(trifluoromethyl)benzyl)-*N*-(3-(2,4-dioxo-3,4-dihydropyrimidin-1(2*H*)-



yl)propyl)-1*H*-imidazole-2-carboxamide (123). The synthesis of **123** was conducted according to general procedure E with **102** (0.316 g, 0.80 mmol) in dry THF (5 mL). The benzoyl protected product was treated with 7 N NH₃/MeOH (4 mL) for 2 h. The crude product was purified by washing with EtOAc. The product **123** (0.131 g, 0.27 mmol, 33%) was obtained as a white solid. **R_f**: 0.36 (EtOAc:MeOH 9:1). **¹H NMR** (400 MHz, DMSO-*d*₆) δ 11.23 (s, 1H), 8.69 (t, *J* = 6.2 Hz, 1H), 8.05 (s, 1H), 7.95 (s, 2H), 7.70 – 7.63 (m, 2H), 7.10 (d, *J* = 1.1 Hz, 1H), 5.83 (s, 2H), 5.52 (d, *J* = 7.8 Hz, 1H), 3.65 (t, *J* = 7.0 Hz, 2H), 3.22 (q, *J* = 6.6 Hz, 2H), 1.78 (p, *J* = 6.8 Hz, 2H). **¹³C NMR** (101 MHz, DMSO-*d*₆) δ 163.7, 158.9, 151.0, 145.6, 141.4, 138.3, 130.4 (q, 33 Hz), 128.3 (m), 128.0, 125.2, 123.2 (q, 273 Hz), 121.4 (m), 100.8, 49.2, 45.4, 35.6, 28.7. **FTIR** (neat): 3294, 3041, 3015, 2955, 2817, 1704, 1689, 1655, 1283, 1127, 668 cm⁻¹. **HRMS** (ESI): calculated for C₂₀H₁₈F₆N₅O₃ [M+H]⁺ 490.1308; found: 490.1311.

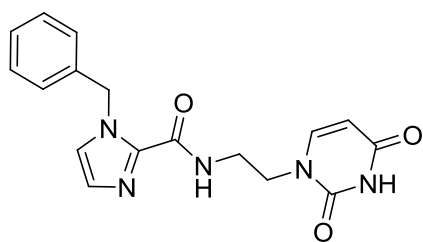
1-(4-*tert*-Butylbenzyl)-*N*-(3-(2,4-dioxo-3,4-dihydropyrimidin-1(2*H*)-yl)propyl)-1*H*-



imidazole-2-carboxamide (126). The synthesis of **126** was conducted according to general procedure E with **109** (0.237 g, 0.75 mmol) in dry THF (5 mL). The benzoyl protected product was treated with 7 N NH₃/MeOH (4 mL) for 2 h. The crude product was purified by washing with EtOAc. The product **126** (0.147 g, 0.36 mmol, 48%)

was obtained as a white solid. **R_f**: 0.36 (EtOAc:MeOH 9:1). **¹H NMR** (400 MHz, DMSO-*d*₆) δ 11.24 (s, 1H), 8.59 (t, *J* = 6.1 Hz, 1H), 7.65 (d, *J* = 7.8 Hz, 1H), 7.45 (s, 1H), 7.36 – 7.30 (m, 2H), 7.18 – 7.12 (m, 2H), 7.01 (s, 1H), 5.64 (s, 2H), 5.52 (d, *J* = 7.8 Hz, 1H), 3.65 (t, *J* = 6.9 Hz, 2H), 3.22 (q, *J* = 6.4 Hz, 2H), 1.79 (p, *J* = 6.9 Hz, 2H), 1.23 (s, 9H). **¹³C NMR** (101 MHz, DMSO-*d*₆) δ 163.7, 159.0, 151.0, 149.9, 145.7, 138.2, 135.1, 127.5, 127.0, 125.3, 125.1, 100.8, 49.7, 45.5, 35.6, 34.2, 31.1, 28.7. **FTIR** (neat): 3335, 3123, 3096, 2962, 2866, 2802, 1715, 1678, 1659, 1439, 762 cm⁻¹. **HRMS** (ESI): calculated for C₂₂H₂₈N₅O₃ [M+H]⁺ 410.2187; found: 410.2189.

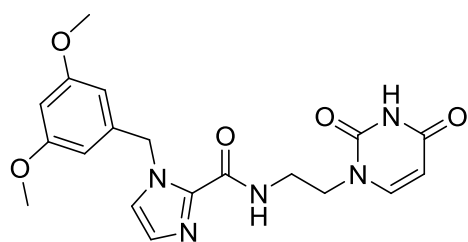
1-Benzyl-*N*-(2-(2,4-dioxo-3,4-dihydropyrimidin-1(2*H*)-yl)ethyl)-1*H*-imidazole-2-



carboxamide (115). The synthesis of **115** was conducted according to general procedure E with **97** (0.245 g, 1.00 mmol) in dry THF (6 mL). The benzoyl protected product was treated with 7 N NH₃/MeOH (3 mL) for 2 h. The crude product was purified by washing with DCM. The product **115** (0.116 g, 0.34 mmol, 34%) was obtained as a

white solid. **R_f**: 0.29 (EtOAc:MeOH 9:1). **¹H NMR** (400 MHz, DMSO-*d*₆) δ 11.20 (s, 1H), 8.69 (t, *J* = 6.2 Hz, 1H), 7.45 (d, *J* = 1.0 Hz, 1H), 7.40 – 7.18 (m, 6H), 7.02 (d, *J* = 1.0 Hz, 1H), 5.65 (s, 2H), 5.41 (d, *J* = 7.8 Hz, 1H), 3.80 (t, *J* = 5.4 Hz, 2H), 3.47 (q, *J* = 6.0 Hz, 2H). **¹³C NMR** (101 MHz, DMSO-*d*₆) δ 163.9, 159.3, 151.0, 145.8, 138.0, 138.0, 128.6, 127.7, 127.5, 127.4, 125.1, 100.4, 49.9, 47.7, 37.1. **FTIR** (neat): 3286, 3041, 3015, 2959, 2821, 1678, 1700, 1678, 1652, 1462, 709 cm⁻¹. **HRMS** (ESI): calculated for C₁₇H₁₇N₅O₃Na [M+Na]⁺ 362.1224; found: 362.1227.

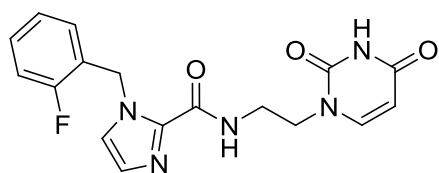
1-(3,5-Dimethoxybenzyl)-N-(2-(2,4-dioxo-3,4-dihydropyrimidin-1(2H)-yl)ethyl)-1H-



imidazole-2-carboxamide (119). The synthesis of **119** was conducted according to general procedure E with **106** (0.305 g, 1.00 mmol) in dry THF (6 mL). The benzoyl protected product was treated with 7 N NH₃/MeOH (5 mL) for 3 h. The crude product was purified by washing with CHCl₃. The product **119**

(0.120 g, 0.30 mmol, 30%) was obtained as a white solid. *R_f*: 0.29 (EtOAc:MeOH 9:1). ¹H NMR (400 MHz, DMSO-*d*₆) δ 11.18 (s, 1H), 8.70 (t, *J* = 6.1 Hz, 1H), 7.44 (s, 1H), 7.36 (d, *J* = 7.8 Hz, 1H), 7.02 (s, 1H), 6.40 (t, *J* = 2.3 Hz, 1H), 6.34 (d, *J* = 2.3 Hz, 2H), 5.56 (s, 2H), 5.40 (d, *J* = 7.8 Hz, 1H), 3.80 (t, *J* = 5.2 Hz, 2H), 3.69 (s, 6H), 3.45 (q, *J* = 5.7 Hz, 2H). ¹³C NMR (101 MHz, DMSO-*d*₆) δ 163.9, 160.6, 159.3, 151.0, 145.8, 140.2, 138.1, 127.6, 125.2, 105.4, 100.4, 98.8, 55.1, 49.9, 47.6, 37.3. FTIR (neat): 3260, 3093, 3033, 3011, 2944, 2840, 1707, 1674, 1655, 1614, 1473, 1436, 1205, 1164, 1141, 769, 750, 665 cm⁻¹. HRMS (ESI): calculated for C₁₉H₂₂N₅O₅ [M+H]⁺ 400.1615; found: 400.1617.

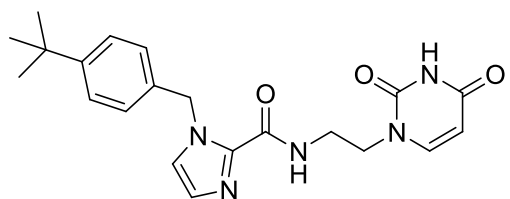
N-(2-(2,4-dioxo-3,4-dihydropyrimidin-1(2H)-yl)ethyl)-1-(2-fluorobenzyl)-1H-imidazole-



2-carboxamide (121). The synthesis of **121** was conducted according to general procedure E with **110** (0.211 g, 0.80 mmol) in dry THF (5 mL). The benzoyl protected product was treated with 7 N NH₃/MeOH (4 mL) for 2 h. The crude product was purified by washing

with DCM. The product **121** (0.118 g, 0.33 mmol, 41%) was obtained as a white solid. *R_f*: 0.31 (EtOAc:MeOH 9:1). ¹H NMR (400 MHz, DMSO-*d*₆) δ 11.18 (s, 1H), 8.71 (t, *J* = 6.2 Hz, 1H), 7.41 – 7.30 (m, 3H), 7.26 – 7.17 (m, 1H), 7.14 (t, *J* = 7.5 Hz, 1H), 7.07 – 7.03 (m, 1H), 6.97 – 6.88 (m, 1H), 5.72 (s, 2H), 5.40 (dd, *J* = 7.8, 2.2 Hz, 1H), 3.79 (t, *J* = 5.4 Hz, 2H), 3.45 (q, *J* = 5.8 Hz, 2H). ¹³C NMR (101 MHz, DMSO-*d*₆) δ 163.9, 159.6 (d, 245 Hz), 159.2, 151.0, 145.8, 138.3, 129.7 (d, 8 Hz), 128.8 (d, 4 Hz), 127.8, 125.3, 124.9 (d, 15 Hz), 124.7 (d, 4 Hz), 115.3 (d, 21 Hz), 100.4, 47.6, 44.1 (d, 4 Hz), 37.2. FTIR (neat): 3290, 3022, 2817, 1707, 1674, 1655, 1465, 1432, 754 cm⁻¹. HRMS (ESI): calculated for C₁₇H₁₇FN₅O₃ [M+H]⁺ 358.1310; found: 358.1310.

1-(4-*tert*-Butylbenzyl)-*N*-(2-(2,4-dioxo-3,4-dihydropyrimidin-1(2*H*)-yl)ethyl)-1*H*-



imidazole-2-carboxamide (125). The synthesis of **125** was conducted according to general procedure E with **108** (0.241 g, 0.80 mmol) in dry THF (5 mL). The benzoyl protected product was treated with 7 N NH₃/MeOH (4 mL) for 2 h. The crude

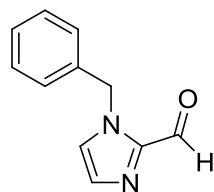
product was purified by washing with EtOAc. The product **125** (0.121 g, 0.31 mmol, 38%) was obtained as a white solid. **R_f**: 0.36 (EtOAc:MeOH 9:1) **¹H NMR** (400 MHz, DMSO-*d*₆) δ 11.21 (s, 1H), 8.69 (t, *J* = 6.1 Hz, 1H), 7.43 (d, *J* = 1.1 Hz, 1H), 7.39 – 7.30 (m, 3H), 7.18 – 7.11 (m, 2H), 7.00 (d, *J* = 1.1 Hz, 1H), 5.60 (s, 2H), 5.40 (dd, *J* = 7.8, 2.3 Hz, 1H), 3.81 (t, *J* = 5.4 Hz, 2H), 3.48 (q, *J* = 6.0 Hz, 2H), 1.24 (s, 9H). **¹³C NMR** (101 MHz, DMSO-*d*₆) δ 163.9, 159.3, 151.0, 150.0, 145.8, 137.9, 135.0, 127.6, 127.2, 125.3, 125.0, 100.4, 49.6, 47.7, 37.1, 34.2, 31.1. **FTIR** (neat): 3305, 3029, 2962, 2840, 1704, 1674, 1659, 1462, 1369, 803, 758, 706 cm⁻¹. **HRMS** (ESI): calculated for C₂₁H₂₅N₅O₃Na [M+Na]⁺ 418.1850; found: 418.1843.

11.2.4 Synthesis discussed in section 4.6

General procedure F: Alkylation of 1*H*-imidazole-2-carbaldehydes

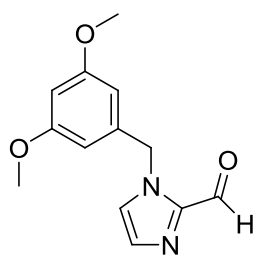
1*H*-imidazole-2-carbaldehyde (X) (1.0 eq.) and K₂CO₃ (1.2 eq.) were suspended in dry DMF (1.5 mL per mmol) at 0 °C. The alkyl halide (1.2 eq.) was added dropwise or in portions over 1 minute. The reaction was allowed to warm to room temperature and was stirred overnight. The mixture was concentrated and the resulting residue diluted with water and DCM. The aqueous layer was extracted (3x). The combined organic layers were washed with water (1x) and brine (1x) and were dried over Na₂SO₄. The solvent was removed under reduced pressure. The crude product was purified by silica column chromatography (EtOAc).

1-Benzyl-1*H*-imidazole-2-carbaldehyde (128). The synthesis of **128** was conducted according to general procedure F with 1*H*-imidazole-2-carbaldehyde (0.480 g, 5.00 mmol) and benzyl bromide (0.71 mL, 6.00 mmol). The product **128** (0.590 g, 3.17 mmol, 63%) was obtained as a pale orange oil.

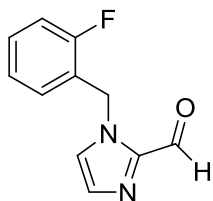


R_f: 0.49 (EtOAc). **¹H NMR** (400 MHz, CDCl₃) δ 9.85 (d, *J* = 0.9 Hz, 1H), 7.39 – 7.28 (m, 4H), 7.24 – 7.16 (m, 2H), 7.16 – 7.11 (m, 1H), 5.61 (s, 2H). **¹³C NMR** (101 MHz, CDCl₃) δ 182.3, 143.4, 135.9, 132.0, 129.1, 128.5, 127.9, 126.4, 51.1. **FTIR** (neat): 3357, 3111, 3033, 2836, 1678, 1410, 1339, 769, 713, 695 cm⁻¹. **HRMS** (ESI): calculated for C₁₁H₁₁N₂O [M+H]⁺ 187.0866; found: 187.0864.

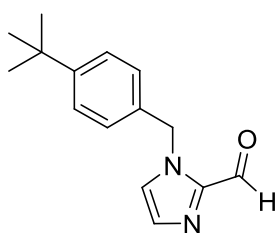
1-(3,5-Dimethoxybenzyl)-1H-imidazole-2-carbaldehyde (134). The synthesis of **134** was conducted according to general procedure F with 1H-imidazole-2-carbaldehyde (0.480 g, 5.00 mmol) and 3,5-dimethoxybenzyl bromide (1.387 g, 6.00 mmol). The product **134** (0.891 g, 3.62 mmol, 72%) was obtained as a white solid. *R_f*: 0.47 (EtOAc). ¹H NMR (400 MHz, CDCl₃) δ 9.86 (d, *J* = 1.0 Hz, 1H), 7.30 (d, *J* = 1.0 Hz, 1H), 7.16 – 7.12 (m, 1H), 6.39 (t, *J* = 2.3 Hz, 1H), 6.32 (d, *J* = 2.3 Hz, 2H), 5.54 (s, 2H), 3.75 (s, 6H). ¹³C NMR (101 MHz, CDCl₃) δ 182.3, 161.4, 143.3, 138.1, 131.9, 126.4, 105.9, 100.0, 55.5, 51.0. FTIR (neat): 3115, 3003, 2959, 2836, 1681, 1603, 1335, 1212, 1156, 1060, 840, 795, 776, 758, 691 cm⁻¹. HRMS (ESI): calculated for C₁₃H₁₅N₂O₃ [M+H]⁺ 247.1077; found: 247.1081.



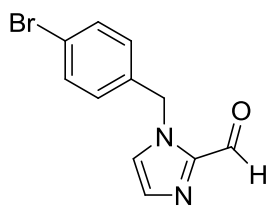
1-(2-Fluorobenzyl)-1H-imidazole-2-carbaldehyde (127). The synthesis of **127** was conducted according to general procedure F with 1H-imidazole-2-carbaldehyde (0.480 g, 5.00 mmol) and 2-fluorobenzyl bromide (0.72 mL, 6.00 mmol). The product **127** (0.792 g, 3.88 mmol, 78%) was obtained as a white solid. *R_f*: 0.53 (EtOAc). ¹H NMR (400 MHz, CDCl₃) δ 9.87 (s, 1H), 7.39 – 7.22 (m, 4H), 7.17 – 7.05 (m, 2H), 5.70 (s, 2H). ¹³C NMR (101 MHz, CDCl₃) δ 182.4, 160.9 (d, 247 Hz), 143.4, 132.0, 130.7 (d, 8 Hz), 130.4 (d, 3 Hz), 126.7 (d, 3 Hz), 124.8 (d, 4 Hz), 123.3 (d, 15 Hz), 115.8 (d, 21 Hz), 44.8 (d, 4 Hz). FTIR (neat): 3137, 3093, 2854, 1670, 1421, 1402, 1339, 1235, 754, 691 cm⁻¹. HRMS (ESI): calculated for C₁₁H₁₀FN₂O [M+H]⁺ 205.0772; found: 205.0772.



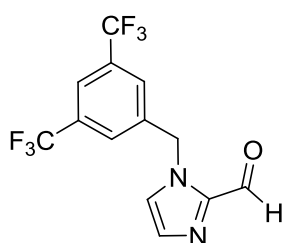
1-(4-tert-Butylbenzyl)-1H-imidazole-2-carbaldehyde (132). The synthesis of **132** was conducted according to general procedure F with 1H-imidazole-2-carbaldehyde (0.961 g, 10.00 mmol) and 4-tert-butylbenzyl bromide (2.21 mL, 12.00 mmol). The product **132** (1.618 g, 6.67 mmol, 67%) was obtained as a white solid. *R_f*: 0.57 (EtOAc). ¹H NMR (400 MHz, CDCl₃) δ 9.85 (d, *J* = 0.9 Hz, 1H), 7.42 – 7.30 (m, 2H), 7.28 (d, *J* = 1.0 Hz, 1H), 7.18 – 7.11 (m, 3H), 5.58 (s, 2H), 1.30 (s, 9H). ¹³C NMR (101 MHz, CDCl₃) δ 182.4, 151.6, 143.4, 132.8, 131.9, 127.7, 126.4, 126.0, 50.7, 34.7, 31.4. FTIR (neat): 3108, 2959, 2907, 2866, 2843, 1689, 1417, 1343, 821, 806, 780, 762 cm⁻¹. HRMS (ESI): calculated for C₁₅H₁₉N₂O [M+H]⁺ 243.1492; found: 243.1489.



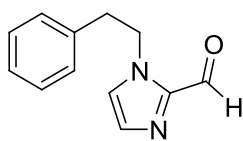
1-(4-Bromobenzyl)-1*H*-imidazole-2-carbaldehyde (129). The synthesis of **129** was conducted according to general procedure F with 1*H*-imidazole-2-carbaldehyde (0.961 g, 10.00 mmol) and 4-bromobenzyl bromide (3.00 g, 12.00 mmol). The product **129** (1.625 g, 6.13 mmol, 61%) was obtained as a white solid. **R_f**: 0.47 (EtOAc). **¹H NMR** (400 MHz, CDCl₃) δ 9.86 – 9.83 (m, 1H), 7.50 – 7.45 (m, 2H), 7.32 (d, *J* = 0.8 Hz, 1H), 7.16 – 7.12 (m, 1H), 7.11 – 7.03 (m, 2H), 5.56 (s, 2H). **¹³C NMR** (101 MHz, CDCl₃) δ 182.3, 143.3, 134.9, 132.3, 132.1, 129.5, 126.2, 122.6, 50.5. **FTIR** (neat): 3141, 3100, 1666, 1413, 1398, 1343, 1164, 1074, 1011, 799, 765 cm⁻¹. **HRMS** (ESI): calculated for C₁₁H₁₀BrN₂O [M+H]⁺ 264.9971; found: 264.9975.



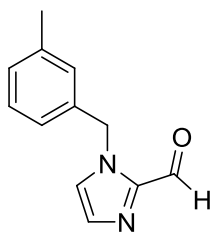
1-(3,5-Bis(trifluoromethyl)benzyl)-1*H*-imidazole-2-carbaldehyde (135). The synthesis of **135** was conducted according to general procedure F with 1*H*-imidazole-2-carbaldehyde (0.961 g, 10.00 mmol), and 3,5-bis(trifluoromethyl)benzyl bromide (2.20 mL, 12.00 mmol). The product **135** (2.310 g, 7.12 mmol, 72%) was obtained as a pale yellow solid. **R_f**: 0.53(EtOAc). **¹H NMR** (400 MHz, CDCl₃) δ 9.83 (d, *J* = 0.9 Hz, 1H), 7.83 (s, 1H), 7.62 (s, 2H), 7.39 (d, *J* = 1.0 Hz, 1H), 7.26 – 7.21 (m, 1H), 5.73 (s, 2H). **¹³C NMR** (101 MHz, CDCl₃) δ 182.4, 143.2, 138.6, 132.7, 132.6 (q, 33 Hz), 127.7 (m), 126.3, 123.1 (q, 273 Hz), 122.6 (m), 50.1. **FTIR** (neat): 3119, 3152, 3074, 2862, 1681, 1279, 1167, 1123, 877, 765, 683 cm⁻¹. **HRMS** (ESI): calculated for C₁₃H₉F₆N₂O [M+H]⁺ 323.0614; found: 323.0616.



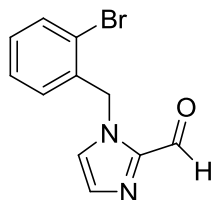
1-Phenethyl-1*H*-imidazole-2-carbaldehyde (136). The synthesis of **136** was conducted according to general procedure F with 1*H*-imidazole-2-carbaldehyde (0.961 g, 10.00 mmol) and (2-bromoethyl)benzene (1.64 mL, 12.00 mmol). The product **136** (1.530 g, 7.64 mmol, 77%) was obtained as a pale green oil. **R_f**: 0.47 (EtOAc). **¹H NMR** (400 MHz, CDCl₃) δ 9.81 (d, *J* = 1.0 Hz, 1H), 7.31 – 7.20 (m, 3H), 7.19 (d, *J* = 1.0 Hz, 1H), 7.12 – 7.05 (m, 2H), 6.89 – 6.84 (m, 1H), 4.60 (t, *J* = 7.2 Hz, 2H), 3.05 (t, *J* = 7.2 Hz, 2H). **¹³C NMR** (101 MHz, CDCl₃) δ 182.1, 143.2, 137.2, 131.4, 128.9, 128.8, 127.1, 126.7, 49.5, 37.6. **FTIR** (neat): 3357, 3111, 3029, 2933, 2836, 1678, 1477, 1410, 1339, 780, 762, 702 cm⁻¹. **HRMS** (ESI): calculated for C₁₂H₁₃N₂O [M+H]⁺ 201.1022; found: 201.1019.



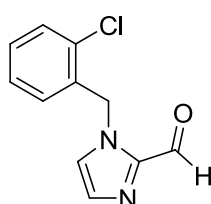
1-(3-Methylbenzyl)-1*H*-imidazole-2-carbaldehyde (130). The synthesis of **130** was conducted according to general procedure F with 1*H*-imidazole-2-carbaldehyde (0.961 g, 10.00 mmol) and 3-methylbenzyl bromide (1.62 mL, 12.00 mmol). The product **130** (1.485 g, 7.42 mmol, 74%) was obtained as a pale yellow solid. *R_f*: 0.50 (EtOAc). ¹H NMR (400 MHz, CDCl₃) δ 9.85 (d, *J* = 0.9 Hz, 1H), 7.29 (d, *J* = 1.0 Hz, 1H), 7.25 – 7.19 (m, 1H), 7.15 – 7.09 (m, 2H), 7.01 – 6.96 (m, 2H), 5.57 (s, 2H), 2.32 (s, 3H). ¹³C NMR (101 MHz, CDCl₃) δ 182.3, 143.4, 138.9, 135.8, 132.0, 129.2, 129.0, 128.5, 126.4, 124.9, 51.0, 21.5. FTIR (neat): 3353, 3100, 2962, 2843, 1681, 1410, 1339, 1160, 803, 765, 732, 687 cm⁻¹. HRMS (ESI): calculated for C₁₂H₁₃N₂O [M+H]⁺ 201.1022; found: 201.1022.



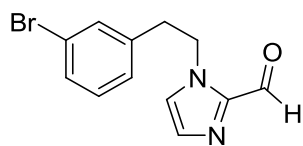
1-(2-Bromobenzyl)-1*H*-imidazole-2-carbaldehyde (131). The synthesis of **131** was conducted according to general procedure F with 1*H*-imidazole-2-carbaldehyde (0.480 g, 5.00 mmol) and 2-bromobenzyl bromide (1.500 g, 6.00 mmol). The product **131** (1.015 g, 3.96 mmol, 77%) was obtained as a pale yellow solid. *R_f*: 0.49 (EtOAc). ¹H NMR (400 MHz, CDCl₃) δ 9.87 (d, *J* = 1.0 Hz, 1H), 7.61 (dd, *J* = 7.9, 1.4 Hz, 1H), 7.32 (d, *J* = 1.0 Hz, 1H), 7.30 – 7.23 (m, 1H), 7.20 (td, *J* = 7.7, 1.8 Hz, 1H), 7.17 – 7.12 (m, 1H), 6.91 (dd, *J* = 7.6, 1.8 Hz, 1H), 5.73 (s, 2H). ¹³C NMR (101 MHz, CDCl₃) δ 182.3, 143.5, 135.3, 133.3, 132.1, 130.1, 129.3, 128.2, 126.3, 123.5, 51.0. FTIR (neat): 3137, 3111, 2851, 1678, 1413, 1343, 1253, 1030, 784, 769, 754, 672cm⁻¹. HRMS (ESI): calculated for C₁₁H₁₀BrN₂O [M+H]⁺ 264.9971; found: 264.9976.



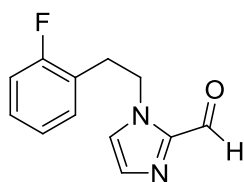
1-(2-Chlorobenzyl)-1*H*-imidazole-2-carbaldehyde (133). The synthesis of **133** was conducted according to general procedure F with 1*H*-imidazole-2-carbaldehyde (0.961 g, 10.00 mmol) and 2-chlorobenzyl bromide (1.56 mL, 12.00 mmol). The product **133** (1.581 g, 7.16 mmol, 72%) was obtained as a pale yellow solid. *R_f*: 0.53 (EtOAc). ¹H NMR (400 MHz, CDCl₃) δ 9.86 (d, *J* = 0.9 Hz, 1H), 7.42 (dd, *J* = 7.9, 1.4 Hz, 1H), 7.34 – 7.24 (m, 2H), 7.21 (td, *J* = 7.5, 1.4 Hz, 1H), 7.16 (d, *J* = 1.0 Hz, 1H), 6.98 (dd, *J* = 7.6, 1.8 Hz, 1H), 5.74 (s, 2H). ¹³C NMR (101 MHz, CDCl₃) δ 182.3, 143.5, 133.7, 133.5, 132.0, 130.0, 129.9, 129.4, 127.6, 126.4, 48.5. FTIR (neat): 3339, 3145, 3104, 2858, 1674, 1421, 1402, 1421, 1343, 765, 743, 683 cm⁻¹. HRMS (ESI): calculated for C₁₁H₁₀ClN₂O [M+H]⁺ 221.0476; found: 221.0479.



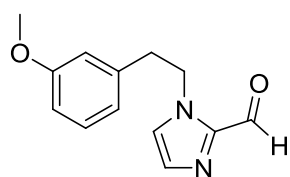
1-(3-Bromophenethyl)-1*H*-imidazole-2-carbaldehyde (142). The synthesis of **142** was conducted according to general procedure F with 1*H*-imidazole-2-carbaldehyde (0.480 g, 5.00 mmol) and 3-bromophenethyl bromide (0.92 mL, 6.00 mmol). The product **142** (0.830 g, 2.97 mmol, 59%) was obtained as a white solid. **R_f**: 0.49 (EtOAc). **¹H NMR** (400 MHz, CDCl₃) δ 9.83 (d, *J* = 0.9 Hz, 1H), 7.41 – 7.35 (m, 1H), 7.29 – 7.26 (m, 1H), 7.22 (d, *J* = 0.8 Hz, 1H), 7.14 (t, *J* = 7.8 Hz, 1H), 7.04 – 6.97 (m, 1H), 6.92 – 6.87 (m, 1H), 4.58 (t, *J* = 7.2 Hz, 2H), 3.03 (t, *J* = 7.3 Hz, 2H). **¹³C NMR** (101 MHz, CDCl₃) δ 182.1, 143.1, 139.5, 132.0, 131.5, 130.4, 130.3, 127.6, 126.6, 122.8, 49.2, 37.2. **FTIR** (neat): 3350, 3104, 3085, 3048, 2966, 2936, 2847, 1685, 1477, 1413, 1343, 668, 784, 765, 695, 668 cm⁻¹. **HRMS** (ESI): calculated for C₁₂H₁₂BrN₂O [M+H]⁺ 279.0128; found: 279.0132.



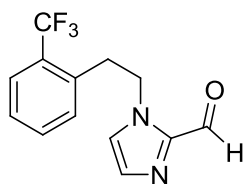
1-(2-Fluorophenethyl)-1*H*-imidazole-2-carbaldehyde (138). The synthesis of **138** was conducted according to general procedure F with 1*H*-imidazole-2-carbaldehyde (0.961 g, 10.00 mmol), and 2-fluorophenethyl bromide (1.69 mL, 12.00 mmol). The product **138** (1.492 g, 6.83 mmol, 68%) was obtained as a pale yellow solid. **R_f**: 0.53 (EtOAc). **¹H NMR** (400 MHz, CDCl₃) δ 9.80 (d, *J* = 1.1 Hz, 1H), 7.25 – 7.15 (m, 2H), 7.06 – 6.94 (m, 3H), 6.90 – 6.85 (m, 1H), 4.61 (t, *J* = 7.0 Hz, 2H), 3.11 (t, *J* = 7.1 Hz, 2H). **¹³C NMR** (101 MHz, CDCl₃) δ 182.0, 161.4 (d, 246 Hz), 143.2, 131.5, 131.3 (d, 5 Hz), 129.0 (d, 8 Hz), 126.6, 124.4 (d, 4 Hz), 124.1 (d, 15 Hz), 115.5 (d, 22 Hz), 47.9 (d, 2 Hz), 31.0 (d, 2 Hz). **FTIR** (neat): 3108, 2944, 2843, 1689, 1480, 1413, 1343, 1227, 717, 758, 691 cm⁻¹. **HRMS** (ESI): calculated for C₁₂H₁₂FN₂O [M+H]⁺ 219.0928; found: 219.0931.



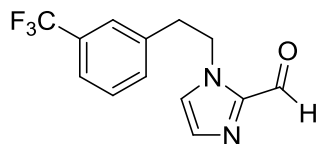
1-(3-Methoxyphenethyl)-1*H*-imidazole-2-carbaldehyde (137). The synthesis of **137** was conducted according to general procedure F with 1*H*-imidazole-2-carbaldehyde (0.961 g, 10.00 mmol) and 3-methoxyphenethyl bromide (1.88 mL, 12.00 mmol). The product **137** (1.740 g, 7.56 mmol, 76%) was obtained as a pale yellow oil. **R_f**: 0.47 (EtOAc). **¹H NMR** (400 MHz, CDCl₃) δ 9.82 (s, 1H), 7.23 – 7.14 (m, 2H), 6.90 – 6.85 (m, 1H), 6.80 – 6.73 (m, 1H), 6.71 – 6.64 (m, 1H), 6.64 – 6.58 (m, 1H), 4.59 (t, *J* = 7.2 Hz, 2H), 3.76 (s, 3H), 3.02 (t, *J* = 7.2 Hz, 2H). **¹³C NMR** (101 MHz, CDCl₃) δ 182.1, 159.9, 143.2, 138.8, 131.4, 129.8, 126.7, 121.2, 114.5, 112.5, 55.3, 49.4, 37.6. **FTIR** (neat): 3108, 3003, 2940, 2836, 1678, 1588, 1477, 1410, 1339, 1264, 1156, 1045, 773, 698 cm⁻¹. **HRMS** (ESI): calculated for C₁₃H₁₅N₂O₂ [M+H]⁺ 231.1128; found: 231.1131.



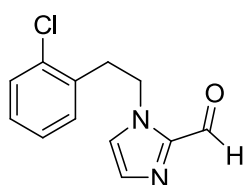
1-(2-(Trifluoromethyl)phenethyl)-1*H*-imidazole-2-carbaldehyde (140). The synthesis of **140** was conducted according to general procedure F with 1*H*-imidazole-2-carbaldehyde (0.961 g, 10.00 mmol), and 2-(trifluoromethyl)phenethyl bromide (2.00 mL, 12.00 mmol). The product **140** (0.730 g, 2.72 mmol, 27%) was obtained as a pale yellow solid. *R_f*: 0.51 (EtOAc). ¹H NMR (400 MHz, CDCl₃) δ 9.86 (d, *J* = 0.9 Hz, 1H), 7.69 – 7.62 (m, 1H), 7.49 – 7.41 (m, 1H), 7.40 – 7.31 (m, 1H), 7.29 – 7.18 (m, 2H), 6.97 – 6.92 (m, 1H), 4.59 (t, *J* = 7.4 Hz, 2H), 3.24 (t, *J* = 7.4 Hz, 2H). ¹³C NMR (101 MHz, CDCl₃) δ 182.1, 143.2, 135.7 (q, 2 Hz), 132.3 (q, 1 Hz), 132.0, 131.6, 128.8 (q, 30 Hz), 127.4, 126.6, 126.4 (q, 6 Hz), 124.7 (q, 274 Hz), 49.0 (q, 1 Hz), 34.6 (q, 2 Hz). FTIR (neat): 3350, 3100, 2974, 2854, 1689, 1413, 1316, 1104, 1067, 1041, 791, 765 cm⁻¹. HRMS (ESI): calculated for C₁₃H₁₂F₃N₂O [M+H]⁺ 269.0896; found: 269.0899.



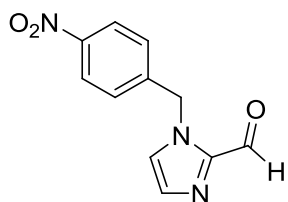
1-(3-(Trifluoromethyl)phenethyl)-1*H*-imidazole-2-carbaldehyde (141). The synthesis of **141** was conducted according to general procedure F with 1*H*-imidazole-2-carbaldehyde (0.480 g, 5.00 mmol) and 3-(trifluoromethyl)phenethyl bromide (1.00 ml, 6.00 mmol). The product **141** (0.818 g, 3.05 mmol, 61%) was obtained as a pale yellow solid. *R_f*: 0.49 (EtOAc). ¹H NMR (400 MHz, CDCl₃) δ 9.82 (d, *J* = 0.9 Hz, 1H), 7.54 – 7.47 (m, 1H), 7.44 – 7.33 (m, 2H), 7.31 – 7.25 (m, 1H), 7.22 (d, *J* = 0.9 Hz, 1H), 6.92 – 6.87 (m, 1H), 4.63 (t, *J* = 7.3 Hz, 2H), 3.12 (t, *J* = 7.3 Hz, 2H). ¹³C NMR (101 MHz, CDCl₃) δ 182.1, 143.2, 138.2, 132.4 (q, 1 Hz), 131.6, 131.3 (q, 32 Hz), 129.4, 126.5, 125.6 (q, 4 Hz), 124.1 (q, 272 Hz), 124.1 (q, 4 Hz), 49.1, 37.4. FTIR (neat): 3357, 3108, 3018, 2970, 2866, 1689, 1413, 1331, 1119, 1071, 814, 791, 765, 709, 661 cm⁻¹. HRMS (ESI): calculated for C₁₃H₁₂ON₂F₃ [M+H]⁺ 269.0896; found: 269.0896.



1-(2-Chlorophenethyl)-1*H*-imidazole-2-carbaldehyde (139). The synthesis of **139** was conducted according to general procedure F with 1*H*-imidazole-2-carbaldehyde (0.961 g, 10.00 mmol) and 2-chlorophenethyl bromide (1.80 mL, 12.00 mmol). The product **139** (0.824 g, 3.51 mmol, 35%) was obtained as pale a yellow solid. *R_f*: 0.51 (EtOAc). ¹H NMR (400 MHz, CDCl₃) δ 9.82 (d, *J* = 1.0 Hz, 1H), 7.36 (dd, *J* = 7.9, 1.4 Hz, 1H), 7.22 – 7.15 (m, 2H), 7.13 (td, *J* = 7.5, 1.5 Hz, 1H), 7.00 (dd, *J* = 7.5, 1.8 Hz, 1H), 6.85 (d, *J* = 0.9 Hz, 1H), 4.63 (t, *J* = 7.1 Hz, 2H), 3.21 (t, *J* = 7.1 Hz, 2H). ¹³C NMR (101 MHz, CDCl₃) δ 182.1, 143.3, 134.9, 134.2, 131.5, 131.3, 129.7, 128.7, 127.3, 126.7, 47.4, 35.2. FTIR (neat): 3119, 3104, 2840, 1689, 1477, 1410, 1339, 791, 762, 747, 691 cm⁻¹. HRMS (ESI): calculated for C₁₂H₁₂ClN₂O [M+H]⁺ 235.0633; found: 235.0636.



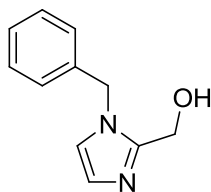
1-(4-Nitrobenzyl)-1H-imidazole-2-carbaldehyde (143). The synthesis of **143** was conducted according to general procedure F with 1H-imidazole-2-carbaldehyde (0.480 g, 5.00 mmol) and 4-nitrobenzyl bromide (1.296 g, 6.00 mmol). The product **143** (0.326 g, 1.41 mmol, 28%) was obtained as a beige solid. **R_f**: 0.40 (EtOAc). **¹H NMR** (400 MHz, CDCl₃) δ 9.82 (s, 1H), 8.23 – 8.16 (m, 2H), 7.40 – 7.36 (m, 1H), 7.34 – 7.28 (m, 2H), 7.24 – 7.17 (m, 1H), 5.71 (s, 2H). **¹³C NMR** (101 MHz, CDCl₃) δ 182.3, 148.0, 143.4, 143.0, 132.5, 128.2, 126.4, 124.4, 50.3. **FTIR** (neat): 3141, 3082, 2948, 2866, 1678, 1518, 1417, 1343, 769, 736 cm⁻¹. **HRMS** (ESI): calculated for C₁₂H₁₄O₄N₃ (MeOH hemiacetal) [M+H]⁺ 264.0979; found: 264.0982.



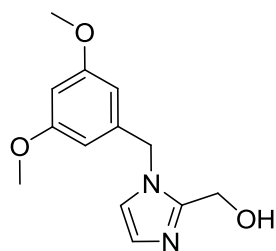
General procedure G: Reduction of *N*-alkyl-1H-imidazole-2-carbaldehydes

The *N*-alkyl-1H-imidazole-2-carbaldehyde (1.0 eq) was dissolved or suspended in MeOH (2 mL per mmol) in an open flask. NaBH₄ (2.0 eq) was added in portions at 0°C. The reaction mixture was allowed to warm to room temperature. The reaction was stirred for 3-4 h and quenched with acetone. The mixture was concentrated under reduced pressure. DCM and water were added to the residue and the aqueous layer was extracted (3x). The combined organic layer was washed with water (1x) and brine (1x) and dried over Na₂SO₄. The solvent was removed under reduced pressure and the product was obtained without further purification.

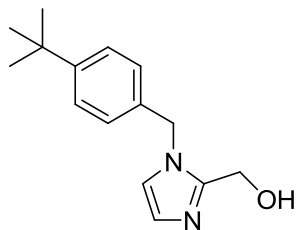
(1-Benzyl-1H-imidazol-2-yl)methanol (145). The synthesis of **145** was conducted according to general procedure G with **128** (0.559 g, 3.00 mmol). The product **145** (0.534 g, 2.83 mmol, 95%) was obtained as a white solid. **R_f**: 0.24 (EtOAc:MeOH 9:1). **¹H NMR** (400 MHz, CD₃OD) δ 7.39 – 7.26 (m, 3H), 7.24 – 7.18 (m, 2H), 7.05 (d, *J* = 1.4 Hz, 1H), 6.90 (d, *J* = 1.4 Hz, 1H), 5.30 (s, 2H), 4.59 (s, 2H). **¹³C NMR** (101 MHz, CD₃OD) δ 148.4, 138.2, 129.9, 129.0, 128.5, 127.4, 122.6, 57.0, 50.6. **FTIR** (neat): 3167, 3119, 3067, 3033, 2940, 2858, 1499, 1436, 1130, 1030, 728, 695 cm⁻¹. **HRMS** (ESI): calculated for C₁₁H₁₃N₂O [M+H]⁺ 189.1022; found: 189.1022.



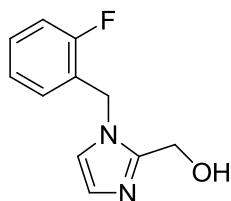
(1-(3,5-Dimethoxybenzyl)-1H-imidazol-2-yl)methanol (151). The synthesis of **151** was conducted according to general procedure G with **134** (0.739 g, 3.00 mmol). The product **151** (0.700 g, 2.98 mmol, 94%) was obtained as a white solid. **R_f**: 0.24 (EtOAc:MeOH 9:1). **¹H NMR** (400 MHz, CD₃OD) δ 7.06 (d, *J* = 1.4 Hz, 1H), 6.91 (d, *J* = 1.4 Hz, 1H), 6.41 (t, *J* = 2.3 Hz, 1H), 6.36 (d, *J* = 2.2 Hz, 2H), 5.22 (s, 2H), 4.60 (s, 2H), 3.73 (s, 6H). **¹³C NMR** (101 MHz, CD₃OD) δ 162.8, 148.5, 140.4, 127.4, 122.7, 106.4, 100.6, 57.0, 55.8, 50.6. **FTIR** (neat): 3145, 3119, 2996, 2944, 2843, 1599, 1432, 1357, 1208, 1153, 1056, 1033, 773, 747 cm⁻¹. **HRMS** (ESI): calculated for C₁₃H₁₇N₂O₃ [M+H]⁺ 249.1234; found: 249.1234.



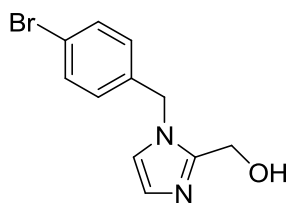
(1-(4-tert-Butylbenzyl)-1H-imidazol-2-yl)methanol (149). The synthesis of **149** was conducted according to general procedure G with **132** (0.727 g, 3.00 mmol). The product **149** (0.700 g, 2.86 mmol, 95%) was obtained as a white solid. **R_f**: 0.34 (EtOAc:MeOH 9:1). **¹H NMR** (400 MHz, CDCl₃) δ 7.39 – 7.32 (m, 2H), 7.12 – 7.06 (m, 2H), 6.93 – 6.88 (m, 1H), 6.85 – 6.80 (m, 1H), 5.19 (s, 2H), 4.65 (s, 2H), 1.30 (d, *J* = 1.2 Hz, 9H). **¹³C NMR** (101 MHz, CDCl₃) δ 151.3, 148.1, 133.4, 127.1, 127.1, 126.0, 120.8, 56.2, 49.5, 34.7, 31.4. **FTIR** (neat): 3145, 3119, 2951, 2903, 2869, 2735, 1473, 1417, 1037, 985, 821, 750 cm⁻¹. **HRMS** (ESI): calculated for C₁₅H₂₁N₂O [M+H]⁺ 245.1648; found: 245.1649.



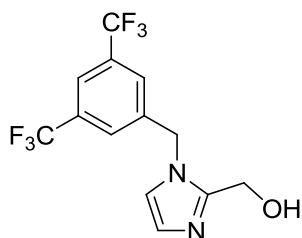
(1-(2-Fluorobenzyl)-1H-imidazol-2-yl)methanol (144). The synthesis of **144** was conducted according to general procedure G with **127** (0.613 g, 3.00 mmol). The product **144** (0.574 g, 2.78 mmol, 93%) was obtained as a white solid. **R_f**: 0.31 (EtOAc:MeOH 9:1). **¹H NMR** (400 MHz, CD₃OD) δ 7.42 – 7.32 (m, 1H), 7.21 – 7.11 (m, 3H), 7.09 – 7.04 (m, 1H), 6.91 (d, *J* = 1.5 Hz, 1H), 5.38 (s, 2H), 4.65 (s, 2H). **¹³C NMR** (101 MHz, CD₃OD) δ 162.0 (d, 246 Hz), 148.5, 131.3 (d, 8 Hz), 130.8 (d, 4 Hz), 127.6, 125.8 (d, 4 Hz), 125.2 (d, 15 Hz), 122.5, 116.5 (d, 22 Hz), 57.0, 44.5 (d, 5 Hz). **FTIR** (neat): 3126, 2832, 1495, 1443, 1212, 1033, 758, 665 cm⁻¹. **HRMS** (ESI): calculated for C₁₁H₁₂FN₂O [M+H]⁺ 207.0928; found: 207.0926.



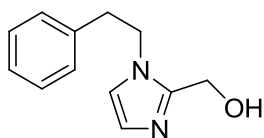
(1-(4-Bromobenzyl)-1H-imidazol-2-yl)methanol (146). The synthesis of **146** was conducted according to general procedure G with **129** (1.326 g, 5.00 mmol). The product **146** (1.161 g, 4.35 mmol, 85%) was obtained as a white solid. **R_f**: 0.24 (EtOAc:MeOH 9:1). **¹H NMR** (400 MHz, CD₃OD) δ 7.54 – 7.45 (m, 2H), 7.18 – 7.10 (m, 2H), 7.06 (d, *J* = 1.3 Hz, 1H), 6.91 (d, *J* = 1.4 Hz, 1H), 5.28 (s, 2H), 4.60 (s, 2H). **¹³C NMR** (101 MHz, CD₃OD) δ 148.5, 137.6, 133.0, 130.4, 127.6, 122.8, 122.6, 57.0, 49.9. **FTIR** (neat): 3111, 3029, 2836, 1491, 1056, 1015, 788, 747, 668 cm⁻¹. **HRMS** (ESI): calculated for C₁₁H₁₂BrN₂O [M+H]⁺ 267.0128; found: 267.0129.



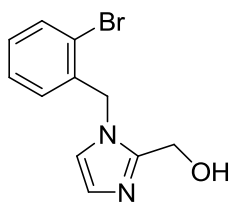
(1-(3,5-Bis(trifluoromethyl)benzyl)-1H-imidazol-2-yl)methanol (152). The synthesis of **152** was conducted according to general procedure G with **135** (1.611 g, 5.00 mmol). The product **152** (1.503 g, 4.63 mmol, 93%) was obtained as a white solid. **R_f**: 0.40 (EtOAc:MeOH 9:1). **¹H NMR** (400 MHz, CD₃OD) δ 7.92 (s, 1H), 7.84 (s, 2H), 7.16 (d, *J* = 1.4 Hz, 1H), 6.98 (d, *J* = 1.4 Hz, 1H), 5.51 (s, 2H), 4.65 (s, 2H). **¹³C NMR** (101 MHz, CD₃OD) δ 148.9, 142.0, 133.1 (q, 33 Hz), 129.0 (m), 128.2, 124.7 (q, 272 Hz), 122.7 (m), 122.5, 56.9, 49.5. **FTIR** (neat): 3111, 2810, 2754, 1279, 1175, 1115, 1022, 743, 687 cm⁻¹. **HRMS** (ESI): calculated for C₁₃H₁₁F₆N₂O [M+H]⁺ 325.0770; found: 325.0772.



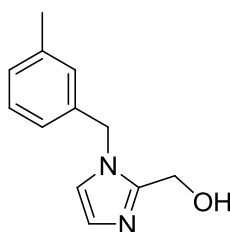
(1-Phenethyl-1H-imidazol-2-yl)methanol (153). The synthesis of **153** was conducted according to general procedure G with **136** (1.001 g, 5.00 mmol). The product **153** (0.922 g, 4.56 mmol, 91%) was obtained as a white solid. **R_f**: 0.23 (EtOAc:MeOH 9:1). **¹H NMR** (400 MHz, CD₃OD) δ 7.28 – 7.17 (m, 3H), 7.12 – 7.06 (m, 2H), 7.02 – 6.98 (m, 1H), 6.83 (d, *J* = 1.4 Hz, 1H), 4.34 – 4.26 (m, 4H), 3.07 (t, *J* = 7.1 Hz, 2H). **¹³C NMR** (101 MHz, CD₃OD) δ 148.3, 139.5, 129.9, 129.6, 127.8, 127.2, 122.1, 56.7, 38.5. (1 alkyl signal behind solvent). **FTIR** (neat): 3111, 3029, 2921, 2892, 2847, 1495, 1458, 1436, 1048, 762, 736, 706 cm⁻¹. **HRMS** (ESI): calculated for C₁₂H₁₅N₂O [M+H]⁺ 203.1179; found: 203.1175.



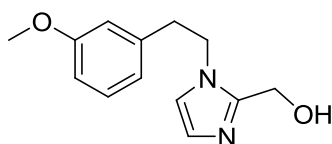
(1-(2-Bromobenzyl)-1*H*-imidazol-2-yl)methanol (148). The synthesis of **148** was conducted according to general procedure G with **131** (0.795 g, 3.00 mmol). The product **148** (0.690 g, 2.58 mmol, 86%) was obtained as a pale yellow solid. **R_f**: 0.30 (EtOAc:MeOH 9:1). **¹H NMR** (400 MHz, CD₃OD) δ 7.65 (dd, *J* = 7.9, 1.4 Hz, 1H), 7.32 (td, *J* = 7.5, 1.4 Hz, 1H), 7.24 (td, *J* = 7.7, 1.8 Hz, 1H), 7.01 (d, *J* = 1.4 Hz, 1H), 6.95 (d, *J* = 1.5 Hz, 1H), 6.89 (dd, *J* = 7.6, 1.8 Hz, 1H), 5.41 (s, 2H), 4.63 (s, 2H). **¹³C NMR** (100 MHz, CD₃OD) δ 148.7, 137.4, 134.1, 130.8, 130.0, 129.2, 127.7, 123.7, 122.6, 57.1, 50.8. **FTIR** (neat): 3141, 3104, 2929, 2817, 1443, 1030, 743, 661 cm⁻¹. **HRMS** (ESI): calculated for C₁₁H₁₂BrN₂O [M+H]⁺ 267.0128; found: 267.0133.



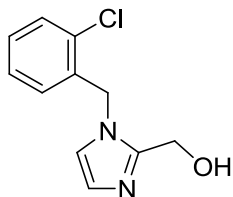
(1-(3-Methylbenzyl)-1*H*-imidazol-2-yl)methanol (147). The synthesis of **147** was conducted according to general procedure G with **130** (1.201 g, 6.00 mmol). The product **147** (1.175 g, 5.81 mmol, 97%) was obtained as a pale yellow solid. **R_f**: 0.33 (EtOAc:MeOH 9:1). **¹H NMR** (400 MHz, CD₃OD) δ 7.21 (t, *J* = 7.6 Hz, 1H), 7.14 – 7.09 (m, 1H), 7.06 – 7.01 (m, 2H), 7.02 – 6.96 (m, 1H), 6.89 (d, *J* = 1.4 Hz, 1H), 5.25 (s, 2H), 4.59 (s, 2H), 2.30 (s, 3H). **¹³C NMR** (101 MHz, CD₃OD) δ 148.4, 139.8, 138.1, 129.8, 129.7, 129.1, 127.4, 125.5, 122.6, 57.0, 50.6, 21.4. **FTIR** (neat): 3082, 2918, 2806, 2687, 1495, 1134, 1048, 747, 695 cm⁻¹. **HRMS** (ESI): calculated for C₁₂H₁₅N₂O [M+H]⁺ 203.1179; found: 203.1182.



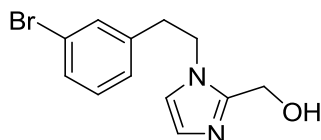
(1-(3-Methoxyphenethyl)-1*H*-imidazol-2-yl)methanol (154). The synthesis of **154** was conducted according to general procedure G with **137** (1.382 g, 6.00 mmol). The product **154** (1.320 g, 5.68 mmol, 95%) was obtained as a white solid. **R_f**: 0.27 (EtOAc:MeOH 9:1). **¹H NMR** (400 MHz, CD₃OD) δ 7.21 – 7.13 (m, 1H), 7.03 (d, *J* = 1.3 Hz, 1H), 6.85 (d, *J* = 1.3 Hz, 1H), 6.81 – 6.75 (m, 1H), 6.73 – 6.67 (m, 1H), 6.62 – 6.58 (m, 1H), 4.38 – 4.26 (m, 4H), 3.72 (s, 3H), 3.05 (t, *J* = 7.0 Hz, 2H). **¹³C NMR** (101 MHz, CD₃OD) δ 161.3, 148.3, 141.0, 130.6, 127.2, 122.1, 122.1, 115.3, 113.5, 56.7, 55.6, 48.7, 38.5. **FTIR** (neat): 3119, 3119, 3000, 2903, 2840, 1596, 1495, 1465, 1432, 1279, 1249, 1164, 1028, 803, 747, 695 cm⁻¹. **HRMS** (ESI): calculated for C₁₃H₁₇N₂O₂ [M+H]⁺ 233.1285; found: 233.1287.



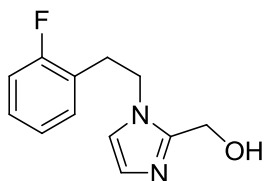
(1-(2-Chlorophenyl)-1*H*-imidazol-2-yl)methanol (150). The synthesis of **150** was conducted according to general procedure G with **139** (1.324 g, 6.00 mmol). The product **150** (1.275 g, 5.73 mmol, 95%) was obtained as a pale yellow solid. **R_f**: 0.31 (EtOAc:MeOH 9:1). **¹H NMR** (400 MHz, CD₃OD) δ 7.47 (dd, *J* = 7.7, 1.6 Hz, 1H), 7.37 – 7.25 (m, 2H), 7.03 (d, *J* = 1.4 Hz, 1H), 6.98 – 6.91 (m, 2H), 5.44 (s, 2H), 4.63 (s, 2H). **¹³C NMR** (101 MHz, CD₃OD) δ 148.7, 135.7, 134.0, 130.8, 130.7, 130.0, 128.6, 127.7, 122.6, 57.1. (1 alkyl signal under solvent signal). **FTIR** (neat): 3123, 2996, 2832, 1439, 1033, 747 cm⁻¹. **HRMS** (ESI): calculated for C₁₁H₁₂ClN₂O [M+H]⁺ 223.0633; found: 223.0631.



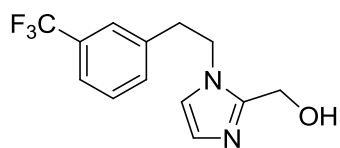
(1-(3-Bromophenethyl)-1*H*-imidazol-2-yl)methanol (160). The synthesis of **160** was conducted according to general procedure G with **142** (0.558 g, 2.00 mmol) and NaBH₄ (0.151 g, 4.00 mmol) in MeOH (4 mL). The product **160** (0.553 g, 1.97 mmol, 98%) was obtained as a colorless oil. **R_f**: 0.26 (EtOAc:MeOH 9:1). **¹H NMR** (400 MHz, CD₃OD) δ 7.39 (ddd, *J* = 7.8, 2.0, 1.0 Hz, 1H), 7.32 (t, *J* = 1.9 Hz, 1H), 7.19 (t, *J* = 7.8 Hz, 1H), 7.11 (dt, *J* = 7.6, 1.0 suHz, 1H), 7.01 (d, *J* = 1.3 Hz, 1H), 6.85 (d, *J* = 1.3 Hz, 1H), 4.41 (s, 2H), 4.31 (t, *J* = 7.1 Hz, 2H), 3.09 (t, *J* = 7.1 Hz, 2H). **¹³C NMR** (101 MHz, CD₃OD) δ 148.2, 142.1, 133.0, 131.4, 130.9, 128.8, 127.2, 123.5, 122.1, 56.8, 48.4, 38.0. **FTIR** (neat): 3111, 2929, 2851, 1570, 1495, 1477, 1432, 1033, 784, 739, 691, 668 cm⁻¹. **HRMS** (ESI): calculated for C₁₂H₁₄ON₂Br [M+H]⁺ 281.0284 ; found: 281.0289.



1-(2-Fluorophenethyl)-1*H*-imidazol-2-yl)methanol (155). The synthesis of **155** was conducted according to general procedure G with **138** (1.091 g, 5.00 mmol). The product **155** (1.039 g, 4.72 mmol, 94%) was obtained as a pale yellow solid. **R_f**: 0.26 (EtOAc:MeOH 9:1). **¹H NMR** (400 MHz, CD₃OD) δ 7.31 – 7.21 (m, 1H), 7.13 – 7.01 (m, 3H), 6.98 (d, *J* = 1.4 Hz, 1H), 6.83 (d, *J* = 1.4 Hz, 1H), 4.42 (s, 2H), 4.33 (t, *J* = 7.1 Hz, 2H), 3.15 (t, *J* = 7.0 Hz, 2H). **¹³C NMR** (101 MHz, CD₃OD) δ 162.7 (d, 243 Hz), 148.2, 132.4 (d, 5 Hz), 130.0 (d, 8.0 Hz), 127.2, 126.1 (d, 16 Hz), 125.5 (d, 4 Hz), 122.1, 116.2 (d, 22 Hz), 56.7, 47.2 (d, 2 Hz) 31.8 (d, 2 Hz). **FTIR** (neat): 3141, 3108, 2948, 2925, 2858, 1495, 1454, 1231, 1041, 762, 743, 661 cm⁻¹. **HRMS** (ESI): calculated for C₁₂H₁₄FN₂O [M+H]⁺ 221.1085; found: 221.1084.

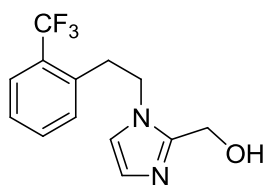


(1-(3-(Trifluoromethyl)phenethyl)-1*H*-imidazol-2-yl)methanol (158). The synthesis of **158**



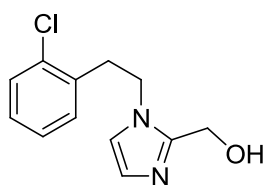
was conducted according to general procedure G with **141** (0.671 g, 2.50 mmol). The product **158** (0.660 g, 2.44 mmol, 98%) was obtained as a pale yellow solid. **R_f**: 0.21 (EtOAc:MeOH 9:1). **¹H NMR** (400 MHz, CD₃OD) δ 7.56 – 7.36 (m, 4H), 7.00 (d, *J* = 1.4 Hz, 1H), 6.84 (d, *J* = 1.4 Hz, 1H), 4.40 (s, 2H), 4.34 (t, *J* = 7.1 Hz, 2H), 3.19 (t, *J* = 7.1 Hz, 2H). **¹³C NMR** (101 MHz, CD₃OD) δ 148.2, 140.9, 133.8 (q, 1 Hz), 131.9 (q, 32 Hz), 130.4, 127.3, 127.0 (q, 4 Hz), 125.6 (q, 271 Hz), 124.6 (q, 4 Hz), 122.1, 56.8, 48.3, 38.0. **FTIR** (neat): 3078, 2929, 2810, 2679, 1495, 1339, 1167, 1115, 1078, 1048, 736, 709, 661 cm⁻¹. **HRMS** (ESI): calculated for C₁₃H₁₄F₃N₂O [M+H]⁺ 271.1053; found: 271.1052.

(1-(2-(Trifluoromethyl)phenethyl)-1*H*-imidazol-2-yl)methanol (157). The synthesis of **157**



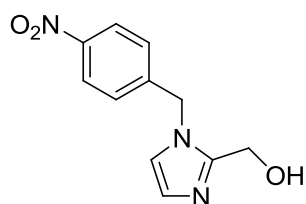
was conducted according to general procedure G with **140** (0.671 g, 2.50 mmol). The product **157** (0.668 g, 2.47 mmol, 99%) was obtained as a pale yellow solid. **R_f**: 0.21 (EtOAc:MeOH 9:1). **¹H NMR** (400 MHz, CD₃OD) δ 7.69 (d, *J* = 7.6 Hz, 1H), 7.52 – 7.38 (m, 2H), 7.19 (d, *J* = 7.6 Hz, 1H), 7.00 (d, *J* = 1.4 Hz, 1H), 6.87 (d, *J* = 1.4 Hz, 1H), 4.41 (s, 2H), 4.33 (t, *J* = 7.3 Hz, 2H), 3.31 – 3.24 (m, 2H). **¹³C NMR** (101 MHz, CD₃OD) δ 148.3, 137.8 (q, 2 Hz), 133.4 (q, 1 Hz), 133.1, 129.8 (q, 30 Hz), 128.4, 127.4, 127.2 (q, 6 Hz), 126.1 (q, 273 Hz), 122.1, 56.7, 48.2 (q, 1 Hz), 35.4 (q, 2 Hz). **FTIR** (neat): 3115, 2854, 1316, 1294, 1108, 1037, 780, 750 cm⁻¹. **HRMS** (ESI): calculated for C₁₃H₁₄F₃N₂O [M+H]⁺ 271.1053; found: 271.1052.

(1-(2-Chlorophenethyl)-1*H*-imidazol-2-yl)methanol (156). The synthesis of **156** was



conducted according to general procedure G with **156** (0.704 g, 3.00 mmol). The product **156** (0.666 g, 2.81 mmol, 94%) was obtained as a pale yellow solid. **R_f**: 0.24 (EtOAc:MeOH 9:1). **¹H NMR** (400 MHz, CD₃OD) δ 7.38 (dd, *J* = 7.9, 1.3 Hz, 1H), 7.22 (td, *J* = 7.6, 1.8 Hz, 1H), 7.15 (td, *J* = 7.6, 1.4 Hz, 1H), 7.07 (dd, *J* = 7.5, 1.8 Hz, 1H), 6.96 (d, *J* = 1.4 Hz, 1H), 6.82 (d, *J* = 1.4 Hz, 1H), 4.40 (s, 2H), 4.34 (t, *J* = 7.1 Hz, 2H), 3.23 (t, *J* = 7.1 Hz, 2H). **¹³C NMR** (101 MHz, CD₃OD) δ 148.2, 136.9, 135.2, 132.4, 130.6, 129.7, 128.3, 127.3, 122.1, 56.7, 46.7, 36.2. **FTIR** (neat): 3137, 3108, 2992, 2948, 2921, 2854, 1480, 1439, 1037, 769, 743, 683, 661 cm⁻¹. **HRMS** (ESI): calculated for C₁₂H₁₄ON₂Cl [M+H]⁺ 237.0789; found: 237.0787.

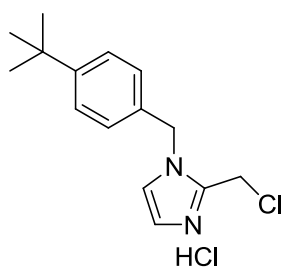
(1-(4-Nitrobenzyl)-1H-imidazol-2-yl)methanol (159) dutpase233. The synthesis of **159** was conducted according to general procedure G with **143** (0.347 g, 1.50 mmol). The product **159** (0.315 g, 1.35 mmol, 90%) was obtained as an orange solid. **R_f**: 0.20 (EtOAc:MeOH 9:1). **¹H NMR** (400 MHz, CD₃OD) δ 8.26 – 8.18 (m, 2H), 7.46 – 7.39 (m, 2H), 7.14 (d, *J* = 1.4 Hz, 1H), 6.97 (d, *J* = 1.4 Hz, 1H), 5.48 (s, 2H), 4.62 (s, 2H). **¹³C NMR** (101 MHz, CD₃OD) δ 149.0, 148.7, 145.9, 129.3, 127.9, 124.9, 122.7, 57.0, 49.9. **FTIR** (neat): 3152, 3130, 3082, 2847, 1521, 1350, 1026, 758, 728 cm⁻¹. **HRMS** (ESI): calculated for C₁₁H₁₂O₃N₃ [M+H]⁺ 234.0873; found: 234.0860.



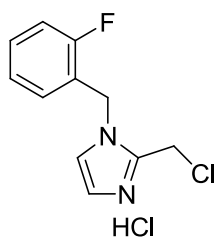
General procedure H: Halogenation of alkylated 1H-Imidazole-2-yl-methanols

To a stirring solution or suspension of alkylated 1H-Imidazol-2-yl-methanol (1.0 eq.) in CHCl₃ (3 mL per mmol), SOCl₂ (1 mL per mmol) was added dropwise over 1 minute at room temperature. The reaction was conducted open to air. After full addition, the reaction mixture was heated to reflux for 3 h. The mixture was concentrated using a nitrogen stream. The resulting crude solid was washed with Et₂O and dried under reduced pressure. The product was used without further purification in the next reaction.

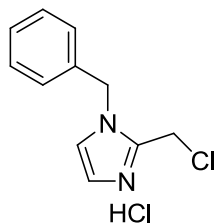
1-(4-tert-Butylbenzyl)-2-(chloromethyl)-1H-imidazole hydrochloride (167). The synthesis of **167** was conducted according to general procedure H with **149** (0.489 g, 2.00 mmol). The product **167** (0.500 g, 1.67 mmol, 84%) was afforded as a white solid. **¹H NMR** (400 MHz, CD₃OD) δ 7.61 (d, *J* = 2.1 Hz, 1H), 7.56 (d, *J* = 2.1 Hz, 1H), 7.52 – 7.45 (m, 2H), 7.36 – 7.30 (m, 2H), 5.47 (s, 2H), 5.09 (s, 2H), 1.31 (s, 9H). **¹³C NMR** (101 MHz, CD₃OD) δ 153.7, 143.5, 131.7, 129.3, 127.4, 124.8, 121.1, 52.2, 35.6, 32.5, 31.6. **FTIR** (neat): 3052, 2962, 2869, 2620, 1521, 1458, 1272, 1238, 817, 769, 739, 702 cm⁻¹. **HRMS** (ESI): calculated for C₁₅H₂₀ClN₂ [M+H]⁺ 263.1310; found: 263.1313.



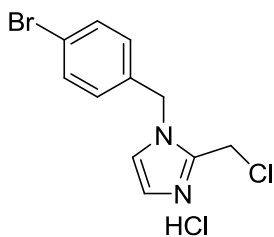
2-(Chloromethyl)-1-(2-fluorobenzyl)-1H-imidazole hydrochloride (163). The synthesis of **163** was conducted according to general procedure H with **144** (0.516 g, 2.50 mmol). The product **163** (0.605 g, 2.32 mmol, 93%) was afforded as a white solid. ¹H NMR (400 MHz, CD₃OD) δ 7.62 (d, *J* = 2.1 Hz, 1H), 7.58 (d, *J* = 2.1 Hz, 1H), 7.52 – 7.42 (m, 2H), 7.30 – 7.15 (m, 2H), 5.57 (s, 2H), 5.10 (s, 2H). ¹³C NMR (101 MHz, CD₃OD) δ 162.4 (d, 247 Hz), 143.7, 133.0 (d, 9 Hz), 132.1 (d, 3 Hz), 126.4 (d, 4 Hz), 124.9 (d, 2 Hz), 121.8 (d, 14 Hz), 121.2, 117.1 (d, 21 Hz), 47.0 (d, 4 Hz), 32.4 (d, 2 Hz). FTIR (neat): 3156, 3123, 3067, 3000, 2948, 2467, 2430, 1231, 1458, 776, 747, 721 cm⁻¹. HRMS (ESI): calculated for C₁₁H₁₁ClFN₂ [M+H]⁺ 225.0589; found: 225.0593.



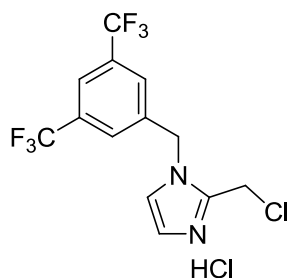
1-Benzyl-2-(chloromethyl)-1H-imidazole hydrochloride (162). The synthesis of **162** was conducted according to general procedure H with **145** (0.753 g, 4.00 mmol). The product **162** (0.931 g, 3.83 mmol, 96%) was afforded as a white solid. ¹H NMR (400 MHz, CD₃OD) δ 7.63 (d, *J* = 2.1 Hz, 1H), 7.59 (d, *J* = 2.1 Hz, 1H), 7.49 – 7.36 (m, 5H), 5.51 (s, 2H), 5.10 (s, 2H). ¹³C NMR (101 MHz, CD₃OD) δ 143.6, 134.7, 130.4, 130.3, 129.5, 124.9, 121.2, 52.5, 32.4. FTIR (neat): 3100, 3067, 3000, 2981, 2951, 2463, 2434, 709 cm⁻¹. HRMS (ESI): calculated for C₁₁H₁₂N₂Cl [M+H]⁺ 207.0684; found: 207.0682.



1-(4-Bromobenzyl)-2-(chloromethyl)-1H-imidazole hydrochloride (164). The synthesis of **164** was conducted according to general procedure H with **146** (1.068 g, 4.00 mmol). The product **164** (1.198 g, 3.72 mmol, 93%) was afforded as a white solid. ¹H NMR (400 MHz, CD₃OD) δ 7.67 – 7.55 (m, 4H), 7.35 – 7.28 (m, 2H), 5.49 (s, 2H), 5.09 (s, 2H). ¹³C NMR (101 MHz, CD₃OD) δ 143.8, 134.0, 133.5, 131.3, 124.9, 124.3, 121.4, 51.7, 32.4. FTIR (neat): 3137, 3100, 3063, 3000, 2948, 2534, 2501, 1235, 795, 728 cm⁻¹. HRMS (ESI): calculated for C₁₁H₁₁BrClN₂ [M+H]⁺ 284.9789; found: 284.9792.

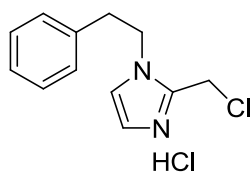


1-(3,5-Bis(trifluoromethyl)benzyl)-2-(chloromethyl)-1H-imidazole hydrochloride (170).



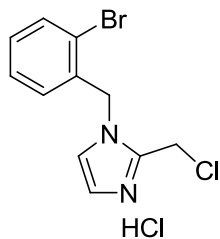
The synthesis of **170** was conducted according to general procedure H with **152** (0.973 g, 3.00 mmol). The product **170** (1.012 g, 2.67 mmol, 89%) was afforded as a white solid. $^1\text{H NMR}$ (400 MHz, CD_3OD) δ 8.04 (s, 3H), 7.73 (d, $J = 2.1$ Hz, 1H), 7.69 (d, $J = 2.1$ Hz, 1H), 5.74 (s, 2H), 5.16 (s, 2H). $^{13}\text{C NMR}$ (101 MHz, CD_3OD) δ 144.3, 138.1, 133.6 (q, 34 Hz), 130.2 (m), 124.9, 124.5 (q, 272 Hz), 124.0 (m), 121.8, 51.1, 32.4. **FTIR** (neat): 3108, 3085, 3059, 2948, 2877, 2627, 1287, 1130, 687cm^{-1} . **HRMS** (ESI): calculated for $\text{C}_{13}\text{H}_{10}\text{N}_2\text{ClF}_6$ $[\text{M}+\text{H}]^+$ 343.0431; found: 343.0434.

2-(Chloromethyl)-1-phenethyl-1H-imidazole hydrochloride (171).



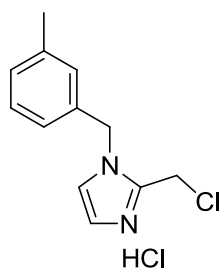
The synthesis of **171** was conducted according to general procedure H with **153** (0.607 g, 3.00 mmol). The product **171** (0.735 g, 2.86 mmol, 95%) was afforded as a white solid. $^1\text{H NMR}$ (400 MHz, CD_3OD) δ 7.62 – 7.55 (m, 2H), 7.40 – 7.24 (m, 3H), 7.22 – 7.15 (m, 2H), 4.76 (s, 2H), 4.55 (t, $J = 7.0$ Hz, 2H), 3.22 (t, $J = 7.0$ Hz, 2H). $^{13}\text{C NMR}$ (101 MHz, CD_3OD) δ 143.4, 137.8, 130.1, 130.0, 128.6, 124.9, 120.9, 50.6, 37.0, 32.1. **FTIR** (neat): 3171, 3067, 3026, 2955, 2497, 2463, 911, 776, 754, 713cm^{-1} . **HRMS** (ESI): calculated for $\text{C}_{12}\text{H}_{14}\text{N}_2\text{Cl}$ $[\text{M}+\text{H}]^+$ 221.0840; found: 221.0840.

1-(2-Bromobenzyl)-2-(chloromethyl)-1H-imidazole hydrochloride (166).

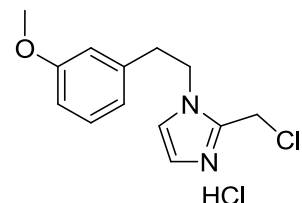


The synthesis of **166** was conducted according to general procedure H with **148** (0.534 g, 2.00 mmol). The product **166** (0.560 g, 1.74 mmol, 87%) was afforded as a white solid. $^1\text{H NMR}$ (400 MHz, CD_3OD) δ 7.76 – 7.69 (m, 1H), 7.67 – 7.62 (m, 1H), 7.50 – 7.42 (m, 2H), 7.41 – 7.32 (m, 2H), 5.61 (s, 2H), 5.13 (s, 2H). $^{13}\text{C NMR}$ (101 MHz, CD_3OD) δ 143.9, 134.8, 133.6, 132.5, 132.1, 129.8, 124.9, 124.7, 121.3, 52.8, 32.6. **FTIR** (neat): 3149, 3093, 3063, 3003, 2951, 2534, 2501, 2478, 795, 754, 732cm^{-1} . **HRMS** (ESI): calculated for $\text{C}_{11}\text{H}_{11}\text{N}_2\text{BrCl}$ $[\text{M}+\text{H}]^+$ 284.9789; found: 284.9794.

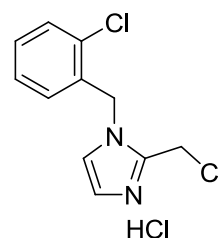
2-(Chloromethyl)-1-(3-methylbenzyl)-1*H*-imidazole hydrochloride (165). The synthesis of **165** was conducted according to general procedure H with **147** (0.809 g, 4.00 mmol). The product **165** (0.956 g, 3.72 mmol, 93%) was afforded as a white solid. ¹H NMR (400 MHz, CD₃OD) δ 7.63 (d, *J* = 2.1 Hz, 1H), 7.58 (d, *J* = 2.1 Hz, 1H), 7.36 – 7.28 (m, 1H), 7.26 – 7.21 (m, 2H), 7.21 – 7.15 (m, 1H), 5.47 (s, 2H), 5.10 (s, 2H), 2.35 (s, 3H). ¹³C NMR (101 MHz, CD₃OD) δ 143.5, 140.6, 134.5, 131.0, 130.3, 130.1, 126.5, 124.9, 121.1, 52.5, 32.5, 21.3. FTIR (neat): 3152, 3096, 2988, 2948, 2854, 2825, 2493, 2441, 754, 721 cm⁻¹. HRMS (ESI): calculated for C₁₂H₁₄N₂Cl [M+H]⁺ 221.0840; found: 221.0843.



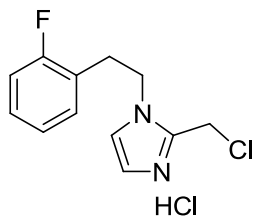
2-(Chloromethyl)-1-(3-methoxyphenethyl)-1*H*-imidazole hydrochloride (172). The synthesis of **172** was conducted according to general procedure H with **154** (0.697 g, 3.00 mmol). The product **172** (0.724 g, 2.52 mmol, 84%) was afforded as a grey solid. ¹H NMR (400 MHz, CD₃OD) δ 7.61 – 7.57 (m, 2H), 7.23 (t, *J* = 8.1 Hz, 1H), 6.88 – 6.81 (m, 1H), 6.78 – 6.71 (m, 2H), 4.77 (s, 2H), 4.55 (t, *J* = 6.9 Hz, 2H), 3.77 (s, 3H), 3.18 (t, *J* = 6.9 Hz, 2H). ¹³C NMR (101 MHz, CD₃OD) δ 161.7, 143.4, 139.3, 131.1, 124.9, 122.1, 120.9, 115.6, 113.9, 55.7, 50.6, 37.0, 32.1. FTIR (neat): 3134, 3119, 3096, 2948, 2873, 2553, 784 cm⁻¹. HRMS (ESI): calculated for C₁₃H₁₆ON₂Cl [M+H]⁺ 251.0946; found: 251.0947.



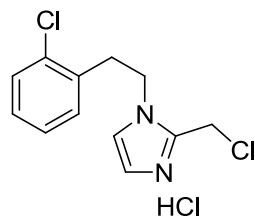
1-(2-Chlorobenzyl)-2-(chloromethyl)-1*H*-imidazole hydrochloride (168). The synthesis of **168** was conducted according to general procedure H with **150** (0.668 g, 3.00 mmol). The product **168** (0.675 g, 2.43 mmol, 81%) was afforded as a white solid. ¹H NMR (400 MHz, CD₃OD) δ 7.65 (d, *J* = 2.1 Hz, 1H), 7.55 (dd, *J* = 7.7, 1.5 Hz, 1H), 7.51 – 7.35 (m, 4H), 5.64 (s, 2H), 5.12 (s, 2H). ¹³C NMR (101 MHz, CD₃OD) δ 143.9, 135.1, 132.4, 132.0, 132.0, 131.4, 129.2, 124.8, 121.3, 50.6, 32.6. FTIR (neat): 3145, 3104, 3059, 3000, 2948, 2411, 799, 743, 724 cm⁻¹. HRMS (ESI): calculated for C₁₁H₁₁N₂Cl₂ [M+H]⁺ 241.0294; found: 241.0296.



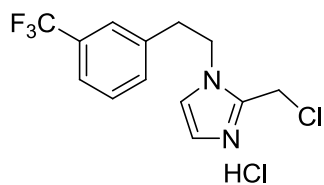
2-(Chloromethyl)-1-(2-fluorophenethyl)-1*H*-imidazole hydrochloride (173). The synthesis of **173** was conducted according to general procedure H with **155** (0.604 g, 2.50 mmol). The product **173** (0.666 g, 2.42 mmol, 97%) was afforded as a white solid. ¹H NMR (400 MHz, CD₃OD) δ 7.54 (d, *J* = 2.1 Hz, 1H), 7.52 (d, *J* = 2.0 Hz, 1H), 7.32 – 7.17 (m, 2H), 7.13 – 7.00 (m, 2H), 4.87 (s, 2H), 4.51 (t, *J* = 7.0 Hz, 2H), 3.28 – 3.20 (m, 2H). ¹³C NMR (101 MHz, CD₃OD) δ 162.7 (d, 243 Hz), 143.4, 132.5 (d, 4 Hz), 130.8 (d, 8 Hz), 125.9 (d, 4 Hz), 124.9, 124.5 (d, 16 Hz), 121.0, 116.5 (d, 22 Hz), 49.30 (d, 2 Hz), 32.1, 30.5 (d, 3 Hz). FTIR (neat): 3104, 3067, 3011, 2951, 2426, 1495, 1231, 765, 702 cm⁻¹. HRMS (ESI): calculated for C₁₂H₁₃N₂ClF [M+H]⁺ 239.0746; found: 239.0747.



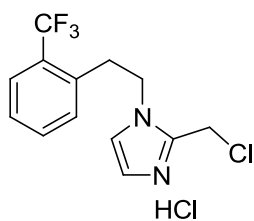
2-(Chloromethyl)-1-(2-chlorophenethyl)-1*H*-imidazole hydrochloride (174). The synthesis of **174** was conducted according to general procedure H with **156** (0.592 g, 2.50 mmol). The product **174** (0.661 g, 2.27 mmol, 91%) was afforded as a white solid. ¹H NMR (400 MHz, CD₃OD) δ 7.59 (d, *J* = 2.0 Hz, 1H), 7.54 (d, *J* = 2.1 Hz, 1H), 7.48 – 7.38 (m, 1H), 7.35 – 7.22 (m, 3H), 4.90 (s, 3H), 4.57 (t, *J* = 7.1 Hz, 2H), 3.38 (t, *J* = 7.1 Hz, 2H). ¹³C NMR (101 MHz, CD₃OD) δ 143.4, 135.3, 135.3, 132.5, 130.9, 130.5, 128.8, 125.0, 121.0, 48.9, 34.7, 32.1. FTIR (neat): 3141, 3123, 3096, 2996, 2944, 2408, 1480, 758, 743, 724 cm⁻¹. HRMS (ESI): calculated for C₁₂H₁₃N₂Cl₂ [M+H]⁺ 255.0450; found: 255.0453.



2-(Chloromethyl)-1-(3-(trifluoromethyl)phenethyl)-1*H*-imidazole hydrochloride (176). The synthesis of **176** was conducted according to general procedure H with **158** (0.541 g, 2.00 mmol). The product **176** (0.602 g, 1.85 mmol, 93%) was afforded as a white solid. ¹H NMR (400 MHz, CD₃OD) δ 7.64 (d, *J* = 2.1 Hz, 1H), 7.61 (d, *J* = 2.1 Hz, 1H), 7.60 – 7.48 (m, 4H), 4.95 (s, 2H), 4.58 (t, *J* = 7.2 Hz, 2H), 3.33 (t, *J* = 7.2 Hz, 2H). ¹³C NMR (101 MHz, CD₃OD) δ 143.5, 139.1, 134.0 (q, 1 Hz), 132.2 (q, 32 Hz), 130.9, 126.8 (q, 4 Hz), 125.5 (q, 271 Hz), 125.2 (q, 4 Hz), 124.8, 121.1, 50.0, 36.5, 32.2. FTIR (neat): 3141, 3115, 3003, 2951, 2430, 1335, 1123, 1074, 791, 702 cm⁻¹. HRMS (ESI): calculated for C₁₃H₁₃N₂ClF₃ [M+H]⁺ 289.0714; found: 289.0718.

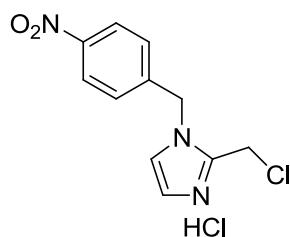


2-(Chloromethyl)-1-(2-(trifluoromethyl)phenethyl)-1H-imidazole hydrochloride (175).



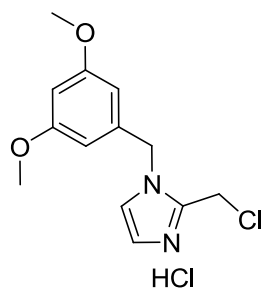
The synthesis of **175** was conducted according to general procedure H with **157** (0.541 g, 2.00 mmol). The product **175** (0.535 g, 1.65 mmol, 82%) was afforded as a white solid. $^1\text{H NMR}$ (400 MHz, CD_3OD) δ 7.75 – 7.69 (m, 1H), 7.63 – 7.55 (m, 2H), 7.53 (d, $J = 2.0$ Hz, 1H), 7.51 – 7.40 (m, 2H), 4.91 (s, 3H), 4.55 (t, $J = 7.4$ Hz, 2H), 3.40 (t, $J = 7.4$ Hz, 2H). $^{13}\text{C NMR}$ (101 MHz, CD_3OD) δ 143.5, 136.2 (q, 2 Hz), 133.9 (q, 1 Hz), 133.1, 129.9 (q, 30 Hz), 129.1, 127.5 (q, 6 Hz), 126.0 (q, 273 Hz), 124.8, 121.5, 50.0 (q, 2 Hz), 34.0 (q, 2 Hz), 32.3. **FTIR** (neat): 3454, 3413, 3111, 3134, 3015, 2962, 2597, 2519, 1316, 1108, 773, 747 cm^{-1} . **HRMS** (ESI): calculated for $\text{C}_{13}\text{H}_{13}\text{N}_2\text{ClF}_3$ $[\text{M}+\text{H}]^+$ 289.0714; found: 289.0718.

2-(Chloromethyl)-1-(4-nitrobenzyl)-1H-imidazole hydrochloride (177). The synthesis of



177 was conducted according to general procedure H with **159** (0.233 g, 1.00 mmol). The product **177** (0.231 g, 0.80 mmol, 80%) was afforded as a yellow solid. $^1\text{H NMR}$ (400 MHz, CD_3OD) δ 8.36 – 8.24 (m, 2H), 7.75 – 7.69 (m, 2H), 7.65 – 7.56 (m, 2H), 5.71 (s, 2H), 5.12 (s, 2H). $^{13}\text{C NMR}$ (101 MHz, CD_3OD) δ 149.7, 144.2, 141.9, 130.3, 125.3, 125.2, 121.6, 51.5, 32.4. **FTIR** (neat): 3164, 3130, 3007, 2981, 2959, 2743, 2478, 1518, 1350, 1227, 862, 769, 747, 721 cm^{-1} . **HRMS** (ESI): calculated for $\text{C}_{11}\text{H}_{11}\text{ClN}_3\text{O}_2$ $[\text{M}+\text{H}]^+$ 252.0534; found: 252.0528.

2-(Chloromethyl)-1-(3,5-dimethoxybenzyl)-1H-imidazole hydrochloride (169). The

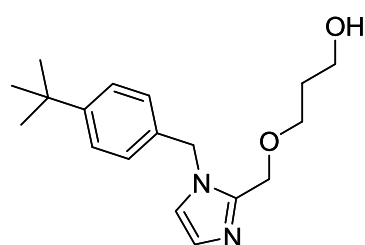


synthesis of **169** was conducted according to general procedure H with **151** (0.621 g, 2.50 mmol). The product **169** (0.700 g, 2.31 mmol, 92%) was afforded as a beige solid. $^1\text{H NMR}$ (400 MHz, CD_3OD) δ 7.68 – 7.58 (m, 2H), 6.59 – 6.48 (m, 3H), 5.44 (s, 2H), 5.11 (s, 1H), 3.83 – 3.73 (m, 6H). $^{13}\text{C NMR}$ (101 MHz, CD_3OD) δ 163.1, 143.6, 136.6, 124.9, 121.1, 101.7, 56.0, 52.5, 32.4. **HRMS** (ESI): calculated for $\text{C}_{13}\text{H}_{16}\text{O}_2\text{N}_2\text{Cl}$ $[\text{M}+\text{H}]^+$ 267.0895; found: 267.0898.

General procedure I: Synthesis of alkylated 1*H*-imidazole hydroxy-alkyl ether

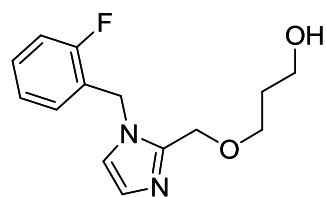
1,3-Propanediol or 1,2-ethanediol (1 mL per mmol halide, dried over Na₂SO₄) was added dropwise to a stirred mixture of Na *tert*-butoxide (3 eq) in dry THF (10 mL per mmol halide) at room temperature. The formed suspension was stirred for 5 minutes before substituted 2-(chloromethyl)-1*H*-imidazole hydrochloride (1.0 eq) was added. The suspension was stirred at 70 °C overnight. The reaction mixture was concentrated under reduced pressure and the residue diluted with water and EtOAc. The aqueous layer was extracted (3x) and the combined organic layers were washed with water (1x) and brine (1x). The solution was dried over Na₂SO₄ and the solvent was removed under reduced pressure. The crude product was purified by silica column chromatography (EtOAc → EtOAc:MeOH 9:1).

3-((1-(4-*tert*-Butylbenzyl)-1*H*-imidazol-2-yl)methoxy)propan-1-ol (184). The synthesis of



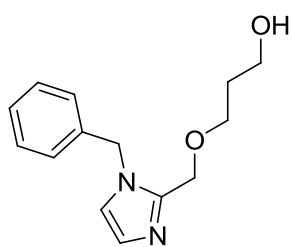
184 was conducted according to general procedure I with **167** (0.299 g, 1.00 mmol) and 1,3-propanediol (1 mL). The product **184** (0.296 g, 0.98 mmol, 98%) was obtained as a pale orange oil. *R_f*: 0.23 (EtOAc:MeOH 9:1). ¹H NMR (400 MHz, CD₃OD) δ 7.43 – 7.37 (m, 2H), 7.17 – 7.11 (m, 2H), 7.09 (d, *J* = 1.3 Hz, 1H), 6.93 (d, *J* = 1.4 Hz, 1H), 5.23 (s, 2H), 4.52 (s, 2H), 3.58 (t, *J* = 6.4 Hz, 2H), 3.52 (t, *J* = 6.3 Hz, 2H), 1.72 (p, *J* = 6.3 Hz, 2H), 1.31 (s, 9H). ¹³C NMR (101 MHz, CD₃OD) δ 152.2, 146.1, 135.1, 128.2, 127.5, 126.8, 123.0, 68.4, 65.3, 59.8, 50.4, 35.4, 33.6, 31.7. FTIR (neat): 3238, 2955, 2869, 1086, 1026, 743, 717, 683 cm⁻¹. HRMS (ESI): calculated for C₁₈H₂₇N₂O₂ [M+H]⁺ 303.2067; found: 303.2069.

3-((1-(2-Fluorobenzyl)-1*H*-imidazol-2-yl)methoxy)propan-1-ol (179). The synthesis of **179**

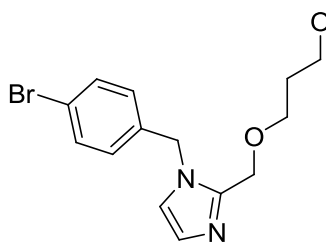


was conducted according to general procedure I with **163** (0.261 g, 1.00 mmol) and 1,3-propanediol (1 mL). The product **179** (0.222 g, 0.84 mmol, 84%) was obtained as a pale orange oil. *R_f*: 0.27 (EtOAc:MeOH 9:1). ¹H NMR (400 MHz, CD₃OD) δ 7.43 – 7.33 (m, 1H), 7.22 – 7.10 (m, 4H), 6.96 (d, *J* = 1.4 Hz, 1H), 5.36 (s, 2H), 4.58 (s, 2H), 3.62 – 3.50 (m, 4H), 1.73 (p, *J* = 6.4 Hz, 2H). ¹³C NMR (101 MHz, CD₃OD) δ 161.9 (d, 246 Hz), 146.2, 131.3 (d, 8 Hz), 130.8 (d, 4 Hz), 127.7, 125.8 (d, 4 Hz), 125.2 (d, 14 Hz), 122.9 (d, 1 Hz), 116.5 (d, 22 Hz), 68.4, 65.3, 59.8, 44.6 (d, 5 Hz), 33.5. FTIR (neat): 3238, 2929, 2866, 1495, 1462, 1235, 1086, 758, 702, 676 cm⁻¹. HRMS (ESI): calculated for C₁₄H₁₈FN₂O₂ [M+H]⁺ 265.1347; found: 265.1348.

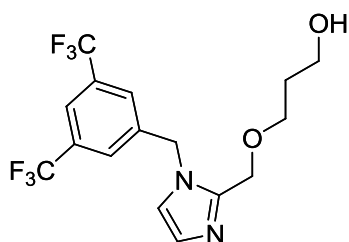
3-((1-Benzyl-1*H*-imidazol-2-yl)methoxy)propan-1-ol (161). The synthesis of **161** was conducted according to general procedure I with **162** (0.243 g, 1.00 mmol) and 1,3-propanediol (1 mL). The product **161** (0.199 g, 0.81 mmol, 81%) was obtained as a pale yellow solid. **R_f**: 0.17 (EtOAc:MeOH 9:1). **¹H NMR** (400 MHz, CD₃OD) δ 7.39 – 7.24 (m, 3H), 7.23 – 7.14 (m, 2H), 7.08 (d, *J* = 1.4 Hz, 1H), 6.93 (d, *J* = 1.4 Hz, 1H), 5.25 (s, 2H), 4.50 (s, 2H), 3.55 (t, *J* = 6.4 Hz, 2H), 3.50 (t, *J* = 6.3 Hz, 2H), 1.71 (p, *J* = 6.3 Hz, 2H). **¹³C NMR** (101 MHz, CD₃OD) δ 146.1, 138.2, 129.9, 129.0, 128.4, 127.6, 123.0, 68.4, 65.3, 59.8, 50.7, 33.5. **FTIR** (neat): 3193, 3104, 2948, 2858, 1088, 1056, 1030, 978, 769, 721, 702, 676 cm⁻¹. **HRMS** (ESI): calculated for C₁₄H₁₉N₂O₂ [M+H]⁺ 247.1441; found: 247.1446.



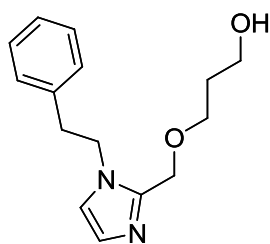
3-((1-(4-Bromobenzyl)-1*H*-imidazol-2-yl)methoxy)propan-1-ol (186). The synthesis of **186** was conducted according to general procedure I with **164** (0.483 g, 1.50 mmol) and 1,3-propanediol (1.5 mL). The product **186** (0.393 g, 1.21 mmol, 81%) was obtained as a pale yellow oil. **R_f**: 0.30 (EtOAc:MeOH 9:1). **¹H NMR** (400 MHz, CD₃OD) δ 7.52 – 7.46 (m, 2H), 7.15 – 7.08 (m, 3H), 6.94 (d, *J* = 1.3 Hz, 1H), 5.24 (s, 2H), 4.51 (s, 2H), 3.59 – 3.47 (m, 4H), 1.70 (p, *J* = 6.3 Hz, 2H). **¹³C NMR** (101 MHz, CD₃OD) δ 146.2, 137.6, 132.9, 130.3, 127.8, 122.9, 122.8, 68.4, 65.2, 59.7, 50.0, 33.5. **FTIR** (neat): 3234, 3111, 2925, 2866, 1491, 1074, 1015, 806, 743 cm⁻¹. **HRMS** (ESI): calculated C₁₄H₁₈BrN₂O₂ [M+H]⁺ 325.0546; found: 325.0549.



3-((1-(3,5-Bis(trifluoromethyl)benzyl)-1*H*-imidazol-2-yl)methoxy)propan-1-ol (194). The synthesis of **194** was conducted according to general procedure I with **170** (0.343 g, 0.90 mmol) and 1,3-propanediol (1 mL). The product **194** (0.299 g, 0.78 mmol, 87%) was obtained as a pale yellow solid. **R_f**: 0.33 (EtOAc:MeOH 9:1). **¹H NMR** (400 MHz, CD₃OD) δ 7.92 (s, 1H), 7.77 (s, 2H), 7.21 (d, *J* = 1.4 Hz, 1H), 7.02 (d, *J* = 1.4 Hz, 1H), 5.48 (s, 2H), 4.57 (s, 2H), 3.55 – 3.43 (m, 4H), 1.61 (p, *J* = 6.3 Hz, 2H). **¹³C NMR** (101 MHz, CD₃OD) δ 146.6, 142.1, 133.1 (q, 33 Hz), 128.8 (m), 128.4, 124.7 (q, 272 Hz), 122.9, 122.6 (m), 68.6, 65.2, 59.5, 49.6, 33.4. **FTIR** (neat): 3379, 3119, 2940, 2880, 1279, 1167, 1130, 1086, 1071, 907, 687 cm⁻¹. **HRMS** (ESI): calculated for C₁₆H₁₇F₆N₂O₂ [M+H]⁺ 383.1189; found: 383.1194.

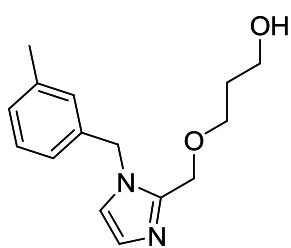


3-((1-Phenethyl-1H-imidazol-2-yl)methoxy)propan-1-ol (198). The synthesis of **198** was



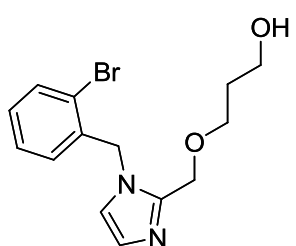
conducted according to general procedure I with **171** (0.257 g, 1.00 mmol) and 1,3-propanediol (1 mL). The product **198** (0.210 g, 0.81 mmol, 81%) was obtained as a pale yellow solid. **R_f**: 0.27 (EtOAc:MeOH 9:1). **¹H NMR** (400 MHz, CD₃OD) δ 7.31 – 7.18 (m, 3H), 7.13 – 7.07 (m, 2H), 7.05 – 7.02 (m, 1H), 6.87 (d, *J* = 1.4 Hz, 1H), 4.32 – 4.25 (m, 2H), 4.24 (s, 2H), 3.61 (t, *J* = 6.4 Hz, 2H), 3.49 (t, *J* = 6.3 Hz, 2H), 3.07 (t, *J* = 6.9 Hz, 2H), 1.76 (p, *J* = 6.4 Hz, 2H). **¹³C NMR** (101 MHz, CD₃OD) δ 146.0, 139.5, 129.9, 129.7, 127.8, 127.4, 122.4, 68.4, 65.0, 59.8, 38.5, 33.6. (1 alkyl signal under solvent). **FTIR** (neat): 3134, 3111, 2940, 2918, 2858, 1495, 1089, 1060, 978, 765, 736, 702, 665 cm⁻¹. **HRMS** (ESI): calculated for C₁₅H₂₁N₂O₂ [M+H]⁺ 261.1598; found: 261.1602.

3-((1-(3-Methylbenzyl)-1H-imidazol-2-yl)methoxy)propan-1-ol (188). The synthesis of



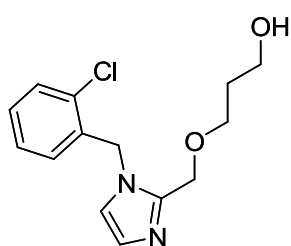
188 was conducted according to general procedure I with **165** (0.257 g, 1.00 mmol) and 1,3-propanediol (1 mL). The product **188** (0.205 g, 0.79 mmol, 79%) was obtained as a colorless oil. **R_f**: 0.30 (EtOAc:MeOH 9:1). **¹H NMR** (400 MHz, CD₃OD) δ 7.22 (t, *J* = 7.6 Hz, 1H), 7.14 – 7.06 (m, 2H), 7.04 – 6.95 (m, 2H), 6.93 (d, *J* = 1.4 Hz, 1H), 5.22 (s, 2H), 4.50 (s, 2H), 3.57 (t, *J* = 6.4 Hz, 2H), 3.51 (t, *J* = 6.3 Hz, 2H), 2.30 (s, 3H), 1.72 (p, *J* = 6.3 Hz, 2H). **¹³C NMR** (101 MHz, CD₃OD) δ 146.1, 139.8, 138.1, 129.8, 129.7, 129.0, 127.6, 125.5, 123.0, 68.4, 65.3, 59.8, 50.7, 33.6, 21.4. **FTIR** (neat): 3219, 2921, 2866, 1495, 1439, 1086, 1056, 736, 695 cm⁻¹. **HRMS** (ESI): calculated for C₁₅H₂₁N₂O₂ [M+H]⁺ 261.1598; found: 261.1602.

3-((1-(2-Bromobenzyl)-1H-imidazol-2-yl)methoxy)propan-1-ol (190). The synthesis of **190**

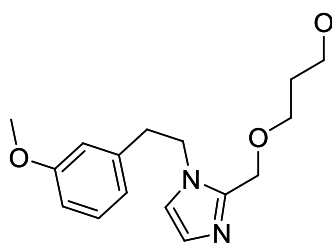


was conducted according to general procedure I with **166** (0.225 g, 0.70 mmol) and 1,3-propanediol (0.7 mL). The product **190** (0.188 g, 0.58 mmol, 83%) was obtained as a colorless oil. **R_f**: 0.26 (EtOAc:MeOH 9:1). **¹H NMR** (400 MHz, CD₃OD) δ 7.65 (dd, *J* = 7.9, 1.3 Hz, 1H), 7.32 (td, *J* = 7.6, 1.3 Hz, 1H), 7.24 (td, *J* = 7.7, 1.8 Hz, 1H), 7.08 (d, *J* = 1.4 Hz, 1H), 6.98 (d, *J* = 1.4 Hz, 1H), 6.85 (dd, *J* = 7.7, 1.8 Hz, 1H), 5.37 (s, 2H), 4.54 (s, 2H), 3.56 – 3.47 (m, 4H), 1.67 (p, *J* = 6.4 Hz, 2H). **¹³C NMR** (101 MHz, CD₃OD) δ 146.4, 137.4, 134.1, 130.8, 129.8, 129.2, 127.8, 123.6, 123.0, 68.5, 65.4, 59.8, 50.9, 33.5. **FTIR** (neat): 3231, 2925, 2866, 1443, 1074, 1052, 1030, 743, 702, 665 cm⁻¹. **HRMS** (ESI): calculated for C₁₄H₁₈BrN₂O₂ [M+H]⁺ 325.0546; found: 325.0551.

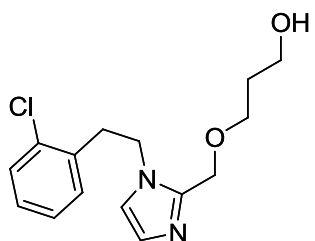
3-((1-(2-Chlorobenzyl)-1H-imidazol-2-yl)methoxy)propan-1-ol (192). The synthesis of **192** was conducted according to general procedure I with **168** (0.278 g, 1.00 mmol) and 1,3-propanediol (1 mL). The product **192** (0.235 g, 0.84 mmol, 84%) was obtained as a pale yellow oil. **R_f**: 0.20 (EtOAc:MeOH 9:1). **¹H NMR** (400 MHz, CD₃OD) δ 7.46 (dd, *J* = 7.8, 1.5 Hz, 1H), 7.36 – 7.22 (m, 2H), 7.08 (d, *J* = 1.4 Hz, 1H), 6.97 (d, *J* = 1.4 Hz, 1H), 6.93 – 6.87 (m, 1H), 5.39 (s, 2H), 4.54 (s, 2H), 3.56 – 3.47 (m, 4H), 1.67 (p, *J* = 6.3 Hz, 2H). **¹³C NMR** (101 MHz, CD₃OD) δ 146.4, 135.7, 133.9, 130.7, 130.6, 129.9, 128.6, 127.8, 123.1, 68.5, 65.4, 59.8, 48.4, 33.5. **FTIR** (neat): 3238, 2925, 2866, 1074, 1056, 747 cm⁻¹. **HRMS** (ESI): calculated for C₁₄H₁₇ClN₂O₂Na [M+Na]⁺ 303.0871; found: 303.0868.



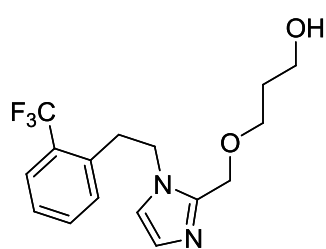
3-((1-(3-Methoxyphenethyl)-1H-imidazol-2-yl)methoxy)propan-1-ol (200). The synthesis of **200** was conducted according to general procedure I with **172** (0.287 g, 1.00 mmol) and 1,3-propanediol (1 mL). The product **200** (0.180 g, 0.62 mmol, 62%) was obtained as a pale yellow oil. **R_f**: 0.20 (EtOAc:MeOH 9:1). **¹H NMR** (400 MHz, CD₃OD) δ 7.20 – 7.13 (m, 1H), 7.04 (d, *J* = 1.4 Hz, 1H), 6.87 (d, *J* = 1.4 Hz, 1H), 6.80 – 6.75 (m, 1H), 6.71 – 6.66 (m, 1H), 6.60 – 6.57 (m, 1H), 4.27 (t, *J* = 6.9 Hz, 2H), 4.22 (s, 2H), 3.71 (s, 3H), 3.60 (t, *J* = 6.4 Hz, 2H), 3.48 (t, *J* = 6.3 Hz, 2H), 3.03 (t, *J* = 6.9 Hz, 2H), 1.76 (p, *J* = 6.3 Hz, 2H). **¹³C NMR** (101 MHz, CD₃OD) δ 161.3, 146.0, 141.0, 130.6, 127.3, 122.4, 122.1, 115.3, 113.5, 68.4, 65.0, 59.8, 55.6, 48.7, 38.5, 33.6. **FTIR** (neat): 3204, 2940, 2866, 1588, 1495, 1439, 1264, 1156, 1086, 1052, 780, 747, 698 cm⁻¹. **HRMS** (ESI): calculated for C₁₆H₂₃N₂O₃ [M+H]⁺ 291.1703; found: 291.1695.



3-((1-(2-Chlorophenethyl)-1H-imidazol-2-yl)methoxy)propan-1-ol (204). The synthesis of **204** was conducted according to general procedure I with **174** (0.204 g, 0.70 mmol) and 1,3-propanediol (0.7 mL). The product **204** (0.180 g, 0.61 mmol, 87%) was obtained as a pale yellow oil. **R_f**: 0.19 (EtOAc:MeOH 9:1). **¹H NMR** (400 MHz, CD₃OD) δ 7.40 (dd, *J* = 7.9, 1.3 Hz, 1H), 7.24 (td, *J* = 7.7, 1.8 Hz, 1H), 7.17 (td, *J* = 7.5, 1.4 Hz, 1H), 7.07 (dd, *J* = 7.5, 1.7 Hz, 1H), 7.01 (d, *J* = 1.3 Hz, 1H), 6.86 (d, *J* = 1.3 Hz, 1H), 4.33 (t, *J* = 7.0 Hz, 2H), 4.30 (s, 2H), 3.61 (t, *J* = 6.4 Hz, 2H), 3.51 (t, *J* = 6.3 Hz, 2H), 3.23 (t, *J* = 7.0 Hz, 2H), 1.78 (p, *J* = 6.4 Hz, 2H). **¹³C NMR** (101 MHz, CD₃OD) δ 145.9, 136.8, 135.2, 132.4, 130.6, 129.8, 128.3, 127.5, 122.4, 68.5, 65.0, 59.9, 46.7, 36.2, 33.6. **FTIR** (neat): 3234, 2933, 2866, 1480, 1439, 1086, 1056, 750, 680 cm⁻¹. **HRMS** (ESI): calculated for C₁₅H₂₀ClN₂O₂ [M+H]⁺ 295.1208; found: 295.1210.

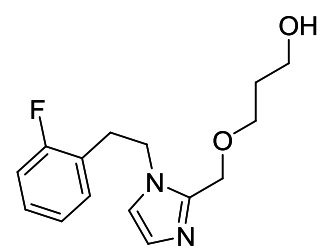


3-((1-(2-(Trifluoromethyl)phenethyl)-1H-imidazol-2-yl)methoxy)propan-1-ol (206).



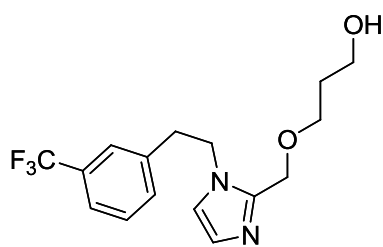
The synthesis of **206** was conducted according to general procedure I with **175** (0.228 g, 0.70 mmol) and 1,3-propanediol (0.7 mL). The product **206** (0.199 g, 6.06 mmol, 87%) was obtained as a pale yellow solid. R_f : 0.20 (EtOAc:MeOH 9:1). $^1\text{H NMR}$ (400 MHz, CD_3OD) δ 7.71 (d, $J = 7.6$ Hz, 1H), 7.54 – 7.40 (m, 2H), 7.17 (d, $J = 7.6$ Hz, 1H), 7.03 (d, $J = 1.4$ Hz, 1H), 6.90 (d, $J = 1.3$ Hz, 1H), 4.38 – 4.28 (m, 4H), 3.60 (t, $J = 6.4$ Hz, 2H), 3.51 (t, $J = 6.3$ Hz, 2H), 3.32 – 3.24 (m, 2H), 1.77 (p, $J = 6.4$ Hz, 2H). $^{13}\text{C NMR}$ (101 MHz, CD_3OD) δ 146.0, 137.7 (q, 2 Hz), 133.5 (q, 1Hz), 133.1, 129.8 (q, 30 Hz), 128.5, 127.6, 127.2 (q, 6 Hz), 126.1 (q, 273 Hz), 122.4, 68.5, 65.0, 59.8, 48.2 (q, 2 Hz), 35.4 (q, 2 Hz), 33.6. **FTIR** (neat): 3216, 2918, 2866, 1324, 1298, 1171, 1153, 1100, 1082, 1048, 776, 747 cm^{-1} . **HRMS** (ESI): calculated for $\text{C}_{16}\text{H}_{20}\text{F}_3\text{N}_2\text{O}_2$ $[\text{M}+\text{H}]^+$ 329.1471; found: 329.1473.

3-((1-(2-Fluorophenethyl)-1H-imidazol-2-yl)methoxy)propan-1-ol (202).



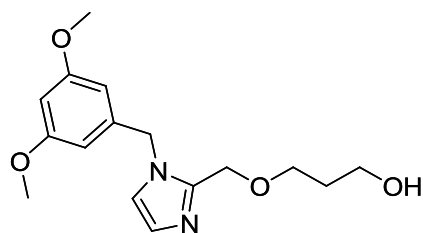
The synthesis of **202** was conducted according to general procedure I with **173** (0.275 g, 1.00 mmol) and 1,3-propanediol (1 mL). The product **202** (0.188 g, 0.68 mmol, 68%) was obtained as pale yellow oil. R_f : 0.20 (EtOAc:MeOH 9:1). $^1\text{H NMR}$ (400 MHz, CD_3OD) δ 7.32 – 7.22 (m, 1H), 7.14 – 7.03 (m, 3H), 7.00 (d, $J = 1.3$ Hz, 1H), 6.86 (d, $J = 1.4$ Hz, 1H), 4.37 – 4.25 (m, 4H), 3.61 (t, $J = 6.4$ Hz, 2H), 3.52 (t, $J = 6.3$ Hz, 2H), 3.14 (t, $J = 7.0$ Hz, 2H), 1.78 (p, $J = 6.4$ Hz, 2H). $^{13}\text{C NMR}$ (101 MHz, CD_3OD) δ 162.7 (d, 244 Hz), 145.9, 132.5 (d, 5 Hz), 130.1 (d, 8 Hz), 127.4, 126.1 (d, 16 Hz), 125.5 (d, 3 Hz), 122.4, 116.3 (d, 22 Hz), 68.4, 65.0, 59.9, 47.3 (d, 2 Hz), 33.6, 31.8 (d, 2 Hz). **FTIR** (neat): 3234, 2929, 2866, 2495, 1495, 1235, 1074, 762 cm^{-1} . **HRMS** (ESI): calculated for $\text{C}_{15}\text{H}_{20}\text{FN}_2\text{O}_2$ $[\text{M}+\text{H}]^+$ 279.1503; found: 279.1505.

3-((1-(3-(Trifluoromethyl)phenethyl)-1H-imidazol-2-yl)methoxy)propan-1-ol (196). The



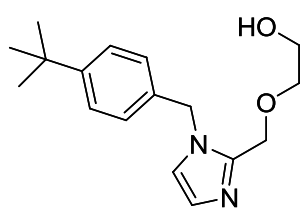
synthesis of **196** was conducted according to general procedure I with **176** (0.228 g, 0.70 mmol) and 1,3-propanediol (0.7 mL). The product **196** (0.207 g, 0.63 mmol, 90%) was obtained as pale yellow solid. **R_f**: 0.20 (EtOAc:MeOH 9:1). **¹H NMR** (400 MHz, CD₃OD) δ 7.56 – 7.43 (m, 2H), 7.42 – 7.36 (m, 2H), 7.03 (d, *J* = 1.4 Hz, 1H), 6.87 (d, *J* = 1.4 Hz, 1H), 4.40 – 4.24 (m, 4H), 3.61 (t, *J* = 6.4 Hz, 2H), 3.52 (t, *J* = 6.3 Hz, 2H), 3.18 (t, *J* = 7.0 Hz, 2H), 1.77 (p, *J* = 6.4 Hz, 2H). **¹³C NMR** (101 MHz, CD₃OD) δ 145.9, 140.8, 133.8 (q, 1 Hz), 131.9 (q, 32 Hz), 130.4, 127.5, 126.7 (q, 4 Hz), 125.6 (q, 271 Hz), 124.6 (q, 4 Hz), 122.4, 68.4, 65.0, 59.8, 38.0, 33.6. **FTIR** (neat): 3219, 2940, 2866, 1339, 1156, 1097, 1074, 754, 706, 661 cm⁻¹. **HRMS** (ESI): calculated for C₁₆H₂₀F₃N₂O₂ [M+H]⁺ 329.1471; found: 329.1475.

3-((1-(3,5-Dimethoxybenzyl)-1H-imidazol-2-yl)methoxy)propan-1-ol (182) Sodium



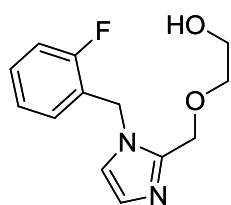
hydroxide (0.120 g, 3.00 mmol) was suspended in 1,3-propanediol (2 mL) and heated to 40 °C. **169** (0.303 g, 1.00 mmol) was added and the reaction mixture was stirred at 80 °C overnight. Water and EtOAc were added to the reaction mixture. The aqueous layer was extracted (3x). The combined organic layers were washed with water (3x) and brine (1x). The organic phase was dried over Na₂SO₄ and the solvent removed under reduced pressure. The crude product was purified by silica column chromatography (EtOAc:MeOH 9:1). **182** (0.131 g, 0.43 mmol, 43%) was obtained as pale orange oil. **¹H NMR** (400 MHz, CDCl₃) δ 7.02 (d, *J* = 1.3 Hz, 1H), 6.91 (d, *J* = 1.3 Hz, 1H), 6.38 (t, *J* = 2.3 Hz, 1H), 6.23 (d, *J* = 2.2 Hz, 2H), 5.09 (s, 2H), 4.57 (s, 2H), 3.76 – 3.69 (m, 6H), 3.64 (t, *J* = 5.9 Hz, 2H), 1.77 (p, *J* = 5.8 Hz, 2H). **¹³C NMR** (101 MHz, CDCl₃) δ 161.4, 144.8, 138.6, 127.7, 121.5, 105.2, 99.7, 68.7, 64.9, 60.6, 55.5, 49.9, 32.3. **HRMS** (ESI): calculated for C₁₆H₂₃N₂O₄ [M+H]⁺ 307.1652; found: 307.1651.

2-((1-(4-*tert*-Butylbenzyl)-1*H*-imidazol-2-yl)methoxy)ethanol (183). The synthesis of **183**



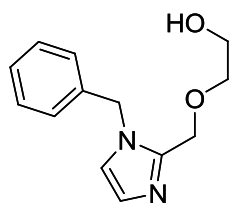
was conducted according to general procedure I with **167** (0.419 g, 1.40 mmol) and 1,2-ethanediol (1.4 mL). The product **183** (0.325 g, 1.12 mmol, 80%) was obtained as a pale orange oil. **R_f**: 0.27 (EtOAc:MeOH 9:1). **¹H NMR** (400 MHz, CD₃OD) δ 7.43 – 7.37 (m, 2H), 7.19 – 7.12 (m, 2H), 7.10 (d, *J* = 1.4 Hz, 1H), 6.93 (d, *J* = 1.3 Hz, 1H), 5.26 (s, 2H), 4.56 (s, 2H), 3.64 – 3.59 (m, 2H), 3.53 – 3.47 (m, 2H), 1.31 (s, 9H). **¹³C NMR** (101 MHz, CD₃OD) δ 152.2, 145.9, 135.1, 128.3, 127.5, 126.8, 123.0, 72.9, 65.4, 62.0, 50.4, 35.4, 31.7. **FTIR** (neat): 3197, 3108, 2962, 2907, 2869, 1491, 1272, 1112, 1082, 1056, 992, 754, 721 cm⁻¹. **HRMS** (ESI): calculated for C₁₇H₂₅N₂O₂ [M+H]⁺ 289.1911; found: 289.1912.

2-((1-(2-Fluorobenzyl)-1*H*-imidazol-2-yl)methoxy)ethanol (178). The synthesis of **178** was



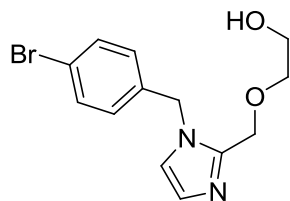
conducted according to general procedure I with **163** (0.261 g, 1.00 mmol) and 1,2-ethanediol (1.0 mL). The product **178** (0.205 g, 0.82 mmol, 82%) was obtained as a pale orange oil. **R_f**: 0.20 (EtOAc:MeOH 9:1). **¹H NMR** (400 MHz, CD₃OD) δ 7.42 – 7.32 (m, 1H), 7.23 – 7.09 (m, 4H), 6.94 (d, *J* = 1.4 Hz, 1H), 5.37 (s, 2H), 4.62 (s, 2H), 3.65 – 3.58 (m, 2H), 3.54 – 3.48 (m, 2H). **¹³C NMR** (101 MHz, CD₃OD) δ 162.0 (d, 246 Hz), 146.1, 131.4 (d, 8 Hz), 131.0 (d, 4 Hz), 127.7, 125.8 (d, 4 Hz), 125.1 (d, 15 Hz), 123.0 (d, 1 Hz), 116.5 (d, 21 Hz), 72.9, 65.4, 62.0, 44.7 (d, 4 Hz). **FTIR** (neat): 3208, 2921, 2862, 1495, 1458, 1235, 1104, 1071, 1033, 754, 702, 676 cm⁻¹. **HRMS** (ESI): calculated for C₁₃H₁₆FN₂O₂ [M+H]⁺ 251.1190; found: 251.1191.

2-((1-Benzyl-1*H*-imidazol-2-yl)methoxy)ethanol (180). The synthesis of **180** was conducted

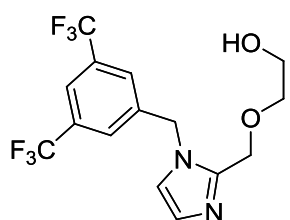


according to general procedure I with **162** (0.243 g, 1.00 mmol) and 1,2-ethanediol (1.0 mL). The product **180** (0.171 g, 0.74 mmol, 74%) was obtained as a pale yellow solid. **R_f**: 0.17 (EtOAc:MeOH 9:1). **¹H NMR** (400 MHz, CD₃OD) δ 7.40 – 7.27 (m, 3H), 7.26 – 7.18 (m, 2H), 7.12 (d, *J* = 1.4 Hz, 1H), 6.94 (d, *J* = 1.4 Hz, 1H), 5.30 (s, 2H), 4.56 (s, 2H), 3.64 – 3.59 (m, 2H), 3.52 – 3.47 (m, 2H). **¹³C NMR** (101 MHz, CD₃OD) δ 146.0, 138.1, 129.9, 129.0, 128.5, 127.6, 123.1, 72.9, 65.4, 62.0, 50.7. **FTIR** (neat): 3175, 3100, 2918, 2869, 1100, 1060, 989, 769, 721, 698, 676 cm⁻¹. **HRMS** (ESI): calculated for C₁₃H₁₇N₂O₂ [M+H]⁺ 233.1285; found: 233.1287.

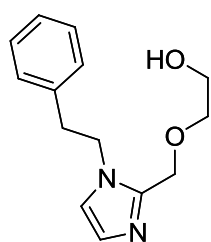
2-((1-(4-Bromobenzyl)-1H-imidazol-2-yl)methoxy)ethanol (185). The synthesis of **185** was conducted according to general procedure I with **164** (0.483 g, 1.50 mmol) and 1,2-ethanediol (1.5 mL). The product **185** (0.301 g, 0.97 mmol, 65%) was obtained as a pale yellow oil. **R_f**: 0.24 (EtOAc:MeOH 9:1). **¹H NMR** (400 MHz, CD₃OD) δ 7.54 – 7.46 (m, 2H), 7.20 – 7.10 (m, 3H), 6.95 (d, *J* = 1.4 Hz, 1H), 5.27 (s, 2H), 4.56 (s, 2H), 3.65 – 3.58 (m, 2H), 3.53 – 3.46 (m, 2H). **¹³C NMR** (101 MHz, CD₃OD) δ 146.0, 137.5, 133.0, 130.5, 127.8, 123.0, 122.8, 72.9, 65.4, 62.0, 50.0. **FTIR** (neat): 3186, 3111, 2910, 2858, 1491, 1112, 1071, 1015, 806, 743 cm⁻¹. **HRMS** (ESI): calculated for C₁₃H₁₆BrN₂O₂ [M+H]⁺ 311.0390; found: 311.0395.



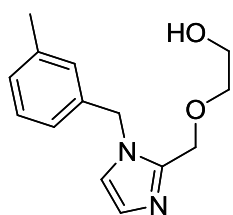
2-((1-(3,5-Bis(trifluoromethyl)benzyl)-1H-imidazol-2-yl)methoxy)ethanol (193). The synthesis of **193** was conducted according to general procedure I with **170** (0.343 g, 0.90 mmol) and 1,2-ethanediol (0.9 mL). The product **193** (0.303 g, 0.82 mmol, 91%) was obtained as pale yellow solid. **R_f**: 0.27 (EtOAc:MeOH 9:1). **¹H NMR** (400 MHz, CD₃OD) δ 7.93 (s, 1H), 7.81 (s, 2H), 7.22 (d, *J* = 1.4 Hz, 1H), 7.02 (d, *J* = 1.4 Hz, 1H), 5.52 (s, 2H), 4.61 (s, 2H), 3.59 – 3.52 (m, 2H), 3.52 – 3.46 (m, 2H). **¹³C NMR** (101 MHz, CD₃OD) δ 146.4, 142.0, 133.1(q, 33 Hz), 129.0 (m), 128.4, 124.7 (q, 272 Hz), 123.0, 122.7(m), 73.0, 65.3, 61.8, 49.6. **FTIR** (neat): 3193, 3059, 2925, 2862, 1380, 1367, 1283, 1167, 1130, 1112, 1074, 1030, 884, 713, 687 cm⁻¹. **HRMS** (ESI): calculated for C₁₅H₁₅F₆N₂O₂ [M+H]⁺ 369.1032; found: 369.1034.



2-((1-Phenethyl)-1H-imidazol-2-yl)methoxy)ethanol (197). The synthesis of **197** was conducted according to general procedure I with **171** (0.257 g, 1.00 mmol) and 1,2-ethanediol (1.0 mL). The product **197** (0.174 g, 0.71 mmol, 71%) was obtained as a pale yellow oil. **R_f**: 0.24 (EtOAc:MeOH 9:1). **¹H NMR** (400 MHz, CD₃OD) δ 7.30 – 7.18 (m, 3H), 7.14 – 7.08 (m, 2H), 7.05 (d, *J* = 1.4 Hz, 1H), 6.87 (d, *J* = 1.4 Hz, 1H), 4.36 – 4.23 (m, 4H), 3.69 – 3.60 (m, 2H), 3.50 – 3.42 (m, 2H), 3.08 (t, *J* = 7.0 Hz, 2H). **¹³C NMR** (101 MHz, CD₃OD) δ 145.9, 139.5, 130.0, 129.6, 127.8, 127.4, 122.4, 72.8, 65.1, 62.0, 48.8, 38.4. **FTIR** (neat): 3204, 3029, 2921, 2858, 1495, 1458, 1439, 1071, 1033, 989, 750, 702 cm⁻¹. **HRMS** (ESI): calculated for C₁₄H₁₉N₂O₂ [M+H]⁺ 265.1347; found: 265.1347.

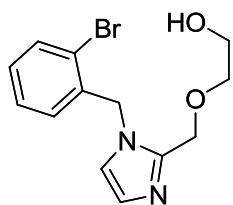


2-((1-(3-Methylbenzyl)-1H-imidazol-2-yl)methoxy)ethanol (187). The synthesis of **187** was



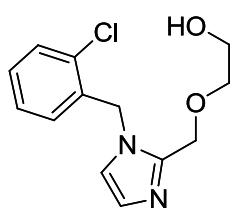
conducted according to general procedure I with **165** (0.257 g, 1.00 mmol) and 1,2-ethanediol (1.0 mL). The product **187** (0.198 g, 0.80 mmol, 80%) was obtained as a pale yellow solid. **R_f**: 0.16 (EtOAc:MeOH 9:1). **¹H NMR** (400 MHz, CD₃OD) δ 7.26 – 7.19 (m, 1H), 7.15 – 7.08 (m, 2H), 7.07 – 6.97 (m, 2H), 6.93 (d, *J* = 1.3 Hz, 1H), 5.25 (s, 2H), 4.55 (s, 2H), 3.66 – 3.55 (m, 2H), 3.56 – 3.44 (m, 2H), 2.31 (s, 3H). **¹³C NMR** (101 MHz, CD₃OD) δ 146.0, 139.8, 138.0, 129.8, 129.7, 129.1, 127.5, 125.6, 123.1, 72.9, 65.4, 62.0, 50.7, 21.4. **FTIR** (neat): 3193, 3111, 2895, 2869, 1097, 1060, 985, 773, 743, 698 cm⁻¹. **HRMS** (ESI): calculated for C₁₄H₁₉N₂O₂ [M+H]⁺ 247.1441; found: 247.1440.

2-((1-(2-Bromobenzyl)-1H-imidazol-2-yl)methoxy)ethanol (189). The synthesis of **189** was



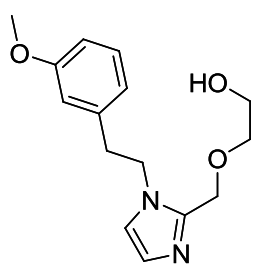
conducted according to general procedure I with **166** (0.225 g, 0.70 mmol) and 1,2-ethanediol (0.7 mL). The product **189** (0.184 g, 0.59 mmol, 84%) was obtained as a pale yellow solid. **R_f**: 0.19 (EtOAc:MeOH 9:1). **¹H NMR** (400 MHz, CD₃OD) δ 7.69 – 7.61 (m, 1H), 7.37 – 7.29 (m, 1H), 7.29 – 7.20 (m, 1H), 7.08 – 7.04 (m, 1H), 6.98 (d, *J* = 1.3 Hz, 1H), 6.95 – 6.88 (m, 1H), 5.39 (s, 2H), 4.60 (s, 2H), 3.65 – 3.56 (m, 2H), 3.56 – 3.46 (m, 2H). **¹³C NMR** (101 MHz, CD₃OD) δ 146.3, 137.3, 134.2, 130.9, 130.2, 129.2, 127.8, 123.8, 123.0, 72.9, 65.5, 62.0, 50.9. **FTIR** (neat): 3257, 3119, 2962, 2929, 2903, 2862, 1439, 1346, 1272, 1112, 1078, 1045, 1026, 996, 877, 776, 747, 702, 672 cm⁻¹. **HRMS** (ESI): calculated for C₁₃H₁₆BrN₂O₂ [M+H]⁺ 311.0390; found: 311.0396.

2-((1-(2-Chlorobenzyl)-1H-imidazol-2-yl)methoxy)ethanol (191). The synthesis of **191** was

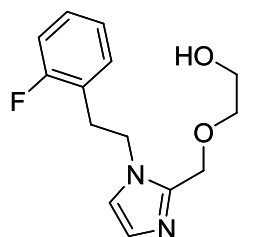


conducted according to general procedure I with **168** (0.241 g, 0.87 mmol) and 1,2-ethanediol (1.0 mL). The product **191** (0.189 g, 0.71 mmol, 82%) was obtained as a pale yellow solid. **R_f**: 0.21 (EtOAc:MeOH 9:1). **¹H NMR** (400 MHz, CD₃OD) δ 7.46 (dd, *J* = 7.8, 1.4 Hz, 1H), 7.38 – 7.22 (m, 2H), 7.07 (d, *J* = 1.4 Hz, 1H), 7.01 – 6.93 (m, 2H), 5.42 (s, 2H), 4.59 (s, 2H), 3.61 – 3.53 (m, 2H), 3.53 – 3.46 (m, 2H). **¹³C NMR** (101 MHz, CD₃OD) δ 146.3, 135.6, 134.1, 130.8, 130.7, 130.2, 128.6, 127.8, 123.0, 72.9, 65.4, 62.0, 48.5. **FTIR** (neat): 3253, 2962, 2899, 2862, 1443, 1346, 1275, 1112, 1078, 1041, 996, 877, 747, 706 cm⁻¹. **HRMS** (ESI): calculated for C₁₃H₁₆ClN₂O₂ [M+H]⁺ 267.0895; found: 267.0900.

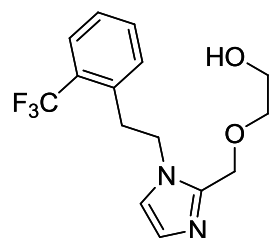
2-((1-(3-Methoxyphenethyl)-1H-imidazol-2-yl)methoxy)ethanol (199). The synthesis of **199** was conducted according to general procedure I with **172** (0.287 g, 1.00 mmol) and 1,2-ethanediol (1.0 mL). The product **199** (0.184 g, 0.67 mmol, 67%) was obtained a pale orange oil. **R_f**: 0.17 (EtOAc:MeOH 9:1). ¹H NMR (400 MHz, CD₃OD) δ 7.20 – 7.13 (m, 1H), 7.06 (d, *J* = 1.4 Hz, 1H), 6.88 (d, *J* = 1.4 Hz, 1H), 6.80 – 6.75 (m, 1H), 6.72 – 6.67 (m, 1H), 6.61 – 6.58 (m, 1H), 4.36 – 4.24 (m, 4H), 3.71 (s, 3H), 3.67 – 3.60 (m, 2H), 3.48 – 3.43 (m, 2H), 3.03 (t, *J* = 6.9 Hz, 2H). ¹³C NMR (101 MHz, CD₃OD) δ 161.3, 145.9, 141.0, 130.6, 127.4, 122.4, 122.2, 115.3, 113.5, 72.8, 65.1, 62.0, 55.6, 48.7, 38.4. **FTIR** (neat): 3193, 2921, 2862, 1588, 1495, 1439, 1261, 1156, 1056, 1041, 780, 750, 698 cm⁻¹. **HRMS** (ESI): calculated for C₁₅H₂₁N₂O₃ [M+H]⁺ 277.1547; found: 277.1550.



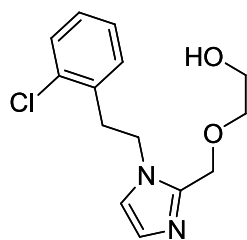
2-((1-(2-Fluorophenethyl)-1H-imidazol-2-yl)methoxy)ethanol (201). The synthesis of **201** was conducted according to general procedure I with **173** (0.275 g, 1.00 mmol) and 1,2-ethanediol (1.0 mL). The product **201** (0.206 g, 0.78 mmol, 78%) was obtained as a pale orange oil. **R_f**: 0.19 (EtOAc:MeOH 9:1). ¹H NMR (400 MHz, CD₃OD) δ 7.31 – 7.21 (m, 1H), 7.15 – 7.02 (m, 3H), 7.00 (d, *J* = 1.4 Hz, 1H), 6.86 (d, *J* = 1.3 Hz, 1H), 4.40 (s, 2H), 4.32 (t, *J* = 7.0 Hz, 2H), 3.68 – 3.62 (m, 2H), 3.52 – 3.45 (m, 2H), 3.14 (t, *J* = 7.0 Hz, 2H). ¹³C NMR (101 MHz, CD₃OD) δ 162.7 (d, 244 Hz), 145.8, 132.5 (d, 4 Hz), 130.0 (d, 8 Hz), 127.4, 126.1 (d, 16 Hz), 125.5 (d, 4 Hz), 122.5, 116.2 (d, 22 Hz), 72.9, 65.1, 62.0, 47.3 (d, 2 Hz), 31.7 (d, 2 Hz). **FTIR** (neat): 3197, 2921, 2862, 2495, 1231, 1104, 1071, 762 cm⁻¹. **HRMS** (ESI): calculated for C₁₄H₁₈FN₂O₂ [M+H]⁺ 265.1347; found: 265.1343.



2-((1-(2-(Trifluoromethyl)phenethyl)-1H-imidazol-2-yl)methoxy)ethanol (195). The synthesis of **195** was conducted according to general procedure I with **175** (0.228 g, 0.70 mmol) and 1,2-ethanediol (0.7 mL). The product **195** (0.176 g, 0.56 mmol, 80%) was obtained as a pale yellow solid. **R_f**: 0.14 (EtOAc:MeOH 9:1). ¹H NMR (400 MHz, CD₃OD) δ 7.71 (d, *J* = 7.8 Hz, 1H), 7.54 – 7.46 (m, 1H), 7.46 – 7.38 (m, 1H), 7.22 (d, *J* = 7.6 Hz, 1H), 7.04 (d, *J* = 1.4 Hz, 1H), 6.91 (d, *J* = 1.4 Hz, 1H), 4.39 (s, 2H), 4.34 (t, *J* = 7.3 Hz, 2H), 3.70 – 3.61 (m, 2H), 3.53 – 3.46 (m, 2H), 3.31 – 3.25 (m, 2H). ¹³C NMR (101 MHz, CD₃OD) δ 145.9, 137.7 (q, 2 Hz), 133.4 (q, 1 Hz), 133.2, 129.8 (q, 30 Hz), 128.4, 127.6, 127.2 (q, 6 Hz), 126.1 (q, 273 Hz), 122.4, 73.0, 65.1, 62.0, 48.2 (q, 2 Hz), 35.3 (q, 2 Hz). **FTIR** (neat): 3171, 2903, 2873, 1316, 1294, 1179, 1104, 1078, 1063, 1041, 992, 773, 750, 728 cm⁻¹. **HRMS** (ESI): calculated for C₁₅H₁₈F₃N₂O₂ [M+H]⁺ 315.1315; found: 315.1320.

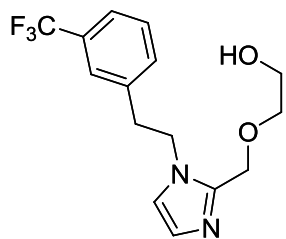


2-((1-(2-Chlorophenethyl)-1H-imidazol-2-yl)methoxy)ethanol (203). The synthesis of **203**



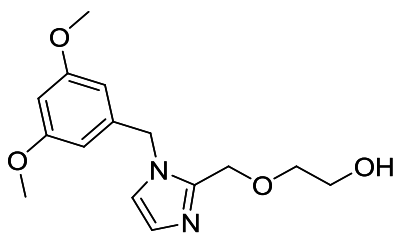
was conducted according to general procedure I with **174** (0.204 g, 0.70 mmol) and 1,2-ethanediol (0.7 mL). The product **203** (0.148 g, 0.53 mmol, 75%) was obtained as a white solid. **R_f**: 0.14 (EtOAc:MeOH 9:1). **¹H NMR** (400 MHz, CD₃OD) δ 7.39 (dd, *J* = 7.9, 1.2 Hz, 1H), 7.26 – 7.20 (m, 1H), 7.17 (td, *J* = 7.4, 1.4 Hz, 1H), 7.09 (dd, *J* = 7.5, 1.8 Hz, 1H), 7.01 (d, *J* = 1.3 Hz, 1H), 6.87 (d, *J* = 1.3 Hz, 1H), 4.40 – 4.28 (m, 4H), 3.70 – 3.61 (m, 2H), 3.52 – 3.45 (m, 2H), 3.23 (t, *J* = 7.0 Hz, 2H). **¹³C NMR** (101 MHz, CD₃OD) δ 145.8, 136.9, 135.2, 132.5, 130.6, 129.8, 128.3, 127.5, 122.5, 73.0, 65.1, 62.0, 46.8, 36.1. **FTIR** (neat): 3126, 2914, 2884, 2851, 1439, 1354, 1112, 1078, 1037, 992, 762, 747, 717, 676 cm⁻¹. **HRMS** (ESI): calculated for C₁₄H₁₈ClN₂O₂ [M+H]⁺ 281.1051; found: 281.1051.

2-((1-(3-(Trifluoromethyl)phenethyl)-1H-imidazol-2-yl)methoxy)ethanol (195). The



synthesis of **195** was conducted according to general procedure I with **176** (0.228 g, 0.70 mmol) and 1,2-ethanediol (0.7 mL). The product **195** (0.188 g, 0.59 mmol, 84%) was obtained as pale yellow solid. **R_f**: 0.13 (EtOAc:MeOH 9:1). **¹H NMR** (400 MHz, CD₃OD) δ 7.56 – 7.38 (m, 4H), 7.05 (d, *J* = 1.4 Hz, 1H), 6.88 (d, *J* = 1.3 Hz, 1H), 4.39 – 4.30 (m, 4H), 3.68 – 3.63 (m, 2H), 3.52 – 3.46 (m, 2H), 3.20 (t, *J* = 7.1 Hz, 2H). **¹³C NMR** (101 MHz, CD₃OD) δ 145.8, 140.9, 133.9 (q, 1 Hz), 131.9 (q, 32 Hz), 130.4, 127.5, 126.7 (q, 4 Hz), 125.6 (q, 271 Hz), 124.6 (q, 4 Hz), 122.4, 72.9, 65.1, 62.0, 48.4, 37.9. **FTIR** (neat): 3186, 2925, 2854, 1331, 1305, 1160, 1130, 1112, 1078, 1041, 996, 709, 683 cm⁻¹. **HRMS** (ESI): calculated for C₁₅H₁₈O₂N₂F₃ [M+H]⁺ 315.1315; found: 315.1312.

2-((1-(3,5-Dimethoxybenzyl)-1H-imidazol-2-yl)methoxy)ethanol (181). Sodium hydroxide



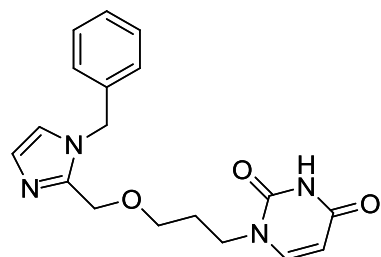
(0.120 g, 3.00 mmol) was suspended in 1,2-ethanediol (2 mL) and heated to 40 °C. **169** (0.303 g, 1.00 mmol) was added and the reaction mixture was stirred at 80 °C overnight. Water and EtOAc were added to the reaction mixture. The aqueous layer was extracted (3x). The combined organic layers were washed with water (3x) and brine (1x). The organic phase was dried over Na₂SO₄ and the solvent removed under reduced pressure. The crude product was purified by silica column chromatography (EtOAc:MeOH 9:1). **181** (0.091 g, 0.31 mmol, 31%) was obtained as a pale yellow solid. **¹H NMR** (400 MHz, CDCl₃) δ 7.01 (d, *J* = 1.3 Hz, 1H), 6.91 (d, *J* = 1.4 Hz, 1H), 6.37 (t, *J* = 2.3 Hz, 1H), 6.23 (d, *J* = 2.2 Hz, 2H), 5.11 (s, 2H), 4.60 (s, 2H), 3.74 (s, 6H), 3.71 – 3.66 (m, 2H), 3.62 – 3.57 (m, 2H). **¹³C NMR** (101 MHz, CDCl₃) δ 161.4, 144.9, 138.8, 127.9, 121.5, 105.1, 99.6,

72.2, 64.9, 61.8, 55.5, 49.8. **HRMS** (ESI): calculated for C₁₅H₂₁N₂O₄ [M+H]⁺ 293.1496; found: 293.1499.

General procedure J: Synthesis of ether-type final compounds (type E)

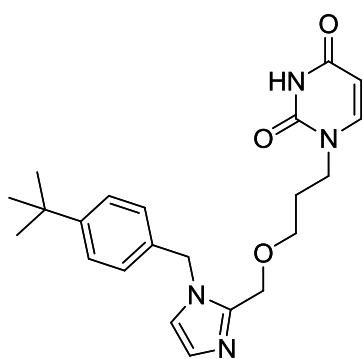
1*H*-substituted imidazole hydroxyalkyl ether (1 eq), N³-benzoyl uracil (**53**) (1.1 eq) and PPh₃ (2.0 eq) were suspended in dry THF (normally 1 mL per 0.2 mmol alcohol). DIAD (2.0 eq) was added dropwise at 0 °C. The mixture was allowed to warm to room temperature and was stirred overnight. The solvent was removed under reduced pressure and the residue was purified by silica column chromatography (EtOAc → EtOAc:MeOH 9:1) to obtain the N³-benzoyl protected product. 7 N NH₃/MeOH (2-3 mL for 0.2-0.4 mmol batch) was added to the N³-benzoyl protected product at 0 °C (cooled flask). The resulting solution was allowed to warm to room temperature and was stirred for 3-4 h. The solvent and the volatiles were removed by a nitrogen gas stream. The crude product was purified by silica column chromatography (EtOAc → EtOAc:MeOH 9:1).

1-(3-((1-Benzyl-1*H*-imidazol-2-yl)methoxy)propyl)pyrimidine-2,4(1*H*,3*H*)-dione (**210**).



The synthesis of **210** was conducted according to general procedure J with **161** (0.246 g, 1.00 mmol). The product **210** (0.230 g, 0.68 mmol, 68%) was obtained as a pale yellow solid. **R_f**: 0.10 (EtOAc:MeOH 9:1). **¹H NMR** (400 MHz, CDCl₃) δ 9.50 (bs, 1H), 7.37 – 7.27 (m, 3H), 7.13 – 7.04 (m, 2H), 6.99 (d, *J* = 7.9 Hz, 1H), 6.93 (d, *J* = 1.3 Hz, 1H), 5.58 (d, *J* = 7.9 Hz, 1H), 5.20 (s, 2H), 4.57 (s, 2H), 3.68 (t, *J* = 6.8 Hz, 2H), 3.47 (t, *J* = 5.7 Hz, 2H), 1.85 (p, *J* = 6.6 Hz, 2H). **¹³C NMR** (101 MHz, CDCl₃) δ 164.0, 151.0, 145.1, 144.4, 136.4, 129.1, 128.3, 127.7, 126.9, 121.6, 101.9, 66.8, 64.6, 49.9, 46.3, 28.6. **FTIR** (neat): 3108, 2966, 2925, 2851, 2735, 1707, 1678, 1443, 1093, 803, 732 cm⁻¹. **HRMS** (ESI): calculated for C₁₈H₂₁N₄O₃ [M+H]⁺ 341.1608; found: 341.1611.

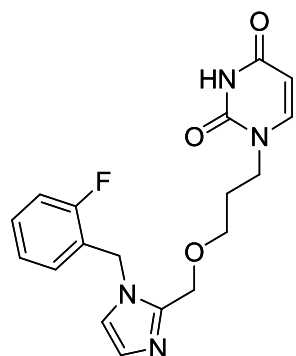
1-(3-((1-(4-*tert*-Butylbenzyl)-1*H*-imidazol-2-yl)methoxy)propyl)pyrimidine-2,4(1*H*,3*H*)-



dione (218). The synthesis of **218** was conducted according to general procedure J with **184** (0.121 g, 0.40 mmol) The product **218** (0.113 g, 0.29 mmol, 71%) was obtained as a white solid. **R_f**: 0.09 (EtOAc:MeOH 9:1). **¹H NMR** (400 MHz, CDCl₃) δ 9.66 (bs, 1H), 7.38 – 7.31 (m, 2H), 7.07 – 6.97 (m, 4H), 6.92 (d, *J* = 1.3 Hz, 1H), 5.57 (d, *J* = 7.9 Hz, 1H), 5.16 (s, 2H), 4.57 (s, 2H), 3.69 (t, *J* = 6.8 Hz, 2H), 3.48 (t, *J* = 5.7 Hz, 2H), 1.86 (p, *J* = 6.3 Hz, 2H), 1.28 (s, 9H). **¹³C NMR** (101 MHz, CDCl₃) δ 164.0, 151.4, 151.0, 145.2, 144.4, 133.4,

127.7, 126.7, 125.9, 121.5, 101.9, 66.6, 64.6, 49.6, 46.3, 34.7, 31.4, 28.6. **FTIR** (neat): 2959, 2869, 2784, 1674, 1439, 1097, 810, 750, 721 cm⁻¹. **HRMS** (ESI): calculated for C₂₂H₂₉N₄O₃ [M+H]⁺ 397.2234; found: 397.2238.

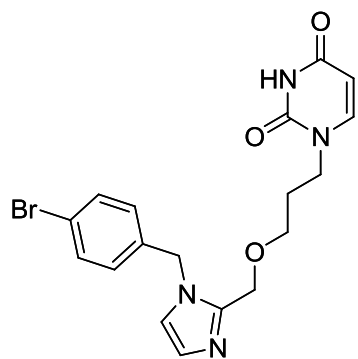
1-(3-((1-(2-Fluorobenzyl)-1*H*-imidazol-2-yl)methoxy)propyl)pyrimidine-2,4(1*H*,3*H*)-



dione (208). The synthesis of **208** was conducted according to general procedure J with **179** (0.106 g, 0.40 mmol). The product **208** (0.080 g, 0.21 mmol, 53%) was obtained as a white solid. **R_f**: 0.13 (EtOAc:MeOH 9:1). **¹H NMR** (400 MHz, CDCl₃) δ 9.20 (bs, 1H), 7.41 – 7.27 (m, 1H), 7.17 – 6.89 (m, 6H), 5.59 (d, *J* = 7.9 Hz, 1H), 5.25 (s, 2H), 4.61 (s, 2H), 3.71 (t, *J* = 6.7 Hz, 2H), 3.50 (t, *J* = 5.7 Hz, 2H), 2.01 – 1.73 (m, 2H). **¹³C NMR** (101 MHz, CDCl₃) δ 163.8, 160.2 (d, 247 Hz), 150.9, 145.1, 144.4, 130.4 (d, 8 Hz), 129.2 (d, 4 Hz), 127.6, 124.8 (d, 4 Hz), 123.6 (d, 15 Hz), 121.6, 115.8 (d, 21 Hz), 101.9, 66.8, 64.5, 46.3, 43.9 (d, 5 Hz), 28.6. **FTIR** (neat): 3104, 2955, 2750, 1685, 1439,

1354, 1231, 1164, 1108, 773 cm⁻¹. **HRMS** (ESI): calculated for C₁₈H₂₀FN₄O₃ [M+H]⁺ 359.1514; found: 359.1516.

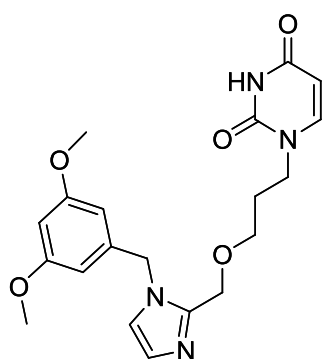
1-(3-((1-(4-Bromobenzyl)-1H-imidazol-2-yl)methoxy)propyl)pyrimidine-2,4(1H,3H)-



dione (212). The synthesis of **212** was conducted according to general procedure J with **186** (0.195 g, 0.60 mmol). The product **212** (0.174 g, 0.42 mmol, 69%) was obtained as a white solid. R_f : 0.09 (EtOAc:MeOH 9:1). $^1\text{H NMR}$ (400 MHz, CDCl_3) δ 9.25 (bs, 1H), 7.50 – 7.42 (m, 2H), 7.06 (d, $J = 1.3$ Hz, 1H), 7.02 (d, $J = 7.9$ Hz, 2H), 7.00 – 6.95 (m, 2H), 6.91 (d, $J = 1.3$ Hz, 1H), 5.61 (dd, $J = 7.9, 1.6$ Hz, 1H), 5.15 (s, 2H), 4.54 (s, 2H), 3.68 (t, $J = 6.8$ Hz, 2H), 3.47 (t, $J = 5.7$ Hz, 2H), 1.85 (p, $J = 6.3$ Hz, 2H). $^{13}\text{C NMR}$ (101 MHz, CDCl_3) δ 163.8, 150.9, 144.9, 144.5, 135.7, 132.2, 128.6, 128.2, 122.2, 121.5, 102.1, 66.9,

64.8, 49.3, 46.3, 28.7. **FTIR** (neat): 3048, 2959, 2869, 2784, 1670, 1436, 1074, 806, 747 cm^{-1} . **HRMS** (ESI): calculated for $\text{C}_{18}\text{H}_{20}\text{BrN}_4\text{O}_3$ $[\text{M}+\text{H}]^+$ 419.0713; found: 419.0715.

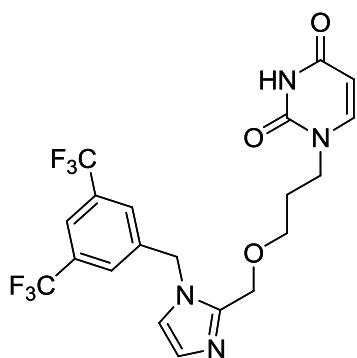
1-(3-((1-(3,5-Dimethoxybenzyl)-1H-imidazol-2-yl)methoxy)propyl)pyrimidine-



2,4(1H,3H)-dione (222). The synthesis of **222** was conducted according to general procedure J with **182** (0.123 g, 0.40 mmol). The product **222** (0.108 g, 0.27 mmol, 67%) was obtained as a white solid. R_f : 0.09 (EtOAc:MeOH 9:1). $^1\text{H NMR}$ (400 MHz, CDCl_3) δ 8.59 (bs, 1H), 7.10 – 6.99 (m, 2H), 6.94 (d, $J = 1.1$ Hz, 1H), 6.37 (t, $J = 2.3$ Hz, 1H), 6.23 (d, $J = 2.2$ Hz, 2H), 5.59 (dd, $J = 7.9, 1.9$ Hz, 1H), 5.12 (s, 2H), 4.57 (s, 2H), 3.81 – 3.65 (m, 8H), 3.50 (t, $J = 5.7$ Hz, 2H), 1.88 (p, $J = 6.3$ Hz, 2H). $^{13}\text{C NMR}$ (101 MHz, CDCl_3) δ 163.5, 161.5, 150.7, 145.2, 144.4, 138.8, 127.7,

121.7, 105.2, 101.9, 99.4, 66.8, 64.6, 55.5, 49.9, 46.3, 28.7. **FTIR** (neat): 2955, 2892, 2843, 2765, 1707, 1663, 1599, 1439, 1354, 1208, 1164, 1086, 1056, 754 cm^{-1} . **HRMS** (ESI): calculated for $\text{C}_{20}\text{H}_{25}\text{N}_4\text{O}_5$ $[\text{M}+\text{H}]^+$ 401.1819; found: 401.1818.

1-(3-((1-(3,5-Bis(trifluoromethyl)benzyl)-1H-imidazol-2-yl)methoxy)propyl)pyrimidine-

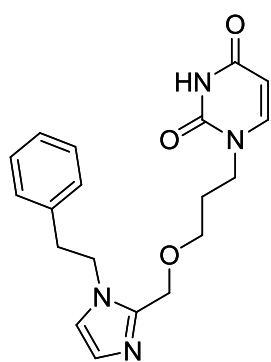


2,4(1H,3H)-dione (224). The synthesis of **224** was conducted according to general procedure J with **194** (0.153 g, 0.40 mmol). The product **224** (0.127 g, 0.27 mmol, 67%) was obtained as a white solid. R_f : 0.19 (EtOAc:MeOH 9:1). $^1\text{H NMR}$ (400 MHz, CDCl_3) δ 8.84 (bs, 1H), 7.85 (s, 1H), 7.62 (s, 2H), 7.16 (s, 1H), 7.10 (d, $J = 7.9$ Hz, 1H), 6.97 (s, 1H), 5.65 (d, $J = 7.9$ Hz, 1H), 5.41 (s, 2H), 4.67 (s, 2H), 3.70 (t, $J = 6.7$ Hz, 2H), 3.53 (t, $J = 5.7$ Hz, 2H), 1.85 (p, $J = 6.3$ Hz, 2H). $^{13}\text{C NMR}$ (101 MHz, CDCl_3) δ 163.9, 151.2, 144.7, 144.6, 139.6, 132.3 (q, 34 Hz),

128.8, 127.3 (m), 123.1 (q, 273 Hz), 122.3 (m), 121.2, 102.3, 66.9, 64.7, 49.0, 45.9, 28.7.

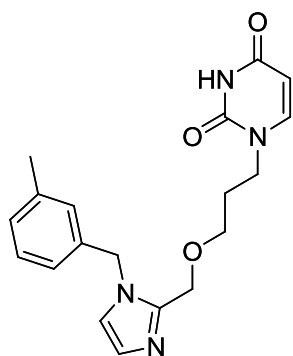
FTIR (neat): 3141, 3119, 3059, 2936, 2869, 2758, 1681, 1287, 1171, 1127, 1100, 683 cm^{-1}
HRMS (ESI): calculated for $\text{C}_{20}\text{H}_{19}\text{F}_6\text{N}_4\text{O}_3$ $[\text{M}+\text{H}]^+$ 477.1356; found: 477.1357.

1-(3-((1-Phenethyl-1*H*-imidazol-2-yl)methoxy)propyl)pyrimidine-2,4(1*H*,3*H*)-dione



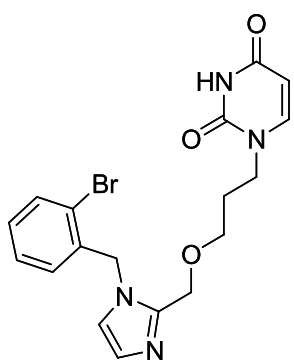
(226). The synthesis of **226** was conducted according to general procedure J with **198** (0.104 g, 0.40 mmol). The product **226** (0.118 g, 0.33 mmol, 83%) was obtained as a white solid. **R_f**: 0.10 (EtOAc:MeOH 9:1). **¹H NMR** (400 MHz, CDCl_3) δ 8.82 (bs, 1H), 7.33 – 7.20 (m, 3H), 7.11 (d, $J = 7.9$ Hz, 1H), 7.07 – 6.98 (m, 3H), 6.85 (d, $J = 1.3$ Hz, 1H), 5.59 (d, $J = 8.0$ Hz, 1H), 4.31 (s, 2H), 4.22 (t, $J = 7.1$ Hz, 2H), 3.77 (t, $J = 6.7$ Hz, 2H), 3.46 (t, $J = 5.7$ Hz, 2H), 3.04 (t, $J = 7.0$ Hz, 2H), 1.92 (p, $J = 6.3$ Hz, 2H). **¹³C NMR** (101 MHz, CDCl_3) δ 163.6, 150.8, 145.2, 144.1, 137.6, 129.0, 128.8, 127.4, 127.3, 120.7, 101.9, 66.7, 64.2, 47.9, 46.4, 37.8, 28.7. **FTIR** (neat): 3119, 2951, 2873, 2765, 1700, 1685, 1439, 1089, 765, 706 cm^{-1} . **HRMS** (ESI): calculated for $\text{C}_{19}\text{H}_{23}\text{N}_4\text{O}_3$ $[\text{M}+\text{H}]^+$ 355.1766; found: 355.1768.

1-(3-((1-(3-Methylbenzyl)-1*H*-imidazol-2-yl)methoxy)propyl)pyrimidine-2,4(1*H*,3*H*)-dione (214).



The synthesis of **214** was conducted according to general procedure J with **188** (0.104 g, 0.40 mmol). The product **214** (0.100 g, 0.28 mmol, 71%) was obtained as a white solid. **R_f**: 0.14 (EtOAc:MeOH 9:1). **¹H NMR** (400 MHz, CDCl_3) δ 10.46 (bs, 1H), 7.19 (t, $J = 7.5$ Hz, 1H), 7.12 – 7.01 (m, 2H), 6.97 (d, $J = 7.9$ Hz, 1H), 6.93 – 6.82 (m, 3H), 5.55 (d, $J = 7.8$ Hz, 1H), 5.13 (s, 2H), 4.55 (s, 2H), 3.66 (t, $J = 6.8$ Hz, 2H), 3.45 (t, $J = 5.7$ Hz, 2H), 2.28 (s, 3H), 1.84 (p, $J = 6.3$ Hz, 2H). **¹³C NMR** (101 MHz, CDCl_3) δ 164.4, 151.2, 145.1, 144.4, 138.7, 136.4, 128.8, 127.8, 127.5, 123.9, 121.5, 101.8, 77.4, 66.5, 64.5, 49.7, 46.1, 28.5, 21.4. **FTIR** (neat): 3108, 3011, 2955, 2925, 2869, 2787, 1670, 1436, 1097, 750 cm^{-1} . **HRMS** (ESI): calculated for $\text{C}_{19}\text{H}_{23}\text{N}_4\text{O}_3$ $[\text{M}+\text{H}]^+$ 355.1765; found: 355.1767.

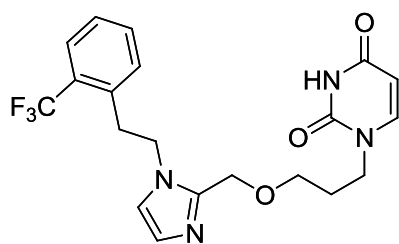
1-(3-((1-(2-Bromobenzyl)-1*H*-imidazol-2-yl)methoxy)propyl)pyrimidine-2,4(1*H*,3*H*)-



dione (216). The synthesis of **216** was conducted according to general procedure J with **190** (0.130 g, 0.40 mmol). The product **216** (0.146 g, 0.35 mmol, 87%) was obtained as a white solid. **R_f**: 0.17 (EtOAc:MeOH 9:1). **¹H NMR** (400 MHz, CDCl₃) δ 8.81 (bs, 1H), 7.60 (dd, *J* = 7.8, 1.3 Hz, 1H), 7.30 – 7.23 (m, 1H), 7.19 (td, *J* = 7.6, 1.8 Hz, 1H), 7.10 (d, *J* = 1.3 Hz, 1H), 7.01 (d, *J* = 7.9 Hz, 1H), 6.93 (d, *J* = 1.4 Hz, 1H), 6.70 (dd, *J* = 7.7, 1.7 Hz, 1H), 5.60 (dd, *J* = 7.8, 1.8 Hz, 1H), 5.27 (s, 2H), 4.58 (s, 2H), 3.65 (t, *J* = 6.8 Hz, 2H), 3.48 (t, *J* = 5.7 Hz, 2H), 1.83 (p, *J* = 6.7 Hz, 2H). **¹³C NMR** (101 MHz, CDCl₃) δ 163.6, 150.8, 145.2, 144.6, 135.9, 133.2, 129.8, 128.3, 128.2, 127.8, 122.5, 121.7,

101.9, 66.9, 64.7, 50.2, 46.3, 28.6. **FTIR** (neat): 3052, 2959, 2869, 2787, 1670, 1432, 1354, 1097, 1030, 747 cm⁻¹. **HRMS** (ESI): calculated for C₁₈H₂₀BrN₄O₃ [M+H]⁺ 419.0713; found: 419.0718.

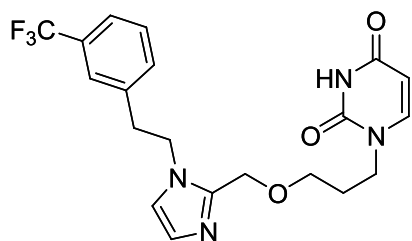
1-(3-((1-(2-(Trifluoromethyl)phenethyl)-1*H*-imidazol-2-yl)methoxy)propyl)pyrimidine-



2,4(1*H*,3*H*)-dione (234). The synthesis of **234** was conducted according to general procedure J with **206** (0.126 g, 0.40 mmol). The product **234** (0.108 g, 2.56 mmol, 64%) was obtained as white solid. **R_f**: 0.13 (EtOAc:MeOH 9:1).

¹H NMR (400 MHz, CDCl₃) δ 9.02 (bs, 1H), 7.68 (d, *J* = 7.7 Hz, 1H), 7.49 – 7.41 (m, 1H), 7.41 – 7.33 (m, 1H), 7.14 (d, *J* = 7.9 Hz, 1H), 7.06 – 6.99 (m, 2H), 6.88 (d, *J* = 1.3 Hz, 1H), 5.60 (d, *J* = 7.8 Hz, 1H), 4.39 (s, 2H), 4.23 (t, *J* = 7.4 Hz, 2H), 3.78 (t, *J* = 6.7 Hz, 2H), 3.49 (t, *J* = 5.7 Hz, 2H), 3.23 (t, *J* = 7.4 Hz, 2H), 1.93 (p, *J* = 6.3 Hz, 2H). **¹³C NMR** (101 MHz, CDCl₃) δ 163.7, 150.9, 145.2, 144.1, 135.8 (q, 2 Hz), 132.4 (q, 1 Hz), 131.8, 128.9 (q, 30 Hz), 127.5, 127.5, 126.7 (q, 6 Hz), 124.6 (q, 274 Hz), 120.8, 102.0, 66.9, 64.1, 47.4, 46.4, 34.9 (q, 2 Hz), 28.6. **FTIR** (neat): 2970, 2665, 2455, 1707, 1659, 1443, 1320, 1104, 1063, 1045, 773, 747 cm⁻¹. **HRMS** (ESI): calculated for C₂₀H₂₂F₃N₄O₃ [M+H]⁺ 423.1639; found: 423.1640.

1-(3-((1-(3-(Trifluoromethyl)phenethyl)-1*H*-imidazol-2-yl)methoxy)propyl)pyrimidine-

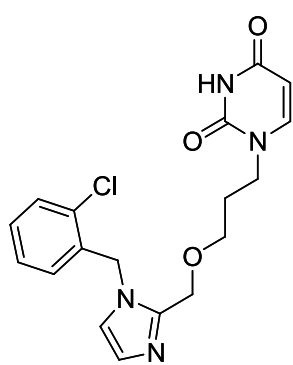


2,4(1*H*,3*H*)-dione (236). The synthesis of **236** was conducted according to general procedure J with **196** (0.126 g, 0.40 mmol). The product **236** (0.099 g, 0.23 mmol, 59%) was obtained as a pale yellow solid. **R_f**: 0.13 (EtOAc:MeOH 9:1). **¹H NMR** (400 MHz, CDCl₃) δ 9.36 (bs, 1H), 7.54 – 7.48 (m, 1H), 7.44 – 7.32 (m, 2H), 7.21 –

7.15 (m, 1H), 7.11 (d, *J* = 7.8 Hz, 1H), 6.99 (d, *J* = 1.3 Hz, 1H), 6.80 (d, *J* = 1.3 Hz, 1H), 5.61 (d, *J* = 7.8 Hz, 1H), 4.40 (s, 2H), 4.38 (s, 2H), 4.24 (t, *J* = 7.1 Hz, 2H), 3.77 (t, *J* = 6.8 Hz,

2H), 3.48 (t, $J = 5.7$ Hz, 2H), 3.11 (t, $J = 7.1$ Hz, 2H), 1.92 (p, $J = 6.4$ Hz, 2H). ^{13}C NMR (101 MHz, CDCl_3) δ 163.9, 151.0, 145.0, 144.1, 138.6, 132.3 (q, 1 Hz), 131.3 (q, 32 Hz), 129.4, 127.9 (m), 125.5 (q, 4 Hz), 124.1 (q, 272 Hz), 124.1 (q, 4 Hz), 120.7, 102.1, 66.8, 64.4, 47.4, 46.3, 37.6, 28.7. **FTIR** (neat): 2959, 2869, 2713, 1715, 1663, 1443, 1343, 1153, 1108, 1074, 706 cm^{-1} . **HRMS** (ESI): calculated for $\text{C}_{20}\text{H}_{22}\text{F}_3\text{N}_4\text{O}_3$ $[\text{M}+\text{H}]^+$ 423.1639; found: 423.1637.

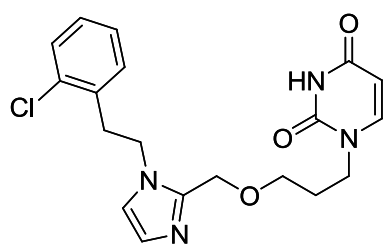
1-(3-((1-(2-Chlorobenzyl)-1H-imidazol-2-yl)methoxy)propyl)pyrimidine-2,4(1H,3H)-



dione (220). The synthesis of **220** was conducted according to general procedure J with **192** (0.107 g, 0.40 mmol). The product **220** (0.090 g, 0.24 mmol, 60%) was obtained as a white solid. R_f : 0.14 (EtOAc:MeOH 9:1). ^1H NMR (400 MHz, CDCl_3) δ 9.84 (bs, 1H), 7.43 – 7.37 (m, 1H), 7.29 – 7.16 (m, 2H), 7.08 (d, $J = 1.3$ Hz, 1H), 6.99 (d, $J = 7.8$ Hz, 1H), 6.94 – 6.90 (m, 1H), 6.77 – 6.71 (m, 1H), 5.58 (d, $J = 7.8$ Hz, 1H), 5.28 (s, 2H), 4.57 (s, 2H), 3.64 (t, $J = 6.8$ Hz, 2H), 3.46 (t, $J = 5.7$ Hz, 2H), 1.82 (p, $J = 6.2$ Hz, 2H). ^{13}C NMR (101 MHz, CDCl_3) δ 164.1, 151.0, 145.1, 144.6, 134.3, 132.6, 129.8,

129.5, 128.2, 128.0, 127.5, 121.6, 101.9, 66.8, 64.7, 47.6, 46.2, 28.6. **FTIR** (neat): 3111, 2959, 2925, 2862, 2739, 1707, 1670, 1439, 1354, 1089, 758, 680 cm^{-1} . **HRMS** (ESI): calculated for $\text{C}_{18}\text{H}_{20}\text{ClN}_4\text{O}_3$ $[\text{M}+\text{H}]^+$ 375.1218; found: 375.1223.

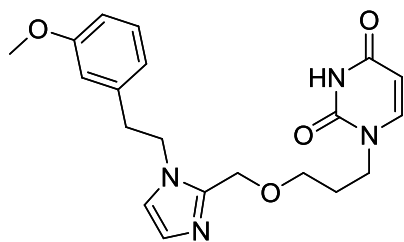
1-(3-((1-(2-Chlorophenethyl)-1H-imidazol-2-yl)methoxy)propyl)pyrimidine-2,4(1H,3H)-



dione (232). The synthesis of **232** was conducted according to general procedure J with **204** (0.112 g, 0.40 mmol). The product **232** (0.105 g, 0.27 mmol, 68%) was obtained as a white solid. R_f : 0.11 (EtOAc:MeOH 9:1). ^1H NMR (400 MHz, CDCl_3) δ 10.00 (bs, 1H), 7.40 – 7.33 (m, 1H), 7.23 – 7.17 (m, 1H), 7.17 – 7.08 (m, 2H), 7.04 – 6.93 (m, 2H), 6.86

– 6.81 (m, 1H), 5.58 (d, $J = 7.8$ Hz, 1H), 4.38 (s, 2H), 4.23 (t, $J = 7.2$ Hz, 2H), 3.77 (t, $J = 6.7$ Hz, 2H), 3.46 (t, $J = 5.7$ Hz, 2H), 3.15 (t, $J = 7.2$ Hz, 2H), 1.92 (p, $J = 6.3$ Hz, 2H). ^{13}C NMR (101 MHz, CDCl_3) δ 164.2, 151.1, 145.2, 144.1, 135.1, 134.0, 131.1, 129.8, 128.8, 127.7, 127.3, 120.7, 101.9, 66.7, 64.2, 46.3, 45.6, 35.8, 28.6. **FTIR** (neat): 2955, 2862, 2754, 1707, 1666, 1436, 1100, 765, 736 cm^{-1} . **HRMS** (ESI): calculated for $\text{C}_{19}\text{H}_{22}\text{ClN}_4\text{O}_3$ $[\text{M}+\text{H}]^+$ 389.1375; found: 389.1379.

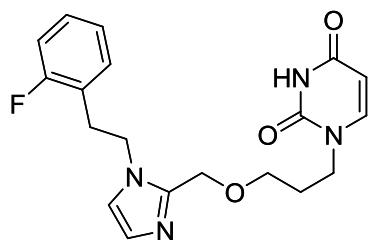
1-(3-((1-(3-Methoxyphenethyl)-1*H*-imidazol-2-yl)methoxy)propyl)pyrimidine-



2,4(1*H*,3*H*)-dione (228). The synthesis of **228** was conducted according to general procedure J with **200** (0.111 g, 0.40 mmol). The product **228** (0.092 g, 0.24 mmol, 60%) was obtained as a white solid. **R_f**: 0.10 (EtOAc:MeOH 9:1). **¹H NMR** (400 MHz, CDCl₃) δ 9.84 (bs, 1H), 7.18 (t, *J* = 7.9 Hz, 1H), 7.10 (d, *J* = 7.9 Hz, 1H), 6.99 (d, *J* = 1.3 Hz, 1H),

6.84 (d, *J* = 1.3 Hz, 1H), 6.81 – 6.73 (m, 1H), 6.68 – 6.59 (m, 1H), 6.57 – 6.51 (m, 1H), 5.58 (d, *J* = 7.8 Hz, 1H), 4.34 (s, 2H), 4.20 (t, *J* = 7.1 Hz, 2H), 3.85 – 3.67 (m, 6H), 3.45 (t, *J* = 5.7 Hz, 2H), 2.99 (t, *J* = 7.1 Hz, 2H), 1.91 (p, *J* = 6.4 Hz, 2H). **¹³C NMR** (101 MHz, CDCl₃) δ 164.1, 159.9, 151.1, 145.1, 144.2, 139.1, 129.9, 127.5, 121.0, 120.7, 114.6, 112.3, 101.9, 66.6, 64.2, 55.3, 47.7, 46.3, 37.8, 28.6. **FTIR** (neat): 3149, 3123, 2940, 2862, 2832, 2739, 1678, 1439, 702 cm⁻¹. **HRMS** (ESI): calculated for C₂₀H₂₅N₄O₄ [M+H]⁺ 385.1870; found: 385.1873.

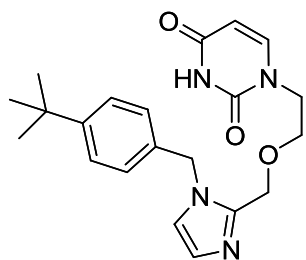
1-(3-((1-(2-Fluorophenethyl)-1*H*-imidazol-2-yl)methoxy)propyl)pyrimidine-2,4(1*H*,3*H*)-



dione (230). The synthesis of **230** was conducted according to general procedure J with **202** (0.106 g, 0.40 mmol). The product **230** (0.096 g, 0.26 mmol, 64%) was obtained as white solid. **R_f**: 0.09 (EtOAc:MeOH 9:1). **¹H NMR** (400 MHz, CDCl₃) δ 9.58 (bs, 1H), 7.28 – 7.19 (m, 1H), 7.13 (d, *J* = 7.9 Hz, 1H), 7.08 – 6.93 (m, 4H), 6.83 (d, *J* = 1.3 Hz, 1H), 5.60 (d, *J* = 7.8 Hz, 1H), 4.43 (s, 2H), 4.22 (t, *J* = 7.3 Hz, 2H), 3.78 (t, *J*

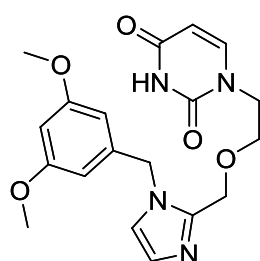
= 6.7 Hz, 2H), 3.49 (t, *J* = 5.7 Hz, 2H), 3.08 (t, *J* = 7.3 Hz, 2H), 1.93 (p, *J* = 6.4 Hz, 2H). **¹³C NMR** (101 MHz, CDCl₃) δ 164.0, 161.3 (d, 245 Hz), 151.0, 145.2, 144.1, 131.2 (d, 5 Hz), 129.2 (d, 8 Hz), 127.6, 124.6 (d, 4 Hz), 124.4 (d, 16Hz), 120.7, 115.6 (d, 22 Hz), 101.9, 66.7, 64.3, 46.4, 46.3 (d, 2 Hz), 31.5 (d, 2 Hz), 28.6. **FTIR** (neat): 2929, 2962, 2873, 2735, 1711, 1674, 1439, 1350, 1343, 1227, 1056, 758, 717 cm⁻¹. **HRMS** (ESI): calculated for C₂₀H₂₅N₄O₄ [M+H]⁺ 373.1670; found: 373.1671.

1-(2-((1-(4-*tert*-Butylbenzyl)-1*H*-imidazol-2-yl)methoxy)ethyl)pyrimidine-2,4(1*H*,3*H*)-



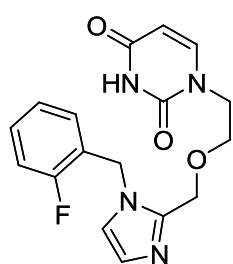
dione (217). The synthesis of **217** was conducted according to general procedure J with **184** (0.174 g, 0.60 mmol). The product **217** (0.151 g, 0.39 mmol, 66%) was obtained as a white solid. **R_f**: 0.13 (EtOAc:MeOH 9:1). **¹H NMR** (400 MHz, CDCl₃) δ 9.38 (bs, 1H), 7.39 – 7.32 (m, 2H), 7.06 (d, *J* = 1.3 Hz, 1H), 7.04 – 6.96 (m, 3H), 6.93 (d, *J* = 1.4 Hz, 1H), 5.52 (d, *J* = 7.9 Hz, 1H), 5.11 (s, 2H), 4.62 (s, 2H), 3.82 – 3.75 (m, 2H), 3.71 – 3.64 (m, 2H), 1.29 (s, 9H). **¹³C NMR** (101 MHz, CDCl₃) δ 163.8, 151.6, 150.9, 145.7, 144.0, 133.2, 127.5, 126.6, 126.0, 121.8, 101.6, 68.0, 64.7, 49.6, 48.3, 34.7, 31.4. **FTIR** (neat): 2959, 2869, 1674, 1439, 1346, 1246, 1097, 810, 747 cm⁻¹. **HRMS** (ESI): calculated for C₂₁H₂₇N₄O₃ [M+H]⁺ 383.2078; found: 383.2079.

1-(2-((1-(3,5-Dimethoxybenzyl)-1*H*-imidazol-2-yl)methoxy)ethyl)pyrimidine-2,4(1*H*,3*H*)-



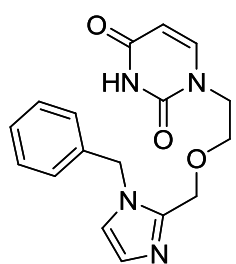
dione (221). The synthesis of **221** was conducted according to general procedure J with **181** (0.088 g, 0.30 mmol). The product **221** (0.076 g, 0.20 mmol, 66%) was obtained as a white solid. **¹H NMR** (400 MHz, CDCl₃) δ 9.55 (bs, 1H), 7.05 (d, *J* = 1.3 Hz, 1H), 7.00 (d, *J* = 7.8 Hz, 1H), 6.93 (d, *J* = 1.3 Hz, 1H), 6.37 (t, *J* = 2.3 Hz, 1H), 6.16 (d, *J* = 2.2 Hz, 2H), 5.52 (d, *J* = 7.9 Hz, 1H), 5.06 (s, 2H), 4.59 (s, 2H), 3.82 – 3.75 (m, 3H), 3.73 (s, 6H), 3.70 – 3.63 (m, 2H). **¹³C NMR** (101 MHz, CDCl₃) δ 163.9, 161.4, 151.0, 145.7, 144.1, 138.9, 128.1, 121.9, 104.9, 101.5, 99.4, 68.0, 64.9, 55.5, 49.8, 48.3. **FTIR** (neat): cm⁻¹. **HRMS** (ESI): calculated for C₁₉H₂₃N₄O₅ [M+H]⁺ 387.1663; found: 387.1665.

1-(2-((1-(2-Fluorobenzyl)-1*H*-imidazol-2-yl)methoxy)ethyl)pyrimidine-2,4(1*H*,3*H*)-



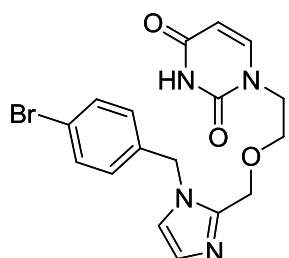
dione (207). The synthesis of **207** was conducted according to general procedure J with **178** (0.075 g, 0.30 mmol). The product **207** (0.048 g, 0.14 mmol, 46%) was obtained as a white solid. **R_f**: 0.10 (EtOAc:MeOH 9:1). **¹H NMR** (400 MHz, CDCl₃) δ 8.85 (bs, 1H), 7.39 – 7.28 (m, 1H), 7.16 – 7.04 (m, 4H), 7.01 – 6.91 (m, 2H), 5.56 (dd, *J* = 7.8, 1.7 Hz, 1H), 5.20 (s, 2H), 4.68 (s, 2H), 3.90 – 3.82 (m, 2H), 3.76 – 3.66 (m, 2H). **¹³C NMR** (101 MHz, CDCl₃) δ 163.6, 160.4 (d, 247 Hz), 150.8, 145.6, 143.9, 130.6 (d, 8 Hz), 129.1 (d, 4 Hz), 127.2, 124.9 (d, 4 Hz), 123.2 (d, 15 Hz), 121.7, 116.0 (d, 21 Hz), 101.7, 68.2, 64.5, 48.3, 44.1 (d, 5 Hz). **FTIR** (neat): 3074, 3044, 2970, 2929, 2866, 2758, 1711, 1655, 1439, 1354, 1097, 985, 754 cm⁻¹. **HRMS** (ESI): calculated for C₁₇H₁₈FN₄O₃ [M+H]⁺ 345.1357; found: 345.1359.

1-(2-((1-Benzyl-1*H*-imidazol-2-yl)methoxy)ethyl)pyrimidine-2,4(1*H*,3*H*)-dione (209).



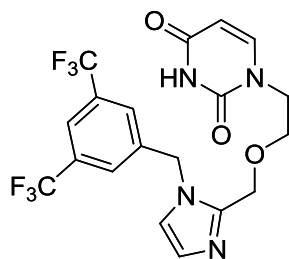
The synthesis of **209** was conducted according to general procedure J with **180** (0.087 g, 0.40 mmol). The product **209** (0.062 g, 0.19 mmol, 47%) was obtained as a white solid. **R_f**: 0.09 (EtOAc:MeOH 9:1). **¹H NMR** (400 MHz, CDCl₃) δ 9.05 (bs, 1H), 7.41 – 7.29 (m, 3H), 7.10 – 7.03 (m, 3H), 6.98 (d, *J* = 7.9 Hz, 1H), 6.95 (d, *J* = 1.3 Hz, 1H), 5.53 (dd, *J* = 7.9, 1.8 Hz, 1H), 5.17 (s, 2H), 4.61 (s, 2H), 3.83 – 3.76 (m, 2H), 3.72 – 3.65 (m, 2H). **¹³C NMR** (101 MHz, CDCl₃) δ 163.6, 150.8, 145.6, 144.1, 136.5, 129.1, 128.3, 128.1, 126.7, 121.8, 101.5, 68.0, 65.0, 49.8, 48.3. **FTIR** (neat): 2955, 2877, 2758, 1700, 1681, 1436, 1246, 1097, 1026, 806, 728 cm⁻¹. **HRMS** (ESI): calculated for C₁₇H₁₉N₄O₃ [M+H]⁺ 327.1452; found: 327.1455.

1-(2-((1-(4-Bromobenzyl)-1*H*-imidazol-2-yl)methoxy)ethyl)pyrimidine-2,4(1*H*,3*H*)-dione (211).



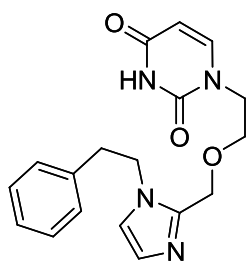
The synthesis of **211** was conducted according to general procedure J with **180** (0.178 g, 0.60 mmol). The product **211** (0.154 g, 0.38 mmol, 63%) was obtained as a white solid. **R_f**: 0.06 (EtOAc:MeOH 9:1). **¹H NMR** (400 MHz, CDCl₃) δ 9.20 (bs, 1H), 7.51 – 7.43 (m, 2H), 7.06 (d, *J* = 1.3 Hz, 1H), 7.01 (d, *J* = 7.9 Hz, 1H), 6.96 – 6.87 (m, 3H), 5.55 (dd, *J* = 7.9, 1.8 Hz, 1H), 5.09 (s, 2H), 4.57 (s, 2H), 3.85 – 3.78 (m, 2H), 3.70 – 3.63 (m, 2H). **¹³C NMR** (101 MHz, CDCl₃) δ 163.7, 150.8, 145.5, 144.1, 135.4, 132.3, 128.5, 128.4, 122.3, 121.6, 101.7, 68.0, 65.0, 49.2, 48.3. **FTIR** (neat): 3108, 2955, 2873, 2750, 1700, 1681, 1436, 1346, 1246, 1093, 810, 706 cm⁻¹. **HRMS** (ESI): calculated for C₁₇H₁₈BrN₄O₃ [M+H]⁺ 405.0557; found: 405.0558.

1-(2-((1-(3,5-Bis(trifluoromethyl)benzyl)-1*H*-imidazol-2-yl)methoxy)ethyl)pyrimidine-2,4(1*H*,3*H*)-dione (223).



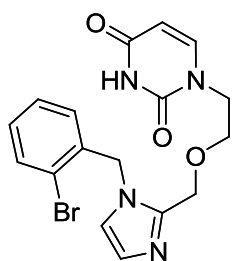
The synthesis of **223** was conducted according to general procedure J with **193** (0.147 g, 0.40 mmol). The product **223** (0.140 g, 0.30 mmol, 76%) was obtained as a white solid. **R_f**: 0.19 (EtOAc:MeOH 9:1). **¹H NMR** (400 MHz, CDCl₃) δ 9.09 (bs, 1H), 7.85 (s, 1H), 7.54 (s, 2H), 7.13 (d, *J* = 1.4 Hz, 1H), 7.04 (d, *J* = 7.9 Hz, 1H), 6.95 (d, *J* = 1.4 Hz, 1H), 5.57 (d, *J* = 7.8 Hz, 1H), 5.30 (d, *J* = 1.6 Hz, 2H), 4.63 (s, 2H), 3.85 – 3.78 (m, 2H), 3.74 – 3.67 (m, 2H). **¹³C NMR** (101 MHz, CDCl₃) δ 163.9, 151.0, 145.2, 144.1, 139.1, 132.7 (q, 34 Hz), 128.7, 127.1 (m), 123.0 (q, 273 Hz), 122.4 (m), 121.4, 101.9, 68.2, 64.6, 49.0, 48.1. **FTIR** (neat): 3108, 2962, 27765, 1711, 1674, 1354, 1283, 1167, 1127, 1086, 1045 cm⁻¹. **HRMS** (ESI): calculated for C₁₉H₁₇F₆N₄O₃ [M+H]⁺ 463.1199; found: 463.1202.

1-(2-((1-Phenethyl-1*H*-imidazol-2-yl)methoxy)ethyl)pyrimidine-2,4(1*H*,3*H*)-dione (225).



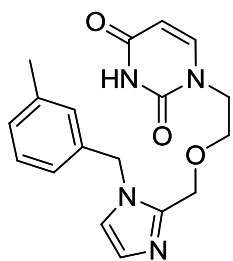
The synthesis of **225** was conducted according to general procedure J with **197** (0.099 g, 0.40 mmol). The product **225** (0.099 g, 0.29 mmol, 73%) was obtained as a white solid. **R_f**: 0.11 (EtOAc:MeOH 9:1). **¹H NMR** (400 MHz, CDCl₃) δ 10.08 (bs, 1H), 7.34 – 7.22 (m, 3H), 7.16 (d, *J* = 7.9 Hz, 1H), 7.05 – 6.98 (m, 3H), 6.84 (d, *J* = 1.3 Hz, 1H), 5.58 (d, *J* = 7.9 Hz, 1H), 4.37 (s, 2H), 4.17 (t, *J* = 7.0 Hz, 2H), 3.88 (t, *J* = 4.9 Hz, 2H), 3.66 (t, *J* = 4.9 Hz, 2H), 3.01 (t, *J* = 7.0 Hz, 2H). **¹³C NMR** (101 MHz, CDCl₃) δ 164.1, 151.1, 145.6, 143.8, 137.5, 128.9, 128.7, 127.8, 127.2, 120.8, 101.6, 67.8, 64.4, 48.3, 47.7, 37.7. **FTIR** (neat): 3020, 2951, 2854, 2799, 1696, 1454, 1242, 1104, 1030, 754, 706 cm⁻¹. **HRMS** (ESI): calculated for C₁₈H₂₁N₄O₃ [M+H]⁺ 341.1608; found: 341.1614.

1-(2-((1-(2-Bromobenzyl)-1*H*-imidazol-2-yl)methoxy)ethyl)pyrimidine-2,4(1*H*,3*H*)-dione (215).



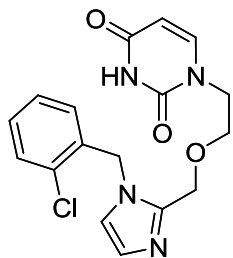
The synthesis of **215** was conducted according to general procedure J with **189** (0.124 g, 0.40 mmol). The product **215** (0.098 g, 0.24 mmol, 60%) was obtained as a white solid. **R_f**: 0.11 (EtOAc:MeOH 9:1). **¹H NMR** (400 MHz, CDCl₃) δ 9.21 (bs, 1H), 7.61 (dd, *J* = 7.8, 1.4 Hz, 1H), 7.29 – 7.16 (m, 2H), 7.10 (d, *J* = 1.3 Hz, 1H), 6.97 (d, *J* = 7.9 Hz, 1H), 6.92 (d, *J* = 1.3 Hz, 1H), 6.68 – 6.61 (m, 1H), 5.53 (dd, *J* = 7.9, 1.6 Hz, 1H), 5.21 (s, 2H), 4.61 (s, 2H), 3.80 – 3.73 (m, 2H), 3.69 – 3.63 (m, 2H). **¹³C NMR** (101 MHz, CDCl₃) δ 163.8, 150.8, 145.6, 144.3, 135.8, 133.2, 129.9, 128.2, 128.1, 128.0, 122.5, 121.8, 101.7, 68.2, 64.9, 50.1, 48.3. **FTIR** (neat): 2925, 2880, 2702, 1704, 1674, 1447, 1432, 1089, 1041, 1004, 750 cm⁻¹. **HRMS** (ESI): calculated for C₁₇H₁₈BrN₄O₃ [M+H]⁺ 405.0557; found: 405.0559.

1-(2-((1-(3-Methylbenzyl)-1*H*-imidazol-2-yl)methoxy)ethyl)pyrimidine-2,4(1*H*,3*H*)-dione (213).



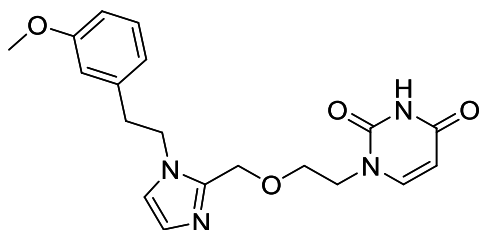
The synthesis of **213** was conducted according to general procedure J with **187** (0.099 g, 0.40 mmol). The product **213** (0.100 g, 0.29 mmol, 74%) was obtained as a white solid. **R_f**: 0.13 (EtOAc:MeOH 9:1). **¹H NMR** (400 MHz, CDCl₃) δ 9.53 (bs, 1H), 7.22 (t, *J* = 7.5 Hz, 1H), 7.14 – 7.08 (m, 1H), 7.06 (d, *J* = 1.3 Hz, 1H), 6.99 (d, *J* = 7.9 Hz, 1H), 6.92 (d, *J* = 1.3 Hz, 1H), 6.87 – 6.80 (m, 2H), 5.51 (d, *J* = 7.9 Hz, 1H), 5.10 (s, 2H), 4.59 (s, 2H), 3.82 – 3.75 (m, 2H), 3.70 – 3.63 (m, 2H), 2.31 (s, 3H). **¹³C NMR** (101 MHz, CDCl₃) δ 163.9, 150.9, 145.6, 144.1, 139.0, 136.3, 129.0, 129.0, 127.8, 127.4, 123.8, 121.8, 101.6, 68.0, 64.9, 49.8, 48.3, 21.5. **FTIR** (neat): 2951, 2921, 2750, 1700, 1678, 1436, 1097, 806, 739 cm⁻¹. **HRMS** (ESI): calculated for 341.1608 [M+H]⁺ 341.1608; found: 341.1609.

1-(2-((1-(2-Chlorobenzyl)-1*H*-imidazol-2-yl)methoxy)ethyl)pyrimidine-2,4(1*H*,3*H*)-dione



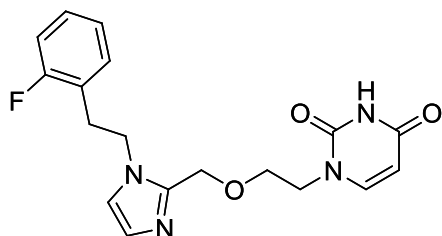
(**219**). The synthesis of **219** was conducted according to general procedure J with **191** (0.107 g, 0.40 mmol). The product **219** (0.085 g, 0.24 mmol, 59%) was obtained as a white solid. **R_f**: 0.11 (EtOAc:MeOH 9:1). **¹H NMR** (400 MHz, CDCl₃) δ 8.71 (bs, 1H), 7.44 (dd, *J* = 7.9, 1.4 Hz, 1H), 7.34 – 7.20 (m, 2H), 7.13 (d, *J* = 1.4 Hz, 1H), 7.07 (d, *J* = 7.9 Hz, 1H), 6.94 (d, *J* = 1.4 Hz, 1H), 6.79 – 6.72 (m, 1H), 5.55 (dd, *J* = 7.9, 1.9 Hz, 1H), 5.26 (s, 2H), 4.68 (s, 2H), 3.85 – 3.78 (m, 2H), 3.73 – 3.67 (m, 2H). **¹³C NMR** (101 MHz, CDCl₃) δ 163.9, 150.9, 145.6, 144.2, 134.2, 132.7, 129.9, 129.6, 128.0, 128.0, 127.5, 121.8, 101.6, 68.2, 64.9, 48.3, 47.6. **FTIR** (neat): 2925, 2880, 2653, 1704, 1674, 1447, 1432, 1089, 1041, 1004, 754 cm⁻¹. **HRMS** (ESI): calculated for C₁₇H₁₈ClN₄O₃ [M+H]⁺ 361.1062; found: 361.1064.

1-(2-((1-(3-Methoxyphenethyl)-1*H*-imidazol-2-yl)methoxy)ethyl)pyrimidine-2,4(1*H*,3*H*)-dione



(**227**). The synthesis of **227** was conducted according to general procedure J with **199** (0.110 g, 0.40 mmol). The product **227** (0.090 g, 0.24 mmol, 61%) was obtained as a white solid. **R_f**: 0.10 (EtOAc:MeOH 9:1). **¹H NMR** (400 MHz, CDCl₃) δ 9.16 (bs, 1H), 7.23 – 7.13 (m, 2H), 7.00 (d, *J* = 1.3 Hz, 1H), 6.84 (d, *J* = 1.3 Hz, 1H), 6.81 – 6.74 (m, 1H), 6.62 – 6.56 (m, 1H), 6.53 – 6.47 (m, 1H), 5.56 (d, *J* = 7.9 Hz, 1H), 4.36 (s, 2H), 4.15 (t, *J* = 7.0 Hz, 2H), 3.87 (t, *J* = 4.9 Hz, 2H), 3.74 (s, 3H), 3.65 (t, *J* = 4.9 Hz, 2H), 2.96 (t, *J* = 7.0 Hz, 2H). **¹³C NMR** (101 MHz, CDCl₃) δ 163.7, 160.0, 150.9, 145.6, 143.8, 138.9, 130.0, 127.5, 121.0, 120.9, 114.6, 112.4, 101.7, 67.9, 64.4, 55.3, 48.3, 47.8, 37.7. **FTIR** (neat): 3115, 2970, 2929, 2877, 2836, 2758, 1678, 1436, 1246, 1045, 750, 769 cm⁻¹. **HRMS** (ESI): calculated for C₁₉H₂₃N₄O₄ [M+H]⁺ 371.1714; found: 371.1717.

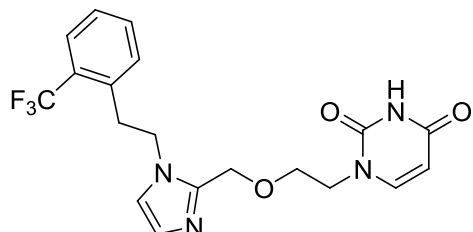
1-(2-((1-(2-Fluorophenethyl)-1*H*-imidazol-2-yl)methoxy)ethyl)pyrimidine-2,4(1*H*,3*H*)-dione



(**229**). The synthesis of **229** was conducted according to general procedure J with **201** (0.106 g, 0.40 mmol). The product **229** (0.098 g, 0.27 mmol, 68%) was obtained as a white solid. **R_f**: 0.11 (EtOAc:MeOH 9:1). **¹H NMR** (400 MHz, CDCl₃) δ 9.29 (bs, 1H), 7.29 – 7.20 (m, 1H), 7.19 (d, *J* = 7.9 Hz, 1H), 7.09 – 6.91 (m, 4H), 6.83 (d, *J* = 1.4 Hz, 1H), 5.56 (d, *J* = 7.9 Hz, 1H), 4.46 (s, 2H), 4.17 (t, *J* = 7.2 Hz, 2H), 3.96 – 3.83 (m, 2H), 3.74 – 3.63 (m, 2H), 3.05 (t, *J* = 7.2 Hz, 2H). **¹³C NMR** (101 MHz, CDCl₃) δ 163.8, 161.3 (d, 245 Hz), 150.9, 145.7, 143.7, 131.1 (d, 5 Hz), 129.3 (d, 8 Hz), 127.6, 124.7 (d, 4 Hz), 124.2 (d, 16 Hz), 120.9, 115.7 (d, 22 Hz),

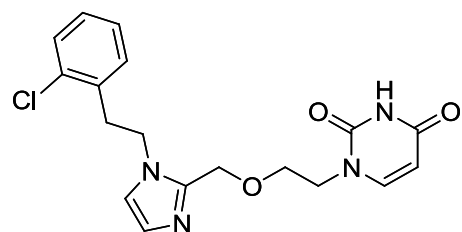
101.6, 68.0, 64.5, 48.4, 46.3 (d, 2 Hz), 31.5 (d, 2 Hz). **FTIR** (neat): 3115, 2699, 2858, 2769, 1678, 1436, 1343, 1056, 758 cm^{-1} . **HRMS** (ESI): calculated for $\text{C}_{18}\text{H}_{20}\text{FN}_4\text{O}_3$ $[\text{M}+\text{H}]^+$ 359.1514; found: 359.1516.

1-(2-((1-(2-(Trifluoromethyl)phenethyl)-1H-imidazol-2-yl)methoxy)ethyl)pyrimidine-2,4(1H,3H)-dione (233).



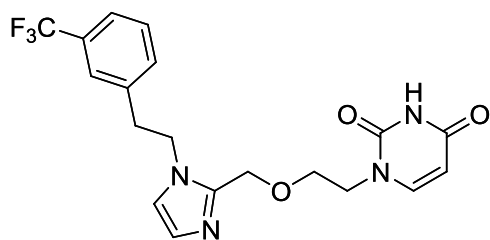
The synthesis of **233** was conducted according to general procedure J with **205** (0.126 g, 0.40 mmol). The product **233** (0.082 g, 0.20 mmol, 50%) was obtained as a white solid. **R_f**: 0.13 (EtOAc:MeOH 9:1). **¹H NMR** (400 MHz, CDCl_3) δ 9.22 (bs, 1H), 7.72 – 7.64 (m, 1H), 7.47 – 7.33 (m, 2H), 7.17 (d, $J = 7.9$ Hz, 1H), 7.03 (d, $J = 1.3$ Hz, 1H), 7.00 – 6.93 (m, 1H), 6.88 (d, $J = 1.3$ Hz, 1H), 5.54 (d, $J = 7.9$ Hz, 1H), 4.40 (s, 2H), 4.17 (t, $J = 7.4$ Hz, 2H), 3.93 – 3.85 (m, 2H), 3.72 – 3.64 (m, 2H), 3.20 (t, $J = 7.4$ Hz, 2H). **¹³C NMR** (101 MHz, CDCl_3) δ 163.7, 150.9, 145.6, 143.8, 135.7 (q, 2 Hz), 132.4 (q, 1 Hz), 131.7, 128.8 (q, 30 Hz) 127.8, 127.6, 126.6 (q, 6 Hz), 124.6 (q, 274 Hz), 121.0, 101.6, 68.0, 64.3, 48.3, 47.3 (q, 2 Hz), 34.9 (q, 2 Hz). **FTIR** (neat): 3078, 3037, 2966, 2907, 2866, 2717, 1711, 1663, 1443, 1316, 1097, 1045, 989, 763 cm^{-1} . **HRMS** (ESI): calculated for $\text{C}_{19}\text{H}_{20}\text{F}_3\text{N}_4\text{O}_3$ $[\text{M}+\text{H}]^+$ 409.1482; found: 409.1481.

1-(2-((1-(2-Chlorophenethyl)-1H-imidazol-2-yl)methoxy)ethyl)pyrimidine-2,4(1H,3H)-



dione (231). The synthesis of **231** was conducted according to general procedure J with **203** (0.112 g, 0.40 mmol). The product **231** (0.091 g, 0.24 mmol, 61%) was obtained as a white solid. **R_f**: 0.13 (EtOAc:MeOH 9:1). **¹H NMR** (400 MHz, CDCl_3) δ 8.98 (bs, 1H), 7.38 (dd, $J = 7.9, 1.4$ Hz, 1H), 7.26 – 7.18 (m, 2H), 7.14 (td, $J = 7.4, 1.4$ Hz, 1H), 7.02 (d, $J = 1.4$ Hz, 1H), 6.93 (dd, $J = 7.5, 1.8$ Hz, 1H), 6.86 (d, $J = 1.4$ Hz, 1H), 5.56 (d, $J = 7.8$ Hz, 1H), 4.42 (s, 2H), 4.22 (t, $J = 7.1$ Hz, 2H), 3.93 – 3.86 (m, 2H), 3.73 – 3.63 (m, 2H), 3.14 (t, $J = 7.1$ Hz, 2H). **¹³C NMR** (101 MHz, CDCl_3) δ 163.6, 150.8, 145.7, 143.7, 134.8, 134.0, 131.1, 129.9, 129.1, 127.5, 127.3, 121.0, 101.6, 68.1, 64.3, 48.4, 45.8, 35.8. **FTIR** (neat): 2955, 2862, 2754, 1707, 1666, 1436, 1100, 765, 736 cm^{-1} . **HRMS** (ESI): calculated for $\text{C}_{18}\text{H}_{20}\text{ClN}_4\text{O}_3$ $[\text{M}+\text{H}]^+$ 375.1218; found: 375.1221.

1-(2-((1-(3-(Trifluoromethyl)phenethyl)-1*H*-imidazol-2-yl)methoxy)ethyl)pyrimidine-



2,4(1*H*,3*H*)-dione (235). The synthesis of **235** was conducted according to general procedure J with **205** (0.126 g, 0.40 mmol). The product **235** (0.081 g, 0.20 mmol, 50%) was obtained as a white solid. **R_f**: 0.10 (EtOAc:MeOH 9:1). **¹H NMR** (400 MHz, CDCl₃) δ 9.46 (bs, 1H), 7.55 – 7.48 (m, 1H), 7.43 – 7.35 (m,

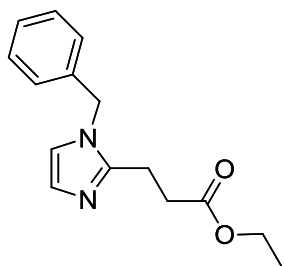
1H), 7.33 – 7.28 (m, 1H), 7.18 – 7.10 (m, 2H), 7.00 (d, *J* = 1.3 Hz, 1H), 6.78 (d, *J* = 1.3 Hz, 1H), 5.56 (d, *J* = 7.9 Hz, 1H), 4.42 (s, 2H), 4.18 (t, *J* = 7.0 Hz, 2H), 3.93 – 3.84 (m, 2H), 3.73 – 3.63 (m, 2H), 3.07 (t, *J* = 7.0 Hz, 2H). **¹³C NMR** (101 MHz, CDCl₃) δ 163.8, 150.9, 145.5, 143.6, 138.4, 132.3 (m), 131.3 (q, 32 Hz), 129.5, 127.8, 125.5 (q, 4 Hz), 124.2 (q, 4 Hz), 124.0 (q, 272 Hz), 120.9, 101.7, 67.8, 64.3, 48.3, 47.4, 37.5. **FTIR** (neat): 2966, 2873, 2717, 1715, 1659, 1443, 1343, 1153, 1093, 1074, 754, 702 cm⁻¹. **HRMS** (ESI): calculated for C₁₉H₂₀F₃N₄O₃ [M+H]⁺ 409.1482; found: 409.1483.

11.2.5 Synthesis discussed in section 4.7

General procedure K: Reduction of unsaturated esters

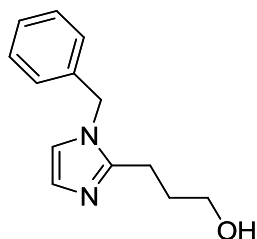
Substituted (*E*)-ethyl 3-(1*H*-imidazol-2-yl)acrylate (1.0 eq.) and cobalt(II)-chloride hexahydrate (6 mol%) were dissolved in 99% ethanol (5 mL per mmol SM). NaBH₄ (3.0 eq) was added in portions at room temperature. The reaction mixture was heated for 3 h at 50 °C. The reaction mixture was concentrated and the residue diluted with dry THF (5 mL per mmol SM). A solution of 2 M LiBH₄ in THF (1 mL per mmol SM) was added dropwise at room temperature. The reaction mixture was heated to 40°C overnight. The reaction was quenched with acetone and was concentrated under reduced pressure. The residue was diluted with DCM and water. The aqueous layer was extracted with DCM (3x) and the combined fractions were washed with water (1x) and brine (1x) and dried over Na₂SO₄. The solvent was removed under reduced pressure and the residue was purified by silica column chromatography (EtOAc → EtOAc:MeOH 9:1).

Ethyl 3-(1-benzyl-1*H*-imidazol-2-yl)propanoate (237). **36** (2.947 g, 11.5 mmol) and CoCl₂ x 6 H₂O (0.083 g, 3 mol%) were dissolved in 99% ethanol (60 mL). NaBH₄ (1.310 g, 34.5 mmol) was added in portions over 10 min. The reaction mixture was stirred at room temperature overnight. The reaction was quenched with acetone and was concentrated under reduced pressure. Water and DCM were added and the aqueous layer was extracted (3x). The combined organic layers were washed with water (2x) and brine (1x) and dried over Na₂SO₄.

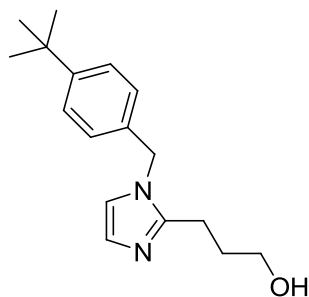


The solvent was removed under reduced pressure. The product **237** (2.460 g, 9.52 mmol, 83%) was obtained as an orange oil and was used without further purification. **R_f**: 0.26 (EtOAc). **¹H NMR** (400 MHz, CD₃OD) δ 7.41 – 7.26 (m, 3H), 7.19 – 7.12 (m, 2H), 7.07 – 7.03 (m, 1H), 6.93 – 6.88 (m, 1H), 5.23 (s, 2H), 4.09 (q, *J* = 7.1 Hz, 2H), 2.90 (t, *J* = 7.4 Hz, 2H), 2.68 (t, *J* = 7.4 Hz, 2H), 1.21 (t, *J* = 7.1 Hz, 3H). **¹³C NMR** (101 MHz, CD₃OD) δ 173.9, 148.4, 138.3, 130.0, 129.0, 128.0, 127.3, 121.8, 61.7, 50.4, 32.8, 22.6, 14.5. **HRMS** (ESI): calculated for C₁₅H₁₉N₂O₂ [M+H]⁺ 259.1441; found: 259.1436.

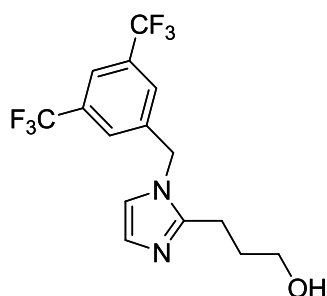
3-(1-Benzyl-1*H*-imidazol-2-yl)propan-1-ol (78): 1 M DIBAL-H in DCM (20.9 mmol, 2.2 eq.) was added dropwise (over 5 minutes) to a solution of **237** (2.450 g, 9.50 mmol) in dry DCM (50 mL) at -78°C. The reaction mixture was allowed to warm to room temperature and was stirred for 2.5 h. The DIBAL-H excess was quenched with a small amount of MeOH (1-2ml). Saturated Rochelle-salt solution was added and the mixture was stirred overnight. The layers were separated and the aqueous layer extracted with DCM 2x). The combined organic layers were washed with brine (1x) and dried over Na₂SO₄. The solvent was removed under reduced pressure. The product **78** (1.993 g, 9.22 mmol, 97%) was obtained as an orange oil and was used without further purification. **¹H NMR** (400 MHz, CD₃OD) δ 7.38 – 7.25 (m, 3H), 7.16 – 7.09 (m, 2H), 7.03 (d, *J* = 1.4 Hz, 1H), 6.90 (d, *J* = 1.4 Hz, 1H), 5.20 (s, 2H), 3.54 (t, *J* = 6.2 Hz, 2H), 2.76 – 2.68 (m, 2H), 1.89 – 1.76 (m, 2H). **¹³C NMR** (101 MHz, CD₃OD) δ 149.6, 138.4, 129.9, 128.9, 127.9, 127.2, 121.6, 62.0, 50.3, 31.8, 23.9. **HRMS** (ESI): calculated for C₁₃H₁₇N₂O [M+H]⁺ 217.1335; found: 217.1338.



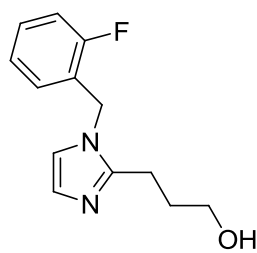
3-(1-(4-*tert*-Butylbenzyl)-1*H*-imidazol-2-yl)propan-1-ol (239). The synthesis of **239** was conducted according to general procedure K with **41** (0.312 g, 1.00 mmol). The product **244** (0.097 g, 0.36 mmol, 36%) was obtained as a colorless oil. **R_f**: 0.11 (EtOAc). **¹H NMR** (400 MHz, CDCl₃) δ 7.39 – 7.33 (m, 2H), 7.03 – 6.94 (m, 3H), 6.86 – 6.82 (m, 1H), 5.04 (s, 2H), 3.76 – 3.70 (m, 2H), 2.84 – 2.76 (m, 2H), 2.03 – 1.92 (m, 2H), 1.30 (s, 9H). **¹³C NMR** (101 MHz, CDCl₃) δ 151.3, 148.4, 133.2, 126.7, 126.5, 126.1, 120.2, 62.7, 49.5, 34.7, 31.4, 29.6, 25.2. **FTIR** (neat): 3193, 2959, 2869, 1417, 1272, 1067, 1045, 728 cm⁻¹. **HRMS** (ESI): calculated for C₁₇H₂₅N₂O [M+H]⁺ 273.1961; found: 273.1964.



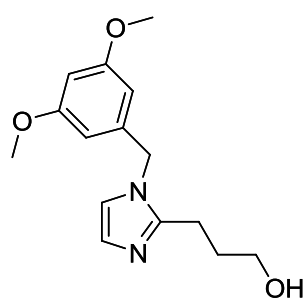
3-(1-(3,5-Bis(trifluoromethyl)benzyl)-1*H*-imidazol-2-yl)propan-1-ol (83). The synthesis of **83** was conducted according to general procedure K with **37** (0.785 g, 2.00 mmol). The product **83** (0.342 g, 0.97 mmol, 49%) was obtained as a grey solid. **R_f**: 0.17 (EtOAc:MeOH 9:1). **¹H NMR** (400 MHz, CD₃OD) δ 7.93 (s, 1H), 7.67 (s, 2H), 7.14 (s, 1H), 7.00 (s, 1H), 5.44 (s, 2H), 3.54 (t, *J* = 6.2 Hz, 2H), 2.72 (t, *J* = 7.7 Hz, 2H), 1.84 (p, *J* = 6.4 Hz, 2H). **¹³C NMR** (101 MHz, CD₃OD) δ 149.9, 142.2, 133.3 (q, 33 Hz), 128.3 (m), 128.0, 126.0, 124.6 (q, 272 Hz), 122.7 (m), 121.6, 61.8, 31.8, 23.8. **FTIR** (neat): 3160, 2929, 2858, 1279, 1164, 1127, 1082, 1045, 724, 706, 687 cm⁻¹. **HRMS** (ESI): calculated for C₁₅H₁₅F₆N₂O [M+H]⁺ 353.1094; found: 353.1087.



3-(1-(2-Fluorobenzyl)-1*H*-imidazol-2-yl)propan-1-ol (240). The synthesis of **240** was conducted according to general procedure K with **40** (0.411 g, 1.50 mmol). The product **240** (0.177 g, 0.76 mmol, 50%) was obtained as colorless oil. **R_f**: 0.17 (EtOAc:MeOH 9:1). **¹H NMR** (400 MHz, CDCl₃) δ 7.35 – 7.27 (m, 1H), 7.15 – 7.03 (m, 2H), 7.01 – 6.93 (m, 1H), 6.92 – 6.81 (m, 2H), 5.11 (s, 2H), 3.77 – 3.70 (m, 2H), 2.85 – 2.78 (m, 2H), 2.05 – 1.93 (m, 2H). **¹³C NMR** (101 MHz, CDCl₃) δ 160.3 (d, 246 Hz), 148.4, 130.1 (d, 8 Hz), 128.8 (d, 4 Hz), 127.0, 124.8 (d, 4 Hz), 123.6 (15 Hz), 120.1, 115.8 (d, 21 Hz), 62.6, 43.6 (d, 5 Hz), 29.6, 25.1. **FTIR** (neat): 3178, 3111, 2933, 2866, 1495, 1458, 1231, 1067, 1041, 758, 736, 676 cm⁻¹. **HRMS** (ESI): calculated for C₁₃H₁₆FN₂O [M+H]⁺ 235.1241; found: 235.1242.



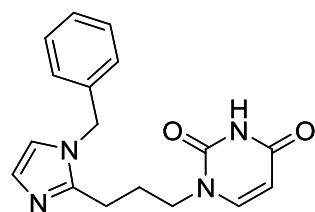
3-(1-(3,5-Dimethoxybenzyl)-1H-imidazol-2-yl)propan-1-ol (82). The synthesis of **82** was conducted according to general procedure K with **38** (0.633 g, 2.00 mmol). The product **82** (0.300 g, 1.09 mmol, 54%) was obtained as a colorless oil. **R_f**: 0.16 (EtOAc:MeOH 9:1). **¹H NMR** (400 MHz, CDCl₃) δ 6.98 – 6.93 (m, 1H), 6.87 – 6.82 (m, 1H), 6.37 (t, *J* = 2.2 Hz, 1H), 6.17 (d, *J* = 2.3 Hz, 2H), 4.99 (s, 2H), 3.78 – 3.69 (m, 8H), 2.77 (t, *J* = 6.5 Hz, 2H), 1.97 (p, *J* = 6.1 Hz, 2H). **¹³C NMR** (101 MHz, CDCl₃) δ 161.5, 148.5, 138.8, 126.9, 120.3, 104.8, 99.6, 62.6, 55.5, 49.7, 29.6, 25.1. **FTIR** (neat): 3190, 2936, 2840, 1599, 1462, 1432, 1208, 1156, 1056, 736 cm⁻¹. **HRMS** (ESI): calculated for C₁₅H₂₀N₂O₃Na [M+Na]⁺ 299.1366; found: 299.1359.



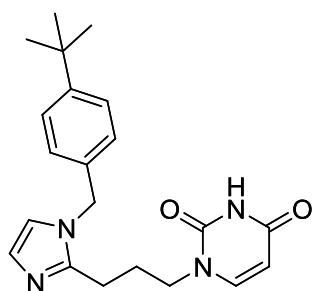
General procedure L: Synthesis of alkyl-type final compounds (type C)

Substituted 1*H*-imidazol-2-yl)propan-1-ol (1.0 eq), N³-benzoyl uracil (**53**) (1.1 eq) and PPh₃ (2.0 eq) were suspended in dry THF (1 mL per 0.2 mmol alcohol). DIAD (2.0 eq) was added dropwise at 0 °C. The mixture was allowed to warm to room temperature and was stirred overnight. The solvent was removed under reduced pressure and the residue purified by silica column chromatography (EtOAc → EtOAc:MeOH 9:1) to afford the benzoyl-protected product. 7 N NH₃/MeOH (3-4 mL for 0.2-0.4 mmol batch) was added to the benzoyl-protected product at 0 °C. The resulting solution was allowed to warm to room temperature. After stirring for 3 h, the volatiles were removed with a nitrogen gas stream. The crude product was purified by silica column chromatography (EtOAc → EtOAc:MeOH 9:1).

1-(3-(1-Benzyl-1H-imidazol-2-yl)propyl)pyrimidine-2,4(1H,3H)-dione (238). The synthesis of **238** was conducted according to general procedure L with **78** (0.230 g, 1.06 mmol). The product **238** (0.090 g, 0.29 mmol, 27%) was obtained as a white solid. **R_f**: **0.07** (EtOAc:MeOH 9:1). **¹H NMR** (400 MHz, CDCl₃) δ 9.27 (bs, 1H), 7.38 – 7.27 (m, 4H), 7.07 – 7.00 (m, 3H), 6.89 (d, *J* = 1.4 Hz, 1H), 5.62 (d, *J* = 7.9 Hz, 1H), 5.06 (s, 2H), 3.82 (t, *J* = 7.0 Hz, 2H), 2.66 (t, *J* = 7.0 Hz, 2H), 2.11 (p, *J* = 7.0 Hz, 2H). **¹³C NMR** (101 MHz, CDCl₃) δ 163.9, 151.1, 146.6, 145.2, 136.1, 129.2, 128.4, 127.1, 126.7, 120.6, 102.1, 49.8, 47.7, 26.3, 23.1. **FTIR** (neat): 3033, 2955, 2780, 1666, 1432, 1354, 810, 717 cm⁻¹. **HRMS** (ESI): calculated for C₁₇H₁₉N₄O₂ [M+H]⁺ 311.1503; found: 311.1506.

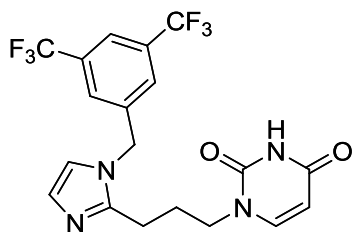


1-(3-(1-(4-*tert*-Butylbenzyl)-1*H*-imidazol-2-yl)propyl)pyrimidine-2,4(1*H*,3*H*)-dione (**242**).



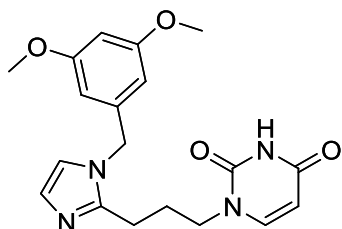
The synthesis of **242** was conducted according to general procedure L with **239** (0.082 g, 0.30 mmol). The product **242** (0.061 g, 0.17 mmol, 55%) was obtained as a white-yellow solid. **R_f**: **0.09** (EtOAc:MeOH 9:1). **¹H NMR** (400 MHz, CDCl₃) δ 8.66 (bs, 1H), 7.40 – 7.31 (m, 3H), 7.03 – 6.94 (m, 3H), 6.88 (d, *J* = 1.3 Hz, 1H), 5.63 (d, *J* = 7.9 Hz, 1H), 5.02 (s, 2H), 3.84 (t, *J* = 7.0 Hz, 2H), 2.67 (t, *J* = 6.9 Hz, 2H), 2.12 (p, *J* = 7.0 Hz, 2H), 1.30 (s, 9H). **¹³C NMR** (101 MHz, CDCl₃) δ 163.8, 151.5, 151.1, 146.5, 145.2, 133.0, 126.9, 126.6, 126.1, 120.6, 102.1, 49.5, 47.7, 34.7, 31.4, 26.3, 23.1. **FTIR** (neat): 3052, 2962, 2869, 1674, 1436, 810, 765, 721 cm⁻¹. **HRMS** (ESI): calculated for C₂₁H₂₇N₄O₂ [M+H]⁺ 367.2129; found: 367.2132.

1-(3-(1-(3,5-bis(Trifluoromethyl)benzyl)-1*H*-imidazol-2-yl)propyl)pyrimidine-

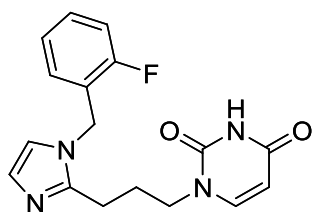


2,4(1*H*,3*H*)-dione (243**).** The synthesis of **243** was conducted according to general procedure L with **83** (0.141 g, 0.40 mmol). The product **243** (0.092 g, 0.21 mmol, 52%) was obtained as a white solid. **R_f**: 0.14 (EtOAc:MeOH 9:1). **¹H NMR** (400 MHz, CDCl₃) δ 9.14 (s, 1H), 7.84 (bs, 1H), 7.47 (s, 2H), 7.36 (d, *J* = 7.8 Hz, 1H), 7.08 (d, *J* = 1.4 Hz, 1H), 6.88 (d, *J* = 1.4 Hz, 1H), 5.66 (d, *J* = 7.9 Hz, 1H), 5.21 (s, 2H), 3.86 (t, *J* = 6.9 Hz, 2H), 2.65 (t, *J* = 6.9 Hz, 2H), 2.17 (p, *J* = 6.9 Hz, 2H). **¹³C NMR** (101 MHz, CDCl₃) δ 163.7, 151.2, 146.6, 145.0, 139.2, 132.8 (q, 34 Hz), 128.6, 126.7 (m), 123.0 (q, 274 Hz), 122.4 (m), 120.2, 102.3, 48.6, 47.7, 26.4, 23.2. **FTIR** (neat): 3052, 2795, 1674, 1279, 1171, 1127, 683 cm⁻¹. **HRMS** (ESI): calculated for C₁₉H₁₇F₆N₄O₂ [M+H]⁺ 447.1250; found: 447.1253.

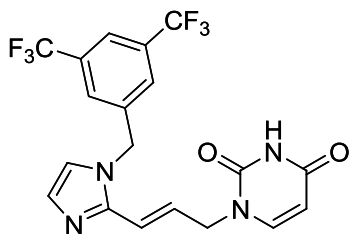
1-(3-(1-(3,5-Dimethoxybenzyl)-1*H*-imidazol-2-yl)propyl)pyrimidine-2,4(1*H*,3*H*)-dione



(244**).** The synthesis of **244** was conducted according to general procedure L with **82** (0.111g, 0.40 mmol). The product **244** (0.073 g, 0.20 mmol, 50%) was obtained as a pale yellow solid. **R_f**: **0.09** (EtOAc:MeOH 9:1). **¹H NMR** (400 MHz, CDCl₃) δ 8.76 (bs, 1H), 7.33 (d, *J* = 7.8 Hz, 1H), 7.06 – 7.01 (m, 1H), 6.93 – 6.88 (m, 1H), 6.38 (t, *J* = 2.3 Hz, 1H), 6.15 (d, *J* = 2.1 Hz, 2H), 5.62 (d, *J* = 7.9 Hz, 1H), 4.99 (s, 2H), 3.85 (t, *J* = 6.9 Hz, 2H), 3.75 (s, 6H), 2.68 (t, *J* = 7.0 Hz, 2H), 2.14 (p, *J* = 7.1 Hz, 2H). **¹³C NMR** (101 MHz, CDCl₃) δ 163.6, 161.6, 151.0, 146.6, 145.2, 138.2, 126.6, 120.8, 104.9, 102.1, 99.5, 55.5, 49.9, 47.7, 26.2, 23.0. **FTIR** (neat): 3164, 3104, 3048, 2940, 2840, 1674, 1596, 1458, 1432, 1208, 1156, 1067, 810, 765 cm⁻¹. **HRMS** (ESI): calculated for C₁₉H₂₃N₄O₄ [M+H]⁺ 371.1714; found: 371.1717.

1-(3-(1-(2-Fluorobenzyl)-1H-imidazol-2-yl)propyl)pyrimidine-2,4(1H,3H)-dione (245).

The synthesis of **245** was conducted according to general procedure L, with **240** (0.094 g, 0.40 mmol). The product **245** (0.081 g, 0.25 mmol, 62%) was obtained as a pale yellow solid. R_f : 0.11 (EtOAc:MeOH 9:1). $^1\text{H NMR}$ (400 MHz, CDCl_3) δ 9.08 (bs, 1H), 7.39 – 7.28 (m, 2H), 7.15 – 7.05 (m, 2H), 7.01 (d, $J = 1.4$ Hz, 1H), 6.97 – 6.85 (m, 2H), 5.63 (d, $J = 7.9$ Hz, 1H), 5.09 (s, 2H), 3.87 (t, $J = 6.9$ Hz, 2H), 2.72 (t, $J = 7.0$ Hz, 2H), 2.17 (p, $J = 6.9$ Hz, 2H). $^{13}\text{C NMR}$ (101 MHz, CDCl_3) δ 163.8, 160.4 (d, 247 Hz), 151.1, 146.5, 145.2, 130.4 (d, 8 Hz), 129.0 (d, 4 Hz), 127.2, 124.9 (d, 4 Hz), 123.3 (d, 14 Hz), 120.4, 115.9 (d, 21 Hz), 102.1, 47.7, 43.7 (d, 5 Hz), 26.3, 23.0. **FTIR** (neat): 3104, 3048, 2959, 2784, 1670, 1432, 1231, 758 cm^{-1} . **HRMS** (ESI): calculated for $\text{C}_{17}\text{H}_{18}\text{FN}_4\text{O}_2$ $[\text{M}+\text{H}]^+$ 329.1408; found: 329.1411.

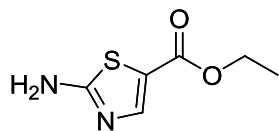
(E)-1-(3-(1-(3,5-Bis(trifluoromethyl)benzyl)-1H-imidazol-2-yl)allyl)pyrimidine-

2,4(1H,3H)-dione (250). **43** (0.210 g, 0.60 mmol) was dissolved in chloroform (4 mL). SOCl_2 (0.6 mL) was added dropwise and the reaction mixture was stirred at reflux for 3 h. The volatiles were removed and the solid residue was washed with Et_2O . The solid was dried and redissolved in dry DMF (2 mL). N^3 -benzoyl uracil (**53**) (0.143 g, 0.66 mmol) and K_2CO_3 (0.249 g, 1.80 mmol) were added and the reaction mixture was stirred at room temperature overnight. Water and EtOAc were added and the aqueous layer was extracted (3x). The combined organic layers were washed with water (1x) and brine (1x) and dried over Na_2SO_4 . The solvent was removed under reduced pressure to afford the benzoyl-protected product. The crude benzoyl-protected product was dissolved in 7 N NH_3/MeOH (4 mL) at 0 °C. The reaction mixture was stirred for 3 h at room temperature. The mixture was concentrated using a stream of nitrogen. The crude solid product was washed with EtOAc and MeOH. The product **250** (0.115 g, 0.26 mmol, 43%) was obtained as a white solid. $^1\text{H NMR}$ (400 MHz, $\text{DMSO}-d_6$) δ 11.25 (s, 1H), 8.07 (s, 1H), 7.81 (s, 2H), 7.53 (d, $J = 7.9$ Hz, 1H), 7.38 (d, $J = 1.2$ Hz, 1H), 7.00 (d, $J = 1.2$ Hz, 1H), 6.72 (d, $J = 15.4$ Hz, 1H), 6.48 (dt, $J = 15.4, 6.3$ Hz, 1H), 5.51 (d, $J = 8.0$ Hz, 3H), 4.44 – 4.37 (m, 2H). $^{13}\text{C NMR}$ (101 MHz, $\text{DMSO}-d_6$) δ 163.6, 150.8, 144.8, 143.6, 141.1, 130.6 (q, 33 Hz), 129.0, 127.9, 127.8 (m), 123.0 (q, 272 Hz), 121.6 (m), 121.5, 119.2, 101.2, 48.3, 47.1. **HRMS** (ESI): calculated for $\text{C}_{19}\text{H}_{15}\text{O}_2\text{N}_4\text{F}_6$ $[\text{M}+\text{H}]^+$ 445.1094; found: 445.1092.

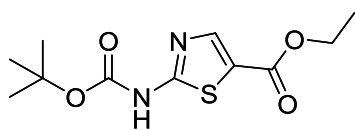
11.3 Supporting information project 2

11.3.1 Synthesis of dasatinib scaffold

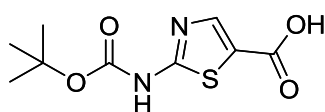
Ethyl 2-aminothiazole-5-carboxylate (275). **275** was synthesized based on a literature procedure.¹⁸³ NBS (6.247 g, 35.10 mmol) was added in portions to a mixture of ethyl β -ethoxyacrylate (4.600 g, 31.90 mmol) in dioxane/water (1:1, 32 mL) at -9 °C. The solution was allowed to warm to room temperature and stirred for 1.5 h. Thiourea (2.428 g, 31.90 mmol) was added and the mixture heated to 80 °C for 1.5 h. The solution was cooled to room temperature and concentrated ammonium hydroxide solution (7 mL) was added. The precipitated product was filtrated and washed with water and dried under reduced pressure. The product **275** (4.477 g, 26.00 mmol, 81%) was obtained as pale yellow powder. ¹H NMR (400 MHz, CDCl₃) δ 7.77 (s, 1H), 6.13 (bs, 2H), 4.30 (q, J = 7.1 Hz, 2H), 1.34 (t, J = 7.1 Hz, 3H). ¹³C NMR (101 MHz, CDCl₃) δ 172.3, 161.8, 145.8, 118.7, 61.3, 14.5. HRMS (ESI): calculated for C₆H₉N₂O₂S [M+H]⁺ 173.0379; found: 171.0375.



Ethyl-2-[[*tert*-butyloxy]carbonyl]-amino]-1,3-thiazole-5-carboxylate (276). **276** was synthesized according to a literature procedure.¹⁸¹ X (2.583 g, 15.00 mmol) and di-*tert*-butyl dicarbonate (3.929 g, 18.00 mmol) were dissolved in dry THF (45 mL). DMAP (0.122 g, 1.00 mmol) was added and the reaction mixture was stirred at room temperature overnight. The reaction solvent was removed. The residue was suspended in DCM (150 mL) and filtrated. The obtained solution was washed with 1M HCl (1x), water (1x) and brine (1x) and was dried over MgSO₄. The solvent was removed under reduced pressure. The solid residue was washed with n-hexane. The product **276** (3.060 g, 11.24 mmol, 75%) was obtained as a yellow solid. ¹H NMR (400 MHz, CDCl₃) δ 12.04 (s, 1H), 8.03 (s, 1H), 4.33 (q, J = 7.1 Hz, 2H), 1.60 (s, 9H), 1.35 (t, J = 7.1 Hz, 3H). ¹³C NMR (101 MHz, CDCl₃) δ 165.9, 162.0, 152.6, 144.3, 122.0, 83.2, 61.3, 28.3, 14.4. HRMS (ESI): calculated C₁₁H₁₆N₂O₄SNa for [M+Na]⁺ 295.0723; found: 295.0725.

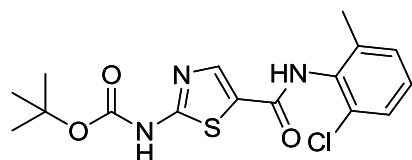


2-[[*tert*-Butyloxy]carbonyl]-amino]-1,3-thiazole-5-carboxylic acid (277). **277** was synthesized according to a literature procedure.¹⁸¹ **276** (1.721 g, 6.32 mmol) was dissolved in a mixture of THF:EtOH (2:3, 40 mL) and 6 N KOH solution (30 mL) and stirred at 55 °C overnight. The reaction mixture was concentrated under reduced pressure until the organic solvents were mostly removed. The solution was acidified to pH 1 with concentrated HCl under vigorous stirring. The precipitated product was washed with water and Et₂O and dried under



reduced pressure. The product **277** (1.351 g, 5.53 mmol, 87%) was obtained as a white solid. $^1\text{H NMR}$ (400 MHz, DMSO- d_6) δ 12.99 (bs, 1H), 11.95 (bs, 1H), 7.95 (s, 1H), 1.49 (s, 9H). $^{13}\text{C NMR}$ (101 MHz, DMSO- d_6) δ 164.1, 162.8, 152.7, 145.0, 122.3, 82.0, 27.8. **HRMS** (ESI): calculated for $\text{C}_9\text{H}_{11}\text{N}_2\text{O}_4\text{S}$ $[\text{M}-\text{H}]^-$ 243.0445; found: 243.0445.

2-[[*tert*-Butyloxy]carbonyl]-amino]-*N*-(2-chloro-6-methylphenyl)-1,3-thiazole-5-

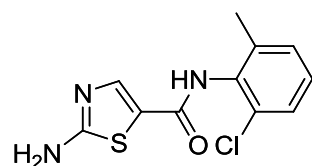


carboxamide (278). **278** was synthesized according to a literature procedure.¹⁸¹ **277** (3.640 g, 14.90 mmol) was mixed with dry DCM (40 mL) and was cooled to 0 °C. Oxalyl chloride (1.53 mL, 18.0 mmol) was added. The reaction was initialized by addition of a few drops of DMF

and was allowed to slowly warm to room temperature. The reaction mixture was stirred for further 2 h. The solvent and the reagent excess were removed under reduced pressure and the residue was dissolved in dry DCM (40 mL). 2-Chloro-6-methylaniline (2.634 g, 18.60 mmol) was added to the reaction mixture at 0 °C. The mixture was stirred for 5 minutes before DIPEA (3.40 mL, 19.50 mmol) was added. The reaction mixture was allowed to warm to room temperature, stirred overnight and was then concentrated under reduced pressure. The obtained residue was suspended in EtOAc, the white solid was filtrated and further washed with 1 M HCl and water. The product **278** (4.013 g, 10.91 mmol, 73%) was afforded as a white solid. $^1\text{H NMR}$ (400 MHz, DMSO- d_6) δ 11.82 (bs, 1H), 10.05 (bs, 1H), 8.24 (s, 1H), 7.42 – 7.33 (m, 1H), 7.31 – 7.21 (m, 2H), 2.22 (s, 3H), 1.50 (s, 9H). $^{13}\text{C NMR}$ (101 MHz, DMSO- d_6) δ 163.0, 159.4, 152.7, 141.0, 138.7, 133.3, 132.3, 129.1, 128.3, 127.0, 126.4, 81.8, 27.8, 18.3. **HRMS** (ESI): calculated for $\text{C}_{16}\text{H}_{17}\text{ClN}_3\text{O}_3\text{S}$ $[\text{M}-\text{H}]^-$ 366.0685; found: 366.0682.

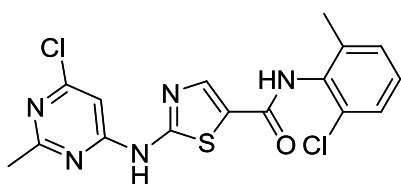
2-Amino-*N*-(2-chloro-6-methylphenyl)-thiazole-5-carboxamide (279).

279 was synthesized according to a literature procedure.¹⁸¹ **278** (4.013 g,



10.91 mmol) was mixed with cold TFA (15 mL) and was stirred for 3.5 h at 0-5 °C and 45 minutes at room temperature. The solution was diluted with water and EtOAc. The pH was adjusted with sodium hydroxide solution to pH 9-10. The aqueous layer was extracted with EtOAc (3x). The combined organic layers were washed with brine (1x) were dried over Na_2SO_4 . The solvent was removed under reduced pressure. The product **279** (2.390 g, 8.93 mmol, 82%) was obtained as a pale yellow solid. $^1\text{H NMR}$ (400 MHz, DMSO- d_6) δ 9.65 (bs, 1H), 7.87 (bs, 1H), 7.61 (bs, 2H), 7.43 – 7.15 (m, 3H), 2.21 (s, 3H). $^{13}\text{C NMR}$ (101 MHz, DMSO- d_6) δ 172.2, 159.6, 143.2, 138.9, 133.7, 132.5, 129.0, 128.0, 127.0, 120.7, 18.3. **HRMS** (ESI): calculated for $\text{C}_{11}\text{H}_{19}\text{ClN}_3\text{OS}$ $[\text{M}-\text{H}]^-$ 266.0160; found: 266.0160.

2-(6-Chloro-2-methylpyrimidin-4-ylamino)-N-(2-chloro-6-methylphenyl)-thiazole-5-

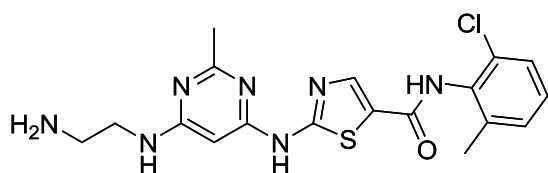


carboxamide (273). **273** was synthesized according to a literature procedure.^{184,185} A solution of X (1.976 g, 7.38 mmol) and 4,6-dichloro-2-methylpyrimidine (1.306 g, 8.01 mmol) in dry THF (25 mL) were stirred for 10 minutes at 0 °C. NaOtBu (2.483 g, 25.83 mmol) was added in portions

over 10 minutes and the reaction mixtures allowed to warm up to room temperature. The reaction was stirred for 2-3 h. Water (10 mL) was added to the reaction mixture at 0 °C. The pH was adjusted to pH 5-6 with 4M HCL and 1M HCl. The resulting yellow suspension was stirred at room temperature overnight. The crude solid was filtrated, was washed with THF, water, and THF and was dried under reduced pressure. The product **273** (1.850 g, 4.69 mmol, 63%) was afforded as a pale yellow powder. ¹H NMR (400 MHz, DMSO-*d*₆) δ 12.24 (s, 1H), 10.02 (s, 1H), 8.32 (s, 1H), 7.44 – 7.38 (m, 1H), 7.33 – 7.23 (m, 2H), 6.95 (s, 1H), 2.59 (s, 3H), 2.24 (s, 3H). ¹³C NMR (101 MHz, DMSO-*d*₆) δ 173.8, 167.4, 161.3, 159.6, 158.5, 157.5, 140.9, 138.8, 133.3, 132.4, 129.1, 128.3, 127.1, 103.4, 25.2, 18.3. HRMS (ESI): calculated for C₁₆H₁₃Cl₂N₅OS [M-H]⁻ 392.0145; found: 392.0143.

11.3.2 Linker synthesis

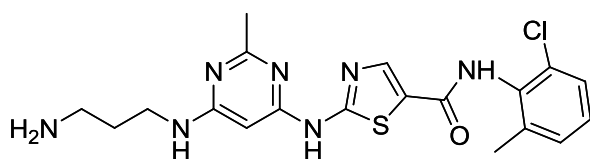
2-(6-(2-Aminoethylamino)-2-methylpyrimidin-4-ylamino)-N-(2-chloro-6-methylphenyl)-



thiazole-5-carboxamide (280). **273** (0.394 g, 1.0 mmol) was dissolved in 1,2-ethanediamine (2 mL) and stirred at 70 °C overnight. Water (30 mL) was added to the reaction mixture at room temperature. The precipitating solid was filtered,

was washed with water and was dried under reduced pressure. The product **280** (0.360 g, 0.86 mmol, 86%) was obtained as pale yellow solid. ¹H NMR (400 MHz, CD₃OD) δ 8.16 (s, 1H), 7.41 – 7.34 (m, 1H), 7.31 – 7.20 (m, 2H), 5.88 (s, 1H), 3.44 – 3.35 (m, 2H), 2.90 – 2.83 (m, 2H), 2.48 (s, 3H), 2.34 (s, 3H). HRMS (ESI): calculated for C₁₈H₂₁ON₇ClS [M+H]⁺ 418.1211; found: 418.1211.

2-(6-(3-Aminopropylamino)-2-methylpyrimidin-4-ylamino)-N-(2-chloro-6-

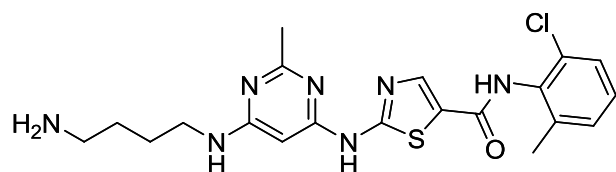


methylphenyl)thiazole-5-carboxamide (281). **273** (0.197 g, 0.46 mmol) was dissolved in 1,3-diaminopropane (1 mL) and was stirred at 70 °C overnight. Water (20 mL) was added to the reaction mixture at room

temperature. The precipitating solid was filtered, was washed with water and was dried under

reduced pressure. **281** (0.165 g, 0.38 mmol, 83%) was obtained as pale yellow solid. $^1\text{H NMR}$ (400 MHz, CD_3OD) δ 8.16 (s, 1H), 7.39 – 7.17 (m, 3H), 5.87 (s, 1H), 3.43 – 3.35 (m, 2H), 2.75 (t, $J = 6.9$ Hz, 2H), 2.47 (s, 3H), 2.34 (s, 3H), 1.78 (p, $J = 6.8$ Hz, 2H). $^{13}\text{C NMR}$ (101 MHz, , $\text{DMSO-}d_6$) δ 165.2, 163.1, 163.0, 162.8, 159.9, 140.9, 138.8, 133.5, 132.4, 129.0, 128.1, 127.0, 125.3, 39.1, 32.5, 25.4, 18.3. **HRMS** (ESI): calculated for $\text{C}_{19}\text{H}_{21}\text{ON}_7\text{ClS}$ [M-H] $^-$ 430.1222; found: 430.1221.

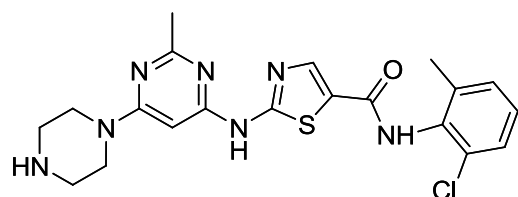
2-(6-(4-Aminobutylamino)-2-methylpyrimidin-4-ylamino)-N-(2-chloro-6-methylphenyl)thiazole-5-carboxamide (282).



273 (0.394 g, 1.0 mmol) was mixed with solid 1,4-butanediamine (1.763, 20.0 mmol) in DMSO (2 mL). The mixture was stirred at 70 °C overnight. Water (30 mL)

was added to the reaction mixture at room temperature. The precipitated solid was filtered, was washed with water and was dried under reduced pressure. **282** (0.405 g, 0.9 mmol, 90%) was obtained as pale yellow solid. $^1\text{H NMR}$ (400 MHz, $\text{DMSO-}d_6$) δ 9.85 (bs, 1H), 8.20 (s, 1H), 7.43 – 7.33 (m, 1H), 7.32 – 7.16 (m, 3H), 5.85 (s, 1H), 3.19 – 3.14 (m, 2H), 2.60 – 2.53 (m, 2H), 2.36 (s, 3H), 2.23 (s, 3H), 1.58 – 1.46 (m, 2H), 1.45 – 1.34 (m, 2H). $^{13}\text{C NMR}$ (101 MHz, $\text{DMSO-}d_6$) δ 165.3, 163.1, 162.8, 160.0, 140.8, 138.8, 133.6, 132.4, 129.0, 128.2, 127.0, 125.3, 48.6, 41.2, 30.2, 26.1, 25.4, 18.3 (2 pyrimidine carbon not visible). **HRMS** (ESI): calculated for $\text{C}_{20}\text{H}_{25}\text{ON}_7\text{ClS}$ [M+H] $^+$ 446.1524; found: 446.1517.

N-(2-Chloro-6-methylphenyl)-2-(2-methyl-6-(piperazin-1-yl)pyrimidin-4-ylamino)thiazole-5-carboxamide (283).

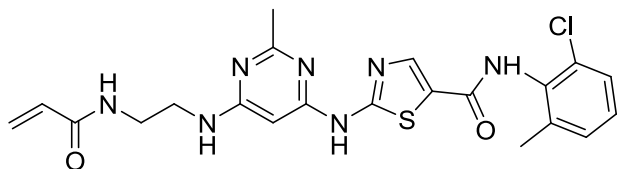


273 (0.200 g, 0.51 mmol) and piperazine (0.500 g, 5.80 mmol) were mixed in DMSO (1 mL) and stirred at 70 °C overnight. Water (20 mL) was added to the reaction mixture at room temperature. The precipitated solid was filtered, was washed with

water and was dried under reduced pressure. The product **283** (0.201 g, 0.45 mmol, 88%) was obtained as pale yellow solid. $^1\text{H NMR}$ (400 MHz, $\text{DMSO-}d_6$) δ 9.87 (bs, 1H), 8.22 (s, 1H), 7.46 – 7.19 (m, 3H), 6.02 (s, 1H), 3.49 – 3.40 (m, 4H), 2.81 – 2.68 (m, 4H), 2.40 (s, 3H), 2.24 (s, 3H). $^{13}\text{C NMR}$ (101 MHz, $\text{DMSO-}d_6$) δ 165.1, 162.6, 162.5, 159.9, 156.9, 140.8, 138.8, 133.5, 132.4, 129.0, 128.2, 127.0, 125.6, 82.4, 45.3, 44.8, 25.6, 18.3. **HRMS** (ESI): calculated for $\text{C}_{20}\text{H}_{23}\text{ON}_7\text{ClS}$ [M+H] $^+$ 444.1368; found: 444.1370.

11.3.3 Final compounds

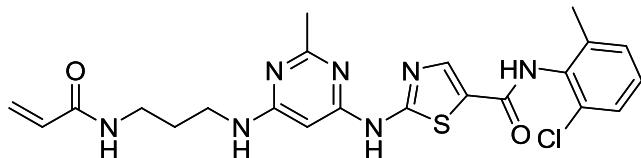
2-(6-(2-Acrylamidoethylamino)-2-methylpyrimidin-4-ylamino)-N-(2-chloro-6-methylphenyl)thiazole-5-carboxamide (284). **280** (0.104 g, 0.25 mmol) and K_2CO_3 (0.069g,



0.5 mmol) were mixed in dry DMF (2 mL). A solution of acryloyl chloride (0.020 mL, 0.25 mmol) in dry DMF (1 mL) was added dropwise (over 10 min) at $-40\text{ }^\circ\text{C}$. The reaction mixture was stirred at room

temperature for 4 h. The reaction was stopped by addition of 0.1 M AcOH (20 mL). The precipitated solid was filtrated and was washed with water. The crude product was purified by reverse phase chromatography (MeCN:H₂O). The product **284** (0.031 g, 0.066 mmol, 26%) was obtained as a white solid. **¹H NMR** (400 MHz, DMSO-*d*₆) δ 11.36 (s, 1H), 9.85 (s, 1H), 8.26 – 8.14 (m, 2H), 7.44 – 7.20 (m, 5H), 6.25 – 6.02 (m, 2H), 5.88 (s, 1H), 5.59 (dd, $J = 10.0, 2.4$ Hz, 1H), 3.33 – 3.26 (m, 4H), 2.37 (s, 3H), 2.24 (s, 3H). **¹³C NMR** (101 MHz, DMSO-*d*₆) δ 165.4, 164.9, 163.0, 162.8, 160.0, 140.9, 138.8, 133.5, 132.4, 131.8, 129.0, 128.2, 127.0, 125.4, 125.1, 38.4, 38.3, 25.5, 18.3 (2 pyrimidine carbon not visible). **HRMS** (ESI): calculated for C₂₁H₂₃O₂N₇ClS [M+H]⁺ 472.1317; found: 472.1315.

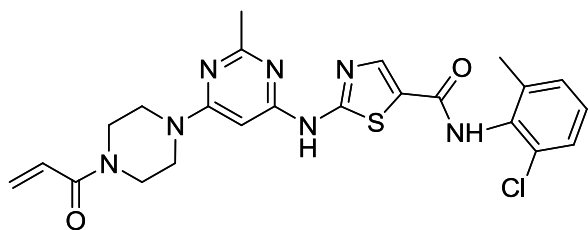
2-(6-(3-Acrylamidopropylamino)-2-methylpyrimidin-4-ylamino)-N-(2-chloro-6-methylphenyl)thiazole-5-carboxamide (285). **281** (0.108 g, 0.25 mmol) and



K_2CO_3 (0.069g, 0.5 mmol) were mixed in dry DMF (2 mL). A solution of acryloyl chloride (0.020 mL, 0.25 mmol) in dry

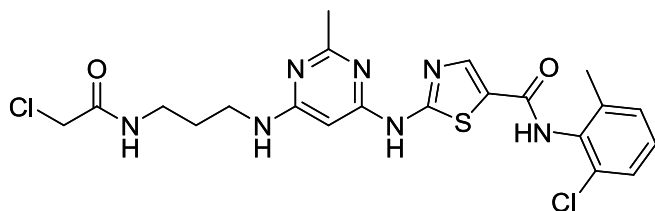
DMF (1 mL) was added dropwise (over 10 min) at $-40\text{ }^\circ\text{C}$. The reaction mixture was stirred at room temperature for 4 h. The reaction was stopped by addition of 0.1 M AcOH (20 mL). The precipitated solid was filtrated and was washed with water. The crude product was purified by reverse phase chromatography (MeCN:H₂O). The product **285** (0.050 g, 0.10 mmol, 40%) was obtained as a white solid. **¹H NMR** (400 MHz, DMSO-*d*₆) δ 11.34 (bs, 1H), 9.85 (s, 1H), 8.20 (s, 1H), 8.11 (t, $J = 5.6$ Hz, 1H), 7.40 (dd, $J = 7.4, 2.0$ Hz, 1H), 7.33 – 7.09 (m, 3H), 6.29 – 6.15 (m, 1H), 6.12 – 5.99 (m, 1H), 5.86 (s, 1H), 5.58 (dd, $J = 10.1, 2.3$ Hz, 1H), 3.31 – 3.04 (m, 4H), 2.36 (s, 3H), 2.24 (s, 3H), 1.68 (p, $J = 6.9$ Hz, 2H). **¹³C NMR** (101 MHz, DMSO-*d*₆) δ 165.3, 164.6, 163.0, 162.8, 160.0, 140.9, 138.8, 133.6, 132.4, 131.8, 129.0, 128.1, 127.0, 125.4, 124.9, 38.1, 36.4, 25.4, 18.3 (2 pyrimidine carbon not visible, 1 CH₂ behind solvent). **HRMS** (ESI): calculated for C₂₂H₂₅O₂N₇ClS [M+H]⁺ 486.1473; found: 486.1474.

2-(6-(4-acryloylpiperazin-1-yl)-2-methylpyrimidin-4-ylamino)-N-(2-chloro-6-methylphenyl)thiazole-5-carboxamide (**286**). **283** (0.111 g, 0.25 mmol) and K₂CO₃ (0.069g, 0.5 mmol) were mixed in dry DMF (2 mL). A solution of acryloyl chloride (0.020 mL, 0.25 mmol) in dry DMF (0.5 mL) was added dropwise (over



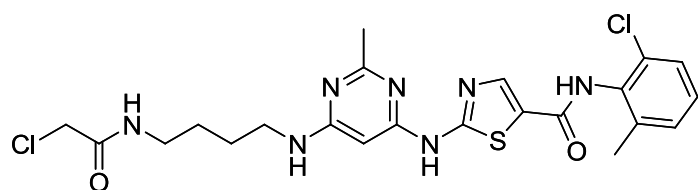
10 min) at -40 °C. After completion, the reaction mixture was stirred at room temperature for 4 h. The reaction mixture was stirred at room temperature for 4 h. The reaction was stopped by addition of 0.1 M AcOH (20 mL). The precipitated solid was filtrated and was washed with water. The crude product was purified by reverse phase chromatography (MeCN:H₂O). The product **286** (0.040 g, 0.080 mmol, 32%) was obtained as a white solid. ¹H NMR (400 MHz, DMSO-*d*₆) δ 11.52 (s, 1H), 9.88 (s, 1H), 8.23 (s, 1H), 7.40 (dd, *J* = 7.5, 2.0 Hz, 1H), 7.33 – 7.21 (m, 2H), 6.83 (dd, *J* = 16.7, 10.5 Hz, 1H), 6.16 (dd, *J* = 16.7, 2.4 Hz, 1H), 6.07 (s, 1H), 5.73 (dd, *J* = 10.4, 2.4 Hz, 1H), 3.71 – 3.61 (m, 4H), 3.61 – 3.56 (m, 4H), 2.43 (s, 3H), 2.24 (s, 3H). ¹³C NMR (101 MHz, DMSO-*d*₆) δ 165.2, 164.4, 162.5, 162.2, 159.9, 157.0, 140.8, 138.8, 133.5, 132.4, 129.0, 128.2, 128.1, 127.7, 127.0, 125.8, 82.8, 44.4, 43.7, 43.2, 40.9, 25.6, 18.3. HRMS (ESI): calculated for C₂₃H₂₅O₂N₇ClS [M+H]⁺ 498.1473; found: 498.1473.

N-(2-chloro-6-methylphenyl)-2-(6-(3-(2-chloroacetamido)propylamino)-2-methylpyrimidin-4-ylamino)thiazole-5-carboxamide (**287**). **281** (0.108 g, 0.25 mmol) and K₂CO₃ (0.035g, 0.25 mmol) were mixed in dry DMF (2 mL). A solution of chloroacetyl chloride (0.020 mL, 0.25 mmol) in DMF (1 mL)



was added dropwise (over 10 min) at -40 °C. The reaction mixture was stirred at room temperature for 2 h. The reaction was stopped by addition of 0.1 M AcOH (20 mL). The precipitated solid was filtrated and was washed with water. The crude product was purified by reverse phase chromatography (MeCN:H₂O). The product **287** (0.050 g, 0.093 mmol, 37%) was obtained as a white solid. ¹H NMR (400 MHz, DMSO-*d*₆) δ 11.39 (s, 1H), 9.85 (s, 1H), 8.28 – 8.14 (m, 2H), 7.40 (dd, *J* = 7.6, 1.9 Hz, 1H), 7.30 – 7.09 (m, 3H), 5.86 (s, 1H), 4.06 (s, 2H), 3.31 – 3.07 (m, 4H), 2.37 (s, 3H), 2.24 (s, 3H), 1.67 (p, *J* = 6.8 Hz, 2H). ¹³C NMR (101 MHz, DMSO) δ 165.9, 165.4, 163.1, 162.8, 160.0, 140.9, 138.8, 133.6, 132.4, 129.0, 128.2, 127.0, 125.4, 42.7, 37.9, 36.8, 28.7, 25.4, 18.3 (2 pyrimidine signals not visible). HRMS (ESI): calculated for C₂₁H₂₄O₂N₇Cl₂S [M+H]⁺ 508.1084; found: 508.1088.

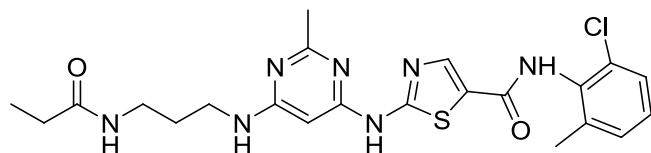
***N*-(2-chloro-6-methylphenyl)-2-(6-(4-(2-chloroacetamido)butylamino)-2-methylpyrimidin-4-ylamino)thiazole-5-carboxamide (288).**



To a suspension of **282** (0.100 g, 0.22 mmol) and K_2CO_3 (0.062 g, 0.45 mmol) were mixed in dry DMF (1 mL). A solution of chloroacetyl chloride (0.018 mL, 0.22 mmol) in DMF (0.5 mL) was added dropwise

(over 10 min) at $-40\text{ }^\circ\text{C}$. The reaction mixture was stirred at room temperature for 2 h. The reaction was stopped by addition of 0.1 M AcOH (10 mL). The precipitated solid was filtrated and was washed with water. The crude product was purified by reverse phase chromatography (MeCN:H₂O). The product **288** (0.044 g, 0.084 mmol, 38%) was obtained as a white solid. **¹H NMR** (400 MHz, DMSO-*d*₆) δ 11.36 (s, 1H), 9.85 (s, 1H), 8.32 – 8.08 (m, 2H), 7.48 – 7.07 (m, 4H), 5.85 (s, 1H), 4.03 (s, 2H), 3.30 – 3.01 (m, 4H), 2.36 (s, 3H), 2.24 (s, 3H), 1.62 – 1.33 (m, 4H). **¹³C NMR** (101 MHz, DMSO-*d*₆) δ 165.8, 165.3, 163.1, 162.8, 160.0, 140.9, 138.8, 133.6, 132.4, 129.0, 128.2, 127.0, 125.4, 42.7, 38.7, 26.4, 26.4, 25.5, 18.3 (1CH₂ group and 2 pyrimidine carbons not visible). **HRMS** (ESI): calculated for C₂₂H₂₆O₂N₇Cl₂S [M+H]⁺ 522.1240; found: 522.1240.

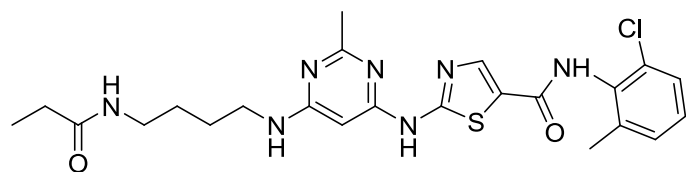
***N*-(2-chloro-6-methylphenyl)-2-(2-methyl-6-(3-propionamidopropylamino)pyrimidin-4-ylamino)thiazole-5-carboxamide (289).**



281 (0.130 g, 0.30 mmol) and K_2CO_3 (0.081 g, 0.60 mmol) were mixed in dry DMF (2 mL). A solution of propionic anhydride (0.039 g, 0.30 mmol) in dry

DMF (0.5 mL) was added dropwise (over 10 min) at $-40\text{ }^\circ\text{C}$. The reaction mixture was stirred at room temperature for 2 h. The reaction was stopped by addition of 0.1 M AcOH (20 mL). The precipitated solid was filtrated and was washed with water. The crude product was purified by reverse phase chromatography (MeCN:H₂O). The product **289** (0.026 g, 0.053 mmol, 18%) was afforded as a white solid. **¹H NMR** (400 MHz, DMSO-*d*₆) δ 11.38 (s, 1H), 9.85 (s, 1H), 8.20 (s, 1H), 7.75 (bs, 1H), 7.40 (dd, $J = 7.6, 2.0$ Hz, 1H), 7.33 – 7.21 (m, 2H), 7.16 (bs, 1H), 5.86 (s, 1H), 3.28 – 3.15 (m, 2H), 3.09 (q, $J = 6.6$ Hz, 2H), 2.37 (s, 3H), 2.24 (s, 3H), 2.07 (q, $J = 7.6$ Hz, 2H), 1.63 (p, $J = 7.0$ Hz, 2H), 0.99 (t, $J = 7.6$ Hz, 3H). **¹³C NMR** (101 MHz, DMSO-*d*₆) δ 172.8, 165.3, 163.0, 162.8, 160.0, 140.9, 138.8, 133.6, 132.5, 129.0, 128.2, 127.0, 125.4, 38.2, 36.3, 28.9, 28.5, 25.4, 18.3, 10.0. (2 pyrimidine carbon not visible) **HRMS** (ESI): calculated for C₂₂H₂₇O₂N₇ClS [M+H]⁺ 488.1630; found: 488.1630.

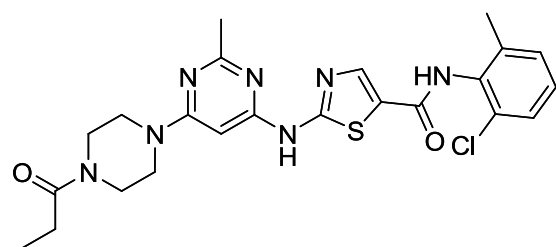
***N*-(2-chloro-6-methylphenyl)-2-(2-methyl-6-(4-propionamidobutylamino)pyrimidin-4-ylamino)thiazole-5-carboxamide**



(290). 282 (0.062 g, 0.14 mmol) and K_2CO_3 (0.019 g, 0.14 mmol) were mixed in dry DMF (1 mL). Propionic

anhydride (0.018 mL, 0.14 mmol) was added at 0 °C. The reaction mixture was stirred at room temperature for 24 h. The reaction was stopped by addition of 0.1 M AcOH (10 mL). The precipitated solid was filtrated and was washed with water. The product **290** (0.062 g, 0.12 mmol, 88%) was obtained as a pale yellow solid. 1H NMR (400 MHz, DMSO- d_6) δ 11.34 (bs, 1H), 9.85 (s, 1H), 8.19 (d, $J = 7.2$ Hz, 1H), 7.72 (t, $J = 5.6$ Hz, 1H), 7.40 (dd, $J = 7.5, 2.0$ Hz, 1H), 7.32 – 7.13 (m, 3H), 5.85 (s, 1H), 3.26 – 3.12 (m, 2H), 3.14 (d, $J = 23.8$ Hz, 2H), 3.05 (q, $J = 6.4$ Hz, 2H), 2.36 (s, 3H), 2.24 (s, 3H), 2.05 (q, $J = 7.6$ Hz, 2H), 1.54 – 1.37 (m, 4H), 0.98 (t, $J = 7.6$ Hz, 3H). ^{13}C NMR (101 MHz, DMSO- d_6) δ 172.7, 165.3, 163.1, 162.8, 160.0, 140.8, 138.8, 133.6, 132.4, 129.0, 128.2, 127.0, 125.4, 38.2, 28.5, 26.7, 26.7, 25.4, 18.3, 10.0 (2 pyrimidine carbon not visible, 1 CH_2 behind solvent). HRMS (ESI): calculated for $C_{23}H_{29}O_2N_7ClS$ $[M+H]^+$ 502.1786; found: 502.1786.

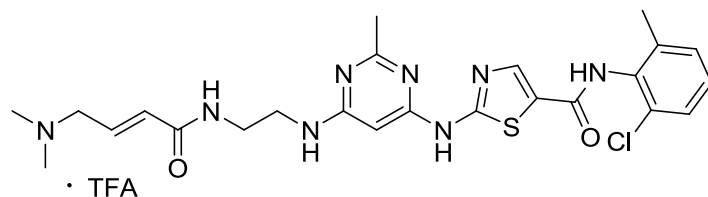
***N*-(2-chloro-6-methylphenyl)-2-(2-methyl-6-(4-propionylpiperazin-1-yl)pyrimidin-4-ylamino)thiazole-5-carboxamide** (291). 283



(0.062 g, 0.14 mmol) and K_2CO_3 (0.019 g, 0.14 mmol) were mixed in dry DMF (1 mL). The mixture was cooled to 0 °C. Propionic anhydride (0.018 mL, 0.14 mmol) was added. The reaction mixture was stirred at room temperature for 24 h. The reaction was stopped by addition of 0.1 M AcOH (10 mL). The

precipitated solid was filtrated and was washed with water. The product **291** (0.070 g, 0.14 mmol, quant.) was obtained as a white solid. 1H NMR (400 MHz, DMSO- d_6) δ 11.52 (s, 1H), 9.89 (s, 1H), 8.23 (s, 1H), 7.41 (dd, $J = 7.5, 2.0$ Hz, 1H), 7.33 – 7.22 (m, 2H), 6.07 (s, 1H), 3.64 – 3.49 (m, 8H), 2.43 (s, 3H), 2.36 (q, $J = 7.4$ Hz, 2H), 2.25 (s, 3H), 1.01 (t, $J = 7.4$ Hz, 3H). ^{13}C NMR (101 MHz, DMSO- d_6) δ 171.6, 165.2, 162.5, 162.2, 159.9, 157.0, 140.8, 138.8, 133.5, 132.4, 129.0, 128.2, 127.0, 125.8, 82.8, 44.0, 43.5, 43.2, 40.5, 25.6, 25.6, 18.3, 9.3. HRMS (ESI): calculated for $C_{23}H_{26}O_2N_7ClNaS$ $[M+H]^+$ 522.1449; found: 522.1448.

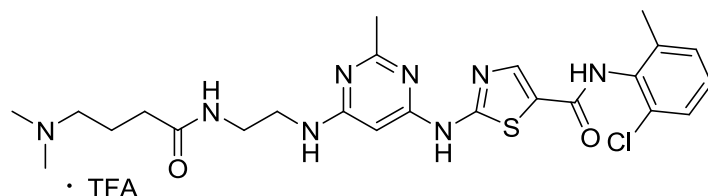
(E)-N-(2-chloro-6-methylphenyl)-2-(6-(2-(4-(dimethylamino)but-2-enamido)ethylamino)-2-methylpyrimidin-4-ylamino)thiazole-5-carboxamide TFA salt



(292). 4-dimethylamino crotonic acid hydrochloride (0.028 g, 0.17 mmol), HBTU (0.064 g, 0.17 mmol) and DIPEA (0.073 mL, 0.42 mmol) were mixed in dry DMF (1 mL) at 0 °C. **280** (0.058 g, 0.14 mmol) was

added after 5 minutes and the reaction mixture was stirred at room temperature for 2 h. The reaction was stopped by addition of water (10 mL). The precipitated solid was filtrated and was washed with water. The crude product was purified by reverse phase chromatography (MeCN:H₂O with 0.1% TFA). **292** (0.043 g, 0.067 mmol, 48%) was afforded as a white solid. ¹H NMR (400 MHz, DMSO-*d*₆) δ 11.63 (bs, 1H), 9.92 (s, 2H), 8.45 (s, 1H), 8.23 (s, 1H), 7.65 (bs, 1H), 7.43 – 7.37 (m, 1H), 7.33 – 7.21 (m, 2H), 6.64 – 6.52 (m, 1H), 6.28 – 6.19 (m, 1H), 6.00 (s, 1H), 3.87 (d, *J* = 6.0 Hz, 2H), 3.48 – 3.24 (m, 4H), 2.76 (s, 6H), 2.42 (s, 3H), 2.24 (s, 3H). ¹³C NMR (101 MHz DMSO-*d*₆) δ 163.7, 162.5, 158.3 (q, 34 Hz), 157.8, 140.7, 138.8, 133.4, 132.4, 131.9, 130.1, 129.0, 128.2, 127.0, 125.9, 120.7, 116.3 (q, 295 Hz), 56.7, 41.9, 38.4, 38.2, 24.7, 18.3. (2 pyrimidine carbon and thiazol carbon not visible). HRMS (ESI): calculated for C₂₄H₃₀O₂N₈ClS [M+H]⁺ 529.1895; found: 529.1889.

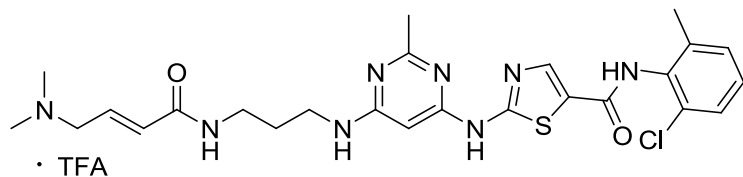
N-(2-chloro-6-methylphenyl)-2-(6-(2-(4-(dimethylamino)butanamido)ethylamino)-2-methylpyrimidin-4-ylamino)thiazole-5-carboxamide TFA salt (296)



(4-(dimethylamino)butyric acid hydrochloride (0.028 g, 0.17 mmol), HBTU (0.064 g, 0.17 mmol) and DIPEA (0.073 mL, 0.42 mmol) were mixed in dry DMF (1 mL) at 0 °C. **280** (0.058 g, 0.14 mmol) was

added after 5 minutes and the reaction mixture was stirred at room temperature for 2 h. The reaction was stopped by addition of water (10 mL). The precipitated solid was filtrated and was washed with water. The crude product was purified by reverse phase chromatography (MeCN:H₂O with 0.1% TFA). **296** (0.043 g, 0.067 mmol, 48%) was afforded as a white solid. ¹H NMR (400 MHz, DMSO-*d*₆) δ 11.62 (bs, 1H), 9.93 (s, 1H), 9.67 (bs, 1H), 8.24 (s, 1H), 8.13 (bs, 1H), 7.40 (dd, *J* = 7.4, 2.0 Hz, 1H), 7.33 – 7.22 (m, 2H), 6.03 (s, 1H), 3.39 – 3.20 (m, 4H), 3.08 – 2.94 (m, 2H), 2.77 (d, *J* = 4.7 Hz, 6H), 2.44 (s, 3H), 2.24 (s, 3H), 2.17 (t, *J* = 7.2 Hz, 2H), 1.83 (p, *J* = 7.3 Hz, 2H). ¹³C NMR (101 MHz, DMSO-*d*₆) δ 171.3, 162.6, 159.8, 140.8, 138.8, 133.4, 132.4, 129.1, 128.2, 127.0, 116.3 (q, 295 Hz), 56.4, 42.2, 38.2, 31.8, 24.2, 19.9, 18.3 (1 carbon of TFA, 1 thiazole and 4 pyrimidine carbons not visible, 1 CH₂ group behind solvent). HRMS (ESI): calculated for C₂₄H₃₂O₂N₈ClS [M+H]⁺ 531.2052; found: 531.2047.

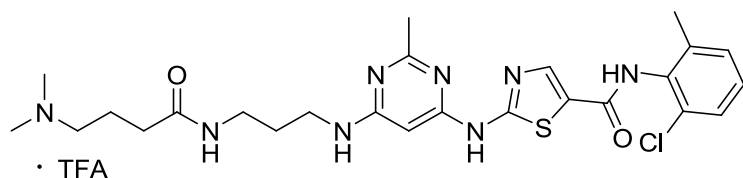
(E)-N-(2-chloro-6-methylphenyl)-2-(6-(3-(4-(dimethylamino)but-2-enamido)propylamino)-2-methylpyrimidin-4-ylamino)thiazole-5-carboxamide TFA salt



(293). 4-dimethylamino crotonic acid hydrochloride (0.028 g, 0.17 mmol), HBTU (0.064 g, 0.17 mmol) and DIPEA (0.073 mL, 0.42 mmol) were mixed in dry

DMF (1 mL) at 0 °C. **281** (0.058 g, 0.14 mmol) was added after 5 minutes and the reaction mixture was stirred at room temperature for 2 h. The reaction was stopped by addition of water (10 mL). The precipitated solid was filtrated and was washed with water. The crude product was purified by reverse phase chromatography (MeCN:H₂O with 0.1% TFA). **293** (0.064 g, 0.097 mmol, 70%) was afforded as a white solid. **¹H NMR** (400 MHz, DMSO-*d*₆) δ 11.72 (bs, 1H), 10.09 – 9.86 (m, 2H), 8.36 (t, *J* = 5.6 Hz, 1H), 8.24 (s, 1H), 7.40 (dd, *J* = 7.5, 2.0 Hz, 1H), 7.34 – 7.17 (m, 2H), 6.57 (dt, *J* = 14.8, 7.2 Hz, 1H), 6.30 – 6.20 (m, 1H), 6.12 – 5.95 (m, 1H), 3.87 (d, *J* = 7.2 Hz, 2H), 3.37 – 3.13 (m, 4H), 2.76 (s, 6H), 2.44 (s, 3H), 2.24 (s, 3H), 1.73 (q, *J* = 7.0 Hz, 2H). **¹³C NMR** (101 MHz, DMSO-*d*₆) δ 163.5, 162.5, 159.7, 158.5 (q, 34 Hz), 140.8, 138.8, 133.4, 132.4, 132.1, 129.9, 129.1, 128.3, 127.0, 116.4 (q, 295 Hz), 56.8, 41.9, 36.4, 28.5, 23.9, 18.3 (3 pyrimidine and 2 thiazole carbon not visible, 1 CH₂ behind solvent). **HRMS** (ESI): calculated for C₂₅H₃₂O₂N₈ClS [M+H]⁺ 543.2063; found: 543.2051.

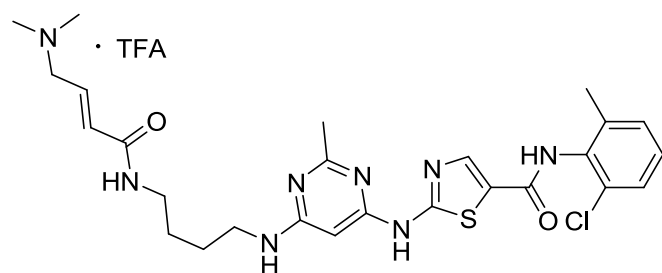
N-(2-chloro-6-methylphenyl)-2-(6-(3-(4-(dimethylamino)butanamido)propylamino)-2-methylpyrimidin-4-ylamino)thiazole-5-carboxamide TFA salt (297).



(4-(dimethylamino)butyric acid hydrochloride (0.020 g, 0.12 mmol), HBTU (0.046 g, 0.12 mmol) and DIPEA (0.052 mL, 0.30 mmol) were mixed in dry

DMF (1 mL) at 0 °C. **281** (0.043 g, 0.10 mmol) was added after 5 minutes and the reaction mixture was stirred at room temperature overnight. The reaction was stopped by addition of water (10 mL). The precipitated solid was filtrated and was washed with water. The crude product was purified by reverse phase chromatography (MeCN:H₂O with 0.1% TFA). **297** (0.048 g, 0.073 mmol, 73%) was afforded as a white solid. **¹H NMR** (400 MHz, DMSO-*d*₆) δ 11.75 (bs, 1H), 9.95 (s, 1H), 9.66 (bs, 1H), 8.25 (s, 1H), 8.02 (t, *J* = 5.5 Hz, 1H), 7.40 (dd, *J* = 7.5, 2.0 Hz, 1H), 7.37 – 7.17 (m, 2H), 6.04 (s, 1H), 3.34 – 3.17 (m, 3H), 3.13 (q, *J* = 6.6 Hz, 2H), 3.07 – 2.98 (m, 2H), 2.77 (d, *J* = 4.6 Hz, 6H), 2.45 (s, 3H), 2.24 (s, 3H), 2.18 (t, *J* = 7.2 Hz, 2H), 1.90 – 1.77 (m, 2H), 1.68 (p, *J* = 7.2 Hz, 2H). **¹³C NMR** (101 MHz, DMSO-*d*₆) δ 171.0, 162.6, 162.4, 159.7, 158.5 (q, 34 Hz), 140.8, 138.8, 133.4, 132.4, 129.1, 128.3, 127.0, 116.3 (q, 295 Hz), 56.4, 42.2, 36.3, 31.9, 28.5, 20.0, 18.3. CH₃-group of pyrimidine-, 3 pyrimidine carbon-, 1 thiazole carbon not visible 1 CH₂-group behind solvent). **HRMS** (ESI): calculated for C₂₅H₃₄O₂N₈ClS [M+H]⁺ 545.2214; found: 545.2190.

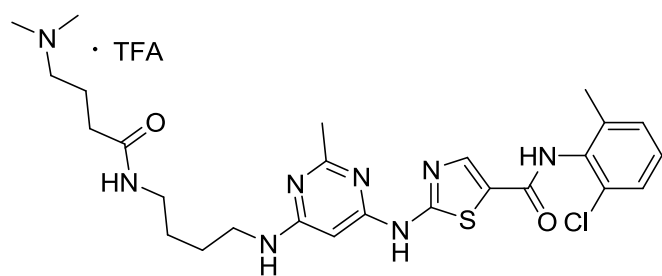
(E)-N-(2-chloro-6-methylphenyl)-2-(6-(4-(4-(dimethylamino)but-2-enamido)butylamino)-2-methylpyrimidin-4-ylamino)thiazole-5-carboxamide TFA salt



(294). 4-dimethylamino crotonic acid hydrochloride (0.028 g, 0.17 mmol), HBTU (0.064 g, 0.17 mmol) and DIPEA (0.073 mL, 0.42 mmol) were mixed in dry DMF (1 mL) at 0 °C. **282** (0.062 g, 0.14 mmol) was added after 5 minutes and the reaction mixture was

stirred at room temperature for 2 h. The reaction was stopped by addition of water (10 mL). The precipitated solid was filtrated and was washed with water. The crude product was purified by reverse phase chromatography (MeCN:H₂O with 0.1% TFA). **294** (0.024 g, 0.036 mmol, 26%) was afforded as a white solid. ¹H NMR (400 MHz, DMSO-*d*₆) δ 11.71 (bs, 1H), 9.94 (s, 2H), 8.31 (t, *J* = 5.7 Hz, 1H), 8.24 (s, 1H), 7.40 (dd, *J* = 7.4, 2.0 Hz, 1H), 7.33 – 7.22 (m, 2H), 6.62 – 6.50 (m, 1H), 6.29 – 6.20 (m, 1H), 6.03 (s, 1H), 3.86 (d, *J* = 7.1 Hz, 2H), 3.34 – 3.10 (m, 4H), 2.76 (s, 6H), 2.44 (s, 3H), 2.24 (s, 3H), 1.57 – 1.45 (m, 4H). ¹³C NMR (101 MHz, DMSO-*d*₆) δ 163.3, 159.7, 158.4 (q, 34 Hz), 140.8, 138.8, 133.4, 132.4, 132.1, 129.7, 129.0, 128.2, 127.0, 116.3 (q, 295 Hz), 56.8, 41.9, 38.3, 26.5, 25.9, 18.3 (4 pyrimidine and 2 thiazole carbons, pyrimidine CH₃ and 1 CH₂ group not visible). HRMS (ESI): calculated for C₂₆H₃₄O₂N₈ClS [M+H]⁺557.2208; found:557.3304.

N-(2-chloro-6-methylphenyl)-2-(6-(4-(4-(dimethylamino)butanamido)butylamino)-2-methylpyrimidin-4-ylamino)thiazole-5-carboxamide TFA salt (298)

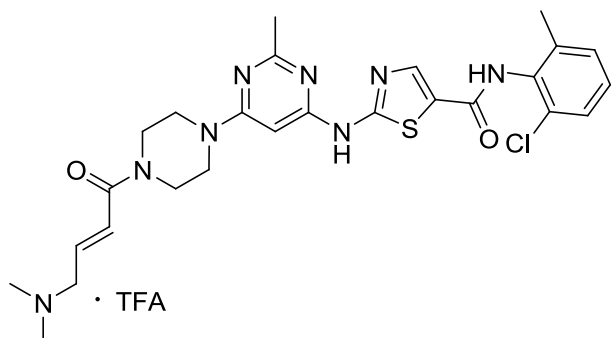


(298). (4-(dimethylamino)butyric acid hydrochloride (0.022 g, 0.13 mmol), HBTU (0.049 g, 0.13 mmol) and DIPEA (0.057 mL, 0.33 mmol) were mixed in ry DMF (1 mL) at 0 °C. **282** (0.050 g, 0.11 mmol) was added after 5

minutes and the reaction mixture was stirred at room temperature overnight. The reaction was stopped by addition of water (10 mL). The precipitated solid was filtrated and was washed with water. The crude product was purified by reverse phase chromatography (MeCN:H₂O with 0.1% TFA). **298** (0.024 g, 0.036 mmol, 32%) was afforded as a white solid. ¹H NMR (400 MHz, DMSO-*d*₆) δ 11.85 (bs, 1H), 9.98 (s, 1H), 9.72 (bs, 1H), 8.26 (s, 1H), 7.99 (t, *J* = 5.6 Hz, 1H), 7.39 (dd, *J* = 7.5, 2.0 Hz, 1H), 7.33 – 7.21 (m, 2H), 6.11 (s, 1H), 3.24 (s, 2H), 3.13 – 2.96 (m, 4H), 2.76 (d, *J* = 4.5 Hz, 6H), 2.47 (s, 3H), 2.23 (s, 3H), 2.16 (t, *J* = 7.2 Hz, 2H), 1.89 – 1.73 (m, 2H), 1.62 – 1.36 (m, 4H). ¹³C NMR (101 MHz, DMSO-*d*₆) δ 170.9, 159.6, 158.7 (q, 34 Hz) 140.7, 138.8, 133.4, 132.4, 129.1, 128.3, 127.0, 116.3 (q, 295 Hz), 56.5, 42.2, 38.2, 31.9, 26.5, 26.5, 20.0, 18.3 (CH₃ and 3 pyrimidine and 2 thiazole carbon not

detectable, 2 CH₂ group behind solvent). **HRMS** (ESI): calculated for C₂₆H₃₆O₂N₈ClS [M+H]⁺ 559.2365; found: 559.2368.

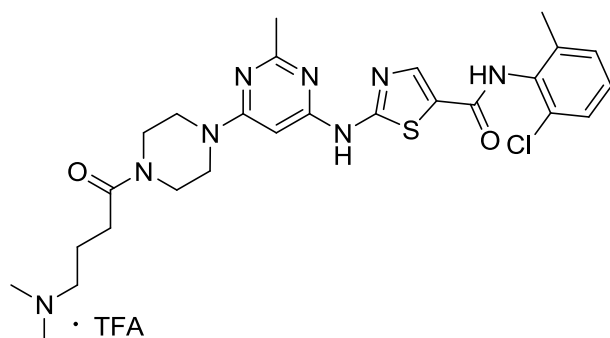
(E)-N-(2-chloro-6-methylphenyl)-2-(6-(4-(4-(dimethylamino)but-2-enoyl)piperazin-1-yl)-2-methylpyrimidin-4-ylamino)thiazole-5-carboxamide TFA salt (295).



4-dimethylamino crotonic acid hydrochloride (0.028 g, 0.17 mmol), HBTU (0.064 g, 0.17 mmol) and DIPEA (0.073 mL, 0.42 mmol) were mixed in dry DMF (1 mL) at 0 °C. **283** (0.062 g, 0.14 mmol) was added after 5 minutes and the reaction mixture was stirred at room temperature for 2 h. The reaction was

stopped by addition of water (10 mL). The precipitated solid was filtrated and was washed with water. The crude product was purified by reverse phase chromatography (MeCN:H₂O with 0.1% TFA). **295** (0.058 g, 0.087 mmol, 62%) was afforded as a white solid. ¹H NMR (400 MHz, DMSO-*d*₆) δ 11.57 (s, 1H), 10.05 (s, 1H), 9.90 (s, 1H), 8.23 (s, 1H), 7.43 – 7.36 (m, 1H), 7.33 – 7.21 (m, 2H), 6.97 – 6.89 (m, 1H), 6.68 – 6.58 (m, 1H), 6.11 (s, 1H), 3.90 (d, *J* = 7.0 Hz, 2H), 3.77 – 3.52 (m, 8H), 2.79 (s, 6H), 2.43 (s, 3H), 2.24 (s, 3H). ¹³C NMR (101 MHz, DMSO-*d*₆) δ 165.2, 163.2, 162.5, 162.1, 159.9, 153.3 (q, 35 Hz), 157.0, 140.8, 138.8, 133.5, 132.4, 132.2, 129.1, 128.9, 128.2, 127.0, 125.8, 116.2 (q, 295 Hz), 82.9, 57.1, 44.5, 43.6, 43.2, 42.1, 41.0, 25.5, 18.3. **HRMS** (ESI): calculated for C₂₆H₃₂O₂N₈ClS [M+H]⁺ 555.2052; found: 555.2059.

N-(2-chloro-6-methylphenyl)-2-(6-(4-(4-(dimethylamino)butanoyl)piperazin-1-yl)-2-methylpyrimidin-4-ylamino)thiazole-5-carboxamide TFA salt (299).

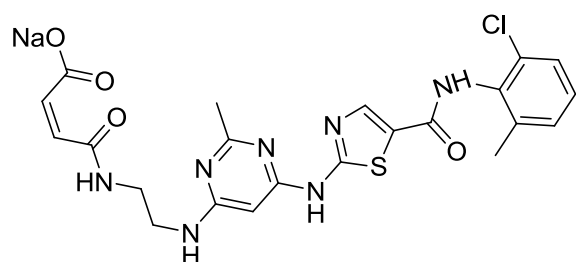


(4-(dimethylamino)butyric acid hydrochloride (0.025 g, 0.15 mmol), HBTU (0.057 g, 0.15 mmol) and DIPEA (0.070 mL, 0.40 mmol) were mixed in dry DMF (1 mL) at 0 °C. **283** (0.044 g, 0.10 mmol) was added after 5 minutes and the reaction mixture was stirred at room temperature overnight. The

reaction was stopped by addition of water (10 mL). The precipitated solid was filtrated and was washed with water. The crude product was purified by reverse phase chromatography (MeCN:H₂O with 0.1% TFA). **299** (0.035 g, 0.052 mmol, 52%) was afforded as a white solid. ¹H NMR (400 MHz, DMSO-*d*₆) δ 11.55 (bs, 1H), 9.90 (s, 1H), 9.59 (bs, 1H), 8.23 (s, 1H), 7.43 – 7.36 (m, 1H), 7.33 – 7.21 (m, 2H), 6.09 (s, 1H), 3.70 – 3.47 (m, 8H), 3.11 – 3.02 (m,

2H), 2.79 (d, $J = 4.8$ Hz, 6H), 2.49 – 2.36 (m, 5H), 2.24 (s, 3H), 1.86 (p, $J = 7.0$ Hz, 2H). ^{13}C NMR (101 MHz, DMSO- d_6) δ 169.8, 165.1, 162.5, 162.2, 159.9, 158.3 (q, 35 Hz), 157.0, 140.8, 138.8, 133.5, 132.4, 129.0, 128.2, 127.0, 125.8, 116.2 (q, 295 Hz), 82.8, 56.5, 44.0, 43.4, 43.2, 42.2, 40.6, 29.1, 25.5, 19.5, 18.3. HRMS (ESI): calculated for $\text{C}_{26}\text{H}_{34}\text{O}_2\text{N}_8\text{ClS}$ $[\text{M}+\text{H}]^+$ 557.2208; found: 557.2206.

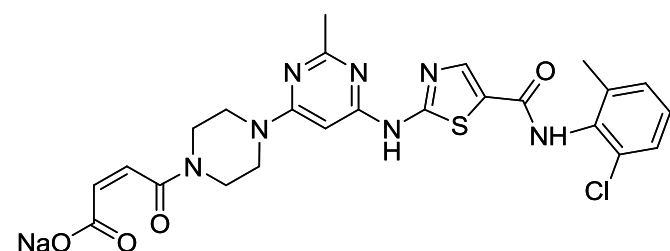
Sodium (Z)-4-(3-(6-(5-(2-chloro-6-methylphenylcarbamoyl)thiazol-2-ylamino)-2-



methylpyrimidin-4-ylamino)propylamino)-4-oxobut-2-enoate (300). 281 (0.065 g, 0.15 mmol) and Na_2CO_3 (0.048 g, 0.45 mmol) were mixed in dry DMF (1 mL). Maleic anhydride (0.014 g, 0.15 mmol) was added to the suspension at -40 °C. The reaction mixture was stirred at room temperature for 2 h. DCM and

Et_2O were added until precipitation occurred. The solid was filtrated and was washed with diethylether. The crude product was purified by reverse phase chromatography (MeCN: H_2O). The product **300** (0.035 g, 0.063 mmol, 42%) was afforded as a white solid. ^1H NMR (400 MHz DMSO- d_6) δ 11.27 (bs, 1H), 9.86 (s, 1H), 8.20 (s, 1H), 7.40 (dd, $J = 7.6, 2.0$ Hz, 1H), 7.32 – 7.22 (m, 2H), 7.14 (bs, 1H), 6.29 – 5.95 (m, 2H), 5.60 (d, $J = 13.1$ Hz, 1H), 3.24 – 3.12 (m, 4H), 2.36 (s, 3H), 2.24 (s, 3H), 1.69 – 1.57 (m, 2H). ^{13}C NMR (101 MHz, DMSO- d_6) δ 169.3, 165.7, 165.1, 163.0, 162.8, 160.1, 141.0, 138.9, 138.3, 138.3, 133.6, 132.5, 129.0, 128.1, 127.0, 125.2, 38.4, 35.8, 29.1, 25.3, 18.4. (2 pyrimidine carbon not visible). HRMS (ESI): calculated for $\text{C}_{23}\text{H}_{23}\text{O}_4\text{N}_7\text{ClS}$ $[\text{M}-\text{H}]^-$ 528.1226; found: 528.1221.

Sodium (Z)-4-(4-(6-(5-(2-chloro-6-methylphenylcarbamoyl)thiazol-2-ylamino)-2-



methylpyrimidin-4-yl)piperazin-1-yl)-4-oxobut-2-enoate (301). 283 (0.111 g, 0.25 mmol) and K_2CO_3 (0.069 g, 0.50 mmol) were mixed in dry DMF (1 mL). Maleic anhydride (0.024 g, 0.25 mmol) was added to the suspension at -25 °C. The reaction was stirred at room temperature for 2 h. 1 M HCl (15 mL) was added to the reaction mixture. The

precipitated solid was filtrated and was washed with water. Saturated Na_2CO_3 solution (1 mL) was added to the crude product and the mixture purified by reverse phase chromatography (MeCN: H_2O). The product **301** (0.026 g, 0.05 mmol, 18%) was obtained as a beige solid. ^1H NMR (400 MHz, DMSO- d_6) δ 9.80 (s, 1H), 8.18 (s, 1H), 7.38 (dd, $J = 7.7, 1.9$ Hz, 1H), 7.31 – 7.19 (m, 2H), 6.16 (s, 1H), 5.94 – 5.83 (m, 2H), 3.60 – 3.43 (m, 8H), 2.38 (s, 3H), 2.24 (s, 3H). ^{13}C NMR (101 MHz, DMSO- d_6) δ 169.1, 168.4, 164.7, 162.4, 160.3, 141.4, 138.9,

134.4, 133.9, 132.5, 129.0, 128.0, 127.1, 126.9, 84.3, 45.3, 43.7, 42.9, 25.7, 18.4. (1 CH₂ behind solvent, 3 aromatic carbons not visible). **HRMS** (ESI): calculated for C₂₄H₂₃O₄N₇ClS [M-H]⁻ 540.1226; found: 540.1221.

12. References

- (1) National Cancer Institute. About cancer. Understanding cancer. <https://www.cancer.gov/about-cancer/understanding> (accessed Dec 13, 2019).
- (2) World Health Organization. Newsroom/Fact sheets/Detail/Cancer. <https://www.who.int/en/news-room/fact-sheets/detail/cancer> (accessed Dec 13, 2019).
- (3) Krefregisteret "Cancer in Norway (2018); Cancer incidence, mortality, survival and prevalence in Norway," **2019**.
- (4) Steinhilber, D.; Schubert-Zsilavec, M.; Roth, H. J. *Medizinische Chemie; Targets und Arzneistoffe*; Deutscher Apotheker Verlag: Stuttgart, **2005**; Vol. 1.
- (5) Robertson, G. S.; LaCasse, E. C.; Holcik, M. In *Pharmacology*; Hacker, M., Messer, W., Bachmann, K., Eds.; Academic Press: San Diego, **2009**, p 455.
- (6) Bafico, A.; Grumolato, L.; Aaronson, S. A. In *The Molecular Basis of Cancer (Third Edition)*; Mendelsohn, J., Howley, P. M., Israel, M. A., Gray, J. W., Thompson, C. B., Eds.; W.B. Saunders: Philadelphia, **2008**, p 17.
- (7) Cooper GM. *The Cell: A Molecular Approach*. 2nd edition. Sunderland (MA): Sinauer Associates; **2000**. The Development and Causes of Cancer.
- (8) *Deutsches Krebsforschungszentrum. Krebsentstehung*. <https://www.krebsinformationsdienst.de/tumorarten/grundlagen/krebsentstehung.php> (accessed Dec 13, 2019).
- (9) Wu, S.; Zhu, W.; Thompson, P.; Hannun, Y. A. *Nature Communications* **2018**, *9*, 3490.
- (10) Croce, C. M. *New England Journal of Medicine* **2008**, *358*, 502.
- (11) Lodish H, B. A., Zipursky SL, et al. *Molecular Cell Biology*. 4th edition. New York: W. H. Freeman; **2000**. Section 24.2, Proto-Oncogenes and Tumor-Suppressor Genes.
- (12) Levine, A. J.; Hu, W.; Feng, Z. In *The Molecular Basis of Cancer (Third Edition)*; Mendelsohn, J., Howley, P. M., Israel, M. A., Gray, J. W., Thompson, C. B., Eds.; W.B. Saunders: Philadelphia, **2008**, p 31.
- (13) Aktories, K.; Förstermann, U.; Hofmann, F.; Starke, K. *Allgemeine und spezielle Pharmakologie und Toxikologie*; Urban und Fischer Verlag: Munich, **2009**; Vol. 10.
- (14) Basu, A. K. *Int J Mol Sci* **2018**, *19*, 970.
- (15) Fouad, Y. A.; Aanei, C. *Am J Cancer Res* **2017**, *7*, 1016.
- (16) Baskar, R.; Lee, K. A.; Yeo, R.; Yeoh, K.-W. *Int J Med Sci* **2012**, *9*, 193.
- (17) Santos, S. B.; Sousa Lobo, J. M.; Silva, A. C. *Drug Discovery Today* **2019**, *24*, 293.
- (18) American Cancer Society. Treatments and Side Effects. Learn about Treatments. <https://www.cancer.org/treatment/treatments-and-side-effects/treatment-types/surgery.html> (accessed Dez 13, 2019).
- (19) Mihlon, F. t.; Ray, C. E., Jr.; Messersmith, W. *Semin Intervent Radiol* **2010**, *27*, 384.
- (20) Bhullar, K. S.; Lagarón, N. O.; McGowan, E. M.; Parmar, I.; Jha, A.; Hubbard, B. P.; Rupasinghe, H. P. V. *Molecular Cancer* **2018**, *17*, 48.
- (21) Remesh, A. *2017* **2017**, *1*, 11.
- (22) Housman, G.; Byler, S.; Heerboth, S.; Lapinska, K.; Longacre, M.; Snyder, N.; Sarkar, S. *Cancers (Basel)* **2014**, *6*, 1769.
- (23) Alberts B, J. A., Lewis J, et al. *Molecular Biology of the Cell*. 4th edition. New York: Garland Science; 2002. The Structure and Function of DNA.
- (24) Lindahl, T. *Nature* **1993**, *362*, 709.
- (25) Pearl, L. H.; Savva, R. *Nature Structural Biology* **1996**, *3*, 485.

- (26) Scitable by nature Education. Discovery of DNA Structure and Function: Watson and Crick. <https://www.nature.com/scitable/topicpage/discovery-of-dna-structure-and-function-watson-397/> (accessed Dec 13, 2019).
- (27) Vértessy, B. G.; Tóth, J. *Accounts of Chemical Research* **2009**, *42*, 97.
- (28) Visnes, T.; Doseth, B.; Pettersen Henrik, S.; Hagen, L.; Sousa Mirta, M. L.; Akbari, M.; Otterlei, M.; Kavli, B.; Slupphaug, G.; Krokan Hans, E. *Philosophical Transactions of the Royal Society B: Biological Sciences* **2009**, *364*, 563.
- (29) Baldo, A. M.; McClure, M. A. *J Virol* **1999**, *73*, 7710.
- (30) Robert, D. L. *Current Protein & Peptide Science* **2001**, *2*, 361.
- (31) Krokan, H. E.; Drabløs, F.; Slupphaug, G. *Oncogene* **2002**, *21*, 8935.
- (32) Visnes, T.; Doseth, B.; Pettersen, H. S.; Hagen, L.; Sousa, M. M. L.; Akbari, M.; Otterlei, M.; Kavli, B.; Slupphaug, G.; Krokan, H. E. *Philos Trans R Soc Lond B Biol Sci* **2009**, *364*, 563.
- (33) Papamichael, D. *The Oncologist* **1999**, *4*, 478.
- (34) Wilson, P. M.; Danenberg, P. V.; Johnston, P. G.; Lenz, H.-J.; Ladner, R. D. *Nat Rev Clin Oncol* **2014**, *11*, 282.
- (35) Longley, D. B.; Harkin, D. P.; Johnston, P. G. *Nature Reviews Cancer* **2003**, *3*, 330.
- (36) Langenbach, R. J.; Danenberg, P. V.; Heidelberger, C. *Biochemical and Biophysical Research Communications* **1972**, *48*, 1565.
- (37) Ward, W. H. J.; Kimbell, R.; Jackman, A. L. *Biochemical Pharmacology* **1992**, *43*, 2029.
- (38) Curtin, N. J.; Hughes, A. N. *The Lancet Oncology* **2001**, *2*, 298.
- (39) Elstein, K. H.; Mole, M. L.; Setzer, R. W.; Zucker, R. M.; Kavlock, R. J.; Rogers, J. M.; Lau, C. *Toxicology and Applied Pharmacology* **1997**, *146*, 29.
- (40) Yoshioka, A.; Tanaka, S.; Hiraoka, O.; Koyama, Y.; Hirota, Y.; Ayusawa, D.; Seno, T.; Garrett, C.; Wataya, Y. *Journal of Biological Chemistry* **1987**, *262*, 8235.
- (41) CARADONNA, S. J.; CHENG, Y.-C. *Molecular Pharmacology* **1980**, *18*, 513.
- (42) Curtin, N. J.; Harris, A. L.; Aherne, G. W. *Cancer Research* **1991**, *51*, 2346.
- (43) Harris, J. M.; McIntosh, E. M.; Muscat, G. E. O. *Journal of Molecular Biology* **1999**, *288*, 275.
- (44) Kerepesi, C.; Szabó, J. E.; Papp-Kádár, V.; Dobay, O.; Szabó, D.; Grolmusz, V.; Vértessy, B. G. *Frontiers in microbiology* **2016**, *7*, 1768.
- (45) Gadsden, M. H.; McIntosh, E. M.; Game, J. C.; Wilson, P. J.; Haynes, R. H. *The EMBO journal* **1993**, *12*, 4425.
- (46) el-Hajj, H. H.; Zhang, H.; Weiss, B. *Journal of Bacteriology* **1988**, *170*, 1069.
- (47) Wilson, P. M.; LaBonte, M. J.; Lenz, H.-J.; Mack, P. C.; Ladner, R. D. *Molecular Cancer Therapeutics* **2012**, *11*, 616.
- (48) Mol, C. D.; Harris, J. M.; McIntosh, E. M.; Tainer, J. A. *Structure* **1996**, *4*, 1077.
- (49) Babkov, D. A.; Chizhov, A. O.; Khandazhinskaya, A. L.; Corona, A.; Esposito, F.; Tramontano, E.; Seley-Radtke, K. L.; Novikov, M. S. *Synthesis* **2015**, *47*, 1413.
- (50) Varga, B.; Barabás, O.; Kovári, J.; Tóth, J.; Hunyadi-Gulyás, É.; Klement, É.; Medzihradsky, K. F.; Tölgyesi, F.; Fidy, J.; Vértessy, B. G. *FEBS Letters* **2007**, *581*, 4783.
- (51) Koehler, S. E.; Ladner, R. D. *Molecular Pharmacology* **2004**, *66*, 620.
- (52) Ladner, R. D.; Lynch, F. J.; Groshen, S.; Xiong, Y. P.; Sherrod, A.; Caradonna, S. J.; Stoehlmacher, J.; Lenz, H.-J. *Cancer Research* **2000**, *60*, 3493.
- (53) Kawahara, A.; Akagi, Y.; Hattori, S.; Mizobe, T.; Shirouzu, K.; Ono, M.; Yanagawa, T.; Kuwano, M.; Kage, M. *Journal of clinical pathology* **2009**, *62*, 364.
- (54) Parsels, L. A.; Parsels, J. D.; Wagner, L. M.; Loney, T. L.; Radany, E. H.; Maybaum, J. *Cancer Chemotherapy and Pharmacology* **1998**, *42*, 357.
- (55) Hagenkort, A.; Paulin, C. B. J.; Desroses, M.; Sarno, A.; Wiita, E.; Mortusewicz, O.; Koolmeister, T.; Loseva, O.; Jemth, A.-S.; Almlöf, I.; Homan, E.; Lundbäck, T.; Gustavsson, A.-L.; Scobie, M.; Helleday, T. *Oncotarget* **2017**, *8*, 23713.

- (56) Zalud, P.; Wachs, W. O.; Nyman, P. O.; Zeppezauer, M. M. In *Purine and Pyrimidine Metabolism in Man VIII*; Sahota, A., Taylor, M. W., Eds.; Springer US: Boston, MA, 1994, p 135.
- (57) Persson, T.; Larsson, G.; Nyman, P. O. *Bioorganic & Medicinal Chemistry* **1996**, *4*, 553.
- (58) Miyakoshi, H.; Miyahara, S.; Yokogawa, T.; Chong, K. T.; Taguchi, J.; Endoh, K.; Yano, W.; Wakasa, T.; Ueno, H.; Takao, Y.; Nomura, M.; Shuto, S.; Nagasawa, H.; Fukuoka, M. *Journal of Medicinal Chemistry* **2012**, *55*, 2960.
- (59) Miyahara, S.; Miyakoshi, H.; Yokogawa, T.; Chong, K. T.; Taguchi, J.; Muto, T.; Endoh, K.; Yano, W.; Wakasa, T.; Ueno, H.; Takao, Y.; Fujioka, A.; Hashimoto, A.; Itou, K.; Yamamura, K.; Nomura, M.; Nagasawa, H.; Shuto, S.; Fukuoka, M. *Journal of Medicinal Chemistry* **2012**, *55*, 2970.
- (60) Tóth, J.; Varga, B.; Kovács, M.; Málnási-Csizmadia, A.; Vértessy, B. G. *Journal of Biological Chemistry* **2007**, *282*, 33572.
- (61) Nguyen, C.; Ruda, G. F.; Schipani, A.; Kasinathan, G.; Leal, I.; Musso-Buendia, A.; Kaiser, M.; Brun, R.; Ruiz-Pérez, L. M.; Sahlberg, B.-L.; Johansson, N. G.; González-Pacanowska, D.; Gilbert, I. H. *Journal of Medicinal Chemistry* **2006**, *49*, 4183.
- (62) Whittingham, J. L.; Leal, I.; Nguyen, C.; Kasinathan, G.; Bell, E.; Jones, A. F.; Berry, C.; Benito, A.; Turkenburg, J. P.; Dodson, E. J.; Perez, L. M. R.; Wilkinson, A. J.; Johansson, N. G.; Brun, R.; Gilbert, I. H.; Pacanowska, D. G.; Wilson, K. S. *Structure* **2005**, *13*, 329.
- (63) Chan, S.; Segelke, B.; Lekin, T.; Krupka, H.; Cho, U. S.; Kim, M.-y.; So, M.; Kim, C.-Y.; Naranjo, C. M.; Rogers, Y. C.; Park, M. S.; Waldo, G. S.; Pashkov, I.; Cascio, D.; Perry, J. L.; Sawaya, M. R. *Journal of Molecular Biology* **2004**, *341*, 503.
- (64) Hampton, S. E.; Baragaña, B.; Schipani, A.; Bosch-Navarrete, C.; Musso-Buendía, J. A.; Recio, E.; Kaiser, M.; Whittingham, J. L.; Roberts, S. M.; Shevtsov, M.; Brannigan, J. A.; Kahnberg, P.; Brun, R.; Wilson, K. S.; González-Pacanowska, D.; Johansson, N. G.; Gilbert, I. H. *ChemMedChem* **2011**, *6*, 1816.
- (65) Nguyen, C.; Kasinathan, G.; Leal-Cortijo, I.; Musso-Buendia, A.; Kaiser, M.; Brun, R.; Ruiz-Pérez, L. M.; Johansson, N. G.; González-Pacanowska, D.; Gilbert, I. H. *Journal of Medicinal Chemistry* **2005**, *48*, 5942.
- (66) Ruda, G. F.; Nguyen, C.; Ziemkowski, P.; Felczak, K.; Kasinathan, G.; Musso-Buendia, A.; Sund, C.; Zhou, X. X.; Kaiser, M.; Ruiz-Pérez, L. M.; Brun, R.; Kulikowski, T.; Johansson, N. G.; González-Pacanowska, D.; Gilbert, I. H. *ChemMedChem* **2011**, *6*, 309.
- (67) Yano, W.; Yokogawa, T.; Wakasa, T.; Yamamura, K.; Fujioka, A.; Yoshisue, K.; Matsushima, E.; Miyahara, S.; Miyakoshi, H.; Taguchi, J.; Chong, K. T.; Takao, Y.; Fukuoka, M.; Matsuo, K. *Molecular Cancer Therapeutics* **2018**, *17*, 1683.
- (68) Miyahara, S.; Miyakoshi, H.; Yokogawa, T.; Chong, K. T.; Taguchi, J.; Muto, T.; Endoh, K.; Yano, W.; Wakasa, T.; Ueno, H.; Takao, Y.; Fujioka, A.; Hashimoto, A.; Itou, K.; Yamamura, K.; Nomura, M.; Nagasawa, H.; Shuto, S.; Fukuoka, M. *Journal of Medicinal Chemistry* **2012**, *55*, 5483.
- (69) Miyakoshi, H.; Miyahara, S.; Yokogawa, T.; Endoh, K.; Muto, T.; Yano, W.; Wakasa, T.; Ueno, H.; Chong, K. T.; Taguchi, J.; Nomura, M.; Takao, Y.; Fujioka, A.; Hashimoto, A.; Itou, K.; Yamamura, K.; Shuto, S.; Nagasawa, H.; Fukuoka, M. *Journal of Medicinal Chemistry* **2012**, *55*, 6427.
- (70) Ladner, R. D.; Giethlen, B. DEOXYURIDINE TRIPHOSPHATASE INHIBITORS. WO 2014/107622 A1, July 10, 2014.
- (71) Spyvee M.; Shirude, P. S. DEOXYURIDINE TRIPHOSPHATASE INHIBITORS CONTAINING CYCLOPROPANO LINKAGE. WO2017006283A1, January 12, 2017.
- (72) Ladner, R. D.; Spyvee M.; Shirude, P. S. DEOXYURIDINE TRIPHOSPHATASE INHIBITORS CONTAINING AMINO SULFONYL LINKAGE. WO 2017/006271 A1, July 8, 2015.
- (73) *European Journal of Cancer* **2018**, *103*, e23.

- (74) Zhang, L.; Peng, X.-M.; Damu, G. L. V.; Geng, R.-X.; Zhou, C.-H. *Medicinal Research Reviews* **2014**, *34*, 340.
- (75) Lu, X.; Liu, X.; Wan, B.; Franzblau, S. G.; Chen, L.; Zhou, C.; You, Q. *European Journal of Medicinal Chemistry* **2012**, *49*, 164.
- (76) Leclaire, J.; Mazari, M.; Zhang, Y.; Bonduelle, C.; Thillaye du Boullay, O.; Martin-Vaca, B.; Bourissou, D.; De Riggi, I.; Fortrie, R.; Fotiadu, F.; Buono, G. *Chemistry – A European Journal* **2013**, *19*, 11301.
- (77) Goff, D. A.; Harris, R. N.; Bottaro, J. C.; Bedford, C. D. *The Journal of Organic Chemistry* **1986**, *51*, 4711.
- (78) Voight, E. A.; Brown, B. S.; Greszler, S. N.; Halvorsen, G. T.; Zhao, G.; Kruger, A. W.; Hartung, J.; Lukin, K. A.; Martinez, S. R.; Moschetta, E. G.; Tudesco, M. T.; Ide, N. D. *The Journal of Organic Chemistry* **2019**, *84*, 4723.
- (79) Novikov, M. S.; Buckheit, R. W.; Temburnikar, K.; Khandazhinskaya, A. L.; Ivanov, A. V.; Seley-Radtke, K. L. *Bioorganic & Medicinal Chemistry* **2010**, *18*, 8310.
- (80) In *Comprehensive Organic Name Reactions and Reagents*.
- (81) Li, N.-S.; Piccirilli, J. A. *Chemical Communications* **2012**, *48*, 8754.
- (82) Khare, P.; Gupta, A. K.; Gajula, P. K.; Sunkari, K. Y.; Jaiswal, A. K.; Das, S.; Bajpai, P.; Chakraborty, T. K.; Dube, A.; Saxena, A. K. *Journal of Chemical Information and Modeling* **2012**, *52*, 777.
- (83) Kita, Y.; Haruta, J.; Segawa, J.; Tamura, Y. *Tetrahedron Letters* **1979**, *20*, 4311.
- (84) Li, N.-S.; Piccirilli, J. A. *Chemical Communications* **2012**, *48*, 8754.
- (85) Welch, C.; Chattopadhyaya, J.; Undheim, K.; Åstrand, I.-M.; Berg, J.-E.; W. Dingle, T.; Vaughan Williams, R.; Mahedevan, R. *3-N-Acyl Uridines: Preparation and Properties of a New Class of Uracil Protecting Group*, 1983; Vol. 37b.
- (86) Lipani, L.; Odadzic, D.; Weizel, L.; Schwed, J.-S.; Sadek, B.; Stark, H. *European Journal of Medicinal Chemistry* **2014**, *86*, 578.
- (87) Frieden, M.; Giraud, M.; B. Reese, C.; Song, Q. *Journal of the Chemical Society, Perkin Transactions 1* **1998**, 2827.
- (88) Čerňová, M.; Čerňa, I.; Pohl, R.; Hocek, M. *The Journal of Organic Chemistry* **2011**, *76*, 5309.
- (89) Weaver, D. F.; Guillain, B. M.; Google Patents: 2006.
- (90) Edstrom, E. D.; Feng, X.; Tumkevicius, S. *Tetrahedron Letters* **1996**, *37*, 759.
- (91) Aleiwi, B. A.; Kurosu, M. *Tetrahedron letters* **2012**, *53*, 3758.
- (92) Spork, A. P.; Wiegmann, D.; Granitzka, M.; Stalke, D.; Ducho, C. *The Journal of Organic Chemistry* **2011**, *76*, 10083.
- (93) Whitten, J. P.; Matthews, D. P.; McCarthy, J. R. *The Journal of Organic Chemistry* **1986**, *51*, 1891.
- (94) Muchowski, J. M.; Solas, D. R. *The Journal of Organic Chemistry* **1984**, *49*, 203.
- (95) In *Encyclopedia of Reagents for Organic Synthesis*.
- (96) Chandra, T.; Broderick, W. E.; Broderick, J. B. *Nucleosides Nucleotides Nucleic Acids* **2010**, *29*, 132.
- (97) Vakalopoulos, A.; Hoffmann, H. M. R. *Organic Letters* **2000**, *2*, 1447.
- (98) Schlessinger, R. H.; Poss, M. A.; Richardson, S. *Journal of the American Chemical Society* **1986**, *108*, 3112.
- (99) Jaime-Figueroa, S.; Zamilpa, A.; Guzmán, A.; Morgans, D. J. *Synthetic Communications* **2001**, *31*, 3739.
- (100) Phadtare, S.; Zemlicka, J. *The Journal of Organic Chemistry* **1989**, *54*, 3675.
- (101) In *Hydrolysis in Drug and Prodrug Metabolism*, p 419.
- (102) Choi-Sledeski, Y. M.; Wermuth, C. G. In *The Practice of Medicinal Chemistry (Fourth Edition)*; Wermuth, C. G., Aldous, D., Raboisson, P., Rognan, D., Eds.; Academic Press: San Diego, 2015, p 657.

- (103) Elizabeth Taylor, H.; Sloan, K. B. *Journal of Pharmaceutical Sciences* **1998**, *87*, 15.
- (104) Loren, J. C.; Krasiński, A.; Fokin, V. V.; Sharpless, K. B. *Synlett* **2005**, *2005*, 2847.
- (105) Pradere, U.; Garnier-Amblard, E. C.; Coats, S. J.; Amblard, F.; Schinazi, R. F. *Chemical Reviews* **2014**, *114*, 9154.
- (106) Koszytkowska-Stawińska, M.; Mironiuk-Puchalska, E.; Rowicki, T. *Tetrahedron* **2012**, *68*, 214.
- (107) Johns, B. A. W., J. G. CHEMICAL COMPOUNDS, WO 2010/011815 A1, January 28, 2010.
- (108) Oyo, M.; Masaaki, Y. *Bulletin of the Chemical Society of Japan* **1967**, *40*, 2380.
- (109) Jeannot, F.; Taillier, T.; Despeyroux, P.; Renard, S.; Rey, A.; Mourez, M.; Poverlein, C.; Khichane, I.; Perrin, M.-A.; Versluys, S.; Stavenger, R. A.; Huang, J.; Germe, T.; Maxwell, A.; Cao, S.; Huseby, D. L.; Hughes, D.; Bacqué, E. *Journal of Medicinal Chemistry* **2018**, *61*, 3565.
- (110) Sindac, J. A.; Barraza, S. J.; Dobry, C. J.; Xiang, J.; Blakely, P. K.; Irani, D. N.; Keep, R. F.; Miller, D. J.; Larsen, S. D. *Journal of Medicinal Chemistry* **2013**, *56*, 9222.
- (111) Yao, Y.; Liao, C.; Li, Z.; Wang, Z.; Sun, Q.; Liu, C.; Yang, Y.; Tu, Z.; Jiang, S. *European Journal of Medicinal Chemistry* **2014**, *86*, 639.
- (112) Shen, J.; Wang, Y.; Wang, K. Azole heterocyclic compound, preparation method, pharmaceutical composition and use. WO2013000267A1, January 3, 2013.
- (113) Mitra, S.; Darira, H.; Chattopadhyay, P. *Synthesis* **2013**, *45*, 85.
- (114) Kleyi, P.; Walmsley, R. S.; Gundhla, I. Z.; Walmsley, T. A.; Jauka, T. I.; Dames, J.; Walker, R. B.; Torto, N.; Tshentu, Z. R. *South African Journal of Chemistry* **2012**, *65*, 231.
- (115) Roper, K. A.; Lange, H.; Polyzos, A.; Berry, M. B.; Baxendale, I. R.; Ley, S. V. *Beilstein J Org Chem* **2011**, *7*, 1648.
- (116) Appel, R. *Angewandte Chemie International Edition in English* **1975**, *14*, 801.
- (117) Kim, J. M. L., R. M.; Mckibben, B.; Tschantz, A.; Yu, H. Substituted benzylimidazoles useful for the treatment of inflammatory diseases. WO2006107923A1, October 12, 2006. .
- (118) Jones, R. G. *Journal of the American Chemical Society* **1949**, *71*, 383.
- (119) Zimmerman, S. C.; Cramer, K. D.; Galan, A. A. *The Journal of Organic Chemistry* **1989**, *54*, 1256.
- (120) Periasamy, M.; Thirumalaikumar, M. *Journal of Organometallic Chemistry* **2000**, *609*, 137.
- (121) Jagdale, A. R.; Paraskar, A. S.; Sudalai, A. *Synthesis* **2009**, *2009*, 660.
- (122) Kawasaki, Y.; Freire, E. *Drug Discovery Today* **2011**, *16*, 985.
- (123) Klebe, G. *Nature Reviews Drug Discovery* **2015**, *14*, 95.
- (124) Martínez-Maqueda, D.; Miralles, B.; Recio, I. In *The Impact of Food Bioactives on Health: in vitro and ex vivo models*; Verhoeckx, K., Cotter, P., López-Expósito, I., Kleiveland, C., Lea, T., Mackie, A., Requena, T., Swiatecka, D., Wichers, H., Eds.; Springer International Publishing: Cham, 2015, p 113.
- (125) COMŞA, Ş.; CÎMPEAN, A. M.; RAICA, M. *Anticancer Research* **2015**, *35*, 3147.
- (126) Miyaura, N.; Suzuki, A. *Chemical Reviews* **1995**, *95*, 2457.
- (127) Nakatake, D.; Yokote, Y.; Matsushima, Y.; Yazaki, R.; Ohshima, T. *Green Chemistry* **2016**, *18*, 1524.
- (128) Mor, M.; Rivara, S.; Lodola, A.; Plazzi, P. V.; Tarzia, G.; Duranti, A.; Tontini, A.; Piersanti, G.; Kathuria, S.; Piomelli, D. *Journal of Medicinal Chemistry* **2004**, *47*, 4998.
- (129) Acharya, R. B., D.; Bursavich, M. G.; Cook, A. S.; Harrison, B. A.; Mcriner, A. J. AMINOBENZISOXAZOLE COMPOUNDS AS AGONISTS OF A7-NICOTINIC ACETYLCHOLINE RECEPTORS. WO 2016/201096 A1, December 25, 2016.
- (130) Wang, D.; Zou, L.; Jin, Q.; Hou, J.; Ge, G.; Yang, L. *Acta Pharmaceutica Sinica B* **2018**, *8*, 699.
- (131) Paul, M. K.; Mukhopadhyay, A. K. *Int J Med Sci* **2004**, *1*, 101.
- (132) Ardito, F.; Giuliani, M.; Perrone, D.; Troiano, G.; Lo Muzio, L. *Int J Mol Med* **2017**, *40*, 271.
- (133) Siveen, K. S.; Prabhu, K. S.; Achkar, I. W.; Kuttikrishnan, S.; Shyam, S.; Khan, A. Q.; Merhi, M.; Dermime, S.; Uddin, S. *Molecular cancer* **2018**, *17*, 31.

- (134) Klebe, G. In *Drug Design: Methodology, Concepts, and Mode-of-Action*; Klebe, G., Ed.; Springer Berlin Heidelberg: Berlin, Heidelberg, 2013, p 599.
- (135) Weber, T. J. In *Comprehensive Toxicology (Second Edition)*; McQueen, C. A., Ed.; Elsevier: Oxford, 2010, p 473.
- (136) Manning, G.; Whyte, D. B.; Martinez, R.; Hunter, T.; Sudarsanam, S. *Science* **2002**, *298*, 1912.
- (137) Hubbard, S. R. In *Handbook of Cell Signaling (Second Edition)*; Bradshaw, R. A., Dennis, E. A., Eds.; Academic Press: San Diego, 2010, p 413.
- (138) Du, Z.; Lovly, C. M. *Molecular Cancer* **2018**, *17*, 58.
- (139) Moustakas, A.; Souchelnytskyi, S.; Heldin, C. H. In *Encyclopedic Reference of Genomics and Proteomics in Molecular Medicine*; Springer Berlin Heidelberg: Berlin, Heidelberg, 2006, p 1603.
- (140) Robinson, D. R.; Wu, Y.-M.; Lin, S.-F. *Oncogene* **2000**, *19*, 5548.
- (141) Toffalini, F.; Demoulin, J.-B. *Blood* **2010**, *116*, 2429.
- (142) Scitable by nature Education. RTK. <https://www.nature.com/scitable/topicpage/rtk-14050230/> (accessed Dez 12, 2019).
- (143) Tsukahara, F.; Maru, Y. In *Chemotherapy for Leukemia: Novel Drugs and Treatment*; Ueda, T., Ed.; Springer Singapore: Singapore, 2017, p 11.
- (144) Wang, J. Y. J. *Molecular and Cellular Biology* **2014**, *34*, 1188.
- (145) Shah, N. H.; Amacher, J. F.; Nocka, L. M.; Kuriyan, J. *Critical Reviews in Biochemistry and Molecular Biology* **2018**, *53*, 535.
- (146) London, C. A. *Veterinary Dermatology* **2013**, *24*, 181.
- (147) Ren, R. *Nature Reviews Cancer* **2005**, *5*, 172.
- (148) Hantschel, O. *Genes Cancer* **2012**, *3*, 436.
- (149) Sattler, M.; Griffin, J. D. *International Journal of Hematology* **2001**, *73*, 278.
- (150) Jiao, Q.; Bi, L.; Ren, Y.; Song, S.; Wang, Q.; Wang, Y.-s. *Molecular Cancer* **2018**, *17*, 36.
- (151) Hehlmann, R.; Lauseker, M.; Saußebe, S.; Pfirrmann, M.; Krause, S.; Kolb, H. J.; Neubauer, A.; Hossfeld, D. K.; Nerl, C.; Gratwohl, A.; Baerlocher, G. M.; Heim, D.; Brümmendorf, T. H.; Fabarius, A.; Haferlach, C.; Schlegelberger, B.; Müller, M. C.; Jeromin, S.; Proetel, U.; Kohlbrenner, K.; Voskanyan, A.; Rinaldetti, S.; Seifarth, W.; Spieß, B.; Balleisen, L.; Goebeler, M. C.; Hänel, M.; Ho, A.; Dengler, J.; Falge, C.; Kanz, L.; Kremers, S.; Burchert, A.; Kneba, M.; Stegelmann, F.; Köhne, C. A.; Lindemann, H. W.; Waller, C. F.; Pfreundschuh, M.; Spiekermann, K.; Berdel, W. E.; Müller, L.; Edinger, M.; Mayer, J.; Beelen, D. W.; Bentz, M.; Link, H.; Hertenstein, B.; Fuchs, R.; Wernli, M.; Schlegel, F.; Schlag, R.; de Wit, M.; Trümper, L.; Hebart, H.; Hahn, M.; Thomalla, J.; Scheid, C.; Schafhausen, P.; Verbeek, W.; Eckart, M. J.; Gassmann, W.; Pezzutto, A.; Schenk, M.; Brossart, P.; Geer, T.; Bildat, S.; Schäfer, E.; Hochhaus, A.; Hasford, J. *Leukemia* **2017**, *31*, 2398.
- (152) Roskoski, R. *Pharmacological Research* **2019**, *144*, 19.
- (153) Sasaki, K.; Strom, S. S.; O'Brien, S.; Jabbour, E.; Ravandi, F.; Konopleva, M.; Borthakur, G.; Pemmaraju, N.; Daver, N.; Jain, P.; Pierce, S.; Kantarjian, H.; Cortes, J. E. *The Lancet Haematology* **2015**, *2*, e186.
- (154) Bower, H.; Björkholm, M.; Dickman, P. W.; Höglund, M.; Lambert, P. C.; Andersson, T. M.-L. *Journal of Clinical Oncology* **2016**, *34*, 2851.
- (155) Fabbro, D.; Cowan-Jacob, S. W.; Moebitz, H. *Br J Pharmacol* **2015**, *172*, 2675.
- (156) Traxler, P.; Furet, P. *Pharmacology & Therapeutics* **1999**, *82*, 195.
- (157) Le Corre, L.; Girard, A.-L.; Aubertin, J.; Radvanyi, F.; Benoist-Lasselain, C.; Jonquoy, A.; Mugniery, E.; Legeai-Mallet, L.; Busca, P.; Le Merrer, Y. *Organic & Biomolecular Chemistry* **2010**, *8*, 2164.
- (158) Gavrin, L. K.; Saiah, E. *MedChemComm* **2013**, *4*, 41.
- (159) Zuccotto, F.; Ardini, E.; Casale, E.; Angiolini, M. *Journal of Medicinal Chemistry* **2010**, *53*, 2681.
- (160) Ko, B.; Paucar, D.; Halmos, B. *Lung Cancer (Auckl)* **2017**, *8*, 147.

- (161) Rossari, F.; Minutolo, F.; Orciuolo, E. *Journal of Hematology & Oncology* **2018**, *11*, 84.
- (162) Modugno, M.; Casale, E.; Soncini, C.; Rosettani, P.; Colombo, R.; Lupi, R.; Rusconi, L.; Fancelli, D.; Carpinelli, P.; Cameron, A. D.; Isacchi, A.; Moll, J. *Cancer Research* **2007**, *67*, 7987.
- (163) Shah, N. P.; Nicoll, J. M.; Nagar, B.; Gorre, M. E.; Paquette, R. L.; Kuriyan, J.; Sawyers, C. L. *Cancer Cell* **2002**, *2*, 117.
- (164) Tokarski, J. S.; Newitt, J. A.; Chang, C. Y. J.; Cheng, J. D.; Wittekind, M.; Kiefer, S. E.; Kish, K.; Lee, F. Y. F.; Borzilleri, R.; Lombardo, L. J.; Xie, D.; Zhang, Y.; Klei, H. E. *Cancer Research* **2006**, *66*, 5790.
- (165) Lombardo, L. J.; Lee, F. Y.; Chen, P.; Norris, D.; Barrish, J. C.; Behnia, K.; Castaneda, S.; Cornelius, L. A. M.; Das, J.; Doweiko, A. M.; Fairchild, C.; Hunt, J. T.; Inigo, I.; Johnston, K.; Kamath, A.; Kan, D.; Klei, H.; Marathe, P.; Pang, S.; Peterson, R.; Pitt, S.; Schieven, G. L.; Schmidt, R. J.; Tokarski, J.; Wen, M.-L.; Wityak, J.; Borzilleri, R. M. *Journal of Medicinal Chemistry* **2004**, *47*, 6658.
- (166) Hare, T.; Walters, D. K.; Stoffregen, E. P.; Jia, T.; Manley, P. W.; Mestan, J.; Cowan-Jacob, S. W.; Lee, F. Y.; Heinrich, M. C.; Deininger, M. W. N.; Druker, B. J. *Cancer Research* **2005**, *65*, 4500.
- (167) Davis, M. I.; Hunt, J. P.; Herrgard, S.; Ciceri, P.; Wodicka, L. M.; Pallares, G.; Hocker, M.; Treiber, D. K.; Zarrinkar, P. P. *Nature Biotechnology* **2011**, *29*, 1046.
- (168) Lonsdale, R.; Ward, R. A. *Chemical Society Reviews* **2018**, *47*, 3816.
- (169) Singh, J.; Petter, R. C.; Baillie, T. A.; Whitty, A. *Nature Reviews Drug Discovery* **2011**, *10*, 307.
- (170) Barf, T.; Kaptein, A. *Journal of Medicinal Chemistry* **2012**, *55*, 6243.
- (171) Potashman, M. H.; Duggan, M. E. *Journal of Medicinal Chemistry* **2009**, *52*, 1231.
- (172) Macherey, A.-C.; Dansette, P. M. In *The Practice of Medicinal Chemistry (Fourth Edition)*; Wermuth, C. G., Aldous, D., Raboisson, P., Rognan, D., Eds.; Academic Press: San Diego, 2015, p 585.
- (173) Gilbert, A. M. *Pharmaceutical Patent Analyst* **2014**, *3*, 375.
- (174) Liu, Q.; Sabnis, Y.; Zhao, Z.; Zhang, T.; Buhrlage, S. J.; Jones, L. H.; Gray, N. S. *Chem Biol* **2013**, *20*, 146.
- (175) Zhao, Z.; Liu, Q.; Bliven, S.; Xie, L.; Bourne, P. E. *Journal of medicinal chemistry* **2017**, *60*, 2879.
- (176) Leproult, E.; Barluenga, S.; Moras, D.; Wurtz, J.-M.; Winssinger, N. *Journal of Medicinal Chemistry* **2011**, *54*, 1347.
- (177) Rao, S.; Gurbani, D.; Du, G.; Everley, R. A.; Browne, C. M.; Chaikuad, A.; Tan, L.; Schröder, M.; Gondi, S.; Ficarro, S. B.; Sim, T.; Kim, N. D.; Berberich, M. J.; Knapp, S.; Marto, J. A.; Westover, K. D.; Sorger, P. K.; Gray, N. S. *Cell Chemical Biology* **2019**, *26*, 818.
- (178) Chaikuad, A.; Koch, P.; Laufer, S. A.; Knapp, S. *Angewandte Chemie International Edition* **2018**, *57*, 4372.
- (179) Yamaura, T.; Nakatani, T.; Uda, K.; Ogura, H.; Shin, W.; Kurokawa, N.; Saito, K.; Fujikawa, N.; Date, T.; Takasaki, M.; Terada, D.; Hirai, A.; Akashi, A.; Chen, F.; Adachi, Y.; Ishikawa, Y.; Hayakawa, F.; Hagiwara, S.; Naoe, T.; Kiyoi, H. *Blood* **2018**, *131*, 426.
- (180) Kwarcinski, F. E.; Fox, C. C.; Steffey, M. E.; Soellner, M. B. *ACS chemical biology* **2012**, *7*, 1910.
- (181) Das, J.; Chen, P.; Norris, D.; Padmanabha, R.; Lin, J.; Moquin, R. V.; Shen, Z.; Cook, L. S.; Doweiko, A. M.; Pitt, S.; Pang, S.; Shen, D. R.; Fang, Q.; de Fex, H. F.; McIntyre, K. W.; Shuster, D. J.; Gillooly, K. M.; Behnia, K.; Schieven, G. L.; Wityak, J.; Barrish, J. C. *Journal of Medicinal Chemistry* **2006**, *49*, 6819.
- (182) Deadman, B. J.; Hopkin, M. D.; Baxendale, I. R.; Ley, S. V. *Organic & Biomolecular Chemistry* **2013**, *11*, 1766.
- (183) Zhao, R.; Gove, S.; Sundeen, J. E.; Chen, B.-C. *Tetrahedron Letters* **2001**, *42*, 2101.
- (184) Allentoff, A. J.; Lago, M. W.; Ogan, M.; Chen, B.-C.; Zhao, R.; Iyer, R. A.; Christopher, L. J.; Rinehart, J. K.; Balasubramanian, B.; Bonacorsi Jr, S. J. *Journal of Labelled Compounds and Radiopharmaceuticals* **2008**, *51*, 41.

- (185) Chen, B. C.; Zhao, R.; Wang, B.; Droghini, R.; Lajeunesse, J.; Sirard, P.; Endo, M.; Balu, B.; Barrisha, J. C. *Arkivoc* **2010**, 2010, 32.
- (186) Peng, B.; Thorsell, A.-G.; Karlberg, T.; Schüler, H.; Yao, S. Q. *Angewandte Chemie International Edition* **2017**, 56, 248.
- (187) Liu, L.; Hussain, M.; Luo, J.; Duan, A.; Chen, C.; Tu, Z.; Zhang, J. *Chemical Biology & Drug Design* **2017**, 89, 420.
- (188) Zhang, J.; Liu, L.; Chen, C.; Duan, A.; Zhengchao, T.; Yao G. Tyrosine kinase inhibitor and its production and use. CN106749223A, May 31, 2017.
- (189) Pal Singh, S.; Dammeijer, F.; Hendriks, R. W. *Molecular Cancer* **2018**, 17, 57.
- (190) Fletcher, J. A.; Rubin, B. P. *Current Opinion in Genetics & Development* **2007**, 17, 3.
- (191) Dragovich, P. S.; Webber, S. E.; Babine, R. E.; Fuhrman, S. A.; Patick, A. K.; Matthews, D. A.; Lee, C. A.; Reich, S. H.; Prins, T. J.; Marakovits, J. T.; Littlefield, E. S.; Zhou, R.; Tikhe, J.; Ford, C. E.; Wallace, M. B.; Meador, J. W.; Ferre, R. A.; Brown, E. L.; Binford, S. L.; Harr, J. E. V.; DeLisle, D. M.; Worland, S. T. *Journal of Medicinal Chemistry* **1998**, 41, 2806.
- (192) Dahlin JL, Baell J, Walters MA. Assay Interference by Chemical Reactivity. 2015 Sep 18. In: Sittampalam GS, Grossman A, Brimacombe K, et al., editors. *Assay Guidance Manual [Internet]. Bethesda (MD): Eli Lilly & Company and the National Center for Advancing Translational Sciences; 2004-*.
- (193) Flanagan, M. E.; Abramite, J. A.; Anderson, D. P.; Aulabaugh, A.; Dahal, U. P.; Gilbert, A. M.; Li, C.; Montgomery, J.; Oppenheimer, S. R.; Ryder, T.; Schuff, B. P.; Uccello, D. P.; Walker, G. S.; Wu, Y.; Brown, M. F.; Chen, J. M.; Hayward, M. M.; Noe, M. C.; Obach, R. S.; Philippe, L.; Shanmugasundaram, V.; Shapiro, M. J.; Starr, J.; Stroh, J.; Che, Y. *Journal of Medicinal Chemistry* **2014**, 57, 10072.
- (194) Schwartz, P. A.; Kuzmic, P.; Solowiej, J.; Bergqvist, S.; Bolanos, B.; Almaden, C.; Nagata, A.; Ryan, K.; Feng, J.; Dalvie, D.; Kath, J. C.; Xu, M.; Wani, R.; Murray, B. W. *Proc Natl Acad Sci U S A* **2014**, 111, 173.
- (195) Wu, H.; Wang, W.; Liu, F.; Weisberg, E. L.; Tian, B.; Chen, Y.; Li, B.; Wang, A.; Wang, B.; Zhao, Z.; McMillin, D. W.; Hu, C.; Li, H.; Wang, J.; Liang, Y.; Buhrlage, S. J.; Liang, J.; Liu, J.; Yang, G.; Brown, J. R.; Treon, S. P.; Mitsiades, C. S.; Griffin, J. D.; Liu, Q.; Gray, N. S. *ACS chemical biology* **2014**, 9, 1086.
- (196) Quentmeier, H.; Reinhardt, J.; Zaborski, M.; Drexler, H. G. *Leukemia* **2003**, 17, 120.
- (197) Ampasavate, C.; Jutapakdee, W.; Phongpradist, R.; Tima, S.; Tantiworawit, A.; Charoenkwan, P.; Chinwong, D.; Anuchapreeda, S. *Journal of Clinical Laboratory Analysis* **2019**, 33, e22859.
- (198) Guo, W.; Liu, R.; Ono, Y.; Ma, A.-H.; Martinez, A.; Sanchez, E.; Wang, Y.; Huang, W.; Mazloom, A.; Li, J.; Ning, J.; Maverakis, E.; Lam, K. S.; Kung, H.-J. *Molecular Pharmacology* **2012**, 82, 938.
- (199) Hantschel, O.; Rix, U.; Schmidt, U.; Bürckstümmer, T.; Kneidinger, M.; Schütze, G.; Colinge, J.; Bennett, K. L.; Ellmeier, W.; Valent, P.; Superti-Furga, G. *Proc Natl Acad Sci U S A* **2007**, 104, 13283.
- (200) Zapf, C. W.; Gerstenberger, B. S.; Xing, L.; Limburg, D. C.; Anderson, D. R.; Caspers, N.; Han, S.; Aulabaugh, A.; Kurumbail, R.; Shakya, S.; Li, X.; Spaulding, V.; Czerwinski, R. M.; Seth, N.; Medley, Q. G. *Journal of Medicinal Chemistry* **2012**, 55, 10047.
- (201) Declerck, V.; Aitken, D. J. *Amino Acids* **2011**, 41, 587.

Appendix

Enzyme based dUTPase inhibitor assays

Cell based dUTPase inhibitor screening

TKI cell assays

NMR spectra

13. Appendix

Enzyme based dUTPase inhibitor assays

Materials and methods

The pMSE147 vector contains amino acids 112-252 of the DUT_HUMAN P33316 (uniprot accession code) and was provided as a generous gift of Medivir.

Expression

Precultures in LB-media containing ampicillin were started from glycerol stocks of BL21 Star (DE3) transformed with the pMSE147 plasmid. 1 L culture with TB-media containing ampicillin was grown at 37°C to an OD of 0.9 before induction with 0.1 mM IPTG. The temperature was lowered to 20°C for overnight expression. Cells were harvested by centrifugation at 6000 rpm for 30 minutes, and the pellet was frozen.

Purification

The thawed pellet was resuspended in 50 mM HEPES pH 7.5, 500 mM NaCl and sonicated for 15 minutes with 4/6 second pulses. The cell extract was clarified by centrifugation at 20000 rpm for 30 minutes. The clarified cell extract was loaded on a HisTrap HP 5 mL column and eluted with a gradient to 300 mM Imidazole. The main peak was loaded on a HiLoad Superdex 75 26/600 column equilibrated with 10 mM HEPES pH 7.5, 50 mM NaCl, 5 mM MgCl₂ and 0.1 mM TCEP. Following gel filtration the dUTPase was concentrated to 1 mM and flash-frozen with liquid nitrogen and kept at -20°C.

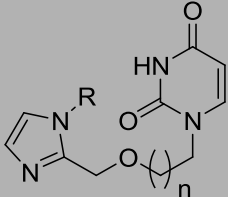
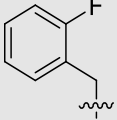
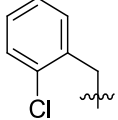
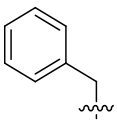
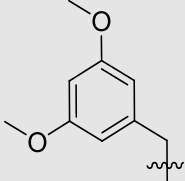
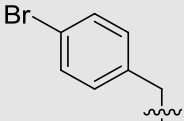
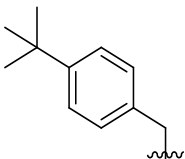
Activity assay using MAK168 pyrophosphate kit

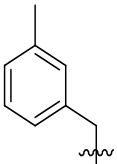
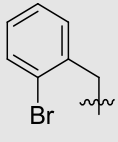
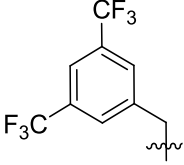
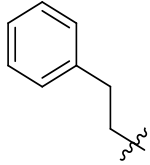
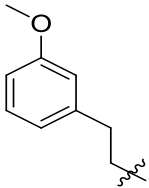
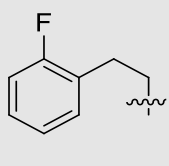
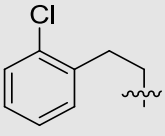
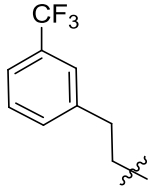
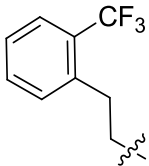

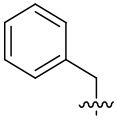
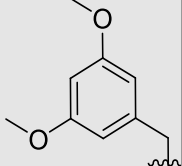
All compounds were diluted from 100 mM to 1 mM by mixing 1 µL thawed stock with 99 µL 50 mM HEPES pH 7.5, 150 mM KCl, 10 mM MgCl₂. 10 µL of the 1 mM stock was added to 40 µL 50 nM dUTPase for 100 µM final concentration of compound and 20 nM enzyme. Reaction was started with the addition of 50 µL PPI sensor/60 µM dUTP in the supplied analysis buffer and monitored at 316/456 for 30 min at 27°C. Negative (no enzyme) fluorescence was subtracted from all, and the percentage calculated from positive (no inhibitor).

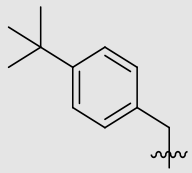
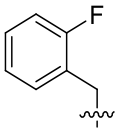
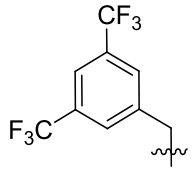
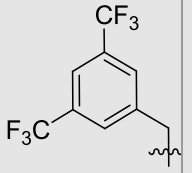
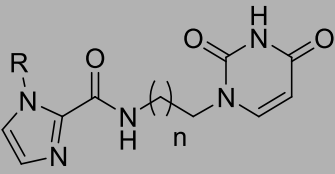
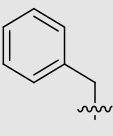
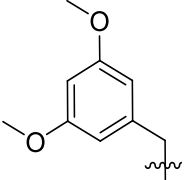
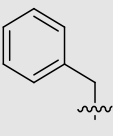
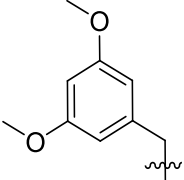
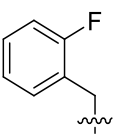
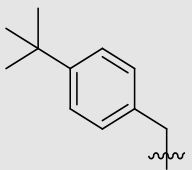
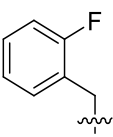
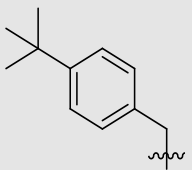
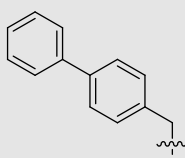
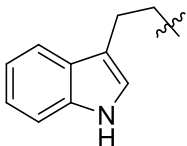
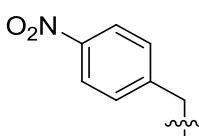
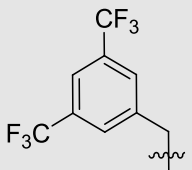
Binding assay using isothermal calorimetry

All experiments were performed at 25°C using a GE LifeScience ITC-200. Enzyme concentration was kept at 0.25 mM, reference power at 11 μ cal/min, stirring speed at 500 rpm and the concentration in the syringe was 2.5 mM. All experiments were performed with 50 mM HEPES, 150 mM KCl, 5 mM MgCl₂ and 2.5 % DMSO. The dUTPase was titrated at least twice with each inhibitor, and a separate buffer-inhibitor titration was also performed for each inhibitor. Data were fitted using PYTC using a single-site model and all global parameter.

Table 28: Overview of all final compounds and their results in the SPR and pyrophosphate assay

substituent	nr	n	SPR test Kd (μ M)	PPi assay Kd (μ M)	substituent	nr	n	SPR test Kd (μ M)	PPi assay Kd (μ M)
α,β -imino-dUTP	11		3.05 \pm 0.36	45%					
DMSO				9%					
									
	207	1	n.d	28%		219	1	n.d	37%
	208	2	unknown	16%		220	2	n.d	71%
	209	1	no	25%		221	1	no	n.d
	210	2	5.44 \pm 0.21	22%		222	2	12 \pm 0.86	24%
	211	1	no	26%		217	1	8.86 \pm 0.84	43%
	212	2	6.28 \pm 0,77	46%		218	2	unknown	9%

	213	1	n.d	-8%		215	1	4.44	8%
	214	2	no	-6%		216	2	50.51±41 nM 50.20±38 nM	52%
	215	1	322±705 nM	58%		225	1	61±90.3 nM	32%
	216	2	no	-2%		226	2	no	35%
	227	1	n.d	61%		229	1	6.51	49%
	228	2	n.d	54%		230	2	n.d	36%
	231	1	4.95	49%		235	1	1.12	18%
	232	2	n.d	71%		236	2	n.d	31%
	233	1	n.d	44%					
	234	2	6.81	36%					
	238	-	17.8±0.33	56%		244	-	no	12%

	242	-	18.5	28%		245	-	no	34%
	243	-	n.d	43%		350	-	n.d	30%
									
	115	1	29±0.28	17%		119	1	7.754	-4%
	116	2	40.9±0.45	7%		120	2	26.47	-14%
	121	1	85.1±26.7	11%		125	1	n.d	n.d
	122	2	unknown	3%		126	2	n.d	n.d
	124	2	33.08	nd		118	2	8.6±0.13	59%
	117	2	31±0.58	7%		123	2	n.d	n.d

n.d = not determined. Test conditions of the SPR measurements were changed or different protein batches used. The results were therefore only used to get an overview of the suitability of the scaffold types. Other test methods exhibit that the results were questionable.

Table 29: ITC raw data of compound **220**, **231**, **232** and the reference α,β -imido dUTP (**11**).

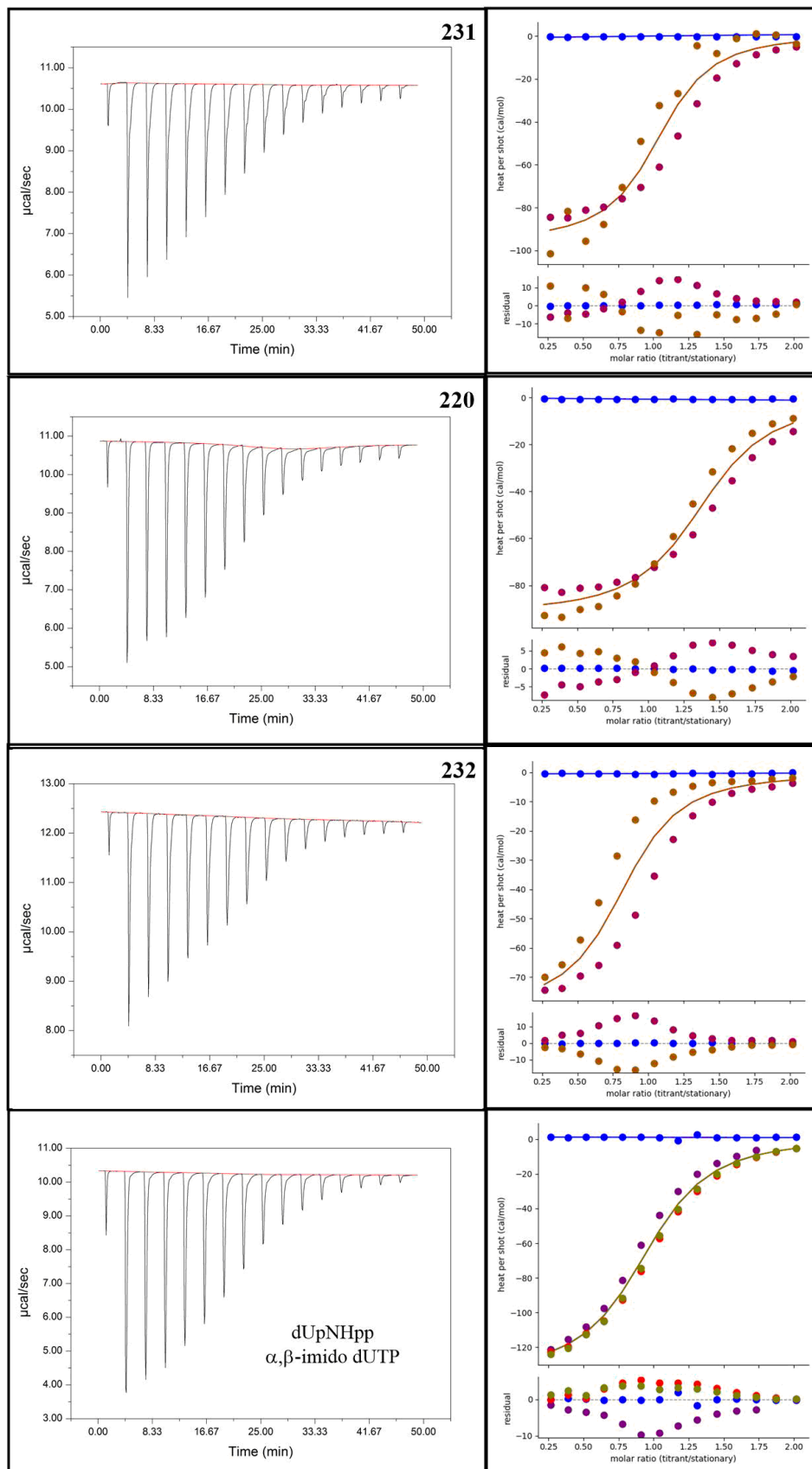
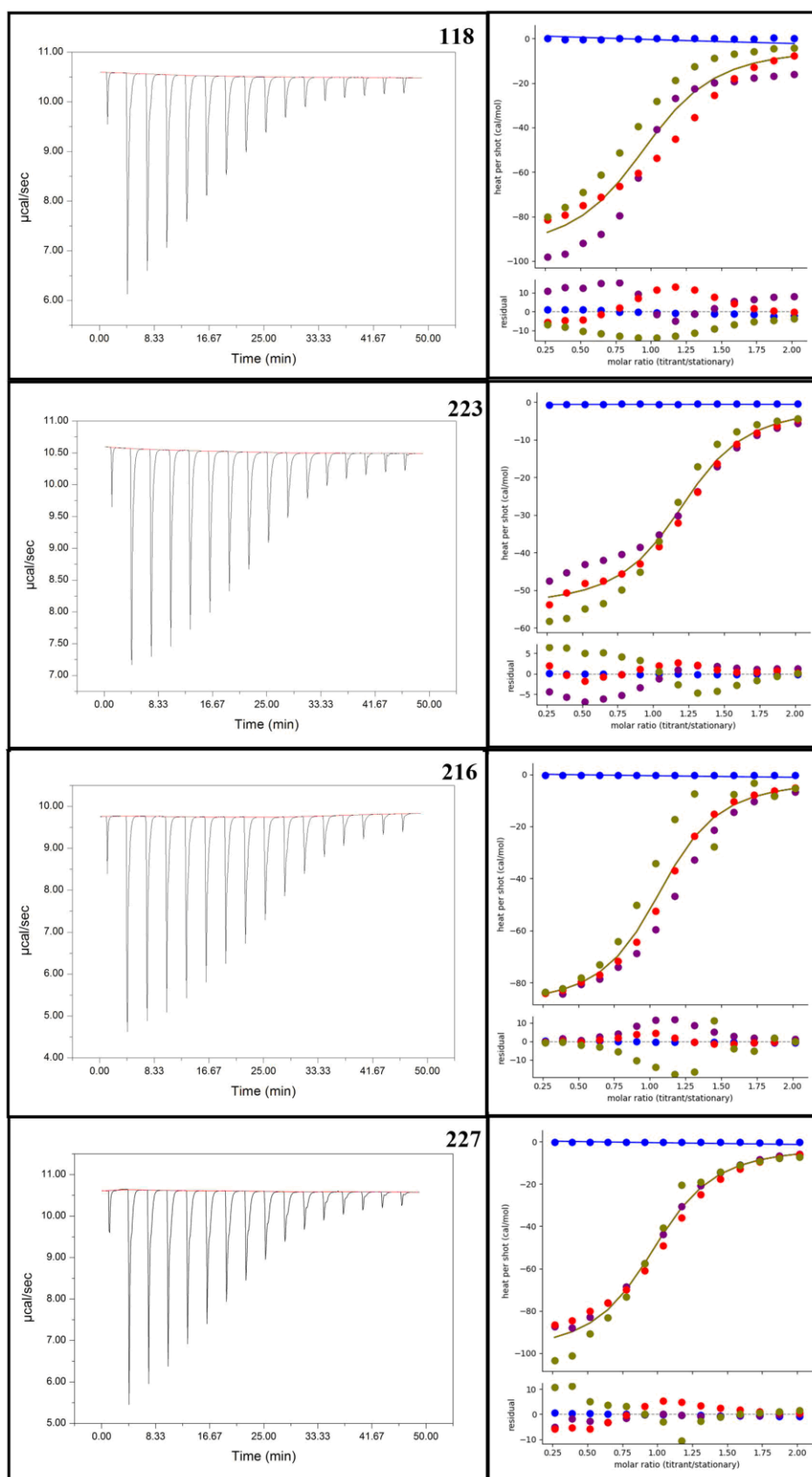


Table 30: ITC raw data of compound **118**, **216**, **223**, and **227**.



Cell based dUTPase inhibitor screening

Cell based dUTPase inhibitor screenings were conducted by **Marbio/Uit Tromsø** using the CellTiter96 Aqueous One Solution Cell Proliferation assay (**MTS assay**). 72 hours cell incubation with the compounds, then measurement of the cell survival.

Cell lines:

HT29 (ATCC-HTB-38) – 2000 cells/well, grown in RPMI (Biochrom FG1385) supplemented with 10 % fetal bovine serum (FBS) and 10 ug/mL Gentamycin.

MCF7 (ECACC accession number: 86012803) – 2000 cells/well, grown in EMEM (Biochrom F4315) supplemented with

10 % FBS (Biochrom),

10 ug/mL Gentamycin (A2712 Biochrom)

2 mM L-alanyl-L-Glutamin (K0302 Biochrom)

Non essential amino acids (K0293 Biochrom)

1 mM Sodium Pyruvat (L0473 Biochrom)

0,15 % NaHCO₃ (L1713 Biochrom)

Table 31: MCF7-cell assays for synergistic effects of FdUrd with dUTPase inhibitors.

COMPOUND	ASSAY_NAME	SURVIVAL	CONCENTRATION	CONC_UNITS
500 nM FdUrd influence on MCF7 cells				
FdUrd	MCF7_MTT	91	500	nM
FdUrd	MCF7_MTT	91	500	nM
FdUrd	MCF7_MTT	87	500	nM
FdUrd	MCF7_MTT	85	500	nM
FdUrd	MCF7_MTT	85	500	nM
FdUrd	MCF7_MTT	83	500	nM
FdUrd	MCF7_MTT	82	500	nM
FdUrd	MCF7_MTT	81	500	nM
500 nM FdUrd in combination with different concentrations dUTPase inhibitors				
11	MCF7_MTT	94	20	μM
11	MCF7_MTT	95	10	μM
11	MCF7_MTT	90	5	μM
11	MCF7_MTT	87	2,5	μM
11	MCF7_MTT	87	1	μM
11	MCF7_MTT	87	750	nM
11	MCF7_MTT	85	500	nM
11	MCF7_MTT	85	100	nM
238	MCF7_MTT	58	20	μM
238	MCF7_MTT	60	2,5	μM
238	MCF7_MTT	59	100	nM
118	MCF7_MTT	55	20	μM
118	MCF7_MTT	59	2,5	μM
118	MCF7_MTT	61	100	nM
218	MCF7_MTT	84	20	μM
218	MCF7_MTT	90	2,5	μM

218	MCF7_MTT	93	100	nM
208	MCF7_MTT	101	20	μM
208	MCF7_MTT	95	2,5	μM
208	MCF7_MTT	97	100	nM
212	MCF7_MTT	87	20	μM
212	MCF7_MTT	82	2,5	μM
212	MCF7_MTT	81	100	nM
242	MCF7_MTT	77	20	μM
242	MCF7_MTT	78	2,5	μM
242	MCF7_MTT	76	100	nM
242	MCF7_MTT	86	20	μM
242	MCF7_MTT	80	2,5	μM
242	MCF7_MTT	82	100	nM
226	MCF7_MTT	85	20	μM
226	MCF7_MTT	81	2,5	μM
226	MCF7_MTT	83	100	nM
332	MCF7_MTT	89	20	μM
332	MCF7_MTT	84	2,5	μM
332	MCF7_MTT	84	100	nM
233	MCF7_MTT	89	20	μM
233	MCF7_MTT	89	2,5	μM
233	MCF7_MTT	87	100	nM
231	MCF7_MTT	94	20	μM
231	MCF7_MTT	89	2,5	μM
231	MCF7_MTT	88	100	nM
235	MCF7_MTT	90	20	μM
235	MCF7_MTT	88	2,5	μM
235	MCF7_MTT	85	100	nM
236	MCF7_MTT	80	20	μM

236	MCF7_MTT	79	2,5	μM
236	MCF7_MTT	78	100	nM
232	MCF7_MTT	83	20	μM
232	MCF7_MTT	80	2,5	μM
232	MCF7_MTT	80	100	nM
228	MCF7_MTT	88	20	μM
228	MCF7_MTT	83	2,5	μM
228	MCF7_MTT	84	100	nM
230	MCF7_MTT	90	20	μM
230	MCF7_MTT	84	2,5	μM
230	MCF7_MTT	82	100	nM

Table 32: Cytotoxicity tests of MCF7 cells treated with 10 μ M dUTPase inhibitors.

COMPOUND	ASSAY_NAME	SURVIVAL	CONCENTRATION	CONC_UNITS
124	MCF7_MTT	104	10	μ M
118	MCF7_MTT	101	10	μ M
218	MCF7_MTT	97	10	μ M
208	MCF7_MTT	98	10	μ M
212	MCF7_MTT	102	10	μ M
242	MCF7_MTT	101	10	nM
242	MCF7_MTT	101	10	nM
226	MCF7_MTT	101	10	nM
332	MCF7_MTT	111	10	μ M
233	MCF7_MTT	108	10	μ M
231	MCF7_MTT	104	10	μ M
235	MCF7_MTT	107	10	μ M
236	MCF7_MTT	108	10	μ M
232	MCF7_MTT	104	10	nM
228	MCF7_MTT	107	10	nM
230	MCF7_MTT	108	10	nM
dUpNHpp	MCF7_MTT	119	10	μ M

Table 33: HT29-cell assays for synergistic effects of FdUrd with dUTPase inhibitors.

COMPOUND	ASSAY_NAME	SURVIVAL	CONCENTRATION	CONC_UNITS
10 nM FdUrd influence on HT-29 cells				
FdUrd	HT29_MTT	86	10	nM
FdUrd	HT29_MTT	84	10	nM
FdUrd	HT29_MTT	80	10	nM
FdUrd	HT29_MTT	81	10	nM
FdUrd	HT29_MTT	80	10	nM

FdUrd	HT29_MTT	83	10	nM
FdUrd	HT29_MTT	80	10	nM
FdUrd	HT29_MTT	82	10	nM
10 nM FdUrd in combination with different concentrations dUTPase inhibitors				
dUpNHpp	HT29_MTT	90	20	μM
dUpNHpp	HT29_MTT	84	10	μM
dUpNHpp	HT29_MTT	84	5	μM
dUpNHpp	HT29_MTT	83	2,5	μM
dUpNHpp	HT29_MTT	81	1	μM
dUpNHpp	HT29_MTT	84	750	nM
dUpNHpp	HT29_MTT	82	500	nM
dUpNHpp	HT29_MTT	83	100	nM
238	HT29_MTT	87	20	μM
238	HT29_MTT	83	2,5	μM
238	HT29_MTT	84	100	nM
118	HT29_MTT	87	20	μM
118	HT29_MTT	82	2,5	μM
118	HT29_MTT	80	100	nM
218	HT29_MTT	88	20	μM
218	HT29_MTT	80	2,5	μM
218	HT29_MTT	81	100	nM
208	HT29_MTT	85	20	μM
208	HT29_MTT	83	2,5	μM
208	HT29_MTT	82	100	nM
212	HT29_MTT	83	20	μM
212	HT29_MTT	81	2,5	μM
212	HT29_MTT	76	100	nM
242	HT29_MTT	94	20	μM

242	HT29_MTT	87	2,5	μM
242	HT29_MTT	82	100	nM
242	HT29_MTT	90	20	μM
242	HT29_MTT	84	2,5	μM
242	HT29_MTT	80	100	nM
226	HT29_MTT	88	20	μM
226	HT29_MTT	87	2,5	μM
226	HT29_MTT	79	100	nM
332	HT29_MTT	83	20	μM
332	HT29_MTT	80	2,5	μM
332	HT29_MTT	77	100	nM
233	HT29_MTT	83	20	μM
233	HT29_MTT	79	2,5	μM
233	HT29_MTT	79	100	nM
231	HT29_MTT	87	20	μM
231	HT29_MTT	80	2,5	μM
231	HT29_MTT	80	100	nM
235	HT29_MTT	81	20	μM
235	HT29_MTT	81	2,5	μM
235	HT29_MTT	81	100	nM
236	HT29_MTT	87	20	μM
236	HT29_MTT	82	2,5	μM
236	HT29_MTT	81	100	nM
232	HT29_MTT	87	20	μM
232	HT29_MTT	81	2,5	μM
232	HT29_MTT	78	100	nM
228	HT29_MTT	88	20	μM
228	HT29_MTT	76	2,5	μM
228	HT29_MTT	78	100	nM

230	HT29_MTT	87	20	μM
230	HT29_MTT	80	2,5	μM
230	HT29_MTT	78	100	nM

Table 34: Cytotoxicity tests of MCF7 cells treated with 10 μM dUTPase inhibitor.

COMPOUND	ASSAY_NAME	SURVIVAL	CONCENTRATION	CONC_UNITS
238	HT29_MTT	101	10	μM
118	HT29_MTT	98	10	μM
218	HT29_MTT	98	10	μM
208	HT29_MTT	102	10	μM
212	HT29_MTT	97	10	μM
242	HT29_MTT	99	10	nM
242	HT29_MTT	98	10	nM
226	HT29_MTT	98	10	nM
332	HT29_MTT	102	10	μM
233	HT29_MTT	100	10	μM
231	HT29_MTT	99	10	μM
235	HT29_MTT	100	10	μM
236	HT29_MTT	101	10	μM
232	HT29_MTT	112	10	nM
228	HT29_MTT	95	10	nM
230	HT29_MTT	94	10	nM
dUpNHpp	HT29_MTT	99	10	μM

TKI cell assay

Cell based dUTPase inhibitor screenings were conducted by **Marbio/Uit Tromsø** using the CellTiter96 Aqueous One Solution Cell Proliferation assay (**MTS assay**). 48 hours cell incubation with the compounds, then measurement of the cell survival.

MV-4-11, MOLM-13, Ramos and MOLT4. were seeded at a density of 40 000 cells/well. MRC5 were seeded 6000 cells per well.

The Molt4 cells were grown and seeded in RPMI 1640 Medium supplemented with 10 % FBS and 10 ug/ml gentamicin.

The MV-4-11 cells were grown and seeded in Iscove Basal Medium supplemented with 10 % FBS and 10 ug/ml gentamicin.

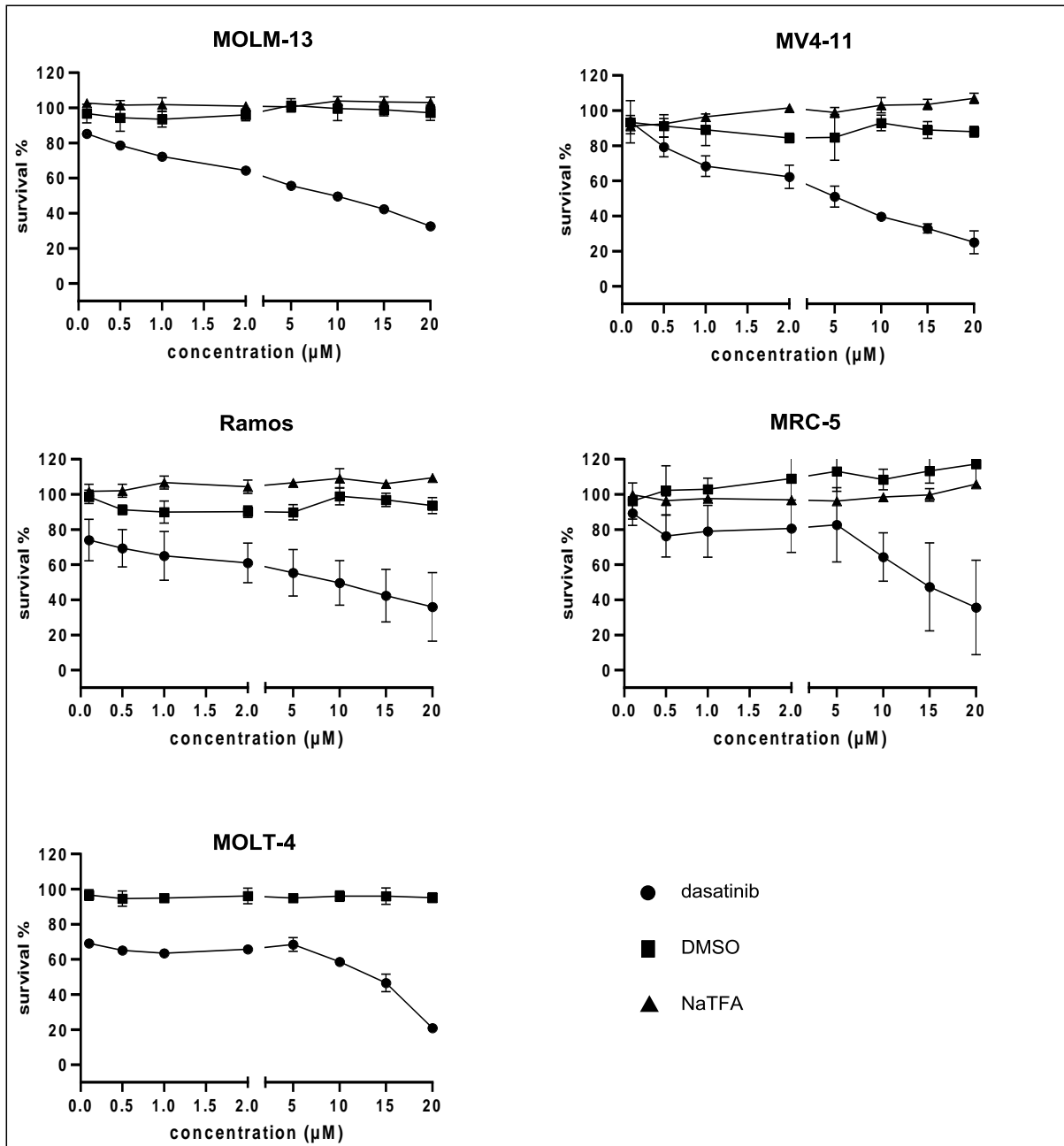


Figure 59: References TKI cell assays. For details see main text.

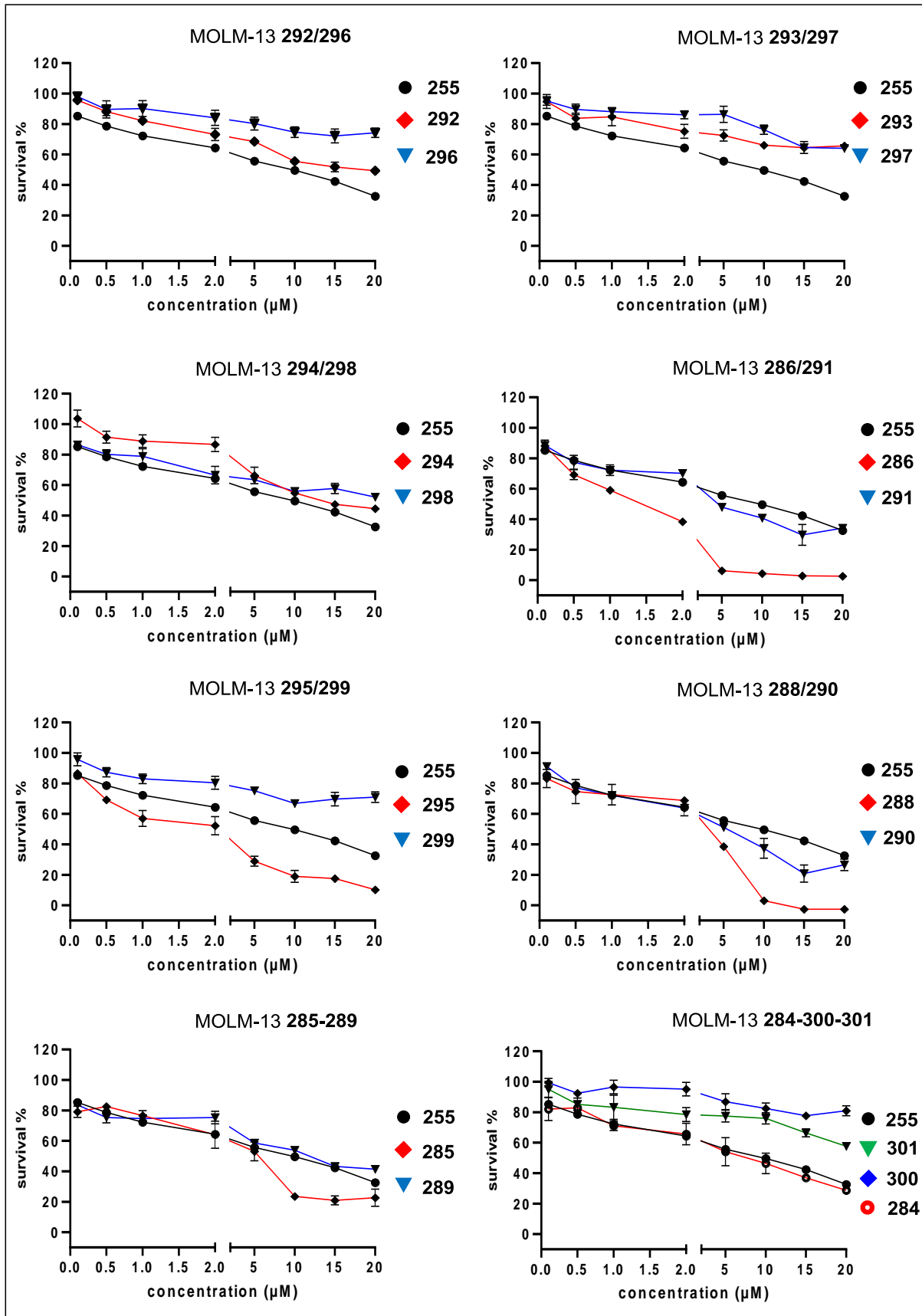


Figure 60 MOLM-13 TKI cell assays. For details see main text.

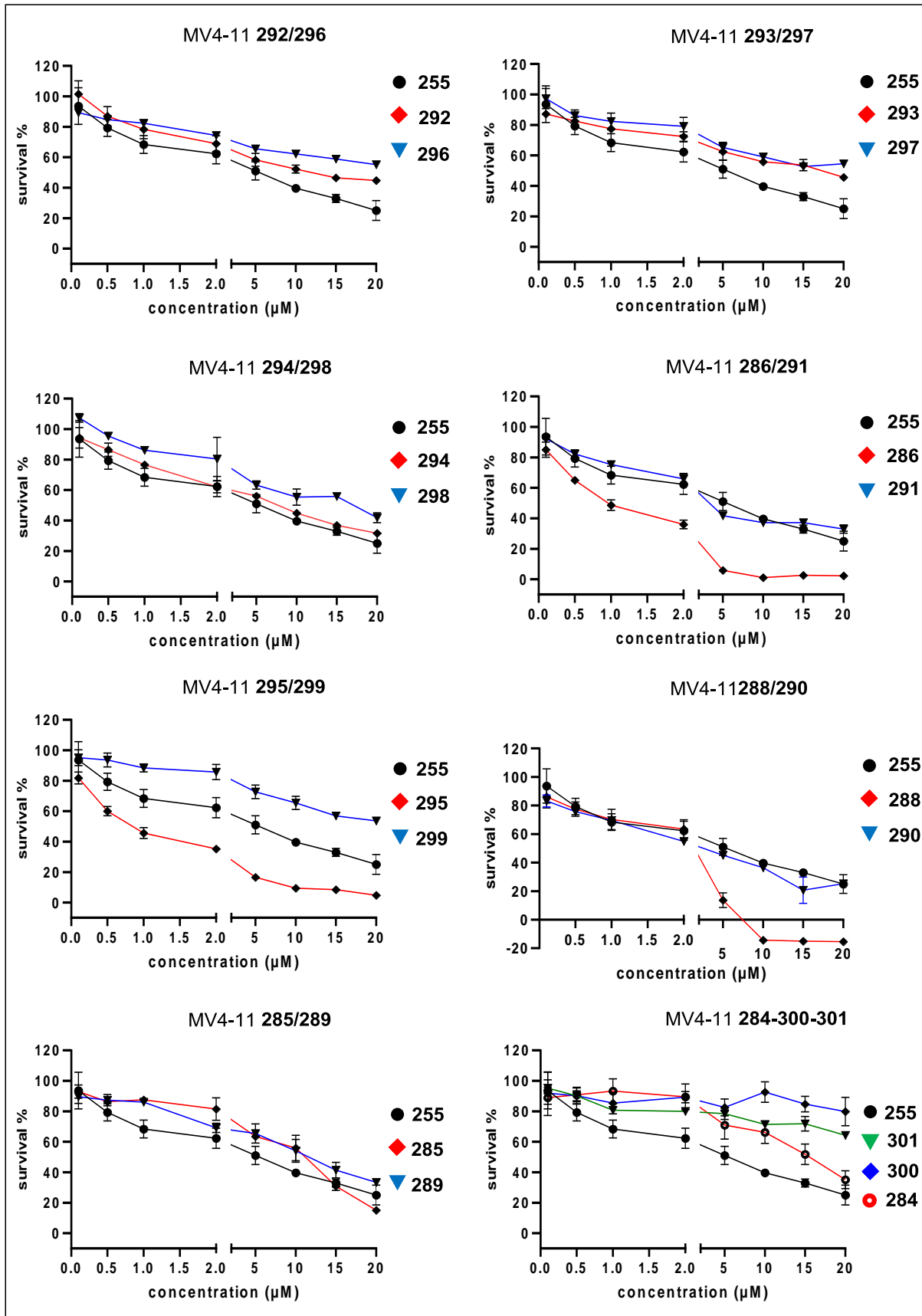


Figure 61: MV4-11 TKI cell assays. For details see main text.

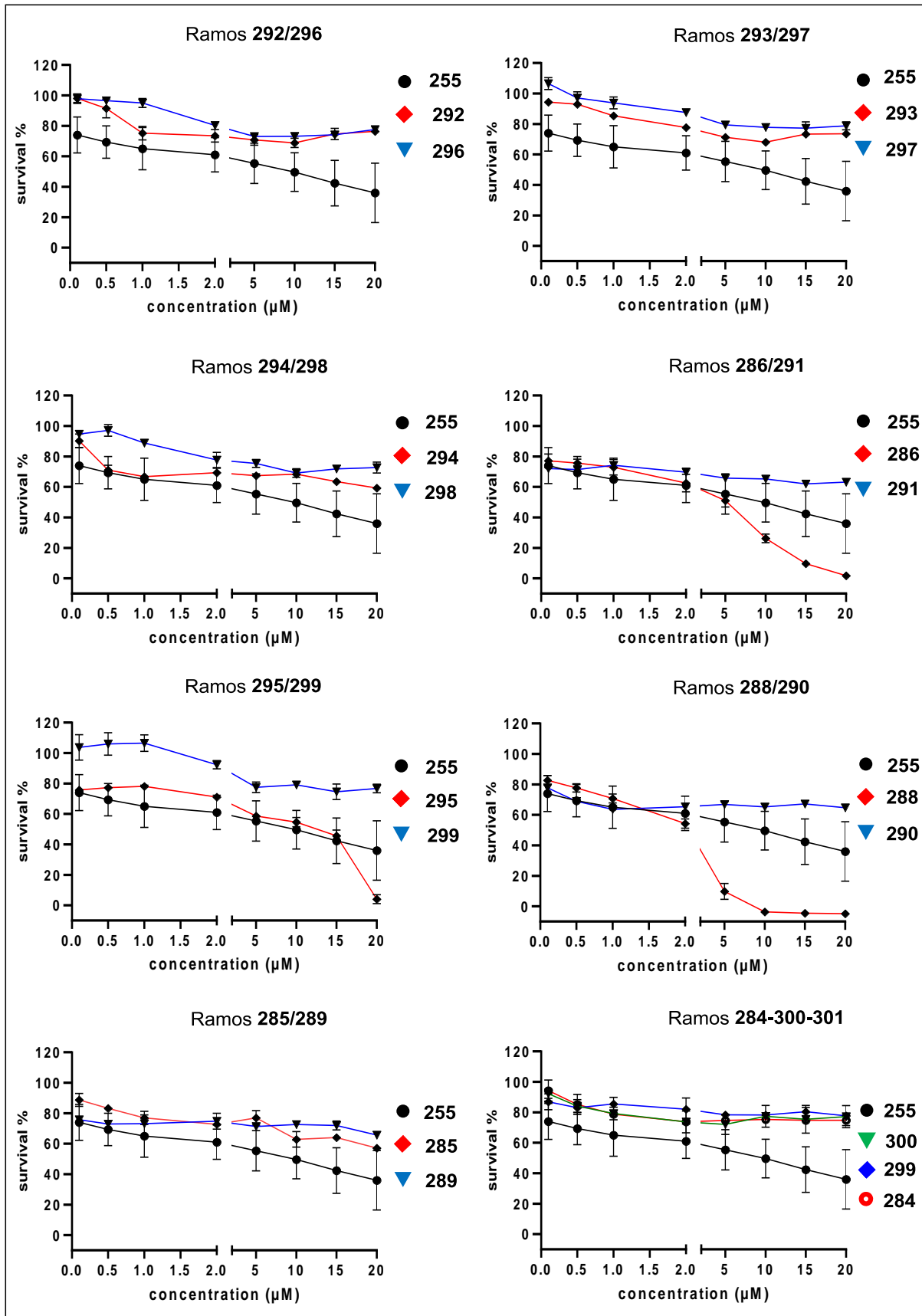


Figure 62: Ramos TKI cell assays. For details see main text.

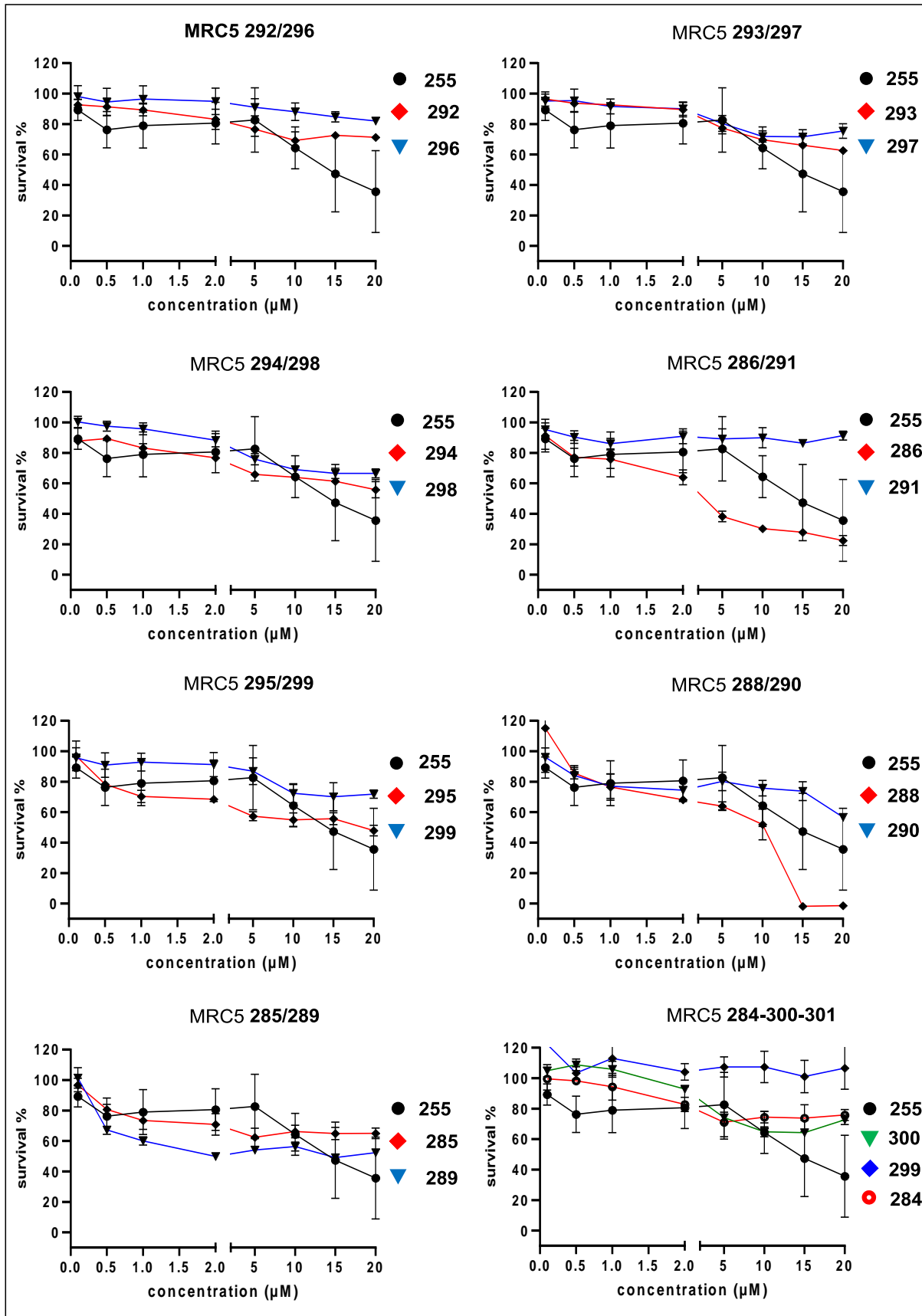


Figure 63: MRC5 TKI cell assays. For details see main text.

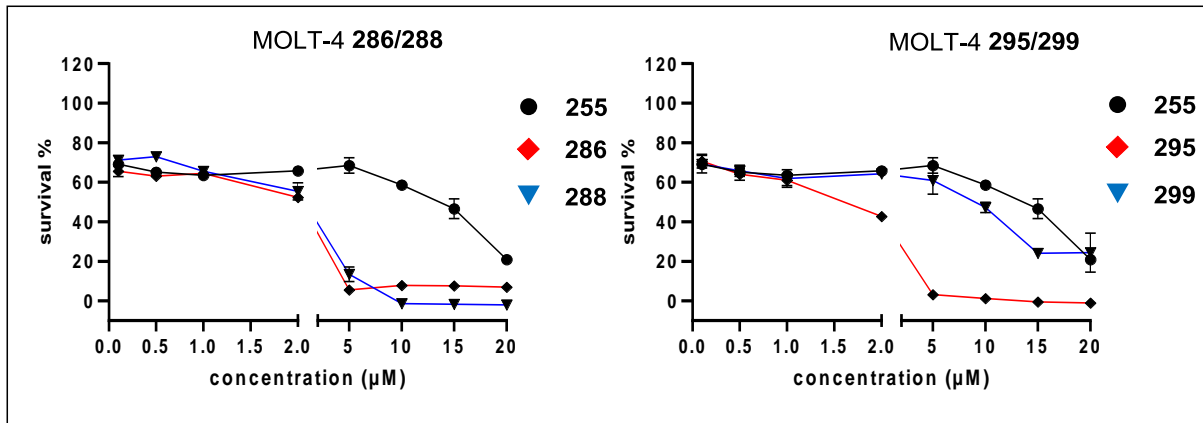
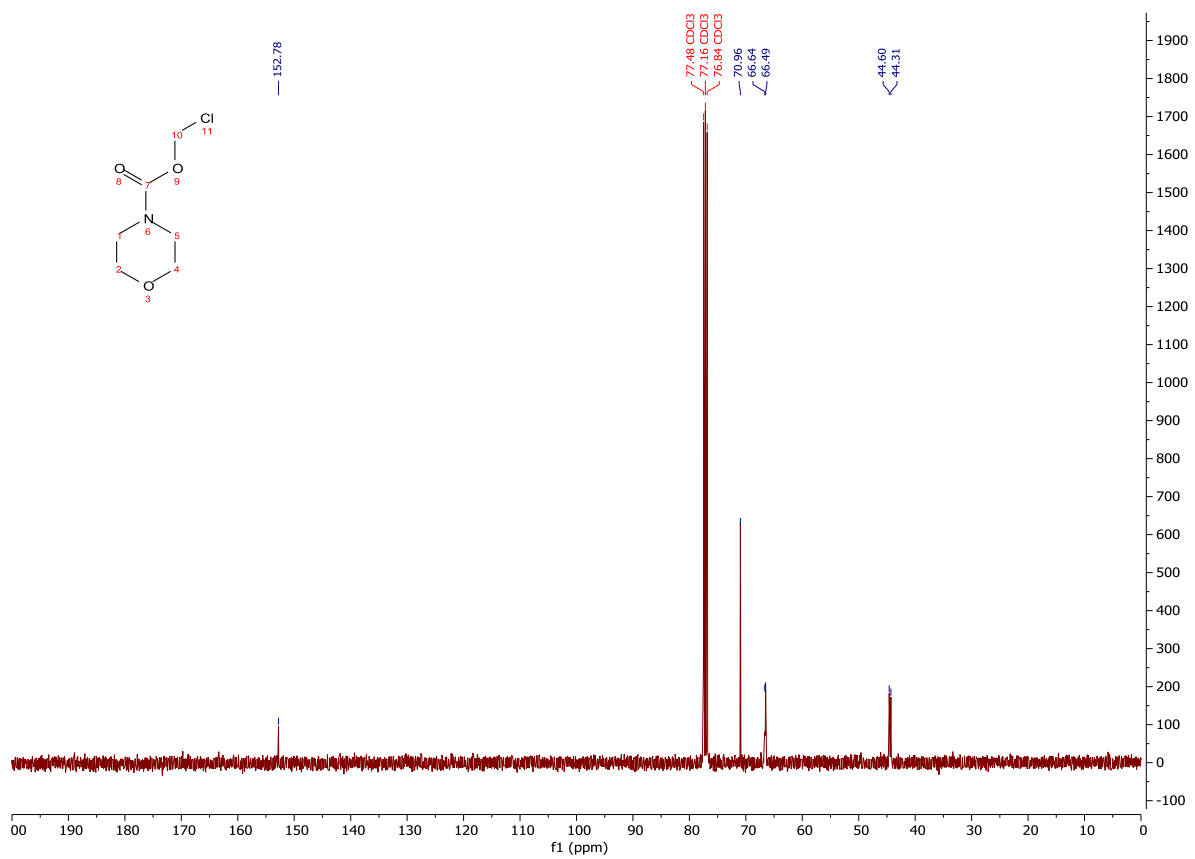
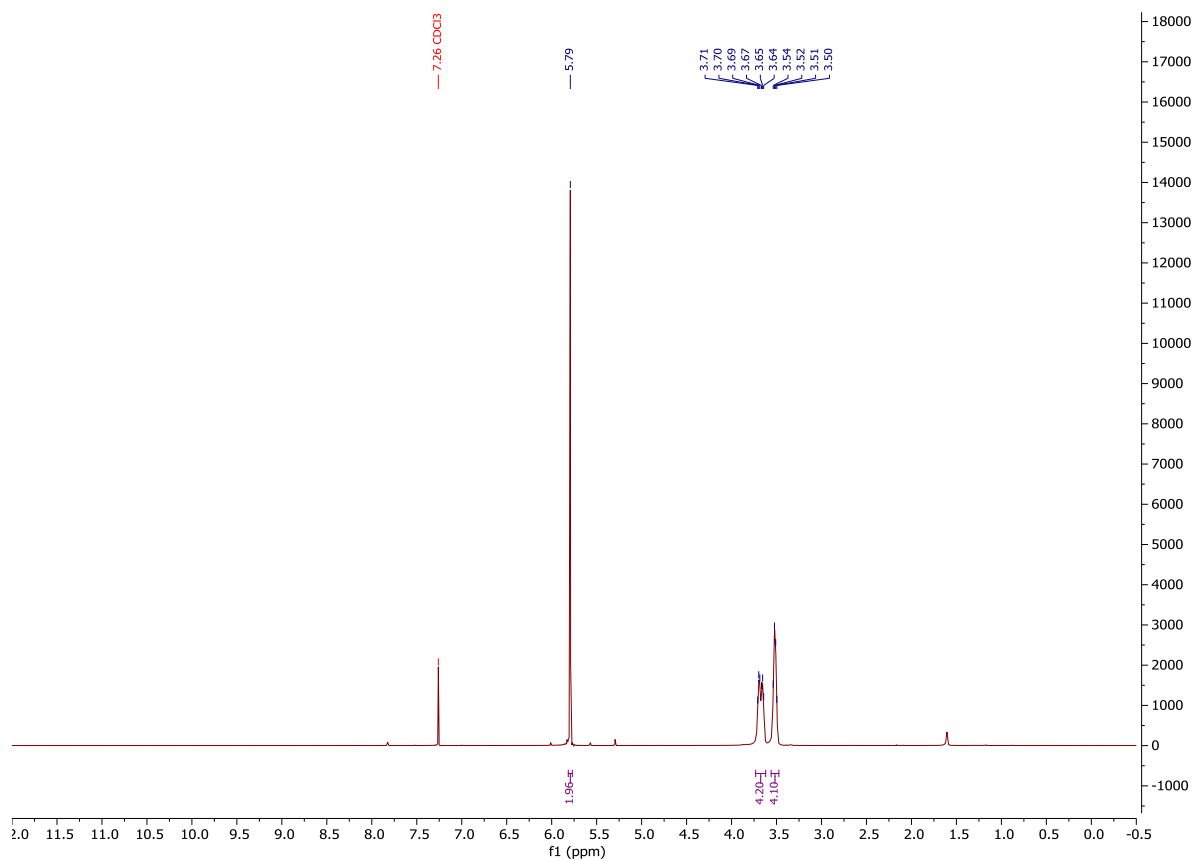


Figure 64: MOLT-4 TKI cell assays. For details see main text.

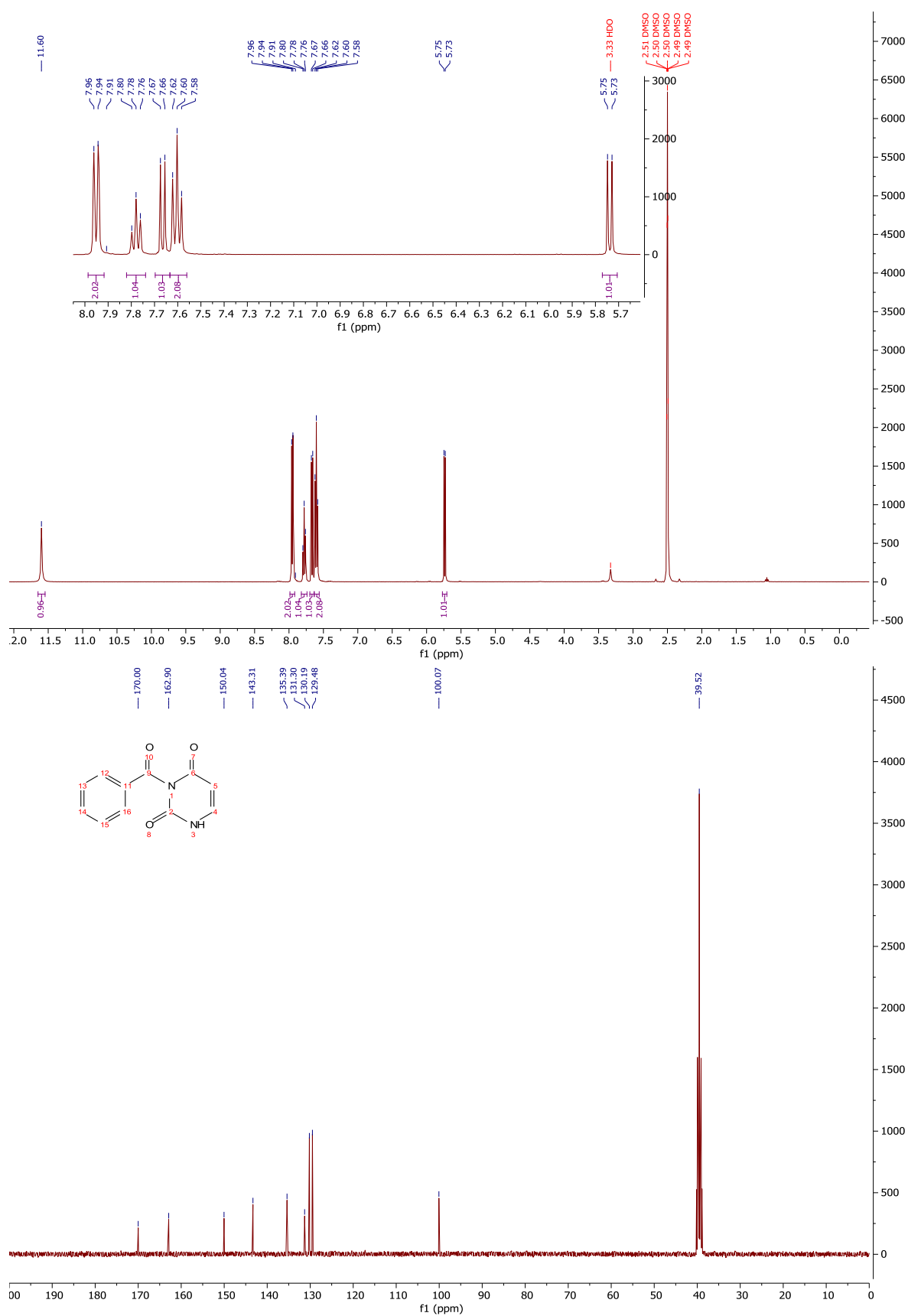
Proton and carbon NMR spectra of project 1

Uracil building blocks

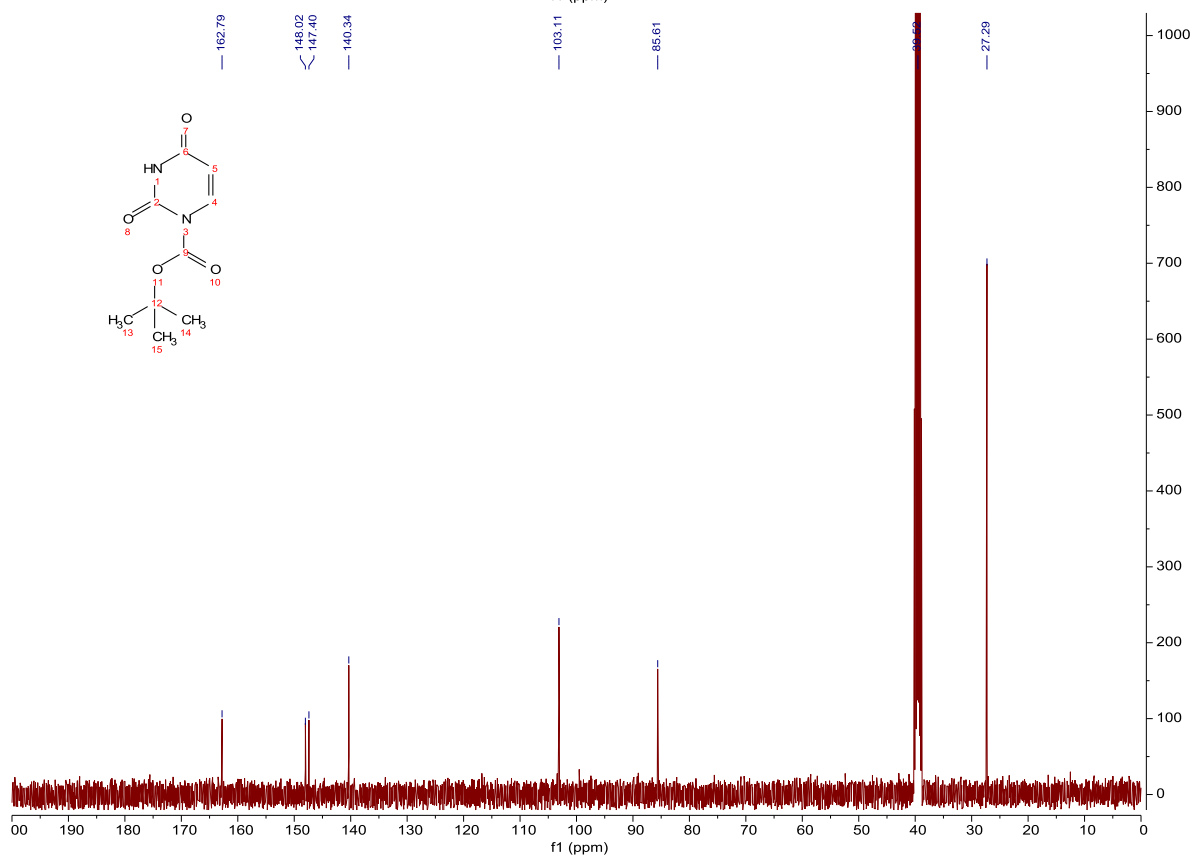
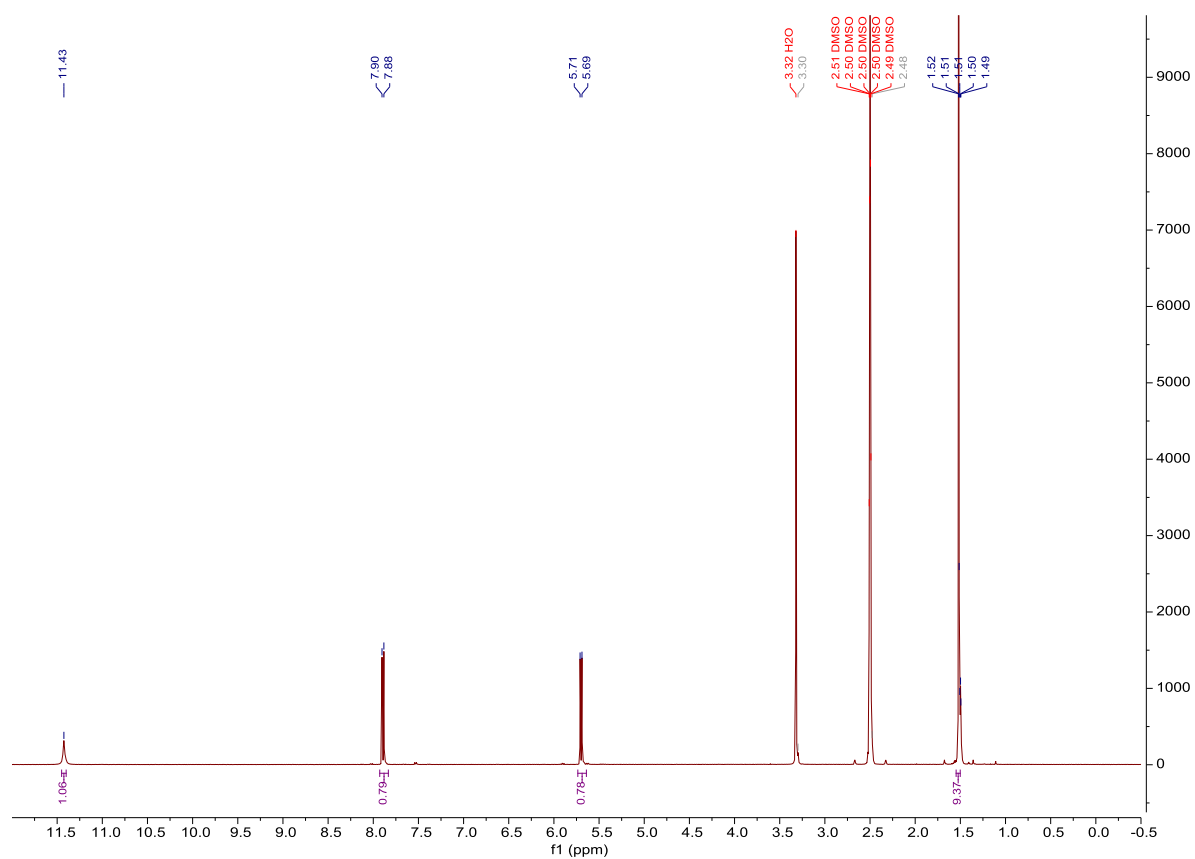
$^1\text{H-NMR}$ and $^{13}\text{C-NMR}$: Compound 076



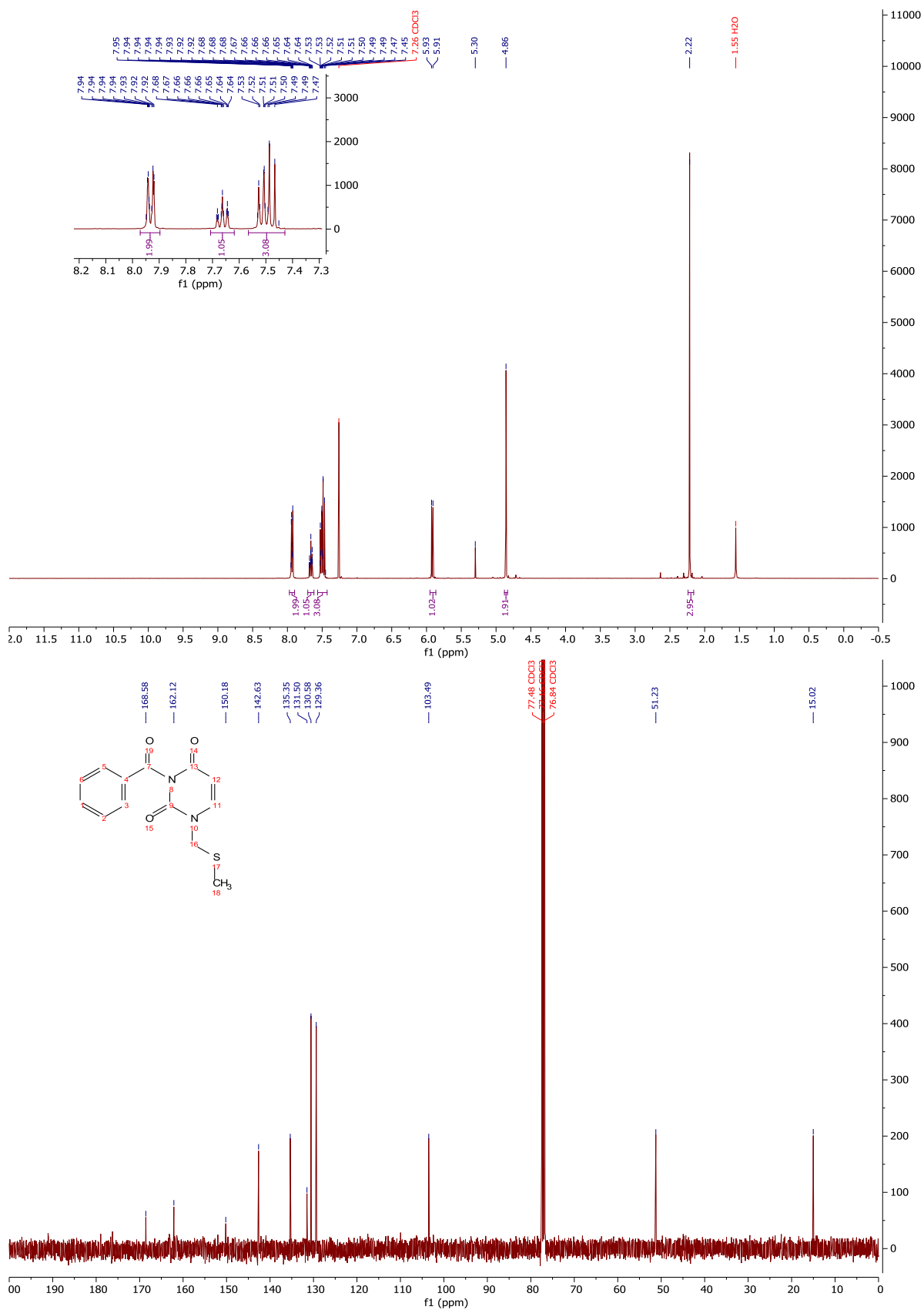
$^1\text{H-NMR}$ and $^{13}\text{C-NMR}$: Compound 53



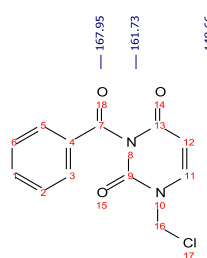
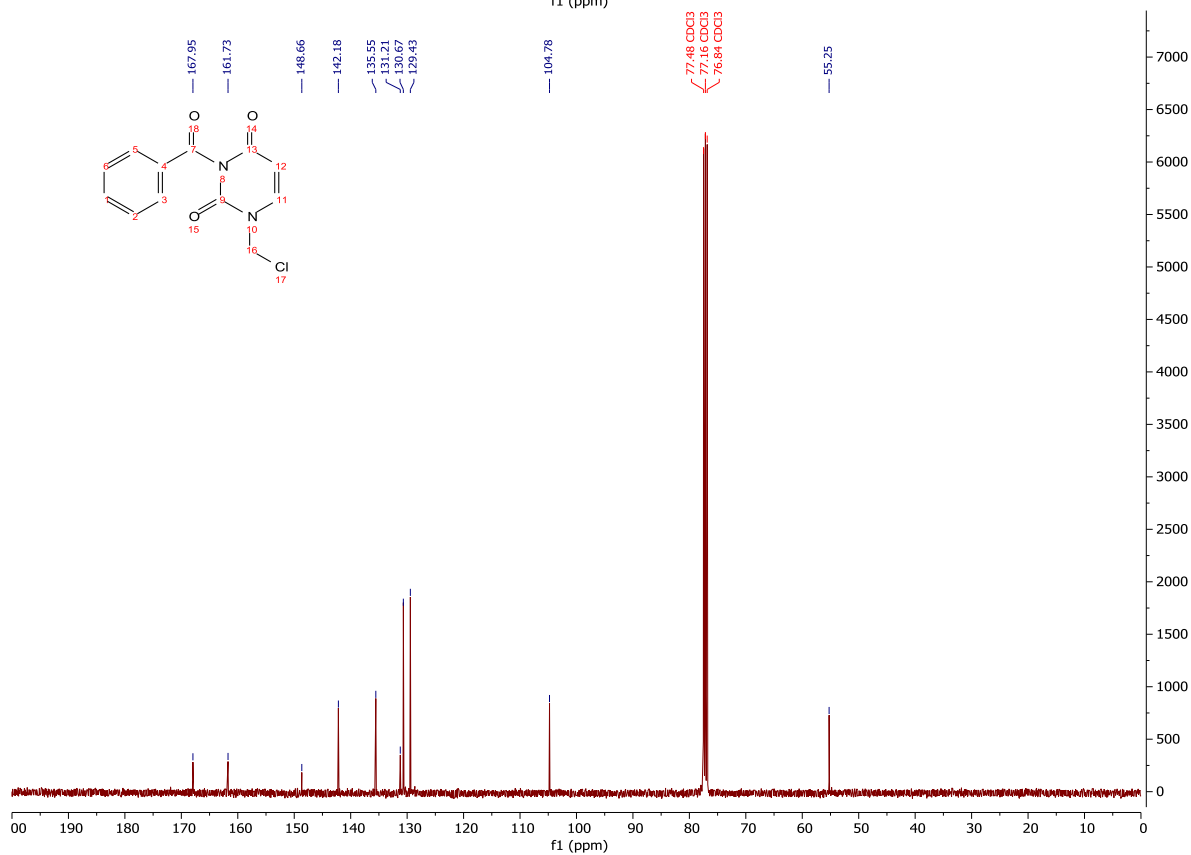
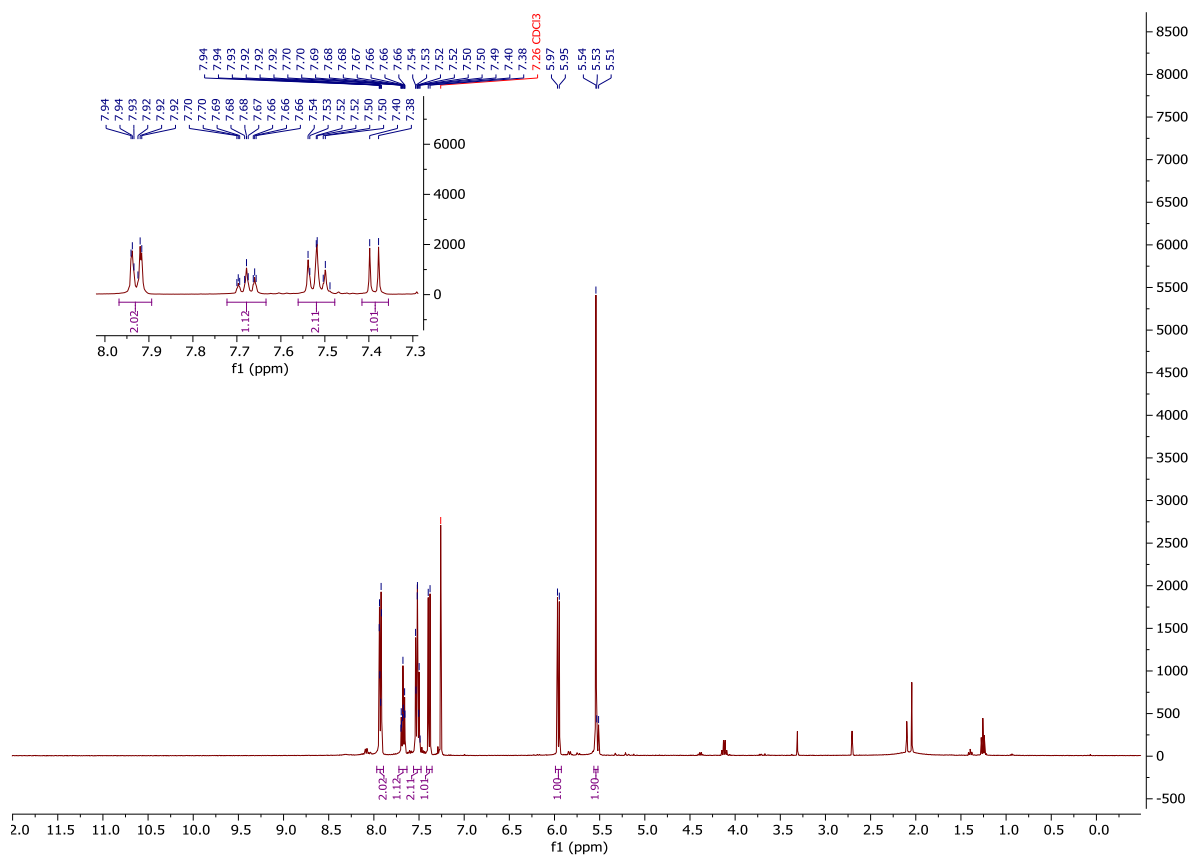
¹H-NMR and ¹³C-NMR: Compound 59



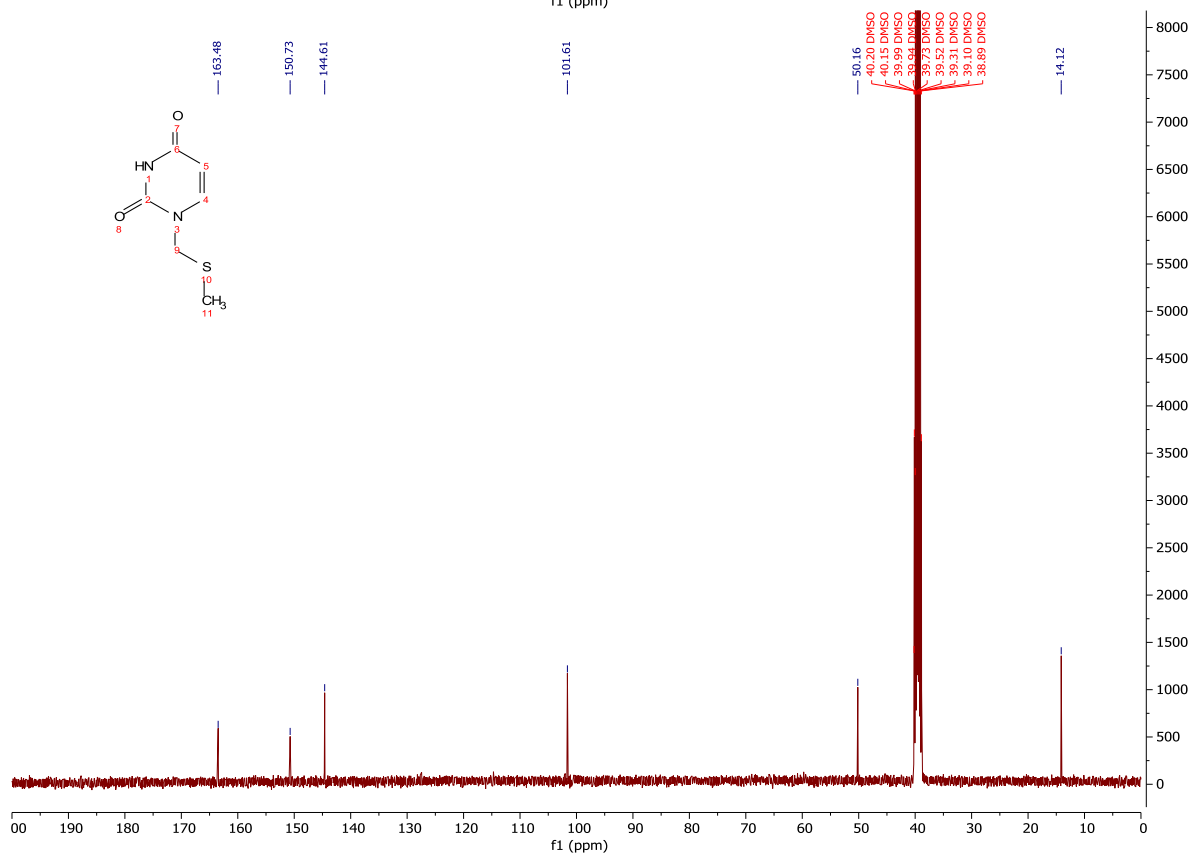
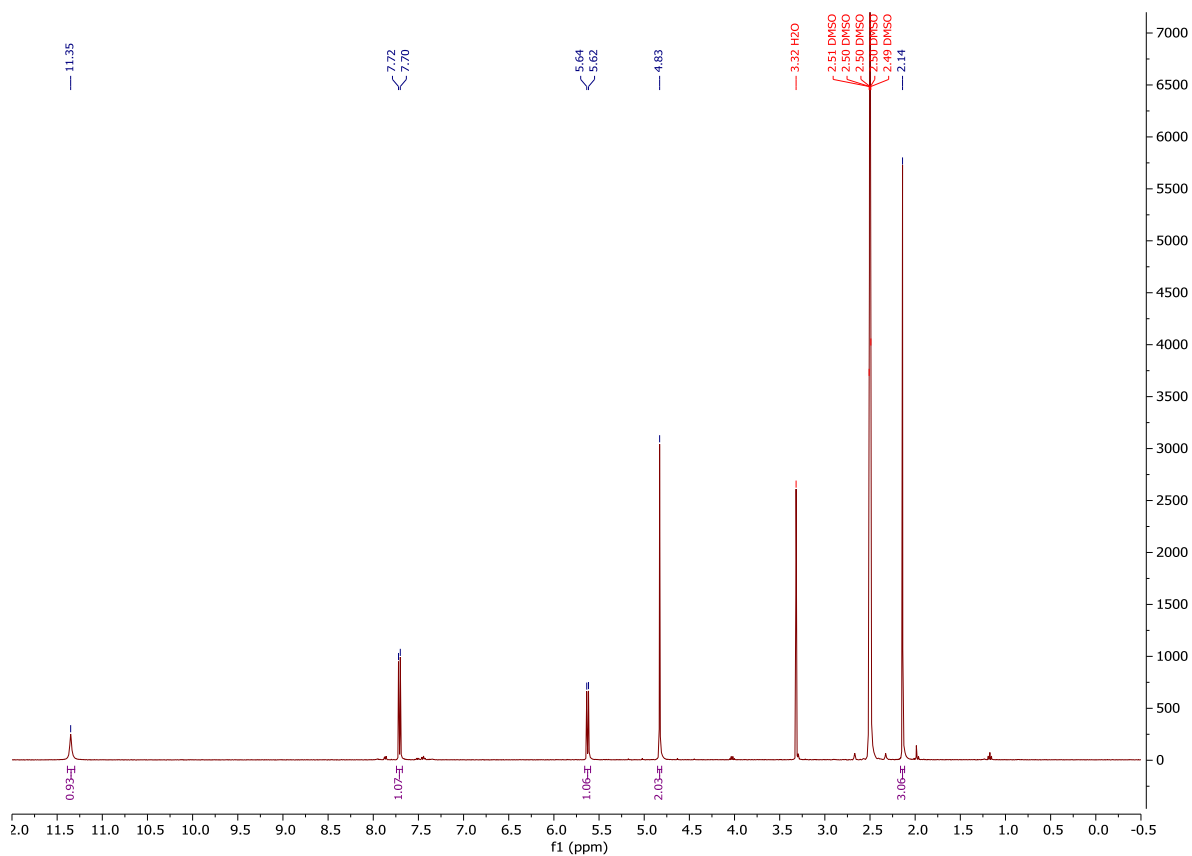
¹H-NMR and ¹³C-NMR: Compound 55



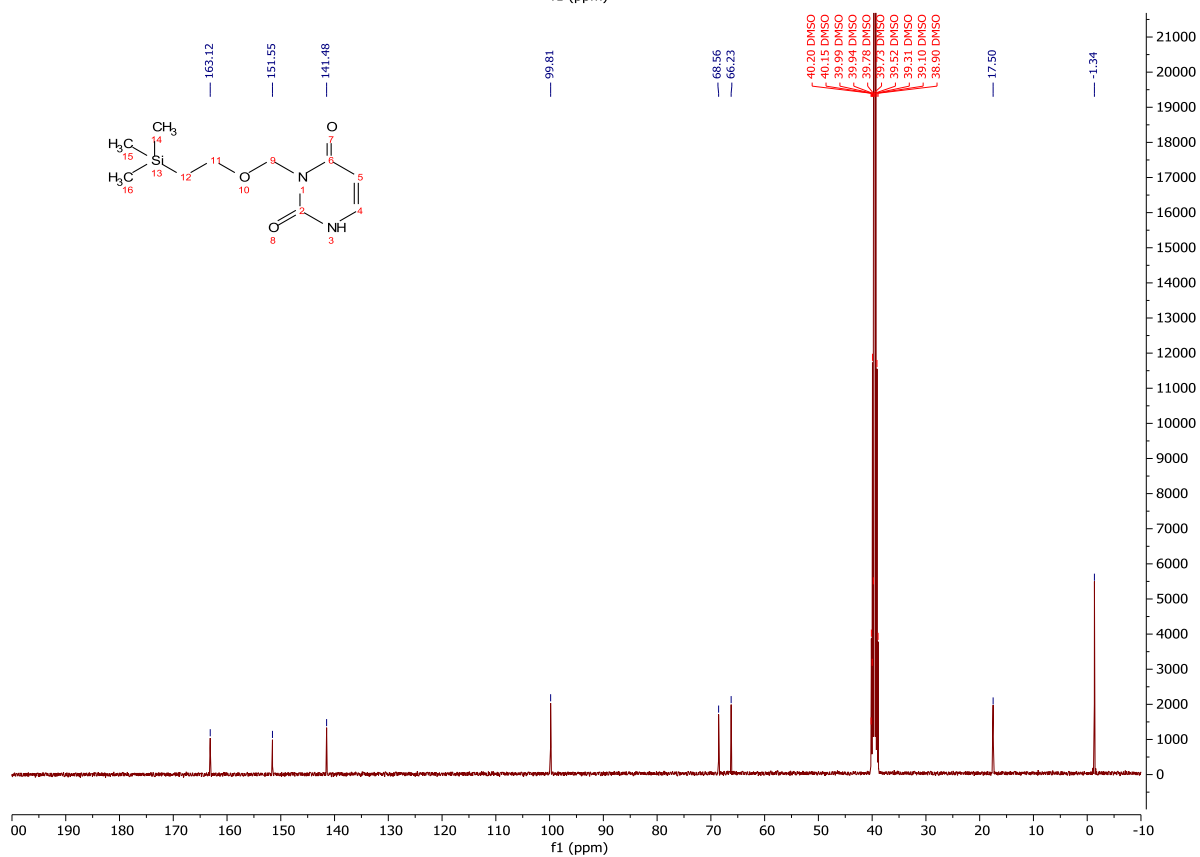
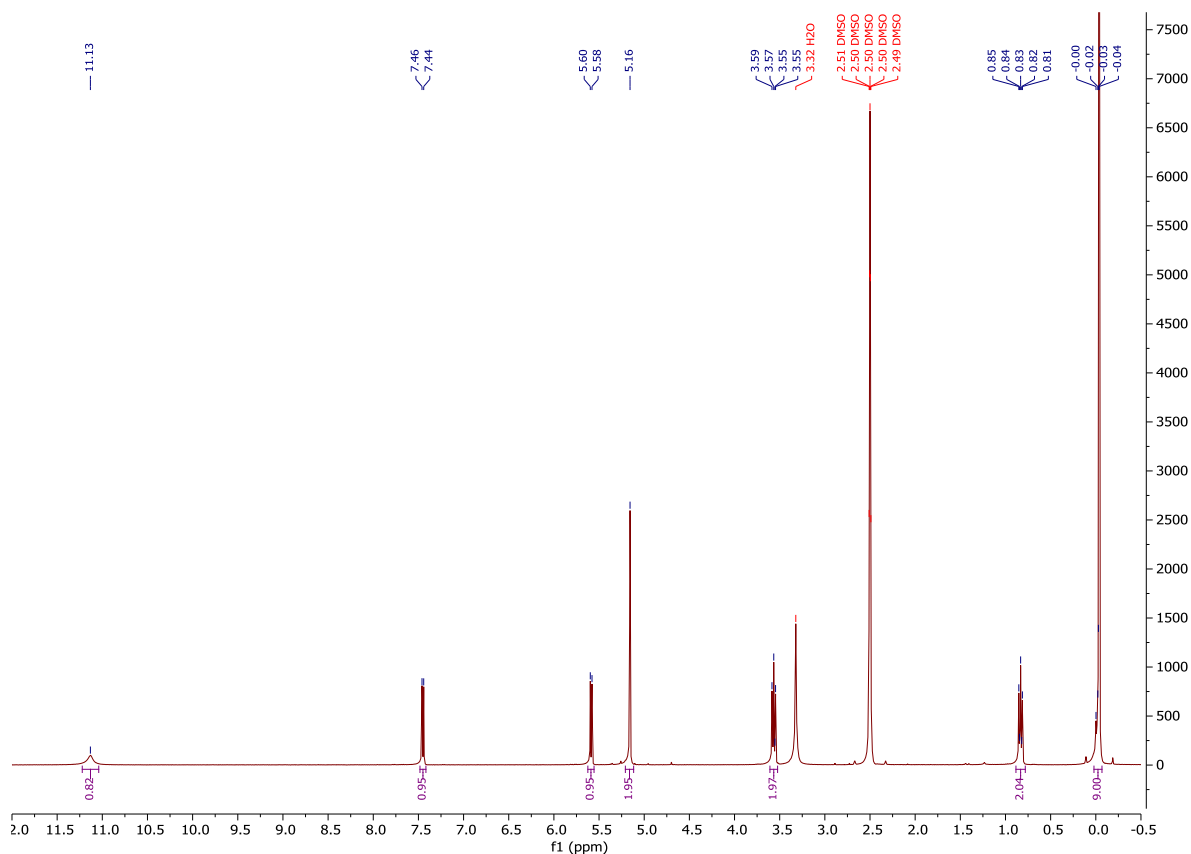
¹H-NMR and ¹³C-NMR: Compound 52



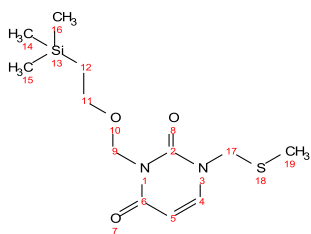
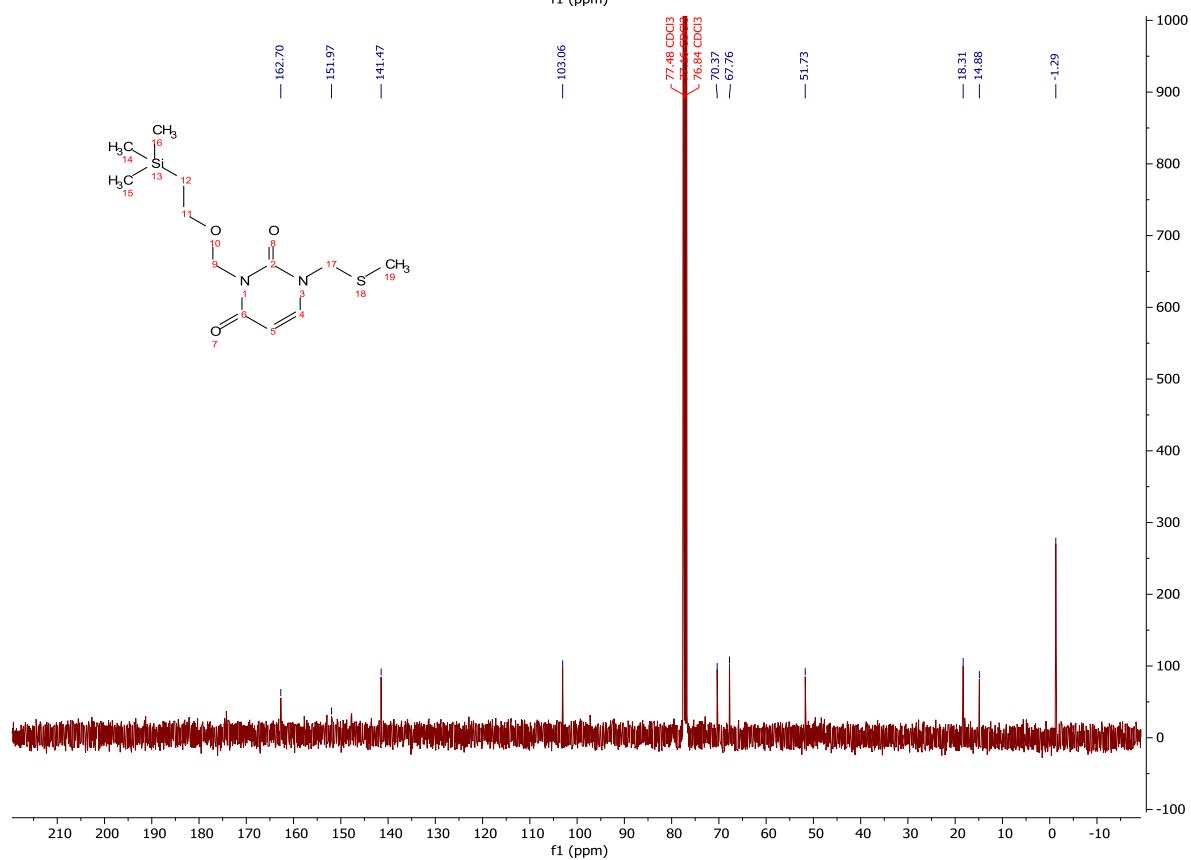
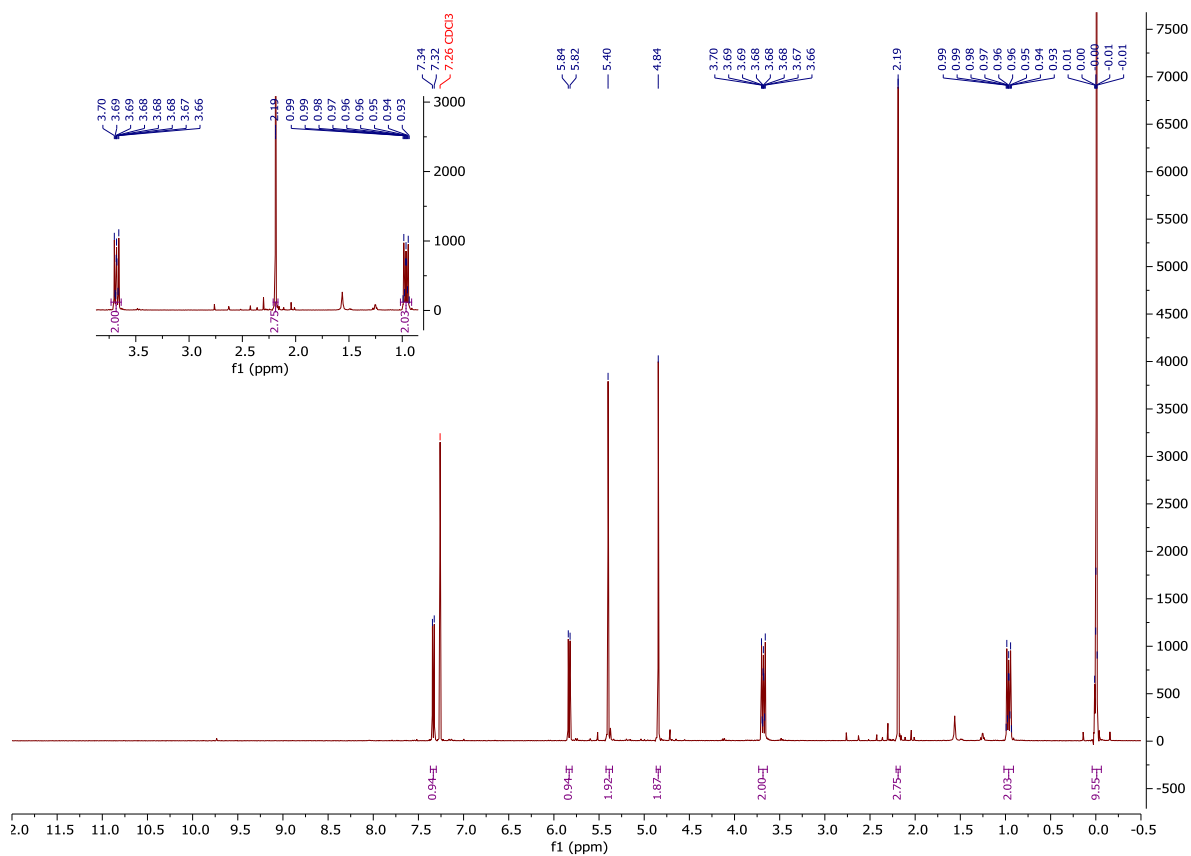
¹H-NMR and ¹³C-NMR: Compound 81



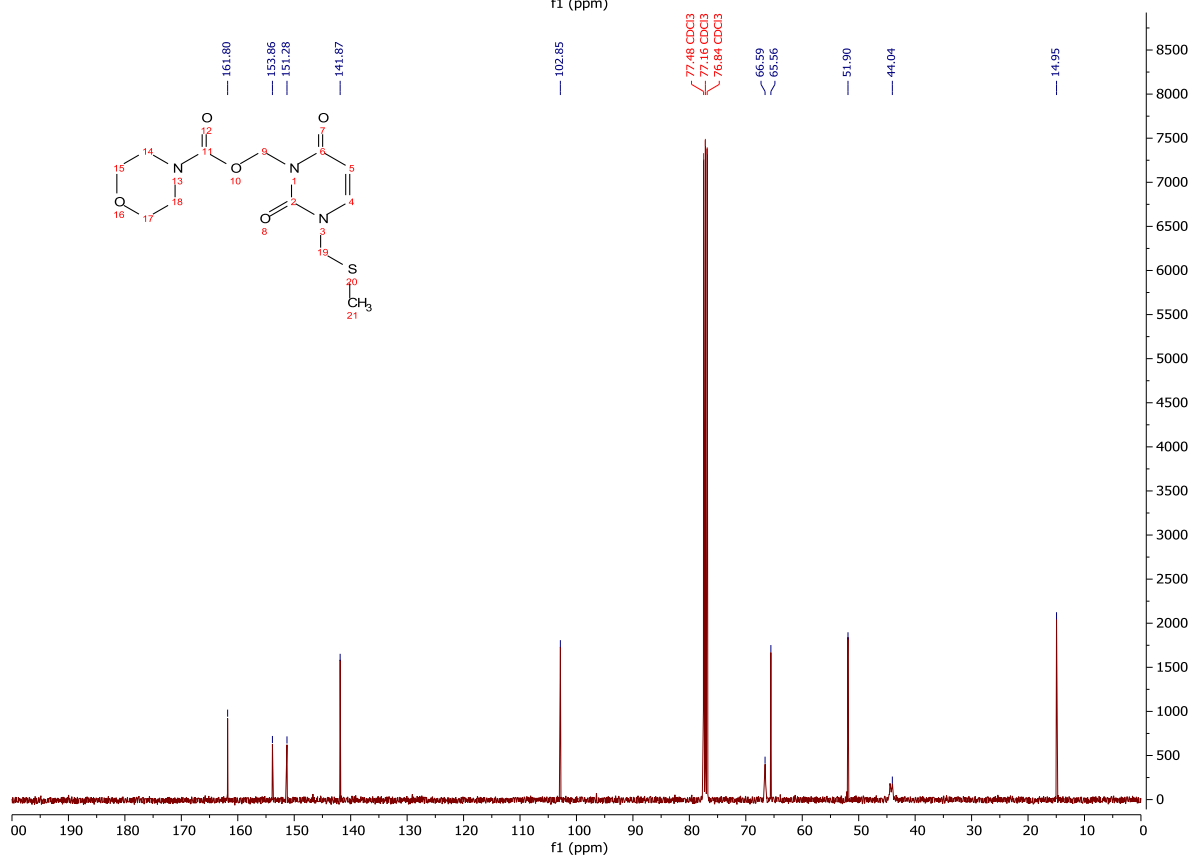
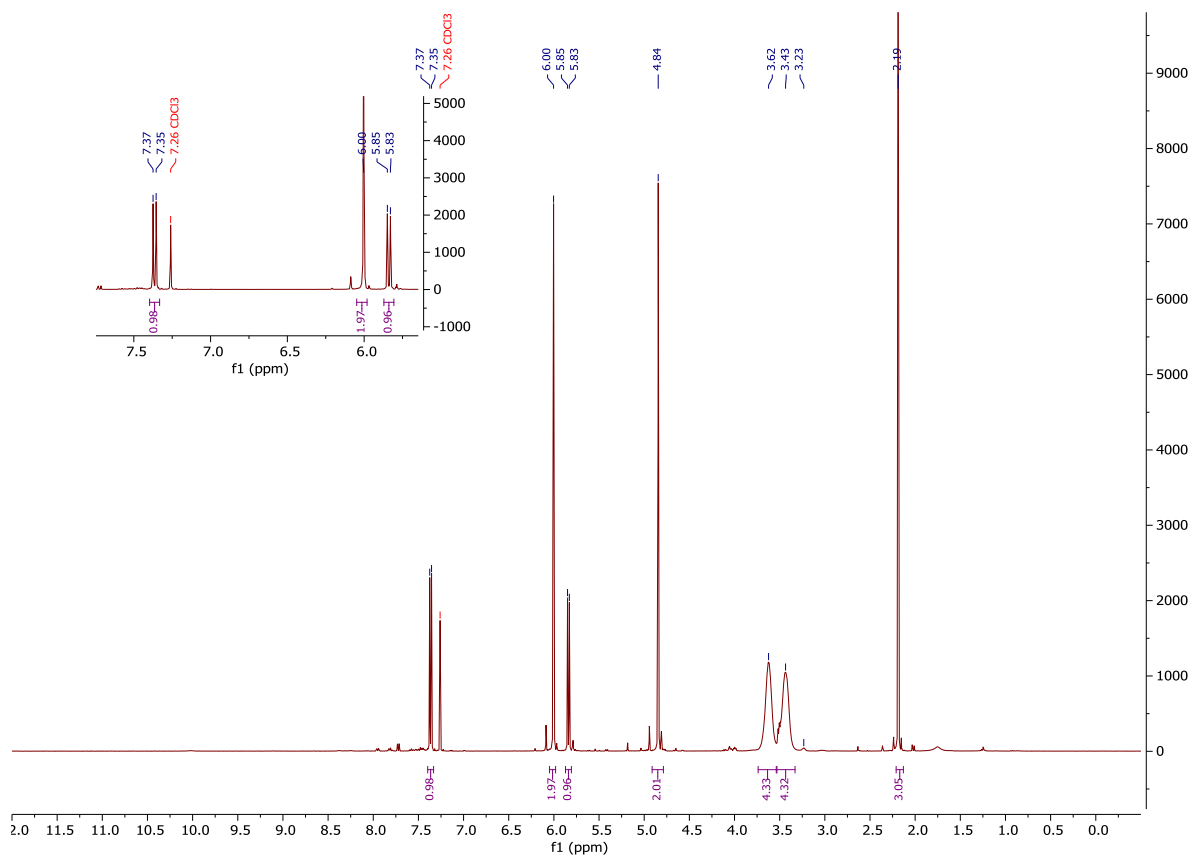
¹H-NMR and ¹³C-NMR: Compound 60



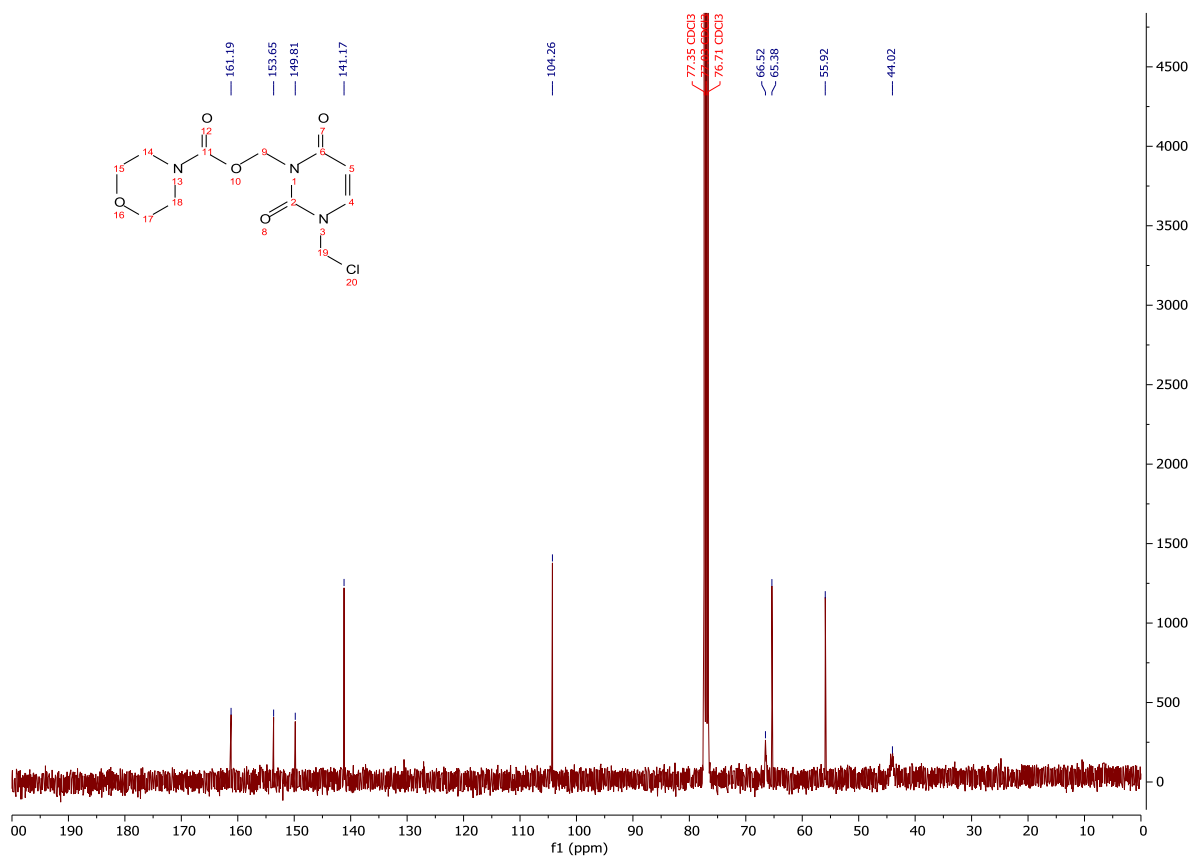
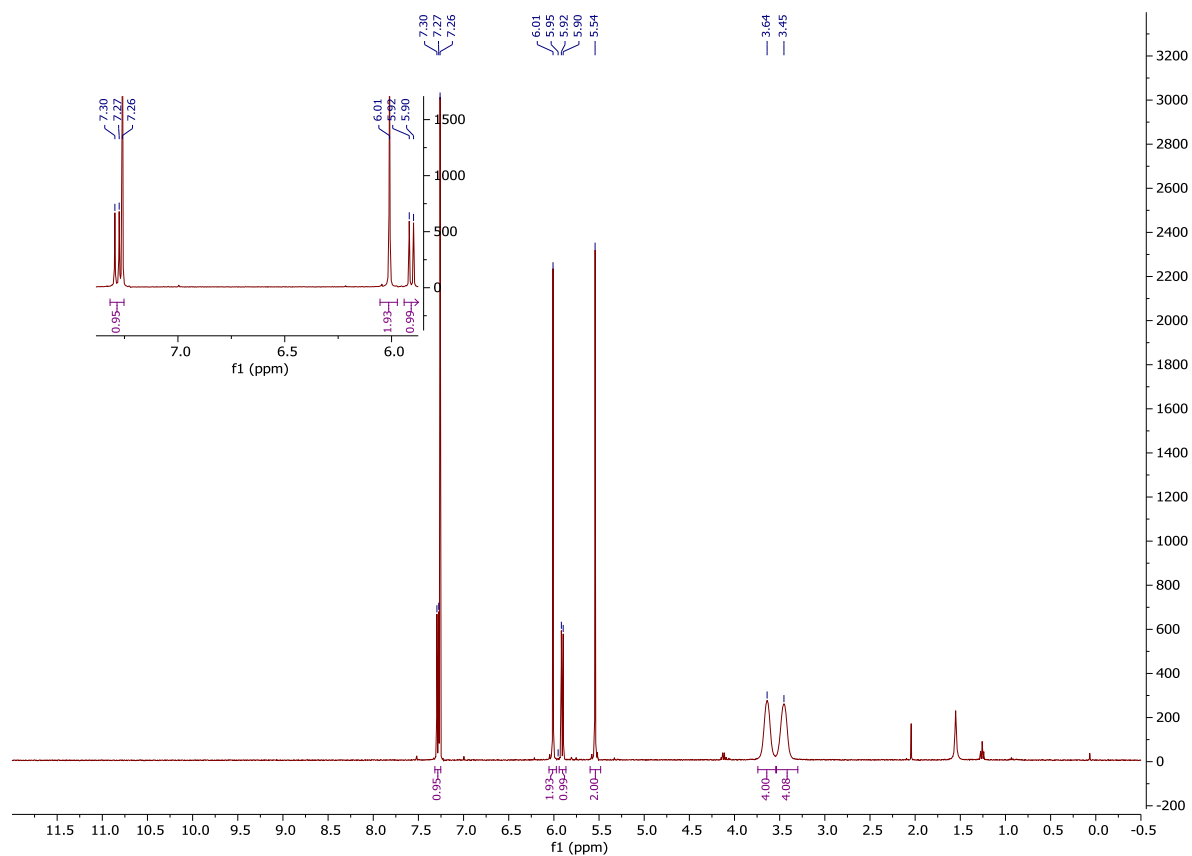
¹H-NMR and ¹³C-NMR: Compound 58



¹H-NMR and ¹³C-NMR: Compound 72

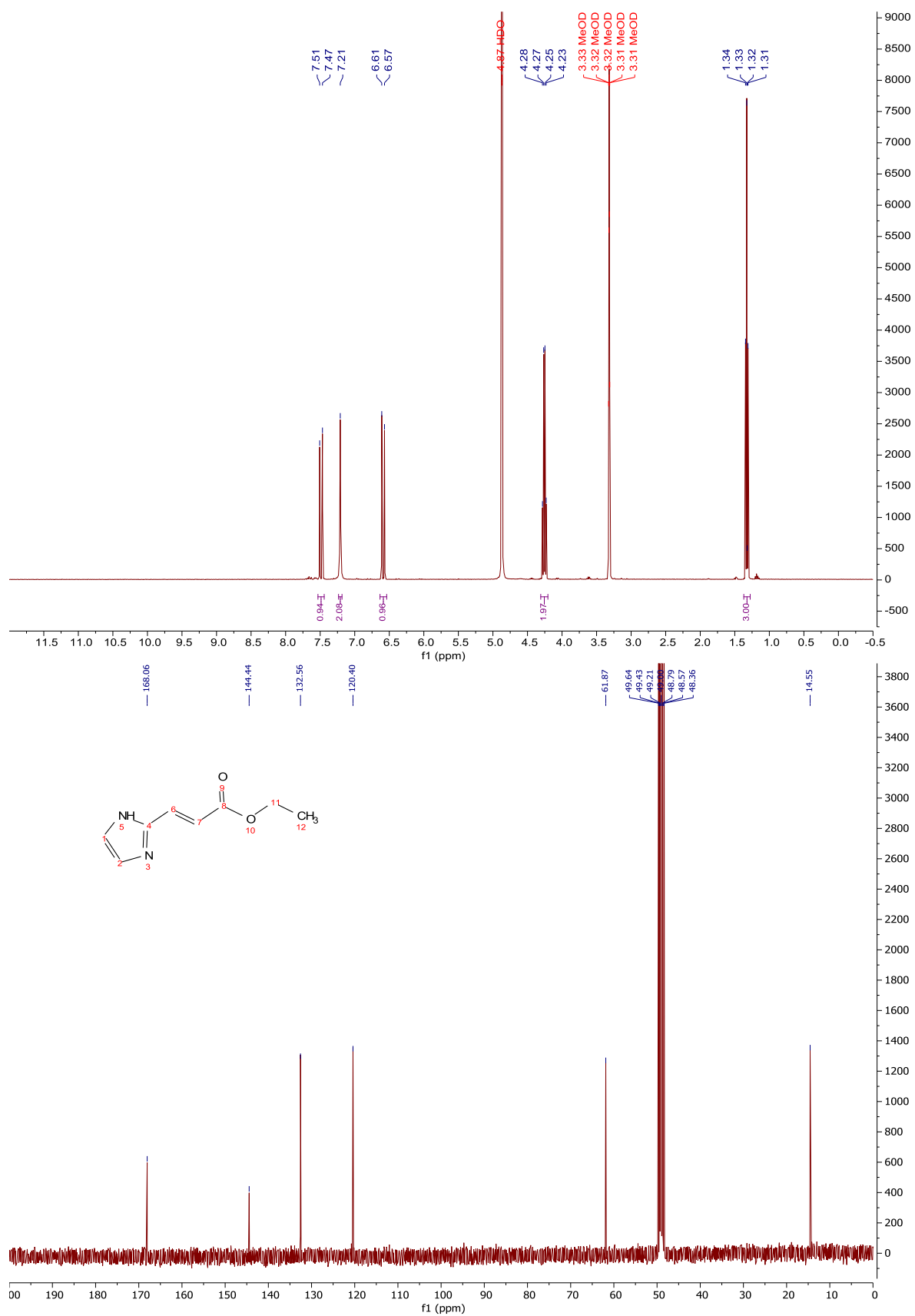


$^1\text{H-NMR}$ and $^{13}\text{C-NMR}$: Compound 70

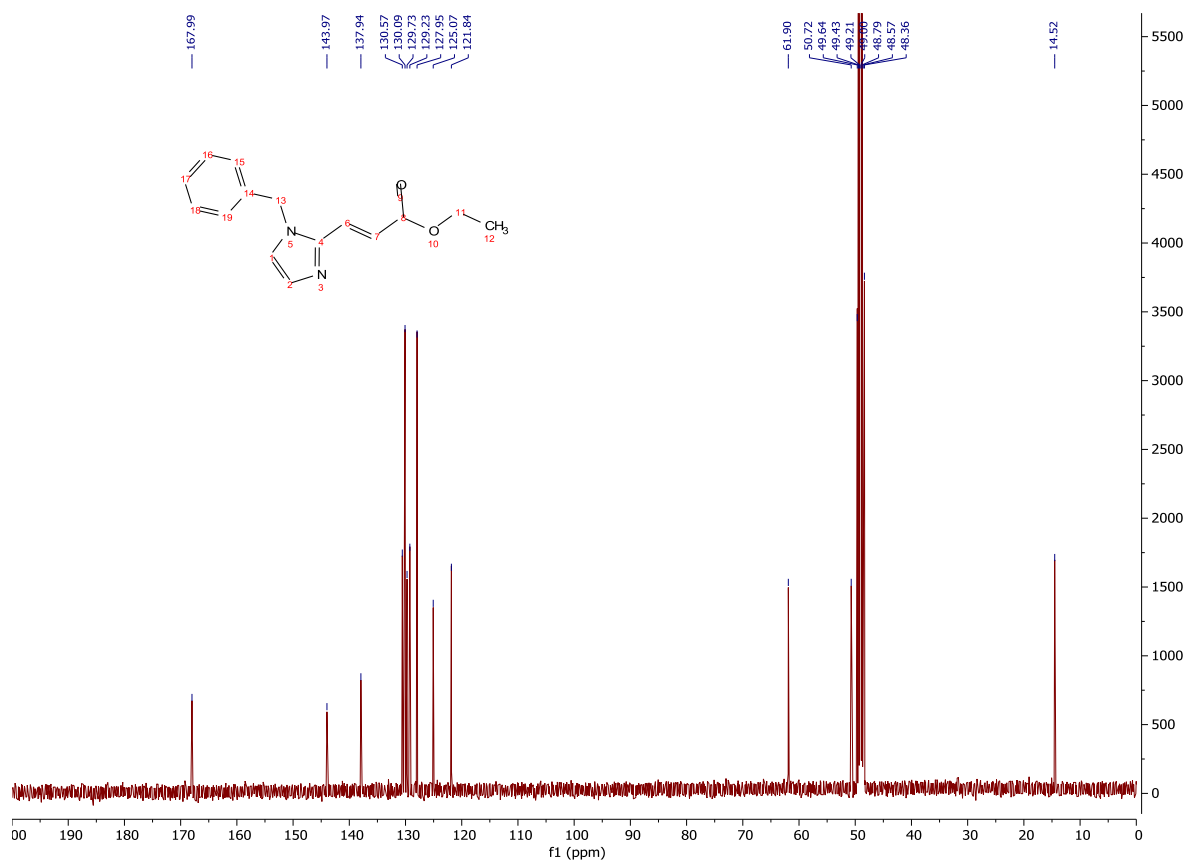
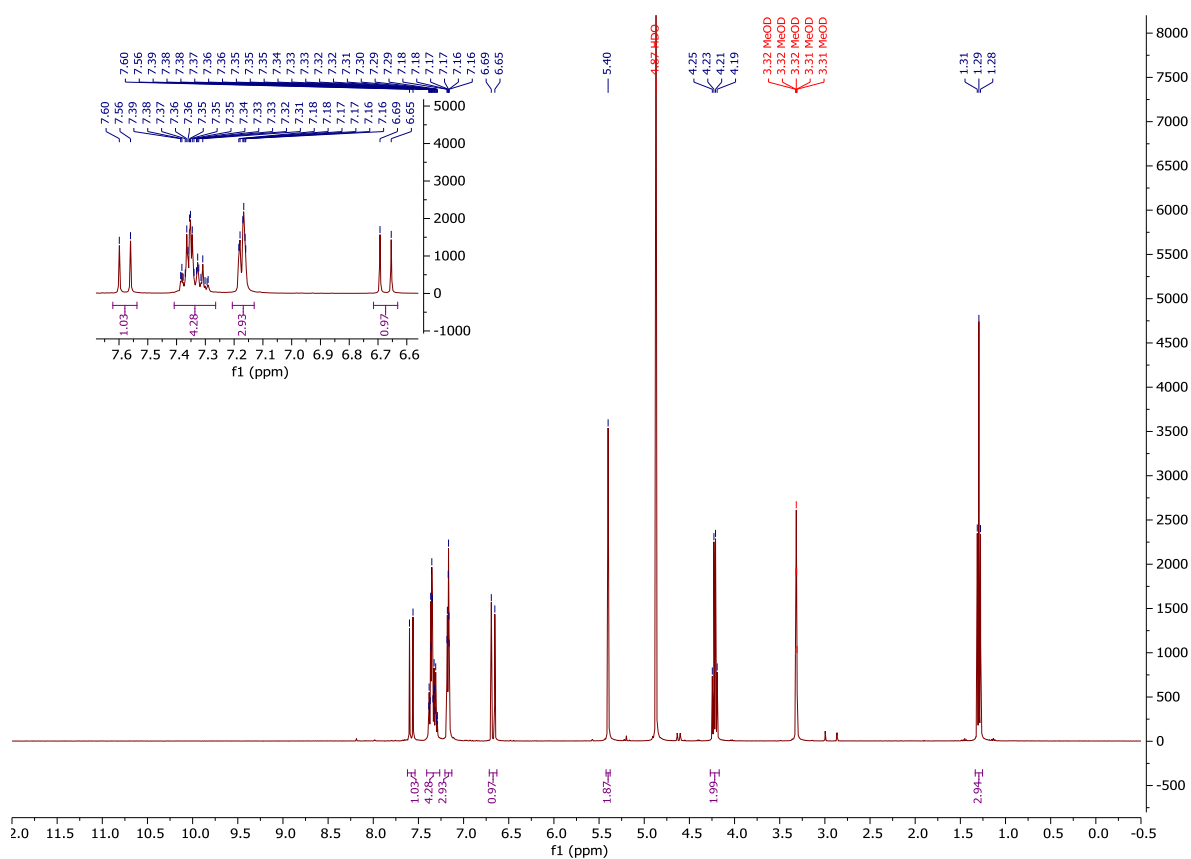


Synthesis discussed in section 4.2

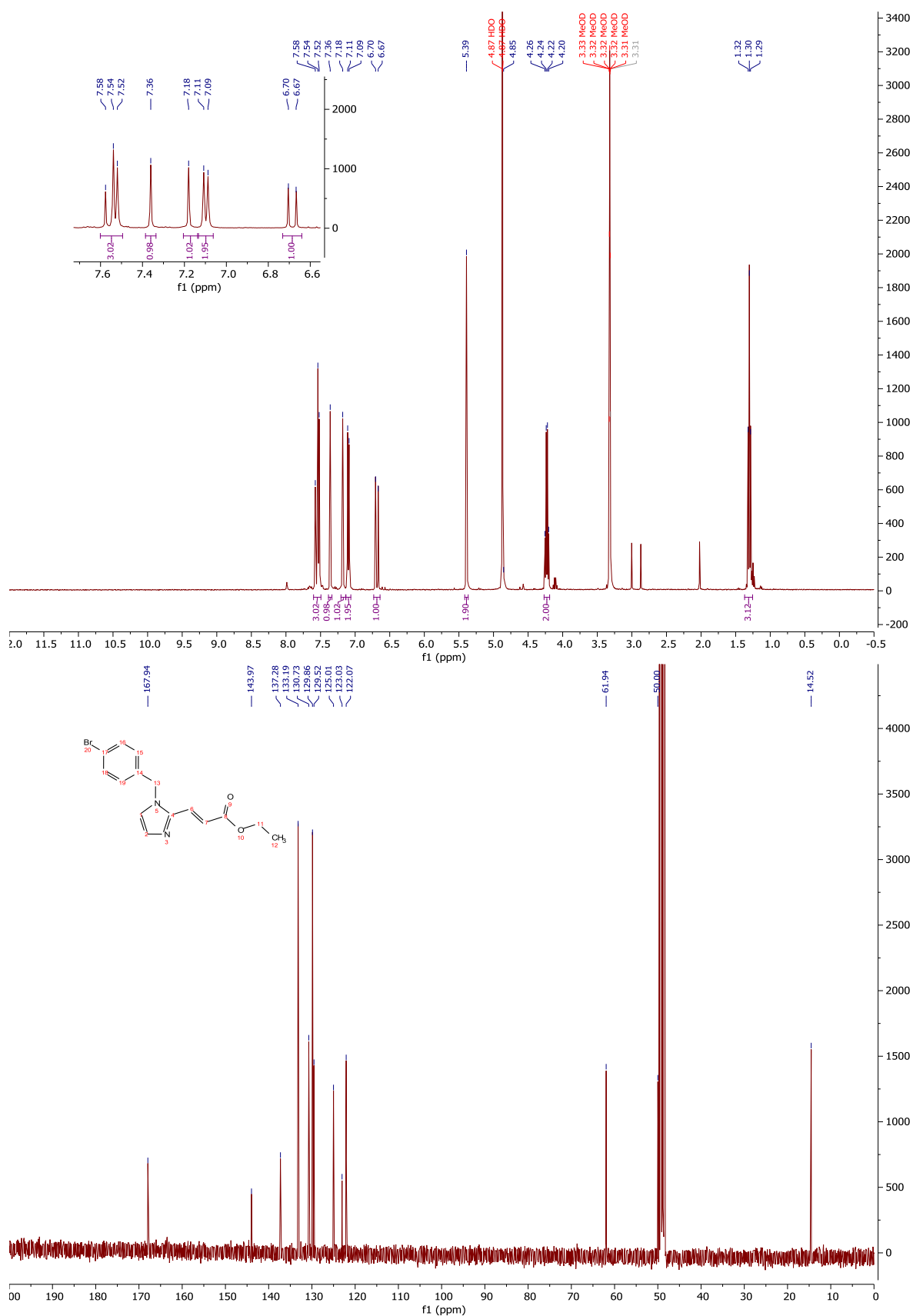
¹H-NMR and ¹³C-NMR: Compound 34



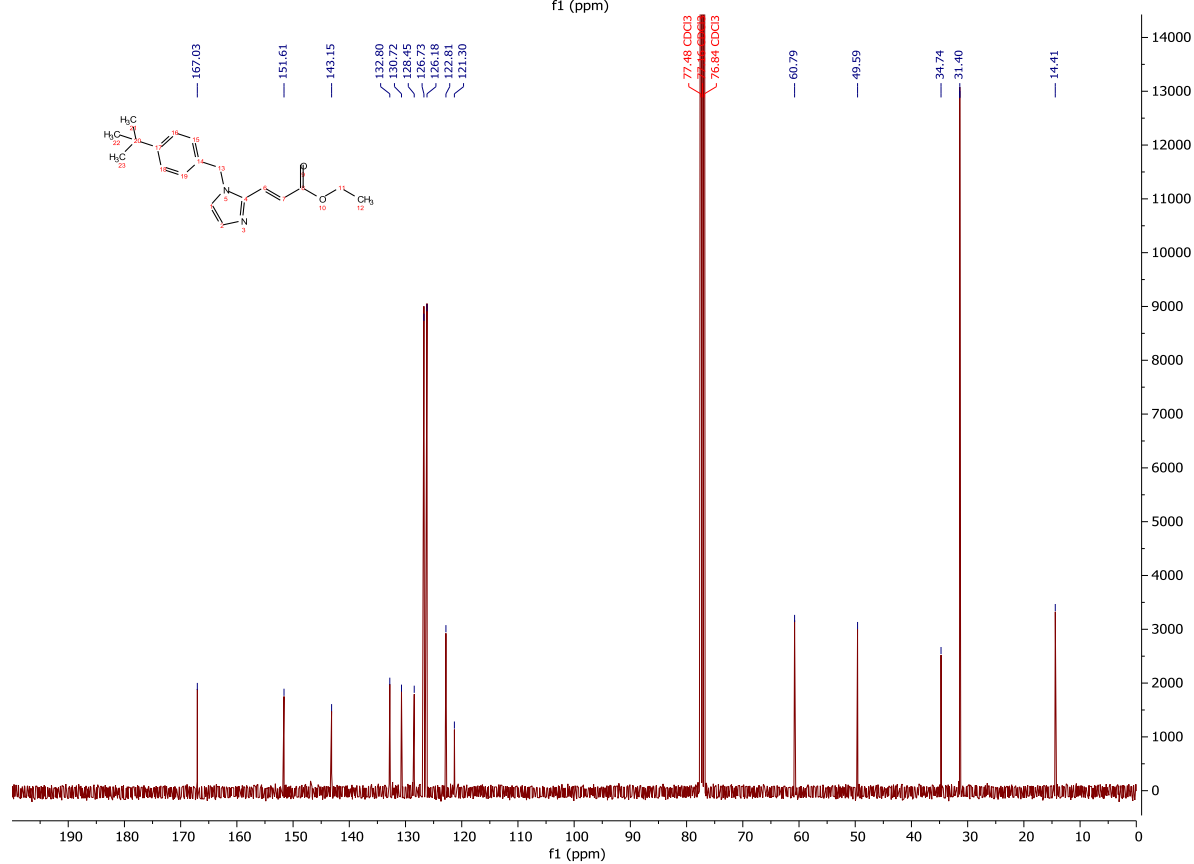
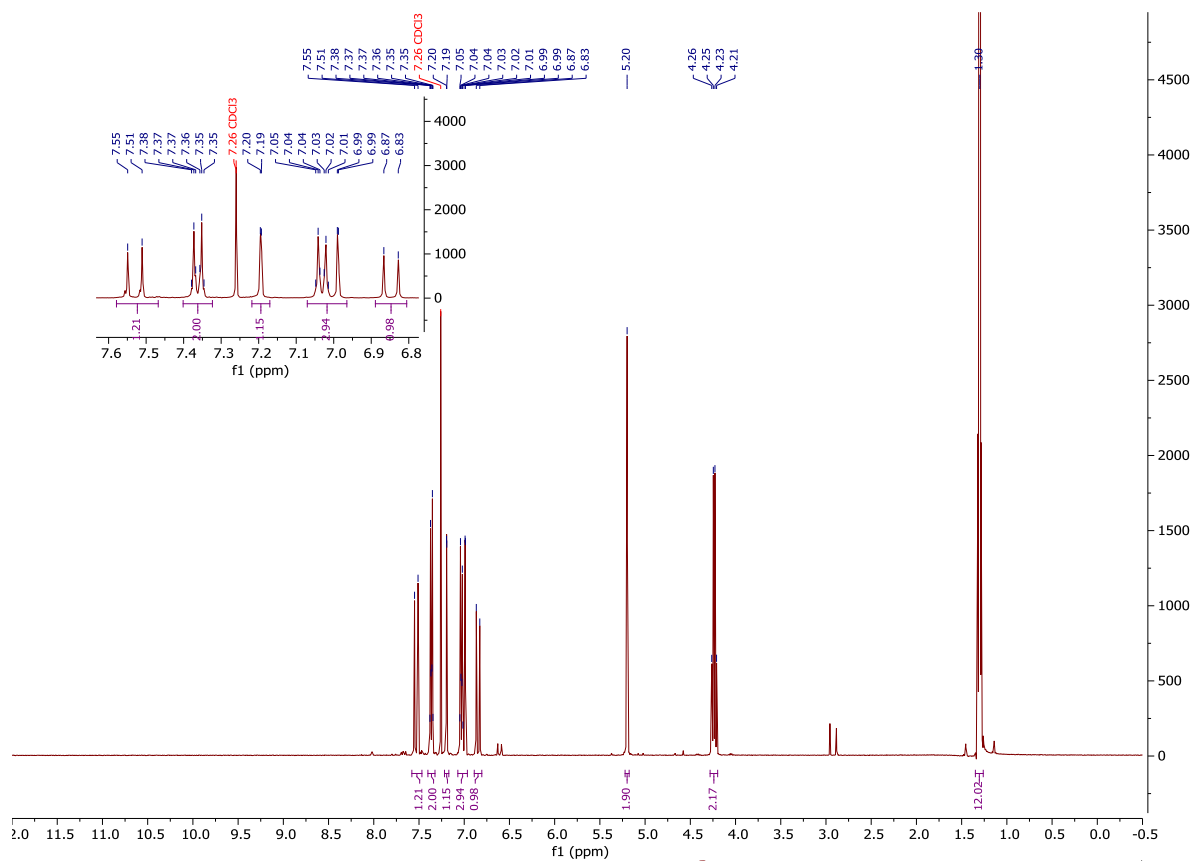
¹H-NMR and ¹³C-NMR: Compound 36



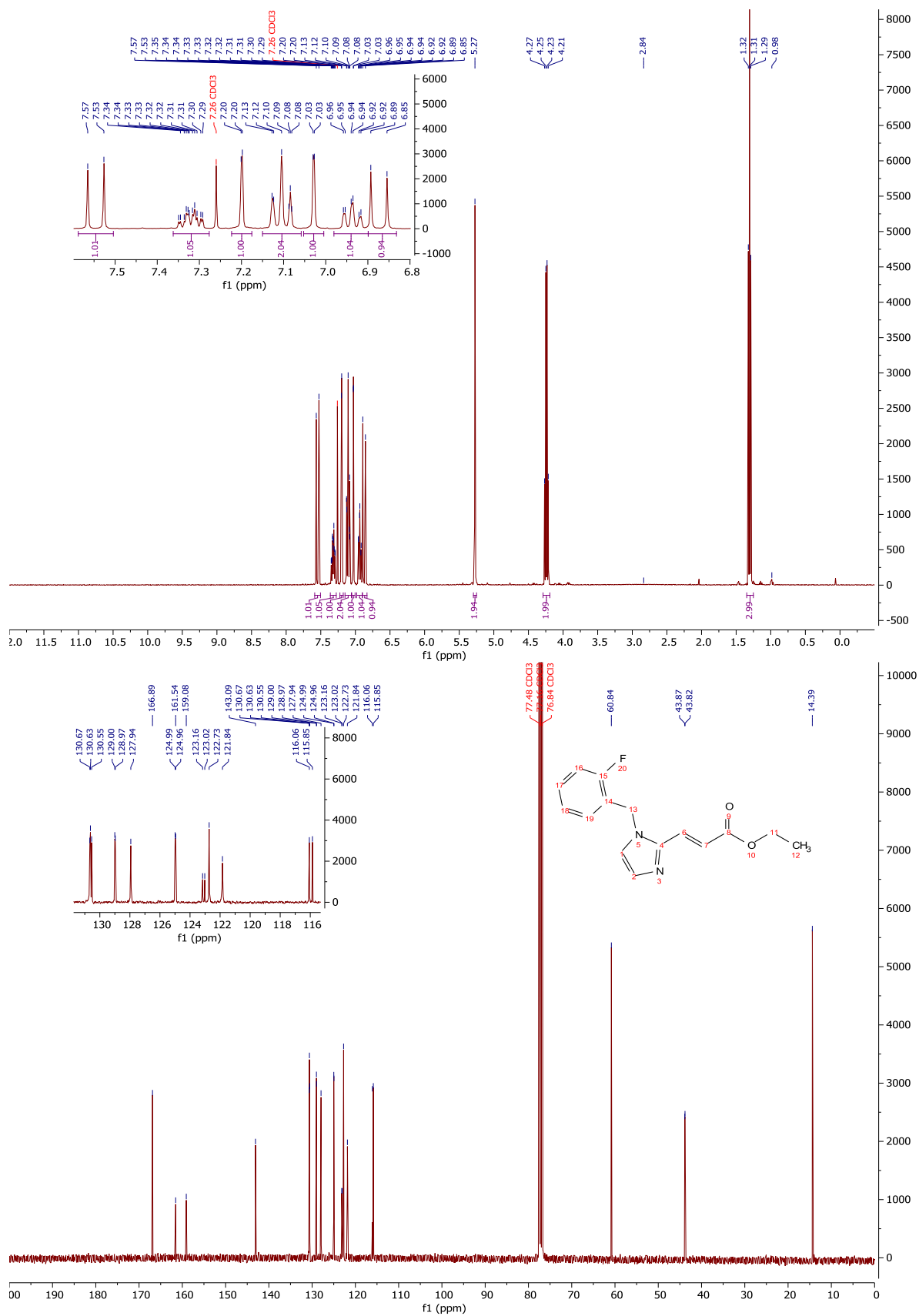
¹H-NMR and ¹³C-NMR: Compound 39



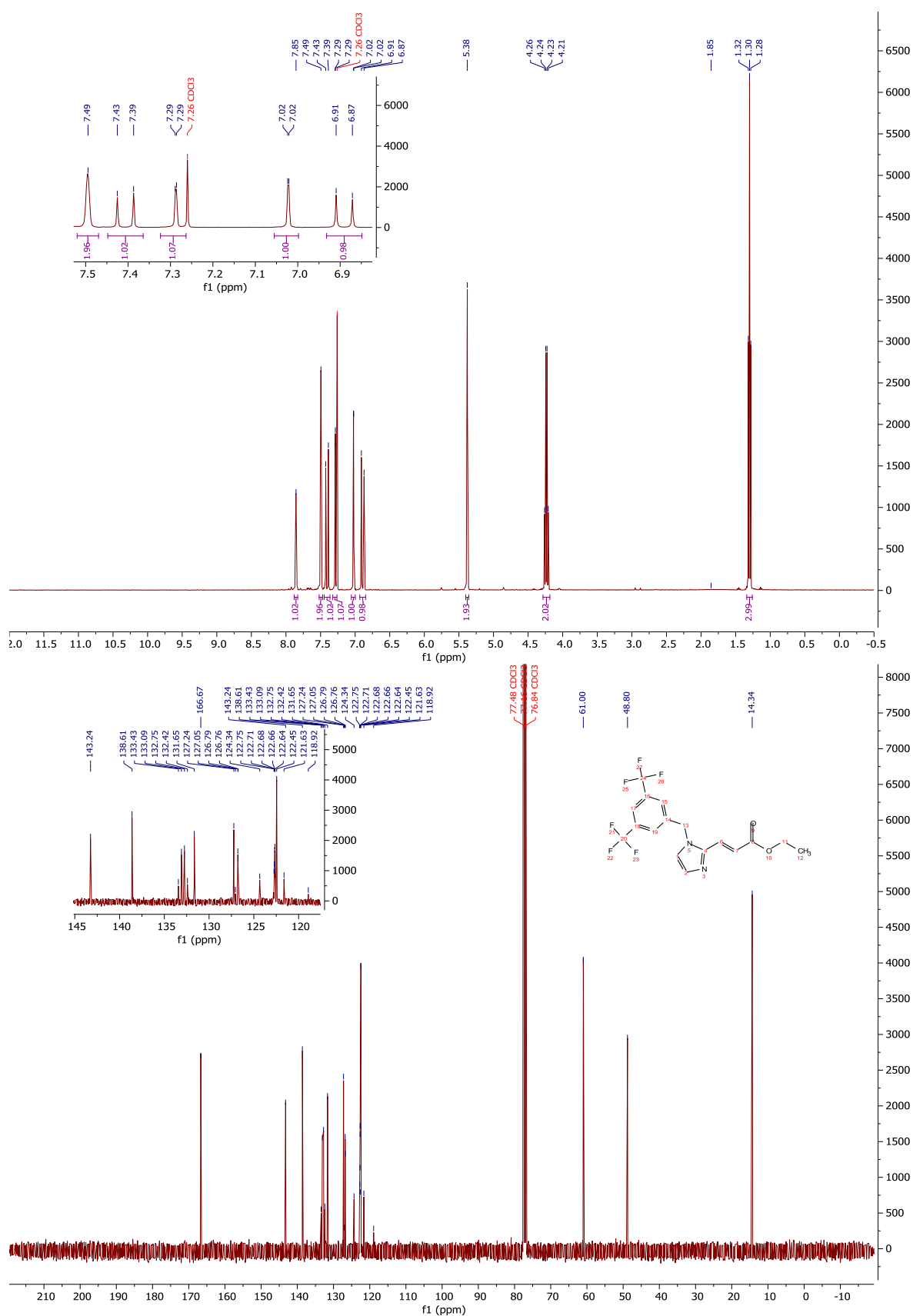
¹H-NMR and ¹³C-NMR: Compound 41



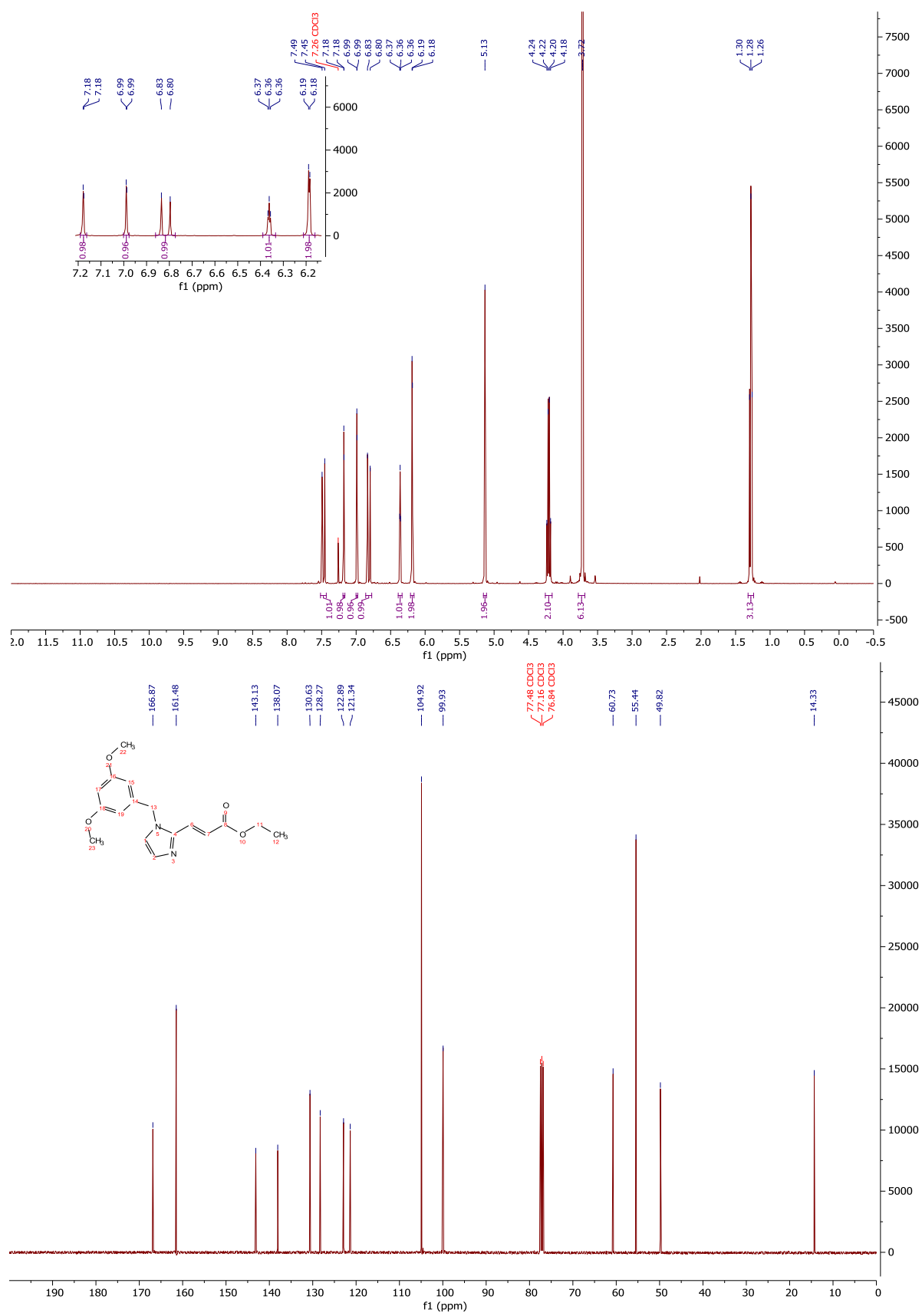
$^1\text{H-NMR}$ and $^{13}\text{C-NMR}$: Compound **40**



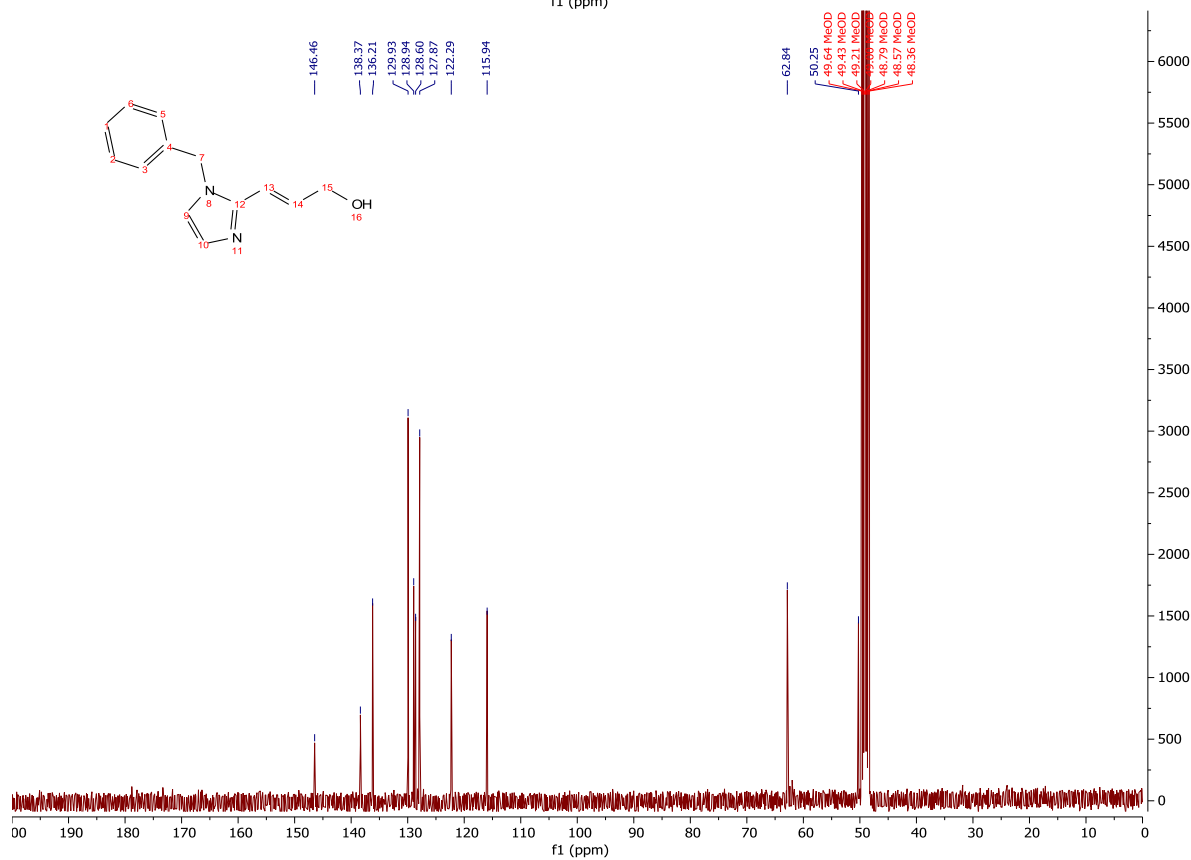
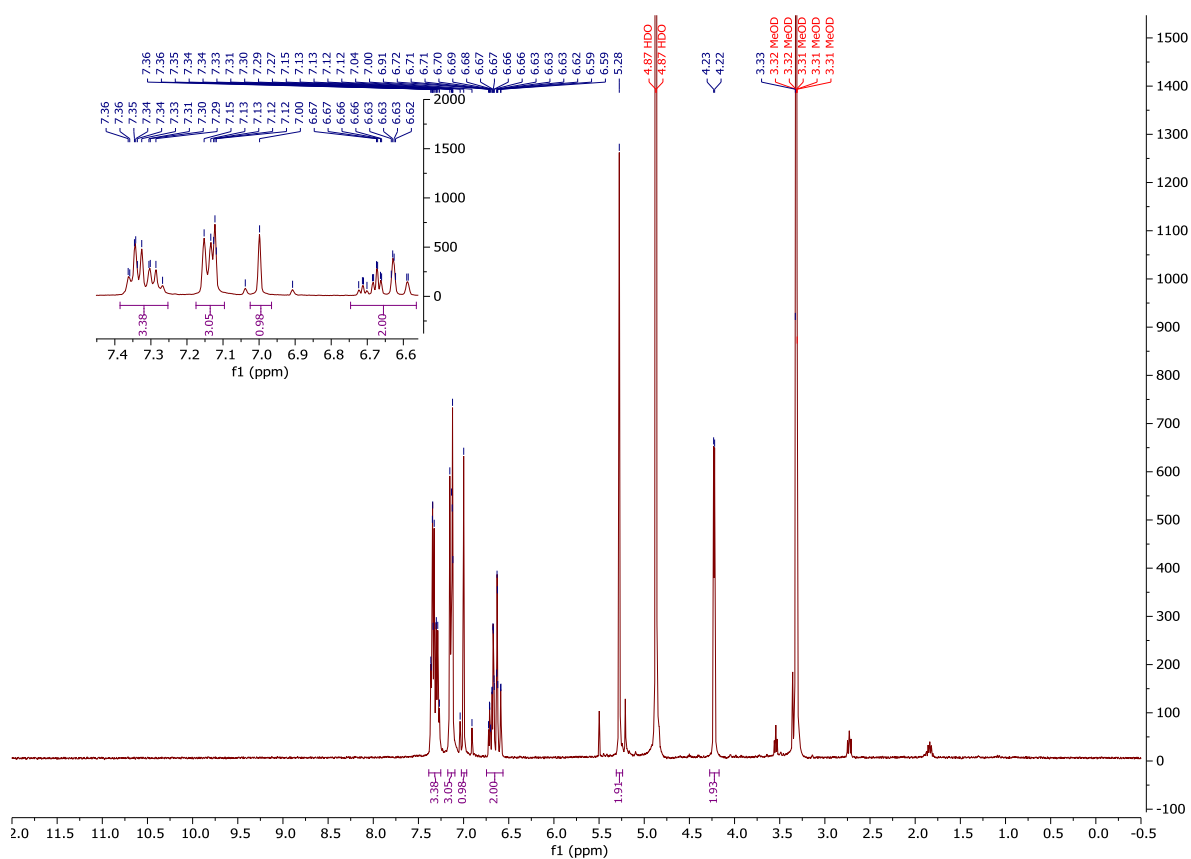
¹H-NMR and ¹³C-NMR: Compound 37



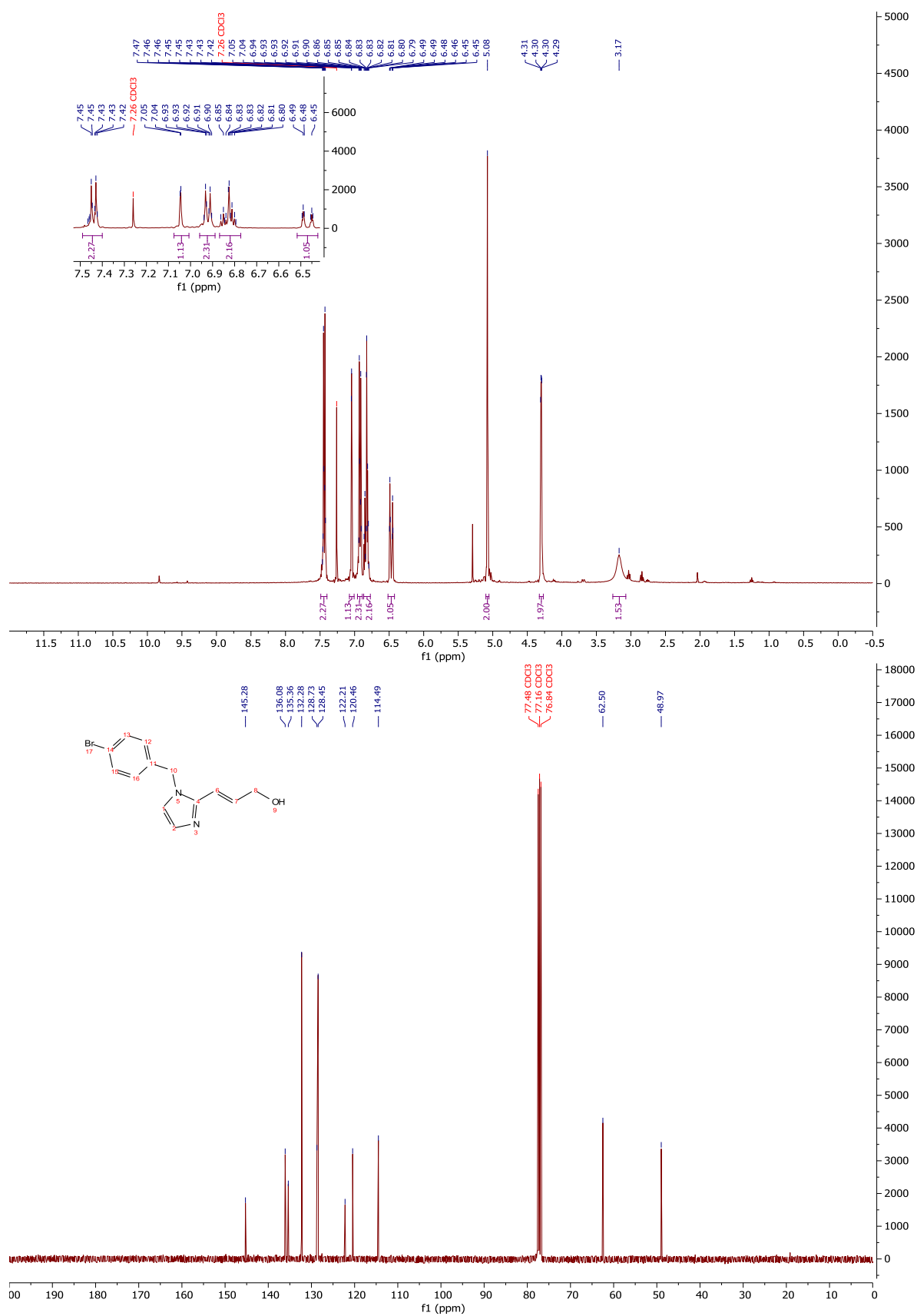
¹H-NMR and ¹³C-NMR: Compound 38



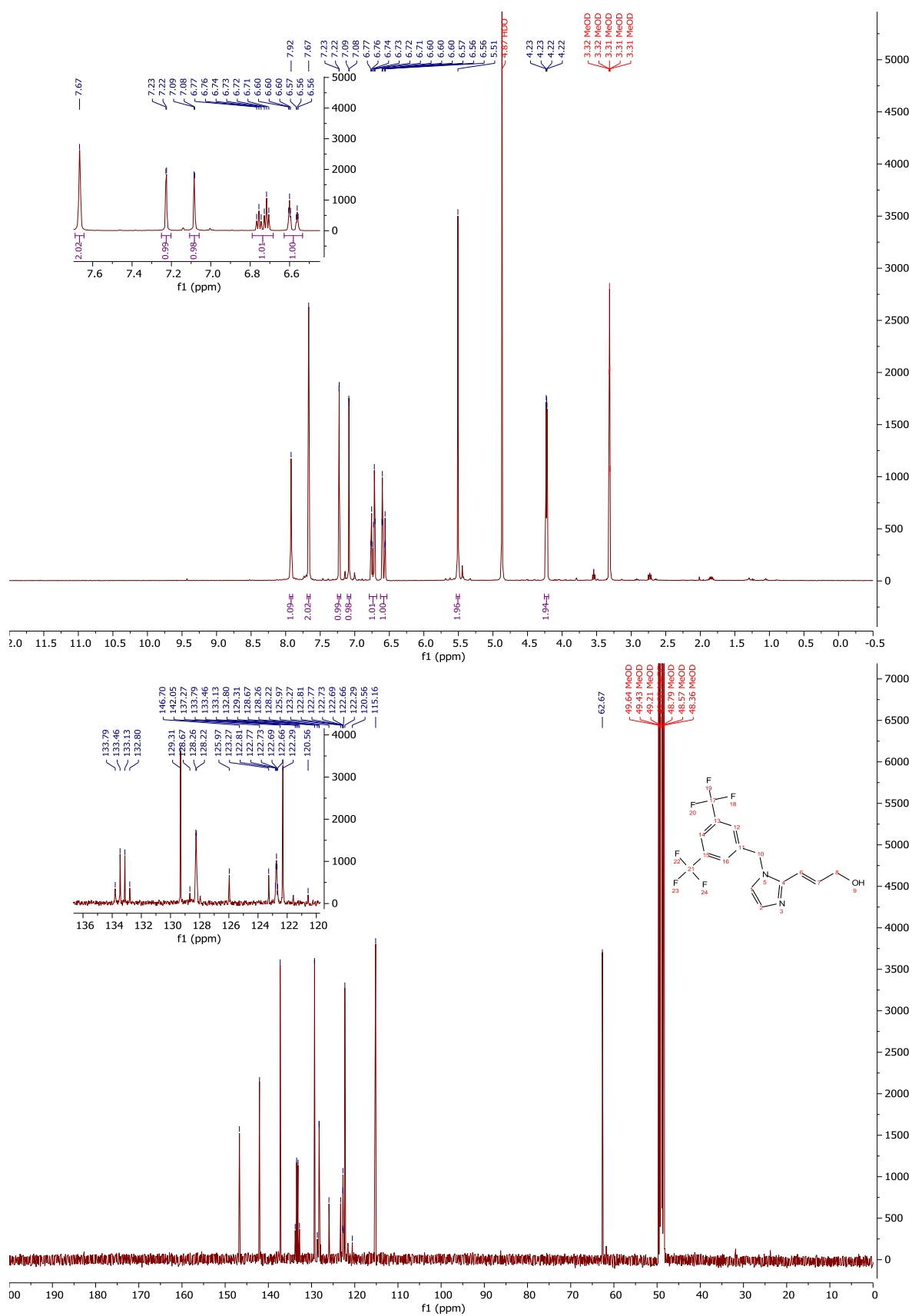
¹H-NMR and ¹³C-NMR: Compound 42



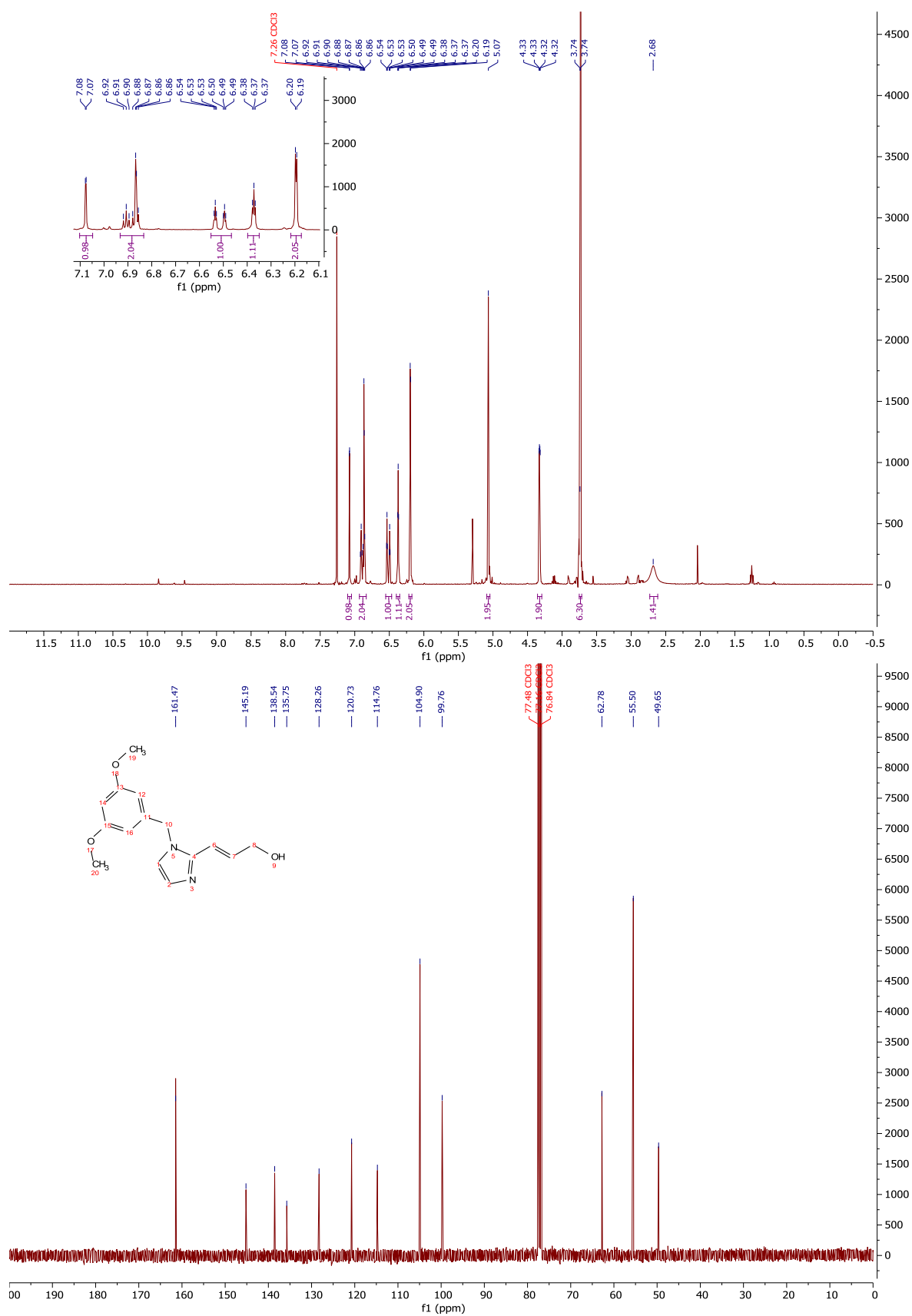
¹H-NMR and ¹³C-NMR: Compound 45



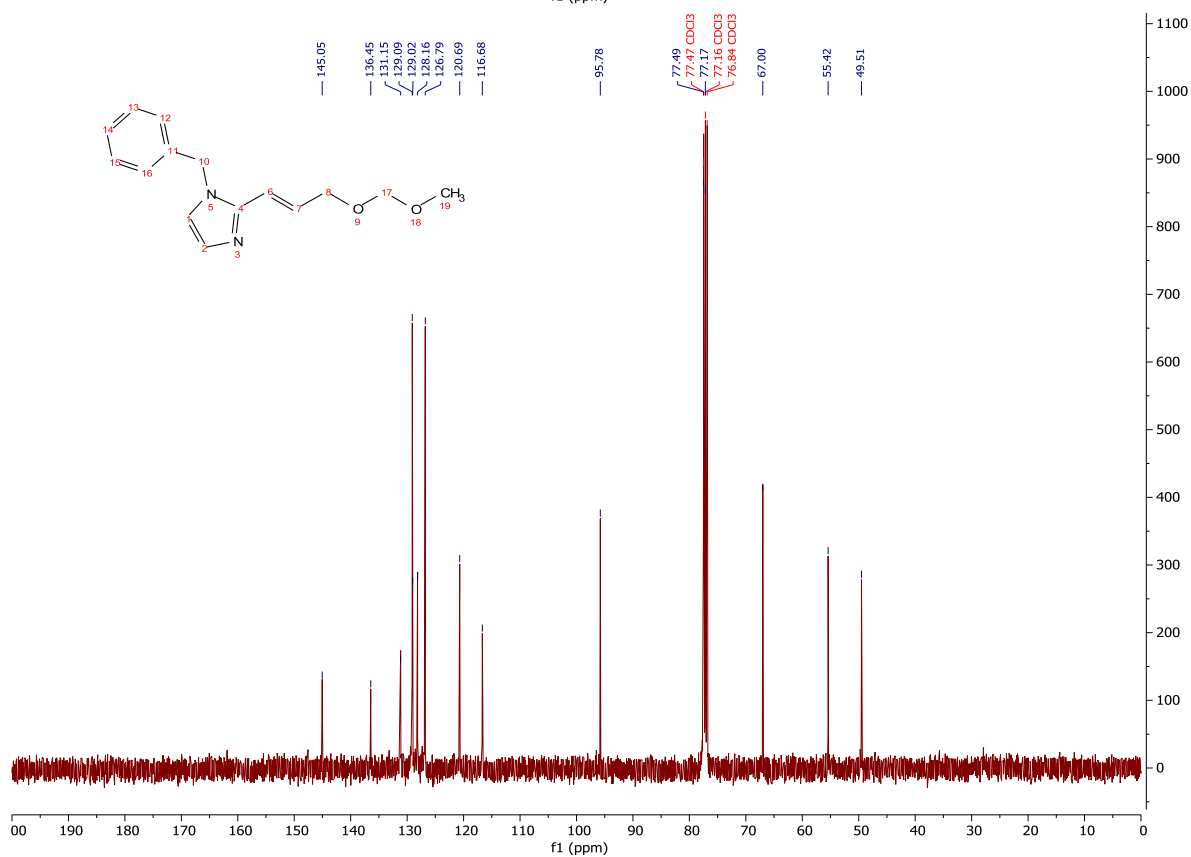
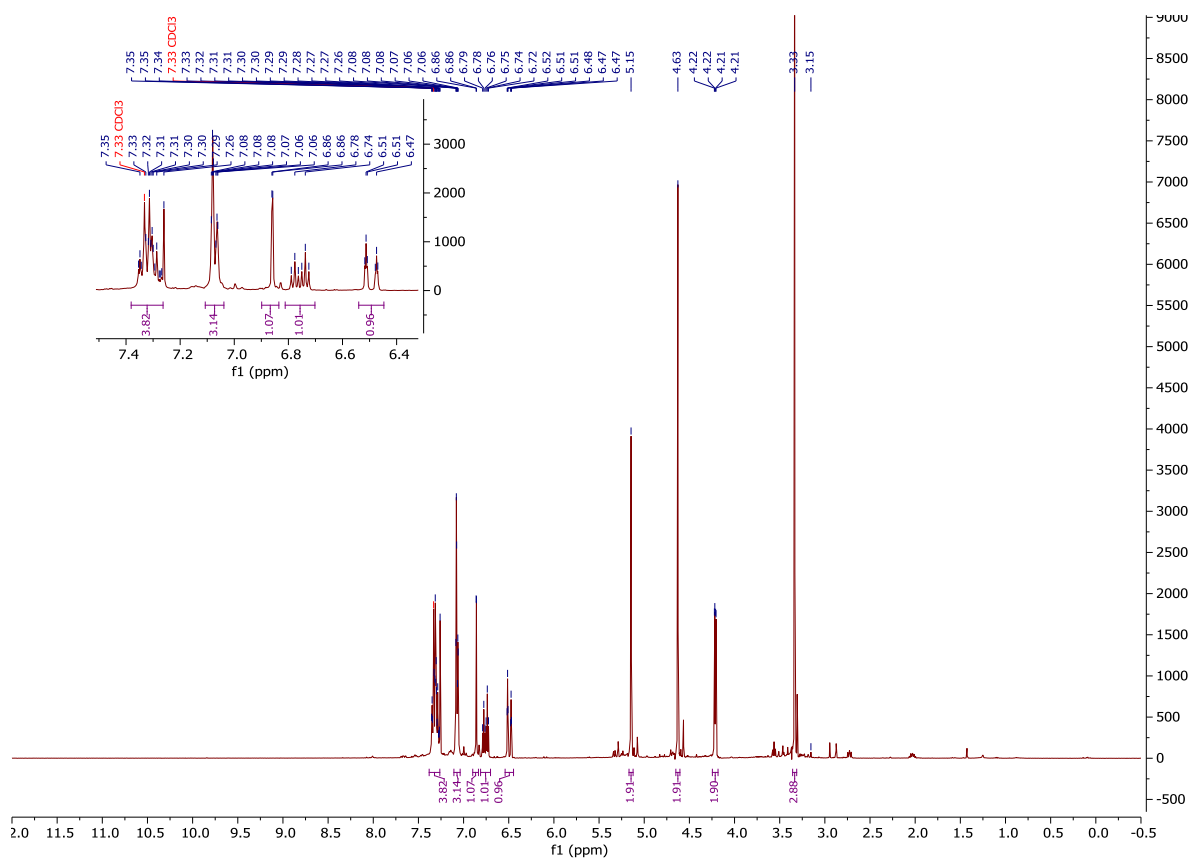
¹H-NMR and ¹³C-NMR: Compound 43



¹H-NMR and ¹³C-NMR: Compound 44

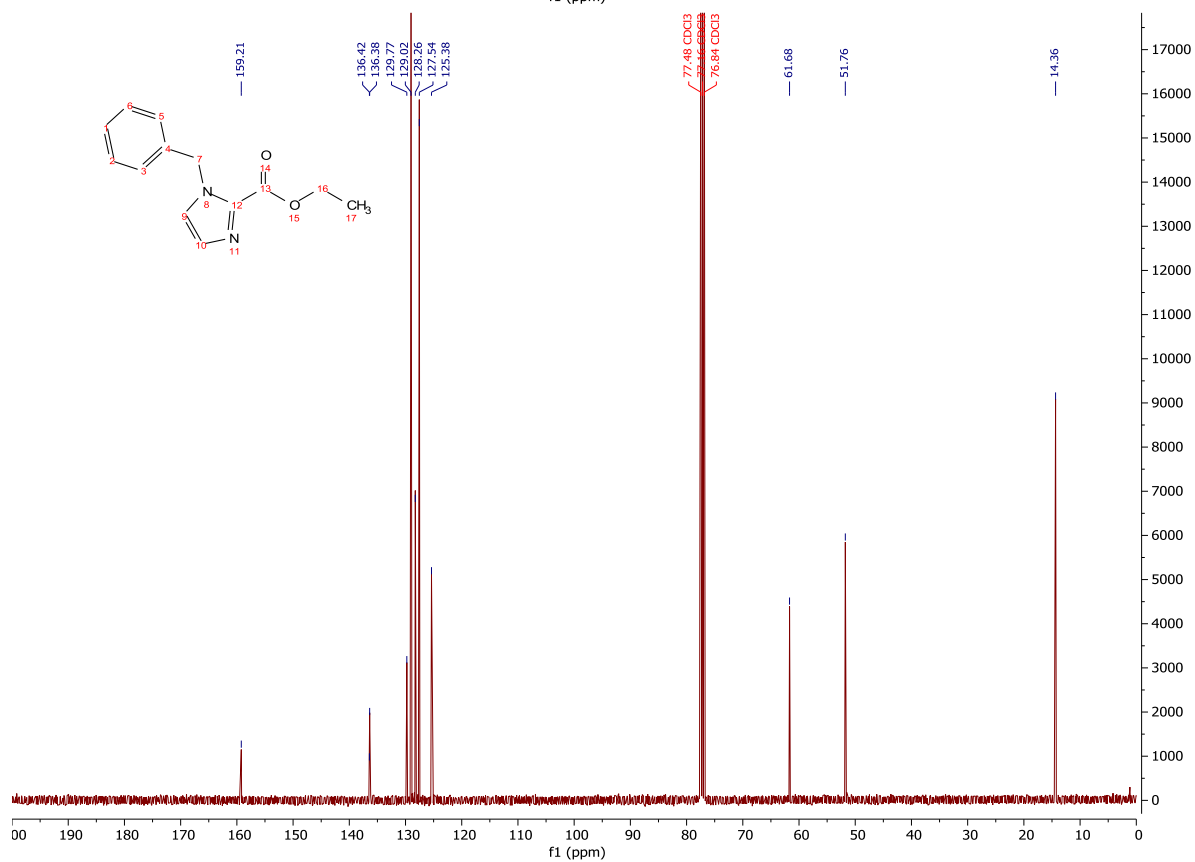
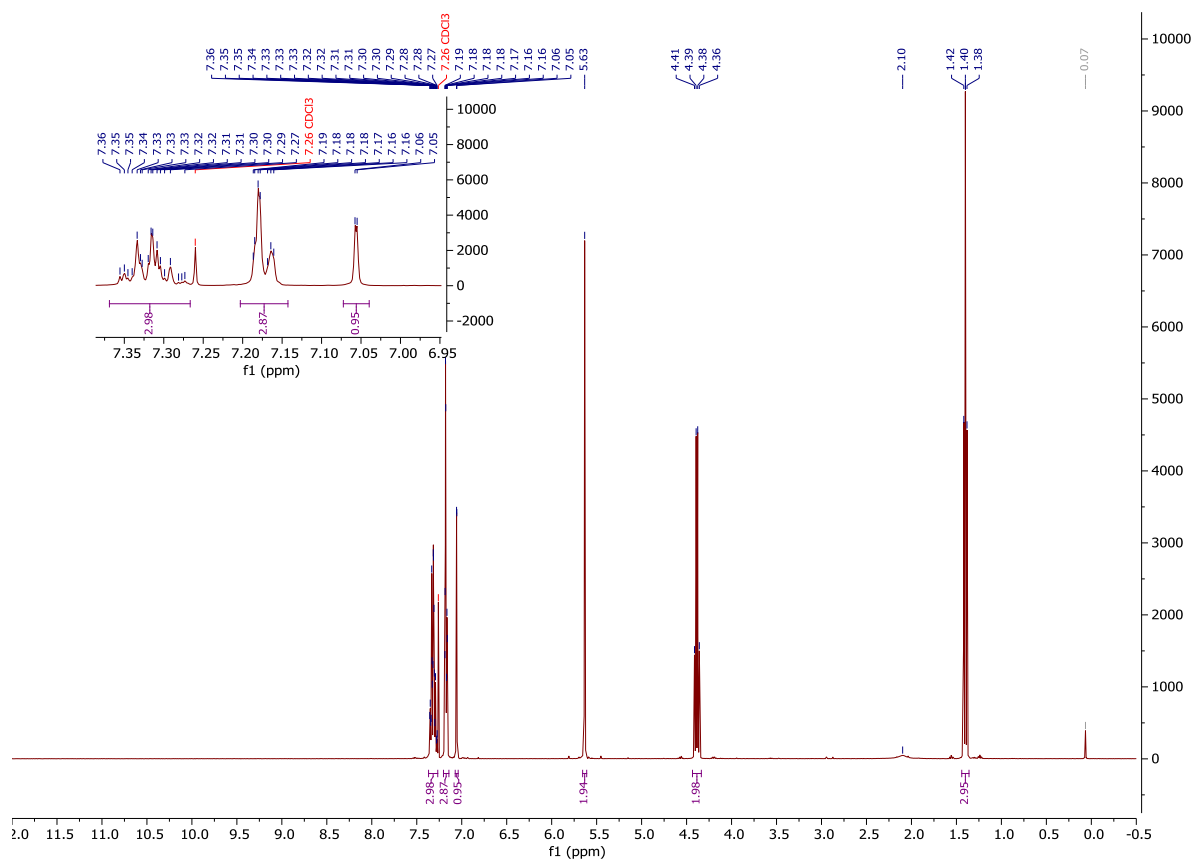


¹H-NMR and ¹³C-NMR: Compound 46

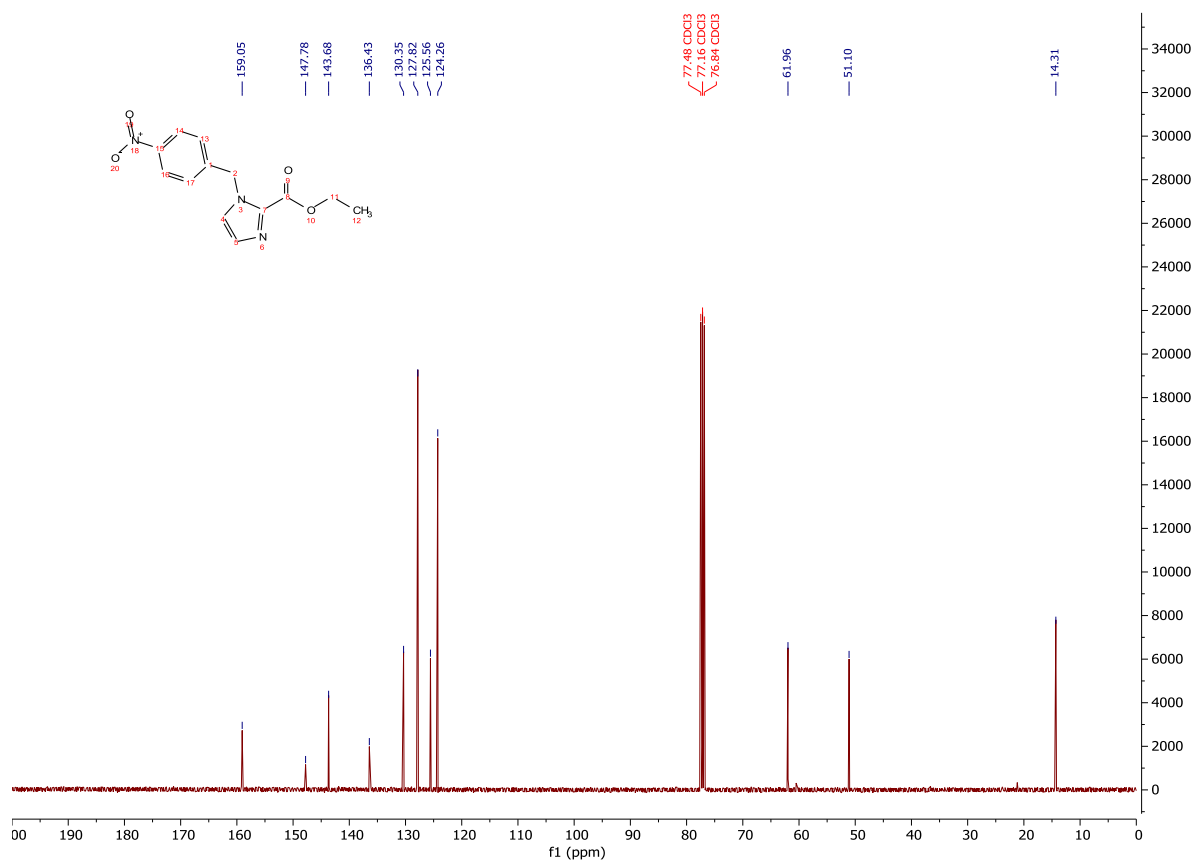
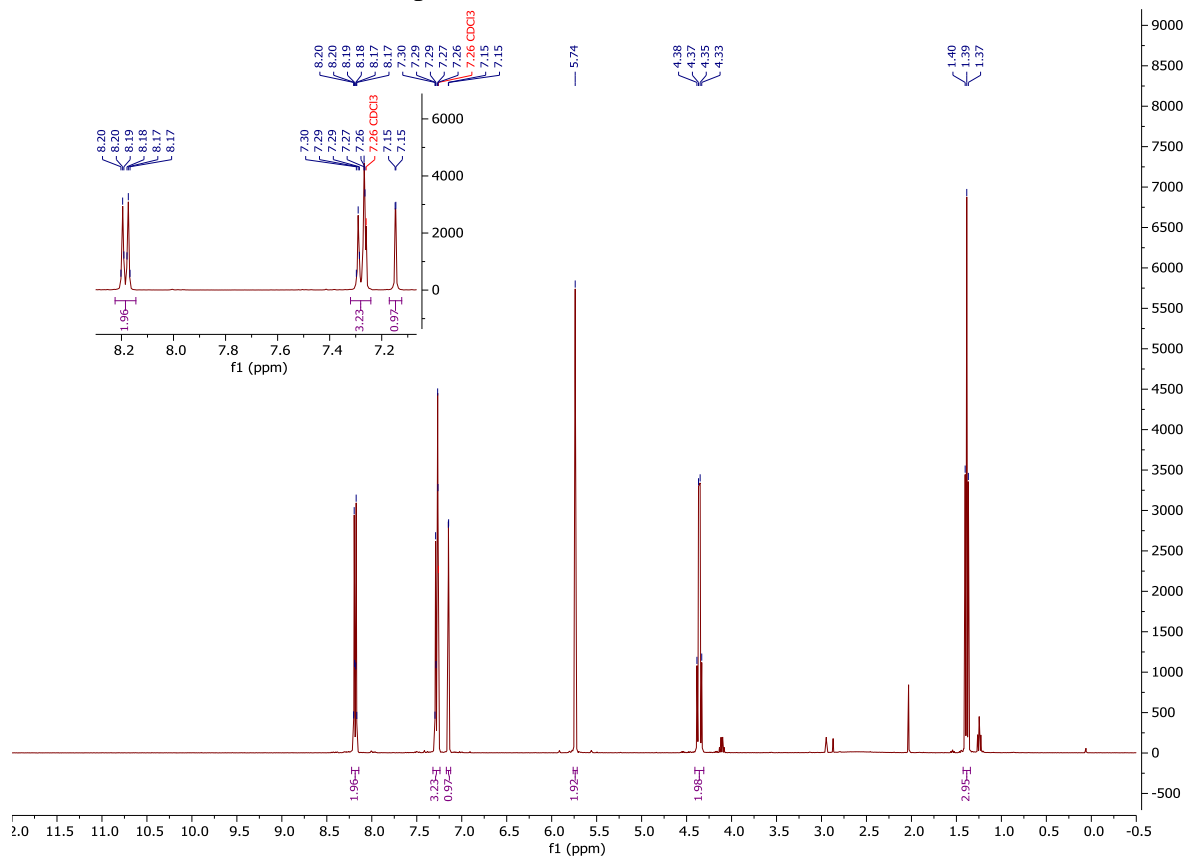


Synthesis discussed in section 4.5

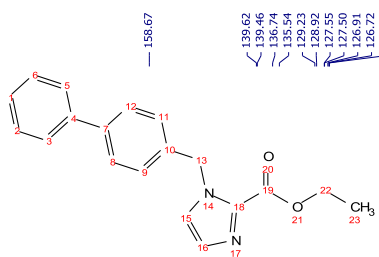
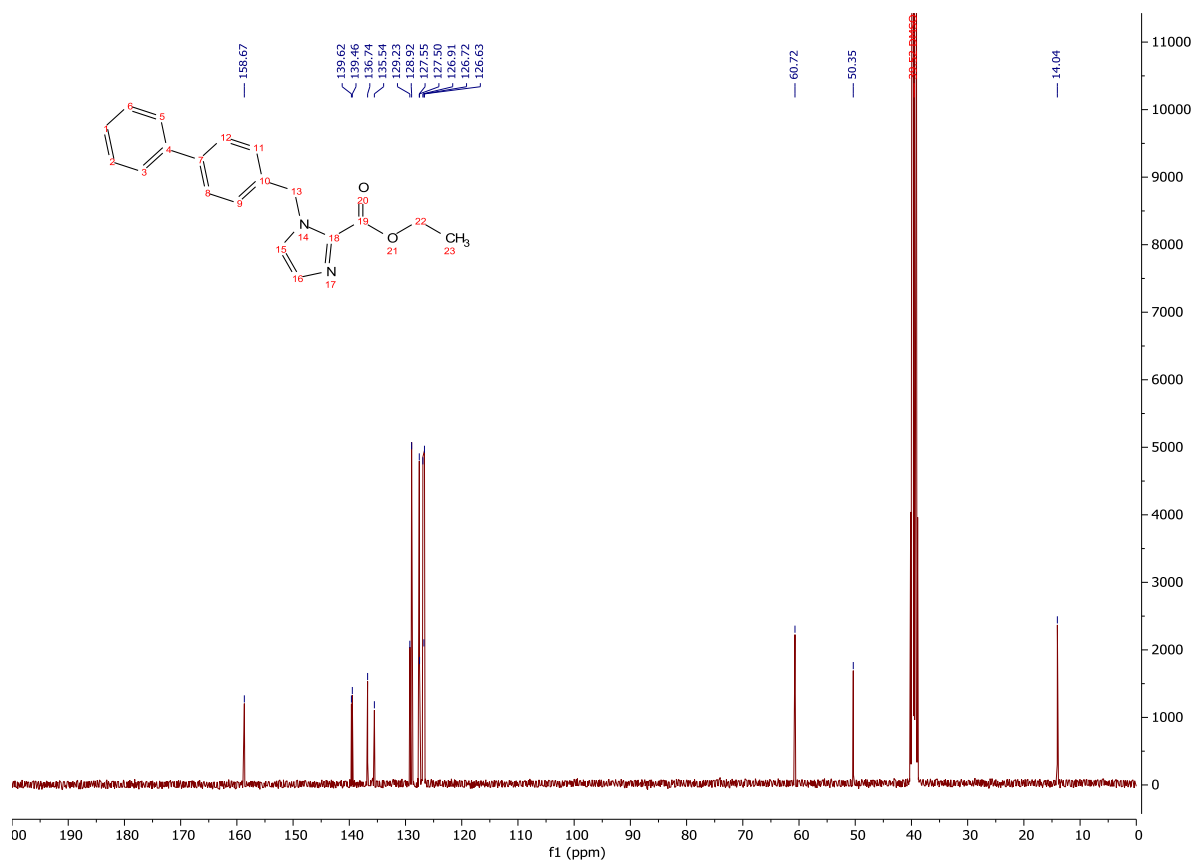
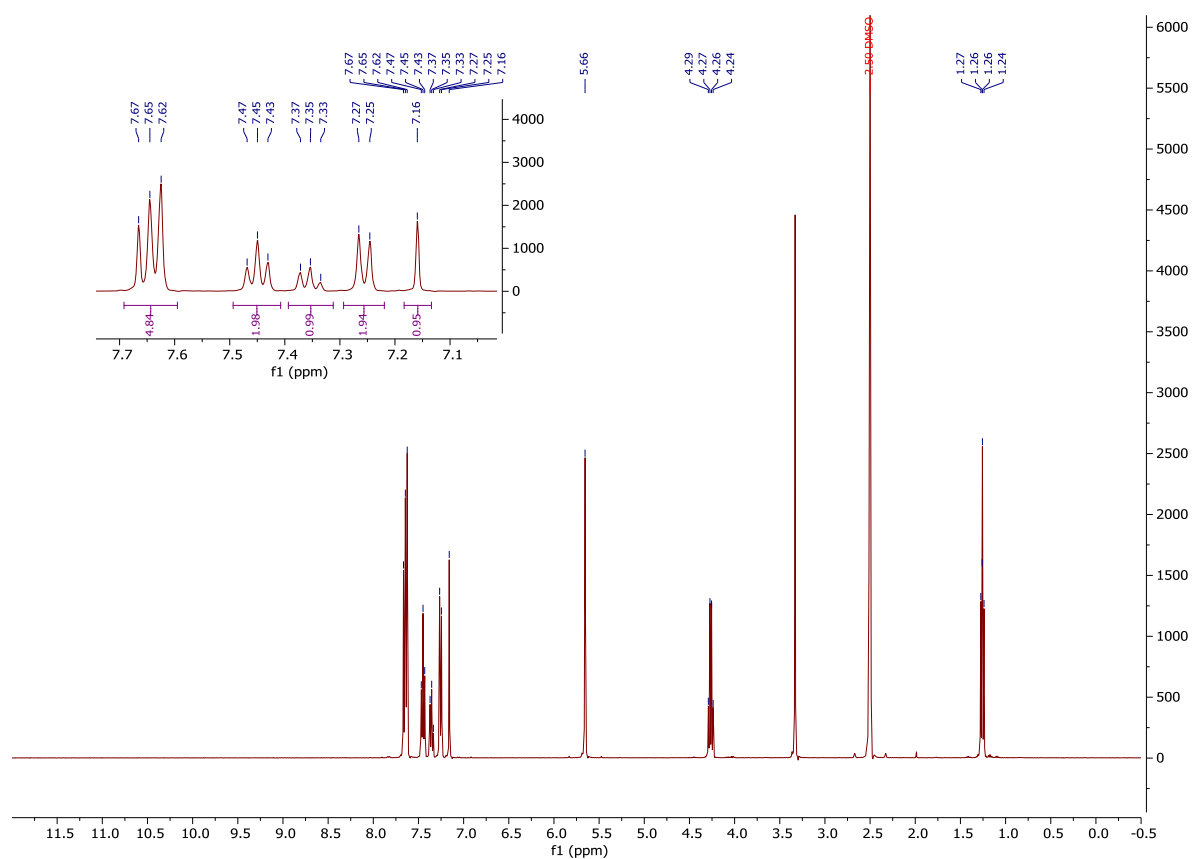
¹H-NMR and ¹³C-NMR: Compound 87



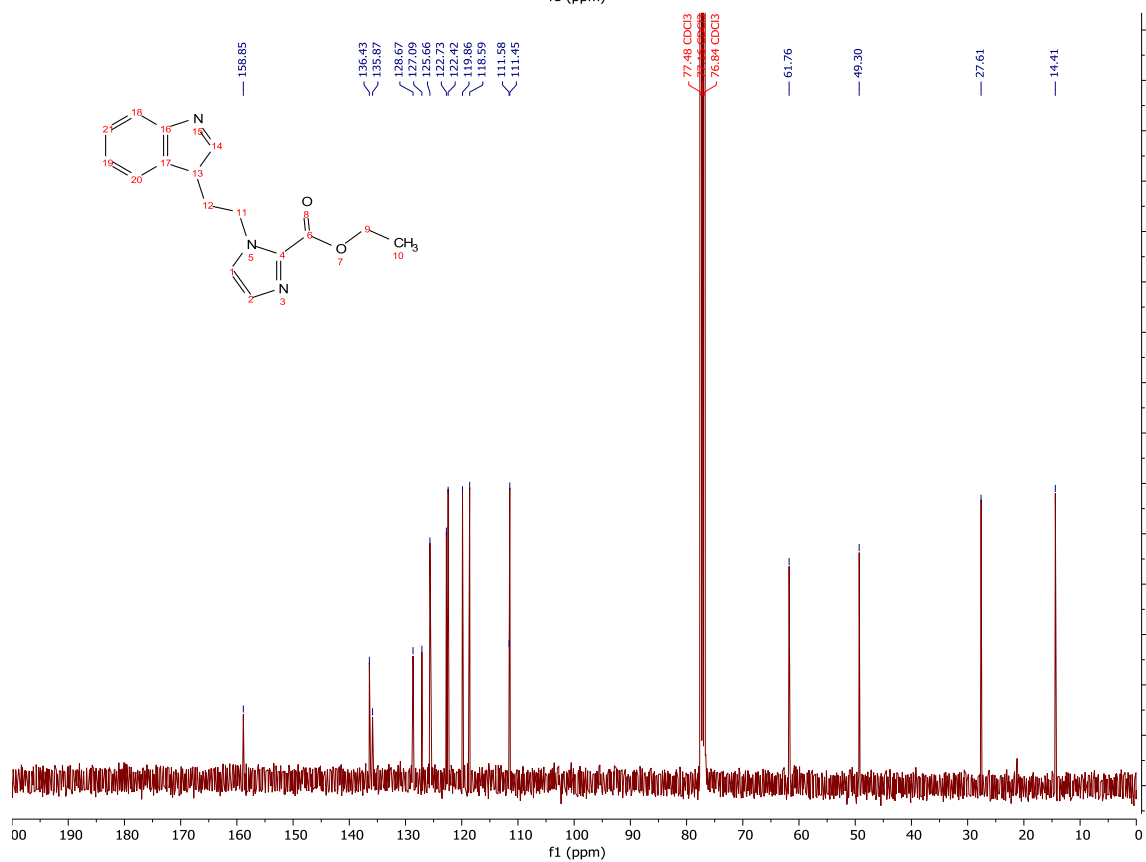
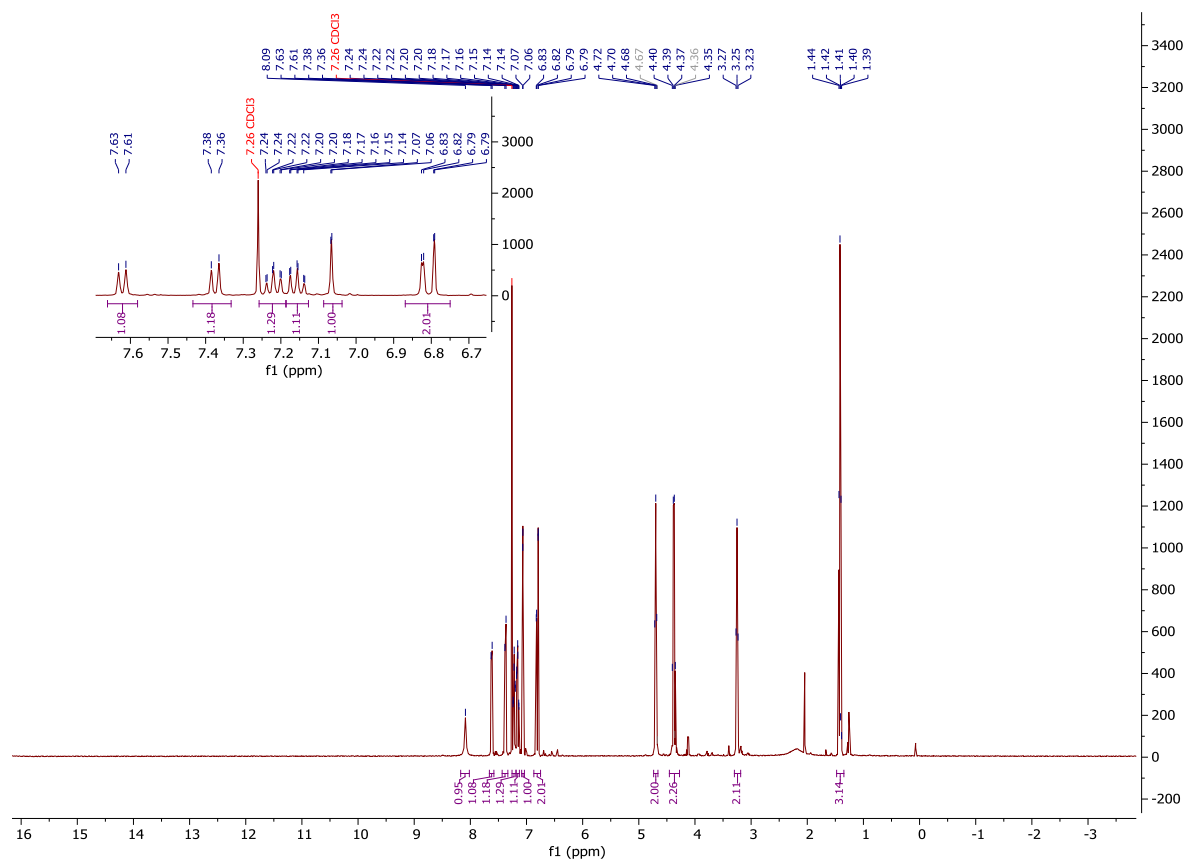
¹H-NMR and ¹³C-NMR: Compound 88



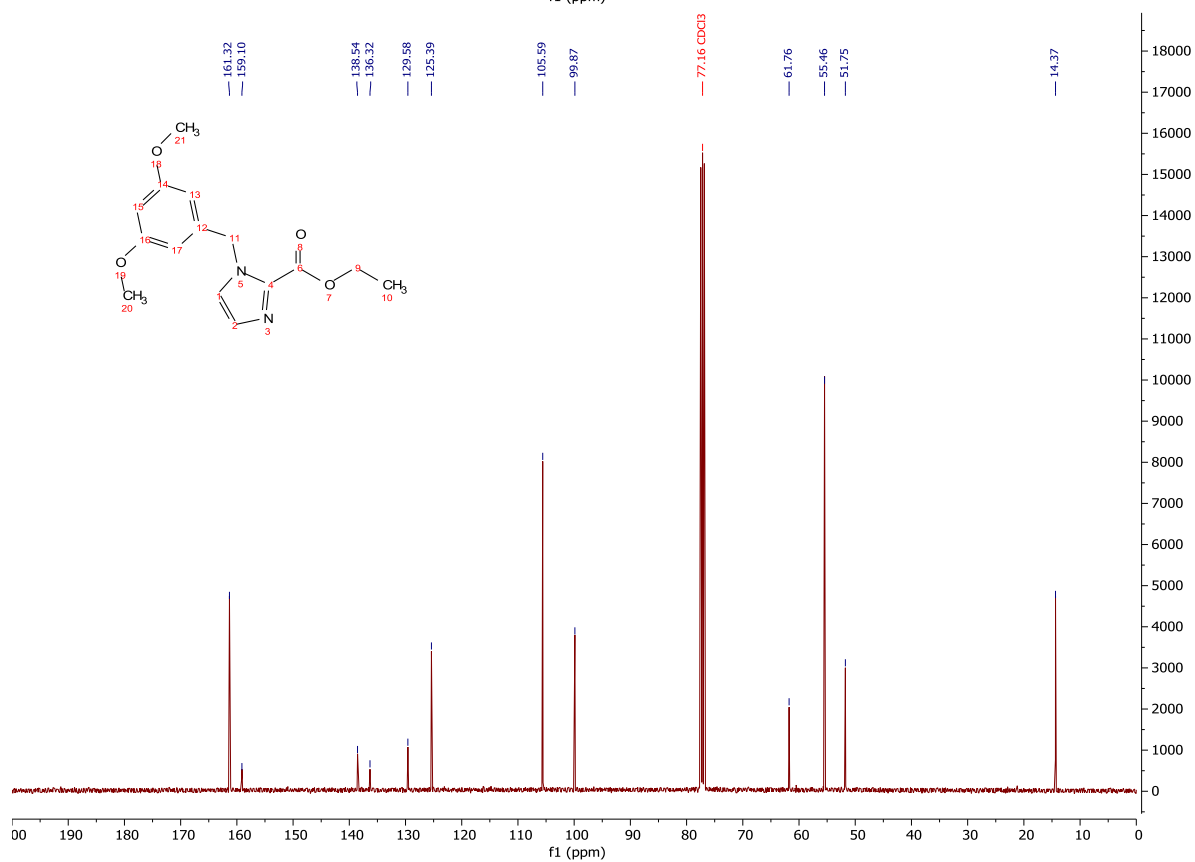
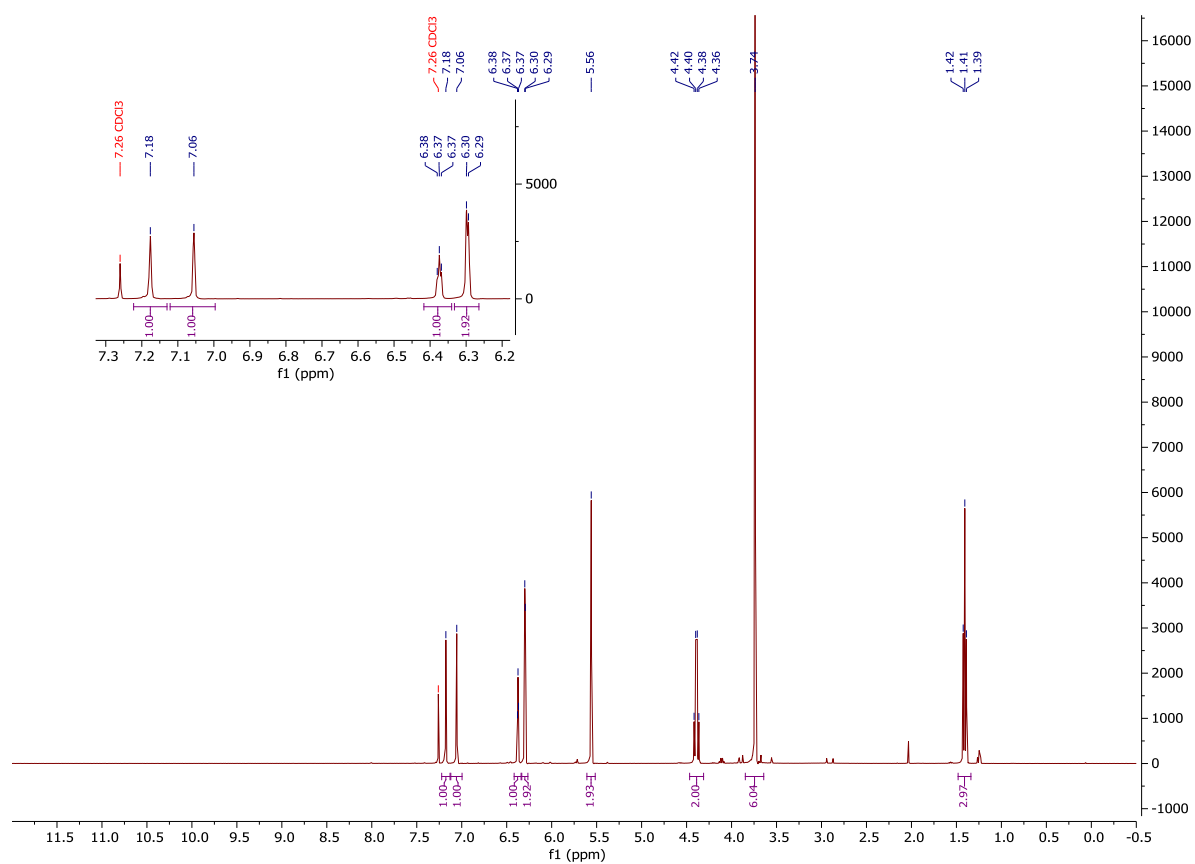
$^1\text{H-NMR}$ and $^{13}\text{C-NMR}$: Compound **89**



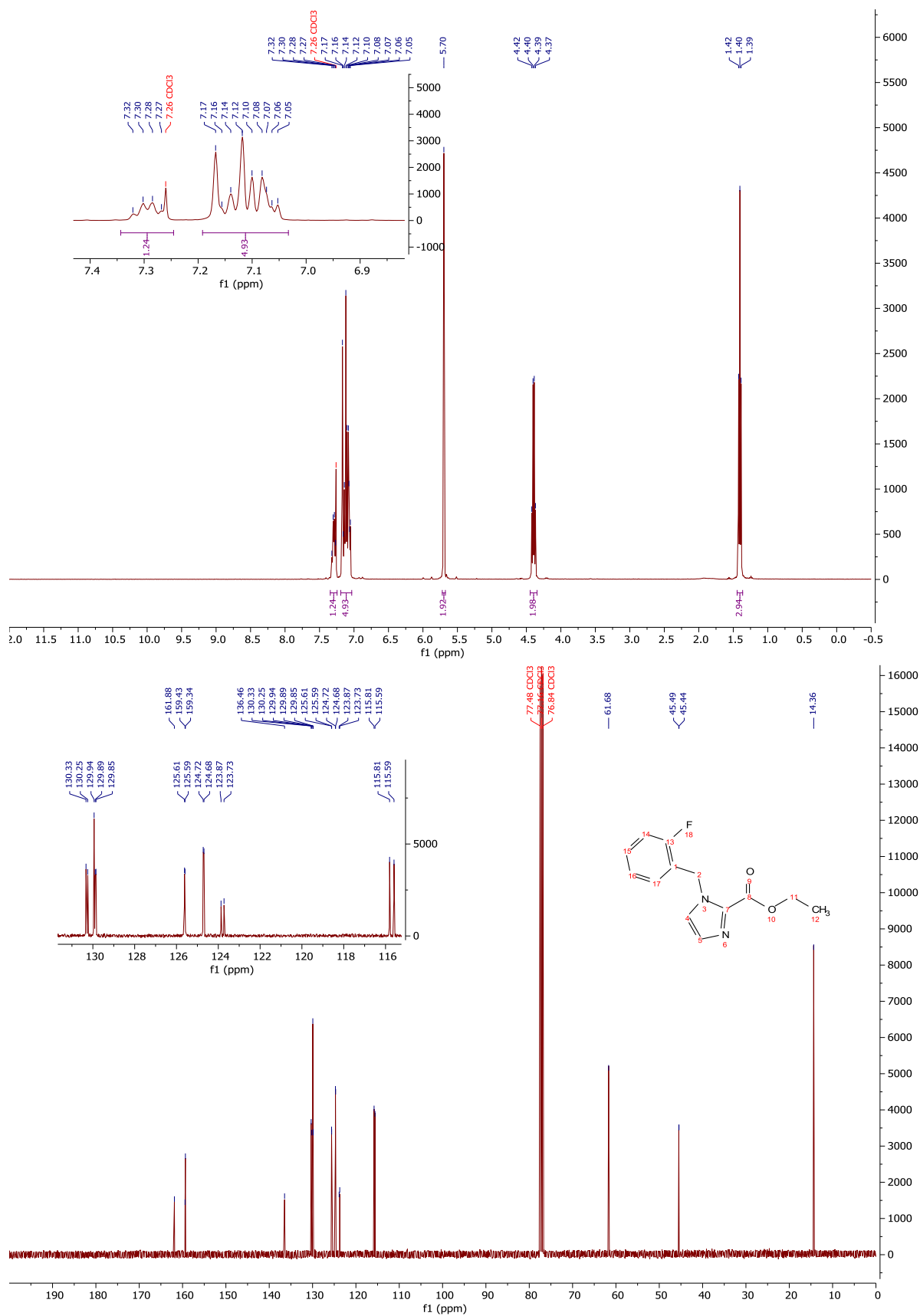
¹H-NMR and ¹³C-NMR: Compound 92



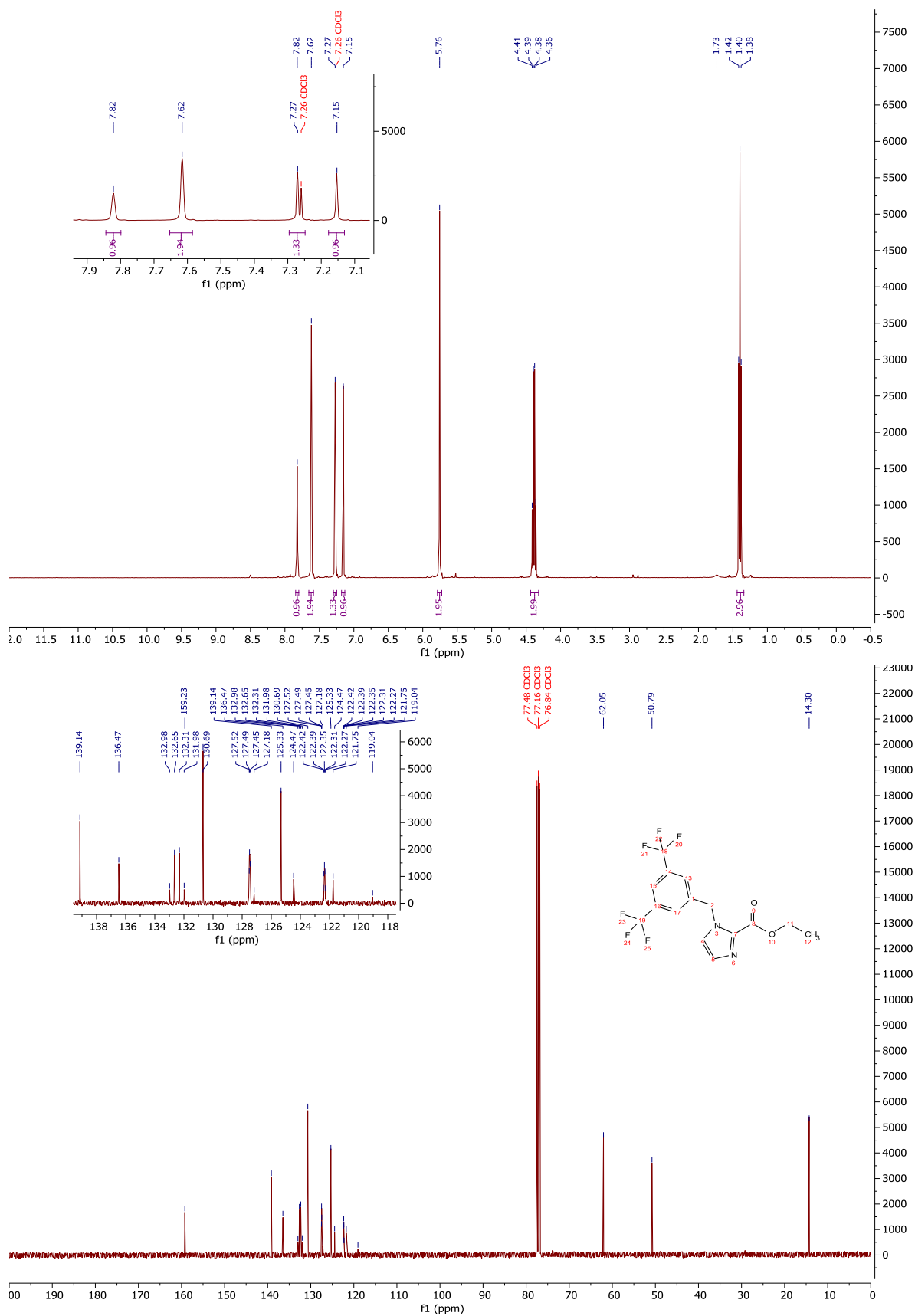
¹H-NMR and ¹³C-NMR: Compound 93



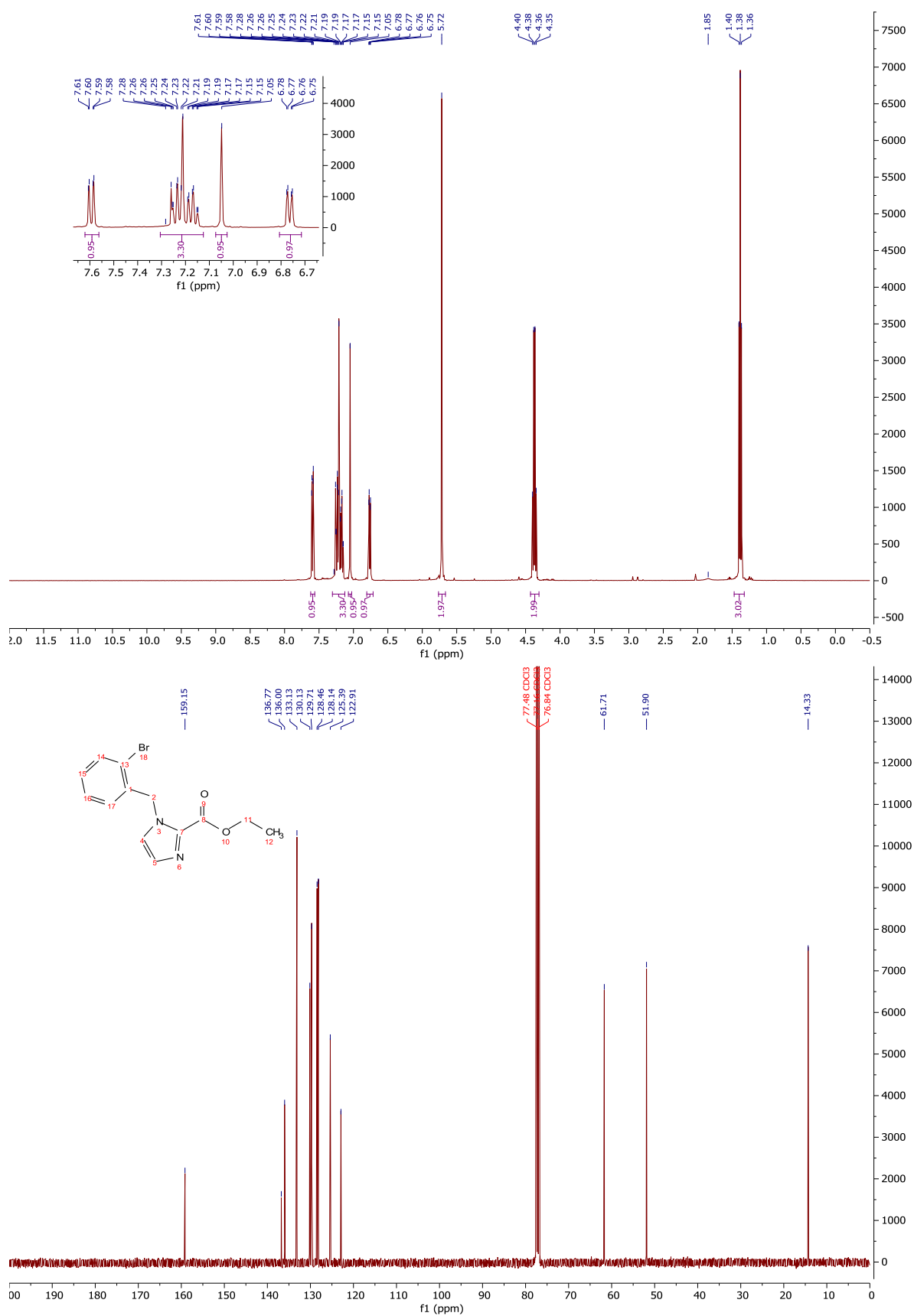
¹H-NMR and ¹³C-NMR: Compound 96



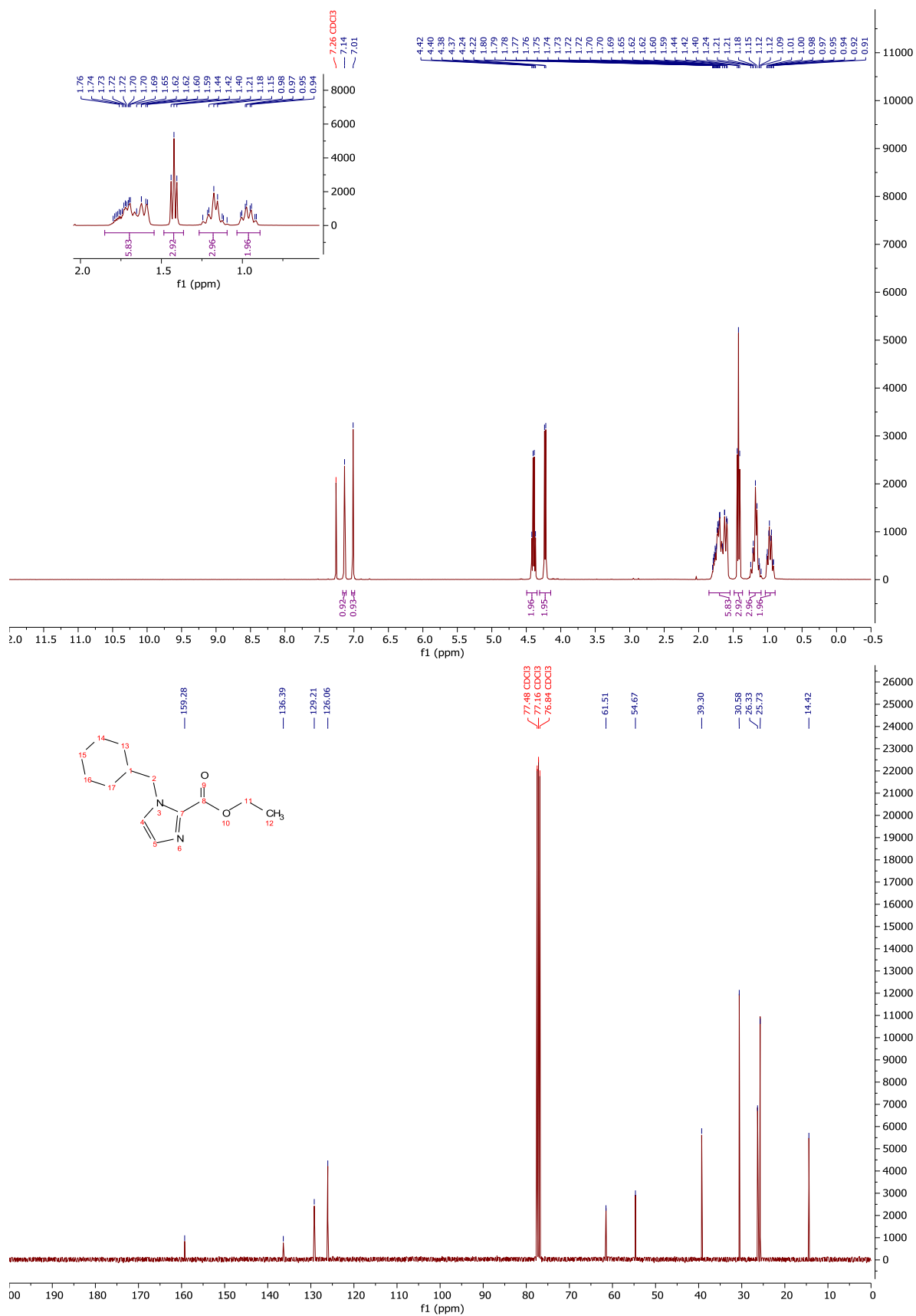
¹H-NMR and ¹³C-NMR: Compound 90



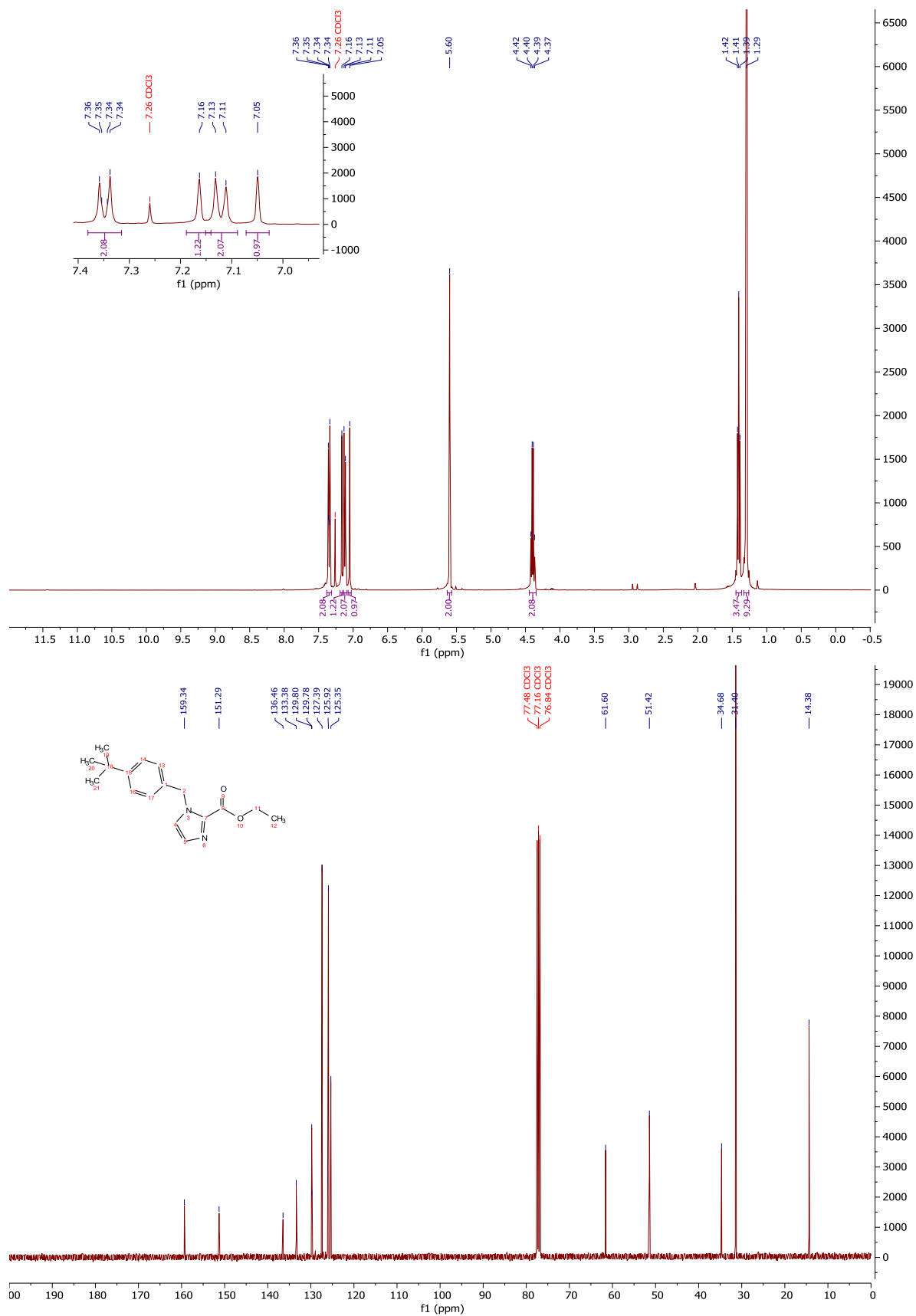
$^1\text{H-NMR}$ and $^{13}\text{C-NMR}$: Compound **95**



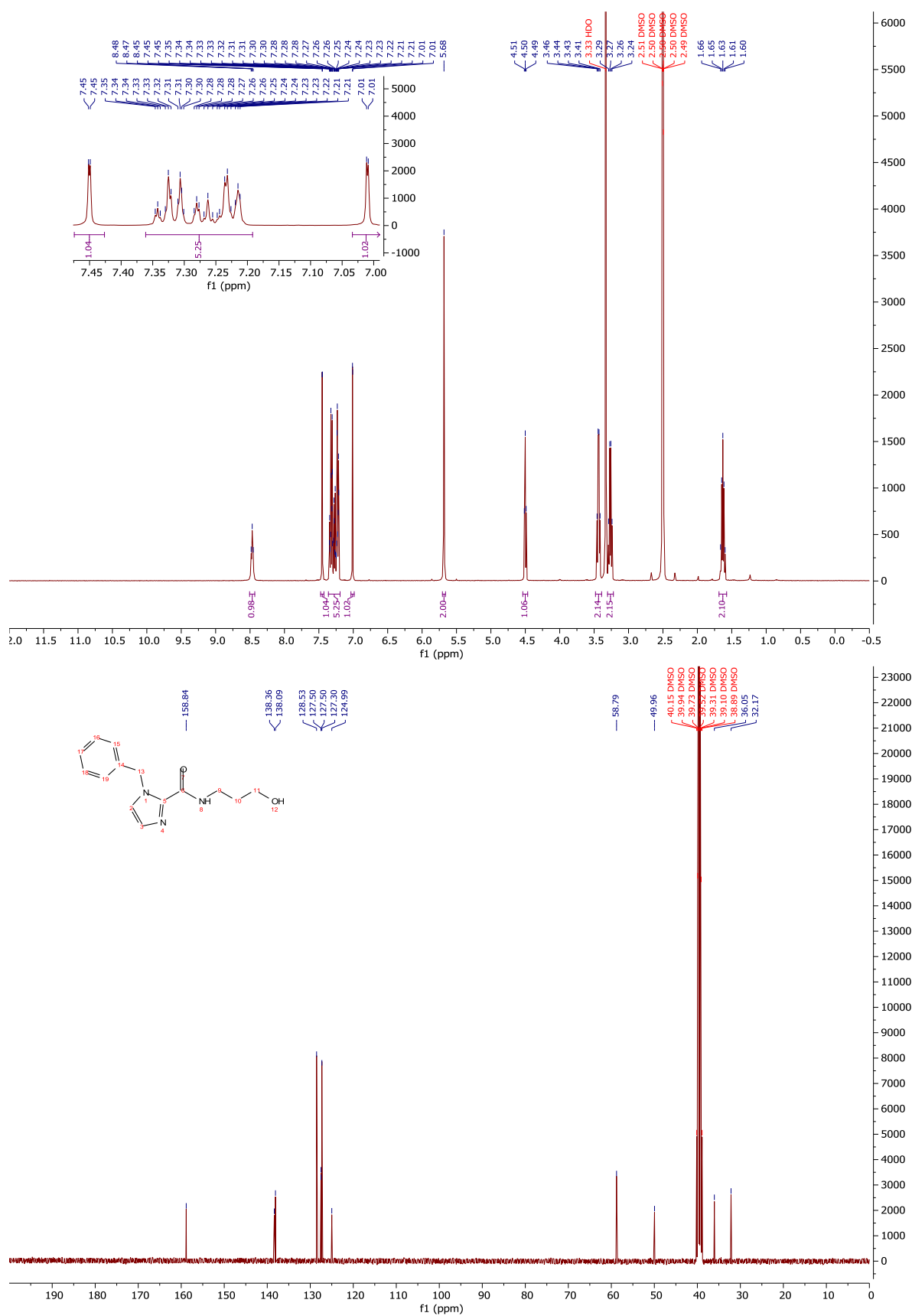
$^1\text{H-NMR}$ and $^{13}\text{C-NMR}$: Compound **91**



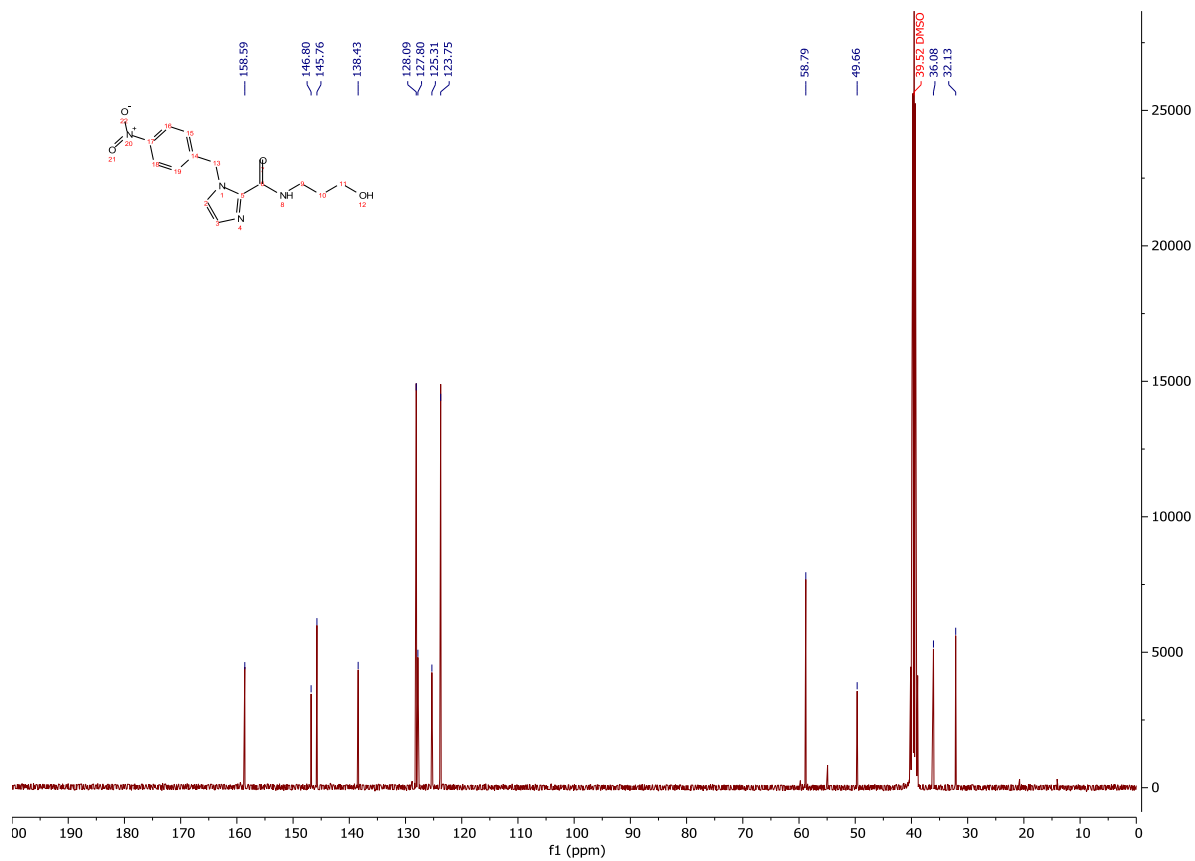
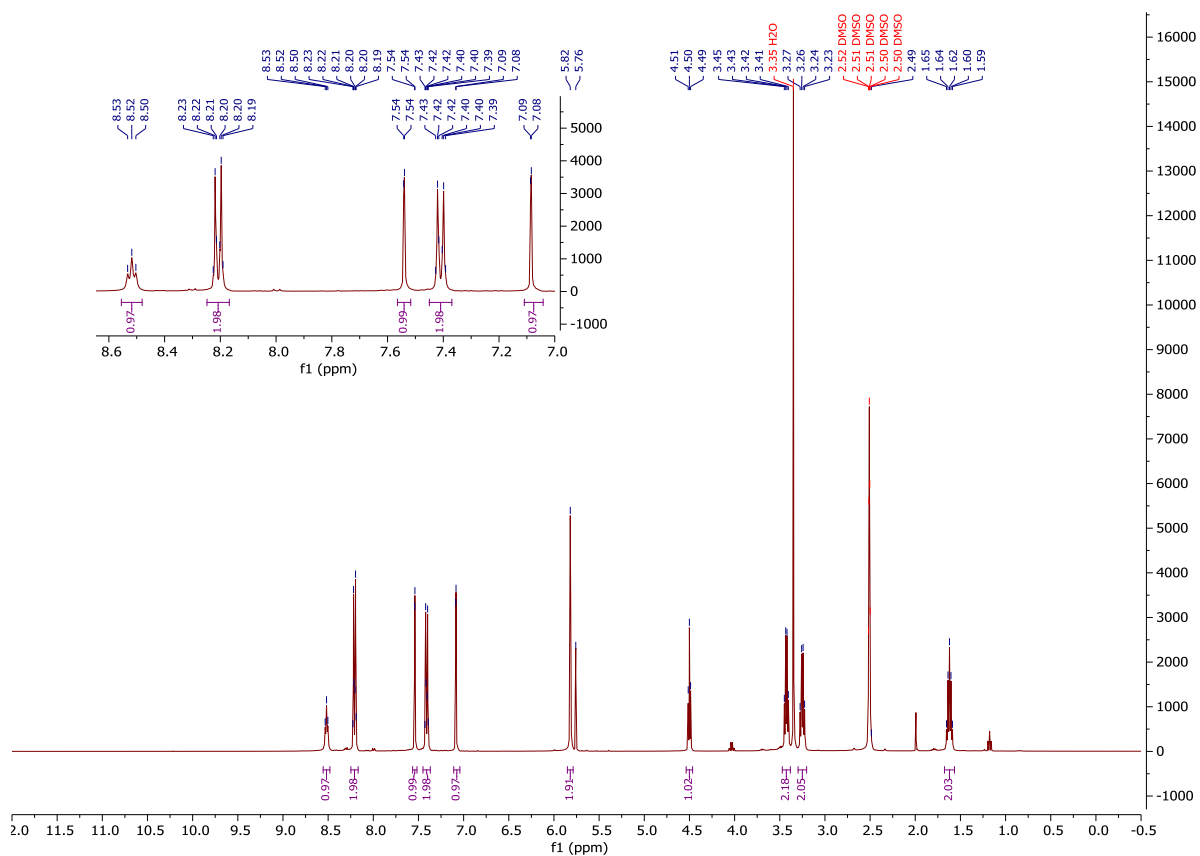
¹H-NMR and ¹³C-NMR: Compound 94



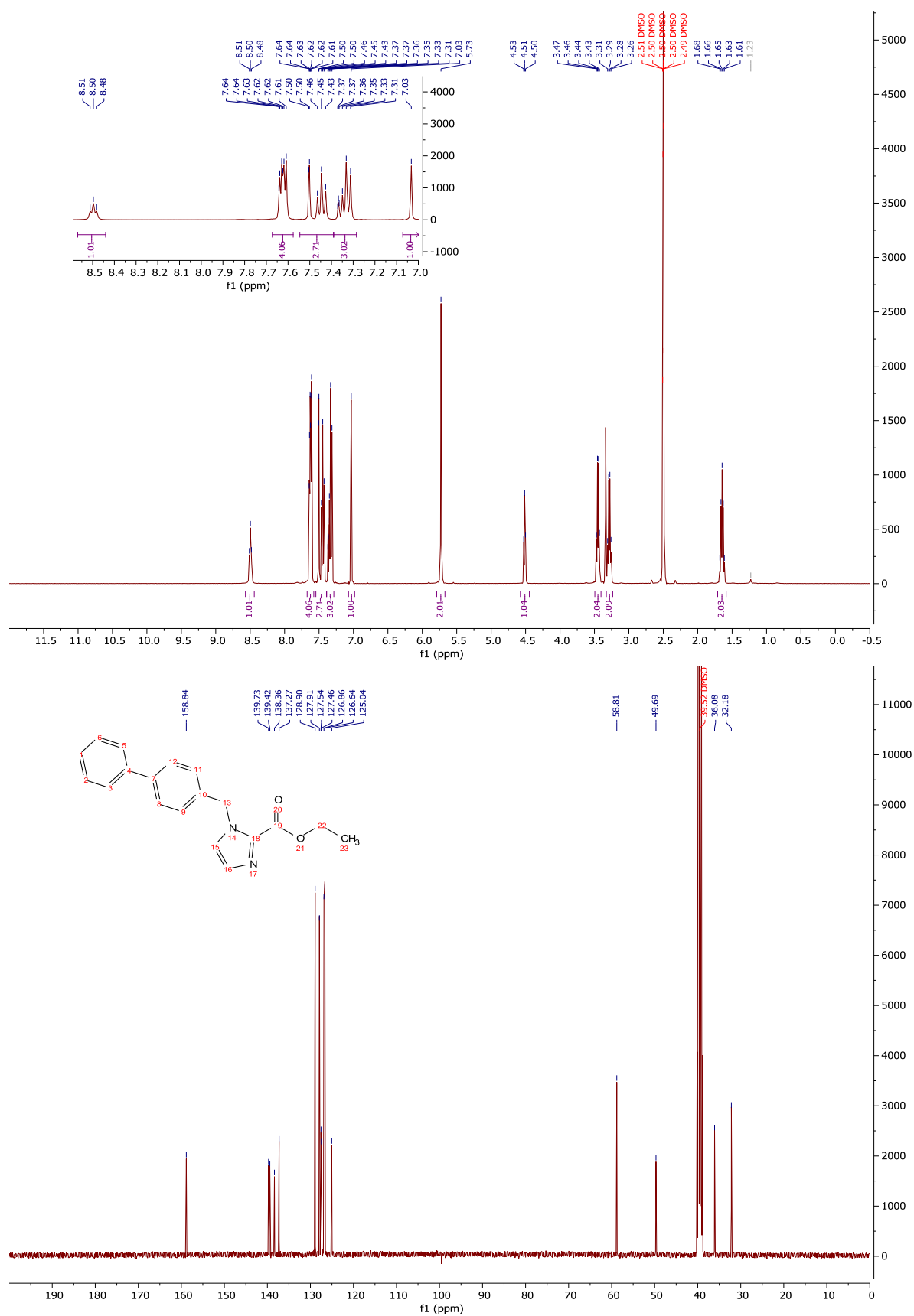
¹H-NMR and ¹³C-NMR: Compound 98



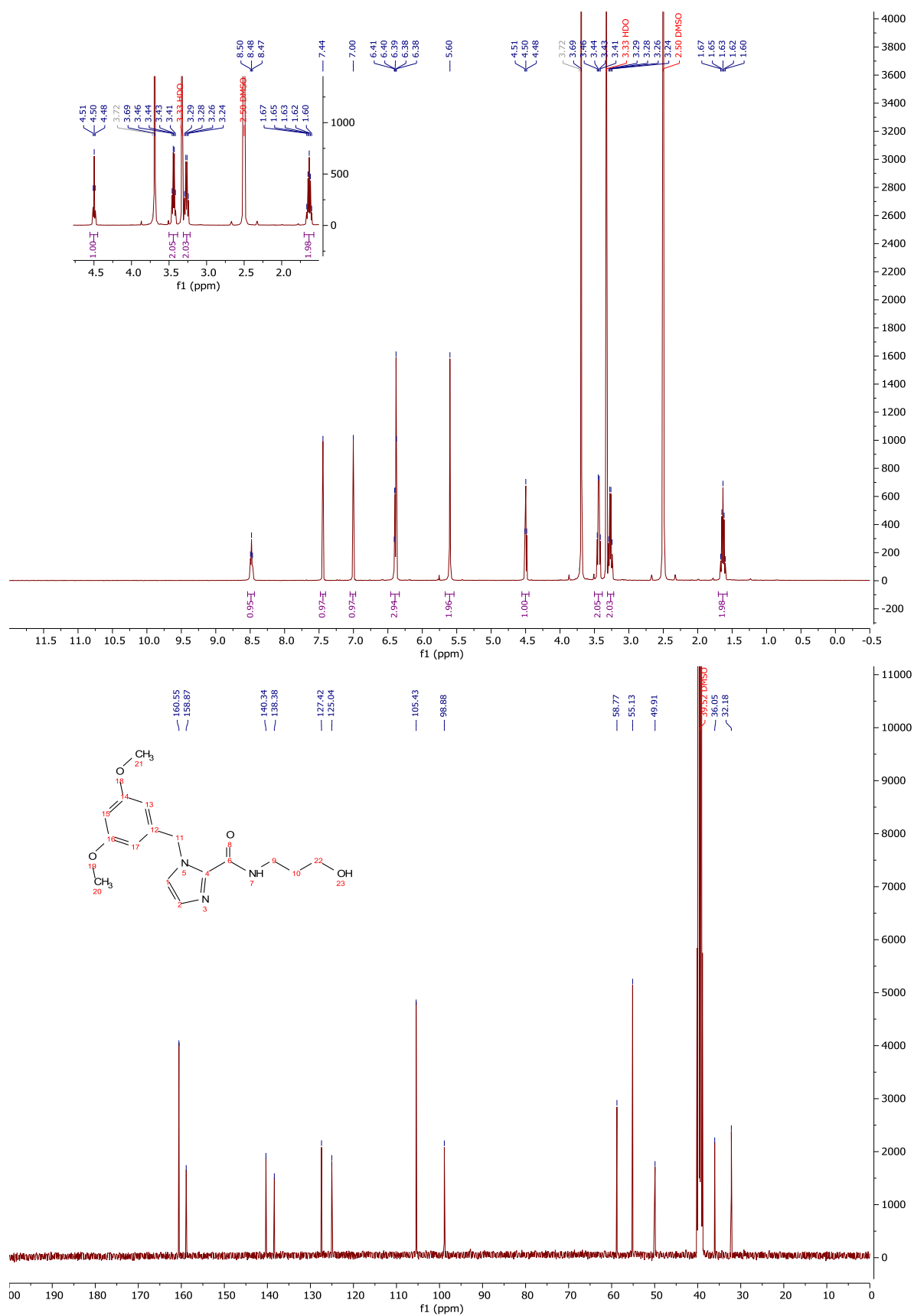
¹H-NMR and ¹³C-NMR: Compound 99



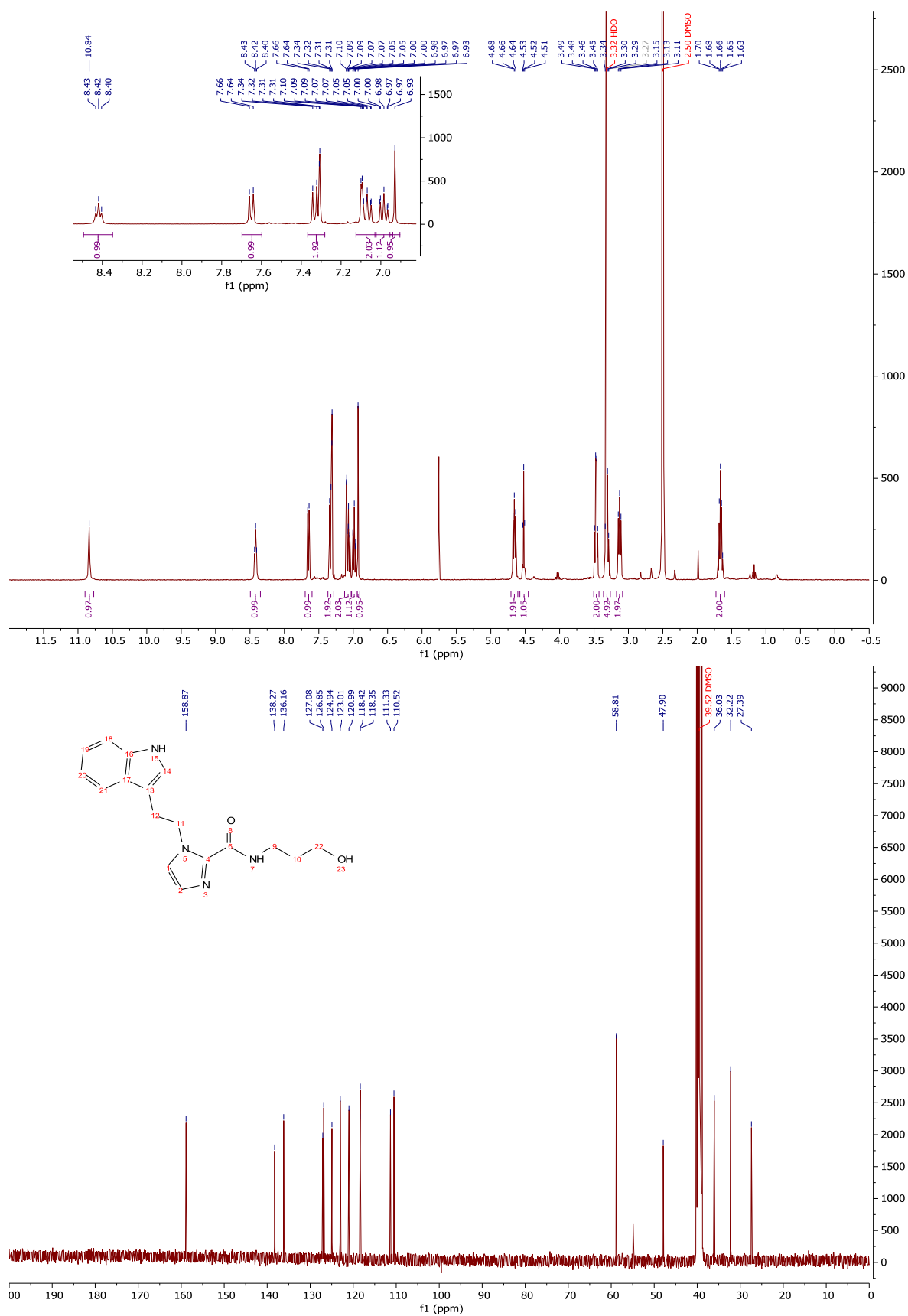
$^1\text{H-NMR}$ and $^{13}\text{C-NMR}$: Compound 100



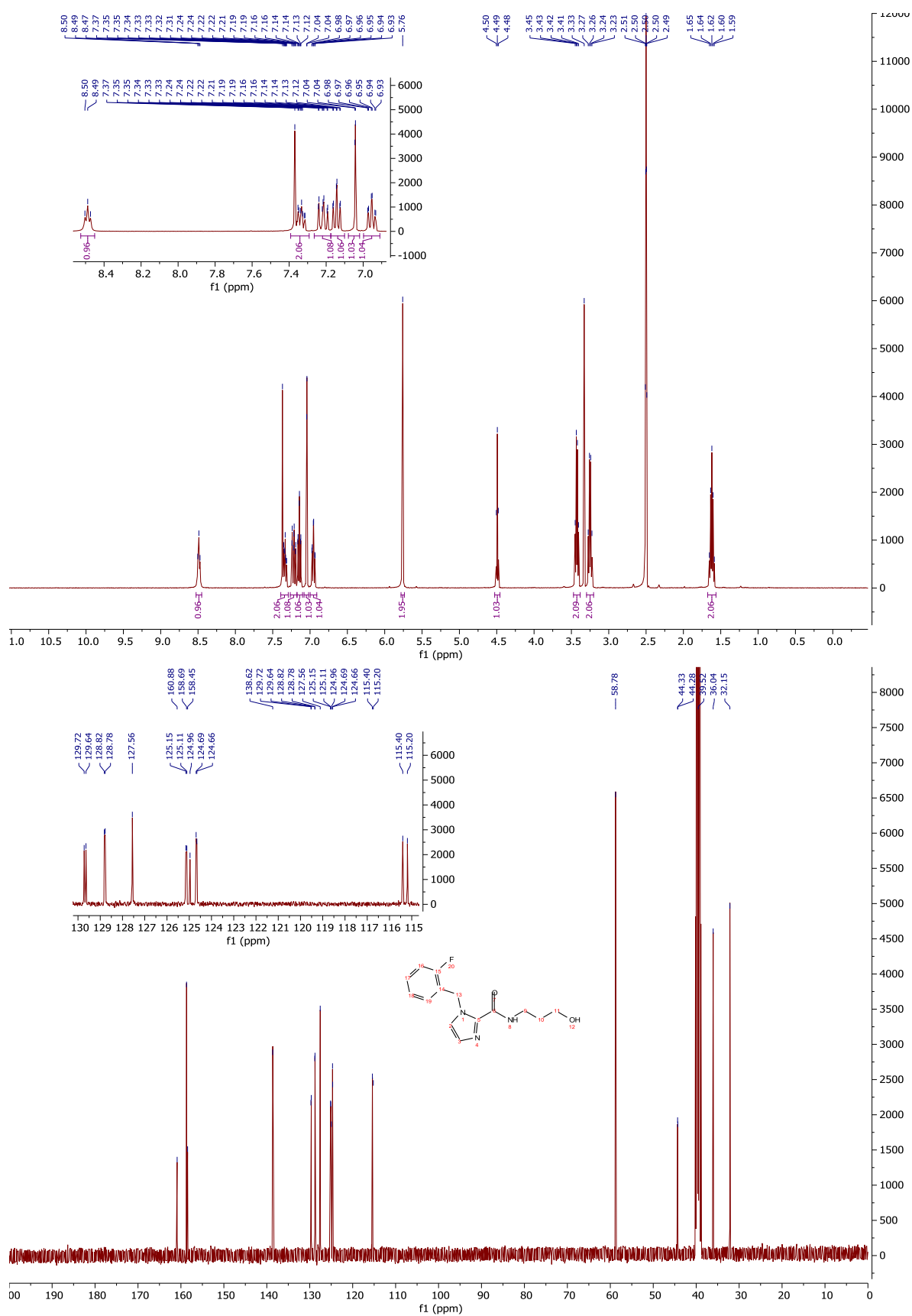
¹H-NMR and ¹³C-NMR: Compound 107



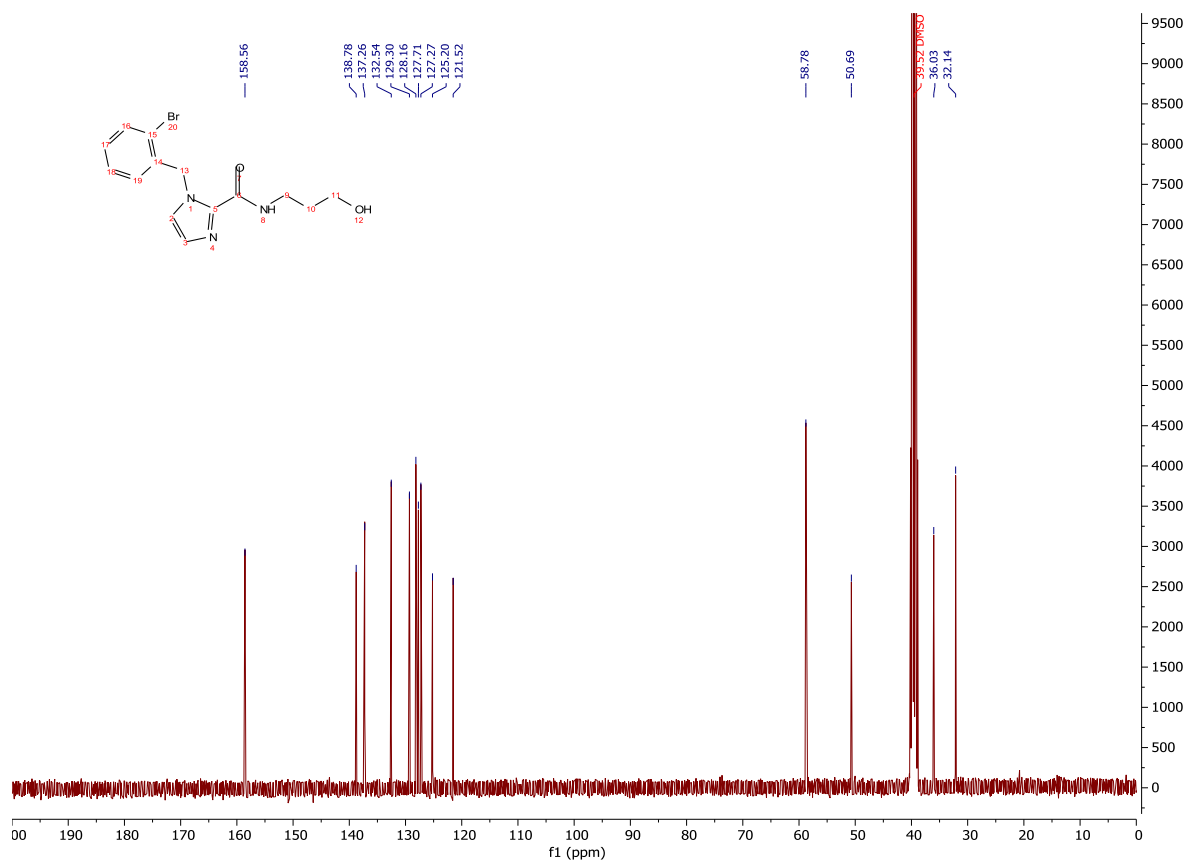
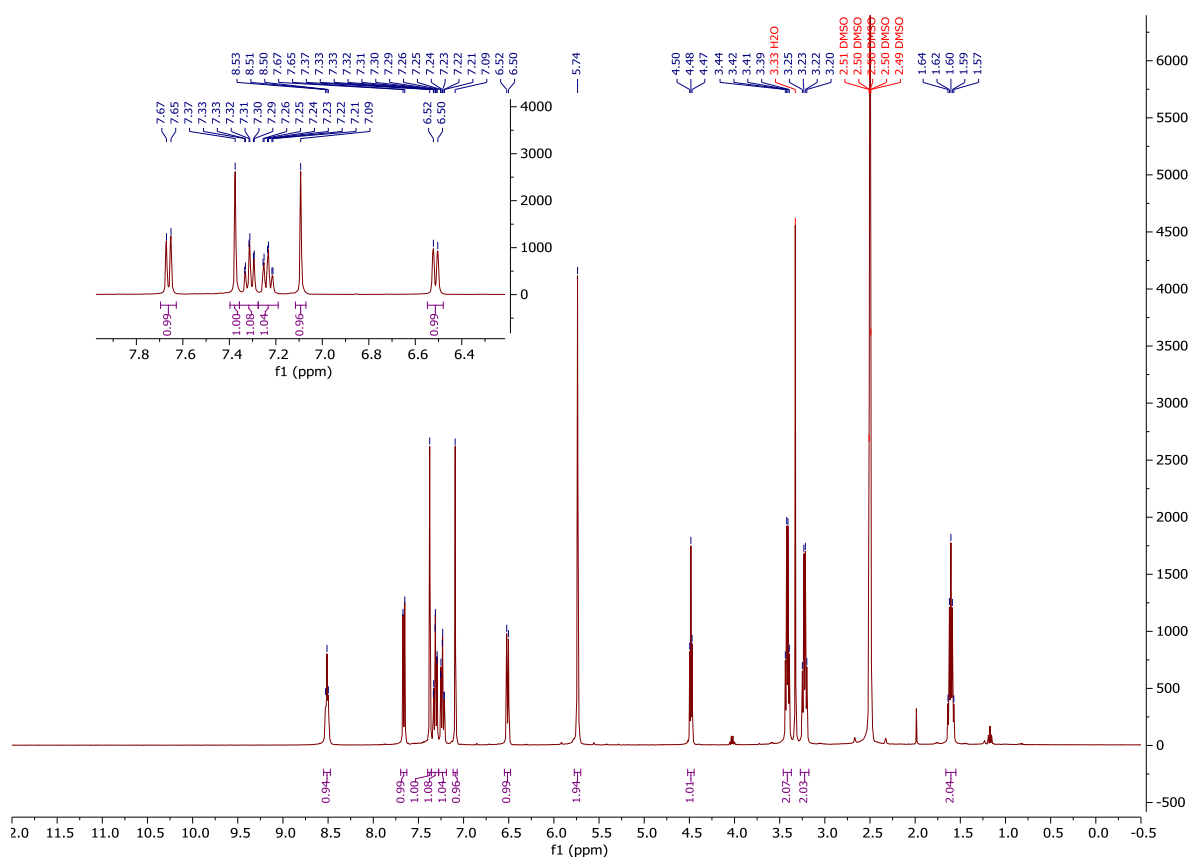
$^1\text{H-NMR}$ and $^{13}\text{C-NMR}$: Compound 105



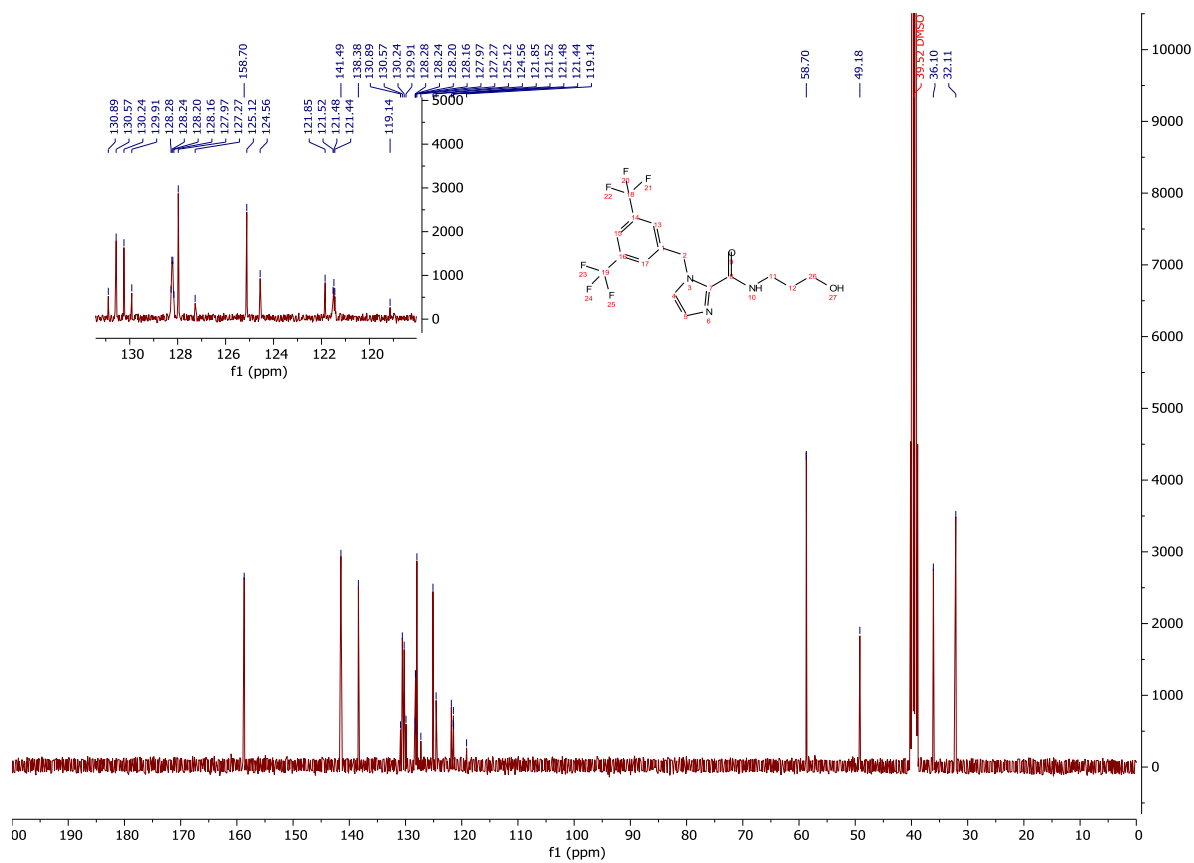
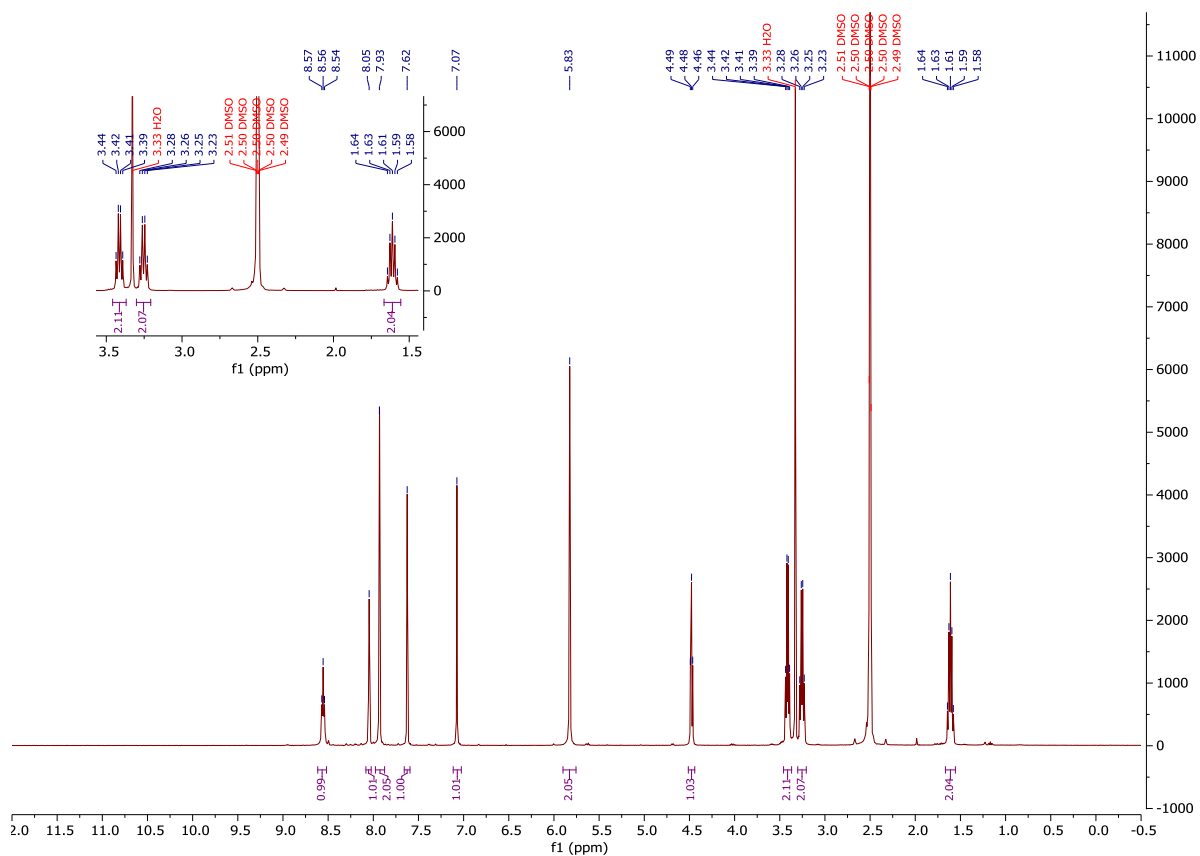
¹H-NMR and ¹³C-NMR: Compound 111



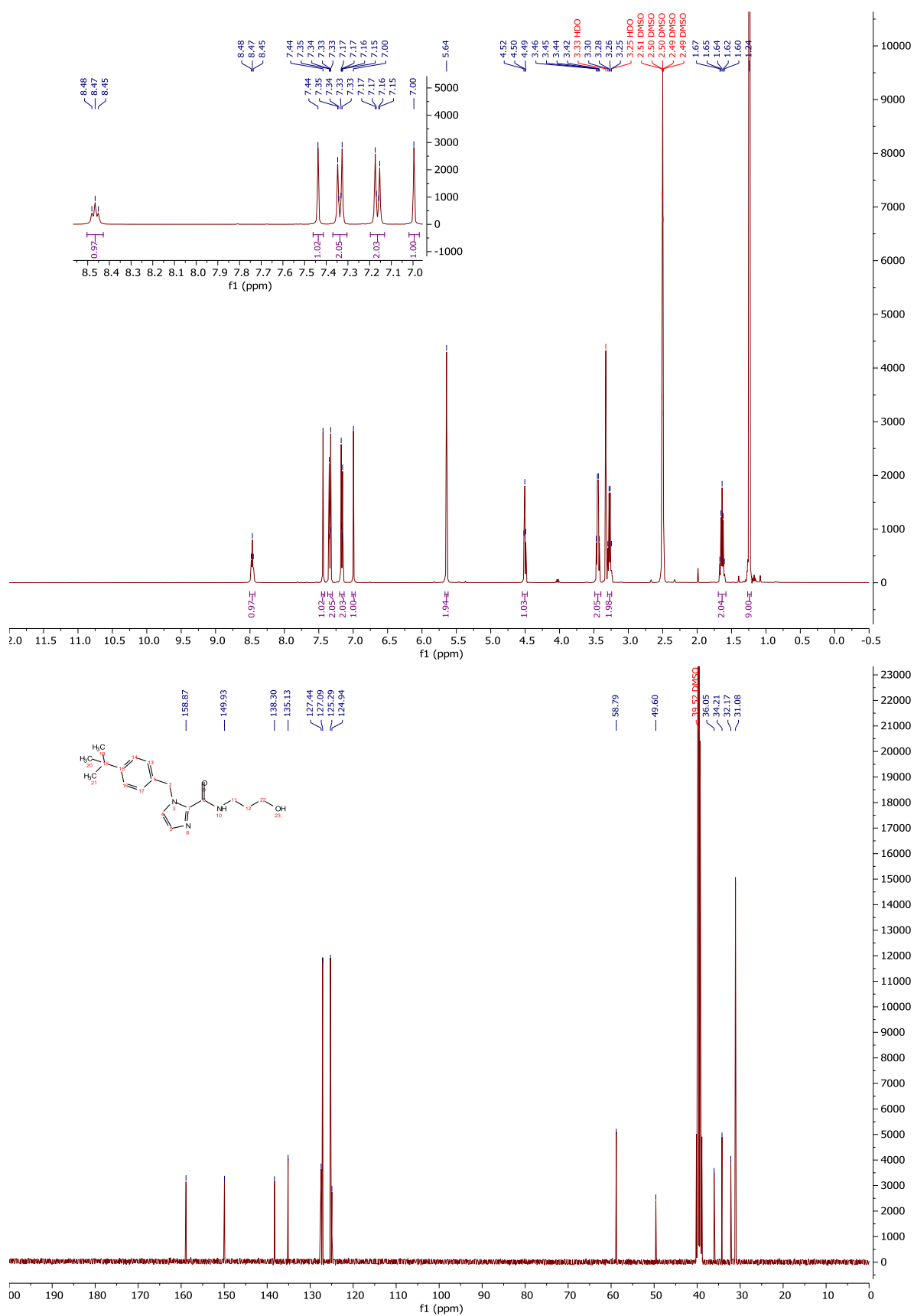
¹H-NMR and ¹³C-NMR: Compound 114



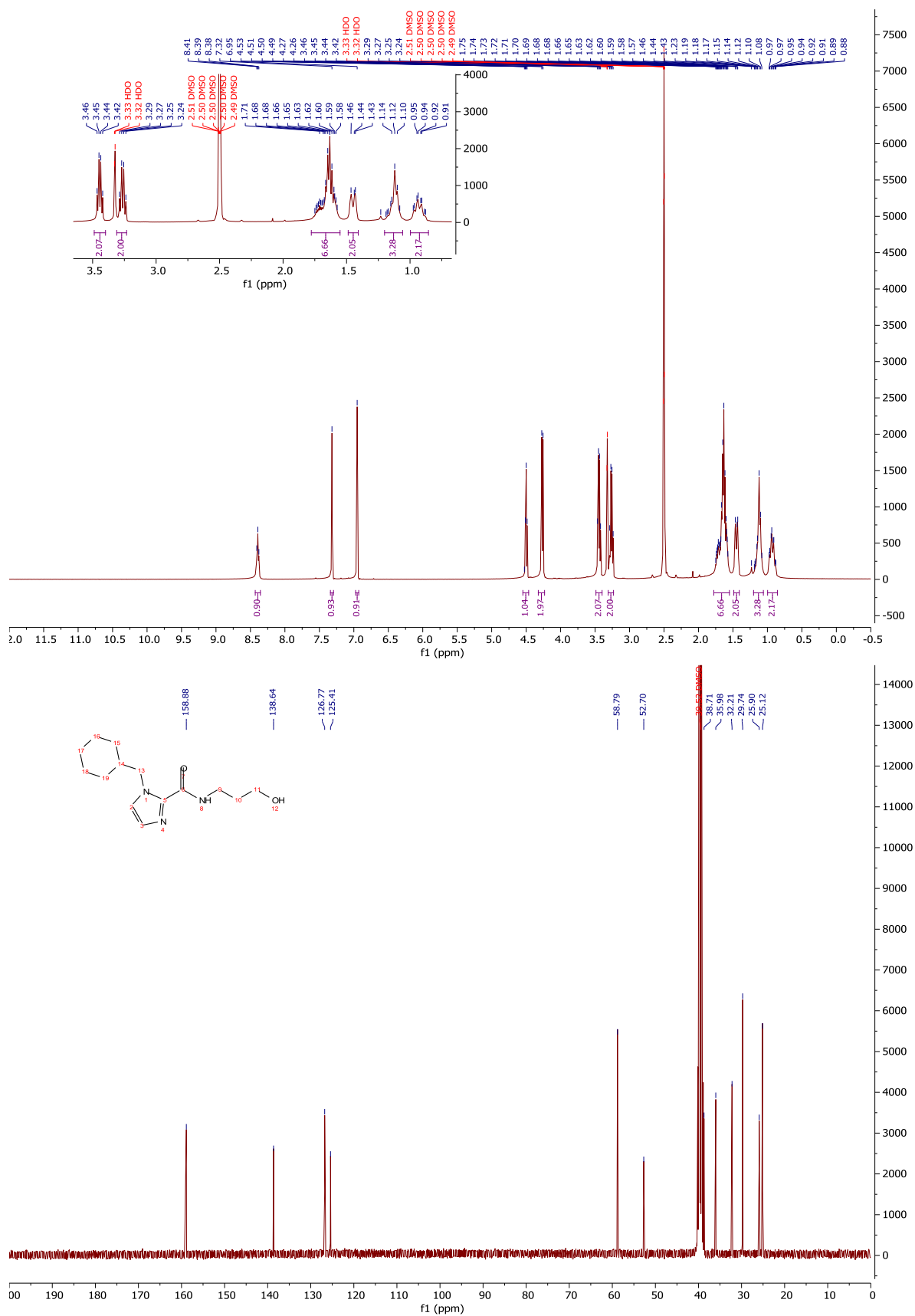
¹H-NMR and ¹³C-NMR: Compound 102



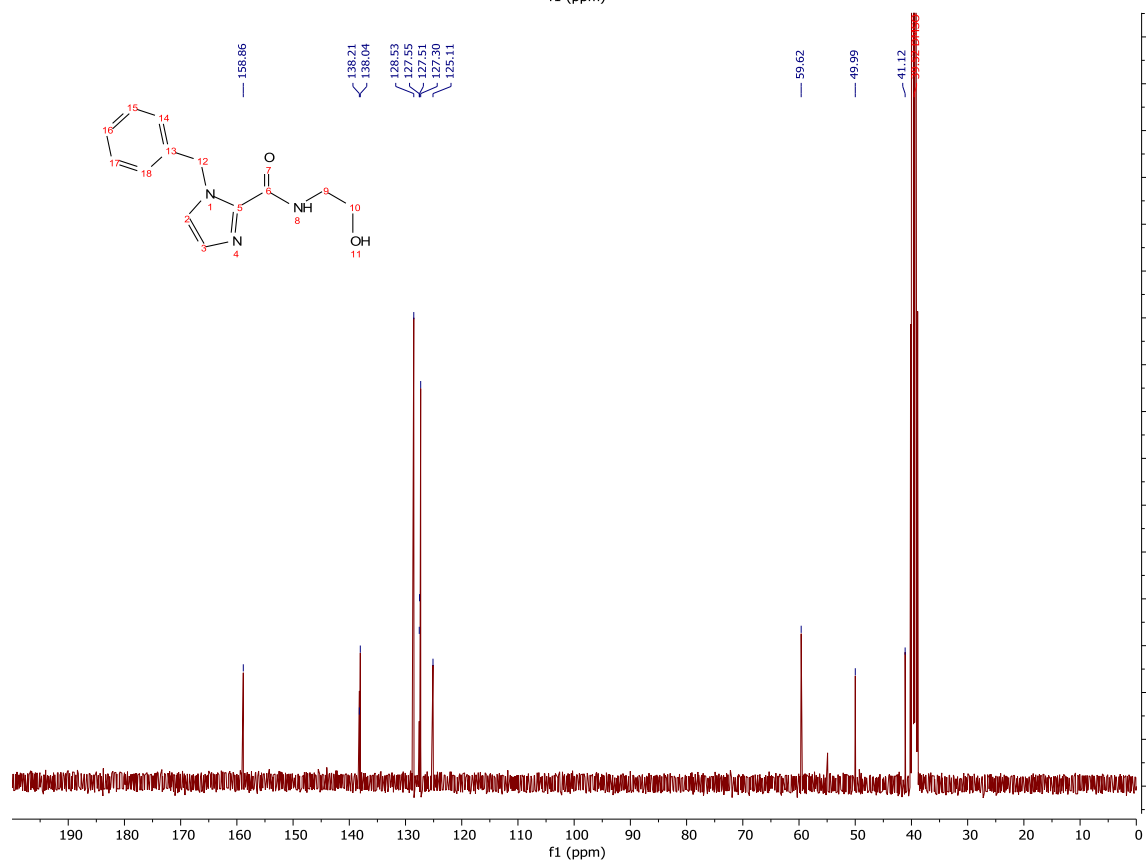
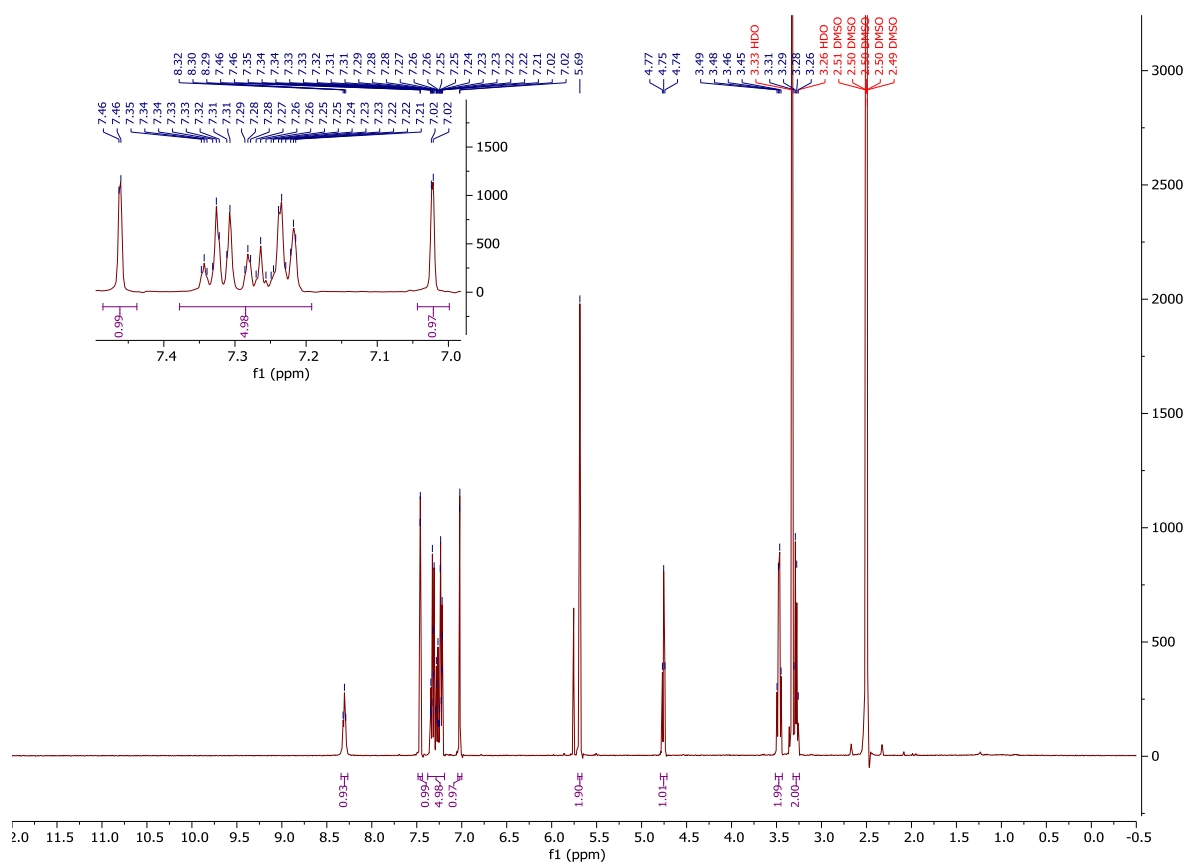
¹H-NMR and ¹³C-NMR: Compound 109



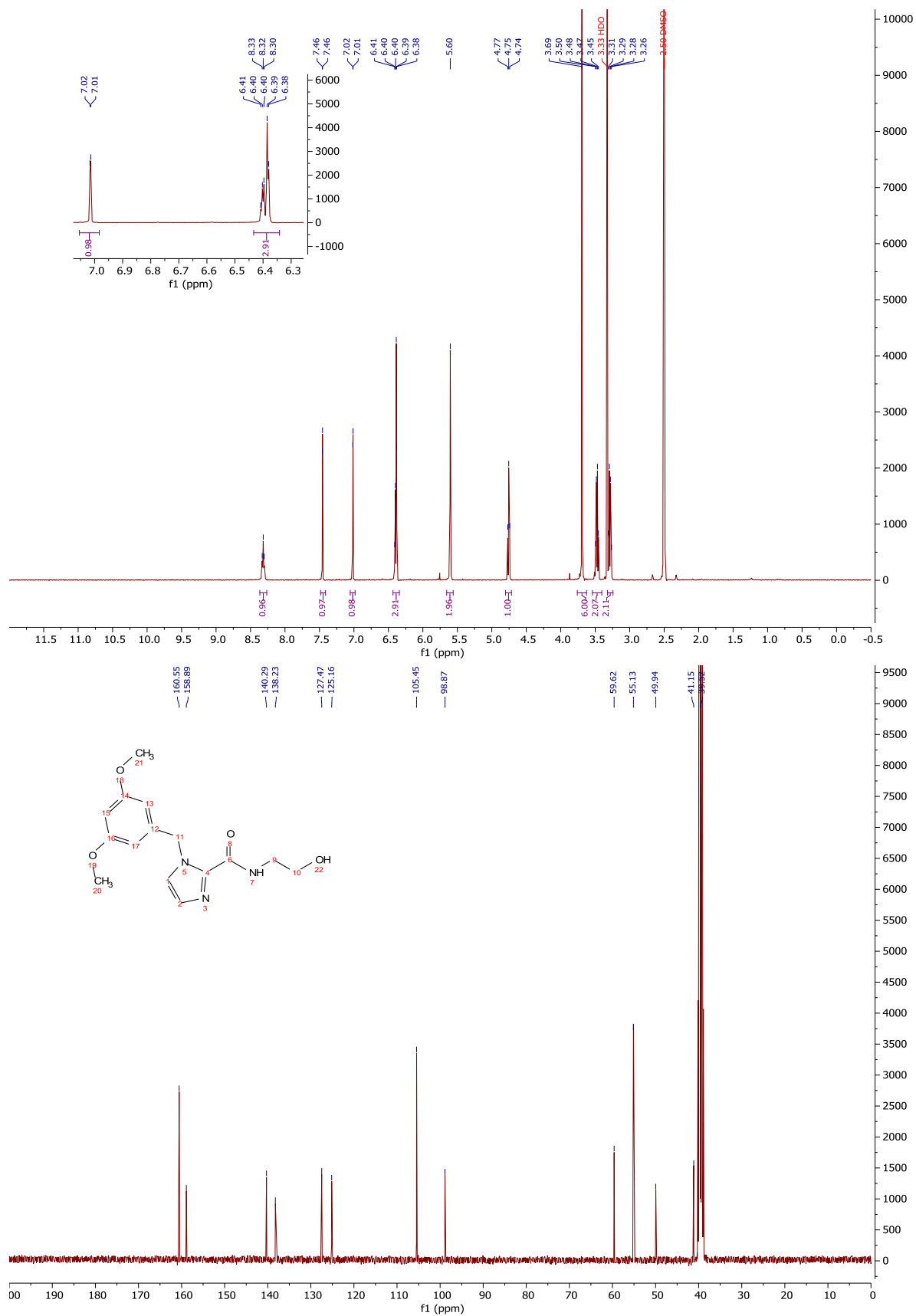
¹H-NMR and ¹³C-NMR: Compound 104



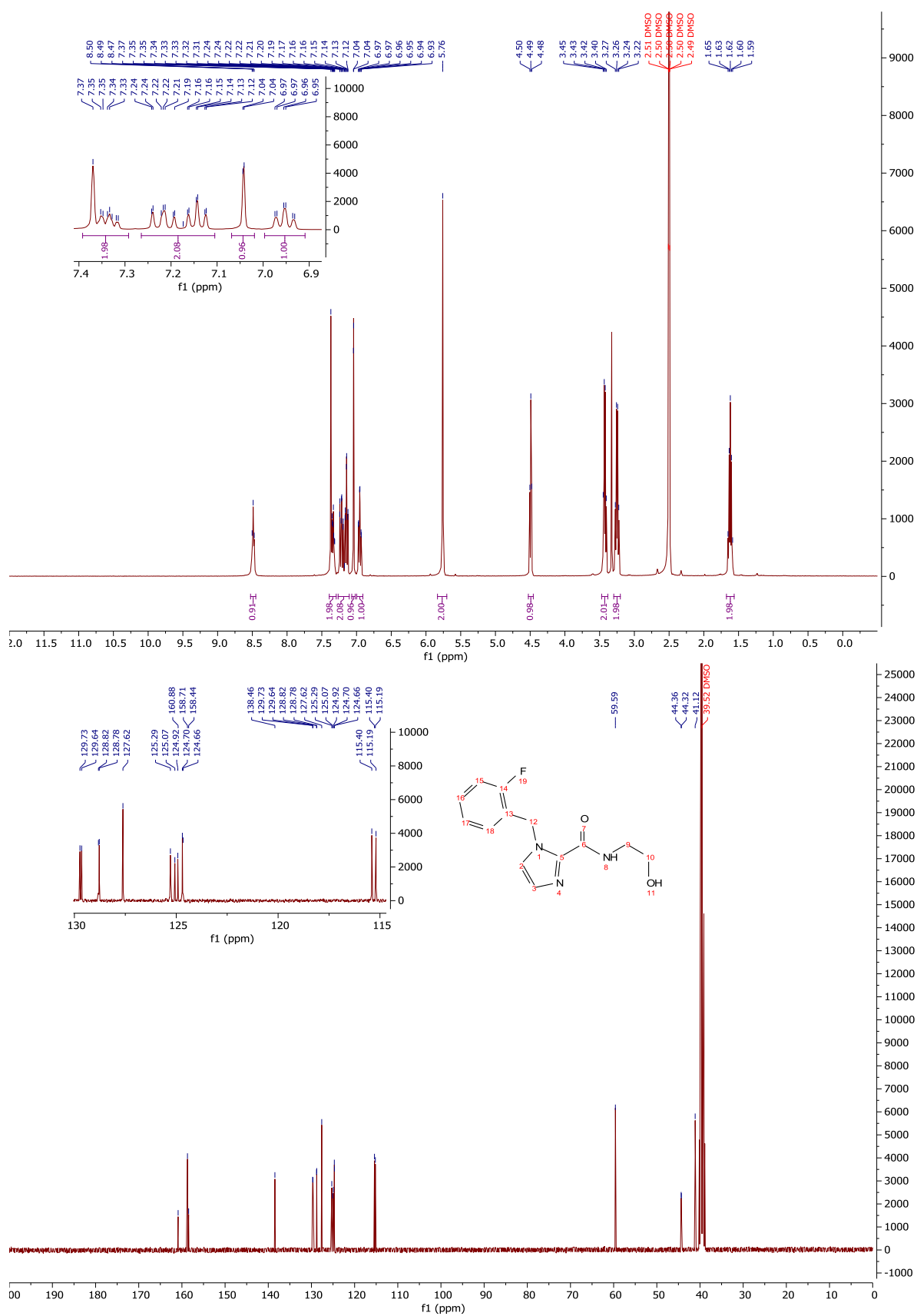
¹H-NMR and ¹³C-NMR: Compound 97



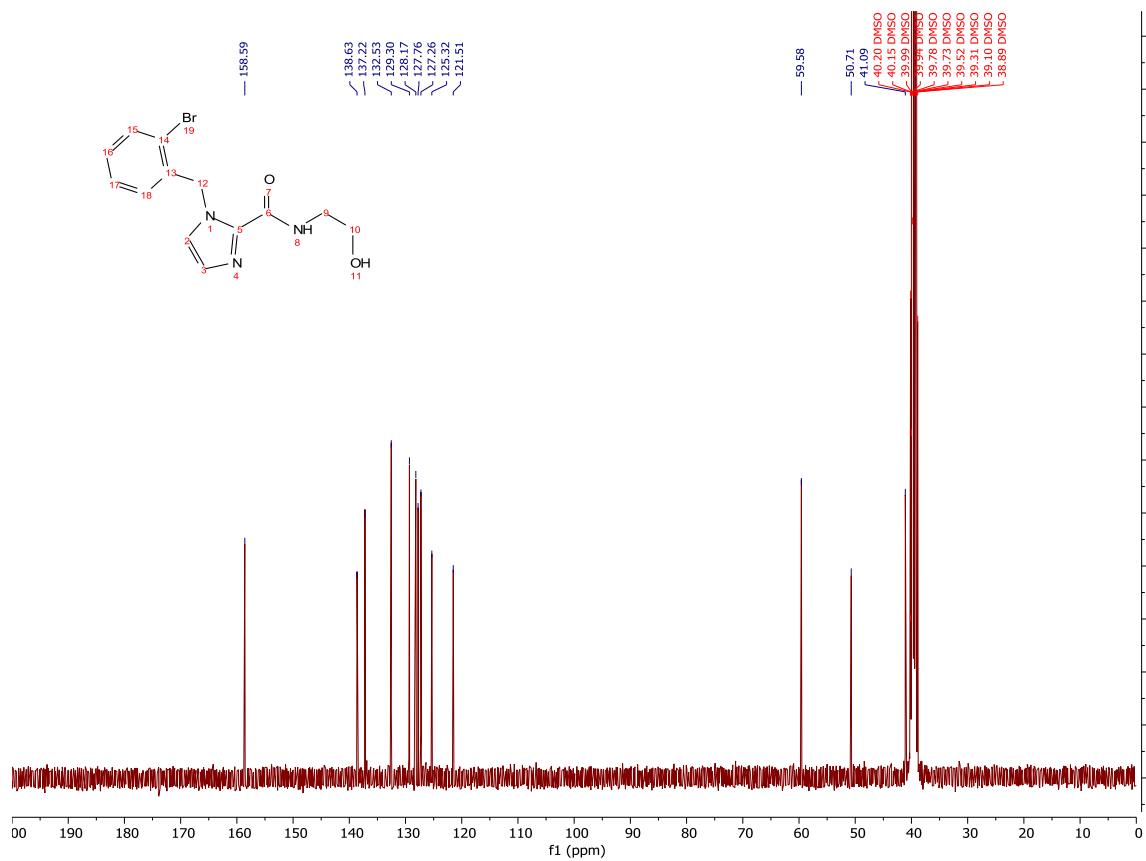
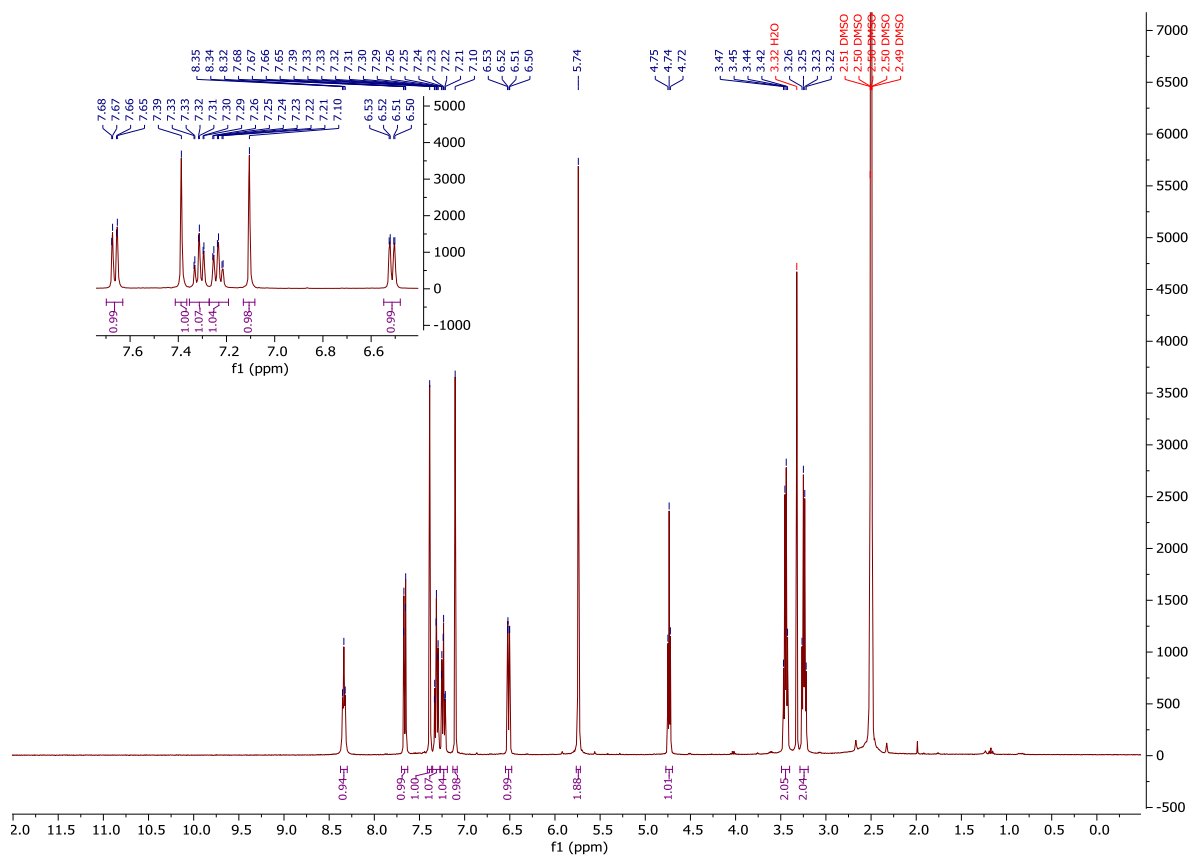
¹H-NMR and ¹³C-NMR: Compound 101



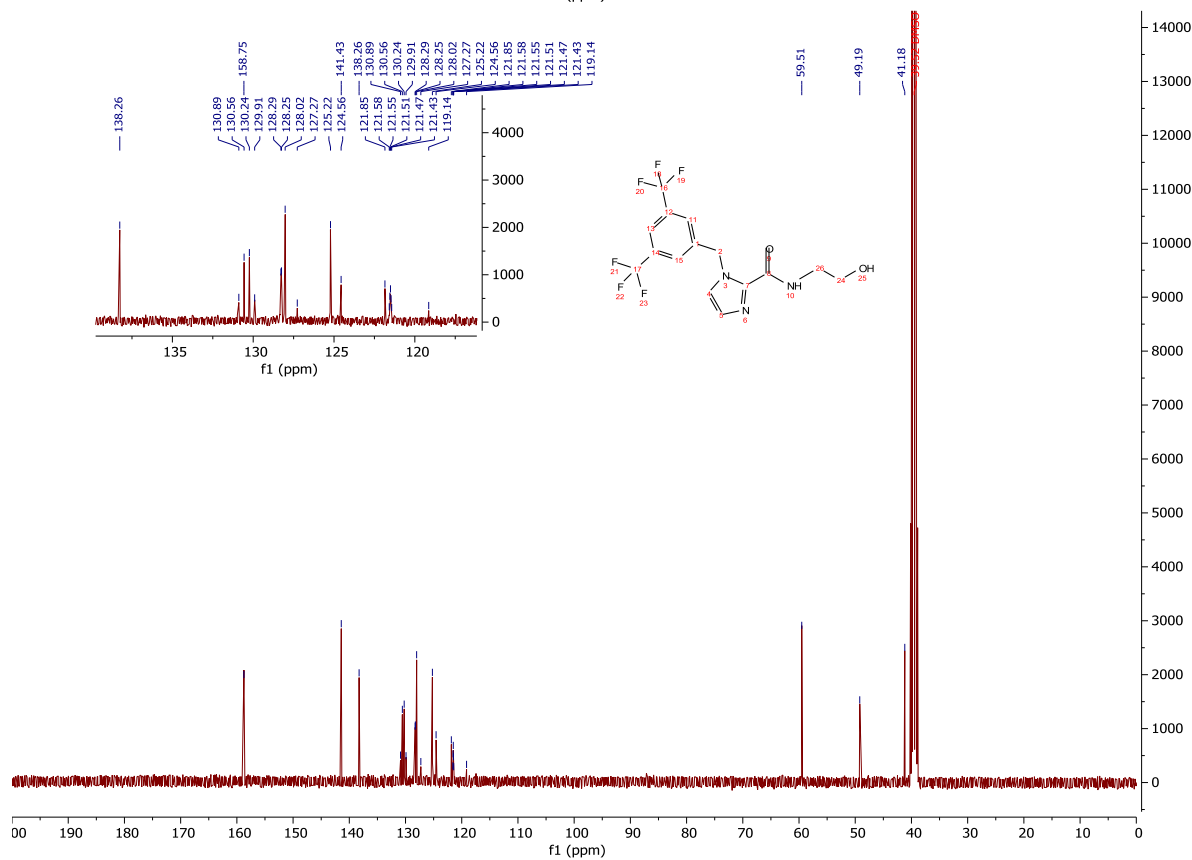
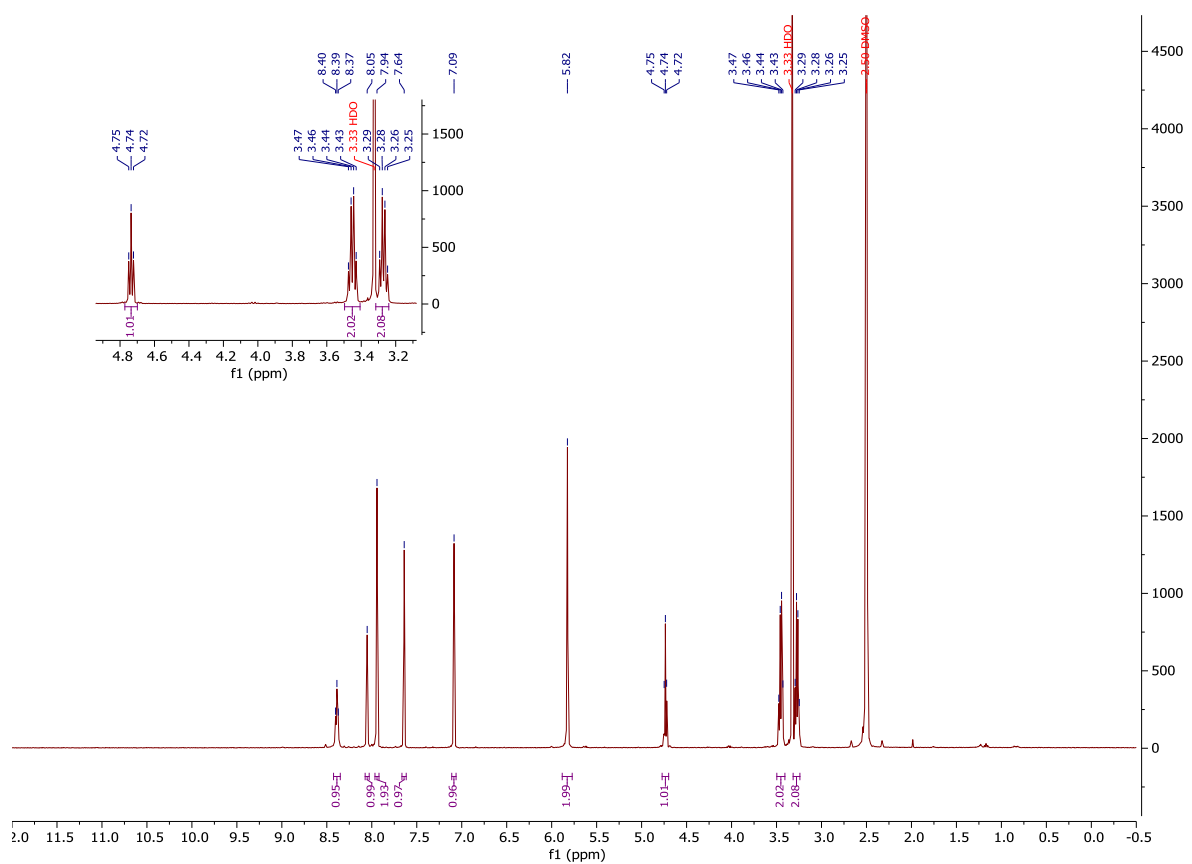
¹H-NMR and ¹³C-NMR: Compound 110



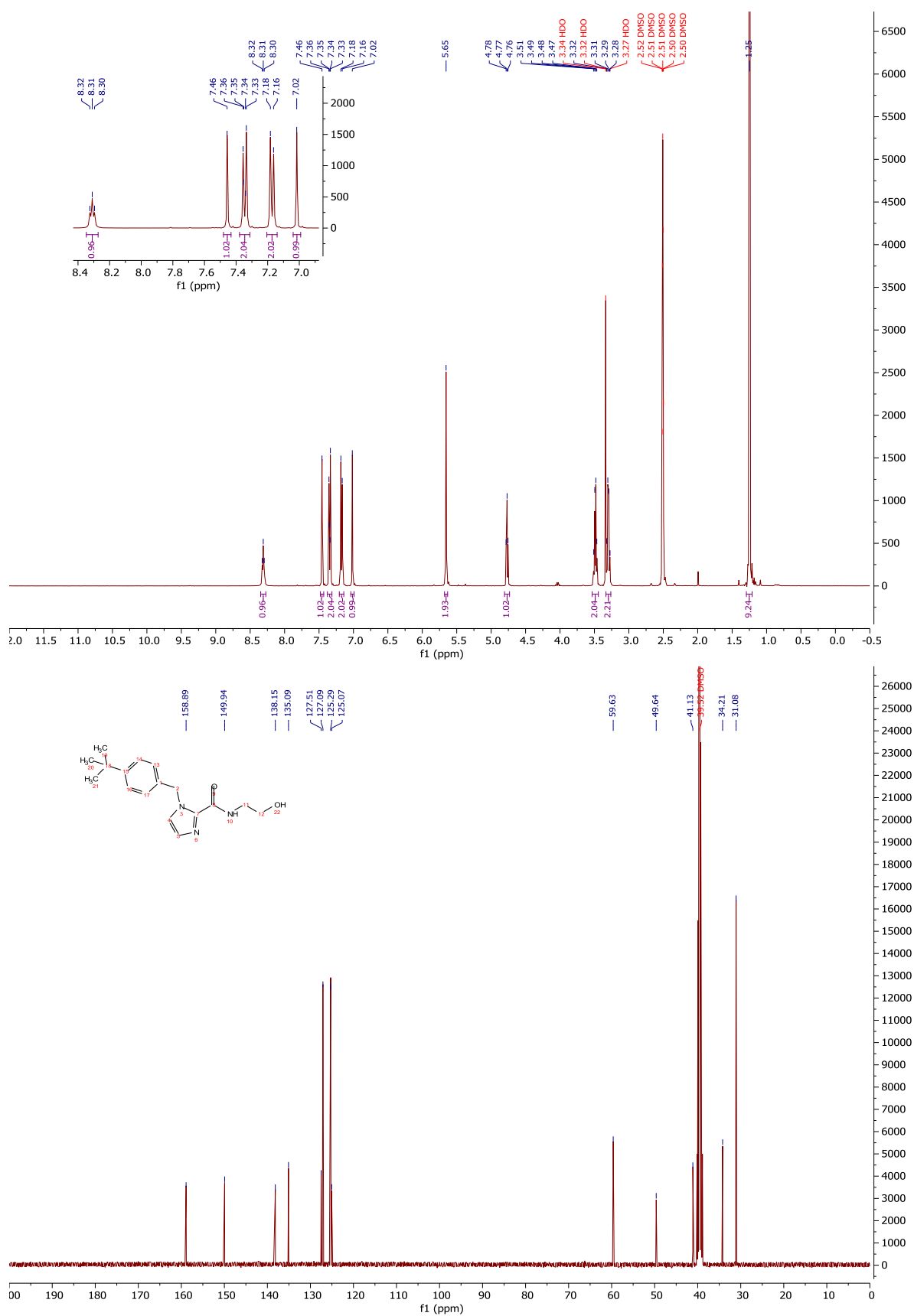
$^1\text{H-NMR}$ and $^{13}\text{C-NMR}$: Compound 113



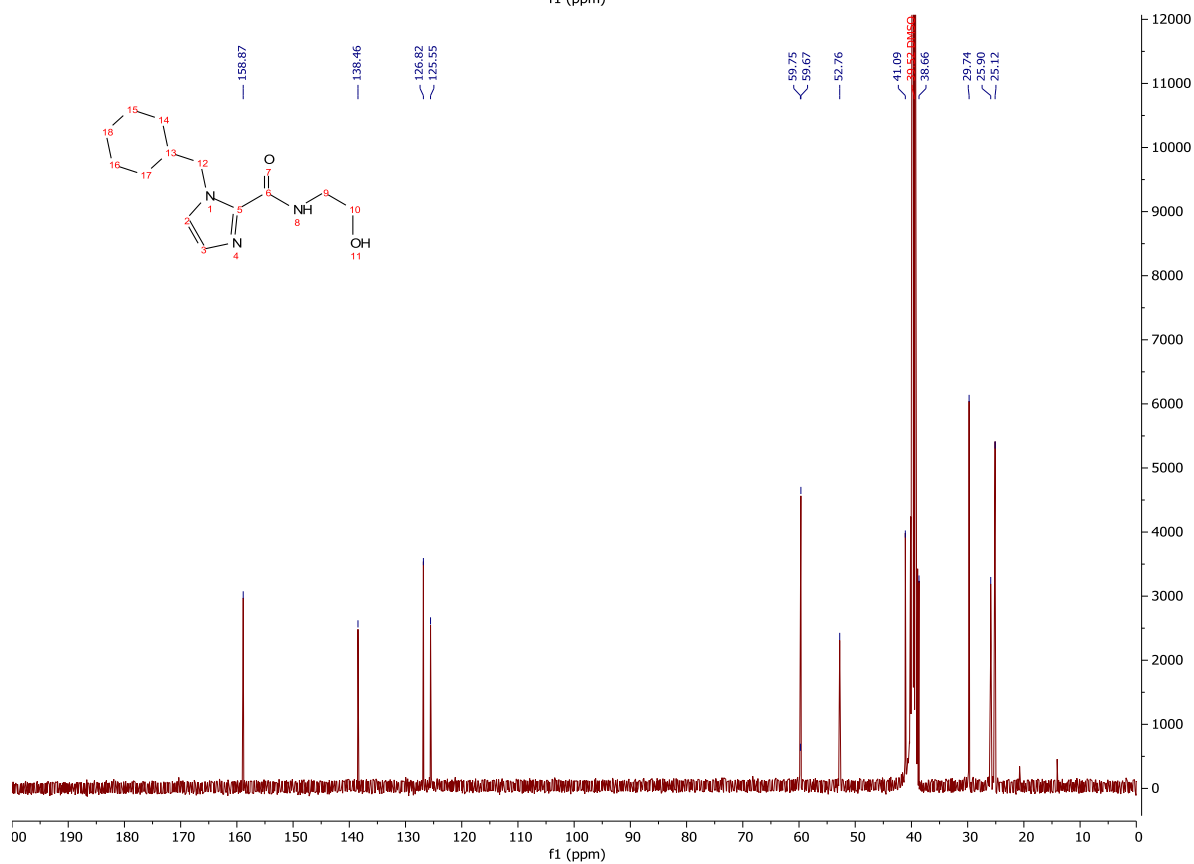
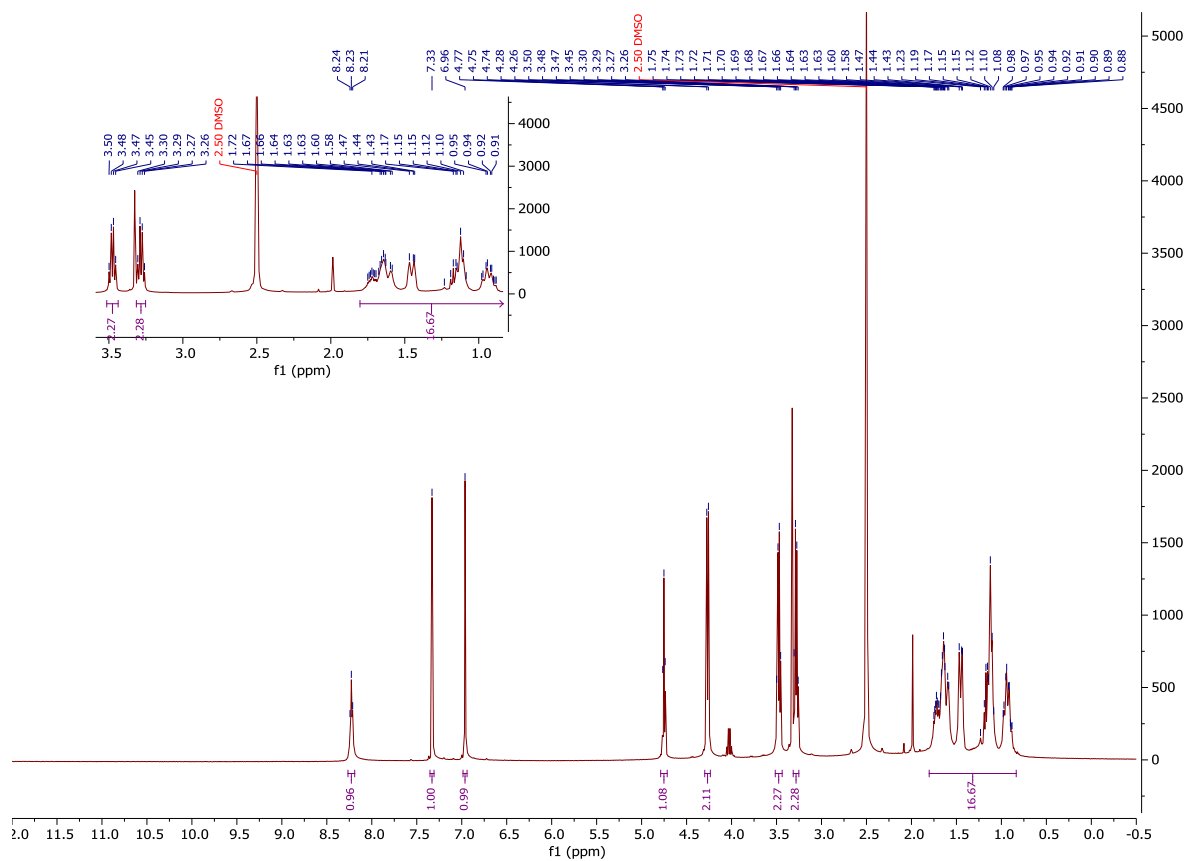
¹H-NMR and ¹³C-NMR: Compound 101



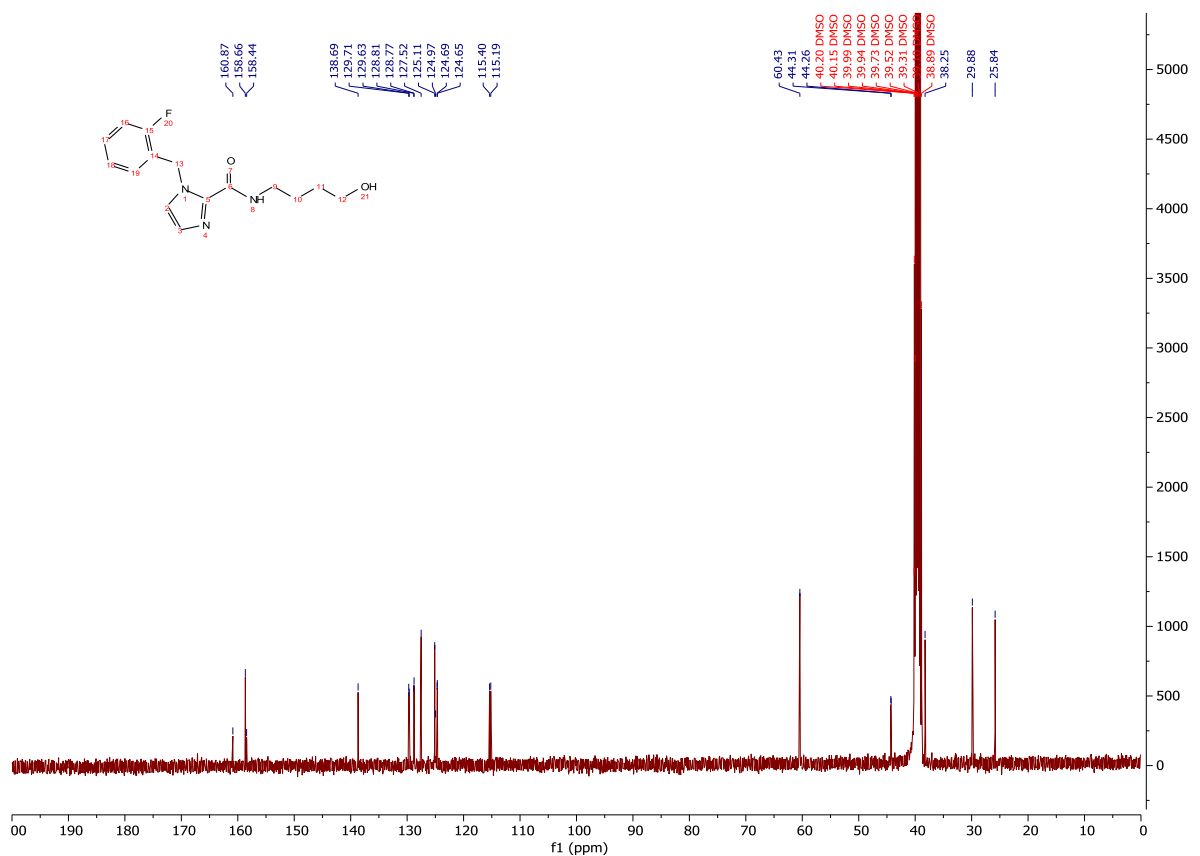
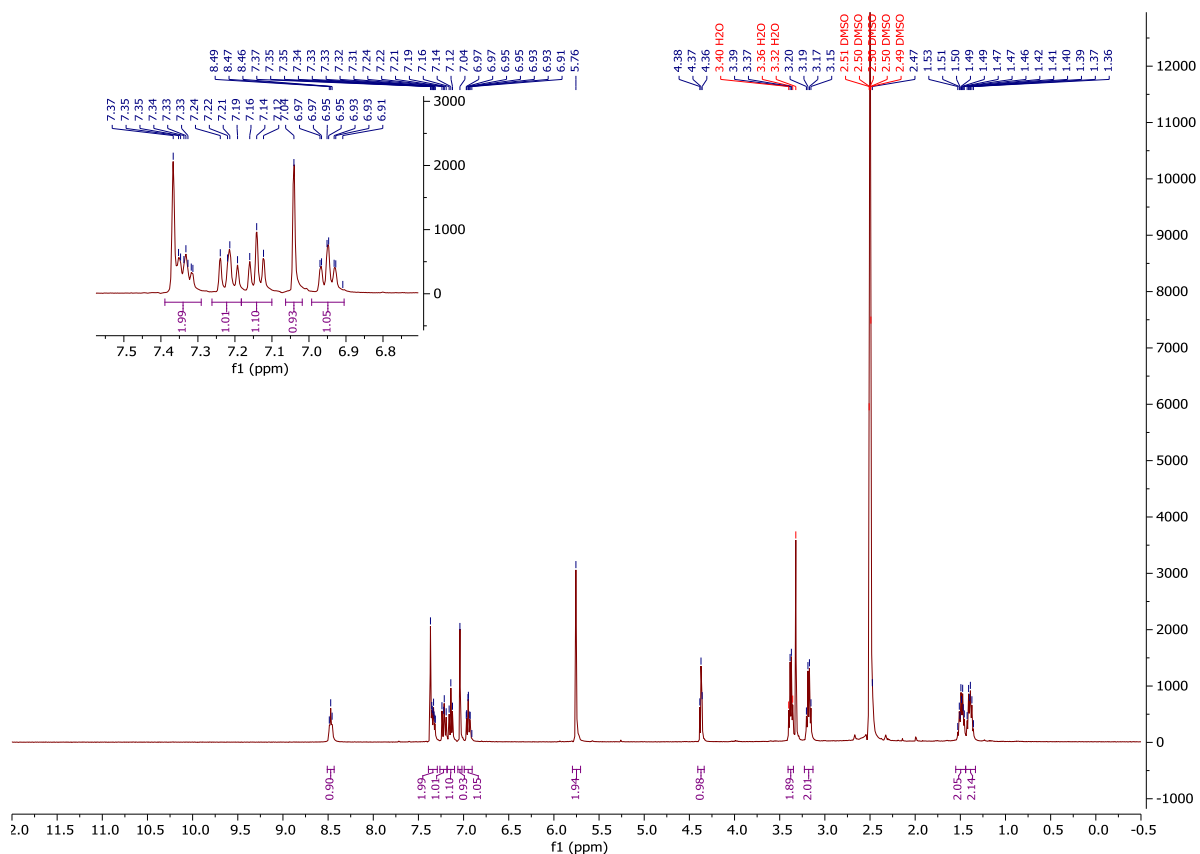
¹H-NMR and ¹³C-NMR: Compound 108



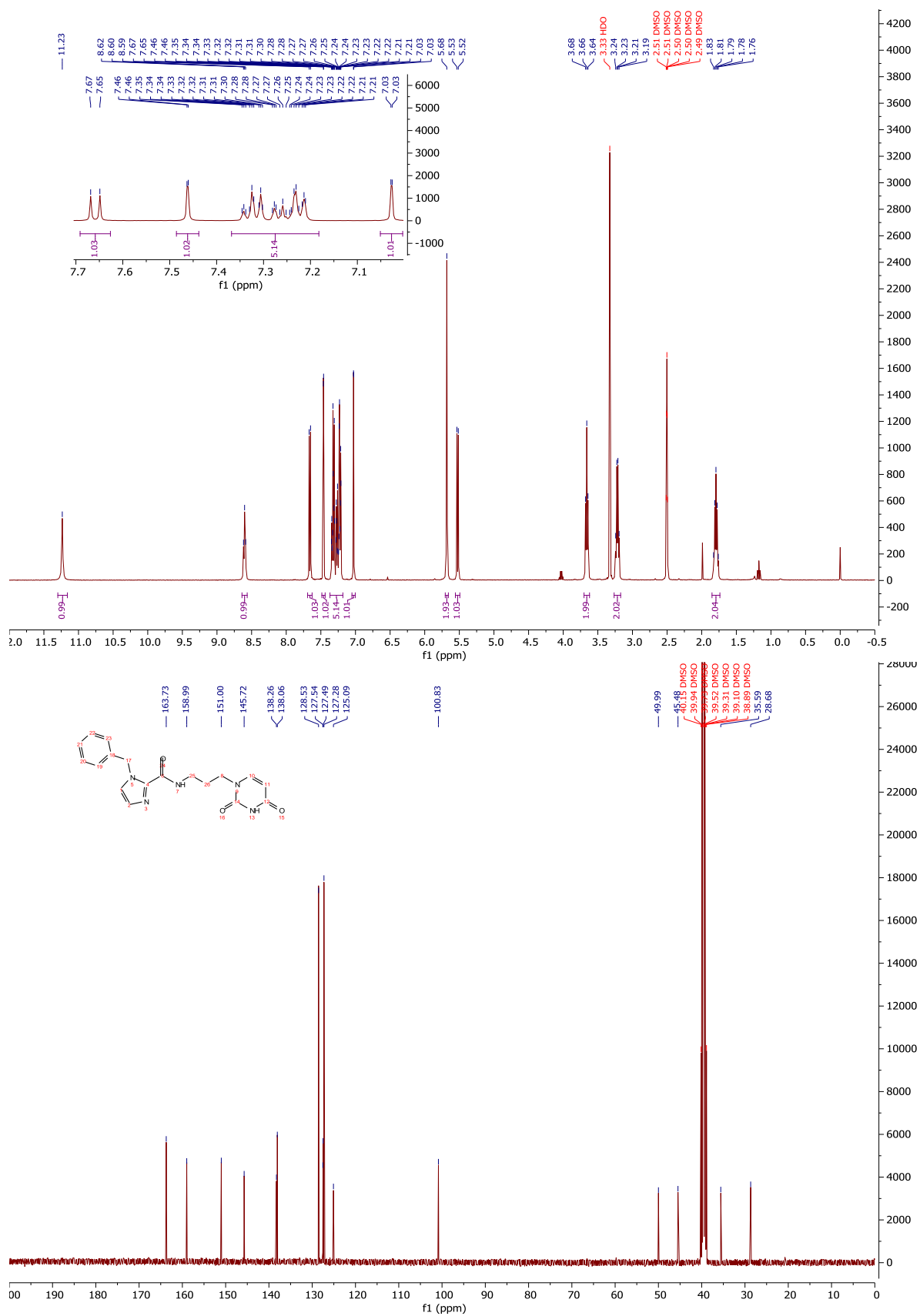
¹H-NMR and ¹³C-NMR: Compound 103



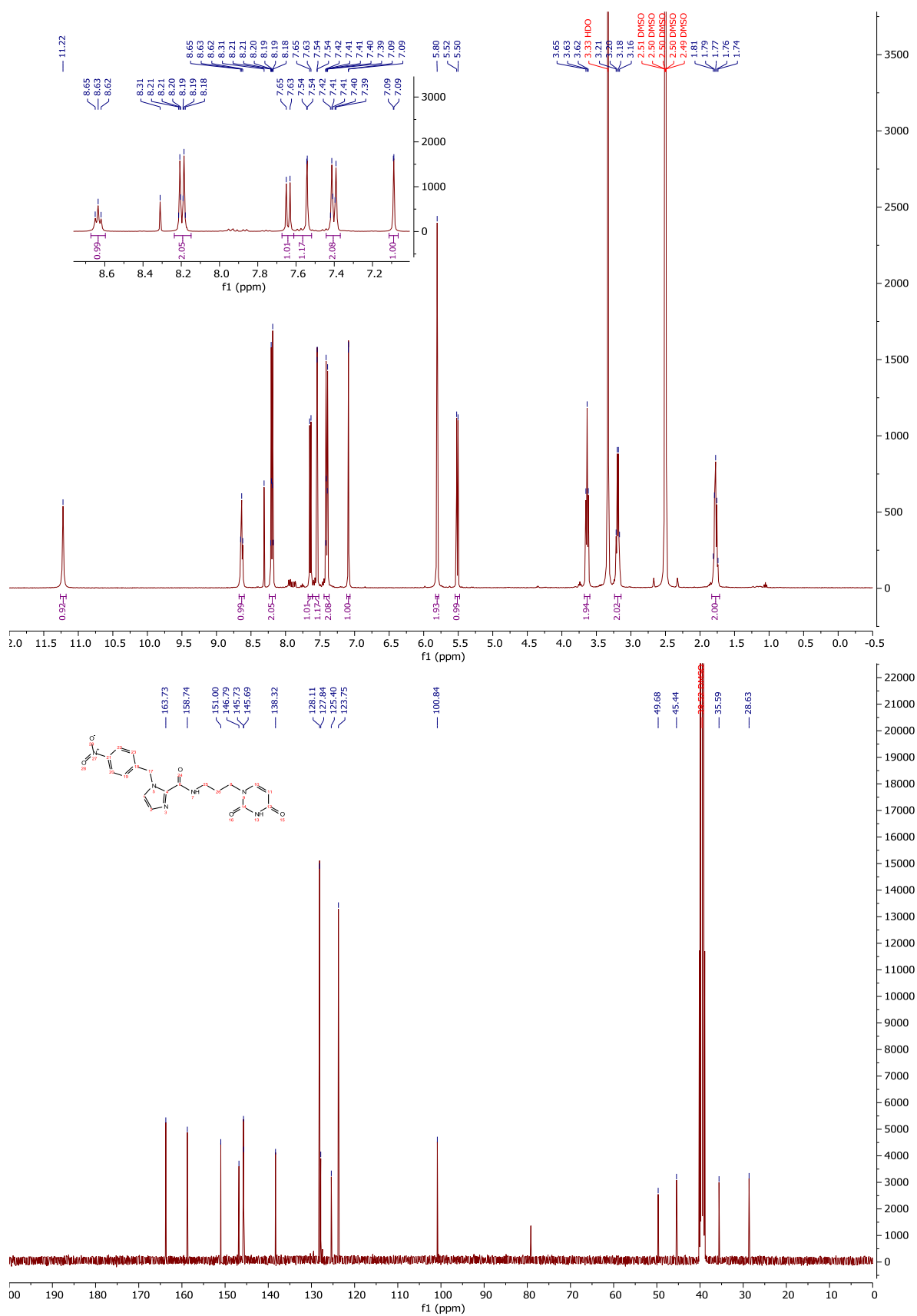
¹H-NMR and ¹³C-NMR: Compound 112



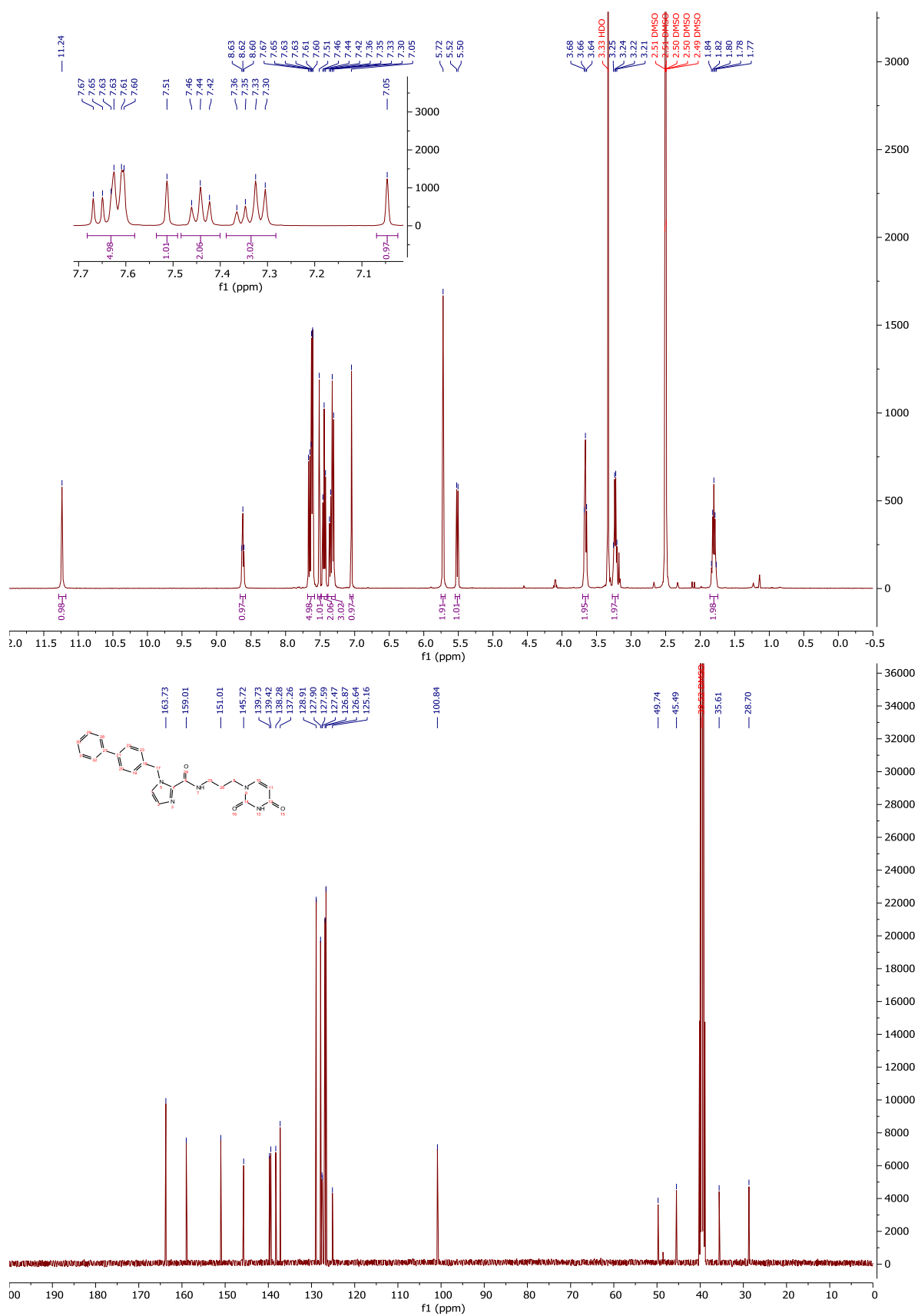
¹H-NMR and ¹³C-NMR: Compound 116



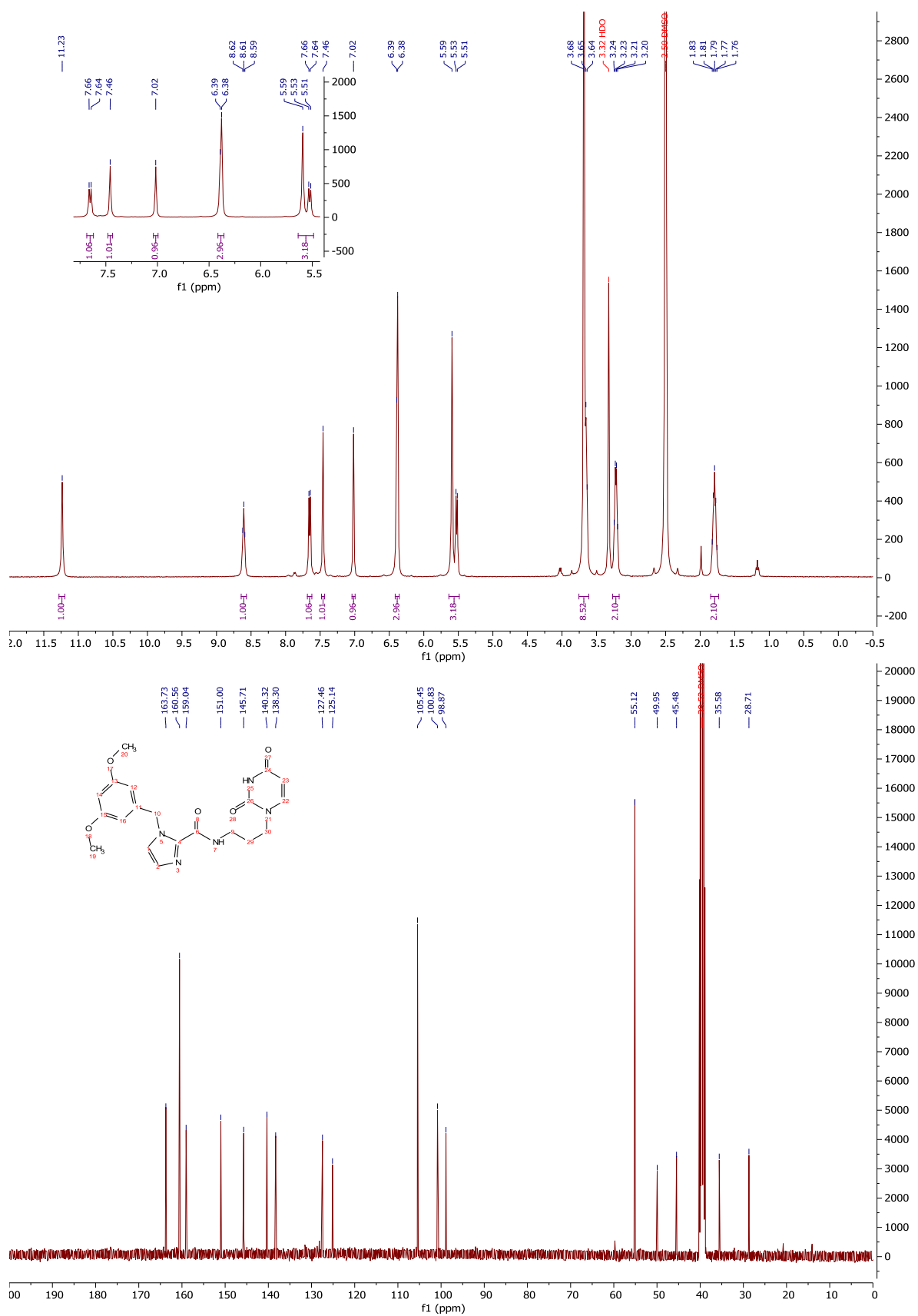
¹H-NMR and ¹³C-NMR: Compound 117



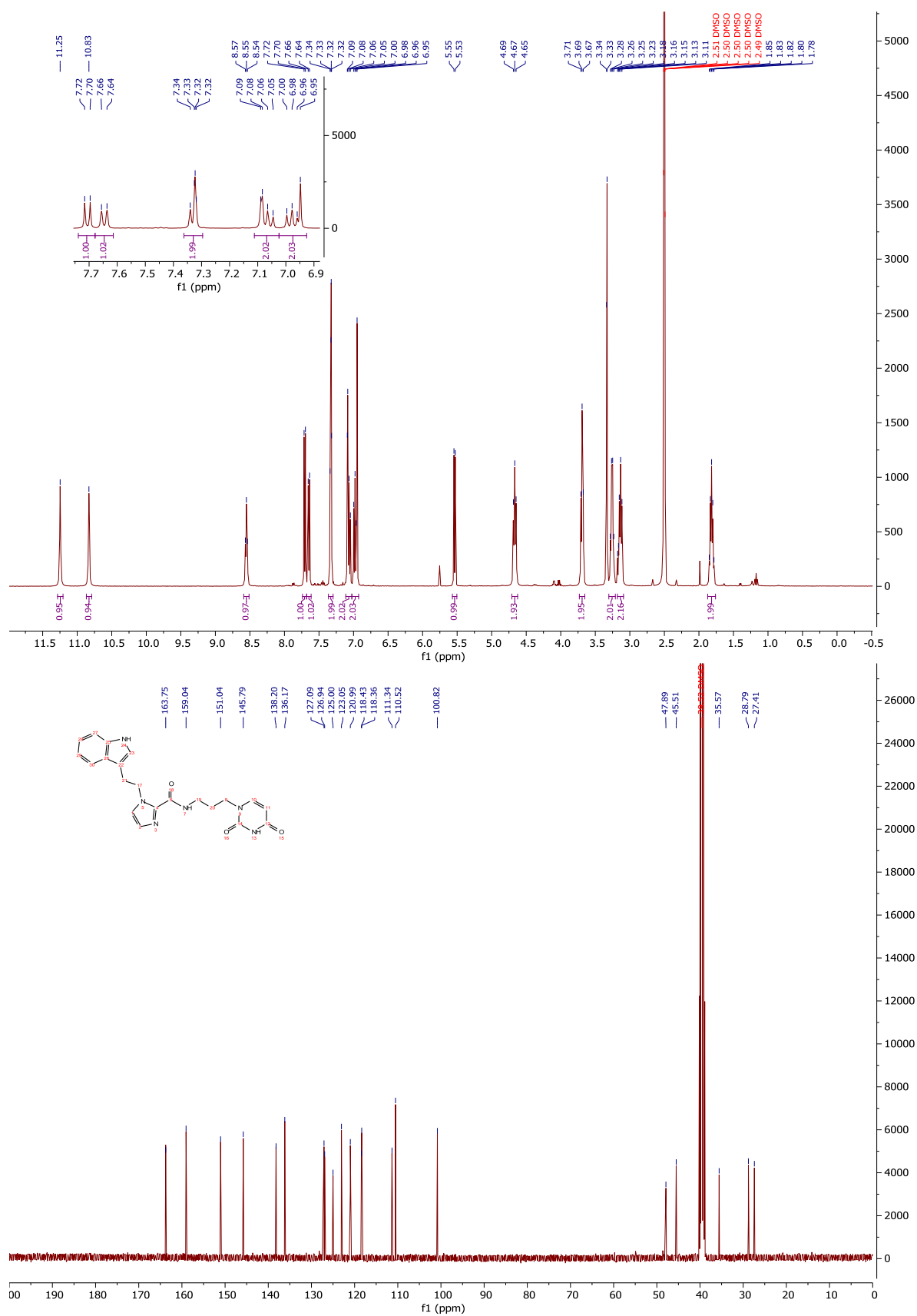
¹H-NMR and ¹³C-NMR: Compound 124



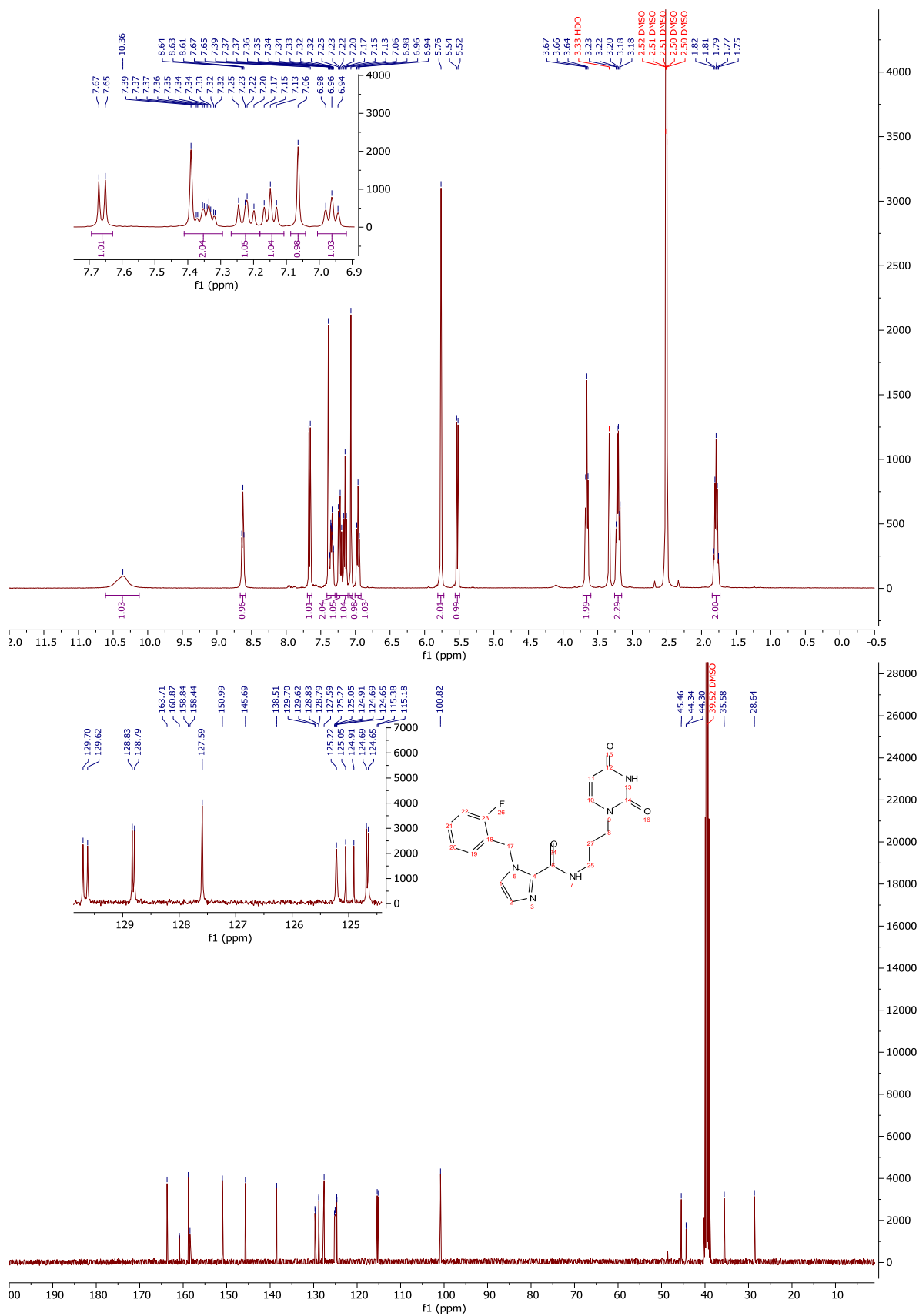
¹H-NMR and ¹³C-NMR: Compound 119



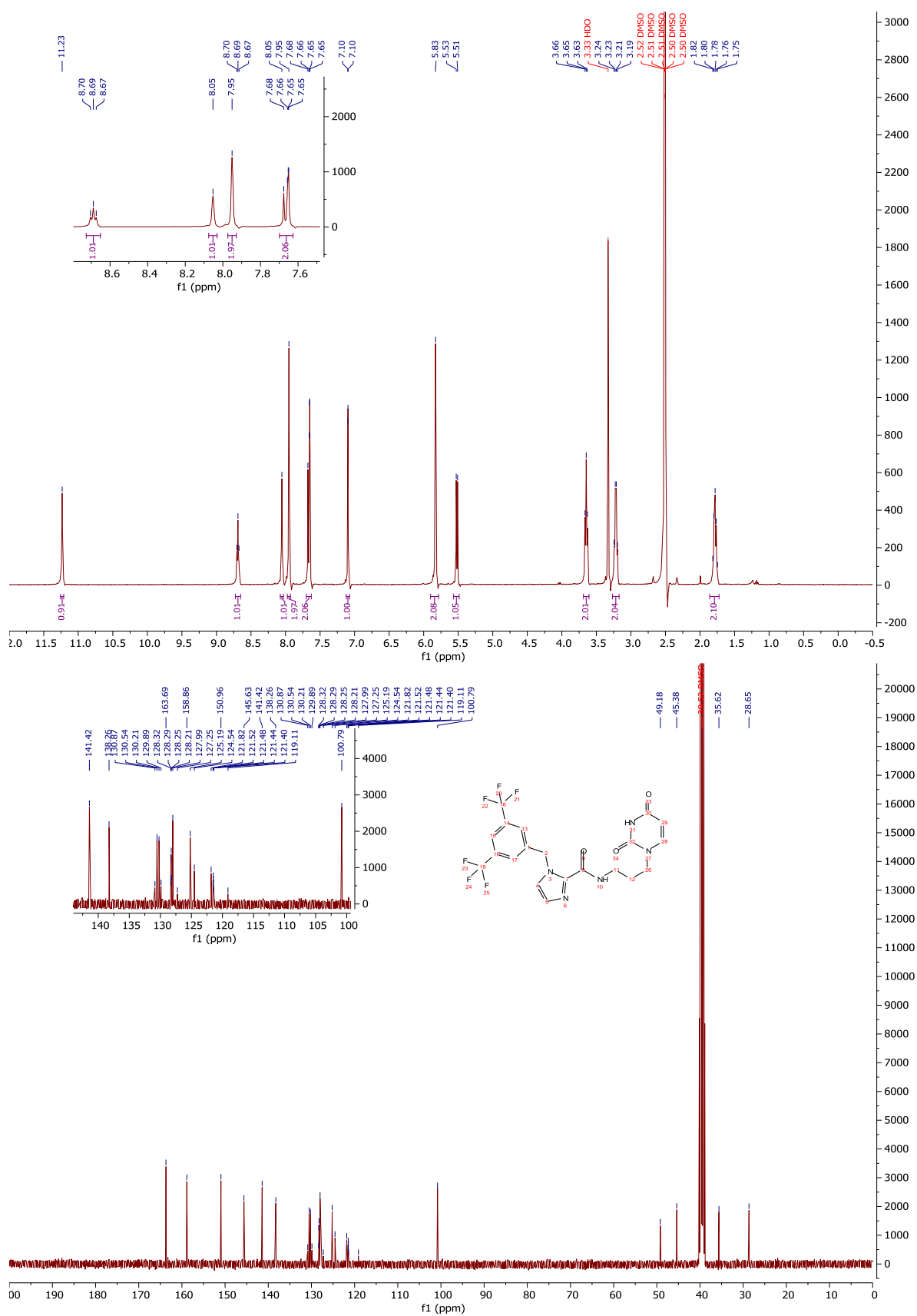
¹H-NMR and ¹³C-NMR: Compound 118



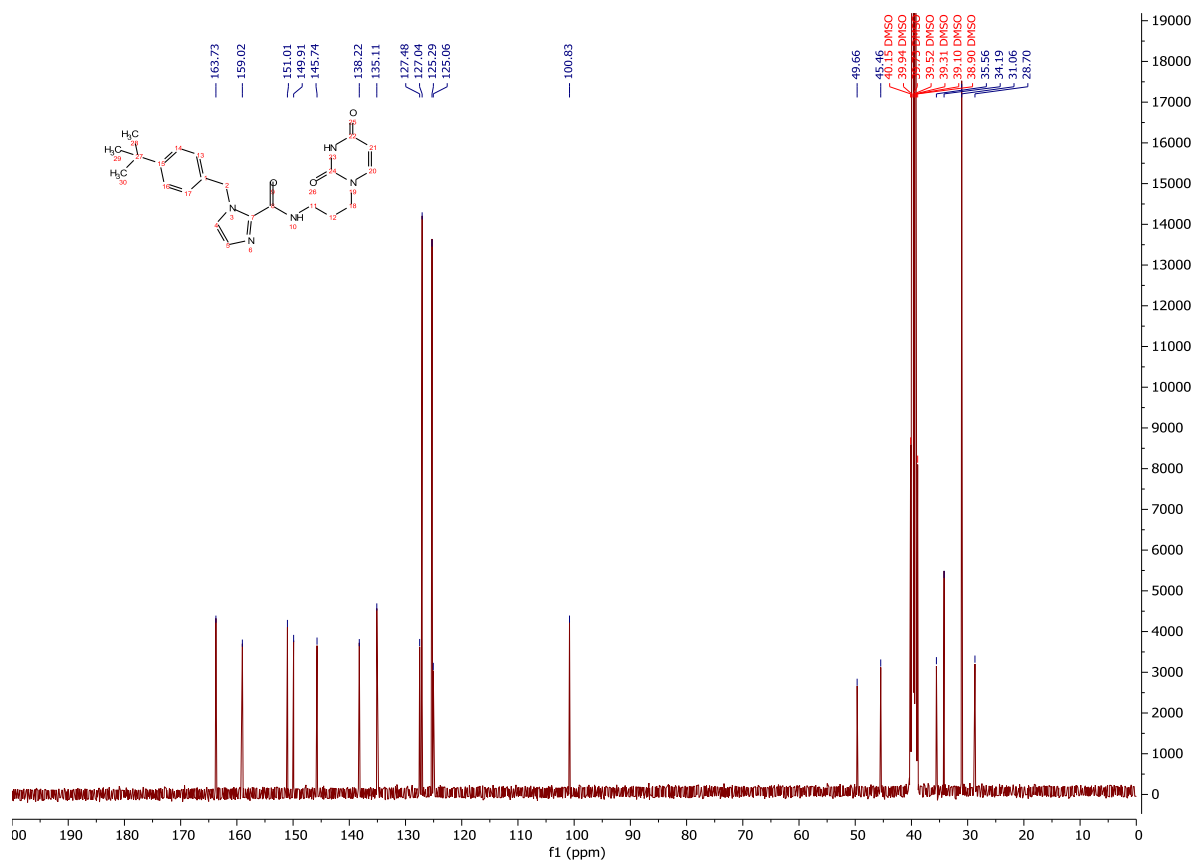
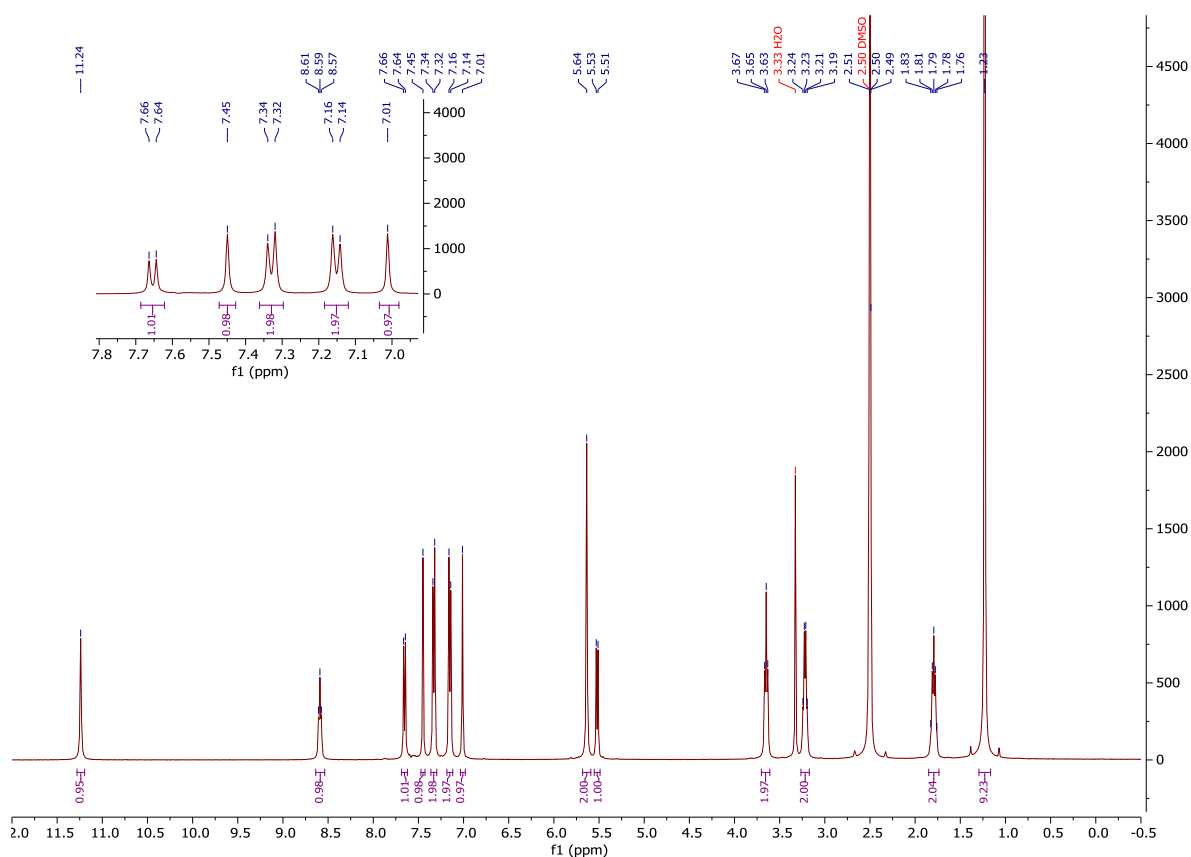
¹H-NMR and ¹³C-NMR: Compound 122



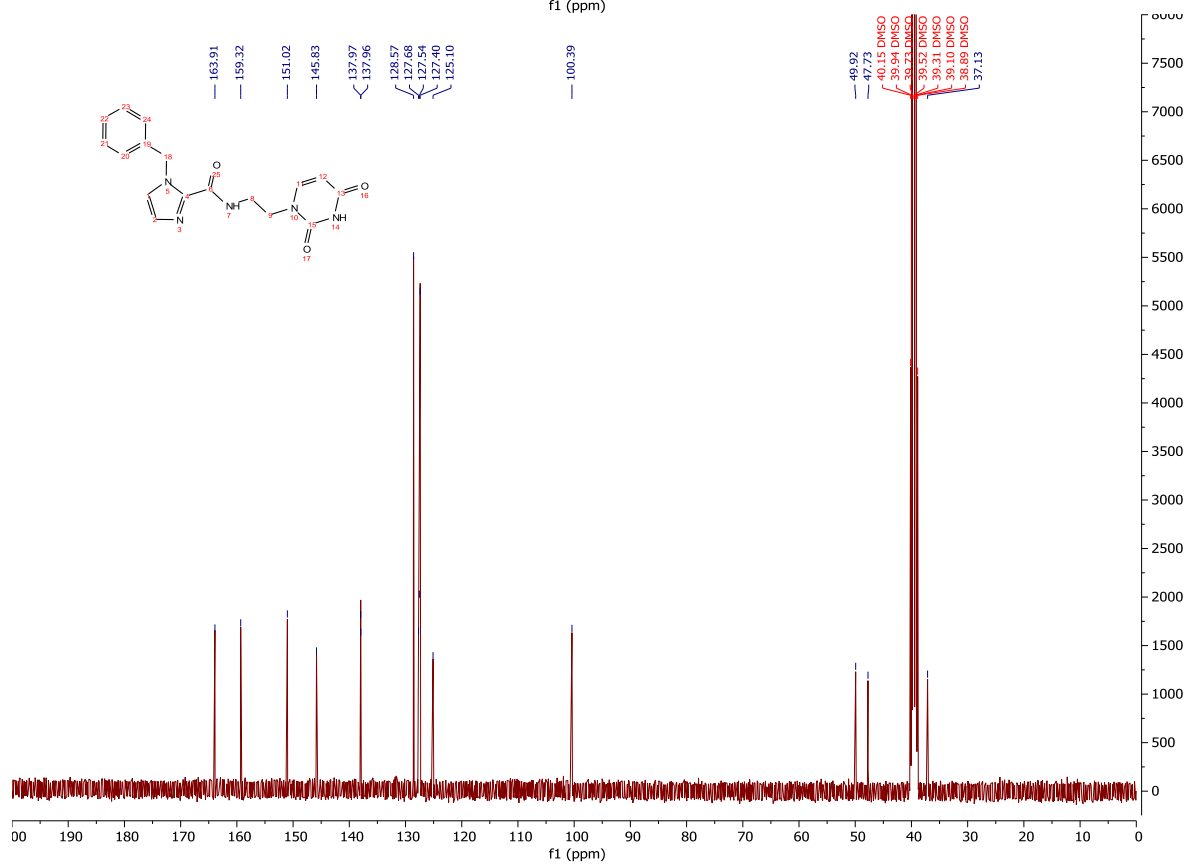
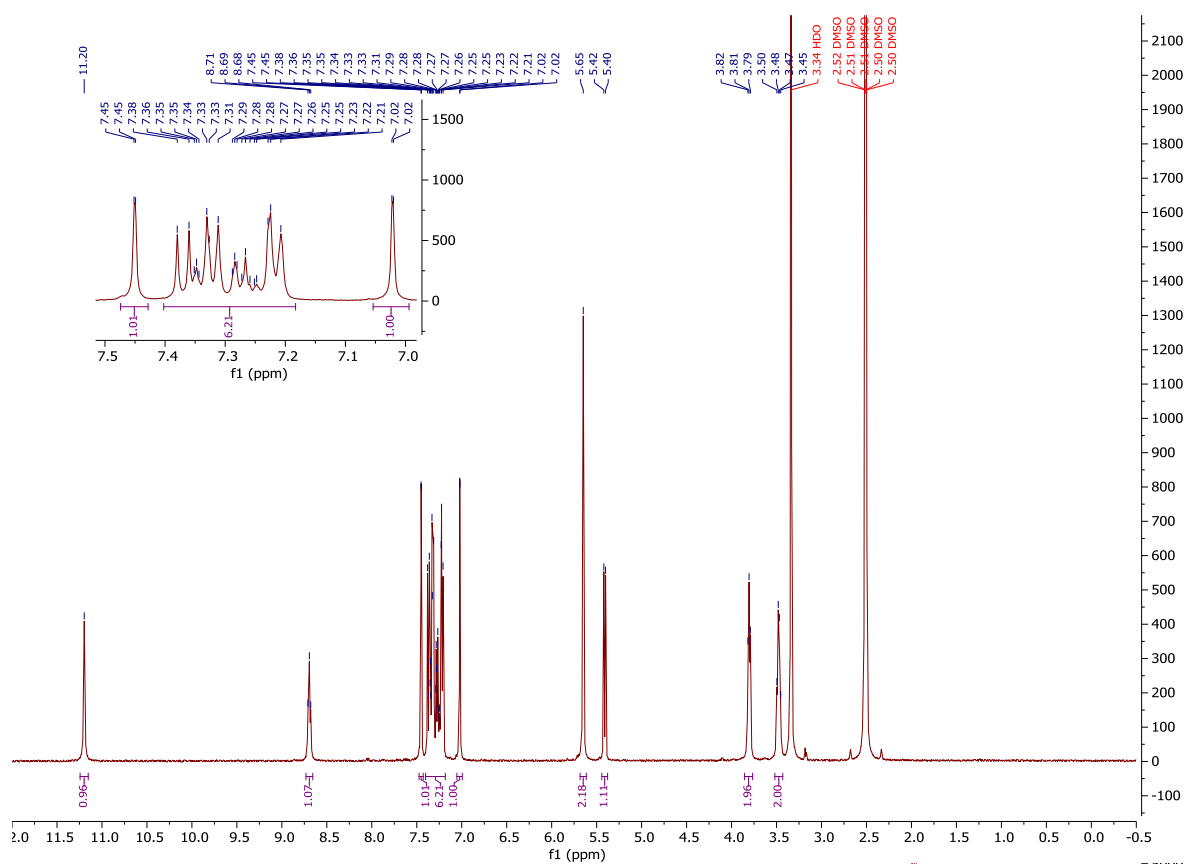
¹H-NMR and ¹³C-NMR: Compound 123



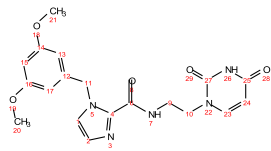
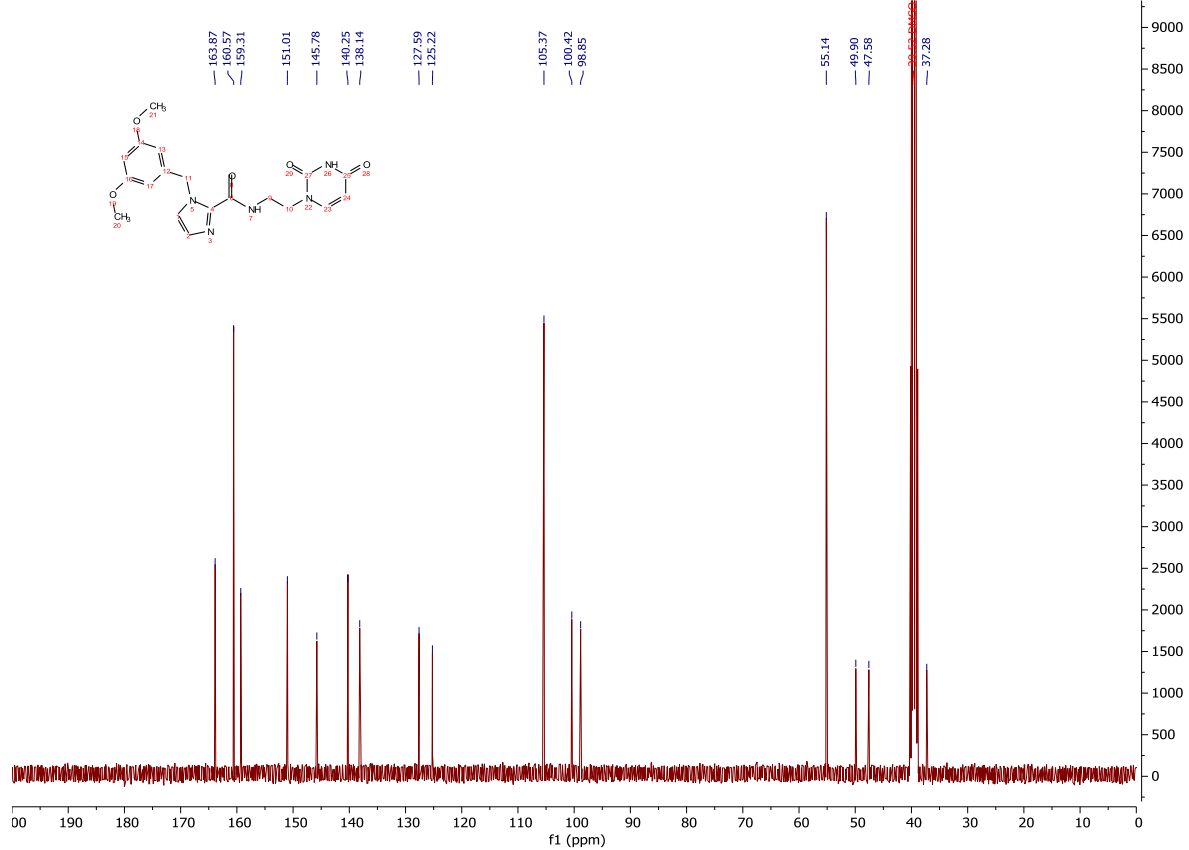
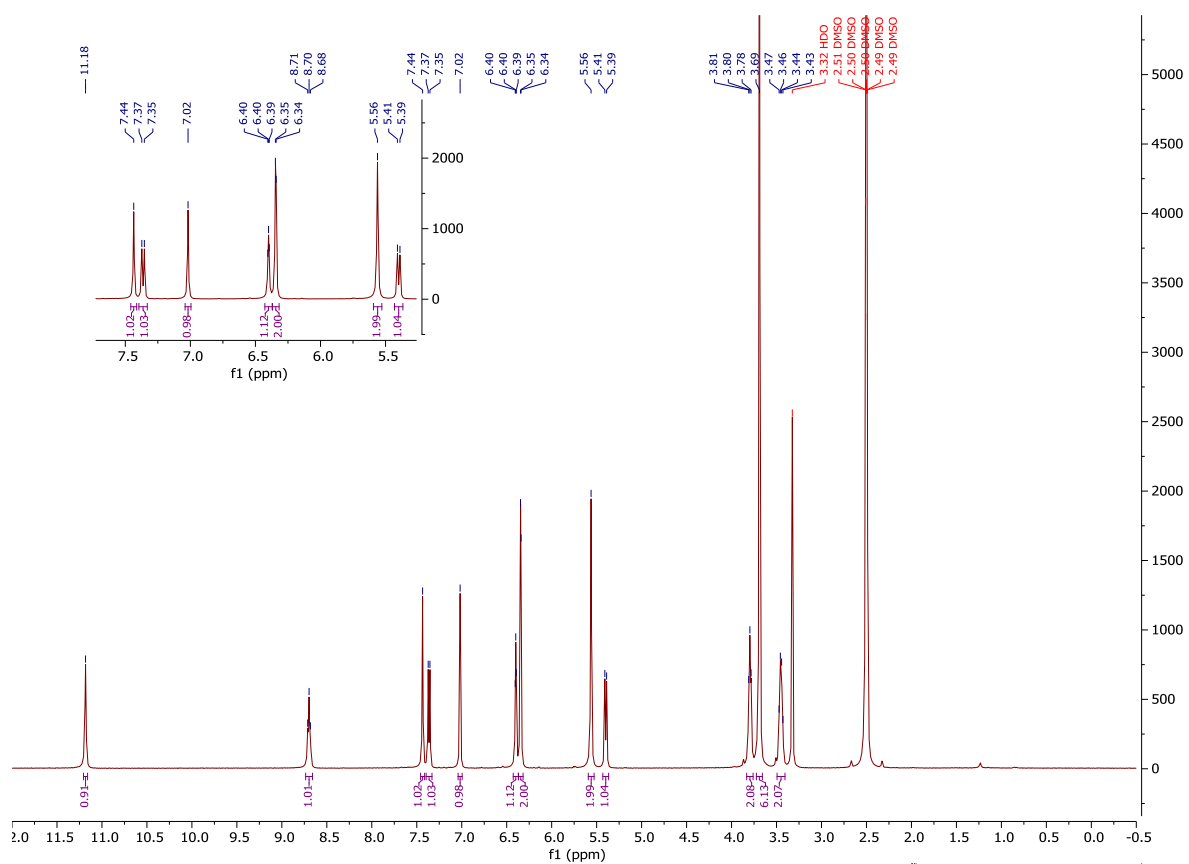
¹H-NMR and ¹³C-NMR: Compound 126



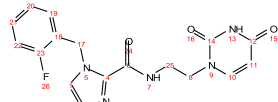
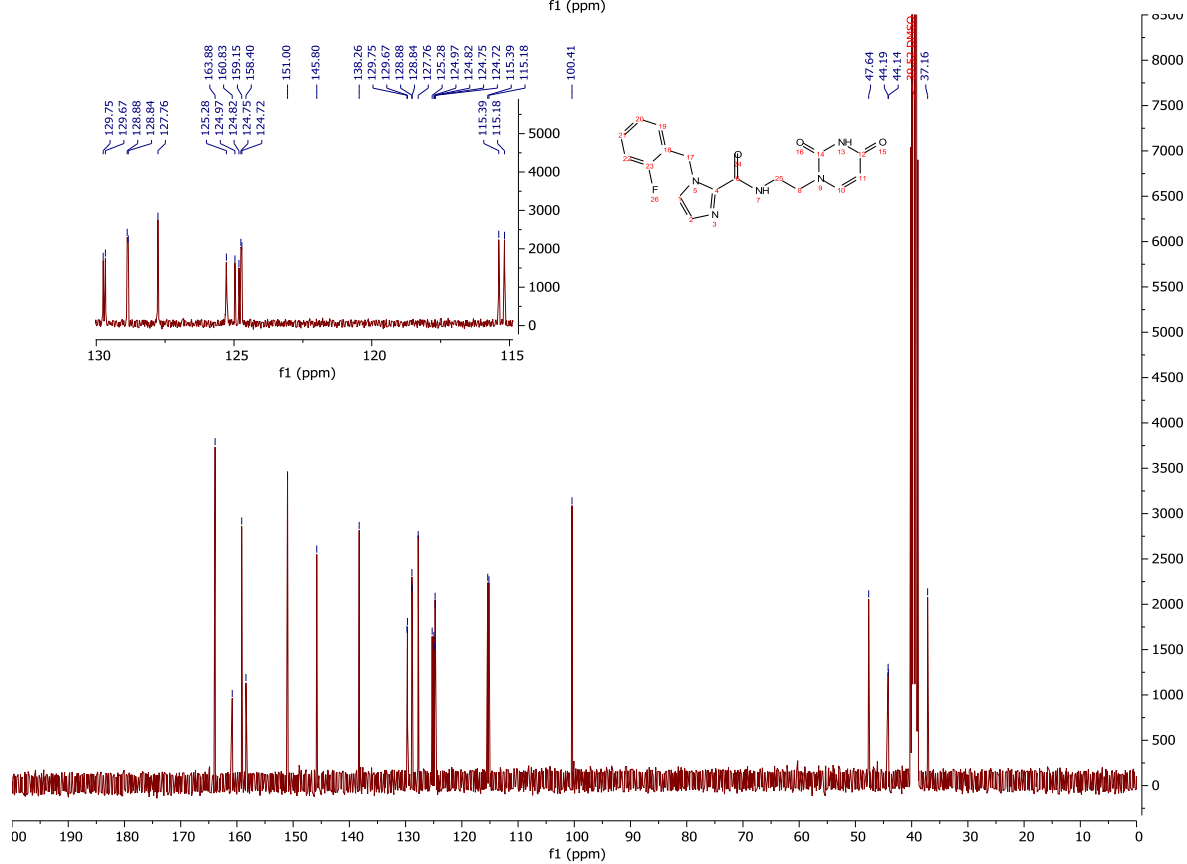
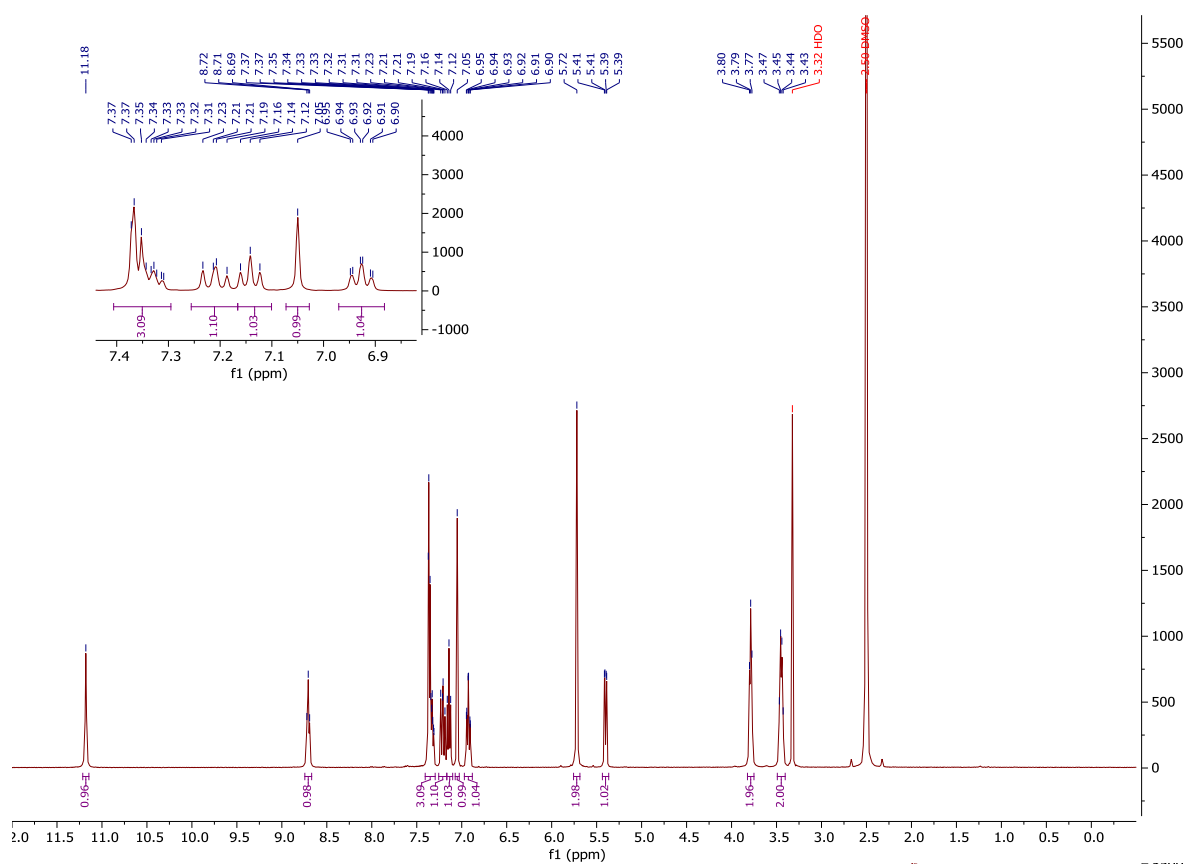
$^1\text{H-NMR}$ and $^{13}\text{C-NMR}$: Compound 115



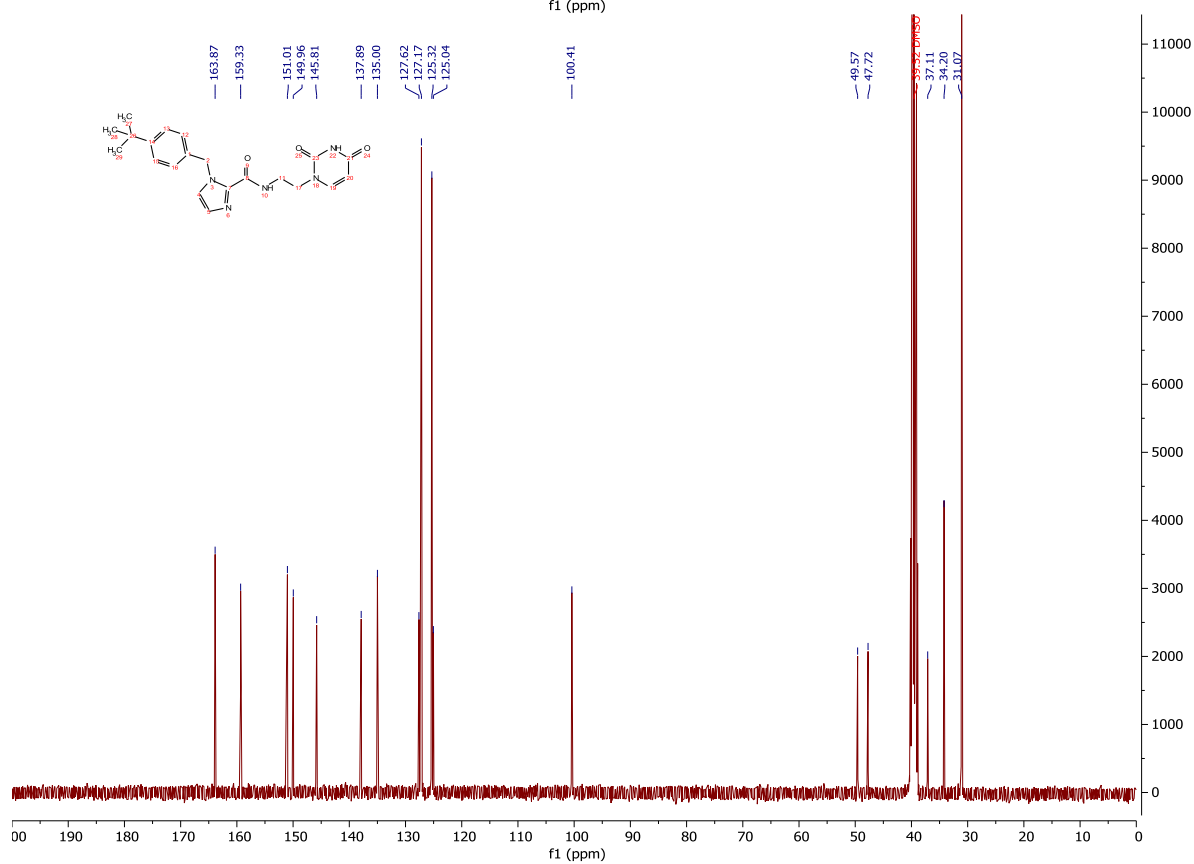
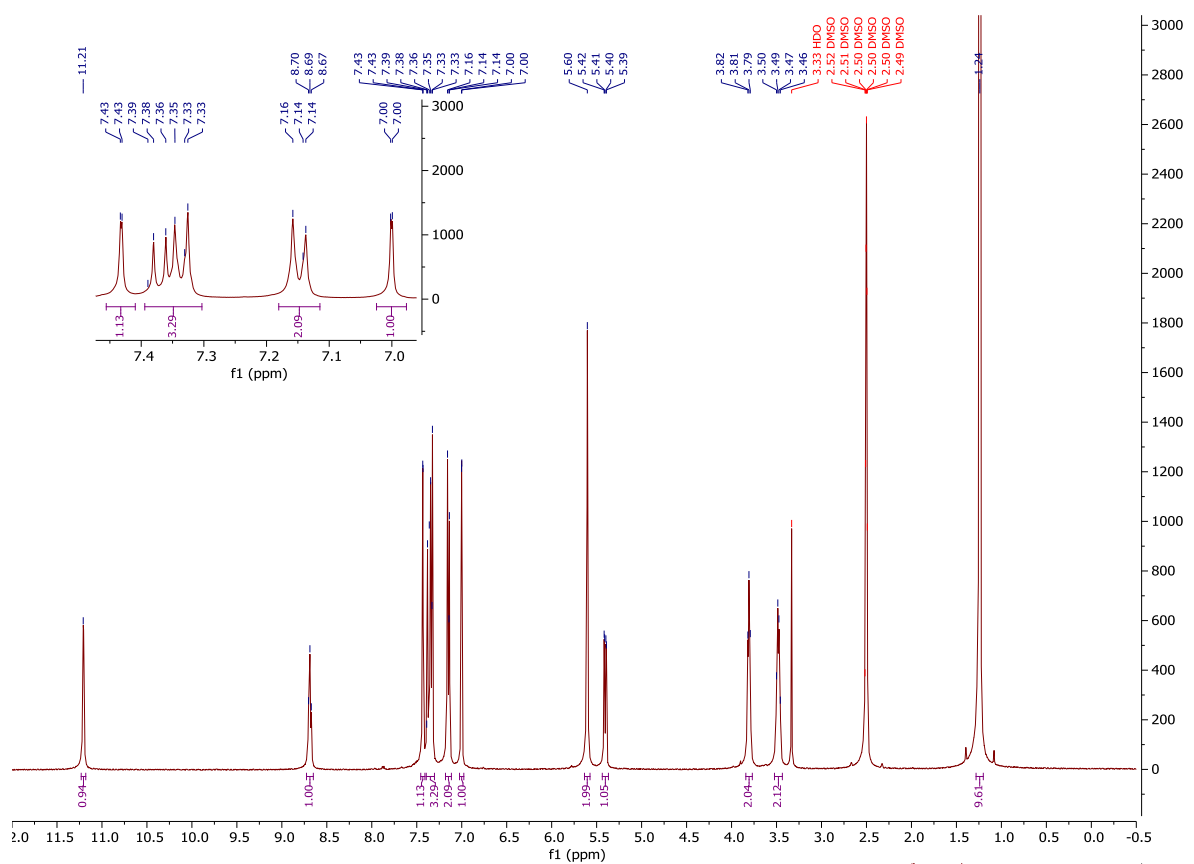
¹H-NMR and ¹³C-NMR: Compound 119



$^1\text{H-NMR}$ and $^{13}\text{C-NMR}$: Compound 121

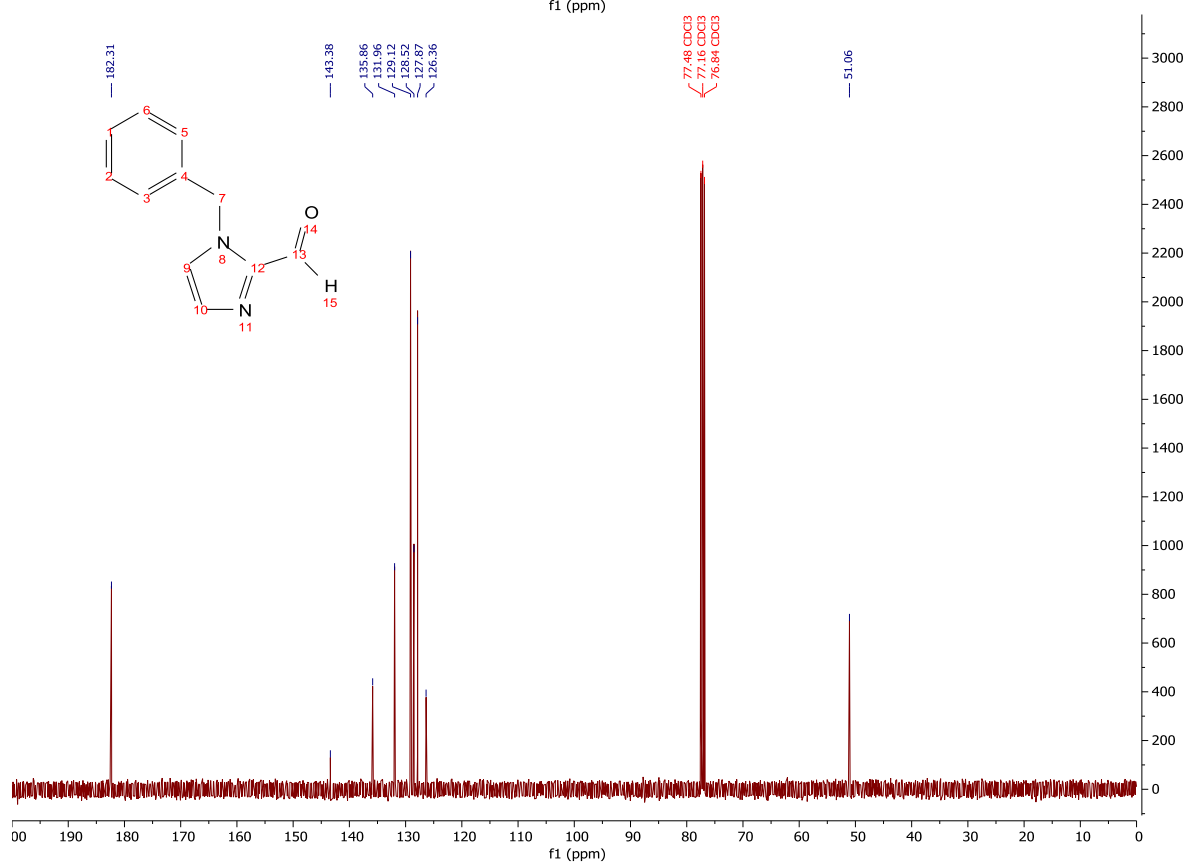
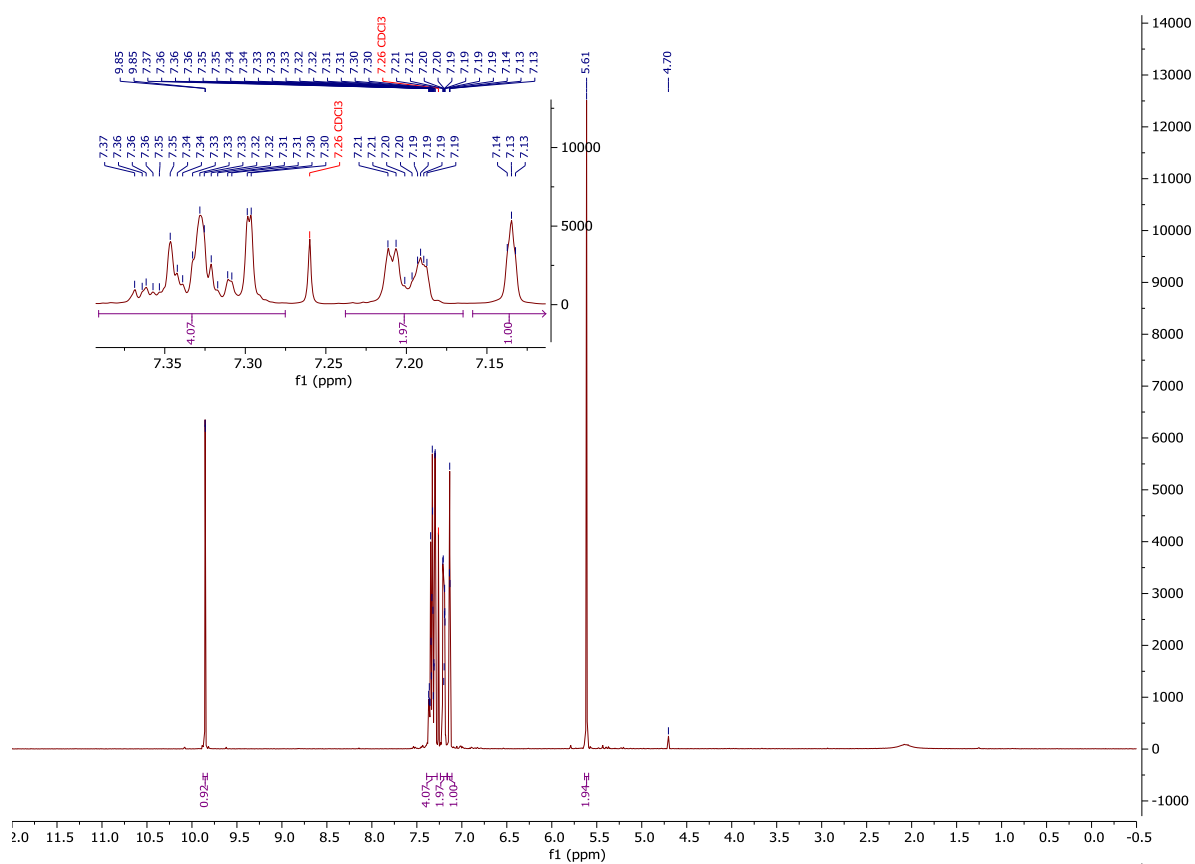


¹H-NMR and ¹³C-NMR: Compound 125

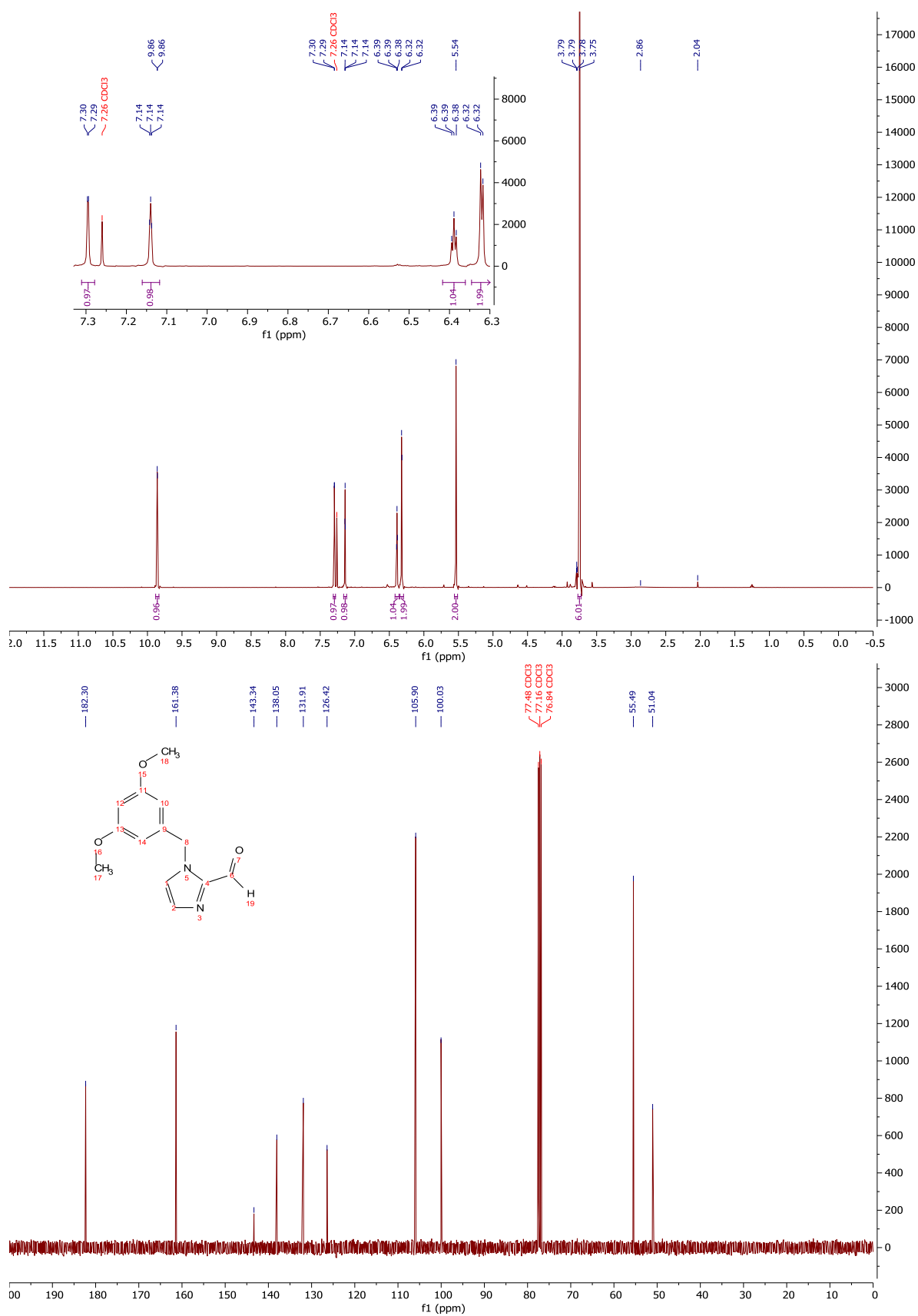


Synthesis discussed in section 4.6

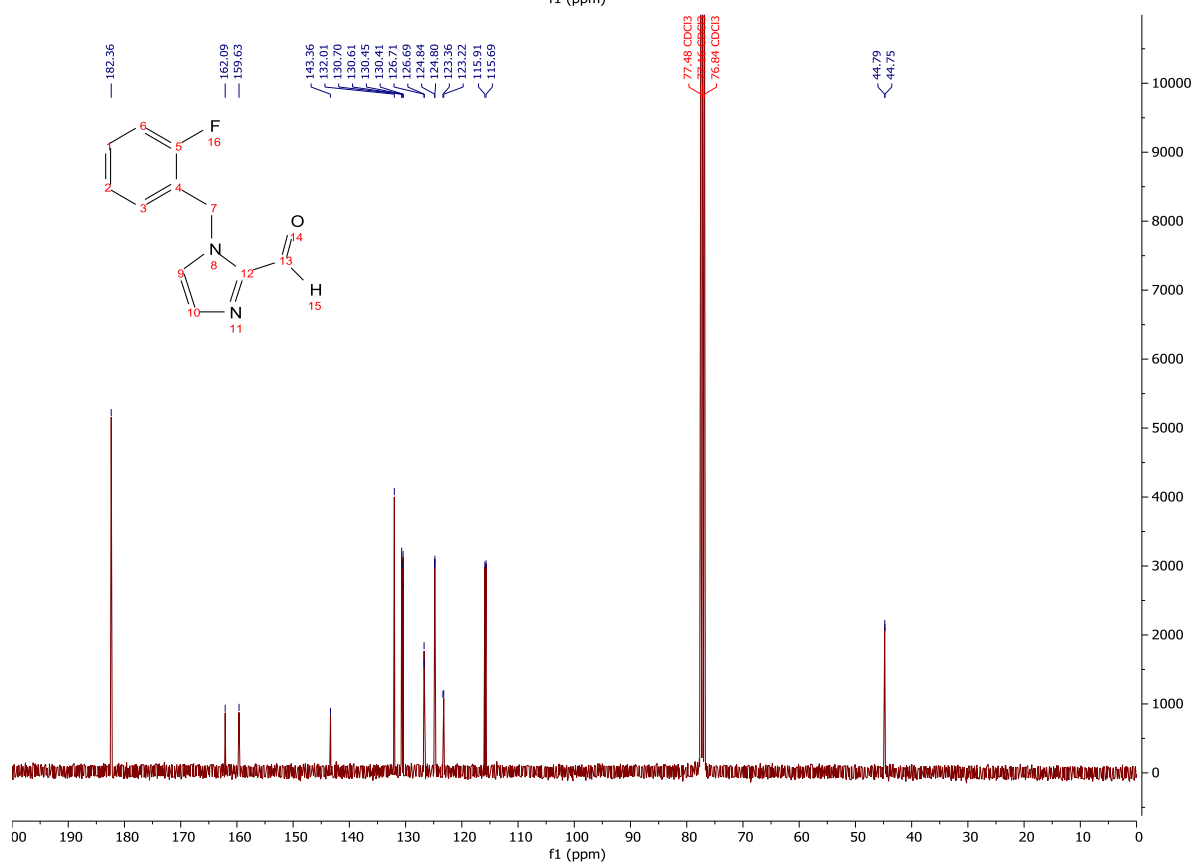
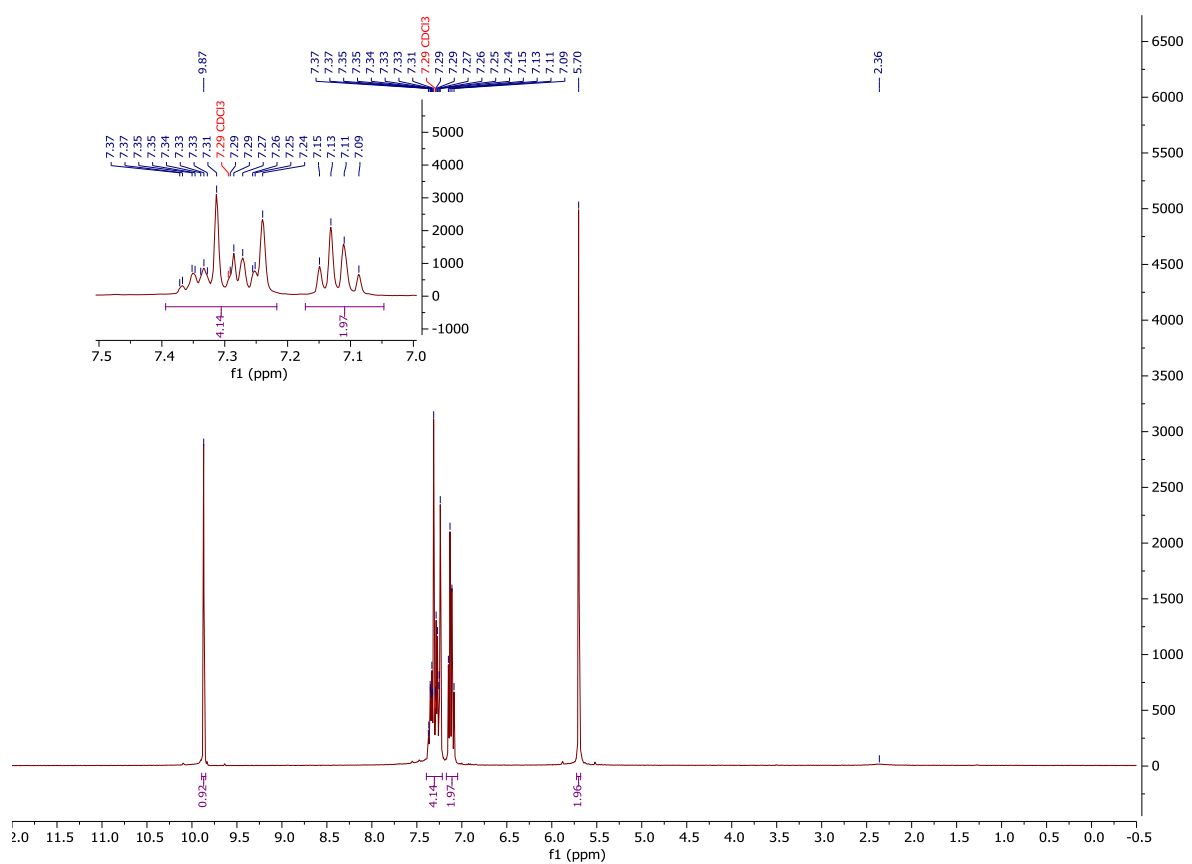
¹H-NMR and ¹³C-NMR: Compound 128



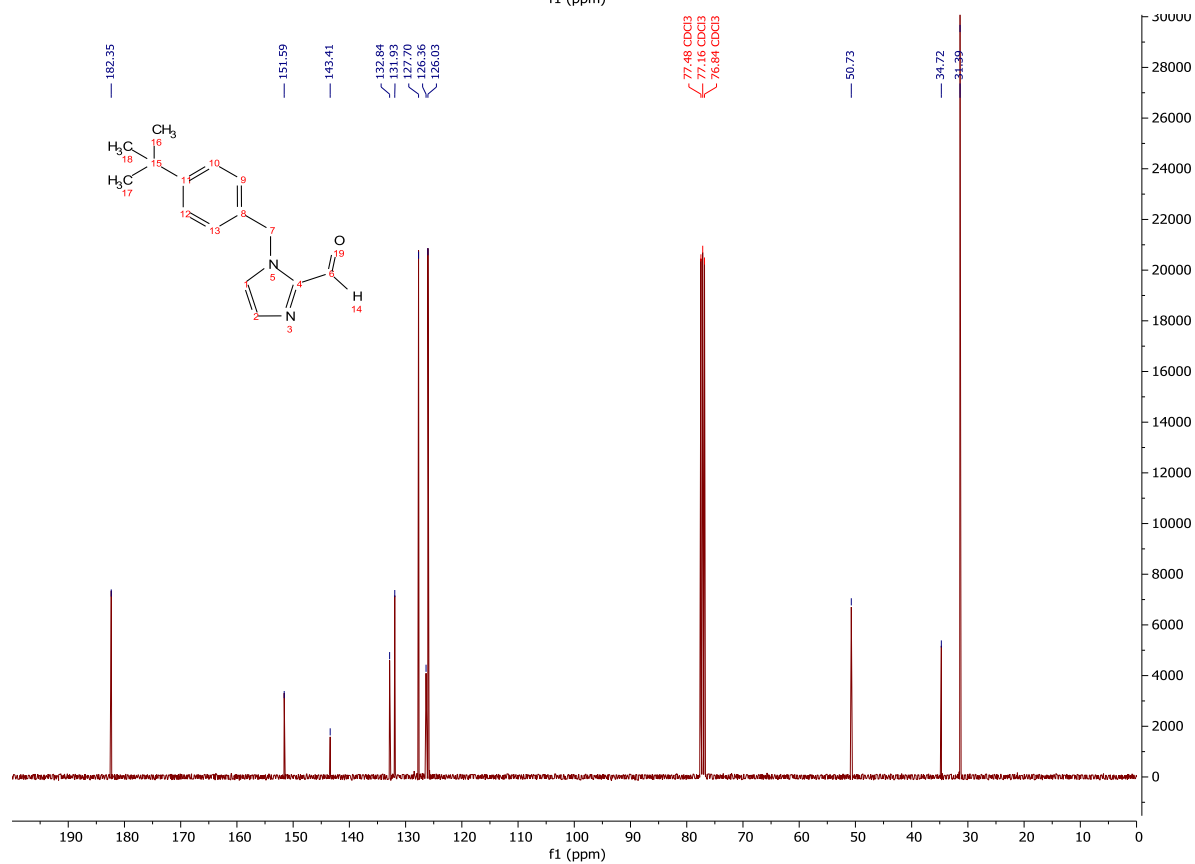
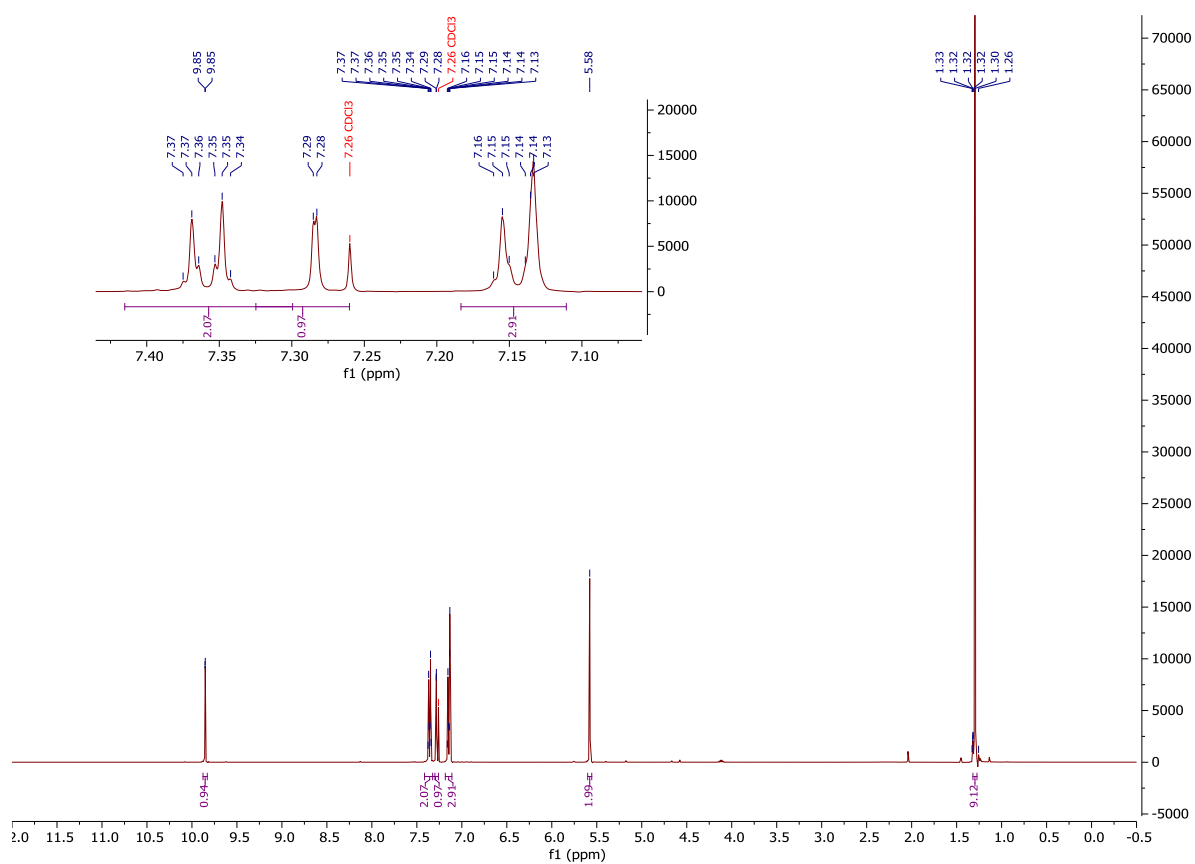
¹H-NMR and ¹³C-NMR: Compound 134



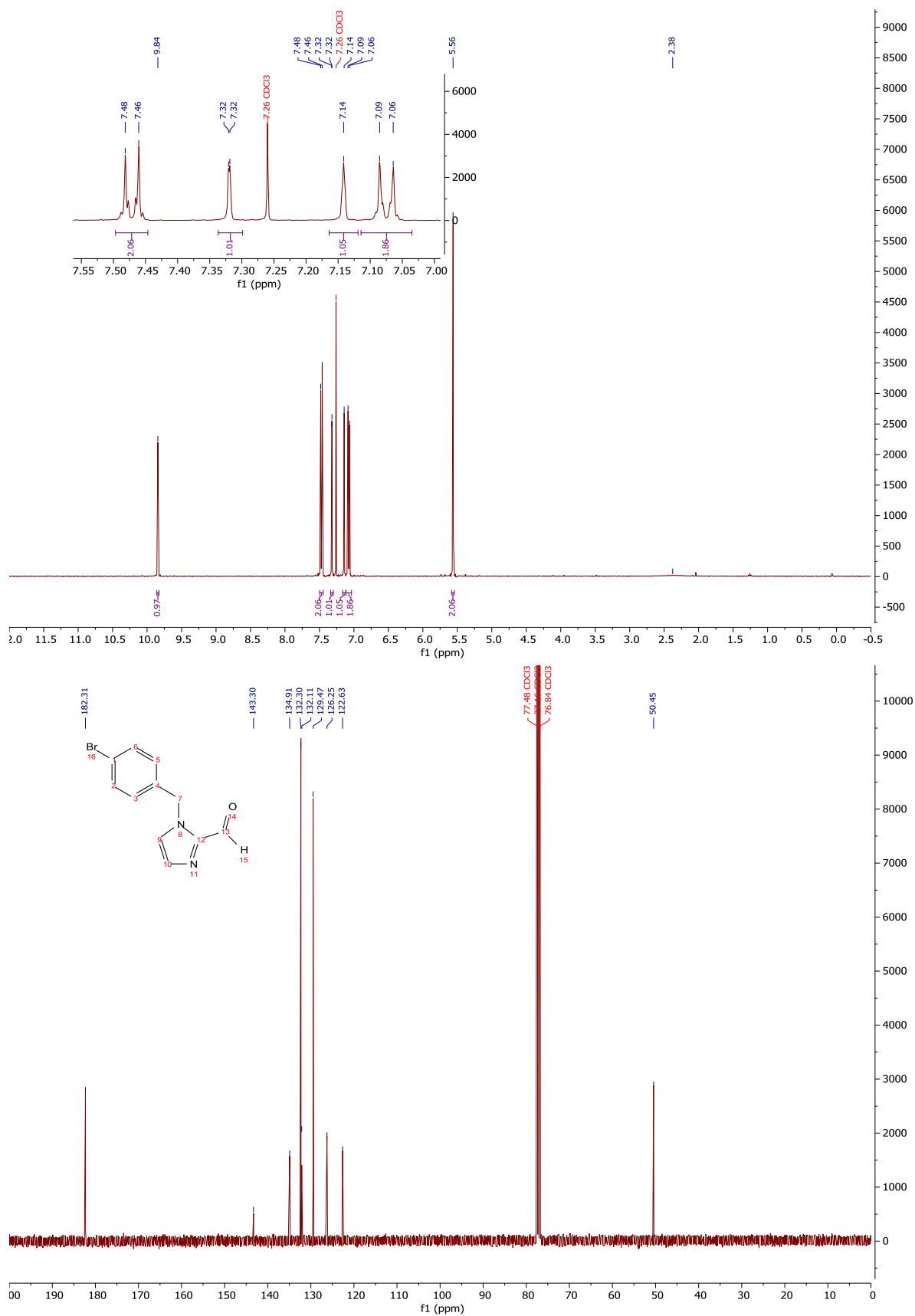
¹H-NMR and ¹³C-NMR: Compound 127



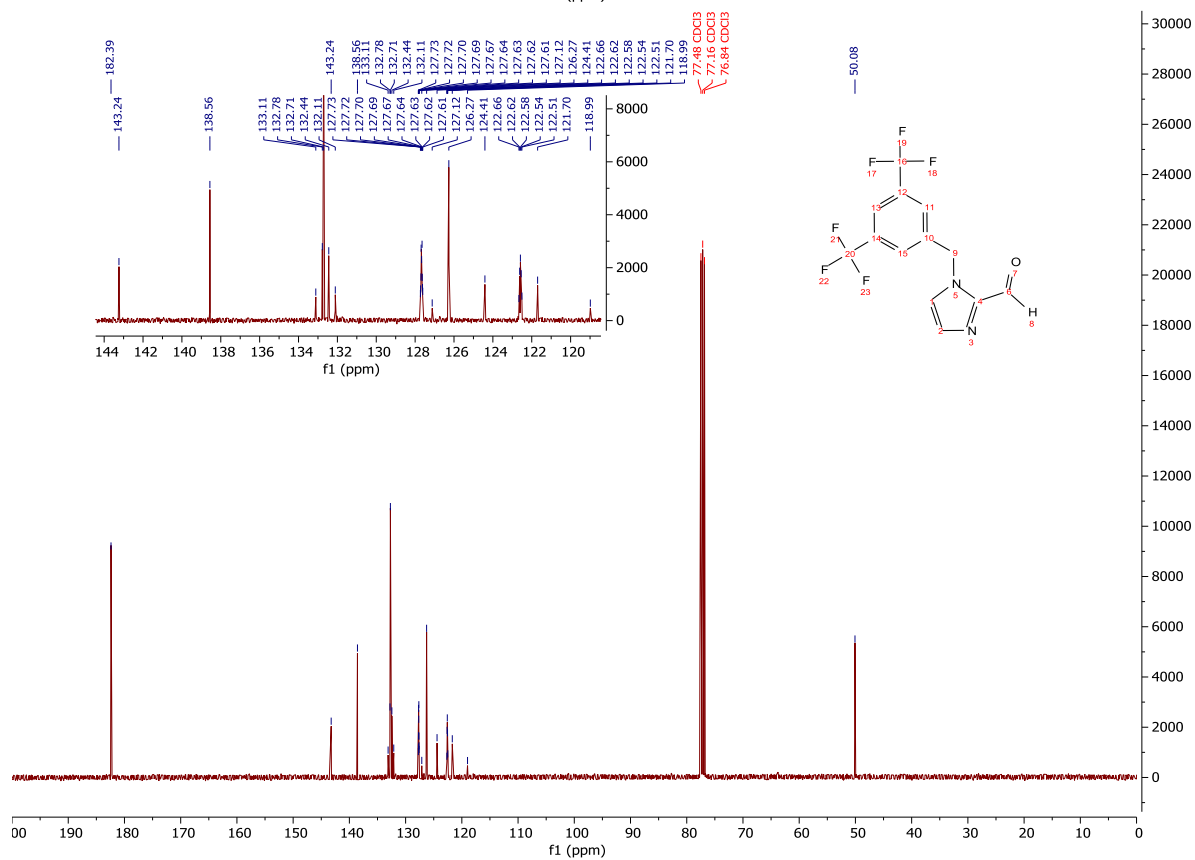
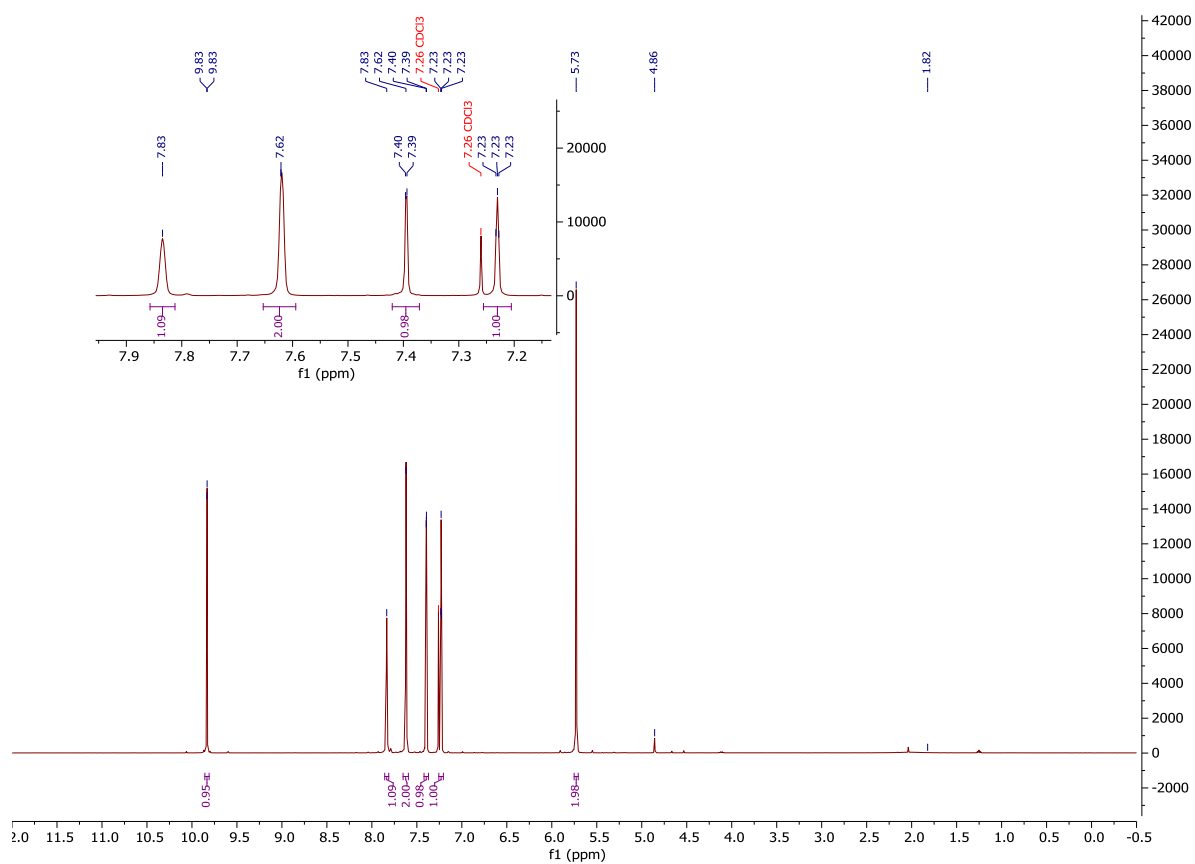
¹H-NMR and ¹³C-NMR: Compound 132



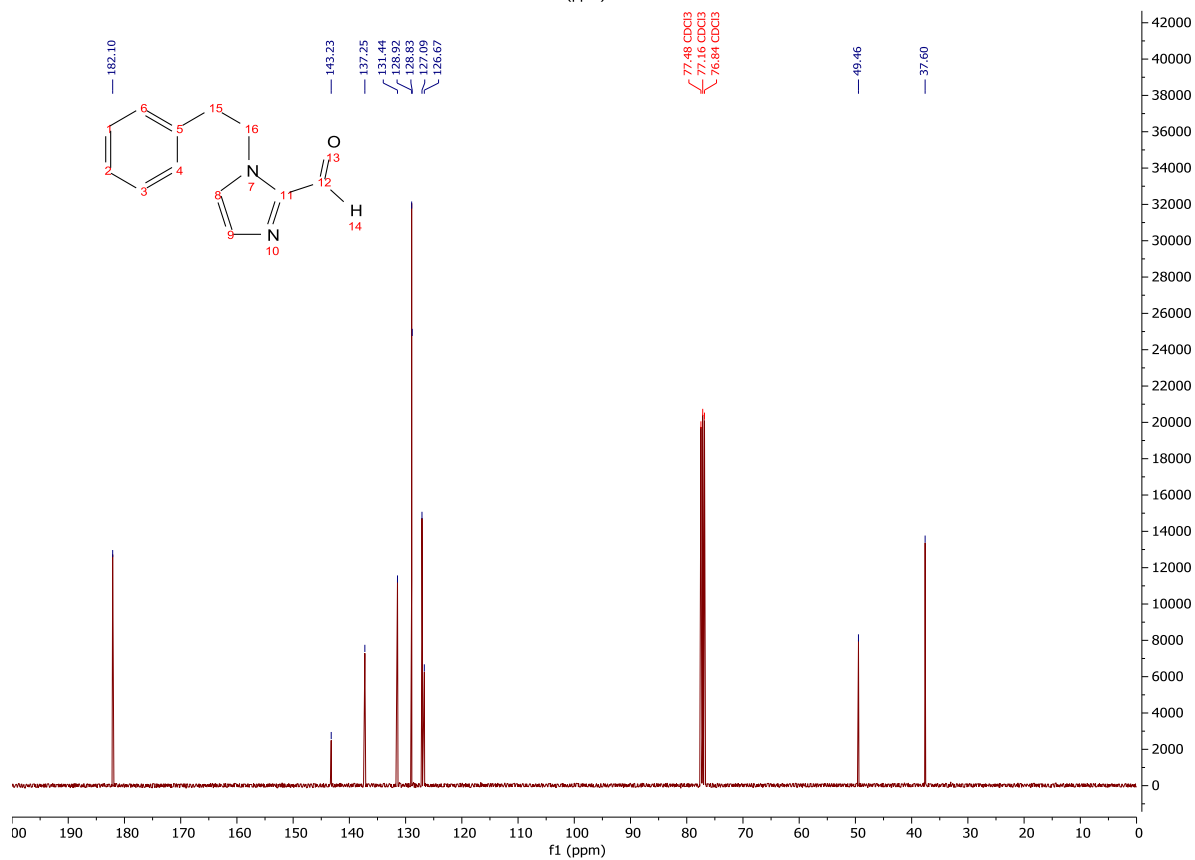
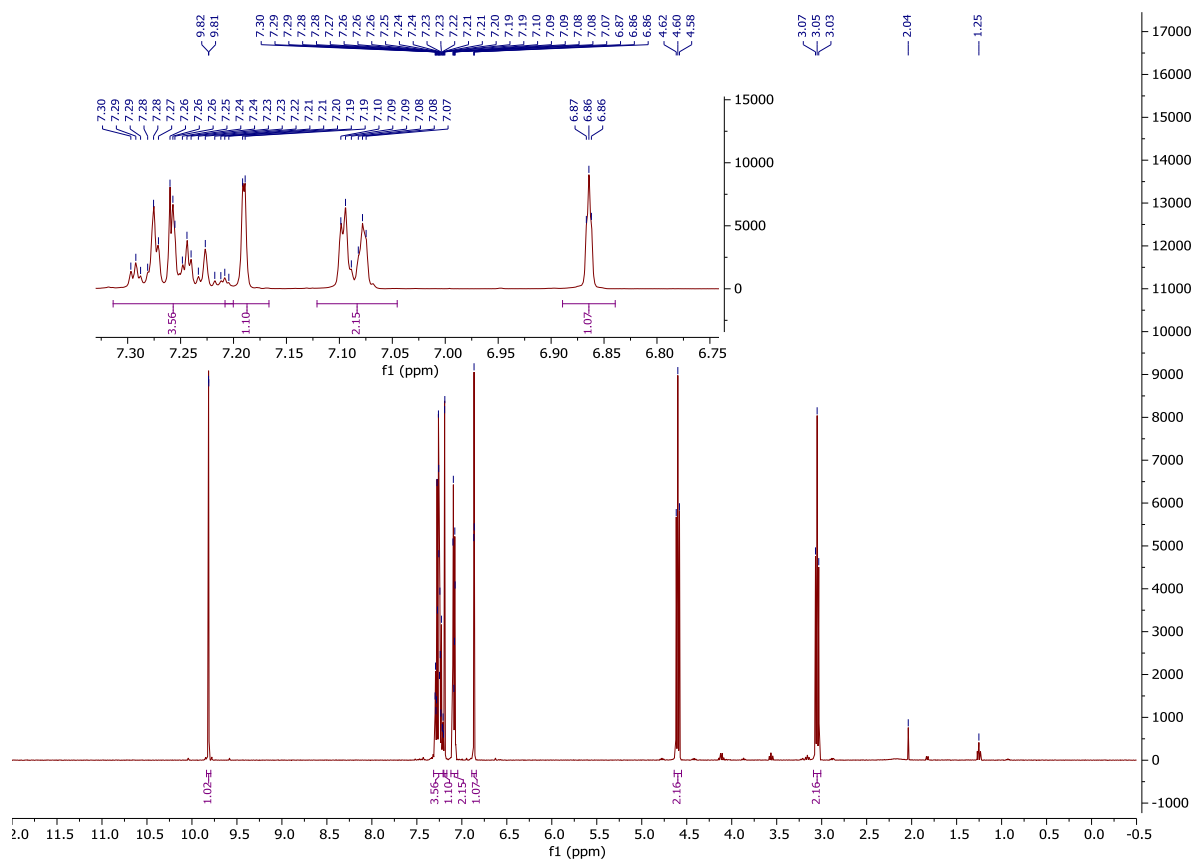
$^1\text{H-NMR}$ and $^{13}\text{C-NMR}$: Compound 129



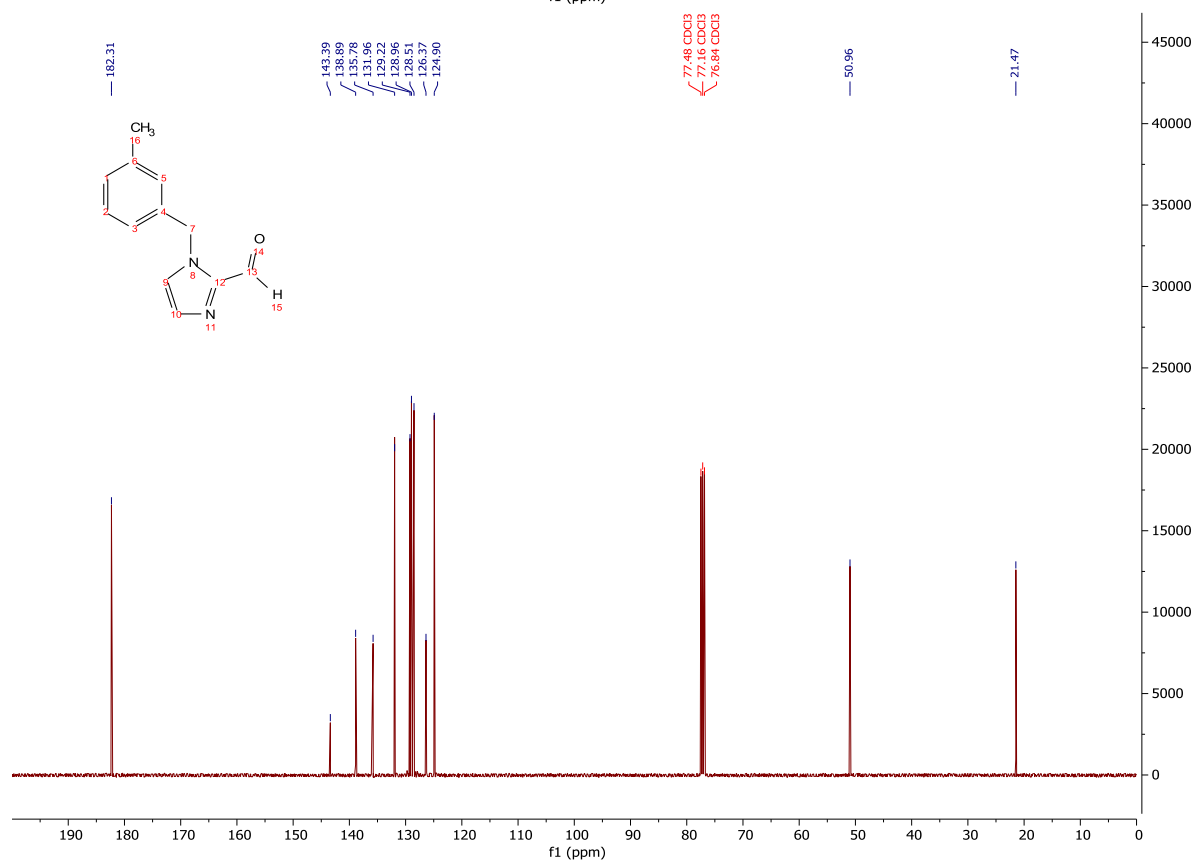
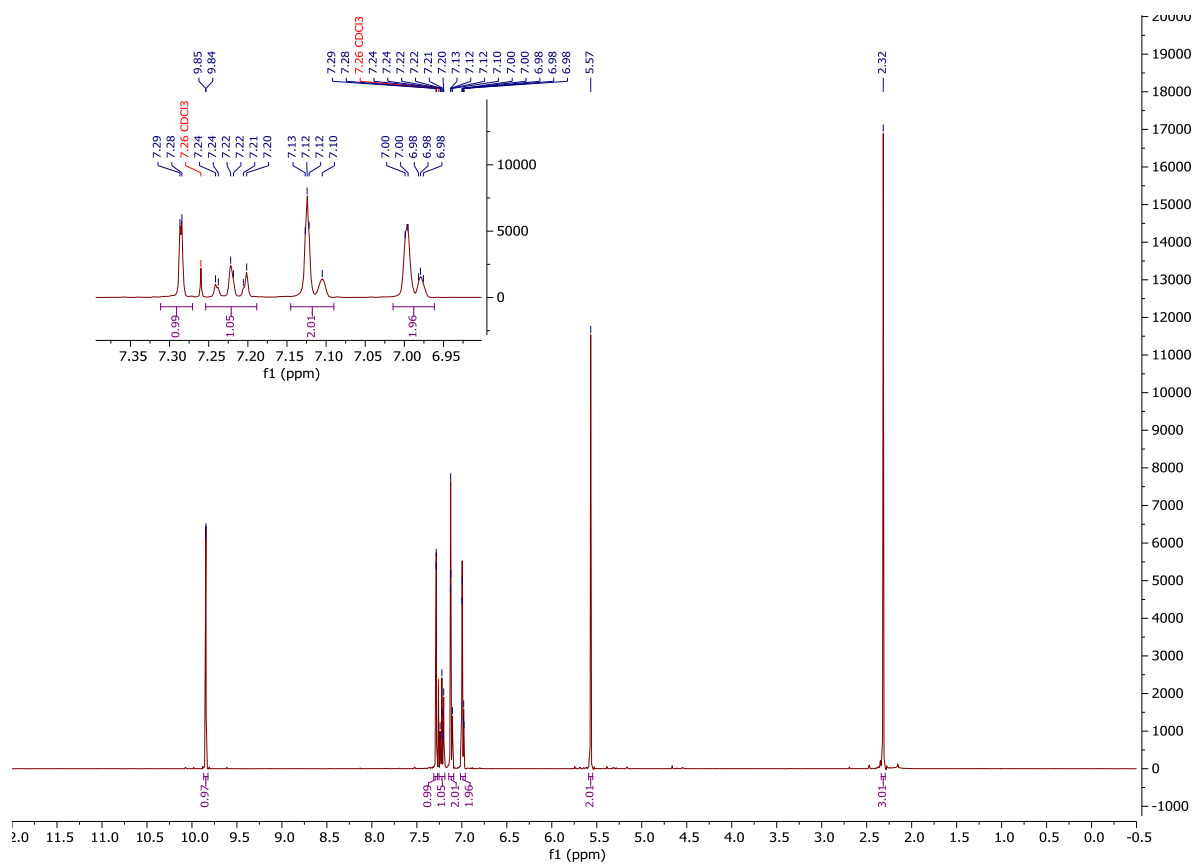
¹H-NMR and ¹³C-NMR: Compound 135



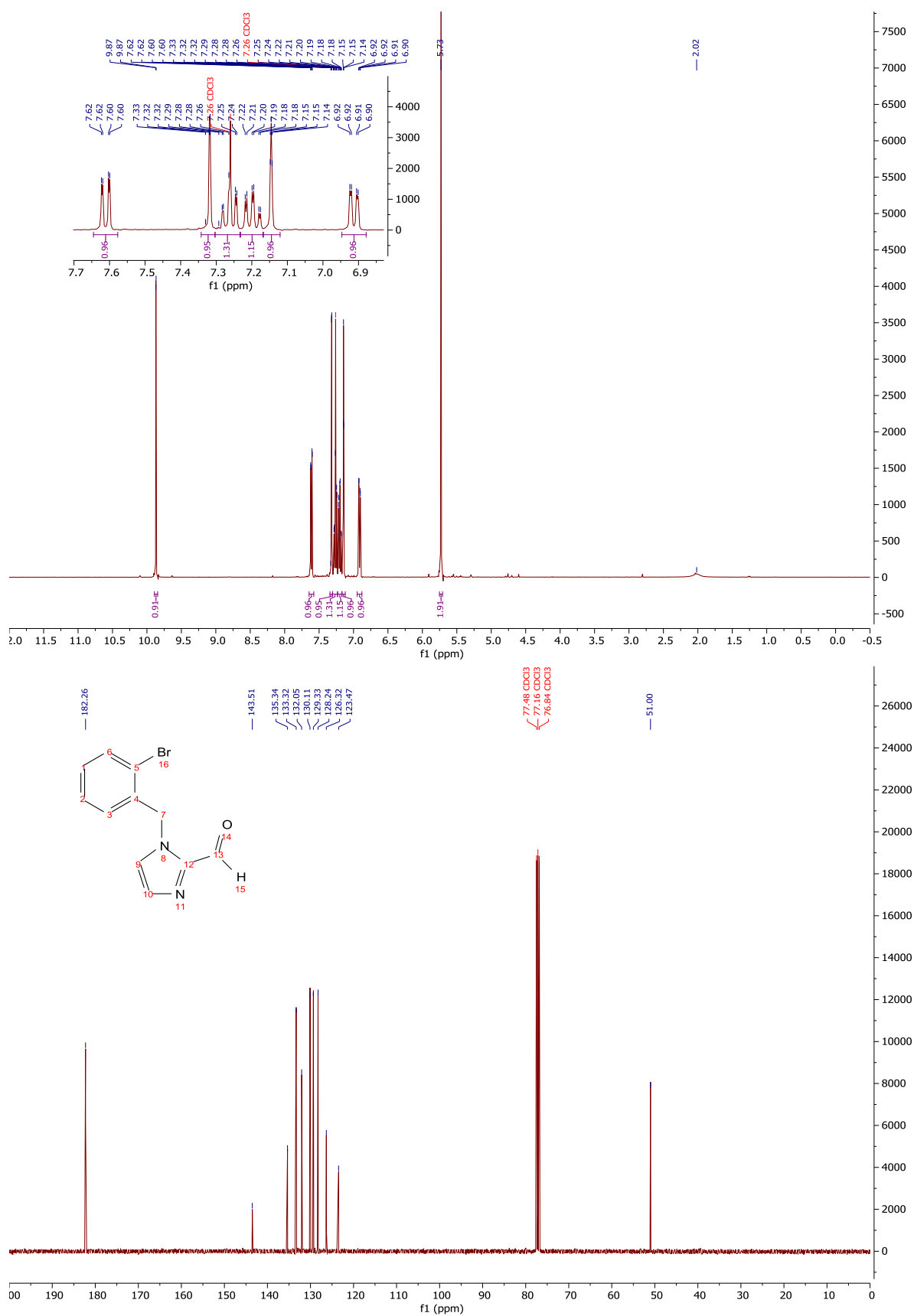
¹H-NMR and ¹³C-NMR: Compound 136



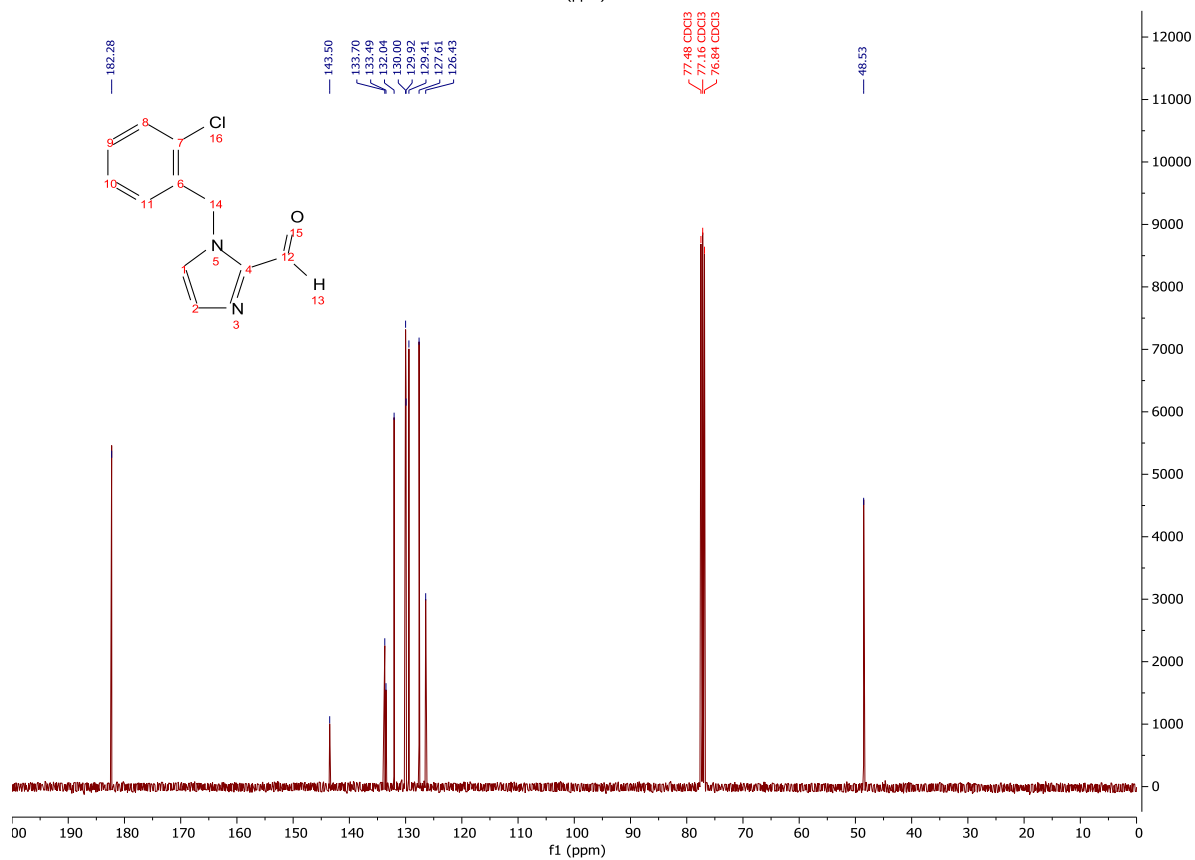
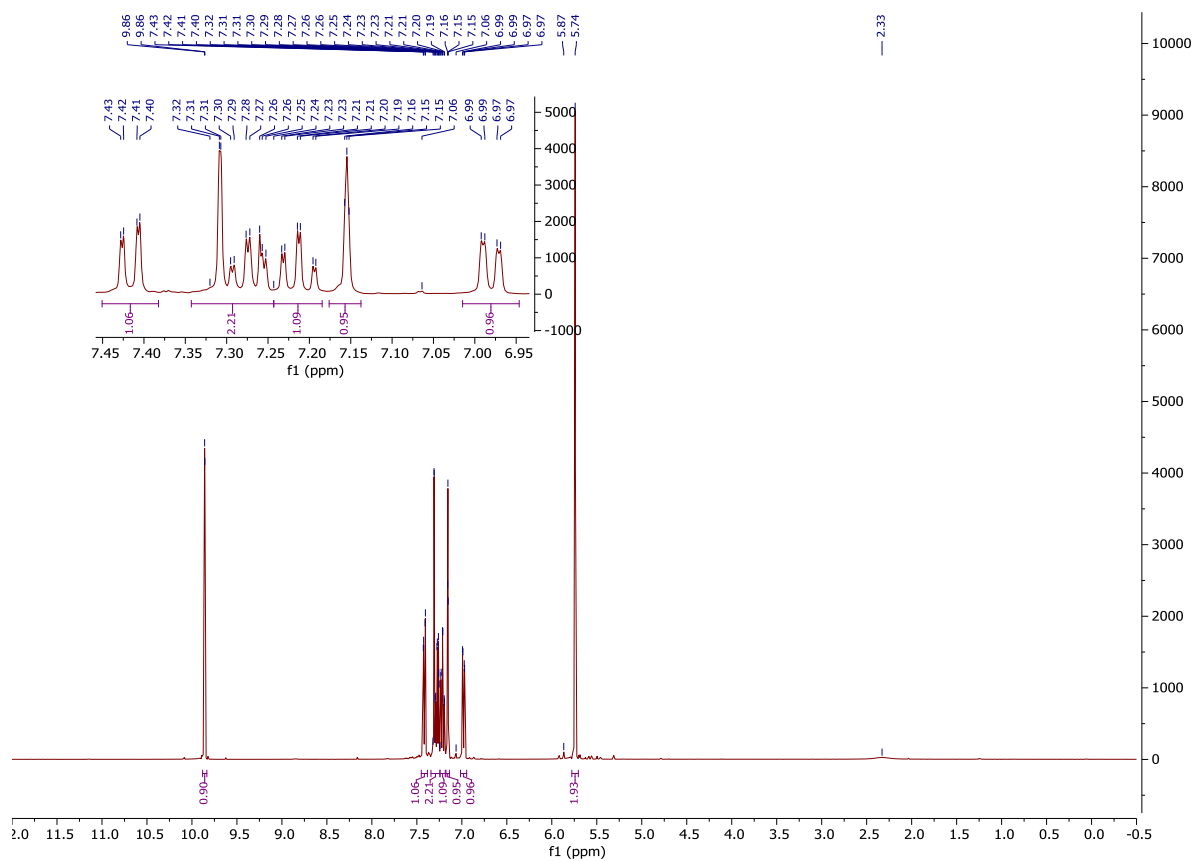
¹H-NMR and ¹³C-NMR: Compound 130



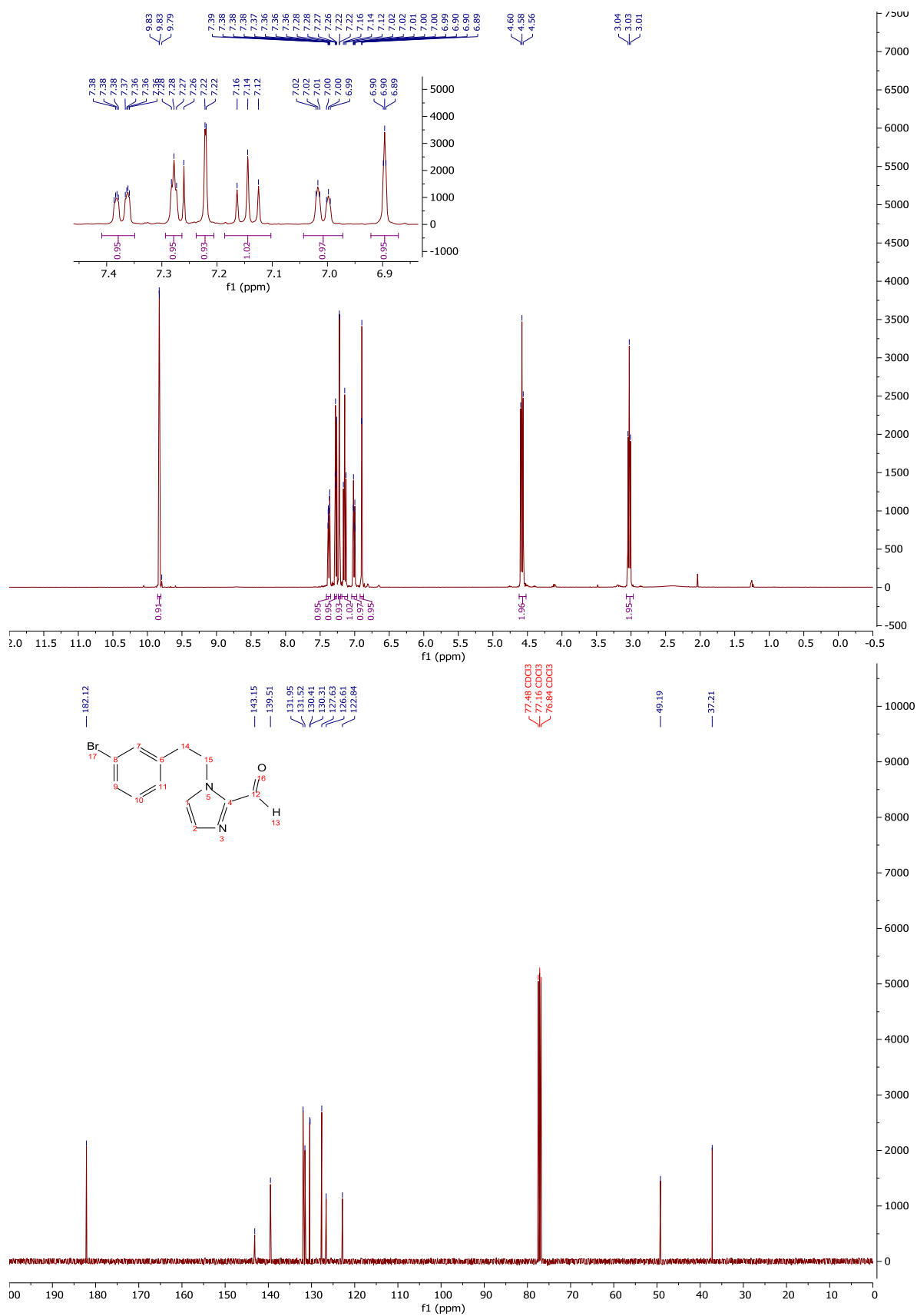
¹H-NMR and ¹³C-NMR: Compound 131



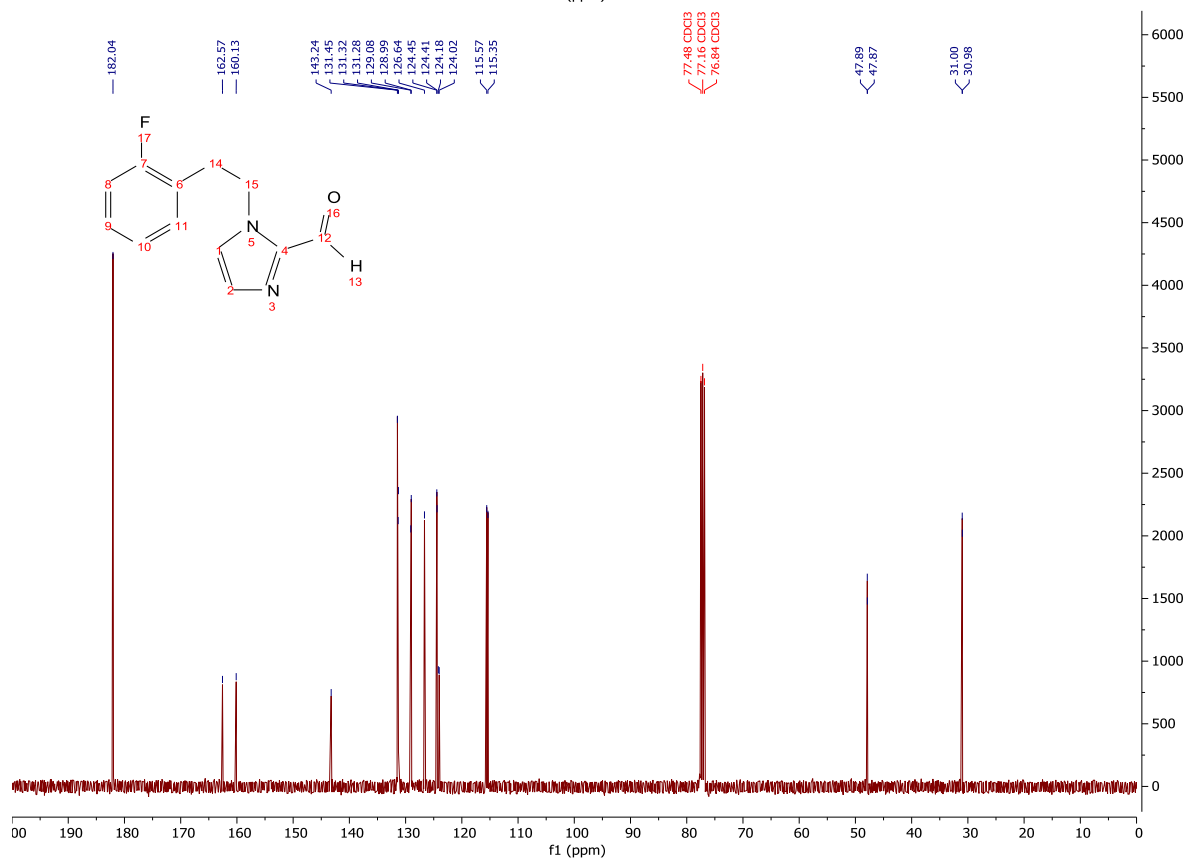
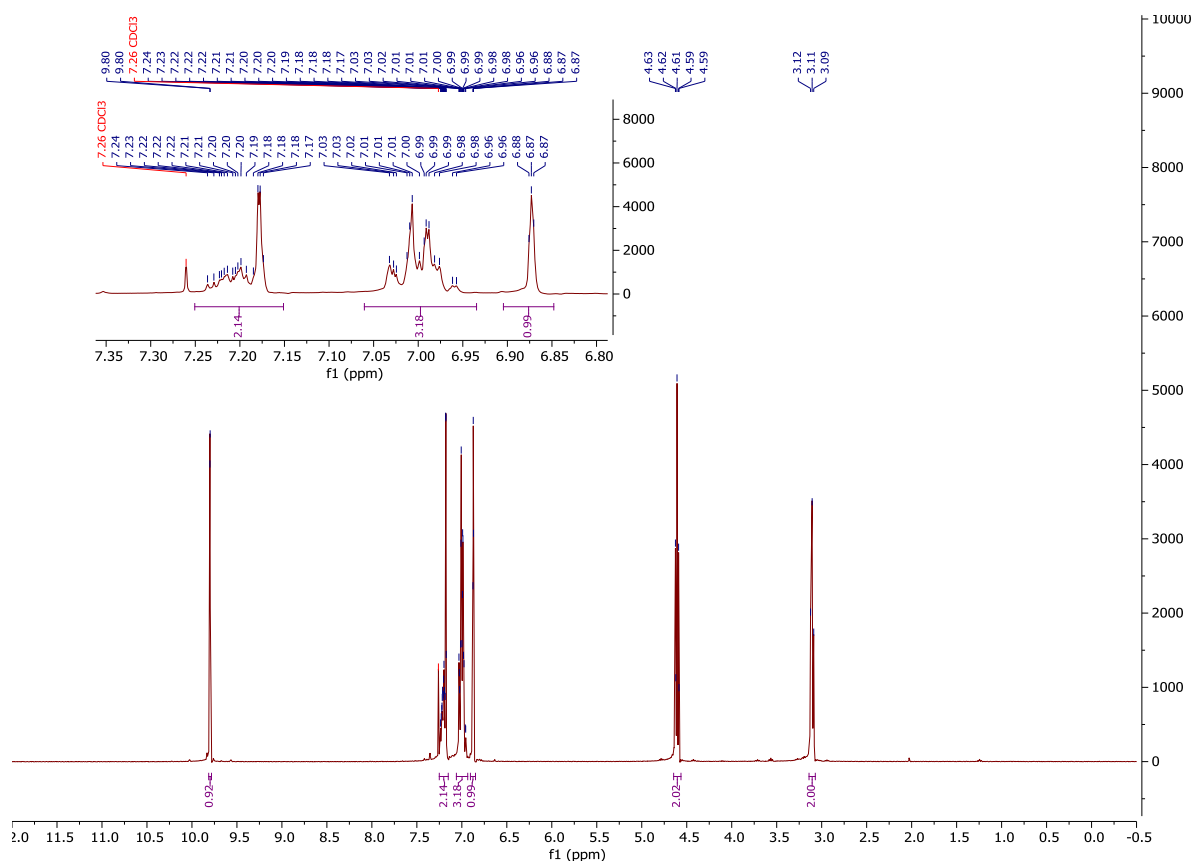
¹H-NMR and ¹³C-NMR: Compound 133



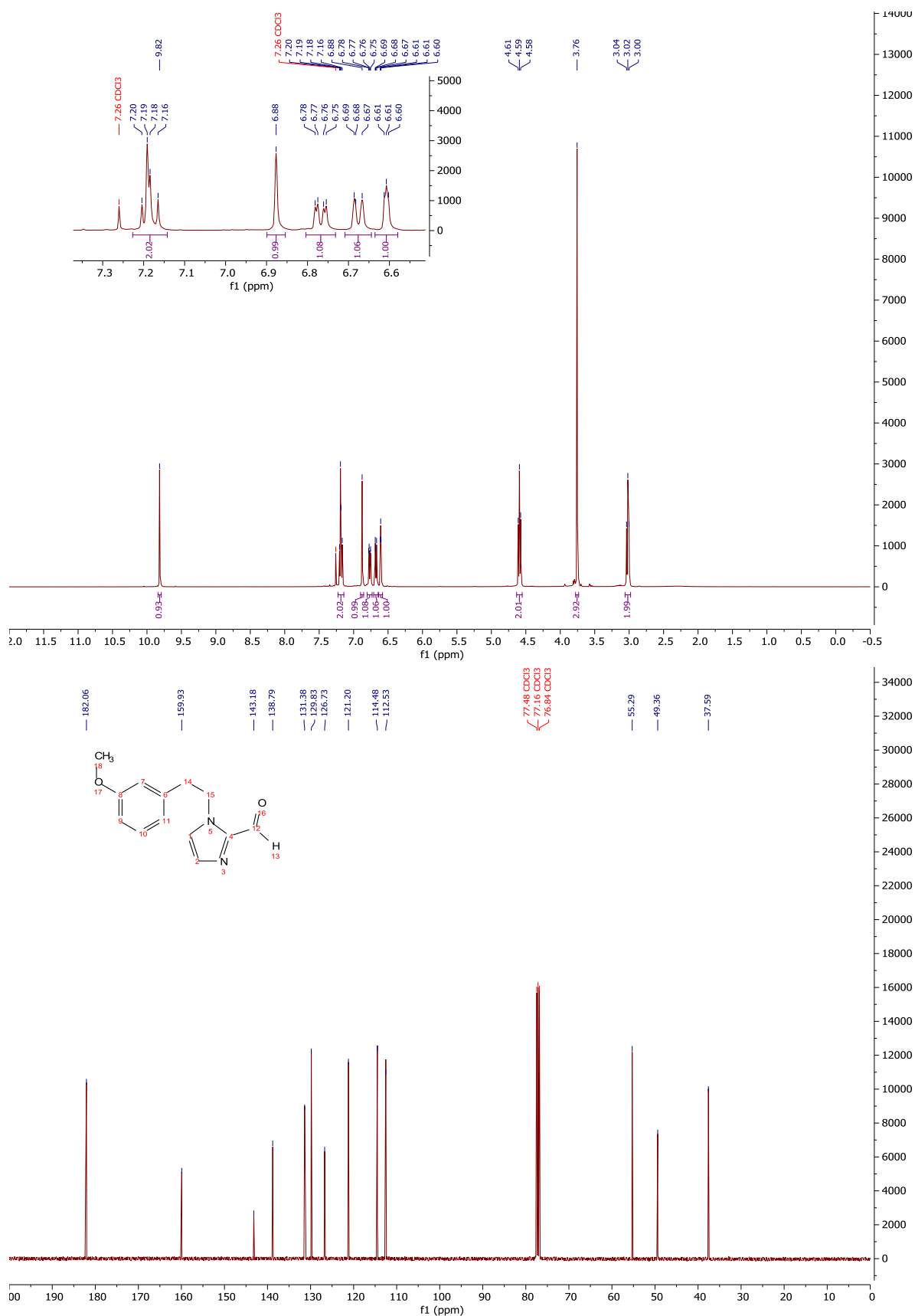
¹H-NMR and ¹³C-NMR: Compound 142



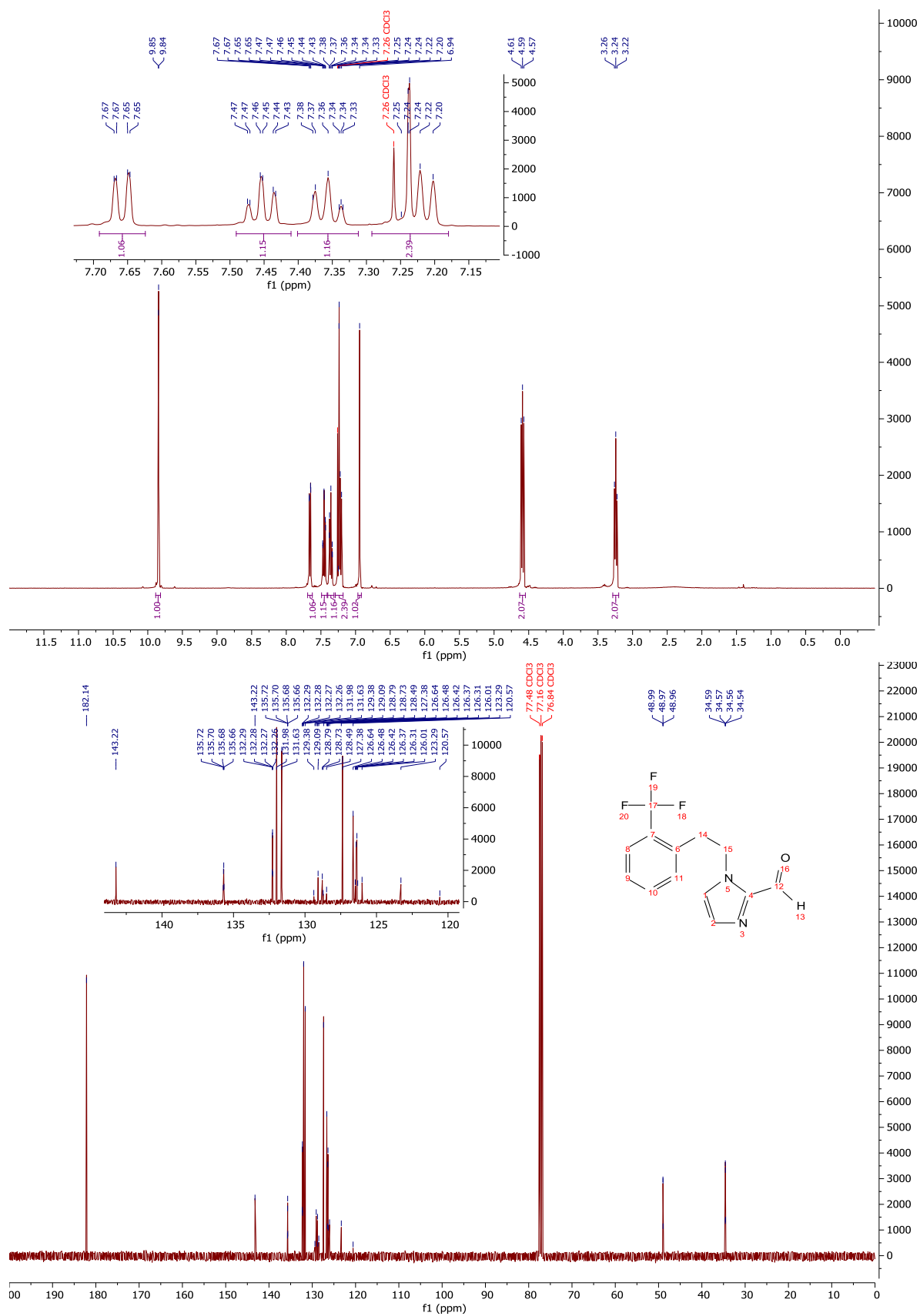
¹H-NMR and ¹³C-NMR: Compound 138



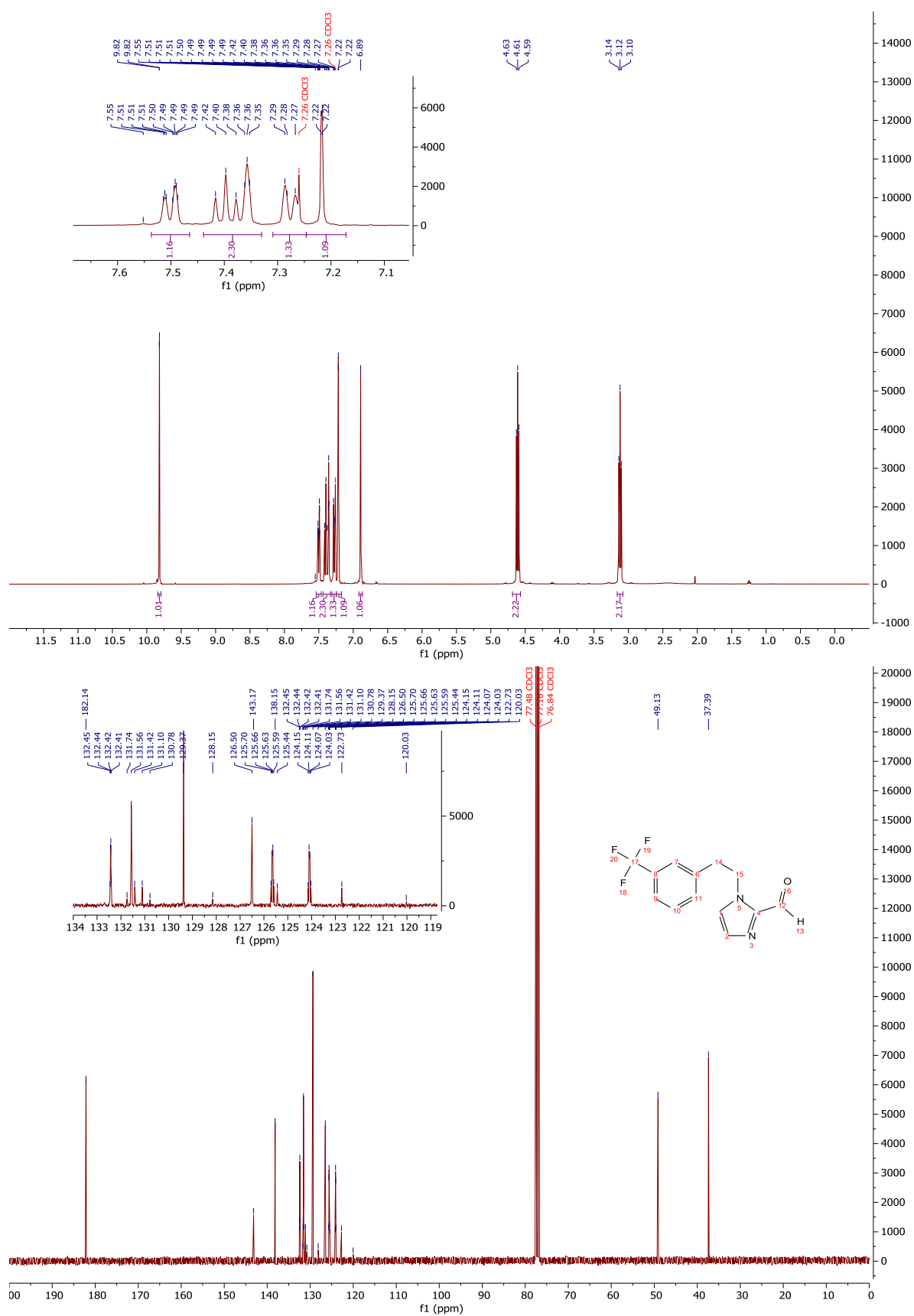
$^1\text{H-NMR}$ and $^{13}\text{C-NMR}$: Compound 137



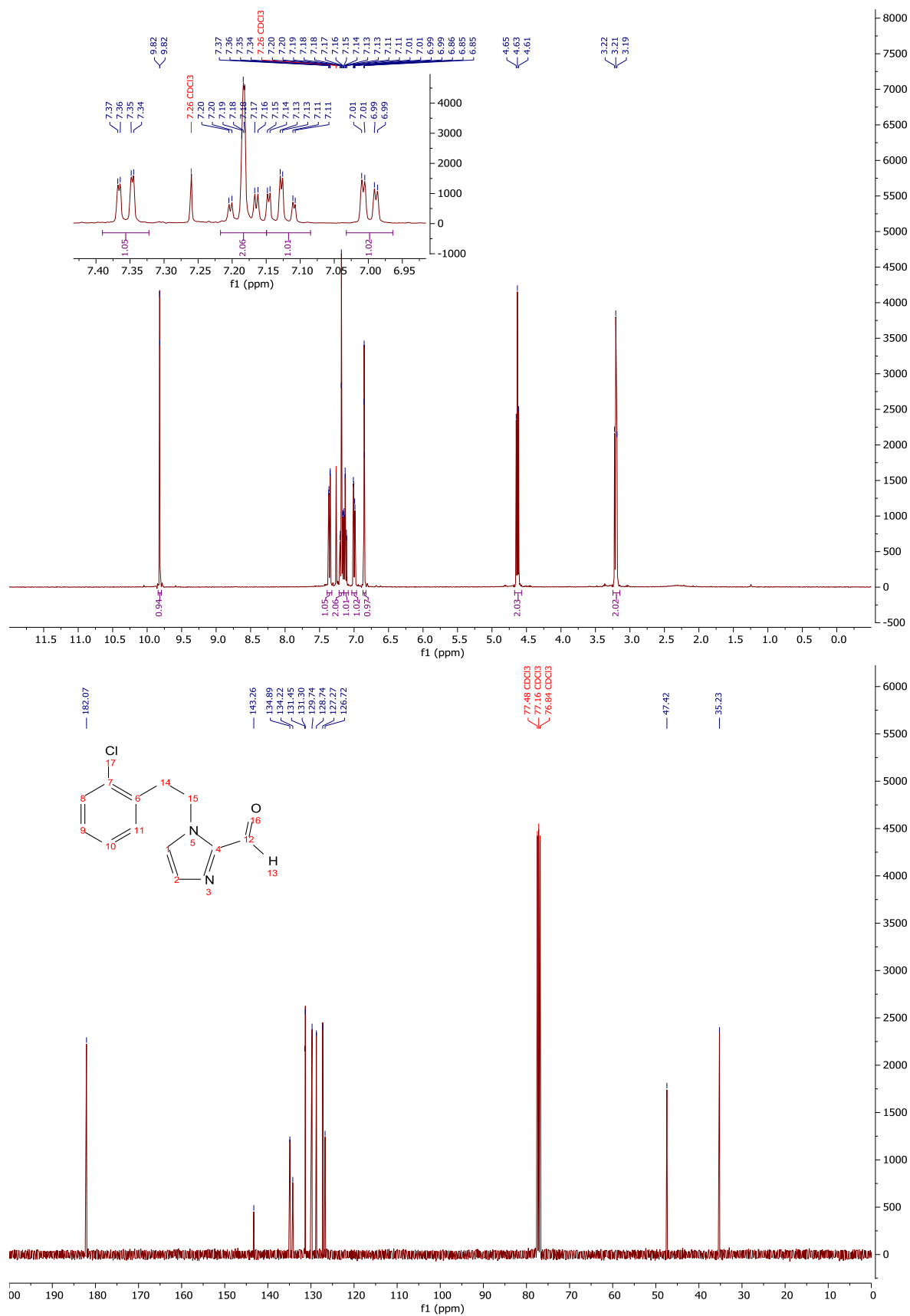
¹H-NMR and ¹³C-NMR: Compound 140



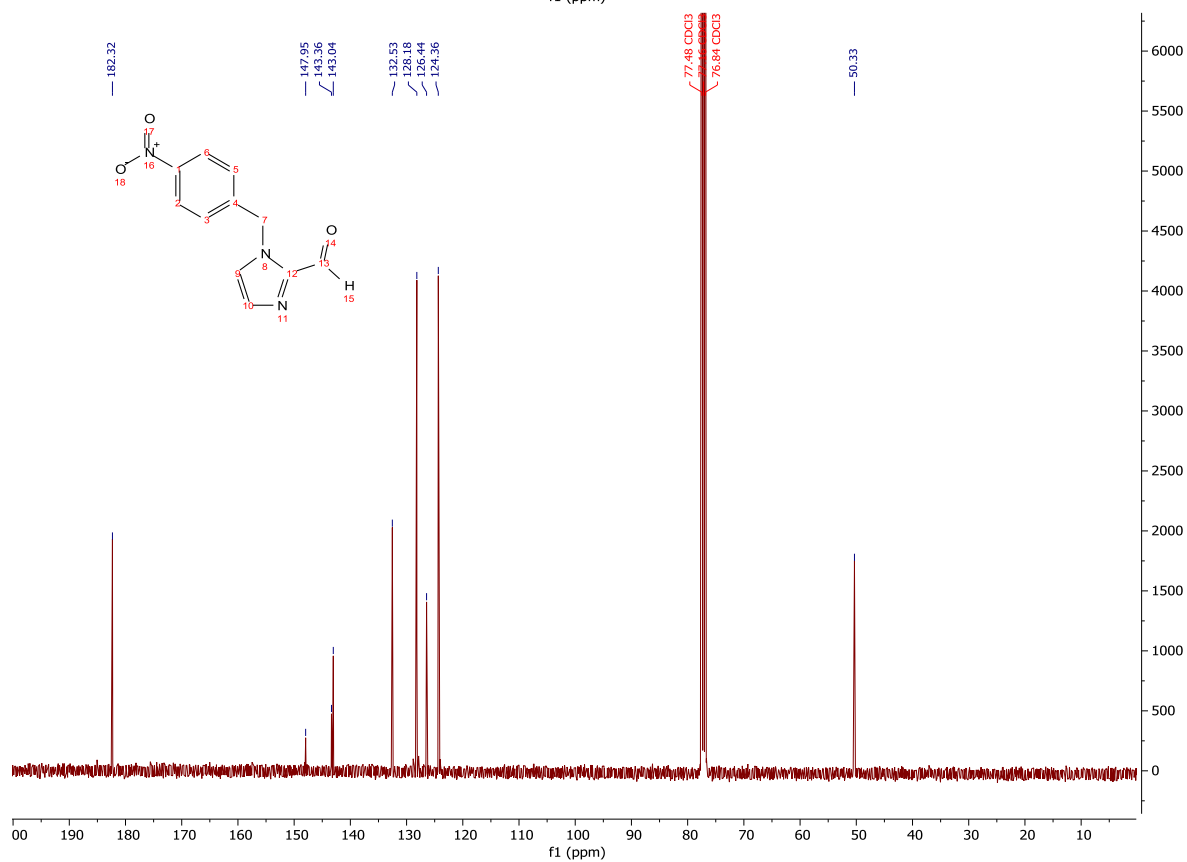
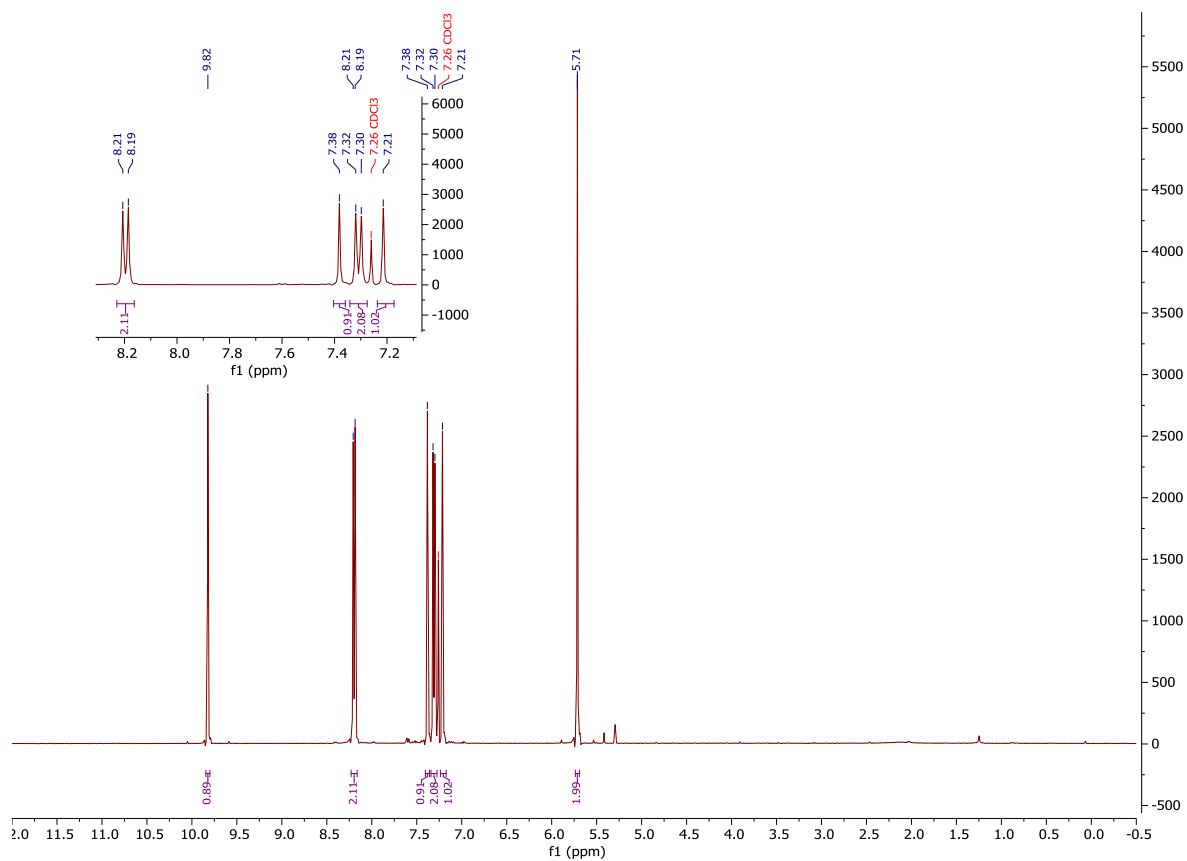
¹H-NMR and ¹³C-NMR: Compound 141



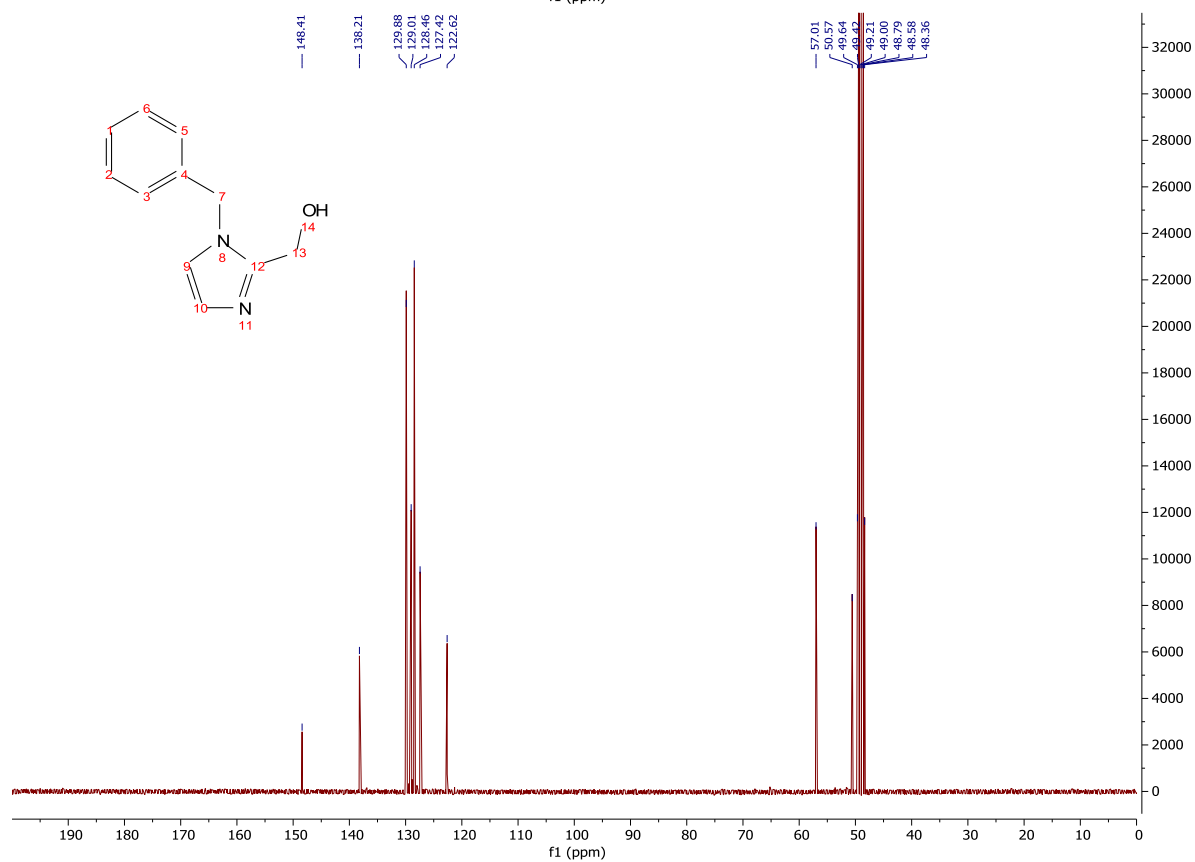
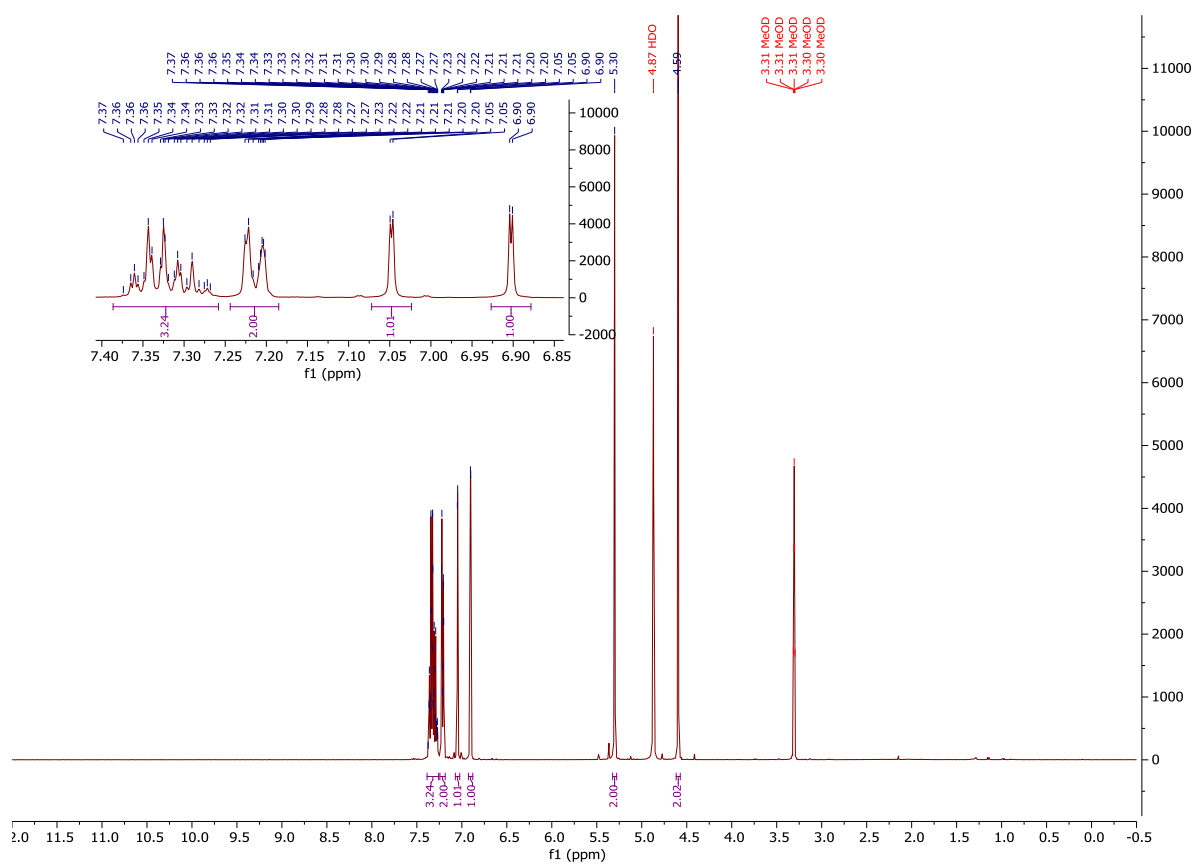
¹H-NMR and ¹³C-NMR: Compound 139



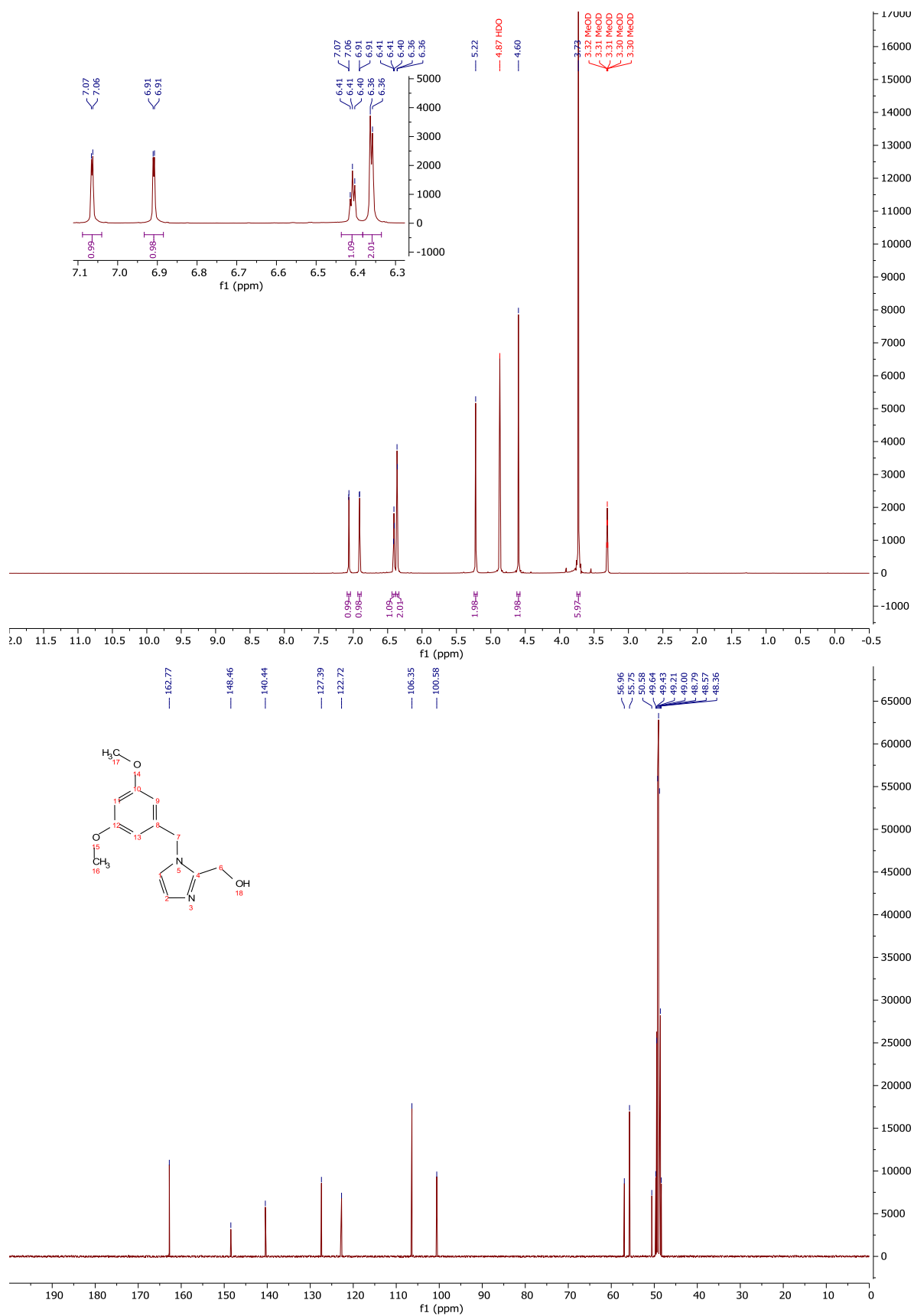
$^1\text{H-NMR}$ and $^{13}\text{C-NMR}$: Compound 143



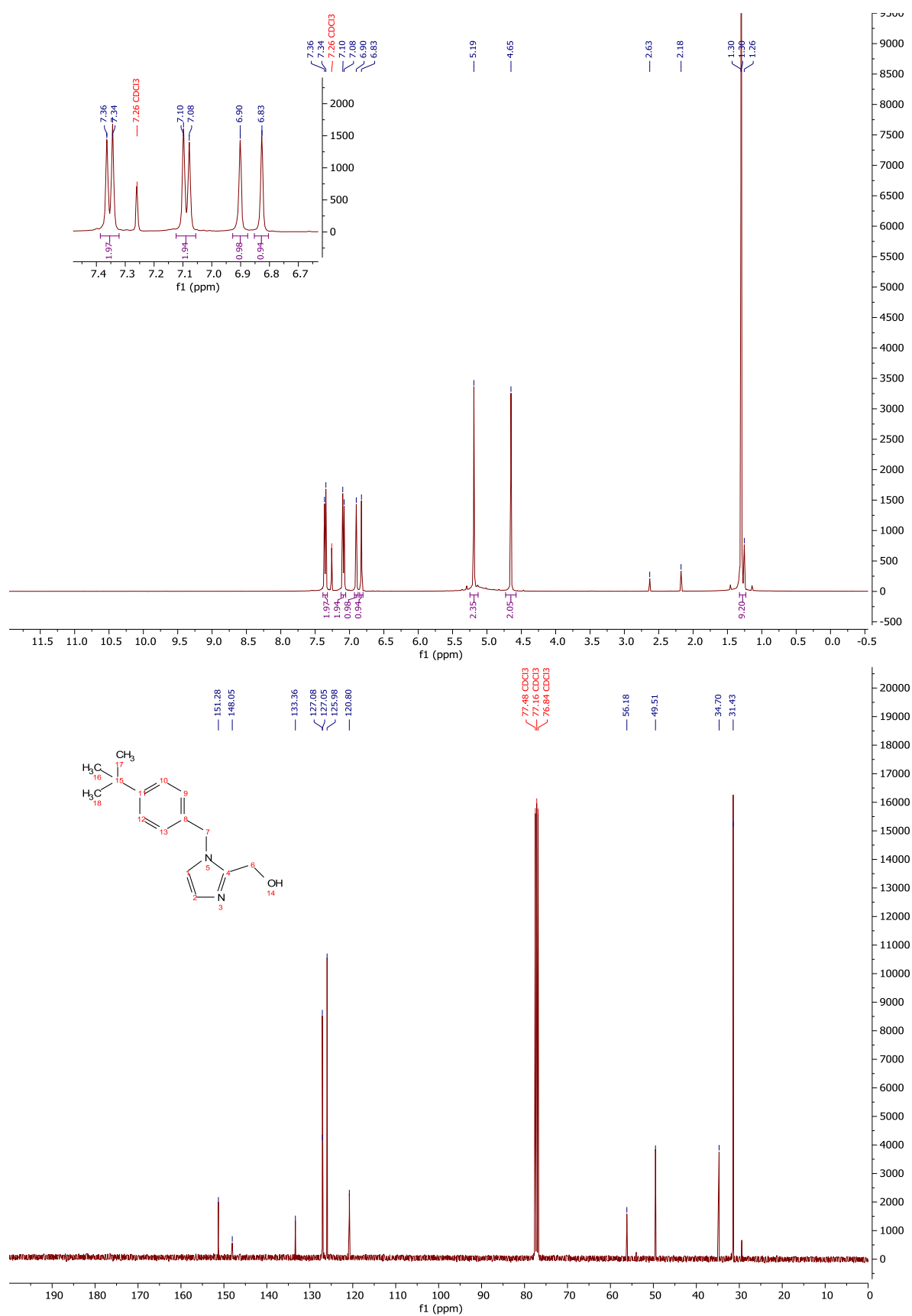
¹H-NMR and ¹³C-NMR: Compound 145



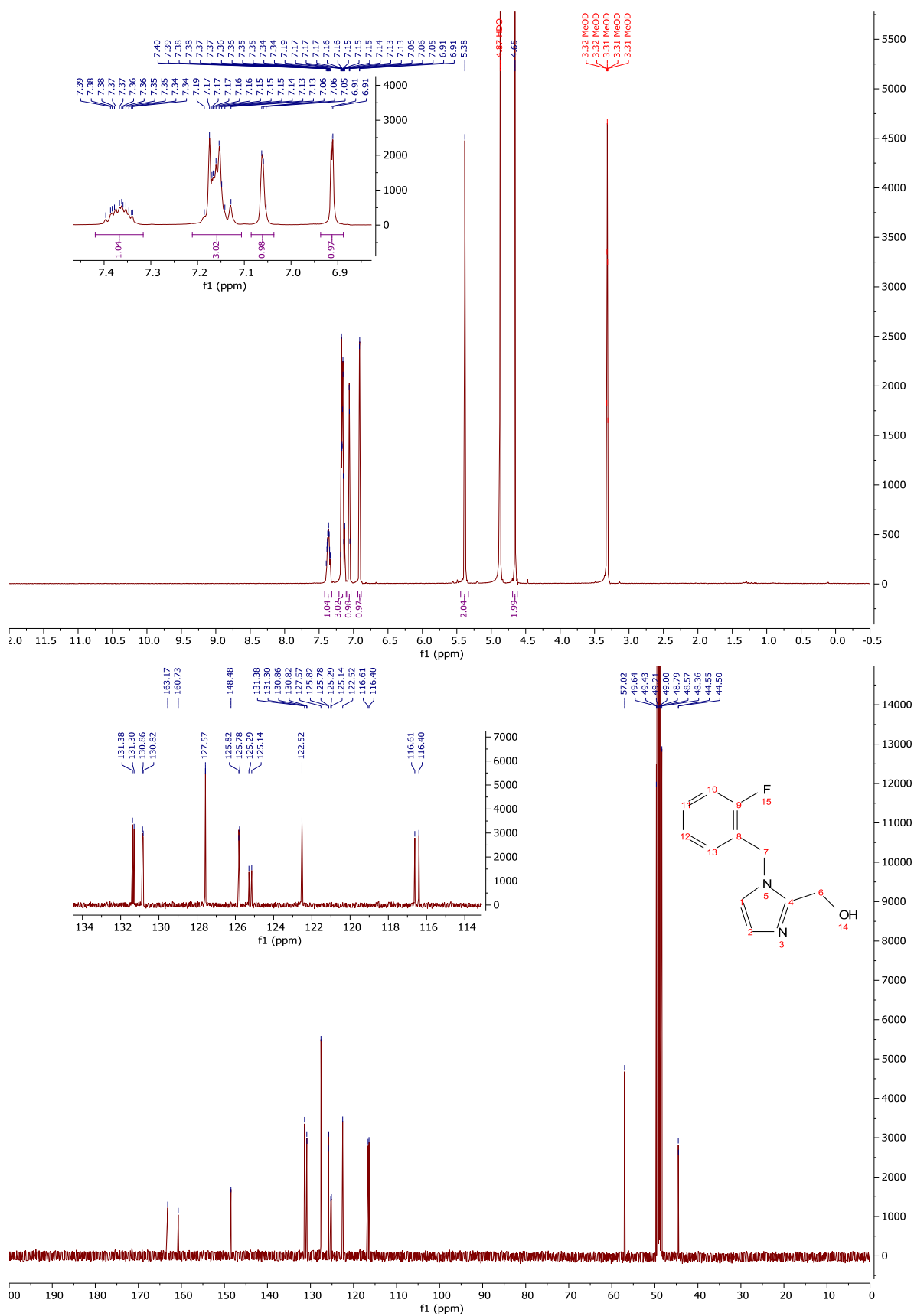
¹H-NMR and ¹³C-NMR: Compound 151



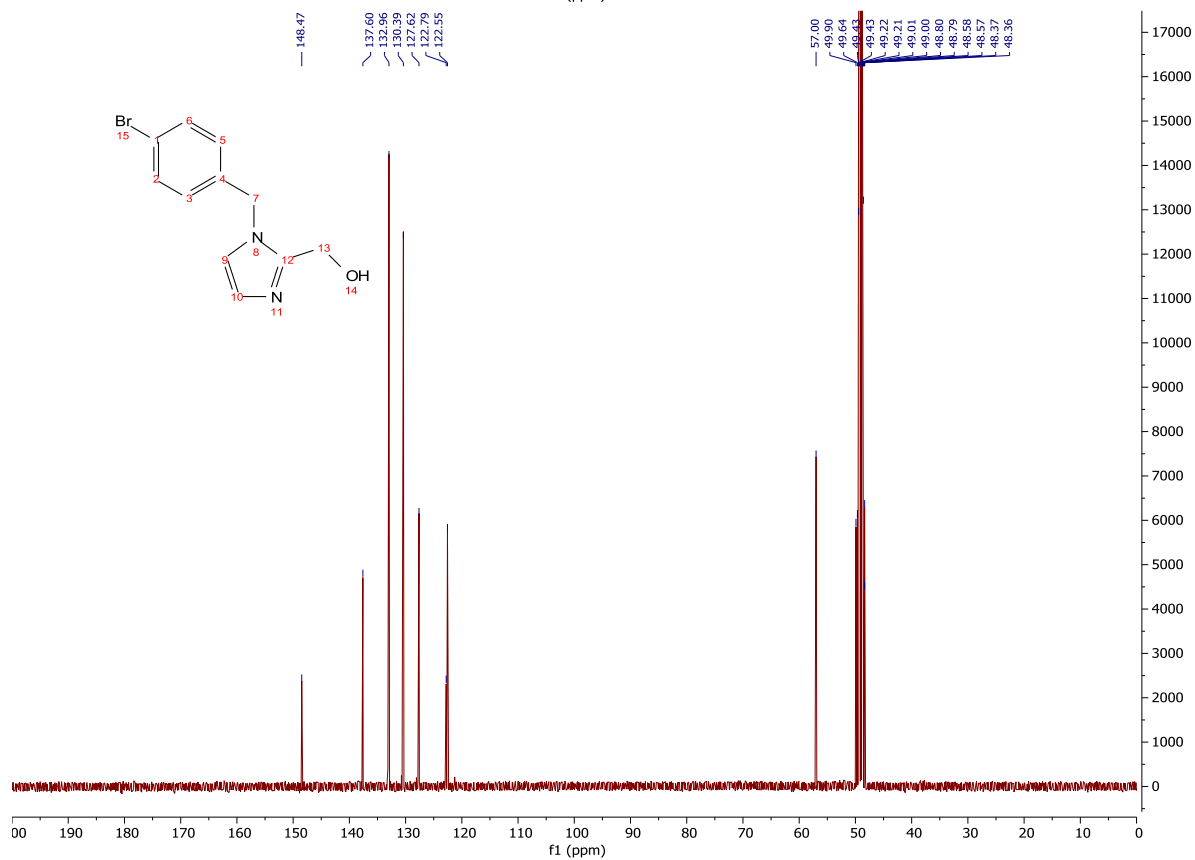
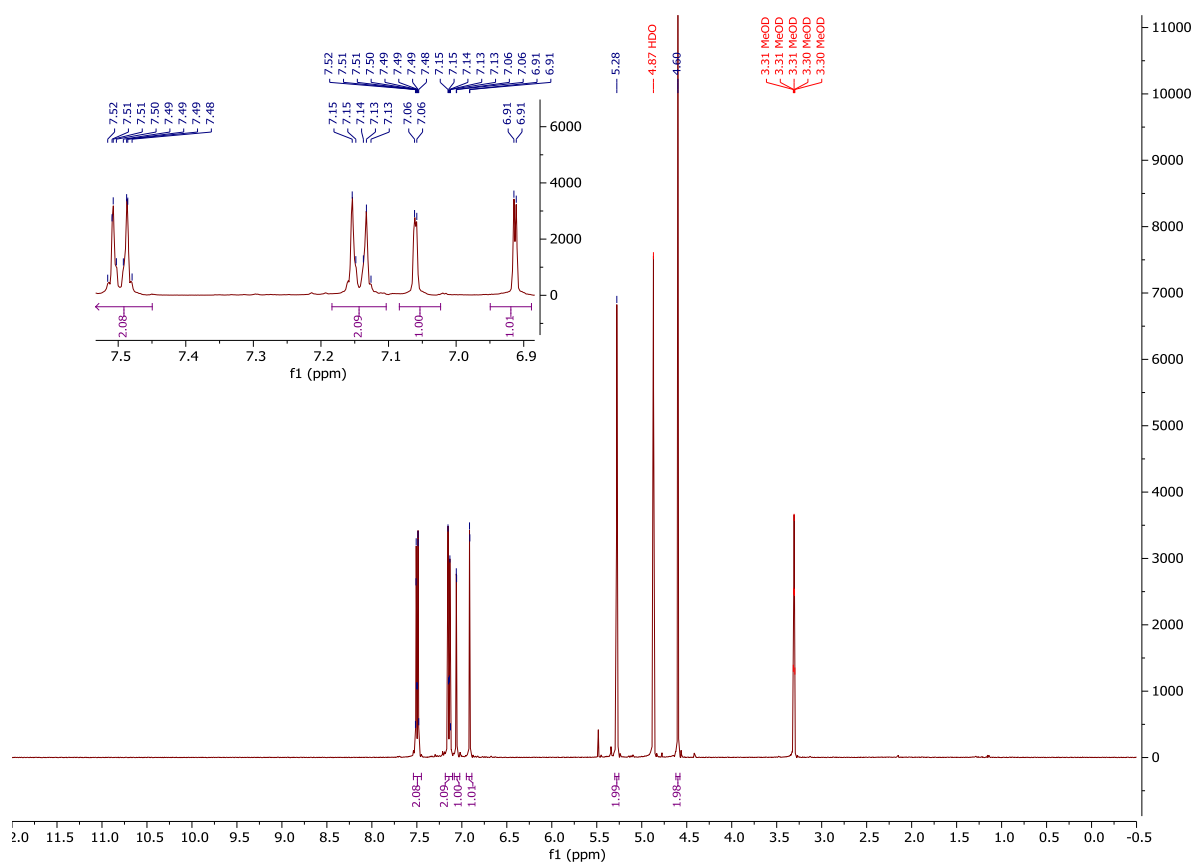
$^1\text{H-NMR}$ and $^{13}\text{C-NMR}$: Compound 149



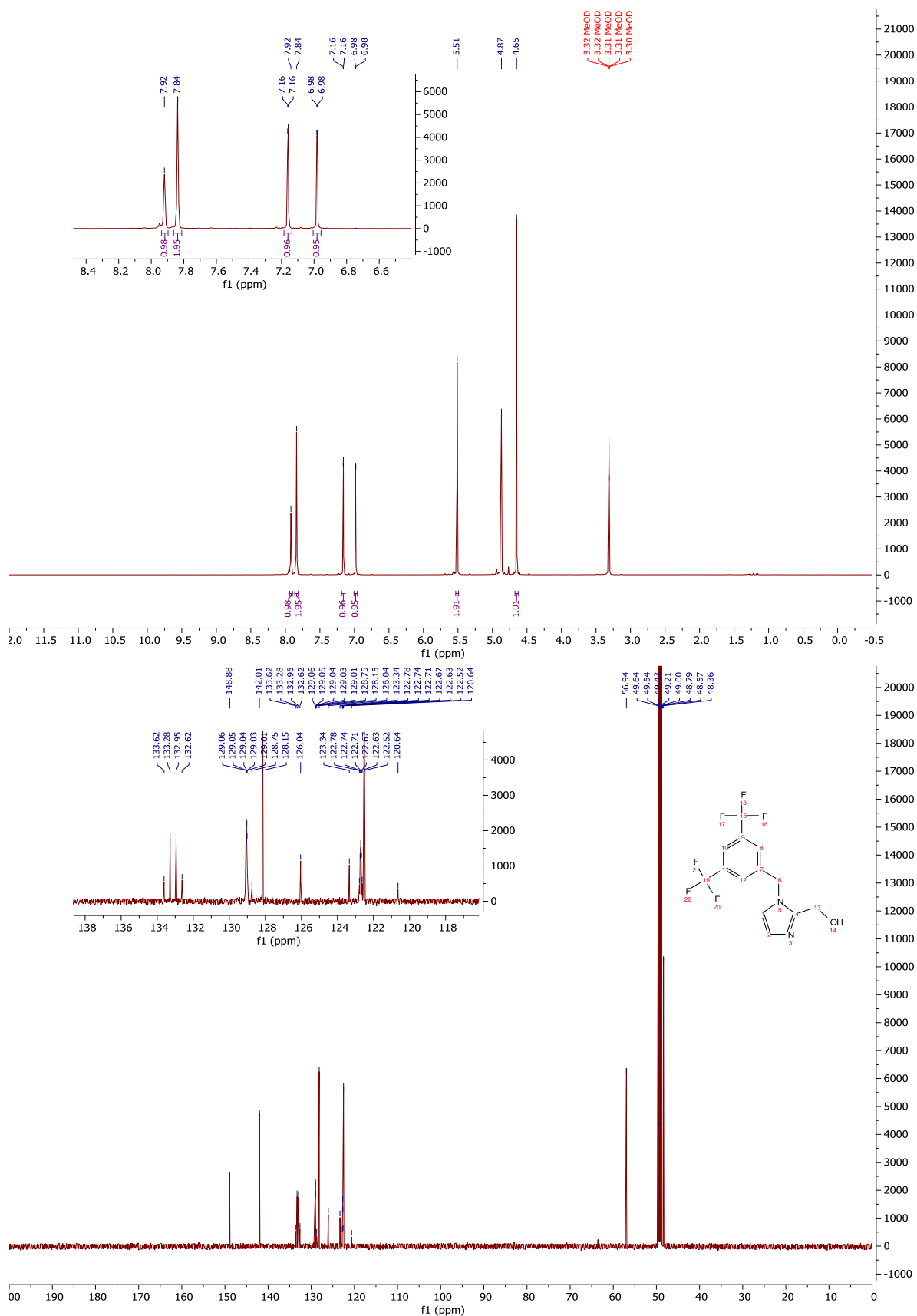
¹H-NMR and ¹³C-NMR: Compound 144



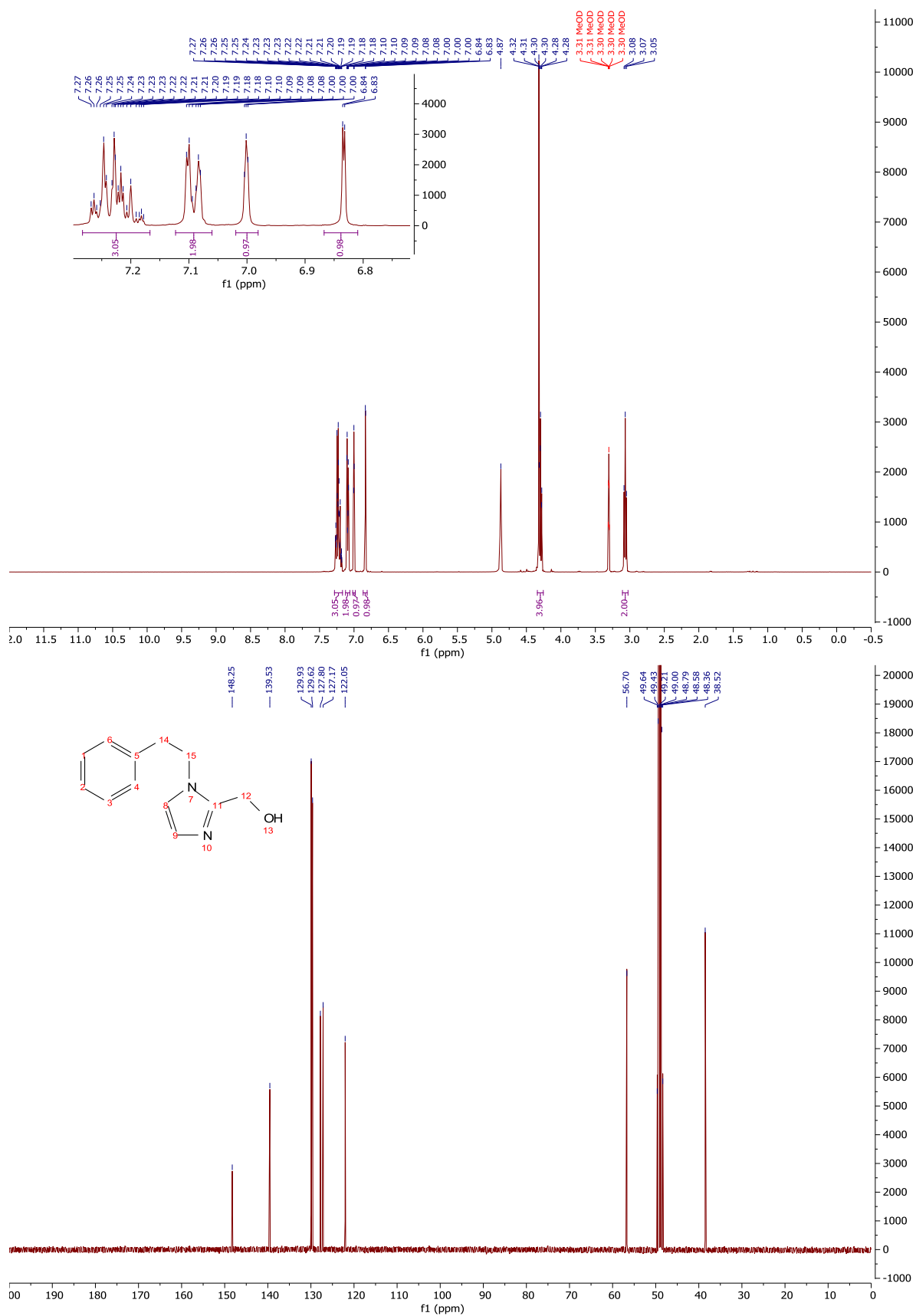
¹H-NMR and ¹³C-NMR: Compound 146



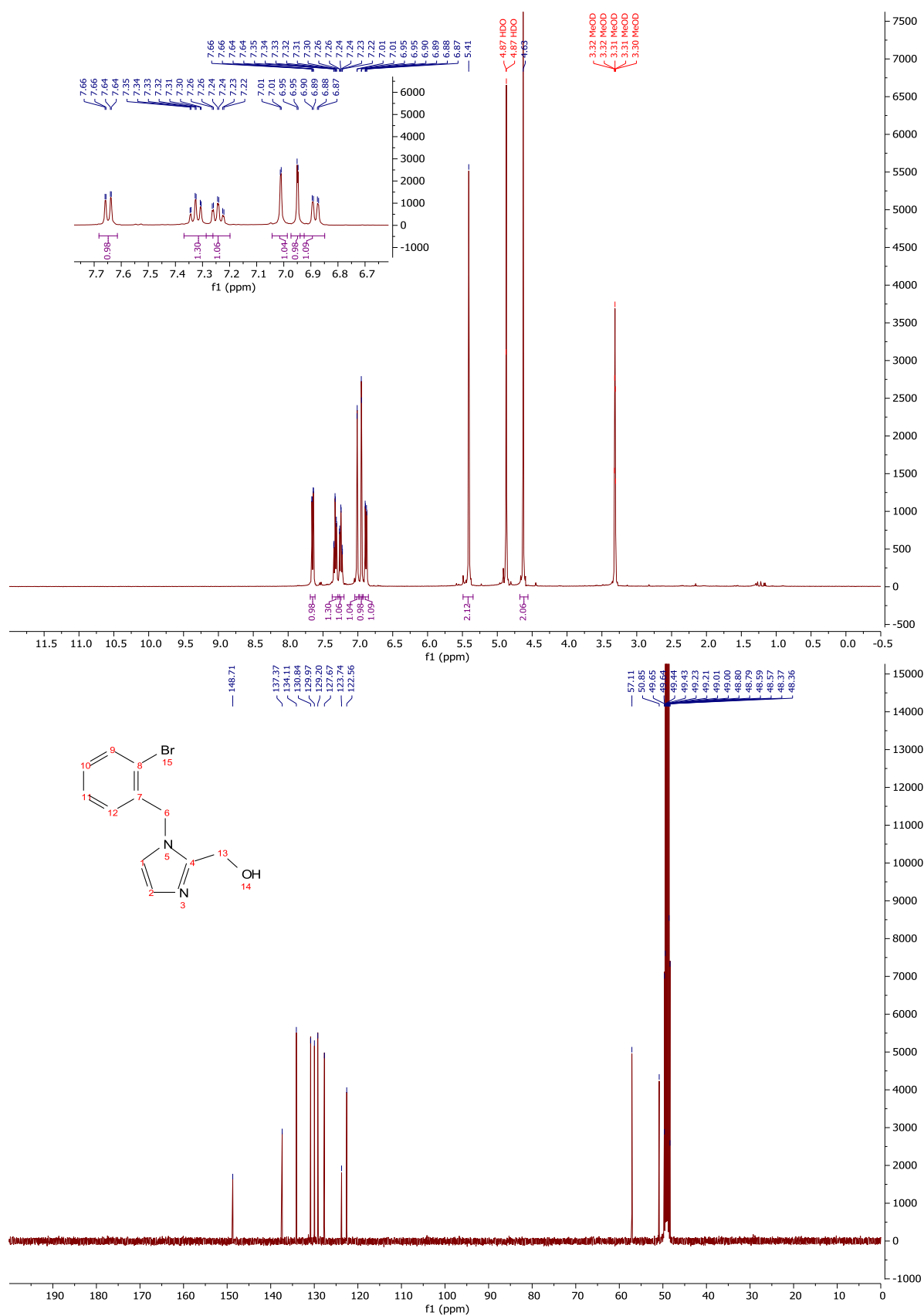
$^1\text{H-NMR}$ and $^{13}\text{C-NMR}$: Compound 152



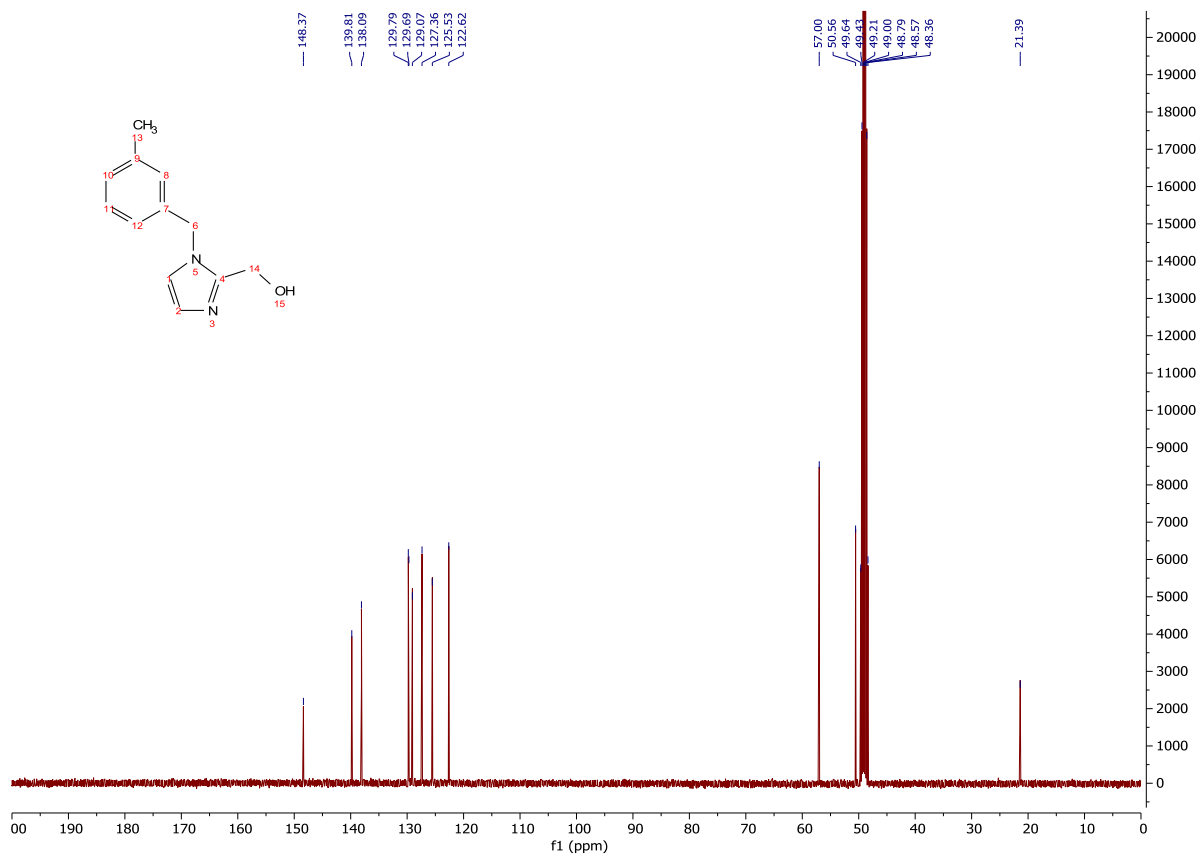
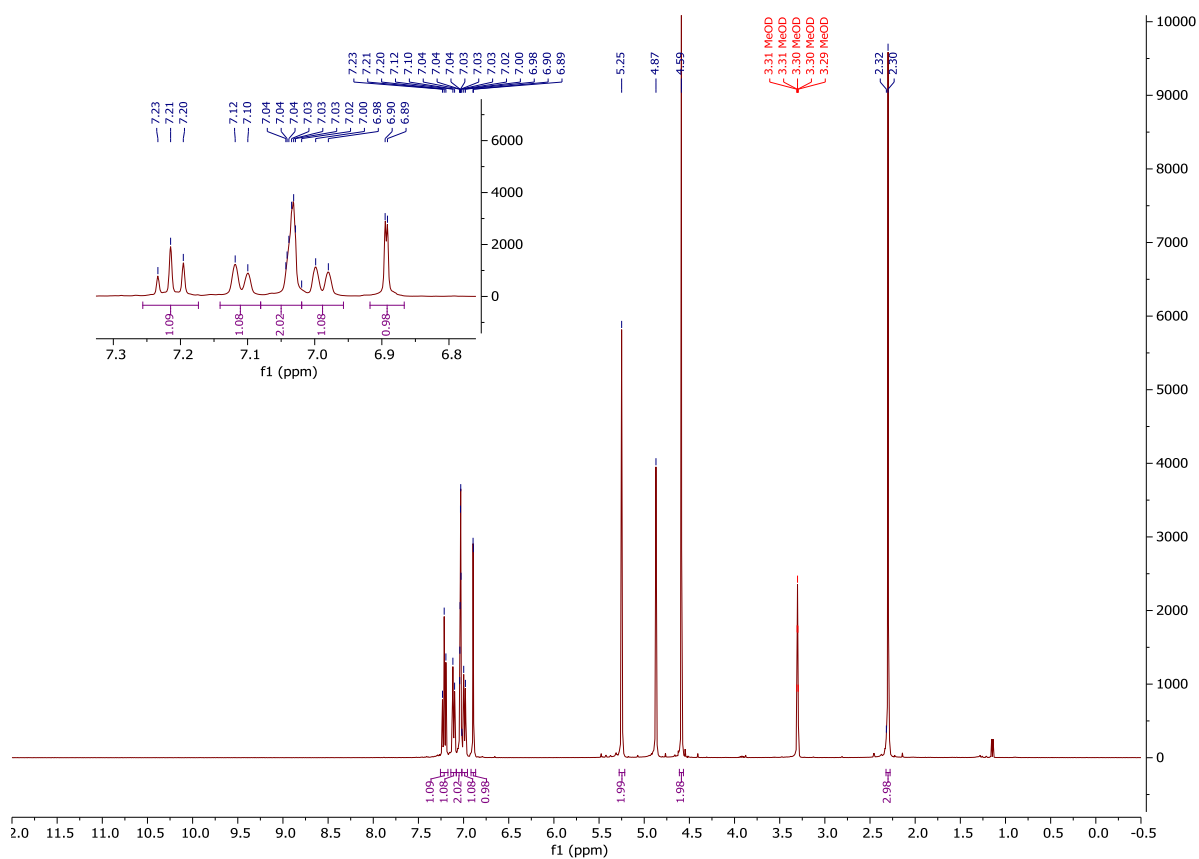
¹H-NMR and ¹³C-NMR: Compound 153



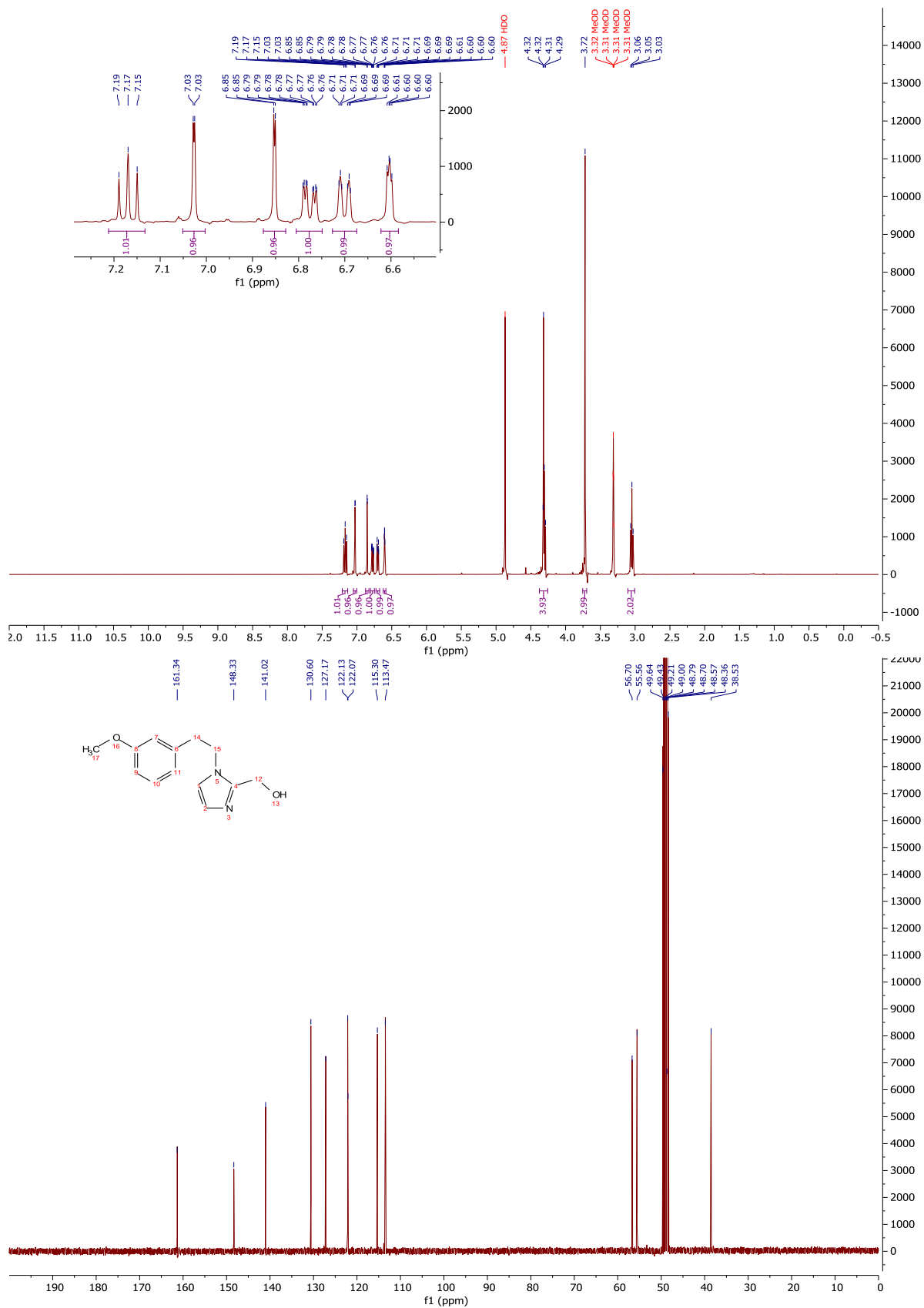
¹H-NMR and ¹³C-NMR: Compound 148



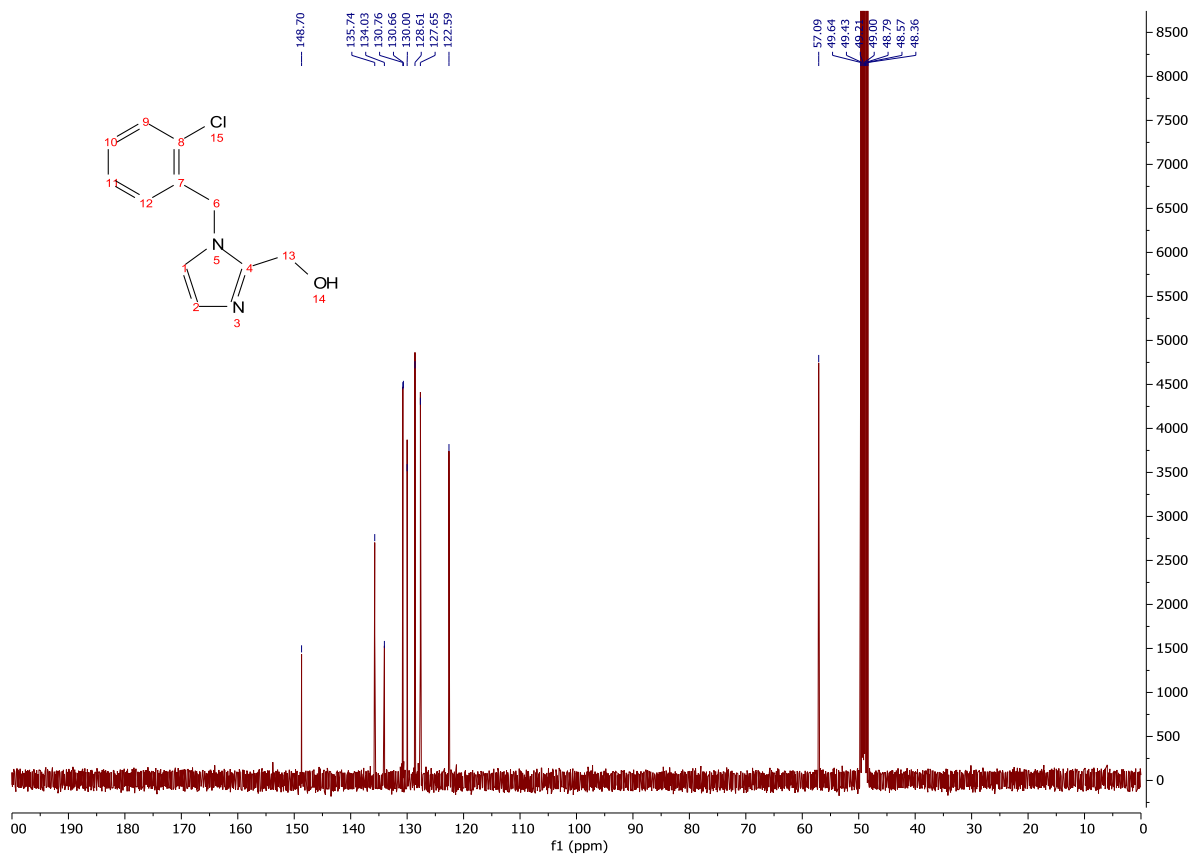
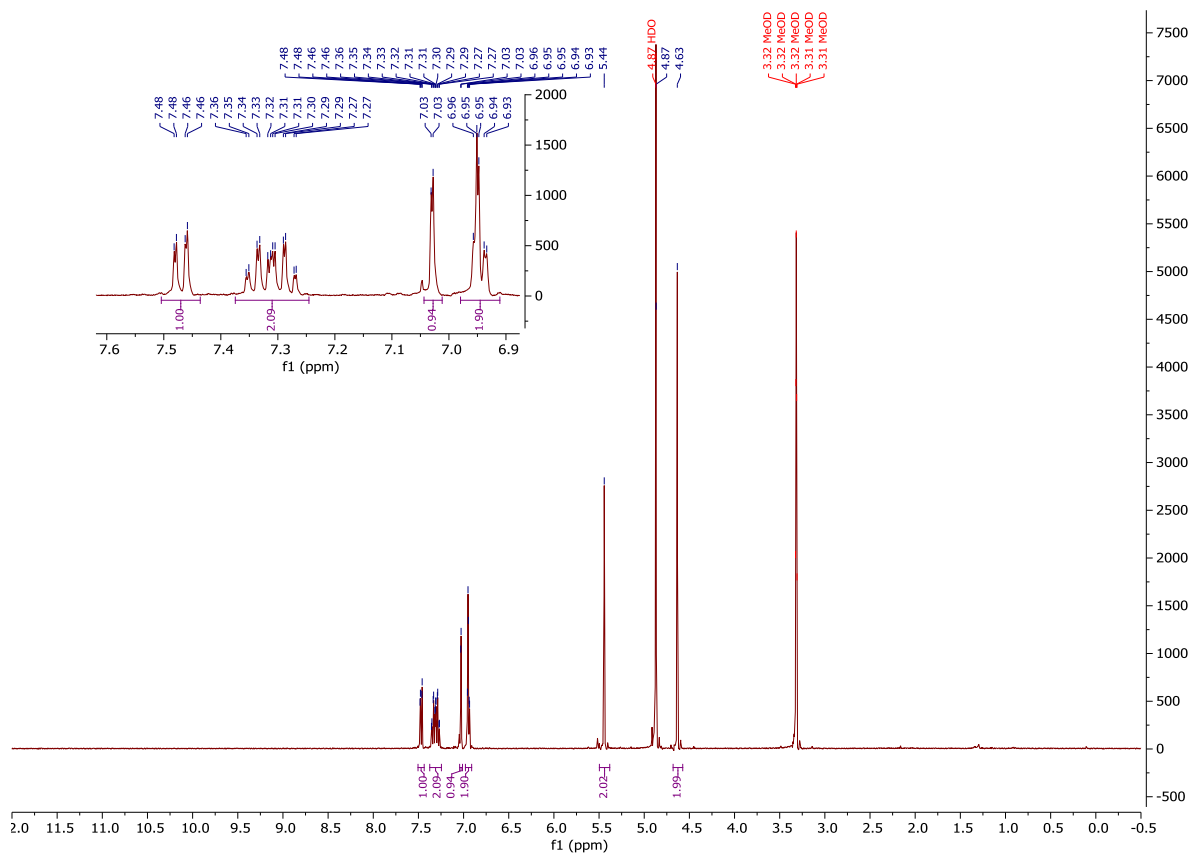
¹H-NMR and ¹³C-NMR: Compound 147



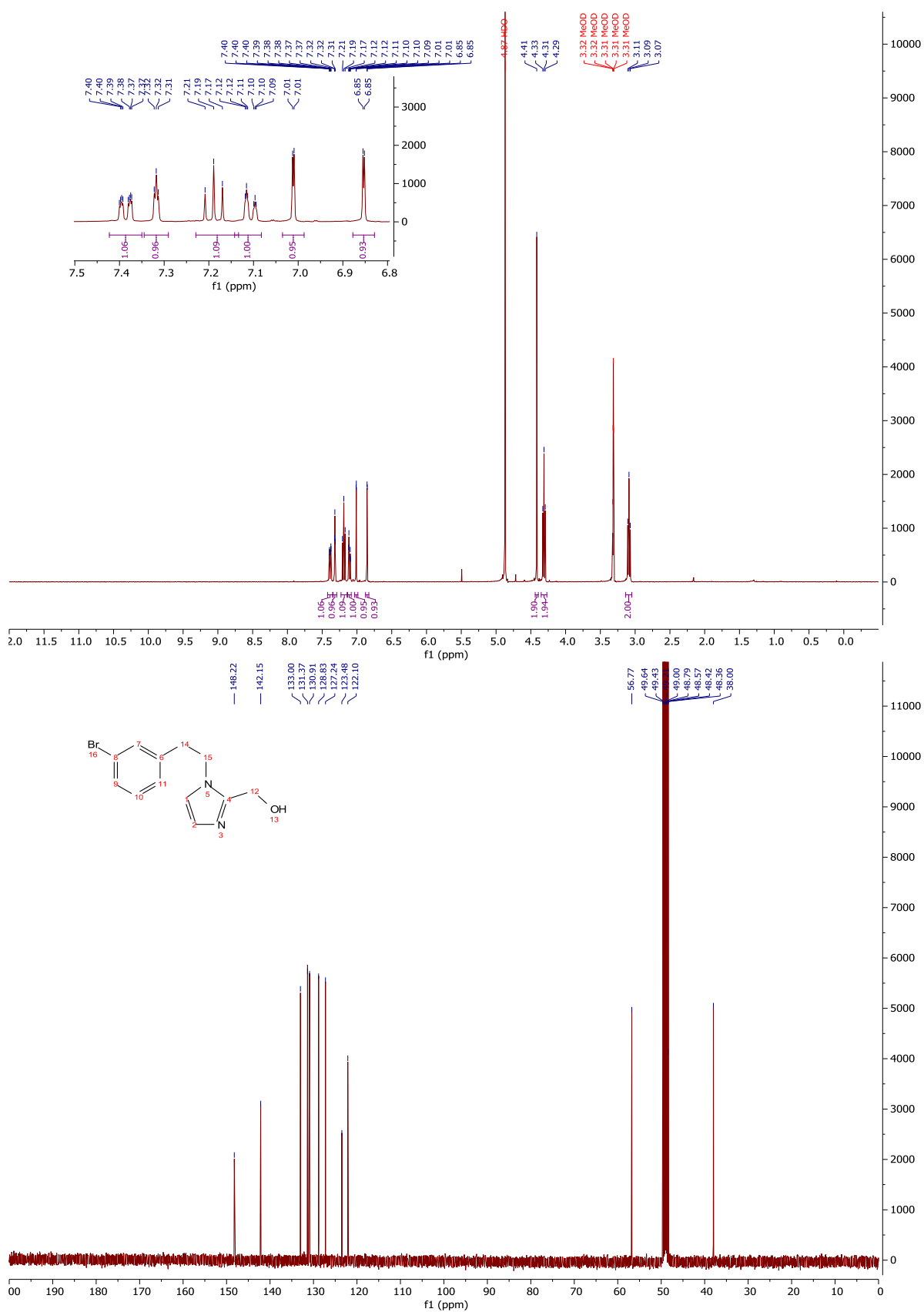
¹H-NMR and ¹³C-NMR: Compound 154



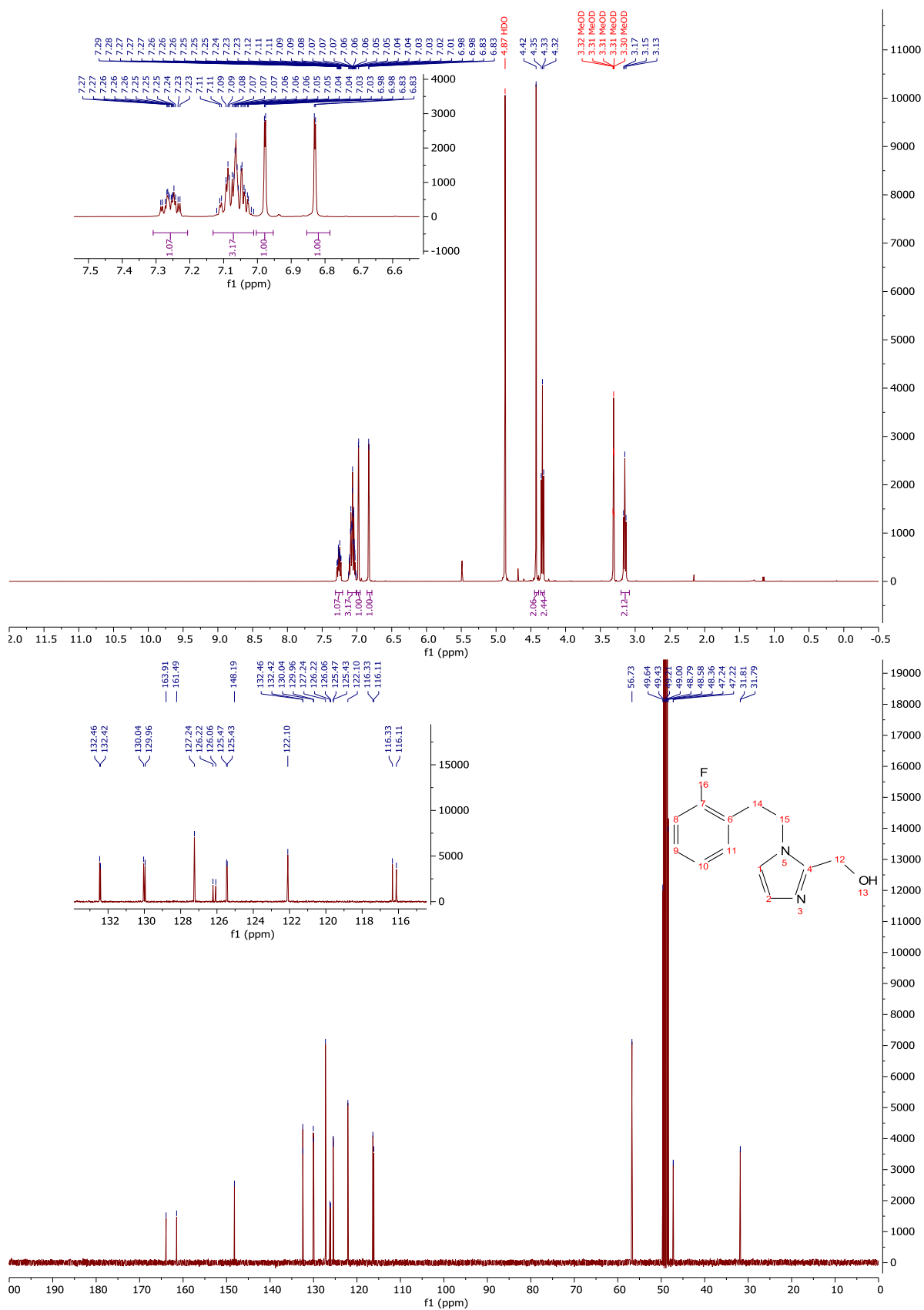
¹H-NMR and ¹³C-NMR: Compound 150



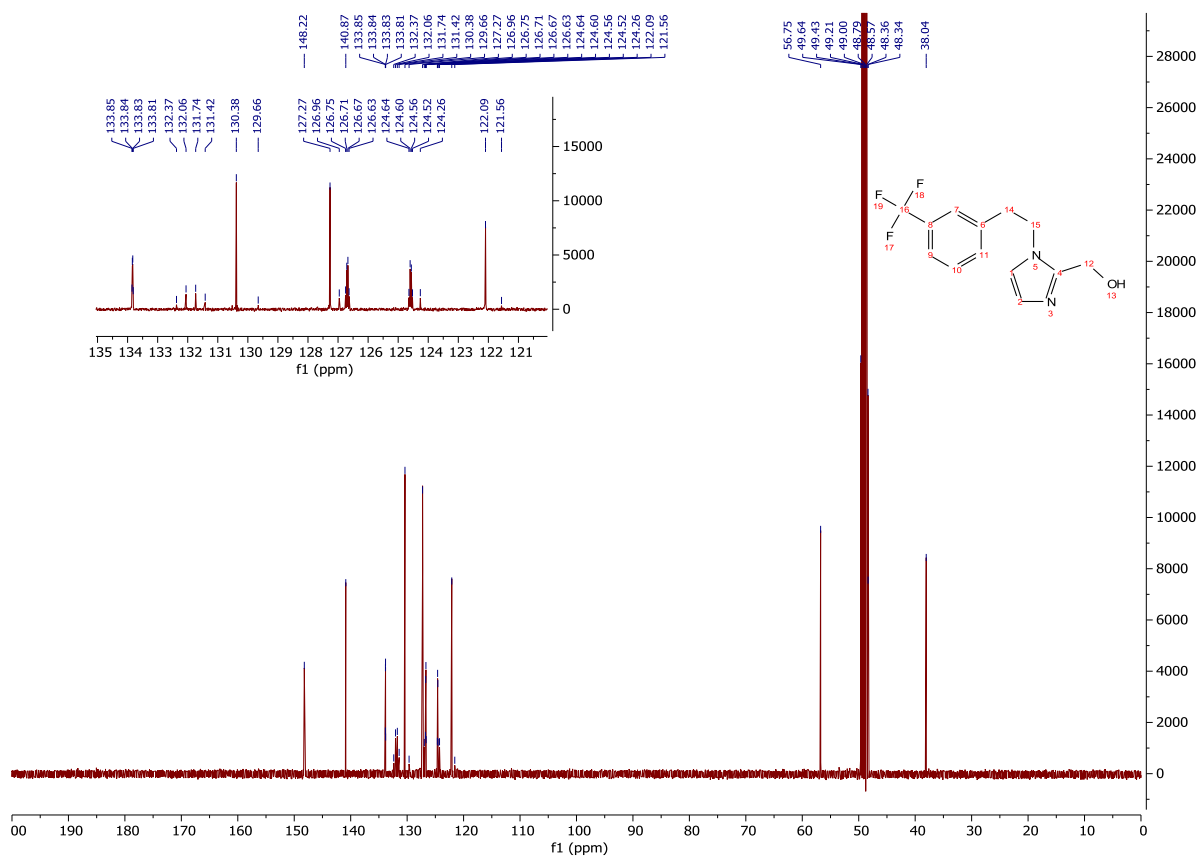
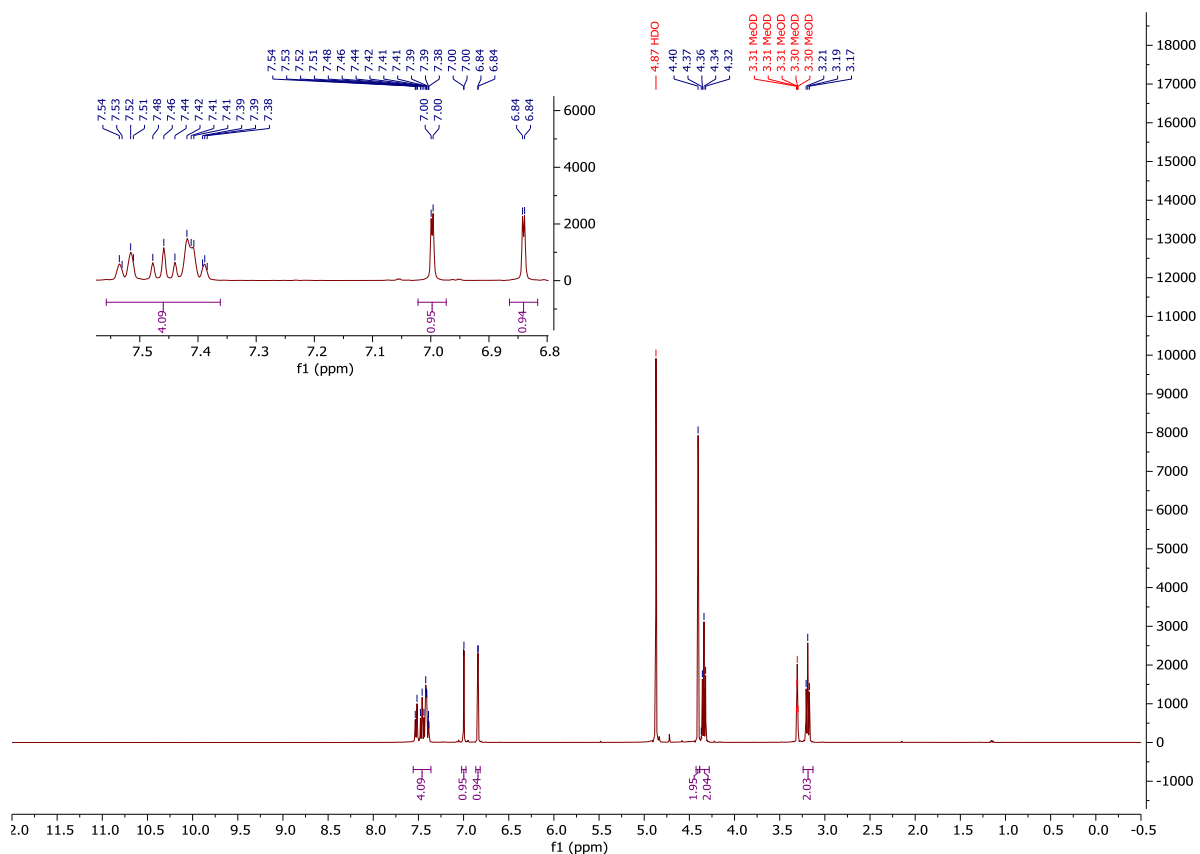
¹H-NMR and ¹³C-NMR: Compound 160



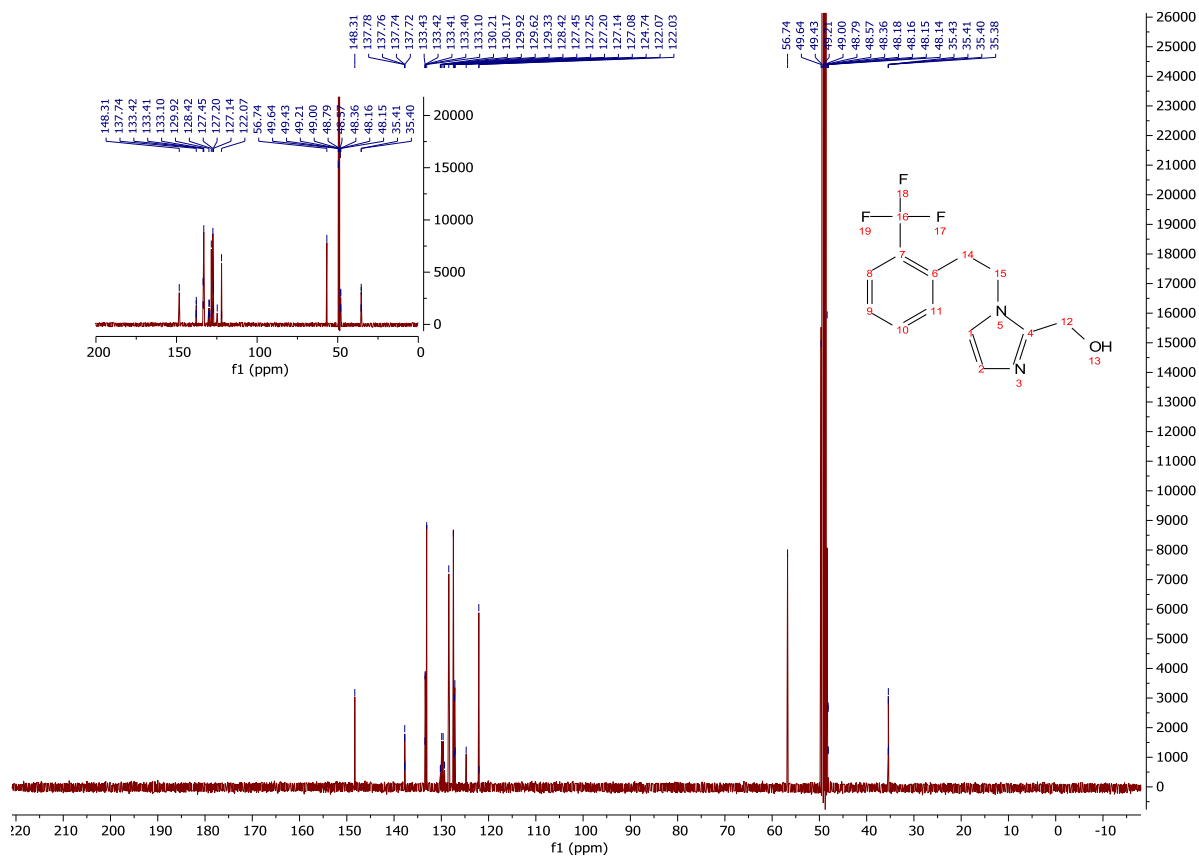
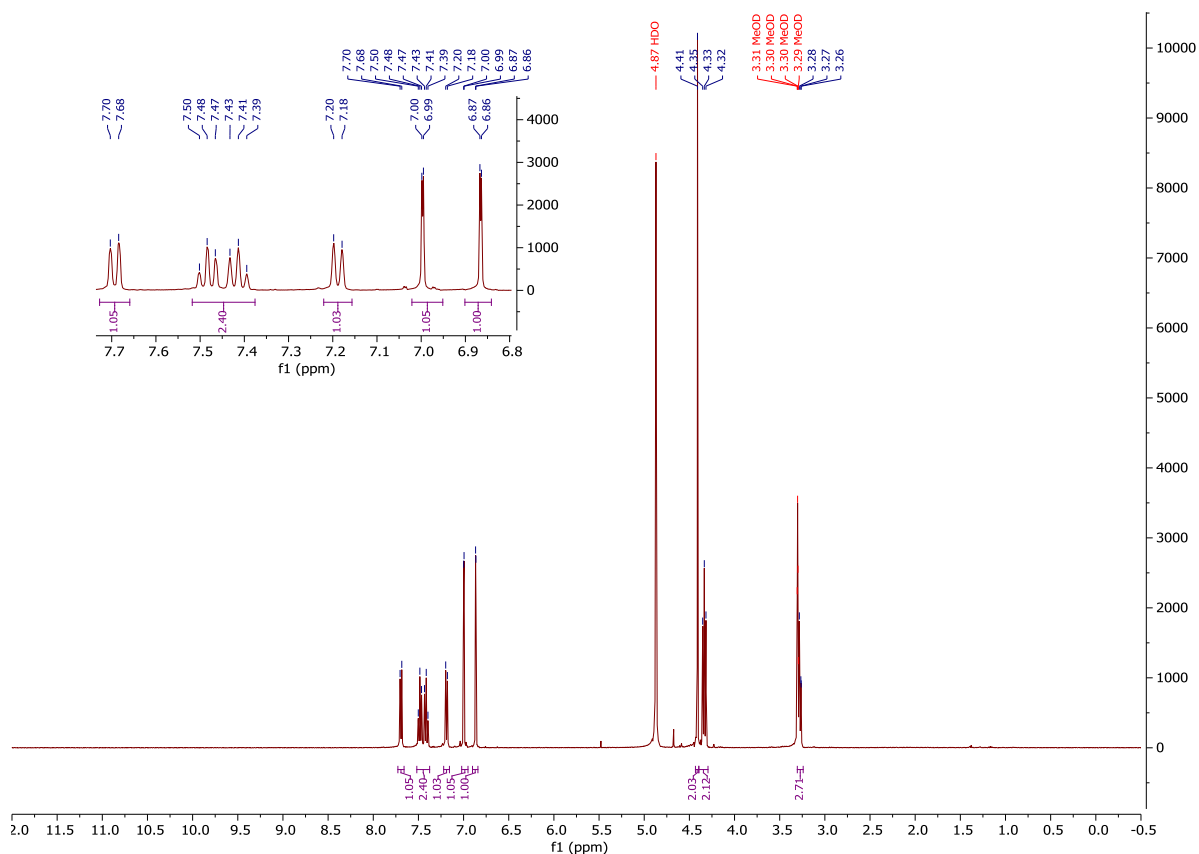
¹H-NMR and ¹³C-NMR: Compound 155



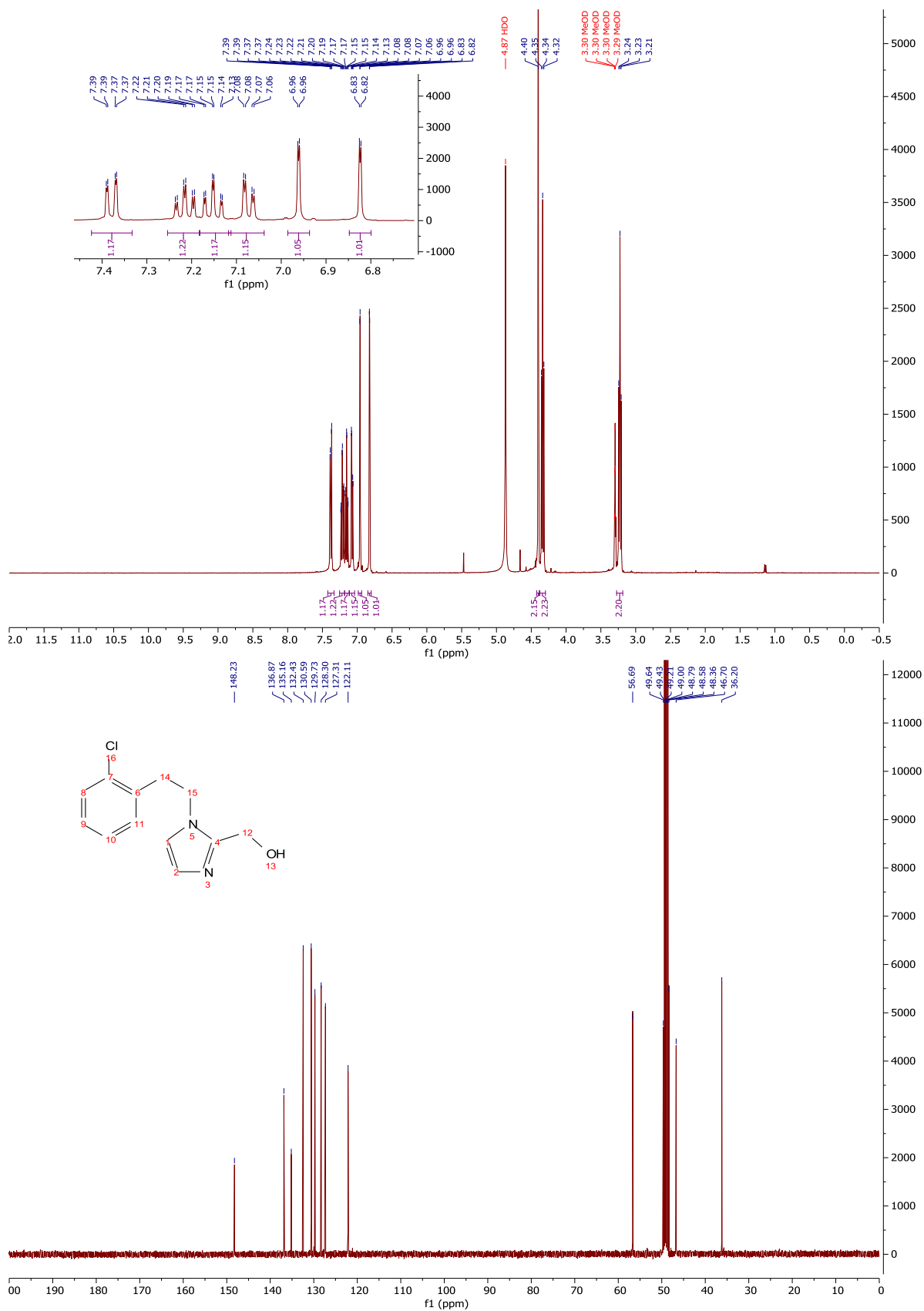
¹H-NMR and ¹³C-NMR: Compound 158



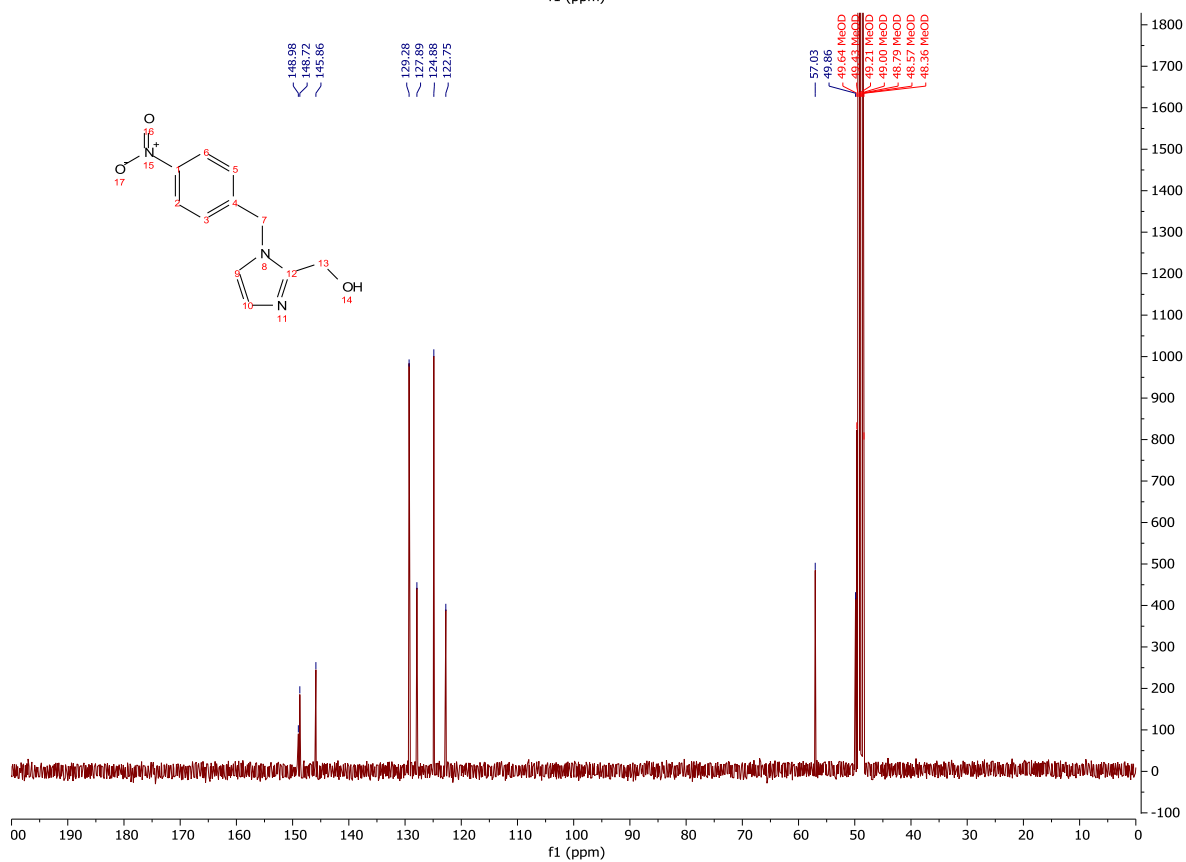
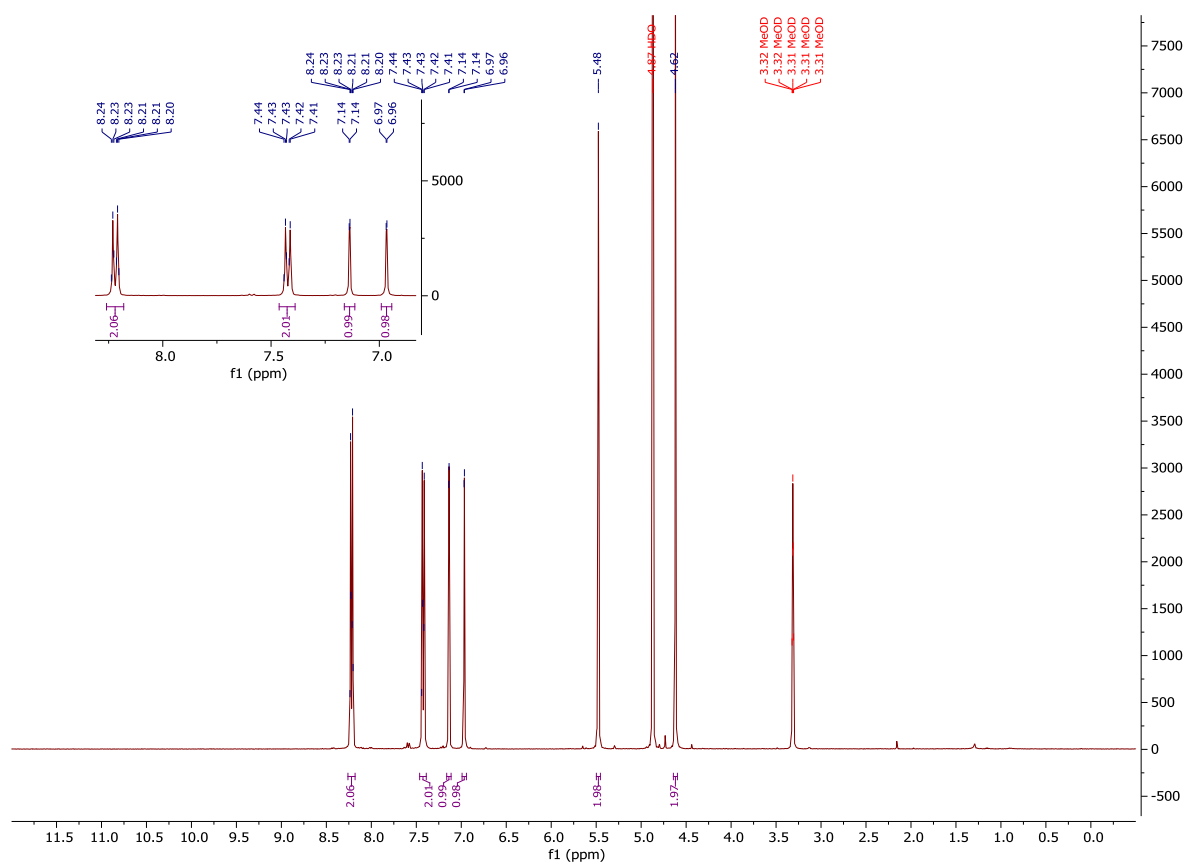
¹H-NMR and ¹³C-NMR: Compound 157



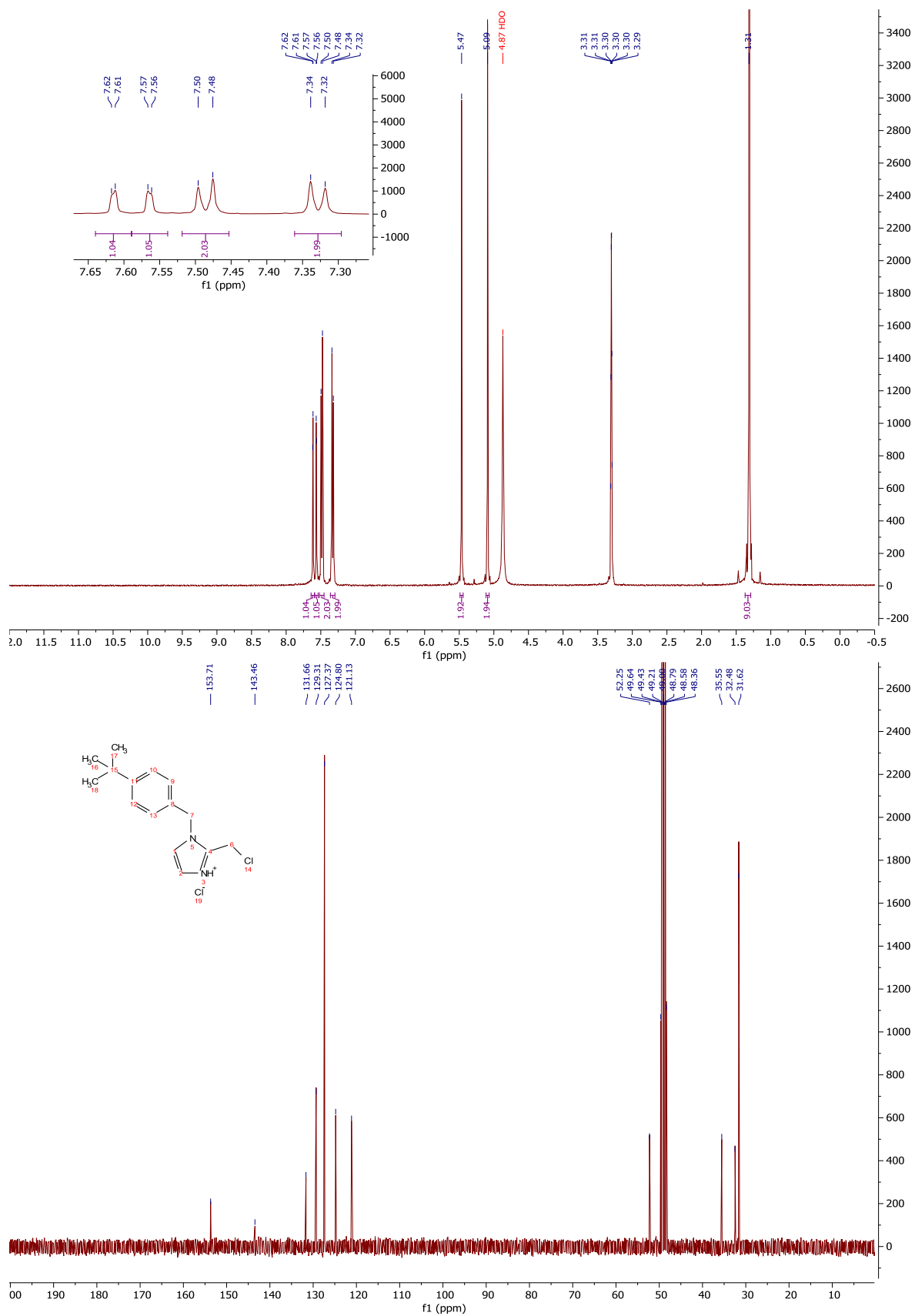
¹H-NMR and ¹³C-NMR: Compound 156



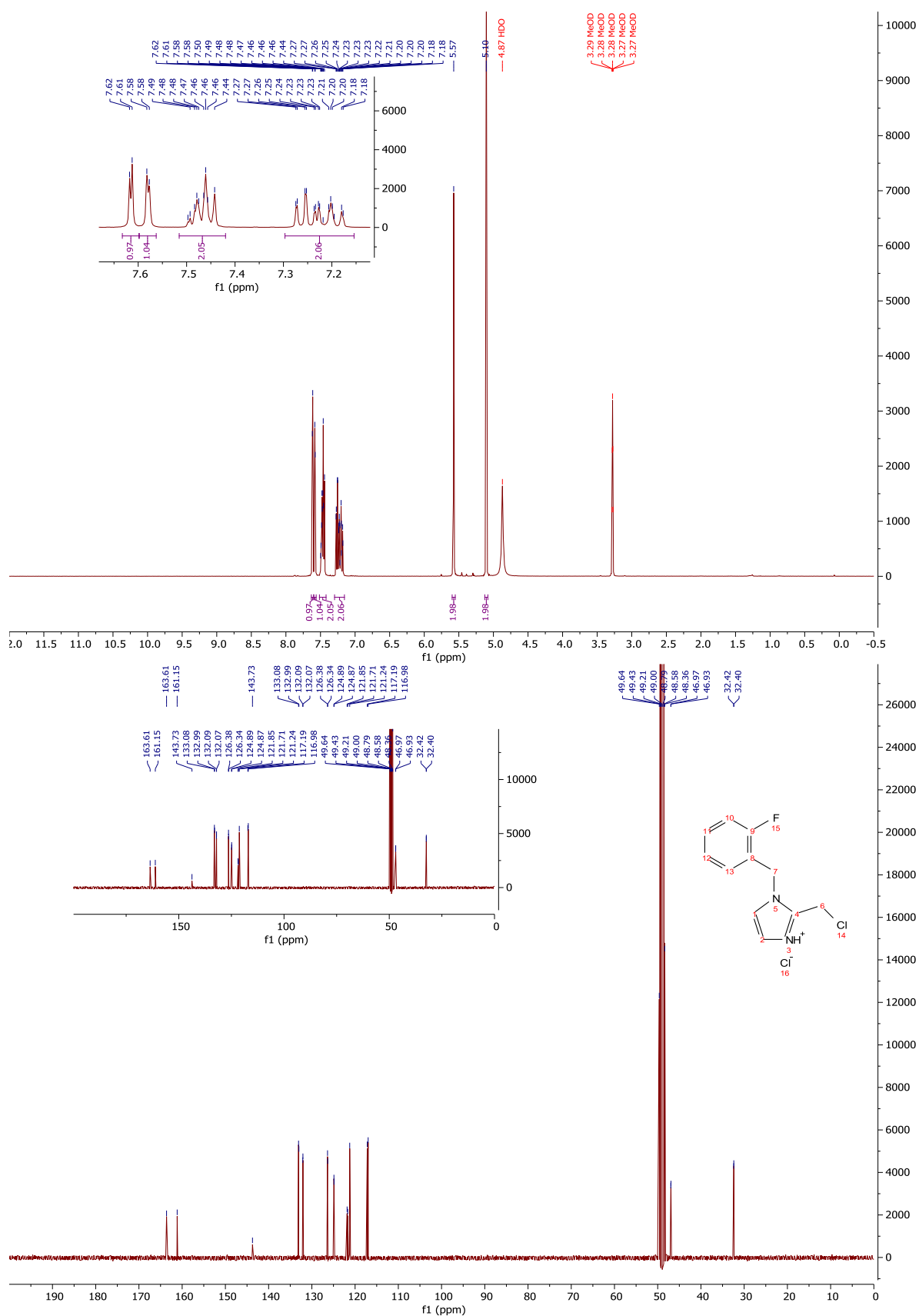
¹H-NMR and ¹³C-NMR: Compound 159



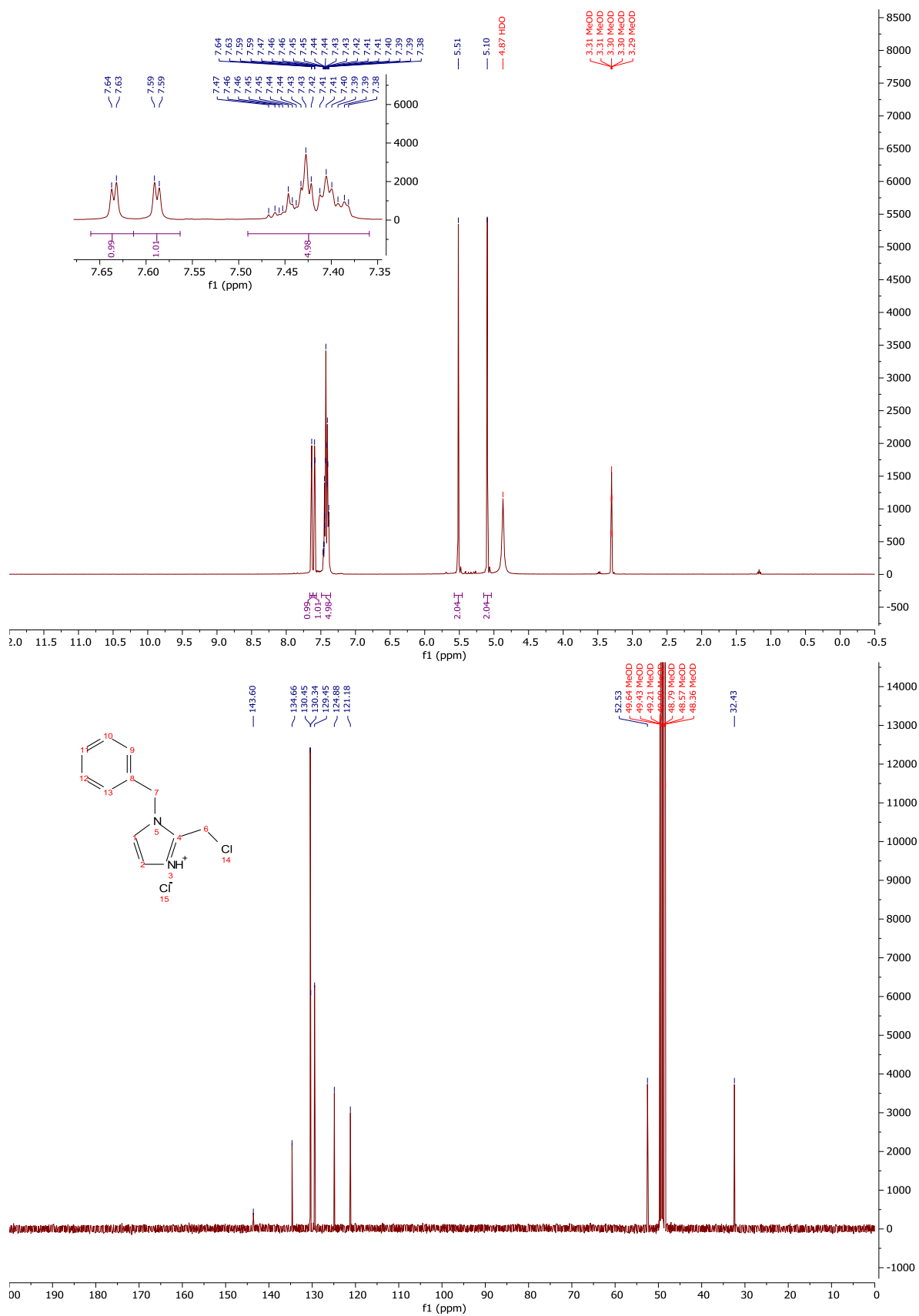
$^1\text{H-NMR}$ and $^{13}\text{C-NMR}$: Compound 167



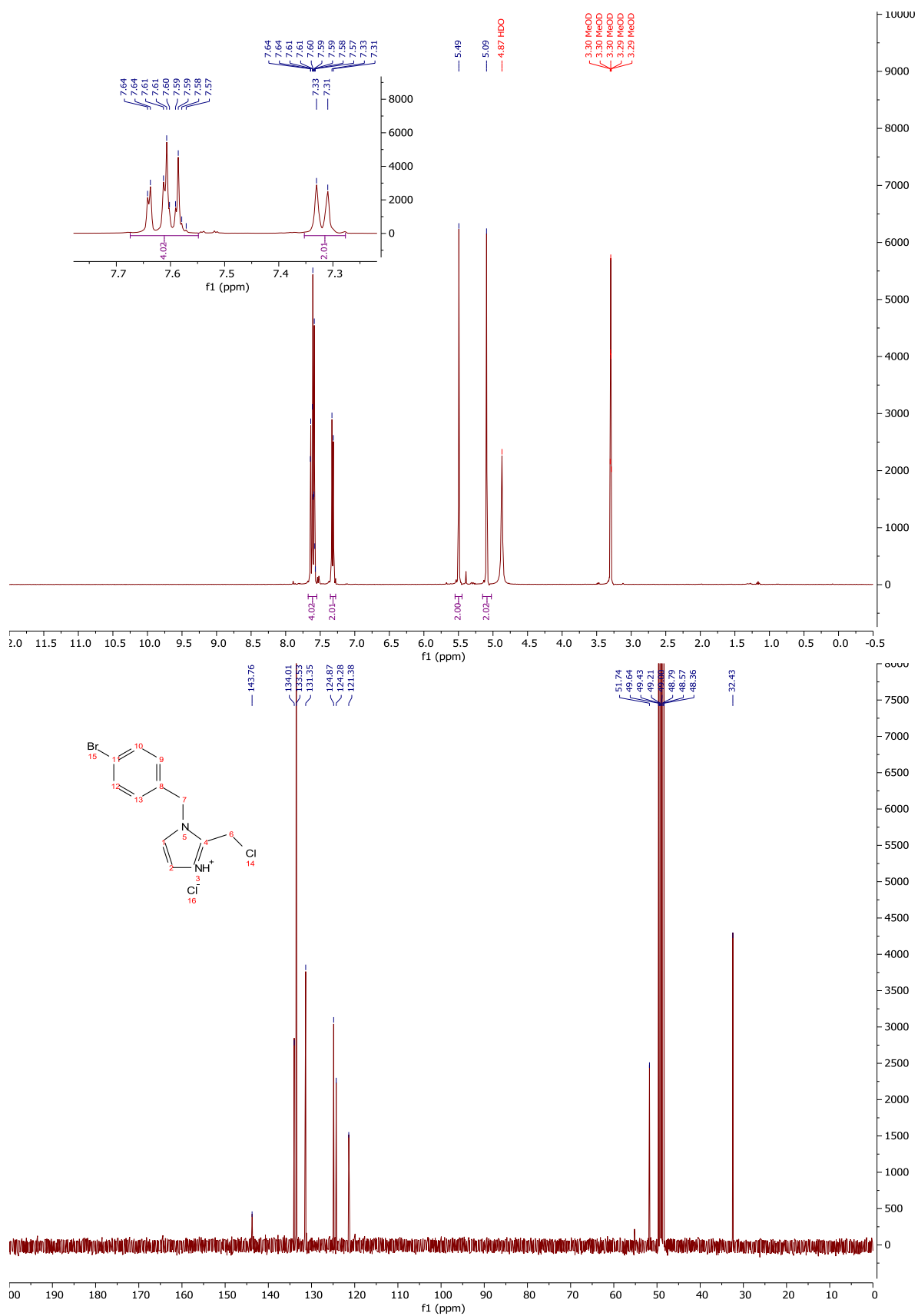
¹H-NMR and ¹³C-NMR: Compound 163



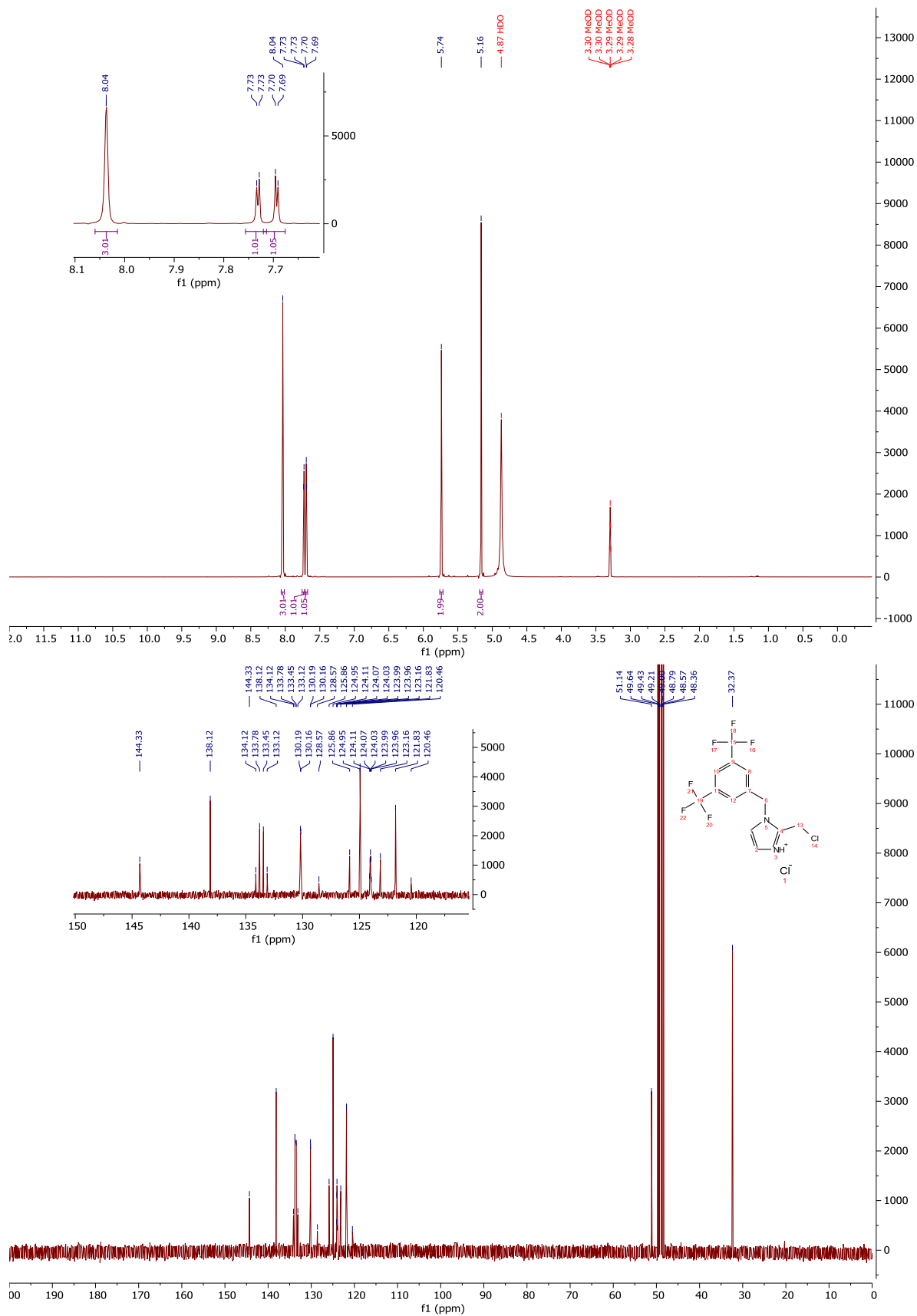
¹H-NMR and ¹³C-NMR: Compound 162



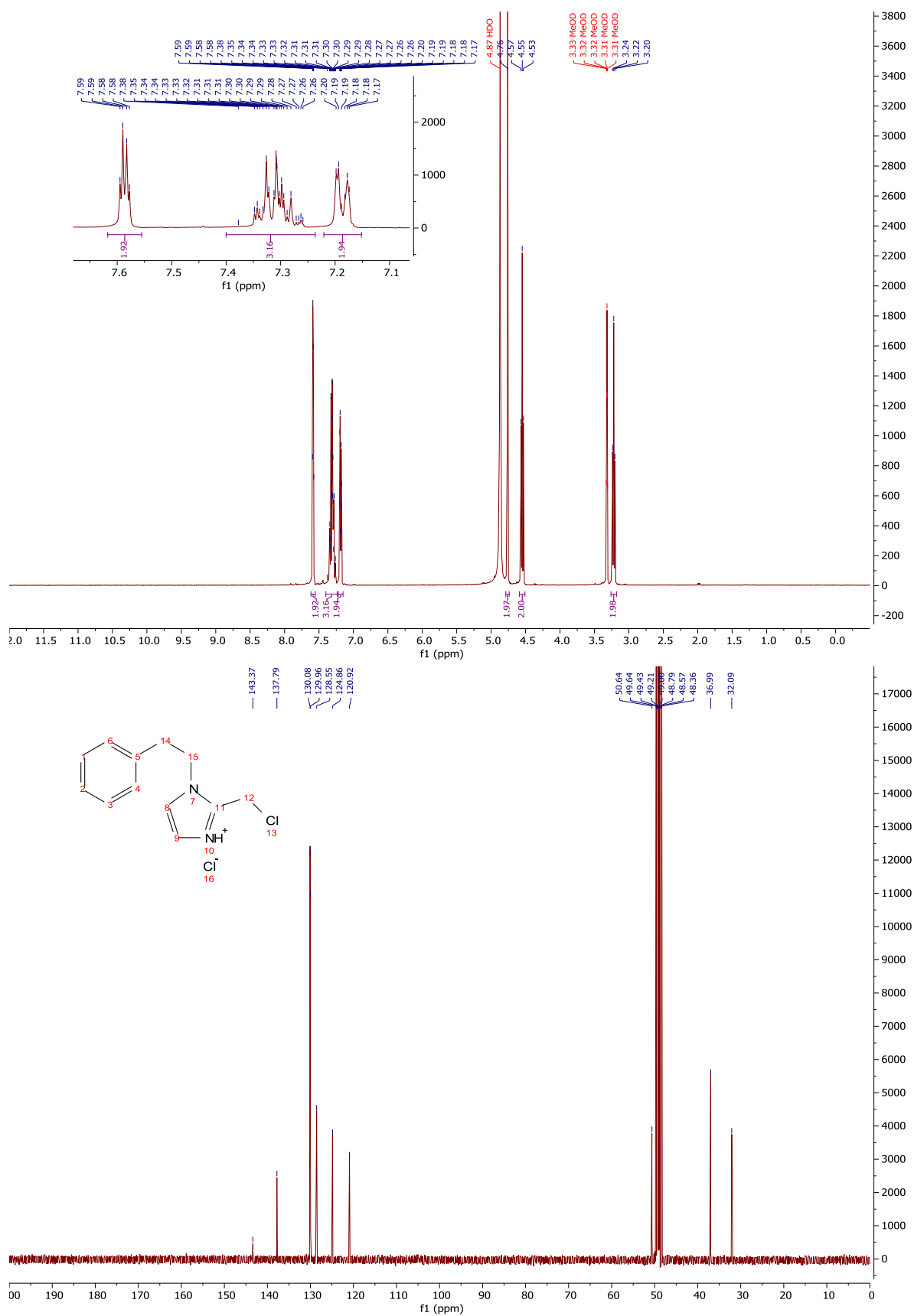
$^1\text{H-NMR}$ and $^{13}\text{C-NMR}$: Compound 164



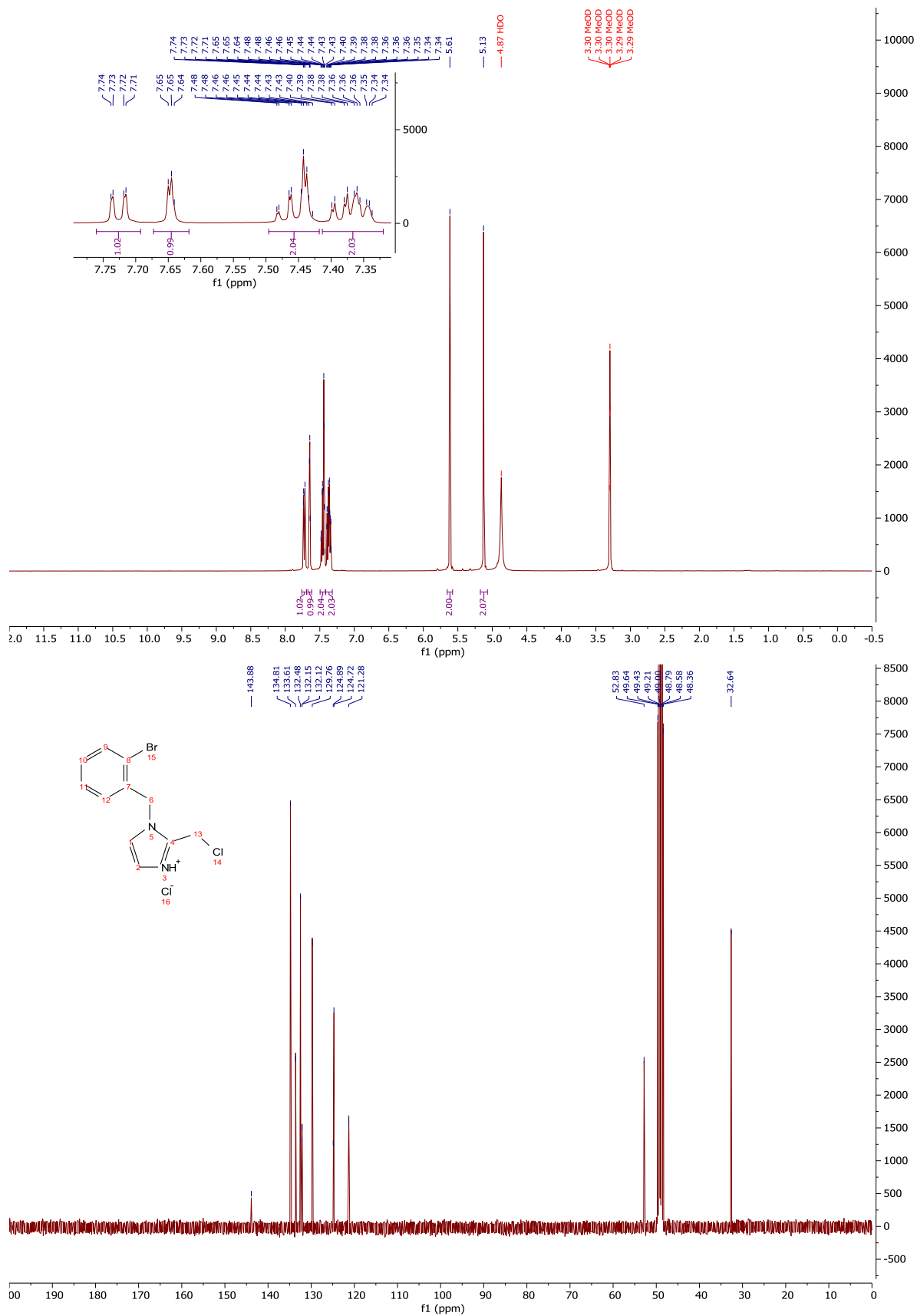
¹H-NMR and ¹³C-NMR: Compound 170



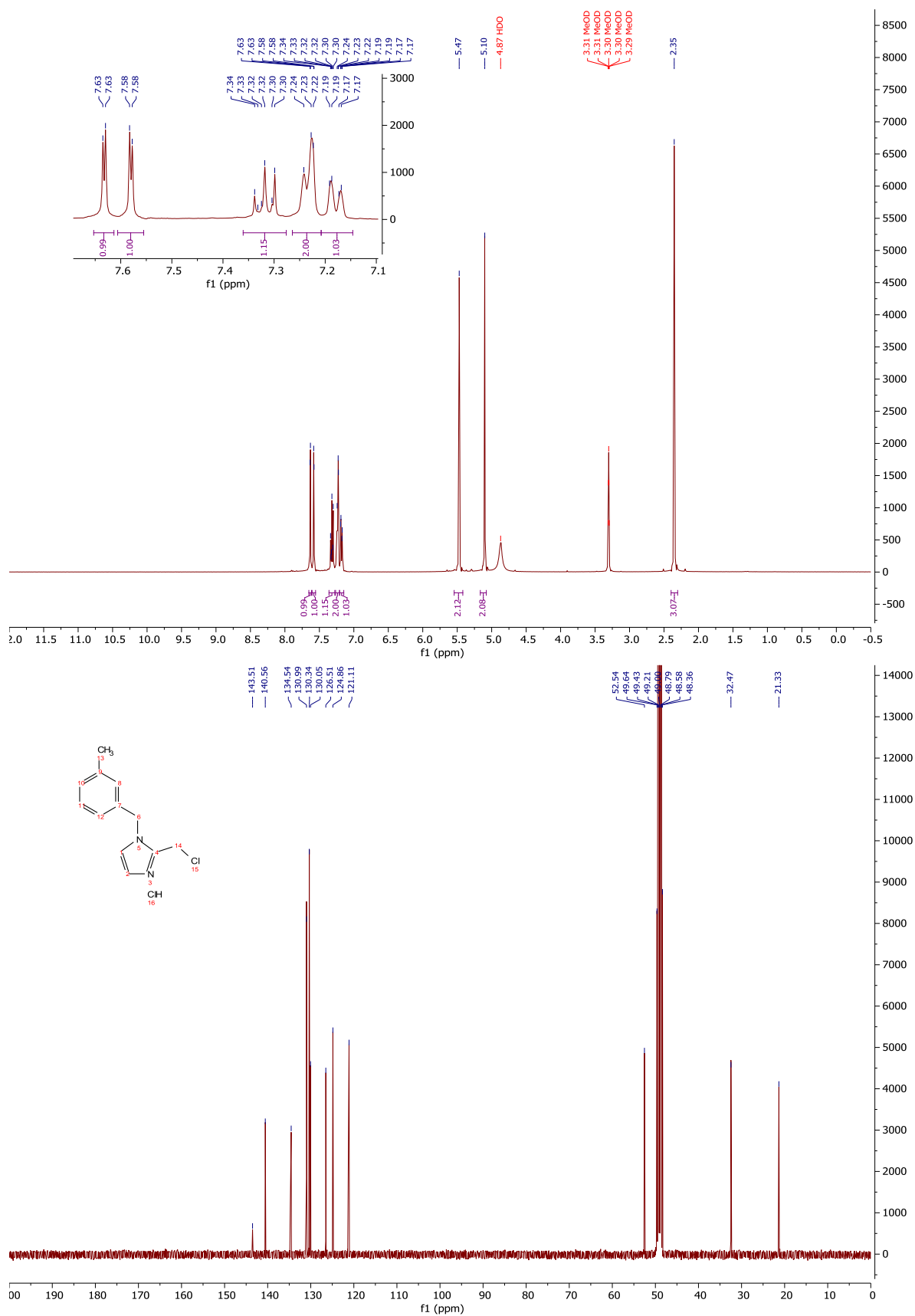
¹H-NMR and ¹³C-NMR: Compound 171



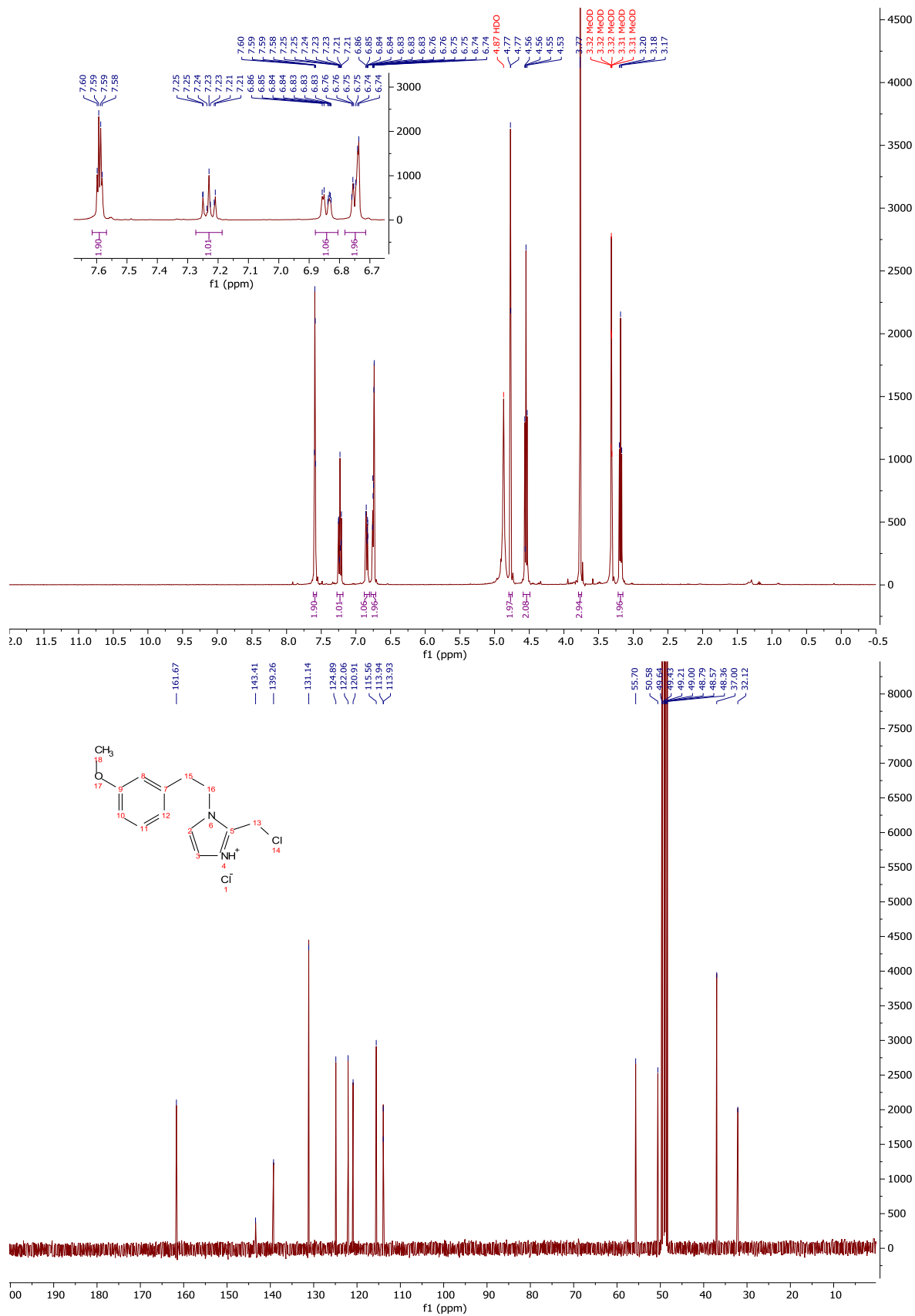
¹H-NMR and ¹³C-NMR: Compound 166



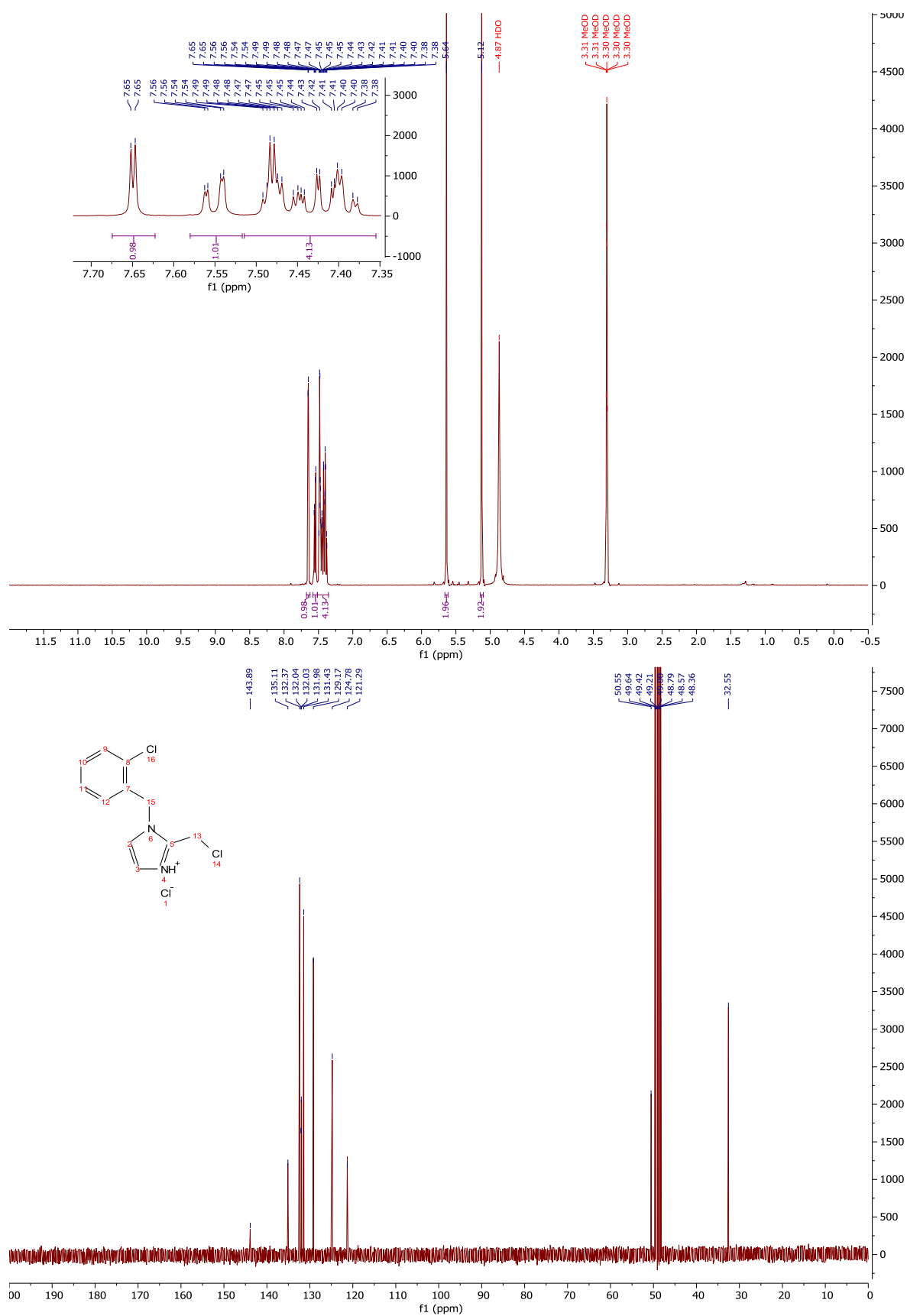
¹H-NMR and ¹³C-NMR: Compound 165



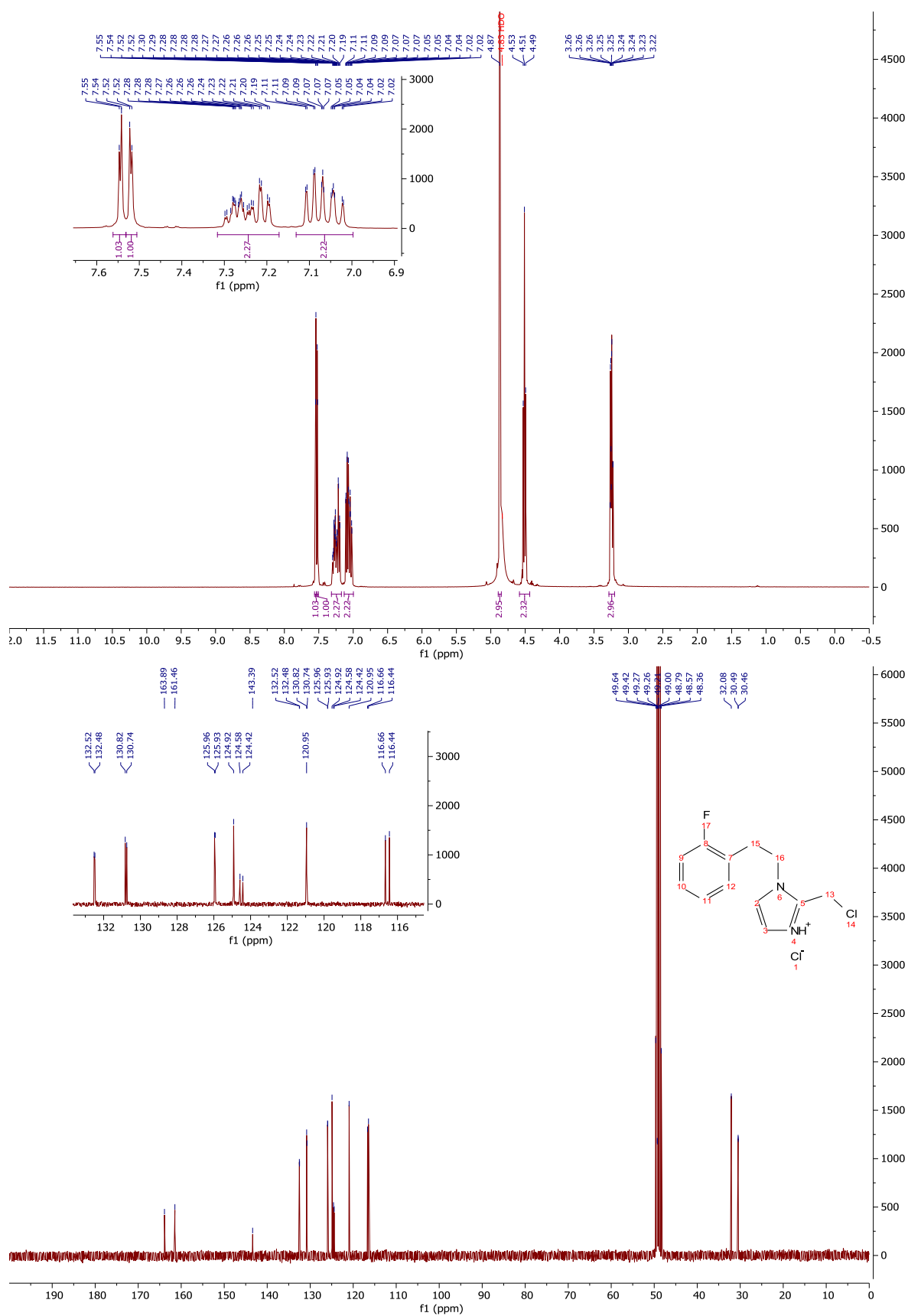
¹H-NMR and ¹³C-NMR: Compound 172



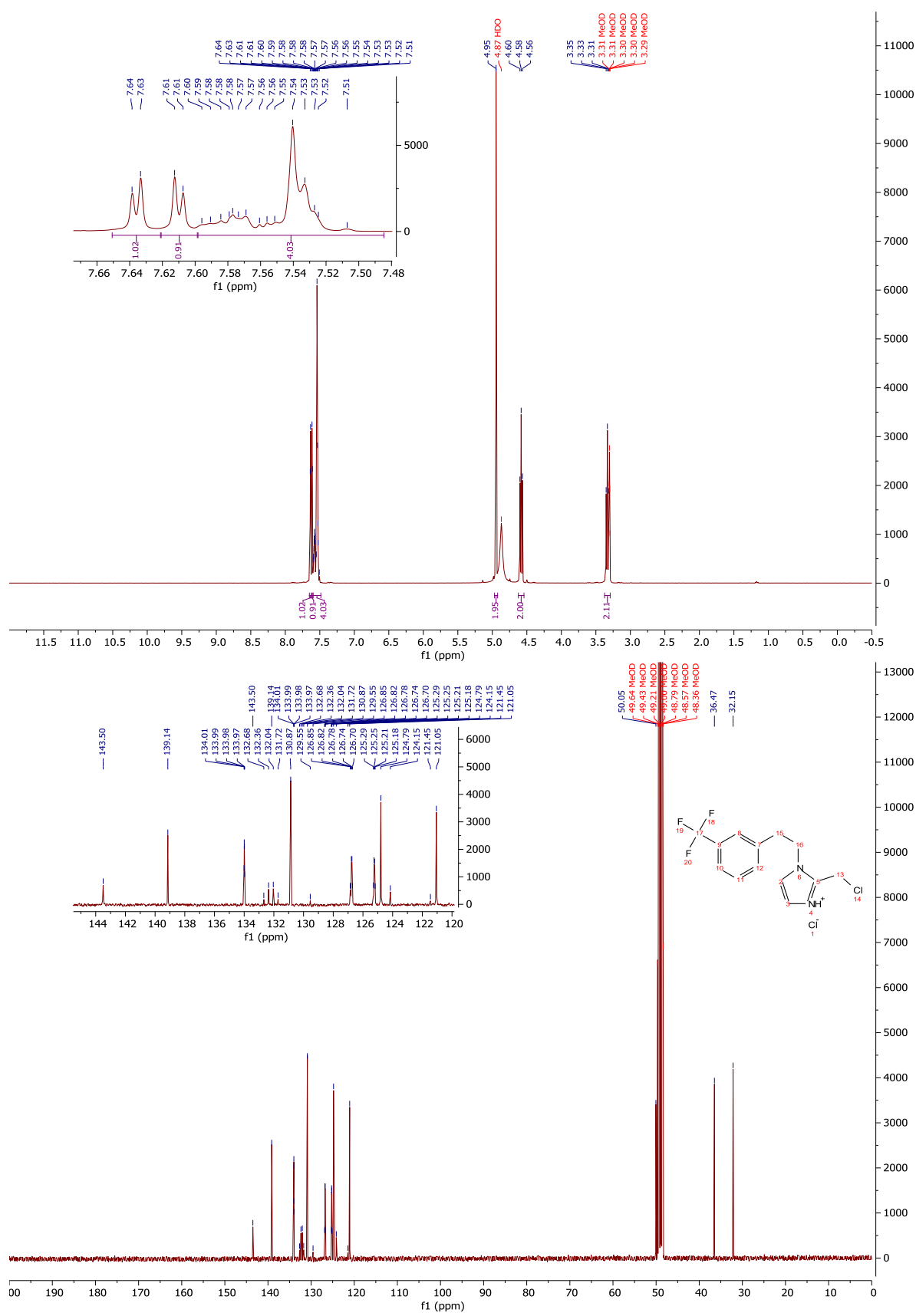
¹H-NMR and ¹³C-NMR: Compound 168



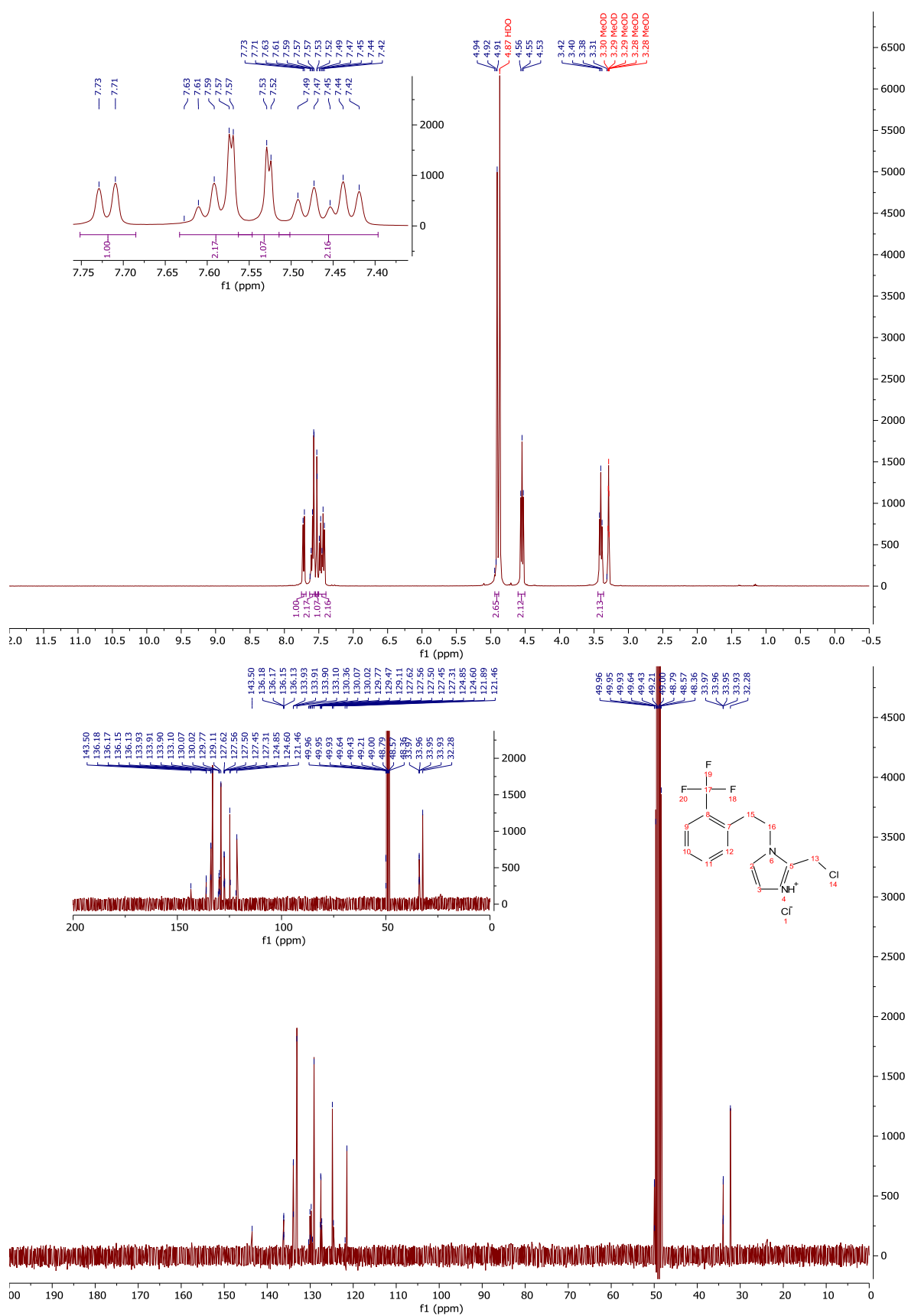
¹H-NMR and ¹³C-NMR: Compound 173



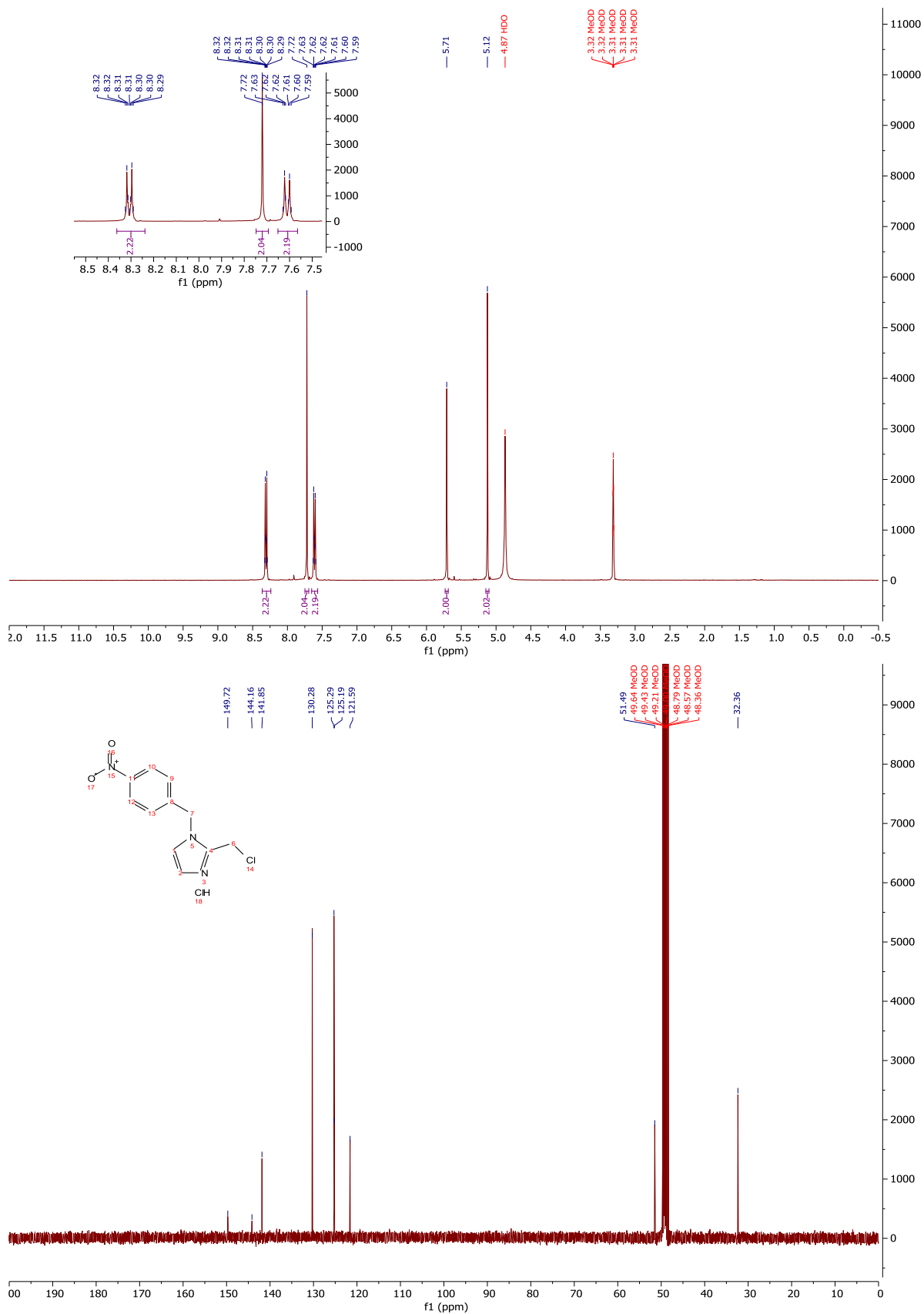
¹H-NMR and ¹³C-NMR: Compound 176



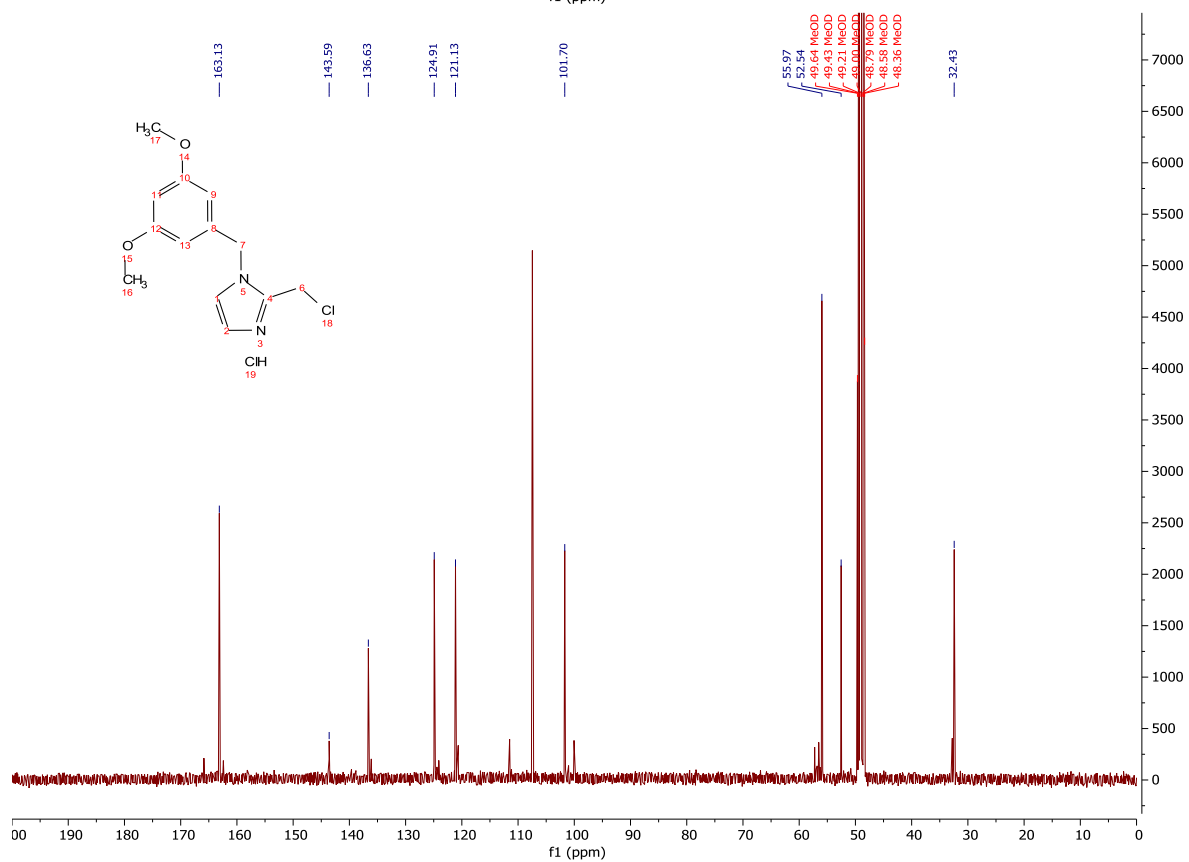
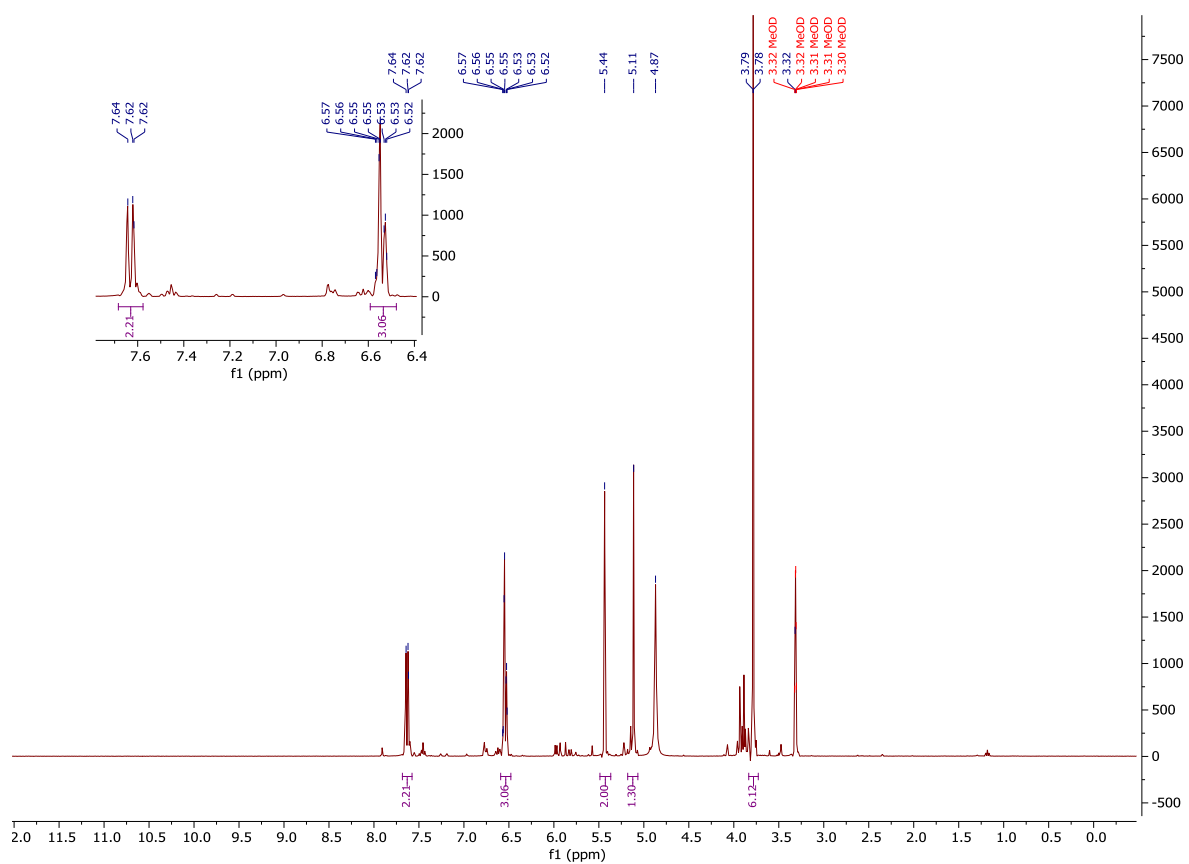
¹H-NMR and ¹³C-NMR: Compound 175



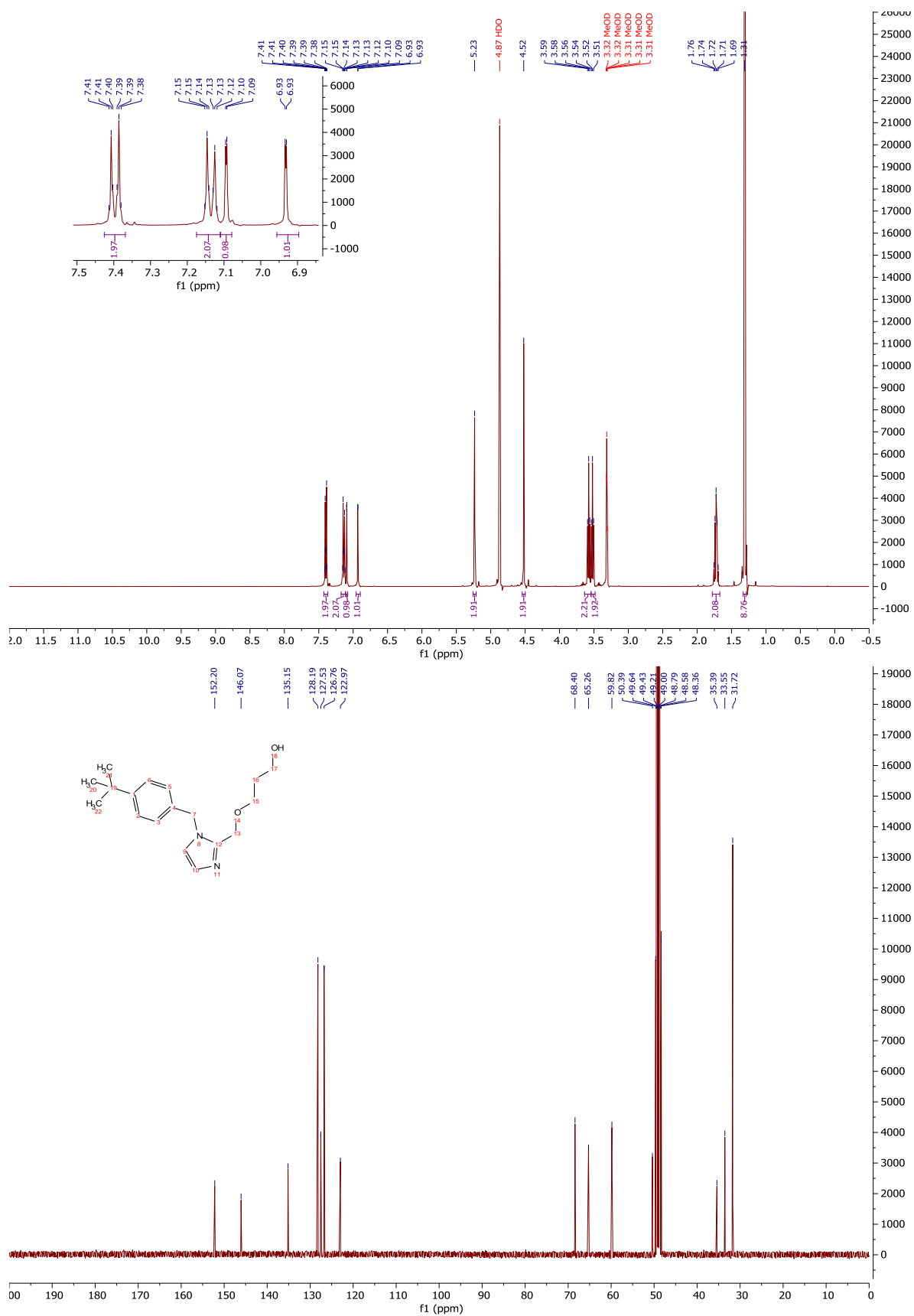
¹H-NMR and ¹³C-NMR: Compound 177



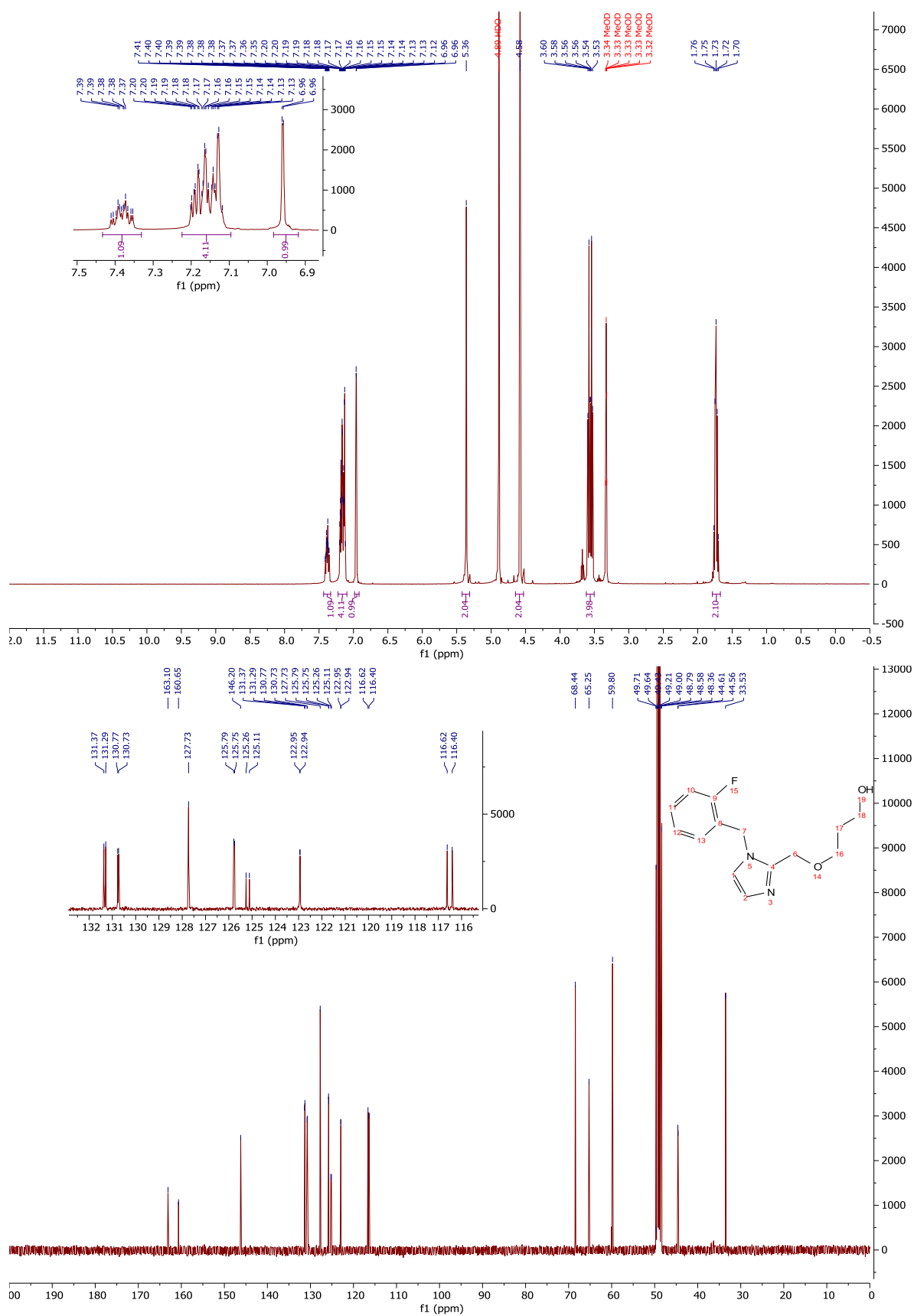
$^1\text{H-NMR}$ and $^{13}\text{C-NMR}$: Compound 169



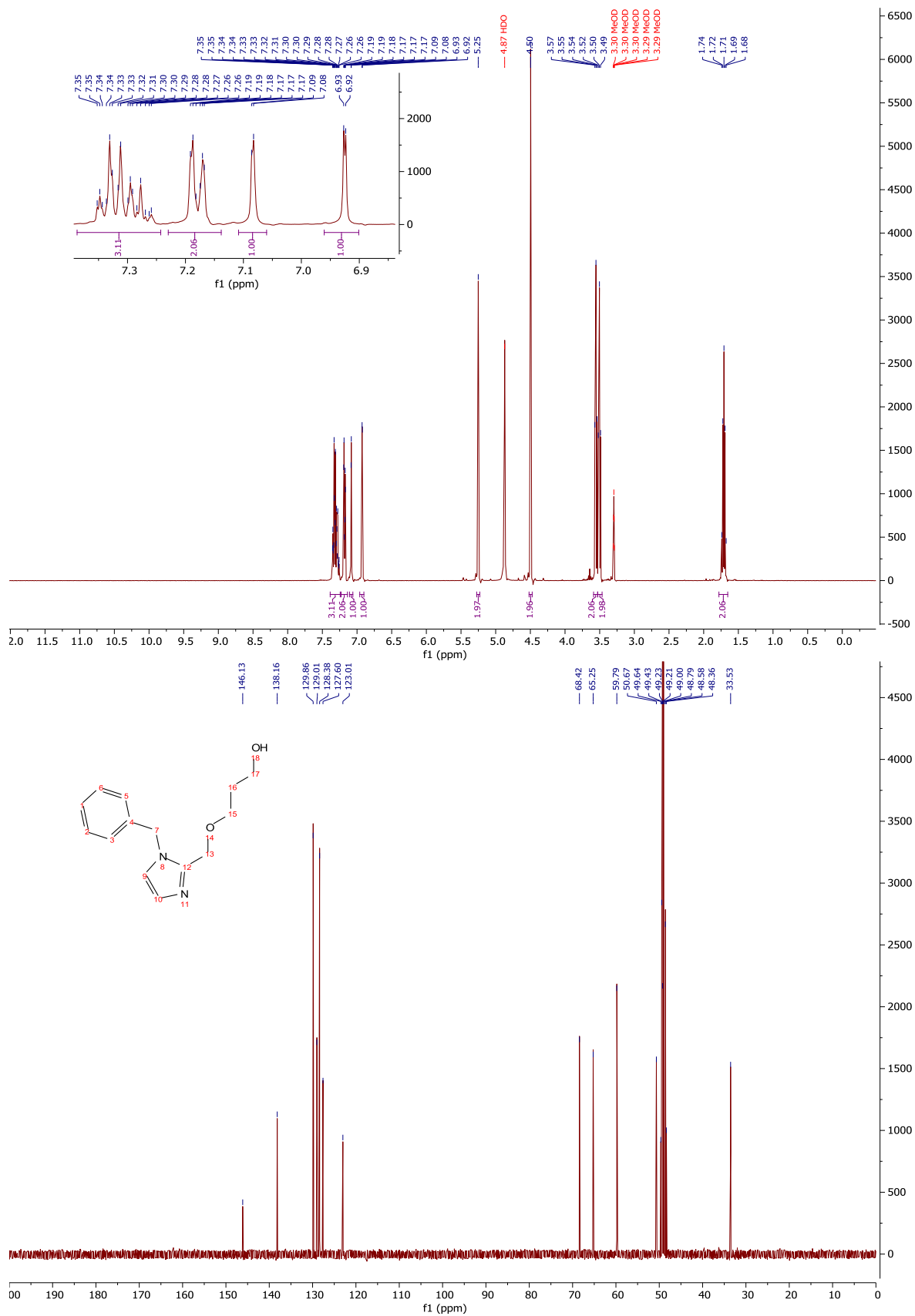
¹H-NMR and ¹³C-NMR: Compound 184



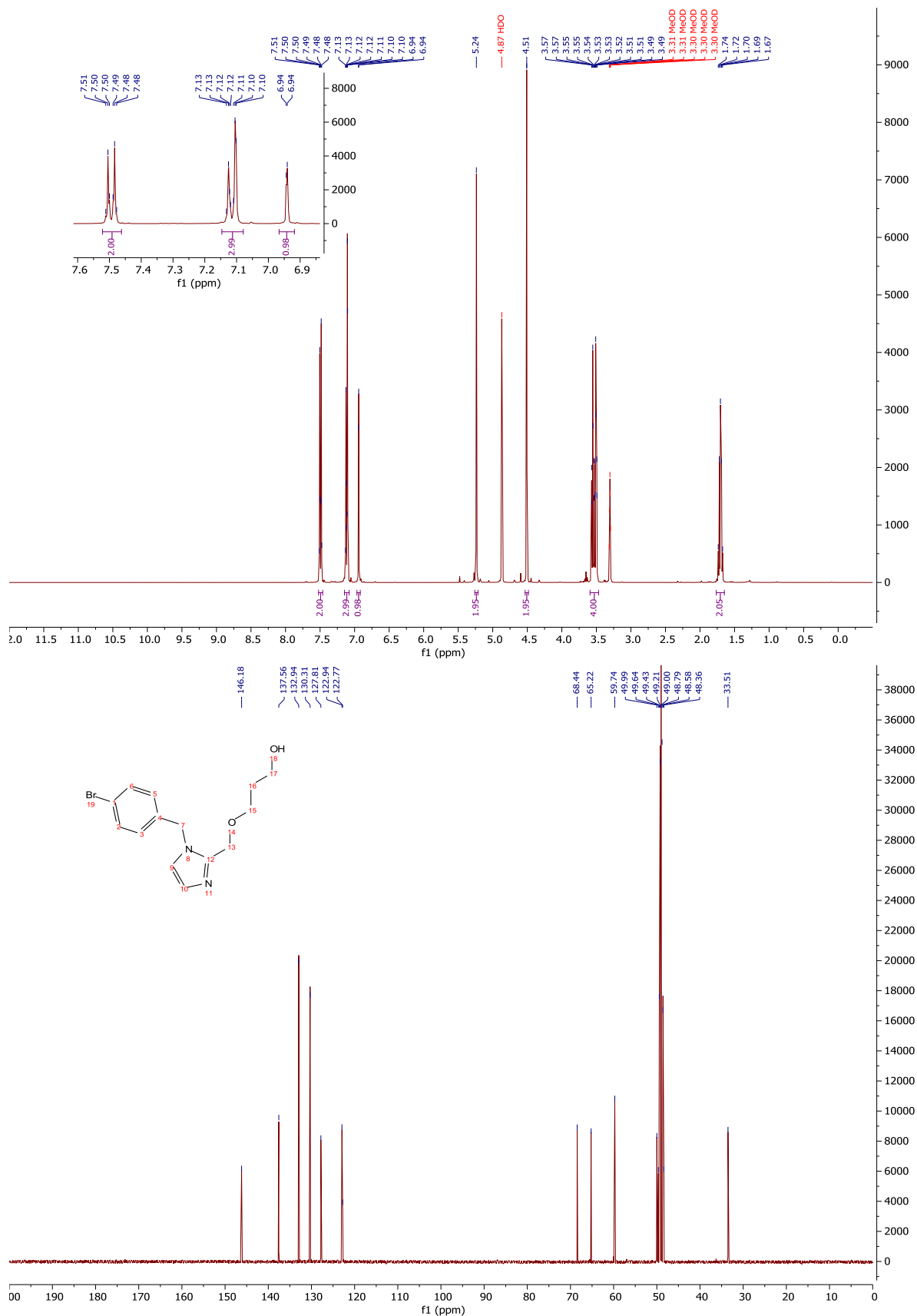
¹H-NMR and ¹³C-NMR: Compound 179



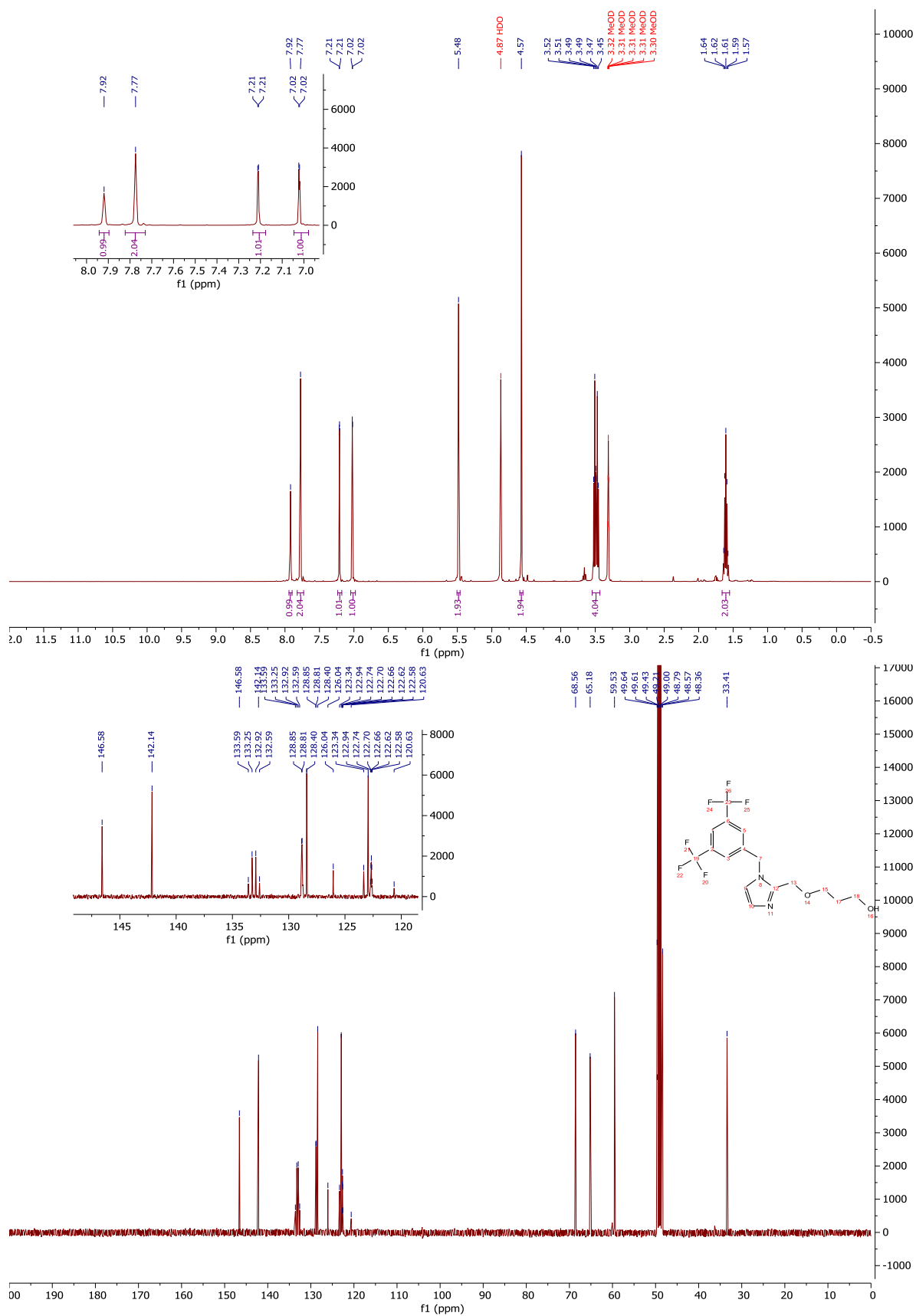
¹H-NMR and ¹³C-NMR: Compound 161



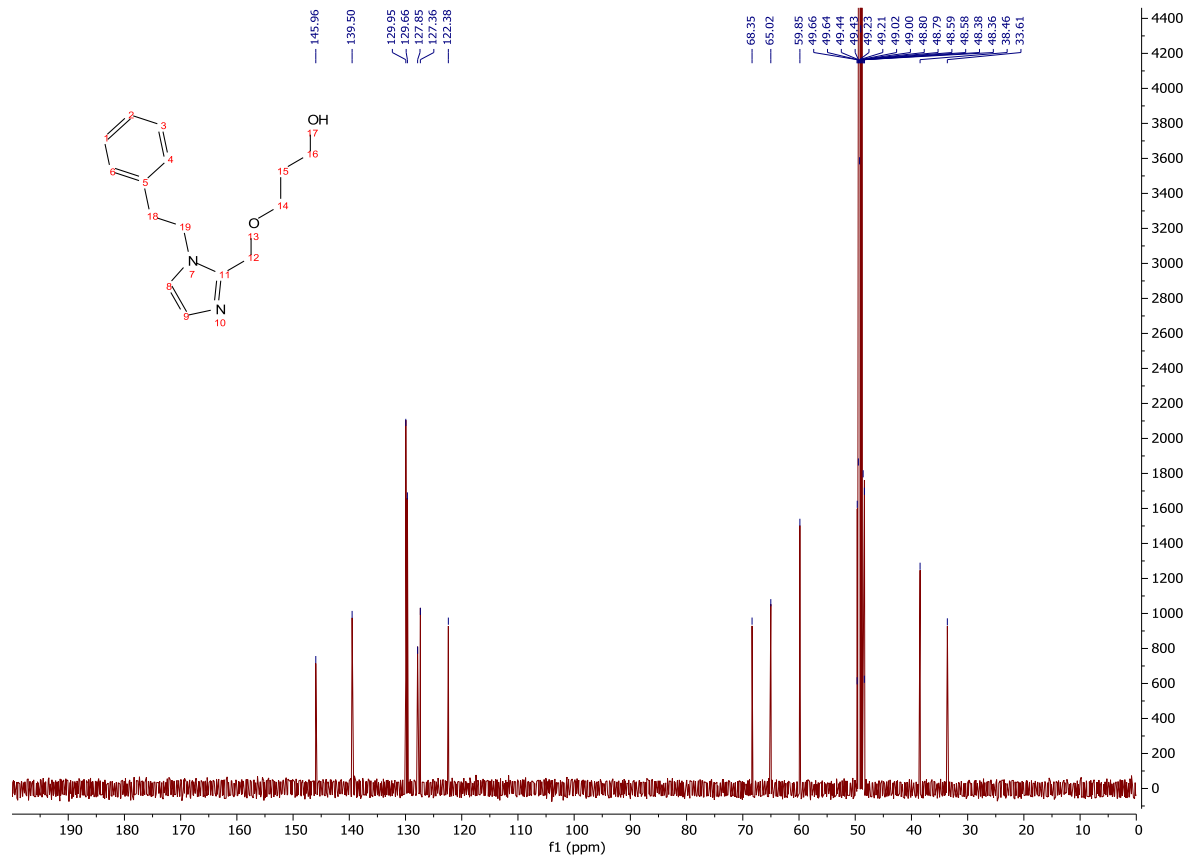
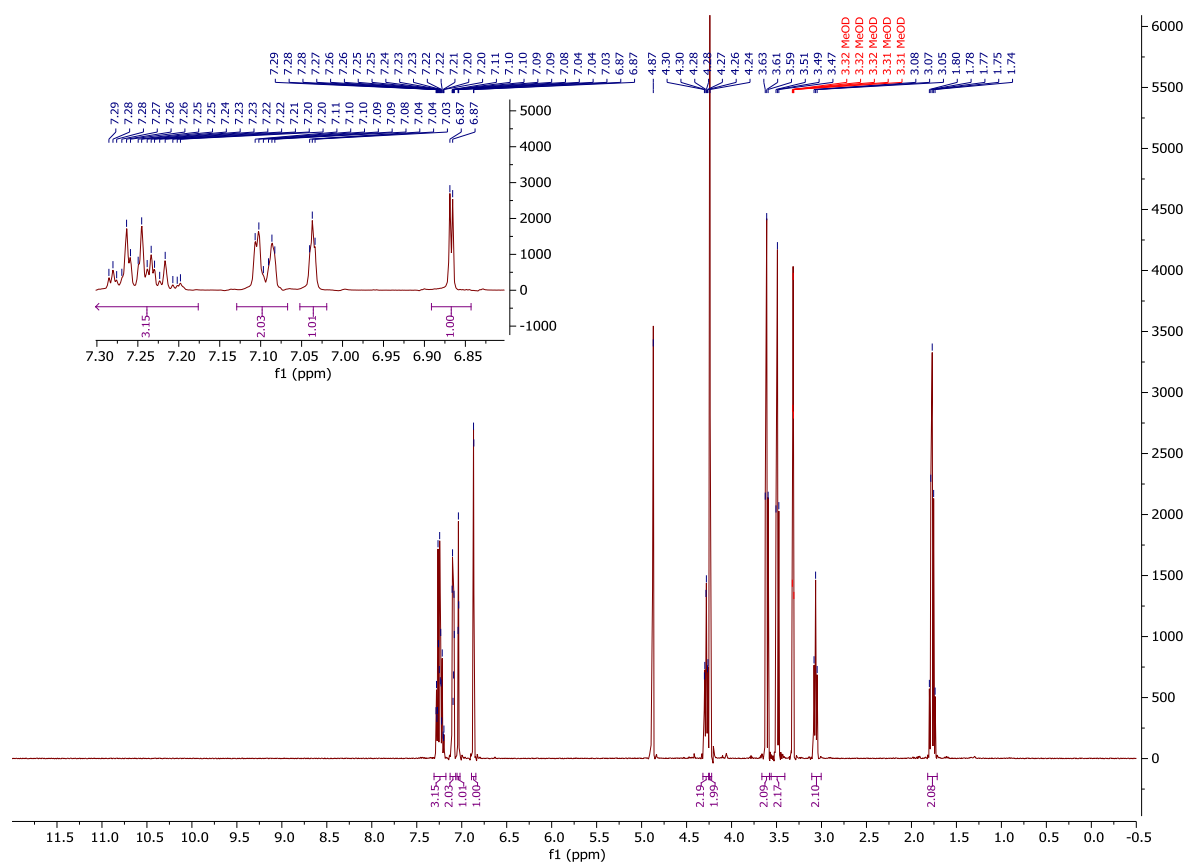
$^1\text{H-NMR}$ and $^{13}\text{C-NMR}$: Compound 186



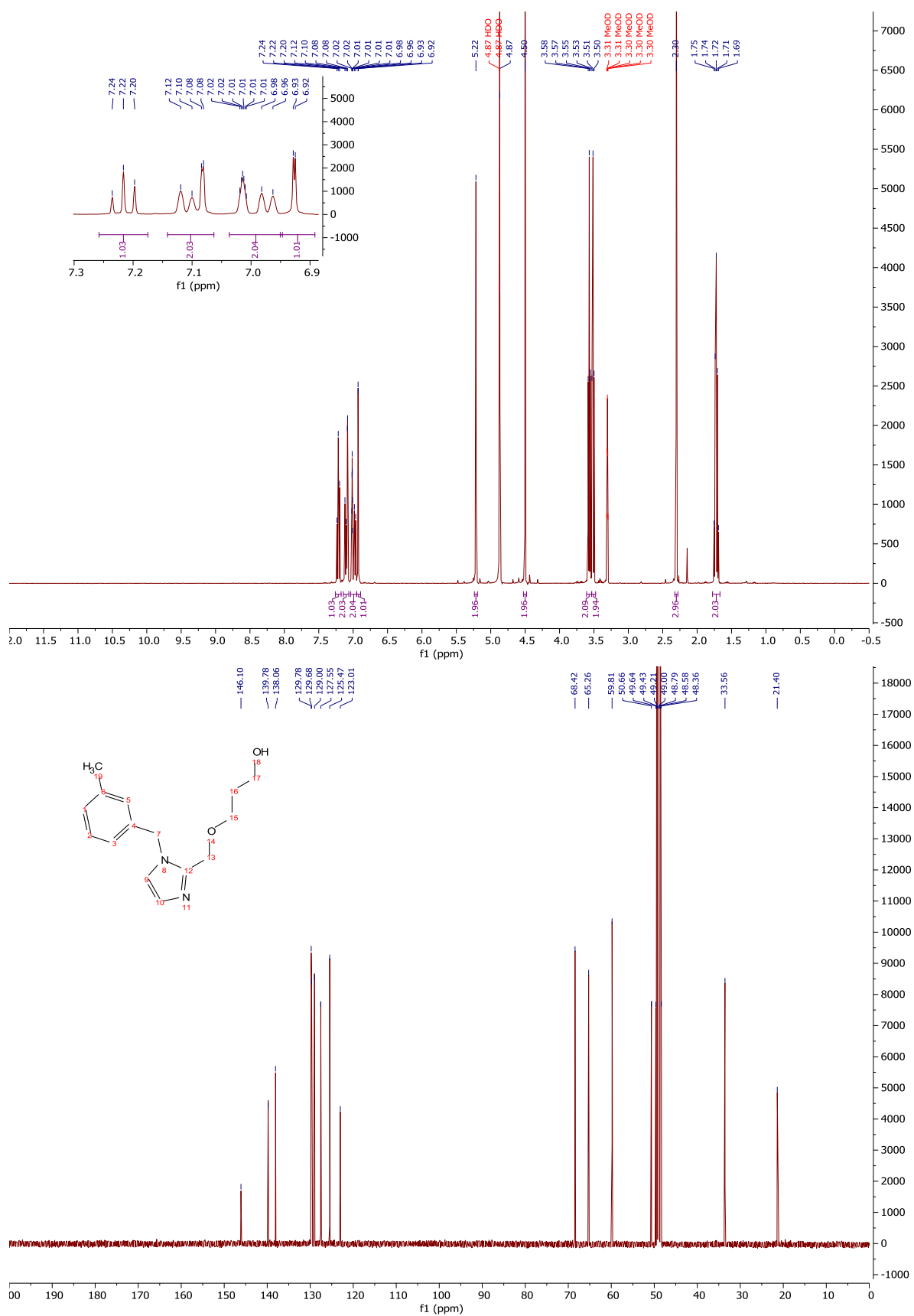
¹H-NMR and ¹³C-NMR: Compound 194



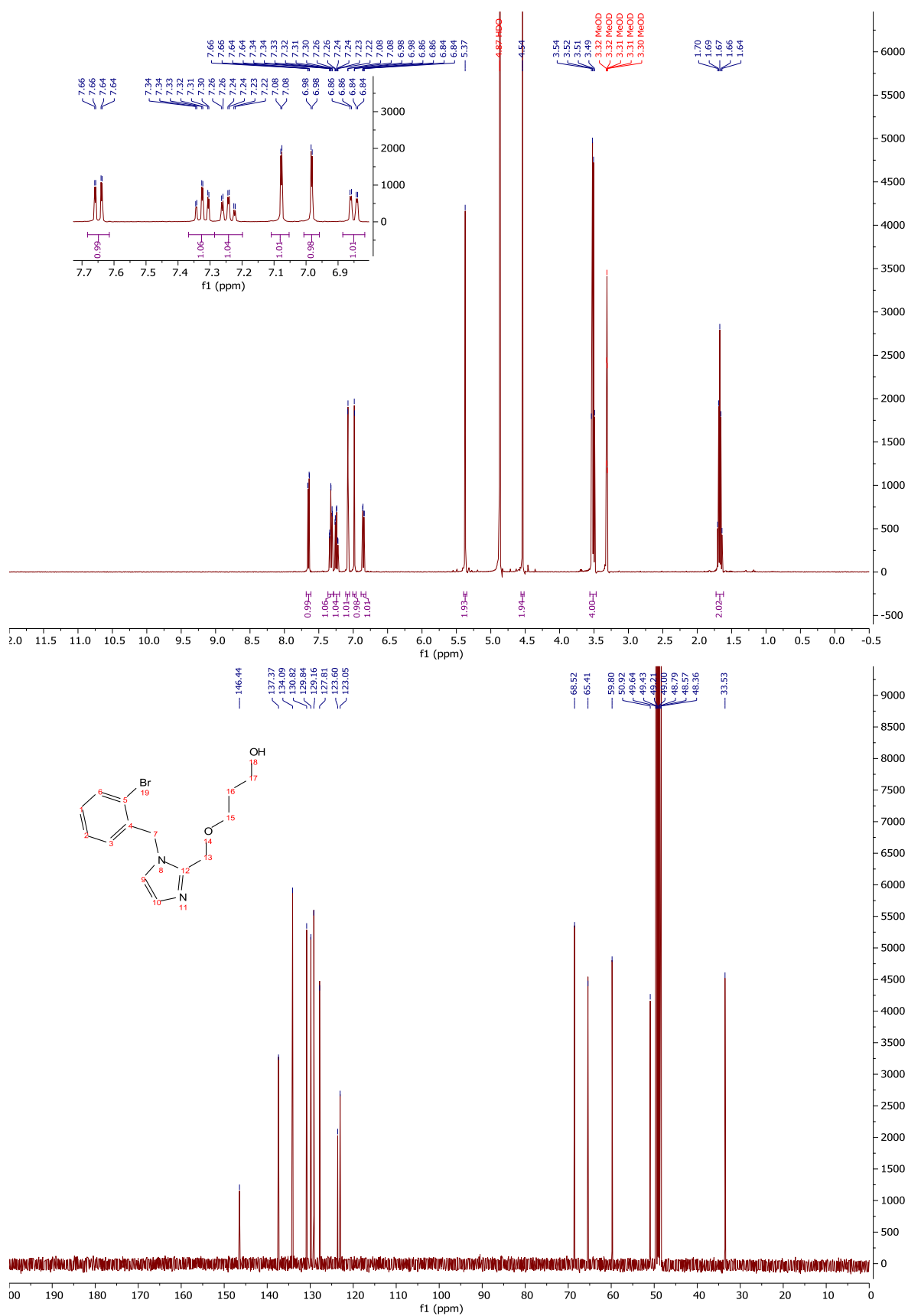
¹H-NMR and ¹³C-NMR: Compound 198



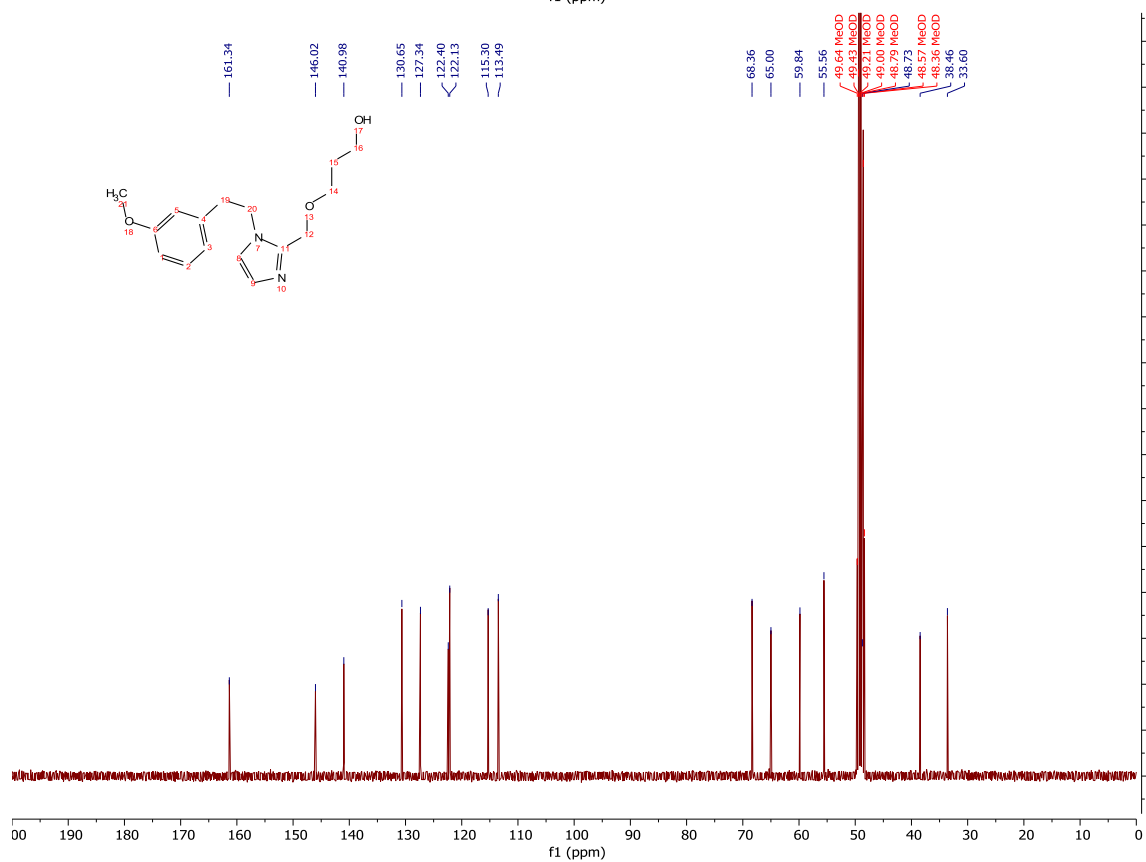
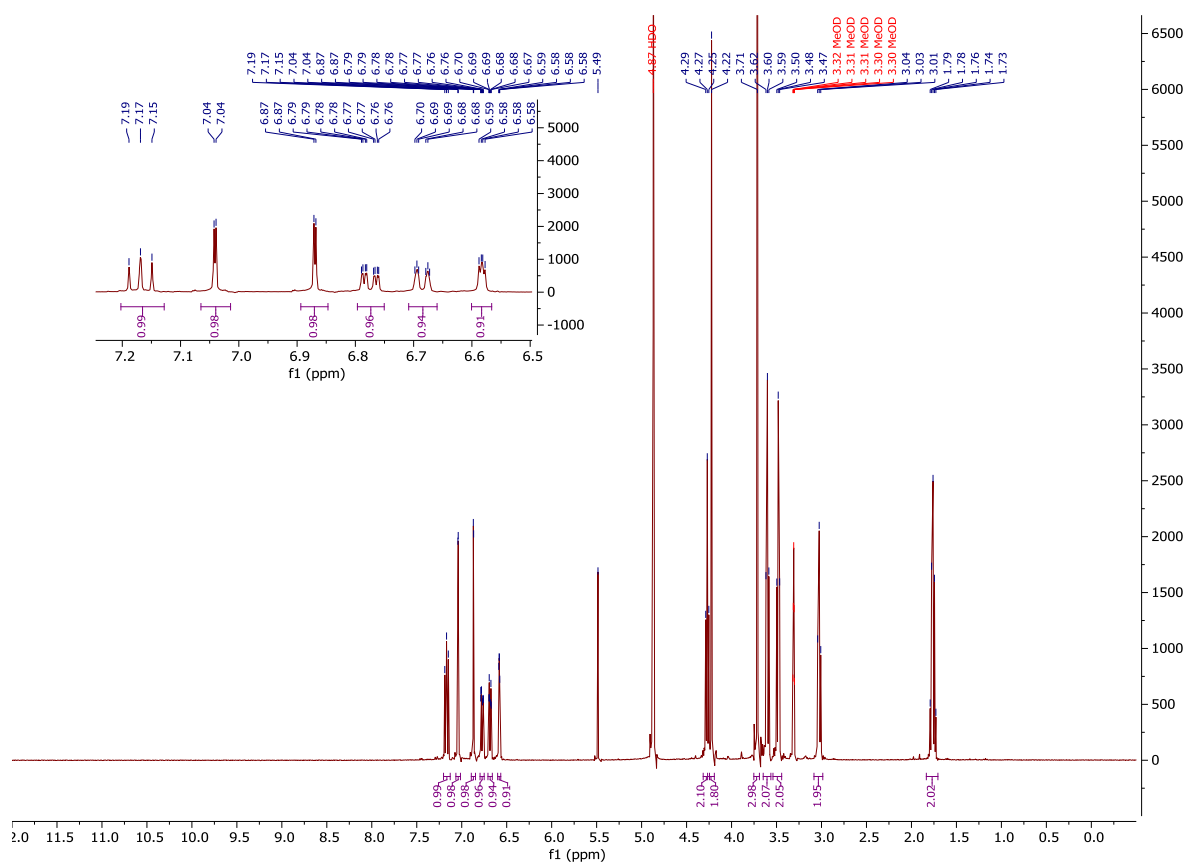
¹H-NMR and ¹³C-NMR: Compound 188



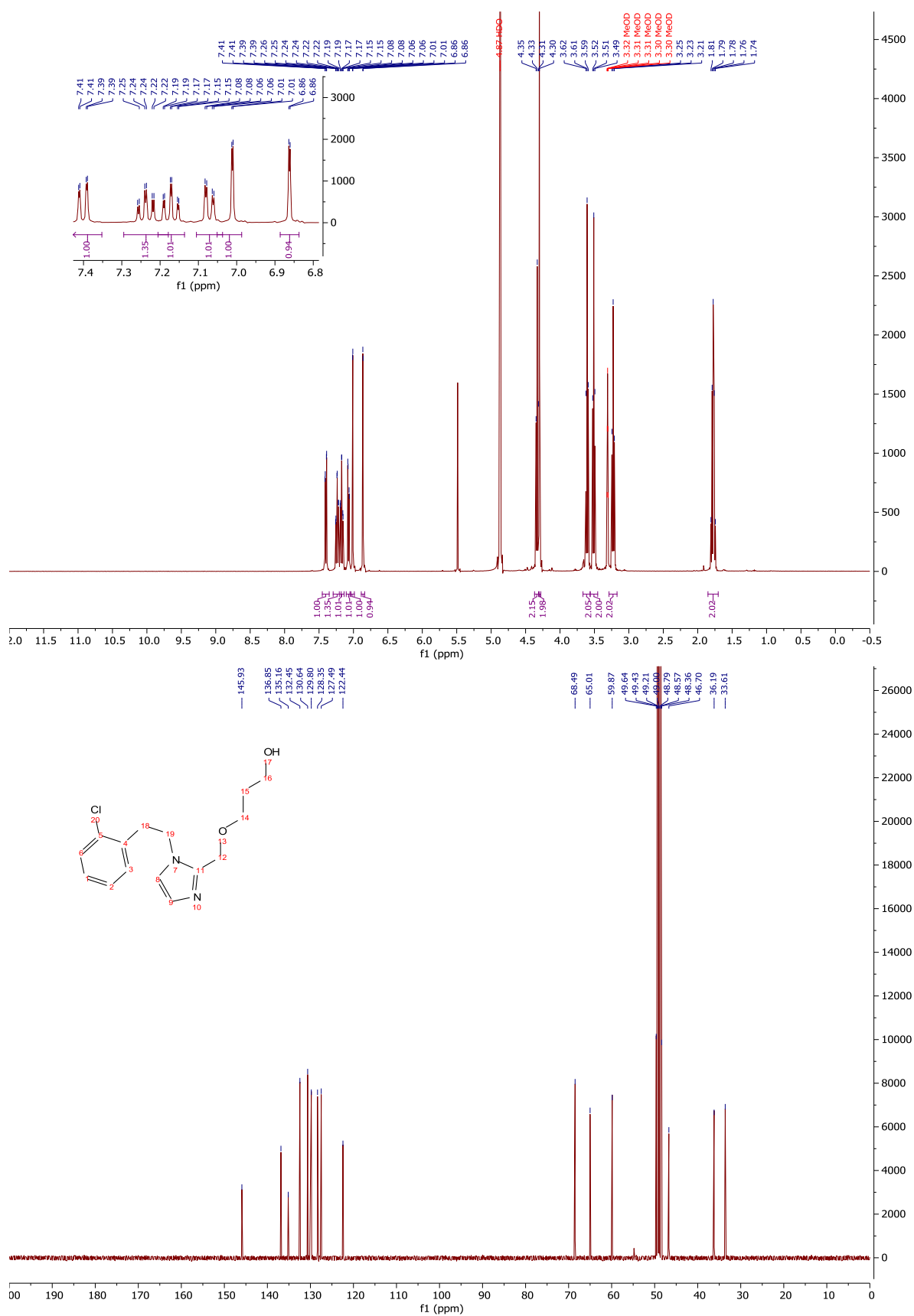
¹H-NMR and ¹³C-NMR: Compound 190



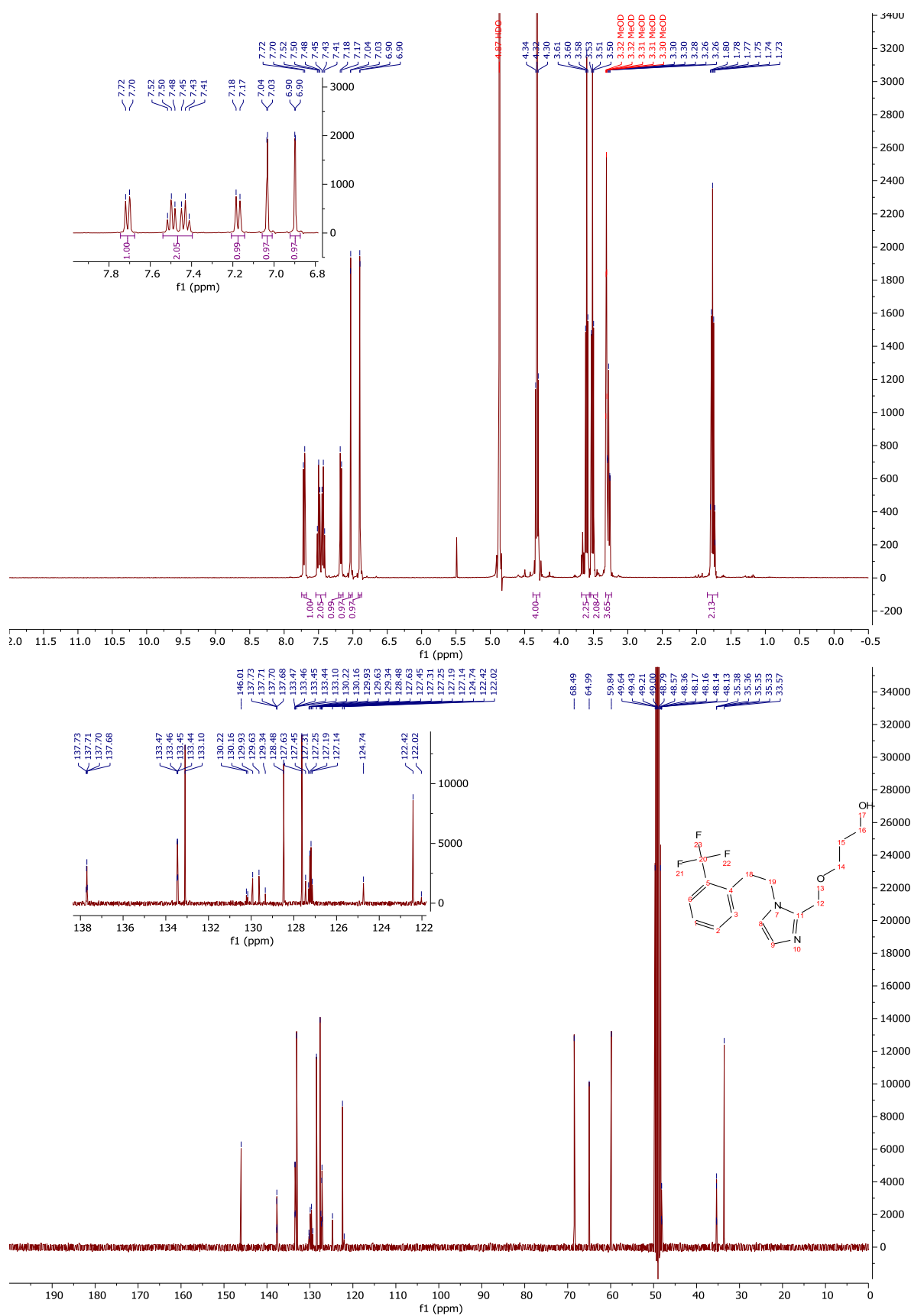
¹H-NMR and ¹³C-NMR: Compound 200



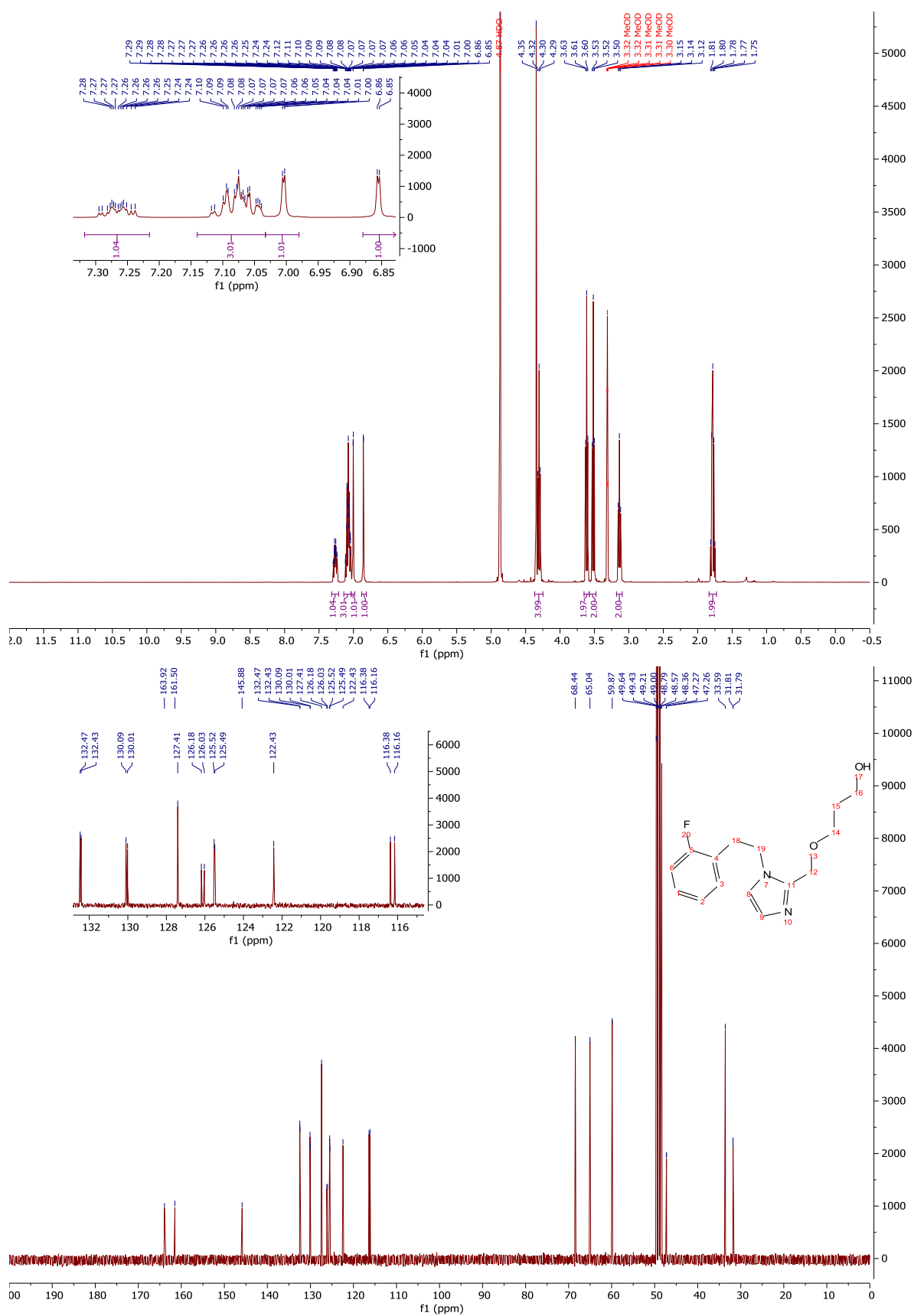
¹H-NMR and ¹³C-NMR: Compound 204



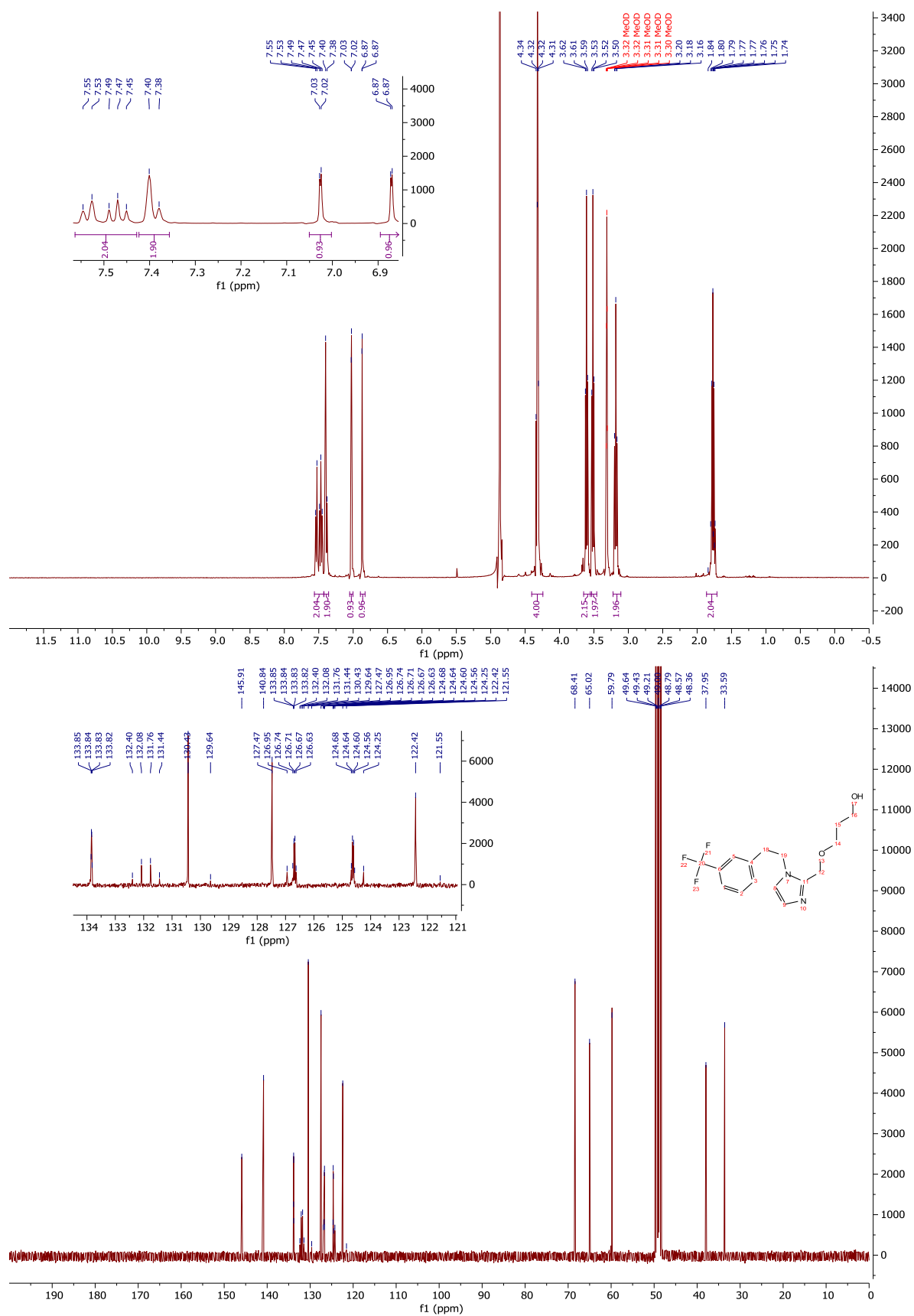
$^1\text{H-NMR}$ and $^{13}\text{C-NMR}$: Compound 206



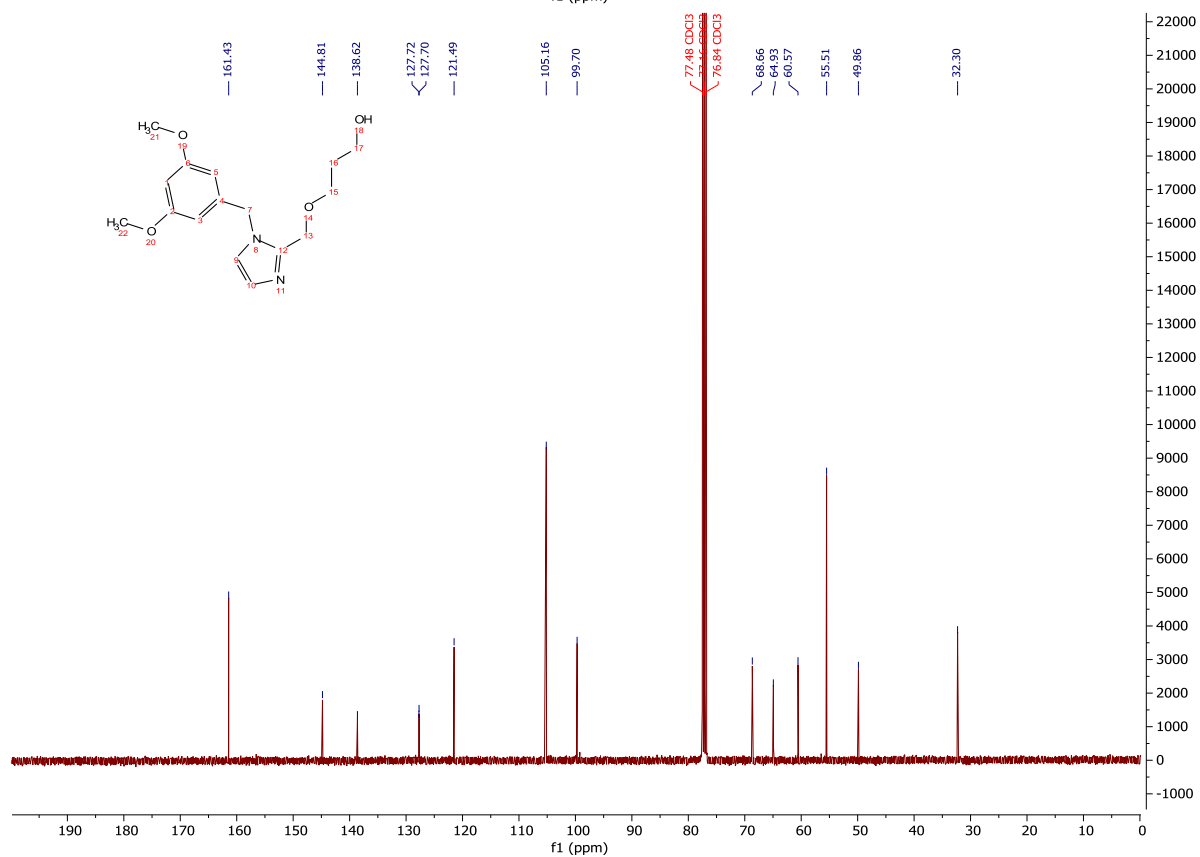
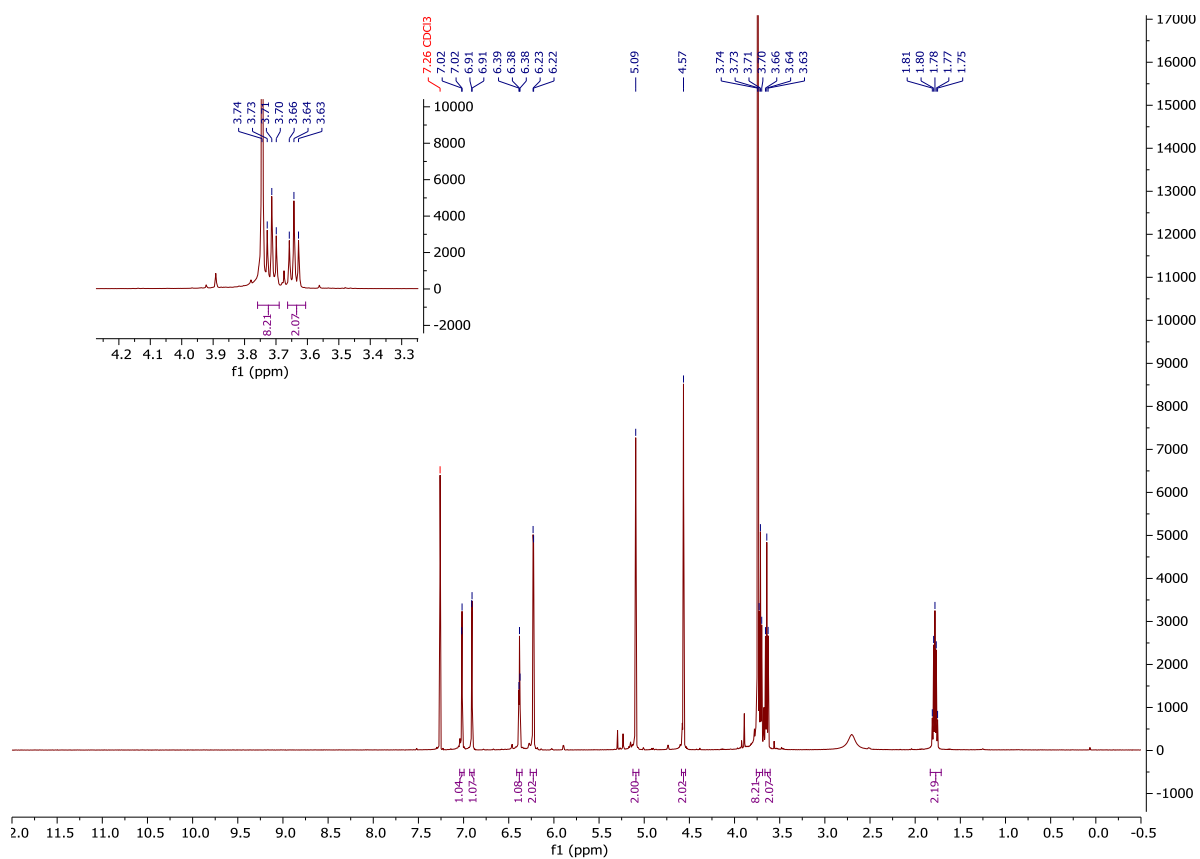
¹H-NMR and ¹³C-NMR: Compound 202



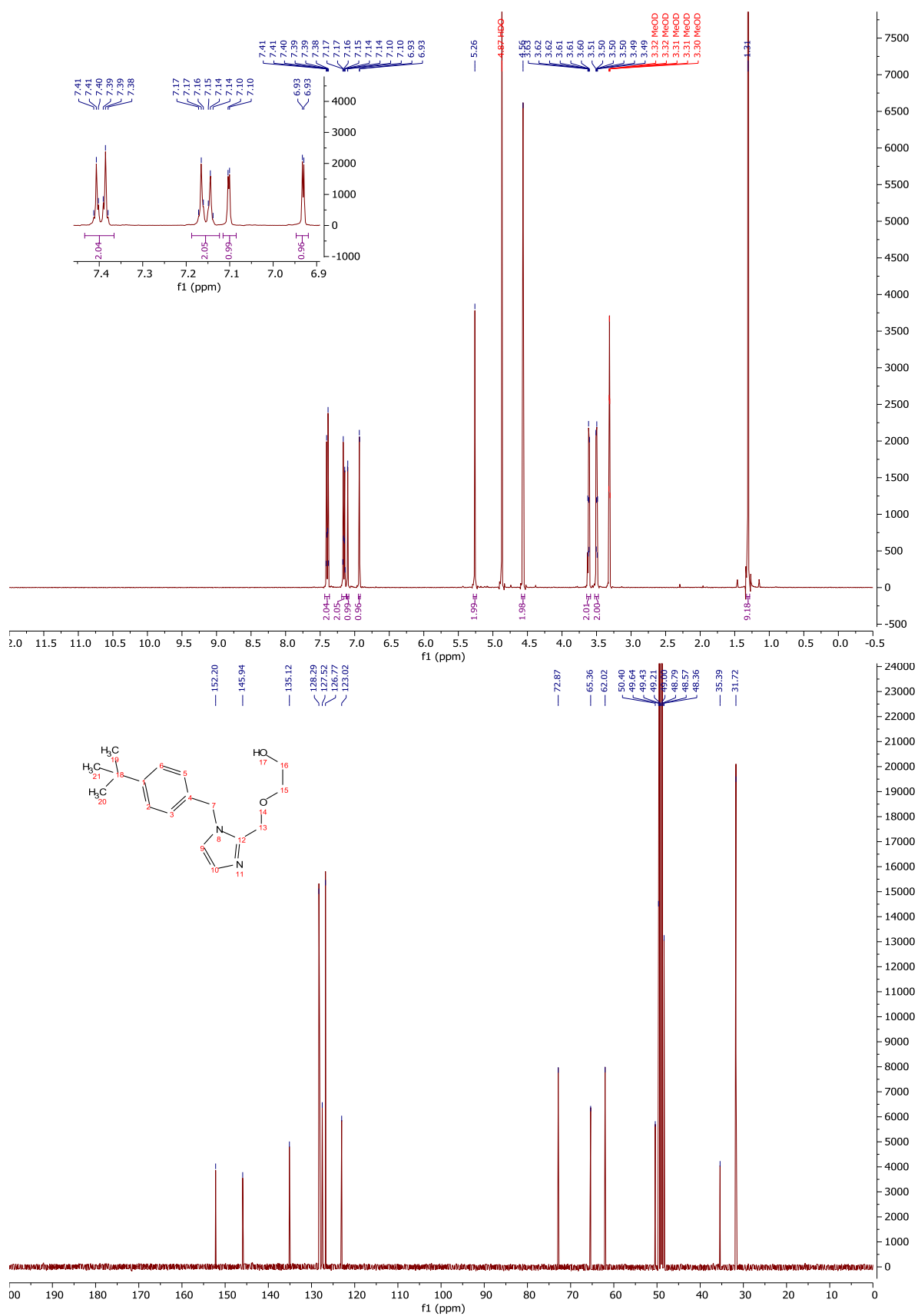
¹H-NMR and ¹³C-NMR: Compound 196



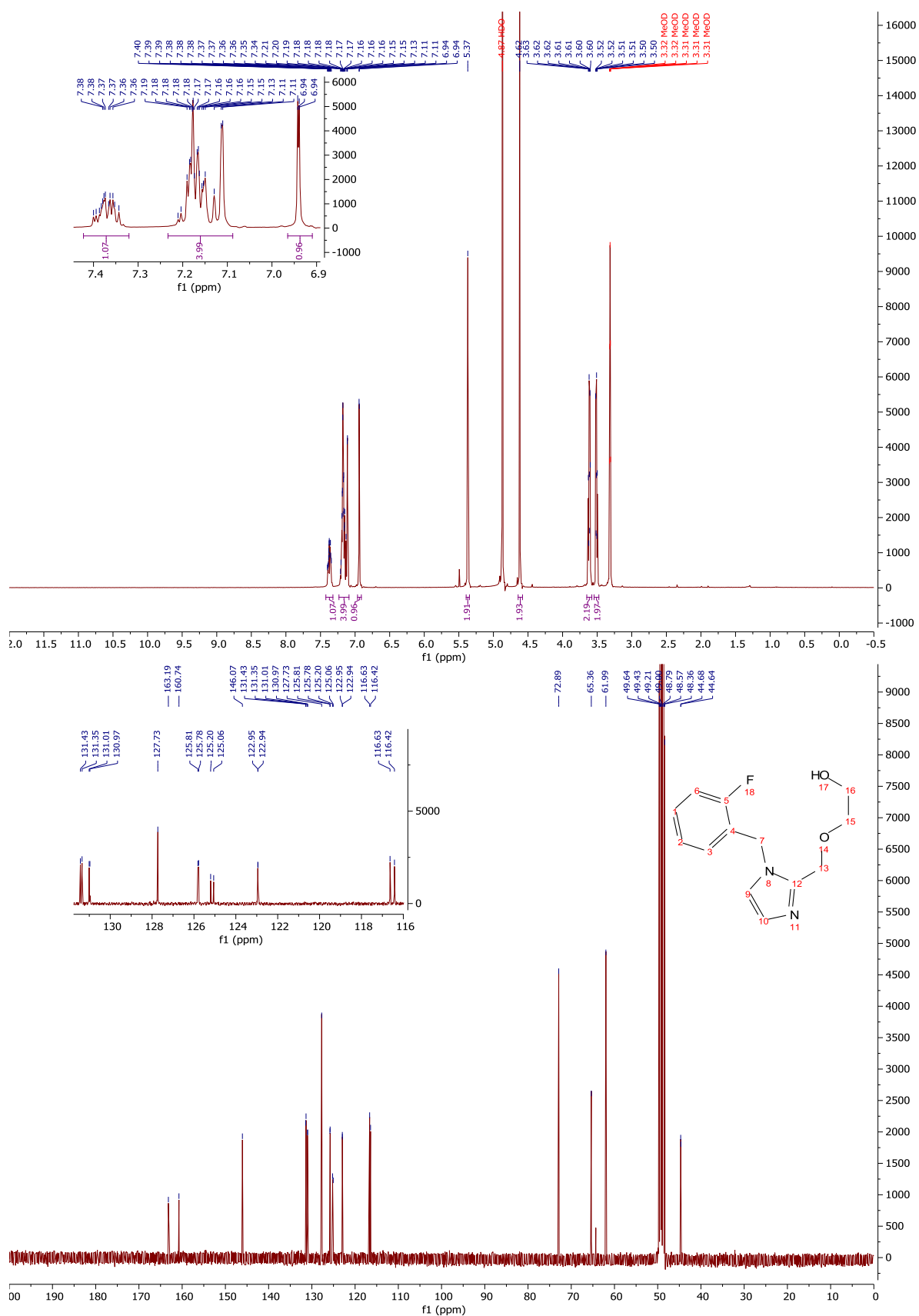
¹H-NMR and ¹³C-NMR: Compound 182



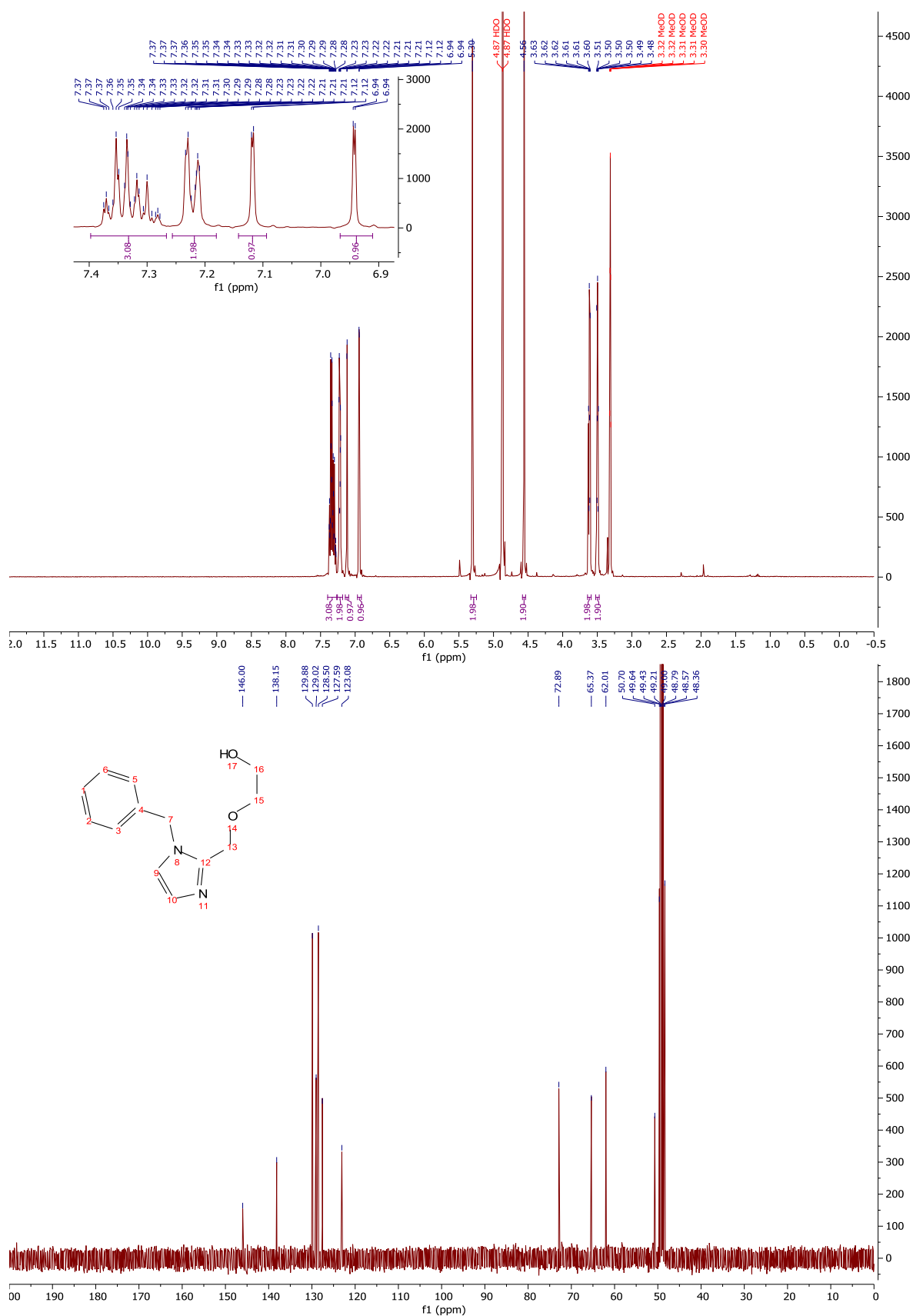
¹H-NMR and ¹³C-NMR: Compound 183



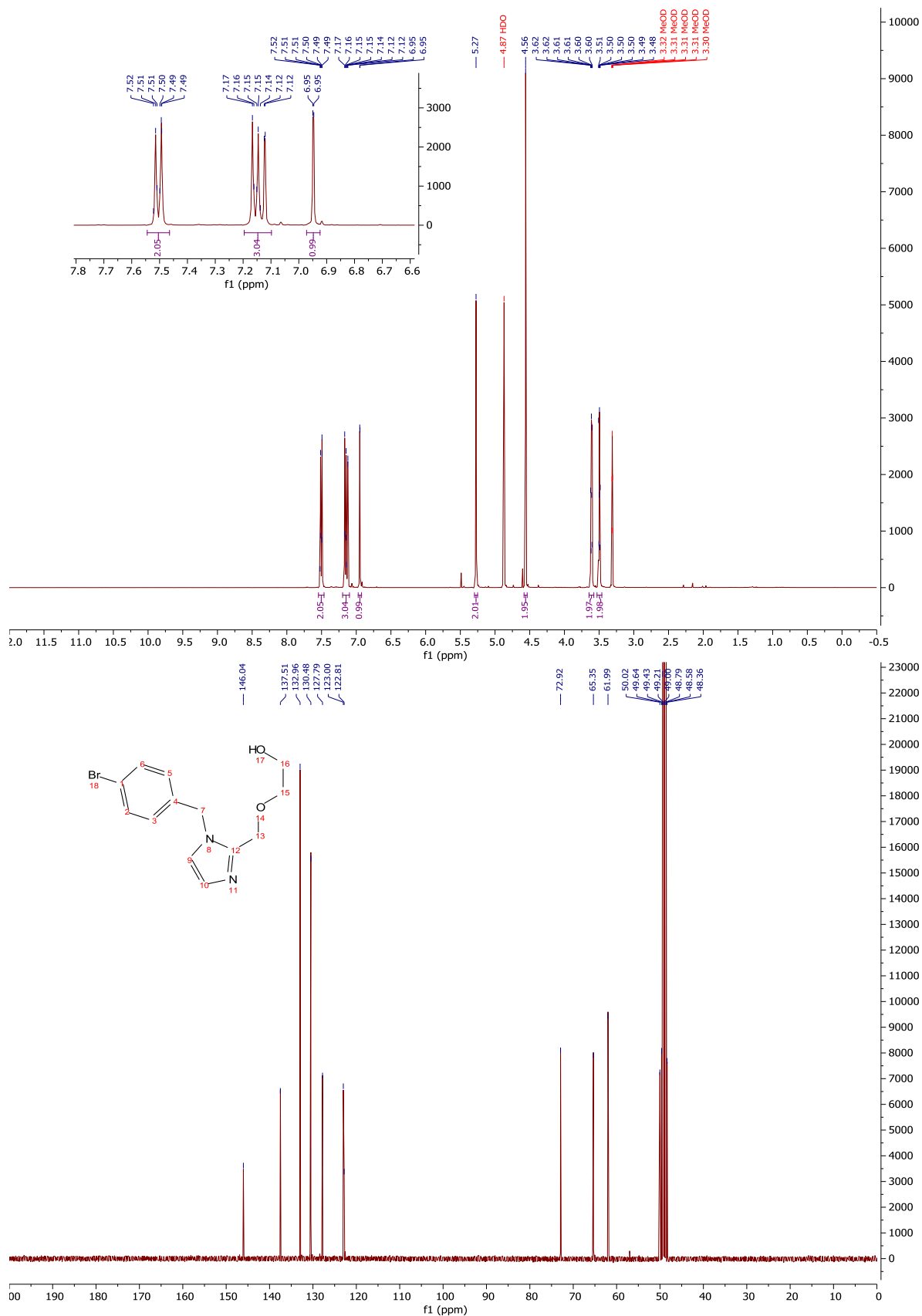
¹H-NMR and ¹³C-NMR: Compound 178



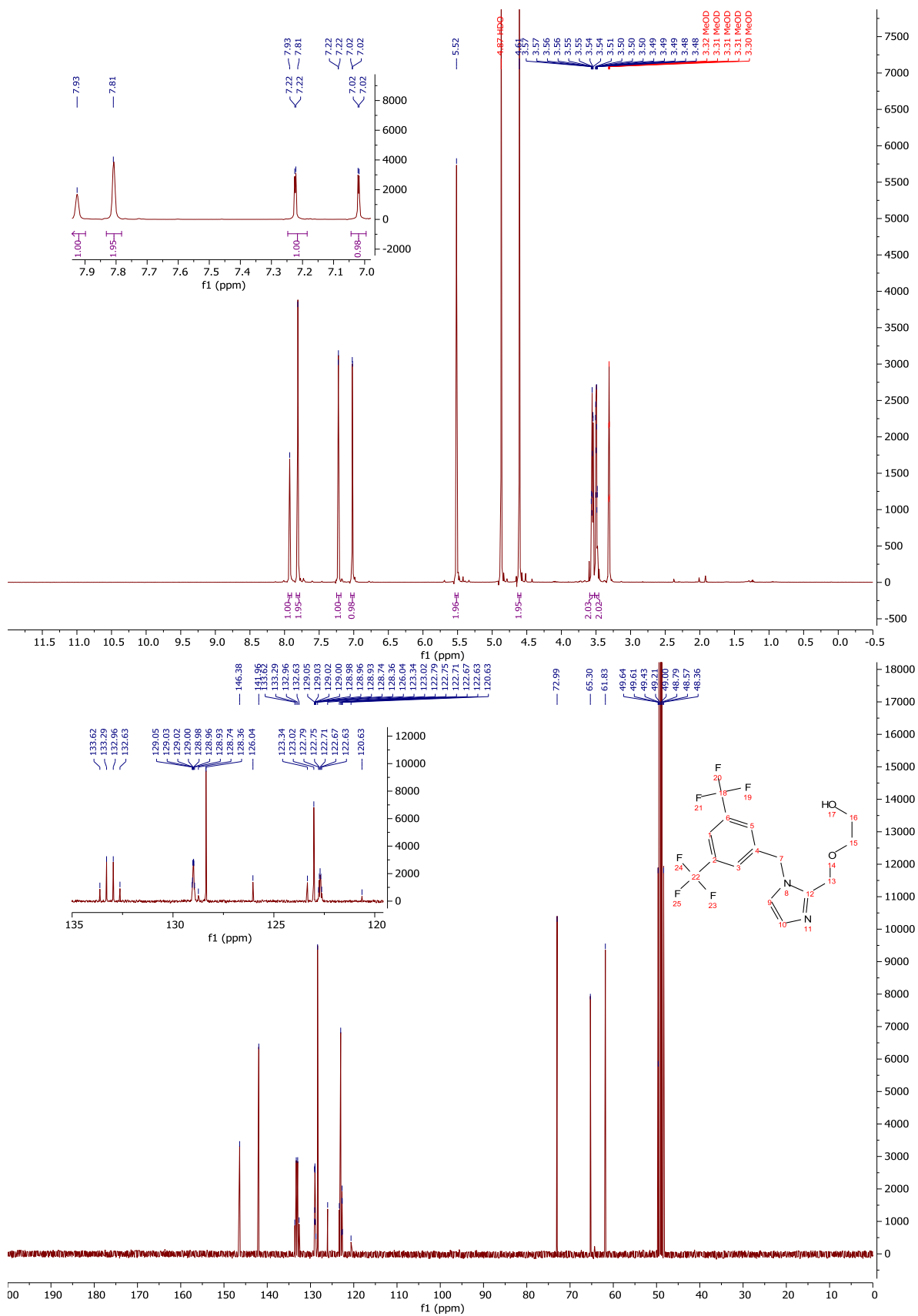
¹H-NMR and ¹³C-NMR: Compound 180



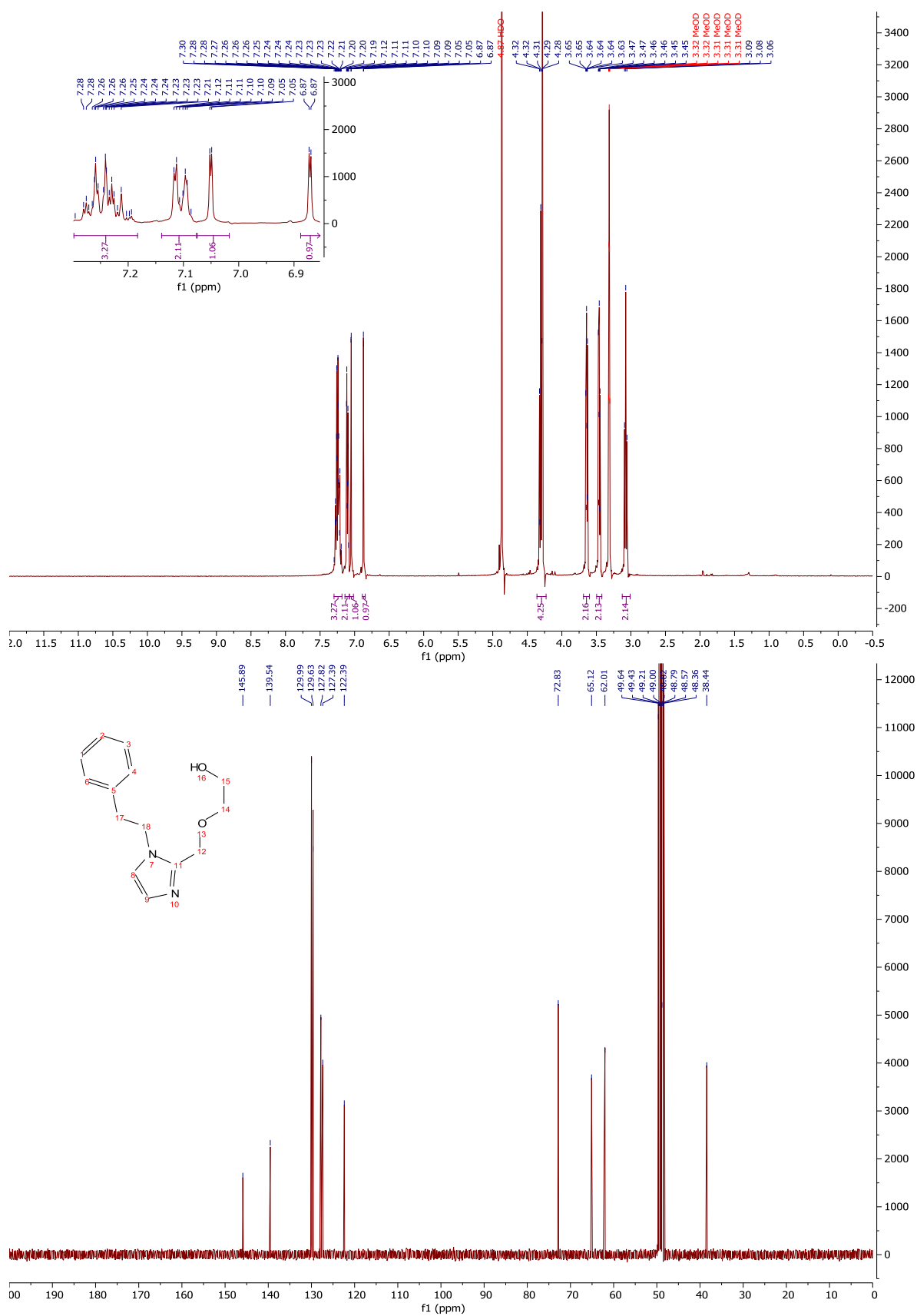
¹H-NMR and ¹³C-NMR: Compound 185



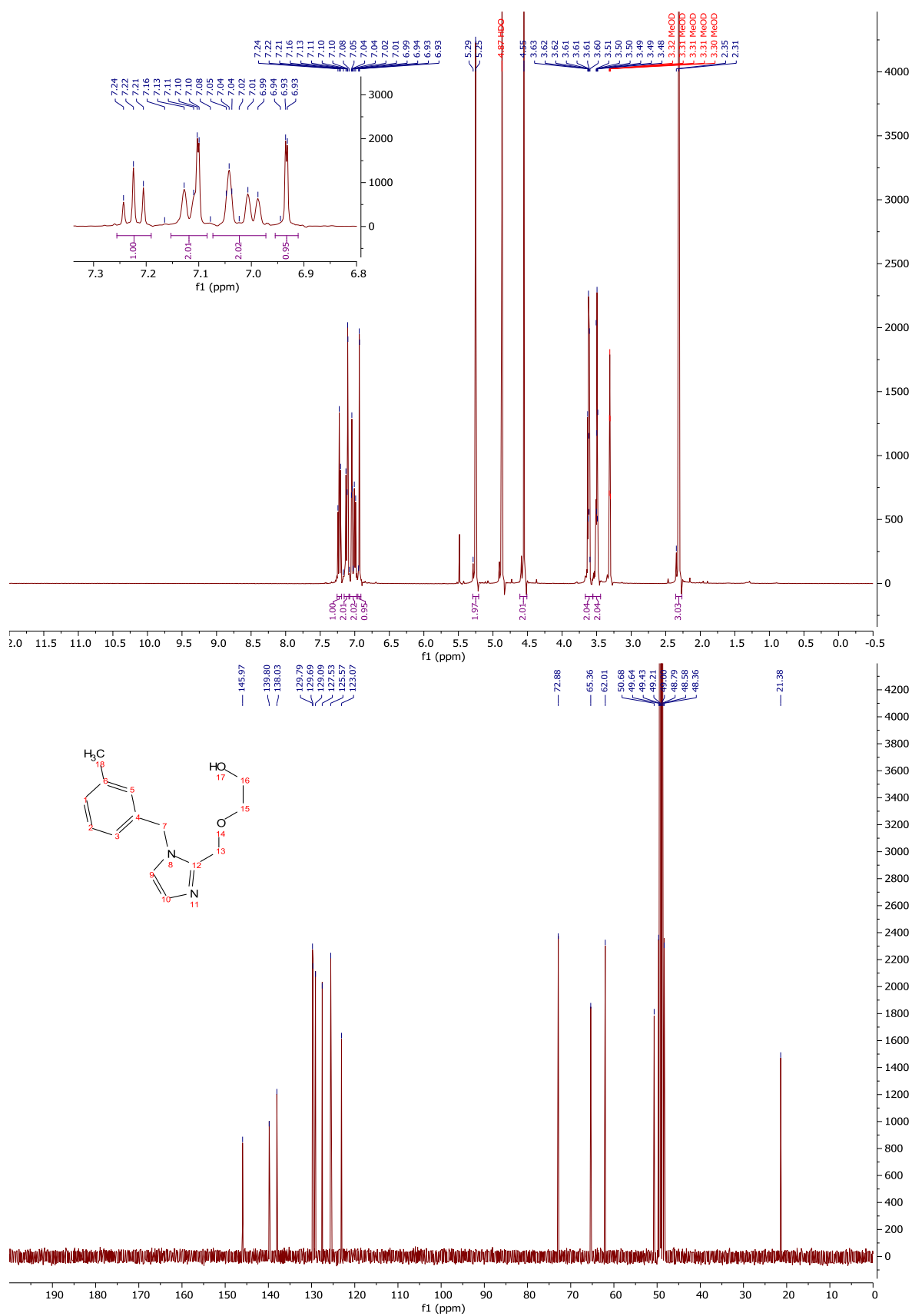
$^1\text{H-NMR}$ and $^{13}\text{C-NMR}$: Compound 193



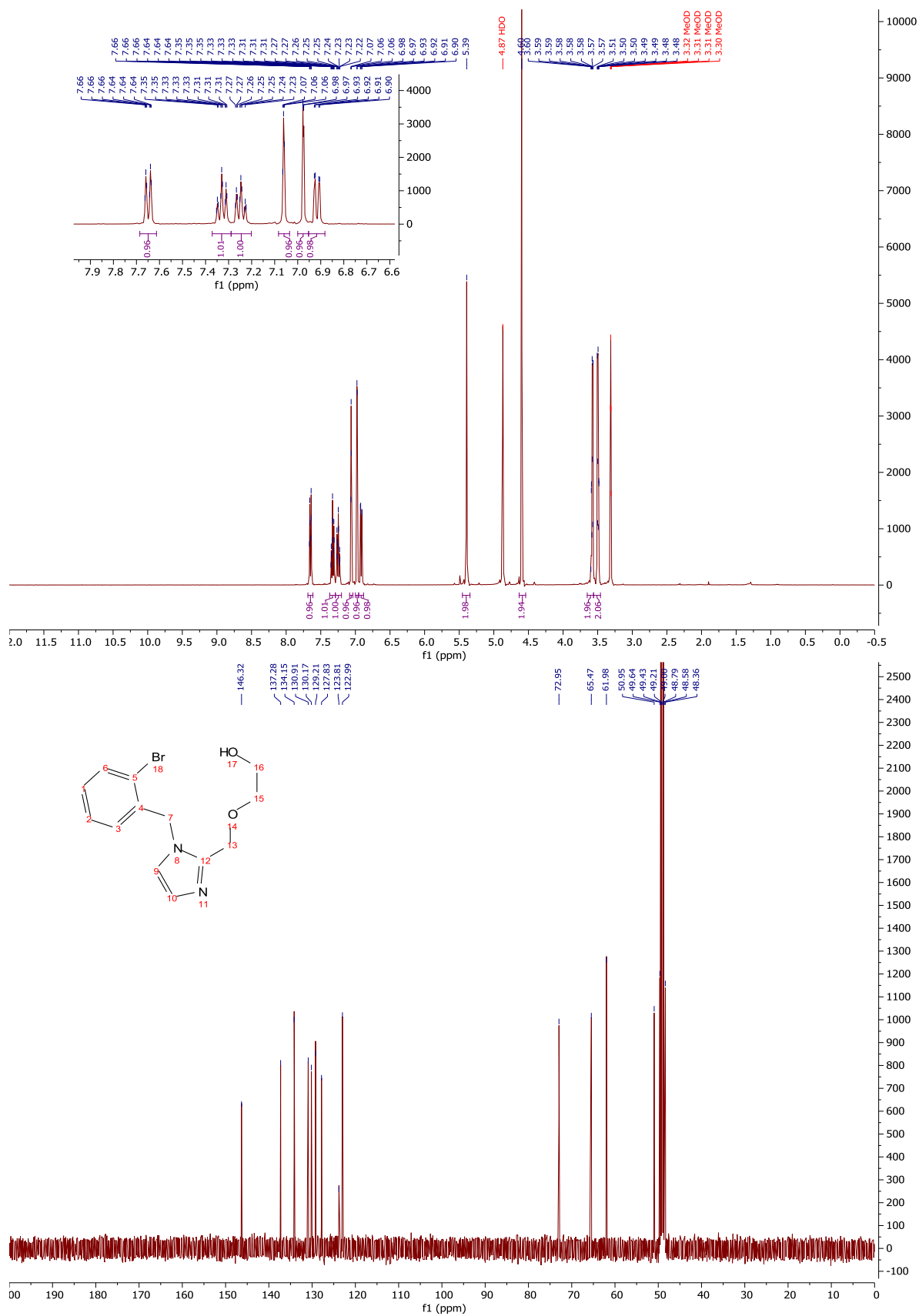
¹H-NMR and ¹³C-NMR: Compound 197



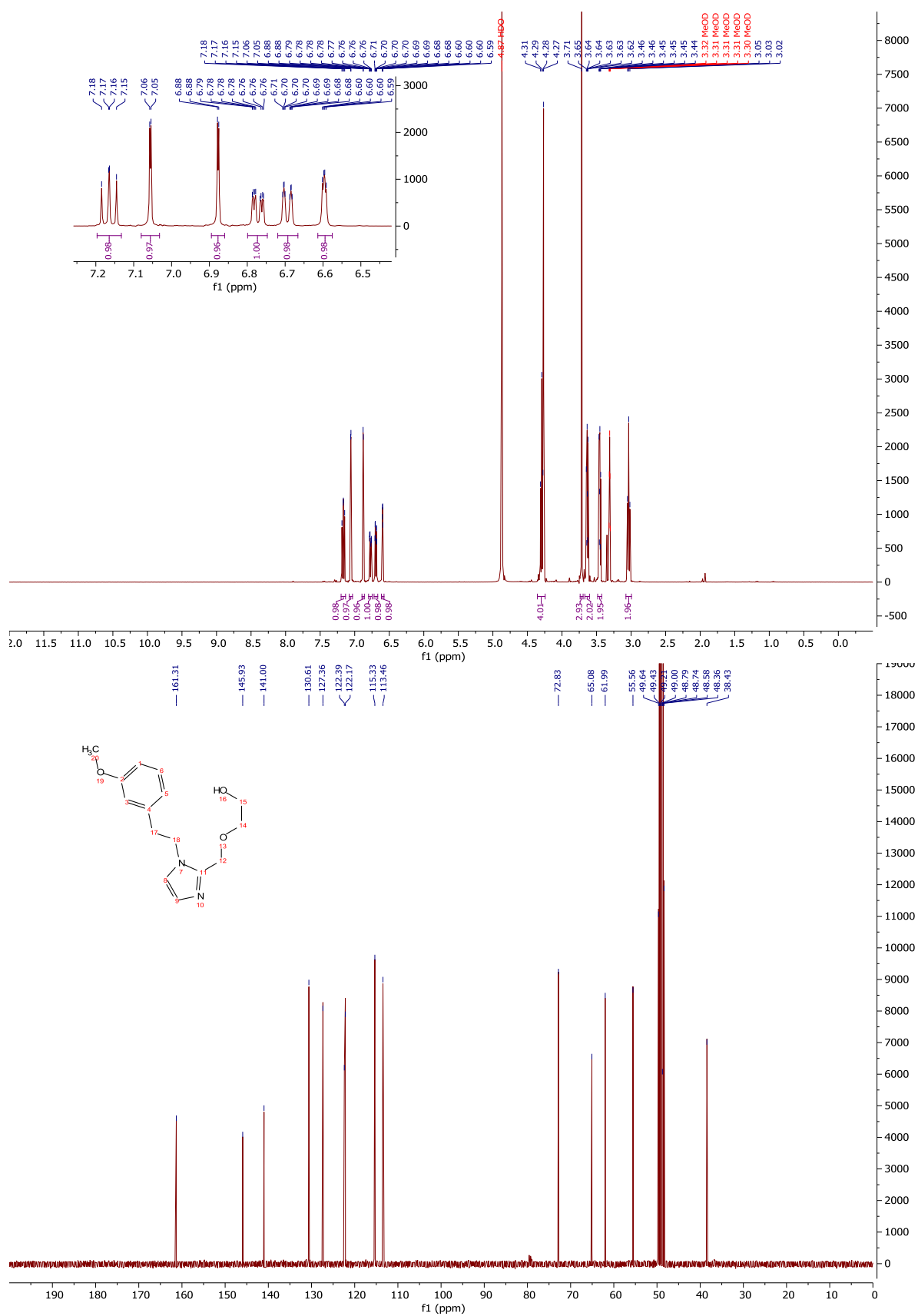
¹H-NMR and ¹³C-NMR: Compound 187



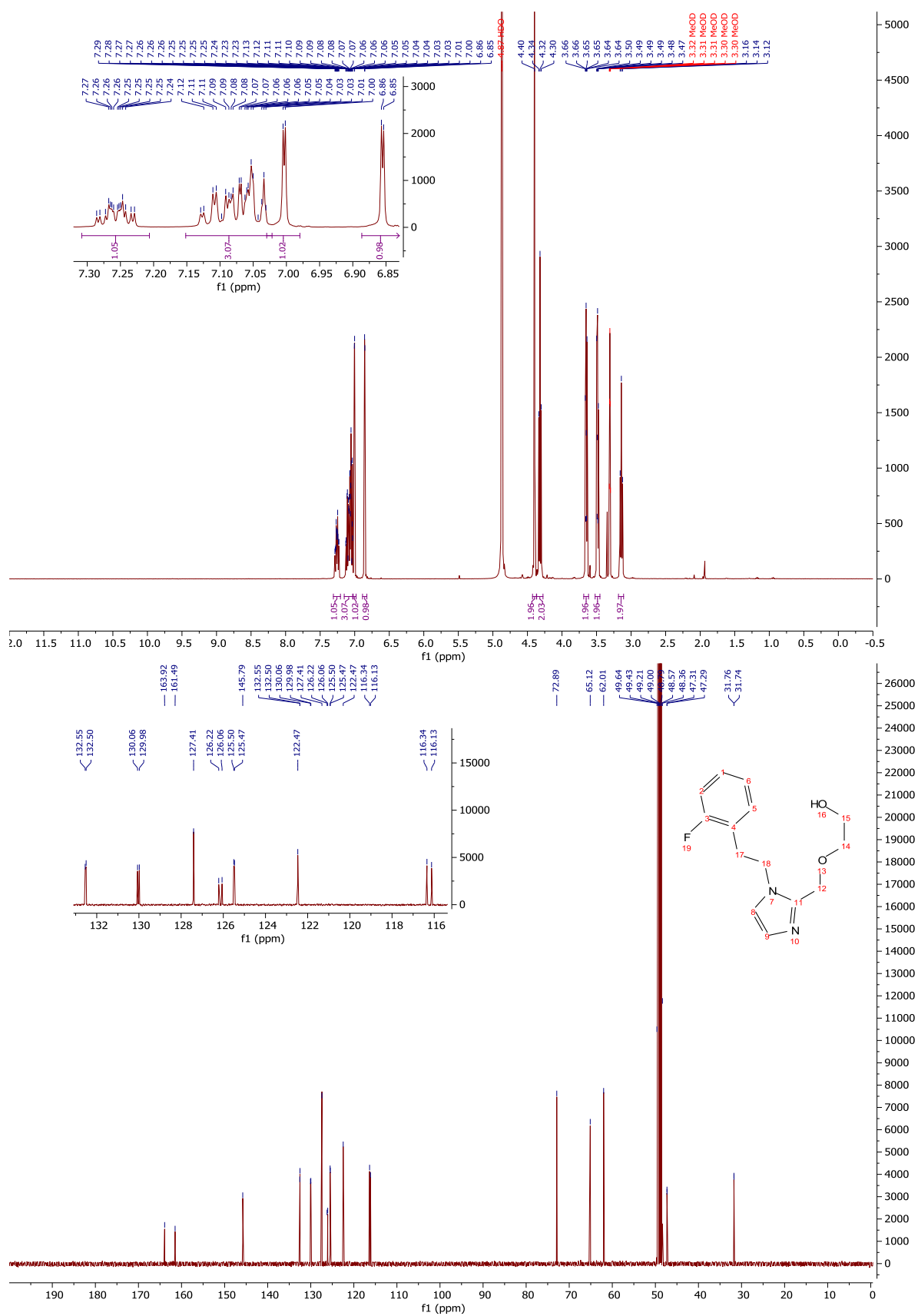
¹H-NMR and ¹³C-NMR: Compound 189



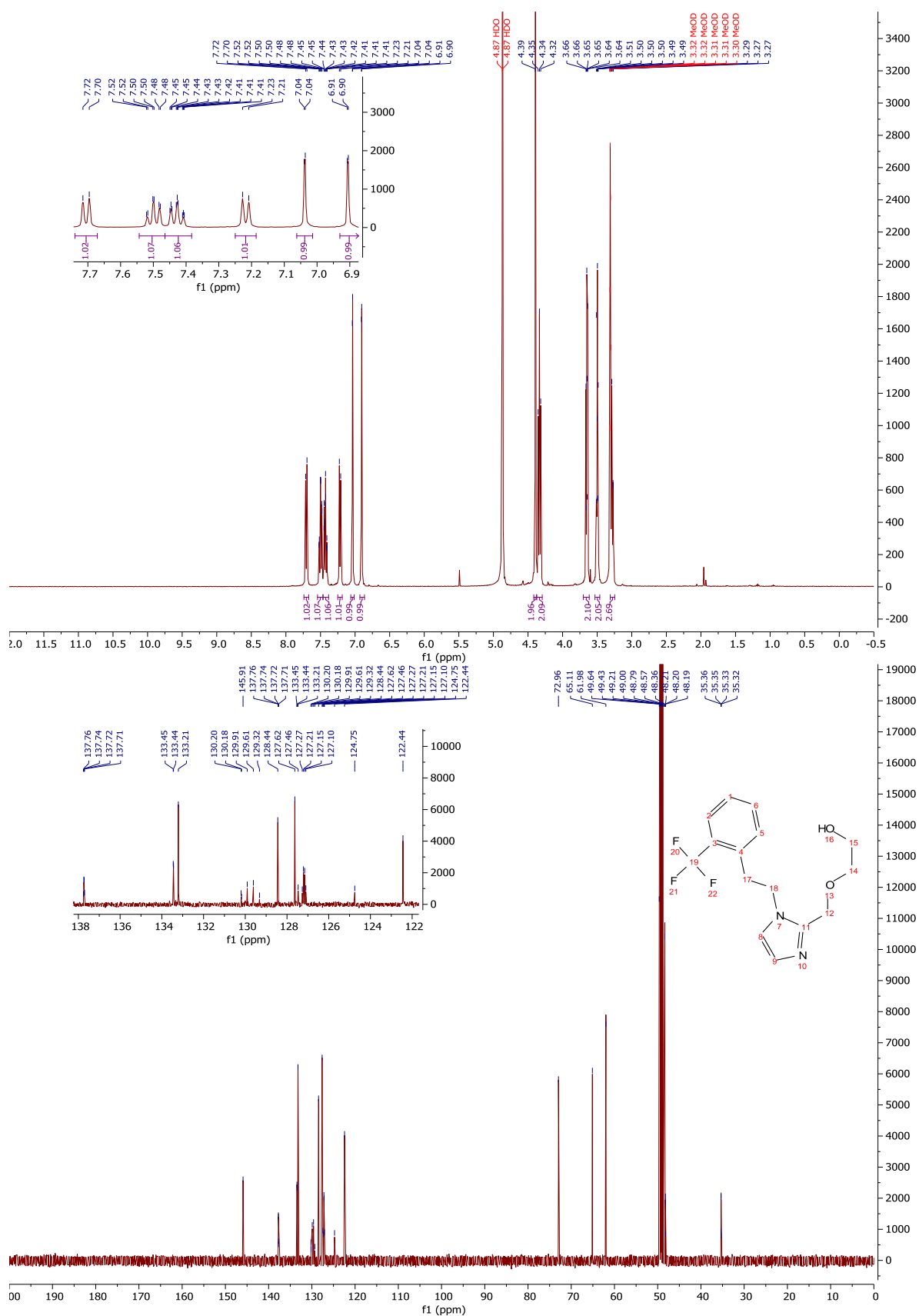
¹H-NMR and ¹³C-NMR: Compound 199



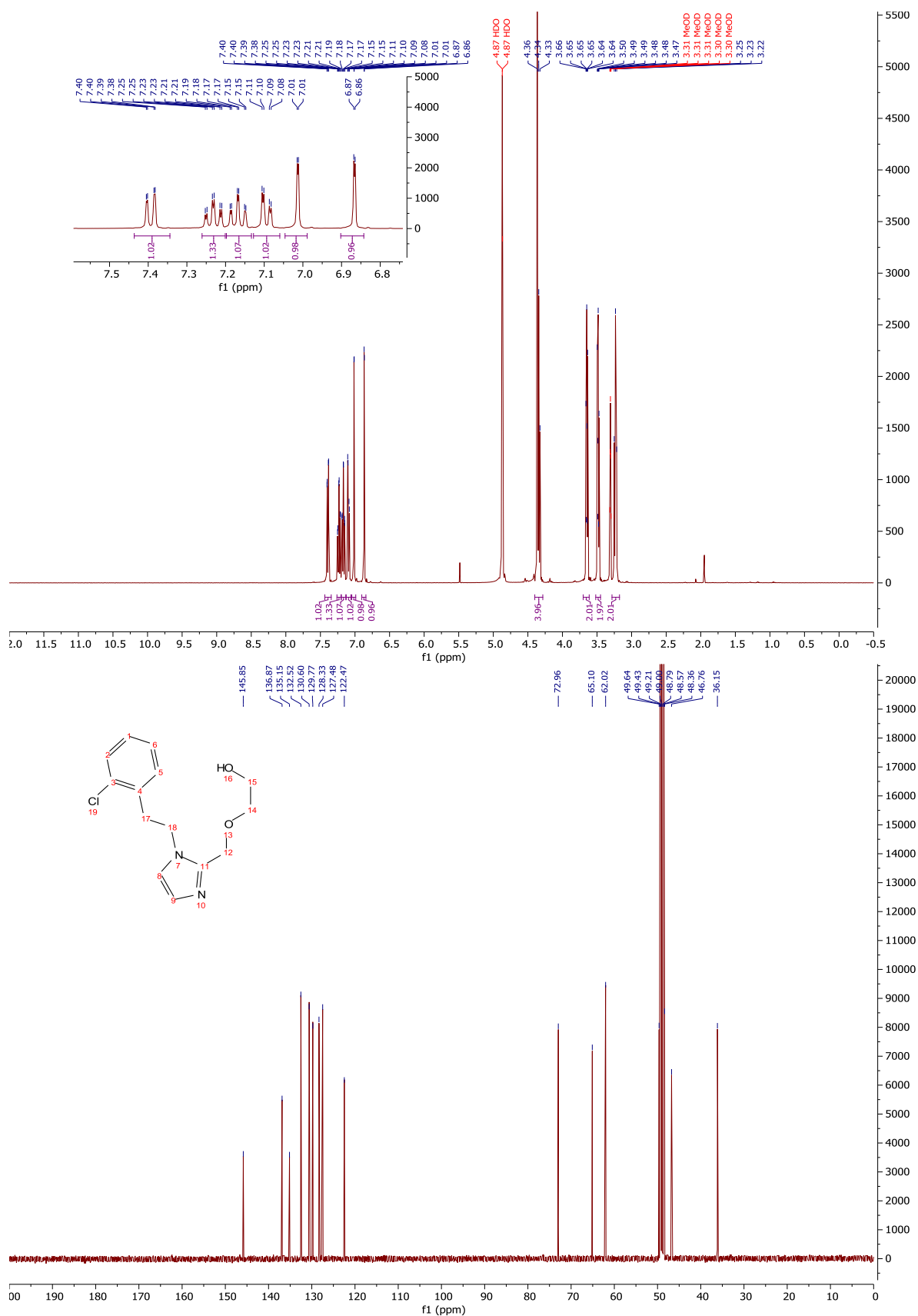
¹H-NMR and ¹³C-NMR: Compound 201



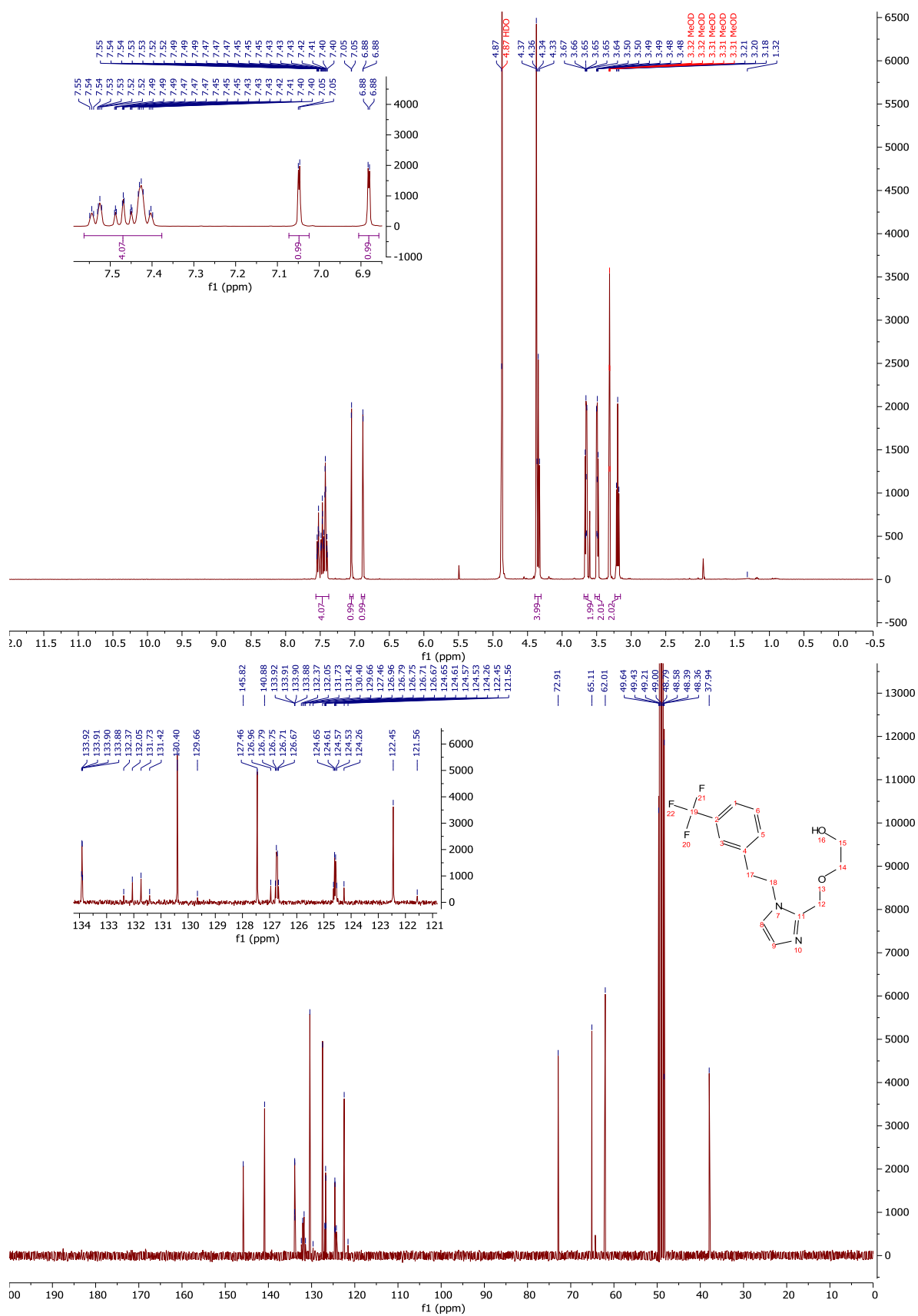
¹H-NMR and ¹³C-NMR: Compound 195



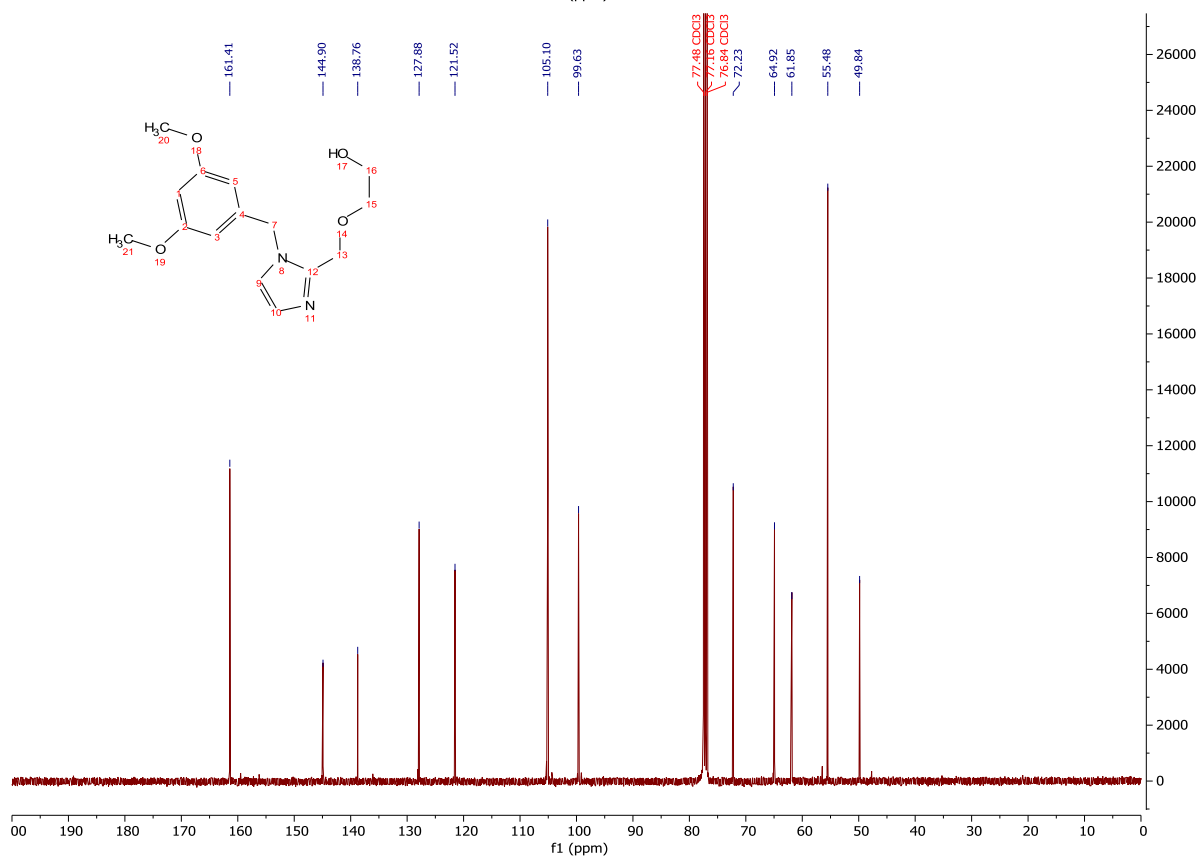
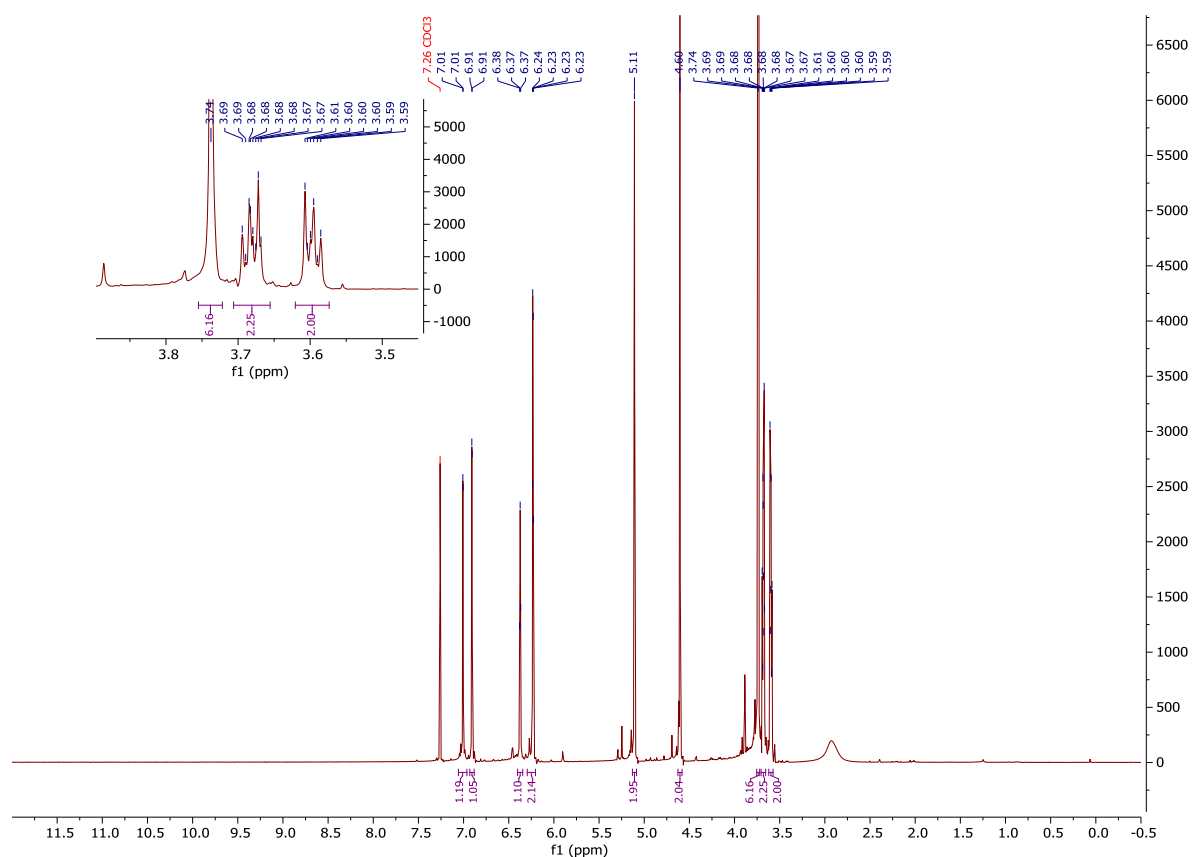
¹H-NMR and ¹³C-NMR: Compound 203



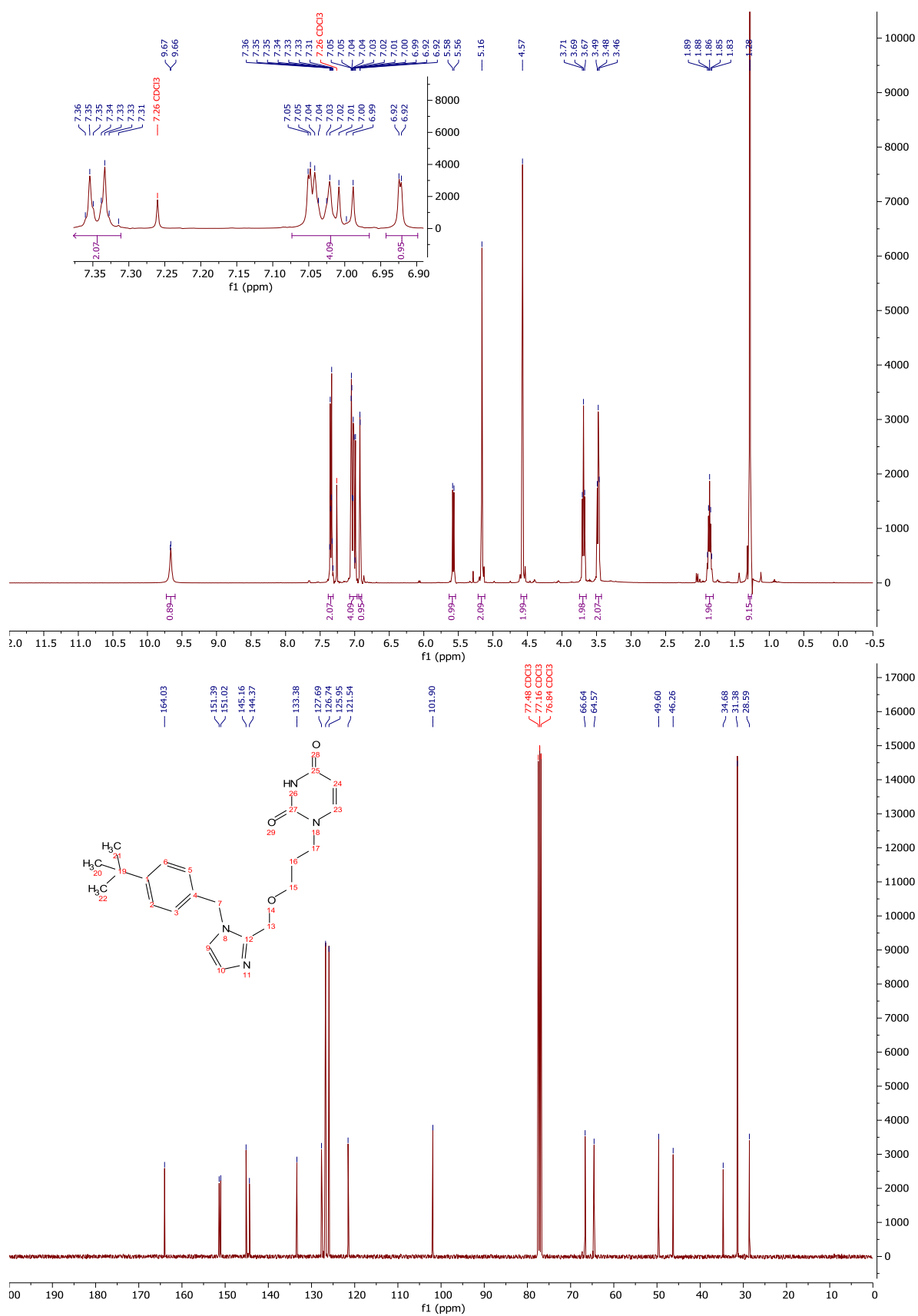
¹H-NMR and ¹³C-NMR: Compound 195



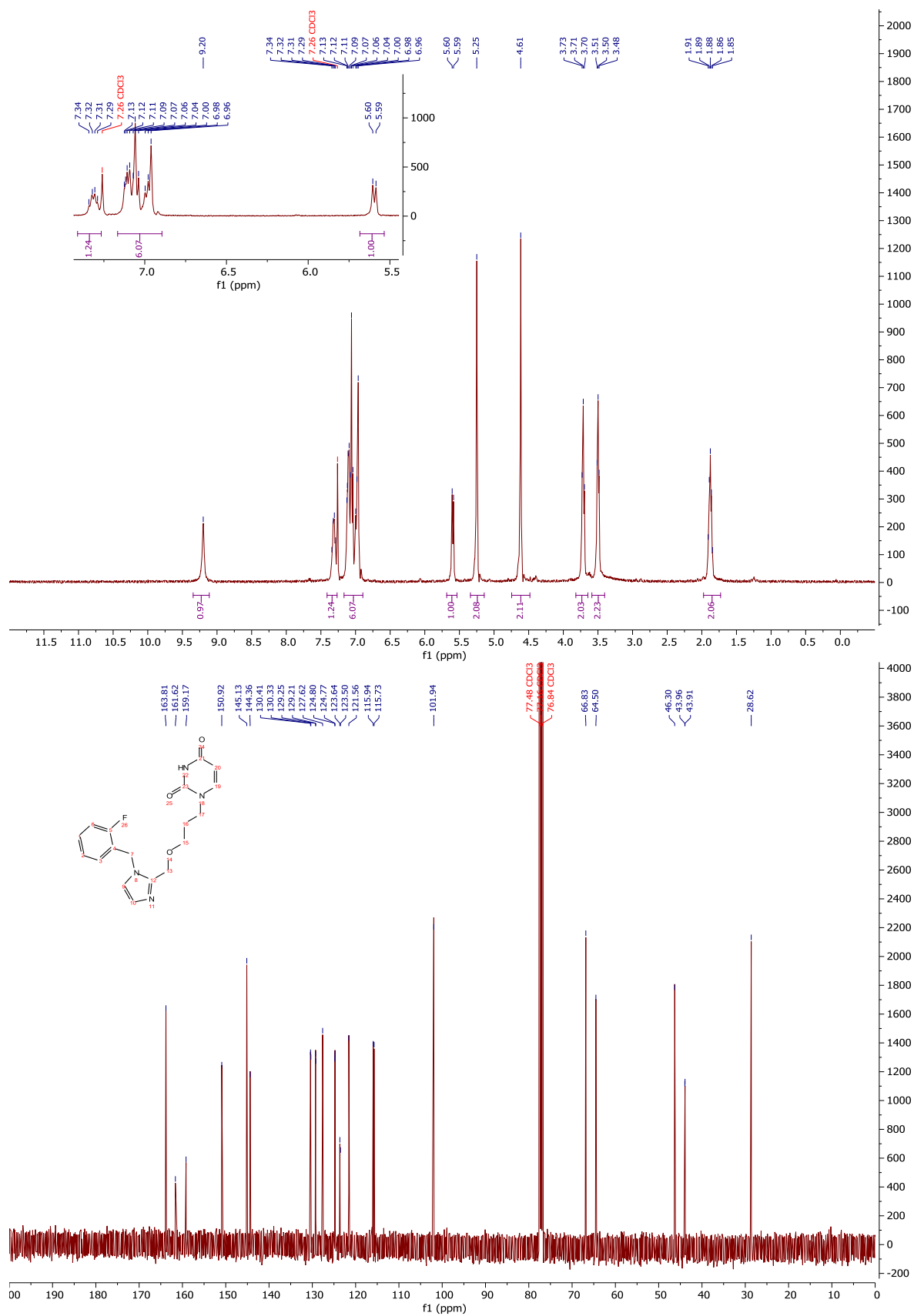
¹H-NMR and ¹³C-NMR: Compound 181



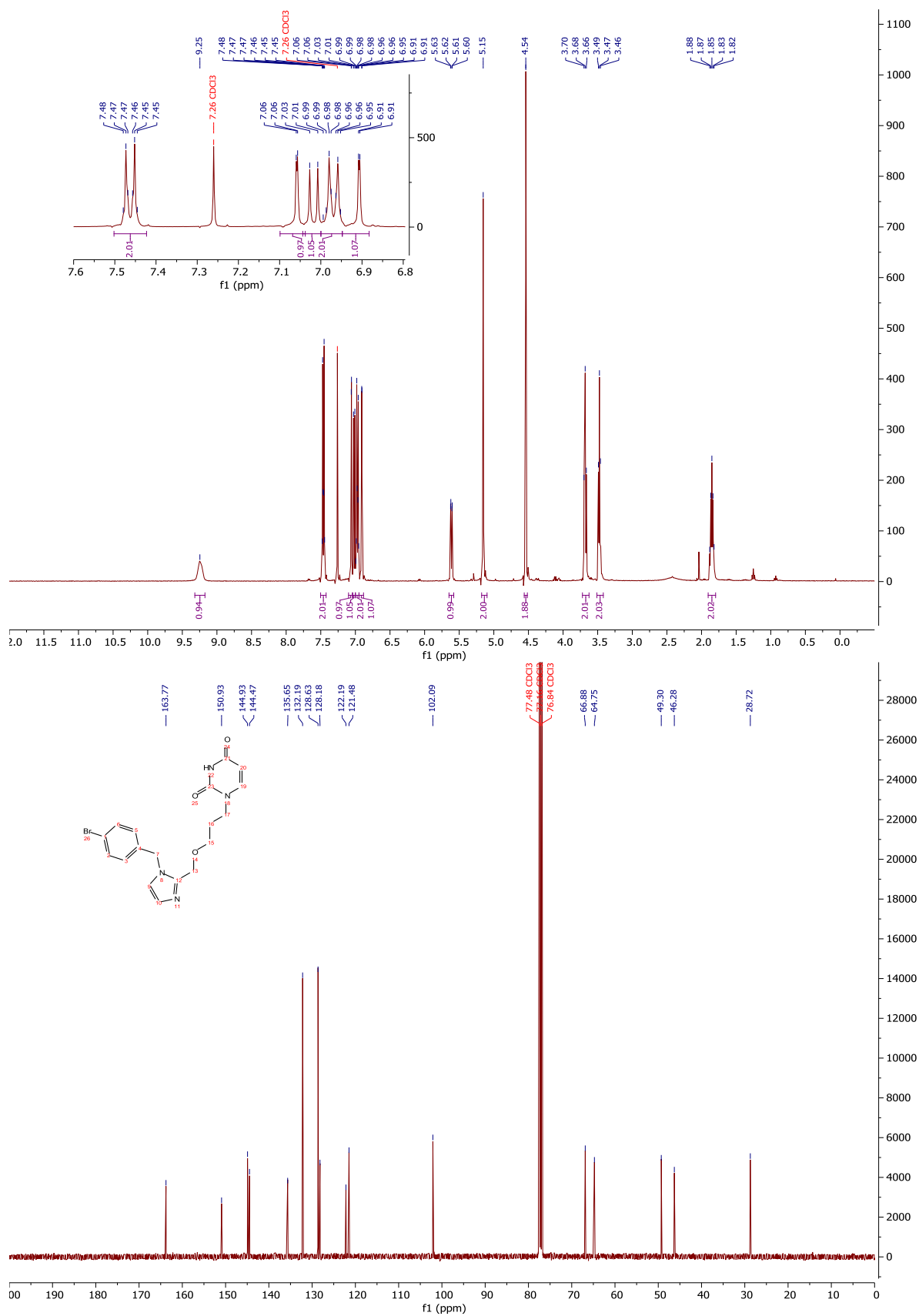
¹H-NMR and ¹³C-NMR: Compound 218



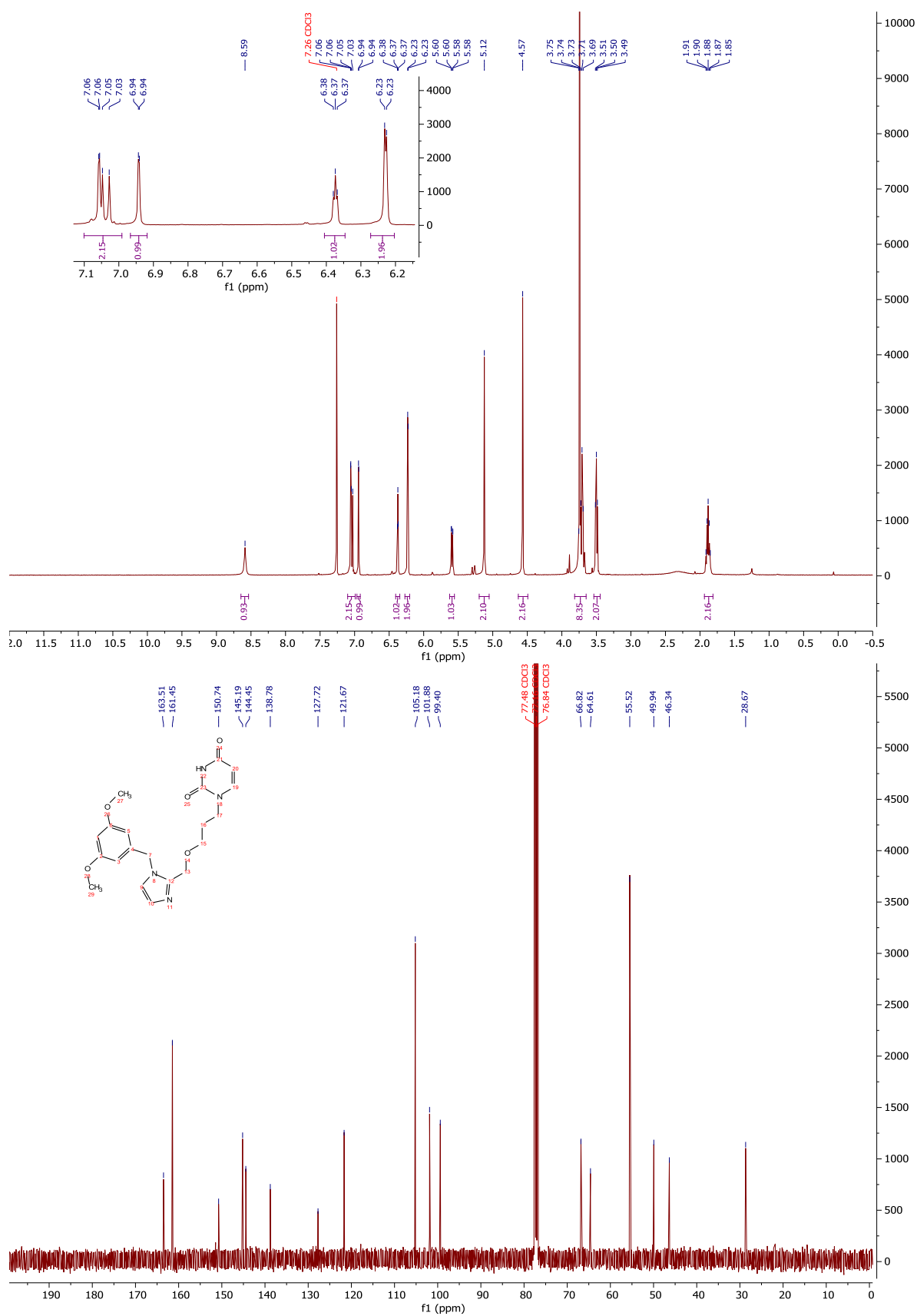
¹H-NMR and ¹³C-NMR: Compound 208



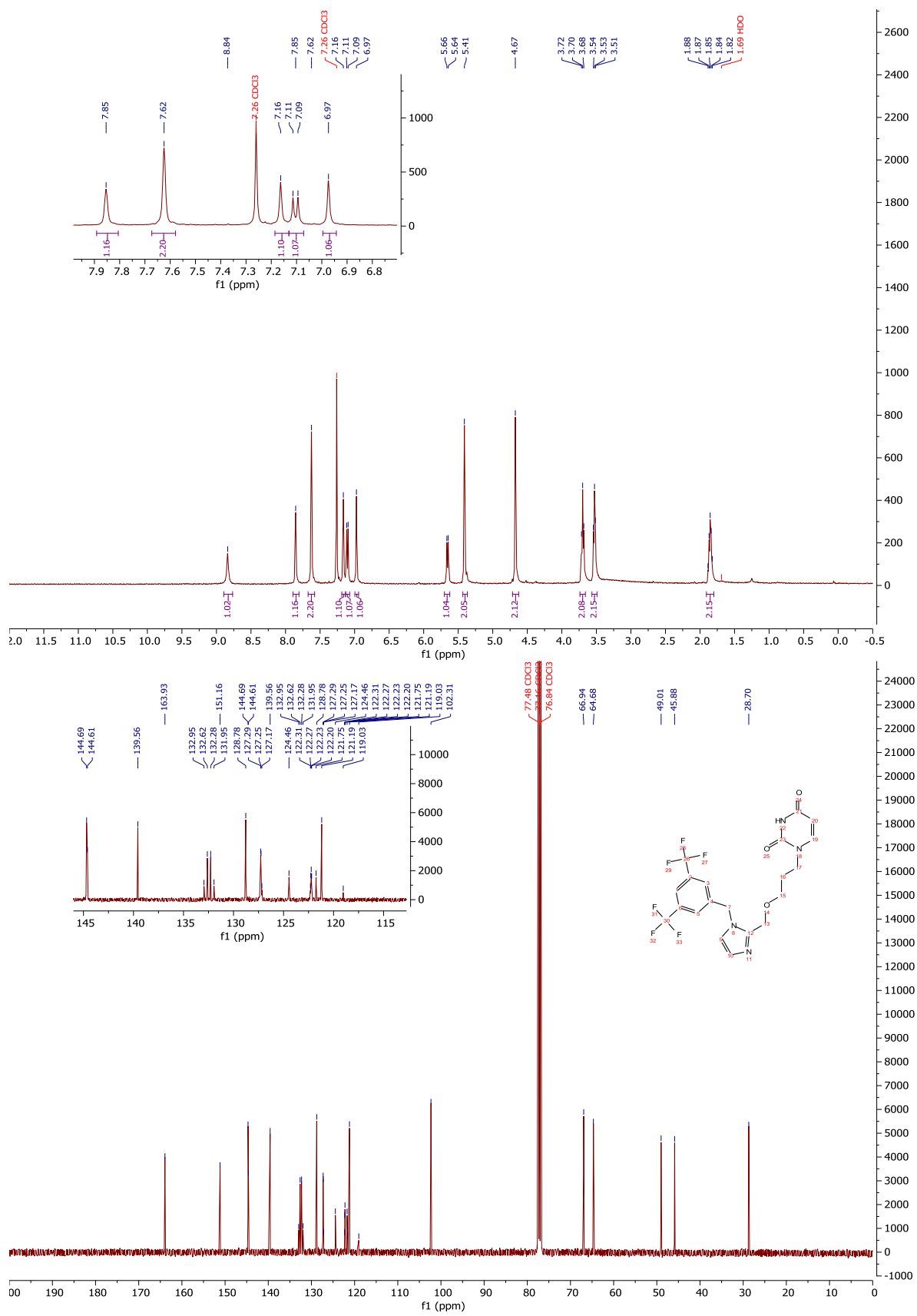
¹H-NMR and ¹³C-NMR: Compound 212



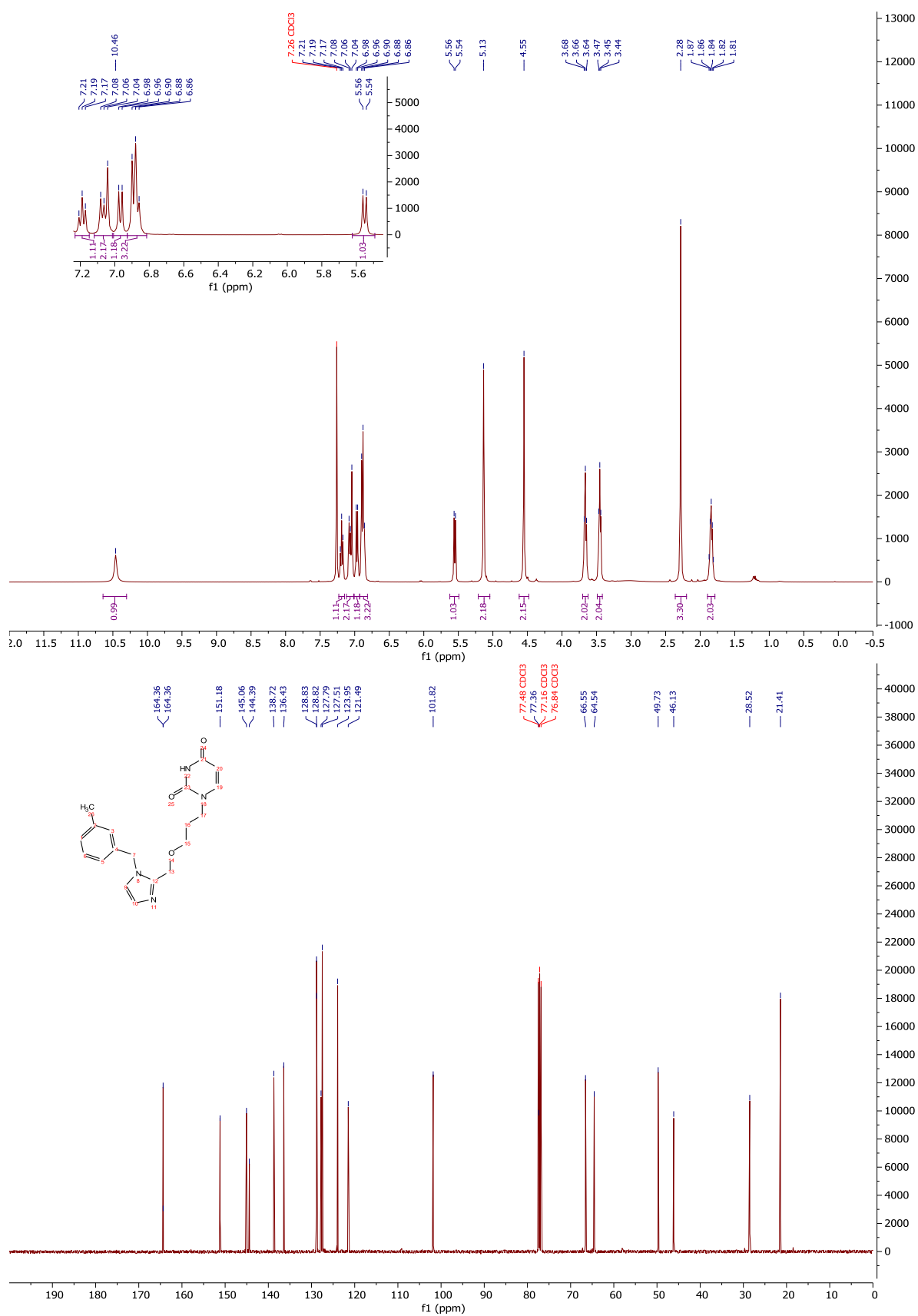
¹H-NMR and ¹³C-NMR: Compound 222



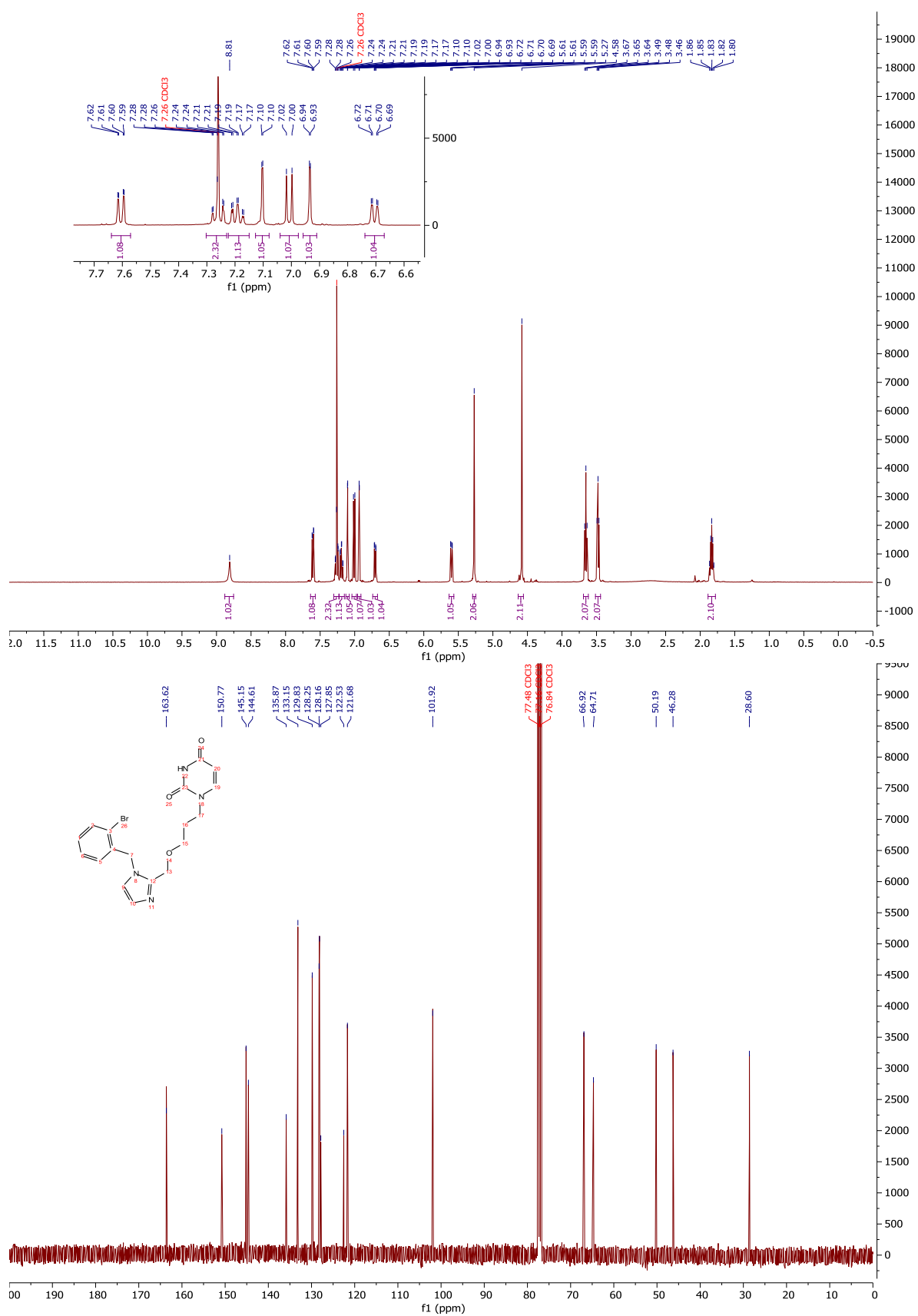
¹H-NMR and ¹³C-NMR: Compound 224



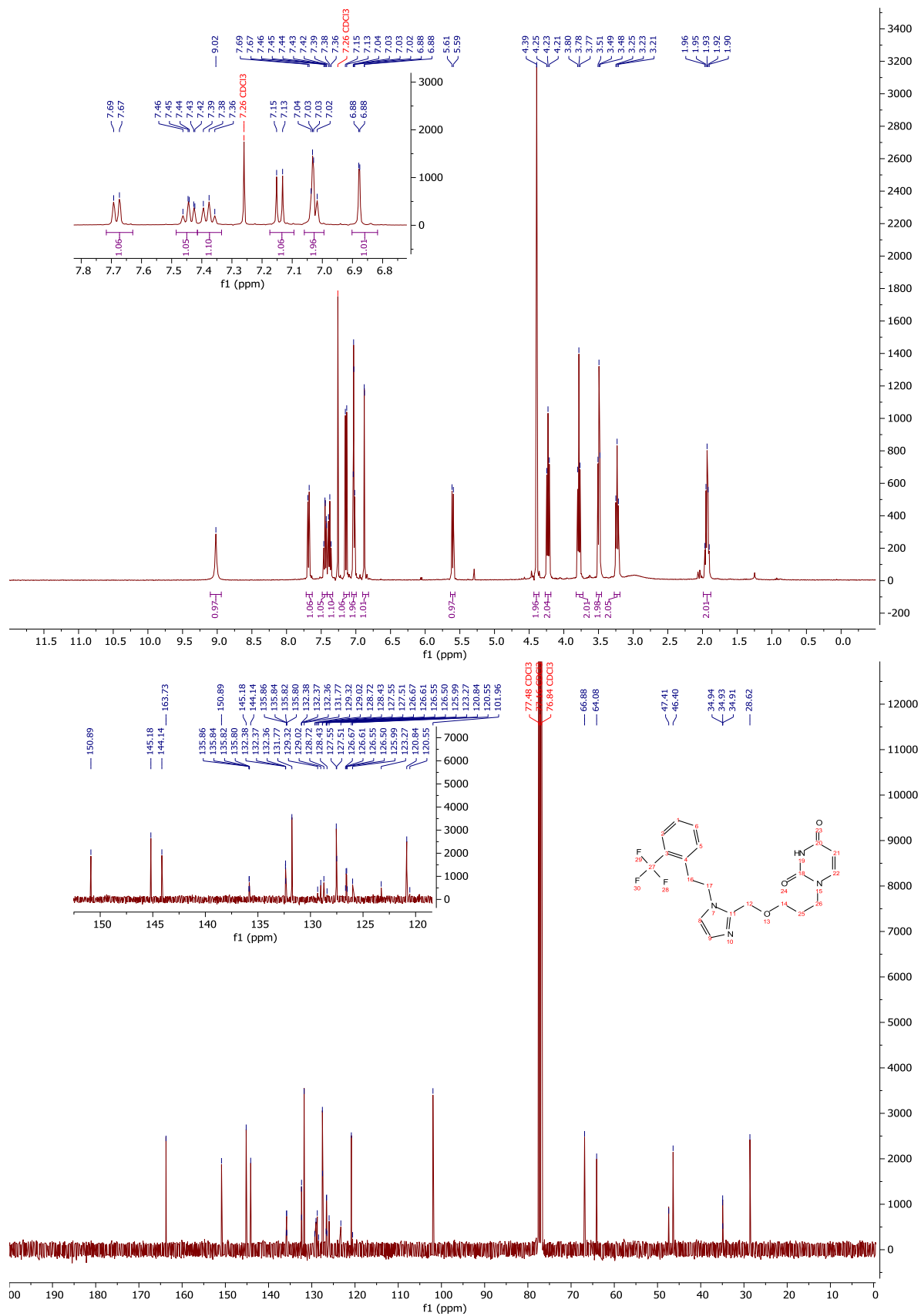
¹H-NMR and ¹³C-NMR: Compound 214



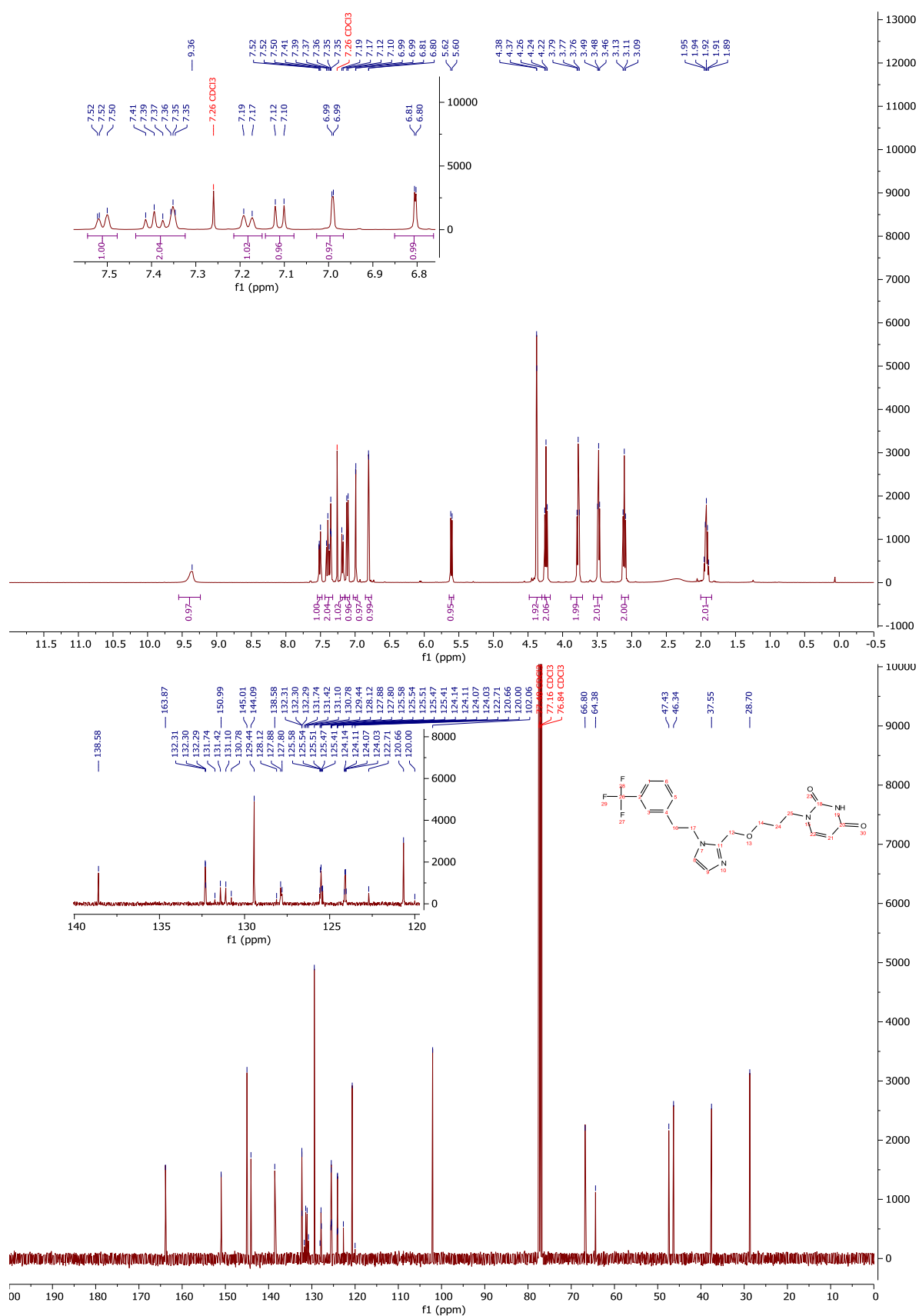
¹H-NMR and ¹³C-NMR: Compound 216



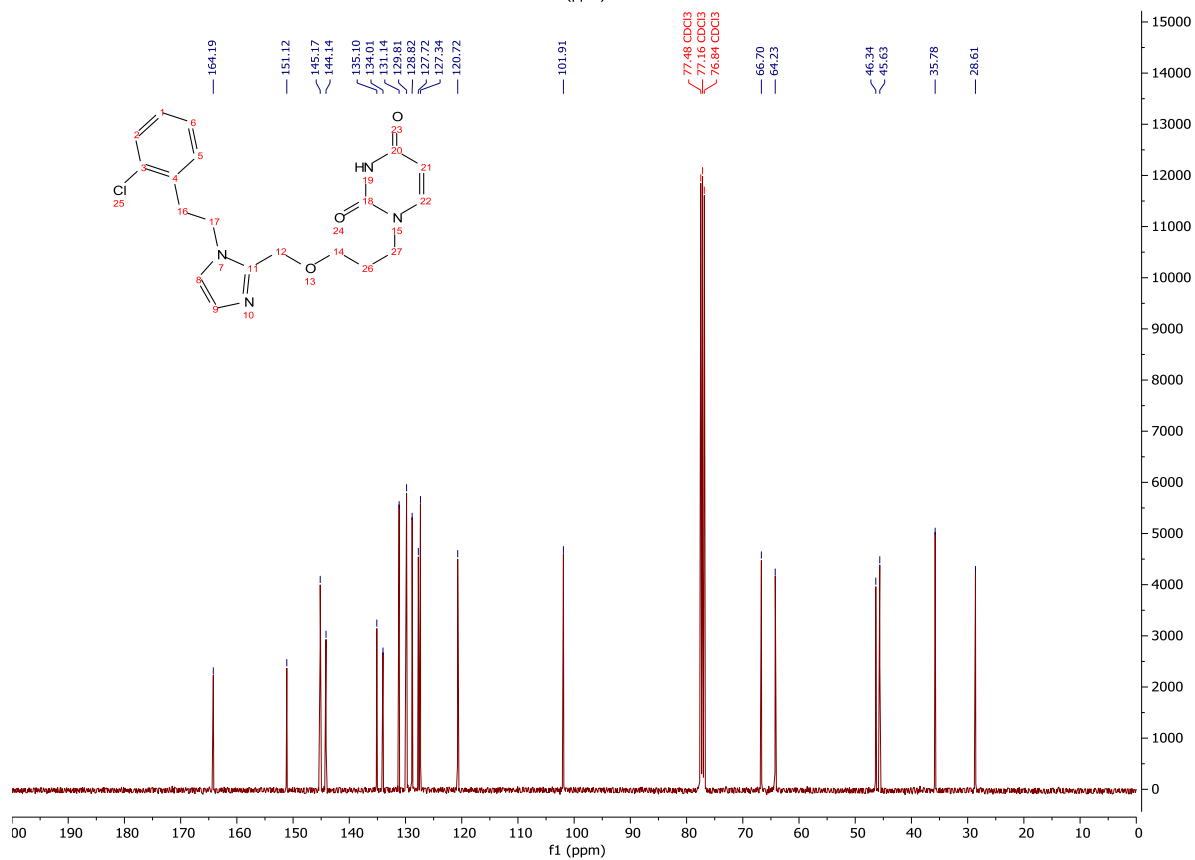
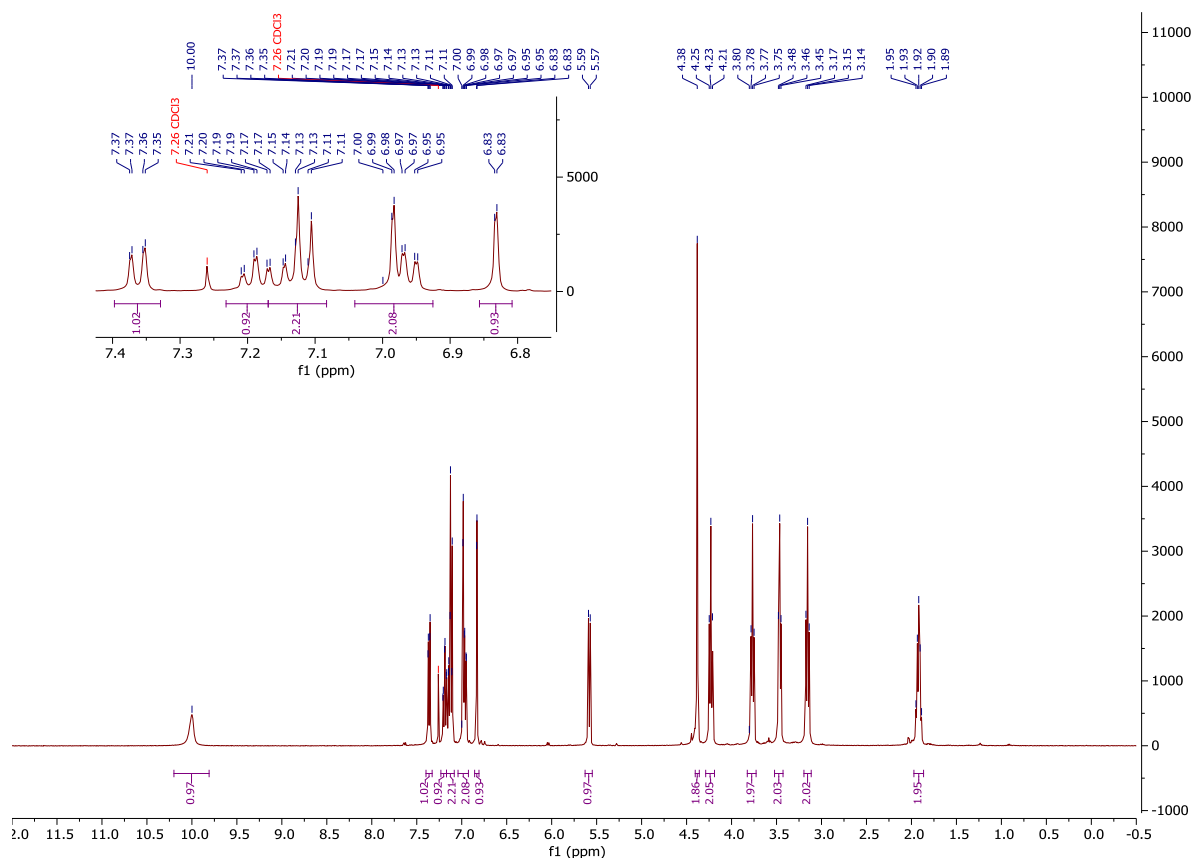
$^1\text{H-NMR}$ and $^{13}\text{C-NMR}$: Compound 234



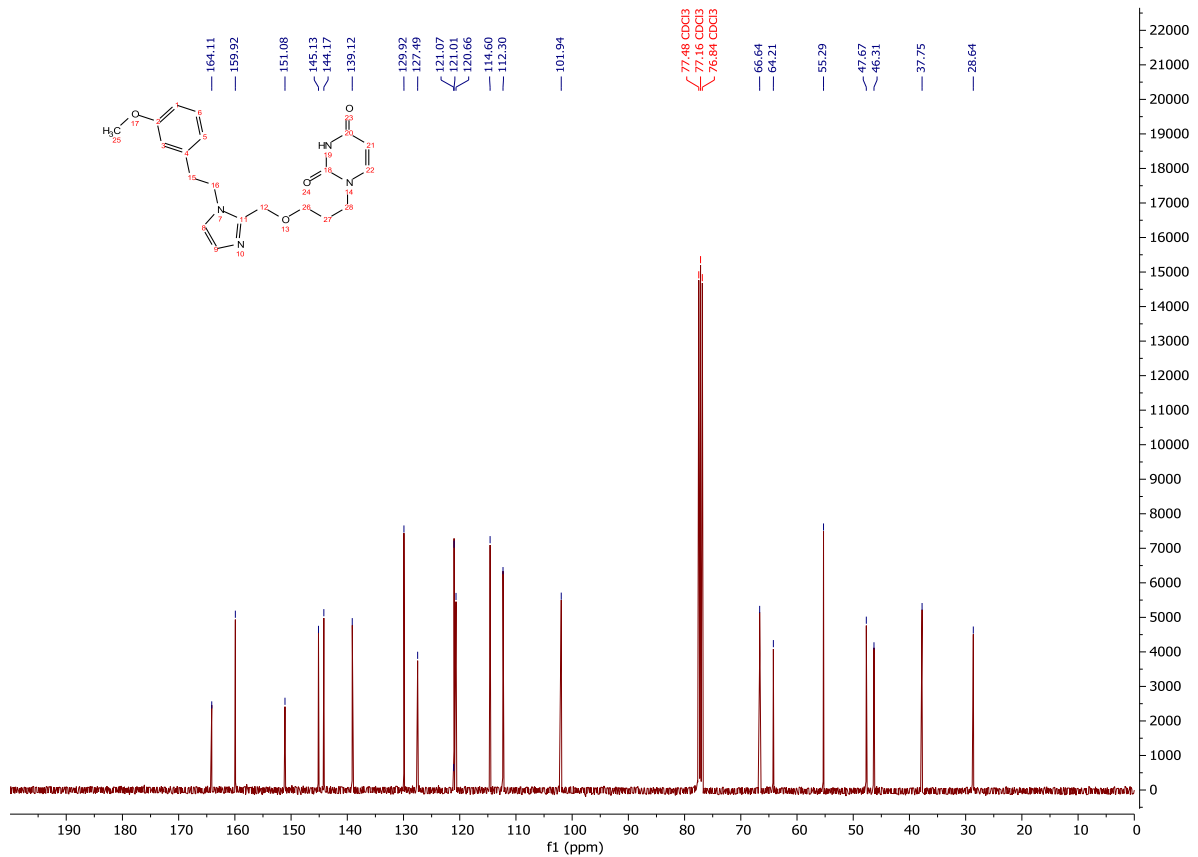
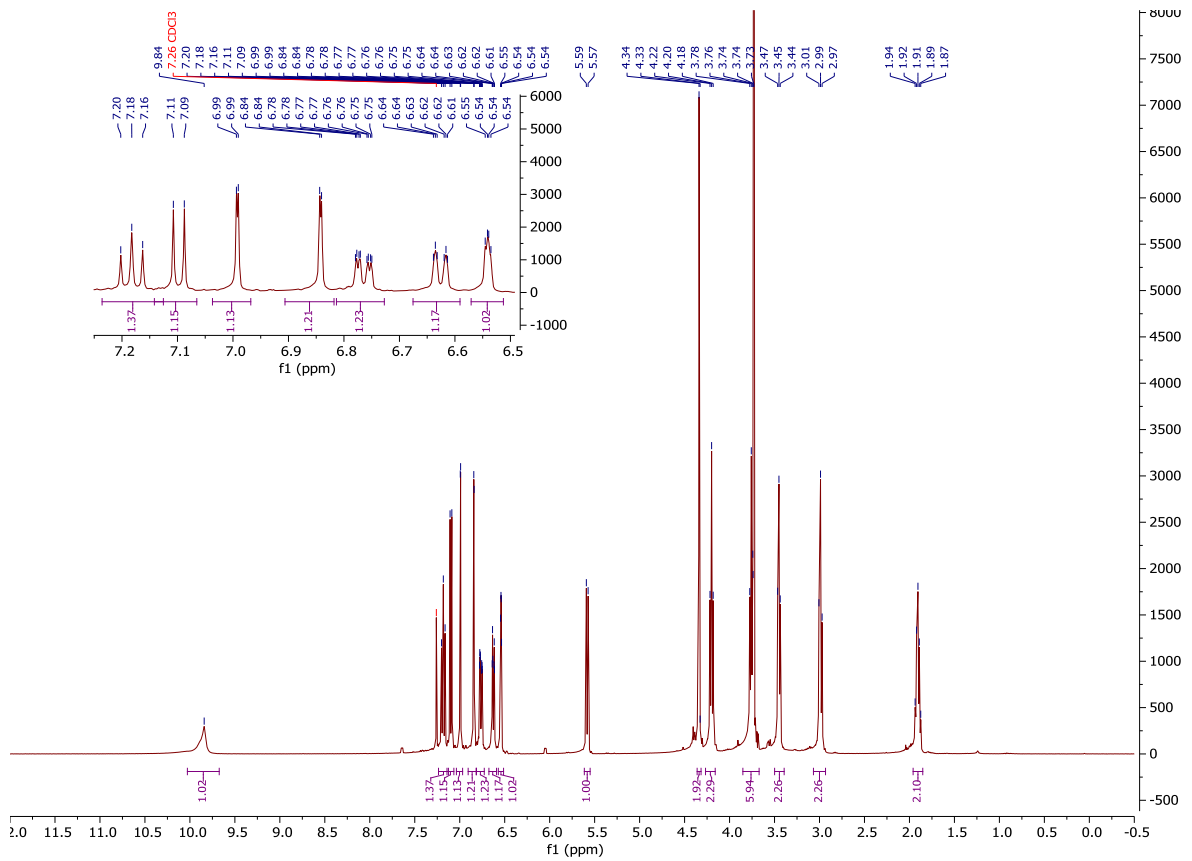
¹H-NMR and ¹³C-NMR: Compound 236



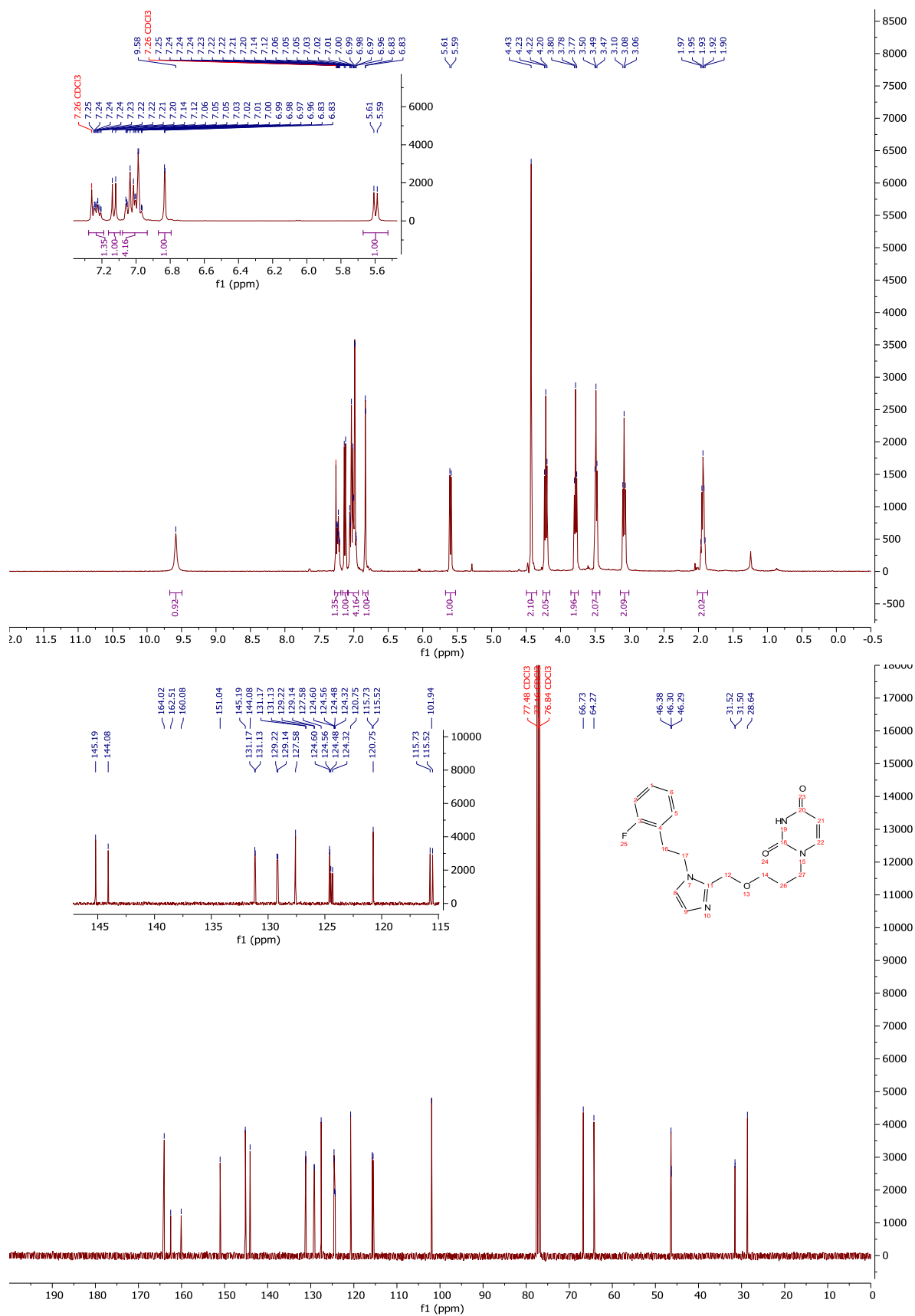
¹H-NMR and ¹³C-NMR: Compound 232



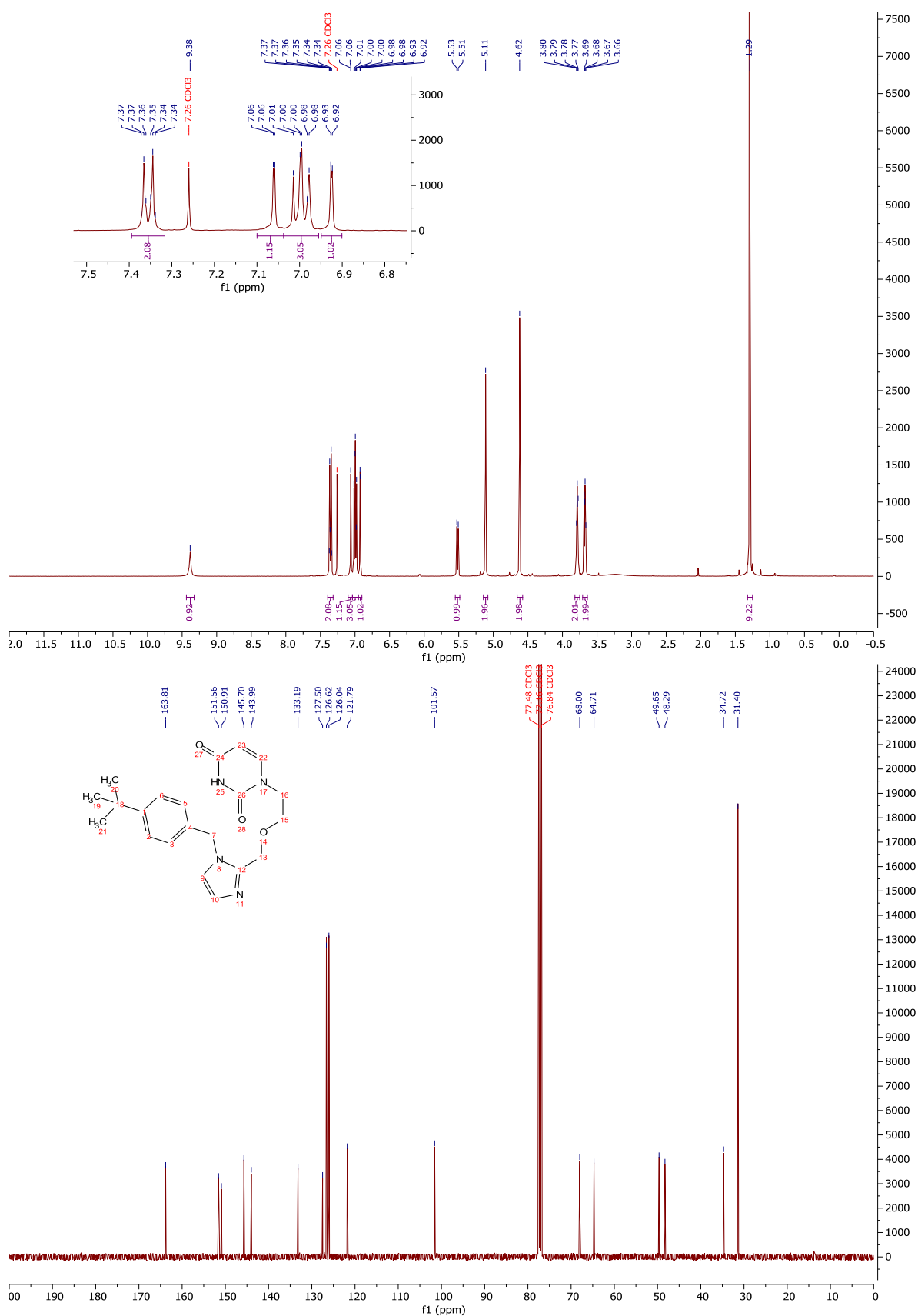
¹H-NMR and ¹³C-NMR: Compound 228



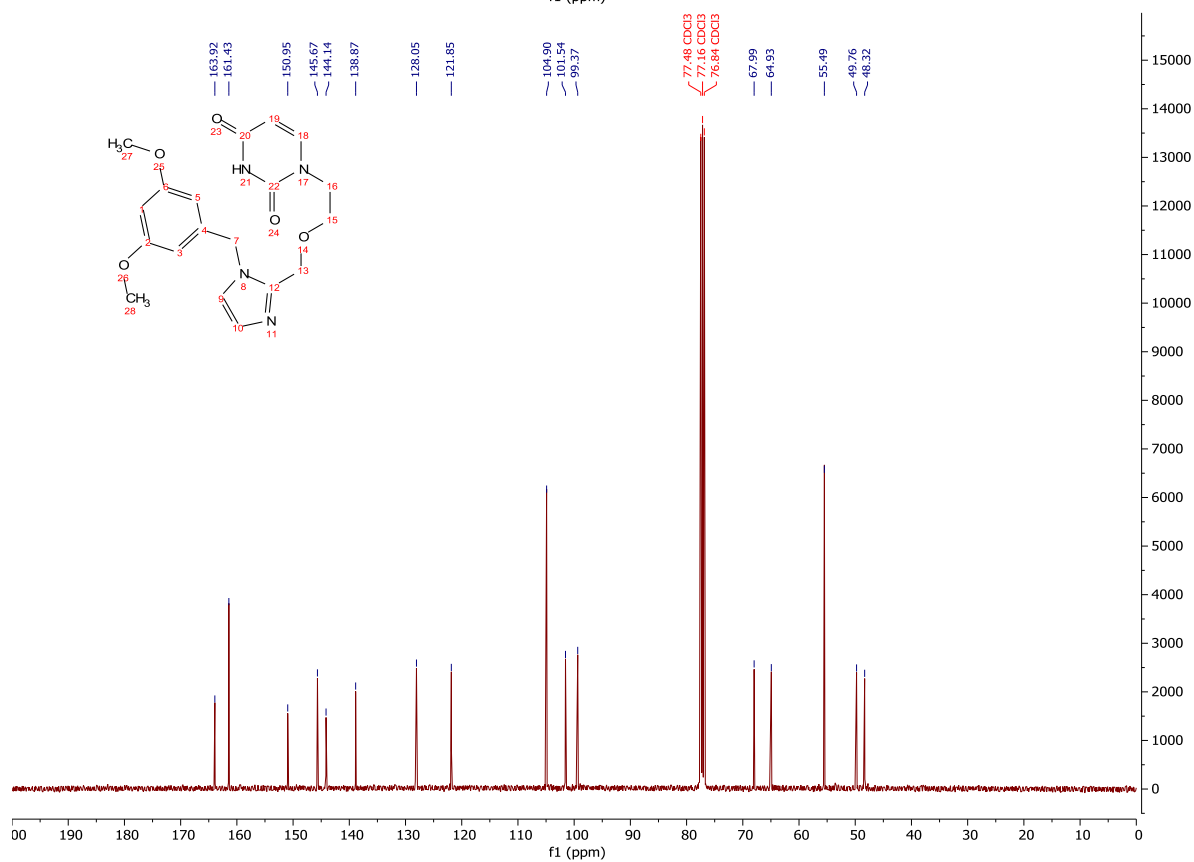
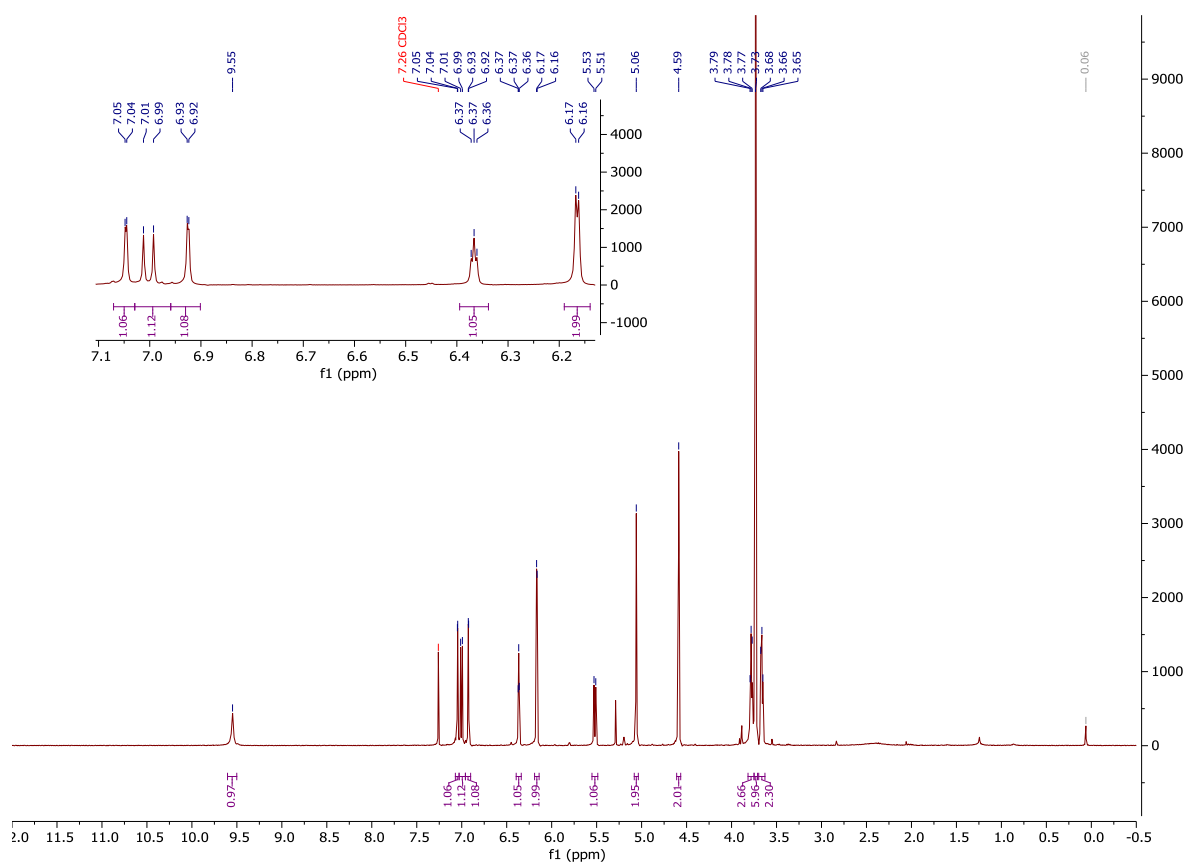
¹H-NMR and ¹³C-NMR: Compound 230



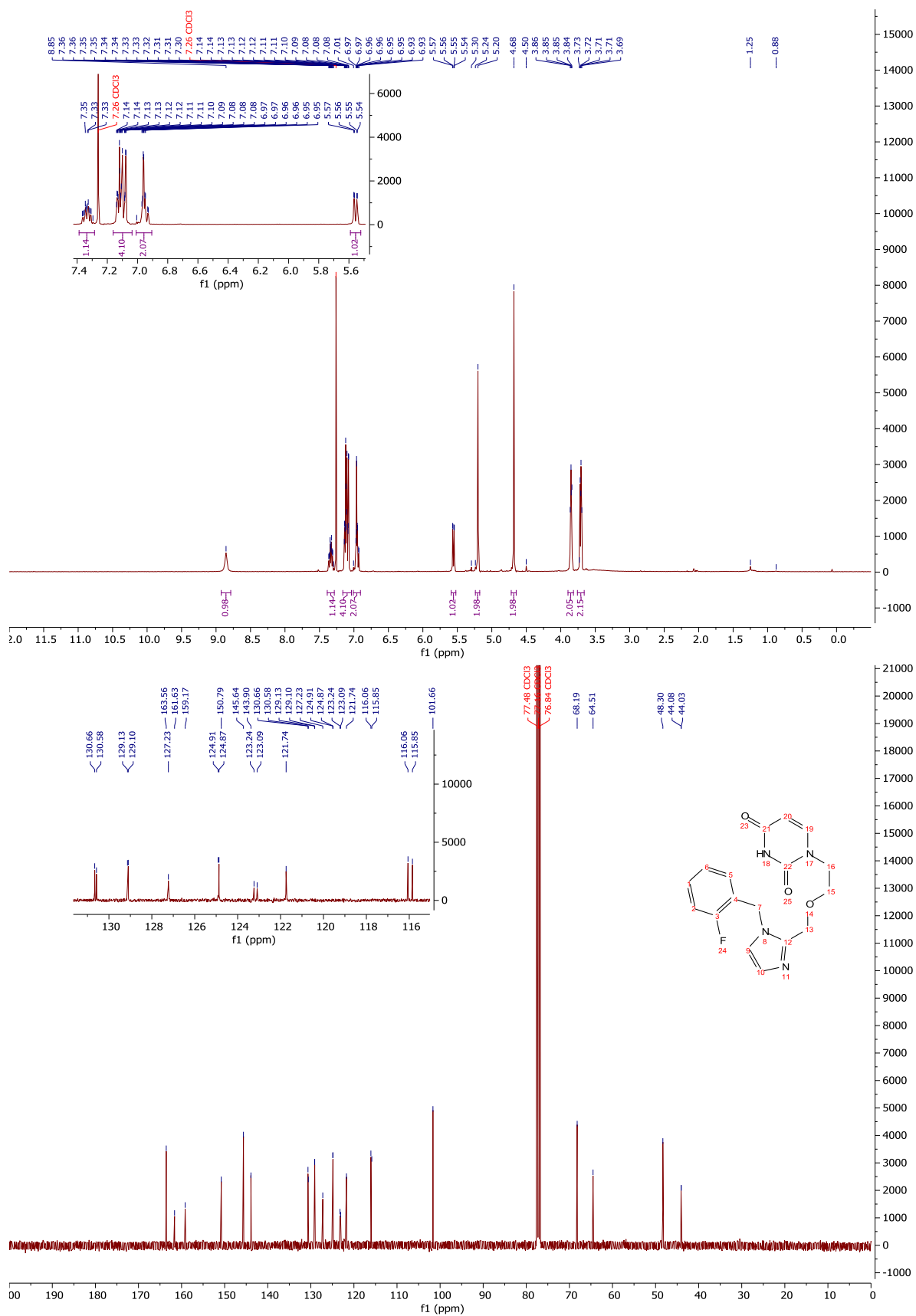
¹H-NMR and ¹³C-NMR: Compound 217



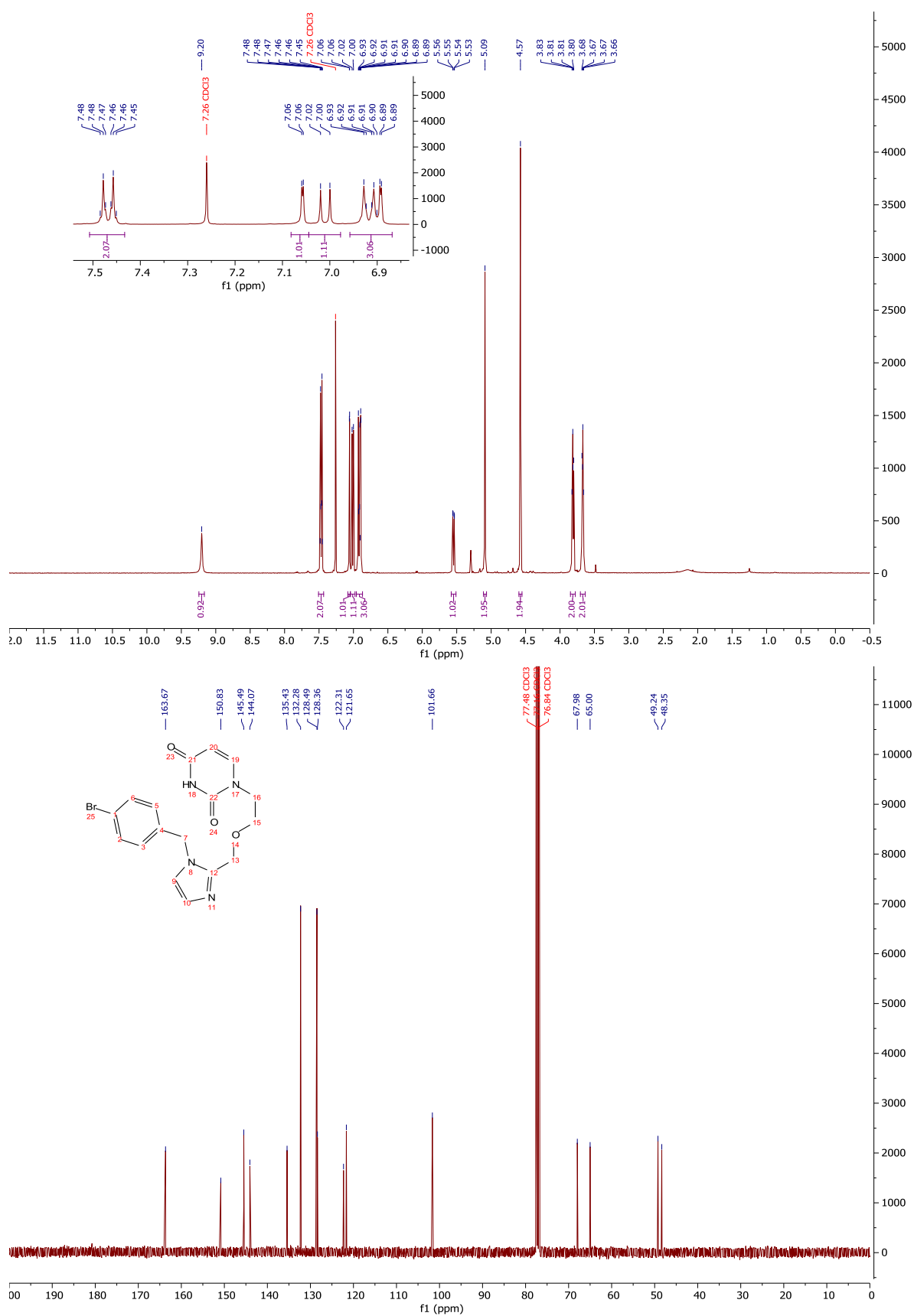
¹H-NMR and ¹³C-NMR: Compound 221



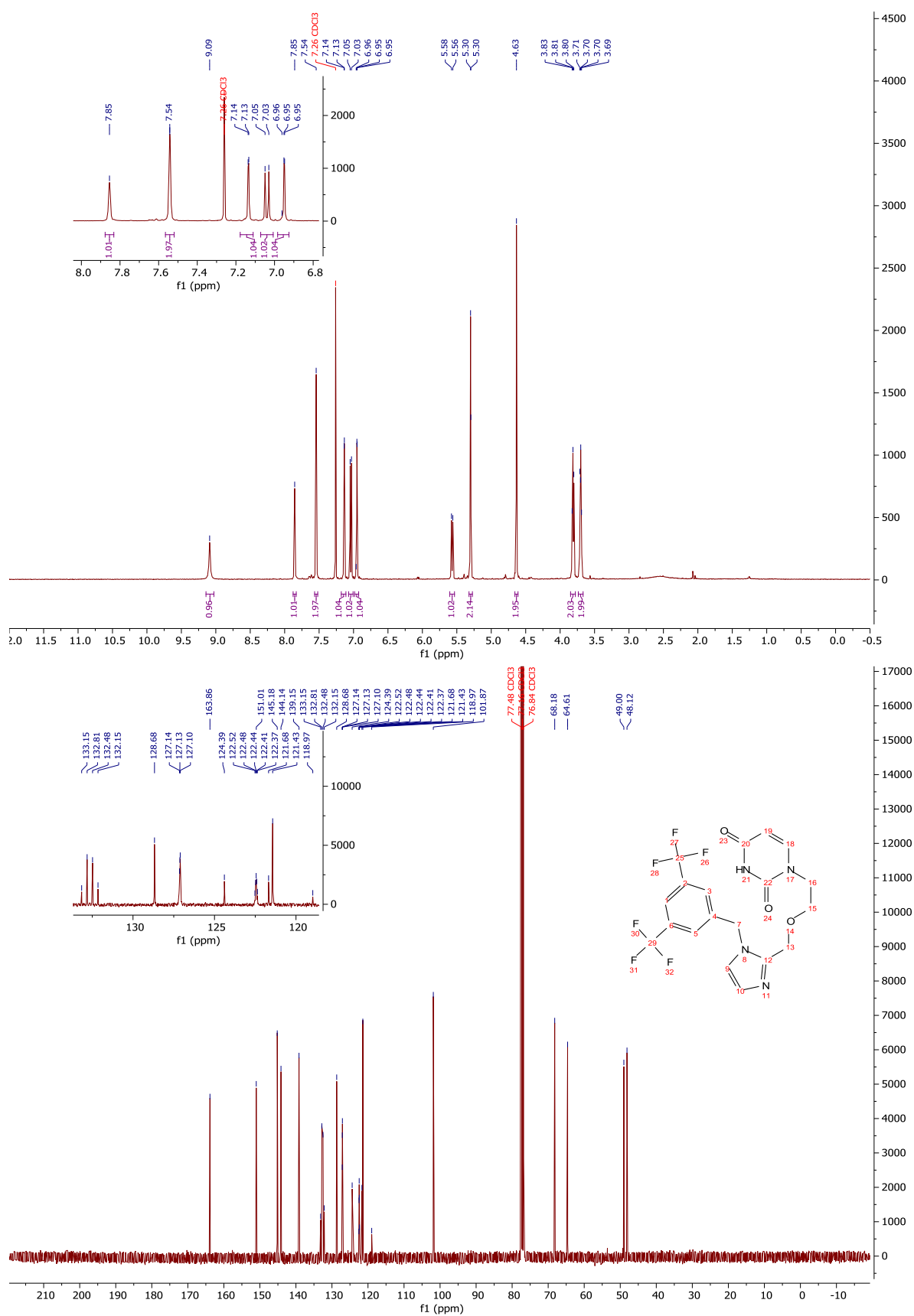
$^1\text{H-NMR}$ and $^{13}\text{C-NMR}$: Compound 207



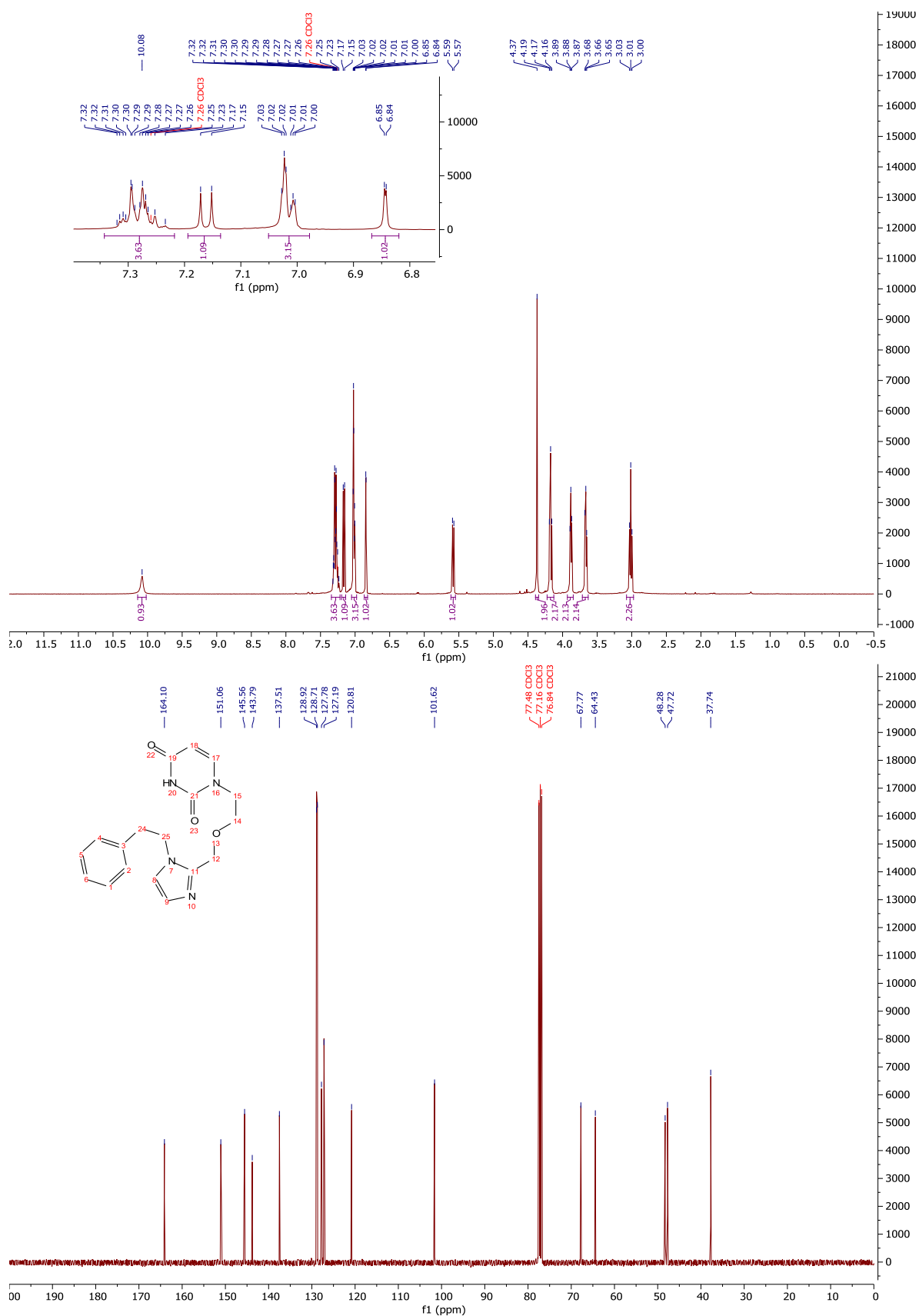
¹H-NMR and ¹³C-NMR: Compound 211



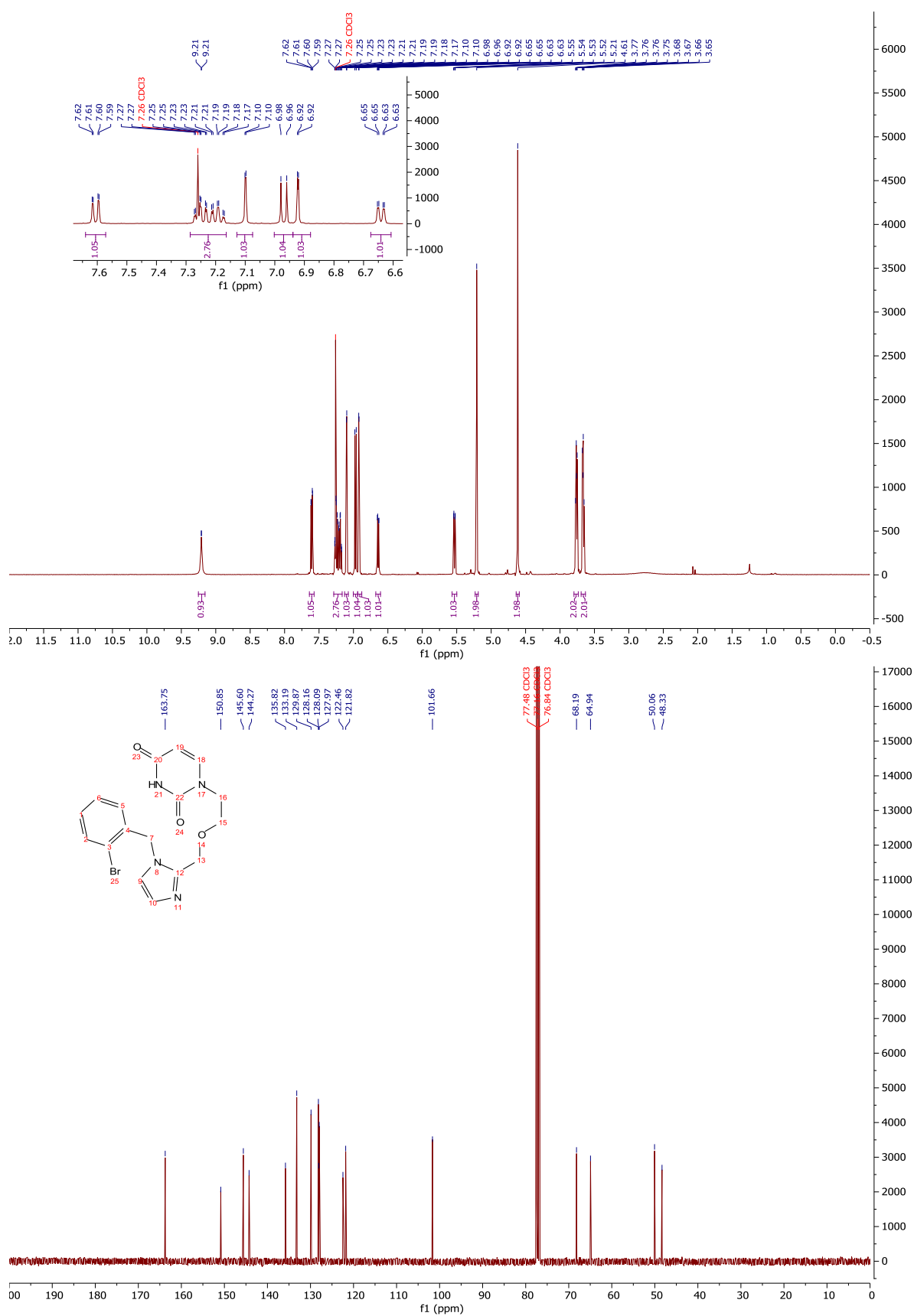
¹H-NMR and ¹³C-NMR: Compound 223



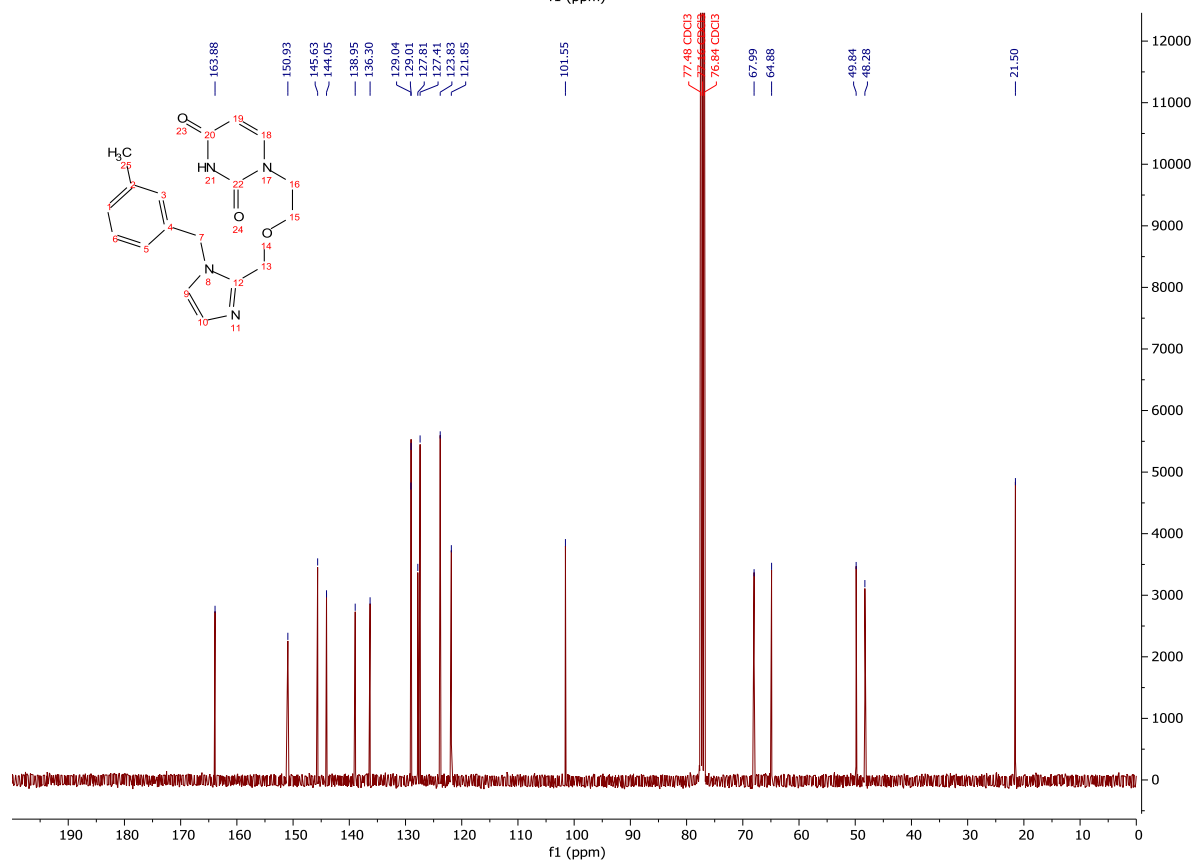
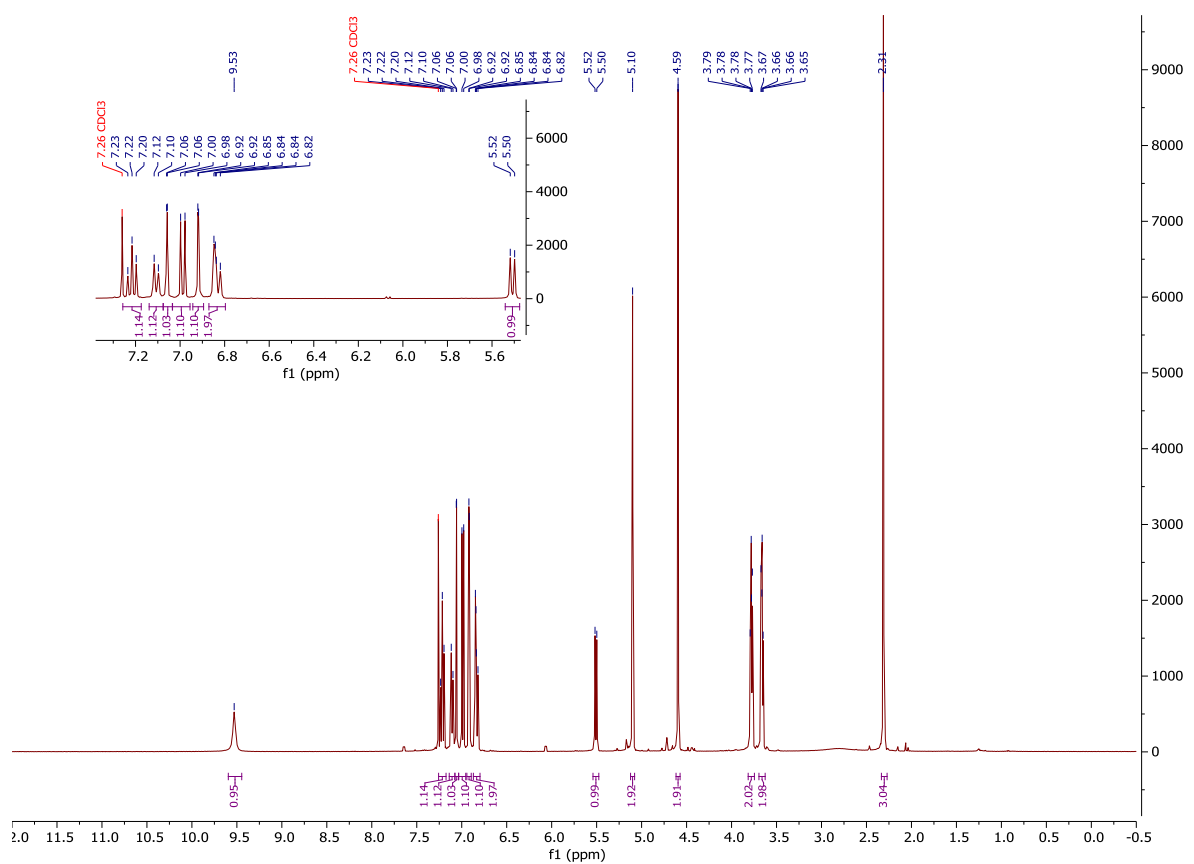
¹H-NMR and ¹³C-NMR: Compound 225



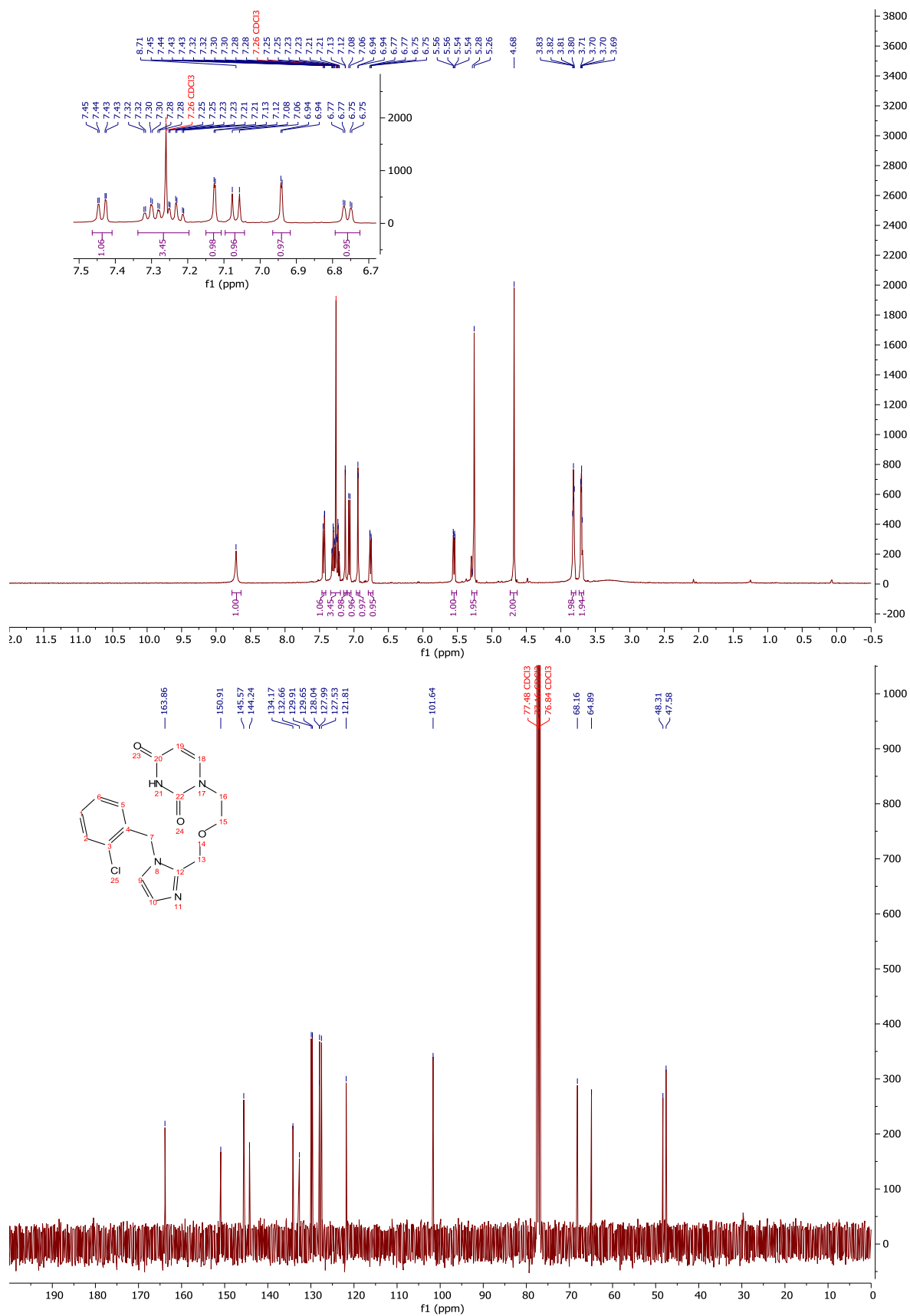
¹H-NMR and ¹³C-NMR: Compound 215



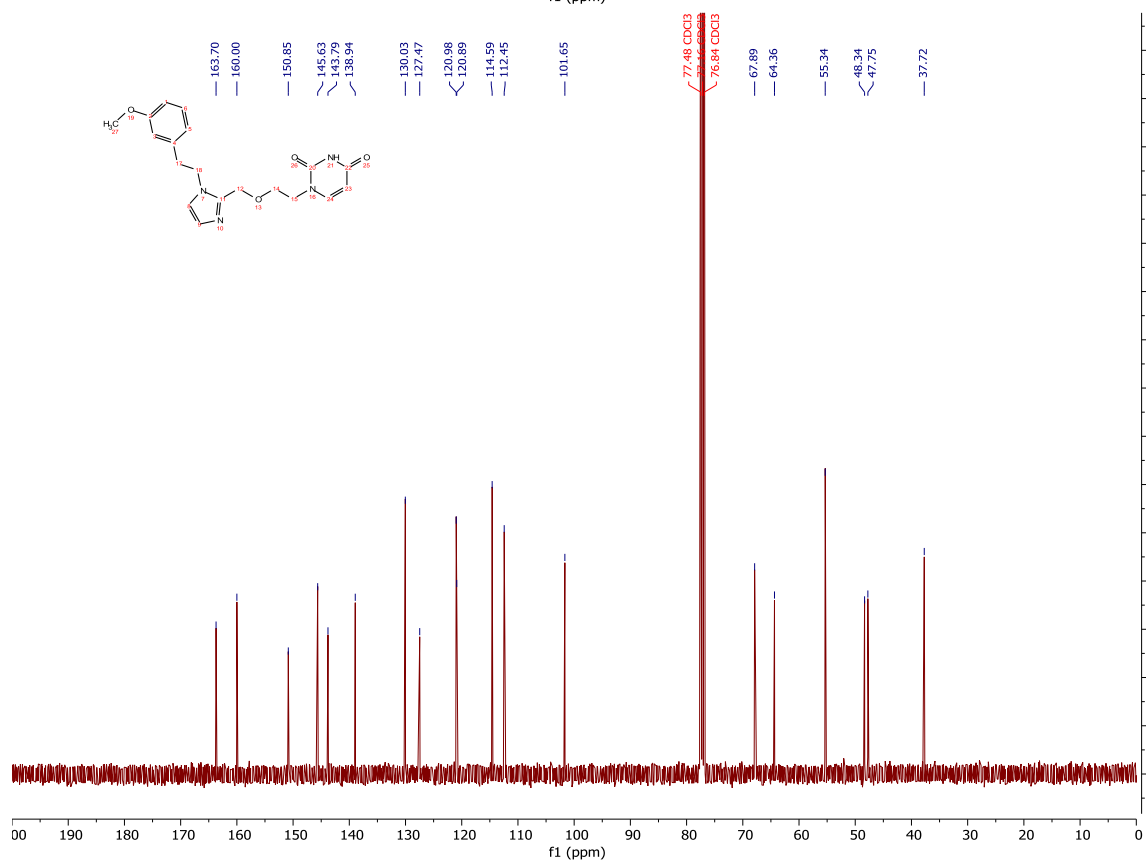
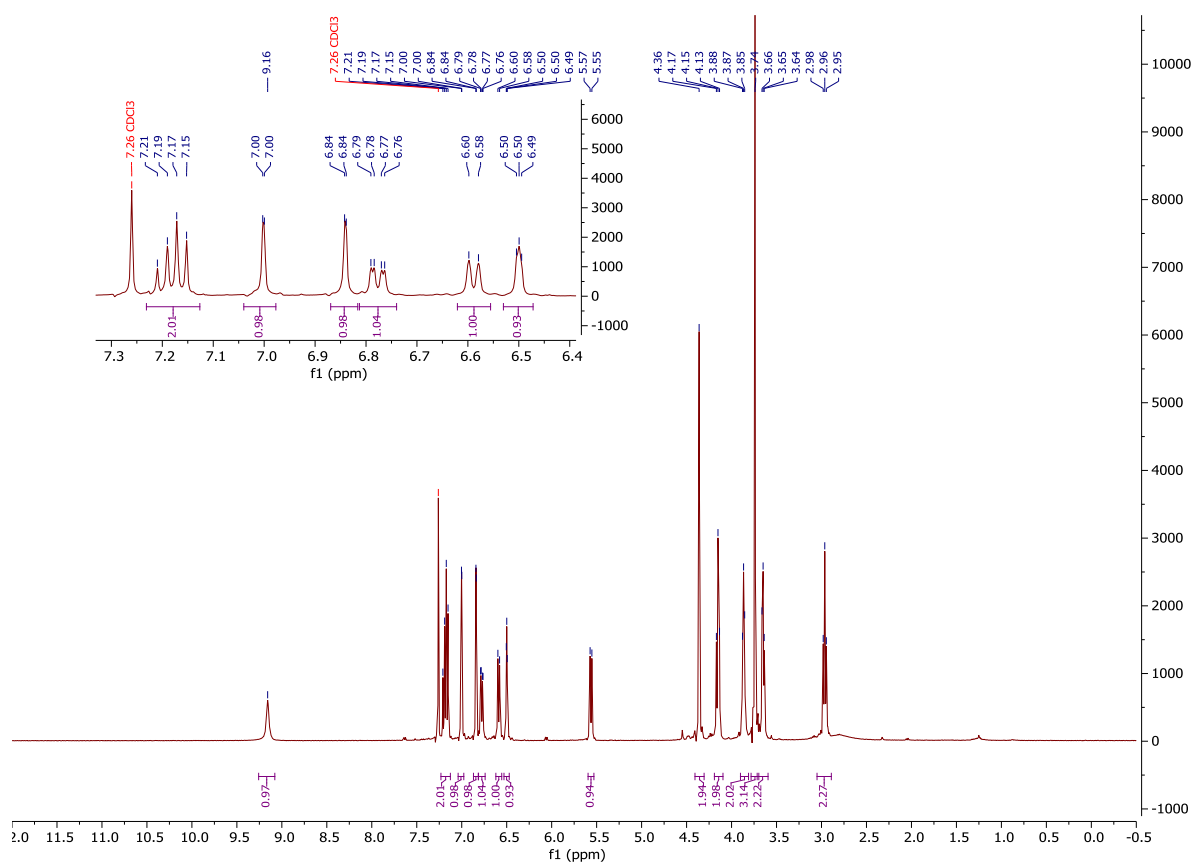
¹H-NMR and ¹³C-NMR: Compound 213



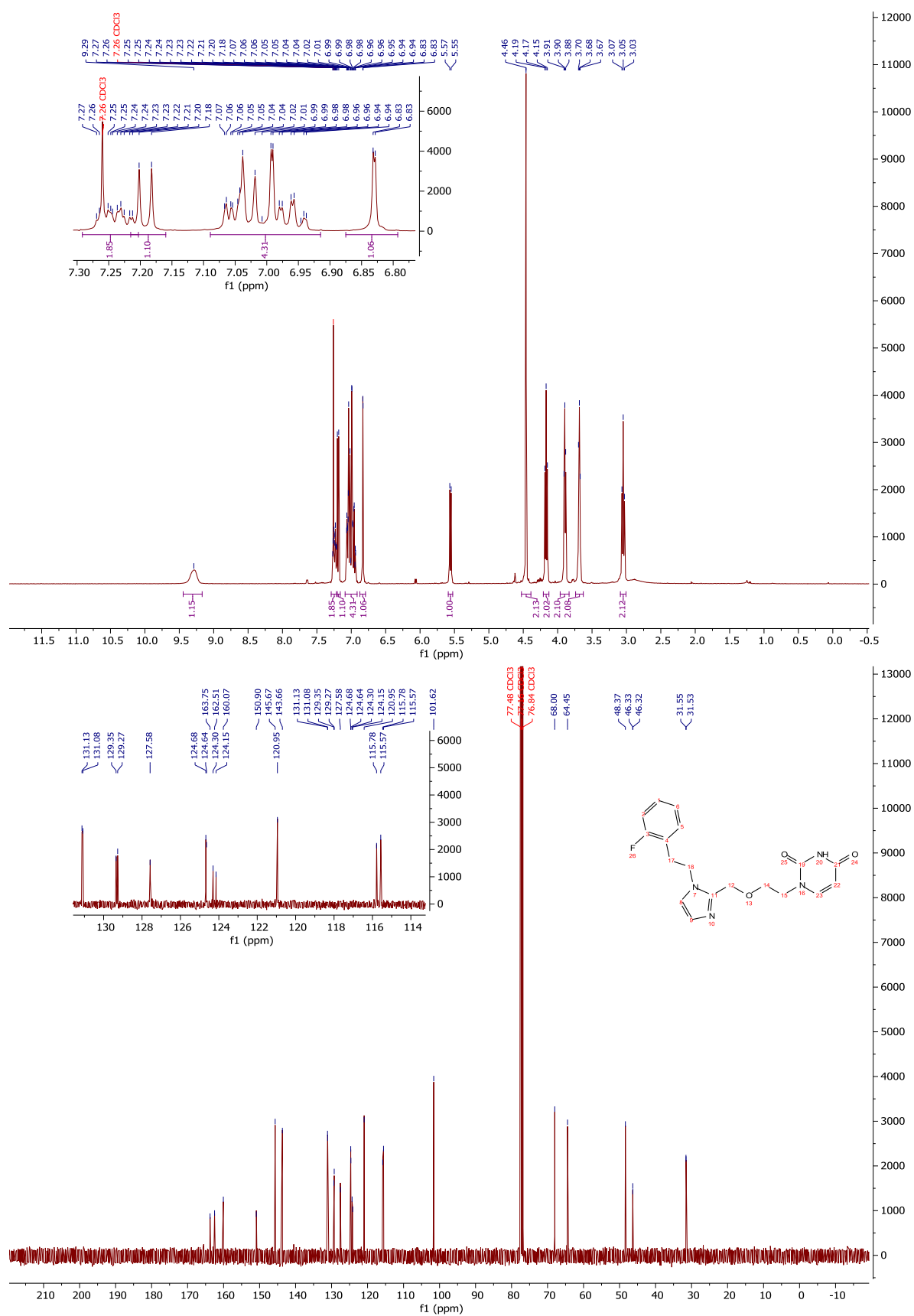
¹H-NMR and ¹³C-NMR: Compound 219



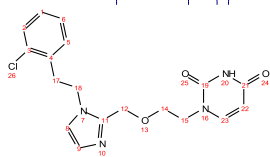
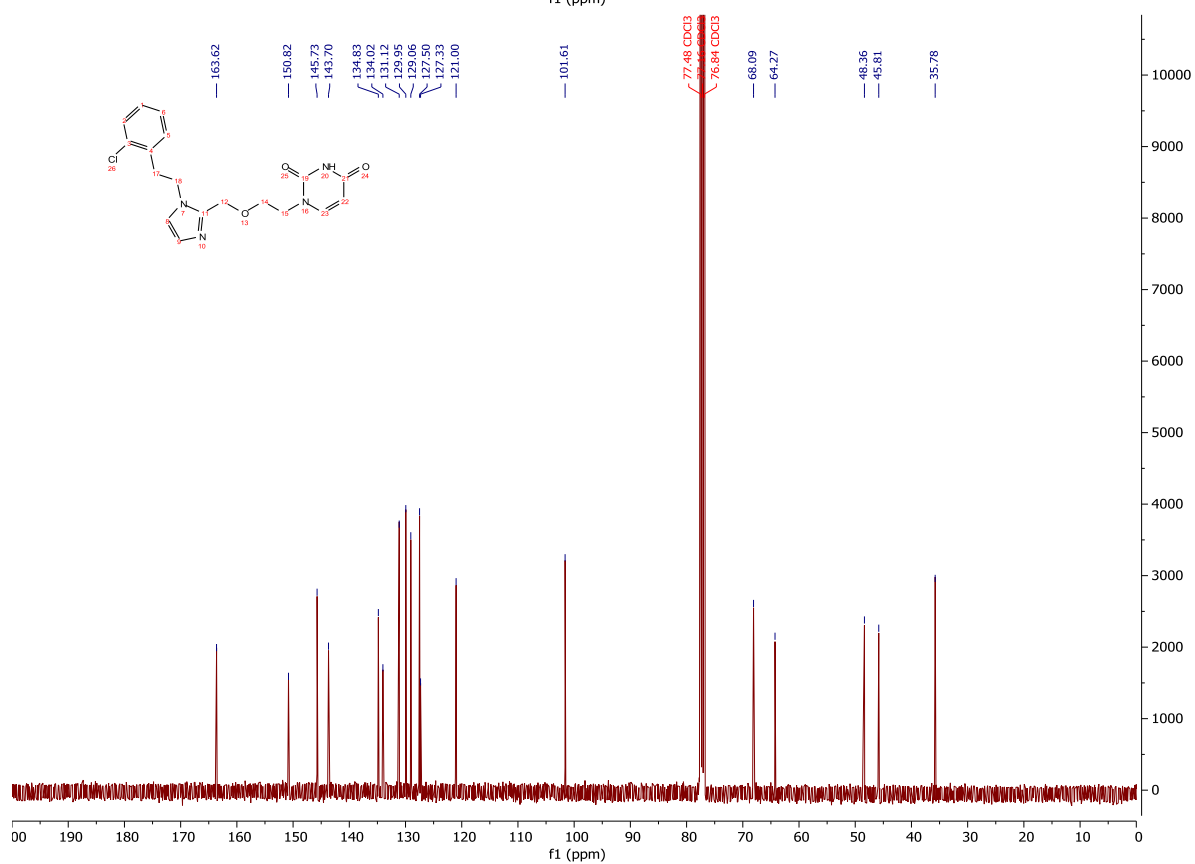
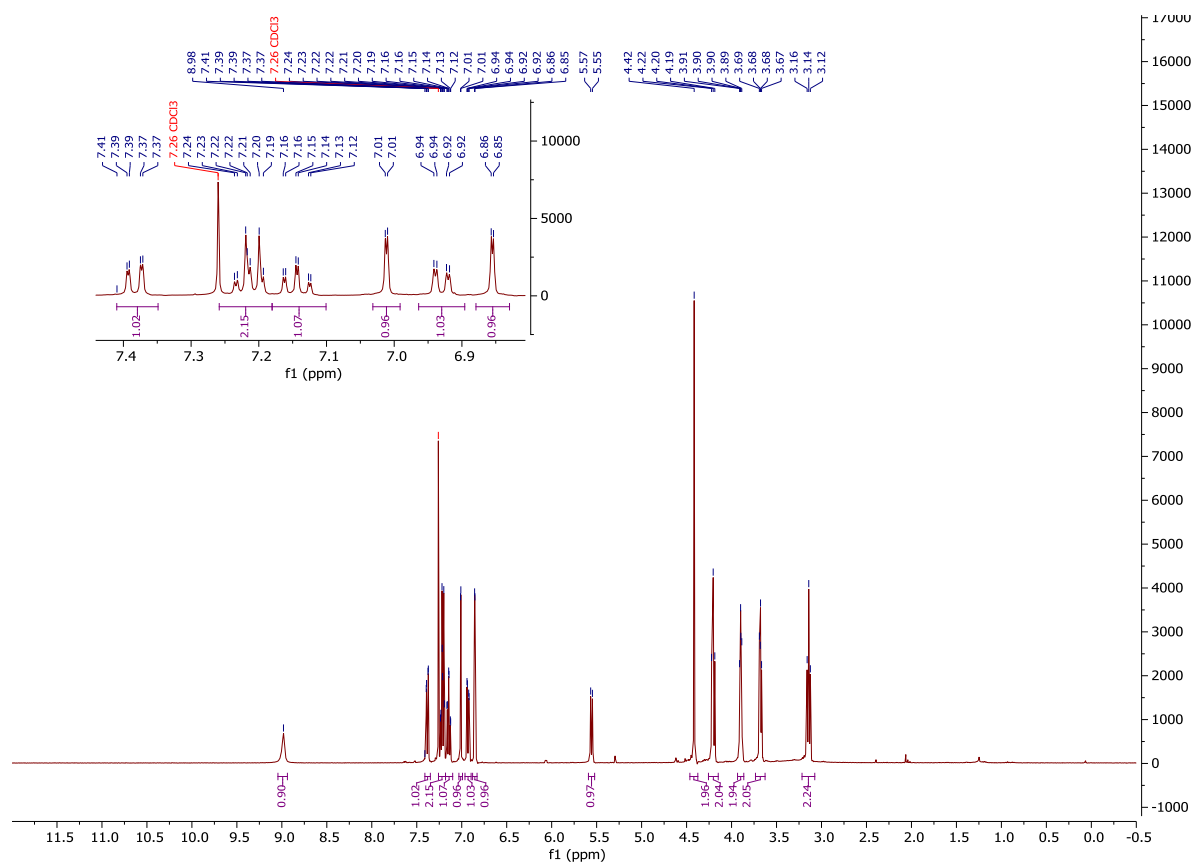
¹H-NMR and ¹³C-NMR: Compound 227



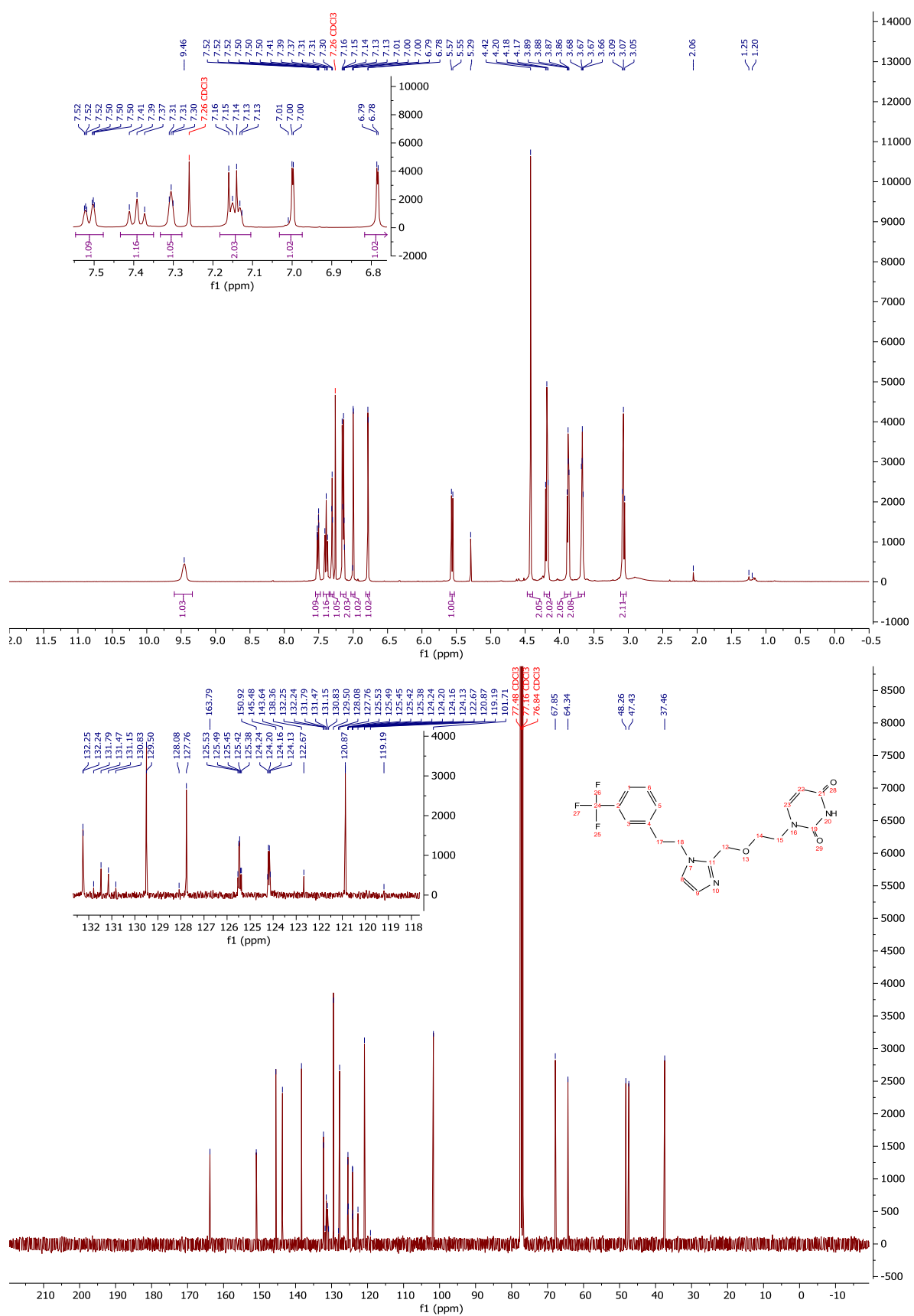
¹H-NMR and ¹³C-NMR: Compound 229



¹H-NMR and ¹³C-NMR: Compound 231

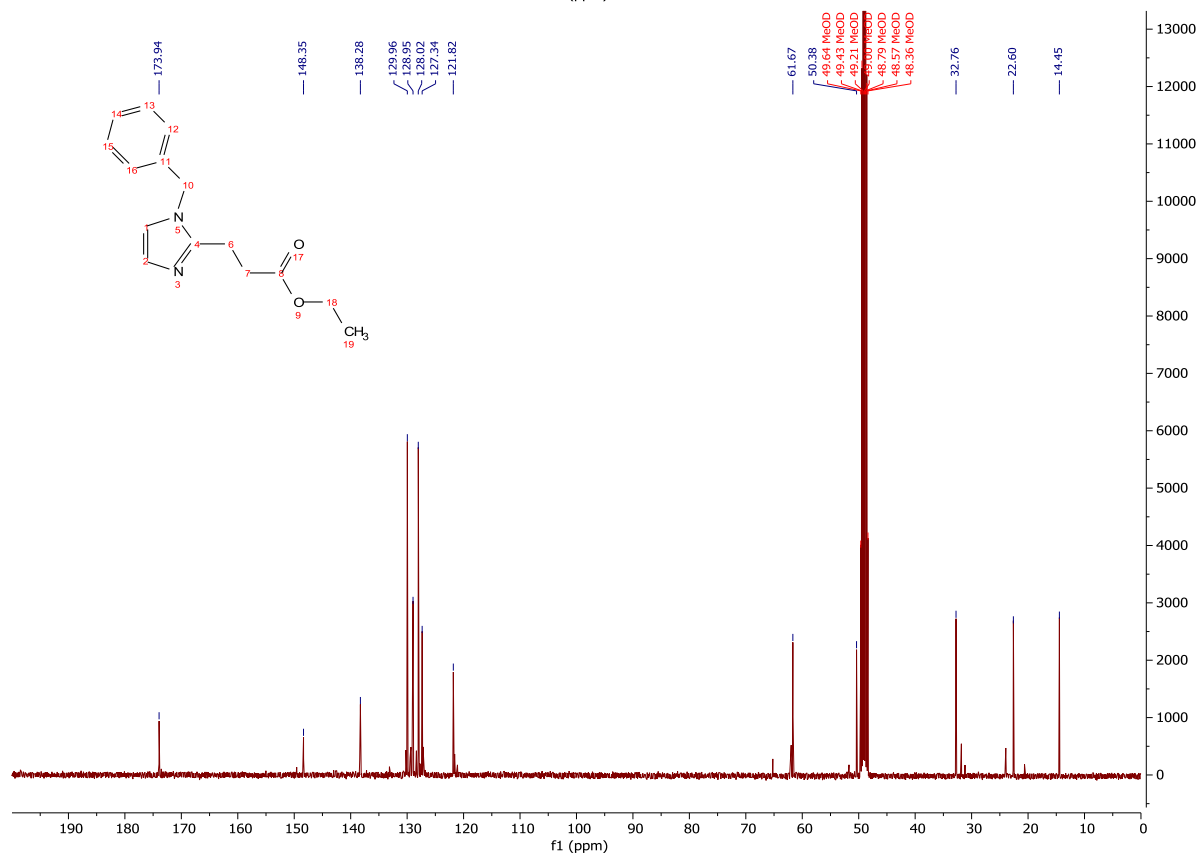
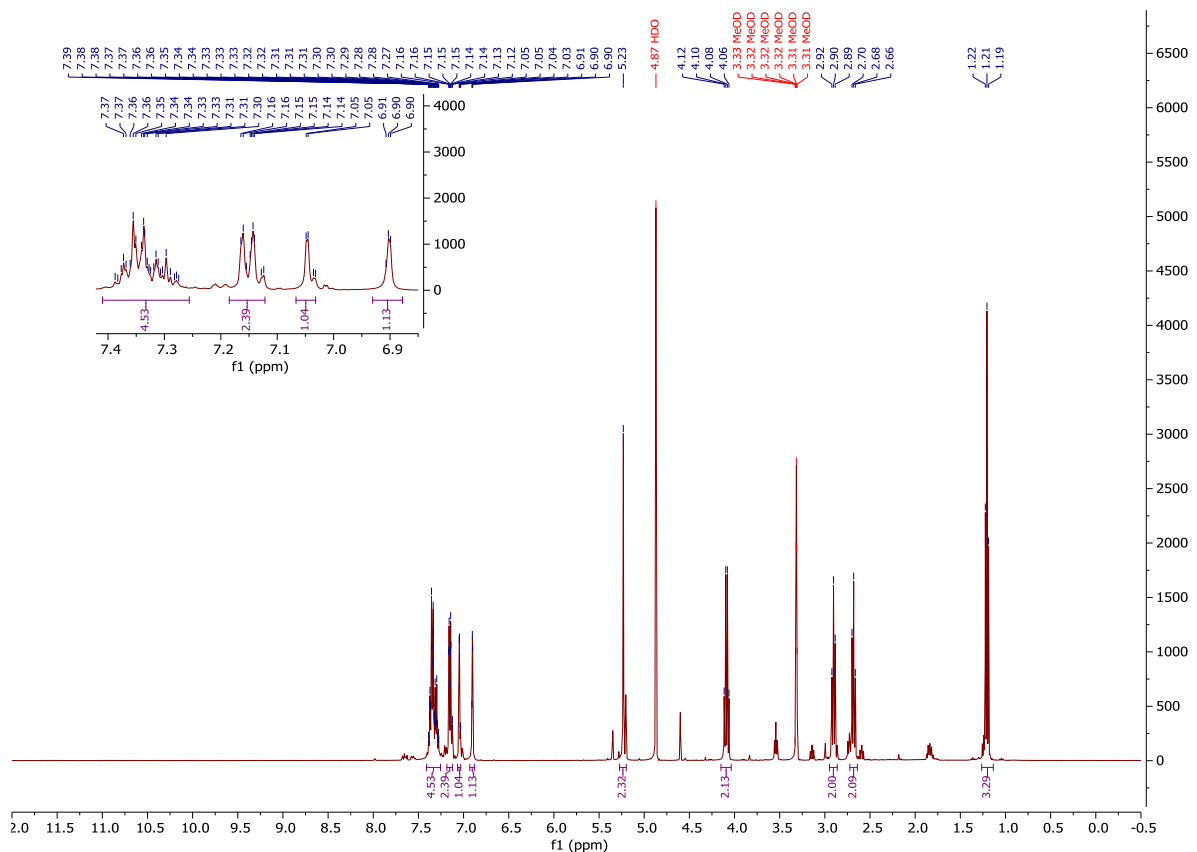


$^1\text{H-NMR}$ and $^{13}\text{C-NMR}$: Compound 235

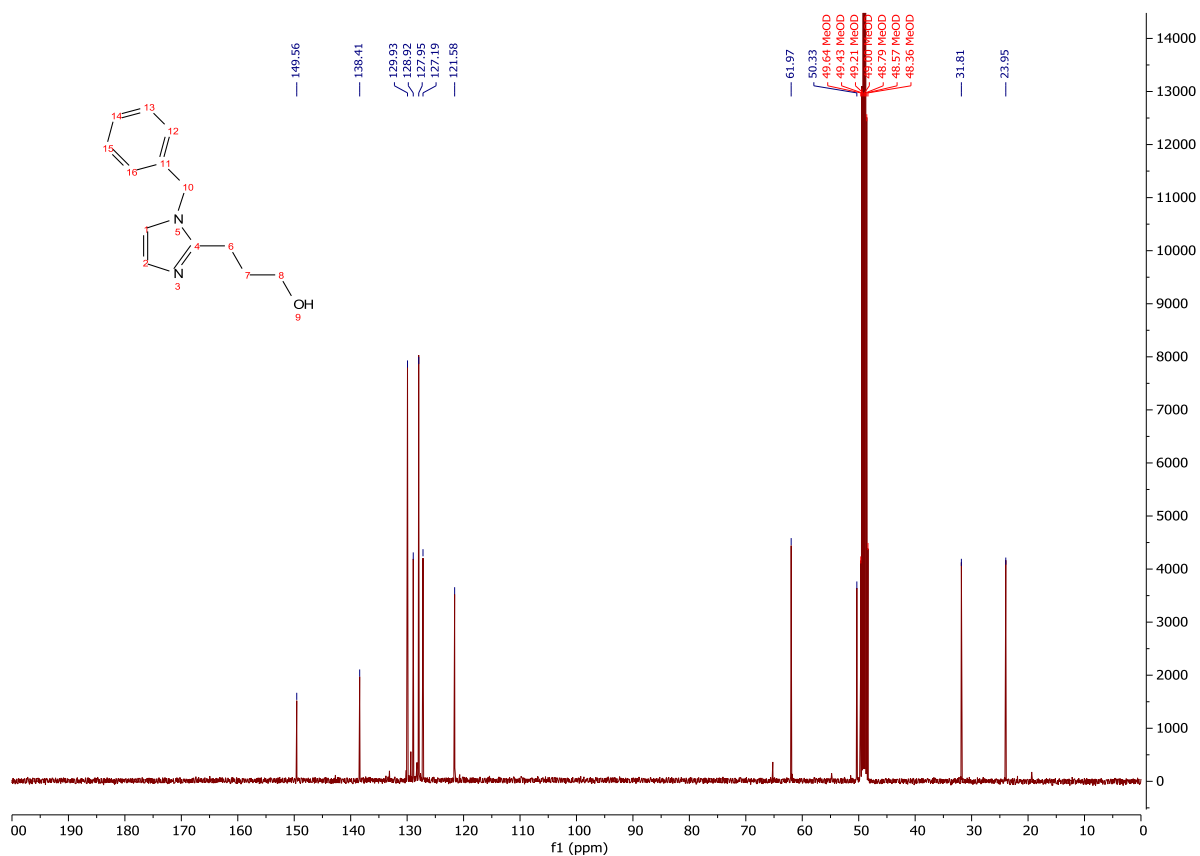
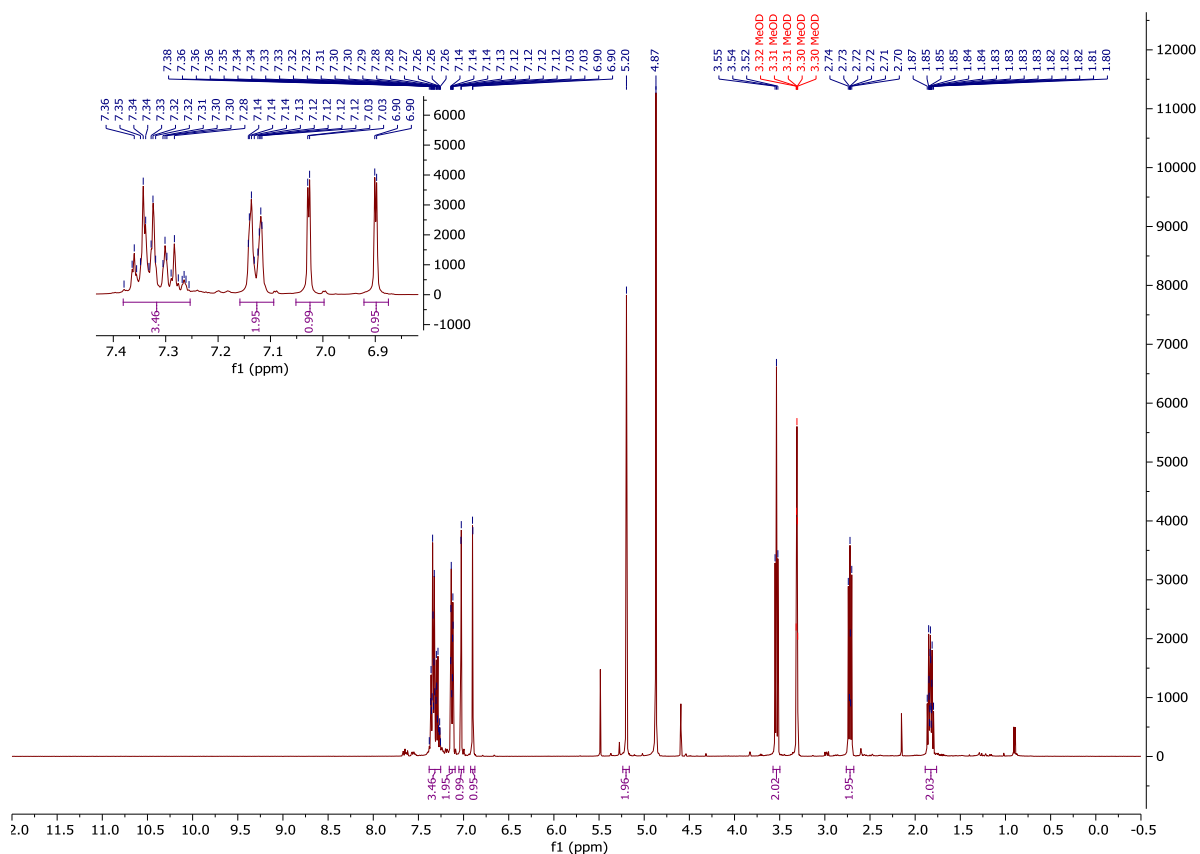


Synthesis discussed in section 4.7

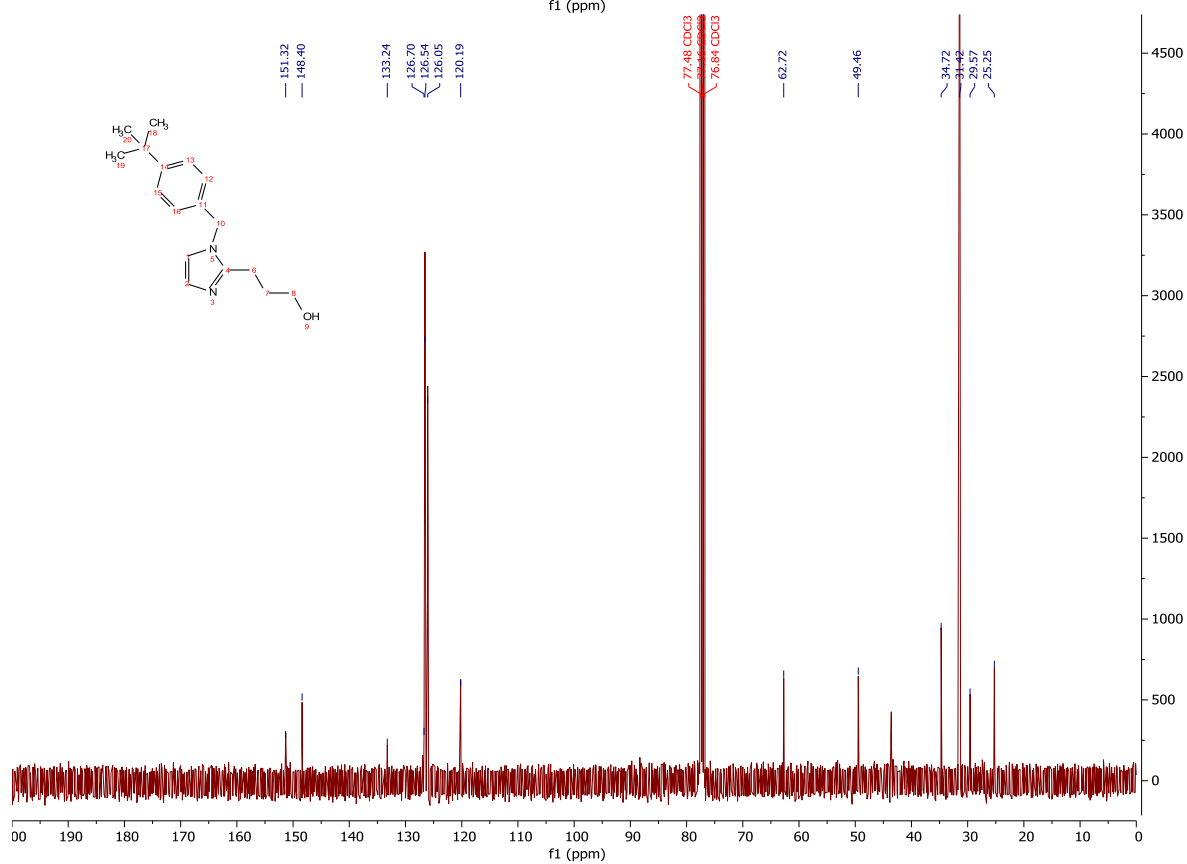
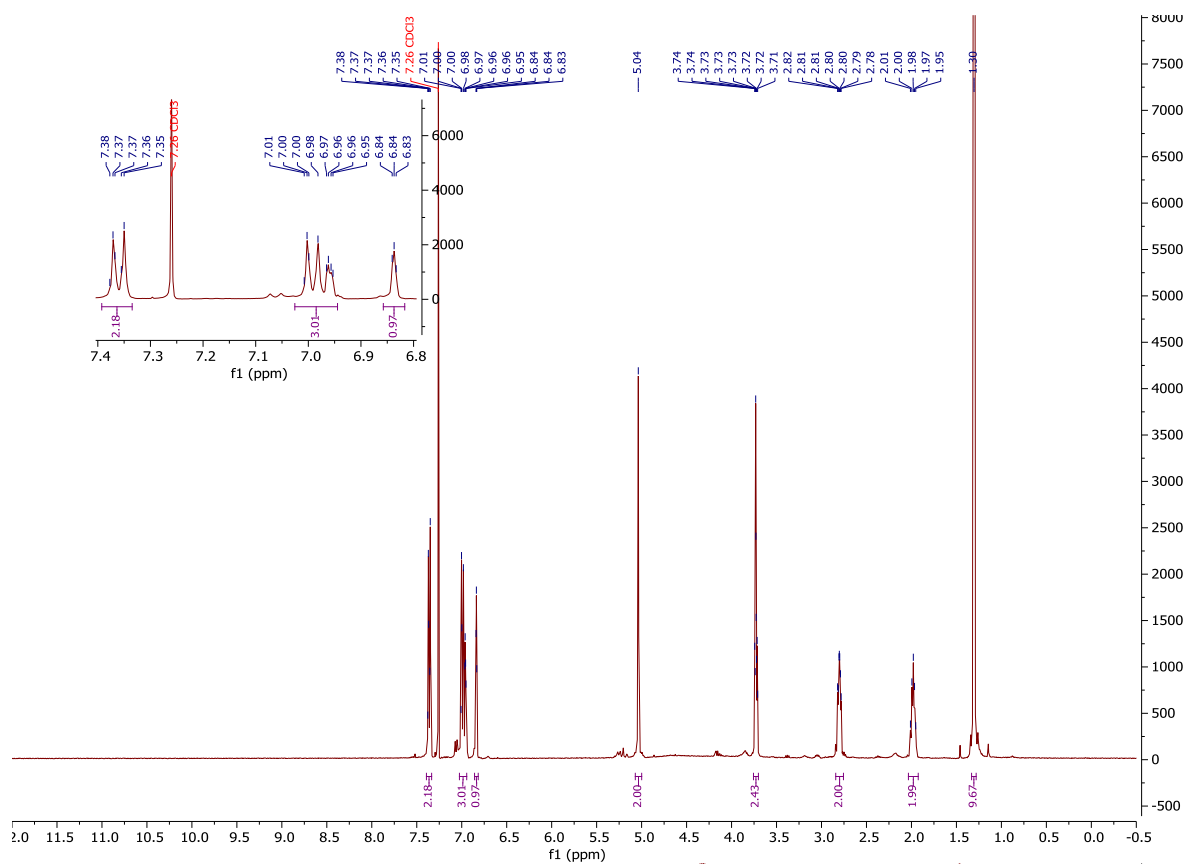
¹H-NMR and ¹³C-NMR: Compound 237



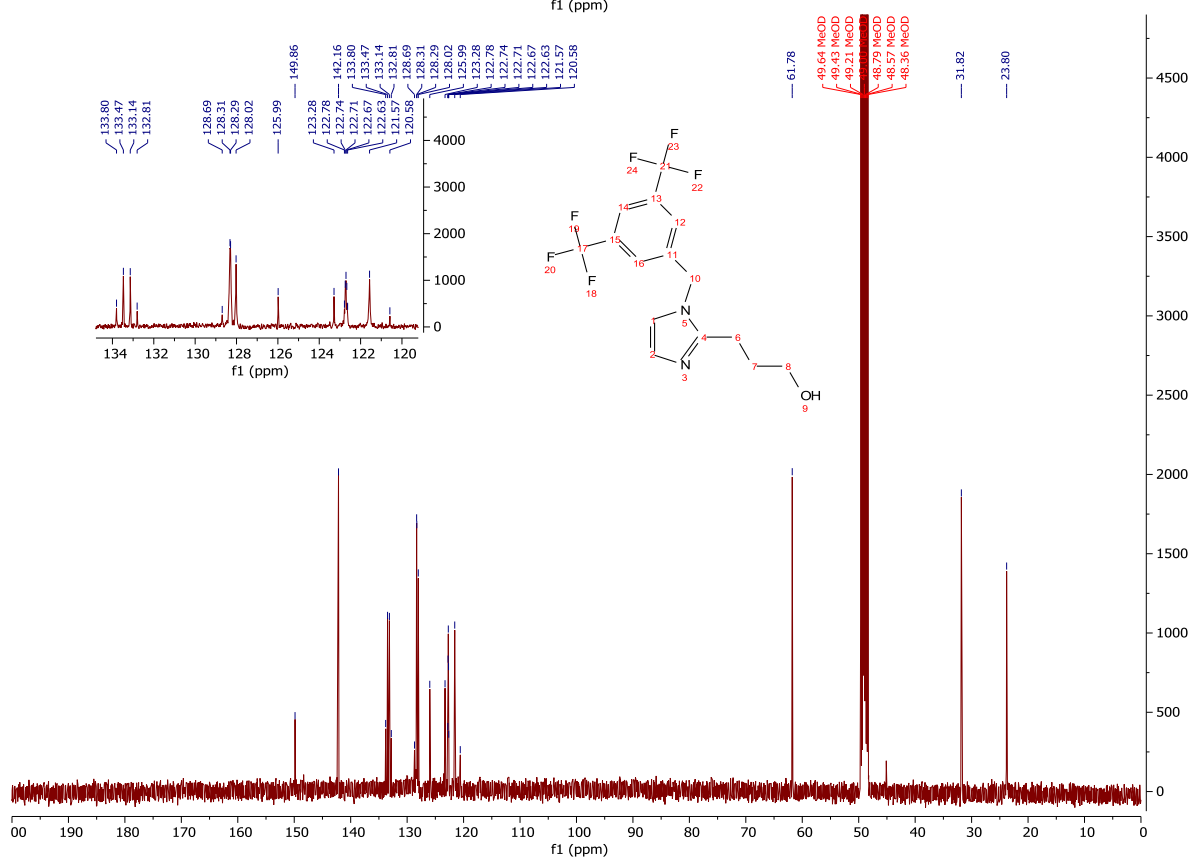
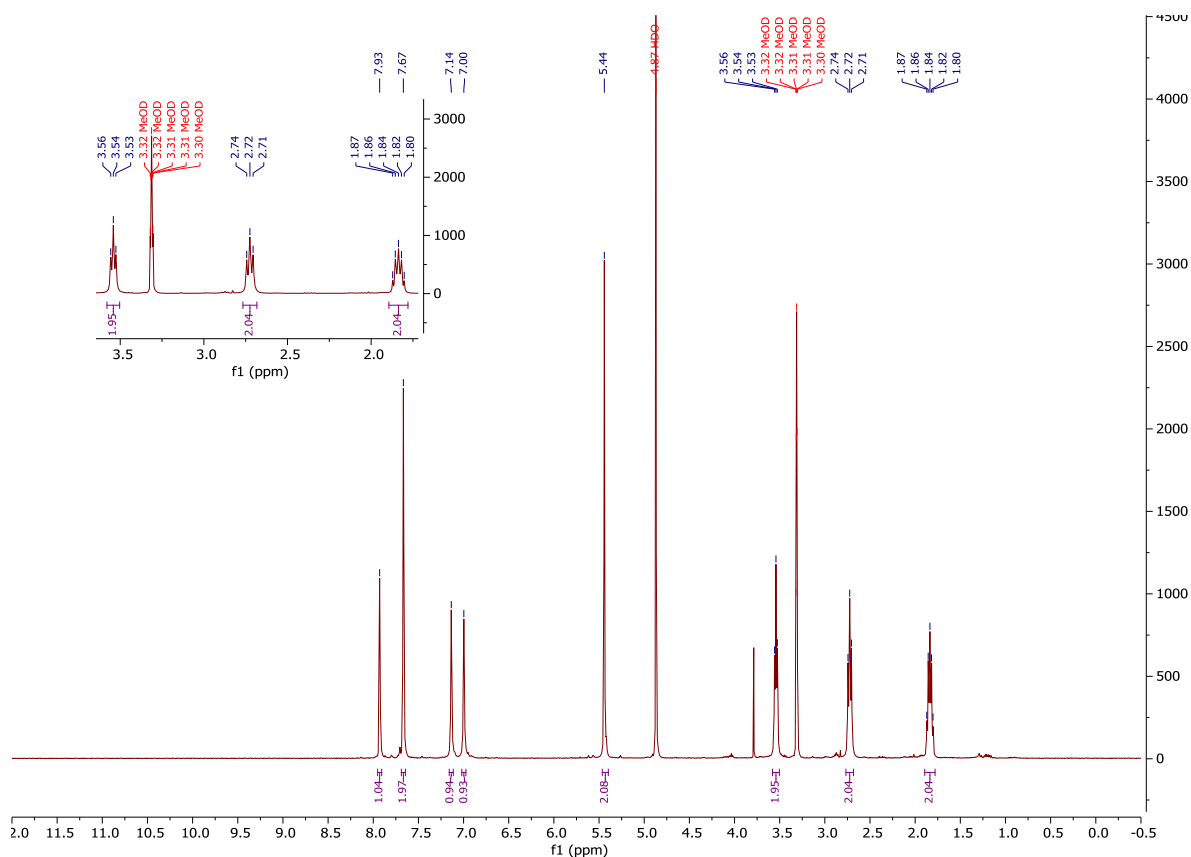
¹H-NMR and ¹³C-NMR: Compound 78



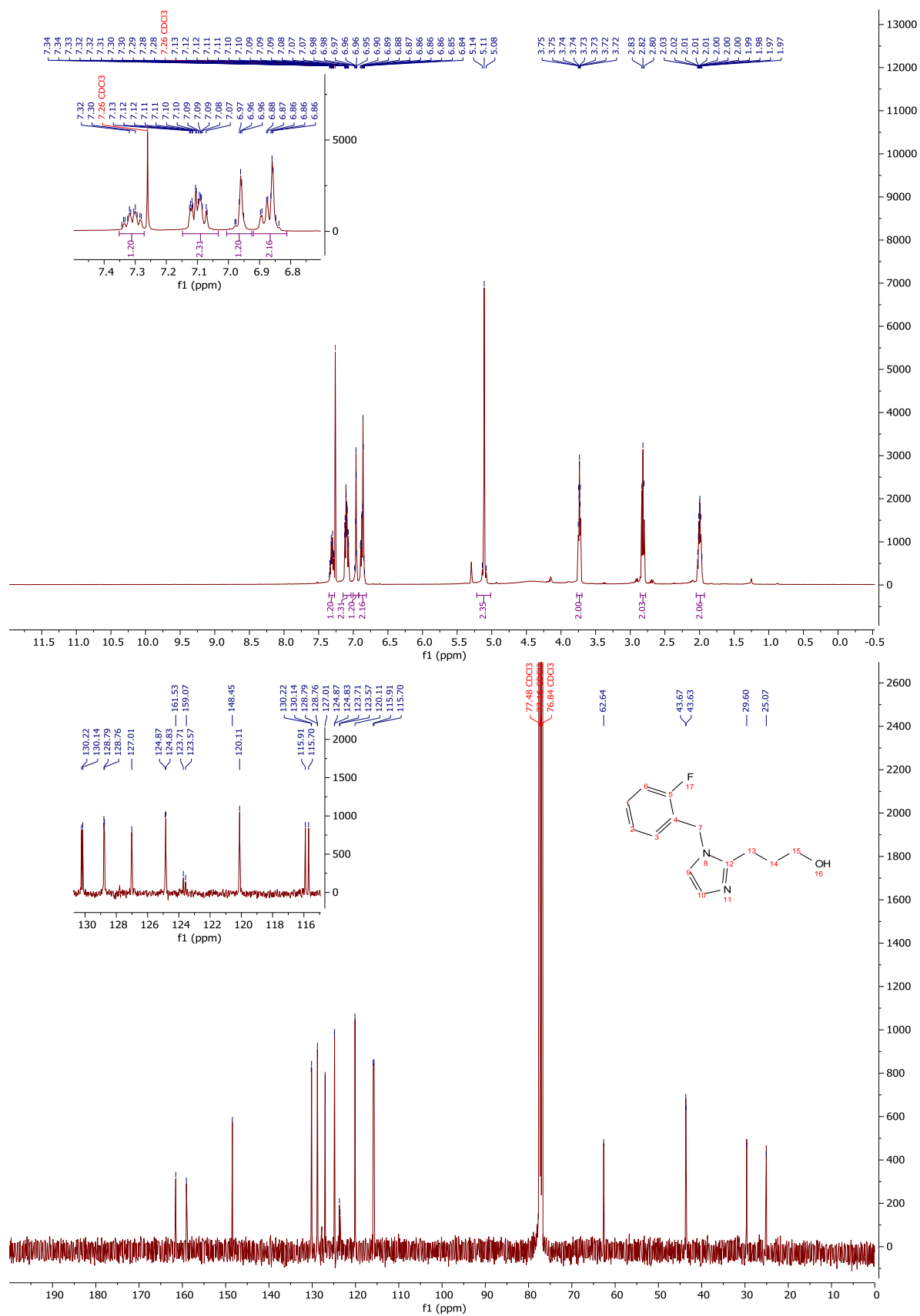
¹H-NMR and ¹³C-NMR: Compound 239



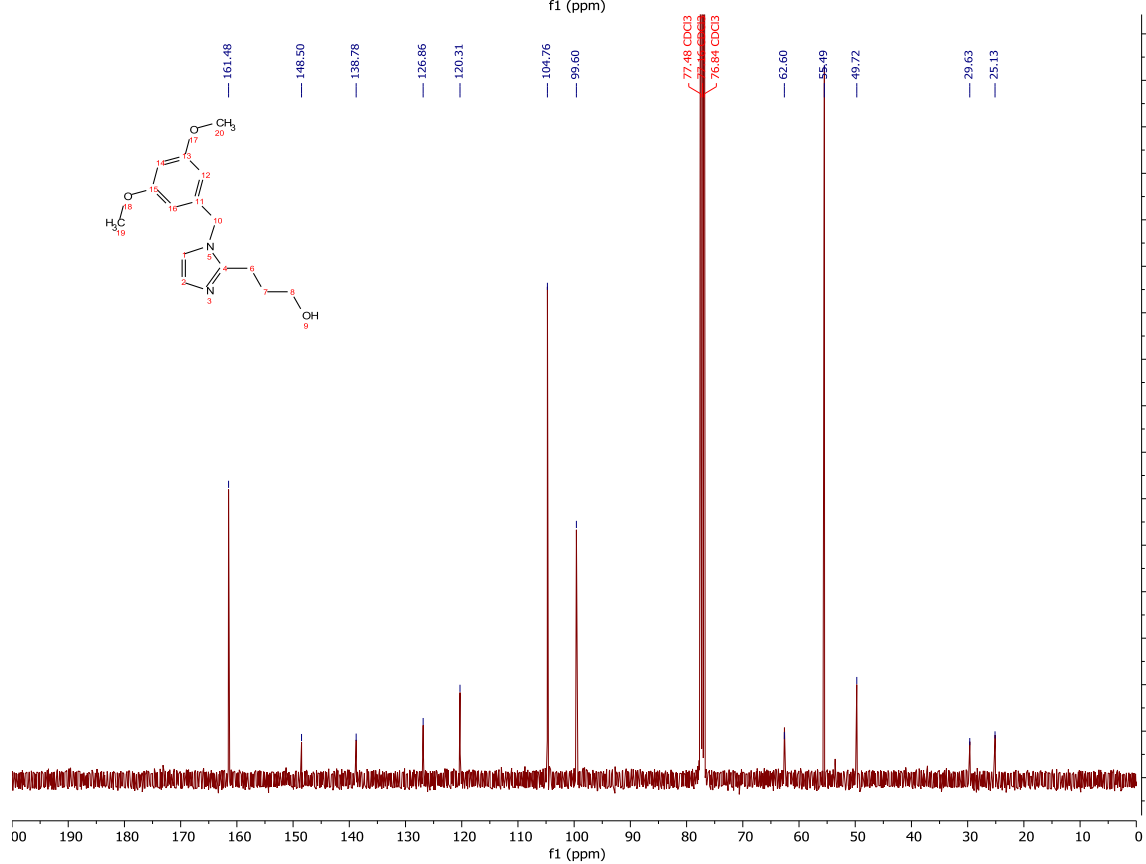
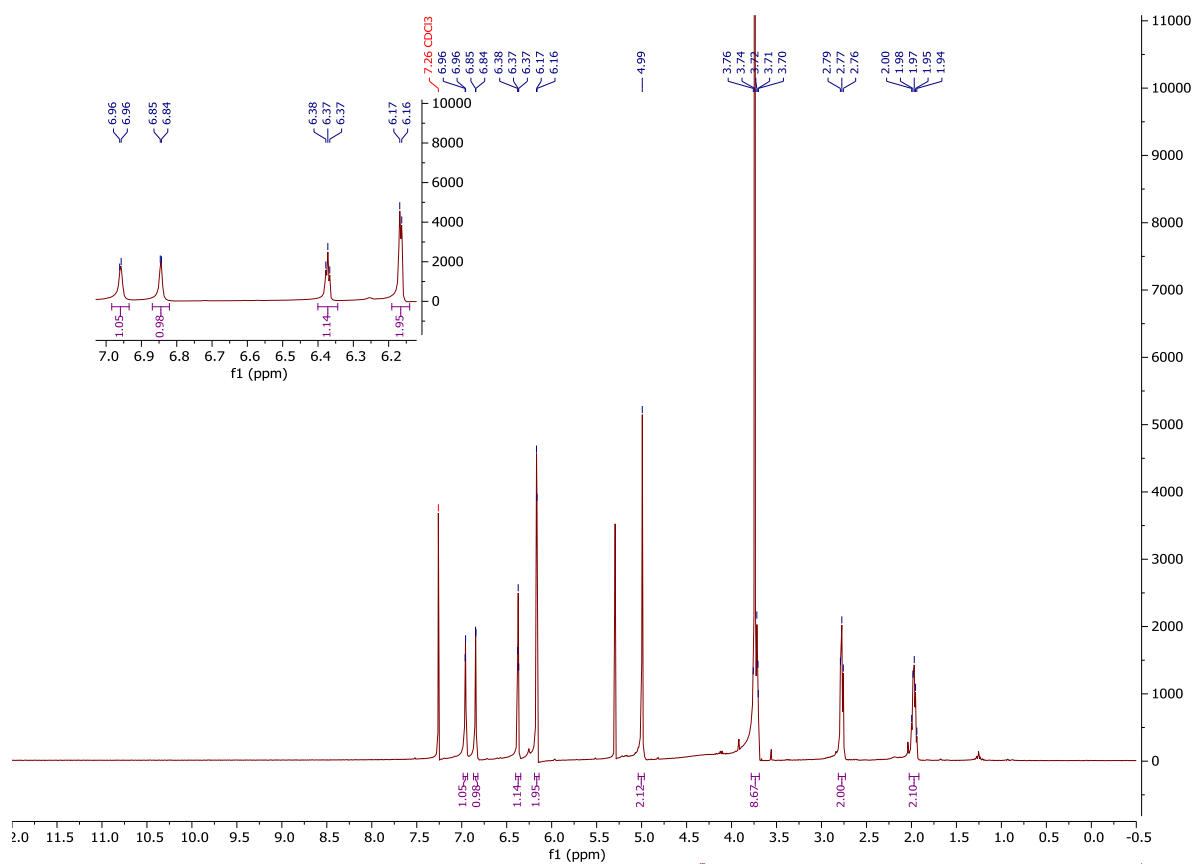
¹H-NMR and ¹³C-NMR: Compound 83



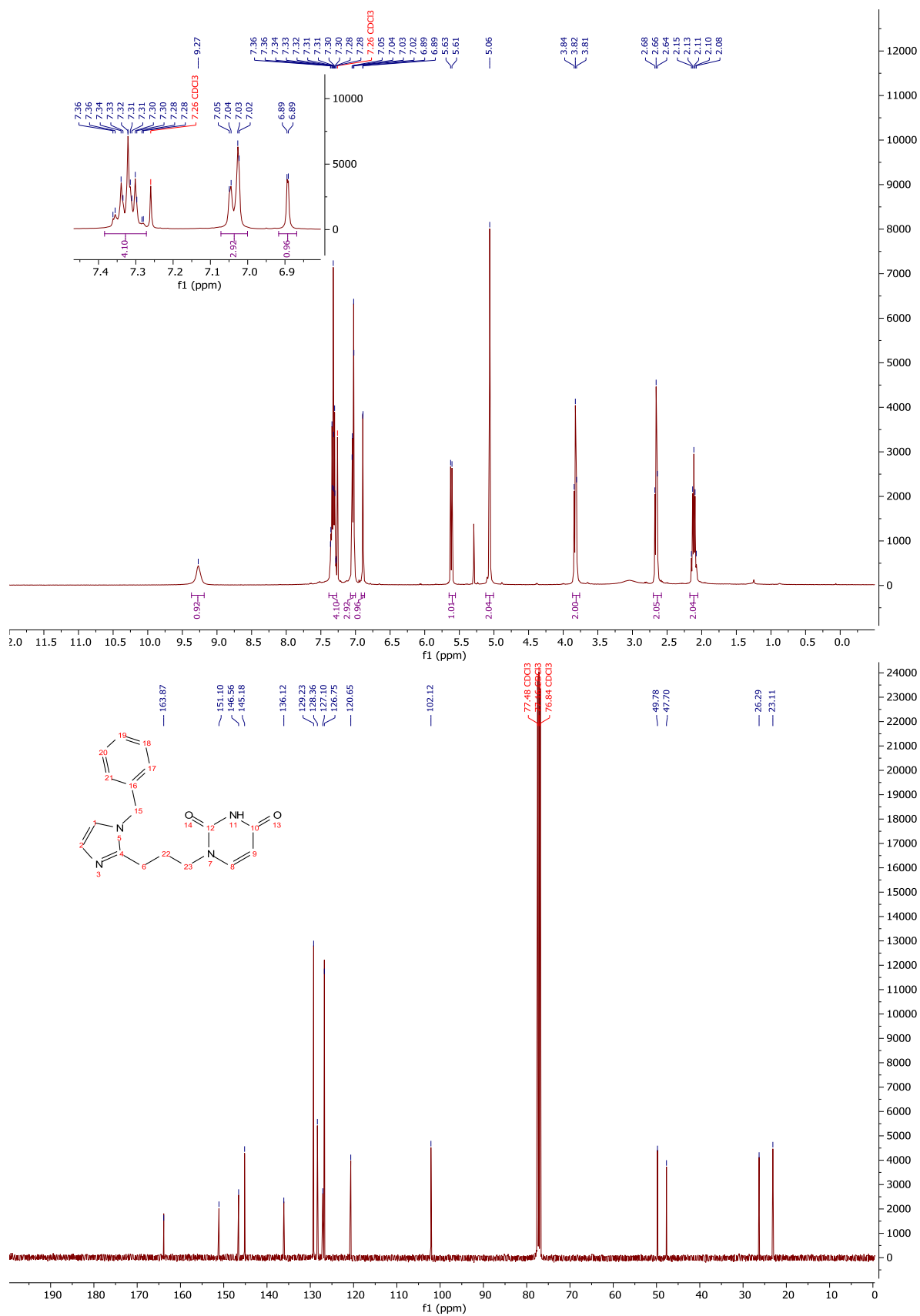
¹H-NMR and ¹³C-NMR: Compound 240



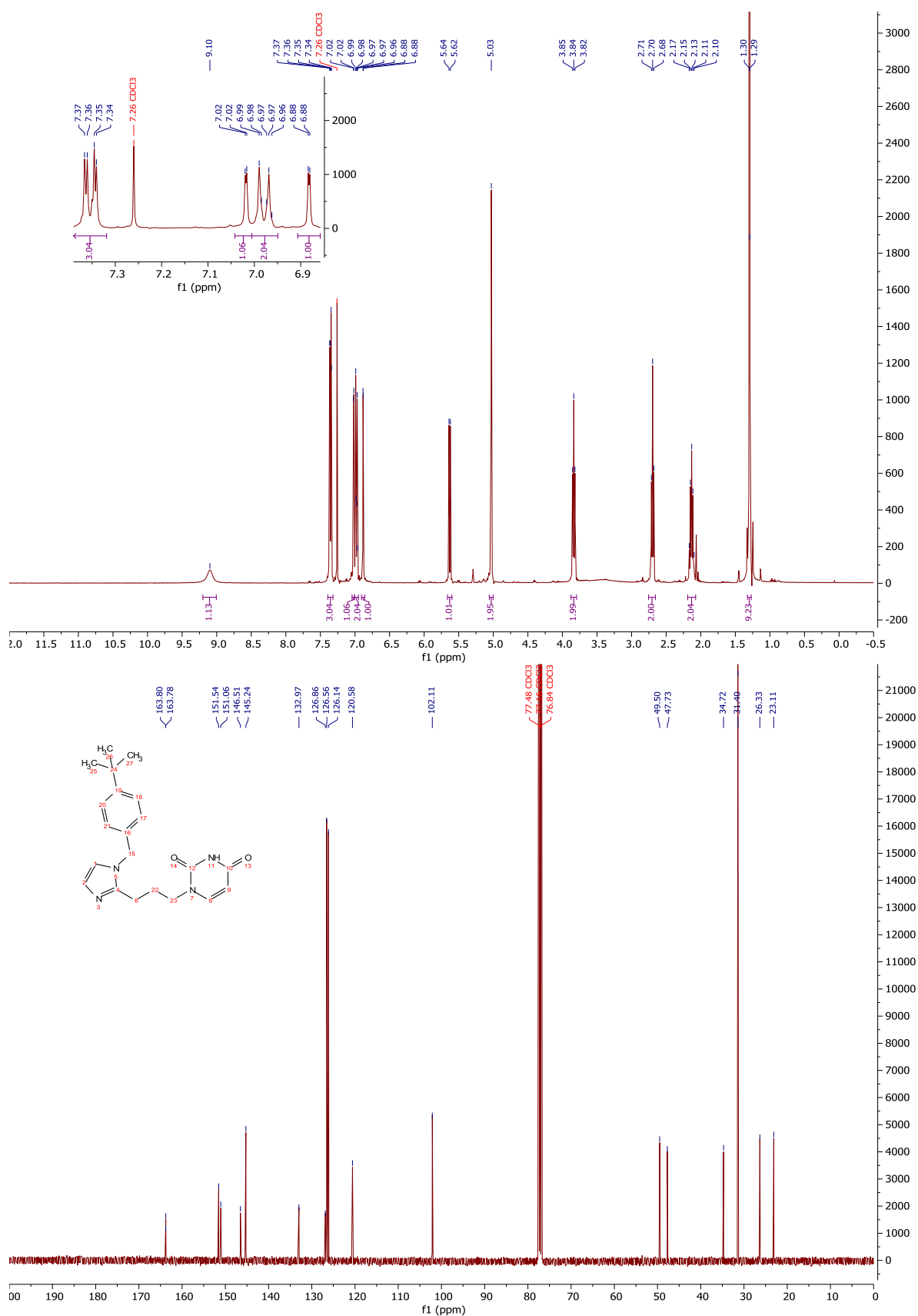
$^1\text{H-NMR}$ and $^{13}\text{C-NMR}$: Compound 82



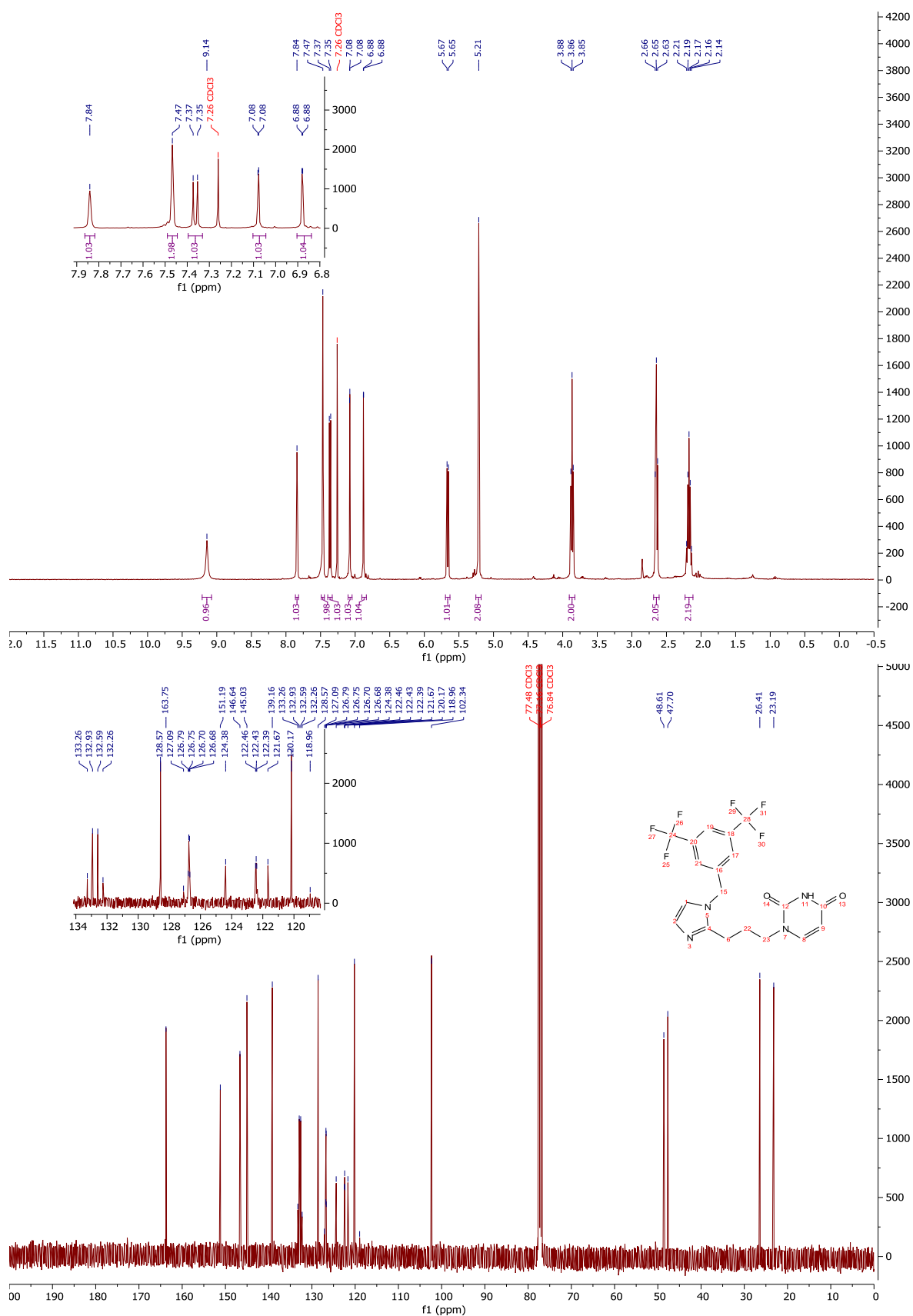
¹H-NMR and ¹³C-NMR: Compound 238



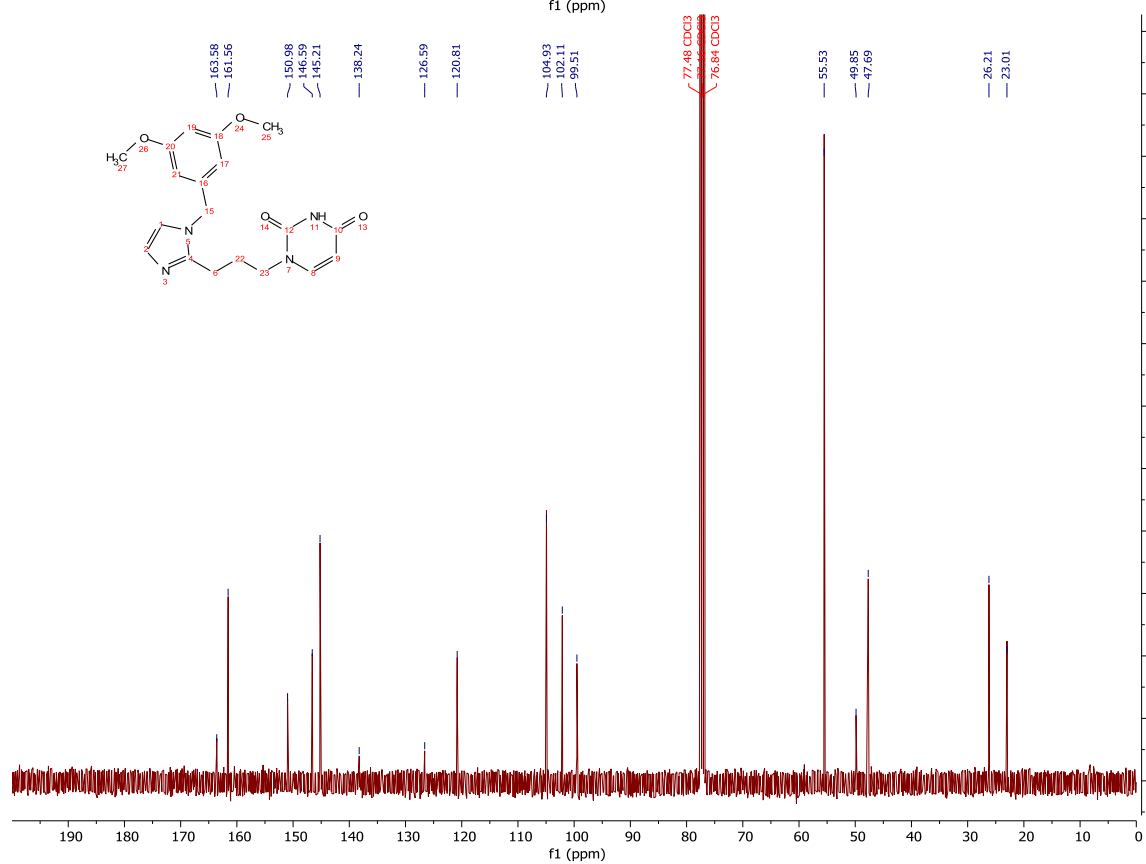
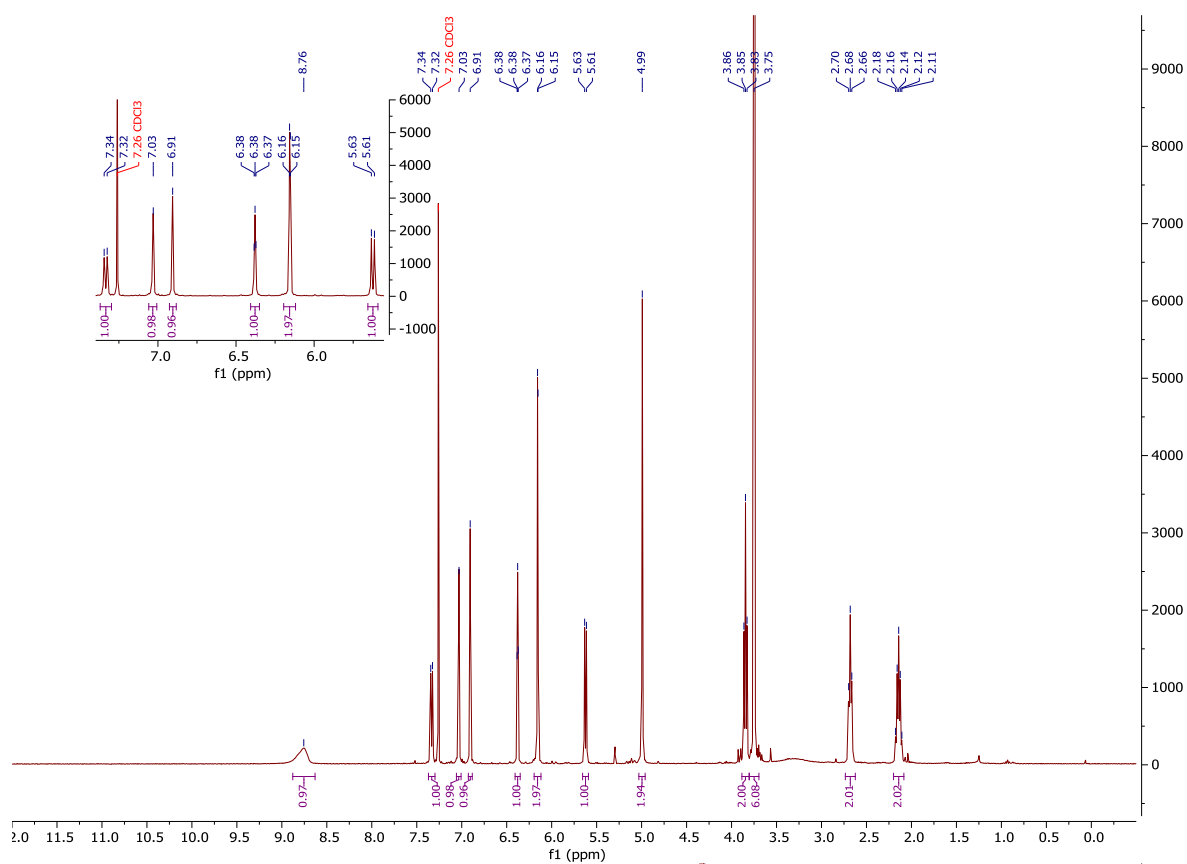
¹H-NMR and ¹³C-NMR: Compound 242



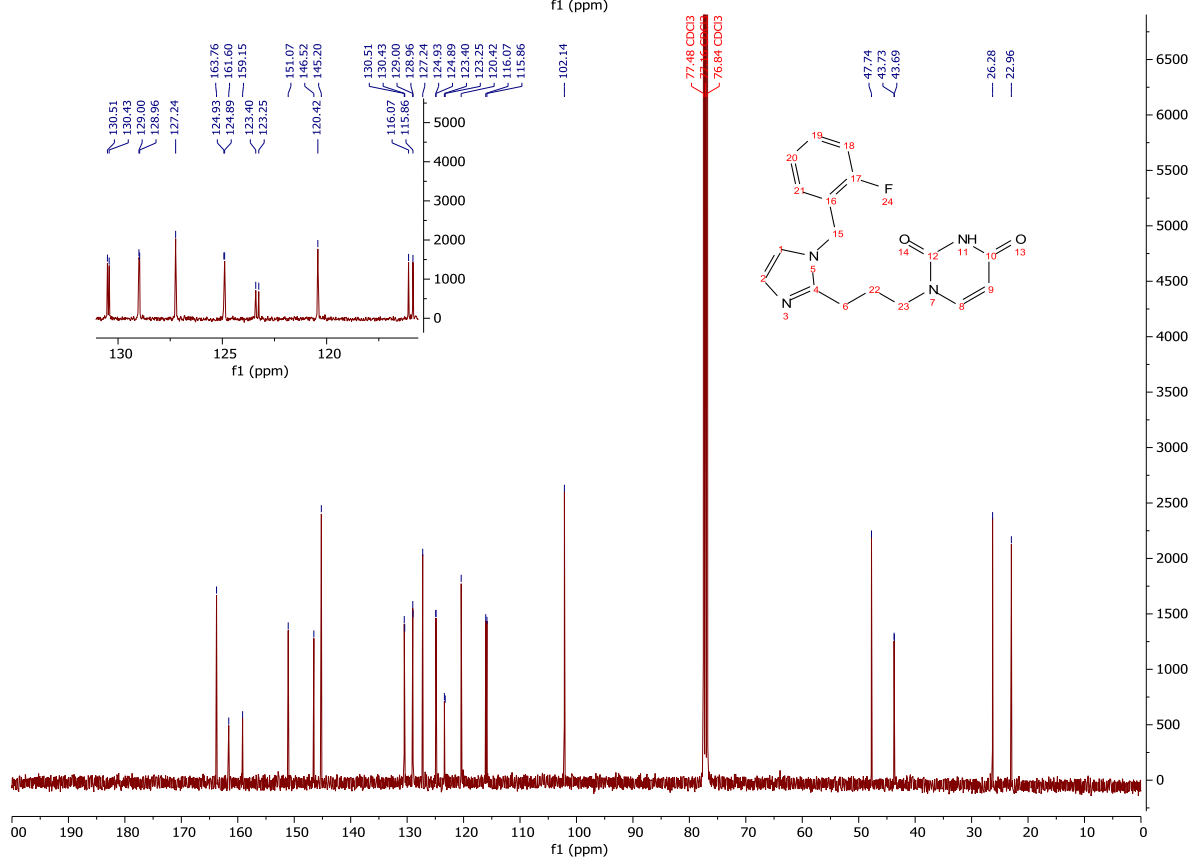
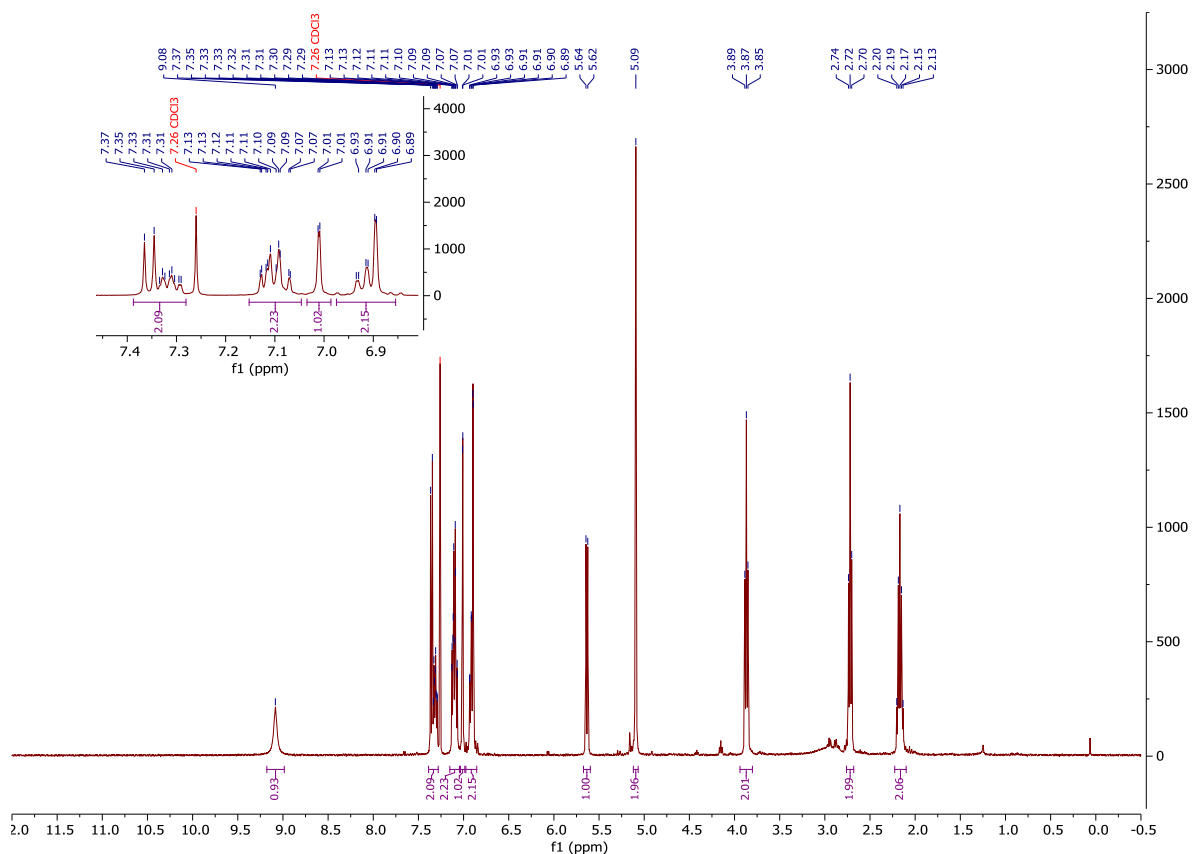
¹H-NMR and ¹³C-NMR: Compound 243



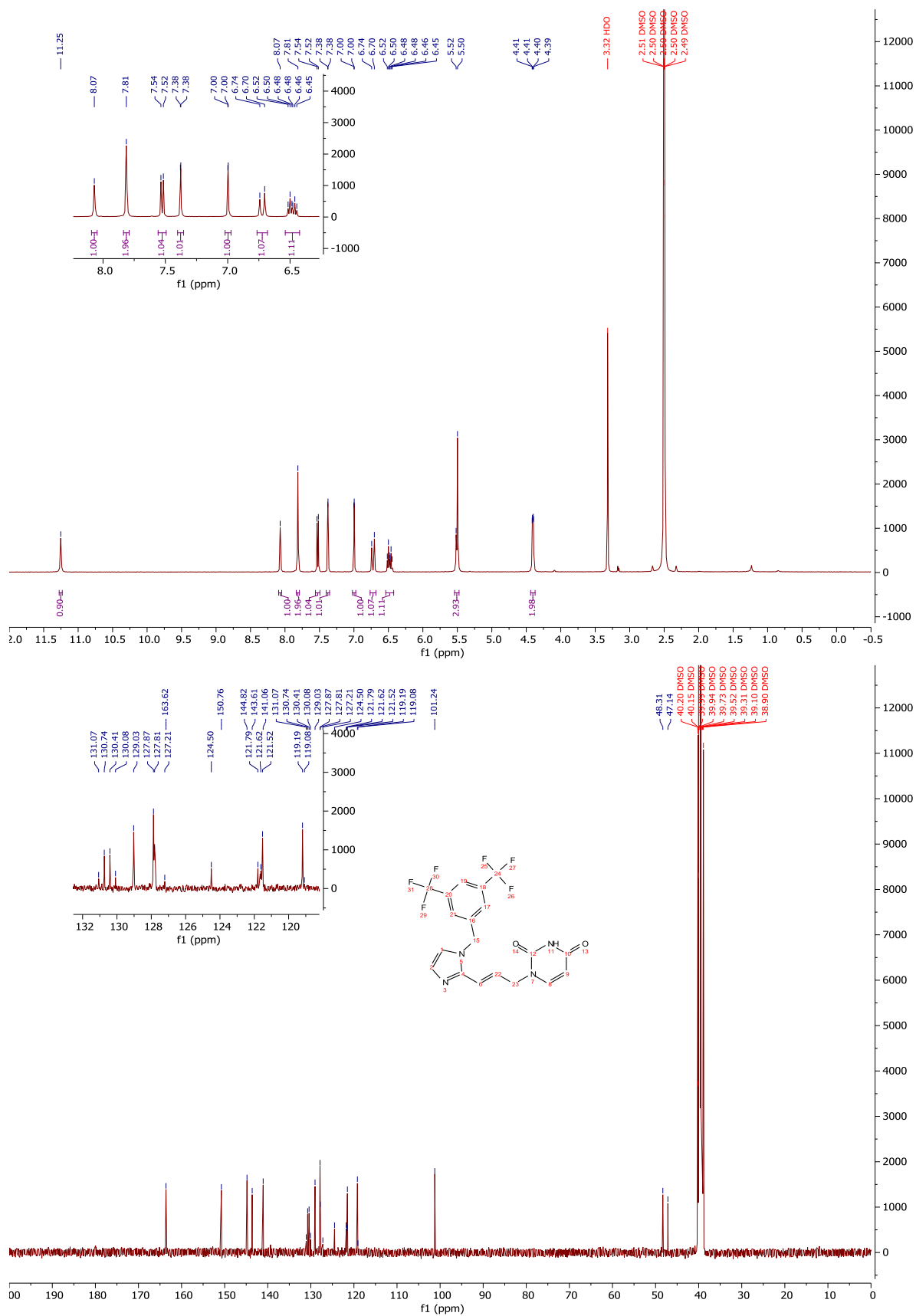
¹H-NMR and ¹³C-NMR: Compound 244



¹H-NMR and ¹³C-NMR: Compound 245



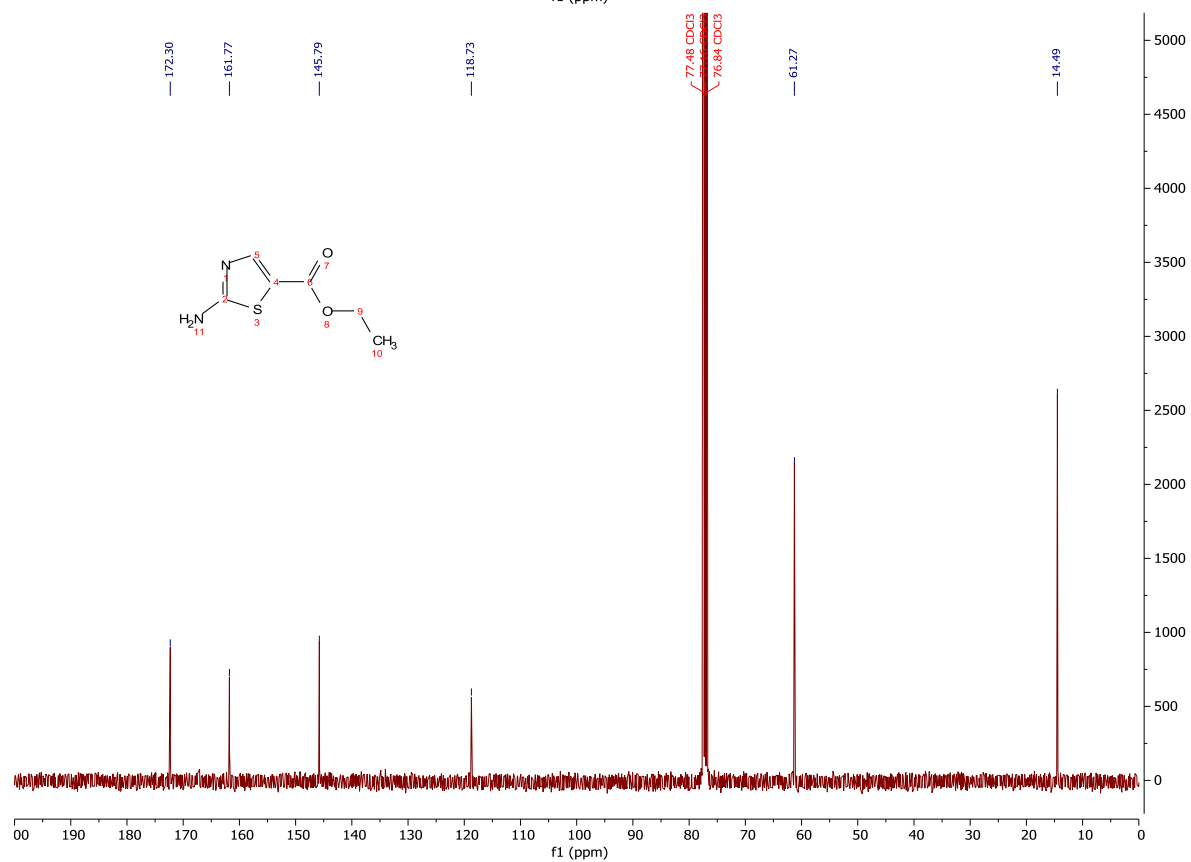
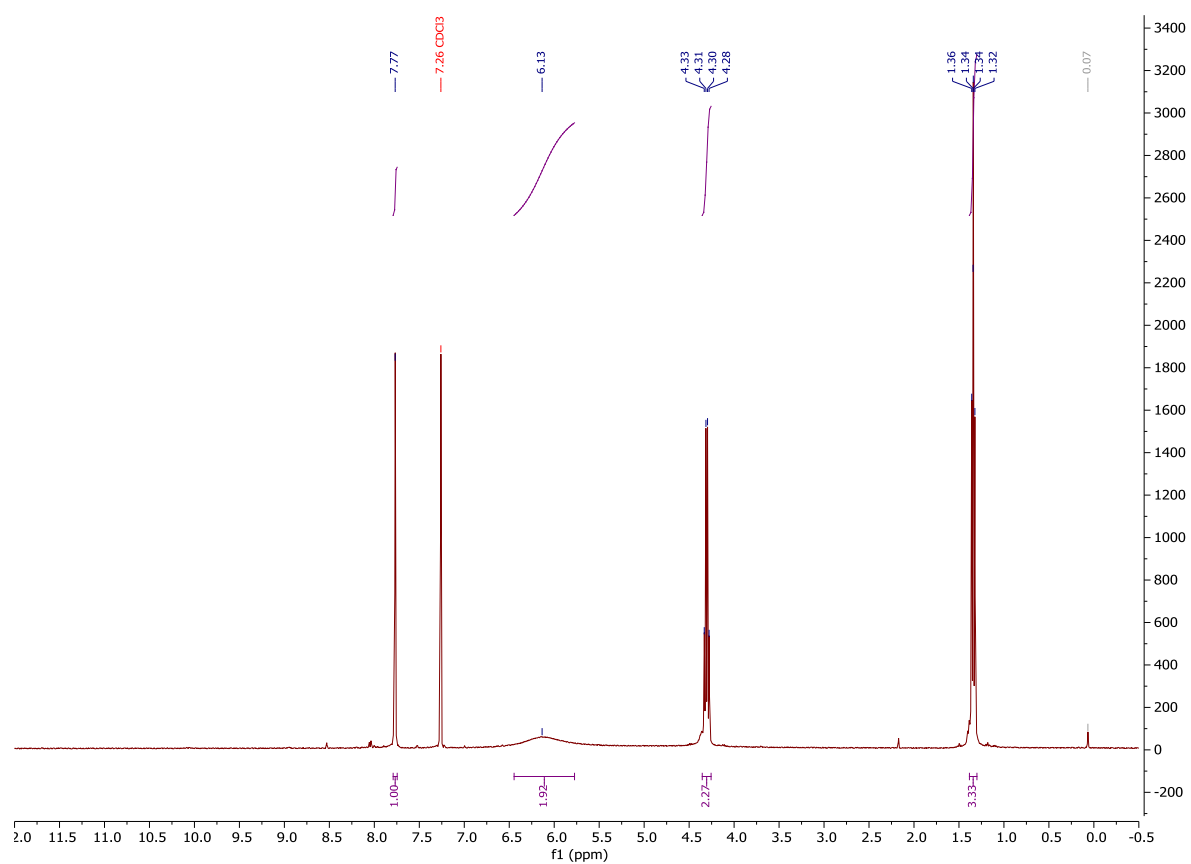
¹H-NMR and ¹³C-NMR: Compound 250



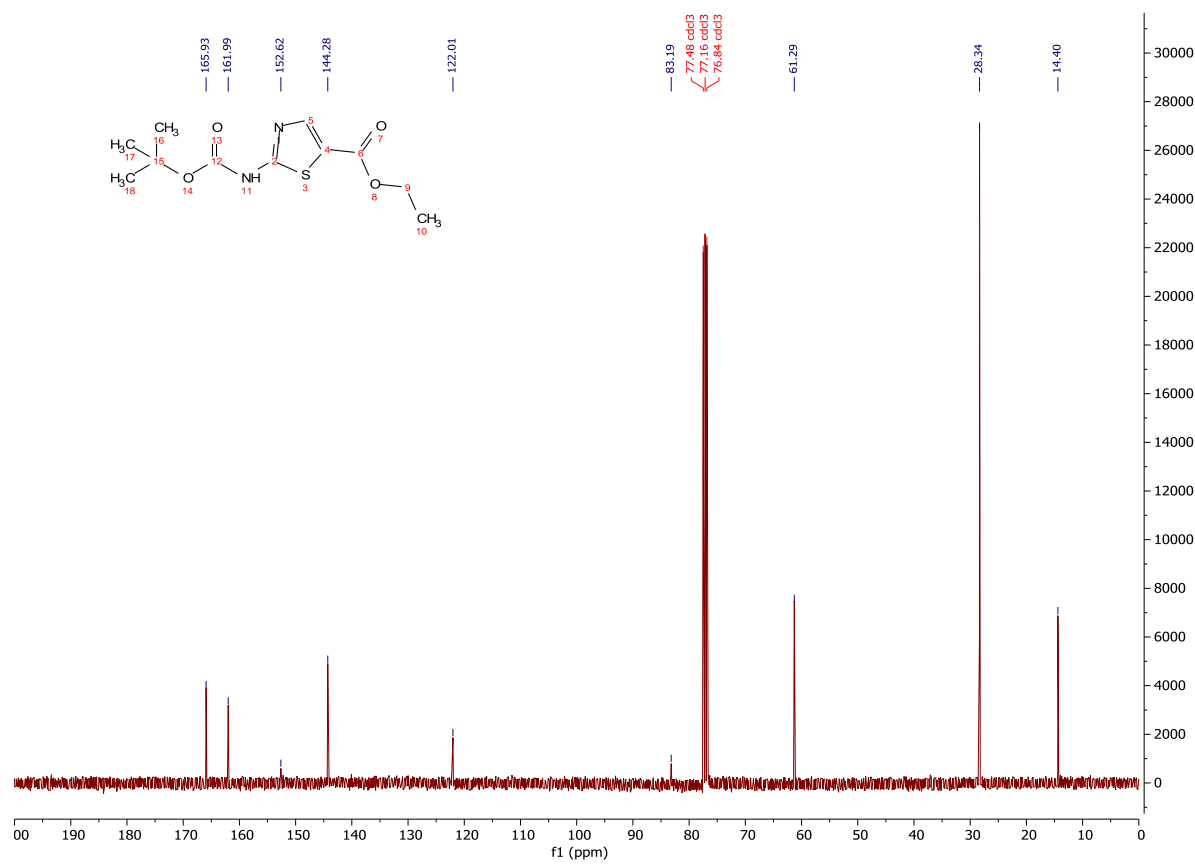
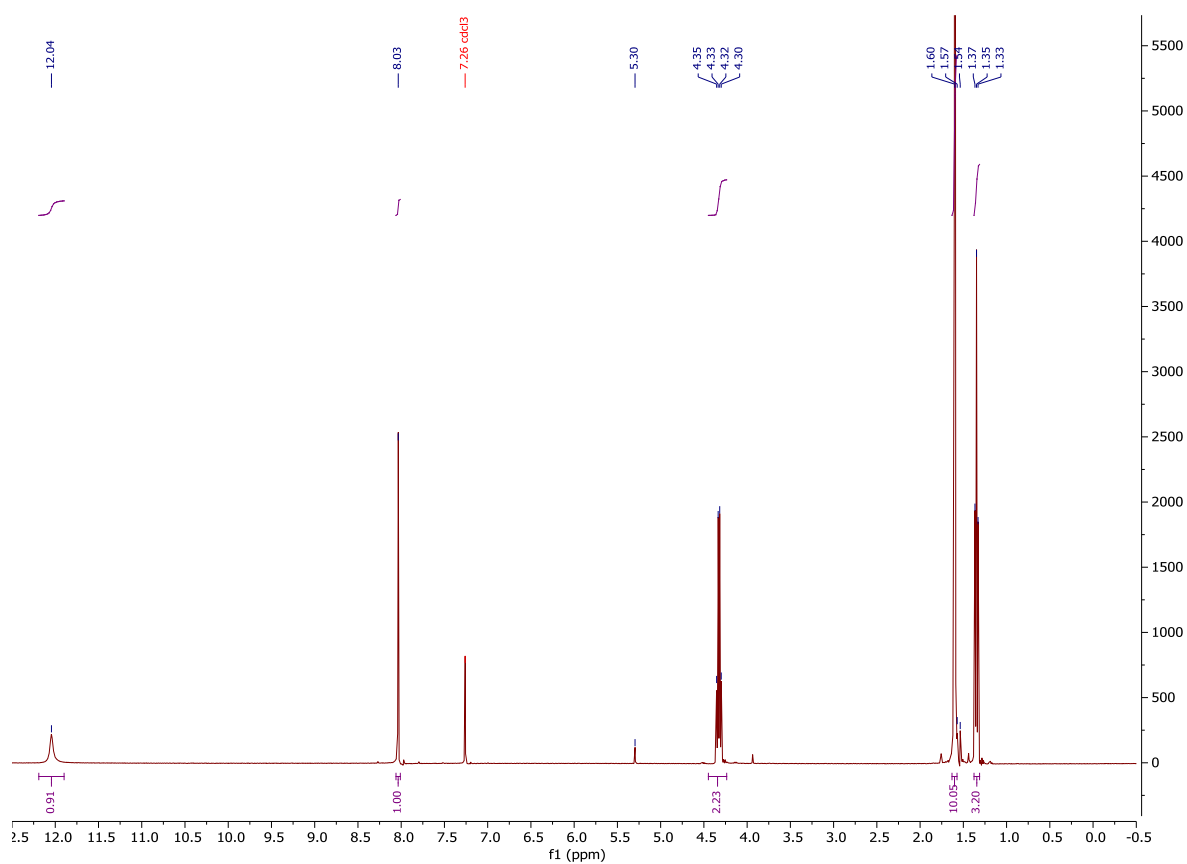
Proton and Carbon NMR spectra of project 2

Scaffold synthesis

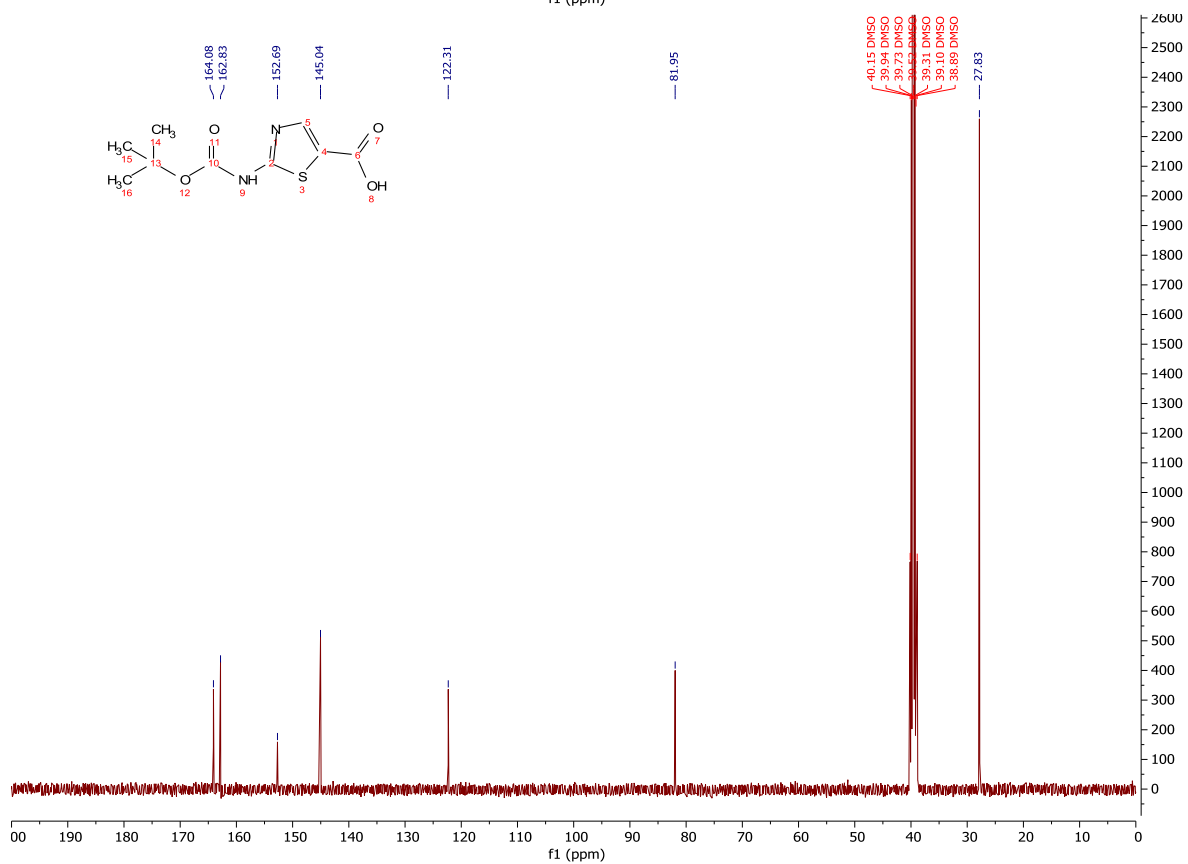
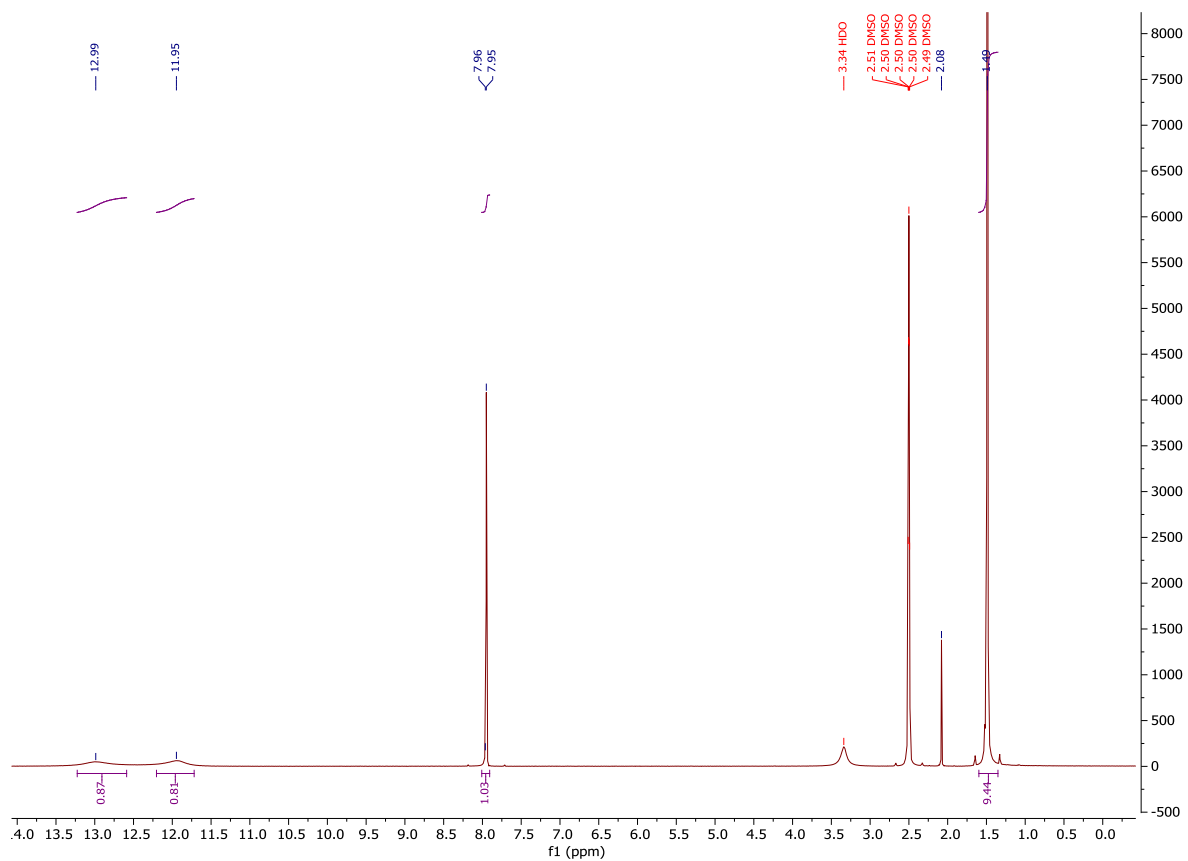
¹H-NMR and ¹³C-NMR: Compound 275



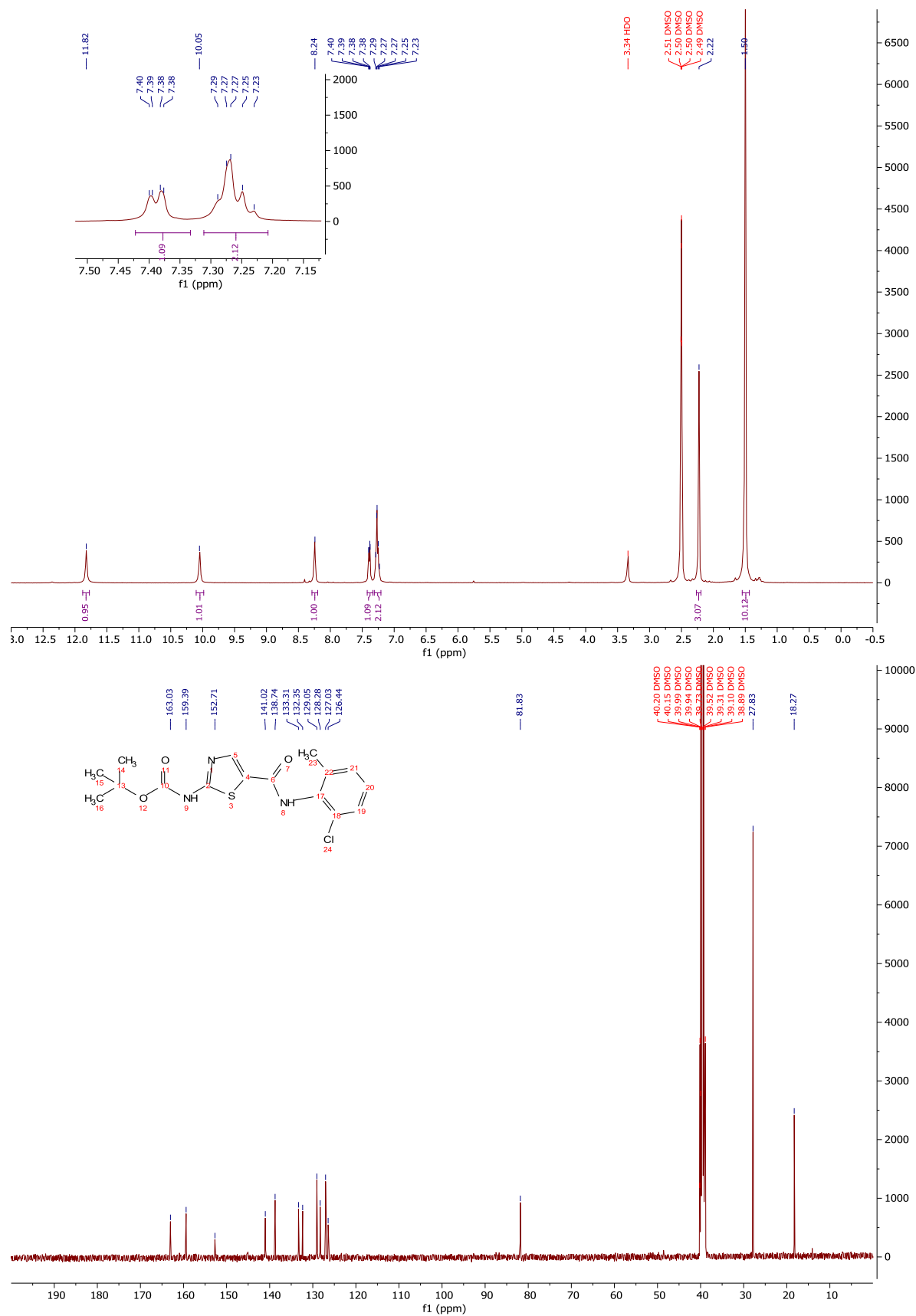
¹H-NMR and ¹³C-NMR: Compound 276



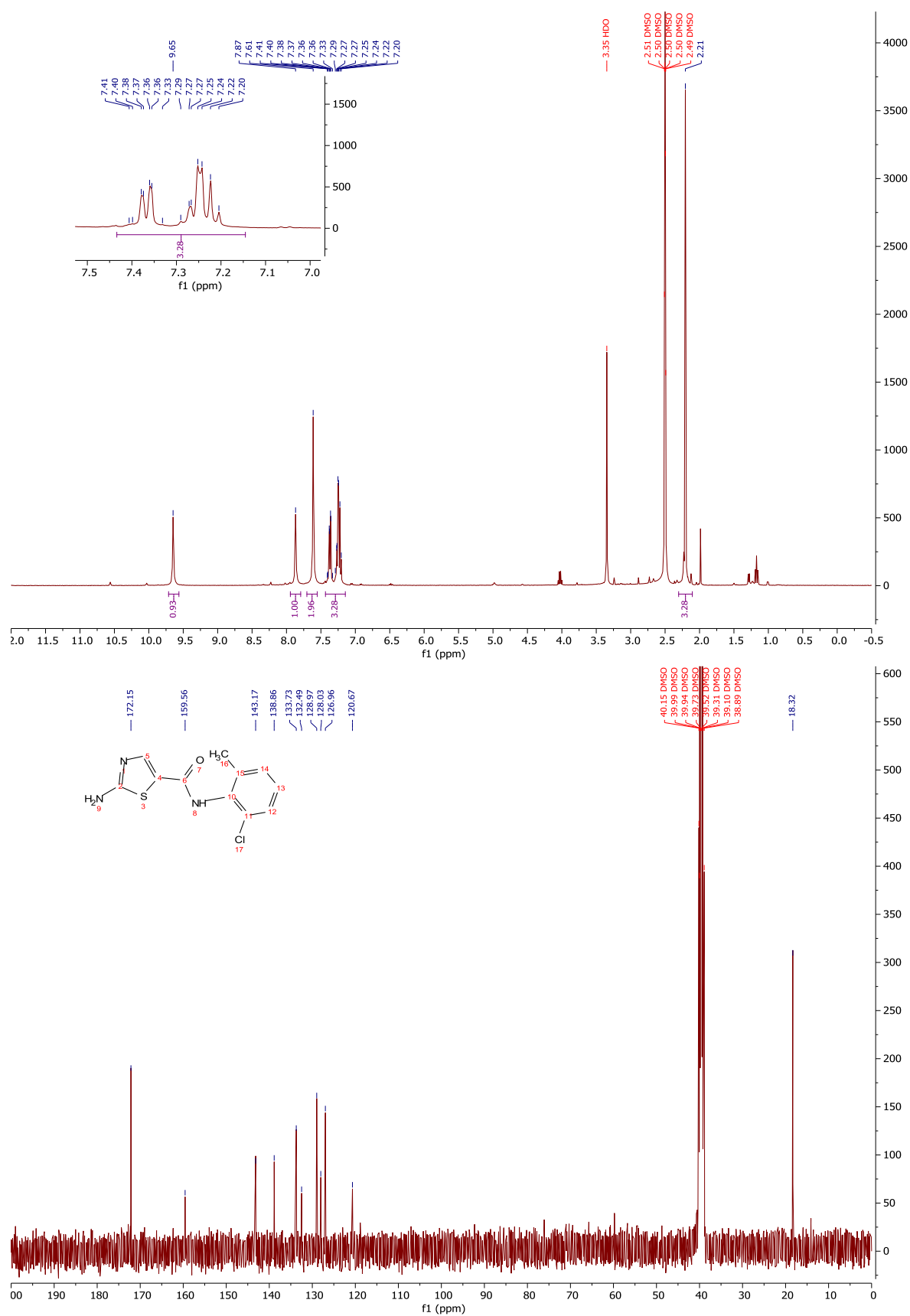
$^1\text{H-NMR}$ and $^{13}\text{C-NMR}$: Compound 277



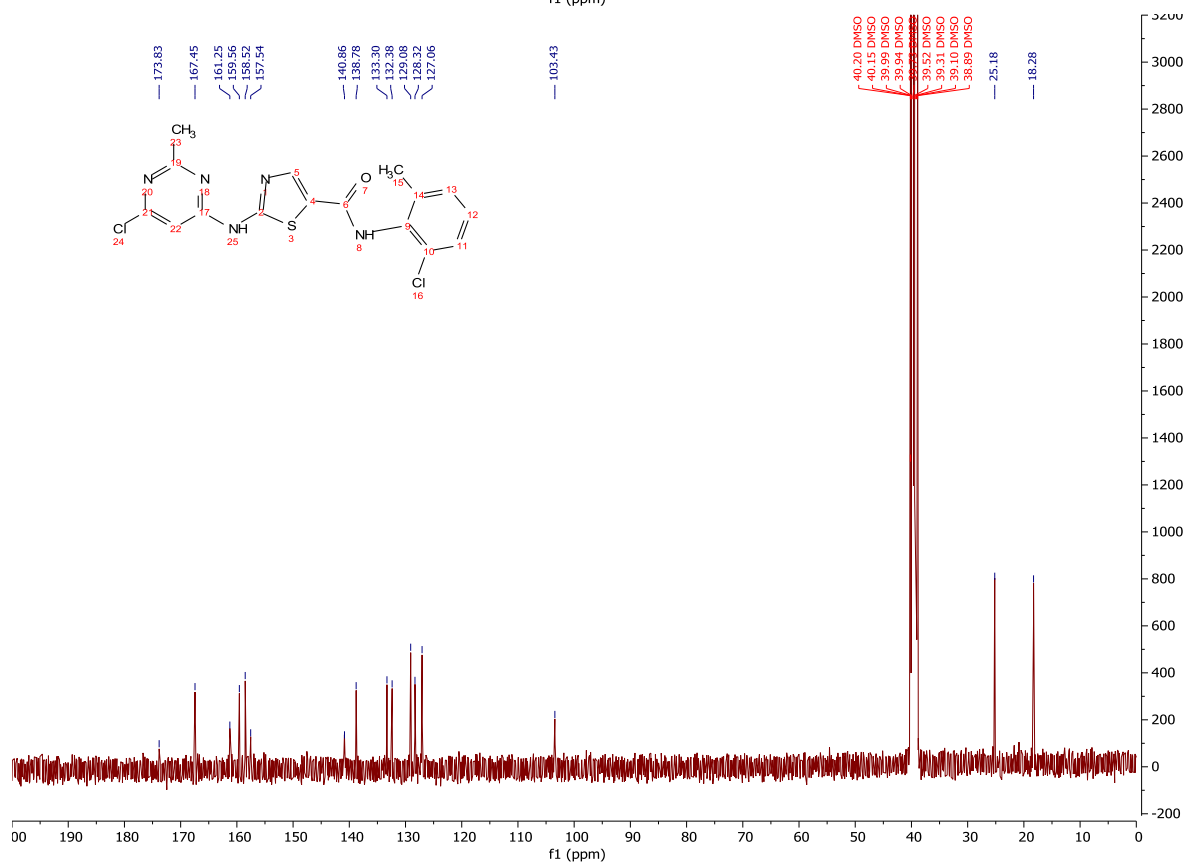
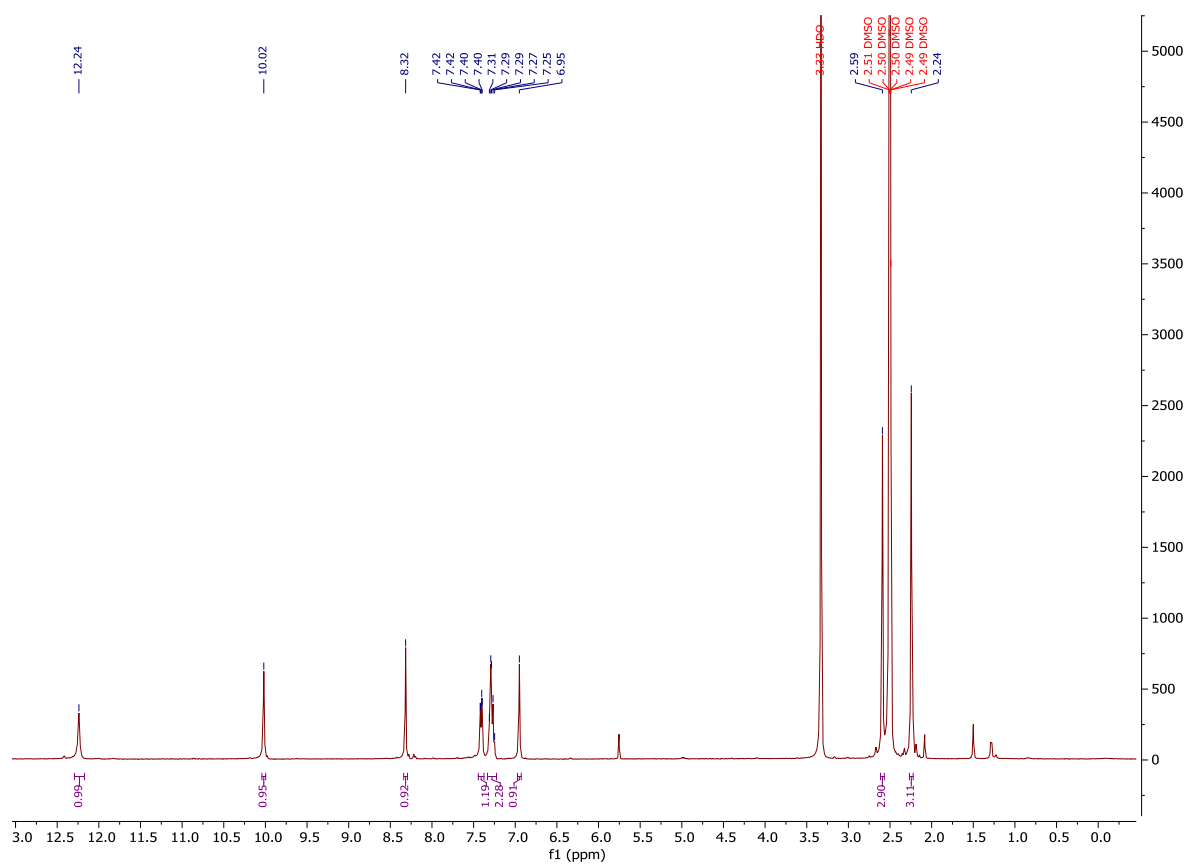
¹H-NMR and ¹³C-NMR: Compound 278



$^1\text{H-NMR}$ and $^{13}\text{C-NMR}$: Compound 279

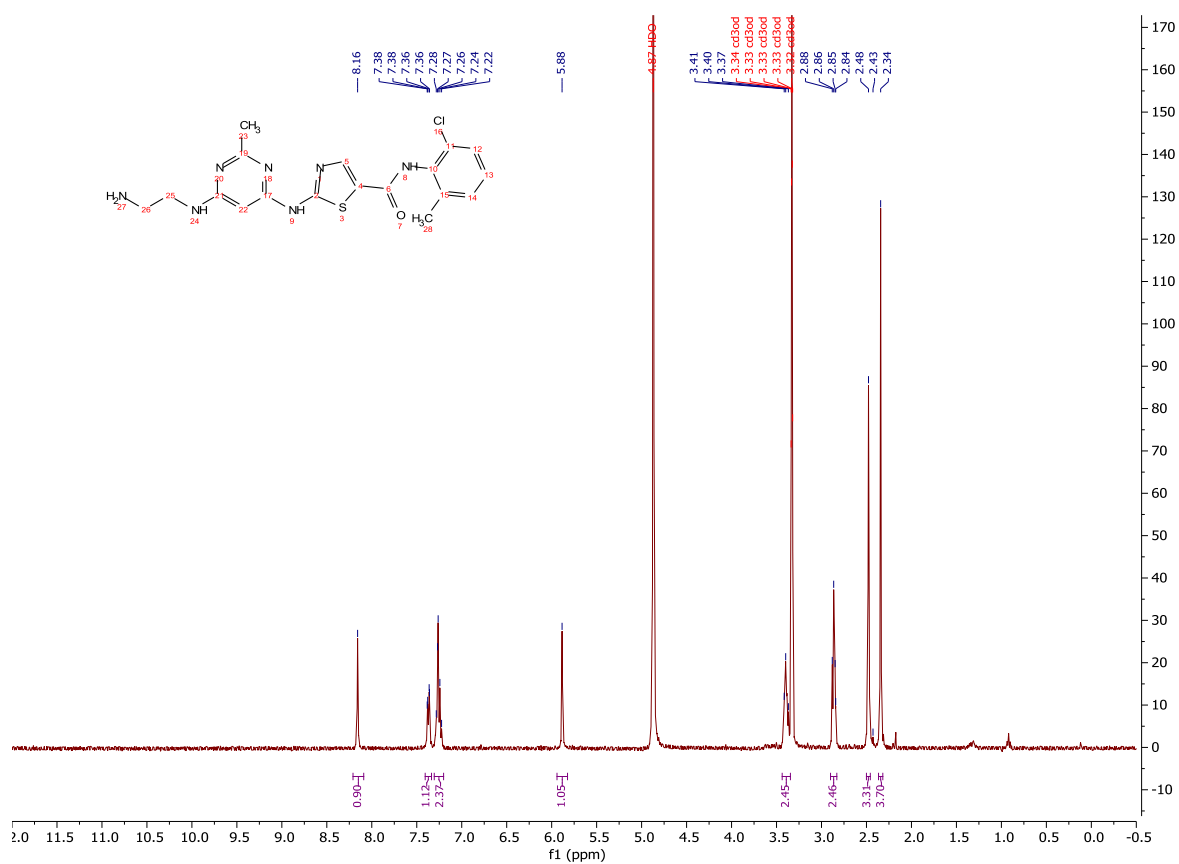


¹H-NMR and ¹³C-NMR: Compound 273

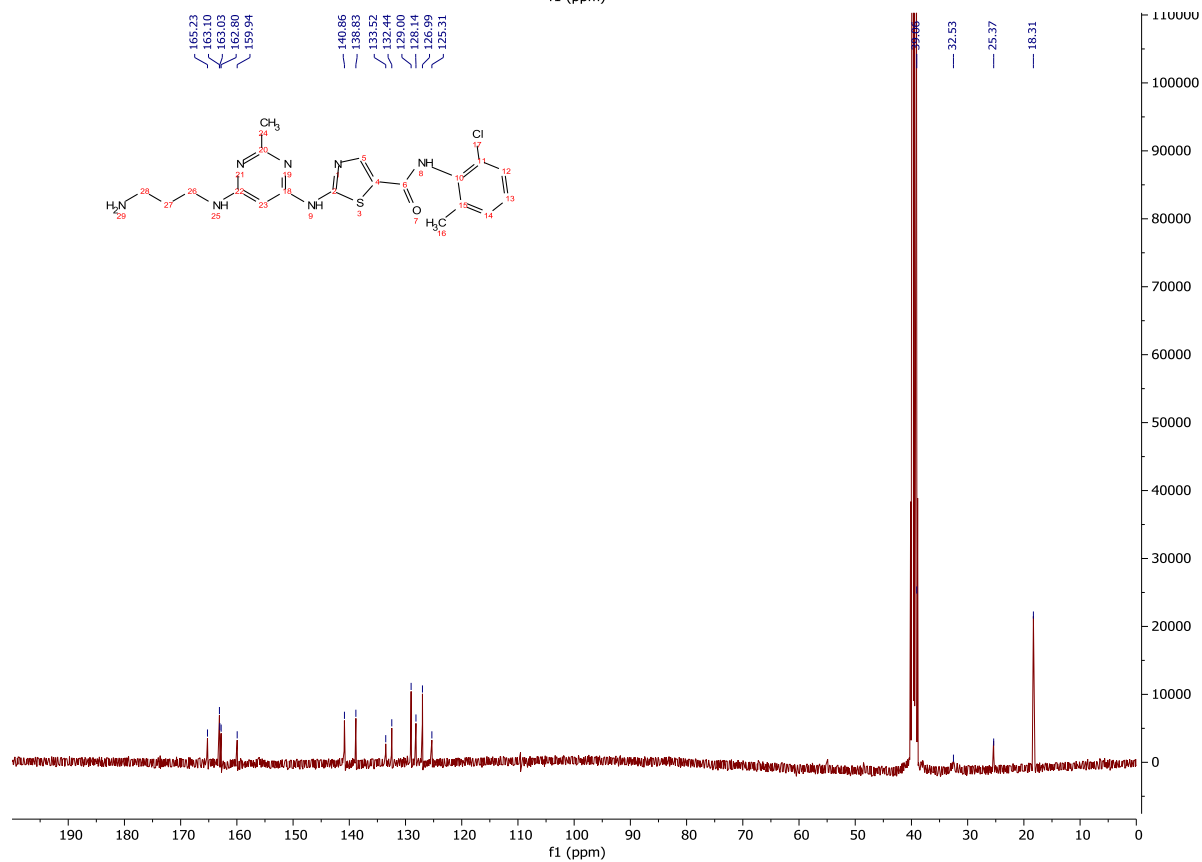
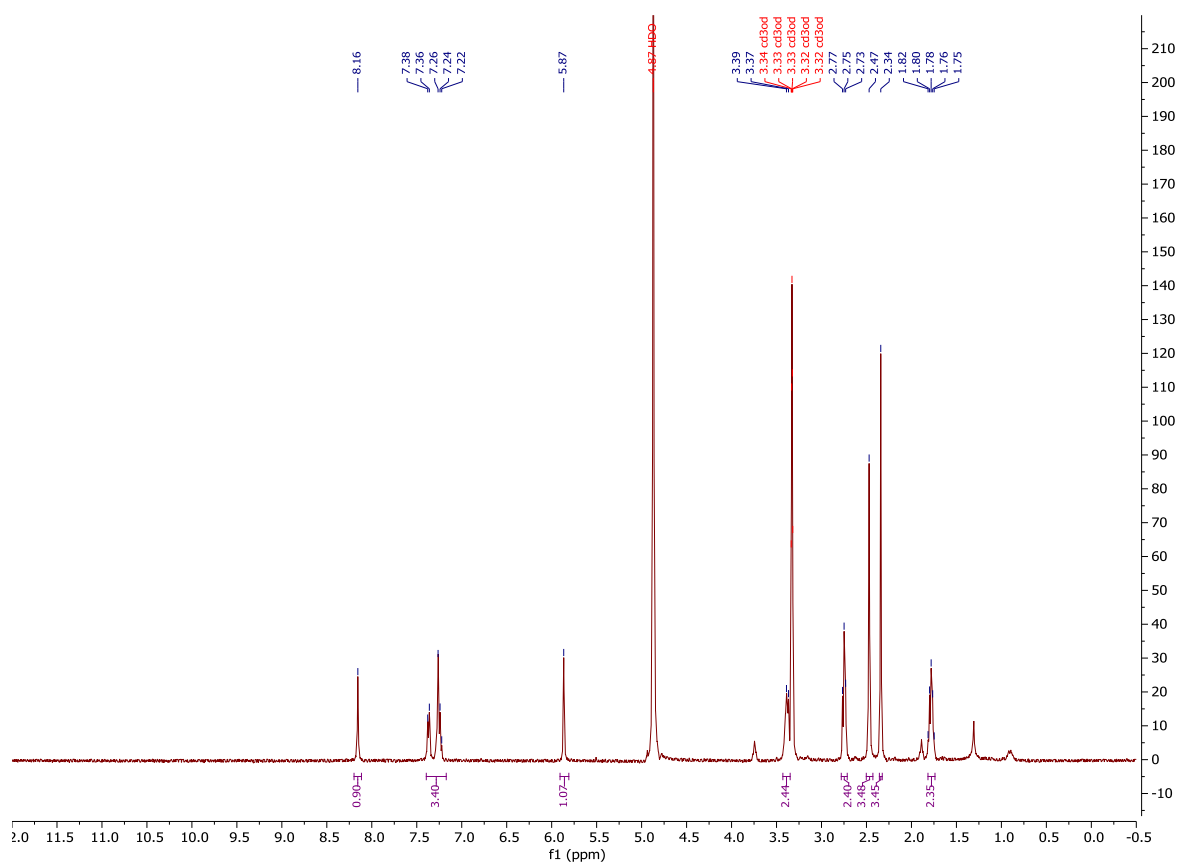


Linker synthesis

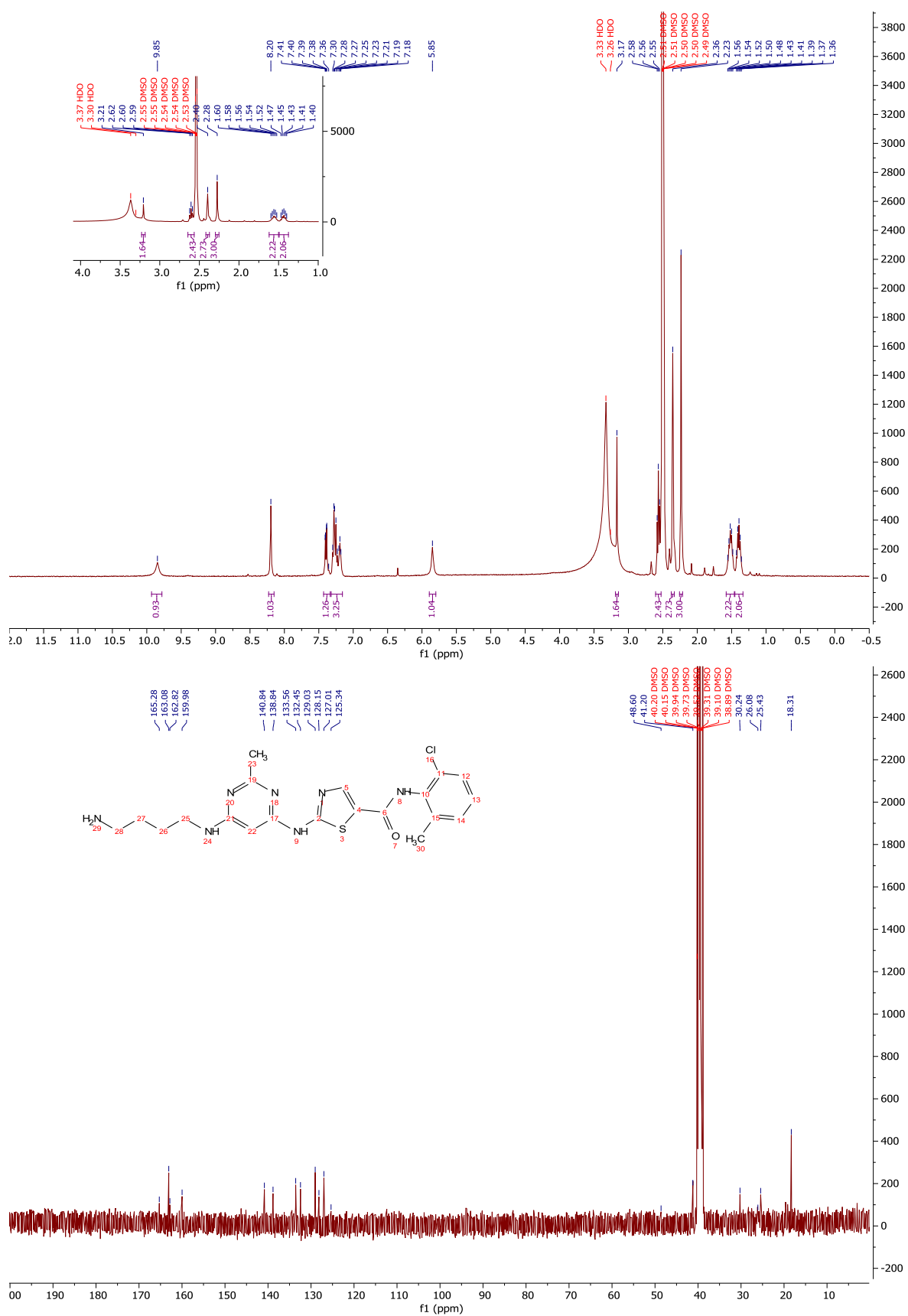
¹H-NMR and ¹³C-NMR: Compound 280



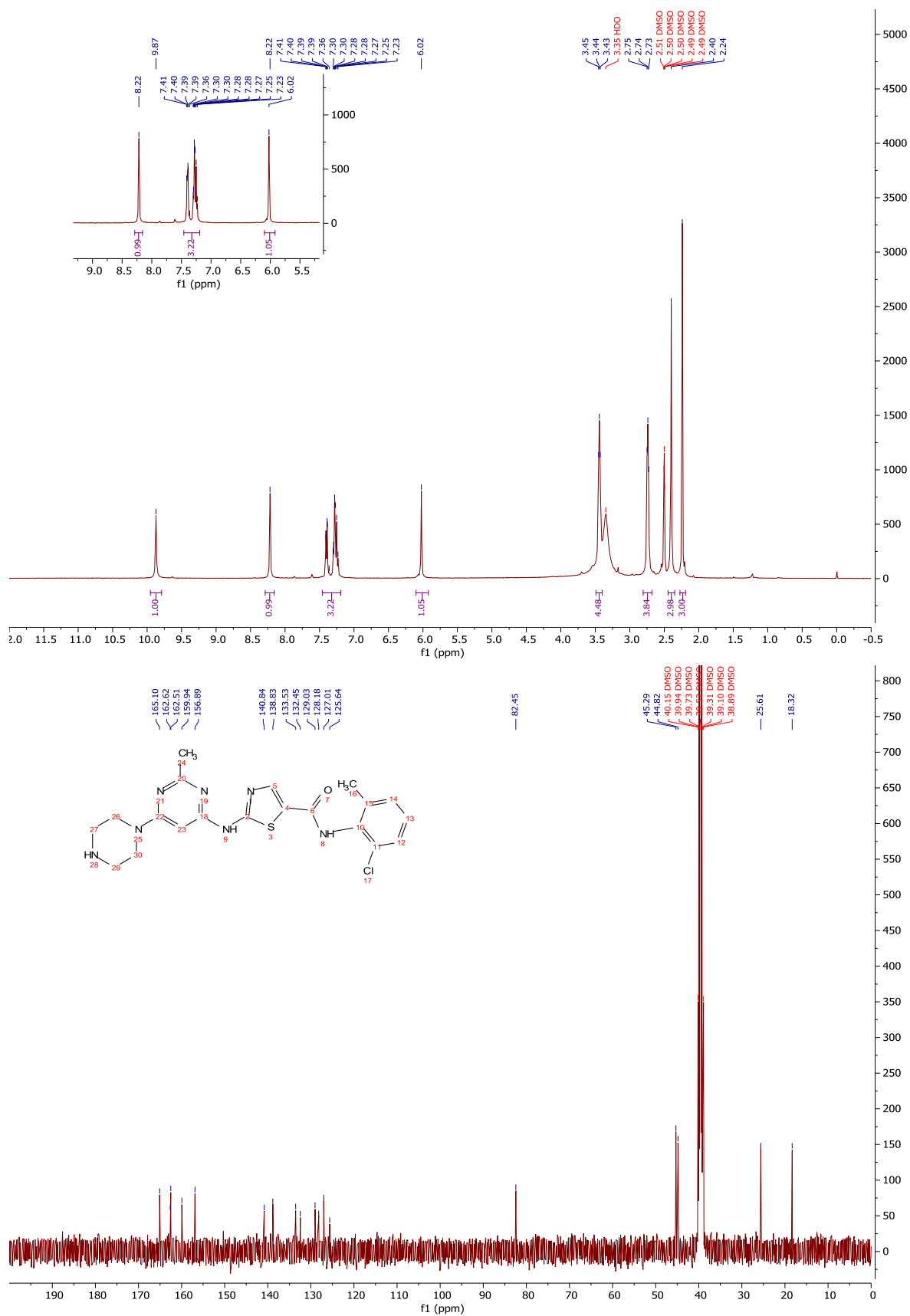
¹H-NMR and ¹³C-NMR: Compound 281



¹H-NMR and ¹³C-NMR: Compound 282

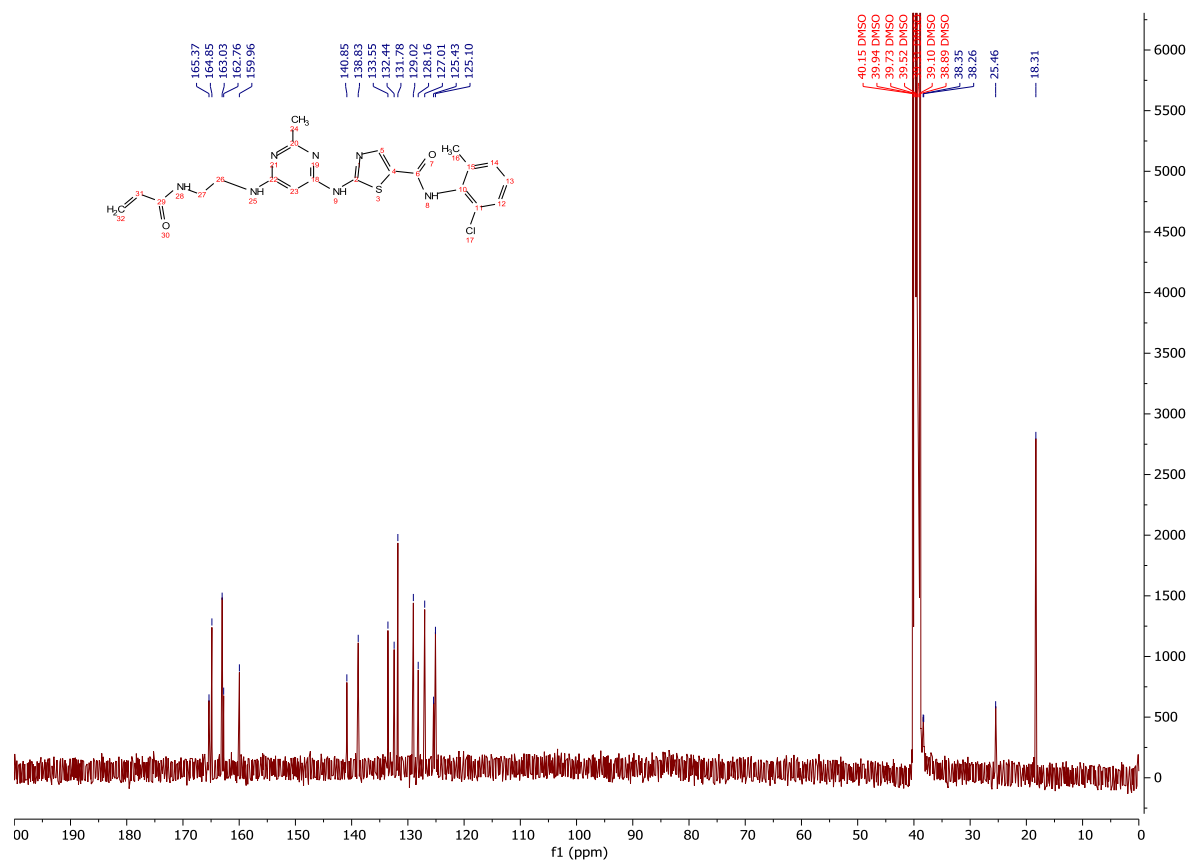
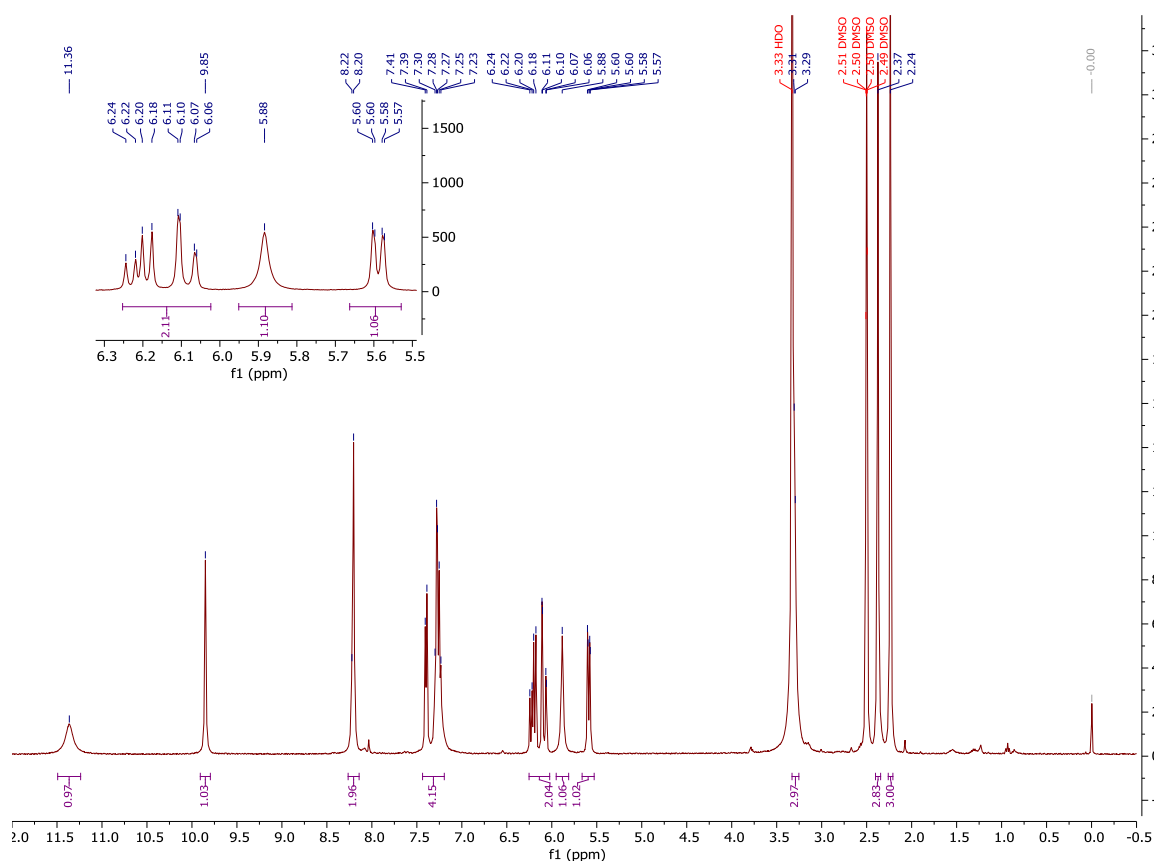


¹H-NMR and ¹³C-NMR: Compound 283

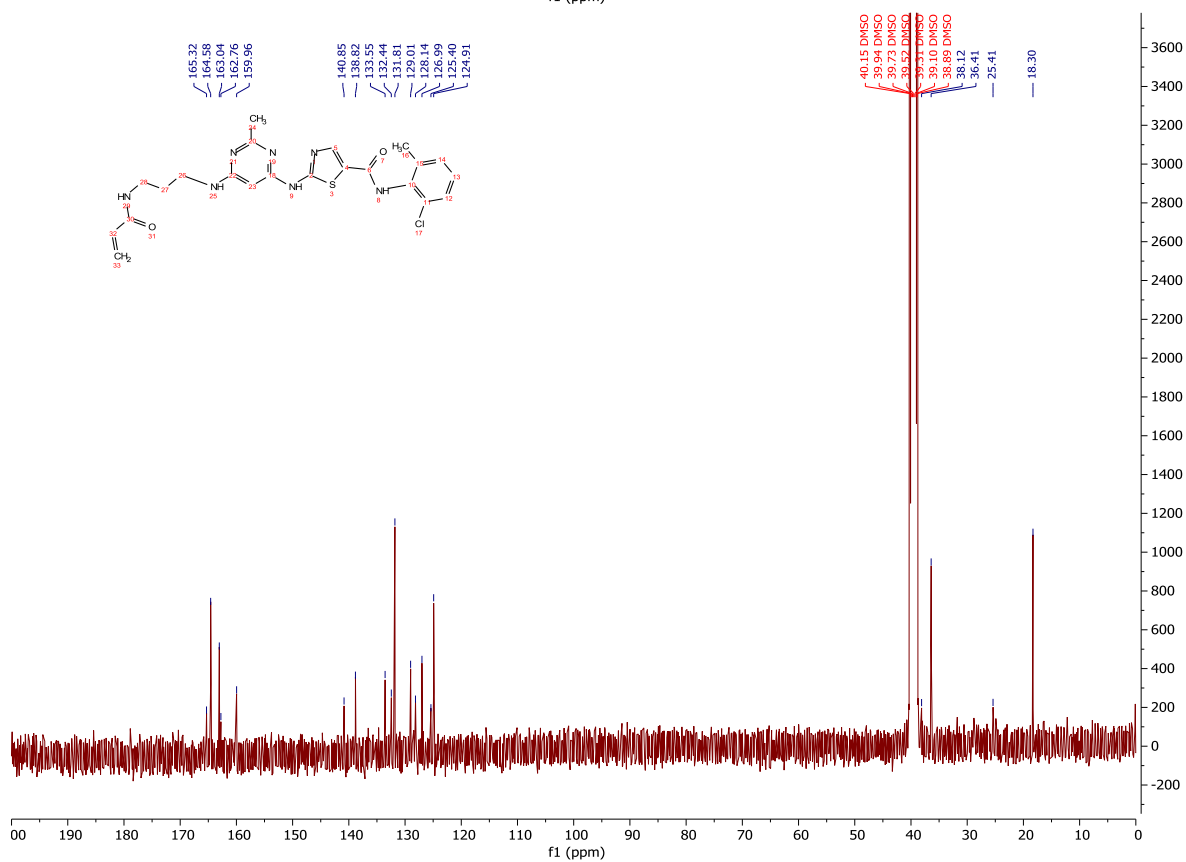
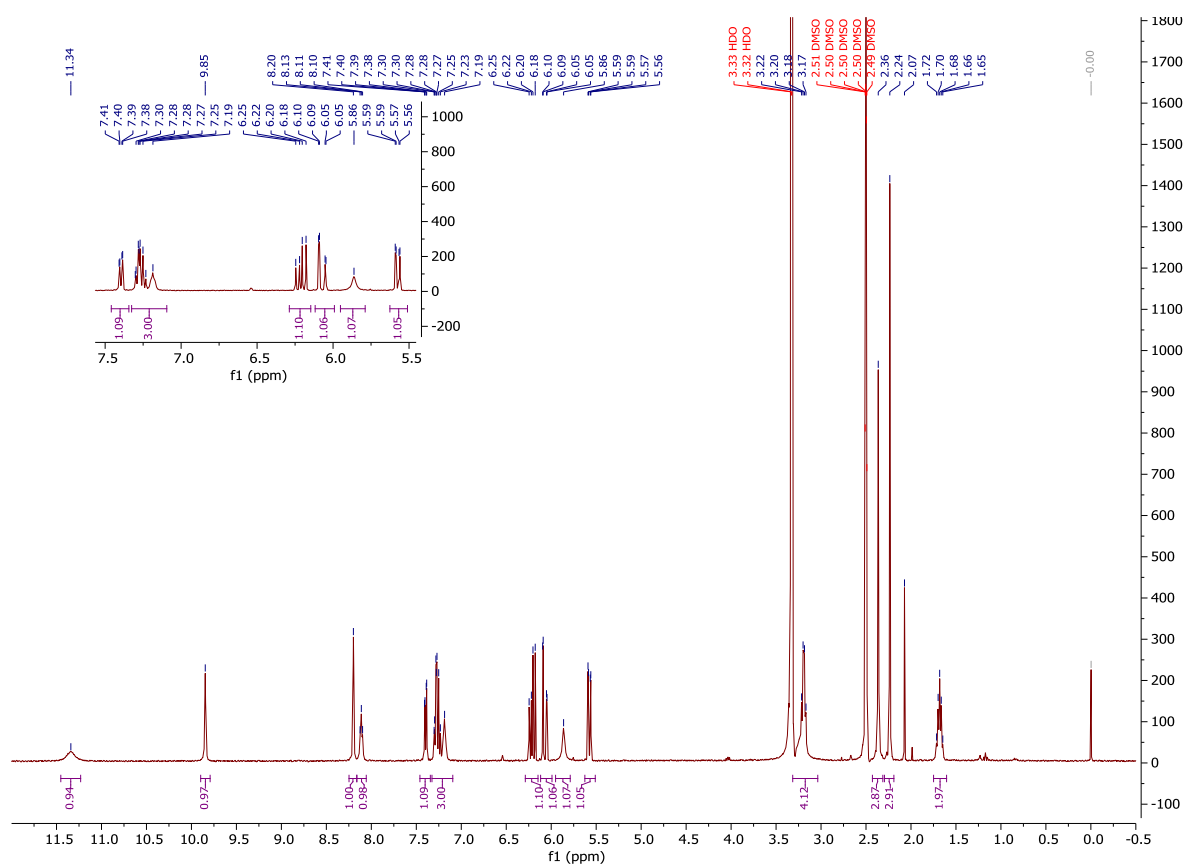


Final Compounds

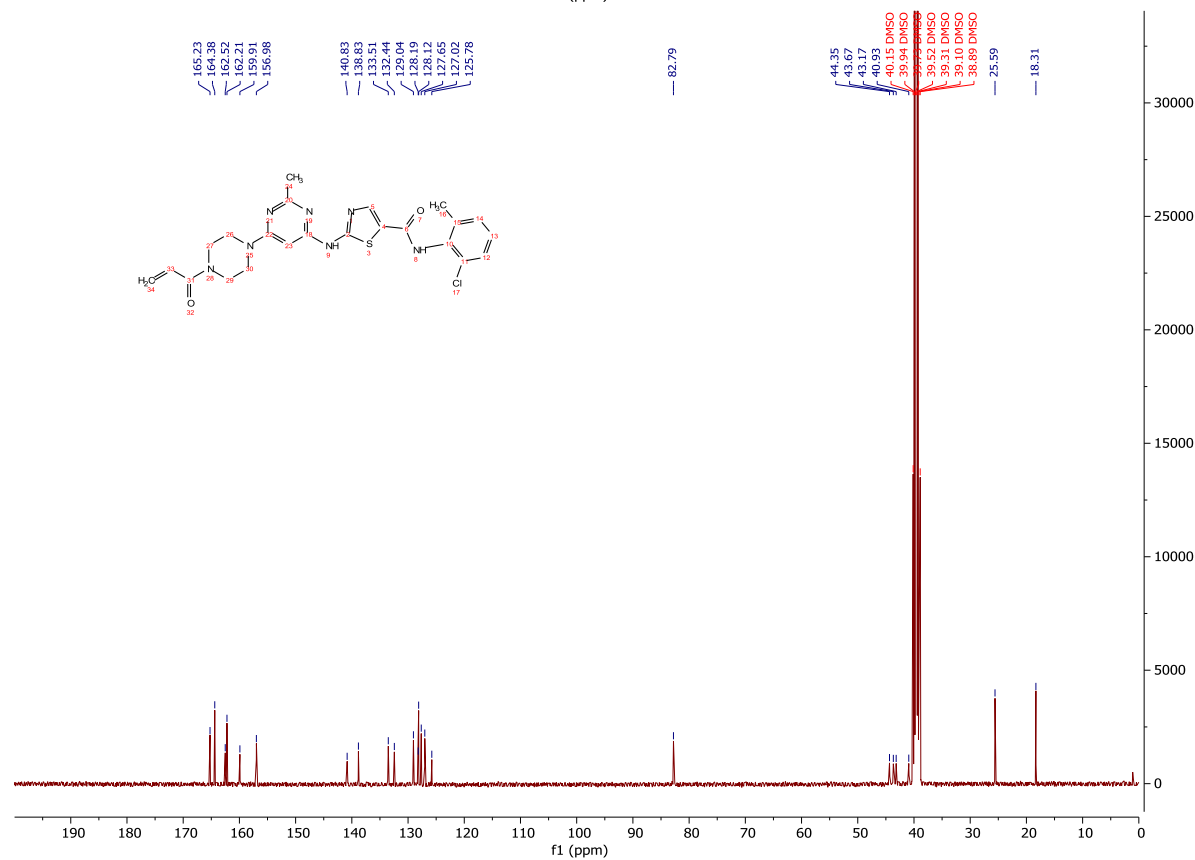
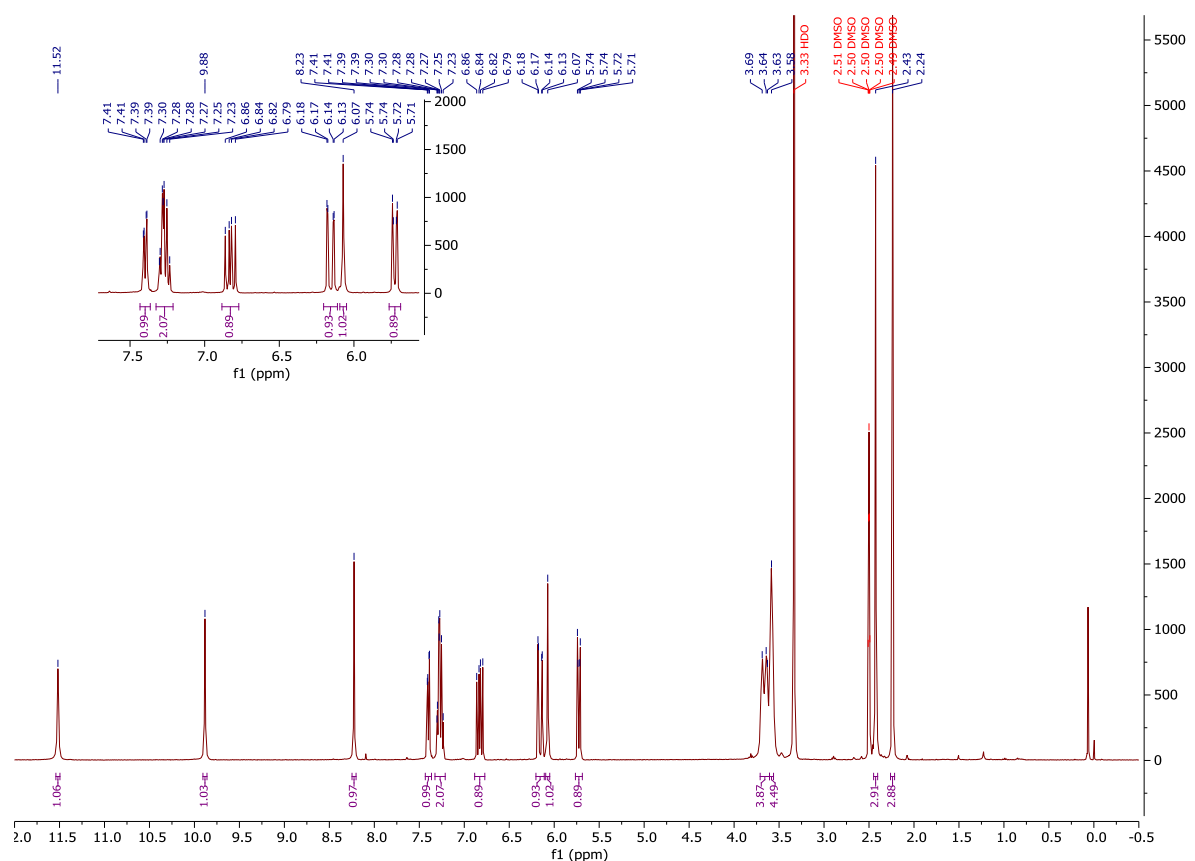
¹H-NMR and ¹³C-NMR: Compound 284



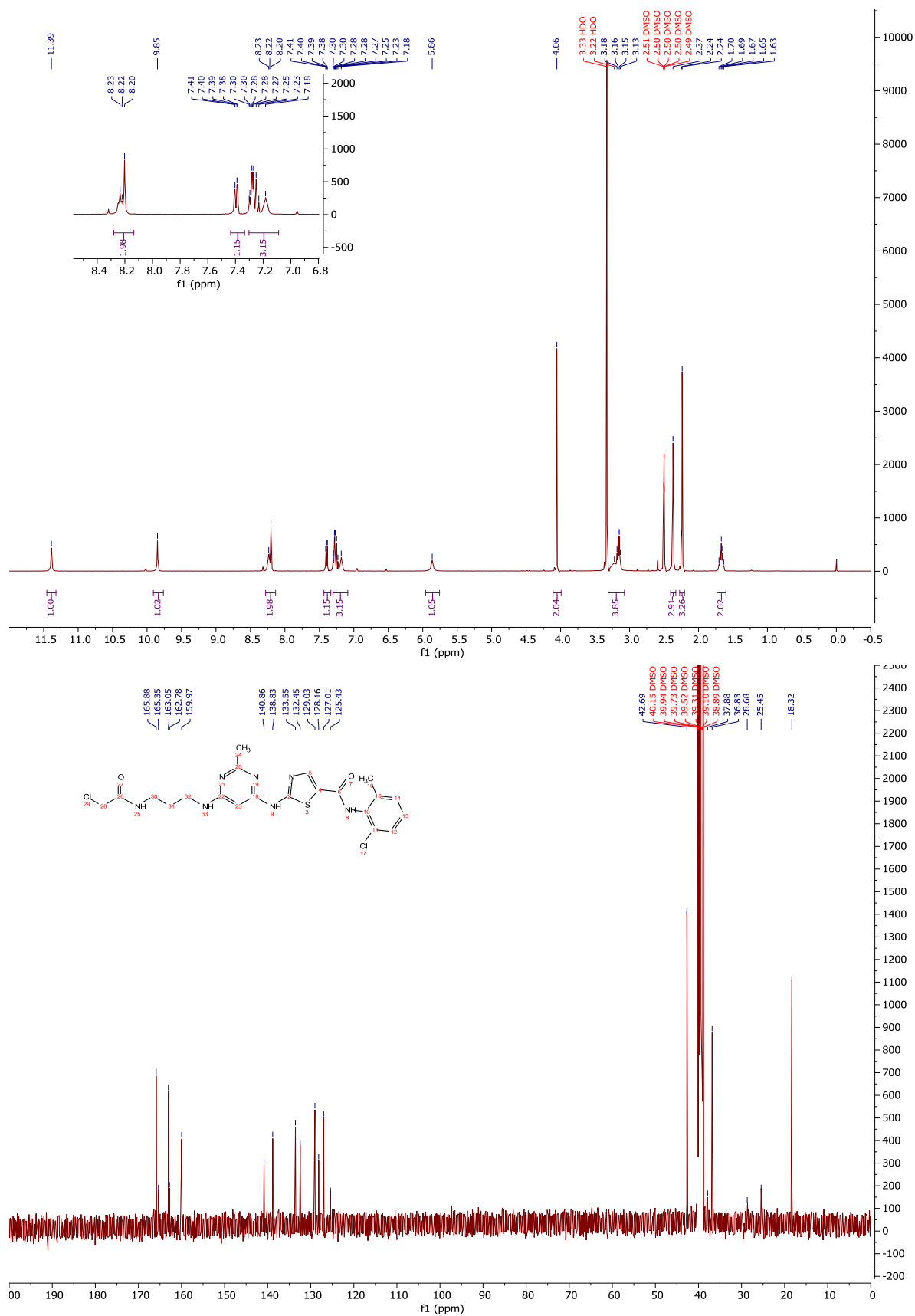
¹H-NMR and ¹³C-NMR: Compound 285



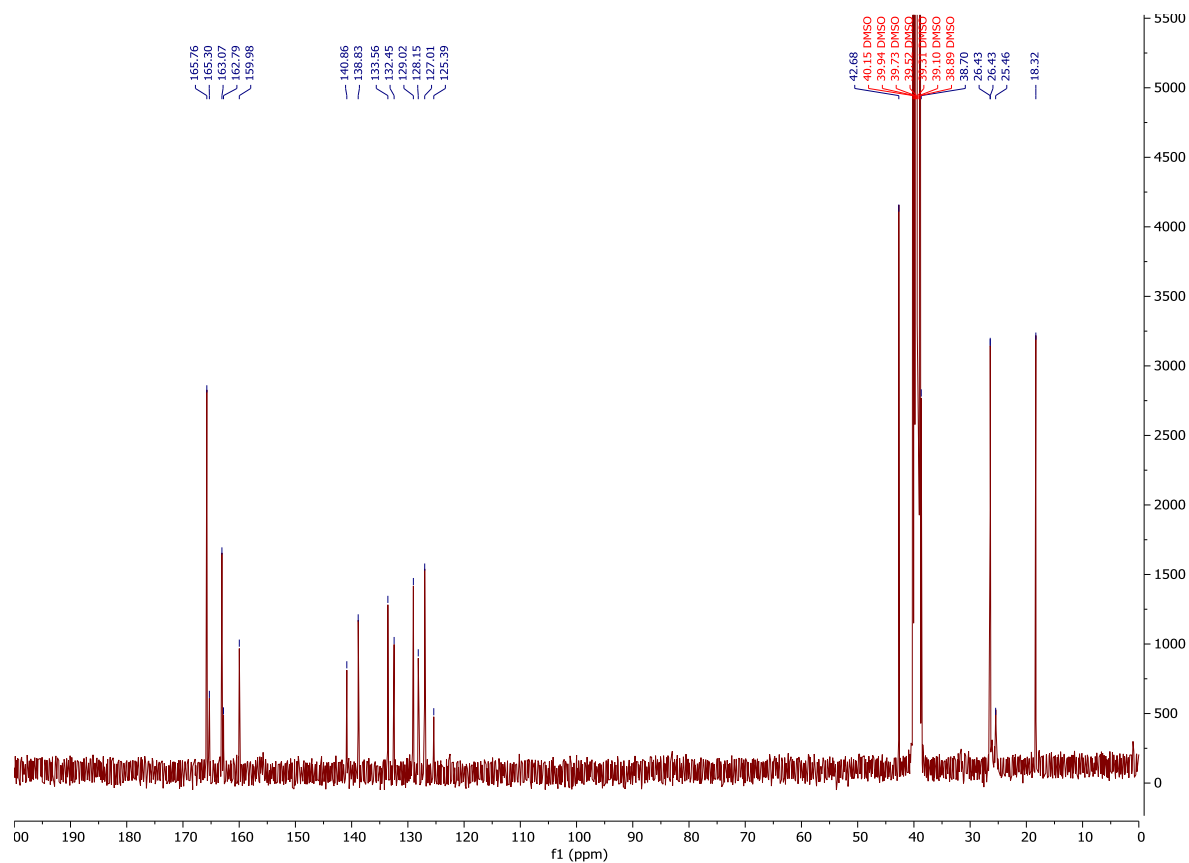
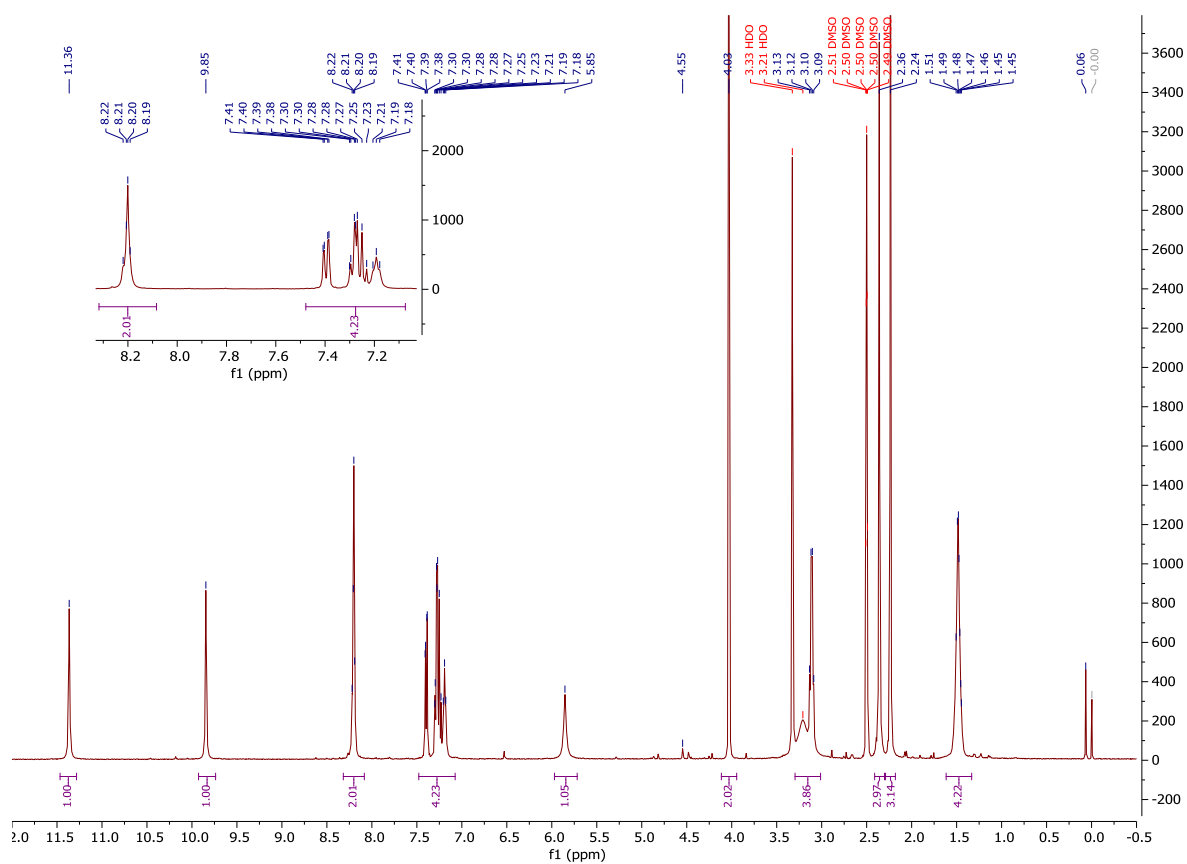
¹H-NMR and ¹³C-NMR: Compound 286



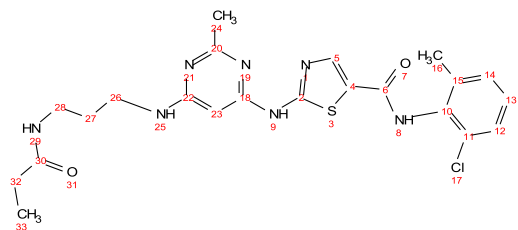
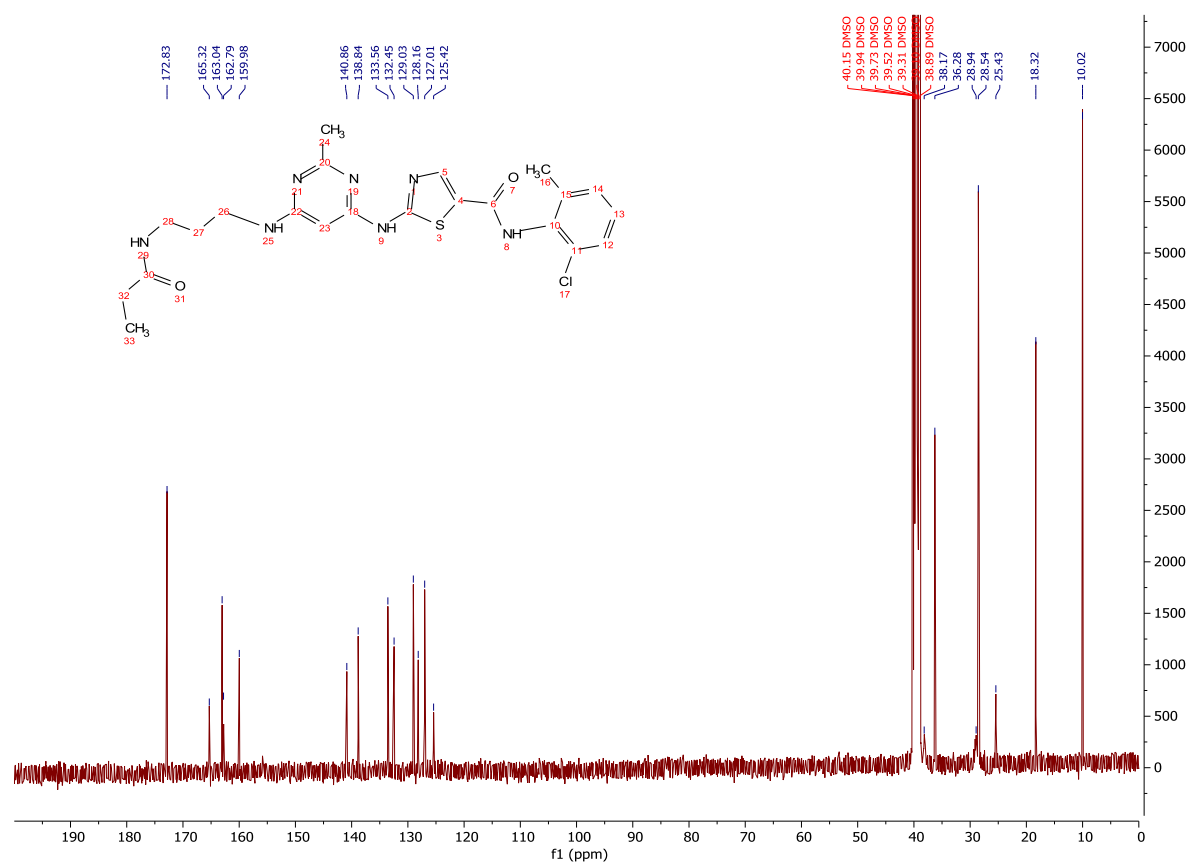
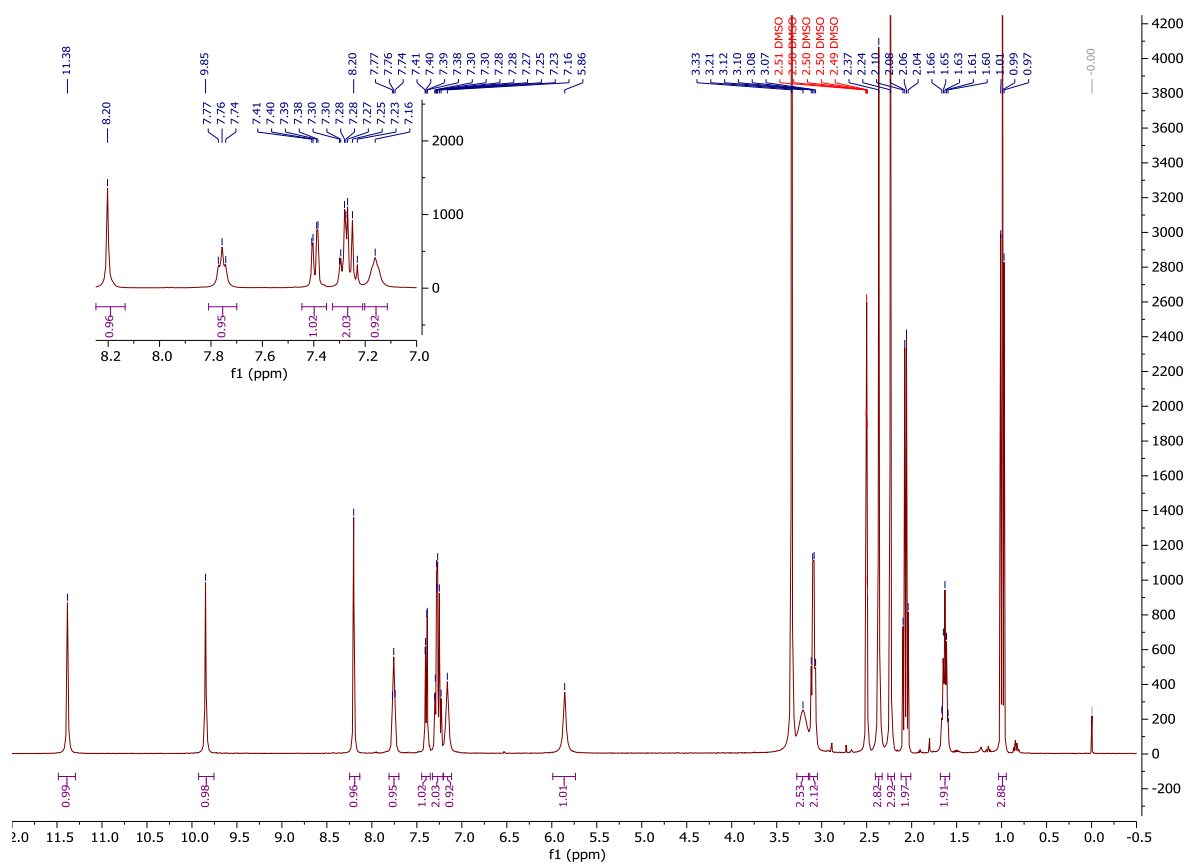
¹H-NMR and ¹³C-NMR: Compound 287



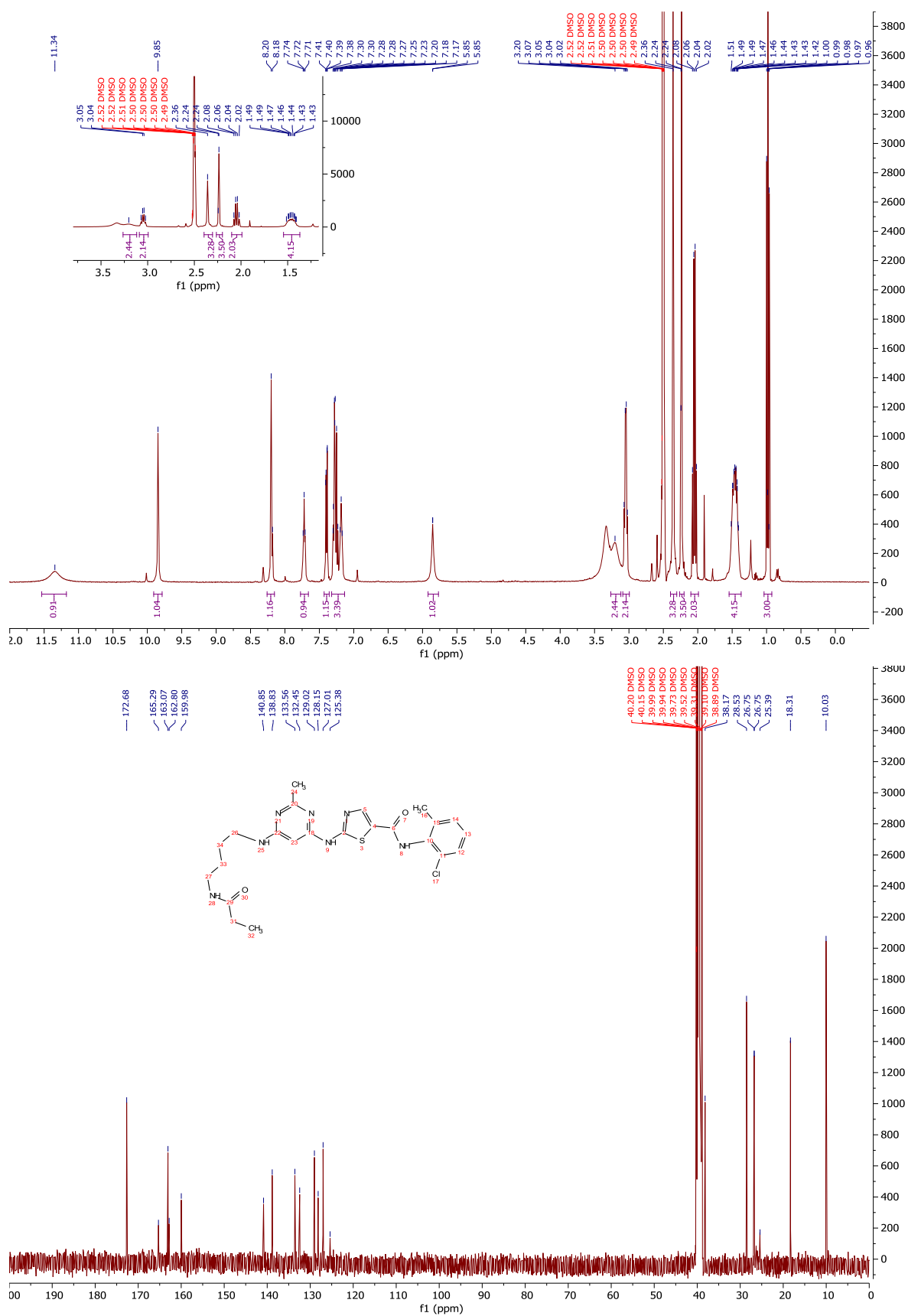
¹H-NMR and ¹³C-NMR: Compound 288



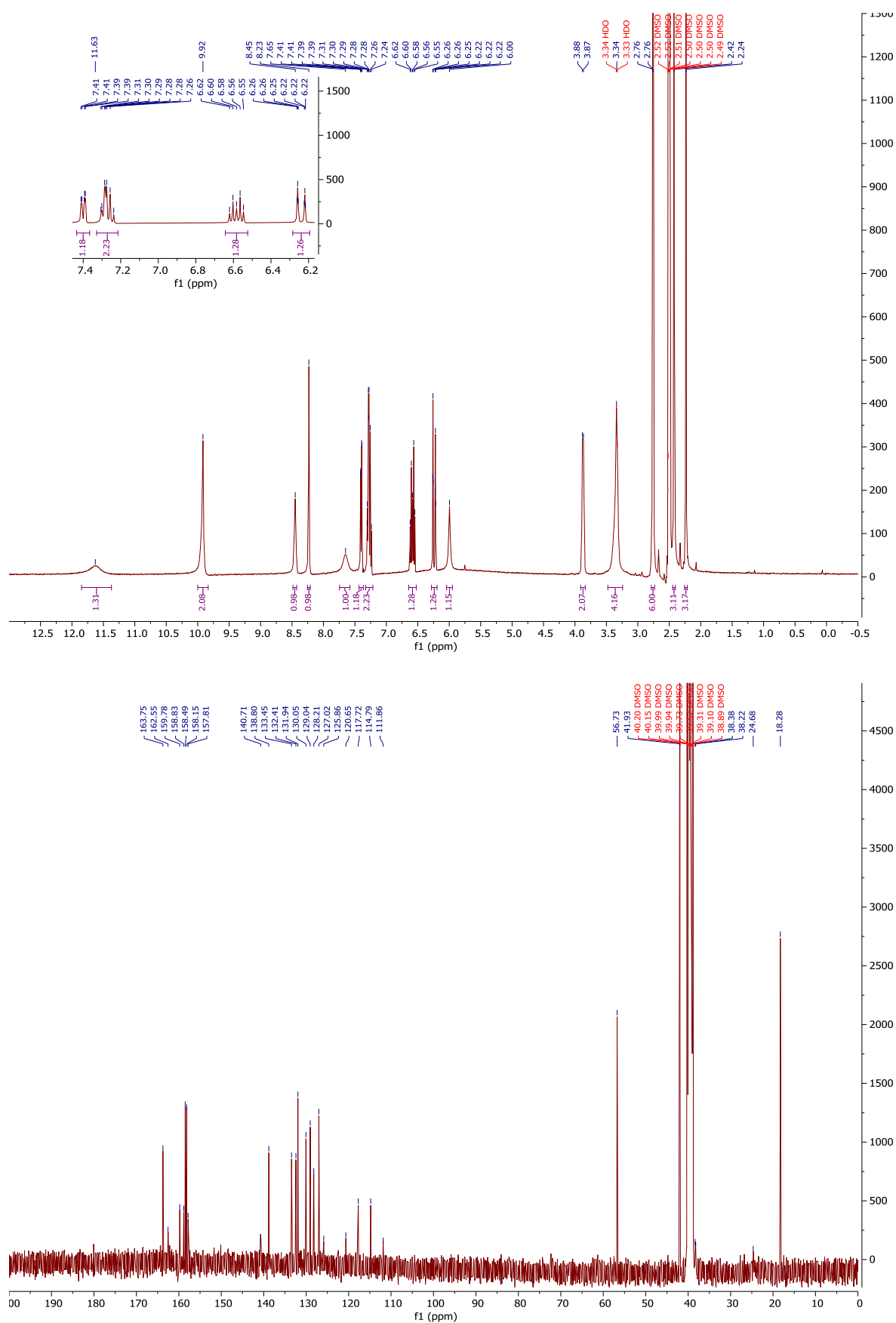
¹H-NMR and ¹³C-NMR: Compound 289



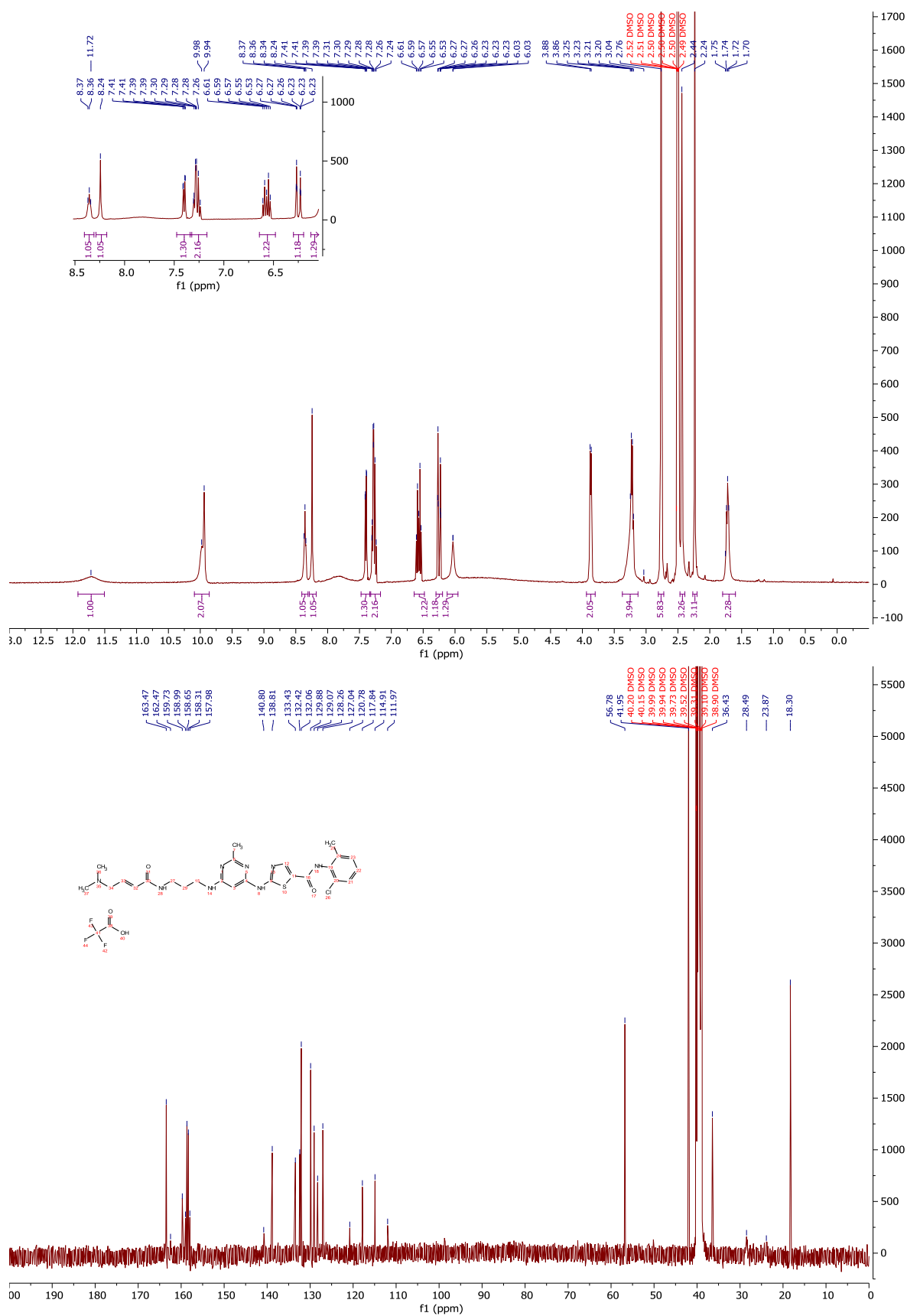
¹H-NMR and ¹³C-NMR: Compound 290



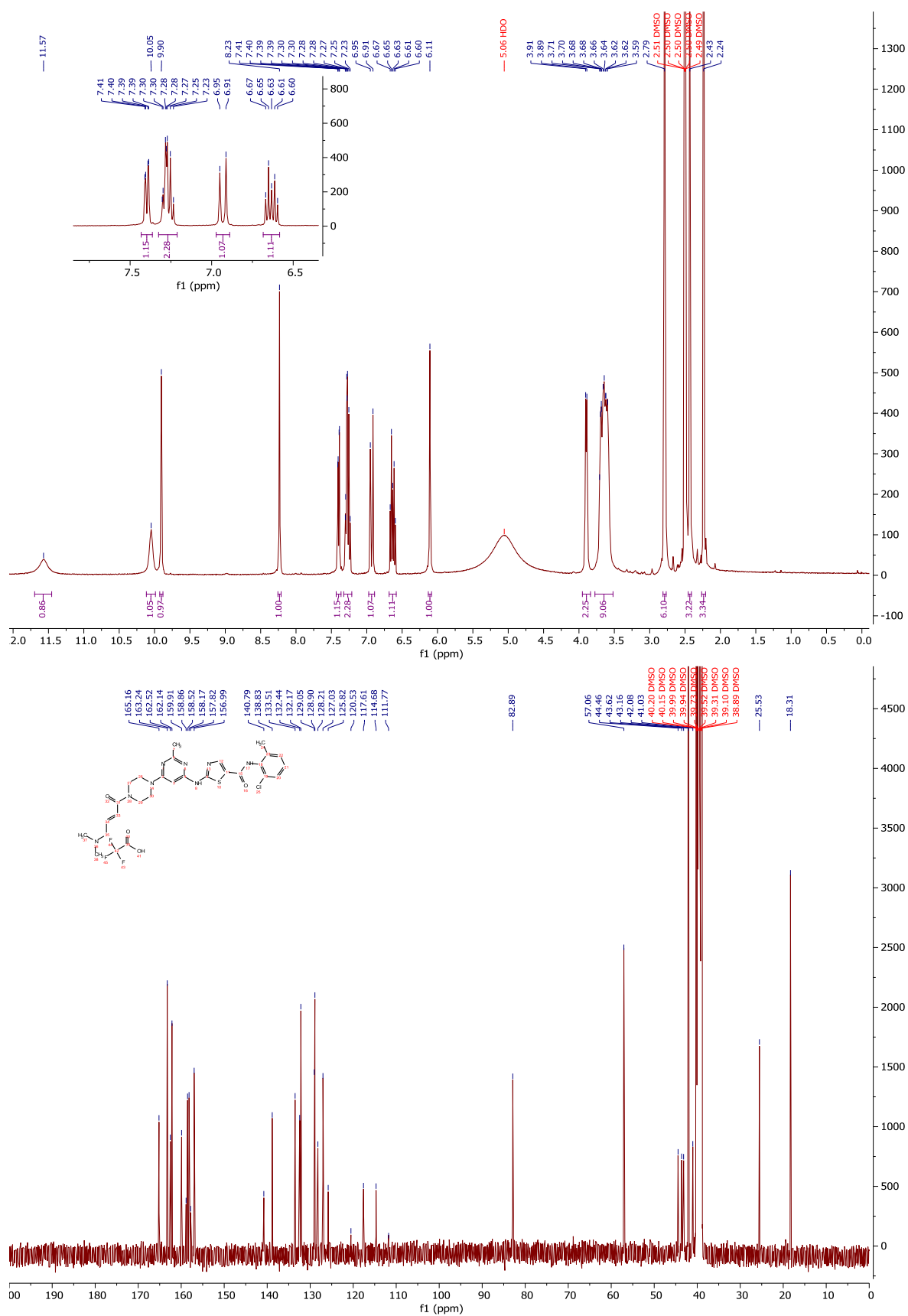
¹H-NMR and ¹³C-NMR: Compound 292



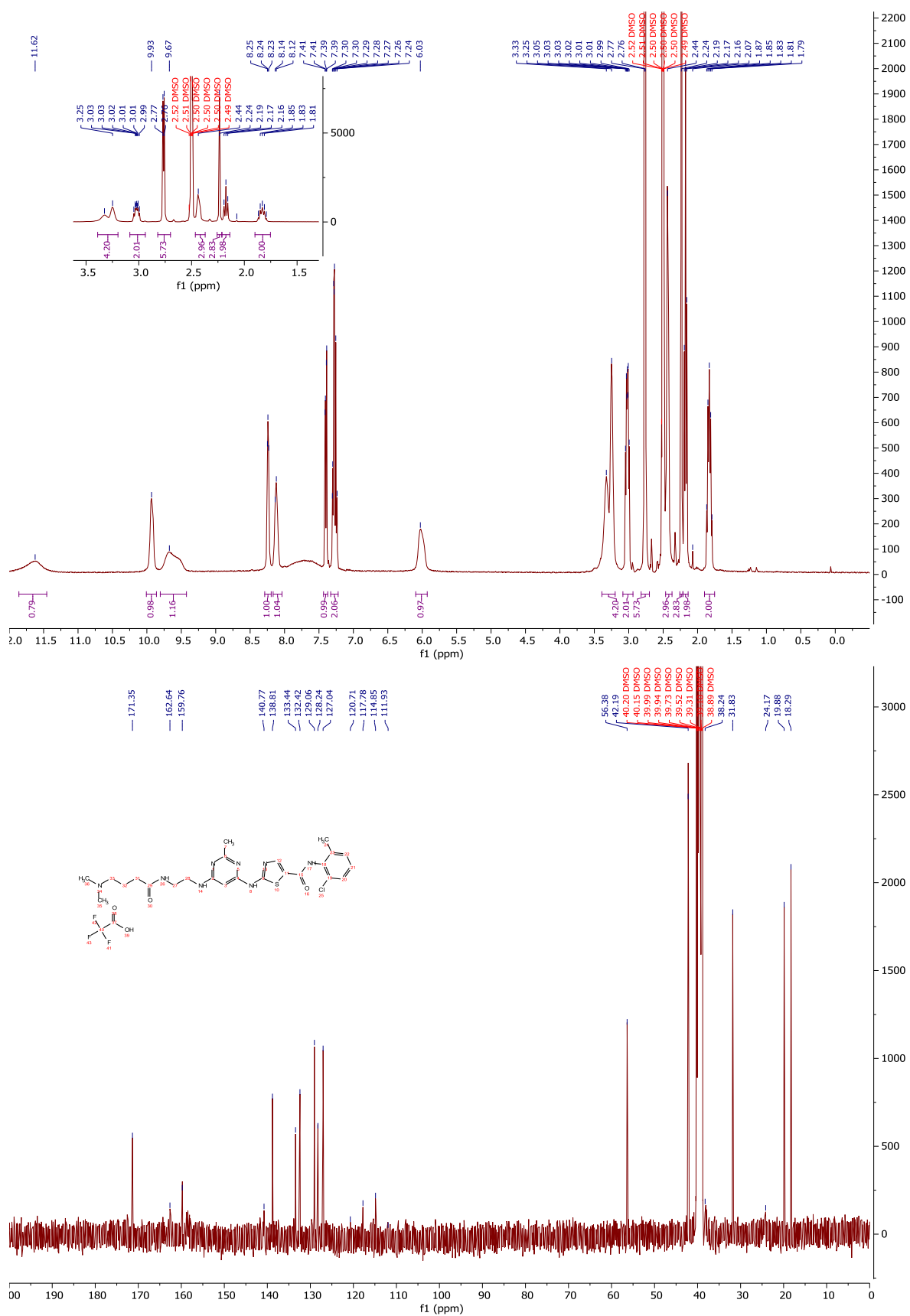
¹H-NMR and ¹³C-NMR: Compound 293



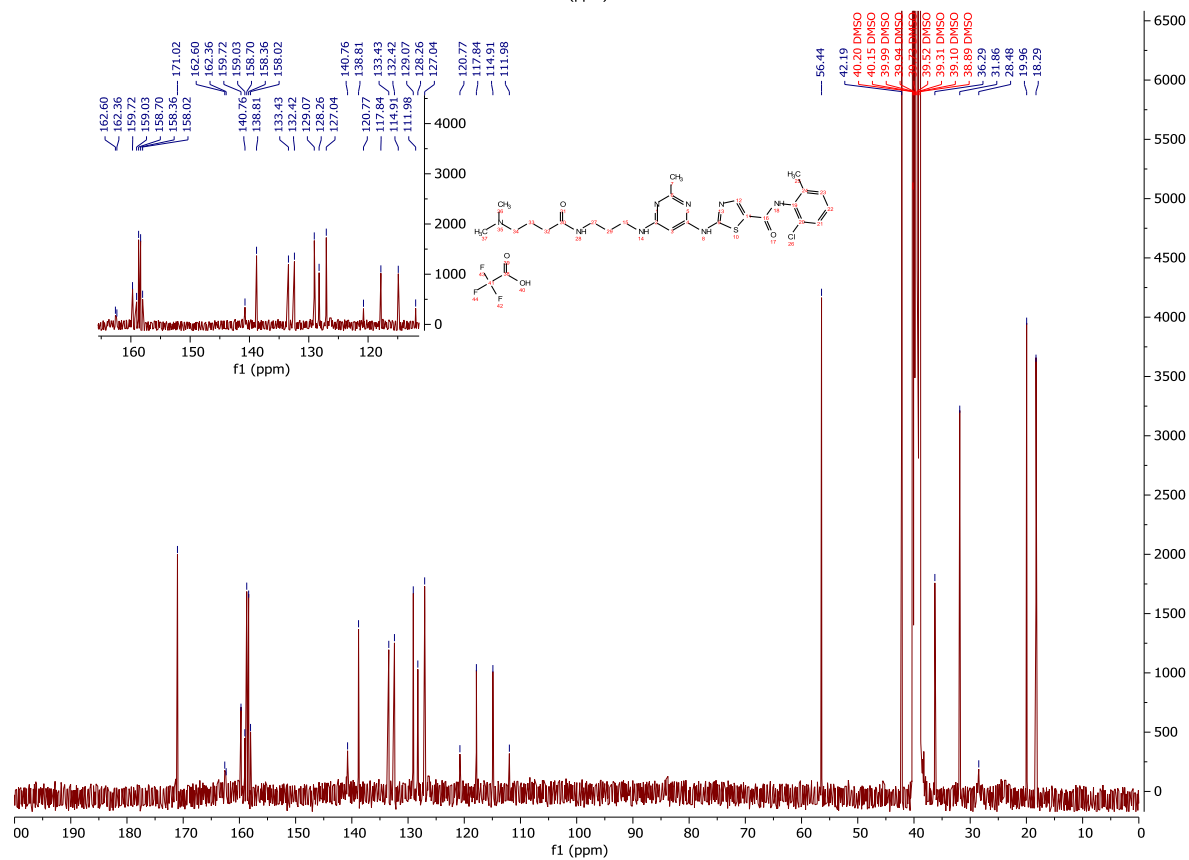
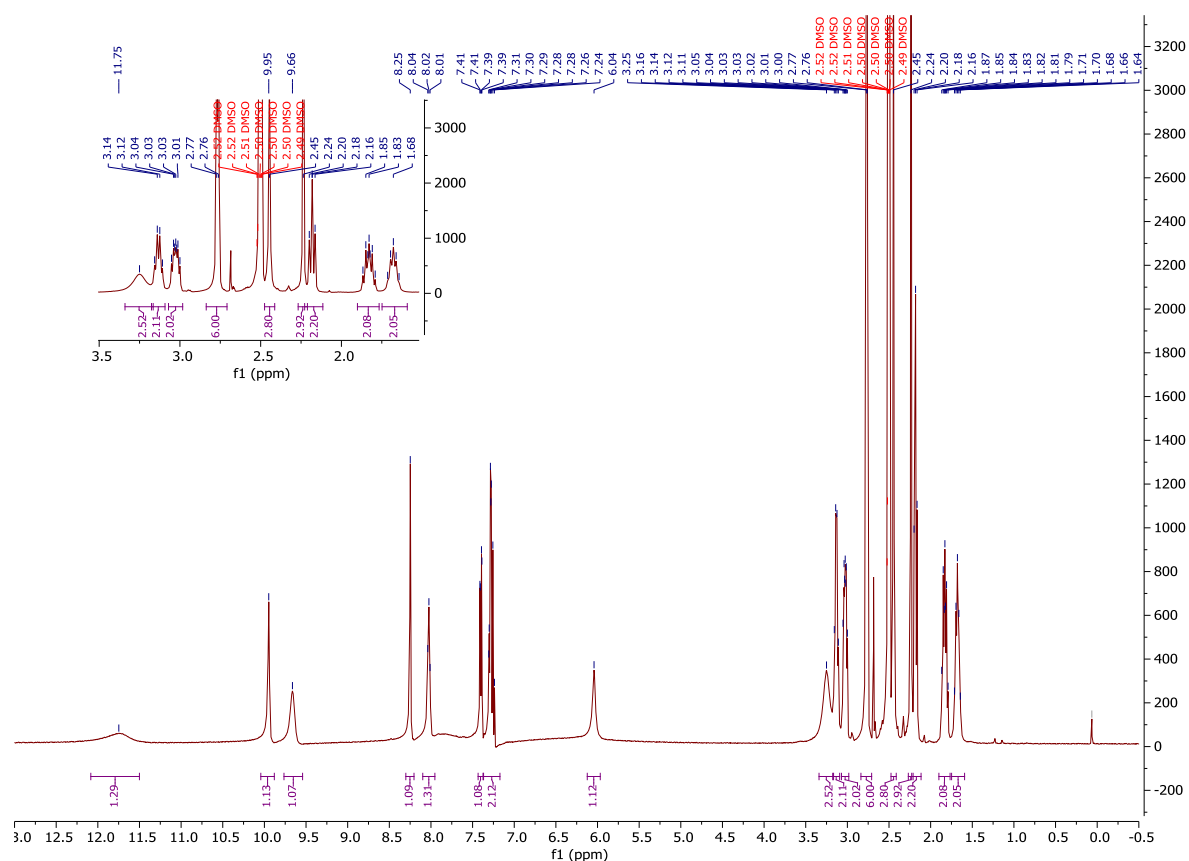
¹H-NMR and ¹³C-NMR: Compound 295



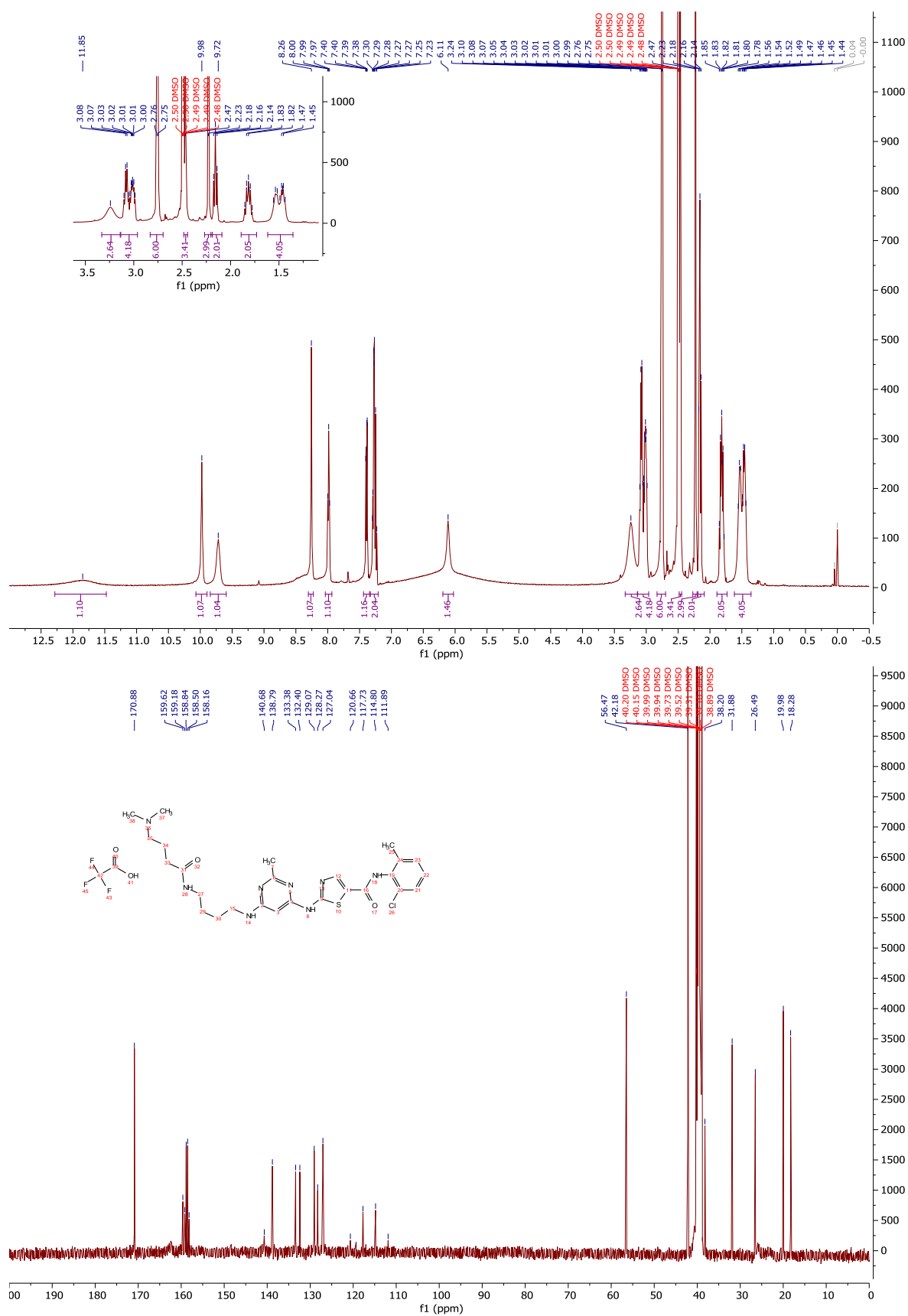
¹H-NMR and ¹³C-NMR: Compound 296



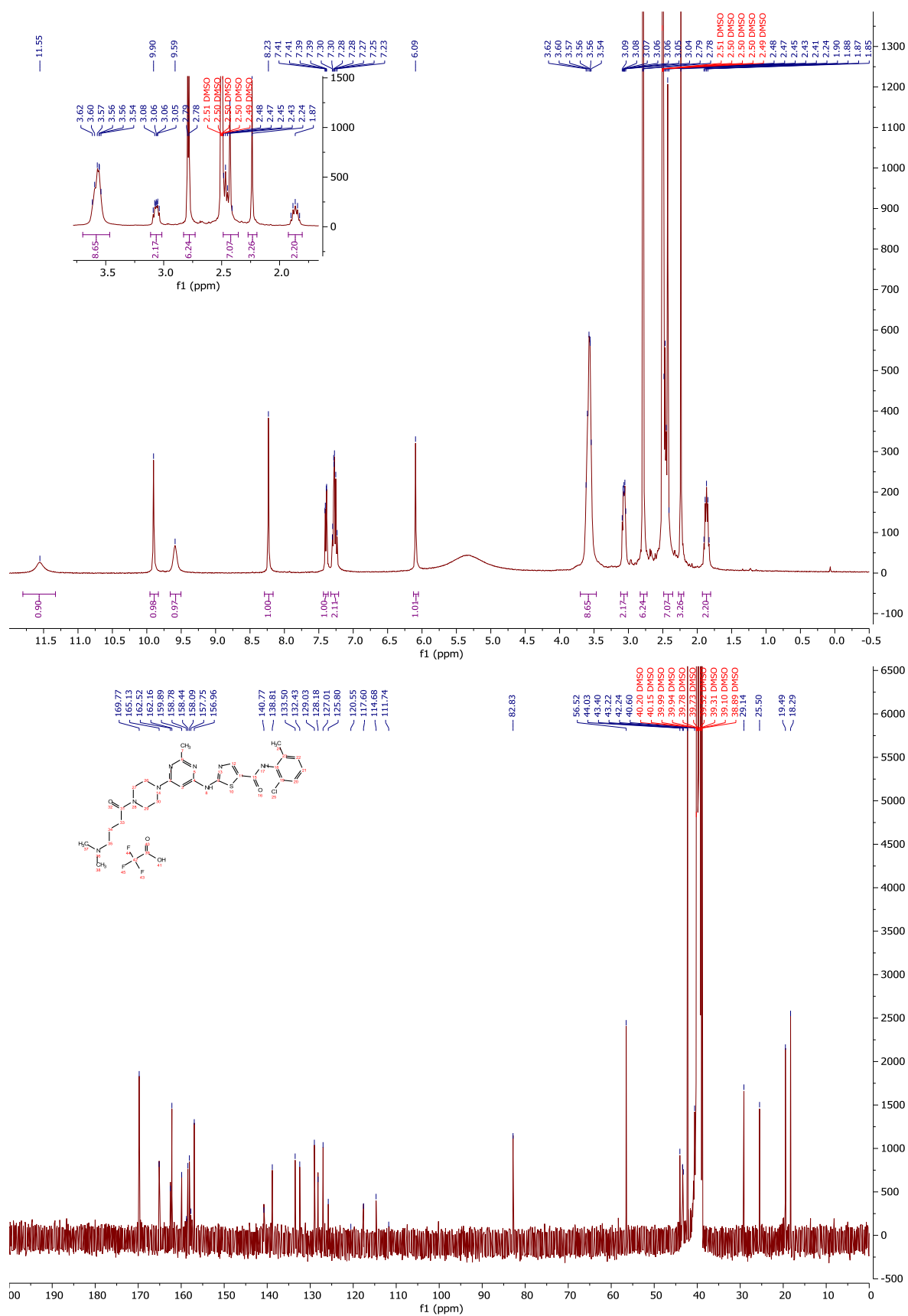
¹H-NMR and ¹³C-NMR: Compound 297



¹H-NMR and ¹³C-NMR: Compound 298



¹H-NMR and ¹³C-NMR: Compound 299



¹H-NMR and ¹³C-NMR: Compound 300

